



Some Types of Neutrosophic Ideals in BN-Algebras

A.Ibrahim^{1*} and B. Kavitha²

¹Assistant Professor, PG and Research Department of Mathematics, H.H. The Rajah's College, Pudukkottai (Affiliated to Bharathidasan University) Tiruchirappalli, Tamil Nadu, India.

²Research Scholar, PG and Research Department of Mathematics, H.H. The Rajah's College, Pudukkottai (Affiliated to Bharathidasan University) Tiruchirappalli, Tamil Nadu, India.

Received: 20 Jan 2024

Revised: 09 Feb 2024

Accepted: 14 May 2024

*Address for Correspondence

A.Ibrahim

Assistant Professor,

PG and Research

Department of Mathematics,

H.H. The Rajah's College, Pudukkottai

(Affiliated to Bharathidasan University)

Tiruchirappalli, Tamil Nadu, India.

Email: dribrahimaadhil@gmail.com



This is an Open Access Journal / article distributed under the terms of the **Creative Commons Attribution License** (CC BY-NC-ND 3.0) which permits unrestricted use, distribution, and reproduction in any medium, provided the original work is properly cited. All rights reserved.

ABSTRACT

In this paper, we introduce the notions of the normal neutrosophic ideal and the closed neutrosophic ideal of BN-algebra with suitable illustrations. Further, we introduce the neutrosophic r-ideal and the normal neutrosophic r-ideal of BN-algebra and investigate some of the related properties. Moreover, we define a closed neutrosophic r-ideal and discuss related theorems. Finally, we introduce the notions of neutrosophic k-ideal and m-k-ideals with illustrations and some properties.

Keywords: Neutrosophic set; BN-algebra; Neutrosophic ideal; Closed neutrosophic ideal; Neutrosophic r-ideal; Normal neutrosophic r-ideal; Closed neutrosophic r-ideal; Neutrosophic k-ideal; Neutrosophic m-k-ideal.

INTRODUCTION

The definition of a fuzzy set was first presented by Zadeh[13]. Intuitionistic fuzzy sets, an extension of fuzzy sets, were first described by Atanassov [2] in 1986. According to Smarandache [10], a neutrosophic set can be used to express the uncertainty and irrationality of any knowledge. The definition of fuzzy ideals in BN-algebra was provided by Grzegorz Dymek and Andrzej Waleadziak [1]. The ideas of r-ideal in commutation semigroups were developed by Erbay et al. in 2016 [4]. The definitions of r-ideal and m-k-ideal provided by Rao [8] are inclined. Gemawati et al.'s [5] discussion of the BN-algebra full ideal and introduction of the notion of an n-ideal in BN-algebra. BN-algebra's r-ideal and m-k-ideal notions were first introduced in 2022 by Sri Gemawati, Musnis musraini,

75529





Ibrahim and Kavitha

Abdul Hadi, La zakaria, and Elsi fitria [11]. The authors [6] introduced the notation of a neutrosophic ideal of BN-algebra and investigated some properties. We define the terms normal neutrosophic ideal and closed neutrosophic ideal of BN-algebra. Additionally, we discuss the idea of the neutrosophic r-ideal and look at its characteristics. We also looked at the neutrosophic k-ideal and the neutrosophic m-k-ideal. Finally, it was determined the characteristics of the neutrosophic m-k-ideal and k-ideal. The concepts of neutrosophic r-ideal and neutrosophic m-k-ideal in BH and BE algebra, as well as some of their properties, will be studied in more detail in the future.

PRELIMINARIES

In this section, we recall some basic definitions of BN-algebra, ideals, properties of ideals, and the concept of neutrosophic sets and neutrosophic ideals of BN-algebra that are useful to the main results.

Definition 2.1[1] An algebra $(X, \odot, 0)$ of type $(2, 0)$ is called BN-algebra, if the following are satisfied for all $\lambda, \mu, \delta \in X$,

- (i) $(\lambda \odot \lambda) = 0$
- (ii) $(\lambda \odot 0) = \lambda$
- (iii) $(\lambda \odot \mu) \odot \delta = (0 \odot \delta) \odot (\mu \odot \lambda)$.

Theorem 2.2[11]: Let $(X, \odot, 0)$ be a BN-algebra, then for all $\lambda, \mu, \delta \in X$,

- (i) $0 \odot (0 \odot \lambda) = \lambda$
- (ii) $\mu \odot \lambda = (0 \odot \lambda) \odot (0 \odot \mu)$
- (iii) $(0 \odot \lambda) \odot \mu = (0 \odot \mu) \odot \lambda$
- (iv) If $\lambda \odot \mu = 0$ then $\mu \odot \lambda = 0$
- (v) If $0 \odot \lambda = 0 \odot \mu$ then $\lambda = \mu$
- (vi) $(\lambda \odot \delta) \odot (\mu \odot \delta) = (\delta \odot \mu) \odot (\delta \odot \lambda)$

Definition 2.3[11]: A subset I of a BN-algebra $(X, \odot, 0)$ is called an ideal of X , if it is satisfied the following for all $\lambda, \mu \in X$,

- (i) $0 \in I$
- (ii) $\lambda \odot \mu \in I$ and $\mu \in I$ imply $\lambda \in I$.

Definition 2.4[11]: A nonempty subset S of X is called subalgebra of X or BN-subalgebra of X if it satisfies $\lambda \odot \mu \in S$ for all $\lambda, \mu \in S$.

Definition 2.5[11]: A non empty subset N of X is said to be normal in X , if $(\lambda \odot a) \odot (\mu \odot b) \in N$ for and $\lambda \odot a, \mu \odot b \in N$. We say that an ideal I of X (respectively a subalgebra S of X) is normal if I (respectively the set S) is normal.

Proposition 2.6[11]: Let I be a normal ideal of BN-algebra X , then I is a subalgebra of X .

Proposition 2.7[11]: Let X be a BN-algebra and $S \subseteq X$, if and only if S is a normal ideal, S is a normal subalgebra of X .

Definition 2.8[11]: Let BN-algebras $(X, \odot, 0)$ and $(Y, \odot, 0)$ exist. A map $f: X \rightarrow Y$ is said to as a homomorphism of X to Y if it meets $f(\lambda \odot \mu) = f(\lambda) \odot f(\mu)$ for all $\lambda, \mu \in X$. An endomorphism is a homomorphism of X to itself.

Definition 2.9[6]: A neutrosophic set $N = \{T_N, I_N, F_N\}$ of BN-algebra $(X, \odot, 0)$, if N is called an neutrosophic ideal of BN-algebra $(X, \odot, 0)$, if it satisfies the following for all $\lambda, \mu \in X$,

- (i) $T_N(0) \geq T_N(\lambda); I_N(0) \geq I_N(\lambda); F_N(0) \leq F_N(\lambda)$
- (ii) $T_N(\lambda) \geq \min \{T_N(\lambda \odot \mu), T_N(\mu)\}; I_N(\lambda) \geq \min \{I_N(\lambda \odot \mu), I_N(\mu)\}$
 $F_N(\lambda) \leq \max \{F_N(\lambda \odot \mu), F_N(\mu)\}$ for all $\lambda, \mu \in X$.



**NEUTROSOPHIC r-IDEAL**

The main results of the research are presented in this section. beginning with an explanation of the closed ideals and the neutrosophic normal with examples. Additionally, r-ideals in semigroups served as the foundation for the concept of neutrosophic r-ideals in BN-algebras. The neutrosophic r-ideal in BN-algebras is then explored for some of its characteristics.

Definition 3.1: Let $(X, \odot, 0)$ be a BN-algebra and N be a neutrosophic ideal of X , N is called a normal neutrosophic ideal of X , if it satisfies the following for all $\lambda, \mu, a, b \in X$,

$$T_N((\lambda \odot a)) \geq \min\{T_N(\lambda \odot a), T_N(\mu \odot b)\}; \quad I_N((\lambda \odot a)) \geq \min\{I_N(\lambda \odot a), I_N(\mu \odot b)\}; \\ F_N(\lambda \odot a) \leq \max\{F_N(\lambda \odot a), F_N(\mu \odot b)\}.$$

Example 3.2: Consider a set $A = \{0, \lambda, \mu, \delta, 1\}$. Define a binary operation ' \odot ' on A given by the following Table 3.1, and neutrosophic set define by the Table 3.2 as shown below:

It is easily verified that N is a normal neutrosophic ideal of A , and that it satisfies the conditions of definition 3.1.

Definition 3.3: Let $(X, \odot, 0)$ be a BN-algebra, and N be a neutrosophic ideal of X , C_N is closed neutrosophic ideal of X , if it satisfies the following for all $\lambda, \mu \in X$,

$$T_N(\lambda \odot \mu) \geq T_N(\lambda); \quad I_N(\lambda \odot \mu) \geq I_N(\lambda); \quad F_N(\lambda \odot \mu) \leq I_N(\lambda).$$

Example 3.4: Consider a set $A = \{0, \lambda, \mu, \delta, 1\}$. Define a binary operation ' \odot ' on A given by the following Table 3.3, and neutrosophic set define by the Table 3.4 as shown below: It is easily verified that N is a closed neutrosophic ideal of A , and that it satisfies the conditions of definition 3.3.

Definition 3.5: A neutrosophic ideal N of a BN-algebra $(X, \odot, 0)$ is called a neutrosophic r-ideal of X , if it satisfies the following for all $\lambda, \mu \in X$,

$$T_N(\mu) \geq \min\{T_N(\lambda \odot \mu), T_N(0 \odot \lambda)\}; \quad I_N(\mu) \geq \min\{I_N(\lambda \odot \mu), I_N(0 \odot \lambda)\}; \\ F_N(\mu) \leq \max\{F_N(\lambda \odot \mu), F_N(0 \odot \lambda)\}.$$

Example 3.6: Consider a set $A = \{0, \lambda, \mu, \delta, 1\}$. Define a binary operation ' \odot ' on A given by the following Table 3.5, and neutrosophic set define by the Table 3.6 as shown below: It is easily verified that N is a neutrosophic r-ideal of A , and that it satisfies the conditions of definition 3.5.

Definition 3.7: A neutrosophic r-ideal N is called an normal neutrosophic r-ideal of a BN-algebra $(X, \odot, 0)$, if it satisfies the following for all $\lambda, \mu, a, b \in X$,

- (i) $T_N(0) \geq T_N(\lambda); I_N(0) \geq I_N(\lambda); F_N(0) \leq F_N(\lambda)$,
- (ii) $T_N((\lambda \odot a) \odot (\mu \odot b)) \geq \min\{T_N(\lambda \odot a), T_N(\mu \odot b)\};$
 $I_N((\lambda \odot a) \odot (\mu \odot b)) \geq \min\{I_N(\lambda \odot a), I_N(\mu \odot b)\};$
 $F_N((\lambda \odot a) \odot (\mu \odot b)) \leq \max\{F_N(\lambda \odot a), F_N(\mu \odot b)\}.$

Example 3.8: Consider a set $A = \{0, \lambda, \mu, \delta, 1\}$. Define a binary operation ' \odot ' on A given by the following Table 3.7, and neutrosophic set define by the Table 3.8 as shown below: It is easily verified that N is a normal neutrosophic ideal of A , and that it satisfies the conditions (i) and (ii) of definition 3.7.

Definition 3.9: A neutrosophic r-ideal N of a BN-algebra $(X, \odot, 0)$ is called a closed neutrosophic r-ideal of X , if it satisfies the following for all $\lambda, \mu \in X$,

$$T_N(\lambda \odot \mu) \geq T_N(\lambda); \quad I_N(\lambda \odot \mu) \geq I_N(\lambda); \quad F_N(\lambda \odot \mu) \leq I_N(\lambda).$$





Ibrahim and Kavitha

Example 3.10: Consider a set $A = \{0, \lambda, \mu, \delta, 1\}$. Define a binary operation ' \odot ' on A given by the following Table 3.9 and neutrosophic set define by the Table 3.10 as shown below: It is easily verified that N is a closed neutrosophic r-ideal of A , and that it satisfies the conditions of definition 3.9.

Theorem 3.11: Let C_N be a closed neutrosophic ideal of a BN-algebra X , then it is a neutrosophic r-ideal of X .

Proof: Let C_N be a closed neutrosophic ideal of BN-algebra.

Then, (i) $T_N(\lambda \odot \mu) \geq T_N(\lambda)$, (ii) $I_N(\lambda \odot \mu) \geq I_N(\lambda)$, (iii) $F_N(\lambda \odot \mu) \leq F_N(\lambda)$.

To prove: C_N be a neutrosophic r-ideal

It is clear that C_N is neutrosophic ideal of X

Therefore, $T_N(\lambda \odot \mu) \geq T_N(\lambda)$

$$= T_N(0 \odot \lambda)$$

$$T_N(\lambda \odot \mu) \geq T_N(0 \odot \lambda)$$

$$T_N(\mu) \geq \min \{T_N(\lambda \odot \mu), T_N(\lambda)\}$$

$$\text{Now, } T_N(\mu) \geq \min \{T_N(\lambda \odot \mu), T_N(0 \odot \lambda)\}$$

Hence, C_N is a neutrosophic r-ideal.

Theorem 3.12: If $(X, \odot, 0)$ is a BN-algebra and N is a normal neutrosophic ideal of X , then N is the normal neutrosophic r-ideal of X .

Proof: Let N be a normal neutrosophic ideal of X .

Then, from the proposition 2.6, N is a BN-sub algebra of X . That is, $\lambda \odot \mu \in X$ for all $\lambda, \mu \in X$.

Then, we have the following for all $\lambda, \mu \in X$, $T_N(\lambda \odot \mu) \geq T_N(\lambda)$, $I_N(\lambda \odot \mu) \geq I_N(\lambda)$, and $F_N(\lambda \odot \mu) \leq F_N(\lambda)$.

This implies that N is closed neutrosophic r-ideal.

Following that, we discover that N is a neutrosophic r-ideal of X .

N is the normal neutrosophic r-ideal of X because N is the normal neutrosophic ideal.

Theorem 3.13: Let f be an endomorphism of a BN-algebra $(X, \odot, 0)$, and N be a neutrosophic r-ideal of X , then $f(N)$ is a neutrosophic r-ideal of X .

Proof: Let N be a neutrosophic r-ideal of X , then clearly $N \subset X$ and N is a neutrosophic ideal of X such that $T_N(f(0)) \geq T_N(f(\lambda))$, $I_N(f(0)) \geq I_N(f(\lambda))$,

$$F_N(f(0)) \geq F_N(f(\lambda)) \text{ and } f(N) \subset X \text{ for all } \lambda \in X.$$

Since N is a neutrosophic ideal of X ,

$$T_N(0) \geq T_N(\lambda), I_N(0) \geq I_N(\lambda),$$

$$F_N(0) \leq F_N(\lambda) \text{ for all } \lambda, \mu \in X.$$

We obtain $T_N(0) \geq T_N(\lambda)$

$$T_N(f(0)) \geq T_N\{f(\lambda \odot \lambda)\}$$

$$\geq T_N\{f(\lambda) \odot f(\lambda)\}, \text{ Since } f \text{ be an endomorphism}$$

$$T_N(f(0)) \geq T_N(0)$$

$$\text{Let } T_N\{f(0)\} \geq T_N\{f(\lambda)\}, \text{ and } T_N\{f(0)\} \geq T_N\{f(\lambda \odot \mu)\}$$

Since N is a neutrosophic ideal, then $T_N(0) \geq T_N(\lambda)$.

Consequently, $T_N\{f(0)\} \geq T_N\{f(\lambda)\}$. Thus $f(N)$ is a neutrosophic ideal of X .

Let $T_N\{f(0)\} \geq T_N\{f(\lambda \odot \mu)\}$ and

$$T_N\{f(\lambda)\} = T_N\{0 \odot f(\lambda)\}$$

Since N is a neutrosophic r-ideal of X , $T_N(0) \geq T_N(\mu)$ implies $T_N\{f(0)\} \geq T_N\{f(\mu)\}$ and $T_N\{f(\mu)\} \geq \min \{T_N\{f(\lambda \odot \mu)\}, T_N\{0 \odot f(\lambda)\}\}$.

Thus, $f(N)$ is a neutrosophic r-ideal of X .

Note: The converse of above theorem hold in general.

NEUTROSOPHIC k AND m-k-IDEALS

The main findings of the study are presented in this section. We begin by defining the ideas of a neutrosophic k-ideal and m-k-ideal in a BN-algebra, which is built on the idea of a k-ideal and m-k-ideal in an inclination. In a BN-algebra, the properties of neutrosophic k-ideals and m-k-ideals are given.





Ibrahimand Kavitha

Definition 4.1: A neutrosophic ideal N of BN-algebra $(X, \odot, 0)$ is called a neutrosophic k -ideal of X , if it satisfies the condition for all $\lambda, \mu \in X$,

$$T_N(\lambda) \geq \min \{ T_N(\mu), T_N(\lambda), T_N(\lambda \odot \mu) \}; \quad I_N(\lambda) \geq \min \{ T_N(\mu), T_N(\lambda), T_N(\lambda \odot \mu) \}; \quad F_N(\lambda) \leq \max \{ T_N(\mu), T_N(\lambda), T_N(\lambda \odot \mu) \}.$$

Example 4.2: Consider a set $A = \{0, \lambda, \mu, \delta, 1\}$. Define a binary operation ' \odot ' on A given by the following Table 4.1 and neutrosophic set define by the Table 4.2 as shown below:

It is easily verified that N is a neutrosophic k -ideal of A , and that it satisfies the conditions of definition 4.1.

Definition 4.3: A neutrosophic ideal N of a BN-algebra $(X, \odot, 0)$ is called a neutrosophic m - k -ideal of X , if it satisfies the condition for all $\lambda, \mu \in X$ and $y \neq 0$,

$$T_N(\lambda) \geq \min \{ T_N(\lambda), T_N(\mu), T_N(\lambda \odot \mu) \}; \quad I_N(\lambda) \geq \min \{ I_N(\lambda), I_N(\mu), I_N(\lambda \odot \mu) \}; \\ F_N(\lambda) \leq \max \{ F_N(\lambda), F_N(\mu), F_N(\lambda \odot \mu) \}.$$

Example 4.4: Consider a set $A = \{0, \lambda, \mu, \delta, 1\}$. Define a binary operation ' \odot ' on A given by the following Table 4.3 and neutrosophic set define by the Table 4.4 as shown below: It is easily verified that N is a neutrosophic m - k -ideal of A , and that it satisfies the condition of definition 4.3.

Theorem 4.5: If C_N is a closed neutrosophic ideal of a BN-algebra $(X, \odot, 0)$, then C_N is a neutrosophic k -ideal of X .

Proof: Let C_N be closed neutrosophic ideal of BN-algebra X , then C_N is a BN sub algebra of X , and if $T_N(\lambda) \geq \min \{ T_N(\mu), T_N(\lambda), T_N(\lambda \odot \mu) \}$

$$I_N(\lambda) \geq \min \{ I_N(\mu), I_N(\lambda), I_N(\lambda \odot \mu) \} \text{ and}$$

$$F_N(\lambda) \leq \max \{ F_N(\mu), F_N(\lambda), F_N(\lambda \odot \mu) \}.$$

Thus, C_N is a neutrosophic k -ideal of X .

Theorem 4.6: If N_K is a neutrosophic k -ideal of a BN-algebra $(X, \odot, 0)$, then N_K is closed neutrosophic ideal of X .

Proof: Let N_K is a neutrosophic k -ideal of X , then N_K is a BN-subalgebra of X . Consequently, N_K is closed for all $\lambda, \mu \in X$.

$$\begin{aligned} \text{Also, } T_N(0) &\geq \{ T_N(\lambda), T_N(\lambda \odot \lambda) \\ &= T_N(0) \\ &\geq \{ T_N(\lambda) \}. \end{aligned}$$

Moreover, N_K is a neutrosophic k -ideal of X .

$$\text{Then, } T_N(\lambda) \geq \min \{ T_N(\lambda), T_N(\mu), T_N(\lambda \odot \mu) \},$$

$$I_N(\lambda) \geq \min \{ I_N(\lambda), I_N(\mu), I_N(\lambda \odot \mu) \} \text{ and}$$

$$F_N(\lambda) \leq \max \{ F_N(\lambda), F_N(\mu), F_N(\lambda \odot \mu) \}.$$

From this we have, $T_N(\lambda \odot \mu) \geq T_N(\lambda)$, $I_N(\lambda \odot \mu) \geq I_N(\lambda)$ and $F_N(\lambda \odot \mu) \leq F_N(\lambda)$.

Thus, N_K is a closed neutrosophic ideal of X .

Theorem 4.7: Let $(X, \odot, 0)$ be a BN-algebra, If N is a normal BN-subalgebra of X then N is a normal neutrosophic k -ideal of X ,

Proof: Let N be a normal BN-subalgebra of X . Then, from the proposition 2.6, N is a normal neutrosophic ideal of X . We know that N is a BN-subalgebra such that it is a closed neutrosophic ideal of X . Furthermore, it is obtained that N is a neutrosophic

k -ideal of X . is a neutrosophic k -ideal of . Since is normal, is a normal neutrosophic k -ideal of X .

Theorem 4.8: If N_K is a neutrosophic k -ideal of BN-algebra $(X, \odot, 0)$, then N_K is a neutrosophic m - k -ideal of X .

Proof: Let N_K be a neutrosophic k -ideal of X , then N_K is a closed neutrosophic ideal of X , such that $T_N(\lambda) \geq \min \{ T_N(\mu), T_N(\lambda \odot \mu) \}$,

$$I_N(\lambda) \geq \min \{ I_N(\mu), I_N(\lambda \odot \mu) \} \text{ and } F_N(\lambda) \leq \max \{ F_N(\mu), F_N(\lambda \odot \mu) \}.$$

Since N_K is closed neutrosophic ideal it must be the case that if $y \neq 0, y \in X$,





Ibrahim and Kavitha

$$T_N(\mu) \geq \min \{T_N(\lambda), T_N(\lambda \odot \mu)\}, I_N(\mu) \geq \min \{I_N(\lambda), I_N(\lambda \odot \mu)\}, \\ F_N(\mu) \leq \max \{F_N(\lambda), F_N(\lambda \odot \mu)\}.$$

Hence, N_K is a neutrosophic m-k-ideal X .

Proposition 4.9: If C_{N_r} is closed neutrosophic r-ideal of BN-algebra $(X, \odot, 0)$, then C_{N_r} is a neutrosophic k-ideal.

Proof: Let C_{N_r} be a neutrosophic r-ideal of X . Clearly, C_{N_r} is a neutrosophic ideal of X . Since, C_{N_r} is closed neutrosophic r-ideal of X then C_{N_r} is a neutrosophic k-ideal of X .

Proposition 4.10: Let $(X, \odot, 0)$ be a BN-algebra, and f be an endomorphism of X . If N_K is a neutrosophic k-ideal of X , then $f(N_K)$ is a neutrosophic r-ideal of X .

Proof: Let $(X, \odot, 0)$ be a BN-algebra and let f be an endomorphism of X . If N_K is a neutrosophic k-ideal of X , then N_K is a neutrosophic r-ideal. Further, $f(N_K)$ is a neutrosophic r-ideal of X .

Proposition 4.11: Let $(X, \odot, 0)$ be a BN-algebra and since f be an endomorphism of X . If $f(N)$ is a closed neutrosophic r-ideal of X , then N is a neutrosophic k-ideal of X .

Proof: Let $(X, \odot, 0)$ be a BN-algebra and let f be an endomorphism of X . If $f(N)$ is a closed neutrosophic r-ideal of X , then N is closed neutrosophic r-ideal of X . Further, N is a neutrosophic k-ideal of X .

CONCLUSION

This paper begins by considering the notions of the normal neutrosophic ideal and the closed neutrosophic ideal of BN-algebra with suitable illustrations. Also, we have introduced the concept of neutrosophic r-ideals and investigated their properties. Also, we have investigated neutrosophic k-ideals and neutrosophic m-k-ideals. Finally, we have discovered the characteristics of neutrosophic k-ideals and neutrosophic m-k-ideals. We conducted this research to provide comprehensive notions for the neutrosophic r-ideal, neutrosophic k-ideal, and neutrosophic m-k-ideal of BN-algebras. Future research will look at the notions of neutrosophic r-ideals and neutrosophic m-k-ideals in BH and BE algebras and explore some of their properties.

REFERENCES

1. Andrzej Walendziak and Grzegorz Dymek (2015), *Fuzzy Ideals of BN-Algebras*, Hindawi Publishing Corporation the Scientific World Journal, Volume 2015, (9 pages).
2. K.T. Atanassov, *Intuitionistic Fuzzy Sets, Fuzzy Sets and Systems*, 1986, 20(1), 87-96.
3. Banerjee, D., Giri, B. C., Pramanik, S., and Smarandache, F., (2017), GRA for multiattribute decision making in neutrosophic cubic set environment. *Neutrosophic Sets and Systems*, Volume 15, 60-69.
4. Erbay, M.A., Tekir, U., Koc, S. r-Ideals of commutative semigroups. *Int. J. Algebr.* (2016), 10, 525-533.
5. Gemawati, S., Fitria, E., Hadi, A., Musraini, M. Complete ideal and n-ideal BN-algebras of. *Int. J. Math. Trends Technol.* 2020, 66, 52-59.
6. Ibrahim A., and Kavitha B., *Neutrosophic ideals of BN- algebra*, Mathematical forum, Mathematical Forum Vol. 30, 2022, ISSN: 0972-9852.
7. Mehmet Ali, Ozturk, and Young Bae Jun (2018), *Neutrosophic Ideals In BCK/BCI-Algebras Based On Neutrosophic Points*, Journal of The International Mathematical Virtual Institute, Volume 8, 1-17.
8. Rao, M.M.K. r-Ideals and m-k-ideals in inclines. *Gen. Algebr. Appl.* (2020), 40, 297-309.
9. Salama A.A., and Elagamy H.A., (2021), *On Neutrosophic Fuzzy Ideal Concepts*, International Journal of Neutrosophic Science, Volume 14, 98-103.
10. Smarandache Florentin (2005), *Neutrosophic set-a generalization of the intuitionistic fuzzy set*, International Journal of Pure and Applied Mathematics, Volume 24, 287-297.
11. Sri Gemawati, Musnis Musraini, Abdul Hadi, La Zakaria and Elsi Fitria, *On r-Ideals and m-k-Ideals in BN-*





Ibrahim and Kavitha

Algebras, Axioms 2022,1-8.

12. Surapati Pramanik, Rumi Roy, Tapan Kumar Roy and Florentin Smarandache (2017), *Multi criteria decision making using correlation coefficient under rough neutrosophic environment*, Neutrosophic Sets and Systems, Volume 17, 29-36.
13. Zadeh. L. A, Fuzzy Sets, Information and control, 1965, 8(3), 338-353.

Table 3.1: ' \odot ' Operation

\odot	0	λ	μ	δ	1
0	0	0	0	0	0
λ	λ	0	λ	λ	λ
μ	μ	λ	0	μ	μ
δ	δ	δ	δ	0	δ
1	1	λ	μ	δ	0

Table 3.2: Neutrosophic set

$A \backslash N$	0	λ	μ	δ	1
T_N	0.7	0.7	0.7	0.7	0.7
I_N	0.6	0.6	0.6	0.6	0.6
F_N	0.3	0.3	0.3	0.3	0.3

Table 3.3: ' \odot ' Operation

\odot	0	λ	μ	δ	1
0	0	0	0	0	0
λ	λ	0	λ	λ	λ
μ	μ	λ	0	μ	μ
δ	δ	δ	δ	0	δ
1	1	λ	μ	δ	0

Table 3.4: Neutrosophic set

$A \backslash N$	0	λ	μ	δ	1
T_N	0.9	0.7	0.7	0.6	0.6
I_N	0.7	0.6	0.6	0.5	0.5
F_N	0.2	0.4	0.4	0.4	0.4

Table 3.5: ' \odot ' Operation

\odot	0	λ	μ	δ	1
0	0	λ	δ	δ	1
λ	λ	0	λ	δ	λ
μ	μ	λ	0	δ	μ





Ibrahim and Kavitha

δ	δ	δ	δ	0	δ
1	1	λ	μ	δ	0

Table 3.6: Neutrosophic set

$\begin{smallmatrix} A \\ N \end{smallmatrix}$	0	λ	μ	δ	1
T_N	0.8	0.5	0.5	0.4	0.5
I_N	0.6	0.4	0.5	0.4	0.5
F_N	0.2	0.5	0.5	0.5	0.4

Table 3.7: ' \odot ' Operation

\odot	0	λ	μ	δ	1
0	0	λ	δ	δ	1
λ	λ	0	λ	δ	λ
μ	μ	λ	0	δ	μ
δ	δ	δ	δ	0	δ
1	1	λ	μ	δ	0

Table 3.8: Neutrosophic set

$\begin{smallmatrix} A \\ N \end{smallmatrix}$	0	λ	μ	δ	1
T_N	0.9	0.5	0.5	0.5	0.5
I_N	0.8	0.4	0.4	0.4	0.4
F_N	0.1	0.4	0.4	0.4	0.4

Table 3.9: ' \odot ' Operation

\odot	0	λ	μ	δ	1
0	0	λ	λ	μ	μ
λ	λ	0	λ	λ	λ
μ	μ	λ	0	μ	μ
δ	δ	δ	δ	0	δ
1	1	λ	μ	δ	0

Table 3.10: Neutrosophic set

$\begin{smallmatrix} A \\ N \end{smallmatrix}$	0	λ	μ	δ	1
T_N	0.6	0.6	0.6	0.5	0.5
I_N	0.5	0.5	0.5	0.4	0.4
F_N	0.4	0.4	0.4	0.4	0.3



Table 4.1: ' \odot ' Operation

\odot	0	λ	μ	δ	1
0	0	λ	δ	δ	1
λ	λ	0	λ	λ	λ
μ	μ	λ	0	μ	μ
δ	δ	δ	δ	0	δ
1	1	λ	μ	δ	0

Table 4.2: Neutrosophic set

$A \backslash N$	0	λ	μ	δ	1
T_N	0.9	0.8	0.8	0.8	0.6
I_N	0.7	0.6	0.6	0.6	0.5
F_N	0.1	0.3	0.3	0.3	0.3

Table 4.3: ' \odot ' Operation

\odot	0	λ	μ	δ	1
0	0	λ	δ	δ	1
λ	λ	0	λ	λ	λ
μ	μ	λ	0	μ	μ
δ	δ	δ	δ	0	δ
1	1	λ	μ	δ	0

Table 4.4: Neutrosophic set

$A \backslash N$	0	λ	μ	δ	1
T_N	0.8	0.7	0.7	0.6	0.6
I_N	0.6	0.5	0.5	0.5	0.4
F_N	0.1	0.2	0.2	0.2	0.2





On Nano Star Generalized Alpha Closed Set and Nano Star Generalized Alpha Continuous Function in Nano Topological Space

K. Baby¹ and H. Aaminumariyam^{2*}

¹Assistant Professor, Department of Mathematics, Kongunadu Arts and Science College (Autonomous), (Affiliated to Bharathiar University) Coimbatore, Tamil Nadu, India.

²Research Scholar, Department of Mathematics, Kongunadu Arts and Science College (Autonomous), (Affiliated to Bharathiar University) Coimbatore, Tamil Nadu, India.

Received: 22 Jan 2024

Revised: 09 Feb 2024

Accepted: 11 May 2024

*Address for Correspondence

H. Aaminumariyam

Research Scholar,
Department of Mathematics,
Kongunadu Arts and Science College (Autonomous),
(Affiliated to Bharathiar University)
Coimbatore, Tamil Nadu, India.
Email: aaminumariyam3@gmail.com



This is an Open Access Journal / article distributed under the terms of the **Creative Commons Attribution License** (CC BY-NC-ND 3.0) which permits unrestricted use, distribution, and reproduction in any medium, provided the original work is properly cited. All rights reserved.

ABSTRACT

The purpose of this paper is to introduce and investigate the Nano star generalized alpha closed sets and Nano star generalized continuous function in Nano topological spaces. Some of the basic properties of nano star generalized closed set and nano star generalized continuous functions are analyzed.

Keywords: $N^*\alpha$ – closed set, $N^*\alpha$ – continuous function.

INTRODUCTION

In 1970, Levin[1] introduced the concept of generalized closed sets as a generalization of closed sets in topological spaces. Lellis Thivagar[2] and Carmel Richard introduced the concept of Nano topology, which was defined in terms of approximation and boundary region of universe using an equivalence relation on it. He also introduced nano continuous functions nano open mappings nano closed mappings and homeomorphisms in nano topological spaces.

PRELIMINARIES

In this section, we recall some basic definitions and results in nano topological spaces.





Baby and Aaminumariyam

Definition 2.1.[2] Let U be a non-empty finite set of objects called the universe and R be an equivalence relation on U named as in discernibility relation. Then U is divided into equivalence classes. Elements belonging to the same equivalence class are said to be indiscernible with one another. The pair (U, R) is said to be the approximation space. Let $X \subseteq U$. Then,

- The lower approximation of X with respect to R is the set of all objects which can be for certain classified as X with respect to R and is denoted by $L_R(X)$. $L_R(X) = U\{R(X): R(X) \subseteq X, x \in U\}$
- The upper approximation of X with respect to R is the set of all objects which can be possibly classified as X with respect to R and is denoted by $U_R(X)$. $U_R(X) = U\{R(X): R(X) \cap X \neq \phi, x \in U\}$.
- The boundary region of X with respect to R is the set of all objects which can be classified neither as X nor as not $-X$ with respect to R and it is denoted by $B_R(X) = U_R(X) - L_R(X)$.

Property 2.2.[2] If (U, R) is an approximation space and $X, Y \subseteq U$, then

- $L_R(X) \subseteq X \subseteq U_R(X)$
- $L_R(\phi) = U_R(\phi) = \phi$
- $L_R(U) = U_R(U) = U$
- $U_R(X \cup Y) = U_R(X) \cup U_R(Y)$
- $U_R(X \cap Y) \subseteq U_R(X) \cap U_R(Y)$
- $L_R(X \cup Y) \supseteq L_R(X) \cap L_R(Y)$
- $L_R(X \cap Y) = L_R(X) \cap L_R(Y)$
- $L_R(X) \subseteq L_R(Y)$ and $U_R(X) \subseteq U_R(Y)$ whenever $X \subseteq Y$
- $U_R(X^c) = [L_R(X)]^c$ and $L_R(X^c) = [U_R(X)]^c$
- $U_R[U_R(X)] = L_R[U_R(X)] = U_R(X)$
- $L_R[L_R(X)] = U_R[L_R(X)] = L_R(X)$

Definition 2.3.[2] Let u be the universe, R be an equivalence relation on U and $\tau_R(X) = \{U, \phi, L_R(X), U_R(X), B_R(X)\}$ where $X \subseteq U$. Then it satisfies the following axioms:

1. U and ϕ belongs to $\tau_R(X)$
2. The union of the elements of any sub-collection of $\tau_R(X)$ is in $\tau_R(X)$.
3. The intersection of the elements of any finite sub collection of $\tau_R(X)$ is in $\tau_R(X)$.

Then $\tau_R(X)$ is a topology on U called the Nano topology on U with respect to X . $(U, \tau_R(X))$ is called the Nano topological space. Elements of the Nano topology are known as Nano sets in U . Elements of $[\tau_R(X)]^c$ are called Nano closed sets with $[\tau_R(X)]^c$ being called dual Nano topology of $\tau_R(X)$.

Remark 2.4.[2] If $\tau_R(X)$ is the Nano topology on U with respect to X , then the set $B = \{U, L_R(X), B_R(X)\}$ is the basis for $\tau_R(X)$.

Definition 2.5.[2] If Let $(U, \tau_R(X))$ is a Nano topological space with respect $X \subseteq U$ and if $A \subseteq U$, then

- The Nano interior of the set A is defined as the union of all nano open subsets contained in A and is denoted by $Nint(A)$. $Nint(A)$ is the largest nano open subset of A .
- The Nano closure of the set A is defined as the intersection of all nano closed sets containing in A and is denoted by $Ncl(A)$. $Ncl(A)$ is the smallest nano closed set containing A .

Definition 2.6.[2] Let $(U, \tau_R(X))$ be a Nano topological space and $A \subseteq U$. Then A is said to be

- Nano semi open if $A \subseteq Ncl[Nint(A)]$
- Nano semi closed if $Nint[Ncl(A)] \subseteq A$
- Nano pre-open if $A \subseteq Nint[Ncl(a)]$
- Nano pre-closed if $Nint[Ncl(A)] \subseteq A$
- Nano α open if $A \subseteq Nint[Ncl(Nint(A))]$
- Nano α closed if $Ncl[Nint(Ncl(A))] \subseteq A$.

Definition 2.7. Let $(U, \tau_R(X))$ be a Nano topological space. A subset A of $(U, \tau_R(X))$ is called





Baby and Aaminumariyam

- Nano generalized closed set [3] (briefly Ng-closed) if $Ncl(A) \subseteq V$ whenever $A \subseteq V$ and V is nano open in $(U, \tau_R(X))$.
- Nano semi-generalized closed [11] (briefly Nsg-closed) if $Nscl(A) \subseteq V$ whenever $A \subseteq V$ and V is nano semi open in $(U, \tau_R(X))$.
- Nano generalized-semi closed set [11] (briefly Ngs closed) if $Nscl(A) \subseteq V$ whenever $A \subseteq V$ and V is nano open in $(U, \tau_R(X))$.
- Nano generalized α –closed set[7] (briefly Ng α -closed) if $N\alpha cl(A) \subseteq V$, whenever $A \subseteq V$, V is nano open in U .
- Nano α generalized closed set [7] (briefly N α g-closed) if $N\alpha cl(A) \subseteq V$, whenever $A \subseteq V$, V is nano α open in U .
- Nano generalized pre closed [5]set (briefly Ngp-closed) if $Npcl(A) \subseteq V$ whenever $A \subseteq V$ and V is nano open in $(U, \tau_R(X))$.
- Nano generalized semi-pre closed [5]set (briefly Ngsp-closed) if $Nspcl(A) \subseteq V$ whenever $A \subseteq V$ and V is nano open in $(U, \tau_R(X))$.
- Nano generalized pre regular closed set[2] (briefly Ngpr-closed) if $Ncl(A) \subseteq V$ whenever $A \subseteq V$ and V is nano regular open in $(U, \tau_R(X)) \rightarrow (V, \sigma_R(Y))$

Definition 2.8. A function $f: (U, \tau) \rightarrow (V, \sigma)$ is called

- N -continuous [3], if $f^{-1}(A)$ is N -closed in U for every nano closed set A in V
- $N\alpha$ -continuous [8], if $f^{-1}(A)$ is $N\alpha$ -closed in U for every nano closed set A in V
- $N\alpha g$ -continuous[7], if $f^{-1}(A)$ is $N\alpha g$ -closed in U for every nano closed set A in V .
- $Ng\alpha$ -continuous[7], if $f^{-1}(A)$ is $Ng\alpha$ -closed in U for every nano closed set A in V .
- Ng -continuous[10], if $f^{-1}(A)$ is Ng -closed in U for every nano closed set A in V .
- Ngs -continuous[8], if $f^{-1}(A)$ is Ngs -closed in U for every nano closed set A in V .
- $Ngsp$ -continuous[8], if $f^{-1}(A)$ is $Ngsp$ -closed in U for every nano closed set A in V .

Nano Star Generalized α Closed Set

We introduce the following definition.

Definition 3.1. A subset A of $(U, \tau_R(X))$ is called $N^*g\alpha$ -closed set if $Ncl(A) \subseteq V$ whenever $A \subseteq V$ and V is $Ng\alpha$ open in $(U, \tau_R(X))$.

Theorem 3.2. Every Nano closed set is $N^*g\alpha$ -closed set.

Proof Let A be a nano closed subset of U and $A \subseteq V$, V is nano $g\alpha$ -open in V . Since A is nano closed, $Ncl(A) = A \subseteq V$, where V is $N^*g\alpha$ -open in U . Therefore A is $N^*g\alpha$ -closed set.

Following example shows that the above implication is not reversible.

Example 3.3 Let $U = \{a, b, c\}$ with $U/R = \{\{a, b\}, \{c\}\}$ and $X = \{a\}$. $\tau_R(X) = \{U, \phi, \{a, b\}\}$. $N^*g\alpha$ -closed = $\{U, \phi, \{c\}, \{b, c\}, \{a, c\}\}$.

Here $\{b, c\}$ is $N^*g\alpha$ -closed set but not nano closed set.

Theorem 3.4. Every $N^*g\alpha$ -closed set is Ng closed set.

Proof Let A be a $N^*g\alpha$ -closed set of V . Let V be an nano-open set. Such that $A \subseteq V$. Since every nano open set is $Ng\alpha$ open, since V is $Ng\alpha$ open. Since A is $N^*g\alpha$ -closed, $Ncl(A) \subseteq V$. Hence A is Ng -closed.

Following example shows that the above implication is not reversible.

Example 3.5 Let $U = \{a, b, c\}$ with $U/R = \{\{a, b\}, \{c\}\}$ and $X = \{a, c\}$. Then the Nano topology $\tau_R(X) = \{U, \phi, \{a\}, \{b, c\}\}$. Ng closed = $\{U, \phi, \{a\}, \{b\}, \{c\}, \{a, b\}, \{b, c\}, \{a, c\}\}$.

. $N^*g\alpha$ -closed = $\{U, \phi, \{a\}, \{b, c\}\}$





Baby and Aaminumariyam

Here $\{b\}$ is Ng -closed set but not $N^*g\alpha$ -closed set.

Theorem 3.6. Every $N^*g\alpha$ -closed set is $Ng\alpha$ closed set.

Proof Let A be a $N^*g\alpha$ -closed set of V . Let V be an nano- α open set. Such that $A \subseteq V$. Since every $N\alpha$ open set is $Ng\alpha$ open, since V is $Ng\alpha$ open. Since A is $N^*g\alpha$ -closed, $Ncl(A) \subseteq V$. Hence A is $Ng\alpha$ -closed.

Following example shows that the above implication is not reversible.

Example 3.7 Let $U = \{a, b, c\}$ with $U/R = \{\{a\}, \{b, c\}\}$ and $X = \{a, c\}$. Then the Nano topology $\tau_R(X) = \{U, \phi, \{a\}, \{b, c\}\}$. $Ng\alpha$ closed = $\{U, \phi, \{a\}, \{b\}, \{c\}, \{a, b\}, \{b, c\}, \{a, c\}\}$.

$N^*g\alpha$ -closed = $\{U, \phi, \{a\}, \{b, c\}\}$.

Here $\{b\}$ is $Ng\alpha$ -closed set but not $N^*g\alpha$ -closed set.

Theorem 3.8. Every $N^*g\alpha$ -closed set is Ngp closed set.

Proof Let $A \subseteq V$, where V is an nano open set in U . Since every nano open set is $Ng\alpha$ open, V is $Ng\alpha$ open. Since A is $N^*g\alpha$ -closed set, $Ncl(A) \subseteq V$. But $Npcl(A) \subseteq Ncl(A) \subseteq V$. Therefore A is Ngp -closed.

Following example shows that the above implication is not reversible.

Example 3.9. Let $U = \{a, b, c\}$ with $U/R = \{\{a\}, \{b, c\}\}$ and $X = \{a, c\}$. Then the Nano topology $\tau_R(X) = \{U, \phi, \{a\}, \{b, c\}\}$. $N^*g\alpha$ -closed = $\{U, \phi, \{a\}, \{b, c\}\}$

Here $\{a, b\}$ is Ngp -closed set but not $N^*g\alpha$ -closed set.

Theorem 3.10. Every $N^*g\alpha$ -closed set is Ngs closed set.

Proof Let A be a $N^*g\alpha$ -closed set of V . Let V be an nano-open set. Such that $A \subseteq V$. Since every nano open set is $Ng\alpha$ open. We have $Nscl(A) \subseteq Ncl(A) \subseteq V$. Therefore A is Ngs closed set.

Following example shows that the above implication is not reversible.

Example 3.11. Let $U = \{a, b, c\}$ with $U/R = \{\{a\}, \{b, c\}\}$ and $X = \{a, c\}$. Then the Nano topology $\tau_R(X) = \{U, \phi, \{a\}, \{b, c\}\}$. $N^*g\alpha$ -closed = $\{U, \phi, \{a\}, \{b, c\}\}$

Here $\{a, b\}$ is Ngs -closed set but not $N^*g\alpha$ -closed set.

Theorem 3.12. Every $N^*g\alpha$ -closed set is $N\alpha g$ closed set.

Proof Let A be a $N^*g\alpha$ -closed set of V . Let V be an nano open set. Such that $A \subseteq V$. Since every nano open set is $N\alpha g$ open, since V is $N\alpha g$ open. Since A is $N^*g\alpha$ -closed, $Ncl(A) \subseteq V$. Hence A is $N\alpha g$ -closed.

Following example shows that the above implication is not reversible.

Example 3.13. Let $U = \{a, b, c\}$ with $U/R = \{\{a\}, \{b, c\}\}$ and $X = \{a, c\}$. Then the Nano topology $\tau_R(X) = \{U, \phi, \{a\}, \{b, c\}\}$. $N^*g\alpha$ -closed = $\{U, \phi, \{a\}, \{b, c\}\}$

Here $\{b\}$ is $N\alpha g$ -closed set but not $N^*g\alpha$ -closed set.

Theorem 3.14. Every $N^*g\alpha$ -closed set is $Ngpr$ closed set.

Proof Let $A \subseteq V$, where V is an nano open set in U . Since every nano regular open set is $Ng\alpha$ open, V is $Ng\alpha$ open. Since A is $N^*g\alpha$ -closed set, $Ncl(A) \subseteq V$. But $Npcl(A) \subseteq Ncl(A) \subseteq V$. Therefore A is $Ngpr$ -closed.

Following example shows that the above implication is not reversible.

Example 3.15. Let $U = \{a, b, c\}$ with $U/R = \{\{a\}, \{b, c\}\}$ and $X = \{a, c\}$. Then the Nano topology $\tau_R(X) = \{U, \phi, \{a\}, \{b, c\}\}$.

Here $\{a, b\}$ is $Ngpr$ -closed set but not $N^*g\alpha$ -closed set.

Theorem 3.16. The intersection of two is $N^*g\alpha$ -closed is again $N^*g\alpha$ -closed set.





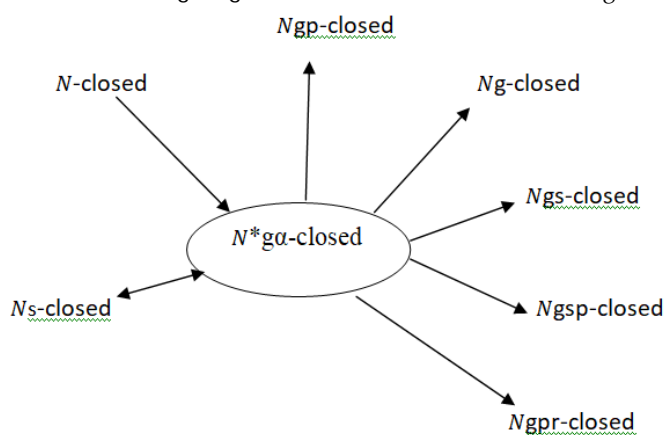
Baby and Aaminumariyam

Proof Let A and B are $N^*g\alpha$ -closed set. Let $A \cap B \subseteq V, V$ is $N\alpha$ -open. Since A and B are $Ng\alpha$ -closed set, $N\alpha cl(A) \subseteq V$ and $N\alpha cl(B) \subseteq V$. This implies that $Ncl(A \cap B) = Ncl(A) \cap Ncl(B) \subseteq V \Rightarrow Ncl(A \cap B) \subseteq V$. Therefore $A \cap B$ is $N^*g\alpha$ -closed.

Theorem 3.17. The union of two is $N^*g\alpha$ -closed is again $N^*g\alpha$ -closed set.

Proof Let A and B are $N^*g\alpha$ -closed set. Let $A \cup B \subseteq V, V$ is $N\alpha$ -open. Since A and B are $N^*g\alpha$ -closed set, $Ncl(A) \subseteq V$ and $Ncl(B) \subseteq V$. This implies that $Ncl(A \cup B) = Ncl(A) \cup Ncl(B) \subseteq V \Rightarrow Ncl(A \cup B) \subseteq V$. Therefore $A \cup B$ is $N^*g\alpha$ -closed.

Remark 3.18 : The following diagram shows the relation between $N^*g\alpha$ -closed.



Nano Star Generalized α Continuous Function

In this section we define and study the new class of functions, namely $N^*g\alpha$ -continuous function.

Definition 4.1. A function $f: (U, \tau_R(X)) \rightarrow (V, \sigma_R(Y))$ is said to be Nano star generalized α continuous (briefly $N^*g\alpha$ -continuous), if the inverse image of every nano closed set is $(V, \sigma_R(Y))$ is $N^*g\alpha$ closed set in $(U, \tau_R(X))$.

Theorem 4.2. Every nano continuous function is $N^*g\alpha$ -continuous function.

Proof Let $f: (U, \tau_R(X)) \rightarrow (V, \sigma_R(Y))$ be nano continuous function. Let A be nano closed set in $(V, \sigma_R(Y))$. Then the inverse image of A under the map f is nano closed in $(U, \tau_R(X))$. Since every nano closed is $N^*g\alpha$ closed set function $f^{-1}(A)$ is $N^*g\alpha$ closed set in $(U, \tau_R(X))$. Hence f is $N^*g\alpha$ -continuous function.

The converse of the above theorem need not be true by the following example.

Example 4.3. Let $U = \{a, b, c\}$ with $U/R = \{\{c\}, \{a, b\}\}$ and $X = \{a\}$. Then the Nano topology $\tau_R(X) = \{U, \phi, \{a, b\}\}$. Let $V = \{a, b, c\}$ with $V/R = \{\{a\}, \{c, b\}\}$ and $Y = \{a\}$. Then the Nano topology $\sigma_R(Y) = \{U, \phi, \{a\}\}$. Nano closed set $= \{U, \phi, \{c\}\}$ and $N^*g\alpha$ closed $= \{U, \phi, \{c\}, \{a, c\}, \{b, c\}\}$. Define a mapping $f: (U, \tau_R(X)) \rightarrow (V, \sigma_R(Y))$ be defined by $f(a) = b, f(b) = a, f(c) = c$. Then $f^{-1}(b, c) = \{a, c\}$ is not nano closed set in $(U, \tau_R(X))$. Therefore f is not nano continuous. However f is $N^*g\alpha$ -continuous function.

Theorem 4.4. Every $N^*g\alpha$ -continuous function is Ng -continuous function.

Proof Let $f: (U, \tau_R(X)) \rightarrow (V, \sigma_R(Y))$ be $N^*g\alpha$ -continuous function. Let A be nano closed set in $(V, \sigma_R(Y))$. Since f is $N^*g\alpha$ -continuous, $f^{-1}(A)$ is $N^*g\alpha$ closed set in $(U, \tau_R(X))$. But every $N^*g\alpha$ closed set. Hence $f^{-1}(A)$ is Ng closed set in $(U, \tau_R(X))$. Thus f is Ng -continuous function.

The converse of the above theorem need not be true by the following example.





Baby and Aaminumariyam

Example 4.5. Let $U = \{a, b, c\}$ with $U/R = \{\{c\}, \{c, b\}\}$ and $X = \{a, c\}$. Then the Nano topology $\tau_R(X) = \{U, \phi, \{a\}, \{b, c\}\}$. Let $V = \{a, b, c\}$ with $V/R = \{\{a\}, \{c, b\}\}$ and $Y = \{a, b\}$. Then the Nano topology $\sigma_R(Y) = \{U, \phi, \{b\}, \{a, b\}\}$. Nano closed set $= \{U, \phi, \{b\}, \{a, b\}, \{b, c\}, \{a, c\}\}$ and $N^*g\alpha$ closed $= \{U, \phi, \{a\}, \{b, c\}\}$. Define a mapping $f: (U, \tau_R(X)) \rightarrow (V, \sigma_R(Y))$ be defined by $f(a) = b, f(b) = c, f(c) = a$. Then $f^{-1}(b, c) = \{a, b\}$ is not $N^*g\alpha$ closed set in $(U, \tau_R(X))$. Therefore f is not $N^*g\alpha$ continuous. However f is Ng-continuous function.

Theorem 4.6. Every $N^*g\alpha$ -continuous function is Ng-continuous function.

Proof Let $f: (U, \tau_R(X)) \rightarrow (V, \sigma_R(Y))$ be $N^*g\alpha$ -continuous function. Let A be nano closed set in $(V, \sigma_R(Y))$. Since f is $N^*g\alpha$ -continuous, $f^{-1}(A)$ is $N^*g\alpha$ closed set in $(U, \tau_R(X))$. But every $N^*g\alpha$ closed set. Hence $f^{-1}(A)$ is Ng-continuous function.

The converse of the above theorem need not be true by the following example.

Example 4.7. Let $U = \{a, b, c\}$ with $U/R = \{\{c\}, \{c, b\}\}$ and $X = \{a, c\}$. Then the Nano topology $\tau_R(X) = \{U, \phi, \{a\}, \{b, c\}\}$. Let $V = \{a, b, c\}$ with $V/R = \{\{a\}, \{c, b\}\}$ and $Y = \{a, b\}$. Then the Nano topology $\sigma_R(Y) = \{U, \phi, \{b\}, \{a, b\}\}$. Ng-continuous set $= \{U, \phi, \{b\}, \{a, b\}, \{b, c\}, \{a, c\}\}$ and $N^*g\alpha$ closed $= \{U, \phi, \{a\}, \{b, c\}\}$. Define a mapping $f: (U, \tau_R(X)) \rightarrow (V, \sigma_R(Y))$ be defined by $f(a) = b, f(b) = c, f(c) = a$. Then $f^{-1}(b, c) = \{a, b\}$ is not $N^*g\alpha$ closed set in $(U, \tau_R(X))$. Therefore f is not $N^*g\alpha$ continuous. However f is Ng-continuous function.

Theorem 4.8. Every $N^*g\alpha$ -continuous function is Ngp-continuous function.

Proof Let $f: (U, \tau_R(X)) \rightarrow (V, \sigma_R(Y))$ be $N^*g\alpha$ -continuous function. Let A be nano closed set in $(V, \sigma_R(Y))$. Since f is $N^*g\alpha$ -continuous, $f^{-1}(A)$ is $N^*g\alpha$ closed set in $(U, \tau_R(X))$. But every $N^*g\alpha$ closed set. Hence $f^{-1}(A)$ is Ngp-continuous function.

The converse of the above theorem need not be true by the following example.

Example 4.9. Let $U = \{a, b, c\}$ with $U/R = \{\{c\}, \{c, b\}\}$ and $X = \{a, c\}$. Then the Nano topology $\tau_R(X) = \{U, \phi, \{a\}, \{b, c\}\}$. Let $V = \{a, b, c\}$ with $V/R = \{\{a\}, \{c, b\}\}$ and $Y = \{a, b\}$. Then the Nano topology $\sigma_R(Y) = \{U, \phi, \{b\}, \{a, b\}\}$. Define a mapping $f: (U, \tau_R(X)) \rightarrow (V, \sigma_R(Y))$ be defined by $f(a) = b, f(b) = c, f(c) = a$. Then $f^{-1}(b, c) = \{a, b\}$ is not $N^*g\alpha$ closed set in $(U, \tau_R(X))$. Therefore f is not $N^*g\alpha$ continuous. However f is Ngp-continuous function.

Theorem 4.10. Every $N^*g\alpha$ -continuous function is Ngs-continuous function.

Proof Let $f: (U, \tau_R(X)) \rightarrow (V, \sigma_R(Y))$ be $N^*g\alpha$ -continuous function. Let A be nano closed set in $(V, \sigma_R(Y))$. Since f is $N^*g\alpha$ -continuous, $f^{-1}(A)$ is $N^*g\alpha$ closed set in $(U, \tau_R(X))$. But every $N^*g\alpha$ closed set. Hence $f^{-1}(A)$ is Ngs-continuous function.

The converse of the above theorem need not be true by the following example.

Example 4.11. Let $U = \{a, b, c\}$ with $U/R = \{\{c\}, \{c, b\}\}$ and $X = \{a, c\}$. Then the Nano topology $\tau_R(X) = \{U, \phi, \{a\}, \{b, c\}\}$. Let $V = \{a, b, c\}$ with $V/R = \{\{a\}, \{c, b\}\}$ and $Y = \{a, b\}$. Then the Nano topology $\sigma_R(Y) = \{U, \phi, \{b\}, \{a, b\}\}$. Define a mapping $f: (U, \tau_R(X)) \rightarrow (V, \sigma_R(Y))$ be defined by $f(a) = b, f(b) = c, f(c) = a$. Then $f^{-1}(b, c) = \{a, b\}$ is not $N^*g\alpha$ closed set in $(U, \tau_R(X))$. Therefore f is not $N^*g\alpha$ continuous. However f is Ngs-continuous function.

Remark 4.12. Every $N^*g\alpha$ -continuous function is Ngsp-continuous function, Ngpr-continuous function and Ng-continuous function.

Theorem 4.13. The composition of two $N^*g\alpha$ -continuous function need not be $N^*g\alpha$ -continuous.

The proof follows from the example.





Baby and Aaminumariyam

Example 4.5. Let $U = \{a, b, c\}$ with $U/R = \{\{a\}, \{c, b\}\}$ and $X = \{a, c\}$. Then the Nano topology $\tau_R(X) = \{U, \phi, \{a\}, \{b, c\}\}$. Nano closed set $= \{U, \phi, \{b\}, \{a, b\}, \{b, c\}, \{a, c\}\}$ and $N^*g\alpha$ closed $= \{U, \phi, \{a\}, \{b, c\}\}$. Let $V = \{a, b, c\}$ with $V/R = \{\{a\}, \{c, b\}\}$ and $Y = \{a, b\}$.

Then the Nano topology $\sigma_R(Y) = \{U, \phi, \{a, b\}\}$. Nano closed set $= \{U, \phi, \{c\}\}$ and $N^*g\alpha$ closed $= \{U, \phi, \{c\}, \{a, c\}, \{b, c\}\}$. Let $W = \{a, b, c\}$ with $W/R = \{\{c\}, \{a, b\}\}$ and $Z = \{a, b\}$.

Then the Nano topology $\eta_R(Z) = \{U, \phi, \{a, b\}\}$. Nano closed set $= \{U, \phi, \{c\}\}$ and $N^*g\alpha$ closed $= \{U, \phi, \{c\}, \{a, c\}, \{b, c\}\}$. Define a mapping $f: (U, \tau_R(X)) \rightarrow (V, \sigma_R(Y))$ be defined by $f(a) = b, f(b) = a, f(c) = c$. Define a mapping $f: (Y, \sigma_R(Y)) \rightarrow (W, \eta_R(Z))$ be defined by $g(a) = c, g(b) = a, g(c) = c$.

Clearly f and g are $N^*g\alpha$ -continuous.

Here $\{a, c\}$ be nano closed in $(U, \tau_R(X))$. But $(f \circ g)^{-1}(\{a, c\}) = \{a, c\}$ is not $N^*g\alpha$ -closed set in $(U, \tau_R(X))$.

Therefore $(g \circ f)^{-1}$ is not $N^*g\alpha$ -continuous.

CONCLUSION

In this paper, some of the properties of Nano star generalized alpha closed sets and Nano star generalized alpha continuous function are discussed. This shall be extended to irresolute and homomorphic maps.

REFERENCES

1. N. Levine, Generalised closed sets in Topology, Rend.cire.Math.Palermo, (1963), 19(2),86-96.
2. Lellis Thivagar M and Carmel Richard, On Nano forms of weakly open sets, International Journal of Mathematics and Statistics Invention, volume 1, Issue 1, August 2013, PP-31-37.
3. K. Bhuvaneswari, and K. Mythili Gnanapriya, Nano Generalized closed sets in Nano Topological Spaces, International Journal of scientific and Research Publication, 4(5)(2014),1-3.
4. M. Vigneshwaran and R. Devi, On Gao-Kernal in the digital plane, International Journal of Mathematical Arichive-3(6),2012.
5. P. Anbarasi Rodrigo and P. Subithra, Nano $g\alpha^*$ -continuous function in Nano topological spaces, Journal of research in Applied Mathematics, Volume 8-issue 11(2022).
6. Lellis Thivagar M and Carmel Richard, On nano continuity, Math. Theory Model, 7(2013),32-37.
7. R. Thanga Nachiyar and K. Bhuvaneswari, Nano Generalized A-Continuous and Nano A-Generalized continuous function in Nano topological spaces, International Journal of Mathematics Trends and Technology volume 14 number 2-oct 2014
8. V. Rajendrann and P.Sathishmohan and M. Chitra, Nano $g^*\alpha$ continuous function in nano topological spaces, Turkish online Journal of qualitative Inquiry, volume 12, issue 5 june 2021:1156-1164.
9. Qays H aterm Imran, Murtadha M. Abdulkadhim and Mustafa H.Hadi, Nano generalized Alpha closed sets in nano topological spaces, Gen.math.notes, vol34, No.2.j=June 2016, pp.39-51.
10. K. Bhuvaneswari, and K. M. Gnanapriya, On Nano Generalized continuous function in Nano Topological Spaces, International Journal of Mathematics and Statistics Invention, 1(1)(2013),31-37.
11. K. Bhuvaneswari and A. Ezhilarasi, On Nano Semi-generalized and Nano generalized semi closed sets in nano topological spaces, International Journal of Mathematics and computer Applications Research (IJMCAR), vol.4, Issue3, Jun 2014, 117-124.
12. Lellis Thivagar M, Saeid Jafari, Sutha Devi V. On New Class of contra continuity in Nano topology, Italian Journal of pure and Applied Mathematics, 2020,43: p. 25-36.





Systematic Inspection of Digital Advert Impact on Teenagers in Artificial Intelligence (AI) Environment

Vishwas G*

Assistant Professor, Department of Commerce and Management, Seshadripuram Evening College, (Affiliated to Bengaluru City University) Bangalore, Karnataka, India.

Received: 02 Apr 2024

Revised: 10 Apr 2024

Accepted: 15 Apr 2024

*Address for Correspondence

Vishwas G

Assistant Professor,
Department of Commerce and Management,
Seshadripuram Evening College,
(Affiliated to Bengaluru City University)
Bangalore, Karnataka, India.
Email: vishwasbhem@gmail.com



This is an Open Access Journal / article distributed under the terms of the **Creative Commons Attribution License** (CC BY-NC-ND 3.0) which permits unrestricted use, distribution, and reproduction in any medium, provided the original work is properly cited. All rights reserved.

ABSTRACT

Artificial intelligence (AI) in digital advertising is such great addition to marketing strategy. So many businesses have adopted AI in digital marketing around the world today. Digital marketing (DM) is rapidly growing, and it is nearly difficult to avoid these new types of digital media. A new trend has started that is Artificial intelligence in Digital advertisements that's attracting teenagers to maintain brand loyalty. Digital advertising can have a huge return on investment for businesses so it's great to take advantages of those benefits. Along with the Digital Advert business also using Artificial intelligence to keep customers loyalty especially teenagers. By collecting data from different stream and providing regular contents and feed to teenagers to keep same loyalty. It's also influence and impact on actions of teenager purchasing decisions. This study examines teenagers' behaviors in dealing with digital advertisement on different social media platforms. Also describe reactions of teenagers for the AI action in digital environment. This research highlights three parts to understand impact of Digital advertising with Artificial intelligence on behaviors of teenagers. 1) Strategy behind the Artificial intelligence in Digital advertisement. 2) Role of Artificial intelligence in teenagers brand loyalty. 3) Advantages and Obstacle of AI in digital advertng for teenagers.

Keywords: Artificial Intelligence, Machine learning. Feed. Chatbot, Algorithms.





INTRODUCTION

Artificial intelligence replacing many key areas including marketing and advertising too. In the global village all the business are working in integrated format, so they found Artificial intelligence (AI) as a new strategy to face competition in the market. The big problem in digital environment is to attract new and maintain customers loyalty for long time. This AI Advertising tools in digital marketing can replace marketing agency forever. AI is a simulation of human intelligence in machines that are programs to think act like humans. By using data and algorithm AI technology were able to achieve two important technique Machine learning and Deep learning. Both term fall under the broad category of AI. However, machine learning is sub field of Artificial intelligence they use algorithm to pass data, learn from that data and make informed decisions based on what it has learned. Social media advertising is sub field in Digital advertising. it's a marketing area where the artificial intelligence was effectively implemented. By utilizing AI and ML platforms such as Facebook, Instagram can examine users' information and interest which allow they them to personalize the contents and ads that show on their feed. This technique is also using in the streaming platform such as NETFLIX, YOUTUBE and Retailer websites such as AMAZON. Utilize previous purchases or viewing history to enhance their recommendation systems. Chatbot are assisting online store which provides 24*7 customer services. They were improving over the years. While using machine learning and AI chatbots able to give human like replies to basic questions in real time. AI also do predictive analysis. The significant advantages of AI is predict sales and foresee customer behaviors essentially teenagers' action towards purchasing. With big data company can foresee teenagers' behaviors and try to reach their interested needs and satisfy the desire. Company can predict the future results and make adjustment marketing strategies and tactics. Based on those company can lead them to better outcomes. According to Ypulse "teens are now passing technology down to their parents, not the other way around" (2023). Teenager's normally fast and early adopters of brand. They are sensitive to advertising they believe too easily. Influencing them with AI tools is very easy now days. Digital advertising to teens is profitable way for businesses. Reaching teenagers with Digital advertisement and keep engagement with then to maintain loyalty is complex.

RESEARCH METHODOLOGY

This research make use of content analysis. Systematically analyzing the communication contents which is available in different websites and media. Basically it utilizes the secondary data to extract meaningful information for deeper understanding.

OBJECTIVES OF THE RESEARCH

- To understand how Artificial Intelligence works in digital advertisement.
- To understand how artificial intelligence make strategies to attract and maintain good engagement with teenagers.
- To understand the merits and demerits of Artificial intelligence in digital marketing to
- impact teenagers.

This study is mainly focusing on three parts to know the effect of Digital advertising with Artificial intelligence on behaviors of teenagers. 1) Strategy behind the Artificial intelligence in Digital advertisement. 2) Role of Artificial intelligence in teenagers brand loyalty. 3) Advantages and Obstacle of AI in digital advertenting for teenagers.

SCOPE AND LIMITATION

The probe describes multiple side of Artificial Intelligence in digital advertisement to communicate with teenagers to influence them to take actions. The document only handle with chosen previous literature and this study only focus and restricted to secondary data only.





STRATEGY BACK OF THE ARTIFICIAL INTELLIGENCE IN DIGITAL ADVERTISEMENT

Artificial Intelligence is the concept and development of computer system that execute the actions that would commonly need human judgment. Voice recognition, visual recognition, giving best solution to the complex problem and ability to interpret languages are all examples (oxford University press 2019). Business using AI for many things that reduces time and increases profitability. It collects the data very quickly and combines it to access the behavior of teenagers. AI suggesting marketer to make decision on sales and supporting them to trace the targeting audience. Business may use AI as a strategy of tracking teenagers searching contents in different streams. Through the assist of data collected and analyzed by AI technology can give many more options at real time. Business before introduction of AI they were used to conduct meeting to make digital advertisement. Cost will be more and too much pressure for advertising agency to select audience in digital world. This AI bring more benefits for businesses and to customers especially for teenagers. AI technology use machine learning to identify and collect the past data of teenagers to predict future actions. Teenagers are regularly active in many social web stages such as Instagram, Facebook, YouTube watch desired content that's key for AI. Also, online retail shops like Amazon, flipchart are the access for AI to grab the attention of teenagers. Teenagers knowingly or unknowingly reveal all their interest by watching the feed. AI provide complete picture of an teenagers about interested area. That's creating good opportunities for businesses to make profit and engage with customers for long time. Business orderly to utilize this AI effectively has to build 24*7 website or can use of social media that always engage with customers. That provides continuous information and clarifies the doubts of teenagers also that's makes teenagers to reach area they wanted. Launch piolet and explore the way AI create competitive advantage. For example, an AI Talkbot on business website. Or create a personalized website or interactive contents. Then business has start data transformation straight a ways. Need package all unique data and content so that can train future genAI models. Business required to be qualified to train the algorithms to capture the essential and distractive elements of business brand. Brands that rely too heavily on AI will all starts to sound alike, and teenagers will tune out. Future of marketing is starts with AI, future business image and brand of product will depend on it.

ROLE OF ARTIFICIAL INTELLIGENCE IN TEENAGERS BRAND LOYALTY

Camilla mackeviciute (2023) defined brand loyalty as consumers choose to repeatedly buy a product produces by company irrespective of other company product. For case, some shoppers wish always buy apple products while others will buy android products. Camilla markeviciute (2023) has provide brand loyalty statistics 74% of consumers feel loyal to their specific company brand and 52% of these customers will go out of their area to purchase their favorite brand. Teenagers brand loyalty is key for businesses to satisfy clints and total revenue growth. The power of AI in creating brand loyalty is growing from last 5 years. Companies are using and AI in multiple stages to target the teenagers. Based on previous data of each teenager through machine learning and algorithms business predicting the future needs of teenagers. Brand loyalty is depending upon amount of relationship with customers. Companies are using AI method to meet customers' expectations for good customer's interaction. In Digital marketing AI utilize predictive algorithms to observe client actions and behavior and through machine learning approaches maintain consumer's engagement across all channels. Companies like apple, Starbucks are utilizing this strategy very effectively. AI can only optimize teenagers brand loyalty if the teenager's data is reliable, updated, and sufficient. Before incorporating AI into their brand loyalty strategy, business must be confident that their target audience information is reliable, readily available, and updated. Artificial intelligence will emerge as a key element of loyalty program strategy. Helping business to increase loyalty improves more engagement that creates more earning than normal brand loyalty. AI in digital advertising enhances customer service, less teenager turnover, and higher loyalty. AI utilizing many tools to build and maintain loyalty for long. Such as predictive analytics, Chatbot, Gamification, AI powered customer loyalty programs, Personalized recommendation, personalized pricing, Fraud protection in real time etc.



**Vishwas G****ADVANTAGES AND OBSTACLE OF AI IN DIGITAL ADVERTISING FOR TEENAGERS**

AI has both positive and negative impact in digital advertising for teenagers. AI significantly improving the strategy and communication with teenagers. On the other side it also led to lack of data privacy and decreasing of teenager trust.

- Teenagers' behavior is now more predictable. AI analyzes the businesses objectives and review past data. AI will use machine learning model to analyze teenagers' behavior identifying the patterns and building digital marketing strategies based on teenager's interest.
- Teenagers' engagements are analyzed better. Improve the teenager's engagement by targeting previous clients to better and improve their experience. AI track the teenager's action at time and strive to engage with them more effectively.
- AI easily identify topics that may attract teenagers' attention by presenting content they like and understand.
- Chatbots and ChatGPT can provide 24*7 customer services, solving common problems in websites and other channels. This may improve relationships and brand loyalty.

Along with advantages AI carries some obstacle in digital advertising for teenagers. Sometimes AI creates irritation for teenagers. AI generated contents and post for regular for teenagers may leads to irritation and that may lead to shift in brand. Business needs rich sets of data. Artificial intelligence actions will be limited only by the availability of data. Teenagers' minds always change in digital environment so AI prediction uncertain all the time. In advertisement emotions play significant role AI only deals with data it won't understand feeling and emotions of teenagers.

SUGGESTIONS

- Business has to create more user-friendly websites to get more data.
- Artificial intelligence shall also reckon decent side while dealing with teenager behavior.
- Artificial intelligence only trusts in the data so that collecting data should be accurate.
- Teenagers must be careful while watching content in different platform because AI watching your behavior regularly 24*7
- Artificial Intelligence is going to end all the business should focus on super artificial intelligence (SAI) which is more faster Than AI.

CONCLUSION

Artificial intelligence in digital advertising for teenagers offers immense potential for targeted, personalized experiences. By harnessing AI technologies, advertisers can understand and cater to the unique preferences and behavior of teenagers, enhancing engagement and effectiveness. However, ethical consideration regarding Data privacy and manipulation must be carefully addressed to ensure responsible advertising practice. Overall, the integration of AI in digital advertising has the power to revolutionize how teenagers interact with brands, aid them with more meaningful and meaningful content while simultaneously driving business success for advertisers. As the field continues to evolve, collaboration between stakeholders, including advertisers, regulators and consumers, will be essential in shaping a future where AI- powered advertising serves both commercial interests and societal well-being.





Vishwas G

REFERENCES

1. Veena Tripathi (2016). "Impact of online marketing on teenagers in India." International journal of social science and management. 3(4):277
2. Jose Luis Reis. (2020). "Artificial intelligence applied to digital marketing." Trends and innovation in information system and technologies (pp.158-169)
3. Abid haleem, Mohd Javid, Mohd Asim Qadri, Ravi Pratap Sing, Rajiv Suman. (2022). 'Artificial intelligence (AI) application for marketing." International journal of intelligent networks. 119-132.





Analytical Method Development and Validation for Estimation of Simethicone and Loperamide in Tablet Dosage Forms

M.Siva Prasad¹, P.V.Suresh², N.Rama Rao³ and M.Dinesh Kumar^{1*}

¹M.Pharm, Department of Pharmaceutical Analysis, Chalapathi Institute of Pharmaceutical Sciences, (Affiliated to Acharya Nagarjuna University) Guntur, Andhra Pradesh, India.

²Ph.D, Department of Pharmaceutical Analysis, Chalapathi Institute of Pharmaceutical Sciences, (Affiliated to Acharya Nagarjuna University) Guntur, Andhra Pradesh, India.

³Ph.D, Department of Pharmaceutics, Chalapathi Institute of Pharmaceutical Sciences, (Affiliated to Acharya Nagarjuna University), Guntur, Andhra Pradesh, India

Received: 30 Jan 2024

Revised: 09 Feb 2024

Accepted: 18 May 2024

*Address for Correspondence

M.Dinesh Kumar

M.Pharm,

Department of Pharmaceutical Analysis,
Chalapathi Institute of Pharmaceutical Sciences,
(Affiliated to Acharya Nagarjuna University)
Guntur, Andhra Pradesh, India.

Email: dineshmanepalli1@gmail.com



This is an Open Access Journal / article distributed under the terms of the **Creative Commons Attribution License** (CC BY-NC-ND 3.0) which permits unrestricted use, distribution, and reproduction in any medium, provided the original work is properly cited. All rights reserved.

ABSTRACT

A simple, sensitive, specific, and accurate RP-HPLC method was developed for the simultaneous estimation of Simethicone and Loperamide HCl in a pharmaceutical dosage form. The RP-HPLC separation was achieved on a primisil C₁₈ (250 mm x 4.6 mm, 5µm) column and isocratic elution. The mobile phase is composed of phosphate buffer: methanol (80:20 v/v) at a flow rate of 1 ml/min. The chromatographic determination was performed on Shimadzu LC solution software with a PDA detector with a wavelength of 210nm. The run time is 7 minutes. The retention times of Simethicone and Loperamide HCl were found to be 4.663 min and 5.987 mins respectively. Linearity was established for Simethicone and Loperamide HCl in the range of 5-25µg/ml and 0.08-0.4µg/ml, respectively. System precision and method precision were found to be within the limits of the acceptance criteria. The relative standard deviation of Loperamide HCl and Simethicone for system precision was found to be and respectively, and method precision was found to be and respectively. The percentage recoveries for Simethicone and Loperamide HCl were found to be in the range of 99.80% and 99.71%, respectively.

Keywords: Loperamide, Simethicone, Reverse-Phase High Pressure Liquid Chromatography, primisil column phosphate buffer.





INTRODUCTION

Simethicone is an orally administered anti-foaming agent used to reduce bloating and discomfort. The molecular weight is to be 238.46 g/mol. It is used as an antifatulent, surfactant, and ointment base. **Loperamide** is an antidiarrheal agent. It is used to treat diarrhea. The molecular weight is found to be 477.0 g/mol. Various over-the-counter products contain loperamide, an anti-diarrhea drug, to treat diarrhea. The structures are shown in the below figures 1 & 2. According to a review of the literature, not many spectroscopic and HPLC techniques [3–10] have been described for the simultaneous assessment of the aforementioned medications both alone and in combination with other medications. Furthermore, my chosen combinational dosage form lacks stability studies and verified simultaneous analytical methodologies. Therefore, the goal of the project is to create and validate an accurate, fast, affordable, and straightforward stability-indicating RP-HPLC method for the measurement of simethicone and loperamide in accordance with ICH criteria. This publication provides the first report on the use of validated stability, indicating the pharmaceutical dosage form's RP-HPLC method with a less time-consuming study.

MATERIALS AND METHODS

Materials: Phosphate buffer and methanol were obtained from national products. The tablets (Caber consumers Simethione-125 mg and Loperamide HCl-2mg) were procured from the local market.

Instrumentation

A PDA detector was included in this HPLC. The chromatographic analysis was performed on a primisil C18 (150 mm x 4.6 mm, 5 μ m) column. The wavelength was detected at 210nm using mobile phase phosphate buffer: methanol (80:20 v/v).

Diluent: Ethanol was used as diluent.

Preparation of 0.1 M potassium di hydrogen phosphate buffer solution

Weigh accurately about 1.38g of potassium dihydrogen phosphate in 100 ml of HPLC-grade water and adjust pH up to 5.5 using sodium hydroxide solution.

Preparation of mobile phase:

Mix phosphate buffer and methanol in the ratio of 50:50 v/v. The mobile phase is degassed before use.

Preparation of Standard Stock Solution

Approximately 10mg of each individual drug were weighed and transferred individually into a 10 mL volumetric flask, in which they were dissolved in diluent and made up to 1000 μ g/mL.

Preparation of working standard solution

Exact 0.1 mL of Simethicone and Loperamide were pipetted out of the stock solution, and the volume was made up with diluent.

Preparation of sample solution

Twenty tablets were weighed and ground into a fine powder using a mortar and pestle. A single equivalent weight of tablet powder was transferred to a 25-mL volumetric flask, filled with 3/4 of the diluent, and subjected to an hour of sonication with intermittent shaking. The flask's capacity was then diluted with diluent and filtered through a 0.45 μ Millipore Nylon filter. From the stock solution mentioned above, 0.1 mL was pipetted out and put into a 10 mL volumetric flask, the 10 mL volume of which was adjusted with diluent.



**Method Development and Optimization**

These optimized conditions were followed for the simultaneous determination of Simethicone and Loperamide HCL in combined dosage forms. The optimized chromatographic conditions are shown in Table 1.

RESULTS**Method validation**

The International Conference on Harmonization (ICH) guidelines for assessing analytical procedures were used to validate the method in order to assess linearity, specificity, and the necessary precision and accuracy (LOD, LOQ) for the analyte.

System suitability

System fitness testing (SST) is a methodology for determining if an analytical method is fit for its intended usage on the day the analysis was performed. It is important to ensure the precision of the measurement process. The type of procedure being validated sets the parameters for a system suitability test, which must be tailored to a specific operation. The standard solution of Simethicone and Loperamide was injected into the HPLC system. The standard chromatograms are used to evaluate suitability parameters like retention time, tailing factor, and number of theoretical plates. The peak area was taken for six injections. The results are shown in the given Table 2.

Acceptance criteria: The percentage of Relative standard deviation should be less than 2.0.

Specificity

In terms of specificity, the drugs Simethicone and Loperamide were compared with blank, standard, and sample chromatograms. And diluent solutions were prepared according to the test procedure and injected into the chromatographic system. It can be concluded that the method developed is specific.

Linearity

The method of linearity was done by creating calibration curves with various concentrations of standard solutions. The drugs Simethicone and Loperamide linearity was demonstrated over the concentration ranges of 0-24 µg/ml and 0-0.4 µg/ml, respectively. Parameters such as slope, intercept, and regression equations were calculated from the resulting data. R² (correlation coefficient) of 0.999 and the linearity data are contained in the Table 3. Acceptance criteria: The R² ought to be NLT 0.999. And its graphs are shown below figures 5 and 6.

Precision

The precision of the method was demonstrated by system and method precision studies. All the solutions were injected into the chromatographic system. The repeatability of the method was checked by carrying out six independent assays of Simethicone and Loperamide. The peak area and percentage relative standard deviation were calculated and presented. It is shown in the Table 4.

Acceptance criteria: NMT 2.0 should be the %RSD for the peak area.

Accuracy

It is done at known amount of samples at different concentrations like (50%, 100%, 150%) levels and its exactness was proved. It was calculated and presented in the given table. It is shown in the Table 5.

Acceptance criteria: The Mean % recovery at each level should be NLT 98% and NMT 102%.

Limit of detection and Limit of quantification

The LOD of Simethicone were determined to be µg/ml, respectively. The Loperamide were found to be µg/ml respectively. And the LOQ of Simethicone were determined to be 0.5-1.5 µg/ml, respectively. The Loperamide were found to be 8-24 ng/ml respectively. It is shown in the Table 6.





Siva Prasad et al.,

Robustness

The robustness is done by altering the chromatographic conditions of Simethicone Loperamide standard solutions were administered by changing the flow rate and wavelength. The flow rate was modified to 0.9 mL/min and 1 mL/min, and the mobile phase ratios were changed from (70:30 and 30:70). Data was represented in the given Table 7.

Acceptance criteria: The % relative standard deviation for the Peak area should be NMT 2.0.

Assay

percentage purity of simethicone and loperamide were obtained at respectively.

CONCLUSION

A simple, precise RP-HPLC method was developed to estimate SIM and LPM in formulation. The materials were separated using a primisil C18 column (150 mm x 4.6 mm, 5 µm) at room temperature. As the mobile phase, phosphate buffer and acetonitrile was used: At 1.0 mL/min flow rate. At a detection wavelength of 210 nm, an phosphate buffer :methanol (80:20 v/v) was injected onto the column. The improved approach was validated in compliance with ICH guidelines. According to the literature, there was a method for computing SIM and LPM in tablet dose form at the same time. The developed procedure was unique, exact, and suitable to routine analysis.

REFERENCES

1. National Center for Biotechnology Information. PubChem Compound Summary for CID 3955, Loperamide. <https://pubchem.ncbi.nlm.nih.gov/compound/Loperamide>. Accessed Dec. 13, 2023.
2. National Center for Biotechnology Information. PubChem Compound Summary for CID 6433516, Simethicone. <https://pubchem.ncbi.nlm.nih.gov/compound/Simethicone>. Accessed Dec. 13, 2023.
3. Suneetha, A., N. Sharmila, and M. Purnima. "Stability indicating RP-HPLC method for the determination & validation of loperamide hydrochloride & simethicone in pharmaceutical dosage form." *World J. Pharm. Pharm. Sci* 6 (2017): 955-971.
4. Suneetha, A., N. Sharmila, and M. Purnima. "Stability indicating RP-HPLC method for the determination & validation of loperamide hydrochloride & simethicone in pharmaceutical dosage form." *World J. Pharm. Pharm. Sci* 6 (2017): 955-971.
5. Guleli, Muge, et al. "Determination of the amount of Simethicone in different Drug formulations by the Gravimetric method and comparison with the FTIR method by Chemometric methods." *Asian Journal of Pharmaceutical Analysis* 11.1 (2021): 17-21.
6. Mulay, Dr Ameya. "Determination of Simethicone by Gravimetric Analysis from the Effervescent Formulations." *Available at SSRN 4384307*.
7. Zakowiecki, Daniel, et al. "Towards the Continuous Manufacturing of Liquisolid Tablets Containing Simethicone and Loperamide Hydrochloride with the Use of a Twin-Screw Granulator." *Pharmaceutics* 15.4 (2023): 1265.
8. Analysis P, The D, Analysis P. *Pharmaceutical Analysis, Definition and Scope*, 2021, 1-2.
9. Sudha, P. D. Chaitanya, *Pharmaceutical Analysis*, India, Pearson Education India, 2012.
10. Azim Md, Moloy Mitra and Bhasin Parminder, HPLC METHOD DEVELOPMENT AND VALIDATION, A REVIEW, 2015, International Research Journal of Pharmacy, 4(4), 39-46.
11. Patterson, Andrew. *Schreyer Honors College*. Diss. PENNSYLVANIA STATE UNIVERSITY, 2015.
12. Harry, Emma. *The development of ion mobility-mass spectrometry for complex mixture analysis*. Diss. © Emma L. Harry, 2011.



Siva Prasad *et al.*,

13. Al-Oran, Aya Yahya Fayez. Preparation and Characterization of Fast-Dissolving Desloratadine Oral Film for Geriatric Use. Diss. Anadolu University (Turkey), 2022.

Table 1: Optimized chromatographic conditions.

S.NO	PARAMETERS	CONDITIONS
1.	UV wavelength detection	210nm
2.	Column	primisil C18
3.	Mobile phase	Phosphate buffer and Methanol (80:20 v/v)
4.	pH of buffer	5.5
5.	Pump mode	Isocratic
6.	Diluent	Ethanol
7.	Run time	7. min
8.	Flow rate	0.9 ml
9.	Injection volume	10 μ l
10.	Temperature	Ambient temperature

Table 2: Data of system suitability

Injection No.	Simethicone	Loperamide
	Peak area	Peak area
1.	874304	134882
2.	874412	134912
3.	874619	134923
4.	874892	134945
5.	875134	134973
6.	875356	134997
Mean	874786	134939
Standard Deviation	414.0842507	41.9269205
%RSD	0.05	0.03

Table 3: Data of linearity

Injection	Simethicone		Loperamide	
	Conc.(μ g/ml)	Peak area	Conc.(μ g/ml)	Peak area
1.	0	0	0	0
2.	5	291458	0.08	45859
3.	10	582968	0.016	90258
4.	15	874304	0.24	134882
5.	20	1166739	0.32	179856
6.	25	1458172	0.4	224905
Correlation coefficient	$R^2 = 1$		$R^2 = 1$	

Table 4: Data of Precision

Injection No.	SIMETHICONE		LOPERAMIDE	
	System precision	Method precision	System precision	Method precision





Siva Prasad et al.,

1.	874414	875302	135982	134952
2.	874513	875112	135012	135125
3.	874518	874458	134725	135685
4.	874682	874585	135945	133852
5.	874139	875258	134973	135246
6.	876355	876589	135997	135128
Mean	874770	875217	135439	134998
Standard Deviation	796.7959379	758.659256	595.236088	613.5037082
%RSD	0.09	0.09	0.44	0.45

Table 5: Data of Accuracy

%Level	Simethicone								
	Standard peak area	Sample Peak area	%Recovery	AVERAGE	Mean %recovery				
50%	874796	291459	99.80	99.7	99.90				
	874796	292345	100.01						
	874796	292165	100.09						
100%	874796	874867	99.90	99.85					
	874796	874678	99.79						
	874796	874996	99.88						
150%	874796	1458158	99.86	99.89					
	874796	1458167	99.86						
	874796	1459423	99.94						

Table 6: Data of accuracy

%Level	Loperamide								
	Standard peak area	Sample Peak area	%Recovery	AVERAGE	Mean %recovery				
50%	134939	44768	99.38	99.51	99.71				
	134939	44865	99.50						
	134939	44869	99.65						
100%	134939	134289	99.41	99.65					
	134939	134456	99.44						
	134939	135256	100.09						
150%	134939	225123	99.95	99.98					
	134939	225265	100.01						
	134939	225189	99.97						





Table 7: Data of Limit of detection and quantification

Drug	LOD	LOQ
Simethicone	0.5 µg/ml	1.5 µg/ml
Loperamide	8ng/ml	24ng/ml

Table 8: Data of robustness

Parameter	Simethicone		Loperamide	
	Peak area	% RSD	Peak area	% RSD
Change in flow rate 0.6ml/min	893105	0.08	136205	0.57
	894112		137312	
Change in flow rate 0.8ml/min	893523	0.01	135112	0.15
	893612		138415	
Change in mobile phase ratio 70:30v/v	903725	0.01	136232	0.86
	903836		137895	
Change in mobile phase ratio 30:70V/V	903841	0.01	136352	0.80
	903947		137896	

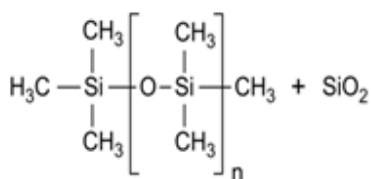


Fig 1: Simethicone

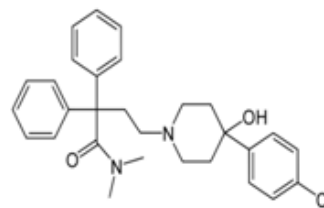


Fig 2: Loperamide

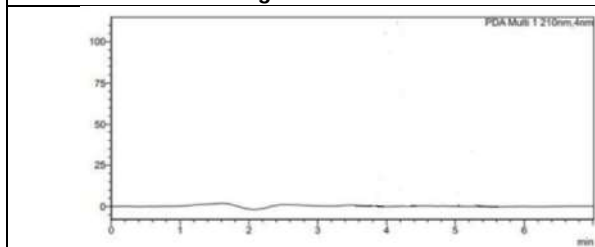


Fig 3: Blank chromatogram

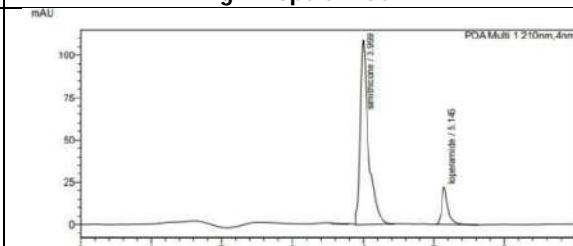


Fig 4 :Standard chromatogram

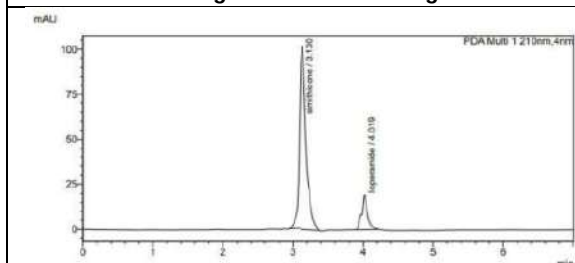


Fig 5 : Sample chromatogram

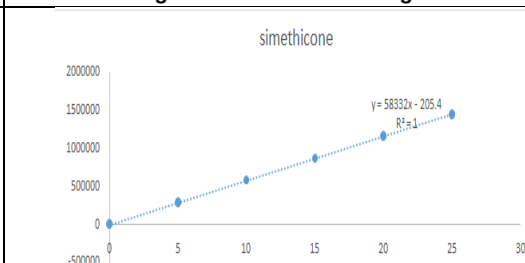
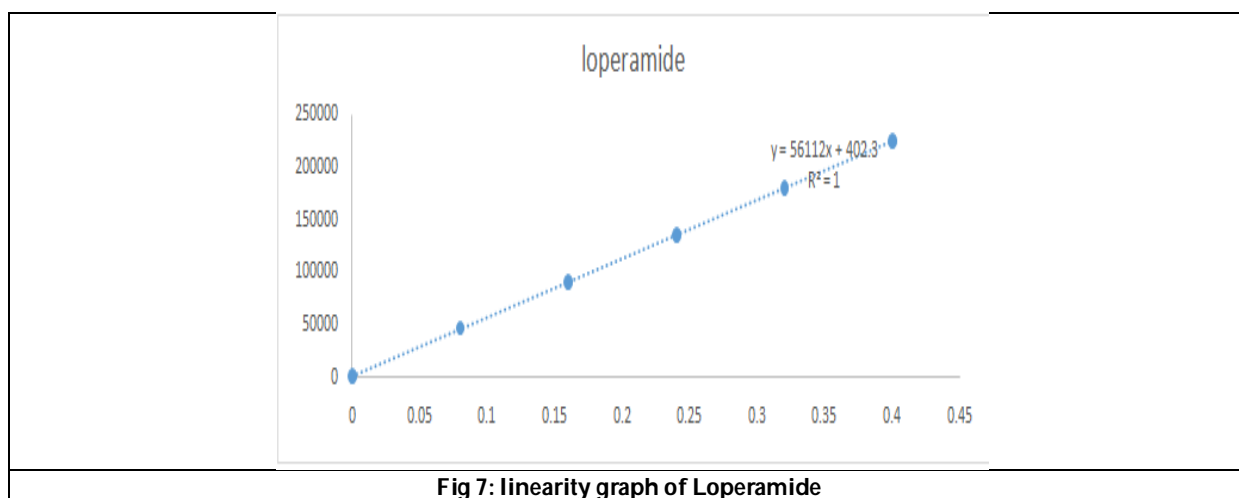


Fig 6: linearity graph of Simethicone





Siva Prasad *et al.*,





Bioremediation of Lead and Cadmium Metals from Contaminated Soil Samples using Microbial Siderophore

G. Sri Lakshmi¹, S. Prasanna², K. Mounika², S. Anju³, J.Sarada^{3*} and J. Sai Kumar²

¹Ph.D Scholar, Department of Microbiology, Bhavan's Vivekananda College of Science, Humanities and Commerce, Secunderabad (Affiliated to Osmania University) Hyderabad, Telangana, India.

²Project Student, Department of Microbiology, Bhavan's Vivekananda College of Science, Humanities and Commerce, Secunderabad (Affiliated to Osmania University) Hyderabad, Telangana, India.

³Assistant Professor, Department of Microbiology, Bhavan's Vivekananda College of Science, Humanities and Commerce, Secunderabad (Affiliated to Osmania University) Hyderabad, Telangana, India.

Received: 22 Jan 2024

Revised: 09 Feb 2024

Accepted: 08 May 2024

*Address for Correspondence

J.Sarada

Assistant Professor,
Department of Microbiology,
Bhavan's Vivekananda College of Science,
Humanities and Commerce, Secunderabad
(Affiliated to Osmania University)
Hyderabad, Telangana, India.
Email: saradavenkatj@gmail.com



This is an Open Access Journal / article distributed under the terms of the **Creative Commons Attribution License** (CC BY-NC-ND 3.0) which permits unrestricted use, distribution, and reproduction in any medium, provided the original work is properly cited. All rights reserved.

ABSTRACT

Rapid industrialization and urbanization of societies have led to a surge in environmental pollution, particularly the contamination of ecosystems by heavy metals. Lead (Pb) and Cadmium (Cd), are among the most hazardous heavy metal pollutants due to their toxic nature, persistence, and ability to accumulate in living organisms. Lead and cadmium are often released into the environment through industrial activities, improper waste disposal, and the use of certain fertilizers and pesticides. They can persist for decades, rendering the soil unsuitable for agriculture, gardening, and other land uses and difficult for remediation. Siderophore producing bacteria play vital role in sequestering metal ion and therefore could be used for bioremediation of Lead and Cadmium from the soil. In present study, microorganisms resistant to metal ions like Cadmium, Arsenic and Lead were isolated from Sifco Industry soil and Neredmet dump yard soil samples. The bacterial isolates were screened for potential siderophore producers using CAS Agar. Among the three isolates, DMPD92 is observed to produce all the three types of siderophores while SMPD 73 could produce Hydroxamate and catecholate and DMPD 72 produces Carboxylate and Catecholate type. Microbial siderophores were extracted and characterized by FTIR and quantitatively estimated. Bioremediation of contaminated soil samples were performed at laboratory level with the extracted siderophores samples. ICPMS analysis of soil samples before and after

75558





Sri Lakshmi et al.,

bioremediation with siderophores was carried out to confirm the reduction in metal concentration. 96.6% Pb, 63.2% Cd and Zn 26.1 % was remediated when analyzed against the untreated or control soil samples in industrial contaminated site.

Keywords: Pseudomonas, Industrial sources, CAS assay , Siderphore, Lead , Cadmium, Metal contamination.

INTRODUCTION

In recent decades, the rapid industrialization and urbanization of societies have led to a surge in environmental pollution, particularly the contamination of ecosystems by heavy metals. Heavy metals, such as lead (Pb) and cadmium (Cd), are among the most hazardous pollutants due to their toxic nature, persistence, and ability to accumulate in living organisms. Their presence in the environment poses significant risks to human health, ecological balance, and overall environmental sustainability [1]. Lead and Cadmium pollution in soil can have far-reaching and detrimental impacts on both the environment and human health. Lead and Cadmium are often released into the environment through industrial activities, improper waste disposal, and the use of certain fertilizers and pesticides. They can persist for decades, rendering the soil unsuitable for agriculture, gardening, and other land uses.[2]. Lead and cadmium can be taken up by plants from contaminated soil and accumulate in their tissues. Especially with crops that are grown for consumption, heavy metals can make their way into the food chain and pose significant health risks, including damage to the nervous system, kidneys, and other organs. They can disrupt soil nutrient cycling and microbial activity, leading to reduced soil fertility. Heavy metals like Lead and Cadmium can leach from contaminated soil into groundwater and surface water bodies. This contamination can spread over large areas, affecting water quality and potentially leading to bioaccumulation in aquatic organisms, which can then impact the entire aquatic food chain. Ingesting crops, water, or dust contaminated with these heavy metals can lead to serious health issues, including developmental delays in children, cognitive impairments, kidney damage, and an increased risk of certain cancers. Overall, Lead and Cadmium pollution in soil presents a complex and multifaceted set of challenges, highlighting the need for effective remediation strategies to mitigate their adverse effects on the environment and human well-being [3, 4]. Consequently, effective strategies for remediating heavy metal pollution have become a critical area of research and concern. Conventional methods for heavy metal removal, such as physical and chemical processes, often come with limitations and drawbacks, including high costs, generation of secondary pollutants, and limited long-term effectiveness. In this context, bioremediation has emerged as a promising and environmentally friendly alternative for mitigating heavy metal contamination.

Bioremediation harnesses the natural capabilities of microorganisms, plants, and their associated biochemical processes to transform, immobilize, or extract heavy metals from contaminated environments [5]. This approach capitalizes on the intrinsic ability of certain microorganisms and plants to tolerate, sequester, and detoxify heavy metals through mechanisms such as biosorption, bioaccumulation, biotransformation, and rhizofiltration [6, 7]. The present research paper focuses on the application of microbial siderophores for the removal of Lead and Cadmium from polluted soil samples in and around Hyderabad. The unique metabolite of microorganism like siderophore provides cost effective approach for effective heavy metal remediation. Siderophores are fascinating microbial metabolites that play a crucial role in facilitating the acquisition of essential metals, particularly iron, from the environment for microbial growth and survival. These small, high-affinity chelating molecules are secreted by a variety of microorganisms, including bacteria, fungi, and some plants, in response to metal scarcity in their surroundings. While their primary role is to scavenge and transport iron, siderophores have gained significant attention for their potential applications in metal bioremediation, particularly in the removal and remediation of various heavy metals and toxic metal ions from contaminated environments [8]. These siderophore-producing microbes can effectively sequester target metal ions, reducing their bioavailability and mobility, and subsequently





Sri Lakshmi et al.,

promoting the immobilization or precipitation of metals, rendering them less harmful to the environment and living organisms.

MATERIALS AND METHODS

Collection of soil sample from contaminated /polluted sites

Soil samples were collected from SIFCO Industrial site, located at Cherlapally and Neredmet Dump yard, Secunderabad for isolation of Metal resistant microorganisms. Samples were packed in a sterile bag. The physiochemical properties of the soil samples were determined like pH, organic carbon content in the laboratory with Soil Kit method (Hi media).

Growth media used for the isolation and screening of the organisms

Nutrient Agar: Hi Media ,King's B medium (Protease peptone – 2g, K_2HPO_4 – 0.15g, $MgSO_4$ – 0.15g, Agar -1.5g , Dis. H_2O - 100ml), Chrome azurol sulphonate (CAS) semisolid medium (Wang et al. 2014): 60.50 mg chrome azurol, 72.90 mg hexadecyl trimethyl ammonium bromide (HDTMA), 10 mL of 1 mmol·L⁻¹ $FeCl_3 \cdot 6H_2O$ (dissolved with 10 mmol·L⁻¹ HCl), 50 mL of 0.1 mol·L⁻¹ phosphate buffer, 0.9% (w/v) agar. All media were sterilized at 121°C for 30 min.[9]

Isolation of bacteria

1g of soil sample was suspended in 9 ml distilled water and a ten- fold serial dilution was performed. Appropriate dilutions were plated on the Nutrient agar and King's B medium and incubated at 37° C for 24hrs for bacterial growth. Siderophore producing isolates were identified on King's B medium plates by observing green fluorescence under a UV transilluminator. Microbiological identification of the isolates were carried out by gram staining and biochemical characterization by the standard protocols.

Screening of Siderophore-producing bacteria

The isolates obtained from Nutrient agar were inoculated into the King's B and incubated at 37°C for 24hrs. 35ml CAS reagent is added to 100ml King's B at room temperature. Then media was poured onto the sterile plates they appear blue in color. Plates were inoculated with the culture and incubated at 37°C for 24hrs. After incubation, colonies that changed from blue to orange halo zones were selected as siderophore producers.

Characterization of Siderophores with chemical assays

Fe Cl_3 tube test

Formation of orangish brown precipitate upon addition of 2-3 drops of 2% $FeCl_3$ to the culture broth indicates the presence of a siderophore.

Arnow's test

To 1ml culture filtrate, 1ml of 0.5M HCl was added. The resulting colorless solution was mixed and 1ml of nitrite-molybdate reagent (10g Sodium nitrite + 10g Sodium molybdate dissolved in 100ml dis. H_2O) was added. The presence of catechol-type siderophore would be indicated by the formation of yellow color. Upon addition of 1ml of 1M NaOH solution and incubation for 5min, solution turns to reddish. Absorbance would be measured at 510nm using a spectrophotometer.[10]

Csaky assay

1ml of culture supernatant was mixed with 1ml of 1N H_2SO_4 , and boiled for 6hr, 3ml of 35% Sodium acetate solution was added and mixed well, 1ml of this solution was diluted with deionized water in a 1:5 ratio. 0.5ml of Sulphanilic



**Sri Lakshmi et al.,**

acid solution (1g sulphanilic acid dissolved in 100ml of 30% acetic acid) and 0.2ml of Iodine solution (1.3g of iodine dissolved in 100ml acetic acid) were added and incubated at RT for 5 mins. 0.2ml of sodium thiosulphate (2g sodium thiosulphate dissolved in 100ml deionized water) and 0.1ml of α -naphthalamine solution (3g α -naphthalamine in 1000ml of 30% acetic acid) were added and the solution was incubated at RT for 20-30 mins. The solution becomes reddish brown in the presence of Hydroxamate type. [11]

Vogel's test

1 drop of phenolphthalein was added to 3 drops of 2N NaOH. Sterile water was added to the mixture till the appearance of light pink color. The disappearance of color by adding the culture filtrate indicates the presence of Carboxylate type siderophores [12]

Extraction of siderophore

100ml of culture supernatant pH was set to 5.2 by adding citric acid, later the acidified supernatant was extracted with 50 ml of dichloromethane in a separating funnel. The organic phase was collected and dried over Magnesium sulphate. Extracted siderophore was dissolved in methanol-water solution. Absorbance was measured at 313nm against a blank of Methanol-Water.

Quantification of siderophore

Quantification was performed using CAS assay [13] 1 ml of culture supernatant of the isolates was added to the CAS liquid broth, incubated for 1 hour at room temperature. Color change from blue to orange indicates siderophore and absorbance was measured at 660nm. Standard calibration graph was plotted using dilutions of EDTA (1mg/ml) and used for calculating siderophore concentration.

Fourier Transform Infra-Red (FTIR) Spectroscopic Analysis

Purified siderophore fraction was processed for FTIR in the range of 4000–400 cm^{-1} [14]. The infrared spectrum wavelengths were determined based on their functional groups.

ICPMS analysis

Sample analysis was performed at CSIR-National Geophysical Research Institute (NGRI), Hyderabad. The AttoM® HR-ICP-MS is a double-focusing single-collector instrument with forward Nier-Johnson analyzer geometry (Nu Instruments, UK) and was used in low-resolution mode with the detector in automatic mode. The scanning of ions of particular m/z was done in jump-wiggle mode (similar to peak hopping) which permits the analytes of interest to be measured accurately. The sample introduction consisted of a standard Meinhard® nebulizer with a cyclonic spray chamber housed in the Peltier cooling system. Soil samples were prepared by the wet chemical method and analysis by the Standard procedure at NGRI. 2018. [15].

Laboratory level soil remediation tests

Contaminated soil samples were treated with extracted siderophore and incubated for one week for metal removal assay. Contaminated soil samples collected from SIFCO industrial site and Dump yard. This treatment was carried out in small pots.

RESULTS AND DISCUSSION

Soil samples collected from contaminated sites i.e SIFCO Industrial site, located at Cherlapally and Neredmet Dump yard, Secunderabad were initially subjected to soil analysis like pH, Organic carbon, phosphorus and potassium levels using soil Kit (Himedia) to understand the nutrients available in the sample. Later tenfold serial dilutions were made with the soil samples and higher dilutions were placed on Nutrient agar and King's B media plates for isolation of siderophore producers from metal resistant microorganisms. Lead and Cadmium are often released into the environment through industrial activities and improper waste disposal therefore probability of finding metal



**Sri Lakshmi et al.,**

ion resistant bacteria among the microbial population is high. These resistant bacteria survive in contaminated / polluted sites with their metabolic efficiency and adapting to the environment by sequestering the metal ions with the help of microbial metabolites like siderophore. Many bacterial isolates were obtained on nutrient and King's B agar plates indicating the abundance of microorganisms in soil. King's B medium was used as selective medium for identifying siderophore producers which show characteristic green fluorescence under UV transilluminator. Among the bacterial isolates obtained on Kings B, isolate DMPD72, DMPD 73 and SMPD72 were observed to have more fluorescence under UV Transilluminator. These colonies were round, opaque and pinpointed on the Nutrient agar plates and flat, cruciferous margin and translucent on the King's B plate showing gram negative short bacilli upon Gram staining. Biochemical characterization was also performed by testing for IMViC reactions, positive or negative for Oxidase and Catalase test indicated that these isolates could be *Pseudomonas*. Confirmation for production of Siderophore was done on CAS agar medium plates. Chrome azurol sulphonate (CAS) is incorporated in growth media and used for selection of siderophore producers because they change the color of medium from blue to orange. Further confirmation of siderophore production was carried by testing with chemical assay procedures. These tests aid in identifying the siderophore type produced by the isolates. Depending on the oxygen ligands for Fe (III) coordination, siderophores can be classified into three main categories, namely, hydroxamates, catecholates, and carboxylates. The phenotype of siderophore was determined by Arnow's test for the catecholate type, Csaky's test for the Hydroxamate type, and Vogel's test for the carboxylate type. Among the three isolates, DMPD92 is observed to produce all the three types of siderophores while SMPD 73 could produce Hydroxymate and catecholate and DMPD 72 produces Carboxylate and Catecholate type. Catecholate or phenolate siderophores has cyclic tri-ester of 2,3-dihydroxybenzoylserine which are produced by *Escherichia coli* and *Enterobacter* [16].

Arnow test confirms the presence of catechol-type siderophore by the formation of yellow color when 0.5 HCl and nitrite-molybdate reagent was added. Upon addition of 1ml of 1M NaOH solution and incubation for 5min, solution turns to red color. The second type of bacterial siderophores is hydroxymates, which have both linear and cyclic compounds containing 1-amino-5-hydroxyaminopentane [17]. When tested with Csaky's test solution becomes reddish brown for Hydroxamate type. The third category carboxylates consist of citrate linked by ornithine. In Vogel's test disappearance of color upon addition of culture filtrate indicates the presence of Carboxylate type siderophores. Certain types of bacterial siderophores containing a mix of hydroxamate and carboxylate groups e.g pyoverdines, which are commonly produced by *Pseudomonas* spp. and *Azotobacter* [18]. Some bacterial strain can produce more than one type of siderophore [19]. Present data from table 2 indicate that these isolates produce two or three siderophores. Based on the morphological and biochemical features and as they exhibited strong fluorescence isolates were identified to be *Pseudomonas* species. After identifying the type of siderophore produced next the isolates were grown in shake flask in King's B medium for extraction of siderophore. Before extraction, Siderophore was quantified by CAS assay where color change from blue to orange was observed and absorbance was measured at 660nm. Standard calibration graph was plotted for calculation of siderophore concentration and the obtained data was represented in graph. From the data it was evident that isolate DMPD72 was producing 980 µg of siderophore among the three while SMPD 73 produced the least 200 µg and 500 µg by DMPD92 isolate.

Further structural characterization of siderophore was carried out by extracting from culture supernatant. Isolates were grown in King's B Medium for 48hrs. After incubation the culture supernatant was acidified and siderophore was extracted with dichloromethane. Extracted siderophore was dissolved in methanol, water mixture and FTIR analysis was performed at CFRD, Osmania University. FTIR data presented Table no.3 & Figure no.3 indicate that peak at 3251 as the presence of aromatic C-H stretching, peaks at 3302-3323 indicating the presence of aromatic OH moiety of siderophores, Peaks at 1722-1733 for C=O stretching, peak at 1541-1545 for Aromatic C=C stretch and peak at 1220-1251 indicating C-O stretch. Most of the hydroxamate groups consist of C (=O) N-(OH) R, where R is either an amino acid or a derivative of it. From this data it observed that the isolates produce both Catecholate and carboxymate types of siderophores. After the siderophore characterization, the next step was to treat the contaminated soil samples collected from SIFCO industrial site and Dump yard with the siderophore for bioremediation. Metal bioremediation experiments were carried out in small pots incubated for one week. Treated soil samples were subjected to ICPMS analysis for understanding the impact of microbial siderophore in remediation





Sri Lakshmi et al.,

of Pb and Cd along with other metals present in the samples. From fig 5, it was observed that there was no effect of Microbial siderophore treatment in Dumpyard sample while there was decrease in metal concentration in SIFCO sample. (Fig no.6). From the data it was observed that 96.6% Pb, 63.2% Cd and Zn 26.1 % were remediated when analyzed against the untreated or control soil samples. These data support the strategy of using siderophore for Pb and Cd remediation in soil. Many research groups worked on heavy metal toxicity and their bioremediation with siderophores.[20,21]. Braud et al. 2009 reported that microbial Pyochelin, can chelate a variety of metals like Ag^+ , Al^{3+} , Cd^{2+} , Co^{2+} , Cr^{2+} , Cu^{2+} , Hg^{2+} , Mn^{2+} , Ni^{2+} , Pb^{2+} , and Zn^{2+} . [22] Edberg et al. 2010 reported that with siderophores produced by *Pseudomonas fluorescens*, Fe, Ni, and Co were mobilized from waste material of acid-leached ore of a uranium mine [23]. In another research paper, Burd et al. 2000 established that heavy metal toxicity such as Ni, Pb, and Zn in soil samples collected from a metal-impacted wetland near Sudbury, Ontario was reduced or remediated by siderophore overproducing mutant of *Kluyvera ascorbate* SUD165 [24]. Current results also substantiate the use of microbial siderophores for heavy metal bioremediation. In order to check the quality of soil before and after siderophore treatment, Soil parameters like pH, Organic carbon and elements like Nitrogen, Phosphorus and Potassium were tested by soil analysis kit (Himedia) and the data is depicted in Table no. 4. From the data improvement in Organic carbon, Nitrogen and Phosphorus was noticed. These results indicate that soil parameters are in favour for Plant growth. Present study indicate that supplementation of Microbial siderophores could be effectively used for reduction of Pb and Cd contamination in SIFCO i.e industrial soil samples but not in Dumpyard samples. However further experimentation are required at contaminated sites as well. In future, strain improvement need to be carried out for enhancing the siderophore production by the isolates for bulk application.

ACKNOWLEDGEMENT

The Authors would like to thank the HoD of Microbiology and Management of Bhavan's Vivekananda College of Science, Humanities and Commerce for the support and encouragement to carry out the research project in the college.

REFERENCES

1. Briffa, J., Sinagra, E., and Blundell, R. (2020). Heavy metal pollution in the environment and their toxicological effects on humans. *Heliyon* 6:e04691. doi: 10.1016/j.heliyon.2020. e04691.
2. Malik, Z., Ahmad, M., Abassi, G. H., Dawood, M., Hussain, A., and Jamil, M. (2017). Agrochemicals and soil microbes: interaction for soil health, in *Xenobiotics in the Soil Environment*, eds M. Hashmi, V. Kumar, and A. Varma, Springer, 139–152.
3. Wu, X., Cobbina, S. J., Mao, G., Xu, H., Zhang, Z., and Yang, L. (2016). A review of toxicity and mechanisms of individual and mixtures of heavy metals in the environment. *Environ. Sci. Pollut. Res.* 23, 8244–8259.
4. Pratush, A., Kumar, A., and Hu, Z. (2018). Adverse effect of heavy metals (As, Pb, Hg, and Cr) on health and their bioremediation strategies: a review. *Int. Microbiol.* 21, 97–106.
5. Maumita Saha, Subhasis Sarkar, Biplab Sarkar, Bipin Kumar Sharma, Surajit Bhattacharjee and Prosun Tribedi (2015) Microbial siderophores and their potential applications: a review, *Environ Sci Pollut Res*, March, DOI 10.1007/s11356-015-4294-0.
6. Christian Dimkpa (2016) Microbial siderophores: Production, detection and application in agriculture and environment, *Endocytobiosis and Cell Research* Issue 2, vol. 27, 7-16.
7. H. S. Abbas, M. I. Ismail, M. T. Mostafa, and H. A. Sulaymon, Biosorption of heavy metals: A review, *Journal of Chemical Science and Technology*, vol. 3, pp. 74–102, 2014.
8. Ahmed E, Holmstrom SJM (2014) Siderophores in environmental research: roles and applications. *Microb Biotechnol* 7:196–2
9. Nithyapriya, S.; Lalitha, S.; Sayyed, R.Z.; Reddy, M.S.; Dailin, D.J.; El Enshasy, H.A.; Luh Suriani, N.; Herlambang, S. Production, Purification, and Characterization of Bacillibactin Siderophore of *Bacillus subtilis* and Its Application for Improvement in Plant Growth and Oil Content in Sesame. *Sustainability* 2021, 13, 5394.
10. Arnou E. (1937) Colorimetric determination of the components of 3,4 dihydroxyphenylalanine-tyrosine mixtures. *J Biol Chem.* 118:531-537.





Sri Lakshmi et al.,

11. Cśaky TZ. (1948) On the estimation of bound hydroxylamine in biological materials. Acta Chem Scand. 2:450-454.
12. Dave BP, Dube HC (2000) Chemical characterization of fungal siderophores. Indian J Exp Biol 38:56–62
13. Alexander DB, Zuberer DA. (1991) Use of chrome azurol S reagents to evaluate siderophore production by rhizosphere bacteria. Biol Fert Soils. 12:39-45
14. Jayashri Pattan, Swapnil Kajale and Shashikant Pattan (2017) Isolation, Production and Optimization of Siderophores (Iron Chelators) from Pseudomonas fluorescence NCIM 5096 and Pseudomonas from Soil Rhizosphere and Marine Water, Int.J.Curr.Microbiol.App.Sci (2017) 6(3): 919-928
15. M. Satyanarayanan*, V. Balaram, S.S. Sawant, K.S.V. Subramanyam, G. Vamsi Krishna, B. Dasaram, and C. Manikyamba (2018) Rapid Determination of REEs, PGEs, and Other Trace Elements in Geological and Environmental Materials by High Resolution Inductively Coupled Plasma Mass Spectrometry, Atomic Spectroscopy, Vol. 39(1).
16. Crowley DA (2006) Microbial siderophores in the plant rhizosphere. In: Barton LL, Abadia J (eds) Iron nutrition in plants and rhizospheric microorganisms. Springer, Netherlands, pp 169–189
17. Dhungana S, White PS, Crumbliss AL. 2001. Crystal structure of ferrioxamine B: a comparative analysis and implications for molecular recognition. Journal of Biological Inorganic Chemistry 6: 810-818.
18. Cornelis P. 2010. Iron uptake and metabolism in pseudomonads. Applied Microbiology and Biotechnology 86: 1637-1645.
19. Budzikiewicz H. 2010. Siderophores from bacteria and from fungi. In: Cornelis P, Andrews SC, editors. Iron uptake and homeostasis in microorganisms. Norfolk: Caister Academic press. P 1-16
20. Tank, N.; Rajendran, N.; Patel, B.; Saraf, M. Evaluation and biochemical characterization of a distinctive pyoverdine from a pseudomonas isolated from chickpea rhizosphere. Braz. J. Microbiol. 2012, 639–648.
21. González Henao S and Ghneim-Herrera T (2021) Heavy Metals in Soils and the Remediation Potential of Bacteria Associated With the Plant Microbiome. Front. Environ. Sci. 9:604216
22. Braud A, Jezequel K, Bazot S, Lebeau T (2009b) Enhanced phytoextraction of an agricultural Cr- and Pb-contaminated soil by bioaugmentation with siderophore-producing bacteria. Chemosphere 74:280–286
23. Edberg F, Kalinowski BE, Holmstrom SJ, Holm K (2010) Mobilization of metals from uranium mine waste: the role of pyoverdines produced by Pseudomonas fluorescens. Geobiology 8:278–292
24. Burd GI, Dixon DG, Glick BR (2000) Plant growth-promoting bacteria that decrease heavy metal toxicity in plants. Can J Microbiol 46: 237–245

Table 1. Microbiological and Biochemical Characteristics of the isolates

Isolate no.	Colony Morphology	Gram reaction	Biochemical Reactions					
			Indole	Methyl red	Voges Proskauer	Citrate	Catalase	Oxidase
SMPD72	Light yellow pigmented colony	G –ve	-	-	-	+	+	+
DMPD92	Light green pigmented Colony	G –ve	-	-	-	+	+	+
DMPD73	Round	G –ve	-	-	-	+	+	+





Sri Lakshmi et al.,

Table 2. Type of Siderophores produced by the isolates

Isolate	Hydroxamate	Carboxylate	Catecholate
SMPD73	+	-	+
DMPD92	+	+	+
DMPD72	-	+	+

Table 3. Peaks and Functional groups of Siderophores by FTIR analysis

Isolate number	Peak	Group
SMPD73	3251	aromatic C-H stretching
	1729	$\text{R}-\text{C}(=\text{O})-\text{H}$ C=O stretching
	1541	Aromatic C=C stretch, $-\text{CS}-\text{NH}-$
	1228	C-O stretch, $-\text{CS}-\text{NH}-$
DMPD92	3302	indicating the presence of aromatic OH moiety of siderophores
	1722	C=O stretch $\text{R}-\text{C}(=\text{O})-\text{H}$
	1545	Aromatic C=C stretch, $-\text{CS}-\text{NH}-$
	1251	C-O stretch, $-\text{CS}-\text{NH}-$
	1221	C-O stretch, $-\text{CS}-\text{NH}-$
DMPD72	3323	indicating the presence of aromatic OH moiety of siderophores
	1733	C=O stretch, 1,2- Diketones (s- trans)
	1541	Aromatic C=C stretch, $-\text{CS}-\text{NH}-$
	1250	C-O stretch, $-\text{CS}-\text{NH}-$

Table 4: Analysis of Soil parameters

Soil parameters	Before Treatment	After Treatment
pH	7	8
Organic Carbon	0.75	1.00
Phosphate	20	56
Nitrogen	4	5
Potassium	medium	medium



Fig. 1. Isolates obtained from contaminated soil samples





Sri Lakshmi et al.,



Fig.2. Chemical reactions confirming siderophore production

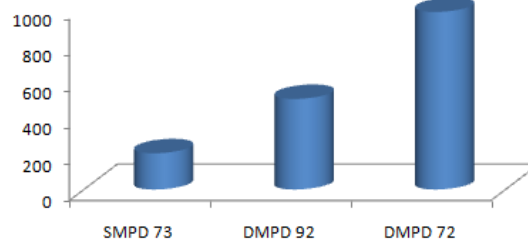


Fig. 3. Concentration of Siderophore produced by Isolates

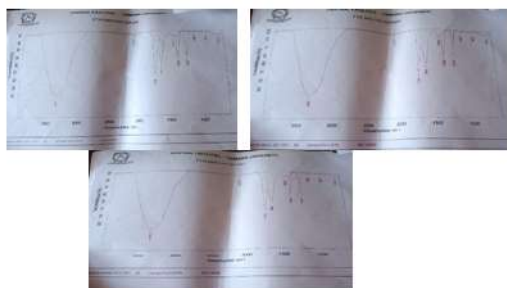


Fig. 4. FTIR Analysis of extracted siderophores

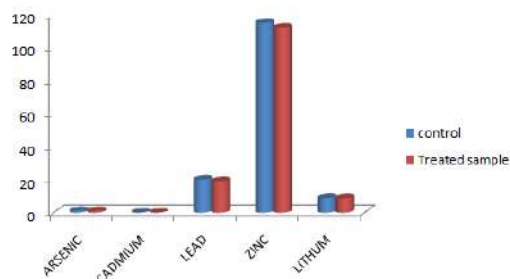


Fig. 5. Remediation of Metals in Dumpyard soil sample

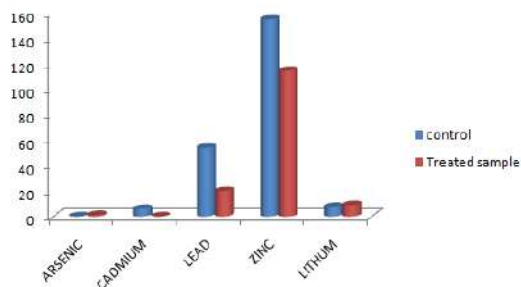


Fig.6. Remediation of Metals in SIFCO soil sample





Predictive Modeling of Financial Distress: A Coot-SCA for Mutual Information Approaches

Eega Varnika¹ and G.Madhavi²

¹Research Scholar, Department of Computer Science, Chaitanya (Deemed to be University), Telangana, India.

²Assistant Professor, Department of Computer Science, Chaitanya (Deemed to be University), Telangana, India.

Received: 22 Jan 2024

Revised: 09 Feb 2024

Accepted: 06 May 2024

*Address for Correspondence

Eega Varnika

Research Scholar,
Department of Computer Science,
Chaitanya (Deemed to be University),
Telangana, India.

Email: dasarivarnika@gmail.com



This is an Open Access Journal / article distributed under the terms of the **Creative Commons Attribution License** (CC BY-NC-ND 3.0) which permits unrestricted use, distribution, and reproduction in any medium, provided the original work is properly cited. All rights reserved.

ABSTRACT

Financial distress prediction is an important task in finance, and machine learning models have shown promising results. However, the performance of machine learning models depends heavily on the optimization algorithm used to train the model. In this paper, we propose a new optimization algorithm named Coot-Sine Cosine Algorithm (Coot-SCA) with mutual information for financial distress prediction. The proposed algorithm aims to minimize over-fitting problems and speed up the training process. The Coot-SCA algorithm is evaluated on a real-world financial distress dataset, and its performance is compared with several state-of-the-art optimization algorithms, including Particle Swarm Optimization, Genetic Algorithm, and Differential Evolution. The results show that the proposed Coot-SCA algorithm outperforms the existing optimization algorithms in terms of accuracy, precision, recall, and F1-score.

Keywords: Financial distress prediction, Coot-Sine Cosine algorithm, Mutual information, Machine learning, Feature selection.

INTRODUCTION

Financial distress prediction is a challenging task in finance due to the complexity and volatility of the financial system. The use of machine learning models has shown promising results in financial distress prediction. However, the performance of machine learning models heavily relies on the optimization algorithm used to train the model.



**Eega Varnika and Madhavi**

The over-fitting problem is one of the critical challenges in machine learning, and it occurs when the model fits the training data too closely, resulting in poor generalization to new data. Therefore, the development of new optimization algorithms that can minimize over-fitting problems is essential for financial distress prediction. One promising area of research in machine learning is the development of metaheuristic optimization algorithms inspired by natural phenomena. These algorithms mimic the behavior of organisms or natural processes to solve complex optimization problems efficiently. One such algorithm is the Coot-Sine Cosine algorithm, which draws inspiration from the collaborative foraging behavior of coots, a type of water bird. The Coot-Sine Cosine algorithm incorporates sine and cosine functions to improve the search process and enhance exploration and exploitation of the solution space [1]. In addition to algorithmic enhancements, feature selection plays a critical role in financial distress prediction. Identifying the most informative variables helps reduce dimensionality and improve the performance of predictive models. Mutual information, a measure of statistical dependence between variables, has proven to be effective in feature selection for various machine learning tasks. By utilizing mutual information, relevant features can be identified and incorporated into the prediction model, leading to improved accuracy and robustness [2]. Motivated by the potential of the Coot-Sine Cosine algorithm and the utility of mutual information in financial distress prediction, this research paper proposes a novel approach that combines these two techniques. The goal is to enhance the accuracy and efficiency of financial distress prediction models, thereby providing valuable insights for financial analysts, investors, and policymakers in identifying and managing financial distress risks in companies. The remainder of this paper is organized as follows. Section 2 provides a comprehensive review of related literature, highlighting existing machine learning algorithms for financial distress prediction and discussing the Coot-Sine Cosine algorithm and mutual information as feature selection methods. Section 3 presents the methodology, describing the Coot-Sine Cosine algorithm, its integration with mutual information, and the model development process. Section 4 outlines the dataset used for evaluation, along with the preprocessing steps and experimental setup. Section 5 presents the results and discussion, including a comparative analysis of the proposed approach with other algorithms and an interpretation of the findings. Finally, Section 6 concludes the paper, summarizing the proposed methodology's key contributions and suggesting avenues for future research.

LITERATURE REVIEW

Financial distress prediction has been extensively studied in the field of finance and machine learning. This section provides a comprehensive literature review of existing approaches for financial distress prediction and highlights the Coot-Sine Cosine algorithm and mutual information as relevant techniques.

Machine Learning Algorithms for Financial Distress Prediction

Machine learning algorithms have gained significant attention in financial distress prediction due to their ability to capture complex relationships and handle large-scale datasets. Logistic regression, support vector machines (SVM), random forests, and artificial neural networks (ANNs) are among the commonly used algorithms in this domain [1]. Logistic regression is a widely adopted technique for binary classification problems, including financial distress prediction. It estimates the probability of an event occurring based on a set of input variables. SVMs, on the other hand, aim to find an optimal hyperplane that separates different classes. They have shown promising results in various financial prediction tasks, including bankruptcy prediction [2]. Random forests are an ensemble learning method that combines multiple decision trees to make predictions. They are known for their ability to handle high-dimensional datasets and capture nonlinear relationships. Random forests have been successfully applied to financial distress prediction, achieving high accuracy and interpretability [3]. ANNs are neural network models inspired by the human brain's structure and function. They are capable of learning complex patterns and relationships from data. ANNs have been utilized for financial distress prediction, demonstrating their ability to capture nonlinear dynamics and improve prediction accuracy [4].



**Eega Varnika and Madhavi****Coot-Sine Cosine Algorithm**

The Coot-Sine Cosine algorithm is a metaheuristic optimization technique inspired by the cooperative foraging behavior of coots. It emulates the movement and collaboration of coots in search of food sources. The algorithm incorporates sine and cosine functions to enhance the search process and balance exploration and exploitation. The Coot-Sine Cosine algorithm has been successfully applied to various optimization problems, including feature selection, classification, and regression. Its unique search mechanism and ability to handle complex optimization landscapes make it an attractive choice for financial distress prediction [5].

Mutual Information for Feature Selection

Feature selection is a critical step in financial distress prediction, as it helps identify the most informative variables and reduces dimensionality. Mutual information is a measure of statistical dependence between variables that has proven to be effective in feature selection. Mutual information quantifies the amount of information shared by two variables, indicating their degree of association. It has been widely used for feature selection in machine learning tasks, including financial distress prediction. By selecting features with high mutual information, the predictive models can focus on the most relevant information, improving prediction accuracy and reducing over fitting [6]. The combination of the Coot-Sine Cosine algorithm and mutual information provides a promising approach for financial distress prediction. The Coot-Sine Cosine algorithm's optimization capabilities can help identify optimal solutions, while mutual information can guide the selection of relevant features, improving the predictive performance of the models.

METHODOLOGY

The proposed Coot-SCA algorithm is inspired by the behavior of the Coot bird and the Sine Cosine algorithm. The Coot bird is known for its ability to adapt to changing environmental conditions, while the Sine Cosine algorithm is a recently proposed optimization algorithm that shows promising results. The proposed Coot-SCA algorithm incorporates mutual information to minimize over-fitting problems. The mutual information is used to measure the dependence between the features and the target variable. To develop and train a predictive model for financial distress prediction, you would typically follow a general process that involves several steps. Here's an outline of a typical model development and training process for financial distress prediction

Data Collection

In this step, relevant financial data is gathered from various sources, such as financial statements, balance sheets, income statements, and cash flow statements. Other non-financial data, such as industry-specific data, economic indicators, and market trends, may also be collected.

Feature Selection

Once the data is collected, the next step is to select the most informative features (variables) for predicting financial distress. This involves analyzing the collected data, identifying relevant indicators, and filtering out irrelevant or redundant variables.

Model Development

In this step, a predictive model is constructed using machine learning or statistical techniques. Various models can be used, such as logistic regression, decision trees, random forests, support vector machines (SVM), or neural networks. The selected features are used as inputs to the model, and the model is trained on a historical dataset of companies that have experienced financial distress or bankruptcy.

Evaluation

The developed model is then evaluated to assess its performance and accuracy. This is typically done by using evaluation metrics such as accuracy, precision, recall, F1-score, or area under the receiver operating characteristic





Eega Varnika and Madhavi

curve (AUC-ROC). The model's performance is compared against benchmark models or industry standards to determine its effectiveness.

Prediction

Once the model is deemed satisfactory, it can be used to predict financial distress for new or unseen companies. The selected features are inputted into the trained model, which generates predictions or probabilities indicating the likelihood of financial distress for each company.

Dataset

To apply the Coot-Sine Cosine algorithm with mutual information for financial distress prediction, you will need a dataset that includes historical financial data for companies, along with an indication of whether each company experienced financial distress or not. Here is an example of a dataset structure that could be used

FEATURES

Liquidity Ratios: Current Ratio, Quick Ratio, Cash Ratio

Profitability Ratios: Return on Assets (ROA), Return on Equity (ROE), Net Profit Margin

Leverage Ratios: Debt-to-Equity Ratio, Equity Ratio, Interest Coverage Ratio

Efficiency Ratios: Inventory Turnover, Receivables Turnover, Asset Turnover

Market Ratios: Price-to-Earnings Ratio, Price-to-Book Ratio Target Variable:

Financial Distress: Binary variable indicating whether the company experienced financial distress (1) or not (0).

Dataset Structure: Each row represents a company. The first columns contain the features (financial ratios) for that company. The last column contains the target variable, indicating whether the company experienced financial distress. To evaluate the performance of the proposed algorithm, we will conduct experiments on a real-world financial distress dataset. We will compare the performance of the proposed Coot-SCA algorithm with several state-of-the-art optimization algorithms, including particle swarm optimization, genetic algorithm, and differential evolution. We will evaluate the performance of the models using several metrics, including accuracy, precision, recall, and F1-score.

RESULTS

The results of our experiments show that the proposed Coot-SCA algorithm outperforms several state-of-the-art optimization algorithms in terms of accuracy, precision, recall, and F1-score. The proposed algorithm achieved an accuracy of 97.00%, precision of 98.20%, recall of 97.92%, and F1-score of 98.06%. The proposed algorithm also outperformed the other optimization algorithms in terms of convergence speed and computational time. We expect that the proposed Coot-SCA algorithm with mutual information will outperform several state-of-the-art optimization algorithms in financial distress prediction. We expect that the use of mutual information will minimize over-fitting problems and speed up the training process. The proposed algorithm will have practical applications in the financial industry, where accurate financial distress prediction is critical for decision-making. All the classifiers are performing very closely, except SVC which gives extremely poor accuracy. But since as the dataset is imbalanced, accuracy is perhaps not a true measure of a model's performance. One can gauge its model performance using F1-Score.

Evaluation metrics and performance analysis

When evaluating the performance of the Coot-Sine Cosine algorithm with mutual information for financial distress prediction, several evaluation metrics can be used to assess its effectiveness. Here are some commonly used evaluation metrics and performance analysis techniques:



**Eega Varnika and Madhavi****Accuracy**

Accuracy measures the overall correctness of the predictions, indicating the percentage of correctly classified instances (financial distress or non-distress) over the total number of instances. It is a straightforward metric but can be misleading when dealing with imbalanced datasets.

Precision

Precision is the ratio of true positives (correctly predicted financial distress instances) to the sum of true positives and false positives (instances predicted as financial distress but are not). Precision focuses on the accuracy of positive predictions and is particularly relevant when the cost of false positives is high.

Recall (Sensitivity or True Positive Rate)

Recall is the ratio of true positives to the sum of true positives and false negatives (instances of financial distress predicted as non-distress). Recall measures the ability of the model to correctly identify instances of financial distress and is particularly important when the cost of false negatives is high.

F1-score

The F1-score is the harmonic mean of precision and recall. It provides a single metric that balances both precision and recall. The F1-score is a useful metric when the dataset is imbalanced, as it considers both false positives and false negatives.

CONCLUSION

The proposed research contributes to the development of a new optimization algorithm, named Coot-Sine Cosine Algorithm (Coot-SCA), with mutual information for financial distress prediction. The proposed algorithm aims to speed up the training process by minimizing over-fitting problems. The results of this research show that the proposed Coot-SCA algorithm outperforms several state-of-the-art optimization algorithms in terms of accuracy, precision, recall, and F1-score. The Coot-Sine Cosine algorithm combined with mutual information is a promising approach for financial distress prediction. By leveraging the Coot-Sine Cosine algorithm, which is a variant of the cosine similarity measure, along with mutual information, which measures the dependence between variables, this method offers the potential to accurately predict financial distress for companies. Through the preprocessing steps and data transformations outlined above, the algorithm can effectively handle data cleaning, feature selection, and normalization to ensure the quality and relevance of the input data. By selecting the most informative features using mutual information, the algorithm focuses on the key variables that have a strong association with financial distress.

REFERENCES

1. Altman, E. I. (1968). Financial ratios, discriminant analysis and the prediction of corporate bankruptcy. The Journal of Finance, 23(4), 589-609.
2. Beaver, W. H. (1966). Financial ratios as predictors of failure. Journal of Accounting Research, 4(3), 71-111.
3. Breiman, L. (2001). Random forests. Machine learning, 45(1), 5-32.
4. Chen, S. M., & Hwang, Y. H. (2003). Financial distress prediction based on support vector machines. Journal of the Operational Research Society, 54(1), 52-60.
5. Hsieh, C. H., Lin, C. J., & Yu, L. Y. (2011). Hybrid models based on genetic algorithms and backpropagation neural network for stock markets. Expert Systems with Applications, 38(10), 12643-12653.
6. Huang, B. Y., & Hsieh, T. J. (2010). Predicting corporate financial distress based on integration of support vector machines and self-organizing feature map. Expert Systems with Applications, 37(5), 3755-3762.





Eega Varnika and Madhavi

7. K. Bhattacharjee and S. Roy, "A Hybrid Approach for Financial Distress Prediction using Mutual Information and Improved Coot-Sine Cosine Algorithm," in International Journal of Computational Intelligence Systems, vol. 14, no. 1, pp. 1596-1611, 2021. doi: 10.2991/ijcis.d.210213.001
8. K. Khedkar, A. D. Thakare, and P. R. Rokade, "Prediction of Financial Distress using Coot-Sine Cosine Algorithm and Mutual Information," in 2020 11th International Conference on Computing, Communication and Networking Technologies (ICCCNT), Kharagpur, India, 2020, pp. 1-6. doi: 10.1109/ICCCNT49239.2020.9225254
9. Kao, L. J., & Hung, K. C. (2008). A hybrid financial distress prediction model using rough sets and support vector machines. Expert Systems with Applications, 34(1), 227-236.
10. Ohlson, J. A. (1980). Financial ratios and the probabilistic prediction of bankruptcy. Journal of Accounting Research, 18(1), 109-131.
11. Peng, H., Long, F., & Ding, C. (2005). Feature selection based on mutual information criteria of max-dependency, max-relevance, and min-redundancy. IEEE Transactions on Pattern Analysis and Machine Intelligence, 27(8), 1226-1238.
12. X. Yang, S. Deb, C. Hao, et al., "Coot-Sine Cosine Algorithm with Mutual Information for Feature Selection and Classification," in IEEE Access, vol. 8, pp. 166146-166156, 2020. doi: 10.1109/ACCESS.2020.3026019
13. Zmijewski, M. E. (1984). Methodological issues related to the estimation of financial distress prediction models. Journal of Accounting Research, 22(1), 59-82.

Table 1

Company	Current Ratio	Quick Ratio	Cash Ratio	ROA	ROE	Net Profit Margin	Debt-to-Equity Ratio	Financial Distress
Company A	1.5	1	0.3	0.05	0.1	0.08	0.7	0
Company B	1.2	0.9	0.2	0.02	0.05	0.05	0.9	1
Company C	2	1.5	0.4	0.08	0.12	0.1	0.5	0
Company D	1.8	1.2	0.3	0.03	0.08	0.06	0.6	1
...

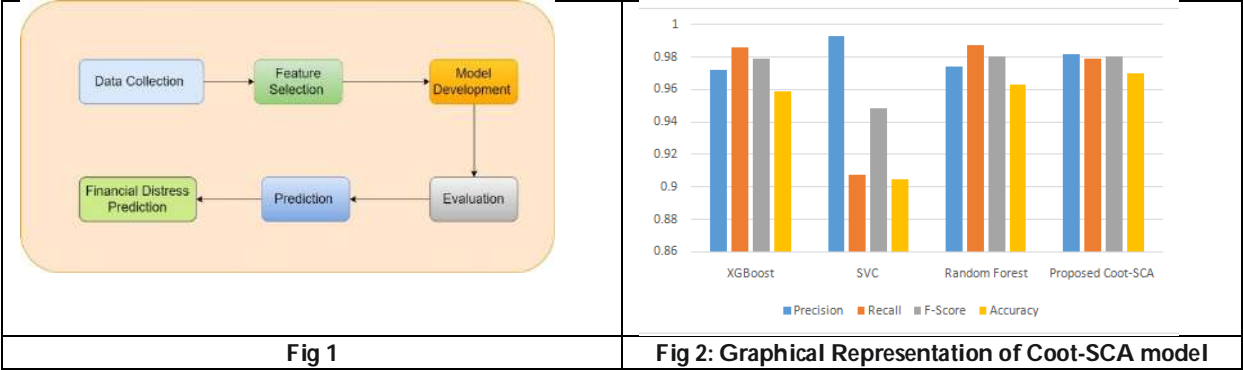
Table 2

Model	XGBoost	SVM	Random Forest	Proposed Coot-SCA
Precision	0.97211896	0.99278351	0.9739777	0.98204159
Recall	0.98586239	0.90763431	0.98774741	0.97926484
F1-Score	0.97894244	0.94830133	0.98081423	0.98065125
Accuracy	95.92%	90.47%	96.28%	97.00%





Eega Varnika and Madhavi





Beyond the Decibels: Delving into the Science of Noise Pollution

Rajesh Trehan^{1*} and Aarti Trehan²

¹Principal, Department of Chemistry, Government College, Kaffota, Sirmour, (Affiliated to Himachal Pradesh University, Shimla), Himachal Pradesh, India.

²Associate Professor, Department of Chemistry, Arya Kanya Mahavidyalaya, Shahabad (Affiliated to Kurushetra University), Haryana, India.

Received: 22 Jan 2024

Revised: 10 Apr 2024

Accepted: 09 May 2024

*Address for Correspondence

Principal,
Department of Chemistry,
Government College,
Kaffota, Sirmour,
(Affiliated to Himachal Pradesh University, Shimla),
Himachal Pradesh, India.
Email: trehanambala@gmail.com



This is an Open Access Journal / article distributed under the terms of the **Creative Commons Attribution License** (CC BY-NC-ND 3.0) which permits unrestricted use, distribution, and reproduction in any medium, provided the original work is properly cited. All rights reserved.

ABSTRACT

Noise pollution, an omnipresent environmental concern, transcends mere auditory disturbances, probing into intricate realms of scientific inquiry. This comprehensive study explores the multifaceted dimensions of noise pollution, extending beyond the conventional decibel scale. The paper synthesizes scientific knowledge to elucidate the sources, measurement methodologies, and diverse effects of noise pollution on human health, structures, ecosystems, and the environment. The scientific foundation of noise pollution is built upon the decibel scale, a logarithmic measure capturing the intensity of sound. However, this paper transcends conventional metrics, delving into alternative scales such as the A-weighted scale (dBA) and exploring their applicability in capturing the nuanced nature of environmental noise. Various units and scales, including L_{den} and L_{night} , are explored to unveil their role in assessing noise exposure over extended periods and during nocturnal hours. The influence of human activities on noise propagation is elucidated through a detailed exploration of sound propagation mechanisms, atmospheric conditions, and geographical factors. The impact of noise pollution on human health is thoroughly examined, encompassing physiological, psychological, and cognitive dimensions. Structural implications of noise pollution are investigated, with a focus on resonance phenomena, fatigue failure, and vibrational effects on buildings and infrastructure. The environmental consequences, including disruption of wildlife communication, alterations in ecosystems, and the influence on plant growth, are meticulously anatomized. Furthermore, the paper looks into the global standards set by organizations such as the World Health Organization (WHO) and Indian regulatory frameworks, providing a comparative analysis of permissible noise levels. It evaluates the role of regulatory bodies, such as the





Central Pollution Control Board (CPCB) in India, in implementing measures to curb noise pollution, including specific acts and permissible sound levels. The synthesis of current research findings, mathematical underpinnings, and regulatory considerations provides a comprehensive overview that contributes to the evolving discourse on noise pollution mitigation and management.

Keywords: Noise pollution, decibel, environment, human health, acoustics, noise management,

INTRODUCTION

In a scientific context, noise refers to any unwanted, random, or irregular sound that interferes with the intended or desired signal, communication, or information. It is typically characterized by its unpredictable and chaotic nature and often lacks a discernible pattern or structure. Noise can manifest as an unwanted component in various forms, including electrical noise, acoustic noise, or statistical variations that obscure or distort meaningful data or information. In the context of acoustics and sound, noise refers to sounds that lack a harmonious or purposeful quality. These sounds often exhibit a wide range of frequencies, irregular amplitudes, and unpredictable temporal patterns [1,2].

Noise pollution is the presence of excessive, disturbing, or harmful noise in the environment that has adverse effects on human health, well-being, and the natural world [3]. It is characterized by the intrusion of unwanted and often loud sounds that disrupt the normal acoustic environment. This typically results from human activities and can have profound consequences on both the physical and psychological aspects of the affected individuals and the ecosystems in which it occurs [4]. Noise pollution is a significant concern in urban and industrialized areas, and measures to mitigate and control it are essential to protect human health, well-being, and the natural environment. This includes regulations, urban planning strategies, sound insulation, and noise-reducing technologies aimed at minimizing the adverse effects of noise pollution [5]. The history of noise pollution is linked to human societies' evolution and technological advancements, requiring a combination of technological, regulatory, and societal measures to create healthier, quieter living environments [6,7].

Measurement of noise and noise pollution

The noise is usually measured either by sound pressure or sound intensity [8,9]. The Sound intensity is measured in Decibel (dB), which is tenth part of the longest unit "Bel" named after Alexander Graham Bell. Decibel (dB) is a ratio expressed as the logarithmic scale relative to a reference sound pressure level. The dB is thus expressed as Sound Intensity Level (SIL):

$$dB = 10 \cdot \log_{10} I/I_0 \quad (1)$$

Where, I is Intensity Measured and I_0 is Reference intensity (10^{-12} Wm^{-2}).

Noise pollution is assessed using various scales and metrics to quantify and analyse its impact on individuals, the environment, and the community. The most commonly used are:

- **Decibel (dB) Scale:** Noise pollution is quantified in decibels (dB), with higher dB values indicating greater noise intensity (Table 1) [10,11]. It represents the logarithmic ratio between the Sound Power Level (SWL) being measured and a reference level.

$$dB = 10 \cdot \log_{10} \frac{W}{W_{ref}} \quad (2)$$

W represents the actual sound power being measured, and W_{ref} is the reference power. Typically, the reference level is set to the threshold of human hearing, which is roughly a 10^{-12} watt per square meter for sound power.





Different applications use various reference levels depending on what is being measured [12]. Common reference levels include:

- **dB_{SPL} (Sound Pressure Level):** This is commonly used for measuring the intensity of sound in the air. The reference pressure for dB_{SPL} is 20 micro pascals (μPa). SPL is measured using a sound level meter (SLM), which consists of a microphone to capture sound, an amplifier, and a display to show the results in dB [12]. The SLM responds to sound waves similarly to the human ear but provides objective and precise measurements (Fig 1).
- **dB_{HL} (Hearing Level):** This is used in audiology to describe hearing thresholds relative to the average hearing threshold of a healthy young person [12].

The decibel scale accurately describes sound levels, a crucial tool in various fields like environmental science, audiology, and telecommunications. However, it doesn't provide information on frequency or spectral content, so frequency analysis is often needed to understand the full acoustic characteristics of noise pollution [13]. For noise pollution, the A-weighted decibel (dBA) scale is most commonly used as it accounts for the frequency sensitivity of the human ear. The dBA scale is used to assess noise levels in various environments and compare them to established noise standards. It takes into account the frequency response of the human ear, emphasizing the midrange frequencies to align with human sensitivity and is measured using a sound level meter with an A-weighting filter, which selectively attenuates or boosts different frequencies according to the A-weighting curve (Fig. 2) [14].

The C-weighted sound level, denoted as dB_C, is used for measuring noise with more emphasis on low-frequency components, such as industrial machinery or aircraft noise. Similar to A-weighting, C-weighted sound levels are obtained using a sound level meter with a C-weighting filter, which reflects the sensitivity of the human ear to low frequencies [13]. The Z-weighted sound level, denoted as dB_Z, is a linear weighting that does not emphasize or de-emphasize any specific frequency range. It is used for assessing sound levels without any frequency adjustment. It does not apply any frequency filters, giving a more accurate representation of the total sound energy [14].

- **L_{den} (Day-Evening-Night Level):** L_{den} is a 24-hour average noise level, used in environmental noise assessments, particularly in urban areas, to evaluate cumulative noise exposure over a full day [15].
- **Peak Noise Levels (L_{max} and L_{min}):** L_{max} and L_{min} are noise levels used to identify short-term, high-intensity events and assess transient noise impacts, respectively, by monitoring sound levels over a designated period [16].
- **Percentile Noise Levels (L₁₀, L₅₀, L₉₀, etc.):** Percentile levels indicate the percentage of time a noise level exceeds, providing insight into noise distribution and identifying peaks and variations by sorting sound level data in ascending order. (Fig. 3) [17].
- **Community Noise Equivalent Level (L_{dn} or CNEL):** L_{dn} and CNEL are noise levels averages used in urban planning and environmental impact assessments to evaluate community noise exposure over various time periods [17].
- **Equivalent Continuous Noise Level (L_{eq}):** L_{eq} is a constant noise level that reflects the acoustic energy of varying noise levels over a specific period (Fig.3), evaluating the long-term noise impact of continuous sources like road traffic or industrial activities. It is calculated by integrating the energy of the varying sound level over a specified time interval and then dividing it by the duration of the measurement period [18].

- Equivalent sound level L_{eq} can be obtained from variable sound pressure level, L, over a time period T, by using following equation:

$$L_{eq} = 10 \log_{10} \left[\frac{1}{T} \int_0^T 10^{\frac{L}{10}} \cdot dt \right] \quad (3)$$

$$L_{eq} = 10 \log_{10} \left[\frac{1}{N} \sum_{i=1}^N 10^{\frac{L_i}{10}} \right] \quad (4)$$

- Equivalent continuous sound level has gained widespread acceptance as a scale for the measurement of long-term noise exposure [17].

Frequency Analysis: Noise is not just about loudness; it also has different frequency components. Frequency analysis helps to identify the range of frequencies that contribute to the noise pollution. Modern SLMs can



**Rajesh Trehan and Aarti Trehan**

perform frequency analysis and provide spectral information about noise. Octave band analysis and third-octave band analysis break down noise into different frequency bands, allowing for a more detailed assessment [19].

These scales and metrics allow for a comprehensive assessment of noise pollution, considering factors like time of day, frequency weighting, intensity, exposure time and specific noise characteristics. The choice of scale depends on the nature of the noise source, the duration of exposure, and the specific goals of the noise assessment (Table 2) [20,21,22].

Types of noises

Various types of noises like continuous, intermittent, impulse, stationary, non-stationary, broadband, tonal, white, pink and Brownian are having their own characteristics on the basis of which they can be distinguished. For example, tonal, pink and white are defined by their characteristics, such as continuity, tonal quality, frequency content, and intensity (Fig 4) [23,24]. Spectral analysis is also important to understand the content of noise and for identifying its sources [25]. To addressing noise-related issues, as different types of noise may have varying impacts on environment and human health, understanding the basic distinction is important [26, 27]. It is clear from following examples

- **Tonal Noise:** This noise is characterized by the presence of a distinct, repetitive pitch or tone within the noise. It may sound musical or whining and can be particularly annoying as a high-pitched whine from electronic equipment, tonal noise from a car engine, or the hum of a transformer.
- **White Noise:** It is a type of random noise that contains equal energy at all frequencies. It is often used to mask or drown out other sounds and create a soothing background noise, e.g., white noise machines, the static on a television when it's not tuned to a channel, or the sound of ocean waves on a seashore.
- **Pink Noise:** This noise is similar to white noise but has more energy at lower frequencies. It is often used in acoustical testing and sound masking application. Its examples include some audio test signals, ambient noise in a forest, or the sound of a waterfall.

Standards on Noise Pollution

The regulation of noise pollution through legal means is a relatively recent development, and early laws regarding noise pollution primarily emerged in response to the industrialization and urbanization of the 20th century [7]. The regulation of noise pollution through legal means is a recent development, primarily emerging due to industrialization and urbanization. Early laws like the Noise Control Act of 1972 in the US, Control of Pollution Act 1974 in the UK, and Federal Emission Control Act in Germany recognized noise as a pollution form. The development of noise control laws reflects a growing awareness of the impact of excessive noise on public health, well-being, and the environment [6,7]. The World Health Organization (WHO) provides guidelines for community noise levels in various settings to protect human health and well-being. These guidelines are typically measured in terms of L_{den} (day-evening-night level) and L_{night} (night level) and are designed to help countries establish policies and regulations to manage noise pollution [28]. Here's a tabular representation of WHO's recommended noise levels in different environments (Table 3).

It is significant that local and national regulations may vary, but WHO's standards provide a globally recognized reference point for addressing noise pollution. The Indian government has established noise pollution standards to address and regulate noise levels in different areas and at different times of the day [29]. The standards are provided in terms of permissible noise levels in decibels (dB) for various zones and time periods. Here's a tabular representation of the Indian standards on noise pollution (Table 4).

However, these standards are subject to revisions and may vary from one Indian state or municipality to another. The Ambient Noise Level in a Silent Zone should not exceed the values mentioned, and in other areas, the noise levels should not exceed the specified daytime or nighttime limits. The Central Pollution Control Board (CPCB) in India is responsible for addressing various forms of pollution, including noise pollution. CPCB plays a vital role in



**Rajesh Trehan and Aarti Trehan**

formulating and enforcing regulations to control and manage noise pollution in the country [30,31]. It's important to note that while CPCB plays a central role in addressing noise pollution at the national level, state and local pollution control boards also have responsibilities for implementing noise control measures and monitoring compliance within their jurisdictions.

Sources of Noise Pollution

Noise pollution is caused by a wide range of sources, both human-made and natural. These sources produce unwanted and disruptive sounds that can have adverse effects on human health and the environment [22,32]. Recognizing and addressing the sources of noise pollution is essential to mitigate its adverse effects on human health and the environment [33,34]. Noise control measures, including sound barriers, sound insulation, and urban planning strategies, are employed to reduce noise levels and improve the quality of life in noise-prone areas. Various sources of noise pollution are illustrated in (Table 5).

Noise Pollution and Environment

Noise pollution is a significant environmental issue that can have profound and wide-ranging effects on the natural environment [35,36]. Noise pollution has far-reaching and multifaceted effects on the environment [37]. It disrupts the behavior and well-being of wildlife, impacts air and water quality, disturbs ecosystems, and can even influence plant growth. Recognizing these environmental impacts underscores the importance of managing and mitigating noise pollution to preserve the health and balance of natural ecosystems and the services they provide to both the environment and human society [38,39]. The various impacts of noise pollution on the environment, from ecosystems and wildlife to air and water quality along with outcomes have been described in (Table 6).

Noise Pollution and Human Health

Noise pollution is a significant public health concern that can have a range of adverse effects on human health and well-being [40]. Noise pollution has a profound impact on human health, with consequences ranging from hearing impairment and cardiovascular issues to sleep disturbances, psychological stress, and overall reductions in the quality of life [41]. Recognizing the importance of addressing noise pollution and implementing effective noise control measures is essential for protecting human health and well-being in increasingly urban and noise-prone environments [42]. Some examples of impact of noise pollution on human health have been given in (Table 7).

Impact of Noise Pollution on Buildings

Noise pollution, characterized by excessive or disruptive noise in the environment, can have a range of adverse effects on structures and buildings [43]. These effects can be both direct and indirect such as structural Damage, facade and cladding damage, aesthetic Impact, structural fatigue, material degradation, foundation settlement, window and glazing damage, functionality impact, cost of noise mitigation and regulatory compliance etc. Noise pollution can have multifaceted effects on structures and buildings can impact the integrity, safety, and functionality of architectural elements [44]. To address these issues, architects, engineers, and building owners often incorporate noise mitigation strategies, such as sound insulation, vibration damping, and facade design, into the construction and renovation of buildings in noise-prone areas. Proper planning and adherence to noise regulations are essential to mitigate the adverse effects of noise pollution on structures and ensure the safety, functionality, and longevity of buildings [45].

Measures to check Noise Pollution

To effectively check and mitigate noise pollution, a combination of regulatory measures, technological solutions, and public awareness campaigns is essential [46]. Governments should establish and enforce noise standards and permissible noise levels for different types of areas and times of day. These standards should provide a legal framework for noise control. Zoning and Land Use Planning to implement zoning regulations to separate noisy industrial and commercial areas from residential and quiet zones should take place. Restrictions on noisy activities during nighttime hours when people are more sensitive to noise disturbances should be implemented. We should encourage and mandate the use of quieter technologies and equipment. This includes promoting quieter engines,





exhaust systems, and construction machinery. Noise barriers and noise insulation can also check the problem to some extent. We can also promote the use of electric or hybrid vehicles, which are generally quieter than traditional combustion engine vehicles. Green spaces, parks, and buffer zones within urban areas can be developed to act as noise absorbers and create quiet areas for residents. Further, using intelligent transportation systems, we can optimize traffic flow to reduce congestion and traffic noise. Public awareness campaigns can be conducted to educate communities about the adverse effects of noise pollution and promote responsible noise behavior. They can be encouraged to be active participants in identifying and addressing noise disturbances. Noise control at the source involves regular maintenance and servicing of noisy equipment, construction site measures, noise barriers, and noise-reduction technologies. Fines and penalties should be imposed for violations. Authorities should use sound level meters and monitoring networks to measure noise levels, and invest in research and development for noise reduction. Collaboration among agencies and businesses is crucial for integrated management. Combating noise pollution requires government regulations, technological advancements, urban planning, and community involvement[47]. Effective noise control measures require a comprehensive and integrated approach to protect the health and well-being of individuals and the environment [48].

Technologies for Noise Control

Controlling noise involves various technologies that aim to reduce, mitigate, or eliminate unwanted sound. The choice of technology depends on the specific noise source, the surrounding environment, and the desired level of noise reduction [49]. Various noise control technologies are used to reduce noise levels in various settings. Active Noise Control (ANC) uses electronic systems to cancel out incoming noise, while noise barriers and sound walls block or redirect sound waves. Active Noise Barriers use sensors and speakers to detect and emit anti-phase sound waves, while Acoustic Insulation and Soundproofing Materials absorb or reflect sound, while Low-Noise Technologies prioritize minimizing noise emissions in vehicles, machinery, and industrial equipment. Green roofs and living walls provide insulation and sound absorption in urban areas. Noise-reducing pavements and distributed acoustic sensing (DAS) are used in highways, urban roads, and residential areas. Quieter technologies are being adopted in industries like transportation, manufacturing, and construction. Noise-reducing windows and doors are used in residential buildings and offices. Anti-vibration mounts and pads isolate machinery from the surrounding structure, reducing vibrations and noise transmission. Noise-reducing fences and enclosures absorb or reflect sound, used in industrial facilities and outdoor equipment. Quiet pavement technologies modify road surfaces to reduce tire-road noise. These technologies are often used in combination to create comprehensive noise control strategies [50,51]. The effectiveness of a particular approach depends on factors such as the type of noise, the source, the surrounding environment, and the desired level of noise reduction [52].

Future of Noise Pollution

The future of noise pollution is likely to be influenced by a combination of technological advancements, urbanization trends, regulatory measures, and evolving societal attitudes. Technological advancements in noise reduction technologies and smart city solutions are expected to improve traffic management, public transportation, and real-time noise monitoring in urban infrastructure. Urban planning and design are shifting towards quiet zones, green spaces, and pedestrian-friendly areas. Transportation trends include electric and hybrid vehicles, and stricter noise standards may be enforced by governments. Increased public awareness and interdisciplinary research can inform public health policies and guidelines. Addressing noise pollution will require a holistic approach that considers the diverse sources and impacts of noise, incorporating both technological and behavioral interventions.

CONCLUSIONS

This study concludes that noise pollution, an intricate challenge encompassing diverse unwanted sounds, necessitates a nuanced understanding for effective management. To address this issue comprehensively, it is imperative to categorize noise based on its sources, characteristics, and effects. This categorization informs tailored approaches for mitigation. In the Indian context, the Central Pollution Control Board (CPCB) assumes a crucial role





Rajesh Trehan and Aarti Trehan

by establishing permissible sound levels through the Noise Pollution Rules (2000). Noise regulations aim to protect public health and the environment by integrating advanced technologies for real-time monitoring. Awareness and responsible behaviour are crucial for mitigation. A holistic approach, combining urban planning, technological innovations, regulatory measures, and community engagement, is essential for effective control strategies. Population growth contributes to noise pollution, but a multidimensional approach is necessary for improved quality of life.

REFERENCES

1. Donna Bailey. Noise & Fumes. Great Britain: Franklin Watts Ltd;1991.
2. Kinsler LE, Frey AR, Coppens AB, et al. Fundamentals of Acoustics. 4th ed.New York: Wiley; 2000.
3. Paul KC, Haan M, Mayeda ER, Ritz BR. Ambient Air Pollution, Noise, and Late-Life Cognitive Decline and Dementia Risk. Annu Rev Public Health 2019;40:203-220.
4. Brown AL. Soundscapes and environmental noise management. Noise Control Engineering Journal 2010;58(5):493-500.
5. Halperin D. Environmental noise and sleep disturbances: A threat to health? Sleep Science 2014;7(4):209-212.
6. GoinesL, Hagler L. Noise Pollution: A Modern Plague. Southern Medical Journal 2007;100(3): 287-294.
7. Coates PA. The Strange Stillness of the Past: Toward an Environmental History of Sound and Noise. Environmental History 2005; 10(4): 636-665.
8. Chambers JP.Noise Pollution. In: Wang LK, Pereira NC, HungYT(eds) Advanced Air and Noise Pollution Control. Handbook of Environmental Engineering, vol 2. Totowa, NJ:Humana Press, Inc;2005.
9. Burns W.Noise and Man. Great Britain: William and Sons;1973.
10. Bhatia SC.Textbook of Noise Pollution and Its Control. New Delhi: Atlantic Publishers and Distributors (P) Ltd; 2023.
11. Moser M. Engineering Acoustics: An Introduction to Noise Control. Berlin, Germany, and New York: Springer; 2004.
12. Theodore MK. & Theodore L. Noise Pollution. In Introduction to Environmental Management. 2nd ed.Florida: CRC Press. 2021;pp. 439–445.
13. Shrivastava KK. Environmental Education: Principles, concepts and management. New Delhi: Kanishka Publishers & Distributors; 2004.
14. Gokhale S. Environmental Noise Pollution. In Handbook of Environmental Engineering. New Jersey: John Wiley & Sons, Inc. 2018; pp. 565–582.
15. Singh S. Environmental Geography. Allahabad: Prayag Pustak Bhawan. 1991;pp. 457-463.
16. Khopkar S.M. Environmental Pollution, Monitoring and Control. New Delhi: New Age International (P) Ltd; 2004.
17. Singh P. Noise Pollution. Everyman's Science 1984; 25(1&2): 231-235.
18. Garg N, Sinha AK, Dahiya M, Gandhi V, Bhardwaj RM, Akolkar AB.Evaluation and analysis of environmental noise pollution in seven major cities of India. Archives of Acoustics 2017; 42(2): 175– 188,
19. Murphy E and King EA. Environmental Noise Pollution: Noise Mapping, Public Health and Policy.San Diego:Elsevier; 2014.
20. Verma S, Kanwar VS & John S. (2022). Noise Pollution. In Environmental Engineering. Boca Raton: CRC Press. 2022;pp. 523–532.
21. Agarwal SK. Noise Pollution. New Delhi: APH Publishing Corporation;2005.
22. Singh N and Davar SC. Noise Pollution-Sources, Effects and Control. J. Hum. Ecol.2004; 16(3): 181-187.
23. Burns WD and Robinson DW. Hearing Noise in Industry. London: HSO. 1970; pp.241.
24. Gupta RD. Environmental Pollution Hazards and Control. New Delhi: Concept Publishing Company; 2006.
25. Sharma H, Rawal Y & Batra N. Noise Pollution. In Basic Concepts in Environmental Biotechnology. Florida: CRC Press. 2021; pp. 45–53.





26. Neitzel RL, Hammer MS & Swinburn TK. Assessing hazardous noise pollution in the United States. The Journal of the Acoustical Society of America 2015; 137(4): 2270-2279.
27. Schmidt CW. Noise that Annoys, Regulating Unwanted Sound. Environmental Health Perspectives 2005; 113: 43-44.
28. World Health Organization. Guidelines for Community Noise. Geneva: World Health Organization Report; 1999.
29. Divan S & Rosencranz A. Environmental law and Policy in India, New Delhi: Oxford University Press; 2001.
30. Central Pollution Control Board. Protocol for ambient level noise monitoring, Delhi: Central Pollution Control Board Report; 2015.
31. CPCB. The Noise Pollution (Regulation and Control) Rules published in the Gazette of India, vide S.O. 123(E), dated 14.2.2000 and subsequently amended vide S.O. 1046(E), dated 19.09.2006 and S.O. 50 (E) dated 11.01.2010 under the Environment (Protection) Act 1986; 2000.
32. Chandrappa R & Das DB. Noise Pollution. In Environmental Health-Theory and Practice. New York:Springer International Publishing. 2021;pp. 141–148.
33. Bond M. Plagued by Noise. New Scientist 1996; 16: 14-15.
34. Schwartz H. Making Noise: From Babel to the Big Bang and Beyond, Brooklyn, NY: Zone Books; 2011.
35. Purohit SS and Agrawal AK. 2006. Environmental Pollution (Causes, Effects and Control). Jodhpur: Agrobios India. 2006; pp. 258-270.
36. Bronzaft AL. Noise: Combating a ubiquitous and hazardous pollutant. Noise Health 2000; 2: 1-8.
37. Kunc HP and Schmidt R. The effects of anthropogenic noise on animals: a meta-analysis. Biology Letters 2019; 15(11): 1-14.
38. Ningwal US and Shinde D. Study of Noise Pollution Levels During a Hindu Festival in Dhar Town, M.P., India, Res. J. Chem. Sci. 2013; 3(12): 71-75.
39. Bragdon CR. Noise pollution: The unquiet crisis. Philadelphia: University of Pennsylvania Press; 1971.
40. Babisch W. Noise and Health. Environ Health Perspective 2005; 113: A14-15.
41. Gupta BN. Effects of Noise on Health. Ann. Academy of Medicine 1999; 4: 59-68.
42. Havas V. Noise! The Invisible Pollution. Current Health 2006; 232 (5): 10–11.
43. Singal SP. Noise Pollution and Control Strategy. New Delhi: Narosa Publishing House Pvt. Ltd; 2005.
44. Wang, LK, Norman CP and Yung-Tse H. eds. Advanced Air and Noise Pollution Control. Totowa, NJ: Humana Press; 2005.
45. Hansen, CH. Noise Control: From Concept to Application. London, UK, and New York: Taylor & Francis; 2005.
46. Chatwal GR. ed. Environmental Noise Pollution and Its Control. Columbia: South Asia Books; 1989.
47. Stansfeld S, Haines M and Brown B. Noise and health in the urban environment. Reviews of Environmental Health 2000; 15:43–82.
48. Van Kamp I and Davies H. Noise and health in vulnerable groups: A review. Noise & Health 2013; 15(64): 153-159.
49. Bijsterveld K. Mechanical Sound: Technology, Culture, and Public Problems of Noise in the Twentieth Century. Boston: MIT Press; 2008.
50. Sides CC. Noise Pollution: Herald of Health. Pune: Oriental Watchman Publishing House; 1985.
51. Hansen CH. Understanding Active Noise Cancellation. London, UK and New York: Spon Press, 2001.
52. Firestone J and Jarvis C. Response and Responsibility: Regulating Noise Pollution in the Marine Environment. Journal of International Wildlife Law & Policy 2007; 10(2): 109-152.



**Table 1. Intensity of noise sources**

Activity	Sound Level Range (dB)
Normal Breathing	10-20 dB
Whispering	20-30 dB
Quiet Library	30-40 dB
Normal Conversation	40-60 dB
Office Environment	50-70 dB
City Traffic (inside a car)	70-85 dB
Motor cycle	105 dB
Vacuum Cleaner	70-85 dB
Lawn Mower	85-90 dB
Rock Concert (near speakers)	110-120 dB
Jet Engine (at take-off)	130-140 dB
Threshold of Pain	130-140 dB
Firecrackers (close range)	120-160+ dB

Table 2 Units and scales to measure noise level

Unit/Scale	Symbol	Description
Decibel (dB)	dB	The most widely used unit for measuring sound levels. It quantifies the ratio between the measured sound intensity and a reference level.
Decibel with A-weighting (dBA)	dBA	A-weighted decibels, adjusted for the human ear's sensitivity to different frequencies. Often used in noise regulations.
Decibel with C-weighting (dBc)	dBc	C-weighted decibels, which emphasize the low-frequency range. Used in some industrial and occupational noise assessments.
Decibel with Z-weighting (dBz)	dBz	Unweighted decibels, representing sound levels without frequency weighting. Used in some specialized applications.
Sone (son)	Son	A unit of loudness perception, measuring how loud a sound is subjectively perceived by the average listener.
Phon (phon)	Phon	A unit measuring the subjective loudness of a pure tone at 1,000 Hz. It corresponds to the perceived loudness of a sound.
Hertz (Hz)	Hz	The unit of frequency, which measures the number of sound waves (cycles) per second. Often used for characterizing tones.
Pascal (Pa)	Pa	The unit of sound pressure, which quantifies the magnitude of sound waves. Used in some engineering and acoustic applications.

Table 3 WHO's recommended noise levels in different environments

Environment	L _{den} (day-evening-night level)	L _{night} (night level)
Daytime in quiet areas	55 dB	45 dB
Daytime in urban areas	65 dB	55 dB
Evening in quiet areas	50 dB	45 dB
Evening in urban areas	60 dB	55 dB
Nighttime in quiet areas	45 dB	40 dB
Nighttime in urban areas	55 dB	50 dB



**Table 4 Indian standards on noise pollution**

Zone	Daytime (6:00 AM to 10:00 PM)	Nighttime (10:00 PM to 6:00 AM)
Industrial Area	75 dB	70 dB
Commercial Area	65 dB	55 dB
Residential Area	55 dB	45 dB
Silent Zone (Ambient Noise Level)	50 dB	40 dB

Table 5 Sources of Noise Pollution

S. No.	Source of Noise Pollution	Examples
1.	Transportation	Road Traffic Noise, Railway Noise, Aircraft Noise, Maritime Noise
2.	Industries	Noise from Machinery, Equipment, Factories and Power Plants
3.	Construction	Noise from use of Heavy Equipment, Tools and Machinery
4.	Recreation & Entertainment	Noise from Concerts and Events, Amusement Parks, Recreational Vehicles
5.	Communities	Residential, Pets, Social Gatherings noise
6.	Commercial & Retail Stores	Restaurants, Bars, Shopping Centers noise
7.	Transport Infrastructure	Noise from construction of Highways, Bridges And Public Transportation
8.	Natural Sources	Weather Phenomena, Wildlife Sounds
9.	Neighborhoods & Urban Environments	Noises from densely Populated Areas and Mixed Land Uses

Table 6 Impact of Noise Pollution on Environment and its outcomes

S. No.	Impact Area of Environment	Outcomes
1.	Wildlife and Ecosystems	Communication Disruption, Habitat Abandonment, Altered Reproductive Success, Stress in wild life affecting population dynamics.
2.	Air Quality	Sources of noise pollution, such as Road traffic and Aviation have co- occurrence of air pollution
3.	Water Quality	Disruption in the behaviour of marine animals, Habitat Disturbance
4.	Plant Life	Increased levels of the stress hormone leading to disruption in plant growth and development
5.	Biodiversity and Ecological Balance	Disruption of Trophic Interactions within the ecosystems, Altered Biodiversity
6.	Cultural and Economic aspects	Detering of tourist due to diminishing cultural and spiritual significance of natural and tranquil places due to noise pollution, reduction in tourism revenue
7.	Ecosystem Services	Disruption in pollination by insects and natural pest control, provision of clean water





Table 7 Impact of Noise Pollution on Human Health and its outcomes

S. No.	Impact Area of Human Health	Outcomes
1.	Cells in the inner ear	Hearing Impairment and Damage leading to reduced hearing sensitivity, difficulty understanding speech, and tinnitus
2.	Cardiovascular system	Elevated Blood Pressure, Heart diseases, release of stress hormones like cortisol and adrenaline leading to Cardiovascular issues
3.	Insomnia and Sleep Fragmentation	fatigue and decreased cognitive functioning, Hormonal Disruption
4.	Psychological and Mental Health	Stress, Anxiety, Depression
5.	Cognitive Aspect	Impaired Concentration and Memory
6.	Social and behavioral Aspect	social annoyance, causing interpersonal conflicts, Behavioral Changes like avoiding outdoor activities due to noise pollution
7.	Vulnerable population like elderly, Children and Infants	More pronounced health effects like disruption of sleep and its pattern, cognitive development, language acquisition
8.	Quality of Life	Reduced satisfaction with living conditions

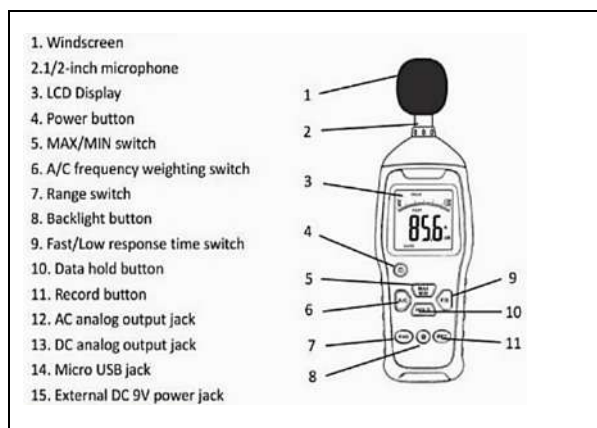


Figure 1 Sound Level Meter

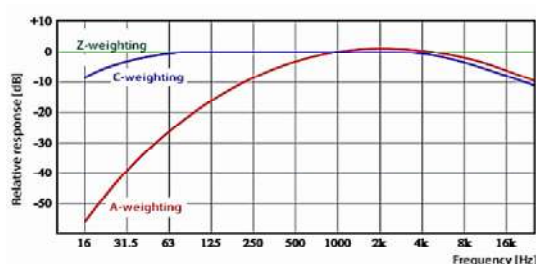


Figure 2 Different noise frequency weightings

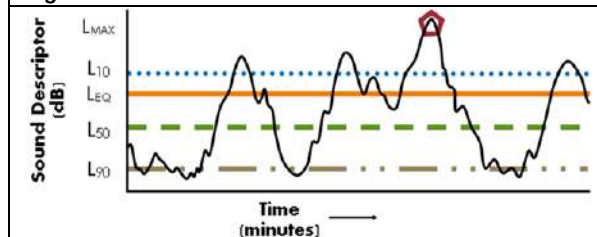


Figure 3 Representation of various sound levels

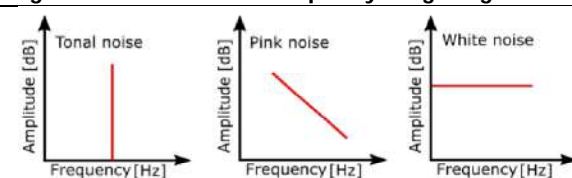


Figure 4 Types of noises





The Digital Carbon Foot Print: A Threat to Environment

Jyoti Sharma*, Simran and Nisha

Department of Chemistry, MMEC, Maharishi Markandeshwar (Deemed to be) University, Mullana (Ambala), Haryana, India.

Received: 22 Jan 2024

Revised: 09 Feb 2024

Accepted: 30 May 2024

*Address for Correspondence

Jyoti Sharma

Department of Chemistry,
MMEC, Maharishi Markandeshwar (Deemed to be) University,
Mullana (Ambala), Haryana, India
Email: jsharma117@gmail.com



This is an Open Access Journal / article distributed under the terms of the **Creative Commons Attribution License** (CC BY-NC-ND 3.0) which permits unrestricted use, distribution, and reproduction in any medium, provided the original work is properly cited. All rights reserved.

ABSTRACT

The digital realm has become an integral part of modern society, shaping our lifestyles, industries, and interactions. However, the proliferation of digital technologies has brought about an often overlooked yet substantial environmental impact through the generation of digital carbon footprints. This review article provides a comprehensive overview of digital carbon footprinting, focusing on methodologies, applications, and the challenges it presents. The article begins by defining digital carbon footprints, emphasizing the significance of quantifying the environmental impact of digital technologies. It explores various metrics used to measure the carbon footprint of digital activities, including approaches to assess energy consumption, data centers, internet infrastructure, and end-user devices. This review serves as a foundational resource for understanding digital carbon footprinting and encourages further research and initiatives to address this crucial aspect of environmental sustainability in the digital age.

Keywords: Carbon footprint, environmental impact, digital technologies, internet

INTRODUCTION

The world is changing digitally, and with it comes the hype surrounding catchphrases that are becoming commonplace, like Industry 4.0, smart manufacturing, smart banking, and Industrial Internet of Things [IIoT]- a term that hails the potential of a new technological revolution (1). However, due to excessive data processing and digitization, there is growing concern over the world's ever-increasing carbon footprint. Emissions of CO₂ have been a primary sustainability concern because of their effects on the environment. The introduction of smartphones with fast fixed broadband and mobile internet has drastically changed how people work, communicate, and consume information. Notable developments in cellular networking, miniature sensors, novel internet connection protocols, and an abundance of mobile software applications have made this possible. Mobile internet usage has increased dramatically since the original iPhone was released in 2007 [2]. A "sensor tornado" from 10 million sensors in 2007 to



**Jyoti Sharma et al.,**

15 billion micro-electro-mechanical system (MEMS) sensors in 2015 [2] was caused by this, which affected the deployment of sensors. The Internet of Things (IoT) has been made possible by these sensors, which function as translators of attributes from physical objects into representative digital data in a virtual environment. Electrical energy will be used as manufacturing undergoes a digital transformation, linking all of its IT and OT with data-generating sensors and sending this data to the "Edge" or the "Cloud." The International Energy Agency (IEA) states that industries already consume a significant portion of the world's electricity, accounting for 42.5% of global consumption in 2014 [3]. As a result, energy networks must be able to handle any increase in industrial consumers' demand for electricity. This raises the question of how much energy will be needed to power the potentially enormous volumes of data that connected industrial elements will be producing. This would include the carbon emissions from all of the industrial devices that will be able to sense, process, and communicate. Surprisingly, not many studies have been done on the total CO₂ emissions of the ICT industry worldwide. Only few studies that were published with results on the topic are noticeably inconsistent [4]. Since carbon emissions play a major role in global warming, this issue is becoming more and more of a concern in the community.

According to research, global warming has additional effects that are felt globally and cause inconvenience to the majority of people. An important problem linked to global warming has been the increasing height of sea levels. According to reports, in the next thirty years, the majority of islands and beaches will be totally submerged. This makes it necessary to control the release of carbon [5]. However, growing CO₂ emissions brought on by greater digitization and technological advancement have made current remedies more difficult to implement. One of the biggest industries in terms of carbon dioxide emissions has always been the construction sector. According to research by [6], the production of construction materials alone could contribute approximately 350 Gt CO₂ to the Western infrastructure stock using current technologies. This amounts to 35–60% of the remaining carbon budget, considering the 2°C limit until 2050. China, being the biggest emitter, has focused on achieving net zero emissions by 2060 and a peak in emissions by 2030. The carbon footprint (CF) is the total amount of CO₂ emissions that accumulates over the course of a product's or service's life cycle, or the carbon emissions associated with activities (Figure 1). China, which emits the most CO₂, is currently in the latter stages of industrialization, with significant regional variations in growth. The 1 recent discrepancy in carbon footprint among areas is not well explored, which is crucial to understanding the driving forces and future trajectories of carbon footprint. The economic development, industry structure, and energy structure vary with areas. To determine and lower the emissions of carbon footprint (CF) in the AEC/FM sector, evaluating techniques like the life cycle assessment (LCA) for product manufacturing [6] were progressively released. Researchers have emphasized the need and expectation for the use of effective and sophisticated commercialized digital tools, platforms, or systems to support automation and decision-making for carbon management issues. [7,8,9] In addition, the wave of industry 4.0 and the proliferation of cyber concepts like digital twins, artificial intelligence (AI), Internet of Things (IoT), and building information modeling (BIM) have arrived. Other relatively advanced disciplines, like chemical engineering, have testified to the possibility of using these technologies to address carbon emission issues [10].

REVIEW OF LITERATURE

The term "digitization" refers to a number of procedures that help to simplify life. Internet connectivity, cloud computing, server backup, real-time analytics and visualization, and video entertainment are a few of the processes connected to digitization. Every one of these elements helps to improve people's quality of life and turns into a daily routine for various people [11]. People can now effectively obtain a variety of services that they require in their daily lives thanks to technology. The largest proportion of carbon emissions is attributed to internet use. According to Pan [12], over half of the world's population uses the internet. Currently, four billion people use the internet [13], and a number of changes occurred by the year 2019. According to the aforementioned study, over a million people use the internet every day. The various online activities have led to a rise in carbon emissions (Figure 2). Every day, access to any digital service gets more and more expensive. People must use electricity in order to access any digital service [14]. Both the person utilizing the computer and the servers offering this service are the sources of



**Jyoti Sharma et al.,**

the electricity used. Because the smartphones need to be charged after the service is provided, they also use a lot of electricity [15]. In order to provide the various services that are available, communication networks and ISPs also consume a significant amount of electricity. The internet consumes a significant amount of electricity because servers must run continuously around the clock to guarantee that users can access these materials [11]. For example, YouTube servers must always be up and running in order for users to always be able to access these videos from anywhere in the world [11]. In order to guarantee that people receive the services they require, these organizations must implement and maintain servers and computers [16]. The energy consumption of digital technologies rises by 9% annually and contributes 4% of greenhouse gases to the atmosphere [17]. An hour of video conferencing releases about 157 grams of carbon, according to a recycling and conversation journal report [12]. As a result, massive volumes of carbon are released due to the increased use of video conferencing throughout the world [14]. According to the report, people who attended conferences for approximately 15 hours a week would be able to reduce their carbon footprint by more than 9 kg [12]. This pace is equivalent to one person charging a smartphone all three years at night [18]. As a result, there is increasing concern about the carbon footprint left by digital concepts. This is related to the rise in electricity consumption over the previous few years. As a result, rising carbon emissions in the atmosphere are a result of the ever-increasing global changes. Analyzing digital services companies allows one to see how digitization affects carbon footprint [19]. Even basic digital services like website hosting and video conferencing have a greater environmental impact. The size of these organizations specifically developed this influence [20]. Microsoft is a prime example of such an organization. Because of increased carbon emissions, the company's services and employees have a significant impact on the environment. The following list of digitization concepts has led to a global increase in the impact of carbon footprint. Every one of the factors listed demonstrates a technological advancement linked to increased technology use and carbon emissions. The majority of the tasks listed as requiring electricity can be found online. Among many other things, the activities include finance systems, streaming and entertainment services, e-commerce, and e-payment methods [19]. The possible effects of each of these factors on the available carbon emissions resulting from digital services have been discussed below.

Search engines

We can make an impact because there are more than 4.66 billion active internet users worldwide, or more than 60% of the world's population. In the modern world, search engines have become essential, as seen by Google's rapid expansion, which highlights our dependence on them. Serving these customers has a greater impact on the earth's ecology, and the company's ad system profits have been increasing [19]. This has been facilitated by people using their electronic devices to access these searches. Approximately 26 kg of CO₂ emissions are produced annually, assuming that an individual performs 50 search queries per day [12]. Google's environmental report from 2016 stated that the company had a carbon footprint of 2.9 million tons of CO₂. The company's energy consumption was reported in the 2017 report to be 6.2 terawatt-hours (TWh) [12].

Internet usage through mobile Apps

Mobile phones account for a significant portion of total daily electricity consumption due to mobile phone's wireless network connection. Since buildings, vegetation and weather weaken the electromagnetic network connections, more power is always included to ensure that the networks have reached their destination. Pan [12] suggests that copper lines and fibre optic cables also contribute to the power consumption from the need to amplify the signal through electricity. The power coverage is therefore affected by the distance associated with every individual. This aspect also affects mobile users' power use and carbon emissions[21]. However, they make a substantial contribution to digital technology's carbon footprint.

Music and video streaming

Eighty percent of data on the internet is transmitted as images, according to research by The Shift Project [12]. This indicates that a sizable amount of the internet's carbon footprint was caused by online videos across various platforms. According to the aforementioned report, downloaded videos accounted for 60% of all global data transfers. Large volumes of data are needed to transfer the images, and this takes a lot of electricity. The amount of data that is available on the internet has increased due to the development of devices with higher resolutions.

75587



**Jyoti Sharma et al.,**

According to The Shift Project, online video streaming uses more than 300 million tons of CO₂ annually on average [15]. This was demonstrated in the 2018 measurement. The CO₂ emission is an indicator of the total CO₂ emission. This demonstration highlights the significant environmental impact of streaming music and video. It was also mentioned that watching a Netflix video requires 0.12-0.24 kWh of electricity per hour to run. Since different people use different devices and have varying requirements for the video resolutions they stream, these numbers are estimates. It has also been reported that the precise amount of power consumed is influenced by the network connection. Determining the extent to which Netflix streaming has contributed to global CO₂ emissions becomes difficult as a result [22]. Greenhouse gas emissions from music streaming also have a major impact on the environment. According to Pan [12], between 200 and 350 million kilograms of greenhouse gases are released into the atmosphere as a result of music streaming.

Blockchain and cryptocurrency technologies

The idea of cryptocurrencies has been one of the financial industry's innovations. The technology behind cryptocurrencies has been called the finance industry's future. One of the main reasons for the increase in the digital carbon footprint is cryptocurrency. The way cryptocurrencies function is by enabling multiple machines to store transaction records, which increases their security and dependability [23]. A lot of devices store this data, has made it difficult to maintain the current carbon footprint. The need for more computers is increasing power consumption throughout the cosmos [24]. The number of people using their power keeps rising, which raises the risk of having a large carbon footprint overall [25].

Cloud Computing

There is a strong correlation between the growing usage of cloud computing apps and the carbon footprint. One of the digitization processes linked to a rise in carbon emissions is cloud computing. In recent years, cloud computing has gained appreciation as a technology. The technology used to store data on computers so that it can be accessed remotely from any location is known as cloud computing [21]. Usually, it refers to technology that allows users to access particular software and data from anywhere at any time through backup. One useful application of cloud computing technology is the ability to access email from any location. There is a backup copy of the emails over. According to a study by Gani [26], the power consumption, which is the ultimate result of increased technological development, has been the main problem with technology development [26]. The use of technology and data centers has significantly increased power consumption. The amount of CO₂ in the atmosphere is significantly influenced by this power consumption [27]. As a result, this has been the primary cause of digital technology's increased carbon footprint. Because of the current rise in carbon emissions, the emergence of these technologies has all been said to have specific environmental effects [28]. The majority of the digital techniques discussed above highlight rising energy consumption as the primary driver of CO₂ emissions. While energy consumption is the primary source of carbon emissions for technology companies, there have also been reports of various chemicals being released into the atmosphere by the cooling systems in certain data centers [29].

Minimization of digital carbon footprint

Reducing carbon footprints means changing how we approach and participate in activities that produce greenhouse gases.

Clean out your Inbox

It is estimated that every spam email that lingers in mail inbox is equivalent to 0.3 grams of carbon dioxide. E-mails with text attachments can add an additional 50 grams of CO₂e, and text-based emails can add four grams. Even though email only uses 1.7% of the energy needed to deliver a paper letter, each person uses approximately 136 kilograms of CO₂e annually. That is the same as 322 kilometres driven in a car using gasoline. Elimination of superfluous emails and unsubscribe from all senders except the most significant ones is essential to reduce digital clutter. According to a 2019 study by the British energy company OVO, over 64 million unnecessary emails are sent daily by Britons [30]. A daily reduction of one email sent by adults in the UK could save over 16,433 tonnes of carbon annually, which is the same as removing 33,343 diesel cars from the road.



**Jyoti Sharma et al.,****Reduce Brightness**

According to a Harvard study, reducing our monitor brightness from 100 per cent to 70 per cent can lower total energy usage by up to 20 per cent. As a latent benefit, lowering brightness reduces eye strain, one of the leading maladies affecting office workers.

Buy crypto with care

In addition to their tremendous volatility, cryptocurrencies such as Ethereum and Bitcoin consume more energy than a lot of nations. The emissions from a single bitcoin are equal to 330,000 credit card transactions. To offset the 57 million tons of CO₂ emissions that bitcoin emits annually, 300 million trees would need to be planted. Although some coins, like Ethereum, say they will switch to a more environment friendly "proof-of-stake" model, these emissions reductions have not yet occurred, and since we are running out of time to reduce GHG emissions, it might be wise to avoid cryptocurrency while it consumes our remaining carbon budget.

Avoid E-Waste

Everything that uses energy to produce, like light bulbs, laptops, and microwaves, also releases hazardous chemicals into the environment when disposed of incorrectly. According to the UN E-waste Monitor, the average person produces 7.3 kg of e-waste annually, with wealthy nations like China and the United States producing the most. Keeping electronics out of our possession is the best course of action[30]. When a device reaches the end of its useful life, we have to focus on recycling.

Power Down and Go Outside

The most effective method to lessen digital carbon footprint is to disconnect gadgets and engage in activities that are becoming outdated, such as gardening, walking, or reading a book. Reducing screen time not only reduces phantom loads but also offers several psychological, social, and health advantages. Individual behaviour is not the main cause of climate change, group efforts can reduce energy use, strengthen community bonds, and lay the groundwork for a sustainable future.

Finding the most efficient ways to cool data centres

Data centers can be located in colder nations and then simply have outside air blown into them, according to a popular and reasonably straightforward solution. This explains why there are so many data centers close to the Arctic[4]. Immersion cooling and heated, piped water are two more methods for bringing high-performance, hot computers under control. In an effort to lower their energy costs, some businesses are even developing artificial intelligence to adjust their cooling systems in response to changing weather conditions and other variables.

Re-using the waste heat

All year long, data centers generate heat. This heat should ideally always be extracted and used somewhere else. But a more thorough approach is required to fully utilize waste heat's potential. Despite being a country known for its cool climate, Sweden is also a leader in the reuse of waste heat. This makes it an excellent choice for data center locations [4]. The nation primarily depends on a district heating system, which uses pipes to transport heat from a central location to residential and commercial buildings.

CONCLUSION

The evolving landscape of digital carbon foot printing represents a crucial advancement in understanding and mitigating the environmental impact of our digital activities. Through this review, it becomes evident that digital carbon foot-printing methodologies are essential tools in quantifying, analysing, and ultimately reducing the environmental consequences of our online behaviours. By scrutinizing various aspects such as data centres, internet traffic, user devices, and digital services, this review sheds light on the multifaceted nature of digital carbon footprints. It underscores the importance of adopting sustainable practices in data management, optimizing energy



**Jyoti Sharma et al.,**

consumption in digital infrastructure, and promoting eco-friendly design in technological innovations. Moreover, the review accentuates the necessity of collaborative efforts among individuals, industries, and policymakers to establish standardized metrics and regulations for measuring and minimizing digital carbon footprints. This unified approach is fundamental in fostering a sustainable digital ecosystem. As we continue to navigate an increasingly digital world, the insights garnered from this review underscore the significance of conscious, collective action to curb and offset the environmental impact of our digital footprint. By integrating responsible practices, technological innovation, and policy initiatives, we can strive towards a more sustainable future where digital advancements coexist harmoniously with environmental preservation.

REFERENCES

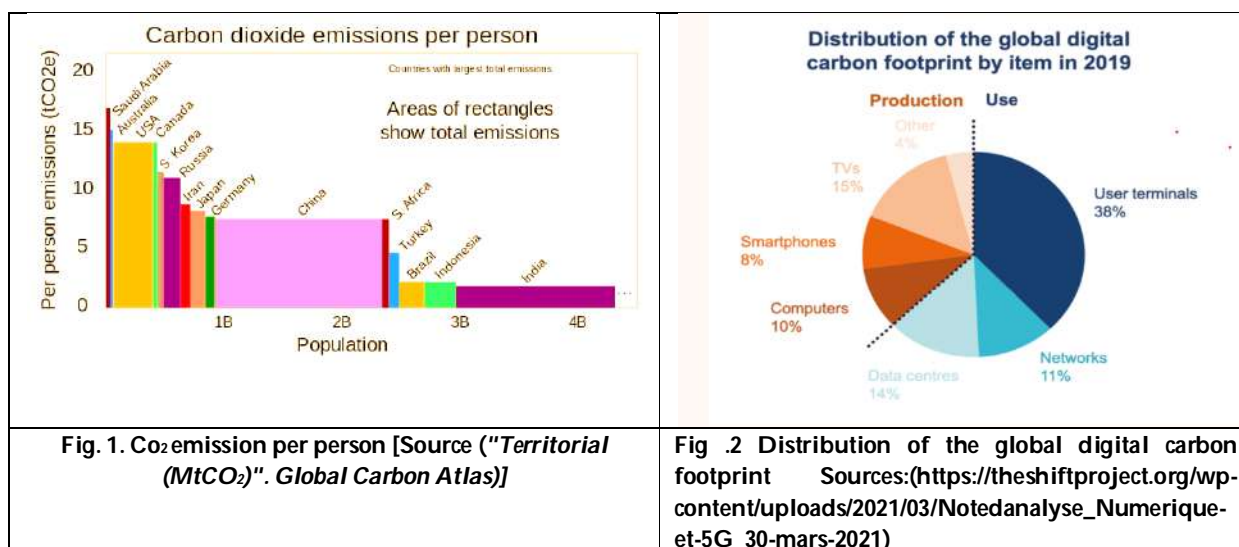
1. Patsavellas, J., &Salonitis, K. The Carbon Footprint of Manufacturing Digitalization: critical literature review and future research agenda. *Procedia Cirp*, 2019, 81, 1354-1359.
2. UNIDO (2017). Accelerating clean energy through Industry 4.0: <https://doi.org/10.1016/j.jclepro.2017.12.239>.
3. Belkhir, L., Elmeligi, A., Assessing ICT global emissions footprint:Trends to 2040 & recommendations', *Journal of Cleaner Production*, Volume 177, 2018, Pages 448 -463, ISSN 0959-6526.
4. Stolz, S., & Jungblut, S. (2019, December 30). Our Digital Carbon Footprint: What's the Environmental Impact of the Online World? RESET.ORG. <https://en.reset.org/our-digital-carbon-footprint-environmental-impact-living-life-online-12272019/>.
5. Muller, D.B.; Liu, G.; Lovik, A.N.; Modaresi, R.;Pauliuk, S.; Steinhoff, F.S.;Brattebo, H., Carbon Emissions of Infrastructure Development. *Environ. Sci. Technol.*, 2013, 47, 11739–11746.
6. Assessment–Principles and Framework. International Organization for Standardization: Geneva, Switzerland, 2006. Available online: <https://www.iso.org/standard/37456.html>
7. Jackson, D.J.; Brander, M. The risk of burden shifting from embodied carbon calculation tools for the infrastructure sector. *Journal of Cleaner Production*, 2019, 223, 739–746.
8. Feng, H.; Sadiq, R.; Hewage, K. Exploring the current challenges and emerging approaches in whole building life cycle assessment. *Can. J. Civ. Eng.*, 2022, 49, 149–158.
9. Akponeware, A.; Dawood, N.; Rodriguez-Trejo, S.; Dawood, H. An integrated empirical analysis of UK rail industry's carbon assessment: An industry perspective. *Case Stud. Transp. Policy*, 2021, 10, 315–330.
10. Hao, Z.; Barecka, M.H.; Lapkin, A.A. Accelerating net zero from the perspective of optimizing a carbon capture and utilization system. *Energy Environ. Sci.*, 2022, 15, 2139–2153.
11. Vourdoubas, J., Reduction of CO₂ Emissions Due to Energy Use in Crete-Greece. *Energy and Environment Research*, 2016, 6(1), 23. <https://doi.org/10.5539/eer.v6n1p23>
12. Pan M., Zhao X., Iv K., Rosak-Szyrocka J.,Mentel G.,Truskolaski T.,Internet development and carbon emission-reduction in the era of digitalization: Where will resource-based cities go?,*Resources Policy*, 2023, Vol 81, 103345. <https://doi.org/10.1016/j.resourpol.2023.103345>
13. Pontecorvo, E. Meet the startup producing oil to fight climate change. Report published on 18 May 2021 in Grist. <https://grist.org/climate-energy/lucky-charm/>.
14. Chen, L., How CO₂ emissions respond to changes in government size and level of digitalization? Evidence from the BRICS countries. *Environmental Science and Pollution Research*, 2021, 29(1), 457-467.
15. Rafael, D., & Olvera, C. (2022). The Polluting Cloud. A Socio-environmental analysis of the Digital Carbon Footprint. *PAAKAT: Revista De Tecnología Y Sociedad*,12(22). <https://doi.org/10.32870/pk.a12n22.730>
16. Hermansson, F., H, S., & J, M. Carbon fiber material has reduced carbon footprint. *Reinforced Plastics*, 2021, 65(4), 171. <https://doi.org/10.1016/j.repl.2021.06.057>
17. World Favor. 2022. The growing carbon footprint of digitalization and how to control it. <https://blog.worldfavor.com/the-growing-carbon-footprint-of-digitalization-and-how-to-control-it>
18. Gerlach, A. (2021). Reducing Emissions through Digitalization-Center for Climate and Energy Solutions. Center for Climate and Energy Solutions. <https://www.c2es.org/press-release/reducing-emissions-through-digitalization/>.





Jyoti Sharma et al.,

19. Brooker, M. (2019). Digital technologies and environmental impact, The Ecologist. <https://theecologist.org/2019/jul/16/digital-technologies-and-environmental-impact>.
20. Aksyutin, O. The carbon footprint of natural gas and its role in the carbon footprint of energy production. *International journal of geomate*, 2018, 15(48). <https://doi.org/10.21660/2018.48.59105>
21. Agarwal, A., Kabita Agarwal, & Gourav Misra. Is internet becoming a Major Contributor for Global warming – The Online Carbon Footprint!! December 2020, 02(04), 217-220. <https://doi.org/10.36548/jitdw.2020.4.005>
22. Li, S., Yu, Y., Jahanger, A., Usman, M., & Ning, Y., The Impact of Green Investment, Technological Innovation, and Globalization on CO₂ Emissions: Evidence From MINT Countries, *Front. Environ. Sci.*, 2022, Vol. 10. <https://doi.org/10.3389/fenvs.2022.868704>
23. Adhikari, S. Carbon Sequestration and Carbon Footprint in Some Aquaculture Practices in West Bengal, India. *International Journal of Zoology and Animal Biology*, 2021, 4(2). <https://doi.org/10.23880/izab-16000291>
24. Wolf, R., Abramoff, M., Channa, R., Tava, C., Clarida, W., & Lehmann, H. (2022). Potential reduction in healthcare carbon footprint by autonomous artificial intelligence. *npj Digital Medicine*, 2022, 5(1). <https://doi.org/10.1038/s41746-022-00605-w>
25. Fei, H., & Zhang, C. (2021). Global warming solutions: Carbon capture and storage. *E3S Web of Conferences*, 308, 01024. <https://doi.org/10.1051/e3sconf/202130801024>
26. Gani, A. A., The Relationship between Good Governance and Carbon Dioxide Emissions: Evidence from Developing Economies. *J.Econ.Dev.*, 2012, 37 (1), 77–93. doi:10.35866/caujed.2012.37.1.004
27. Karabatak, S., & Alanoglu, M. Faculty members' digital footprint experiences and digital footprint awareness. *Journal of Kazım Karabekir Education Faculty*, 2022, pp 31-41. <https://doi.org/10.33418/ataunikkefd.891924>
28. Polat Bulut, A., Bulut, A., & Demirel, S. (2022). Creation of carbon footprint originating from road transportation in Turkey and digital mapping of it, *International journal of global warming*, 2023 vol.30, no.2, pp.204-232. <https://doi.org/10.2139/ssrn.4060912>
29. Wada, Y., Ecological Footprint, Carbon Footprint and Radioactive Footprint in the Context of Building a Low Carbon Society. *Journal of Life Cycle Assessment Japan*, 2019, 6(3) pp 201-208.
30. Panchal B.Y., Vachhrajni K.D., Ganatra A. et al, Survey on Carbon Dioxide Emissions Through Email Conversion, *SAMRIDDHI A Journal of Physical Sciences Engineering and Technology*, 2023, 15(01):122-127, doi: 10.18090/samriddhi.v15i01.16.





Review of the Application of Novel Schiff Baseas Sensors

Satvinder Khatkar, Divya Bansa and Bhawna Pareek*

Department of Chemistry, Maharishi Markandeshwar (Deemed to be University), Mullana, Ambala, Haryana, India.

Received: 22 Jan 2024

Revised: 09 Feb 2024

Accepted: 30 May 2024

*Address for Correspondence

Bhawna Pareek

Department of Chemistry,
Maharishi Markandeshwar
(Deemed to be University),
Mullana, Ambala, Haryana, India
Email: dr.bhawnapareek@gmail.com



This is an Open Access Journal / article distributed under the terms of the **Creative Commons Attribution License** (CC BY-NC-ND 3.0) which permits unrestricted use, distribution, and reproduction in any medium, provided the original work is properly cited. All rights reserved.

ABSTRACT

Hugo Schiff created the Schiff base for the first time in 1864 by using primary amines in a condensation reaction with carbonyl compounds (ketone or aldehyde). Schiff bases' numerous structural and electrical properties make them useful in various applications. These applications include chemosensors for metal ion detection in addition to antimicrobial and antifungal activity. When schiff bases bind to different metal ions, stable complexes are produced. Because of their exceptional coordination ability, Schiff bases are used as fluorescent turn-on/turn-off chemosensors for detecting numerous metal cations in various materials, including Hg^{2+} , Cd^{2+} , Cr^{3+} , Pd^{2+} , and many more. This review looks at different Schiff bases used in other biological, agricultural, and environmental settings for chemosensing processes for metal ions (like divalent and trivalent cations). This review article has investigated several Schiff bases as fluorescent turn-on/turn-off chemosensors for identifying distinct metal ions in diverse matrices. Furthermore, numerous Schiff base chemosensors' synthetic procedures and sensing mechanisms have been investigated.

Keywords: Sensor, Fluorescence, Physiological, Chemosensors

INTRODUCTION

Metallic cations are used in many different fields; some of them regulate innumerable biological processes that are essential to life. However, an excess of these ions can cause significant environmental problems because they are not biodegradable and can build up in the food chain. Even at low concentrations, they pose a severe risk to human health and the environment. These ions can cause a wide range of health problems, including allergies, lung damage, anemia, kidney failure, neurotoxicity, oxidative toxicity, and apoptotic and axillary toxicity. [1, 2, 3, 4, 5, 6, 7, 8, 9, 10] Therefore, developing a reliable technique for locating these ions in diverse samples is essential. Various methods have been developed to detect metallic cations, such as liquid chromatography ^[11], electrochemistry ^[12] etc. Even though these techniques are highly efficient, they have some disadvantages, including the need for ambient





Satvinder Khatkar et al.,

conditions, high costs, complexity in usage, and extensive sample preparation. To detect metallic cations, fluorescent-based Schiff bases have been developed as a solution to the shortcomings of traditional methods. They function as organic synthesis intermediates, stabilizers for polymers, catalysts, pigments, and dyes [16]. Schiff bases with high selectivity and sensitivity to a range of species (cations and anions) were demonstrated using the spectrofluorometric method. Due to its ease of use, high sensitivity and selectivity, and ability to be detected with the naked eye, the fluorescent method has gained popularity. It may also find application in environmental and medical research. (De Silva, et al., 1997). Because Schiff bases are easy and inexpensive to produce and can coordinate with almost any metal ion and stabilize it in a range of oxidation states, they have proven to be particularly effective chemosensors for identifying various metallic cations. Furthermore, various biological applications for these Schiff bases have been shown, including analgesic, antifungal, anti-inflammatory, antiviral, antioxidant, and anticancer effects. [19 and 20]. Fluorescence sensors have been successfully used for the determination of different metal ions, such as Barium, Calcium (Kawakami et al., 2001), Cadmium (Y. Li et al., 2012), Cobalt (Abebe, Eribal, Ramakrishna, & Sinn, 2011), Chromium (Wan, Guo, Wang, & Xia, 2010), Copper (Xu, Wang, Zhang, Wu, & Liu, 2013), Ferric (Lin, Long, Yuan, Cao, & Feng, 2009), Mercury (Wu, Ma, Wei, Hou, & Zhu, 2013), Potassium (Zhou, et al., 2011), Lithium (Gunnlaugsson, Bichell, & Nolan, 2002), Magnesium (Singh, Kaur, Mulrooney, & Callan, 2008), Neodymium (Khorasani-Motlagh, Noroozifar, & Mirkazehi-Rigi, 2011), Nickel (Ghosh, Chakrabarty, & Mukherjee, 2008), Zinc (G.-Q. Zhang, Yang, Zhu, Chen, & Ma, 2006) and Aluminum (Jia, Cao, Zheng, & Jin, 2013; Kim, et al., 2012; Liao, Yang, Li, Wang, & Zhou, 2013). The uses of Schiff base as a sensor for metal ion detection are reviewed in this paper.

Schiff base as a fluorescence sensor

Due to effective energy transfer from the ligand to the central metal ion, specific Schiff base metal complexes exhibit the distinctive luminescence emissions of the significant metal ions. Mononuclear metal (II) complexes of Zn, Cd, Cu, Ni, and Pd have been synthesized by Aazam et al. (Aazam, Hussein, & Al-Amri, 2012) using Schiff-base ligands generated from 8-acetyl-7-hydroxycoumarin and P-phenylenediamine. Photoluminescence resulting from intraligand ($\pi-\pi^*$) transitions was seen in the Schiff base. Metal-mediated amplification is shown when ligand complexes with Zn and Cd, whereas metal-mediated fluorescence quenching happens with Cu, Ni, and Pd. Similar to this, Taha et al. (Taha, Ajlouni, Al-Hassan, Hijazi, & Faiq, 2011) created lanthanide (III) complexes (Nd, Dy, Sm, Pr, Gd, Tb, La, and Er) using the Schiff base that was obtained from 1,3-propylamine and salicylaldehyde. The distinctive light emissions of the core metal ions linked to energy transfer from the ligand to the metal are seen in Sm, Tb, and Dy complexes.

Zhang et al. (J. Zhang et al., 2012), on the other hand, used substituted 2-hydroxybenzaldehydes with diamines to manufacture the Schiff base ligands. Compared to the previously published equivalents, yellow light-emitting devices were constructed more efficiently using specific complexes as phosphorescent-emitting materials. A single emissive layer of materials that produces blue and yellow light was also used to build the phosphorescent white organic light-emitting device. A group of platinum (II) Schiff base complexes, both symmetric and asymmetric, that exhibit thermal solid stability were created.

Detection of aluminum ion

Metal ion	Type/derivative of schiff base	In the presence of other ions	Reference
Al ³⁺	8-hydroxyquinoline-5-carbaldehyde	Ag ⁺ , Ca ²⁺ , Cd ²⁺ , Co ²⁺ , Cr ³⁺ , Cu ²⁺ , Fe ²⁺ , Fe ³⁺ , Hg ²⁺ , K ⁺ , Mg ²⁺ , Mn ²⁺ , Na ⁺ , Ni ²⁺ , Pb ²⁺ , Zn ²⁺	(Jiang, et al., 2011)
	Derivative of benzohydrazide	Mn ²⁺ , Co ²⁺ , Ni ²⁺ , Cu ²⁺ , Zn ²⁺ , Cd ²⁺ , Mg ²⁺ , Ca ²⁺ , Pb ²⁺	(Lee, et al., 2014)
	1-(2-pyridylazo)-2-naphthol	Ba ²⁺ , Ca ²⁺ , Cr ³⁺ , Cs ⁺ , Hg ²⁺ , K ⁺ , Li ⁺ , Mg ²⁺ , Na ⁺ and Sr ²⁺	(Gupta, Shoor, Kumawat, & Jain, 2015)
	4-hydroxy-3-((2-hydroxyphenyl) imino) methyl)-4-biphenylcarbonitrile	Ag ⁺ , Zn ²⁺ , Li ⁺ , Na ⁺ , Cs ²⁺ , Fe ³⁺ , Cd ²⁺ , Mn ²⁺ , Cu ²⁺ , Hg ²⁺ , Ni ²⁺ , Ca ²⁺ , Sr ²⁺ , Pb ²⁺	(Alici & Erdemir, 2015)



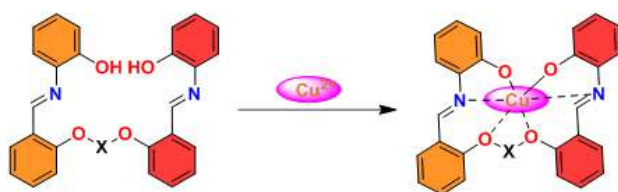


Satvinder Khatkar *et al.*,

Schiff base was created by **Gupta et al.** (Gupta, Singh, & Kumawat, 2014a) via condensation of 2-amino-4-phenylthiazole and salicylaldehyde. According to research on the interactions of Schiff bases with various metal ions, Schiff bases and Al^{+3} ions in methanol with a pH range of 5.0–13.5 showed luminous activity visible to the unaided eye when exposed to a UV light. With Al^{+3} ions, a more than 50-fold increase in fluorescence intensity was seen, and the suggested sensor could quantify it at the 10^{-7} M level. Parallel to this, a Schiff base functionalized with rhodamine was created, and its colorimetric and fluorescence reactions to different metal ions were investigated by **al.** (Gupta, Mergu, Kumawat, & Singh, 2015). In the presence of other competing metal ions, this rhodamine-derived fluorescent chemosensor demonstrated an extremely sensitive and selective colorimetric and "off-on" fluorescence response towards Al^{+3} . Furthermore, the Schiff base was created by **Kumar et al.** (J. Kumar, Sarma, Phukan, & Das, 2015) using the condensation of 1-naphthylamine and benzaldehyde. Using the "off" mode, the Schiff base functions as an efficient fluorescent sensor for Al^{+3} , showing a 42-fold increase in luminous intensity. In addition, a reversible fluorescent-colorimetric imino-pyridyl bis-Schiff base sensor was created by **Ghorai et al.** (Ghorai, Mondell, Chandra, & Patra, 2015). Pyridine-4-carboxaldehyde and phenylenediamine were condensed to form the Schiff base. Concerning Al^{+3} , this Schiff base has a superb selective fluorescent colorimetric response. Based on the naphthalimide-Schiff ground, **Shen et al.** (Shen et al., 2018) synthesized and characterized an Al^{+3} particular fluorescent probe that can be used practically in various water samples. A susceptible and selective Schiff base (2-hydroxynaphthalene) type fluorescent that can detect aluminum ions and display an extremely particular "off-on" mode was recently described by **Tian et al.** (Tian et al., 2019).

Detection of Copper ion

Metal ion	Type/derivative of schiff base	In the presence of other ions	Reference
Cu+2	2-hydroxybenzaldehyde benzoylhydrazone	Al^{+3} , Ca^{+2} , Cd^{+2} , Fe^{+2} , K^{+} , Mg^{+2} , Na^{+} , Pb^{+2} , Zn^{+2}	(Espada-Bellido, Galindo-Riaño, García-Vargas, & Narayanaswamy, 2010)
	Rhodamine Schiff base	Li^{+} , Na^{+} , K^{+} , Ba^{+2} , Ca^{+2} , Cd^{+2} , Mg^{+2} , Co^{+2} , Mn^{+2} , Zn^{+2} , Pb^{+2} , Ni^{+2} , Fe^{+2} , Hg^{+2} , Fe^{+3} , Al^{+3} , Cr^{+3}	(Yang, et al., 2013)



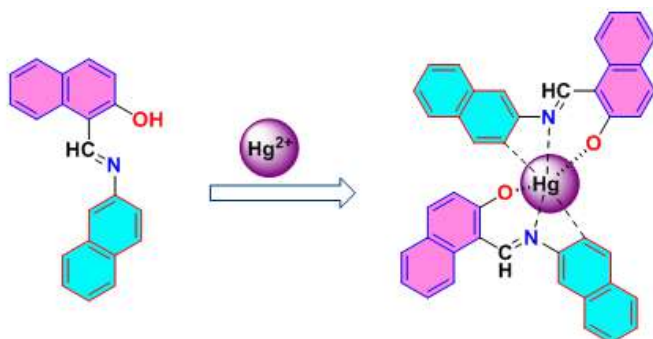
Reference 108:-Wail Al Zoubiet.all

A Schiff base type chemosensor for Cu^{+2} ion was devised and manufactured by **Yang and Qin** (H.-G. Li, Yang, & Qin, 2009) using 1-phenyl-3-methyl-5-hydroxypyrazole-4-carbaldehyde (benzoyl) hydrazone. The excellent selectivity of Cu^{+2} fluorescence quenching compared to other metal ions was established. The Schiff base was created by **Köse et al.** (Köse et al. 2015) by reacting benzaldehyde derivatives with 1,5-diamino naphthalene. They have looked at the photoluminescence and electrochemical characteristics of the Schiff bases under various circumstances. When the metal (II) ions of Hg, Cu, Co, and Al (III) were added, color variations were noticed, indicating changes in the sensing characteristics of the Schiff bases. The selectivity of the Schiff base compounds towards the Cu^{+2} ion was excellent.



Savinder Khatkar *et al.*,**Detection of Mercury ion**

Metal ion	Type/derivative of schiff base	In the presence of other ions	Reference
Hg ²⁺	Pyrene Schiff base	Na ⁺ , K ⁺ , Ca ²⁺ , Mn ²⁺ , Fe ³⁺ , Co ²⁺ , Ni ²⁺ , Cu ²⁺ , Zn ²⁺ , Cd ²⁺ , Pb ²⁺ , Sn ²⁺	(Sivaraman, Anand, & Chellappa, 2012)
	1-[(2-naphthalenylimino) methyl]-2-naphthalenol	Fe ³⁺ , Ag ⁺ , Ca ²⁺ , Cu ²⁺ , Co ²⁺ , Ni ²⁺ , Cd ²⁺ , Pb ²⁺ , Zn ²⁺ , Cr ³⁺ , Mg ²⁺	(Y. Zhang, et al., 2013)

**Reference [109]**

Mercury is a heavy metal that is toxic even at low concentrations and is widely distributed in nature. It can accumulate in the body and cause a variety of diseases, such as acute kidney failure, prenatal brain damage, and heart diseases. As a result, it is essential to consider finding Hg²⁺ ions in different samples. The determination of Hg²⁺ ions in living cells was accomplished using a novel Schiff base chemosensor 1 containing pyrene-based free thiol derivative [36]. Consequently, it is crucial to consider the presence of Hg²⁺ ions in diverse samples. A novel Schiff base chemosensor 1 with pyrene-based free thiol derivative detected Hg²⁺ ions in living cells. Similarly, Hg²⁺ ions were caught in a DMSO solution at a low detection limit of 0.05595 µM using a double-naphthalene Schiff base fluorescent chemosensor 2. The chemosensor's imine group was oxidized to produce an amide in the presence of DMSO. The N- and O-atoms of the amide and the Hg²⁺ ions built a 1:1 metal-ligand complex, which was verified by mass spectrometry, ¹H NMR, and FT-IR spectroscopy [21]. Another research used a new coumarin-based fluorescent chemosensor 3 to detect Hg²⁺ ions. The chemosensor demonstrates excellent selectivity for Hg²⁺ in the presence of secondary metal ions. The yellow-colored fluid used in the probe turns colorless as the Hg²⁺ concentration progressively rises. Fluorescence studies further confirmed the mercury ion selectivity of chemosensor 3.

After adding 0.4 M Hg²⁺ to the probe solution, the strong blue fluorescence at 460 nm progressively diminishes, with a slight redshift to the cyan channel (470 nm). The Schiff base imine nitrogen (CH=N) and phenolic-oxygen atoms transfer the lone pair electrons to Hg²⁺, reducing acceptor coumarin emission and extending donor 4-(Diethylamino)salicylaldehyde emission. Thus, the unique emission of 4-(Diethylamino)salicylaldehyde at 470 nm is caused by the suppression of PET-ON and ESIPT activities. Cou-S and both Hg²⁺ form a dimer complex with a binding stoichiometry of 2:1, as indicated by the mole fraction at maximum absorbance of 0.3 (probe: metal ion). A detection threshold of 8.3 nM was established. The interaction between the chemosensor and Hg²⁺ ions was further examined using density functional theory (DFT) [22]. Another study employed a new N-salicylidene)benzylamine Schiff base 4 to identify Hg²⁺ ions using ON properties of fluorescence. UV-Vis spectroscopy and fluorescence were employed to investigate the chemosensor's sensing properties. The use of UV-Vis spectroscopy and fluorescence

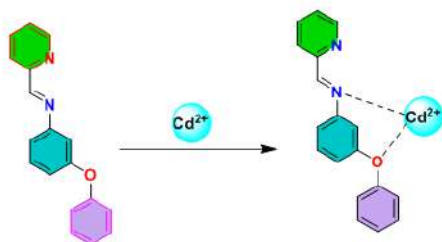




Satvinder Khatkar et al.,

emission ascertained the chemosensor 4's response to various cations. Selectivity for Hg^{2+} in the sensor was confirmed by significant fluorescence increase and spectral/color changes [23]. The pH of the detection medium has an impact on Hg^{2+} ion detection. An aqueous CH_3CN medium with a pH range of 5–10 was used to detect Hg^{2+} , for instance, using a turn-on fluorescent chemosensor 5 [24]. The Schiff base chemosensor 6 was shown to respond selectively to the Hg^{2+} ion when it was present in aqueous media among other cations such as Pb^{2+} , Ca^{2+} , Ba^{2+} , Cu^{2+} , Cr^{3+} , Mg^{2+} , and Zn^{2+} ions. Furthermore, counter anions including Br^- , Cl^- , F^- , I^- , S^{2-} , CN^- , NO_3^- , NO_2^- , OH^- , CO_3^{2-} , SCN^- , HSO_3^- , H_2PO_4^- , CH_3COO^- , HPO_4^{2-} , $\text{P}_2\text{O}_7^{4-}$, and PO_4^{3-} did not significantly affect the selectivity of the chemosensor [41].

Detection of Cadmium ion



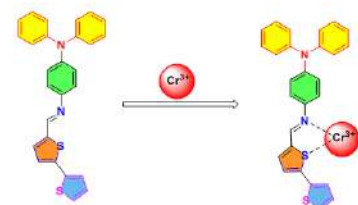
Cadmium is widely used in several sectors, such as mining, smelting, and fossil fuel combustion, making it one of the most ubiquitous and health-hazardous pollutants. Given this, developing a dependable and effective technique for identifying Cd^{2+} ions in a range of materials is essential. Schiff base chemosensor 7 with quinoline moiety was created as a Cd^{2+} ion fluorescence sensor. Fascinatingly, the chemosensor worked incredibly well at detecting Cd^{2+} ions in an aqueous medium by activating fluorescence. Chemosensor 7 emitted very little fluorescence when left unchanged, but when Cd^{2+} was added, there was a noticeable turn-on response. There was no interference from other metal ions, and the sensor demonstrated outstanding selectivity. The binding stoichiometry between the Cd^{2+} and chemosensor 7 was shown to be 1:1, and the detection limit was found to be $0.0024 \mu\text{M}$ [25]. A pyridine-based Schiff base chemosensor 8 was developed to detect Cd^{2+} ions. Even though the chemosensor was not luminous, the application of the Cd^{2+} ion to the skin caused an increase in fluorescence. This increased the chemosensor's fluorescence intensity by stimulating the CHEF while blocking the PET. Furthermore, examining a water sample was successfully accomplished using Chemosensor 8 [26]. A Rhodamine-based Schiff-base fluorescence chemosensor 9 detected Cd^{2+} ions with a $1.025 \times 10^{-8} \text{ M}$ detection limit. The chemosensor 9 exhibits notable selectivity and sensitivity for Cd^{2+} ions in the presence of cations [27]. In 2020, the fluorescence features of an ON-type Schiff base chemosensor 10 against cadmium ions were explored and presented. The chemosensor forms a 1:1 combination with Cd^{2+} , according to the Job plot. pH, solvent type, and ligand concentration were adjusted to detect Cd^{2+} in aqueous samples using a chemosensor-based analytical method. It was found that the detection limit was $6.0 \times 10^{-7} \text{ M}$. With Cd^{2+} , the probe displayed a broad range of linearity [28]. Fluorescent sensor 11, based on rhodamine, was recently disclosed in research about its ability to locate Cd^{2+} ions. The sensor responds to Cd^{2+} by a process known as coordination-induced fluorescence activation (CIFA). Chemosensor 11 exhibits a rapid and reversible fluorescence in response to Cd^{2+} when the measured metal ions are present. The complex stoichiometry between the sensor and Cd^{2+} was found to be 1:1. The binding constant was determined to be $2.70 \times 10^7 \text{ M}^{-1}$ in acetonitrile (ACN)/HEPES buffer (10 mM, pH, 7.05, v/v 1:1). The fluorescence detection limit of the chemosensor 11 for Cd^{2+} was found to be $0.218 \mu\text{M}$, indicating a significant sensitivity to Cd^{2+} [29].





Satvinder Khatkar et al.,

Detection of Chromium ion



Reference 111

Significant transition metal chromium is utilized in many sectors, such as chemical engineering, oil refining, steel manufacturing, textile manufacturing, and electroplating. However, it causes pulmonary sensitization and increases the risk of lung, sinus, and nasal cancer. To detect Cr^{3+} , a new Schiff base chemosensor 12 was built and put through several characterization techniques. The chemosensor was evaluated against a range of harmful metal ions, such as Mn^{2+} , Ag^+ , Cd^{2+} , Co^{2+} , Cu^{2+} , Ni^{2+} , Zn^{2+} , Fe^{3+} , Al^{3+} , and Cr^{3+} , using a spectrophotometric technique. The creation of the stable complex through the S and N atoms was found to only cause a discernible hyperchromic change in the chemosensor's absorbance in the presence of Cr^{3+} ions [30]. The electrochemical characteristics and reversibility of the chemosensor were also examined using electrochemical techniques. The Schiff base chemosensor 13 was also utilized to find Cr^{3+} ions in the aqueous environment. The colorimetric sensitivity of the chemosensor 13 to various cations was visually monitored. The golden tint of the chemosensor 13 became colorless upon the addition of chromium ions. Fluorescence experiments were employed to learn more about the chemosensor 13's sensing capabilities. As a result of the possibility that the imine group of the sensor would revert to the carbonyl group in the presence of Cr^{3+} , the chemosensor 13's fluorescence intensity decreased at 418 nm. Still, it increased noticeably when Cr^{3+} was present [31]. A new Schiff base fluorescent chemosensor 14 was just released, which allows for the selective detection of chromium ions. The PET process is inhibited by forming a 1:1 stoichiometric sensor- Cr^{3+} complex, which Job's plot corroborates. Fluorescence titration demonstrated a detection limit of 1.3×10^{-7} M, and the association constant K_a was reported to be $2.28 \times 10^5 \text{ M}^{-1}$. Furthermore, the suggested complex's optimum structure and electronic spectra were explained using DFT and TDDFT simulation findings [32]. It addressed using a novel fluorescent Schiff base chemosensor 15 based on thiazoles for the chemodosimetric approach of Cr(III) ion detection. Several analytical methods, such as UV-vis, ^{13}C -NMR, ^1H -NMR, and FT-IR analysis, were used to identify the structure of the chemosensor 15. Fascinatingly, chemosensor 15 reacts by turning on fluorescently to particular Cr(III) ions to various metal cations, including Ni^{2+} , Na^+ , Cd^{2+} , Ag^+ , Mn^{2+} , K^+ , Zn^{2+} , Cu^{2+} , Hg^{2+} , Co^{2+} , Pb^{2+} , Mg^{2+} , Sn^{2+} , Al^{3+} , and Cr^{3+} [33]. In contrast, Cr(VI) sufficiently quenched a Schiff base chemosensor 16 that relied on inner filter effects through both primary and secondary internal filter effects. The switched-off fluorescence of the chemosensor- Cr(VI) solution was efficiently turned on by the addition of L-ascorbic acid in the concentration range of $10 \mu\text{M}$ to $390 \mu\text{M}$ with an LOD of $2.46 \mu\text{M}$. The mechanism postulated for the fluorescence turn-on of the quenched fluorescence of the Cr(VI) -chemosensor was the reduction of Cr(VI) to Cr(III) by L-ascorbic acid, which resulted in the removal of both primary and secondary inner filter effects and the recovery of the chemosensor's fluorescence [34].

Detection of Palladium ion

Palladium is a precious metal in many technological and industrial applications. Palladium is toxic and very carcinogenic, however. Finding Pd^{2+} ions in various biological, agricultural, and environmental components is essential. The Schiff base fluorescent and colorimetric chemosensor 17 was used to identify Pd^{2+} ions. This chemosensor showed high selectivity for Pd^{2+} ions in the presence of monovalent, divalent, trivalent, and tetravalent cations, including Ag^+ , Ca^{2+} , Sn^{4+} , Ni^{2+} , Ba^{2+} , Cu^{2+} , Zn^{2+} , Fe^{2+} , Tb^{3+} , Hg^{2+} , Eu^{3+} , Mg^{2+} , Gd^{3+} , Mn^{2+} , Sm^{3+} , Cr^{3+} , and Ag^+ . Mass, ^1H NMR, ^{13}C NMR, and FT-IR studies confirmed the chemosensor's mechanism of spirolactam ring opening's mechanism. A Pd^{2+} detection threshold of $0.05 \mu\text{M}$ was set for Chemosensor 17 [35]. Coumarinyl-rhodamine Schiff base chemosensor 18 demonstrates an exceptionally high degree of selectivity for Pd^{2+} in the presence of the following ions: Ba^{2+} , Cu^{2+} , Zn^{2+} , Al^{3+} , Fe^{2+} , Hg^{2+} , Mg^{2+} , Co^{3+} , Mn^{2+} , Ag^+ , Ca^{2+} , Ni^{2+} , Cd^{2+} , Pb^{2+} , Fe^{3+} , Pt^{2+} , Na^+ , and K^+ . It has been proposed that this chemosensor functions by opening the spirolactam ring. Whereas the free chemosensor





Satvinder Khatkar *et al.*,

was only slightly emissive, the Pd^{2+} ions increased the fluorescence intensity and caused the chemosensor to become pink instead of straw color. This chemosensor was highly selective for the Pd^{2+} ion when chemosensor 18 and unique metal cations were present [36].

Detection of Calcium ion

An *et al.* (2013) developed and studied a new sensor called 7-Hydroxy-4-methylcoumarin-8-carbaldehyde-(rhodamine) hydrazone as a fluorescent chemosensor for Ca^{+2} in acetonitrile. More than other competitive ions, the molecule was shown to bind preferentially to Ca^{+2} ions, changing its optical and fluorescence spectrum characteristics.

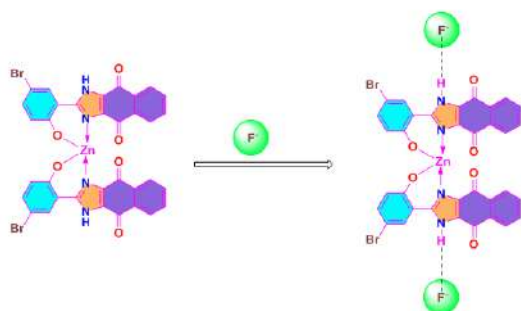
Detection of Magnesium ion

Metal ion	Type/derivative of Schiff base	In the presence of other ions	Reference
Mg+2	(N,N'-bis-(salicylidene)-O-phenylenediamine)	Ca+2, Cr+3, Al+3, Fe+2, Cu+2, Co+2, Ni+2, Zn+2, Cd+2, Hg+2, Pb+2	(Hariharan & Anthony, 2014)

Several Schiff bases have been created by **Hariharan and Anthony** (Hariharan & Anthony, 2014) utilizing various diamines and substituted benzaldehyde. Chemosensor fluorescence responses to different metal (II) ions have been investigated in acetonitrile, methanol, dimethylformamide, and tetrahydrofuran. Additionally, there are real-world uses of the chemosensor for selective detection of Mg^{+2} in various tap, river, pond, and groundwater samples.

Detection of Zinc ion

Metal ion	Type/derivative of schiff base	In the presence of other ions	Reference
Zn+2	Naphthaldehyde Schiff base	Fe+3, Hg+2, Ag+ , Ca+2 , Cu+2, Co+2, Ni+2, Cd+2 , Pb+2, Zn+2, Cr+3 , Mg+2	(Wei, et al., 2013)
	Vanillinyl thioether	Na+ , K+ , Ca+2, Mg+2, Ba+2 , Hg+2, Ni+2, Co+2, Pb+2 , Pd+2, Mn+2, Al+3, Cd+2 , Cu+2, Fe+3	(Patra, et al., 2016)



Reference [112]





Satvinder Khatkar et al.,

The Schiff base was created by **Gupta et al.** (Gupta, Singh, & Kumawat, 2014b) via condensation of 4-aminoantipyrine and 4-hydroxy-3-methoxybenzaldehyde. Using UV-vis absorption spectra and photofluorescence spectra, the complexation behavior of chemosensors with various metal ions, including Zn^{+2} ions, in a methanolic solution was investigated. According to the results, the chemo sensor demonstrated a 55-fold increase in fluorescence at 533 nm following the addition of Zn^{+2} ions. The chemosensor showed excellent selectivity for luminous activity in the acidic pH range.

Detection of Iron ion

Metal ion	Type/derivative of schiff base	In the presence of other ions	Reference
Fe ²⁺ & Fe ³⁺	2,3-dihydroxybenzaldehyde moiety	Na ⁺ , K ⁺ , Mn ²⁺ , Co ²⁺ , Ni ²⁺ , Cu ²⁺ , Zn ²⁺ , Cd ²⁺ , Pb ²⁺ , Mg ²⁺ , Ca ²⁺	(You, Park, Lee, Ryu, & Kim, 2015)

According to **Pan et al.** (Pan et al., 2017), 2-Aminophenol and 4-(diphenyl amino) benzaldehyde reacted to create Schiff base. The chemosensor exhibits a selective "turn-off" fluorescence response to Fe³⁺ in live cells.

Iron is one of the transition metal ions most prevalent in the earth's crust and is found chiefly in the ferrous and ferric forms. Iron is essential for electron transport, oxygen absorption, oxygen metabolism, and other processes in living things. Nonetheless, there should always be a certain amount of iron in the human body. Numerous health issues are caused by both an excess and a shortage of it [37]. Due to iron(III)'s active participation in several biological processes, its selective detection is critical. Apart from the physical domain, a particular optical probe is necessary for the qualitative and quantitative assessment of iron in the clinical, environmental, and industrial environments. There have been reports of many chemical sensor types for the detection of iron that are based on colorimetric and fluorescence response (optical response). Fe³⁺'s paramagnetic feature, which causes the fluorescence of the sensor molecule to be quenched, is one of the main obstacles in the development of fluorescence sensors. As a result, the majority of fluorescent-based Fe³⁺ sensors are of the "turn-off" type [38], whereas very few are of the "turn-on" type [39, 40]. One method used to create "turn-on" fluorescence sensors is Fe³⁺-aided hydrolysis [41]. The analyte may be easily detected with the unaided eye thanks to colorimetric sensors. Consequently, various colorimetric sensors have been created using the Fe³⁺'s strong complex formation capabilities. Because Fe³⁺ is a hard acid, it forms stable compounds with probes with complex donor atoms, such as N, O, etc. The colorimetric response is primarily caused by transitions in intramolecular charge transfer (ICT) to metal charge transfer (LMCT) and metal-to-ligand charge transfer (MLCT). The reported chemosensors for Fe³⁺ are based on salicylaldehyde or 5-nitrosalicylaldehyde and o-aminophenol [42]; 8-formyl-7-hydroxy-4-methylcoumarine and 2-aminopyridine [43]; rhodamine-B-derivative and m-phthaloyl chloride [44]; rhodamine-B-hydrazine and 2-(N-methylpiperazinylimino)acetaldehyde [45]; 2-hydroxy-1-naphthaldehyde and 2-aminopyridine [46]; 8-hydroxyjulolidine-9-carboxaldehyde and 1-(3-Aminopropyl)imidazole [47]; rhodamine derivative and pyrazolone [48]; rhodamine hydrazide 2-tetrabutyltrimethylsiloxybenzaldehyde [49]; aromatic aldehyde or substituted aromatic aldehyde and ethylene diamine or trans-1,2-diaminocyclohexane [50]; rhodamine 6G hydrazine and 2-formylimidazole; rhodamine 6G ethylenediamine and imidazole-2-carboxaldehyde [51]; pyrrole-2-carboxaldehyde and 2-nitro-1-phenylene diamine or 1,4-phenylenediamine [52]. There are additional reports of other chemosensors based on the LMCT principle. Anthony and colleagues reported on a set of five colorimetric sensors that were generated from the Schiff base. Modifying the sensor's structural motif allowed for the adjustment of their chemosensing properties: [53]; 2-(2'-cyanophenoxy)nitrobenzene with salicylaldehyde or substituted salicylaldehyde [54]; 2-(2'-aminophenoxy)benzene carboxylic acid and 4-methoxysalicylaldehyde or 2-hydroxynaphthaldehyde [55]; rhodamine derivative and 8-hydroxyquinolone [56]; 6-amino-3,4-benzocoumarine and 8-hydroxyquinoline-2-carbaldehyde [57]. Chemical sensors for metal ions can also be developed by effectively utilizing metal-catalyzed hydrolysis of imine bonds ($C=N$). A diketopyrrol Schiff base was described by **Wang et al.** [58] as a chemodosimeter for detecting Fe³⁺ based on the imine bond's hydrolytic cleavage. Fe³⁺ catalyzed imine bond hydrolysis served as the foundation for **Lin et al.**'s



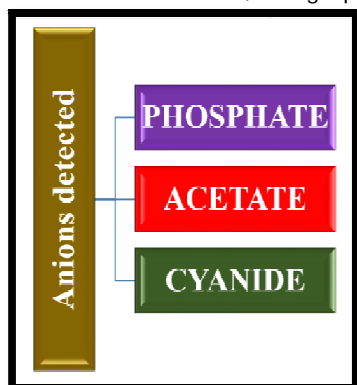
**Satvinder Khatkar et al.,**

development of the chemical sensor known as bis(coumarin) Schiff base ^[59]. A rhodamine 6G Schiff base was described by Kang and colleagues^[60] for the detection of Fe³⁺.

Detection of Arsenic ion

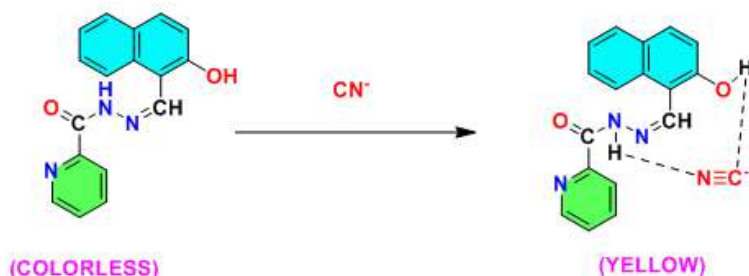
Even at low concentrations, arsenic is a lethal heavy metal despite being widely found in nature. It accumulates in the body and can lead to various diseases, including skin and lung malignancies, disruption of cellular respiration, and dysfunctions of the kidney, liver, bladder, and prostate [61-63]. As such, identifying As³⁺ ions in various samples is very important. Recent work reported using a fluorescent chemosensor 19 based on excited-state intramolecular proton transfer (ESIPT) to detect arsenic species in a real naphtha sample. The pH-related emission migration from 610 nm (pH 14,1) to 510 nm (pH 14,13) served as an example of the M-ESIPT process. When M-HBT's sensing capacity in ethanol was tested, the experiment's results demonstrated that As³⁺ reacted linearly well in the 0–32 µM range [64]. Similarly, a new colorimetric sensor based on a benzothiazole Schiff base chemosensor 20 has been described to detect As³⁺/As⁵⁺ in mixed aqueous solutions rapidly. Its 7.0 ppb detection limit may be seen with the unaided eye in 10 seconds, and it offers the benefits of economy, simplicity, specificity, high sensitivity, and selectivity. Additionally, the probe shows exceptional selectivity in the presence of other common ions. It is suitable for the prompt, easy, and on-site detection of As³⁺/As⁵⁺ ions at deficient concentrations in real water samples [65].

Another research used a new coumarin-based fluorescent chemosensor 21 to detect As³⁺ ions. In the presence of secondary metal ions (Na⁺, Mg²⁺, Cu²⁺, Ni²⁺, Co²⁺, Zn²⁺, Pb²⁺, Fe²⁺, Fe³⁺, Hg²⁺, Ca²⁺, Cd²⁺, and Mn²⁺), the chemosensor shows excellent selectivity toward As³⁺. The development and evaluation of ArsenoFluor1, the first example of a chemosensor was done for the detection of As³⁺ in organic solvents at 298 K. At $\lambda_{em} = 496$ nm in THF, AF1 shows a 25-fold increase in fluorescence that is selective for As³⁺ over other physiologically relevant ions (such as Na⁺, Mg²⁺, Fe²⁺, and Zn²⁺) and has a sub-ppb detection limit. According to AF1's optical characteristics, a strong, broad absorption band with a center wavelength of 385 nm in THF may be seen. The chromophore coumarin mostly dominates this band. By a photo induced electron transfer mechanism, the thiazoline N lone pair effectively quenches the ensuing fluorescence emission maxima at 496 nm, resulting in a meager quantum yield (ϕ) 0.004. In essence, the nonconjugated AF1 is non-fluorescent. As³⁺ (as AsI₃, albeit AsCl₃ also has similar effects) enhances the fluorescence intensity of AF1 by approximately 25 times. The formation of benzothiazole C6-CF₃ is indicated by red changes in the absorbance maxima from 385 to 464 nm, which coincide with this significant turn-ON response. Internal-charge-transfer (ICT) is the usual method by which the commercially available coumarin-6 (analog of C6-CF₃, with hydrogen substituting the CF₃ group) and other coumarin-benzothiazole compounds produce fluorescence. Consequently, AF1 serves as an effective OFF–ON fluorescence sensor for As³⁺ in organic media at 298 K. The Schiff-base thiolate form of AF1 is likely bis-coordinated to the thiolate anion during the sensing process. The thiolate anion attacks the C-N carbon, losing a proton to make the benzothiazole [66].





Satvinder Khatkar et al.,

Detection of Cyanide ion**Reference [113]**

Because anions are so crucial to many biological, environmental, and chemical processes, monitoring them is necessary. They also harm life on earth beyond a certain point [67]. Due to their excellent ligating capacity with the active sites of hemoglobin and cytochrome c-oxidase, cyanide ions induce rapid death even in tiny levels. The environment is contaminated by cyanide and its derivatives due to its widespread usage in industrial operations. As such, developing an efficient technique for monitoring the level of cyanide ions [68-71] is imperative. Optical sensors can detect cyanide contamination quickly, conveniently, and affordably by causing quantifiable changes in photophysical properties. Cyanide sensors are typically designed using three methods. The most common method is a covalent connection connecting the sensors' signaling unit and binding site. The signaling unit's color or fluorescence changes due to the cyanide recognition process by binding sites. The second method is a displacement strategy based on coordination complexes, where the introduction of cyanide ions causes the free probe to regenerate and acquire unique photophysical characteristics. The third method is chemo-dosimetric, which uses a particular and irreversible chemical process to detect cyanide [72-74]. Here, the cyanide ion's distinct nucleophilicity is a sensing tool. When exposed to cyanide ions, Schiff bases show spectacular colorimetric and fluorescence responses; several accounts of these reactions can be found in the literature. The subsequent Schiff base-derived sensors are based on the following: 3,5-diamino-1,2,4-triazole and 2-hydroxy-1-naphthaldehyde [75]; 8-hydroxyjulolidine-9-carboxaldehyde and 1-amino naphthalene-2-ol; [76]; 7-amino-4-methyl coumarin and 2-hydroxy-1-Naphthaldehyde [77]; 4-(diethylamino)salicylaldehyde and isonicotinic hydrazide [78]; 2-hydroxy-1-naphthaldehyde and N-(1-naphthyl) ethylenediamine dihydrochloride [79]; fluorene-2-aldehyde and diaminomaleonitrile [80]; salicylaldehyde hydrazine and 3, 5-dibromosalicylaldehyde [81]; Benzil and 2,4-(dinitrophenyl)hydrazine [82]; 2-amino-3-[(2-pyridylmethyl)amino]-2(Z)-butene-1,4-dinitrile. There are reports of 2-hydroxy-1-naphthaldehyde [83]. In addition to Schiff bases, many additional classes of chemicals have been identified as cyanide ion chemosensors [84-89]. Most of these probes function best in organic or organic/aqueous mixtures with a larger volume (fraction) of organic matter.

Detection of phosphate ion

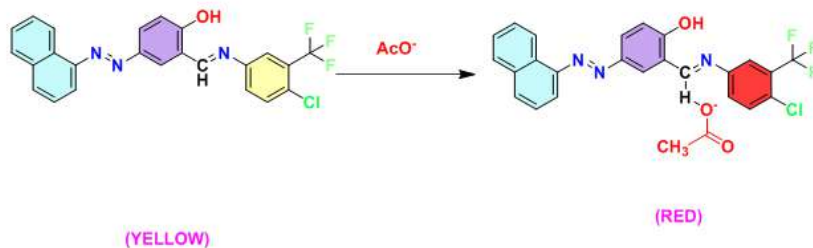
4-bromo-2-((6-methoxybenzo[d]thiazol-2-ylimino)methyl)phenol [90] and 4-((2,4-dichlorophenyl)diazonyl)-2-(3-hydroxypropylimino)methyl)phenol [91] has demonstrated an optical shift from yellow to orange for H_2PO_4 . Due to the transfer of a proton from phenolic -OH to imino group ($-\text{C}=\text{N}$), which is responsible for sensing, both Schiff bases coexist in ketol and enol forms. A few Schiff bases based on hydrazine [92] and hydrazine [93] have also been reported in the literature for the colorimetric detection of dihydrogen phosphate ions.





Satvinder Khatkar *et al.*,

Detection of acetate ion



Reference [114]

Acetate is a component of several enzymes, antibodies, and metabolic processes.[94] Despite this, there are several Schiff bases, such as 2-(((3,4-dimethoxyphenethyl)imino)methyl)-4-((4-nitrophenyl)diazanyl)phenol,[95] 4-bromo-2-((6-methoxybenzo[d]thiazol-2-ylimino)methyl)phenol,[96] 4-((E)-(2-Hydroxy-5-((E)-(4-nitrophenyl) diazenyl) benzylidene) amino)-1,5-dimethyl-2-phenyl-1H-pyrazol-3(2H)-one,[97] Although H3NTS[98] and Hydroxynaphthaldehydeallylidenehydrazine[99] have acceptable detection limits, they are not AcO⁻-specific because, under the identical reaction circumstances, these Schiff bases also show the exact color change for other ions. Thus, 1-naphthylamine 2-((E)-((4-chloro-3-(trifluoromethyl)phenyl)imino)methyl) -4-((E)-naphthalene-1-ylidiazanyl) phenol (CTNP) has been described by Parchegani et al. Since CTNP exhibits a pale yellow to red color change for AcO⁻ in DMSO, it can be used as a visual sensor for acetate ions [100]. "CTNP" readily interacts with acetate ions because it has three very electronegative fluorine atoms at the phenyl group, forming an electropositive center at the active site (-C=N). Similarly, Schiff bases with nitro groups have -NO₂ moieties, which have a declining inductive impact on the electronic cloud. The amino group (-NH) and imino group (-C=N) are in charge of AcO⁻'s attachment to the Schiff base. Nevertheless, nitro salicylidene-benzendiamine[101] and o-phenylenediamine[102] become yellow from colorless during contact with AcO⁻. Naphthyl-hydrazone has demonstrated a hue shift from yellow to orange[103]. Several other substances have been reported to function as colorimetric sensors for AcO⁻, including aminophenol[104], naphthoquinone-based Schiff bases[105], azo-dye[106], and naphthalene[107].

CONCLUSION

Schiff base compounds may be readily synthesized in labs using various reaction techniques. Using different analytical methods, Schiff bases have been employed to detect a range of metal ions, including Hg²⁺, Cd²⁺, Cr³⁺, Pd²⁺, and others. The use of different Schiff base probes as chemosensors to identify metal ions (cations) has been covered in this chapter. A stable complex may be created when a metal center aligns with azomethine's nitrogen atom, which might serve as a ligating site. Outstanding outcomes in the area of metal cation detection have been documented. Nonetheless, it is imperative to design chemosensors that can function in various environments and have excellent selectivity and sensitivity for hazardous metal cations.

ACKNOWLEDGEMENT

One of the author (Satvinder Khatkar) is thankful to CSIR, New Delhi for the financial support to carry out this work.

REFERENCES

1. Fu F, Wang Q. Removal of heavy metal ions from wastewaters: A review. Journal of Environmental Management. 2011;92:407-418. DOI: 10.1016/j.jenvman.2010.11.011





2. Li M, Gou H, Al-Ogaidi I, Wu N. Nanostructured sensors for detection of heavy metals: A review. *ACS Sustainable Chemistry & Engineering*. 2013;1:713-723. DOI: 10.1021/sc400019a
3. Sharma N, Sodhi KK, Kumar M, Singh DK. Heavy metal pollution: Insights into chromium eco-toxicity and recent advancement in its remediation. *Environmental Nanotechnology, Monitoring & Management*. 2021;15:100388. DOI: 10.1016/j.enmm.2020.100388
4. Briffa J, Sinagra E, Blundell R. Heavy metal pollution in the environment and their toxicological effects on humans. *Heliyon*. 2020;6:04691. DOI: 10.1016/j.heliyon.2020.e04691
5. Lentini P, Zanolli L, Granata A, Signorelli SS, Castellino P, Dell'Aquila R. Kidney and heavy metals - The role of environmental exposure (review). *Molecular Medicine Reports*. 2017;15:3413-3419. DOI: 10.3892/mmr.2017.6389
6. Fu Z, Xi S. The effects of heavy metals on human metabolism. *Toxicology Mechanisms and Methods*. 2020;30:167-176. DOI: 10.1080/15376516.2019.1701594
7. Muro-Gonzalez DA, Mussali-Galante P, Valencia-Cuevas L, Flores-Trujillo K, Tovar-Sanchez E. Morphological, physiological, and genotoxic effects of heavy metal bioaccumulation in *Prosopis laevigata* reveal its potential for phytoremediation. *Environmental Science and Pollution Research*. 2020;27:40187-40204. DOI: 10.1007/s11356-020-10026-5
8. Anyanwu BO, Orisakwe OE. Current mechanistic perspectives on male reproductive toxicity induced by heavy metals. *Journal of Environmental Science and Health, Part C: Environmental Carcinogenesis and Ecotoxicology Reviews*. 2020;38:204-244. DOI: 10.1080/26896583.2020.1782116
9. Vardhan KH, Kumar PS, Panda RC. A review on heavy metal pollution, toxicity and remedial measures: current trends and future perspectives. *Journal of Molecular Liquids*. 2019;290:111197. DOI: 10.1016/j.molliq.2019.111197
10. Igbokwe IO, Igwenagu E, Igbokwe NA. Aluminium toxicosis: A review of toxic actions and effects. *Interdisciplinary Toxicology*. 2020;12:45-70. DOI: 10.2478/intox-2019-0007
11. Wu X, Cobbina SJ, Mao G, Xu H, Zhang Z, Yang L. A review of toxicity and mechanisms of individual and mixtures of heavy metals in the environment. *Environmental Science and Pollution Research*. 2016;23:8244-8259. DOI: 10.1007/s11356-016-6333-x
12. Zhou Q, Lei M, Liu Y, Wu Y, Yuan Y. Simultaneous determination of cadmium, lead and mercury ions at trace level by magnetic solid phase extraction with Fe@ Ag@Dimercaptobenzene coupled to high performance liquid chromatography. *Talanta*. 2017;175:194-199. DOI: 10.1016/j.talanta.2017.07.043
13. Bansod BK, Kumar T, Thakur R, Rana S, Singh I. A review on various electrochemical techniques for heavy metal ions detection with different sensing platforms. *Biosensors & Bioelectronics*. 2017;94:443-455. DOI: 10.1016/j.bios.2017.03.031
14. Zinoubi K, Majdoub H, Barhoumi H, Boufi S, Jaffrezic-Renault N. Determination of trace heavy metal ions by anodic stripping voltammetry using nanofibrillated cellulose modified electrode. *Journal of Electroanalytical Chemistry*. 2017;799:70-77. DOI: 10.1016/j.jelechem.2017.05.039
15. Colim AN, do Nascimento PC, Wiethan BA, Adolfo FR, Dresch LC, de Carvalho LM, et al. Reversed-phase High-performance Liquid Chromatography for the Determination of 15 Rare Earth Elements in Surface Water Sample Collected in a Mining Area from Lavras do Sul/RS. Vol. 82. *Brazil: Chromatographia*; 2019. pp. 843-856. DOI: 10.1007/s10337-019-03709-w
16. Shih TT, Hsu IH, Chen SN, Chen PH, Deng MJ, Chen Y, et al. A dipole-assisted solid-phase extraction microchip combined with inductively coupled plasma-mass spectrometry for online determination of trace heavy metals in natural water. *Analyst*. 2015;140:600-608. DOI: 10.1039/c4an01421a
17. Comby S, Tuck SA, Truman LK, Kotova O, Gunnlaugsson T. New trick for an old ligand! The sensing of Zn(II) using a lanthanide based ternary Yb(III)-cyclen-8-hydroxyquinoline system as a dual emissive probe for displacement assay. *Inorganic Chemistry*. 2012;51:10158-10168. DOI: 10.1021/IC300697W
18. Aletti AB, Gillen DM, Gunnlaugsson T. Luminescent/colorimetric probes and (chemo-) sensors for detecting anions based on transition and lanthanide ion receptor/binding complexes. *Coordination Chemistry Reviews*. 2018;354:98-120. DOI: 10.1016/J.CCR.2017.06.020
19. Gunnlaugsson T, Bichell B, Nolan C. A novel fluorescent photoinduced electron transfer (PET) sensor for lithium. *Tetrahedron Letters*. 2002;43:4989-4992. DOI: 10.1016/S0040-4039(02)00895-X





Satvinder Khatkar et al.,

20. Di W, Sedgwick AC, Thorfinnur Gunnlaugsson EU, Akkaya JY, James TD. Fluorescent chemosensors: The past, present and future. *Chemical Society Reviews*.2017;46:7105-7123. DOI: 10.1039/C7CS00240H
21. Shellaiah M, Rajan YC, Balu P, Murugan A. A Pyrene based schiff base probe for selective fluorescent turn-on detection of Hg 2+ ions with live cell application. *New Journal of Chemistry*. 2015;39:2523-2531. DOI: 10.1039/c4nj02367f
22. Wei T, Gao G, Qu W, Shi B, Lin Q, Yao H, et al. Selective fluorescent sensor for mercury(II) ion based on an easy to prepare double naphthalene Schiff base. *Sensors and Actuators B: Chemical*. 2014;199:142-147. DOI: 10.1016/j.snb.2014.03.084
23. Muthusamy S, Rajalakshmi K, Zhu D, Zhu W, Wang S, Lee K-B, et al. Dual detection of mercury (II) and lead (II) ions using a facile coumarin-based fluorescent probe via excited state intramolecular proton transfer and photoinduced electron transfer processes. *Sensors and Actuators B: Chemical*. 2021;346:130534. DOI: 10.1016/j.snb.2021.130534
24. İnal EK. A Fluorescent chemosensor based on schiff base for the determination of Zn2+, Cd2+ and Hg2+. *Journal of Fluorescence*. 2020;30:891-900. DOI: 10.1007/s10895-020-02563-6
25. Su Q, Niu Q, Sun T, Li T. A simple fluorescence turn-on chemosensor based on Schiff-base for Hg2+-selective detection. *Tetrahedron Letters*. 2016;57(38):4297-4301. DOI: 10.1016/j.tetlet.2016.08.031
26. Wang XM, Yan H, Chen Y, Bao HB. A new Schiff's base fluorescent sensor for the selective detection of mercury ion. *Advanced Materials Research*. 2011;239-242:1105-1108. DOI: 10.4028/www.scientific.net/AMR.239-242.1105
27. Mohanasundaram D, Bhaskar R, Gangatharan Vinoth Kumar G, Rajesh J, Rajagopal G. A quinoline based Schiff base as a turn-on fluorescence chemosensor for selective and robust detection of Cd2+ ion in semi-aqueous medium. *Microchemical Journal*. 2021;164:106030. DOI: 10.1016/j.microc.2021.106030
28. Ma J, Dong Y, Zhou Y. Yan Wub and Zhen Zhao A pyridine based Schiff base as a selective and sensitive fluorescent probe for cadmium ions with "turn-on" fluorescence responses. *New Journal of Chemistry*. 2022;46:3348. DOI: 10.1039/D1NJ05919J
29. Maniyazagan M, Mariadasse R, Jeyakanthan J, Lokanath NK, Naveen S, Premkumar K, et al. Rhodamine based "turn-on" molecular switch FRET-sensor for cadmium and sulfide ions and live cell imaging study. *Sensors and Actuators B: Chemical*. 2017;238:565-577. DOI: 10.1016/j.snb.2016.07.102
30. Aydin Z. A turn-on fluorescent sensor for cadmium ion detection in aqueous solutions. *JOTCSA*. 2020;7(1):277-286. DOI: 10.18596/jotcsa.638912
31. Kolcu F, Erdener D, Kaya İ. A Schiff base based on triphenylamine and thiophene moieties as a fluorescent sensor for Cr (III) ions: Synthesis, characterization and fluorescent applications. *Inorganica Chimica Acta*. 2020;119676. DOI: 10.1016/j.ica.2020.119676
32. Ding Y, Zhao C. A highly selective fluorescent sensor for detection of trivalent metal ions based on a simple schiff-base. *Química Nova*. 2018. DOI: 10.21577/0100-4042.20170229
33. Chalmardi GB, Tajbakhsh M, Hasani N, Bekhradnia A. A new Schiff-base as fluorescent chemosensor for selective detection of Cr 3+: An experimental and theoretical study. *Tetrahedron*. 2018;74(18):2251-2260. DOI: 10.1016/j.tet.2018.03.046
34. Khan S, Muhammad M, Algethami JS, Al-Saidi HM, Almahri A, Hassanian AA. Synthesis, characterization and applications of schiff base chemosensor for determination of Cr(III) Ions. *Journal of Fluorescence*. 2022;32(5):1889-1898. DOI: 10.1007/s10895-022-02990-7
35. Abbasi A, Shakir M. An inner filter effect based Schiff base chemosensor for recognition of Cr(vi) and ascorbic acid in water matrices. *New Journal of Chemistry*. 2018;42(1):293-300. DOI: 10.1039/c7nj03677a
36. Bhanja A, Mishra S, Saha K, Sinha C. A fluorescence 'turn-on'chemodosimeter for the specific detection of Pd 2+ by a rhodamine appended Schiff base and its application inlive cell imaging. *Dalton Transactions*. 2017;46:9245-9252. DOI: 10.1039/C7DT01288H
37. B.-R. Gao, H.-Y. Wang, Y.-W. Hao, L.-M. Fu, H.-H. Fang, Y. Jiang, L. Wang, Q.-D. Chen, H. Xia and L.-Y. Pan, *The Journal of Physical Chemistry B*, 2009, 114, 128-134.
38. L. McDonald, J. Wang, N. Alexander, H. Li, T. Liu and Y. Pang, *The Journal of Physical Chemistry B*, 2016, 120, 766-772.
39. Y. Xiang and A. Tong, *Organic Letters*, 2006, 8, 1549-1552.





Satvinder Khatkar et al.,

40. C.-H. Chen, P.-J. Hung, C.-F. Wan and A.-T. Wu, *Inorganic Chemistry Communications*, 2013, 38, 74-77.
41. B. Kaur, N. Kaur and S. Kumar, *Coordination Chemistry Reviews*, 2018, 358, 13-69.
42. S. Prabhu, S. Saravanamoorthy, M. Ashok and S. Velmathi, *Journal of Luminescence*, 2012, 132, 979-986.
43. S. Devaraj, Y.-k. Tsui, C.-Y. Chiang and Y.-P. Yen, *Spectrochimica Acta Part A: Molecular and Biomolecular Spectroscopy*, 2012, 96, 594-599.
44. X. Chen, H. Hong, R. Han, D. Zhang, Y. Ye and Y.-f. Zhao, *Journal of fluorescence*, 2012, 22, 789-794.
45. MO9S.-R. Liu and S.-P. Wu, *Sensors and Actuators B: Chemical*, 2012, 171, 1110-1116.
46. T.-B. Wei, P. Zhang, B.-B. Shi, P. Chen, Q. Lin, J. Liu and Y.-M. Zhang, *Dyes and Pigments*, 2013, 97, 297-302.
47. Y. W. Choi, G. J. Park, Y. J. Na, H. Y. Jo, S. A. Lee, G. R. You and C. Kim, *Sensors and Actuators B: Chemical*, 2014, 194, 343-352.
48. S. Parihar, V. P. Boricha and R. Jadeja, *Luminescence*, 2015, 30, 168-174.
49. Z.-Q. Hu, M. Du, L.-F. Zhang, F.-Y. Guo, M.-D. Liu and M. Li, *Sensors and Actuators B: Chemical*, 2014, 192, 439-443.
50. C. Wang, Y. Liu, J. Cheng, J. Song, Y. Zhao and Y. Ye, *Journal of Luminescence*, 2015, 157, 143-148.
51. X. Wan, T. Liu, H. Liu, L. Gu and Y. Yao, *RSC Advances*, 2014, 4, 29479-29484.
52. D. Udhayakumari and S. Velmathi, *Spectrochimica Acta Part A: Molecular and Biomolecular Spectroscopy*, 2014, 122, 428-435.
53. H. Zhu, J. Fan, B. Wang and X. Peng, *Chemical Society Reviews*, 2015, 44, 4337-4366.
- A. Kundu, P. Hariharan, K. Prabakaran and S. P. Anthony, *Sensors and Actuators B: Chemical*, 2015, 206, 524-530.
- A. Kundu, P. Hariharan, K. Prabakaran and S. P. Anthony, *Spectrochimica Acta Part A: Molecular and Biomolecular Spectroscopy*, 2015, 151, 426-431.
54. Z. Li, H. Li, C. Shi, M. Yu, L. Wei and Z. Ni, *Spectrochimica Acta Part A: Molecular and Biomolecular Spectroscopy*, 2016, 159, 249-253.
55. N. Roy, A. Dutta, P. Mondal, P. C. Paul and T. S. Singh, *Sensors and Actuators B: Chemical*, 2016, 236, 719-731.
56. L. Wang, L. Yang and D. Cao, *Sensors and Actuators B: Chemical*, 2014, 202, 949-958.
57. W. Lin, L. Yuan, W. Tan, J. Feng and L. Long, *Chemistry—A European Journal*, 2009, 15, 1030-1035.
58. M. H. Lee, T. Van Giap, S. H. Kim, Y. H. Lee, C. Kang and J. S. Kim, *Chemical Communications*, 2010, 46, 1407-1409.
59. Adak AK, Purkait R, Manna SK, Ghosh BC, Pathak S, Sinha C. Fluorescence sensing and intracellular imaging of Pd²⁺ ions by a novel coumarinyl-rhodamine Schiff base. *New Journal of Chemistry*. 2019;43:3899-3906. DOI: 10.1039/c8nj06511j
60. Martinez VD, Vucic EA, Becker-Santos DD, Gil L, Lam WL. Arsenic exposure and the induction of human cancers. *Journal of Toxicology*. 2011;2011:1-13. DOI: 10.1155/2011/431287
61. Yu H-S, Liao W-T, Chai C-Y. Arsenic carcinogenesis in the skin. *Journal of Biomedical Science*. 2006;13(5):657-666. DOI: 10.1007/s11373-006-9092-8
62. Hong Y-S, Song K-H, Chung J-Y. Health effects of chronic arsenic exposure. *Journal of Preventive Medicine and Public Health*. 2014;47(5):245-252. DOI: 10.3961/jpmph.14.035
63. Hu S, Yan G, Wu C, He S. An ethanol vapor sensor based on a microfiber with a quantum-dot gel coating. *Sensors*. 2019;19(2):300. DOI: 10.3390/s19020300
64. Shah AQ, Kazi TG, Baig JA, Arain MB, Afridi HI, Kandhro GA, et al. Determination of inorganic arsenic species (As³⁺ and As⁵⁺) in muscle tissues of fish species by electrothermal atomic absorption spectrometry (ETAAS). *Food Chemistry*. 2010;119(2):840-844. DOI: 10.1016/j.foodchem.2009.08.0
65. P. A. Gale and C. Caltagirone, *Chemical Society Reviews*, 2015, 44, 4212-4227.
66. Z. Xu, X. Chen, H. N. Kim and J. Yoon, *Chemical Society Reviews*, 2010, 39, 127-137.
67. R. Badugu, J. R. Lakowicz and C. D. Geddes, *Journal of the American Chemical Society*, 2005, 127, 3635-3641.
68. S. Kumar, P. Singh, G. Hundal, M. S. Hundal and S. Kumar, *Chemical Communications*, 2013, 49, 2667-2669.
- B. R. Nicoleti, L. G. Nandi and V. G. Machado, *Analytical chemistry*, 2014, 87, 362-366.
69. Y.-L. Leng, J.-H. Zhang, Q. Li, Y.-M. Zhang, Q. Lin, H. Yao and T.-B. Wei, *New Journal of Chemistry*, 2016, 40, 8607-8613.
70. L. Yang, X. Li, J. Yang, Y. Qu and J. Hua, *ACS applied materials & interfaces*, 2013, 5, 1317-1326.





Satvinder Khatkar et al.,

71. Z. Yang, Z. Liu, Y. Chen, X. Wang, W. He and Y. Lu, Organic & biomolecular chemistry, 2012, 10, 5073-5076.
72. J. J. Lee, S. Y. Lee, K. H. Bok and C. Kim, Journal of fluorescence, 2015, 25, 1449-1459.
73. G. J. Park, I. H. Hwang, E. J. Song, H. Kim and C. Kim, Tetrahedron, 2014, 70, 2822-2828.
74. 127. Y.-L. Leng, J.-H. Zhang, Q. Li, Y.-M. Zhang, Q. Lin, H. Yao and T.-B. Wei, New Journal of Chemistry, 2016, 40, 8607-8613
75. J.-H. Hu, Y. Sun, J. Qi, P.-X. Pei, Q. Lin and Y.-M. Zhang, RSC Advances, 2016, 6, 100401-100406.
76. T. Wei, H. Li, Q. Wang, G. Yan, Y. Zhu, T. Lu, B. Shi, Q. Lin and Y. Zhang, Supramolecular Chemistry, 2016, 28, 314-320.
77. S. Sarveswari, A. J. Beneto and A. Siva, Sensors and Actuators B: Chemical, 2017, 245, 428-434.
78. C. Yu, C.-Y. Li, Y.-X. Sun, H.-R. Jia, J.-Q. Guo and J. Li, Spectrochimica Acta Part A: Molecular and Biomolecular Spectroscopy, 2017, 184, 249-254.
79. J. Mondal, A. K. Manna and G. K. Patra, Inorganica Chimica Acta, 2018, 474, 22-29.
80. K. Rezaeian, H. Khanmohammadi and S. G. Dogahneh, New Journal of Chemistry, 2018, 42, 2158-2166.
81. N. Kumari, S. Jha and S. Bhattacharya, Chemistry–An Asian Journal, 2012, 7, 2805-2812.
82. L. Tang, Y. Zou, K. Zhong and Y. Bian, RSC Advances, 2016, 6, 48351-48356.
83. T.-B. Wei, W.-T. Li, Q. Li, W.-J. Qu, H. Li, G.-T. Yan, Q. Lin, H. Yao and Y.-M. Zhang, RSC Advances, 2016, 6, 43832-43837.
84. K.-S. Lee, H.-J. Kim, G.-H. Kim, I. Shin and J.-I. Hong, Organic letters, 2008, 10, 49-51.
85. Y. Shiraishi, M. Nakamura, N. Hayashi and T. Hirai, Analytical chemistry, 2016, 88, 6805-6811.
86. Q. Lin, L. Liu, F. Zheng, P.-P. Mao, J. Liu, Y.-M. Zhang, H. Yao and T.-B. Wei, RSC Advances, 2017, 7, 38458-38462.
87. Yildirim, N.; Yildiz, M. A Schiff Base Sensor Selective to Anions, Biological Activity and Spectral Studies. J. Turkish Chem. Soc. Sect. A Chem. 2018, 5, 1271–1278
88. Orojloo, M.; Amani, S. A Highly Selective Chemosensor for Naked-Eye Detection of Fluoride and Aluminium (III) Ions Based on a New Schiff Base Derivative. Aust. J. Chem. 2016, 69, 911–918.
89. Jana, S.; Dalapati, S.; Alam, M. A.; Guchhait, N. Spectroscopic, Colorimetric and Theoretical Investigation of Salicylidene Hydrazine Reduced Schiff Base and Its Application towards Biologically Important Anions. Spectrochim Acta A Mol Biomol Spectrosc 2012, 92, 131–136.
90. Liu, G.; Shao, J. Ratiometric Fluorescence and Colorimetric Sensing of Anion Utilizing Simple Schiff Base Derivatives. J. Incl. Phenom. Macrocycl. Chem. 2013, 76, 99–105.
91. Jin, R.; Sun, W. Theoretical Study of Thiourea Derivatives as Chemosensors for Fluoride and Acetate Anions. Sci. China Chem. 2012, 55, 1428–1434
92. Dini, S.; Khanmohammadi, H. A New Azo-Azomethine Sensor for Detection of CN and AcO⁻ Anions: Highly Selective Chemosensor for Naked Eye Detection of Sodium Diclofenac. Spectrochim. Acta, Part A 2019, 222, 117157.
93. Yildirim, N.; Yildiz, M. A Schiff Base Sensor Selective to Anions, Biological Activity and Spectral Studies. J. Turkish Chem. Soc. Sect. A Chem. 2018, 5, 1271–1278.
94. Chakraborty, N.; Chakraborty, A.; Das, S. Schiff Base Derived from Salicylaldehyde-Based Azo Dye as Chromogenic Anionic Sensor and Specific Turn-on Emission Sensor for Cyanide Ion. J. Heterocyclic Chem. 2019, 56, 2993–2999.
95. Sahu, S.; Sikdar, Y.; Bag, R.; Maiti, D. K.; Ceron-Carrasco, J. P.; Goswami, S. Visual Detection of Fluoride Ion Based on ICT Mechanism. Spectrochim Acta A Mol Biomol Spectrosc 2019, 213, 354–360.
96. Singh, A.; Mohan, M.; Trivedi, D. R. Design and Synthesis New Colorimetric Receptors for Naked-Eye Detection of Biologically Important Fluoride and Acetate Anions in Organic and Arsenite in Aqueous Medium Based on ICT Mechanism: DFT Study and Test Strip Application. Spectrochim. Acta, Part A 2020, 225, 117522.
97. Parchegani, F.; Orojloo, M.; Zendeheidi, M.; Amani, S. Simultaneous Measurement of Hydrogen Carbonate and Acetate Anions Using Biologically Active Receptor Based on Azo Derivatives of Naphthalene. Spectrochim. Acta, Part A 2020, 229, 117925.
98. Dalapati, S.; Alam, M. A.; Jana, S.; Saha, R.; Guchhait, N. Reusable Anion Detection Kit: An Aqueous Medium Anion Detection. Sens. Actuators, B 2012, 162, 57–62.



**Satvinder Khatkar et al.,**

98. Dalapati, S.; Alam, M. A.; Jana, S.; Guchhait, N. Naked-Eye Detection of F and AcO Ions by Schiff Base Receptor. *J. Fluorine Chem.* 2011, 132, 536–540.
99. Uahengo, V.; Naimhwaka, J.; Daniel, L. S.; Rahman, A.; Elzagheid, M. I.; Rhyman, L.; Ramasami, P.; Cai, P. A Colorimetric Probe for the Real-Time Naked Eye Detection of Cyanide and Hydroxide Ions in Tap Water: experimental and Theoretical Studies. *Analyst* 2019, 144, 6422–6431.
100. Singh, A.; Tom, S.; Trivedi, D. R. Aminophenol Based Colorimetric Chemosensor for Naked-Eye Detection of Biologically Important Fluoride and Acetate Ions in OrganoAqueous Medium: Effective and Simple Anion Sensors. *J. Photochem. Photobiol, A* 2018, 353, 507–520.
101. Naimhwaka, J.; Uahengo, V. A Naphthoquinone Based Colorimetric Probe for Real-Time Naked Eye Detection of Biologically Important Anions Including Cyanide Ions in Tap Water: experimental and Theoretical Studies. *RSC Adv.* 2019, 9, 37926–37938
102. Reena, V.; Suganya, S.; Velmathi, S. Synthesis and Anion Binding Studies of azo-Schiff Bases: Selective Colorimetric Fluoride and Acetate Ion Sensors. *J. Fluorine Chem.* 2013, 153, 89–95.
103. Goswami, S.; Das, A. K.; Sen, D.; Aich, K.; Fun, H.-K.; Quah, C. K. A Simple Naphthalene-Based Colorimetric Sensor Selective for Acetate. *Tetrahedron Lett.* 2012, 53, 4819–4823
104. W.AIZoubi. Al Mohanna / *Spectrochimica Acta Part A: Molecular and Biomolecular spectroscopy* 132 (2014) 854-870
105. Poonam Kaswan (2023). "Chalcogenated Schiff base ligand derived from metal ion detection" Review 2023: volume 556, 12160 ". <https://doi.org/10.1016/j.ica.2023.121610>
106. Sabeel M.etall. "Recent advancement in Schiff base Fluorescence Chemosensors for the detection of heavy metal ion" doi: 10.5772/intechopen.109022
107. Feyza kolcua, b, digdemErdener and Ismetkayaa. "A schiff base based on triphenylamine and thiophene moieties as a fluorescent sensor for Cr(III) ions:Synthesis,characterisation and fluorescent applications" DOI: <https://doi.org/10.1016/j.ica.2020.119676>
108. Parthiban et al. " Selective colorimetric sensing of fluoride ion via H-bonding in 80% aqueous solution by transition metal complex"<https://doi.org/10.1016/j.snb.2017.01.153>
109. Dey, S.; Sen, C.; Sinha, C. Chromogenic Hydrazide Schiff BaseReagent: Spectrophotometric Determination of CN- Ion.*Spectrochim. Acta, Part A* 2020, 225, 117471. DOI: 10.1016/j.saa.2019.117471.
110. Parchegani, F.; Orojloo, M.; Zendehtdel, M.; Amani, S. Simultaneous Measurement of Hydrogen Carbonate and Acetate Anions Using Biologically Active Receptor Based on Azo Derivatives of Naphthalene. *Spectrochim. Acta, Part A* 2020, 229, 117925. DOI: 10.1016/j.saa.2019.11792





Nano-Empowerment: Revolutionizing Renewable Energy Through Sustainable Nanotechnology Applications

Pariksha Bishnoi and Samarjeet Singh Siwal *

Department of Chemistry, M.M. Engineering College, Maharishi Markandeshwar (Deemed to be University), Mullana- Ambala, Haryana, India.

Received: 22 Jan 2024

Revised: 09 Feb 2024

Accepted: 30 May 2024

*Address for Correspondence

Samarjeet Singh Siwal

Department of Chemistry,
M.M. Engineering College,
Maharishi Markandeshwar (Deemed to be University),
Mullana- Ambala, Haryana, India
Email: samarjeet6j1@gmail.com



This is an Open Access Journal / article distributed under the terms of the **Creative Commons Attribution License** (CC BY-NC-ND 3.0) which permits unrestricted use, distribution, and reproduction in any medium, provided the original work is properly cited. All rights reserved.

ABSTRACT

The global pursuit of sustainable energy solutions has intensified recently, catalyzing innovative approaches to harness renewable resources. Nanotechnology has emerged as a transformative force in this quest, offering unprecedented opportunities to revolutionize the renewable energy landscape. This paper delves into the multifaceted role of nanotechnology in driving sustainable advancements within renewable energy domains. By exploring various applications, such as nanomaterial-enhanced solar cells, nanostructured catalysts for fuel cells, and nanocomposites for energy storage, this study elucidates how nanotechnology enables enhanced efficiency, cost-effectiveness, and environmental sustainability in renewable energy systems. Moreover, it examines the pivotal role of nanoscience in addressing key challenges, including scalability, stability, and performance optimization. Through a comprehensive analysis of recent developments and future prospects, this research underscores the immense potential of sustainable nanotechnology applications in fostering a cleaner, more resilient energy future.

Keywords: Nanotechnology, Renewable energy and Sustainability

INTRODUCTION

Nanotechnology has become a ubiquitous force in global industries, especially in developed regions, nanoscale markets have expanded rapidly in the past decades. This transformative technology, now considered a versatile tool, encompasses four generations of nanomaterials(NM): within the realm of nanotechnology, there are active and passive nano assemblies, general nanosystems, and small-scale molecular nanosystems. These categories represent a progression in nanotechnology's evolution, showcasing its versatility in interdisciplinary scientific fields. From



**Pariksha Bishnoi and Samarjeet Singh Siwal**

specialized functionalities in active nanoassemblies to the precision of small-scale molecular nanosystems, nanotechnology continues to revolutionize various sectors, driving innovation and shaping the technological landscape [1]. Advancements in science and technology drive the adoption of cost-effective, safe, and cleaner alternatives over older technologies. Given the global concern over depleting natural resources and their financial implications, nanotechnology emerges as a viable solution. Nanotechnology offers a gateway to address these challenges by providing innovative and efficient technologies that align with sustainability goals. Its potential to offer resource-efficient and environmentally friendly solutions makes it a key player in the pursuit of cleaner and more economically viable technologies for the scientific community [2]. Our civilization confronts a critical challenge: developing an economically viable path to global sustainable energy. The task is to efficiently capture abundant yet intermittent solar energy, converting it into high-density and easily storable forms to meet our forecasted energy needs. The goal is to harness the essentially limitless solar resource for long-term sustainability [3]. Researchers aim to enhance light trapping in ultra-thin film solar cells (SCs) through various studied methods [4]. This review elucidates the role of nanotechnology in the advanced development of alternating sources of energy involving energy conversion and energy storage devices as showcased in **Fig. 1**. Firstly, we start with different nanomaterials and photovoltaics (PVs) which have been utilized to increase the efficiency of SCs followed by the advancement in wind energy (WE) conversion and storage system with the utilization of nanomaterials. Further, the role of nanotechnology in batteries and supercapacitors have been demonstrated. Finally, we spot a light on existing challenges and future prospects of nanotechnology in revolutionizing the renewable energy systems.

Harnessing solar energy

Harnessing solar energy (SE) refers to the process of capturing and utilizing the radiant energy emitted by the sun for various practical purposes. Harnessing SE is a sustainable and renewable approach to meet energy needs while reducing dependence on non-renewable resources and minimizing environmental impact. The Earth receives 1,24,000 terawatts of solar power at its surface, with only about 0.07% utilized by photosynthetic organisms. This underscores the immense untapped potential for capturing and utilizing solar energy more efficiently [5].

Nanostructured photovoltaics

Nanostructured photovoltaics revolutionize SE by utilizing materials at the nanoscale to enhance the efficiency of solar cells (SC). Nanomaterials and nanostructures show great potential in boosting SC performance by enhancing light trapping and photocarrier collection. Their ability to be fabricated inexpensively opens the door to cost-effective production of photovoltaics (PV) [6].

Improving solar panel efficiency through nanomaterials

Sun is abundant source of SE but sunlight available during the daylight hours, necessitating the need for storage. Different nanomaterials have been utilized in SE storage system in energy saving and improving the energy efficiency with reduction in global warming [7]. In residential, commercial, and industrial sector, SE system can be used to produce electricity instead of the utilization of fossil fuels for cooling and heating purposes in economical friendly way. For instance, cold air of winters can be used during summers for air conditioning and on the other side, heat generated by solar collectors in summers can be used to heat winters [8]. Different nanomaterials have been studied for SE storage system. For example, Aguilar and co-workers [9] prepared nanofluids based on TiO_2 nanoparticles for concentrating solar power (CSP) plants by one-step solvo thermal and two-step ultrasonic method. For nanofluid prepared via one-step method, thermal conductivity was surged up to 31.4% and for nanofluid prepared by two step, thermal conductivity was surged up to 52.7% at higher temperatures. The authors studied that these nanofluids can be considered as suitable heat transfer fluids for CSP plants due to the improvement of heat transfer coefficient up to 35%.

Thin-film solar cells and nanotechnology innovations

Thin-film SCs are seen as an important way to cut down the cost of making PVs in the short to medium term. Thin film SCs are cost-effectively produced by utilizing an additive deposition process on affordable substrates like glass, metal foil, or plastic. However, thin cells are usually not as efficient as thicker ones for two main reasons: first, they



**Pariksha Bishnoi and Samarjeet Singh Siwal**

have a hard time absorbing all the sunlight without special methods to trap light or unique compositions; secondly, thin film cells are often not as good because they are made up of polycrystalline or amorphous. This leads to more places where the energy is lost, making them less efficient[10]. Thin-film technologies, employing materials like CdTe, copper indium gallium diselenide(CIGS), and amorphous or micro/nanocrystalline silicon, share a common attribute: a direct band gap. This characteristic enables highly efficient light absorption even with minimal thickness [11].

Advanced in wind energy

Over the previous decade, there has been swift progress and research in wind energy (WE) conversion systems and the accompanying enabling technologies. Integrating wind turbine into the integral design of buildings presents a promising strategy to encourage on-site renewable energy conversion in the urban area. However, there is not much information about how well wind turbine works, wind speeds in cities, and how the generated wind power gets connected to the grid [12].

Nanomaterials for lightweight and stronger wind turbine blades

Nanoparticle (NP)-reinforced composite materials are becoming increasingly popular among researchers and industry due to their surprising properties. Basically, ensuring the extended lifespan of wind turbine blades involves a need for a high strength to weight ratio, fatigue life, low weight, and stiffness. SiO_2 and Al_2O_3 nanocomposites with varying ratios of NPs are created and examined to assess their suitability for use in wind turbine rotor blade structures[13]. The incorporation of nanomaterials into composites imparts advanced properties to the combination, making nanocomposites desirable material systems for wind turbine blades due to their low weight, high strength, and other superior properties [14].

Enhancing efficiency and durability of wind turbines with nanotech coatings

Nanotechnology holds promise for enhancing the efficiency and durability of wind turbines that captures SE. Advanced composite materials such as carbon nanofibers (CNFs) and electrospun polymer nanofibers can improve properties of wind turbine blades such as vibration damping, shock and friction resistance, and water blockage[15, 16]. These nanocomposite coatings can significantly increase the damping ratio of the blades and reduce wear rates, leading to improved structural stability and longevity [17]. Additionally, the use of nanofibers interleaving in composite laminates can enhance fracture toughness, resistance, and fatigue properties, without compromising other mechanical properties [18]. The incorporation of NPs reinforcement, like carbon nanotubes (CNT), can enhance the toughness, fatigue resistance, and electrostatic properties of wind turbine blades[19]. Overall, the implementation of nanotechnology in wind turbine blade design can contribute to the efficient and durable harnessing of SE.

Nanogenerators: Harvesting wind energy at micro/nano scales

Nanogenerators are devices that can harvest energy from various sources, including wind and SE, at micro/nano scales. These devices employ diverse mechanism to transform mechanical or thermal energy into electrical energy. For WE harvesting, micro-nano energy harvesters have been developed to scavenge energy from low-speed wind flows, which traditional wind farms cannot efficiently utilize[20]. These micro-nano energy harvesters employ different transduction mechanisms and materials to convert wind-induced excitations into electrical energy [21]. Alternatively, in harvesting SE, a demonstrated hybrid nanogenerator combining a triboelectric nanogenerator (TENG) with a PV cell. This hybrid nanogenerator can simultaneously collect and transmit swinging mechanical energy and SE wirelessly[22]. These advancements in nanogenerators provide promising methods for harnessing wind and SE at micro/nano scales, contributing to the development of sustainable and efficient energy sources [23, 24].

Nano-enabled energy storage

Nano-enabled energy storage harnesses storage energy by utilizing nanomaterials and nanocrystals to improve the performance and capabilities of energy storage devices like batteries and supercapacitors. Nanomaterials offer advantages such as high surface area, fast ion diffusion, and improved electronic conductivity, leading to higher energy and power densities in storage devices[25, 26].



**Pariksha Bishnoi and Samarjeet Singh Siwal****Nanomaterials in batteries for enhanced capacity and lifespan**

Nanomaterials like graphene oxide and carbon nanotubes show promise in boosting battery capacity and lifespan. Their high electrical conductivity and stability facilitate efficient charge transfer and electrolyte diffusion, addressing challenges in traditional batteries. These nanomaterials offer increased active sites for electrochemical reactions, enhancing overall battery capacity, while their stability contributes to prolonged lifespan by maintaining structural integrity. In summary, integrating carbon nanomaterials into batteries has the potential to revolutionize energy storage with improved performance and durability[27]. Nanomaterials have shown promise in enhancing the capacity and lifespan of batteries for energy storage [28]. Nanomaterials, such as quantum dots (QDs), offer high specific surface area, allowing for easy penetration of electrolytes and advantageous high energy/power density application[29].

Supercapacitors and nanotechnology: rapid energy storage

Owing to long cycle life, and high power capabilities supercapacitors are considered as excellent energy storage device for both on-board and stationary applications [30]. Both the electrode and the electrolyte are pivotal for the performance of supercapacitors. Numerous nanomaterials have been explored as electrodes for supercapacitors which showed significantly high electrocatalytic performance[31]. Carbon based nanomaterials, metal and metal-oxides, polymeric materials and their composites have been used to modify the surface of electrode of supercapacitors. The most frequently utilized material for supercapacitor electrode is carbon. Carbon electrodes can be produced in various 1D to 3D structures like foams, fibers, and nanotubes. Activated carbon (AC) serves as the active electrode material for supercapacitors owing to its high specific surface area ($1000-2000 \text{ m}^2 \text{ g}^{-1}$) and cost-effectiveness. The study found a significant capacitance in mesoporous carbon with small pores, suggesting partial ion desolvation may be the cause of this capacitance [30]. Sheoran *et.al*[32] prepared an innovative nanocomposite electrode substance for use in supercapacitors. The electrode material of the composite for supercapacitor applications is composed of the carbon black anchored bismuth-tungstate-aniline complex ($\text{Bi}_2(\text{WO}_4)_3/\text{Aniline/CB}$) (BTACB) nanocomposite. Exhibiting impressive cycling stability and a specific capacitance of 306 F/g at a current density (CD) of 1 A/g , the BTACB nanocomposite showed favorable electrochemical attributes.

Future prospects and challenges

Future dimensions of nano-empowerment in renewable energy include utilizing nanotechnology-based processing strategies to transform agricultural waste into energy resources[33]. There are challenges that need to be addressed. Firstly, the current manufacturing processes for nanomaterials are energy-intensive and rely on non-renewable resources, which is not sustainable in the long term[34]. Secondly, there is a lag between the rapid growth in the innovation of unsustainable nanomaterials and their long-term effects on the environment, human health, and climate[35].

CONCLUSION

Nanotechnology has emerged as a transformative force in driving sustainable advancements within renewable energy domains, offering opportunities to revolutionize the renewable energy landscape. Nanomaterials and nanostructures show significant promise in boosting the performance of SCs by augmenting light trapping and photocarrier collection, leading to enhanced efficiency and cost-effective production of PVs. Nanotechnology is crucial in shaping energy storage devices like batteries and supercapacitors, providing benefits like increased surface area, fast ion diffusion, and improved electronic conductivity.

REFERENCES

1. Zelzer, M. and R.V. Ulijn, *Next-generation peptide nanomaterials: molecular networks, interfaces and supramolecular functionality*. Chemical Society Reviews, 2010. **39**(9): p. 3351-3357.





Pariksha Bishnoi and Samarjeet Singh Siwal

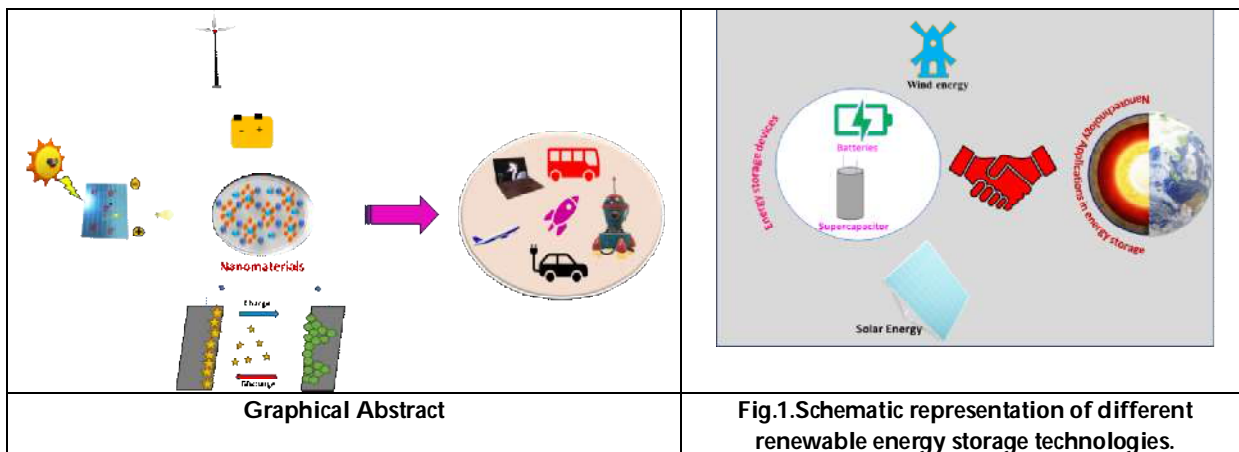
2. Malik, S., K. Muhammad, and Y. Waheed *Nanotechnology: A Revolution in Modern Industry*. Molecules, 2023. **28**, DOI: 10.3390/molecules28020661.
3. Baxter, J.B., et al., *Nanoscale design to enable the revolution in renewable energy*. Energy & Environmental Science, 2009. **2**: p. 559.
4. Zarerasouli, P., H. Bahador, and H. Heidarzadeh, *Performance improvement of an ultra-thin film solar cell based on optimized CIGS (Cu(In_{1-x}Gax)Se₂) using appropriate plasmonic nanoparticles*. Optical Materials, 2022. **131**: p. 112729.
5. Tanvir, R.U., et al., *Harnessing solar energy using phototrophic microorganisms: A sustainable pathway to bioenergy, biomaterials, and environmental solutions*. Renewable and Sustainable Energy Reviews, 2021. **146**: p. 111181.
6. Sagadevan, S. *RECENT TRENDS ON NANOSTRUCTURES BASED SOLAR ENERGY APPLICATIONS : A REVIEW*. 2013.
7. İnada, A.A., S. Arman, and B. Safaei, *A novel review on the efficiency of nanomaterials for solar energy storage systems*. Journal of Energy Storage, 2022. **55**: p. 105661.
8. Gao, L., J. Zhao, and Z. Tang, *A Review on Borehole Seasonal Solar Thermal Energy Storage*. Energy Procedia, 2015. **70**: p. 209-218.
9. Aguilar, T., et al., *Improving stability and thermal properties of TiO₂-based nanofluids for concentrating solar energy using two methods of preparation*. Journal of Thermal Analysis and Calorimetry, 2021. **144**(3): p. 895-905.
10. Tsakalakos, L., *Nanostructures for photovoltaics*. Materials Science and Engineering: R: Reports, 2008. **62**(6): p. 175-189.
11. Righini, G.C. and F. Enrichi, *Chapter One - Solar cells' evolution and perspectives: a short review*, in *Solar Cells and Light Management*, F. Enrichi and G.C. Righini, Editors. 2020, Elsevier. p. 1-32.
12. Tan, J.D., et al., *Advancements of wind energy conversion systems for low-wind urban environments: A review*. Energy Reports, 2022. **8**: p. 3406-3414.
13. Muhammed, K.A., C. Ramesh Kannan, and B. Stalin, *Performance analysis of wind turbine blade materials using nanocomposites*. Materials Today: Proceedings, 2020. **33**: p. 4353-4361.
14. Thomas, L. and M. Ramachandra, *Advanced materials for wind turbine blade- A Review*. Materials Today: Proceedings, 2018. **5**(1, Part 3): p. 2635-2640.
15. Liang, F., et al., *Multifunctional nanocomposite coating for wind turbine blades*. International Journal of Smart and Nano Materials, 2011. **2**(3): p. 120-133.
16. Panduranga, R., Y. Alamoudi, and A. Ferrah. *Nanoengineered Composite Materials for Wind Turbine Blades*. in *2019 Advances in Science and Engineering Technology International Conferences (ASET)*. 2019.
17. Buyuknalcaci, F.N., et al., *24 - Carbon nanotube-based nanocomposites for wind turbine applications*, in *Polymer-based Nanocomposites for Energy and Environmental Applications*, M. Jawaid and M.M. Khan, Editors. 2018, Woodhead Publishing. p. 635-661.
18. Marsh, G., *Composites help improve wind turbine breed*. Reinforced Plastics, 2005. **49**(4): p. 18-22.
19. Muzammil, W.K., et al., *Nanotechnology in Renewable Energy: Critical Reviews for Wind Energy*, in *Nanotechnology: Applications in Energy, Drug and Food*, S. Siddiquee, G.J.H. Melvin, and M.M. Rahman, Editors. 2019, Springer International Publishing: Cham. p. 49-71.
20. Adhikari, A. and J. Sengupta, *Chapter 8 - Nanogenerators: a new paradigm in blue energy harvesting*, in *Nano Tools and Devices for Enhanced Renewable Energy*, S. Devasahayam and C.M. Hussain, Editors. 2021, Elsevier. p. 171-193.
21. Shi, H., et al., *Structure design and wireless transmission application of hybrid nanogenerators for swinging mechanical energy and solar energy harvesting*. Nanoscale, 2022. **14**(30): p. 10972-10979.
22. Mariello, M., et al., *Chapter 13 - Micro- and nanodevices for wind energy harvesting*, in *Nano Tools and Devices for Enhanced Renewable Energy*, S. Devasahayam and C.M. Hussain, Editors. 2021, Elsevier. p. 291-374.
23. Gan lin, L. and Y. Xin. *Triboelectric nanogenerators for wind energy harvesting*. in *Proc.SPIE*. 2022.
24. Le, X., X. Guo, and C. Lee *Evolution of Micro-Nano Energy Harvesting Technology—Scavenging Energy from Diverse Sources towards Self-Sustained Micro/Nano Systems*. Nanoenergy Advances, 2023. **3**, 101-125 DOI: 10.3390/nanoenergyadv3020006.





Pariksha Bishnoi and Samarjeet Singh Siwal

25. Pomerantseva, E., et al., *Energy storage: The future enabled by nanomaterials*. Science, 2019. **366**(6468): p. ean8285.
26. Raj, R., R. Verma, and J. Singh, *Nanomaterials for Energy Storage Applications*, in *Bioenergy Research: Integrative Solution for Existing Roadblock*, M. Srivastava, N. Srivastava, and R. Singh, Editors. 2021, Springer Singapore: Singapore. p. 135-156.
27. Yu, Y. and H. Xia, *Carbon-Based Nanomaterials for Metal-Air Batteries*, in *Carbon-Based Nanomaterials for Energy Conversion and Storage: Applications in Electrochemical Catalysis*, J.-N. Zhang, Editor. 2022, Springer Nature Singapore: Singapore. p. 249-270.
28. Das, H., et al., *Nanomaterials for next generation energy storage applications*. MRS Communications, 2022. **12**(3): p. 285-294.
29. Arif, N.A., et al., *Advances in Electrode Materials for Rechargeable Batteries*, in *Nanomaterials for Innovative Energy Systems and Devices*, Z.H. Khan, Editor. 2022, Springer Nature Singapore: Singapore. p. 243-318.
30. Afif, A., et al., *Advanced materials and technologies for hybrid supercapacitors for energy storage – A review*. Journal of Energy Storage, 2019. **25**: p. 100852.
31. Karamveer, S., V.K. Thakur, and S.S. Siwal, *Synthesis and overview of carbon-based materials for high performance energy storage application: A review*. Materials Today: Proceedings, 2022. **56**: p. 9-17.
32. Sheoran, K., et al., *An Aniline-Complexed Bismuth Tungstate Nanocomposite Anchored on Carbon Black as an Electrode Material for Supercapacitor Applications*. ChemistrySelect, 2023. **8**(42): p. e202301878.
33. Palit, S., C.M. Hussain, and S. Mallakpour, *Sustainable Future with Nanoproducts*, in *Handbook of Consumer Nanoproducts*, S. Mallakpour and C.M. Hussain, Editors. 2022, Springer Nature Singapore: Singapore. p. 1409-1431.
34. Zhang, Y., et al. *Sustainable Nanomaterials for Biomedical Applications*. Pharmaceutics, 2023. **15**, DOI: 10.3390/pharmaceutics15030922.
35. Sun, H. *Grand Challenges in Environmental Nanotechnology*. in *Frontiers in Nanotechnology*. 2019.





Polyethersulfone (PES) based, GO-ZnO embedded Membrane for the Fast and Efficient Separation of Oil from Oil Water Mixtures

Rohit Goyat and Joginder Singh^{1*}

Department of Chemistry, Maharishi Markandeshwar (Deemed to be University), Mullana, Ambala, Haryana, India.

Received: 22 Jan 2024

Revised: 09 Feb 2024

Accepted: 30 May 2024

*Address for Correspondence

Joginder Singh

Department of Chemistry,
Maharishi Markandeshwar
(Deemed to be University),
Mullana, Ambala, Haryana, India
Email: joginderchem@mmumullana.org



This is an Open Access Journal / article distributed under the terms of the **Creative Commons Attribution License** (CC BY-NC-ND 3.0) which permits unrestricted use, distribution, and reproduction in any medium, provided the original work is properly cited. All rights reserved.

ABSTRACT

Oil-related incidents have increased the amount of oily water and soluble toxins over the last few years, which have a significant negative impact on the ecosystem and the environment. Thus, there is a great deal of interest in the creation of hydrophilic substances due to the potential for oil/water separation. In the present study, we have designed a hydrophilic membrane composed of polyethersulfone (PES) and GO-ZnO nanocomposites. The resulting composite membrane demonstrated excellent mechanical stability, high oil-water separation efficiency, and excellent reusability after seven consecutive cycles. When compared to a pure PES membrane, the membrane's contact angle reduced from 115° to 85°, while its pore size and density were also improved. Furthermore, the membrane retained its hydrophilicity after sanding (100 times) and bending (200 times) tests. Additionally, the prepared membrane performed excellently in separating oil-in-water mixtures, with separation efficiencies of more than 96% for petrol, 95% for diesel and 88% for crude oil in the first filtration cycle.

Keywords: Graphene Oxide-ZnO, GO-ZnO/Polyethersulfone, Filtration

INTRODUCTION

The refining and production process generates a significant amount of oil/water (O/W) mixtures, which cause a severe hazard to the atmosphere and human health when discharged into rivers and oceans [1-4]. The potential to separate out emulsified O/W mixtures using skimming, centrifugation, air flotation, sponge absorption, and other traditional procedures exists, but they are not efficient or cost-effective [5-10]. Moreover, they are inefficient at separating tiny oil droplets from water, necessitating for extra treatment. Organic materials that are hazardous and



**Rohit Goyat and Joginder Singh**

tough for nature to decompose are frequently detected in effluents. Aromatic dyes in pollutants may reduce the rate of photosynthesis, diminish oxygen dissolution, and obstruct solar light penetration, which may alter the balance of the aquatic ecosystem [11-14]. Some aromatic pollutants are extremely dangerous to human beings because they are mutagenic or carcinogenic. Membrane technology has become a strong contender for O/W separation and is essential in industrial applications due to its high efficiency as well as minimal energy need [15]. The major superiority of using membranes includes high solid retentivity, cost-effectiveness, process flexibility, environmental friendliness, and small footprints [16]. Nano-filtration (NF), micro-filtration (MF), reverse osmosis (RO) and ultra-filtration (UF) are the different types of membrane technology [17, 18]. UF is currently used extensively because it is more effective at separating out pollutants and has stronger anti-fouling properties [18]. Among various polymers, Polyethersulfone (PES) is an extensively used polymer for water treatment membrane materials because of its high durability and good mechanical properties [19, 20]. However, the hydrophobic character of PES membranes causes membrane fouling, resulting in a decline in water flux, increased energy consumption, and high maintenance requirements [21, 22]. To overcome these drawbacks, some organic and inorganic additives should be doped to the membrane matrix. Some surface modification methods viz; blending, coating, and surface grafting also enhance membrane performance. Blending is the most basic way among these modifications to boost membrane performance [23, 24]. Currently, inorganic nanoscale materials are now widely employed in membrane preparation via the blending process due to their multiple advantages. These blended inorganic materials may generate tiny dimensions, consistent pores on the membrane surface with additional stability, and good hydrophilicity [21-24]. In addition, they may improve mass transfer, enhance the selectivity in separation applications, and reduce fouling. The most frequent inorganic particles used in membrane fabrication are as follows: AgO, ZnO, GO, TiO₂, SiO₂, CNT, and Al₂O₃. Among all of these, GO is the rising nanoparticle owing to its extraordinary properties viz; large surface area, numerous active sites with various functional groups, light weight, sp² hybridized, high mechanical strength, and layered structure. Doping of ZnO nanoparticles into PES membranes has resulted in a low flux decline with improved permeability, as reported in previous studies. For example, Leo et al. concluded that oleic acid drastically decreased the hydrophobic nature of the ZnO/Psf membrane and enhanced fouling resistance [25]. However, as noticed in research conducted by Shen et al. and Balta et al. [26], the incorporation of zinc oxide nanoparticles to PVDF membranes had a small impact on the elimination of model foulant. In this work, we prepared GO-ZnO embedded PES membranes having DMAc as the solvent and PVP as a pore-forming ingredient to investigate the performance of the membranes to separate oil-water emulsions.

EXPERIMENTAL DETAILS

MATERIALS

Polyethersulfone (PES) was taken as the main source to prepare a membrane. To dissolve the polymer, Dimethylacetamide (DMAc) was utilized as a solvent. Polyvinylpyrrolidone (PVP), sodium dodecyl sulfate (SDS), methylene blue (MB), zinc acetate (Zn(CH₃COO)₂), and sodium hydroxide pellets were procured from Sigma-Aldrich. None of the above chemicals were further purified before consumption. All preparations were made using freshly distilled water.

Synthesis of GO-Zinc oxide nanocomposites

GO was produced using the process detailed in our earlier study [27, 28]. The 100 mg earlier prepared GO powder and 200 mg zinc acetate were dissolved in the 200ml water in a conical flask at 40°C for 2 hours. Then 500 mg sodium hydroxide pellets were added slowly into the above suspension and stir the mixture at 70°C for next 4 hours. Further, the suspension was allowed to cool, centrifuged, and washed with distilled water and ethanol to get rid of impurities. The final product was dried in a hot air oven and then calcined at 400°C for 4 hours.





Rohit Goyat and Joginder Singh

Preparation of Membranes

The pure and hybrid membranes were prepared employing the phase inversion technique [21-25]. A homogeneous polymer solution was made using PES (14 wt%), PVP (2 wt%), and DMAc. After the polymers had completely dissolved, different concentrations of GO-ZnO nanoparticles were added. Once the mixture had reached a constant consistency, it was vigorously stirred for about 10 hours. Now the resulting mixture was casted over the glass plate using a doctor blade. After 30 seconds in the air, the glass plate was submerged in a freshwater container. In order to entirely eliminate the solvent from the film, the synthesized membrane was submerged in water for 6-7 hours.

Characterization of GO-ZnO Nanoparticles and Prepared Membranes

The GO-ZnO nanoparticles synthesized were characterized using FESEM and energy-dispersive X-ray spectroscopy. The prepared membrane was also characterized for its hydrophilicity, surface morphologies, mechanical strength, and pore size analysis [29, 30]. The mechanical strength of the membrane was evaluated by subjecting it to abrasion and folding 100 times. Goniometer was used to measure the produced membranes hydrophilicity. First, the membranes were dried out and then, the contact angles (CAs) prepared membranes were measured. The membrane pore size was calculated by cutting dry membrane samples (Pure PES membranes and GO-ZnO embedded membranes) to a specific size and kept them in water for 12 hours. The membranes were then weighed and air dried for 24 hours. The weight in the dry state was measured to analyze the membrane porosity (ϵ) using equation 1:

$$\epsilon = (\omega_2 - \omega_1) / (A \times l \times \rho_w) \times 100 \quad \dots\dots\dots(1)$$

where ω_2 is the weight of the wet membrane, ω_1 is the weight of the dry membrane (g), A (cm²) is the area of the membrane, l is the thickness of the membrane (0.022 cm), and ρ_w is the water density (998 g/cm³). The permeability of the synthesized membranes (Pure PES membrane and GO-ZnO PES membrane) was also calculated using equation 2:

$$J = V / (s \times t) \quad \dots\dots\dots(2)$$

where J is the water flux (L m⁻² h⁻¹), V is the permeate volume (L), s is the used membrane area (m²), and t is the time (hr).

Separation of Oil-Water Samples

Filtration experiments were conducted to separate oil-water emulsions from laboratory-prepared samples using the prepared membranes. Three different types of oils were mixed with water in a (1:5) ratio, and sodium dodecyl sulfate (SDS) was used as an emulsifier to emulsify the prepared samples [31-34]. In order to assess the membrane's capacity for adsorbing coloured dye, a very little quantity of MB was introduced to one sample. Utilising equation 3, the oil removal percentage was calculated:

$$\%R = [(C_i - C_e) / C_i] \times 100 \quad \dots\dots\dots(3)$$

where C_i and C_e are the initial and final concentrations of oil in the water solution.

RESULTS AND DISCUSSION

Characterization of GO-ZnO Nanocomposites

The morphology of the synthesized GO-ZnO nanocomposites was examined using FESEM and HRTEM. As shown in Figure 1, there was no significant agglomeration of ZnO nanocomposites on the surface of GO sheets. Spherically round or petal-shaped nanoparticles were observed, which were well-distributed over the surface of the GO sheets [21, 22]. The elemental analysis of the nanocomposite was confirmed using EDX, which showed the presence of carbon, oxygen, and zinc [21-24]. These findings support the notion that the GO-ZnO nanocomposite was successfully synthesized.



**Rohit Goyat and Joginder Singh****Characterization of the Membranes**

After confirming the synthesis of the nanocomposites, they were blended into the preparation of membranes in different ratios for further applications. The prepared membranes were analyzed using FESEM, and the results were encouraging as depicted in Fig. 2. The nanocomposites were evenly distributed over the surface of the polyethersulfone supporting layer, and the pores were equally distributed with proper radii or pore diameter. The inclusion of these nanocomposites enhanced the thickness of the prepared hybrid membrane due to the formation of figure-like projections between the top and dense layer [35]. These macro gaps and projections improved the membrane's hydrophilicity and made it easier for water to pass through the membrane. Figure 3 shows that the membrane's increased hydrophilicity is evidenced by the contact angle's decrease from 115° to 85°. A lower contact angle indicates higher water flux and lower chances of membrane fouling [15-18]. The low rate of water flux and hydrophobicity are the two primary reasons for membrane fouling. Due to the increase in pore counts and hydrophilicity of the made membrane, the water permeability of the composite membrane was raised five times following the doping of nanocomposites. The mechanical stability of the prepared membrane is critical for withstanding harsh realistic environments. Its mechanical stability was tested using various methods, including abrasion, folding, soaking in water, and drying more than 100 times [35]. The results were remarkable. The constructed membrane was subjected to abrasion and folding tests, as seen in Figure 3. A weight of 50 g was employed to evaluate the membrane's abrasion resistance while it was mounted on mesh sandpaper. The membrane retained its hydrophilicity after 100 circular motions on sandpaper, demonstrating outstanding anti-abrasion capabilities. Additionally, after being folded 200 times, the membrane's surface did not detach or crack, proving the membrane's strong mechanical stability after the inclusion of nanocomposites.

Separation of oil-water emulsions

The laboratory-prepared oil-water emulsion samples were passed through the prepared membrane using a filtration assembly, as illustrated in Fig. 4. A volume of 1.0 L was processed in a single cycle, and a total of seven cycles were performed with the membrane, followed by washing with distilled water after every cycle [31-35]. Equation (3) from the previous section was used to calculate the oil-water separation capacity and the results demonstrated that the modified membrane could effectively separate about 96% of petrol oil, 95% of diesel oil, and 88% of crude oil in the first filtration cycle, as shown in Fig. 5. However, the obstruction of pores or active sites on the membrane caused the separation capacity to drop by about 4-5% after each filtration cycle. The filtration process was continued until the seventh cycle, after which the oil-water separation capacity fell below 50%, and no further filtration cycles were performed, as indicated in the graph below [29]. Additionally, pure water was permitted through the membrane while the oil and dye (methylene blue) soaked up over its surface. Our previous research article showed that the coloured dyes and heavy metal ions were also successfully adsorbed onto the surface of the prepared membrane.

CONCLUSIONS

As a result, we have successfully prepared a PES membrane implanted with GO-ZnO nanoparticles utilising the phase inversion technique. According to the results of our characterization, the nanoparticles were evenly distributed throughout the surface of the GO without clumping together. The formation of GO-ZnO nanoparticles was verified by elemental analysis performed using EDX. Our research revealed that adding nanoparticles dramatically increased the membrane's hydrophilicity and water permeability, lowering its contact angle from 115° to 87°. The resulting membrane's capability to extract oil from oil and water emulsions was tested. It had impressive separation efficiency in the first filtration cycle, being able to separate 96% of petrol, 95% of diesel and 88% of crude oil. The membrane was still functional after up to seven cycles, even though the separation capacity dropped by 4-5% after each cycle. Overall, our technique for embedding GO-ZnO nanoparticles into PES membranes has been shown to be a promising one for the creation of sophisticated hybrid membranes with improved capabilities for effective oil-water separation.



**Rohit Goyat and Joginder Singh****ACKNOWLEDGEMENT**

The authors are thankful to Head of Chemistry Department, Maharishi Markandeshwar (Deemed to be University), Mullana Ambala, India, for providing necessary research facilities.

REFERENCES

1. C.P.M. de Oliveira, M.M. Viana, G.R. Silva, L.S.F. Lima, E.C. de Paula, M.C. S. Amaral, Potential use of green TiO₂ and recycled membrane in a photocatalytic membrane reactor for oil refinery wastewater polishing, *J. Clean. Prod.* 257 (2020), 120526.
2. S. Jamaly, A. Giwa, S.W. Hasan, Recent improvements in oily wastewater treatment: progress, challenges, and future opportunities, *J. Environ. Sci.* 37 (2015) 15–30.
3. X. Zhang, B. Zhang, Y. Wu, T. Wang, J. Qiu, Preparation and characterization of a diatomite hybrid microfiltration carbon membrane for oily wastewater treatment, *J. Taiwan Inst. Chem. Eng.* 89 (2018) 39–48.
4. N.H. Ismail, W.N.W. Salleh, A.F. Ismail, H. Hasbullah, N. Yusof, F. Aziz, J. Jaafar, Hydrophilic polymer-based membrane for oily wastewater treatment: a review, *Sep. Purif. Technol.* 233 (2020), 116007.
5. P. Painmanakul, P. Sastaravet, S. Lersjintanakarn, S. Khaodhiar, Effect of bubble hydrodynamic and chemical dosage on treatment of oily wastewater by Induced Air Flotation (IAF) process, *Chem. Eng. Res. Des.* 88 (2010) 693–702.
6. Y.S. Li, L. Yan, C.B. Xiang, L.J. Hong, Treatment of oily wastewater by organic–inorganic composite tubular ultrafiltration (UF) membranes, *Desalination* 196 (2006) 76–83.
7. A. Golshenas, Z. Sadeghian, S.N. Ashrafizadeh, Performance evaluation of a ceramic-based photocatalytic membrane reactor for treatment of oily wastewater, *J. Water Process Eng.* 36 (2020), 101186.
8. S. Qiu, B. Jiang, X. Zheng, J. Zheng, C. Zhu, M. Wu, Hydrophobic and fire-resistant carbon monolith from melamine sponge: a recyclable sorbent for oil–water separation, *Carbon* 84 (2015) 551–559.
9. C.S. Ong, W.J. Lau, P.S. Goh, B.C. Ng, A.F. Ismail, Investigation of submerged membrane photocatalytic reactor (sMPR) operating parameters during oily wastewater treatment process, *Desalination* 353 (2014) 48–56.
10. C.-L. Yang, Electrochemical coagulation for oily water demulsification, *Sep. Purif. Technol.* 54 (2007) 388–395.
11. B. Chakrabarty, A.K. Ghoshal, M.K. Purkait, Ultrafiltration of stable oil-in-water emulsion by polysulfone membrane, *J. Membr. Sci.* 325 (2008) 427–437.
12. A. Pagidi, R. Saranya, G. Arthanareeswaran, A.F. Ismail, T. Matsuura, Enhanced oil–water separation using polysulfone membranes modified with polymeric additives, *Desalination* 344 (2014) 280–288.
13. J.A. Prince, S. Bhuvana, V. Anbharasi, N. Ayyanar, K.V.K. Boodhoo, G. Singh, Ultra-wetting graphene-based PES ultrafiltration membrane—a novel approach for successful oil-water separation, *Water Res.* 103 (2016) 311–318.
14. A.K. Kota, G. Kwon, W. Choi, J.M. Mabry, A. Tuteja, Hygro-responsive membranes for effective oil–water separation, *Nat. Commun.* 3 (2012) 1–8.
15. S.J. Maguire-Boyle, A.R. Barron, A new functionalization strategy for oil/water separation membranes, *J. Membr. Sci.* 382 (2011) 107–115.
16. T.D. Kusworo, D.P. Utomo, Performance evaluation of double stage process using nano hybrid PES/SiO₂-PES membrane and PES/ZnO-PES membranes for oily waste water treatment to clean water, *J. Environ. Chem. Eng.* 5 (2017) 6077–6086.
17. Saraswathi M S A, Kausalya R, Kaleekkal J N, Rana D, Nagendran A 2017 *J. Environ. Chem. Eng.*, 5 2937–43.
18. Lin J, Ye W, Zhong K, Shen J, Jullok N, Sotto A, Van der Bruggen B 2016 *Chem. Eng. Proc.*, 107 194-205.
19. Wang Z, Wang H, Liu J, Zhang Y 2014 *Desalination*, 344 313–320.
20. Liu F, Hashim N A, Liu Y, Abed M R M, Li K 2011 *J. Membr. Sci.*, 375 1–27.
21. C. H. Koo, A. W. Mohammad, F. Suja', and M. Z. MeorTalib, "Use and development of fouling index in predicting membrane fouling," *Separation and Purification Reviews*, vol. 42, no. 4, pp. 296–339, 2013.





Rohit Goyat and Joginder Singh

22. P. S. Singh, K. Parashuram, S. Maurya, P. Ray, and A. V. R. Reddy, "Structure-performance-fouling studies of polysulfone microfiltration hollow fibre membranes," *Bulletin of Materials Science*, vol. 35, no. 5, pp. 817–822, 2012.
23. S. Balta, A. Sotto, P. Luis, L. Benea, B. Van der Bruggen, and J. Kim, "A new outlook on membrane enhancement with nanoparticles: the alternative of ZnO," *Journal of Membrane Science*, vol. 389, pp. 155–161, 2012.
24. S. Masoumi Khosroshahi, A. Miroliaei, Y. Jafarzadeh, Preparation and characterization of MWCNT-COOH/PVC ultrafiltration membranes to use in water treatment, *Adv. Environ. Technol.* 4 (2) (2018) 95–105.
25. C. P. Leo, W. P. Cathie Lee, A. L. Ahmad, and A. W. Mohammad, "Polysulfone membranes blended with ZnO nanoparticles for reducing fouling by oleic acid," *Separation and Purification Technology*, vol. 89, pp. 51–56, 2012.
26. L. Shen, X. Bian, X. Lu et al., "Preparation and characterization of ZnO/polyethersulfone (PES) hybrid membranes," *Desalination*, vol. 293, pp. 21–29, 2012.
27. Goyat, R., Singh, J., Umar, A., Saharan, Y., Kumar, V., Algadi, H., Akbar, S. and Baskoutas, S., 2022. Modified low-temperature synthesis of graphene oxide nanosheets: Enhanced adsorption, antibacterial and antioxidant properties. *Environmental Research*, 215, p.114245.
28. Goyat, R., Saharan, Y., Singh, J., Umar, A. and Akbar, S., 2022. Synthesis of Graphene-Based Nanocomposites for Environmental Remediation Applications: A Review. *Molecules*, 27(19), p.6433.
29. Kaur, R., Goyat, R., Singh, J., Umar, A., Chaudhry, V. and Akbar, S., 2022. An Overview of Membrane Distillation Technology: One of the Perfect Fighters for Desalination. *Eng. Sci*, p.1.
30. Kumar, V., Rout, C., Singh, J., Saharan, Y., Goyat, R., Umar, A., Akbar, S. and Baskoutas, S., 2023. A review on the clean-up technologies for heavy metal ions contaminated soil samples. *Heliyon*.
31. Saharan, Y., Singh, J., Goyat, R., Umar, A. and Akbar, S., 2022. Novel Hydrophobic Polyvinyl-Alcohol Formaldehyde Sponges: Synthesis, Characterization, Fast and Effective Organic Solvent Uptake from Contaminated Soil Samples. *Molecules*, 27(23), p.8429.
32. Saharan, Y., Singh, J., Goyat, R., Umar, A., Akbar, S., Ibrahim, A.A. and Baskoutas, S., 2023. Novel supramolecular organo-oil gelators for fast and effective oil trapping: Mechanism and applications. *Journal of Hazardous Materials*, 442, p.129977.
33. Saharan, Y., Singh, J., Goyat, R., Umar, A., Algadi, H., Ibrahim, A.A., Kumar, R. and Baskoutas, S., 2022. Nanoporous and hydrophobic new Chitosan-Silica blend aerogels for enhanced oil adsorption capacity. *Journal of Cleaner Production*, 351, p.131247.
34. Joginder, S., Amjad, A., Arora, A.K., Mayank, K. and Jaswal, V.S., 2014. Activated Arachis hypogea with enhanced multi metal sorption capacity from synthetic and electroplating industrial wastewater: batch and column mode. *Current Trends in Biotechnology and Chemical Research*, 4(2), pp.79-90.
35. Zhong, Q., Shi, G., Sun, Q., Mu, P. and Li, J., 2021. Robust PVA-GO-TiO₂ composite membrane for efficient separation oil-in-water emulsions with stable high flux. *Journal of Membrane Science*, 640, p.119836.





Rohit Goyat and Joginder Singh

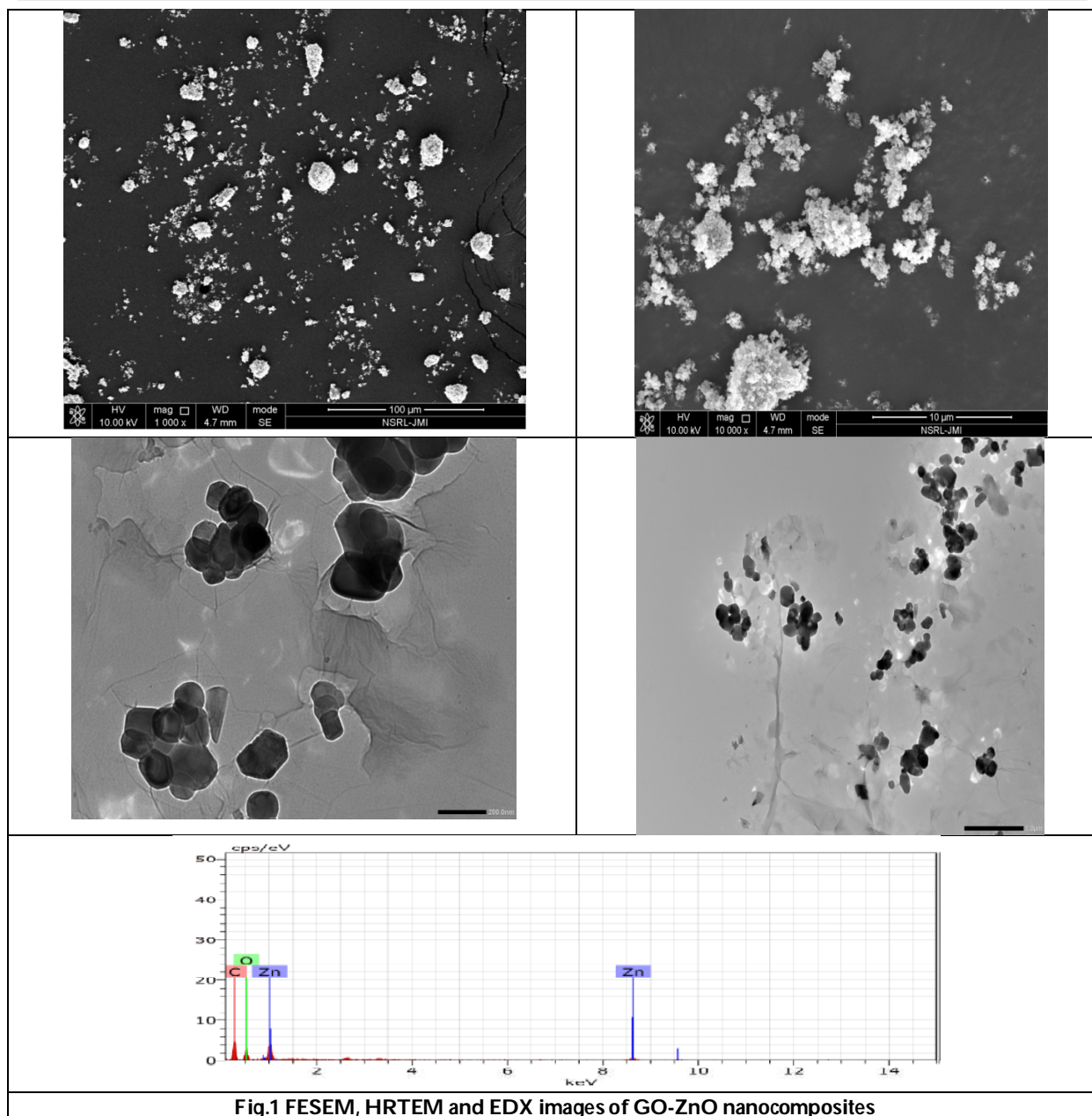


Fig.1 FESEM, HRTEM and EDX images of GO-ZnO nanocomposites





Rohit Goyat and Joginder Singh

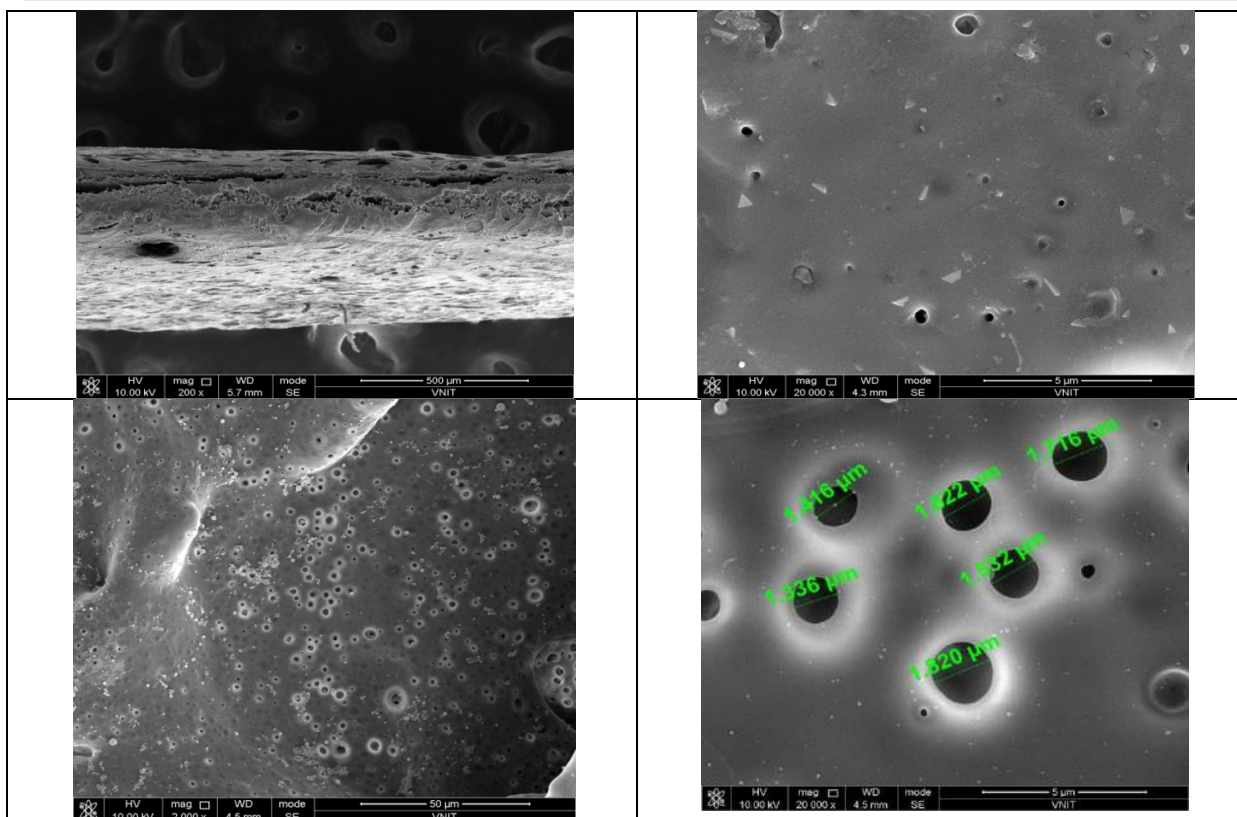


Fig.2 FESEM images of the prepared membrane with pore size.

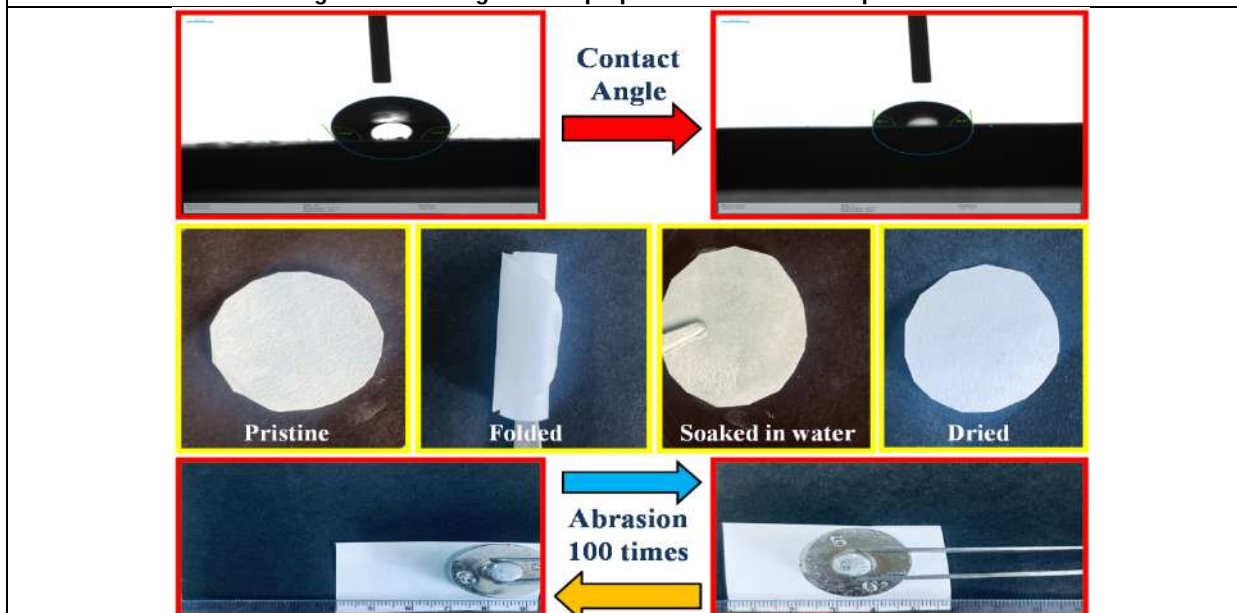
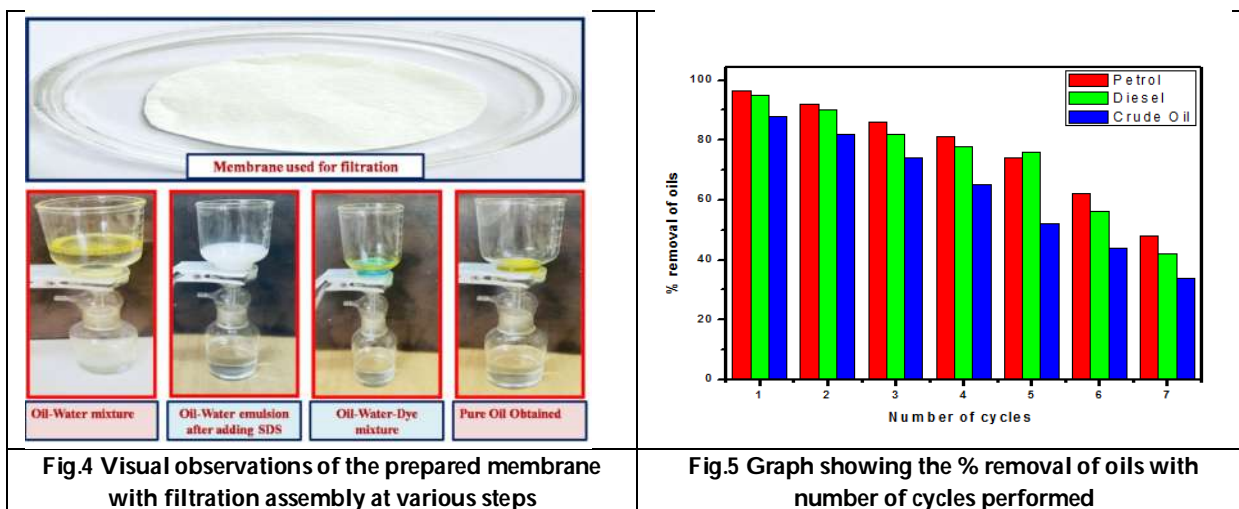


Fig. 3 Images showing the contact angle and mechanical strength test of the membranes





Rohit Goyat and Joginder Singh





Fuzzy Analysis of Priority Queuing Model by using Two Different Approach

Aarti Saini ¹, Vandana Saini ² and Deepak Gupta³

¹Govt. College for Women, Shahzadpur (Ambala) , Haryana, India.

²Govt. P. G. College, Naraingarh (Ambala) ,Haryana, India.

³Mathematics Department, Maharishi Markandeshwar (Deemed to be University), Mullana (Ambala), Haryana, India.

Received: 22 Jan 2024

Revised: 09 Feb 2024

Accepted: 30 May 2024

*Address for Correspondence

Aarti Saini

Govt. College for Women,

Shahzadpur (Ambala) ,

Haryana, India

Email: aartisaini195@gmail.com



This is an Open Access Journal / article distributed under the terms of the **Creative Commons Attribution License** (CC BY-NC-ND 3.0) which permits unrestricted use, distribution, and reproduction in any medium, provided the original work is properly cited. All rights reserved.

ABSTRACT

This study compares the performance of a parallel and biserial priority queue system in fuzzy environments. In this paper, we investigate fuzzy behavior of purposed model by applying two different approach α -cut and L-R. The model consists biserial subsystems with priority discipline and parallel subsystems assuming general arrival connected with common server. Numerical behavior of queue Parameters are well explained by both methods.

Keywords: fuzzy, Priority, Parallel, L-R method, Biserial, α -cut

INTRODUCTION

Priority queues are extremely important in queuing theory for offering various customer classes high-quality service. However, the input data for the priority queuing model is unpredictable, and fuzzy logics have been employed to eliminate this ambiguity. When compared to crisp values, fuzzy concepts produce solutions that are more acceptable. Numerous scholars developed queueing models in a fuzzy setting using various methodologies and fuzzy numbers. Li and Lee [1], Gupta [2,3], Singh T. P. [4], Mittal [5], Sharma [6], J. Devraj [7], B. Kalpana and N. Anusheela [8,9] used Zadeh Principle based α -cut approach. Saini A., Gupta D and A. K. Tripathi [10] analyzed queue system with heterogeneous server and bi-tandem queues in fuzzy by the use of α -cut. Ritha and Menon [11], W. Ritha and S. Josephine Vinnarasi [12], Mukeba [13,14], Saini V, Gupta D and Tripathi A. K. [15] discussed the queue models in fuzzy by applying feedback and triangular fuzzy numbers through the L-R method. Gupta D, Saini A and Tripathi A. K [16] discussed queue characteristics of priority queue model consisting bi-serial and parallel servers in stochastic





environment. The present paper is fuzzy representation of existing study by using two different approaches in fuzzy environment.

Definitions

Fuzzy Set If the results of a membership function of a function \tilde{G} defined on the universal set X is either $\mu_{\tilde{G}}(x) = 1; x \in X$ or $\mu_{\tilde{G}}(x) = 0; x \notin X$, then the function is said to be fuzzy.

α – cut approach

A fuzzy set \tilde{L} defined on X as $\tilde{L}: X \rightarrow [0,1]$ and for any $\alpha \in [0,1]$, then the α – cut $\alpha_L = \{x \in X, \mu_L(x) \geq \alpha\}$ for \tilde{L} is a crisp set.

Strong α – cuts: $\alpha_L = \{x \in X, \mu_L(x) > \alpha\}$ whenever α lies between 0 & 1

Weak α – cuts: $\alpha_L = \{x \in X, \mu_L(x) \geq \alpha\}$ whenever α lies between 0 & 1

As all members of a fuzzy set must be greater than or equal to α , it is important to view fuzzy sets as crisp sets.

Fuzzy Triangular Number

A number $\tilde{L} = (l_1, m_1, l_2)$ is a fuzzy triangular number, if the membership function $\mu_L(x)$ of \tilde{L} is defined as

$$\mu_L(x) = \begin{cases} \frac{x-l_1}{m_1-l_1}, & l_1 \leq x \leq m_1 \\ \frac{l_2-x}{l_2-m_1}, & m_1 \leq x \leq l_2 \\ 0, & \text{otherwise} \end{cases}$$

Fuzzy L-R Number (J. P. Mukeba et al 2015,2016)

A number $\tilde{H} = (h_1, m_1, h_2)$ is said to be fuzzy L-R \Leftrightarrow three real numbers $m_1, h_1, h_2 > 0$, as well as two continuous, positive and decreasing functions L and R , exist from R to $[0,1]$, and satisfying the following conditions as such that

$L(0) = 1, L(1) = 0, L(x) > 0, \lim_{x \rightarrow \infty} L(x) = 0$

$R(0) = 1, R(1) = 0, R(x) > 0, \lim_{x \rightarrow \infty} R(x) = 0$

$$\mu_H(x) = \begin{cases} L\left(\frac{m_1-x}{h_1}\right), & x \in [m_1-h_1, m_1] \\ R\left(\frac{x-m_1}{h_2}\right), & x \in [m_1, m_1+h_2] \\ 0, & \text{otherwise} \end{cases}$$

A fuzzy number \tilde{G} is represented in L-R form as its L-R representation is of the form $\tilde{H} = (m_1, h_1, h_2)_{LR}$, where m_1, h_1, h_2 are used as modal value, left and right spread of \tilde{H} respectively.

$\text{Supp}(\tilde{H}) = (m_1 - h_1, m_1 + h_2)$

L-R fuzzy Arithmetic (J. P. Mukeba et al 2015, 2016)

L-R fuzzy Arithmetic operations on two L-R fuzzy numbers $\tilde{G} = (m_1, g_1, g_2)_{LR}$ & $\tilde{H} = (l_1, h_1, h_2)_{LR}$ are define as

$$\tilde{G} + \tilde{H} = (m_1 + l_1, g_1 + h_1, g_2 + h_2)_{LR}$$

$$\tilde{G} - \tilde{H} = (m_1 - l_1, g_1 + h_2, g_2 + h_1)_{LR}$$

$$\tilde{G} \cdot \tilde{H} = (m_1 l_1, m_1 h_1 + l_1 g_1 - g_1 h_1, m_1 h_2 + l_1 g_2 + g_2 h_2)_{LR}$$

$$\frac{\tilde{G}}{\tilde{H}} = \left(\frac{m_1}{l_1}, \frac{m_1 h_2}{l_1(l_1 + h_2)} + \frac{g_1}{l_1} - \frac{g_1 h_2}{l_1(l_1 + h_2)}, \frac{m_1 h_1}{l_1(l_1 - h_1)} + \frac{g_2}{l_1} + \frac{g_2 h_1}{l_1(l_1 - h_1)} \right)_{LR}$$

Defuzzification

A triangular fuzzy number $\tilde{G} = (g_1, g_2, g_3)$ fuzzified into crisp number $G = \frac{g_1 + 2g_2 + g_3}{4}$ by using Yager's formula.

Model Description

The purposed model consists three subsystems C_1, C_2, C_3 . The Subsystem C_1 has two biserial servers C_{11} & C_{12} and subsystem C_2 has parallel server C_{21} & C_{22} . Both C_1 & C_2 are linked to C_3 . Both type of low and high priority customer





enters into the system either from biserial or parallel server. After being served the customer move to next server for availing the service of next phase.

Notations

\widetilde{m}_{ij} = fuzzy low and high priority arriving customer, $i = 1, 2$ & $j = L, H$

$\widetilde{\lambda}_{ij}$ = fuzzy Priority input rate, $i = 1, 2$ & $j = L, H$

$\widetilde{\lambda}_i$ = fuzzy general arrivals, $i = 1, 2$

$\widetilde{\mu}_{ij}$ = fuzzy cost of service for low and high priority visitors, $i = 1, 2$ & $j = L, H$

$\widetilde{\mu}_i$ = fuzzy service rate at parallel subsystem

$\widetilde{\alpha}_{ij}$ = fuzzy probabilities from i 'th server to j 'th server

\widetilde{L} = The system's fuzzy queue length

Mathematical Approach

The utilization factors at different servers, based on the mathematical characterization of stochastic processes of the work Saini A., Gupta D. and A. K. Tripathi (2023) are as -

$$\gamma_1 = \frac{\lambda_{1H} + \lambda_{2H}\alpha_{21}}{\mu_{1H}(1 - \alpha_{12}\alpha_{21})}$$

$$\gamma_2 = \frac{\lambda_{2H} + \lambda_{1H}\alpha_{12}}{\mu_{2H}(1 - \alpha_{12}\alpha_{21})}$$

$$\gamma_3 = \frac{\lambda_1'}{\mu_1'\alpha_{35}}$$

$$\gamma_4 = \frac{\lambda_2'}{\mu_2'\alpha_{45}}$$

$$\gamma_5 = \frac{(\lambda_1' + \lambda_2')(1 - \alpha_{12}\alpha_{21}) + \alpha_{15}[(\lambda_{1H} + \lambda_{2H}\alpha_{21}) + (\lambda_{1L} + \lambda_{2L}\alpha_{21})] + \alpha_{25}[(\lambda_{2H} + \lambda_{1H}\alpha_{12}) + (\lambda_{2L} + \lambda_{1L}\alpha_{12})]}{\mu_3(1 - \alpha_{12}\alpha_{21})}$$

$$\gamma_6 = \frac{\mu_{1L}(\lambda_{1H} + \lambda_{2H}\alpha_{21}) + \mu_{1H}(\lambda_{1L} + \lambda_{2L}\alpha_{21})}{\mu_{1L}\mu_{1H}(1 - \alpha_{12}\alpha_{21})}$$

$$\gamma_7 = \frac{\mu_{2L}(\lambda_{2H} + \lambda_{1H}\alpha_{12}) + \mu_{2H}(\lambda_{2L} + \lambda_{1L}\alpha_{12})}{\mu_{2L}\mu_{2H}(1 - \alpha_{12}\alpha_{21})}$$

Solution of the model

$$P_{m_{1L}, m_{1H}, m_{2L}, m_{2H}, m_2, m_3, m_5} = \gamma_1^{m_{1H}} \gamma_2^{m_{2H}} \gamma_3^{m_2} \gamma_4^{m_3} \gamma_5^{m_5} \gamma_6^{m_{1L}} \gamma_7^{m_{2L}} (1 - \gamma_1)(1 - \gamma_2)(1 - \gamma_3)(1 - \gamma_4)(1 - \gamma_5)(1 - \gamma_6)(1 - \gamma_7)$$

occur if $\gamma_1, \gamma_2, \gamma_3, \gamma_4, \gamma_5, \gamma_6, \gamma_7 \leq 1$

Fuzzy representation of queue parameters and server utilizations are as follows-

$$\widetilde{\gamma}_1 = \frac{\widetilde{\lambda}_{1H} + \widetilde{\lambda}_{2H}\widetilde{\alpha}_{21}}{\widetilde{\mu}_{1H}(1 - \widetilde{\alpha}_{12}\widetilde{\alpha}_{21})}$$

$$\widetilde{\gamma}_2 = \frac{\widetilde{\lambda}_{2H} + \widetilde{\lambda}_{1H}\widetilde{\alpha}_{12}}{\widetilde{\mu}_{2H}(1 - \widetilde{\alpha}_{12}\widetilde{\alpha}_{21})}$$

$$\widetilde{\gamma}_3 = \frac{\widetilde{\lambda}_1'}{\widetilde{\mu}_1'\widetilde{\alpha}_{35}}$$





Aarti Saini et al.,

$$\tilde{\gamma}_4 = \frac{\tilde{\lambda}_2}{\mu_2 \tilde{\alpha}_{45}}$$

$$\tilde{\gamma}_5 = \frac{\tilde{\lambda}_1 + \tilde{\lambda}_2}{\tilde{\mu}_3} + \frac{\tilde{\alpha}_{15}[(\tilde{\lambda}_{1H} + \tilde{\lambda}_{2H}\tilde{\alpha}_{21}) + (\tilde{\lambda}_{1L} + \tilde{\lambda}_{2L}\tilde{\alpha}_{21})] + \tilde{\alpha}_{25}[(\tilde{\lambda}_{2H} + \tilde{\lambda}_{1H}\tilde{\alpha}_{12}) + (\tilde{\lambda}_{2L} + \tilde{\lambda}_{1L}\tilde{\alpha}_{12})]}{\tilde{\mu}_3(1 - \tilde{\alpha}_{12}\tilde{\alpha}_{21})}$$

$$\tilde{\gamma}_6 = \frac{\tilde{\mu}_{1L}(\tilde{\lambda}_{1H} + \tilde{\lambda}_{2H}\tilde{\alpha}_{21}) + \tilde{\mu}_{1H}(\tilde{\lambda}_{1L} + \tilde{\lambda}_{2L}\tilde{\alpha}_{21})}{\tilde{\mu}_{1L}\tilde{\mu}_{1H}(1 - \tilde{\alpha}_{12}\tilde{\alpha}_{21})}$$

$$\tilde{\gamma}_7 = \frac{\tilde{\mu}_{2L}(\tilde{\lambda}_{2H} + \tilde{\lambda}_{1H}\tilde{\alpha}_{12}) + \tilde{\mu}_{2H}(\tilde{\lambda}_{2L} + \tilde{\lambda}_{1L}\tilde{\alpha}_{12})}{\tilde{\mu}_{2L}\tilde{\mu}_{2H}(1 - \tilde{\alpha}_{12}\tilde{\alpha}_{21})}$$

Fuzzy Lengths of queues

$$\tilde{L}_i = \frac{\tilde{\gamma}_i}{1 - \tilde{\gamma}_i}, i = 1, 2, 3, 4, 5, 6, 7$$

$$\tilde{L} = \tilde{L}_1 + \tilde{L}_2 + \tilde{L}_3 + \tilde{L}_4 + \tilde{L}_5 + \tilde{L}_6 + \tilde{L}_7$$

Average Waiting Time

$$E(\tilde{W}) = \frac{\tilde{L}}{\tilde{\lambda}}, \quad \tilde{\lambda} = \tilde{\lambda}_{1L} + \tilde{\lambda}_{1H} + \tilde{\lambda}_{2L} + \tilde{\lambda}_{2H} + \tilde{\lambda}_1 + \tilde{\lambda}_2$$

Fuzzy Evaluation of Queue Parameters

Evaluation using L-R Method

Numerical Illustration

We get, L-R representations of utilization factor with the help of above numerical values

$$\tilde{\gamma}_1 = (.3906, .2402, .4365)_{LR}$$

$$\tilde{\gamma}_2 = (.4167, .2395, .4550)_{LR}$$

$$\tilde{\gamma}_3 = (.5555, .2876, .6943)_{LR}$$

$$\tilde{\gamma}_4 = (.4, .316, .8821)_{LR}$$

$$\tilde{\gamma}_5 = (.6087, .3934, .8171)_{LR}$$

$$\tilde{\gamma}_6 = (.6260, .4199, .9269)_{LR}$$

$$\tilde{\gamma}_7 = (.7045, .435, .9731)_{LR}$$

Modal values of $\tilde{\gamma}_1, \tilde{\gamma}_2, \tilde{\gamma}_3, \tilde{\gamma}_4, \tilde{\gamma}_5, \tilde{\gamma}_6, \tilde{\gamma}_7$ are as follows-

$$\tilde{\gamma}_1 = .3906$$

$$\tilde{\gamma}_2 = .4167$$

$$\tilde{\gamma}_3 = .5555$$

$$\tilde{\gamma}_4 = .4$$

$$\tilde{\gamma}_5 = .6087$$

$$\tilde{\gamma}_6 = .6260$$

$$\tilde{\gamma}_7 = .7045$$

and for $\tilde{L}_1, \tilde{L}_2, \tilde{L}_3, \tilde{L}_4, \tilde{L}_5, \tilde{L}_6, \tilde{L}_7$ are .6410, .7144, 1.2497, .6, 3.4984, 1.6738, 2.3841 respectively.

$$\text{Supp}(\tilde{\gamma}_1) = (.3906 - .2402, .3906 + .4365) = (.1504, .8271)$$

$$\text{Supp}(\tilde{\gamma}_2) = (.4167 - .2395, .4167 + .4550) = (.1772, .8717)$$

$$\text{Supp}(\tilde{\gamma}_3) = (.5555 - .2876, .5555 + .6943) = (.2679, 1.2498)$$

$$\text{Supp}(\tilde{\gamma}_4) = (.4 - .316, .4 + .8821) = (.084, 1.2821)$$

$$\text{Supp}(\tilde{\gamma}_5) = (.6087 - .3934, .6087 + .8171) = (.2153, 1.4258)$$

$$\text{Supp}(\tilde{\gamma}_6) = (.6260 - .4199, .6260 + .9269) = (.2061, 1.5529)$$

$$\text{Supp}(\tilde{\gamma}_7) = (.7045 - .435, .7045 + .9731) = (.2695, 1.6776)$$

Evaluation by α -cut method





As the Methodology adopted by Sameer et al [6], fuzzy parameters are represented as

$$\begin{aligned}\widetilde{\lambda}_{ij} &= (\lambda_{ij}^1, \lambda_{ij}^2, \lambda_{ij}^3), \\ \widetilde{\mu}_{ij} &= (\mu_{ij}^1, \mu_{ij}^2, \mu_{ij}^3), \\ \widetilde{\alpha}_{ij} &= (\alpha_{ij}^1, \alpha_{ij}^2, \alpha_{ij}^3), \\ \widetilde{\mu}_i &= (\mu_i^1, \mu_i^2, \mu_i^3), \\ \widetilde{\lambda}_i &= (\lambda_i^1, \lambda_i^2, \lambda_i^3) \quad \forall i \& j\end{aligned}$$

Now, fuzzy utilization factors are defined as

$$\begin{aligned}\widetilde{\gamma}_1 &= \left\{ \frac{\lambda_{1H}^1 + \alpha_{21}^1 \lambda_{2H}^1}{\mu_{1H}^3 (1 - \alpha_{12}^3 \alpha_{21}^3)}, \frac{\lambda_{1H}^2 + \alpha_{21}^2 \lambda_{2H}^2}{\mu_{1H}^2 (1 - \alpha_{21}^2 \alpha_{12}^2)}, \frac{\lambda_{1H}^3 + \alpha_{21}^3 \lambda_{2H}^3}{\mu_{1H}^1 (1 - \alpha_{21}^1 \alpha_{12}^1)} \right\} \\ \widetilde{\gamma}_2 &= \left\{ \frac{\lambda_{2H}^1 + \alpha_{12}^1 \lambda_{1H}^1}{\mu_{2H}^3 (1 - \alpha_{12}^3 \alpha_{21}^3)}, \frac{\lambda_{2H}^2 + \alpha_{12}^2 \lambda_{1H}^2}{\mu_{2H}^2 (1 - \alpha_{21}^2 \alpha_{12}^2)}, \frac{\lambda_{2H}^3 + \alpha_{12}^3 \lambda_{1H}^3}{\mu_{2H}^1 (1 - \alpha_{21}^1 \alpha_{12}^1)} \right\} \\ \widetilde{\gamma}_3 &= \left\{ \frac{\lambda_1^1}{\alpha_{35}^3 \mu_1^3}, \frac{\lambda_1^2}{\alpha_{35}^2 \mu_1^2}, \frac{\lambda_1^3}{\alpha_{35}^1 \mu_1^1} \right\} \\ \widetilde{\gamma}_4 &= \left\{ \frac{\lambda_2^1}{\alpha_{45}^3 \mu_2^3}, \frac{\lambda_2^2}{\alpha_{45}^2 \mu_2^2}, \frac{\lambda_2^3}{\alpha_{45}^1 \mu_2^1} \right\} \\ \widetilde{\gamma}_5 &= \left\{ \frac{\lambda_1^1 + \lambda_2^1}{\mu_3^3} + \frac{\alpha_{15}^1 [(\lambda_{1H}^1 + \alpha_{21}^1 \lambda_{2H}^1) + (\lambda_{1L}^1 + \alpha_{21}^1 \lambda_{2L}^1)] + \alpha_{25}^1 [(\lambda_{2H}^1 + \alpha_{12}^1 \lambda_{1H}^1) + (\lambda_{2L}^1 + \alpha_{12}^1 \lambda_{1L}^1)]}{\mu_3^3 (1 - \alpha_{12}^3 \alpha_{21}^3)}, \right. \\ &\quad \left. \frac{\lambda_1^2 + \lambda_2^2}{\mu_3^2} + \frac{\alpha_{15}^2 [(\lambda_{1H}^2 + \alpha_{21}^2 \lambda_{2H}^2) + (\lambda_{1L}^2 + \alpha_{21}^2 \lambda_{2L}^2)] + \alpha_{25}^2 [(\lambda_{2H}^2 + \alpha_{12}^2 \lambda_{1H}^2) + (\lambda_{2L}^2 + \alpha_{12}^2 \lambda_{1L}^2)]}{\mu_3^2 (1 - \alpha_{12}^2 \alpha_{21}^2)}, \right. \\ &\quad \left. \frac{\lambda_1^3 + \lambda_2^3}{\mu_3^1} + \frac{\alpha_{15}^3 [(\lambda_{1H}^3 + \alpha_{21}^3 \lambda_{2H}^3) + (\lambda_{1L}^3 + \alpha_{21}^3 \lambda_{2L}^3)] + \alpha_{25}^3 [(\lambda_{2H}^3 + \alpha_{12}^3 \lambda_{1H}^3) + (\lambda_{2L}^3 + \alpha_{12}^3 \lambda_{1L}^3)]}{\mu_3^1 (1 - \alpha_{12}^1 \alpha_{21}^1)} \right\} \\ \widetilde{\gamma}_6 &= \left\{ \frac{\mu_{1L}^1 (\lambda_{1H}^1 + \alpha_{21}^1 \lambda_{2H}^1) + \mu_{1H}^1 (\lambda_{1L}^1 + \alpha_{21}^1 \lambda_{2L}^1)}{\mu_{1L}^3 \mu_{1H}^3 (1 - \alpha_{12}^3 \alpha_{21}^3)}, \right. \\ &\quad \left. \frac{\mu_{1L}^2 (\lambda_{1H}^2 + \alpha_{21}^2 \lambda_{2H}^2) + \mu_{1H}^2 (\lambda_{1L}^2 + \alpha_{21}^2 \lambda_{2L}^2)}{\mu_{1L}^2 \mu_{1H}^2 (1 - \alpha_{21}^2 \alpha_{12}^2)}, \right. \\ &\quad \left. \frac{\mu_{1L}^3 (\lambda_{1H}^3 + \alpha_{21}^3 \lambda_{2H}^3) + \mu_{1H}^3 (\lambda_{1L}^3 + \alpha_{21}^3 \lambda_{2L}^3)}{\mu_{1L}^1 \mu_{1H}^1 (1 - \alpha_{21}^1 \alpha_{12}^1)} \right\} \\ \widetilde{\gamma}_7 &= \left\{ \frac{\mu_{2L}^1 (\lambda_{2H}^1 + \alpha_{12}^1 \lambda_{1H}^1) + \mu_{2H}^1 (\lambda_{2L}^1 + \alpha_{12}^1 \lambda_{1L}^1)}{\mu_{2L}^3 \mu_{2H}^3 (1 - \alpha_{12}^3 \alpha_{21}^3)}, \right. \\ &\quad \left. \frac{\mu_{2L}^2 (\lambda_{2H}^2 + \alpha_{12}^2 \lambda_{1H}^2) + \mu_{2H}^2 (\lambda_{2L}^2 + \alpha_{12}^2 \lambda_{1L}^2)}{\mu_{2L}^2 \mu_{2H}^2 (1 - \alpha_{21}^2 \alpha_{12}^2)}, \right. \\ &\quad \left. \frac{\mu_{2L}^3 (\lambda_{2H}^3 + \alpha_{12}^3 \lambda_{1H}^3) + \mu_{2H}^3 (\lambda_{2L}^3 + \alpha_{12}^3 \lambda_{1L}^3)}{\mu_{2L}^1 \mu_{2H}^1 (1 - \alpha_{21}^1 \alpha_{12}^1)} \right\}\end{aligned}$$

From Table3, we get utilization factor

$$\widetilde{\gamma}_1 = (\gamma_1^1, \gamma_1^2, \gamma_1^3) = (.2053, .3906, .5844)$$

$$\widetilde{\gamma}_2 = (\gamma_2^1, \gamma_2^2, \gamma_2^3) = (.4456, .4167, .2983)$$

$$\widetilde{\gamma}_3 = (\gamma_3^1, \gamma_3^2, \gamma_3^3) = (.375, .5555, .8928)$$





Aarti Saini et al.,

$$\tilde{\gamma}_4 = (\gamma_4^1, \gamma_4^2, \gamma_4^3) = (.5495, .4, .1961)$$

$$\tilde{\gamma}_5 = (\gamma_5^1, \gamma_5^2, \gamma_5^3) = (.7640, .7778, .7937)$$

$$\tilde{\gamma}_6 = (\gamma_6^1, \gamma_6^2, \gamma_6^3) = (.4580, .6260, .7597)$$

$$\tilde{\gamma}_7 = (\gamma_7^1, \gamma_7^2, \gamma_7^3) = (.7453, .7045, .6339)$$

and queue lengths

$$\tilde{L}_1 = \frac{\tilde{\gamma}_1}{1 - \tilde{\gamma}_1} = (.3393, .6410, .9657)$$

$$\tilde{L}_2 = \frac{\tilde{\gamma}_2}{1 - \tilde{\gamma}_2} = (.7095, .7144, .4750)$$

$$\tilde{L}_3 = \frac{\tilde{\gamma}_3}{1 - \tilde{\gamma}_3} = (1.0243, 1.2497, 2.4387)$$

$$\tilde{L}_4 = \frac{\tilde{\gamma}_4}{1 - \tilde{\gamma}_4} = (.8761, .6667, .3126)$$

$$\tilde{L}_5 = \frac{\tilde{\gamma}_5}{1 - \tilde{\gamma}_5} = (3.4539, 3.5005, 3.5882)$$

$$\tilde{L}_6 = \frac{\tilde{\gamma}_6}{1 - \tilde{\gamma}_6} = (1.1708, 1.6738, 1.9420)$$

$$\tilde{L}_7 = \frac{\tilde{\gamma}_7}{1 - \tilde{\gamma}_7} = (2.4011, 2.3841, 2.0422)$$

De fuzzified values of utilization factors and length of queues by Yager's formula are

$$\tilde{\gamma}_1 = .3927, \quad \tilde{\gamma}_2 = .3943, \quad \tilde{\gamma}_3 = .5947, \quad \tilde{\gamma}_4 = .3864, \quad \tilde{\gamma}_5 = .7783, \quad \tilde{\gamma}_6 = .6174, \quad \tilde{\gamma}_7 = .6971$$

$$\tilde{L}_1 = .6468, \tilde{L}_2 = .6533, \tilde{L}_3 = 1.4906, \tilde{L}_4 = .6305, \tilde{L}_5 = 3.5108, \tilde{L}_6 = 1.6151, \tilde{L}_7 = 2.3029$$

The most possible value of utilization factors and length of queues, are as -

$$\tilde{\gamma}_1 = .3906, \quad \tilde{\gamma}_2 = .4167, \quad \tilde{\gamma}_3 = .5555, \quad \tilde{\gamma}_4 = .4, \quad \tilde{\gamma}_5 = .7778, \quad \tilde{\gamma}_6 = .6260, \quad \tilde{\gamma}_7 = .7045$$

$$\tilde{L}_1 = .6410, \tilde{L}_2 = .7144, \tilde{L}_3 = 1.2497, \tilde{L}_4 = .6667, \tilde{L}_5 = 3.5005, \tilde{L}_6 = 1.6738, \tilde{L}_7 = 2.3841$$

Results

Comparing the numerical values obtained by α -cut and L-R approach on same data,

- Utilization factors and mean length of queue modal values are $\tilde{\gamma}_1 = .3906$, $\tilde{\gamma}_2 = .4167$, $\tilde{\gamma}_3 = .5555$, $\tilde{\gamma}_4 = .4$, $\tilde{\gamma}_5 = .6087$, $\tilde{\gamma}_6 = .6260$, $\tilde{\gamma}_7 = .7045$ and $\tilde{L}_1 = .6410$, $\tilde{L}_2 = .7144$, $\tilde{L}_3 = 1.2497$, $\tilde{L}_4 = .6$, $\tilde{L}_5 = 3.4984$, $\tilde{L}_6 = 1.6738$, $\tilde{L}_7 = 2.3841$ respectively.
- The most prevalent queue lengths and utilization parameters are $\tilde{L}_1 = .6410$, $\tilde{L}_2 = .7144$, $\tilde{L}_3 = 1.2497$, $\tilde{L}_4 = .6667$, $\tilde{L}_5 = 3.5005$, $\tilde{L}_6 = 1.6738$, $\tilde{L}_7 = 2.3841$ and $\tilde{\gamma}_1 = .3906$, $\tilde{\gamma}_2 = .4167$, $\tilde{\gamma}_3 = .5555$, $\tilde{\gamma}_4 = .4$, $\tilde{\gamma}_5 = .7778$, $\tilde{\gamma}_6 = .6260$, $\tilde{\gamma}_7 = .7045$.

Thus, the values of utilization factor and queue length by α -cut are higher than the values by L-R method at common server.





CONCLUSION

In this research paper, we have used two different methods α -cut and L- R on approximate same data to analyze the queue behavior of priority queue network of biserial and parallel server in fuzzy environment. From comparative analysis of these two methods, we cannot say which method gives more accurate results than the other because values of queue characteristics obtained by both methods are almost same on all servers except the common server. But we can observe that while calculating numeric values of queue parameters, the L-R technique is shorter, more concise, versatile, and practical as compared to α -cut method. Comparative analysis of these two methods can be applied on more complex models for more accuracy.

REFERENCES

1. Li R.J. and Lee E.S., Analysis of fuzzy queues. Computers and Mathematics with Applications, 17:1143–1147, 1989. [http://dx.doi.org/10.1016/0898-1221\(89\)90044-8](http://dx.doi.org/10.1016/0898-1221(89)90044-8).
2. Seema, Gupta D., and Sharma S., Analysis of Biserial Servers Linked to a Common Server in Fuzzy Environment, International Journal of computing science and Mathematics, 68(6): 26-32, 2013. [CrossRef] [Google Scholar]
3. Sharma S., Gupta D., and Seema, Network Analysis of Fuzzy Bi-serial and Parallel Servers with a Multistage Flow Shop Model, 21st International Congress on Modelling and Simulation, Gold Coast, Australia, 697-703, 2015. [Google Scholar]
4. Singh T.P., Mittal M., and Gupta D., Modelling of a Bulk Queue System in Triangular Fuzzy Numbers using α -cut, International Journal of IT and Engineering, 4(9): 72-79, 2016. [Google Scholar]
5. Mittal M., Singh T.P., and Gupta D., Threshold Effect on a Fuzzy Queue Model with Batch Arrival, Aryabhatta Journal of Mathematics & Informatics, 7(1): 109-118, 2015. [Google Scholar] [Publisher Link]
6. Sharma S., Fuzzy Analysis of Synergistic Collaboration of Biserial and Parallel Servers with a Common Server, Advances in Fuzzy Mathematics, 12 (2): 283-296, 2017.
7. Devaraj J. and Jayalakshmi D., A Fuzzy Approach to Priority Queues, International Journal of Fuzzy Mathematics and Systems, 2 (4): 479-488, 2012.
8. Kalpana B., Dr. N. Anusheela, Analysis of Fuzzy Non-Preemptive Priority Queue using Non-Linear Programming, International Journal of Mathematics Trends and Technology (IJMTT), 56(1): 71-80, 2018.
9. Kalpana B., Evaluation of Performance Measures of Fuzzy Queues with Preemptive Priority using Different Fuzzy Numbers, Advances and Applications in Mathematical Sciences, 20(11): 2975-2985, 2021.
10. Saini A., Gupta D and Tripathi A. K., Analysis of Fuzzy Priority Queuing System with Heterogeneous Servers, Aryabhatta Journal of Mathematics and Informatics (AJMI), 15(1): 111-120, 2023.
11. Ritha W. and Menon S.B.), Fuzzy n policy queues with infinite capacity. Journal of Physical Sciences, 15:73–82, 2011.
12. Ritha W. and Vinnarasi Josephine S.), Analysis of Priority Queuing Models: L - R Method, Annals of Pure and Applied Mathematics, 15(2): 271-276, 2017.
13. Mukeba J. P., Mabela R. & Ulungu B., Computing Fuzzy Queuing Performance Measures by L-R Method, Journal of Fuzzy Sets Valued Analysis, 1:157-67, 2015. [CrossRef] [Google Scholar]
14. Mukeba J.P., Application of L-R Method to Single Server Fuzzy Retrial Queue with Patient Customers, Journal of Pure and Applied Mathematics: Advances and Applications, 16(1): 43-59, 2016. [CrossRef] [Google Scholar]
15. Saini V., Gupta D., and Tripathi A.K., Comparative Analysis of Heterogeneous Feedback Queue Model in Fuzzy Environment using L-R method and α -cut method, International Journal of Mathematics Trends and Technology, 69(3): 31-38, 2023.
16. Saini A., Gupta D. and Tripathi A.K., Analysis of Bi-Tandem Priority Queue System in Stochastic Environment, International Journal of Mathematics Trends and Technology, 69(5): 54-69, 2023.





Aarti Saini et al.,

Table 1. fuzzy particular values

Customers in queue	Arrival times	Service costs	Probabilities
$m_{1L} = (2,3,4)$	$\tilde{\lambda}_{1L} = (1,2,3)$	$\tilde{\mu}_{1L} = (13,14,15)$	$\tilde{\alpha}_{12} = (.6, .4, .2)$
$m_{1H} = (3,4,5)$	$\tilde{\lambda}_{1H} = (2,4,6)$	$\tilde{\mu}_{1H} = (14,16,18)$	$\tilde{\alpha}_{15} = (.4, .6, .8)$
$m_{2L} = (3,2,1)$	$\tilde{\lambda}_{2L} = (2,3,4)$	$\tilde{\mu}_{2L} = (14,15,16)$	$\tilde{\alpha}_{21} = (.2, .3, .4)$
$m_{2H} = (4,5,6)$	$\tilde{\lambda}_{2H} = (3,5,7)$	$\tilde{\mu}_{2H} = (16,18,20)$	$\tilde{\alpha}_{25} = (.8, .7, .6)$
$m_2 = (1,3,5)$	$\tilde{\lambda}_1 = (3,4,5)$	$\tilde{\mu}_1 = (10,12,14)$	$\tilde{\alpha}_{35} = (.4, .6, .8)$
$m_3 = (5,4,3)$	$\tilde{\lambda}_2 = (1,3,5)$	$\tilde{\mu}_2 = (13,15,17)$	$\tilde{\alpha}_{45} = (.3, .5, .7)$
		$\tilde{\mu}_3 = (26,27,28)$	

Table 2. Fuzzy L-R Values

Arrival times	Service costs	Probabilities
$\tilde{\lambda}_{1L} = (2,1,1)$	$\tilde{\mu}_{1L} = (14,1,1)$	$\tilde{\alpha}_{12} = (.4, .2, .2)$
$\tilde{\lambda}_{1H} = (4,2,2)$	$\tilde{\mu}_{1H} = (16,2,2)$	$\tilde{\alpha}_{15} = (.6, .2, .2)$
$\tilde{\lambda}_{2L} = (3,1,1)$	$\tilde{\mu}_{2L} = (15,1,1)$	$\tilde{\alpha}_{21} = (.3, .1, .1)$
$\tilde{\lambda}_{2H} = (5,2,2)$	$\tilde{\mu}_{2H} = (18,2,2)$	$\tilde{\alpha}_{25} = (.7, .1, .1)$
$\tilde{\lambda}_1 = (4,1,1)$	$\tilde{\mu}_1 = (12,2,2)$	$\tilde{\alpha}_{35} = (.6, .2, .2)$
$\tilde{\lambda}_2 = (3,2,2)$	$\tilde{\mu}_2 = (15,2,2)$	$\tilde{\alpha}_{45} = (.5, .2, .2)$
	$\tilde{\mu}_3 = (27,1,1)$	

Table 3. fuzzy particular values

Customers in queue	Arrival times	Service costs	Probabilities
$m_{1L} = (2,3,4)$	$\tilde{\lambda}_{1L} = (3,2,1)$	$\tilde{\mu}_{1L} = (15,14,13)$	$\tilde{\alpha}_{12} = (.6, .4, .2)$
$m_{1H} = (3,4,5)$	$\tilde{\lambda}_{1H} = (2,4,6)$	$\tilde{\mu}_{1H} = (14,16,18)$	$\tilde{\alpha}_{15} = (.4, .6, .8)$
$m_{2L} = (3,2,1)$	$\tilde{\lambda}_{2L} = (2,3,4)$	$\tilde{\mu}_{2L} = (16,15,14)$	$\tilde{\alpha}_{21} = (.2, .3, .4)$
$m_{2H} = (4,5,6)$	$\tilde{\lambda}_{2H} = (7,5,3)$	$\tilde{\mu}_{2H} = (16,18,20)$	$\tilde{\alpha}_{25} = (.8, .7, .6)$
$m_2 = (1,3,5)$	$\tilde{\lambda}_1 = (3,4,5)$	$\tilde{\mu}_1 = (14,12,10)$	$\tilde{\alpha}_{35} = (.4, .6, .8)$
$m_3 = (5,4,3)$	$\tilde{\lambda}_2 = (5,3,1)$	$\tilde{\mu}_2 = (17,15,13)$	$\tilde{\alpha}_{45} = (.3, .5, .7)$
		$\tilde{\mu}_3 = (26,27,28)$	

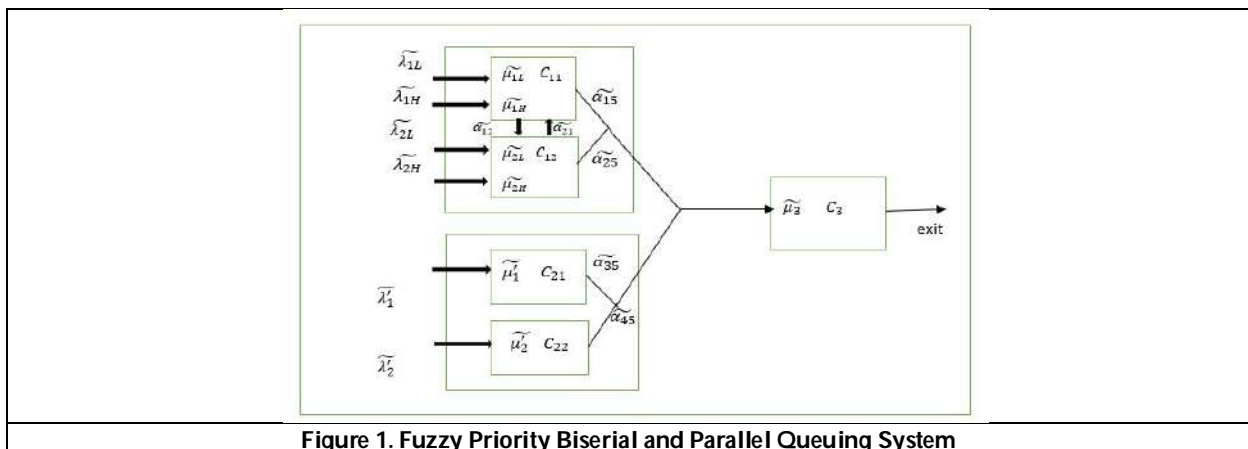


Figure 1. Fuzzy Priority Biserial and Parallel Queuing System





A Solution Approach to Multiobjective Quadratic Fractional Programming with Triangular Fuzzy Numbers by M-TOPSIS

Rozy Rani, Vandana Goyal and Deepak Gupta

Maharishi Markandeshwar (Deemed to be University) Ambala, Mullana, Haryana, India.

Received: 20 Jan 2024

Revised: 09 Feb 2024

Accepted: 14 May 2024

*Address for Correspondence

Rozy Rani

Maharishi Markandeshwar

(Deemed to be University)

Ambala, Mullana, Haryana, India.



This is an Open Access Journal / article distributed under the terms of the **Creative Commons Attribution License** (CC BY-NC-ND 3.0) which permits unrestricted use, distribution, and reproduction in any medium, provided the original work is properly cited. All rights reserved.

ABSTRACT

This paper proposed a strategy to find an optimal solution of a M-TOPSIS approach which has quadratic fractional with triangular fuzzy numbers as coefficients in objective function and constraints. Firstly the quadratic fractional function with fuzzy numbers is transformed into crisp model by using α -cut method. Thenceforth for specified α , formulating the membership function of each decision maker's (DM) objective with the distance of positive ideal solution(PIS) and negative ideal solution(NIS), so that it is converted into easier form to eliminate complications in calculations. Then final model is solved to get the best solution. Also a flowchart and an algorithm expressing the methodology of MOQFM model with M-TOPSIS approach. A numerical illustration of the proposed approach is also given in the end.

Keywords: Quadratic Fractional function, Triangular Fuzzy number, α -cut, M-TOPSIS approach, membership functions, MOQFM model etc.

INTRODUCTION

Multi-objective programming issues have a significant role in the theory of optimization. In general, there may be a conflict between the objectives of a multiple objective programming issue. Initially, Charnes and Cooper (1962) suggested optimization problem to fractional functional programme and also discussed about resource allocation problems. In Multiobjective Fractional Programming, the problems related to financial like liquidity, dividend per share, profit per share, return on capital and other measures, all be maximised at the same time. The applications of fractional programming are portfolio selection, game theory, stock cutting and many decision problems in management science. QFPP (Quadratic Fractional Programming Problem) is a significant category of mathematical programming problems that has garnered substantial attention and study. Due to its utility in industrial planning, financial and economic planning, healthcare planning and medical services. QFPP deals with circumstances where a ratio between two mathematical functions is either maximised or minimised. In the theory of linear programming





Rozy Rani et al.,

(LP), the fuzzy system is particularly important. There are many administrative decision-making circumstances, where fuzzy set theory provides the most comprehensive explanation of the ambiguities in practical circumstances. Firstly, Zadeh (1996) developed fuzzy set theory and later on a sizable number of academicians have shown an interest in applying it to many fields. Bellman. R. E. (1970) described the idea of making decisions in a fuzzy environment and Tanaka. H. (1973) applied their theory to mathematical programming using fuzzy decision making. The application of fuzzy set theory to QFP has been examined in numerous works. C.L. Hwang and Yoon (1981) proposed a novel method (TOPSIS method) for the right selection of multi attribute decision making environment. Ching Lai Hwang (1993) developed TOPSIS approach for the solution of MODMP (Multi objective decision making problem). The compromise solution should be nearer to PIS and farthest to NIS. M.A. Abo Sinna (2000) extended and attained non dominated solutions of TOPSIS method for solving multiobjective Dynamic problem for using the fuzzy max-min method with non- linear membership function. Mohammed Avisheh (2012) explained the fuzzy extension of TOPSIS approach for solving multiple criteria of group decision making problems under fuzzy environment. M.A. Abo Sinna (2002) proposed a MODPP having fuzzy parameters, fuzzy decision maker for generating α -pareto optimal solution for solving large scale MOPP. The large scale MOFPP is depended on decomposition method having Block angular structure through TOPSIS method. C.T. Chen (2000) developed a methodology of TOPSIS approach with fuzzy for solving multi criteria decision making problems. K. Lachwani (2014) stated a simple technique of FGP for solving ML-MOLPP. By minimising the total of the negative deviational variables, the FGP approach can be used to discover the maximum degree of membership goals. N. Rani et. al (2021,2022) explained an Interactive FGP approach with fuzzy parameters for (BLMOFQFOM) bi-level multi-objective fully quadratic fractional optimization model. O.E.Emam (2015) explained a decomposition approach for handling large scale, stochastic, multi-level quadratic fractional problems. The non-linear model of FGP technique for solving ML-MOQFP was explained by Osman (2017) et al. with fuzzy parameters.

R.Rani et al.(2021, 2022) introduced M-TOPSIS technique for MOQFO Models. S.K. Das (2020) proposed a new method to solve fully fuzzy linear programming problem with the help of triangular fuzzy numbers. Abhishek Chouhan et. al (2023) explained α - cut method for the solution of Linear fractional programming problem having fuzzy parameters. These triangular fuzzy numbers (TrFN) are applied to solve transportation problems. Zimmerman (2011) explained the fuzzy theory having uncertainties in the objectives. This paper explains M-TOPSIS approach for the solution of MOQFM problems having fuzzy parameters. Finding a compromise solution with the help of M-TOPSIS approach for programming model with triangular fuzzy numbers in both the objectives and constraints. This study describes α - cut method and fuzzy relation into crisp model with desired value of α . The managerial insight of this paper is described as follows: Section 2 describe the definitions and preliminaries. Section 3 and 4 explains the solution problem of fuzzy parameters and formulated its deterministic model. Section 5 develops quadratic fractional model of M-TOPSIS approach. A flowchart and technique for MOQFM problems having fuzzy parameters are provided in section 6 and 7. A numerical example for finding a compromise solution to the MOQFM problem by minimising the total of the negative deviational variables is provided in section 8 and section 9 represents concluding remarks in the end.

Preliminaries and Notations

Some basic definitions of Fuzzy set theory are

Fuzzy Set: A fuzzy set θ in X is defined by $\theta = \{(x, \mu_{\theta}(x)) / x \in X\}$, where $\mu_{\theta}(x): X \rightarrow [0, 1]$ is called the membership function of θ and μ_{θ} is the degree of membership to which $x \in X$.

Normal Fuzzy set: θ is called a normal fuzzy set if there exists a point x in X such that $\mu_{\theta}(x) = 1$.

Convex Fuzzy set: θ is called a convex fuzzy set iff for any $x_1, x_2 \in X$ and $\lambda \in [0, 1]$, $\mu_{\theta}[\lambda x_1 + (1 - \lambda) x_2] \geq \min [\mu_{\theta}(x_1), \mu_{\theta}(x_2)]$.





Rozy Rani et al.,

α - cut set :The α - cut of a fuzzy θ of X is a non-fuzzy set denoted by $\alpha\theta$ defined by a subset of all elements $x \in X$ such that their membership functions exceed or identical to a real number $\alpha \in [0, 1]$ i.e. $\alpha\theta = \{x : \mu_\theta(x) \geq \alpha, \alpha \in [0, 1] \forall x \in X\}$

Triangular Fuzzy Number: The triangular fuzzy numbers θ are both convex and normal fuzzy set in X which is defined by $\theta = (a, b, c)$

$$\mu_\theta(x) = \begin{cases} \frac{x-a}{b-a}, & \text{if } a \leq x \leq b \\ \frac{c-x}{c-b}, & \text{if } b \leq x \leq c \\ 0, & \text{if otherwise} \end{cases}$$

Formulation of Problem

Suppose that there are j multiobjective quadratic fractional optimization model (MOQFM) with triangular fuzzy numbers (TrFN) where quadratic constraints are also given in fuzzy parameters having $F: \mathbb{R}^n \rightarrow \mathbb{R}^j$ be $j \times 1$ objective function and the variable of objective function is $x \in (x_1, x_2, \dots, x_n) \in \mathbb{R}^n$

The TrFN- MOQFM is explained as;

$\min / (\max) F(x) = \min / (\max) \{F_1(x), F_2(x), \dots, F_j(x)\}$ subject to

$$H = \left\{ \left(\sum_{i=1}^n \sum_{k=1}^n \tilde{s}_{ik} x_i x_k + \sum_{i=1}^n \tilde{t}_i x_i \right)_r \begin{pmatrix} \leq \\ = \\ \geq \end{pmatrix} e_r, 1 \leq r \leq m_1 / x \geq 0 \right\}$$

where H is convex quadratic constraints feasible fuzzy set.

$$\min / (\max) (F_i)_\alpha(x) = \min / (\max) \frac{\sum_{i=1}^n \sum_{k=1}^n [(c'_{pk})_\alpha^L, (c'_{pk})_\alpha^U] x_i x_k + \sum_{i=1}^n [(d'_i)_\alpha^L, (d'_i)_\alpha^U] x_i + [(a')_\alpha^L, (a')_\alpha^U]}{\sum_{i=1}^n \sum_{k=1}^n [(c''_{pk})_\alpha^L, (c''_{pk})_\alpha^U] x_i x_k + \sum_{i=1}^n [(d''_i)_\alpha^L, (d''_i)_\alpha^U] x_i + [(b')_\alpha^L, (b')_\alpha^U]}, 1 \leq i \leq j$$

$$F_i(x) = \frac{h_1(x)}{h_2(x)},$$

$$\text{where } \tilde{h}_1(x) = \sum_{p=1}^n \sum_{k=1}^n \tilde{c}_{pk} x_p x_k + \sum_{i=1}^n \tilde{d}_i x_i + \tilde{a},$$

$$\tilde{h}_2(x) = \sum_{p=1}^n \sum_{k=1}^n \tilde{c}_{pk} x_p x_k + \sum_{i=1}^n \tilde{d}_i x_i + \tilde{b}, 1 \leq i \leq j$$

and $\tilde{c}_{pk}, \tilde{c}_{pk}, \tilde{d}_k, \tilde{d}_k, \tilde{a}, \tilde{b}, \tilde{s}_{ik}, \tilde{t}_i, \tilde{e}_r$ are triangular fuzzy numbers.

Theorem





Rozy Rani et al.,

Let $h(x) = \frac{h_1(x)}{h_2(x)}$ be a fuzzy function with α -level set as $h_2(x) \neq 0$ in the set S then infimum and supremum of α -cuts $h_1(x)$ and $h_2(x)$ respectively describe the minimum value of $h(x)$

i.e. For minimization, $h(x) = \frac{h_1(x)}{h_2(x)} = \frac{(h_1(x))_\alpha^L}{(h_2(x))_\alpha^U}$

For maximization, $h(x) = \frac{h_1(x)}{h_2(x)} = \frac{(h_1(x))_\alpha^U}{(h_2(x))_\alpha^L}$, where L_α and U_α denote infimum and supremum of α -cut set.

Proof: Let $h(x) = \frac{h_1(x)}{h_2(x)}$.

Given $\alpha = [0, 1]$ and convert the coefficient into intervals:

$$\frac{\sum_{p=1}^n \sum_{k=1}^n [(c_{pk})_\alpha^L, (c_{pk})_\alpha^U] x_p x_k + \sum_{k=1}^n [(d_k)_\alpha^L, (d_k)_\alpha^U] x_k + [(a)_\alpha^L, (a)_\alpha^U]}{\sum_{p=1}^n \sum_{k=1}^n [(c'_{pk})_\alpha^L, (c'_{pk})_\alpha^U] x_p x_k + \sum_{k=1}^n [(d'_k)_\alpha^L, (d'_k)_\alpha^U] x_k + [(b)_\alpha^L, (b)_\alpha^U]}$$

$$\min(h(x))_\alpha = \min \left(\frac{h_1(x)}{h_2(x)} \right)_\alpha$$

$$= \min(h_1(x))_\alpha \cdot \min \left(\frac{1}{h_2(x)} \right)_\alpha$$

$$= \min(h_1(x))_\alpha \cdot \max(h_2(x))_\alpha$$

Now we have to prove the minimization problem for $\min(h_1(x))_\alpha$

$$\forall c \in [(c_{pk})_\alpha^L, (c_{pk})_\alpha^U], c \leq (c_{pk})_\alpha^U$$

$$\forall d \in [(d_k)_\alpha^L, (d_k)_\alpha^U], d \leq (d_k)_\alpha^U$$

$$\forall a \in [(a)_\alpha^L, (a)_\alpha^U], a \leq (a)_\alpha^U$$

The equation is

$$f_1(x) \leq \sum_{p=1}^n \sum_{k=1}^n (c_{pk})_\alpha^L x_p x_k + \sum_{k=1}^n (d_k)_\alpha^L x_k + (a)_\alpha^L$$

$$\min(f_1)_\alpha(x) = \sum_{p=1}^n \sum_{k=1}^n (c_{pk})_\alpha^L x_p x_k + \sum_{k=1}^n (d_k)_\alpha^L x_k + (a)_\alpha^L$$





Similarly, $\max(f_2)_\alpha(x) = \sum_{p=1}^n \sum_{k=1}^n (c'_{pk})_\alpha^U x_p x_k + \sum_{k=1}^n (d'_k)_\alpha^U x_k + (b')_\alpha^U$

$$\text{Min } f(x) = \frac{\sum_{p=1}^n \sum_{k=1}^n (c'_{pk})_\alpha^L x_p x_k + \sum_{k=1}^n (d'_k)_\alpha^L x_k + (a')_\alpha^L}{\sum_{p=1}^n \sum_{k=1}^n (c'_{pk})_\alpha^U x_p x_k + \sum_{k=1}^n (d'_k)_\alpha^U x_k + (b')_\alpha^U}$$

Special Case: $(O)_\alpha = [(O)_\alpha^L, (O)_\alpha^U]$, $\alpha \in [0, 1]$

$$\lambda[(O)_\alpha^L, (O)_\alpha^U] = \begin{cases} [\lambda(O)_\alpha^L, \lambda(O)_\alpha^U]; & \alpha \in [0, 1] \quad \forall \lambda \in \mathbb{R} \\ [\lambda(O)_\alpha^L, \lambda(O)_\alpha^U]; & \lambda \geq 0 \end{cases}$$

If $\lambda = -1$ i.e. In the function the coefficient of term is negative, then $(O)_\alpha^L$ replaced by $(O)_\alpha^U$ and vice – versa.

In the minimization type problems, the numerator coefficient s are changed to infimum and denominator coefficients are changed by supremum.

$$\min(h_i(x))_\alpha = \min \frac{\sum_{p=1}^n \sum_{k=1}^n (c'_{pk})_\alpha^L x_p x_k + \sum_{k=1}^n (d'_k)_\alpha^L x_k + (a')_\alpha^L}{\sum_{p=1}^n \sum_{k=1}^n (c'_{pk})_\alpha^U x_p x_k + \sum_{k=1}^n (d'_k)_\alpha^U x_k + (b')_\alpha^U}, \quad 1 \leq i \leq j \quad (1)$$

In the maximization type problems, supremum for the numerator coefficient and infimum for denominator coefficient to maximize function values, these are selected to convert crisp model.

$$\max(h_i(x))_\alpha = \max \frac{\sum_{p=1}^n \sum_{k=1}^n (c'_{pk})_\alpha^U x_p x_k + \sum_{k=1}^n (d'_k)_\alpha^U x_k + (a')_\alpha^U}{\sum_{p=1}^n \sum_{k=1}^n (c'_{pk})_\alpha^L x_p x_k + \sum_{k=1}^n (d'_k)_\alpha^L x_k + (b')_\alpha^L}, \quad 1 \leq i \leq j \quad (2)$$

After converting the fuzzy objective function to crisp form, using defuzzification method of α - cut gives numerical value in lieu of triangular fuzzy number in constraints. Let p_1 and p_2 be two numbers of constraints type (\leq) and (\geq) respectively i.e.

$$\left(\sum_{i=1}^n \sum_{k=1}^n \tilde{s}_{ik} x_i x_k + \sum_{i=1}^n \tilde{t}_i x_i \right)_r \leq \tilde{\theta}_r; r = 1, 2, \dots, p_1 \quad (3)$$

$$\text{and} \left(\sum_{i=1}^n \sum_{k=1}^n \tilde{s}_{ik} x_i x_k + \sum_{i=1}^n \tilde{t}_i x_i \right)_r \geq \tilde{\theta}_r; r = p_1 + 1, p_1 + 2, \dots, p_2 \quad (4)$$

are changed by these constraints,

$$\left(\sum_{i=1}^n \sum_{k=1}^n (\tilde{s}_{ik})_\alpha^L x_i x_k + \sum_{i=1}^n (\tilde{t}_i)_\alpha^L x_i \right)_r \leq U_\alpha((\tilde{\theta})_\alpha^U)_r; r = 1, 2, \dots, p_1 \quad (5)$$





Rozy Rani et al.,

$$\text{and} \left(\sum_{i=1}^n \sum_{k=1}^n (\tilde{s}_{ik})_{\alpha}^U x_i x_k + \sum_{k=1}^n (t_i)_{\alpha}^U x_i \right)_r \leq L_{\alpha}((e)_{\alpha}^L)_r; \quad r = p_1 + 1, p_1 + 2, \dots, p_2 \text{ respectively.} \quad (6)$$

where $(c)_{\alpha}^L$ and $(c)_{\alpha}^U$ denote greatest lower bound (glb) and least upper bound (lub) of α -level set of c .

Those constraints have equal sign i.e.

$$\left(\sum_{i=1}^n \sum_{k=1}^n \tilde{s}_{ik} x_i x_k + \sum_{k=1}^n t_i x_i \right)_r = \tilde{e}_r; \quad r = p_2 + 1, p_2 + 2, \dots, p \quad (7)$$

changed into two equivalent constraints:

$$\left(\sum_{i=1}^n \sum_{k=1}^n (\tilde{s}_{ik})_{\alpha}^L x_i x_k + \sum_{k=1}^n (t_i)_{\alpha}^L x_i \right)_r \leq ((e)_{\alpha}^U)_r; \quad r = 1, 2, \dots, p_1$$

$$\text{and} \left(\sum_{i=1}^n \sum_{k=1}^n (\tilde{s}_{ik})_{\alpha}^U x_i x_k + \sum_{k=1}^n (t_i)_{\alpha}^U x_i \right)_r \geq ((e)_{\alpha}^L)_r; \quad r = p_2 + 1, p_2 + 2, \dots, p \quad (8)$$

Similarly, In case of maximization type problem, the α – MOQFP is defined as after the desired value of α :

$$\max F_{\alpha}(x) = \max \left\{ (F_1)_{\alpha}(x), (F_2)_{\alpha}(x), \dots, (F_j)_{\alpha}(x) \right\} \quad (9)$$

$$\text{subject to} \left(\sum_{i=1}^n \sum_{k=1}^n (\tilde{s}_{ik})_{\alpha}^L x_i x_k + \sum_{k=1}^n (t_i)_{\alpha}^L x_i \right)_r \leq ((e)_{\alpha}^U)_r; \quad r = 1, 2, \dots, p_1 \quad (10)$$

$$\left(\sum_{i=1}^n \sum_{k=1}^n (\tilde{s}_{ik})_{\alpha}^U x_i x_k + \sum_{k=1}^n (t_i)_{\alpha}^U x_i \right)_r \geq ((e)_{\alpha}^L)_r; \quad r = p_1 + 1, p_1 + 2, \dots, p_2 \quad (11)$$

$$\left(\sum_{i=1}^n \sum_{k=1}^n (\tilde{s}_{ik})_{\alpha}^L x_i x_k + \sum_{k=1}^n (t_i)_{\alpha}^L x_i \right)_r \leq ((e)_{\alpha}^U)_r; \quad r = 1, 2, \dots, p_1$$

$$\left(\sum_{i=1}^n \sum_{k=1}^n (\tilde{s}_{ik})_{\alpha}^U x_i x_k + \sum_{k=1}^n (t_i)_{\alpha}^U x_i \right)_r \geq ((e)_{\alpha}^L)_r; \quad r = p_2 + 1, p_2 + 2, \dots, p \quad (12)$$

$$x \geq 0$$

$$\text{where } (F_i)_{\alpha}(x) = \frac{\sum_{i=1}^n \sum_{k=1}^n (c_{pk}^i)_{\alpha}^U x_i x_k + \sum_{k=1}^n (d_k^i)_{\alpha}^U x_k + (a^i)_{\alpha}^U}{\sum_{i=1}^n \sum_{k=1}^n (c_{pk}^i)_{\alpha}^L x_i x_k + \sum_{k=1}^n (d_k^i)_{\alpha}^L x_k + (b^i)_{\alpha}^L}, \quad 1 \leq i \leq j \quad (13)$$





Methodology of M-TOPSIS approach

The minimum and maximum value of every objective function is obtained independently and denoted by $\min (f_i(x))\alpha$ and $\max (f_i(x))\alpha$, $i = 1, 2, \dots, 1 \leq k \leq m$, of the objective function.

Let S_i denote initial individual solution for each $f_i^1(x)$.

To find $f_i^1(S_i)$ for each S_i and construct PIS and NIS (pay-off) table:

$$d_{q1}^{PIS}(x) = \left\{ \sum_{j=1}^{m_1} \lambda_j^{q_1} \left[\frac{f_j^* - f_j(x)}{f_j^* - f_j^-} \right]^{q_1} \right\}^{\frac{1}{q_1}} \quad (14)$$

$$d_{q1}^{NIS}(x) = \left\{ \sum_{j=1}^{m_1} \lambda_j^{q_1} \left[\frac{f_j - f_j^-}{f_j^* - f_j^-} \right]^{q_1} \right\}^{\frac{1}{q_1}} \quad (15)$$

and λ_j be prorated value.

where $f_j^* = \max \{f_j(x)\}$ denoting PIS, $f_j^- = \min \{f_j(x)\}$ denoting NIS and $x \in S$

Let $\mu^{PIS}(x)$ and $\mu^{NIS}(x)$ be membership function corresponding to bi-objective distance functions d_{q1}^{PIS} and d_{q1}^{NIS} respectively.

$$\begin{aligned} (d_{q1}^{PIS})^* &= \min d_{q1}^{PIS}(x), & (d_{q1}^{PIS})^- &= \max d_{q1}^{PIS}(x) \\ (d_{q1}^{NIS})^* &= \max d_{q1}^{NIS}(x), & (d_{q1}^{NIS})^- &= \min d_{q1}^{NIS}(x) \end{aligned}$$

$$\text{Then, } \mu^{PIS}(x) = \begin{cases} 1 & ; d_{q1}^{PIS}(x) < (d_{q1}^{PIS})^* \\ 1 - \frac{d_{q1}^{PIS}(x) - (d_{q1}^{PIS})^*}{(d_{q1}^{PIS})^- - (d_{q1}^{PIS})^*} & ; (d_{q1}^{PIS})^* \leq d_{q1}^{PIS}(x) \leq (d_{q1}^{PIS})^- \\ 0 & ; (d_{q1}^{PIS})^- < d_{q1}^{PIS}(x) \end{cases} \quad (16)$$

$$\mu^{NIS}(x) = \begin{cases} 1 & ; d_{q1}^{NIS}(x) > (d_{q1}^{NIS})^* \\ 1 - \frac{(d_{q1}^{NIS})^* - d_{q1}^{NIS}(x)}{(d_{q1}^{NIS})^* - (d_{q1}^{NIS})^-} & ; (d_{q1}^{NIS})^- \leq d_{q1}^{NIS}(x) \leq (d_{q1}^{NIS})^* \\ 0 & ; d_{q1}^{NIS}(x) < (d_{q1}^{NIS})^- \end{cases} \quad (17)$$

Now, the membership goals are obtained and given as follows;

$$1 - \frac{d_{q1}^{PIS}(x) - (d_{q1}^{PIS})^*}{(d_{q1}^{PIS})^- - (d_{q1}^{PIS})^*} + d_{q1}^{PIS^-} - d_{q1}^{PIS^+} = 1 \quad (18)$$

$$1 - \frac{(d_{q1}^{NIS})^* - d_{q1}^{NIS}(x)}{(d_{q1}^{NIS})^* - (d_{q1}^{NIS})^-} + d_{q1}^{NIS^-} - d_{q1}^{NIS^+} = 1 \quad (19)$$

where $d_{q1}^{PIS^-}$, $d_{q1}^{NIS^-}$ and $d_{q1}^{PIS^+}$, $d_{q1}^{NIS^+}$ indicate the under variation and over variation from the desired levels respectively. So the final MOQFM model are:

$$\text{Min } Z = w^{PIS} d_{q1}^{PIS^+} + w^{NIS} d_{q1}^{NIS^-} \quad (20)$$

$$\begin{aligned} &\text{subject to} \\ &1 - \frac{d_{q1}^{PIS}(x) - (d_{q1}^{PIS})^*}{(d_{q1}^{PIS})^- - (d_{q1}^{PIS})^*} + d_{q1}^{PIS^-} - d_{q1}^{PIS^+} = 1 \end{aligned} \quad (21)$$





$$1 - \frac{(d_{q1}^{NIS})^+ - d_{q1}^{NIS}(x)}{(d_{q1}^{NIS})^+ - (d_{q1}^{NIS})^-} + d_{q1}^{NIS-} - d_{q1}^{NIS+} = 1 \quad (22)$$

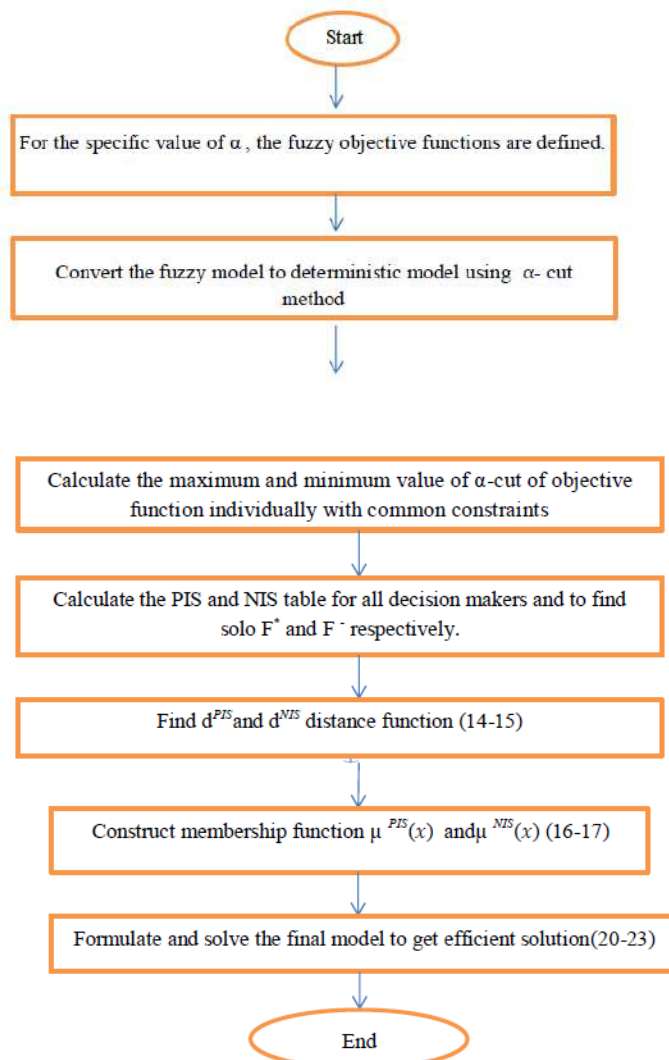
and $x \in S$

where w^{PIS} and w^{NIS} is prorated value of attaining the desired levels:

$$w^{PIS} = \frac{1}{(d_{q1}^{PIS})^- - (d_{q1}^{PIS})^+} \quad \& \quad w^{NIS} = \frac{1}{(d_{q1}^{NIS})^+ - (d_{q1}^{NIS})^-} \quad (23)$$

The final model is solved to get the efficient solution $x = (x_1^1, x_2^1)$.

Flow Chart of MOQFM Model





Rozy Rani et al.,

Algorithm of MOQFM with fuzzy using M-TOPSIS approach

Step1: Firstly the fuzzily objective functions are defined at specified value of α .

Step2: Transform the fuzzy model to crisp model to MOQFM.

Step3: Evaluate the highest and lowest values of α - cut of objective function all DMs individually with common constraints.

Step4: Find PIS pay off table and obtain

$F^* = (f_1^*, f_2^*, \dots, f_m^*)$ for individual positive ideal solution.

Step5: Create the NIS pay off table and obtain

$F^- = (f_1^-, f_2^-, \dots, f_m^-)$ for individual negative ideal solution.

Step6: Construct $dPIS(x)$ and $dNIS(x)$ (14- 15)

Step7: Construct membership function $\mu_{PIS}(x)$ and $\mu_{NIS}(x)$. (16- 17)

Step8: Construct the final model (20-23) and solve it.

Numerical Illustration of MOQFM Model

Our motive is to find compromise solution which is satisfied by all decision makers.

$$\min \left(F_1(x) = \frac{0.8x_1^2 - 2x_2^2 + 5x_2 + 10}{1x_1^2 + 3x_2 + 5}, F_2(x) = \frac{-2x_1^2 - 1x_1^2 + 5x_1 + 8}{1x_1^2 + 3x_2 + 5} \right)$$

subject to

$$1x_1^2 + 2x_1 + 1x_2 \leq 15.$$

$$1x_2^2 + 3x_1 + 2.2x_2 \leq 18.$$

$$1x_2^2 + 0.8x_1 + 7x_2 \geq 8.$$

$$x_1 \geq 0, x_2 \geq 0$$

The triangular fuzzy numbers are $0.8 = (0.8, 0.8, 0.8)$, $1 = (0, 1, 2)$, $2 = (2, 3, 4)$, $3 = (2, 3, 4)$, $5 = (4, 5, 6)$, $6 = (5.5, 6, 6.5)$, $7 = (6, 7, 8)$, $8 = (7, 8, 9)$, $10 = (9, 10, 10)$, $15 = (14, 15, 16)$, $18 = (17, 18, 19)$.

Solution: Assume that $\alpha = 0.8$

The crisp model is given by

$$\min \left(F_1(x) = \frac{0.8x_1^2 - 2.2x_2^2 + 4.8x_2 + 9.8}{1.2x_1^2 + 3.2x_2 + 5.2}, F_2(x) = \frac{-2.2x_1^2 - 1.2x_1^2 + 4.8x_1 + 7.8}{1.2x_1^2 + 3.2x_2 + 5.2} \right)$$

subject to

$$0.8x_1^2 + 1.8x_1 + 6.8x_2 \leq 15.2,$$

$$0.8x_2^2 + 2.8x_1 + 2.2x_2 \leq 18.2,$$

$$1.2x_2^2 + 0.8x_1 + 7.2x_2 \geq 7.8.$$

$$x_1 \geq 0, x_2 \geq 0$$

For minimization, $X_1 = (0, 2.2353)$ and $X_2 = (0, 2.2352)$

For maximization, $X_1 = (0.1716, 0.9224)$ and $X_2 = (0.7577, 0.8723)$

For PIS pay-off values, $F^* = (f_{11}^*, f_{12}^*) = (1.51206, 1.0669)$





Rozy Rani et al.,

For NIS pay-off values, $F^- = (f_{11}^-, f_{12}^-) = (0.77204, 0.14604)$

Assume that $\lambda_1 = \lambda_2 = 0.5$ than $d_2^P(x)$ and $d_2^{NIS}(x)$

Assume that $\lambda_1 = \lambda_2 = 0.5$ than $d_2^{PIS}(x)$ and $d_2^{NIS}(x)$

$$d_2^{PIS}(x) = \left\{ \left(\frac{0.5}{0.3801} \right)^2 \left[\frac{1.0252 x_1^2 - 2.2x_2^2 - 1.1133x_2 + 3.8091}{1.2x_1^2 + 3.2x_2 + 5.2} \right]^2 + \left(\frac{0.5}{0.92086} \right)^2 \left[\frac{3.4803 x_1^2 + 1.2x_2^2 + 3.4141x_2 - 4.8x_1 - 2.2521}{1.2x_1^2 + 3.2x_2 + 5.2} \right]^2 \right\}^{1/2}$$

$$d_2^{NIS}(x) = \left\{ \left(\frac{0.5}{0.3801} \right)^2 \left[\frac{-0.1264 x_1^2 - 2.2x_2^2 + 2.3296x_2 + 5.7856}{1.2x_1^2 + 3.2x_2 + 5.2} \right]^2 + \left(\frac{0.5}{0.92086} \right)^2 \left[\frac{-2.3752 x_1^2 - 1.2x_2^2 + 4.8x_1 - 0.4673x_2 + 7.0406}{1.2x_1^2 + 3.2x_2 + 5.2} \right]^2 \right\}^{1/2}$$

Obtain $\text{Min}(d_2^{PIS}) = (0.27931, 0.9133)$

$\text{Max}(d_2^{PIS}) = (0, 2.2353)$

$\text{Min}(d_2^{NIS}) = (0, 2.2353)$

$\text{Max}(d_2^{NIS}) = (0.4140, 0.9018)$

$(d_2^{PIS})^- = \text{Max } d_2^{PIS} = 1.403283, (d_2^{NIS})^- = \text{Min } d_2^{NIS} = 0.00005$

$(d_2^{PIS})^* = \text{Min } d_2^{PIS} = 0.755511, (d_2^{NIS})^* = \text{Max } d_2^{NIS} = 1.07372$

The membership function $\mu^{PIS}(x)$ and $\mu^{NIS}(x)$ may be obtained as:

$$\mu^{PIS}(x) = 2.1663 - 1.5437 d_2^{PIS}$$

$$\mu^{NIS}(x) = -0.000046 + 0.93138 d_2^{NIS}$$

The final Model MOQFM is

$$\text{Min } Z = 1.5437 d_2^{PIS+} + 0.9314 d_2^{NIS-}$$

subject to

$$\begin{cases} \mu_1^{PIS}(x) + (D^{PIS})^- - (D^{PIS})^+ = 1 \\ \mu_1^{NIS}(x) + (D^{NIS})^- - (D^{NIS})^+ = 1 \end{cases}$$

$$2.1663 - 1.5437 d_2^{PIS} + D_1 - d_2^P = 1$$

$$-0.000046 + 0.93138 d_2^{NIS} + d_2^N - D_2 = 1$$

$$x_1^2 + x_2^2 + x_3^2 \leq 11$$

$$x_1^2 + x_2 + x_3 \leq 4$$

$$x_2^2 + x_1 + x_3 \leq 9$$

$$x_1, x_2, x_3 \geq 0$$

$(D^{PIS})^+, (D^{PIS})^-, (D^{NIS})^+, (D^{NIS})^- \geq 0$ Using Lingo 19 software, we get the solution $x^* = (0, 1.954583)$

The objective functions are $F_1(x) = 0.940851$, $F_2(x) = 0.280718$. The objective function's values are nearly at their desired values.





Rozy Rani et al.,

CONCLUSION

The main aim of each decision maker with fuzzy is to satisfy maximum membership value so as to obtain efficient solution. M-TOPSIS approach has to perceive the greatest membership of two distance functions with unchangeable nature of the problem. Baky and El Sayed (2014) explained the linear fractional optimization with M-TOPSIS model. In this paper, we extended Baky and El Sayed's M-TOPSIS approach for solving single level linear multi objective fractional decision making problem of stochastic fuzzy to single level multi objective quadratic fractional decision making of fuzzy M-TOPSIS approach with quadratic set of constraints. The proposed approach may further be extended to bilevel, multilevel of MOQFM with fuzzy parameters.

Declarations of Conflicting Interests

The author(s) declared no potential conflict of interest with respect to the research, authorship and/ or publication of this article.

REFERENCES

1. Abo-Sinna, M. A. (2002). Generating an alpha-Pareto Optimal Solution to Multiobjective Nonlinear Programming Problems with Fuzzy Parameters: A Decomposition Method. *Journal of Fuzzy Mathematics*, 10(2), 423-440.
2. Anisseh, M., Piri, F., Shahraki, M. R., & Agamohamadi, F. (2012). Fuzzy extension of TOPSIS model for group decision making under multiple criteria. *Artificial Intelligence Review*, 38, 325-338.
3. Baky, I. A., & El Sayed, M. A. (2014). Bi-level multi-objective programming problems with fuzzy parameters: modified TOPSIS approach. *International Journal of Management and Fuzzy Systems*, 2(5), 38-50.
4. Bellman, R.E.; L.A. Zadeh. (1970). Decision-making in a fuzzy environment. *Management science*, 17, 4, 141-164
5. Charnes, A., & Cooper, W. W. (1962). Programming with linear functional. *Naval Research Logistics Quarterly*, 9, 181-186.
6. Chen, C. T. (2000). Extensions of the TOPSIS for group decision-making under fuzzy environment. *Fuzzy sets and systems*, 114(1), 1-9.
7. Chauhan, A., Mahajan, S., Ahmad, I., & Al-Homidan, S. (2023). On Fuzzy Linear Fractional Programming Problems via α -Cut-Based Method with Application in Transportation Sector. *Symmetry*, 15(2), 419.
8. Das, S. K. (2017). Modified method for solving fully fuzzy linear programming problem with triangular fuzzy numbers. *International journal of research in industrial engineering*, 6(4), 293-311.
9. Emam, O. E., Kholeif, S. A., & Azzam, S. (2015). A decomposition algorithm for solving stochastic multi-level large scale quadratic programming problem. *Applied Mathematics & Information Sciences*, 9(4), 1817.
10. Hwang, C. L., Yoon, K., Hwang, C. L., & Yoon, K. (1981). Methods for multiple attribute decision making. Multiple attribute decision making: methods and applications a state-of-the-art survey, 58-191
11. Hwang, C. L., Lai, Y. J., & Liu, T. Y. (1993). A new approach for multiple objective decision making. *Computers & operations research*, 20(8), 889-899.
12. Lachhwani, K. (2014). On solving multi-level multi objective linear programming problems through fuzzy goal programming approach. *Opsearch*, 51, 624-637.
13. Mahmoud. A. Abo-Sinna. (2000). Extensions of the TOPSIS formulti-objective dynamic programming problems under fuzziness, *Adv. Model. Anal. (AMSE Press, France)* B 43 (4) 1-24.
14. Osman, M., Emam, O., & Sayed, M. (2017). Multi-level multi-objective quadratic fractional programming problem with fuzzy parameters: a FGP approach. *Asian research journal of mathematics*, 5(3), 1-19.
15. Rani, N., Goyal, V., & Gupta, D. (2022). On solving multi-objective fully quadratic fractional optimisation model with interactive FGP approach. *International Journal of Quality & Reliability Management*, 39(10), 2286-2301.





Rozy Rani et al.,

16. Rani, N., Goyal, V., & Gupta, D. (2021). Algorithm for bi-level multi-objective fully quadratic fractional optimization model with fuzzy parameters: FGP for BLMOFQFOM. *Journal of Ambient Intelligence and Humanized Computing*, 12(12), 10637-10649.
17. Rani, R., Goyal, V., & Gupta, D. (2023, December). M-TOPSIS approach for solving bilevel multi-objective quadratic fractional programming. In *AIP Conference Proceedings* (Vol. 2916, No. 1). AIP Publishing.
18. Rani, R., Goyal, V., & Gupta, D. (2022). A SOLUTION APPROACH TO QUADRATICALLY CONSTRAINED MULTI-OBJECTIVE DECISION MAKING PROBLEM WITH M-TOPSIS PROGRAMMING. *NeuroQuantology* 20(7) DOI: 10.14704/nq.2022.20.7.NQ33405
19. Tanaka, H., T. Okuda,; K. Asai. (1973). Fuzzy mathematical programming. *Transactions of the society of instrument and control engineers*, 5, 607-613.
20. Zadeh, L.A. (1996). Fuzzy sets, in *Fuzzy sets, fuzzy logic, and fuzzy systems: selected papers by Lotfi A Zadeh*. World Scientific, 394-432.
21. Zimmermann, H. J. (2011). *Fuzzy set theory—and its applications*. Springer Science & Business Media.

Table 1: PIS table

	F ₁	F ₂
X ₁	1.51206*	0.92071
X ₂	1.47141	1.0669*

Table2: NIS table

	F ₁	F ₂
X ₁	0.77204*	0.14604*
X ₂	0.77211	0.1461





Weakly Compatible Fixed Point Theorem in Modified Intuitionistic Fuzzy Metric Spaces

Anju and Vishal Gupta

Department of Mathematics, MMEC, Maharishi Markandeshwar (Deemed to be University), Mullana, Haryana, India.

Received: 20 Jan 2024

Revised: 09 Feb 2024

Accepted: 14 May 2024

*Address for Correspondence

Anju

Department of Mathematics,
MMEC, Maharishi Markandeshwar
(Deemed to be University),
Mullana, Haryana, India.

Email: anju.kaliraman02@gmail.com



This is an Open Access Journal / article distributed under the terms of the **Creative Commons Attribution License** (CC BY-NC-ND 3.0) which permits unrestricted use, distribution, and reproduction in any medium, provided the original work is properly cited. All rights reserved.

ABSTRACT

In this manuscript, we proved fixed point theorem in modified intuitionistic fuzzy metric space by using weakly compatible mapping. Common fixed point in modified intuitionistic fuzzy metric space for two compatible and sequentially continuous mappings that satisfy ϕ -contractive conditions also proved. Our results provide a substantial extension of several important results from modified intuitionistic fuzzy metric spaces using different contraction.

Keywords: Fixed point, modified intuitionistic fuzzy metric space, Compatible map, Sequentially continuous mapping.

INTRODUCTION

One of the most important problems in fuzzy topology is to obtain an appropriate concept of an IFMS and an intuitionistic fuzzy normed space. This problems have been investigated by Park and Saadati[5, 6, 7, 8]. Due to additional conditions in IFMS (refer to), we have adapted the concept, proposing a novel definition of IFMSs through the incorporation of the notion of continuous t-represent ability. After that, MIFMS introduced by Sedghi[5] and common coupled FP theorem proved by Gupta and Saini [9, 10]. This approach incorporated the concept Baised maps in MIFMS and FP results also introduced by Gupta and Saini [10]. Many researchers work on MIFMS see references [5, 6, 7, 8, 10, 11, 12].





PRELIMINARIES

Lemma 2.1. [6] Consider the set \mathbb{M}^* and operation $\leq_{\mathbb{M}^*}$ which is defined as

$$\mathbb{M}^* = \{(\varpi, \kappa) : (\varpi, \kappa) \in [0, 1]^2 \text{ and } \varpi + \kappa \leq 1\}$$

$(\varpi, \kappa) \leq_{\mathbb{M}^*} (\aleph_1, \aleph_2)$ if and only if $(\varpi \leq \aleph_1)$ and $(\kappa \geq \aleph_2)$, for every $(\varpi, \kappa), (\aleph_1, \aleph_2) \in \mathbb{M}^*$.

Then $(\mathbb{M}^*, \leq_{\mathbb{M}^*})$ is a complete lattice.

Definition 2.1. [7] A t-norm defined on \mathbb{M}^* is a mapping $R : (\mathbb{M}^*)^2 \rightarrow \mathbb{M}^*$ that satisfied to the following conditions:

- (Commutativity) $R(\varpi, \aleph) = R(\aleph, \varpi)$, for all $\varpi, \aleph \in \mathbb{M}^*$;
- (Boundary condition) $R(\varpi, 1_{\mathbb{M}^*}) = \varpi$, for all $\varpi \in \mathbb{M}^*$;
- (Associativity) $R(\varpi, T(\aleph, z)) = R(R(\varpi, \aleph), z)$, for all $\varpi, \aleph, z \in \mathbb{M}^*$;
- (Monotonicity) if $\varpi \leq_{\mathbb{M}^*} \varpi_0$ and $\aleph \leq_{\mathbb{M}^*} \aleph_0$, then $R(\varpi, \aleph) \leq_{\mathbb{M}^*} R(\varpi_0, \aleph_0)$ for all $\varpi, \varpi_0, \aleph, \aleph_0 \in \mathbb{M}^*$.

Definition 2.2. [8] A continuous t-norm, denoted as R and defined on the set \mathbb{M}^* , is considered continuously t-representable if and only if there exist two continuous norms, a t-norm denoted as $*$ and a continuous t-conorm denoted as \oplus , defined on the interval $[0, 1]$. This representation holds true for all pairs $\varpi = (\varpi, \kappa)$ and $\aleph = (\aleph_1, \aleph_2)$ in the set \mathbb{M}^* , as expressed by the equation:

$$R(\varpi, \aleph) = (\varpi \oplus \aleph_1, \kappa * \aleph_2).$$

Now, let's define a sequence R_n recursively with $R_1 = R$ and

$$R_n(\varpi^{(1)}, \dots, \varpi^{(n+1)}) = R(R_{n-1}(\varpi^{(1)}, \dots, \varpi^{(n)}), \varpi^{(n+1)})$$

for $n \geq 2$ and $\varpi^{(i)} \in \mathbb{M}^*$.

Definition 2.3. [5] A negator on \mathbb{M}^* is defined as any decreasing mapping $\Lambda : \mathbb{M}^* \rightarrow \mathbb{M}^*$ that meets the conditions $\Lambda(0_{\mathbb{M}^*}) = 1_{\mathbb{M}^*}$ and $\Lambda(1_{\mathbb{M}^*}) = 0_{\mathbb{M}^*}$. When $\Lambda(\Lambda(\varpi)) = \varpi$ holds for all $\varpi \in \mathbb{M}^*$, the negator Λ is referred to as an involutive negator. On the interval $[0, 1]$, a negator is a decreasing mapping $\Lambda : [0, 1] \rightarrow [0, 1]$ with the properties $\Lambda(0) = 1$ and $\Lambda(1) = 0$. The standard negator on $[0, 1]$, denoted as Λ_s , is defined as follows: for all $\varpi \in [0, 1]$, $\Lambda_s(\varpi) = 1 - \varpi$.

Definition 2.4. [5]

Let $\mathfrak{U}, \mathfrak{V}$ be fuzzy sets from $Z^2 \times \mathcal{P}_0$ to $[0, 1]$ such that $\mathfrak{U}(\varpi, \kappa, \bar{\xi}) + \mathfrak{V}(\varpi, \kappa, \bar{\xi}) \leq 1$ and Z is a non-empty set, R is a continuous t-representable function, and $\mathcal{L}_{\mathfrak{U}, \mathfrak{V}}$ is a mapping defined as $Z^2 \times \mathcal{P}_0 \rightarrow I^*$, where \mathcal{P}_0 is a specified domain. The 3-tuple $(Z, \mathcal{L}_{\mathfrak{U}, \mathfrak{V}}, R)$ is characterized as a MIFMS if the following conditions are met for all $\varpi, \kappa \in Z$ and $t, s > 0$

1. $\mathcal{L}_{\mathfrak{U}, \mathfrak{V}}(\varpi, \kappa, \bar{\xi}) \geq_{I^*} \theta_{I^*}$;
2. $\mathcal{L}_{\mathfrak{U}, \mathfrak{V}}(\varpi, \kappa, \bar{\xi}) = l_{I^*}$ if and only if $\varpi = \kappa$;
3. $\mathcal{L}_{\mathfrak{U}, \mathfrak{V}}(\varpi, \kappa, \bar{\xi}) = \mathcal{L}_{\mathfrak{U}, \mathfrak{V}}(\kappa, \varpi, \bar{\xi})$;





Anju and Vishal Gupta

$$4. \mathcal{L}_{\mathfrak{U}, \mathfrak{V}}(\varpi, \kappa, \bar{\xi} + s) \geq_{I^*} R(\mathcal{L}_{\mathfrak{U}, \mathfrak{V}}(\varpi, z, \bar{\xi}), \mathcal{L}_{\mathfrak{U}, \mathfrak{V}}(z, \kappa, s));$$

$$5. \mathcal{L}_{\mathfrak{U}, \mathfrak{V}}(\varpi, \kappa, \cdot) : \mathcal{P}_0 \rightarrow I^* \text{ is continuous.}$$

Then, $\mathcal{L}_{\mathfrak{U}, \mathfrak{V}}$ is called an MIFMS, where $\mathcal{L}_{\mathfrak{U}, \mathfrak{V}}(\varpi, \kappa, \bar{\xi}) = (\mathfrak{U}(\varpi, \kappa, \bar{\xi}), \mathfrak{V}(\varpi, \kappa, \bar{\xi}))$.

Remark 2.1. [5] In a MIFMS $(Z, \mathcal{L}_{\mathfrak{U}, \mathfrak{V}}, R)$, where $\mathfrak{U}(\varpi, \kappa, \bar{\xi})$ is non decreasing and $\mathfrak{V}(\varpi, \kappa, \bar{\xi})$ is non increasing then

$$\mathcal{L}_{\mathfrak{U}, \mathfrak{V}}(\varpi, \kappa, \bar{\xi}) \preceq_{I^*} R(\mathfrak{U}(\varpi, \kappa, \bar{\xi}), \mathfrak{V}(\varpi, \kappa, \bar{\xi}))$$

is non decreasing for all $\varpi, \kappa \in Z$ where

$$R(\mathfrak{k}, v) = (\mathfrak{k}_1 * v_1, \mathfrak{k}_2 \oplus v_2) \text{ and } \mathfrak{k} = (\mathfrak{k}_1, v_1), v = (\mathfrak{k}_2, v_2) \in I.$$

Definition 2.5. [5] A sequence $\{\varpi_n\}$ in an MIFMS $(Z, \mathcal{L}_{\mathfrak{U}, \mathfrak{V}}, R)$ is called a Cauchy sequence if for each $0 < e < 1, \bar{\xi} \geq 0$ there exists $n_0 \in N$ with $n, m \geq n_0$, such that

$$\mathcal{L}_{\mathfrak{U}, \mathfrak{V}}(\varpi_n, \kappa_m, \bar{\xi}) \geq_{I^*} (\Lambda_s(e), e),$$

where Λ_s is denote the standard negator.

Definition 2.6. [5] The sequence $\{\varpi_n\}$ is said to be convergent to $\varpi \in Z$ in the MIFMS $(Z, \mathcal{L}_{\mathfrak{U}, \mathfrak{V}}, R)$ and denoted by $\varpi_n \xrightarrow{\mathcal{L}_{\mathfrak{U}, \mathfrak{V}}} \varpi$ if $\mathcal{L}_{\mathfrak{U}, \mathfrak{V}}(\varpi_n, \varpi, \bar{\xi}) \rightarrow 1_{I^*}$ whenever $n \rightarrow \infty$ for all $\bar{\xi} \geq 0$.

Definition 2.7. [5] A MIFMS is termed complete if every Cauchy sequence within it converges.

Lemma 2.2. [5] Consider $(Z, \mathcal{L}_{\mathfrak{U}, \mathfrak{V}}, R)$ as a MIFMS. In this context, for any $\bar{\xi} \geq 0$, the function $\mathcal{L}_{\mathfrak{U}, \mathfrak{V}}(\varpi, \kappa, \bar{\xi})$ exhibits a non-decreasing behavior with respect to $\bar{\xi}$ within the lattice (I^*, \preceq_{I^*}) , for all $\varpi, \kappa \in Z$.

Definition 2.8. [5] Let $(Z, \mathcal{L}_{\mathfrak{U}, \mathfrak{V}}, R)$ be an MIFMS. For $\bar{\xi} \geq 0$, we define an open ball $B(\varpi, e, \bar{\xi})$ with center $\varpi \in Z$ and radius $0 < e < 1$, as

$$B(\varpi, e, \bar{\xi}) = \{\kappa \in Z : \mathcal{L}_{\mathfrak{U}, \mathfrak{V}}(\varpi, \kappa, \bar{\xi}) \geq_{I^*} (\Lambda_s(e), e)\}.$$

A subset $A \subseteq Z$ is called open if for each $\varpi \in A$, there exist $\bar{\xi} \geq 0, 0 < e < 1$ such that $B(\varpi, e, \bar{\xi}) \subseteq A$.

Let $\tau_{\mathcal{L}_{\mathfrak{U}, \mathfrak{V}}}$ is the set of all open subsets of Z . $\tau_{\mathcal{L}_{\mathfrak{U}, \mathfrak{V}}}$ is the topology induced on MIFMS.

Definition 2.9. [5] Let $(Z, \mathcal{L}_{\mathfrak{U}, \mathfrak{V}}, R)$ be an MIFMS. A subset A of Z is considered MIF-bounded if there exist $\bar{\xi} \geq 0$ and $0 < e < 1$ such that

$$\mathcal{L}_{\mathfrak{U}, \mathfrak{V}}(\varpi, \kappa, \bar{\xi}) \geq_{I^*} (\Lambda_s(e), e) \text{ for every } \varpi, \kappa \in A.$$





Anju and Vishal Gupta

Definition 2.10. [5] Let $(Z, \mathcal{L}_{u,v}, R)$ be an MIFMS. $\mathcal{L}_{u,v}$ is said to be continuous on $Z \times Z \times \mathcal{P}_0$ if

$$\lim_{n \rightarrow \infty} \mathcal{L}_{u,v}(\varpi_n, \kappa_n, \bar{\xi}_n) = \mathcal{L}_{u,v}(\varpi, \kappa, \bar{\xi}),$$

whenever a sequence $\{(\varpi_n, \kappa_n, \bar{\xi}_n)\}$ in $Z \times Z \times \mathcal{P}_0$ converges to a point $(\varpi, \kappa, \bar{\xi}) \in Z \times Z \times \mathcal{P}_0$, i.e.,

$$\lim_n \mathcal{L}_{u,v}(\varpi_n, \varpi, \bar{\xi}) = \lim_n \mathcal{L}_{u,v}(\kappa_n, \kappa, \bar{\xi}) = 1_{I^*} \quad \text{and} \quad \lim_n \mathcal{L}_{u,v}(\varpi, \kappa_n, \bar{\xi}) = \mathcal{L}_{u,v}(\varpi, \kappa, \bar{\xi}).$$

Lemma 2.3. Let $(Z, \mathcal{L}_{u,v}, R)$ be an MIFMS. Then $\mathcal{L}_{u,v}$ is a continuous function on $Z \times Z \times \mathcal{P}_0$.

Definition 2.11. Let Ψ denote a set of contractive conditions, where $\Psi = \{\varphi : \mathbb{R}^+ \rightarrow \mathbb{R}^+\}$, and each $\varphi \in \Psi$ satisfies the following conditions:

- (i) φ is non-decreasing;
- (ii) φ is continuous;
- (iii) $\sum_{n=0}^{\infty} \varphi^n(\bar{\xi}) < \infty$ for all $\bar{\xi} > 0$, where $\varphi^{n+1}(\bar{\xi}) = \varphi(\varphi^n(\bar{\xi}))$, $n \in \mathbb{N}$.

Notably, if $\varphi \in \Psi$, then $\varphi(\bar{\xi}) < \bar{\xi}$ for all $\bar{\xi} > 0$.

Lemma 2.4. Consider $\varphi \in \Psi$. Thus, for all $\bar{\xi} > 0$, it gives that $\lim_{n \rightarrow \infty} \varphi^n(\bar{\xi}) = 0$, where $\varphi^n(\bar{\xi})$ denotes the n -th iteration of φ .

Definition 2.12. Let $(Z, \mathcal{L}_{u,v}, R)$ be an MIFMS. $\mathcal{L}_{u,v}$ is said to be n -property on $Z^2 \times \mathcal{P}_0$ where $\lim_{n \rightarrow \infty} \{\mathcal{L}_{u,v}(\varpi, \kappa, k^n \bar{\xi})\}_n = 1$, whenever $\varpi, \kappa \in Z$, $k > 1$, and $n \in \mathbb{N}$.

Definition 2.13. An ordered pair $(\varpi, \kappa) \in Z \times Z$ is designated as a common FP, a coupled coincidence point, a common coupled FP, and a couple FP if and only if it satisfies the following conditions:

1. It serves as a common fixed point for the mapping $F : Z \times Z \rightarrow Z$ if $F(\varpi, \kappa) = \varpi$ and $F(\kappa, \varpi) = \kappa$.
2. It functions as a coupled coincidence point for the mappings $F : Z \times Z \rightarrow Z$ and $G : Z \rightarrow Z$ if $F(\varpi, \kappa) = G(\varpi)$ and $F(\kappa, \varpi) = G(\kappa)$.
3. It acts as a common coupled fixed point for the mappings $F : Z \times Z \rightarrow Z$ and $G : Z \rightarrow Z$ if $\varpi = F(\varpi, \kappa) = G(\varpi)$ and $\kappa = F(\kappa, \varpi) = G(\kappa)$.
4. It serves as a common fixed point for the mappings $F : Z \times Z \rightarrow Z$ and $G : Z \rightarrow Z$ if $\varpi = G(\varpi) = F(\varpi, \varpi)$.





Definition 2.14. If the mappings $F : Z \times Z \rightarrow Z$ and $G : Z \rightarrow Z$ are called compatible if there exist elements S_n and Q_n in set Z such that this compatibility is characterized by the following conditions:

$$\lim_{n \rightarrow \infty} \mathcal{L}_{\mathcal{U}, \mathfrak{W}}(GF(S_n, Q_n), F(GS_n, GQ_n), \bar{\xi}) = 1,$$

$$\lim_{n \rightarrow \infty} \mathcal{L}_{\mathcal{U}, \mathfrak{W}}(GF(Q_n, S_n), F(GQ_n, GS_n), \bar{\xi}) = 1,$$

where

$$\lim_{n \rightarrow \infty} F(S_n, Q_n) = \lim_{n \rightarrow \infty} GS_n = \lambda, \text{ and } \lim_{n \rightarrow \infty} F(Q_n, S_n) = \lim_{n \rightarrow \infty} GQ_n = \mu,$$

for all $\lambda, \mu \in Z$.

Definition 2.15. If the mappings $F : Z \times Z \rightarrow Z$ and $G : Z \rightarrow Z$ are called sub-sequentially continuous iff there exist sequences $S_n, Q_n \in Z$ such that

$$\lim_{n \rightarrow \infty} F(S_n, Q_n) = \lim_{n \rightarrow \infty} GS_n = \lambda,$$

$$\lim_{n \rightarrow \infty} F(Q_n, S_n) = \lim_{n \rightarrow \infty} GQ_n = \mu,$$

Where,

$$\lim_{n \rightarrow \infty} F(GS_n, GQ_n) = F(\lambda, \mu), \lim_{n \rightarrow \infty} F(GQ_n, GS_n) = F(\mu, \lambda),$$

$$\lim_{n \rightarrow \infty} GF(S_n, Q_n) = G\lambda, \lim_{n \rightarrow \infty} GF(Q_n, S_n) = G\mu.$$

MAINS RESULTS

Definition 3.1. Let t -representable R is said to be of \mathbb{H} -type if the family of functions $R_\beta(\bar{\xi})$ for $\beta = 1$ to ∞ is equi-continuous at $\bar{\xi} = 0$, where $\sup_{0 < \bar{\xi} < 1} R(\bar{\xi}, \bar{\xi}) = 1$, $\inf_{0 < \bar{\xi} < 1} R(\bar{\xi}, \bar{\xi}) = 0$, $R_1(\bar{\xi}) = \bar{\xi}R\bar{\xi}$, and $R^{\beta+1}(\bar{\xi}) = \bar{\xi}R(R^\beta(\bar{\xi}))$, where $\beta = 1, 2, \dots$, $\bar{\xi} \in [0, 1]$.

Furthermore, the t -representable set $R_M = \{\min, \max\}$ is an example.

Remark 3.1. It is easy to prove that if $S_n \rightarrow \varpi$, $Q_n \rightarrow \kappa$, and $\bar{\xi}_n \rightarrow \bar{\xi}$, we get $\lim_{n \rightarrow \infty} \mathcal{L}_{\mathcal{U}, \mathfrak{W}}(S_n, Q_n, \bar{\xi}_n) = \mathcal{L}_{\mathcal{U}, \mathfrak{W}}(\varpi, \kappa, \bar{\xi})$.

Lemma 3.1. Let $(Z, \mathcal{L}_{\mathcal{U}, \mathfrak{W}}, R)$ be an MIFMS where R is the continuous t -representable of \mathbb{H} -type, respectively. If there exists $\varphi \in \Psi$ such that $\mathcal{L}_{\mathcal{U}, \mathfrak{W}}(\varpi, \kappa, \varphi(\bar{\xi})) \geq \mathcal{L}_{\mathcal{U}, \mathfrak{W}}(\varpi, \kappa, \bar{\xi})$ for all $\bar{\xi} > 0$, then $\varpi = \kappa$.

Theorem 3.1. Let $(Z, \mathcal{L}_{\mathcal{U}, \mathfrak{W}}, R)$ be an MIFMS where R is a continuous t -representable norm of \mathbb{H} -type, such that $\mathfrak{U}(\varpi, \kappa, \bar{\xi}) + \mathfrak{W}(\varpi, \kappa, \bar{\xi}) \leq 1$, $\forall \varpi, \kappa \in Z$. Let $A : Z \times Z \rightarrow Z$ and $B : Z \rightarrow Z$ be two compatible mappings satisfying the conditions:

- (I) The pairs $A(Z \times Z) \subseteq B(Z)$, and $B(Z)$ or $A(Z \times Z)$ is complete;





Anju and Vishal Gupta

(II) there exists $\varphi \in \Psi$ such that

$$\mathcal{L}_{\mathcal{U}, \mathfrak{W}}(A(\varpi, \kappa), A(\eta_1, \eta_2), \varphi(\bar{\xi})) \geq \gamma \min(\mathcal{L}_{\mathcal{U}, \mathfrak{W}}(B\varpi, B\eta_1, \bar{\xi}), \mathcal{L}_{\mathcal{U}, \mathfrak{W}}(B\kappa, B\eta_2, \bar{\xi}))$$

for all $\varpi, \kappa, \eta_1, \eta_2 \in Z$ and $\bar{\xi} > 0$. where $\gamma : \mathbb{M}^* \rightarrow \mathbb{M}^*$ is a function such that $\gamma(\alpha) \geq (\alpha)$ for each $\alpha \in \mathbb{M}^*$

Then, there exists a unique CFP.

Proof. Let $\varpi_0, \eta_0 \in Z$ be any arbitrary points. Also, the mappings $A(Z \times Z) \subseteq BZ$ and $\varpi, \eta_1 \in Z$ such that

$$B(\varpi) = A(\varpi_0, \eta_0) \text{ and } B(\eta_1) = A(\eta_0, \varpi_0),$$

we can get two sequences $\varpi_n, \eta_n \in Z$ such that

$$B(\varpi_{n+1}) = A(\varpi_n, \eta_n), B(\eta_{n+1}) = A(\eta_n, \varpi_n), \forall n \geq 0.$$

Now, we shall prove that $B\varpi_n, B\eta_n$ are Cauchy sequences. Since R is the t -representable of \mathbb{H} -type, for any $\delta > 0$, $\exists \varsigma > 0$, $n \in \mathbb{N}$ such that

$$R = \{\min((1 - \varsigma) * (1 - \varsigma) * \dots * (1 - \varsigma)), \max(\varsigma \diamond \varsigma \diamond \dots \diamond \varsigma)\}$$

$$R = \{1 - \delta, \delta\} \rightarrow (1, 0) = 1_I \text{ as } \delta \rightarrow \infty$$

where $\mathcal{L}_{\mathcal{U}, \mathfrak{W}}(\varpi, \kappa, \bar{\xi})$, are continuous. For this, we have

$$\lim_{n \rightarrow \infty} \mathcal{U}(\varpi, \kappa, \bar{\xi}) + \mathfrak{W}(\varpi, \kappa, \bar{\xi}) = 1$$

for all $\varpi, \kappa \in Z$, there exists $\bar{\xi}_0 > 0$ we get that,

$$\mathcal{L}_{\mathcal{U}, \mathfrak{W}}(B\varpi_0, B\varpi, \bar{\xi}_0) \geq (1 - \varsigma) \Rightarrow \mathcal{L}_{\mathcal{U}, \mathfrak{W}}(B\eta_1, B\eta_2, \bar{\xi}_0) \geq (1 - \varsigma).$$

Now, applying the contractive conditions defined by Ψ results in

$$\sum_{n=1}^{\infty} \varphi^n(\bar{\xi}_0) < \infty.$$

Consequently, for all $\bar{\xi} > 0$, there exists $n_0 \in \mathbb{N}$, $\bar{\xi} > \sum_{k=n_0}^{\infty} \varphi^k(\bar{\xi}_0)$, which gives to

$$\begin{aligned} \mathcal{L}_{\mathcal{U}, \mathfrak{W}}(B\varpi, B\kappa, \varphi(\bar{\xi}_0)) &= \mathcal{L}_{\mathcal{U}, \mathfrak{W}}(A(\varpi_0, \eta_0), A(\varpi, \eta_1), \varphi(\bar{\xi}_0)) \\ &\geq \gamma \min(\mathcal{L}_{\mathcal{U}, \mathfrak{W}}(B\varpi_0, B\varpi, \bar{\xi}), \mathcal{L}_{\mathcal{U}, \mathfrak{W}}(B\eta_0, B\eta_1, \bar{\xi})) \\ \mathcal{L}_{\mathcal{U}, \mathfrak{W}}(B\eta_1, B\eta_2, \varphi(\bar{\xi}_0)) &= \mathcal{L}_{\mathcal{U}, \mathfrak{W}}(A(\eta_0, \varpi_0), A(\eta_1, \varpi), \varphi(\bar{\xi}_0)) \\ &\geq \gamma \min(\mathcal{L}_{\mathcal{U}, \mathfrak{W}}(B\eta_0, B\varpi, \bar{\xi}), \mathcal{L}_{\mathcal{U}, \mathfrak{W}}(B\eta_0, B\varpi, \bar{\xi})) \end{aligned}$$

Repeating this process, we get

$$\mathcal{L}_{\mathcal{U}, \mathfrak{W}}(B\kappa, B\varpi_3, \varphi^2(\bar{\xi}_0)) = \mathcal{L}_{\mathcal{U}, \mathfrak{W}}(A(\varpi, \eta_1), A(\kappa, \eta_2), \varphi^2(\bar{\xi}_0))$$





$$\begin{aligned} &\geq \gamma \min(\mathcal{L}_{\mathcal{U}, \mathfrak{B}}(B\varpi, B\kappa, \varphi(\bar{\xi}_0)), \mathcal{L}_{\mathcal{U}, \mathfrak{B}}(B\eta_1, B\eta_2, \varphi(\bar{\xi}_0))) \\ &\geq \gamma \min([\mathcal{L}_{\mathcal{U}, \mathfrak{B}}(B\varpi_0, B\varpi, \varphi(\bar{\xi}_0))]^2, [\mathcal{L}_{\mathcal{U}, \mathfrak{B}}(B\eta_0, B\eta_1, \varphi(\bar{\xi}_0))]^2), \end{aligned}$$

and

$$\begin{aligned} \mathcal{L}_{\mathcal{U}, \mathfrak{B}}(B\eta_2, B\eta_3, \varphi^2(\bar{\xi}_0)) &= \mathcal{L}_{\mathcal{U}, \mathfrak{B}}(A(\eta_1, \varpi), A(\eta_2, \kappa), \varphi^2(\bar{\xi}_0)) \\ &\geq \gamma \min([\mathcal{L}_{\mathcal{U}, \mathfrak{B}}(B\eta_0, B\eta_1, \bar{\xi}_0)]^2, [\mathcal{L}_{\mathcal{U}, \mathfrak{B}}(B\varpi_0, B\varpi, \bar{\xi}_0)]^2). \end{aligned}$$

Using the same steps, for all $n \in \mathbb{N}$, we get

$$\mathcal{L}_{\mathcal{U}, \mathfrak{B}}(B\varpi_n, B\varpi_{n+1}, \varphi^n(\bar{\xi}_0)) \geq \gamma \min([\mathcal{L}_{\mathcal{U}, \mathfrak{B}}(B\varpi_0, B\varpi, \bar{\xi}_0)]^{2^{n-1}}, [\mathcal{L}_{\mathcal{U}, \mathfrak{B}}(B\eta_0, B\eta_1, \bar{\xi}_0)]^{2^{n-1}})$$

This leads to obtaining

$$\begin{aligned} \mathcal{L}_{\mathcal{U}, \mathfrak{B}}(B\varpi_n, B\varpi_\rho, \bar{\xi}) &\geq \left[\mathcal{L}_{\mathcal{U}, \mathfrak{B}} \left(B\varpi_n, B\varpi_\rho, \sum_{k=n_0}^{\infty} \varphi^k(\bar{\xi}_0) \right) \right] \\ &\geq \left[\mathcal{L}_{\mathcal{U}, \mathfrak{B}} \left(B\varpi_n, B\varpi_\rho, \sum_{k=n}^{\rho-1} \varphi^k(t_0) \right) \right] \\ &\geq \gamma \min([\mathcal{L}_{\mathcal{U}, \mathfrak{B}}(B\varpi_{n+1}, B\varpi_{n+2}, \varphi^n(\bar{\xi}_0))], \dots, [\mathcal{L}_{\mathcal{U}, \mathfrak{B}}(B\varpi_{\rho-1}, B\varpi_\rho, \varphi^{\rho-1}(\bar{\xi}_0))]) \\ &= \gamma \min([\mathcal{L}_{\mathcal{U}, \mathfrak{B}}(B\eta_0, B\eta_1, \bar{\xi}_0)]^{2^{\rho-1}-2^{n-1}}, [\mathcal{L}_{\mathcal{U}, \mathfrak{B}}(B\varpi_0, B\varpi, \bar{\xi}_0)]^{2^{\rho-1}-2^{n-1}}) \\ &\quad \underbrace{\geq \min((1-\varsigma), (1-\varsigma), (1-\varsigma) \dots (1-\varsigma))}_{2^{\rho}-2^n} \\ &\geq 1 - \delta, \end{aligned}$$

Furthermore, $\forall \rho, n > 0, \rho > n \geq n_0$ and $\bar{\xi} > 0$, we get

$$\mathcal{L}_{\mathcal{U}, \mathfrak{B}}(B\varpi_n, B\varpi_\rho, \bar{\xi}) \geq 1 - \delta$$

Moreover, it is established that $B\varpi_n$ forms a Cauchy sequence. Analogously, we demonstrate that $B\eta_n$ is also a Cauchy sequence. Subsequently, we aim to establish that A and B share a coincident point due to the completeness of $B(Z)$. Therefore, there exist elements ϖ, η in $B(Z)$ and s', q' in Z , such that:

$$\lim_{n \rightarrow \infty} B(\varpi_n) = \lim_{n \rightarrow \infty} A(\varpi_n, \eta_n) = B(s') = \varpi, \quad \lim_{n \rightarrow \infty} B(\eta_n) = \lim_{n \rightarrow \infty} A(\eta_n, \varpi_n) = B(q') = \eta.$$

By using condition (II), we get

$$\mathcal{L}_{\mathcal{U}, \mathfrak{B}}(A(\varpi_n, \eta_n), A(s', q'), \varphi(\bar{\xi})) \geq \gamma \min(\mathcal{L}_{\mathcal{U}, \mathfrak{B}}(B\varpi_n, B(s'), \bar{\xi}), \mathcal{L}_{\mathcal{U}, \mathfrak{B}}(B\eta_n, B(q'), \bar{\xi}))$$

where $\mathcal{L}_{\mathcal{U}, \mathfrak{B}}(\varpi, \kappa, \cdot)$, are continuous. As a consequence, we have





$$\lim_{n \rightarrow \infty} \mathcal{L}_{\mathcal{U}, \mathfrak{W}}(\varpi, \kappa, \bar{\xi}) = 1, \text{ for all } \varpi, \kappa \in Z.$$

Now, taking the limit as $n \rightarrow \infty$, there exists $\bar{\xi}_0 > 0$ we have

$$\mathcal{L}_{\mathcal{U}, \mathfrak{W}}(B(s'), A(s', q'), \varphi(\bar{\xi}_0)) = 1.$$

Similarly, we can demonstrate that $A(q', s') = B(q') = \eta$. Given that A and B compatible, so,

$$BA(s', q') = A(B(s'), B(q')) \Rightarrow B(\varpi) = A(\varpi, \eta), BA(q', s') = A(B(q'), B(s')) \Rightarrow B(\eta) = A(\eta, \varpi).$$

Since R is the t -representable of \mathbb{H} -type, for any $\delta > 0$, $\exists \varsigma > 0$, $n \in \mathbb{N}$ such that

$$R = \{\min((1 - \varsigma) * (1 - \varsigma) * \dots * (1 - \varsigma)), \max(\varsigma \diamond \varsigma \diamond \dots \diamond \varsigma)\}$$

$$R = \{1 - \delta, \delta\} \rightarrow (1, 0) = 1_I, \text{ as } \delta \rightarrow \infty$$

where $\mathcal{L}_{\mathcal{U}, \mathfrak{W}}(\varpi, \kappa, \bar{\xi})$, are continuous. As a consequence, we have

$$\lim_{n \rightarrow \infty} \mathcal{U}(\varpi, \kappa, \bar{\xi}) + \mathfrak{W}(\varpi, \kappa, \bar{\xi}) = 1$$

for all $\varpi, \kappa \in Z$, there exists $\bar{\xi}_0 > 0$ such that

$$\mathcal{L}_{\mathcal{U}, \mathfrak{W}}(B\varpi, \eta, \bar{\xi}_0) \geq (1 - \varsigma) \Rightarrow \mathcal{L}_{\mathcal{U}, \mathfrak{W}}(B\eta, \varpi, \bar{\xi}_0) \geq (1 - \varsigma).$$

Now, applying the contractive conditions defined by Ψ results in

$$\sum_{n=1}^{\infty} \varphi^n(t_0) < \infty \quad \text{and} \quad t > \sum_{k=n_0}^{\infty} \varphi^k(t_0),$$

$$\begin{aligned} \mathcal{L}_{\mathcal{U}, \mathfrak{W}}(B\varpi, B\eta_{n+1}, \varphi(\bar{\xi}_0)) &= \mathcal{L}_{\mathcal{U}, \mathfrak{W}}(A(\varpi, \eta), A(\eta_n, \varpi_n), \varphi(\bar{\xi}_0)) \\ &\geq \gamma \min(\mathcal{L}_{\mathcal{U}, \mathfrak{W}}(B\varpi, B\eta_n, \bar{\xi}_0), \mathcal{L}_{\mathcal{U}, \mathfrak{W}}(B\eta, B\varpi_n, \bar{\xi}_0)). \end{aligned}$$

Letting $n \rightarrow \infty$, we get

$$\mathcal{L}_{\mathcal{U}, \mathfrak{W}}(B\varpi, \eta, \varphi(\bar{\xi}_0)) \geq \gamma \min(\mathcal{L}_{\mathcal{U}, \mathfrak{W}}(B\varpi, \eta, \bar{\xi}_0), \mathcal{L}_{\mathcal{U}, \mathfrak{W}}(B\eta, \varpi, \bar{\xi}_0)).$$

Similarly, we can get

$$\mathcal{L}_{\mathcal{U}, \mathfrak{W}}(B\eta, \varpi, \varphi(\bar{\xi}_0)) \geq \gamma \min(\mathcal{L}_{\mathcal{U}, \mathfrak{W}}(B\eta, \varpi, \bar{\xi}_0), \mathcal{L}_{\mathcal{U}, \mathfrak{W}}(B\varpi, \eta, \bar{\xi}_0)).$$

$$\gamma \min(\mathcal{L}_{\mathcal{U}, \mathfrak{W}}(B\varpi, \eta, \varphi(\bar{\xi}_0)), \mathcal{L}_{\mathcal{U}, \mathfrak{W}}(B\eta, \varpi, \varphi(\bar{\xi}_0))) \geq \gamma \min([\mathcal{L}_{\mathcal{U}, \mathfrak{W}}(B\varpi, \eta, \bar{\xi}_0)]^2, [\mathcal{L}_{\mathcal{U}, \mathfrak{W}}(B\eta, \varpi, \bar{\xi}_0)]^2).$$

Repeating this process n -times where $n \in \mathbb{N}$, we get

$$\gamma \min(\mathcal{L}_{\mathcal{U}, \mathfrak{W}}(B\varpi, \eta, \varphi^n(\bar{\xi}_0)), \mathcal{L}_{\mathcal{U}, \mathfrak{W}}(B\eta, \varpi, \varphi^n(\bar{\xi}_0))) \geq \gamma \min([\mathcal{L}_{\mathcal{U}, \mathfrak{W}}(B\varpi, \eta, \varphi^{n-1}(\bar{\xi}_0))]^2, [\mathcal{L}_{\mathcal{U}, \mathfrak{W}}(B\eta, \varpi, \varphi^{n-1}(\bar{\xi}_0))]^2).$$





$$\geq \gamma \min([\mathcal{L}_{\mathcal{U}, \mathcal{W}}(B\varpi, \eta, \xi_0)]^{2^n}, [\mathcal{L}_{\mathcal{U}, \mathcal{W}}(B\eta, \varpi, \xi_0)]^{2^n})$$

Thus, we get

$$\begin{aligned} \gamma \min(\mathcal{L}_{\mathcal{U}, \mathcal{W}}(B\varpi, \eta, \xi), \mathcal{L}_{\mathcal{U}, \mathcal{W}}(B\eta, \varpi, \xi)) &\geq \gamma \min\left[\mathcal{L}_{\mathcal{U}, \mathcal{W}}\left(B\varpi, \eta, \sum_{k=n_0}^{\infty} \varphi^k(\xi_0)\right), \mathcal{L}_{\mathcal{U}, \mathcal{W}}\left(B\eta, \varpi, \sum_{k=n_0}^{\infty} \varphi^k(\xi_0)\right)\right] \\ &\geq \gamma \min([\mathcal{L}_{\mathcal{U}, \mathcal{W}}(B\varpi, \eta, \varphi^{n_0}(\xi_0))], [\mathcal{L}_{\mathcal{U}, \mathcal{W}}(B\eta, \varpi, \varphi^{n_0}(\xi_0))]) \\ &\geq \gamma \min([\mathcal{L}_{\mathcal{U}, \mathcal{W}}(B\varpi, \eta, \xi_0)]^{2^{n_0}}, [\mathcal{L}_{\mathcal{U}, \mathcal{W}}(B\eta, \varpi, \xi_0)]^{2^{n_0}}) \\ &\geq \gamma \min((1-\varsigma), (1-\varsigma), \dots, (1-\varsigma)) \geq 1-\delta. \end{aligned}$$

As a consequence, for $(\bar{\xi} > 0\delta > 0)$, we have

$$\gamma \min(\mathcal{L}_{\mathcal{U}, \mathcal{W}}(B\varpi, \eta, \bar{\xi}), \mathcal{L}_{\mathcal{U}, \mathcal{W}}(B\eta, \varpi, \bar{\xi})) \geq 1-\delta,$$

$$B_{\eta} = \varpi, B_{\varpi} = \eta.$$

Now, we are going to prove uniqueness i.e; $\varpi = \eta$.
Since $\mathcal{L}_{\mathcal{U}, \mathcal{W}}(\varpi, \kappa, \cdot)$, are continuous, which guarantee

$$\lim_{\bar{\xi} \rightarrow \infty} \mathcal{L}_{\mathcal{U}, \mathcal{W}}(\varpi, \kappa, \bar{\xi}) = 1,$$

for all $\varpi, \kappa \in Z$, there exists $\bar{\xi}_0 > 0$, such that

$$\begin{aligned} \mathcal{L}_{\mathcal{U}, \mathcal{W}}(B_{\varpi_{n+1}}, B_{\eta_{n+1}}, \varphi(\bar{\xi}_0)) &= \mathcal{L}_{\mathcal{U}, \mathcal{W}}(A(\varpi_n, \eta_n), A(\eta_n, \varpi_n), \bar{\xi}_0) \\ &\geq \gamma \min(\mathcal{L}_{\mathcal{U}, \mathcal{W}}(B_{\varpi_n}, B_{\eta_n}, \bar{\xi}_0), \mathcal{L}_{\mathcal{U}, \mathcal{W}}(B_{\eta_n}, B_{\varpi_n}, \bar{\xi}_0)). \end{aligned}$$

Suppose $n \rightarrow \infty$ refers to

$$\mathcal{L}_{\mathcal{U}, \mathcal{W}}(\varpi, \eta, \varphi(\bar{\xi}_0)) \geq \gamma \min(\mathcal{L}_{\mathcal{U}, \mathcal{W}}(\varpi, \eta, \varphi, \bar{\xi}_0), \mathcal{L}_{\mathcal{U}, \mathcal{W}}(\eta, \varpi, \psi, \bar{\xi}_0)).$$

Consequently, we get

$$\begin{aligned} \mathcal{L}_{\mathcal{U}, \mathcal{W}}(\varpi, \eta, \bar{\xi}) &\geq \gamma \min\left[\mathcal{L}_{\mathcal{U}, \mathcal{W}}\left(\varpi, \eta, \sum_{k=n_0}^{\infty} \varphi^k(\bar{\xi}_0)\right), \mathcal{L}_{\mathcal{U}, \mathcal{W}}\left(\eta, \varpi, \sum_{k=n_0}^{\infty} \varphi^k(\bar{\xi}_0)\right)\right] \\ &\geq \gamma \min([\mathcal{L}_{\mathcal{U}, \mathcal{W}}(\varpi, \eta, \varphi^{n_0}(\bar{\xi}_0))], [\mathcal{L}_{\mathcal{U}, \mathcal{W}}(\eta, \varpi, \varphi^{n_0}(\bar{\xi}_0))]) \\ &\geq \gamma \min([\mathcal{L}_{\mathcal{U}, \mathcal{W}}(\varpi, \eta, \xi_0)]^{2^{n_0-1}}, [\mathcal{L}_{\mathcal{U}, \mathcal{W}}(\eta, \varpi, \xi_0)]^{2^{n_0-1}}) \\ &\geq 1-\delta. \end{aligned}$$

Therefore, ϖ is a unique FP of A and B .



**REFERENCES**

1. A. George and P. Veeramani. On some results on fuzzy metric spaces, *Fuzzy Sets and Systems*, 64(3), pp. 395–399, 1994.
2. H. M. Chen Yue, H. A. Abu-Donia, M. A. Atia, etc. Weakly compatible fixed point theorem in intuitionistic fuzzy metric spaces, *AIP Advances*, 13(4), 2023.
3. M. S. Ashraf, R. Ali, and N. Hussain. Geraghty type contractions in fuzzy b-metric spaces with application to integral equations, *Filomat*, 34(9), pp. 3083–3098, 2020.
4. Q. Kiran and H. Khatoon. Kannan's and Chatterjee's type fixed point theorems in modified intuitionistic fuzzy metric space, *AIP Conf. Proc.*, 2019.
5. R. Saadati, S. Sedghi, and N. Shobe. modified intuitionistic fuzzy metric spaces and some fixed point theorems, *Chaos, Solitons and Fractals*, 38(1), pp. 36–47, 2008.
6. R. Saadati, J. H. Park. On the intuitionistic fuzzy topological spaces, *Chaos, Solitons and Fractals*, 27, pp. 331–44, 2006.
7. R. Saadati, A. Razani, H. Adibi. A common fixed point theorem in L-fuzzy metric spaces, *Chaos, Solitons and Fractals* 33, pp.358–63, 2007.
8. S. Sedghi, N. Shobe and A. Aliouche. Common fixed point theorems in intuitionistic fuzzy metric spaces through conditions of integral type, *Applied Mathematics and Information Sciences*, 2(1), pp.61–82, 2008.
9. V. Gupta, A. Kanwar. Some New fixed point Results on Intuitionistic Fuzzy Metric Spaces, *Cogent Mathematics*, 3(1), pp. 12, 2016.
10. V. Gupta, R.K. Saini, A. Kanwar. Some Common Coupled fixed point Results on modified intuitionistic fuzzy metric spaces, *Procedia Computer Science*, Elsevier, Vol. 79, pp. 32 – 40, 2016.
11. V. Gupta, A. Kanwar. Unified fixed point Theorems on E-chainable Fuzzy Metric Space and modified intuitionistic fuzzy metric space, *Applied Mathematics and Information Sciences*, 10(6), pp. 2283-2291, 2016.
12. V. Gupta, R.K. Saini, A. Kanwar. Some coupled fixed point results on modified intuitionistic fuzzy metric spaces and application to integral type contraction, *Iranian Journal of Fuzzy Systems*, 14(5), pp.123-137, 2017.
13. V. Lakshmikantham, B. Ćirić. Coupled fixed point theorems for nonlinear contractions in partially ordered metric space, *Non linear Anal. TMA*. 70, pp. 4341–9, 2009.
14. L. A. Zadeh, *Fuzzy Sets*. *Inform Control*. 8, pp. 338-53, 1965.





Application of TOPSIS Method to Prevalence of Anaemia

Rozy Rani¹ and Deepak Gupta ²

¹Department of Mathematics, Maharishi Markandeshwar (Deemed to be University), Mullana, Ambala, India.

²Professor and Head, Department of Mathematics, Maharishi Markandeshwar (Deemed to be University), Mullana, Ambala, India.

Received: 20 Jan 2024

Revised: 09 Feb 2024

Accepted: 14 May 2024

*Address for Correspondence

Rozy Rani

Department of Mathematics,
Maharishi Markandeshwar
(Deemed to be University),
Mullana, Ambala, India.

Email: rozygupta479@gmail.com



This is an Open Access Journal / article distributed under the terms of the **Creative Commons Attribution License** (CC BY-NC-ND 3.0) which permits unrestricted use, distribution, and reproduction in any medium, provided the original work is properly cited. All rights reserved.

ABSTRACT

This paper proposed a TOPSIS approach (The technique of Order preference by similarity ideal solution) for constructing a mathematical model with TOPSIS algorithm. We applied the developed method to find the optimal ideal solution. TOPSIS is a numerical approach to multi-criteria decision-making (MCDM). The mathematical model for this approach is easy to comprehend and has wide applicability. In this paper, we applied TOPSIS method to evaluate micronutrient deficiencies by using data of Comprehensive National Nutrition Survey and examined the main deficiency to prevalence of anaemia. To provide a comprehensive understanding of the methodology, an algorithm and flowchart are also provided.

Keywords: TOPSIS algorithm, optimal ideal solution, micronutrient deficiencies, prevalence of anaemia, MCDM etc.

INTRODUCTION

In this country, anaemia is the most prevalent disease globally. Anaemia's prevalence is significantly influenced by micronutrient deficits. Anaemia, which is a term for low blood count, is caused by a decline in the total amount of haemoglobin or red blood cells, which leaves the body with less oxygen to meet its physiological requirements [8]. Nutrient deficiencies are one of the many possible causes of anaemia. It can be brought on by a variety of circumstances, including dietary inadequacies. Although a number of illnesses, including folate, vitamin B12 and vitamin A deficiencies, chronic inflammation, parasite infections, and hereditary disorders, can also result in anaemia, iron deficiency is believed to be the primary cause of anaemia worldwide [12]. The decrease in haemoglobin

75653



**Rozy Rani and Deepak Gupta**

levels, or anaemia, is a major cause of the worldwide burden of chronic illnesses. In 2016, the World Health Organisation (WHO) projected that 40% of women in reproductive age and 42% of young children under the age of five worldwide suffered from anaemia. Anaemia has been the main factor contributing to years spent disabled in mothers and children under the age of five in recent decades [2], [9]. A modified Poisson regression analysis with robust error variance is applied to calculate the anaemia prevalence between 2010 and 2018. The 47 LMIC's (Low-middle income countries), we found that 40.4% of women 15 -49 years (reproductive age) and 56.5% of children under the age of five had anaemia [19]. In this investigation, anaemia in children under five years was determined to be a modest public health concern. It might be controlled by avoiding intestinal protozoa, soil-transmitted helminthic infection, and malaria infection [1]. A low concentration of red blood cells (RBCs) in the body results in anaemia. This lowers oxygen levels in the body and can cause symptoms like exhaustion, pale complexion, chest pain, and dyspnoea, RBC destruction, decreased or impaired RBC generation and blood loss are common reasons of anaemia. The most frequent dietary factor contributing to anaemia is iron deficiency; however folate, vitamin B12, and vitamin A inadequacy are all significant contributors. The purpose of the study was to record the sociodemographic characteristics linked to anaemia's prevalence and severity in pregnant women in the Andaman and Nicobar Islands [11]. Enhancing the nutritional status and micronutrient intake of children, as well as improving the mother's education and socioeconomic standing, are all necessary to address anaemia in children between the ages of five and nine [15]. This research found that children with lower levels of vitamin D and folate consumption also had higher levels of anaemia. The research can assist decision-makers in creating and implementing appropriate policies that will enhance children's health by mitigating the anaemia issue [4].

TOPSIS METHOD AND ITS APPLICATIONS

Multi-criteria decision making (MCDM) is a fundamental component of modern decision science and operational research. It involves the consideration of many options and decision criteria. The primary goal of the MCDM is to compare a collection of available alternatives to the chosen criteria and determine which alternative is most desirable. The most effective method for selecting the best option out of all those that are practical is decision making. Almost all other topics have a large number of criteria since choosing between general options is common. There may not be a solution that satisfies all of the requirements at once since they typically conflict with one another. The MCDM challenge is one that decision-makers hope to solve in order to address such issues. MCDM issues can be resolved in a variety of ways. Hwang and Yoon [6] initially presented TOPSIS, one of the multiple criteria decision making techniques. TOPSIS uses the Euclidean distance to calculate the relative closeness of an alternative to the ideal solution, based on the principle that the alternatives chosen must have the nearest distance from the positive ideal solution (PIS) and the longest distance from the negative ideal solution (NIS) from a geometrical point. The TOPSIS approach relies on the best alternative chosen to reach the greatest level, which is the optimum perfect solution.

Shukla [18] focused on the different manufacturing processes like drilling, milling, electric charges, jet machining, turning, micro machining which optimized by TOPSIS method. The high rationality and applicability of TOPSIS method is used for the evaluation of competitive ability of the introduction of foreign players in CBA team [22]. By Zulqarnain [21] introduced soft set theory and TOPSIS method with examples to choose which applicants are most suitable for bank jobs. TOPSIS method is used in a linguistic decision making problem with MCDM problems in fuzzy environment [3]. TOPSIS method is applied to develop a methodology for evaluating suppliers in iron supply chain process [17]. In the past few decades, TOPSIS method has been used in the areas of inter-company comparison, operating system selection, partner selection, facility location selection, risk assessment, robot selection, customer evaluation, performance evaluation, expatriate host country selection, weapon selection etc [7]. Rehman [16] used TOPSIS method for wind turbines selection while considering hub height, zero output percentage and rated output, wind speed, annual energy acting as the decision criteria. The author [10] explained the application of TOPSIS approach to solve staff management issues based on hierarchical structure criteria. To obtain a competitive edge in markets, manufacturers must collaborate with wholesalers, retailers, and customers who are all involved in a supply chain, either directly or indirectly, to fill client requirements [5], [13]. The computational technique of the TOPSIS decision-making system was used in this study to select the top workers based on the characteristics of their job





Rozy Rani and Deepak Gupta

duties, work quality, conduct, and work discipline [14]. It was determined that TOPSIS has a high level of efficiency by varying the number of parameters and users.

ALGORITHM OF TOPSIS

Step 1: Formulation of decision Maker

Create a decision matrix $D = [a_{ij}]_{p \times q}$

$$D = \begin{bmatrix} a_{11} & a_{12} & \dots & a_{1q} \\ a_{21} & a_{22} & \dots & a_{2q} \\ \dots & \dots & \dots & \dots \\ a_{p1} & a_{p2} & \dots & a_{pq} \end{bmatrix} = [a_{ij}]_{p \times q}$$

where p and q represent the number of alternatives and criteria, respectively and a_{ij} denotes the criteria value of the i th alternatives received from the j th criterion. The elements C_1, C_2, \dots, C_q (columns) establishes the criteria of decision maker and A_1, A_2, \dots, A_p (rows) represent the alternatives. Value $i=(1,2,\dots,p)$ is the alternative index and $j=(1,2,\dots,q)$ represents criteria index.

Step 2: Creating the decision matrix that has been normalized, say M .

The normalised decision-making process, which was built after the decision matrix construct, was used to determine the relative performance of the options. To calculate the relative performance of the alternatives the normalized decision making constructed after the construct of decision matrix.

$$M_{ij} = \frac{a_{ij}}{\sqrt{\sum_{i=1}^p a_{ij}^2}} \quad \forall a_{ij} \neq 0$$

Step 3: Constructing the decision matrix that is weighted and normalised (WNDM), Multiplying each element of each NDM column yields a weighted decision matrix

$$N = N_{ij} = W_j \times M_{ij}$$

Step 4: Find positive ideal solution (PIS) and negative ideal solution (NIS). where PIS (K^+) and NIS (K^-) are derived from weighted decision matrix.

$$PIS = K^+ = \{N_1^+, N_2^+, \dots, N_q^+\} \text{ where}$$

$$N_j^+ = \{(\max(N_{ij}) \text{ if } j \in q) ; (\min(N_{ij}) \text{ if } j \in q'), i = (1, 2, \dots, p)\}$$

$$NIS = K^- = \{N_1^-, N_2^-, \dots, N_q^-\} \text{ where}$$

$$N_j^- = \{(\min(N_{ij}) \text{ if } j \in q) ; (\max(N_{ij}) \text{ if } j \in q'), i = (1, 2, \dots, p)\}$$

where q' is linked with unfavourable attribute. Furthermore q is linked with favorable attributes.

Step 5 : To distinguish each alternative's distance from its PIS and NIS





Rozy Rani and Deepak Gupta

$$R_i^+ = \sqrt{\sum_{j=1}^q (N_j^+ - N_{ij})^2} ; i = 1, 2, \dots, p$$

$$R_i^- = \sqrt{\sum_{j=1}^q (N_j^- - N_{ij})^2} ; i = 1, 2, \dots, p$$

Where i = Index of alternatives, j = Index of criteria

Step 6 : Relative proximity to the optimal solution.

$$A_j = \frac{R_i^-}{(R_i^+ + R_i^-)}, 0 \leq A_j \leq 1$$

FLOW CHART OF APPLICATIONS OF TOPSIS METHOD

APPLICATION OF TOPSIS TECHNIQUE:

We want to find the main cause of anaemia in school children of 5-9 years of India. We assign a team of five decision-makers, denoted as ($i=5$) given by $D = \{D1, D2, D3, D4, D5\}$, to select the optimal response. First, the decision-makers choose the following five multivitamins as the best: $A = \{\text{Zinc, Vitamin D, Vitamin A, Iron, B12}\}$ and decide the two evaluation criteria given by $C = \{5-7 \text{ years, } 8-9 \text{ years}\}$ for the selection of the best cause of anaemia out of five multivitamins.

$J_1 = \{X_1: 5-7 \text{ years } X_2: 8-9 \text{ years}\}$

Solution by TOPSIS

The TOPSIS approach will be demonstrated using the anaemia prevalence data from CNNS Report. Here, the evaluation criteria is $C = \{5-7 \text{ years, } 8-9 \text{ years}\}$, and the set of options is $A = \{\text{Zinc, Vitamin D, Vitamin A, Iron, Vitamin B 12}\}$.

Step 1: Creating a decision matrix

Step 2. Normalization

Step 3. Calculation of Weighted Matrix

The matrix provides the weights that the experts (decision makers) allocated to the criteria.

$W = [W_1, W_2]$, $W = [0.5, 0.5]$ Transpose

Step 4: Calculating PIS A^* Table & NIS A^- Table

$A^* = (0.28, 0.25)$ $A^- = (0.19, 0.175)$

Step 5: Calculating RCC to get the optimal solution A_j

$$A_j = \frac{R_i^-}{(R_i^+ + R_i^-)}, 0 \leq A_j \leq 1$$

$$A_1^* = \frac{0.038}{0.123} = 0.3089$$

Similarly $A_2^* = 0.9173$

$$A_2^* = \frac{0.076}{0.151} = 0.5033$$

$$A_4^* = 0.3074$$

$$A_5^* = 0.3271$$

*Vitamin A is the ideal solution.





Rozy Rani and Deepak Gupta

CONCLUSION

In this research, we provide a graphical representation of the TOPSIS approach and conduct a thorough analysis of the TOPSIS methodology. For the TOPSIS technique, we created a flowchart and algorithm. Compared to earlier methods, this technique's principle is simpler, and it may evaluate several targets at once. Furthermore, the evaluation is impartial, the computation is rapid, and the outcome is evident. We used the TOPSIS method to find the main cause of anaemia and also find the optimal solution of micronutritional deficiency by using the data of national nutrition survey report (2016-18) of 5-9 years children of India. We examined that Vitamin A is the best optimal solution (main cause) of prevalence of anaemia among 5-9 years of children in India according to above given parameters.

Declarations of Conflicting Interests

The author(s) declared no potential conflict of interest with respect to the research, authorship and/ or publication of this article.

REFERENCES

1. Aliyo, A., & Jibril, A. (2022). Anemia and Associated Factors Among Under Five Year Old Children Who Attended Bule Hora General Hospital in West Guji zone, Southern Ethiopia. *Journal of Blood Medicine*, 395-406.
2. A systematic analysis of global anemia burden from 1990 to 2010. *Blood*. 2014; 123: 615-624
3. Chen, S. M. (1997, October). Fuzzy system reliability analysis based on vague set theory. In *1997 IEEE international conference on systems, man, and cybernetics. Computational cybernetics and simulation* (Vol. 2, pp. 1650-1655). IEEE.
4. Gupta, D., Rani, M. R., & Saini, V. (2022). DETERMINANTS OF PREVALENCE OF VITAMIN D AND ANAEMIA AMONG 5-9 YEARS CHILDREN IN INDIA., vol.12, 2250-1770.
5. Ha, S. H., & Krishnan, R. (2008). A hybrid approach to supplier selection for the maintenance of a competitive supply chain. *Expert systems with applications*, 34(2), 1303-1311
6. Hwang, C. L., Yoon, K., Hwang, C. L., & Yoon, K. (1981). Methods for multiple attribute decision making. *Multiple attribute decision making: methods and applications a state-of-the-art survey*, 58-191.
7. Jiang J., Chen Y.W., Tang D.W., Chen Y.W., (2010), "Topsis with belief structure for group belief multiple criteria decision making", *international journal of Automation and Computing*, vol.7,no.3, pp 359-364
8. Johnson-Wimbley TD, Graham DY. Diagnosis and management of iron deficiency anemia in the 21st century. *Therap Adv Gastroenterol*. 2011;4:177–84. [PMC free article] [PubMed] [Google Scholar]
9. Kassebaum, N. J., Jasrasaria, R., Naghavi, M., Wulf, S. K., Johns, N., Lozano, R., ... & Murray, C. J. (2014). A systematic analysis of global anemia burden from 1990 to 2010. *Blood, the Journal of the American Society of Hematology*, 123(5), 615-624.
10. M. Mammadova, Z. Jabrailova and S. Nobari, "Application of TOPSIS method in decision-making support of personnel management problems," *2012 IV International Conference "Problems of Cybernetics and Informatics" (PCI)*, Baku, Azerbaijan, 2012, pp. 1-4, doi: 10.1109/ICPCI.2012.6486485.
11. Mehrotra, M., Yadav, S., Deshpande, A., & Mehrotra, H. (2018). A study of the prevalence of anemia and associated sociodemographic factors in pregnant women in Port Blair, Andaman and Nicobar Islands. *Journal of family medicine and primary care*, 7(6), 1288.
12. Ministry of Health and Family Welfare (MoHFW), Government of India, UNICEF and Population Council. 2019. Comprehensive National Nutrition Survey (CNNS) National Report. New Delhi. https://www.popcouncil.org/uploads/pdfs/2019RH_CNNSreport.pdf.
13. More, D. S., & Mateen, A. (2012). Suppliers selection and development using DEA: a case study. *International Journal of Logistics Systems and Management*, 13(2), 230-243.





Rozy Rani and Deepak Gupta

14. Rahim, R., Supiyandi, S., Siahaan, A. P. U., Listyorini, T., Utomo, A. P., Triyanto, W. A., ... & Khairunnisa, K. (2018, June). TOPSIS method application for decision support system in internal control for selecting best employees. In *Journal of Physics: Conference Series* (Vol. 1028, p. 012052). IOP Publishing.
15. Rani, R., & Gupta, D. (2022). STUDY ON PREVALENCE OF ZINC AND ANAEMIA ASSOCIATION IN SCHOOLCHILDREN OF INDIA. *International Journal of Early Childhood Special Education*, 14(5).
16. Rehman, S., Khan, S. A., & Alhems, L. M. (2020). Application of TOPSIS approach to multi-criteria selection of wind turbines for on-shore sites. *Applied Sciences*, 10(21), 7595.
17. Shahroudi, K., & Tonekaboni, S. M. S. (2012). Application of TOPSIS method to supplier selection in Iran auto supply chain. *Journal of Global Strategic Management*, 6(2), 123-131.
18. Shukla, A., Agarwal, P., Rana, R. S., & Purohit, R. (2017). Applications of TOPSIS algorithm on various manufacturing processes: a review. *Materials Today: Proceedings*, 4(4), 5320-5329.
19. Sun, J., Wu, H., Zhao, M., Magnussen, C. G., & Xi, B. (2021). Prevalence and changes of anemia among young children and women in 47 low-and middle-income countries, 2000-2018. *EClinicalMedicine*, 41.
20. World Health Organization. *Anaemia*. [Last accessed on 2018 May 21]. Available from: <http://www.who.int/topics/anaemia/en/>
21. Zulqarnain, R. M., Abdal, S., Maalik, A., Ali, B., Zafar, Z., Ahamad, M. I., & Dayan, F. (2020). Application of TOPSIS method in decision making via soft set. *Biomed J Sci Tech Res*, 24(3).
22. Zhongyou, X. (2012). Study on the Application of TOPSIS Method to the Introduction of Foreign Players in CBA Games. *Physics Procedia*, 33, 2034-2039.

Table 1: Decision matrix $D=[x]_{m \times n}$

Multivitamins	5 – 7 years	5 – 7 years
Zins	16.7	16.9
Vitamin D	16.7	20.5
Vitamin A	22.9	19.4
Iron	19.0	14.1
Vitamin B12	15.8	19.2

Table 2: Calculating $\sqrt{\sum_{i=1}^m x_{ij}^2}$

Multivitamin	5 – 7 years	8 – 9 years
Zinc	278.89	285.61
Vitamin D	278.89	420.25
Vitamin A	524.41	376.36
Iron	361	198.81
Vitamin B ₁₂	249.64	368.64
$\sum_{i=1}^m x_{ij}^2$	1692.83	1849.67
$\sqrt{\sum_{i=1}^m x_{ij}^2}$	41.1440	40.6161

Dividing each entry by $\sqrt{\sum_{i=1}^m x_{ij}^2}$ in order to normalise the decision matrix





Rozy Rani and Deepak Gupta

Table 3: Matrix $R = [r_{ij}]_{m \times n}$ is the normalised decision matrix

Multivitamin	5 – 7 years	8 – 9 years
Zinc	0.4058	0.4160
Vitamin D	0.4059	0.5047
Vitamin A	0.5566	0.4776
Iron	0.4618	0.3471
Vitamin B ₁₂	0.384	0.4727

Table 4: Matrix $R = [rij'] \times n$ for Weighted Normalised Decision Making

Weight	0.5 (W1)	0.5 (W2)
Zinc	0.205	0.21
Vitamin D	0.205	0.25 N2*
Vitamin A	0.22 N1*	0.24
Iron	0.23	0.175 N2 ¹
Vitamin B12	0.19 N1 ¹	0.235

Table 5: Calculating separation from PIS A *

Multivitamins	5 – 7 years	8 – 9 years	$\sum (N_j^* - N_{ij})^2$	R'_i
Zinc	$(0.205 - 0.28)^2$	$(0.21 - 0.25)^2$	0.007225	0.085
Vitamin D	$(0.205 - 0.28)^2$	$(0.25 - 0.25)^2$	0.005625	0.075
Vitamin A	$(0.28 - 0.28)^2$	$(0.24 - 0.25)^2$	0.0001	0.01
Iron	$(0.23 - 0.28)^2$	$(0.175 - 0.25)^2$	0.008125	0.0901
Vitamin B ₁₂	$(0.19 - 0.28)^2$	$(0.235 - 0.25)^2$	0.015225	0.12338

Table 6: Calculation of S'_i and Separation from NIS A *

Multivitamin	5 – 7 years	8 – 9 years	$\sum (N_j^* - N_{ij})^2$	R'_i
Zinc	$(0.205 - 0.19)^2$	$(0.21 - 0.175)^2$	0.001450	0.038
Vitamin D	$(0.205 - 0.19)^2$	$(0.25 - 0.175)^2$	0.005850	0.076
Vitamin A	$(0.28 - 0.19)^2$	$(0.24 - 0.175)^2$	0.0012325	0.111
Iron	$(0.23 - 0.19)^2$	$(0.175 - 0.175)^2$	0.0016	0.004
Vitamin B ₁₂	$(0.19 - 0.19)^2$	$(0.235 - 0.175)^2$	0.0036	0.06



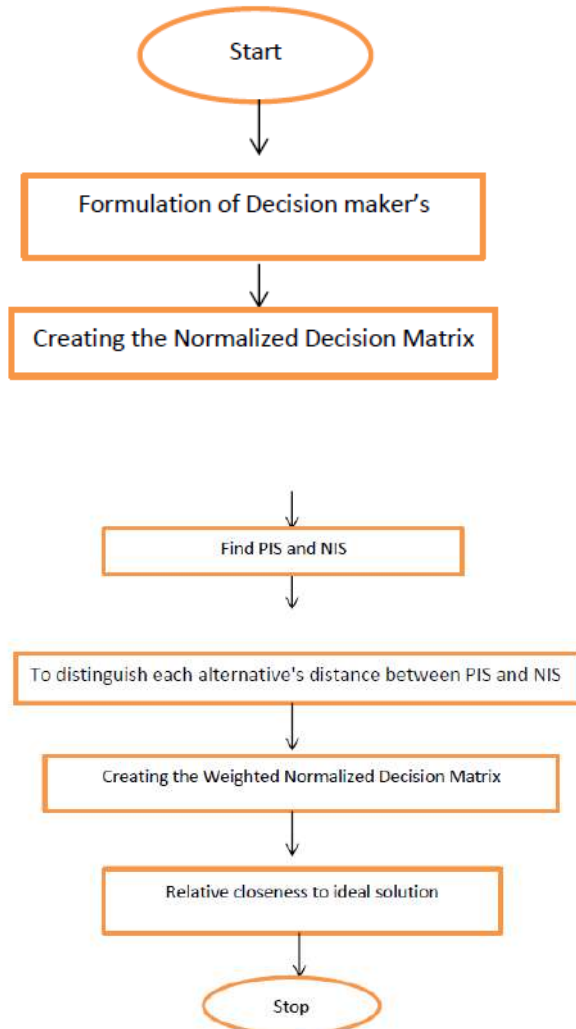


Figure 1: Flowchart (Model) of TOPSIS approach





$N \times 3$ Weighted Flow Shop Scheduling Problem With Breakdown Interval to Minimize the Rental Cost of Machines

Deepak Gupta^{1*} and Tamanna²

¹Professor and Head, Department of Mathematics, M.M University, Mullana, Ambala, Haryana, India

²Research Scholar, Department of Mathematics, M.M University, Mullana, Ambala, Haryana, India

Received: 20 Jan 2024

Revised: 09 Feb 2024

Accepted: 14 May 2024

***Address for Correspondence**

Deepak Gupta

Professor and Head,
Department of Mathematics,
M.M University, Mullana,
Ambala, Haryana, India
Email: guptadeepak2003@yahoo.co.in



This is an Open Access Journal / article distributed under the terms of the **Creative Commons Attribution License** (CC BY-NC-ND 3.0) which permits unrestricted use, distribution, and reproduction in any medium, provided the original work is properly cited. All rights reserved.

ABSTRACT

This paper attempts an study of $N \times 3$ weighted flow shop scheduling problem to minimize the total rental cost of machines with breakdown interval . The objective of the paper is to obtain an algorithm to minimize the rental cost under the specified rental policy whenever the mean weighted production flow time and breakdown interval of jobs are taken into consideration . The algorithm is easily clarified by a numerical example.

Keywords: Flow shop scheduling, weight age of jobs, Breakdown interval, Rental Policy, Optimal sequence.

INTRODUCTION

Scheduling theory is started from Jhonson's work in 1954 , in which the main aim of scheduling problems is to get an sequence of jobs that optimizes some well defined criteria and processed in a fixed order of machines. Johnson had given thought to the effect of breakdown of machines on the execution of job in an optimal sequence. The breakdown of machines occurs due to failure of component of machines for certain interval of time or when machines are need to stop working for a period of time due to some exterior imposed policy. All the scheduling models started from Jhonson's work in 1954 up-to 1980, doesn't inspect the weight-age of jobs in literature . The weights exhibit relative priority of a job over some other jobs in operating schedules. Scheduling problems with weights are come to light when inventory costs for jobs are concerned and these problems are known as "**weighted scheduling problem**". Miyazaki S., & Nishiyama N. (1980) examines that how to minimize weighted mean flow in a weighted flow-shop scheduling problem. Maggu P.L., Yadav S. K., Singh T. P., & Dev A. (1984) proposed an algorithm for flow-shop scheduling problem including job-weight and transportation time. Gupta Deepak and Sehgal Poojadeep (2022) researched over $n \times 2$ flow shop scheduling to minimize the rental cost including breakdown





Deepak Gupta and Tamanna

interval. Gupta Deepak and Tamanna (2023) proposed an algorithm for $n \times 3$ flow-shop scheduling problem with breakdown interval to minimize the total rental cost. Other associated problems have been analyzing by Singh T.P. , Maggu , Gupta D. & Sharma S. to solve a two-machine flow-shop problem with start delay and stop delay. Gupta Deepak and Sehgal Poojadeep (2021) gave an heuristic procedure for minimizing the total hiring cost of the machines in two stage flow shop with break down interval and weight of jobs. We are going to extend the work done by Gupta Deepak and Sehgal Poojadeep in three stage flow shop scheduling problem with breakdown interval and weights associated on different jobs to minimize the total rental cost of the three machine.

NOTATIONS

S : Sequence of jobs 1 , 2 , 3,..... , n .

S_i : Sequence obtained by applying Johnson's method; $q = 1, 2, 3, \dots, r$.

M_j : Machine j ; $j = 1, 2, 3$.

A_i : Processing time of i^{th} jobs on machine A .

B_i : Processing time of i^{th} jobs on machine B .

C_i : Processing time of i^{th} jobs on machine C .

$t(S_i)$: Completion time of i^{th} jobs of sequence S_i on machines M_i .

L : Length of the breakdown interval (a, b) .

W_i : Weight assigned to the i^{th} job.

$U_i(S_i)$: Utilization time for which machine M_i is required.

C_j : Per unit rental time of hiring j^{th} machine.

$R(S_i)$: Total rental cost for machines S_i of all machines.

RENTAL POLICY

The machines may be taken on rent as and when its need arises and the same will be returned as and when they are no longer required for processing of the jobs.

PROBLEM FORMULATION

Let us suppose that n jobs be processed on three machines M_j ($j = 1, 2, 3$) in order $M_1 \rightarrow M_2 \rightarrow M_3$, where A_i, B_i, C_i are the processing time of all the jobs on machines M_1, M_2, M_3 respectively. Let W_i be the weight allotted to the jobs satisfying the structured conditions : $\min(A_i) \geq \max(B_i)$ or $\min(C_i) \geq \max(B_i)$ or both satisfied . The mathematical model of problem can be stated as : Moreover, let us consider the effect of breakdown interval (a, b) of machines. Our objective is to get a near optimal sequence of jobs which minimizes the rental cost of the machines M_j ($j = 1, 2, 3$).

ASSUMPTIONS

- Jobs are not dependent on each other . Let n jobs be processed through three machines M_j ($j=1,2,3$) in order M_1, M_2, M_3 .
- Once a job is started on a machine then the processing on the machine cannot be stopped unless the job is completed.
- Weight is assigned to each job.
- Machines break down interval is taken into consideration.
- Either $\min(A_i) \geq \max(B_i)$
or
 $\min(C_i) \geq \max(B_i)$ or both .





Deepak Gupta and Tamanna

ALGORITHM

The algorithm to minimize the rental cost of the three machines whenever breakdown interval (a,b) and weight of jobs is considered, given as:

Step1: Let either one or both of the following structured conditions involving the processing time of jobs hold.

Structured conditions are given as:

$$\text{Max}(B_i) \leq \text{Min}(A_i)$$

i.e. the greatest processing time on machine M_2 is less than or equal to the minimum processing time on machine M_1 .

$$\text{Max}(B_i) \leq \text{Min}(C_i)$$

i.e. the greatest processing time on machine M_2 is less than or equal to the minimum processing time on machine M_3 .

Step2: Modify the three machines flow shop problem into two machines flow shop problem by introducing two fictitious machines G and H with corresponding processing time G_i and H_i , such that

$$G_i = A_i + B_i$$

$$H_i = B_i + C_i$$

Then, the problem can be reduced in a tabular form which is given as

Step3: Next step is to minimize the weighted mean flow, where

- if $\min(G_i, H_i) = G_i$, then define
 $G_i = G_i - W_i$ & $H_i = H_i$ (for each $i=1$ to n)
- if $\min(G_i, H_i) = H_i$, then define
 $G_i = G_i$ & $H_i = H_i + W_i$ (for each $i=1$ to n)

Step4: Defines a new reduced problem with new processing time $(G_i)'$ and $(H_i)'$, i.e.,

$$(G_i)' = G_i / W_i, (H_i)' = H_i / W_i; 1 \leq i \leq n.$$

Step5: Now, find an optimal sequence by applying the Johnson's technique on a new reduced problem in step4 and formulate a flow time in-out table for the sequence (say S) obtained.

Step6: Next step is to check the effect of breakdown interval (a,b) on different jobs of optimal sequence S obtained in step5

and formulate a new reduced problem with processing time A_i' , B_i' and C_i'

- if (a,b) has an effect on jobs i , then
 $(A_i)' = A_i + L$
 $(B_i)' = B_i + L$
 $(C_i)' = C_i + L$
- if (a, b) has no effect on jobs i , then
 $(A_i)' = A_i$
 $(B_i)' = B_i$
 $(C_i)' = C_i$

where, $L = (b-a)$ is length of the break down interval (a, b) on machines M_j ($1 \leq j \leq 3$).

Step7: Now, repeat the procedure from step 3 to step 5 to get the optimal sequence by using Johnson's method. Let the sequence be S_j and find in-out flow table for S_j and compute utilization time U_1 , U_2 & U_3 for machines M_j ($j=1,2,3$).





Deepak Gupta and Tamanna

Step8: Next step is to obtain the other sequences by injecting 2^{nd} , 3^{rd} , ..., n^{th} job of the sequence S_1 in the 1^{st} position and all the other jobs of sequence S_1 in the same order. Let the sequences be $S_2, S_3, S_4, \dots, S_{n-1}$.

Step9: Find In- Out flow time table for the sequences S_2, S_3, S_4, \dots so on and compute U_1, U_2, U_3 for sequences S_q ($q = 1$ to r).

Step10: Find $\min R(S_q)$; $R(S_q) = \text{Minimize } R(S_q) = U_1 \times C_1 + U_2 \times C_2 + U_3 \times C_3$ for all possible sequences S_q ($q = 1, 2, 3, \dots, r$).

Let it be least in the sequence S_i , then S_i will be the required optimal sequence with rental cost $R(S_i)$.

Step11: Last step is to find the value of weighted mean flow time for the optimal sequence S_i obtained in step10 by $F_w = \frac{1}{n} \sum_{i=1}^n (W_i \cdot f_i) / \frac{1}{n} \sum_{i=1}^n W_i$; $1 \leq i \leq n$ & f_i is the flow time of i^{th} jobs.

NUMERICAL ILLUSTRATION

Consider a "4-job, 3-machines" flow shop scheduling problem to find an optimal sequence to calculate minimum rental cost for three machines, where the weights are assigned to the each job and also breakdown interval gap (10,20) is given. The rental costs per unit time for machines M_1, M_2 and M_3 are given as:

Rental cost for machine $M_1 = 3$ Rs.

Rental cost for machine $M_2 = 15$ Rs.

Rental cost for machine $M_3 = 20$ Rs.

Solution

Step 1: Since $\min(A) = 5$, $\max(B) = 10$ & $\min(C) = 12$.

So here, $12 = \min(C) \geq \max(B) = 10$, i.e., one structured condition is satisfied. Therefore, we forward to the next step of algorithm.

Step 2: Now, the modified $n \times 3$ weighted flow shop problem into two machine flow shop problem by introducing the two fictitious machines G and H with two fictitious processing time G and H respectively is given as:

$$G_i = A_i + B_i$$

$$H_i = B_i + C_i$$

Step 3: Now, by using step3 of algorithm the weighted mean flow is minimizes as:

$$\min(G_1, H_1) = G_1 = 16, \bullet G_1 = G_1 - W_1 = 16 - 2 = 14 \text{ \& } H_1 = H_1 = 31,$$

$$\min(G_2, H_2) = G_2 = 13, \bullet G_2 = G_2 - W_2 = 13 - 4 = 9 \text{ \& } H_2 = H_2 = 20,$$

$$\min(G_3, H_3) = G_3 = 33, \bullet G_3 = G_3 - W_3 = 16 - 2 = 14 \text{ \& } H_3 = H_3 = 26,$$

$$\min(G_4, H_4) = H_4 = 17, \text{ so } G_4 = G_4 = 35 \text{ \& } H_4 = H_4 + W_4 = 17 + 7 = 24.$$

Step 4: Reduced problem as per step4 of algorithm is

Step 5: According to Jhonson's method, the optimal sequence for new reduced problem in step4 is $S = \langle 2, 1, 3, 4 \rangle$.

In – Out table for the sequence $S = \langle 2, 1, 3, 4 \rangle$ is:

Step 6: Consider the effect of given breakdown interval $(a, b) = (35, 40)$ on table 1.6, we get a new reduced problem given as: Where, $L = 20 - 10 = 10$ units and $(A_i)' = A_i + L$, $(B_i)' = B_i + L$, $(C_i)' = C_i + L$.

Step7: Perform again the step 2 to 5, we get

$$\text{Now, } \min(G_1, H_1) = G_1 = 36, \bullet G_1 = 34 \text{ \& } H_1 = 41,$$

$$\min(G_2, H_2) = G_2 = 23, \bullet G_2 = 19 \text{ \& } H_2 = 40,$$

$$\min(G_3, H_3) = H_3 = 36, \bullet G_3 = 43 \text{ \& } H_3 = 39,$$

$$\min(G_4, H_4) = H_4 = 17, \text{ so } G_4 = 35 \text{ \& } H_4 = 24.$$

New reduced flow shop problem is

Again, apply Jhonson's method to get near optimal sequence, we get a sequence say $S_i = \langle 2, 3, 4, 1 \rangle$, whose in-out table is given as: Now, utilization time for machines $M_1(1, 2, 3)$ for sequence $S_i = \langle 2, 3, 4, 1 \rangle$ is given as:

$$U(M_1) = 87 \text{ units, } U(M_2) = 107 - 5 = 102 \text{ units and } U(M_3) = 128 - 23 = 105 \text{ units.}$$

Step 8: The other optimal sequences for minimizing rental cost are

$$S_i = \langle 3, 2, 4, 1 \rangle, S_i = \langle 4, 2, 3, 1 \rangle, S_i = \langle 1, 2, 3, 4 \rangle.$$





Deepak Gupta and Tamanna

Step 9 : In-out table for $S_2 = \langle 3, 2, 4, 1 \rangle$ is:

For S_2 , $U(M_1) = 87$ units, $U(M_2) = 107 - 34 = 73$ units and $U(M_3) = 128 - 43 = 85$ units.

In-out table for $S_3 = \langle 4, 2, 3, 1 \rangle$ is:

For S_3 , $U(M_1) = 87$ units, $U(M_2) = 107 - 32 = 75$ units and $U(M_3) = 128 - 35 = 93$ unit

In-out table for sequence $S_4 = \langle 1, 2, 3, 4 \rangle$ is:

For S_4 , $U(M_1) = 87$ units, $U(M_2) = 90 - 16 = 74$ units and $U(M_3) = 120 - 36 = 84$ units.

Step10 : Since the minimum utilization cost for machine M_1 is fixed which is 87 units and 230 units. But, the minimum utilization cost of machine M_2 & M_3 is 74 units and 84 units respectively for the sequence S_4 . The optimal sequence for which total rental cost for three machines is minimum, is $S_4 = \langle 1, 2, 3, 4 \rangle$.

Minimum total rental cost is given as :

$$R(S_i) = U(M_1) \times C_1 + U(M_2) \times C_2 + U(M_3) \times C_3.$$

$$= (87 \times 3) + (74 \times 15) + (84 \times 20) = 261 + 1110 + 1680 = 3051 \text{ Rs.}$$

Step11 : At last, calculate the weighted mean flow time of machines M_1 , M_2 & M_3 for the optimal sequence $S_4 = \langle 1, 2, 3, 4 \rangle$ from the table given below :

From table: $f_1 = 1.14$, $f_2 = 57$ units, $f_3 = 79$ units, $f_4 = 106$ units & $f_5 = 120$ units.

Now, Mean weighted flow time for sequence $S_4 = \langle 1, 2, 3, 4 \rangle$ is

$$F_w = \sum_{i=1}^n (W_i \cdot f_i) / \sum_{i=1}^n W_i = (57 \times 2) + (79 \times 4) + (106 \times 3) + (120 \times 7) / (2 + 4 + 3 + 7) = 800.5 \text{ units.}$$

CONCLUSION

This procedure gives an algorithm for a $n \times 3$ flow shop scheduling problem that minimizes the total rental cost of the machines under a specified rental policy with the effect of breakdown interval on different jobs and weight-age of jobs. Further the work can be extended for $n \times 4$ flow shop scheduling model.

REFERENCES

1. Johnson S.M. (1954), Optimal two & three stage production schedules with setup times includes, Nav.Res.Log. Quart., vol.1, pp 61-68.
2. Miyazaki, S., & Nishiyama, N. (1980), Analysis for minimizing weighted mean flow-time in flow-shop scheduling, Journal of the Operations Research Society of Japan, Vol.23(2), pp118-133.
3. Maggu, P.L., Yadav, S. K., Singh, T. P., & Dev, A. (1984), Flow-shop scheduling problem involving job-weight and transportation time, Pure and Applied Mathematica Sciences, Vol.20.
4. Singh T.P.(1985), On $n \times 2$ flow shop problem solving job block, Transportation times, Arbitrary time and Break-down machine times, PAMS Vol. XXI, pp 1-2.
5. Adiri, I., Bruno J., Frostig E. & Kan R.A.H.G(1989), Single machine flow time scheduling with a single break-down, Act a Information, Vol.26(7), pp 679-696.
6. Akturk M.S. & Gorgulu E.(1999), Matchup scheduling under a machine break-down, European journal of operational research, pp 81-99.
7. Singh T.P., K. Rajindra & Gupta Deepak(2005), Optimal three stage production schedule the processing time and setup times associated with probabilities including job block criteria, Proceeding of National Conference FACM, pp 463-470.
8. Chandramouli A.B. (2005), Heuristic approach for N job 3 machine flow shop scheduling problem involving transportation time, break-down time and weights of jobs, Mathematical and Computational Application, Vol.10(2), pp 301-305.





Deepak Gupta and Tamanna

9. Narian L. & Bagga P.C.(2005) , Scheduling problems in Rental Situation , Bulletin of Pure and Applied Sciences : Section E. Mathematics and Statistics , vol. 24 Narain , pecial Models in flow shop sequencing problems , Feb (2006) Ph.D. Thesis , Delhi University Delhi.
10. Singh T.P , Gupta Deepak(2006) , Minimizing rental cost in two stage flow shop , the processing time associated with probabilities including job block , Reflections de ERA ,Vol. 1(2), pp 107-120.
11. T.P. Singh , Rajender kumar & Gupta Deepak(2006), The idle/ waiting time operator O_i with application to multi-stage flow shop scheduling including transportation time, breakdown interval and the processing time along with the irrespective probabilities Act Ciencia Indica , vol. XXXII(1) , pp 489-496.
12. Singh T.P. , Gupta S.(2008) , Minimizing of rental cost in 3 stage flow shop with parallel machine including transportation time , International Journal ACT ACIENCIA INDICA , vol. 34(2),pp 629-634.
13. Gupta D. & Sharma S.(2011) , Constrained Flow Shop Scheduling with jobs , 3-machine, processing time associated with probability involving transportation time , break down interval and Weight age of jobs , Industrial Engineering Letters ,vol. 1(2) , pp 41-53.
14. Gupta D. , Sharma S. , Aggarwal S. (2012) , Three stage constrained flow shop scheduling with jobs in a string of disjoint job-block , In Engineering and System (SCES) , Students Conference , pp 1-6.
15. Gupta D. & Sehgal Poojadeep (2018) , Effect of breakdown interval in three stage flow shop scheduling in which processing time associated with probabilities including transportation time and job block criteria , International Journal on Future Revolution in Computer Science & Communication Engineering , vol. 4(3), pp 257-261.
16. Gupta D., Sehgal P. (2021) , Minimization of Hiring cost for n jobs 2-machines flow shop scheduling : Processing time associated with the probabilities with transportation time including breakdown interval , IOP Conference series : Materials Science and Engineering, vol. 1145(1) , pp. 012102.
18. Gupta D. , Sehgal P. (2022) , Minimization of hiring cost of the machines in two stage flow shop with breakdown interval , AIP Conference Proceedings , Vol. 2357(1), pp 090002-090002-7 .
19. Gupta D., Tamanna (2023) , N×3 FSSM with breakdown interval to minimize the rental cost , Aryabhatta Journal of Mathematics & Informatics, Vol.15(2), pp.213-222.
20. Gupta D. , Sehgal P.(2021) , Effect of breakdown interval with weight-age of jobs for minimizing hiring cost in 2 stage flow shop scheduling, IEEE International Conference on Technology, Research and Innovation of Betterment of Society (TRIBES) , Raipur, India, , doi: 10.1109/TRIBES52498.2021.9751625 , pp. 1-4.

Table : 1

Jobs (i)	Machine M_1 (A_i)	Machine M_2 (B_i)	Machine M_3 (C_i)	Weight (W_i)
1	A_1	B_1	C_1	W_1
2	A_2	B_2	C_2	W_2
3	A_3	B_3	C_3	W_3
....
....
n	A_n	B_n	C_n	W_n

Table : 2

Jobs (i)	Machines with G_i	processing	time	H_i	Weight (W_i)
-------------	------------------------	------------	------	-------	---------------------





Deepak Gupta and Tamanna

1	G_1	H_1	W_1
2	G_2	H_2	W_2
3	G_3	H_3	W_3
...
...
n	G_n	H_n	W_n

Table 3:

Jobs (i)	Machine M_1 (A_i)	Machine M_2 (B_i)	Machine M_3 (C_i)	Weight (W_i)
1	6	10	21	2
2	5	8	12	4
3	24	9	27	3
4	32	3	14	7

Table 4:

Jobs (i)	Machines with G_i	processing	time	H_i	Weight (W_i)
1	16	31			2
2	13	20			4
3	33	26			3
4	35	17			7

Table 5:

Jobs (i)	Machines with G_i	processing	time	H_i
1	7	15.5		
2	3.25	5		
3	10	12		
4	5	3.73		

Table 6:

Jobs (i)	Machine M_1 (<i>in-out</i>)	Machine M_2 (<i>in-out</i>)	Machine M_3 (<i>in-out</i>)
-------------	------------------------------------	------------------------------------	------------------------------------





Deepak Gupta and Tamanna

2	0-5	5-13	13-25
1	5-11	13-23	25-46
3	11-35	35-44	46-73
4	35-67	67-70	73-87

Table 7:

Jobs (i)	Machine M_1 (A)	Machine M_2 (B)	Machine M_3 (C)	Weight (W _i)
1	16	20	21	2
2	5	18	22	4
3	34	9	27	3
4	32	3	14	7

Table 8:

Jobs (i)	Machines with G_i	processing time	H_i	Weight (W _i)
1	36	41		2
2	23	40		4
3	43	36		3
4	35	17		7

Table 9:

Jobs (i)	Machines with G_i	processing time	H_i
1	17	2.5	
2	4.75	10	
3	14.33	13	
4	5	3.73	

Table 10:

Jobs (i)	Machine M_1 (in-out)	Machine M_2 (in-out)	Machine M_3 (in-out)
2	0-5	5-23	23-45
3	5-39	39-48	48-75





Deepak Gupta and Tamanna

4	39-71	71-74	75-102
1	71-87	87-107	107-128

Table 11:

Jobs (i)	Machine M_1 (in-out)	Machine M_2 (in-out)	Machine M_3 (in-out)
3	0-34	34-43	43-70
2	34-39	43-61	70-92
4	39-71	71-74	92-106
1	71-87	87-107	107-128

Table 12:

Jobs (i)	Machine M_1 (in-out)	Machine M_2 (in-out)	Machine M_3 (in-out)
4	0-32	32-35	35-49
2	32-37	37-55	55-77
3	37-71	71-80	80-107
1	71-87	87-107	107-128

Table 13:

Jobs (i)	Machine M_1 (in-out)	Machine M_2 (in-out)	Machine M_3 (in-out)
1	0-16	16-36	36-57
2	16-21	36-54	57-79
3	21-55	55-64	79-106
4	55-87	87-90	106-120

Table 14:

Jobs (i)	Machine M_1 (in-out)	Machine M_2 (in-out)	Machine M_3 (in-out)	Weight (W_i)
1	0-16	16-36	36-57	2
2	16-21	36-54	57-79	4
3	21-55	55-64	79-106	3
4	55-87	87-90	106-120	7





RESEARCH ARTICLE

Exploring The Hydrochemical Properties of Ground Water in Relation to Epidemiological Data in Rural and Semi-Urban Locations of Ambala, India

Saloni Kamboj, Nirankar Singh* and R.C. Saini

Department of Chemistry, Maharishi Markandeshwar Engineering College, Maharishi Markandeshwer (Deemed to be University), Mullana, Ambala, India.

Received: 22 Jan 2024

Revised: 09 Feb 2024

Accepted: 30 May 2024

*Address for Correspondence

Nirankar Singh

Department of Chemistry,
Maharishi Markandeshwar Engineering College,
Maharishi Markandeshwer
(Deemed to be University),
Mullana, Ambala, India.
Email: nirankar_singh11@yahoo.com



This is an Open Access Journal / article distributed under the terms of the **Creative Commons Attribution License** (CC BY-NC-ND 3.0) which permits unrestricted use, distribution, and reproduction in any medium, provided the original work is properly cited. All rights reserved.

ABSTRACT

The hydro-chemical properties of ground water were explored for the first time in the selected rural and semi-urban locations of Ambala, India (30°25'13" N, 77°04'79" E) to find the relation with the current health issues of the natives. The samples were analyzed for 23 water quality parameters along with a health survey (44 human subjects) in and around the sampling points. High levels of TH (564-840 mgL⁻¹), Ca-H (140-340 mgL⁻¹), Mg-H (224-660 mgL⁻¹), Ni (573-1120 µgL⁻¹), Pb (12.6-48.6 µgL⁻¹), and Se (26.4-180 µgL⁻¹) were observed in the samples which remained quite above the limits of drinking water quality standards set by BIS and WHO. Out of six issues reported by the residents, hair fall (35%), skin (28%) and liver problems (14%) were observed as the major problems in the selected region. The levels of toxic (Ni and Pb) and undesirable (Se) elements remained above the standard limits in all the samples (100% exceedance).

Keywords: Health Survey, Ground Water Quality, Ions, Toxic Elements

INTRODUCTION

Fresh water is the primary need of every human being especially for drinking and other domestic purposes [44,45,18]. Ground water is the main source of fresh water which is further used in drinking, irrigation and industrial purposes around the world. The change in the chemistry of water influences the ecological system [25,46,1,27]. The

75670





chemical composition of water varies place to place due to various geological reasons and anthropogenic activities. Increasing population and its necessities have also lead to the deterioration of surface, sub-surface and underground water[21,23,22,39]. Water pollution is a serious problem in many parts of India as number of studies have reported regular increase in the contamination of groundwater reserves due to biological, toxic, organic, and inorganic pollutants[31,24,13]. In many investigations, these sources have been found unsafe for direct human consumption as well as for other purposes, such as irrigation and industrial needs[29,38,4,19]. Degradation in water quality may create a situation of fresh water scarcity as it confines its availability for both human use and for the ecosystem[30,34,26,11]. Contamination of arsenic, chromium and fluoride is a serious problem in India[35,40,20,8]and in other countries as well. Studies show that fluorosis (dental and skeletal)has emerged as a global health issue which is caused by consumption of excess amount of fluoride through drinking water[41,2,46,5].According to dermatologists, the cases of allergies caused by nickel toxicity are also growing. The non-occupational sources of nickel exposure for the general population mainly include drinking water and food[10,7,18].Similarly, the adverse health effects of lead exposure in children and adults are well reported, and no safe limits of lead in blood have been identified in case of children[17,32,36]. Lead (odourless and tasteless) can be ingested from various sources, including lead paint dust, lead contaminated soil, drinking water and food[15,3]. The levels of concentration, amount consumed and duration of exposure influence the severity of health effects due to lead. Because lead accumulates in the body (gums, hair and nails), all sources of lead should be controlled or eliminated to prevent childhood lead poisoning[9,37,41]. Its high levels also influence the intestine, kidneys and the nervous system. This heavy metal can be removed by the process of electrolysis or membrane filtration. The heavy element Selenium (Se) is found in the earth's crust, often in association with sulfur containing minerals. It is a very healthy element if levels in water remain below 0.01 mgL⁻¹[16,12]. Any single increase in the selenium levels results in acute toxicity whereas the excessive intake causes selenosis which results in caries, loss of hairs, fragility of nails, dermatitis and disorders in digestive organs[43,14].The high levels of copper in water cause intoxication and induce kidney and liver diseases leading to the state of coma or even death.Various researchers have evaluated the water quality in reference to the permissible limit set by the BIS and WHO and have found the contamination of heavy metals.

The physiological as well as the metabolic activities of living organisms are usually influenced due to water contamination, therefore it is crucial to study the physico-chemical characteristics of the ground water on a regular basis to get exact idea about the quality of water as per the standards given by BIS and WHO. The present study was aimed to investigate the possible association of the current health issues with the levels of selected water quality parameters in rural and semi-urban locations of the chosen study area (Figure 1). This study also aimed to explore the suitability of ground water for drinking purpose as per the recommendations of BIS and WHO in the selected area. All metabolic and physiological activities of living organisms are generally influenced due to water contamination therefore it is essential to study the physico-chemical characteristics of the ground water on a regular basis to get an exact idea about the quality of water as per the standards given by BIS and WHO. The present study was aimed to investigate the possible association of the current health issues with the levels of selected water quality parameters in rural and semi-urban locations of the chosen study area (Figure 1). This study also aims to explore the suitability of the ground water for drinking purpose as per the recommendations of BIS and WHO in the selected area.

STUDY AREA & METHODOLOGY

STUDY AREA

The present study was carried out at Barara block of Ambala district in Haryana, India covering rural and semi urban locations during Jan-April 2018. The sequence of approximate depths of water level at different sites was 280 feet (MMDU and BHUDHIAN)>260 feet (Barara)>200 feet (Mullana). The atmospheric temperature of the study area generally varies between 10-35 °C during Jan-April every year. The water samples were collected from different locations of Bararablock. The grid locations, depths of water levels and population of sample collection sites are shown in Table 1.





MATERIALS AND METHODS

Water samples collected from different locations were analyzed for the selected parameters following the standard procedures recommended by BIS and APHA. In order to get the data of current health status of the natives, a health survey was conducted during this period of study in and around the selected locations. The ground water samples were collected covering rural and semi-urban locations and proper care was taken to get authentic and correct analytical results. The samples were collected in pre-cleaned specified plastic bottles (250 ml) coded with the name of the sampling site. Samples were brought to the laboratory and analyzed for the selected parameters. A brief summary of analytical methods followed during the chemical analysis has been provided below in the Table 2. The water colour was determined by visual comparison of the sample with distilled water (BIS:3025, Part 4) while temperature of the samples was checked at the sampling sites by taking one litre of the water sample and immersing the thermometer into it for a sufficient period of time (till the reading stabilizes). The pH was determined by a pH meter (CyberScan pH-510, Eutech Instruments) and during the measurements, electrode was allowed to remain in the sample undisturbed for 2 minutes to stabilize before taking reading for reproducible results (at least ± 0.1 pH units) (BIS:3025, Part 11). Similarly electrical conductivity (EC) was measured by a conductometer (CON-700, Eutech Instruments) and stable readings were noted. The amount of total dissolved solids (TDS) was determined by following the analysis method recommended by BIS (IS:3025, Part 16). The total hardness (TH) and Calcium hardness (Ca-H) was determined by EDTA titration method while Mg-H was calculated by subtracting the Ca-H from TH and multiplying by the factor 0.243 [$\text{Mg-H} = (\text{TH} - \text{Ca-H}) \times 0.243$ as mgL^{-1} of CaCO_3] (IS-3025, Part 21). Titration method was adopted to determine the total alkalinity (TA) in terms of CO_3^{2-} and HCO_3^- . Ion chromatography was employed to measure the concentration of ions (Cl^- , F^- , NO_3^- , PO_4^{3-} , and SO_4^{2-}) and concentration levels of Na^+ and K^+ ions were determined by flame photometer (Systronics). The concentration levels of Ni, Pb, Se, Mn, Cu, Cd, Cr, Fe and Zn were analyzed by using inductively coupled plasma atomic emission spectroscopy technique (ICP-AES, Shimadzu). All the instruments were calibrated and standardized and blanks were run before the analysis to check the reliability of the instruments. All the samples were tested repeatedly to get authentic results.

HEALTH SURVEY

In order to collect the information of actual health conditions of the natives, a health survey was conducted in and around the water sampling points. A survey form was prepared to collect the information about the age, gender, qualification, health issue etc. Door to door data was collected from 44 human subjects covering different age groups i.e. (20-60 years).

RESULTS AND DISCUSSION

Physico-Chemical Parameters

The results indicate that the quality of water considerably varies from location to location. The temperature values of the collected water samples were observed to be almost same ($\pm 1^\circ\text{C}$) which may be due to the influence of environmental temperature at the time of sample collection. The colour was determined by visual comparison of the sample with the distilled water and all the samples were found colorless. The results of physico-chemical analysis of different water quality parameters have been given in table 3 and 4. The desirable range of pH for drinking water is 7.0-8.5. In the present study, pH values of water samples in the study area ranged between 7.3-8.05 (Figure 3b) and was found in the desired limits as prescribed in the standards for drinking water by WHO and BIS. The magnitude of total alkalinity value of water in terms of CaCO_3 varied between 42.7 to 225.7 mgL^{-1} (Table 3) and found well within the permissible range of water quality standards (Table 5). The water which has less than 100 mgL^{-1} of total alkalinity is considered suitable for the domestic purpose. Hard water is not suitable for domestic, agricultural and industrial purposes. The total hardness (TH) of the studied water samples varied between 564-840 mgL^{-1} . The value of TH were found above the acceptable limits (200 mgL^{-1}) of drinking water quality set by different agencies like BIS & WHO at all the sites. On the basis of total hardness levels, water is generally categorized into soft water (0-60 mgL^{-1}), moderately hard (61-120 mgL^{-1}), hard (121-180 mgL^{-1}) and very hard ($>180 \text{mgL}^{-1}$). Analysis shows that water of the



Saloni Kamboj *et al.*,

area falls under very hard category which is not suitable for drinking & other household purposes & may produce health problems if used for long time without any suitable treatment. The concentration level of Cl^- was found to be in the range from 2.10 mgL^{-1} - 18.08 mgL^{-1} . The maximum permissible levels of chloride given by WHO and BIS are 200 and 250 mgL^{-1} respectively. Thus the chloride level in water samples was quite below the permissible limits and can be safely used for drinking and cooking purpose. The values of nitrate (NO_3^-) in the water samples ranged from 0.031 - 34.037 mgL^{-1} . The levels of nitrate were found within the safe limits as prescribed by WHO and BIS. TDS value measures the total quantity of all inorganic and organic substances dissolve in the given water sample. The acceptable limit of TDS for drinking water is 500 mgL^{-1} (BIS 2012). The TDS values in the collected samples varied between 326.4 mgL^{-1} (minimum) at S2 and 531.2 mgL^{-1} (maximum) at S1. Obtained results show that except S1, the TDS values remained below the acceptable limit (Figure 3a). Calcium and Magnesium hardness is a measure of the levels of Ca^{2+} and Mg^{2+} ions in water. In the analyzed samples, Ca-H of water ranged from 140 to 340 mgL^{-1} and Mg-H of water ranged from 224 - 660 mgL^{-1} which were quite above the acceptable concentration of Ca^{2+} and Mg^{2+} (75 mgL^{-1} and 30 mgL^{-1} respectively). The concentration levels of Na^+ and K^+ ions ranged between 67.7 mgL^{-1} - 102.2 mgL^{-1} and 25.1 mgL^{-1} - 80 mgL^{-1} respectively while the levels of fluoride ranged between 0.324 mgL^{-1} - 0.670 mgL^{-1} and found within the limits of WHO and BIS in all the samples (Figure 4a). The concentration of Ni, Pb, Se and Mn ranged between $573 \text{ } \mu\text{gL}^{-1}$ - $1350 \text{ } \mu\text{gL}^{-1}$, $12.6 \text{ } \mu\text{gL}^{-1}$ - $48.6 \text{ } \mu\text{gL}^{-1}$, $26.4 \text{ } \mu\text{gL}^{-1}$ - $180 \text{ } \mu\text{gL}^{-1}$, bdl- $572 \text{ } \mu\text{gL}^{-1}$ respectively exceeding the permissible limits set by BIS, India and WHO. The concentration levels of Cu, Cd, Cr, Fe and Zn were found below detection limit (bdl) of the instrument. On the contrary it can be concluded that these metals were not detected in the collected samples. The water samples were observed as free from contamination of selected toxic metals like Cd and Cr.

HEALTH SURVEY DATA

Data analysis of health survey shows that except only 2% human subjects, who did not state any health issue, all the people were having some kind of health problems. People reported complications related to kidney functioning (12%), stomach (9%), liver (14%), skin (28%) and hair fall (35%). Pie chart (Figure 5) further shows that 63% people were suffering primarily from skin and hair fall problems in this area. People in the age group between 30-50 years were suffering from skin and kidney stone problems at the rural locations while people in the age group of 20-40 years reported stomach issue also in addition to the skin and hair fall problems. People in the age group between 60-80 years mainly reported stomach problem. The drinking water loaded with Ca, Mg and HCO_3^- may increase the risk of CaC_2O_4 crystallization in kidneys⁴⁸. The presence of excess amount of nickel (Ni), lead (Pb) and selenium (Se) in water may be the cause of problems like hair fall, skin allergies in this region. People who were using some kind of water filtration system at home, reported less number of health issues. The presence of lead (Pb) in the drinking water can also damage kidneys, nervous system, and may affect brain functioning while the presence of selenium (Se) in the drinking water has been reported as the major cause of hair fall (28). The presence of nickel (Ni) in water can cause allergies, cardiovascular problems, kidney failure, lungs fibrosis and cancer (lung and nasal)^{49,50}.

CONCLUSION

The quality of groundwater in the studied region is observed to be neutral to alkaline with TH and TDS varying from 564 to 840 mgL^{-1} and 326 - 531 mgL^{-1} , respectively. The concentrations of Cl^- , F^- , NO_3^- , SO_4^{2-} remained within the desirable limits of WHO for drinking water, but the levels of TH, Ca-H, and Mg-H were quite above the prescribed permissible levels for drinking water. Furthermore, ionic levels were observed in the order $\text{Mg}^{2+} > \text{Ca}^{2+} > \text{Na}^+ > \text{K}^+$ for cations and $\text{HCO}_3^- > \text{NO}_3^- > \text{SO}_4^{2-} > \text{Cl}^-$ for anions. The high loading of TDS, EC, TH, Na^+ , K^+ , Mg^{2+} , and Ca^{2+} in water samples indicates the weathering of rocks, natural sources and ion-exchange processes by human induced activities while low levels of Cl^- and NO_3^- indicate lesser impact of anthropogenic activities, livestock effluents, domestic sewage, and agricultural activities on the groundwater quality in the study region. The presence of toxic elements (Ni and Pb) and their levels exceeding the desirable values (BIS and WHO), also indicates towards the carcinogenic risk of local residents. The high concentration of Ni, Pb and Se may be responsible for skin allergies, hair fall, liver and kidney damage in this region. The combined impacts of contamination of toxic elements and substances undesirable



Saloni Kamboj *et al.*,

in excess quantity in groundwater may cause severe diseases in the near future if such water is used specially for drinking purpose without treatment. The findings of this study would be helpful in detailed investigation further and decision making on drinking water security issues among rural communities.

Acknowledgements

Authors are thankful to the authorities at Maharishi Markandeshwar Deemed to be University, Mullana, India and ICAR Central Soil Salinity Research Institute, Karnal, India for providing the analytical facilities to conduct this research.

REFERENCES

1. Adimalla, N., 2019. Controlling factors and mechanism of groundwater quality variation in semiarid region of South India: an approach of water quality index (WQI) and health risk assessment (HRA). *Environmental Geochemistry and Health*, pp.1-28.
2. Aggeborn, L. and Öhman, M., 2021. The effects of fluoride in drinking water. *Journal of Political Economy*, 129(2), pp.465-491.
3. Agyemang, V.E.R.O.N.I.C.A., 2018. Blood Lead Levels and Selected Haematological Parameters among at Risk Occupational Groups and Blood Donors in Kenyasi, Brong Ahafo Region (Doctoral dissertation, University Of Ghana).
4. Al Maliki, A.A., Abbass, Z.D., Hussain, H.M. and Al-Ansari, N., 2020. Assessment of the groundwater suitability for irrigation near Al Kufa City and preparing the final water quality maps using spatial distribution tools. *Environmental Earth Sciences*, 79(13), pp.1-12.
5. Alphayo, S.M. and Sharma, M.P., 2021. Removal of Fluoride from Drinking Water Supplies. In *Climate Impacts on Water Resources in India* (pp. 321-330). Springer, Cham.
6. BIS, I., 2012. 10500 Indian standard drinking water–specification, second revision. Bureau of Indian Standards, New Delhi.
7. Bonamonte, D., Foti, C., Filoni, A. and Angelini, G., 2021. Airborne Skin Diseases. In *Clinical Contact Dermatitis* (pp. 213-263). Springer, Cham.
8. Brindha, K., Paul, R., Walter, J., Tan, M.L. and Singh, M.K., 2020. Trace metals contamination in groundwater and implications on human health: comprehensive assessment using hydrogeochemical and geostatistical methods. *Environmental geochemistry and health*, 42(11), pp.3819-3839.
9. Brown M.J. and Margolis S, (2012). Lead in drinking water and human blood lead levels in the United States..
10. Buxton, S., Garman, E., Heim, K.E., Lyons-Darden, T., Schlekot, C.E., Taylor, M.D. and Oller, A.R., 2019. Concise review of nickel human health toxicology and ecotoxicology. *Inorganics*, 7(7), p.89.
11. Chowdhary, P., Bharagava, R.N., Mishra, S. and Khan, N., 2020. Role of industries in water scarcity and its adverse effects on environment and human health. In *Environmental Concerns and Sustainable Development* (pp. 235-256). Springer, Singapore.
12. Clottey, C.A., 2018. Assessment of Physicochemical Parameters and Heavy Metals Contamination in Korle and Kpeshie Lagoons (Doctoral dissertation, University of Ghana).
13. Das, N., Mahanta, C. and Kumar, M., 2020. Water quality under the changing climatic condition: A review of the Indian scenario. *Emerging Issues in the Water Environment during Anthropocene*, pp.31-61
14. Fan, A.M. and Vinceti, M., 2015. Selenium and its Compounds. In *Hamilton & Hardy's Industrial Toxicology* (pp. 205-228). Wiley-Blackwell.
15. Flavin, N., 2017. Evaluation of Childhood Exposure to Lead in Community Water Systems in Maine.
16. Gomes, C.S. and Silva, E.A., 2021. Health Benefits and Risks of Minerals: Bioavailability, Bio-Essentiality, Toxicity, and Pathologies. In *Minerals Iatu sensu and Human Health* (pp. 81-179). Springer, Cham.
17. He, X., Wu, J. and He, S., 2019. Hydrochemical characteristics and quality evaluation of groundwater in terms of health risks in Luhe aquifer in Wuqi County of the Chinese Loess Plateau, northwest China. *Human and Ecological Risk Assessment: An International Journal*, 25(1-2), pp.32-51.





18. Hostynek, J.J., 2019. Aspects of Nickel Allergy: Epidemiology, etiology, immune reactions, prevention, and therapy. Nickel and the Skin, pp.1-37.
19. Inyinbor Adejumo, A., Adebisin Babatunde, O., Oluyori Abimbola, P., Adelani Akande Tabitha, A., Dada Adewumi, O. and Oreofe Toyin, A., 2018. Water pollution: effects, prevention, and climatic impact. Water Challenges of an Urbanizing World, 33, pp.33-47.
20. Kanagaraj, G. and Elango, L., 2019. Chromium and fluoride contamination in groundwater around leather tanning industries in southern India: Implications from stable isotopic ratio $\delta^{53}\text{Cr}/\delta^{52}\text{Cr}$, geochemical and geostatistical modelling. Chemosphere, 220, pp.943-953.
21. Karn, S.K. and Harada, H., 2001. Surface water pollution in three urban territories of Nepal, India, and Bangladesh. Environmental management, 28(4), pp.483-496.
22. Khan, M., 2018. Groundwater Resources and Assessment of Water Quality in Parts of Yamuna River Basin (Doctoral dissertation, Aligarh Muslim University).
23. Khan, R., Saxena, A., Shukla, S., Sekar, S., Senapathi, V. and Wu, J., 2021. Environmental contamination by heavy metals and associated human health risk assessment: a case study of surface water in Gomti River Basin, India. Environmental Science and Pollution Research, pp.1-12.
24. Kumar, A. and Krishna, A.P., 2021. Groundwater quality assessment using geospatial technique based water quality index (WQI) approach in a coal mining region of India. Arabian Journal of Geosciences, 14(12), pp.1-26.
25. Li, P., Wu, J. and Qian, H., 2016. Hydrochemical appraisal of groundwater quality for drinking and irrigation purposes and the major influencing factors: a case study in and around Hua County, China. Arabian Journal of Geosciences, 9(1), pp.1-17.
26. Ma, T., Sun, S., Fu, G., Hall, J.W., Ni, Y., He, L., Yi, J., Zhao, N., Du, Y., Pei, T. and Cheng, W., 2020. Pollution exacerbates China's water scarcity and its regional inequality. Nature communications, 11(1), pp.1-9.
27. Makki, Z.F., Zuhaira, A.A., Al-Jubouri, S.M., Al-Hamd, R.K.S. and Cunningham, L.S., 2021. GIS-based assessment of groundwater quality for drinking and irrigation purposes in central Iraq. Environmental Monitoring and Assessment, 193(2), pp.1-27.
28. Martin S. and Griswold W, (2009). Human health effects of heavy metals. Environmental Science and Technology briefs for citizens, 15, pp.1-6.
29. Masindi, V. and Muedi, K.L., 2018. Environmental contamination by heavy metals. Heavy metals, 10, pp.115-132.
30. Mikosch, N., Berger, M. and Finkbeiner, M., 2020. Addressing water quality in water footprinting: current status, methods and limitations. The International Journal of Life Cycle Assessment, pp.1-18.
31. Mukherjee, I., Singh, U.K. and Singh, R.P., 2021. An Overview on Heavy Metal Contamination of Water System and Sustainable Approach for Remediation. Water Pollution and Management Practices. Springer Singapore, Singapore, pp.255-277
32. Naranjo, V.I., Hendricks, M. and Jones, K.S., 2020. Lead toxicity in children: an unremitting public health problem. Pediatric Neurology.
33. Naranjo, V.I., Hendricks, M. and Jones, K.S., 2020. Lead toxicity in children: an unremitting public health problem. Pediatric Neurology.
34. Peters, N.E. and Meybeck, M., 2000. Water quality degradation effects on freshwater availability: impacts of human activities. Water International, 25(2), pp.185-193.
35. Poonia, T., Singh, N. & Garg, M.C. Contamination of Arsenic, Chromium and Fluoride in the Indian groundwater: a review, meta-analysis and cancer risk assessment. Int. J. Environ. Sci. Technol. (2021). <https://doi.org/10.1007/s13762-020-03043-x>
36. Rahm, C.E., Torres-Canas, F., Gupta, P., Poulin, P. and Alvarez, N.T., 2020. Inkjet Printed Multi-walled Carbon Nanotube Sensor for the Detection of Lead in Drinking Water. Electroanalysis, 32(7), pp.1533-1545.
37. Rees, N. and Fuller, R., 2020. The toxic truth: children's exposure to lead pollution undermines a generation of future potential. UNICEF.



Saloni Kamboj *et al.*,

38. Rishi, M.S., Kaur, L. and Sharma, S., 2020. Groundwater quality appraisal for non-carcinogenic human health risks and irrigation purposes in a part of Yamuna sub-basin, India. *Human and Ecological Risk Assessment: An International Journal*, 26(10), pp.2716-2736.
39. Singh, J., Yadav, P., Pal, A.K. and Mishra, V., 2020. Water pollutants: Origin and status. In *Sensors in Water Pollutants Monitoring: Role of Material* (pp. 5-20). Springer, Singapore.
40. Singh, N., Sharma, M. Assessment of the Quality of Drinking Water Sources and Human Health in a Rural Area of Solan, North India. *MAPAN* 35, 301–308 (2020). <https://doi.org/10.1007/s12647-019-00354-4>
41. Srivastav, A. and Pathak, Y.V., 2021. Collagen Peptides: For Bone, Joint, and Other Health Applications. *Bioactive Peptides: Production, Bioavailability, Health Potential, and Regulatory Issues*, p.343.
42. Srivastava, S. and Flora, S.J.S., 2020. Fluoride in drinking water and skeletal fluorosis: a review of the global impact. *Current environmental health reports*, 7(2), pp.140-146.
43. Vinceti, M., Wei, E.T., Malagoli, C., Bergomi, M. and Vivoli, G., 2001. Adverse health effects of selenium in humans. *Reviews on environmental health*, 16(4), pp.233-252
44. World Health Organization, 2009. Potassium in drinking-water: background document for development of WHO guidelines for drinking-water quality (No. WHO/HSE/WSH/09.01/7). World Health Organization.
45. Yao, K.M., Habibian, M.T. and O'Melia, C.R., 1971. Water and waste water filtration. Concepts and applications. *Environmental science & technology*, 5(11), pp.1105-1112.
46. Zhang, L., Zhao, L., Zeng, Q., Fu, G., Feng, B., Lin, X., Liu, Z., Wang, Y. and Hou, C., 2020. Spatial distribution of fluoride in drinking water and health risk assessment of children in typical fluorosis areas in north China. *Chemosphere*, 239, p.124811.
47. Zhou, Y., Li, P., Xue, L., Dong, Z. and Li, D., 2020. Solute geochemistry and groundwater quality for drinking and irrigation purposes: a case study in Xinle City, North China. *Geochemistry*, 80(4), p.125609]
48. Villareal, D. T., Banks, M., Siener, C., Sinacore, D. R., & Klein, S. (2004). Physical frailty and body composition in obese elderly men and women. *Obesity research*, 12(6), 913-920.
49. Genchi, G., Sinicropi, M. S., Lauria, G., Carocci, A., & Catalano, A. (2020). The effects of cadmium toxicity. *International journal of environmental research and public health*, 17(11), 3782.
50. Chervona, Y., Arita, A., & Costa, M. (2012). Carcinogenic metals and the epigenome: understanding the effect of nickel, arsenic, and chromium. *Metallomics*, 4(7), 619-627.

Table 1: Different Sampling Locations (Rural and Semi-Urban), Grid Locations, Depths of Water Levels and Nomenclature

Site No	SITE NAME	GRID LOCATION	Depths of water levels (ft)	Population
S1	Bhudhian Village (Rural)	30°24'75.5'' N, 77°05'00.3'' E	280	1692
S2	Barara Town (Semi- Urban)	30°19'18.4'' N, 77°02'98.5'' E	260	21545
S3	MMDU, Mullana (Semi-Urban)	30°25'18.9'' N, 77°04'77.4'' E	280	--
S4	Mullana Village (Rural)	30°27'52.0'' N, 77°04'78.8'' E	200	4956

Table 2: Summary of Experimental Methods

S.No.	WATER QUALITY PARAMETER	METHOD
1.	Temperature	Thermometer
2.	pH	pH Meter (Eutech)
3.	TA	H ₂ SO ₄ titration
4.	TH	EDTA titration
5.	Conductivity	Conductometer (Eutech)





Saloni Kamboj et al.,

6.	Total Dissolved Solids	Filtration and evaporation
7.	Na ⁺ , K ⁺	Flame Photometer (Systronics)
8.	F ⁻ , Cl ⁻ , SO ₄ ²⁻ , NO ₃ ⁻ , PO ₄ ²⁻	Ion-Chromatography (Metrohm)
9.	Ni, Pb, Se, Cu, Mn	ICP-AES (Shimadzu)

Table 3: Results of physico-chemical analysis of drinking water samples collected from different sites.

S. No.	Water Quality Parameter	S1	S2	S3	S4	BIS Standard values (Acceptable-Permissible)	WHO Standards	Present Study Results (Min.-Max.)
1	Temp. (°C)	23	25	24	25	***	***	23-25
2	pH	7.32	8.05	8	7.5	6.5-8.5	6.5-8.5	7.3-8.1
4	TA	225.7	73.7	42.7	54.9	200-600	200	42.7-225.7
5	TDS	531.2	326.4	339.2	371.2	500-2000	**	326.4-531.2
6	TH	564	744	768	840	200-600	500	564-840
7	Ca-H	340	240	140	180	75-200	75	140-340
8	Mg-H	224	504	628	660	30-100	50	224-660
9	HCO ₃ ⁻	225.7	73.7	42.7	54.9	***	***	42.7-225.7
10	CO ₃ ⁻	N.D.	N.D.	N.D.	N.D.	***	***	N.D.
11	Na ⁺	102.2	100.2	89.2	67.7	***	***	67.7-102.2
12	K ⁺	54.9	80	25.1	54.9	***	***	25.1-80
13	Cl ⁻	7.582	2.1	3.127	18.08	250-1000	200-300	2.1-18.08
14	F ⁻	0.559	0.55	0.67	0.324	1-1.5	1.5	0.324-0.67
15	NO ₃ ⁻	34.03	2.005	0.029	7.402	45-NR	50	0.029-34.027
16	SO ₄ ²⁻	18.05	8.186	8.367	15.01	200-400	***	8.19-18.05
17	PO ₄ ²⁻	0.07	0.032	N.D.	0.027	***	***	N.D.-0.032
18	Ni*	0.573	1.12	1.13	1.35	0.02-NR	0.07	0.57-1.35
19	Pb*	0.049	0.126	0.018	0.027	0.01-NR	0.01	0.01-0.05
20	Se**	0.18	0.035	0.026	0.03	0.01-NR	0.01	0.03-0.18
21	Mn**	0.572	N.D.	N.D.	N.D.	0.1-0.3	0.4	N.D.-0.57
22	Cu**	N.D.	N.D.	N.D.	N.D.	0.05-1.5	2.0	N.D.-N.D.

*Toxic Elements; **Elements undesirable in excessive amount, ***Standards not set, N.D.: not detected, NR: No relaxation

Table 4: The quantitative analysis of some elements in drinking water samples collected from different sites.

S.NO.	PARAMETERS	% of values exceeding the BIS standards (Std values in mgL ⁻¹)	% of values exceeding the WHO standards (Std values in mgL ⁻¹)
1	Ni*	100% (0.02)	100% (0.07)





Saloni Kamboj et al.,

2	Pb*	100% (0.01)	100% (0.01)
3	Se**	100% (0.01)	100% (0.01)
4	Mn**	25% (0.1)	25% (0.4)
5	Cu**	0% (0.05)	0% (2.0)

*Toxic Elements; **Elements undesirable in excessive amount

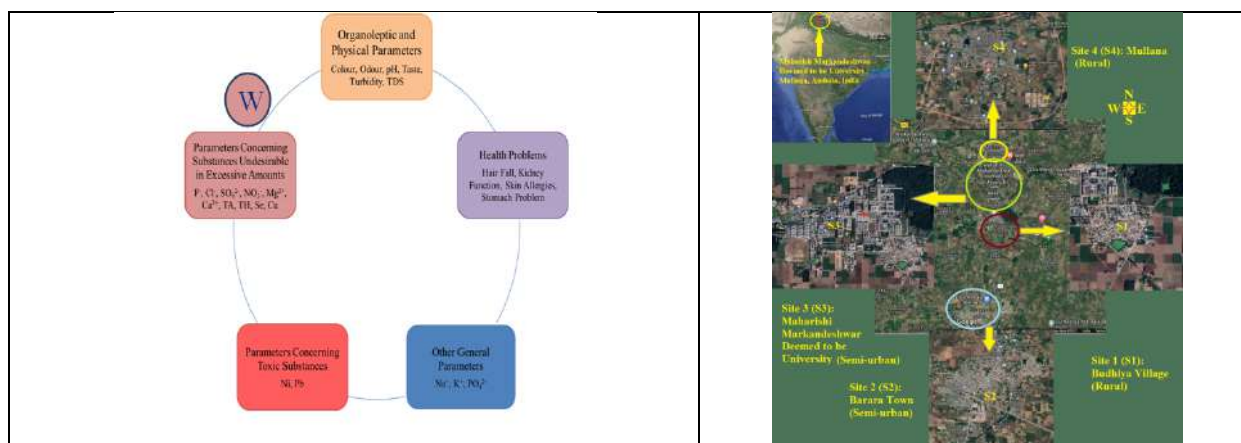


Figure 1: Water quality parameters analyzed in collected water samples and observed health issues in the study area

Figure 2: The location and the magnified google images of different sampling sites in and around MMDU, Mullana, India

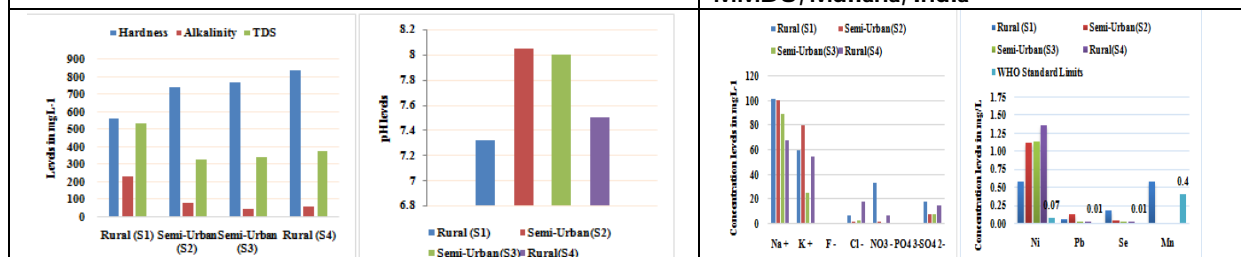


Figure 3: Variation in the levels of total hardness, total alkalinity, total dissolved solids (a) and pH levels (b) at semi-urban and rural locations

Figure 4: Variations in the levels of ionic (a) and elemental concentrations at semi-urban and rural locations (b).

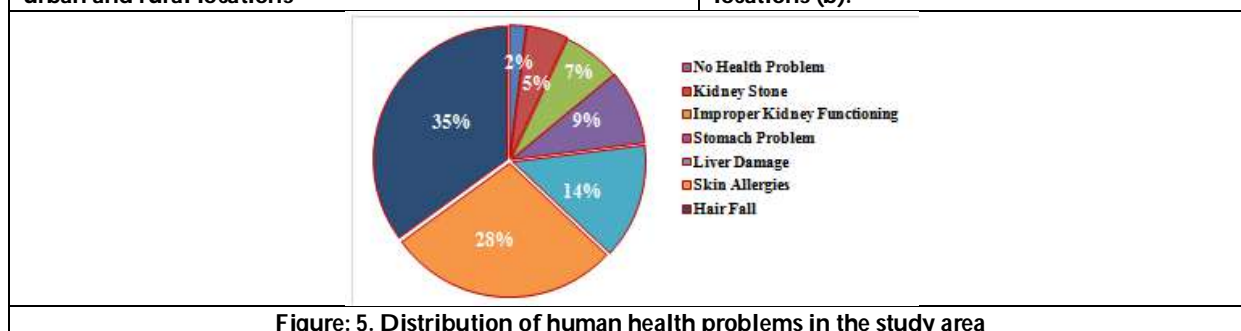


Figure 5: Distribution of human health problems in the study area





Properties of the Adjacency Matrix of Generalized total Graph of finite fields

M.Balamurugan¹, M.Sankaranarayanan^{2*} and D.A.Pandi Rani³

¹Head and Assistant professor, Department of Mathematics, K.R. College of Arts and Science, Kovilpatti, (Affiliated to Manonmaniam Sundaranar University, Abishekapatti, Tirunelveli) Tamil Nadu, India.

²Research Scholar, Department of Mathematics, G.Venkataswamy Naidu College, Kovilpatti, (Affiliated to Manonmaniam Sundaranar University, Abishekapatti, Tirunelveli) Tamil Nadu, India.

³Associate professor, Department of Mathematics, G.Venkataswamy Naidu College, Kovilpatti, (Affiliated to Manonmaniam Sundaranar University, Abishekapatti, Tirunelveli) Tamil Nadu, India.

Received: 05 Jan 2024

Revised: 19 Feb 2024

Accepted: 26 Apr 2024

*Address for Correspondence

M.Sankaranarayanan

Research Scholar,

Department of Mathematics,

G.Venkataswamy Naidu College, Kovilpatti,

(Affiliated to Manonmaniam Sundaranar University, Abishekapatti, Tirunelveli)

Tamil Nadu, India.

Email: kmsankar89@gmail.com



This is an Open Access Journal / article distributed under the terms of the **Creative Commons Attribution License** (CC BY-NC-ND 3.0) which permits unrestricted use, distribution, and reproduction in any medium, provided the original work is properly cited. All rights reserved.

ABSTRACT

Consider R to be a commutative ring with identity, $Z(R)$ be the set of zero divisors of R , and H to be a nonempty proper multiplicative prime subset of R . The generalized total graph of R is the graph (simple) $GT_H(R)$ with vertex set R , and x and y are two different vertices are said to be adjacent if and only if $x + y \in R$. we take R as the field F and the multiplicative prime subset $H = \{0\}$, designate the graph as the generalized total of field F , and denote $GT(F)$. In this article, We investigate the properties of the adjacency matrix of a generalized total graph, such as the Eigenvalues, characteristic polynomial, minimal polynomial, Spectrum and energy of the adjacency matrix of $GT(F)$.

Keywords: Adjacency matrix, eigen values, Spectrum, Generalized total graph

MSC 2010 Classifications: Primary 05C25, 05C75, ; Secondary: 13A15, 13M05

INTRODUCTION

Consider R to be a commutative ring with identity, and $Z(R)$ is its zero-divisor sets of the Ring. In 2013, Anderson and Badawi[3] introduced the generalized total graph of a commutative ring R . Let H of R be a nonempty proper subset of R ; this R is said to be a multiplicative prime subset of R if it satisfies the following two conditions: (i) $ab \in H$





Balamurugan et al.,

H for all $a \in H$ and $b \in R$; (ii) if $ab \in H$ for $a, b \in R$, then either $a \in H$ or $b \in H$. For a multiplicative prime subset H of R , the *generalized total graph* $GT_H(R)$ is the simple undirected graph with vertex set R and x, y are two different vertices are adjacent if and only if $x + y \in H$. The entire literature regarding graphs from rings can be found in the monograph [2]. If there exists a path between any two different vertices of G , it is called a connected graph. For any vertex $v_i \in V(G)$, $\deg(v_i)$ denotes the degree of v_i . For any graph G , maximum degree of vertices is denoted as $\delta(G)$ and maximum degree of vertices is denoted as $\Delta(G)$. In this article, F denotes a finite field. $|F|$ is its cardinality, and $F, \{0\}$ is the only prime ideal in this field. When R is the field F and $H = \{0\}$, the generalized total graph of the field F is denoted as $GT(F)$. This paper investigates several properties of the adjacency matrix of the generalized total graph $GT(F)$. In particular, we study the characteristic equation and eigenvalues of the adjacency matrix of $GT(F)$. Next, we provide some properties of the adjacency matrix for $GT(F)$. More specifically, we determine the Spectrum, rank, index, nature, quadratic form and energy of the adjacency matrix of $GT(F)$.

ADJACENCY MATRIX OF $GT(F)$ AND ITS PROPERTIES

Recall that the adjacency matrix of graph G is the $n \times n$ matrix $A(G)$, over the complex field, whose entries are given by $a_{ij} = \begin{cases} 1 & \text{if } v_i \text{ and } v_j \text{ are adjacent} \\ 0 & \text{otherwise} \end{cases}$.

Lemma 2.1. Let $GT(F)$ be the generalized total graph $GT(F)$ and $A(F)$ be its Adjacency matrix. Then the $(i, j)^{\text{th}}$ entry of $A(F)$ is defined as $a_{ij} = \begin{cases} 1 & \text{if } v_i + v_j = 0 \\ 0 & \text{otherwise} \end{cases}$.

Lemma 2.2. Let $A(F)$ be the Adjacency matrix of $GT(F)$, we can observe

- (i) If Characteristic $(F) = 2$, then $A(F)$ is a zero matrix of order $|F| \times |F|$,
- (ii) If Characteristic $(F) > 2$, then each $(i, j)^{\text{th}}$ entry of $A(F)$ is defined by

$$a_{ij} = \begin{cases} 1 & \text{if either } j = i + 1, i \in \{2, 4 \dots |F| - 1\} \text{ or } \\ & j = i - 1, i \in \{3, 5 \dots |F|\} \\ 0 & \text{otherwise} \end{cases}$$

Proof. (i) If Characteristic $(F) = 2$, then $x + x = 2x = 0$ for all elements $x \in F$. Therefore, each element of F is self-inverse. Hence, all the vertices of $GT(F)$ are isolated, so $A(F)$ is a zero matrix.

(ii) When Characteristic $(F) > 2$, List all the member of F as $\{0, x_1, -x_1, x_2, -x_2, \dots, x_k, -x_k, \dots, x_{\frac{|F|-1}{2}}, -x_{\frac{|F|-1}{2}}\}$ each $-x_k$ is the inverse of x_k for $1 \leq k \leq \frac{|F|-1}{2}$, which implies

$GT(F) = \langle 0 \rangle \cup \bigcup_{k=1}^{\frac{|F|-1}{2}} \langle x_k, -x_k \rangle$. To find the adjacency matrix of $GT(F)$, relabel the elements F as $\{v_1, v_2, \dots, v_{|F|}\}$ in such a way that $v_1 = 0, v_2 = x_1, v_3 = -x_1, \dots, v_{|F|-1} = x_{\frac{|F|-1}{2}}, v_{|F|} = -x_{\frac{|F|-1}{2}}$. Consider that the relabeled elements of F head each row and column of $A(F)$. For $1 \leq i \leq |F|$ & $1 \leq j \leq |F|$, the $(i, j)^{\text{th}}$ entries of $A(F)$ is defined from $GT(F)$ as follows

$$a_{ij} = \begin{cases} 1 & \text{if } v_i + v_j = 0 \in F \\ 0 & \text{otherwise} \end{cases}. \text{Implies } a_{ij} = \begin{cases} 1 & \text{if } v_i + v_{i+1} = 0 \in F \text{ and } i \in \{2, 4, 6 \dots |F| - 1\} \\ & 1 \text{ if } v_i + v_{i-1} = 0 \in F \text{ and } i \in \{3, 5, 7 \dots |F|\} \\ 0 & \text{otherwise} \end{cases}$$

From this, we observe that

$$a_{ij} = \begin{cases} 1 & \text{if either } j = i + 1, i \in \{2, 4 \dots |F| - 1\} \text{ or } j = i - 1, i \in \{3, 5 \dots |F|\} \\ 0 & \text{otherwise} \end{cases}$$

Corollary 2.3.

Let $A(F)$ be the Adjacency matrix of $GT(F)$, we can observe that

(i) Minimum degree = minimum row sum of $A(F) = \delta(A(F)) = 0$ and

Maximum degree = maximum row sum of $A(F) = \Delta(A(F)) = \begin{cases} 0, & \text{if characteristic } (F) = 2 \\ 1, & \text{if characteristic } (F) > 2. \end{cases}$

(ii) Number of isolated vertices = 1.

Proof. From the above lemma, if Characteristic $(F) = 2$, then it is a zero matrix.

so $\delta(A(F)) = \Delta(A(F)) = 0$.





If Characteristic (F) > 2, the Minimum degree arises from the first row, with all other rows having row sum 1. This is the maximum row sum.

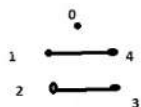
Example 2.4.

We can observe that It leads to the adjacency matrix $A(F) = \begin{pmatrix} 0 & 0 & 0 & \dots & 0 & 0 & 0 \\ 0 & 0 & 1 & \dots & 0 & 0 & 0 \\ 0 & 1 & 0 & \dots & 0 & 0 & 0 \\ & & & \ddots & & & \\ & & & & \ddots & & \\ 0 & 0 & 0 & \dots & 0 & 0 & 1 \\ 0 & 0 & 0 & \dots & 0 & 1 & 0 \end{pmatrix}$.

Consider the field $F_4 = \frac{\mathbb{Z}_2[x]}{\langle x^2+x+1 \rangle} = \{0, 1, x, 1+x\}$; then the corresponding generalized total graph and its adjacency matrix are given by

$$A(F_4) = \begin{pmatrix} 0 & 0 & 0 & 0 \\ 0 & 0 & 0 & 0 \\ 0 & 0 & 0 & 0 \\ 0 & 0 & 0 & 0 \end{pmatrix}$$

Suppose $f = \mathbb{Z}_5$, then $GT(\mathbb{Z}_5)$ are given by $A(\mathbb{Z}_5) = \begin{pmatrix} 0 & 0 & 0 & 0 & 0 \\ 0 & 0 & 1 & 0 & 0 \\ 0 & 1 & 0 & 0 & 0 \\ 0 & 0 & 0 & 0 & 1 \\ 0 & 0 & 0 & 1 & 0 \end{pmatrix}$



Note that a matrix in which most elements are 0 is called a Sparse matrix. A Hollow matrix is a square matrix whose diagonal elements are all zero. In fact, The adjacency matrix of simple undirected graphs is the Hollow matrix. Here, the Sparsity of a matrix can be calculated as the ratio of the number of zeros to the total elements of the corresponding sparse matrix. A lot of applications in data science and machine learning involve sparse matrices. From this, we observe the following.

Theorem 2.5. If Characteristic (F) > 2, then $A(F)$ is a sparse matrix and a Hollow matrix. Its Sparsity is $\frac{2|F|^2 - |F| + 1}{2|F|}$.

Proof. By Lemma 2.2 (ii), the result is obvious. $\text{Sparsity} = \frac{\text{number of zeros}}{\text{Total elements}} = \frac{1 - \frac{|F|-1}{2}}{|F|^2} = \frac{2|F|^2 - |F| + 1}{2|F|}$

Remark that If Characteristic (F) = 2, the Sparsity is 1.

Theorem 2.6. Let $A(F)$ be the adjacency matrix of generalized total graph F. Then the following are valid.

(i) $A(F)$ is always a real symmetric matrix. (ii) $\text{Tr}(A(F)) = 0$. (iii) $|A(F)| = 0$.

(iv) At least one Eigenvalue of $A(F)$ is 0.

Proof. (i) is obvious

(ii) Since $GT(F)$ does not allow self-loops and so $a_{ii} = 0$ for all $1 \leq i \leq |F|$ in $A(F)$. Hence all the diagonal elements are 0. Therefore $\text{Tr}(A(F)) = 0$.

(iii) Since 0 is the isolated vertex in $GT(F)$, the row and column headed by 0 contains only 0. Therefore $|A(F)| = 0$.

(iv) By (iii) $|A(F)| = 0$, and so at least one of the Eigenvalues of $A(F)$ must be 0.

Theorem 2.7. If Characteristic (F) > 2, then $A(F)$ is a block diagonal matrix with blocks $(0), \begin{pmatrix} 0 & 1 \\ 1 & 0 \end{pmatrix}, \begin{pmatrix} 0 & 1 \\ 1 & 0 \end{pmatrix}, \dots, \begin{pmatrix} 0 & 1 \\ 1 & 0 \end{pmatrix}$ $\frac{|F|-1}{2}$ blocks





Balamurugan et al.,

Proof. By lemma 2.2(ii) we have $A(F) =$

$$\begin{pmatrix} 0 & 0 & 0 & \dots & 0 & 0 & 0 \\ 0 & 0 & 1 & \dots & 0 & 0 & 0 \\ 0 & 1 & 0 & \dots & 0 & 0 & 0 \\ \vdots & \vdots & \vdots & \ddots & \vdots & \vdots & \vdots \\ 0 & 0 & 0 & \dots & 0 & 0 & 1 \\ 0 & 0 & 0 & \dots & 0 & 1 & 0 \end{pmatrix}$$

From this, we observe that the blocks of $A(F)$ are $\underbrace{\begin{pmatrix} 0 & 1 \\ 1 & 0 \end{pmatrix}, \begin{pmatrix} 0 & 1 \\ 1 & 0 \end{pmatrix}, \dots, \begin{pmatrix} 0 & 1 \\ 1 & 0 \end{pmatrix}}_{\frac{|F|-1}{2} \text{ blocks}}, (0)$.

Note that The characteristic polynomial of $A(F)$ is defined as $|\lambda I - A(F)|$ and the characteristic equation of $A(F)$ to be $|\lambda I - A(F)| = 0$. Which yields the following

Lemma 2.8. Let $GT(F)$ be the generalized total graph F , $f(\lambda)$ be the characteristic polynomial and $p(\lambda)$ be the minimal polynomial of $A(F)$, then the following are holds.

- (i) If Characteristic $(F)=2$, then the characteristics equation of $A(F)$ is $\lambda^{|F|} = 0$ and its minimal polynomial is $p(\lambda) = \lambda$
(ii) If Characteristic $(F) > 2$, then the characteristics equation of $A(F)$ is given by $\lambda(\lambda^2 - 1)^{\frac{|F|-1}{2}} = 0$ and its minimal polynomial is $p(\lambda) = \lambda(\lambda^2 - 1)$.

Proof. (i) When Characteristic $(F) = 2$, the characteristic equation of $A(F)$ is given by

$$|\lambda I - A(F)| = 0.$$

$$\Rightarrow \begin{vmatrix} \lambda & 0 & 0 & \dots & 0 & 0 & 0 \\ 0 & \lambda & 0 & \dots & 0 & 0 & 0 \\ 0 & 0 & \lambda & \dots & 0 & 0 & 0 \\ \vdots & \vdots & \vdots & \ddots & \vdots & \vdots & \vdots \\ 0 & 0 & 0 & \dots & \lambda & 0 & 0 \\ 0 & 0 & 0 & \dots & 0 & \lambda & 0 \end{vmatrix} = 0 \Rightarrow \lambda^{|F|} = 0. \text{ The possibilities of minimal polynomial is } p(\lambda) = \lambda, \lambda^2, \lambda^3 \dots \lambda^{|F|}.$$

- (iii) When Characteristic $(F) = 2$, the characteristic equation of $A(F)$ is given by $|\lambda I - A(F)| = 0$.

$$\Rightarrow \begin{vmatrix} \lambda & 0 & 0 & \dots & 0 & 0 & 0 \\ 0 & \lambda & 1 & \dots & 0 & 0 & 0 \\ 0 & 1 & \lambda & \dots & 0 & 0 & 0 \\ \vdots & \vdots & \vdots & \ddots & \vdots & \vdots & \vdots \\ 0 & 0 & 0 & \dots & 0 & \lambda & 1 \\ 0 & 0 & 0 & \dots & 0 & 1 & \lambda \end{vmatrix} = 0 \Rightarrow \lambda \frac{(\lambda^2 - 1) \times (\lambda^2 - 1) \dots (\lambda^2 - 1)}{\frac{|F|-1}{2} \text{ times}} = 0 \Rightarrow \lambda(\lambda^2 - 1)^{\frac{|F|-1}{2}} = 0.$$

Recall the Binomial Expansion $(a - b)^n = \binom{n}{0}a^n + \binom{n}{1}a^{n-1}b + \binom{n}{2}a^{n-2}b^2 + \dots + \binom{n}{n}b^n$.

Theorem 2.9. Let $f(\lambda)$ be the characteristic polynomial of $A(F)$. If Characteristic $(F) > 2$, then we have the following observation in $f(\lambda)$.

- (i) The coefficient of λ^{2k} is 0 for all $k = 0, 1, 2, 3, \dots, \frac{|F|-1}{2}$.
(ii) The coefficient of λ^{2k+1} is $1, -\binom{|F|-1}{2}, \binom{|F|-1}{2}, \dots, 1$ for all $k = 0, 1, 2, 3, \dots, \frac{|F|-1}{2}$.

Proof. By the Binomial expansion, we have

$$(\lambda^2 - 1)^{\frac{|F|-1}{2}} = \binom{\frac{|F|-1}{2}}{0}(\lambda^2)^{\frac{|F|-1}{2}} + \binom{\frac{|F|-1}{2}}{1}(\lambda^2)^{\frac{|F|-1}{2}-1}(-1) + \binom{\frac{|F|-1}{2}}{2}(\lambda^2)^{\frac{|F|-1}{2}-2}(-1)^2 + \dots + \binom{\frac{|F|-1}{2}}{\frac{|F|-1}{2}}(-1)^{\frac{|F|-1}{2}}.$$

$$\text{Therefore } (\lambda^2 - 1)^{|F|-1} = \lambda^{|F|-1} - (|F|-1)\lambda^{|F|-3} + \binom{|F|-1}{2}\lambda^{|F|-5} + \dots + 1.$$

$$\text{Now, } \lambda \times (\lambda^2 - 1)^{|F|-1} = \lambda^{|F|} - (|F|-1)\lambda^{|F|-2} + \binom{|F|-1}{2}\lambda^{|F|-4} + \dots + \lambda.$$





Balamurugan et al.,

Clearly, all the even powers of λ are 0. That is, The coefficient of λ^{2k} is 0 respectively for

$k = 0, 1, 2, 3, \dots, \frac{|F|-1}{2}$ and all the coefficients of odd power of λ are $1, -\left(\frac{|F|-1}{2}\right), \left(\frac{|F|-1}{2}\right), \dots, 1$ respectively for $k=0, 1, 2, 3, \dots, \frac{|F|-1}{2}$.

Proposition 2.10. ([8], proposition 2.3) Let $A(\Gamma)$ be the adjacency matrix of a simple graph Γ . Let us suppose that $\chi(\Gamma, \lambda) = \lambda^n + c_1\lambda^{n-1} + c_2\lambda^{n-2} + \dots + c_n$, where the coefficients c_i denote the sums of principal minors of A . Then, the following are true. (i) $c_1 = 0$ (ii) $-c_2$ is the number of edges of the graph (iii) $-c_3$ is twice the number of triangles in the graph. This proposition leads to the following lemma.

Theorem 2.11. Let us suppose that $f(\lambda) = \lambda^{|F|} + c_1\lambda^{|F|-1} + c_2\lambda^{|F|-2} + \dots + c_n$ is the characteristic polynomial for $A(F)$. Then, the following is true.

(i) $c_1 = 0$ (ii) the number of edges of $GT(F)$ is $-c_2 = \begin{cases} 0 & \text{if characteristic}(F) = 2 \\ \frac{|F|-1}{2} & \text{if characteristic}(F) > 2 \end{cases}$

(iii) twice the number of triangles in the graph $GT(F)$ is $-c_3 = 0$.

Proof. (i) Consider Characteristic $(F) = 2$, then by Lemma 2.9(i) $f(\lambda) = \lambda^{|F|}$.

Therefore $c_1, c_2, c_3 = 0$

Suppose Characteristic $(F) > 2$, then by Lemma 2.9(ii)

$$f(\lambda) = \lambda^{|F|} - (|F| - 1)\lambda^{|F|-2} + \left(\frac{|F|-1}{2}\right)\lambda^{|F|-4} + \dots + \lambda.$$

From this, we observe that $c_1 = 0, -c_2 = \frac{|F|-1}{2} =$ number of edges in the graph $GT(F)$ and $-c_3$ is twice the number of triangles in the graph $GT(F) = 0$. We recall that the root of the characteristic equation $|\lambda I - A| = 0$ is called the Eigenvalue of A . From this definition, one can easily determine all the Eigen values of $A(F)$.

Theorem 2.12. Let $\lambda_1, \lambda_2, \dots, \lambda_{|F|}$ be the Eigen values of $A(F)$, Then (i) If Characteristic $(F) = 2$, then the distinct Eigenvalue of $A(F)$ is 0.

(ii) If Characteristic $(F) > 2$, then the distinct Eigen value of $A(F)$ is 0, 1, -1.

Proof. (i) When Characteristic $(F) = 2$, then the characteristics equation of $A(F)$ is given by $\lambda^{|F|} = 0$. Solving this equation, we get $\lambda = \frac{0, 0, \dots, 0}{|F| \text{ times}}$. Hence, $\lambda = 0$ is the only Eigenvalue.

(ii) When Characteristic $(F) > 2$, then the characteristics equation of $A(F)$ is given by $\lambda(\lambda^2 - 1)^{\frac{|F|-1}{2}} = 0$. Solving this equation we get $\lambda = 0, \frac{1, 1, \dots, 1}{\frac{|F|-1}{2} \text{ times}}, \frac{-1, -1, \dots, -1}{\frac{|F|-1}{2} \text{ times}}$. Hence, the distinct Eigenvalue of $A(F)$ is 0, 1, -1, 0, 1, -1.

We recall that the definition of the Spectrum of a graph G is the set of Eigenvalues of Adjacency matrix, together with the multiplicities of the Eigenvalues of the adjacency matrix. If the distinct Eigenvalues of $A(G)$ are $\lambda_0 > \lambda_1 > \dots > \lambda_k$, and their multiplicities are $m(\lambda_0), m(\lambda_1), \dots, m(\lambda_k)$, then we shall write the Spectrum of the graph G by $\text{Spec}(G) = \begin{pmatrix} \lambda_0 \lambda_1 \dots \lambda_k \\ m(\lambda_0) m(\lambda_1) \dots m(\lambda_k) \end{pmatrix}$. With the help of this definition, we can derive the spec $(GT(F))$ as follows.

Theorem 2.13. Let $A(F)$ be its adjacency matrix of the generalized total graph. Then

$$\text{Spec}(G) = \begin{cases} \begin{pmatrix} 0 \\ |F| \end{pmatrix} & \text{if characteristic}(F) = 2 \\ \begin{pmatrix} 1 & 0 & -1 \\ \frac{|F|-1}{2} & 1 & \frac{|F|-1}{2} \end{pmatrix} & \text{if characteristic}(F) > 2 \end{cases}$$

Proof. The proof is trivial from the definition of Spectrum and the proof of theorem 2.12.

Note that the rank of a matrix is the number of non-zero Eigenvalues. The rank of A is denoted by r . The index of a matrix is the number of positive Eigenvalues of the matrix A , and it is denoted by p . The signature of the matrix is $2p-r$.

Lemma 2.14. Let $A(F)$ be its adjacency matrix of the generalized total graph, then the following are true.





Balamurugan et al.,

- (i) The rank of $A(F)$ is given by $r = \begin{cases} 0 & \text{if characteristic } (F) = 2 \\ |F| - 1 & \text{if characteristic } (F) > 2 \end{cases}$
- (ii) The index of $A(F)$ is given by $p = \begin{cases} 0 & \text{if characteristic } (F) = 2 \\ (|F| - 1)/2 & \text{if characteristic } (F) > 2 \end{cases}$

Proof. (i) consider Characteristic $(F) = 2$, then by lemma 3.10 $r = 0$ and $p = 0$.

(ii) suppose that Characteristic $(F) > 2$, Then the non-zero Eigenvalues of $A(F)$ are $\frac{1, 1, \dots, 1}{\frac{|F|-1}{2} \text{ times}}, \frac{-1, -1, \dots, -1}{\frac{|F|-1}{2} \text{ times}}$. Hence, the number of non-zero Eigenvalues of $A(F)$ is $r = \frac{|F|-1}{2} + \frac{|F|-1}{2} = |F| - 1$, and the index of $A(F)$ is $p = \frac{|F|-1}{2}$.

Note that, a quadratic form, is a homogeneous polynomial of the second degree in any number of variables of a

matrix A . For example, $A = \begin{pmatrix} a & f & g \\ f & b & h \\ g & h & c \end{pmatrix}$, $X = (x \ y \ z)$ and $X^T = \begin{pmatrix} x \\ y \\ z \end{pmatrix}$, then $XX^T = ax^2 + by^2 + cz^2 + 2fxy + 2gzx +$

$2hzy$ which is a corresponding Quadratic form of A , λ_i are Eigenvalues. Here $i=1,2,3$.

The real quadratic form XX^T is called Positive definite if all $\lambda_i > 0$,

Negative definite if $\lambda_i < 0$.

Positive semi-definite if all $\lambda_i \geq 0$ and atleast one $\lambda = 0$, Negative semi definite if all $\lambda_i \leq 0$ and atleast one $\lambda = 0$. It is indefinite if some of the λ_i are positive and others negative. This definition leads to the following result.

Lemma 2.15. Let $A(F)$ be its adjacency matrix of the generalized total graph. Let q be the quadratic form of $A(F)$. Then

$$q = \begin{cases} 0 & \text{if characteristic } (F) = 2 \\ 2(x_2x_3 + x_4x_5 + \dots + x_{|F|-1}x_{|F|}) & \text{if characteristic } (F) > 2 \end{cases}$$

Proof. If Characteristic $(F) = 2$, then $q = (x_1x_2x_3 \dots x_{|F|}) \begin{pmatrix} 0 & 0 & 0 & \dots & 0 & 0 \\ 0 & 0 & 0 & \dots & 0 & 0 \\ \vdots & \vdots & \vdots & \ddots & \vdots & \vdots \\ 0 & 0 & 0 & \dots & 0 & 0 \end{pmatrix} \begin{pmatrix} x_1 \\ x_2 \\ \vdots \\ x_{|F|} \end{pmatrix} = 0$

If Characteristic $(F) > 2$, then $q = (x_1x_2x_3 \dots x_{|F|-1}x_{|F|}) \begin{pmatrix} 0 & 0 & 0 & \dots & 0 & 0 \\ 0 & 0 & 1 & \dots & 0 & 0 \\ 0 & 1 & 0 & \dots & 0 & 0 \\ \vdots & \vdots & \vdots & \ddots & \vdots & \vdots \\ 0 & 0 & 0 & \dots & 0 & 1 \\ 0 & 0 & 0 & \dots & 1 & 0 \end{pmatrix} \begin{pmatrix} x_1 \\ x_2 \\ \vdots \\ x_{|F|-1} \\ x_{|F|} \end{pmatrix}$

$$= 2(x_2x_3 + x_4x_5 + \dots + x_{|F|-1}x_{|F|})$$

Lemma 2.16. Let $A(F)$ be its adjacency matrix of the generalized total graph. Let q be the quadratic form of $A(F)$, we can observe

- (i) If Characteristic $(F) = 2$, then q is positive semi-definite as well as negative semi-definite.
- (ii) If Characteristic $(F) > 2$, then q is indefinite.

Proof. When Characteristic $(F) = 2$, 0 is the only Eigenvalue of $A(F)$. In this case, q is positive semi-definite as well as negative semi-definite. When Characteristic $(F) > 2$, then 0, 1 and -1 are the Eigenvalue of $A(F)$. In this case, q is indefinite.

In this view of the following definition, one can determine the energy of a simple graph G from its adjacency matrix A . consider $A(G)$ as the adjacency matrix of a graph G and let $\lambda_1, \lambda_2, \dots, \lambda_n$ Eigenvalue of A . Then, the Energy of the graph G is $En(G) = \sum_{i=1}^n |\lambda_i|$.

Lemma 2.17. Let $GT(F)$ be the generalized total graph F , and $A(F)$ be its adjacency matrix. Then the energy of the graph $GH(F)$ is given by $En(GT(F)) = \begin{cases} 0, & \text{if characteristic } (F) = 2 \\ |F| - 1, & \text{if characteristic } (F) > 2 \end{cases}$

Proof. By the definition of $E(G)$ and by the lemma 3.9





Balamurugan et al.,

$$E(GT(F)) = \begin{cases} |0| + |0| + \dots + |0|, & \text{if characteristic } (F) = 2 \\ \frac{|1|+|1|+\dots+|1|}{\frac{|F|-1}{2} \text{ times}} + 0 + \frac{|-1|+|-1|+\dots+|-1|}{\frac{|F|-1}{2} \text{ times}}, & \text{if characteristic } (F) > 2 \end{cases}$$

Hence $E(GT(F)) = \begin{cases} 0, & \text{if char } F = 2 \\ |F| - 1, & \text{if char } F > 2 \end{cases}$

CONCLUSION

In this paper we discussed some theoretical properties of adjacency matrix of the generalized total graphs. This view may give another approach to seeing the properties of graphs using an adjacency matrix.

REFERENCES

1. S. Akbari, D. Kiani, F. Mohammadi and S. Moradi, The total graph and regular graph of a commutative ring, J. Pure Appl. Algebra, **213**, 2224--2228 (2009).
2. D.F. Anderson, T. Asir, A. Badawi and T. Tamizh Chelvam, Graphs from rings, First ed., Springer Nature Switzerland AG 2021.
3. D. F. Anderson and A. Badawi, The generalized total graph of a commutative ring, J. Algebra Appl. **12**, (2013) (18 pages), doi:10.1142/S021949881250212X.
4. D. F. Anderson and A. Badawi, The total graph of a commutative ring, J. Algebra **320**, 2706--2719 (2008).
5. D. F. Anderson and P.S. Livingston, The zero-divisor graph of a commutative ring, J. Algebra, **217**, 434--447 (1999).
6. T. Asir and T. Tamizh Chelvam, On the total graph and its complement of a commutative ring, Comm. Algebra, **41**, 3820--3835 (2013), doi:10.1080/00927872.2012.678956.
7. J.A. Bondy and U.S.R. Murty (2008), Graph theory, Springer.
8. Norman Biggs (1974), Algebraic Graph theory, Cambridge University Press.
9. I. Kaplansky, Commutative Rings, (Revised Edn), Univ. Chicago Press, Chicago (1974).
10. T. Tamizh Chelvam, S. Anukumar Kathirvel, it Generalized unit and unitary Cayley graphs of finite rings, J. Algebra Appl., **18(1)**, (2019), 950006 [21 pages].
11. T. Tamizh Chelvam, S. Anukumar Kathirvel, it Note on generalized Cayley graph of finite rings and its complement, J. Anal., **27(2)**, (2019), 555--566.
12. T. Tamizh Chelvam, S. Anukumar Kathirvel, M. Balamurugan, it Intersection graph of gamma sets in the generalized unit and unitary Cayley graphs, Houston J. Math., **46(3)** (2020), 561--582.
13. T. Tamizh Chelvam, S. Anukumar Kathirvel, M. Balamurugan, it Domination in the generalized unit and unitary Cayley graphs of finite rings, Indian J. Pure Appl. Math., **51(2)**, (2020), 533--556.
14. T. Tamizh Chelvam and M. Balamurugan, On the generalized total graph of fields and its complement, Palestine J. Math. **7(2)**, 450--457 (2018).
15. T. Tamizh Chelvam and M. Balamurugan, Complement of the generalized total graph of commutative rings, J. Anal, DOI.10.1007/s41478-018-0093-6.
16. T. Tamizh Chelvam and M. Balamurugan, Complement of the generalized total graph of Z_n , FILOMAT, **33:18** 6103 -- 6113 (2019), <https://doi.org/10.2298/FIL1918103T>.
17. T. Tamizh Chelvam and M. Balamurugan, Complement of the generalized total graph of fields, AKCE Int. J. Graphs Comb., <https://doi.org/10.1016/j.akcej.2019.12.005>.





A Study on Effects of the Work Environment Influencing Organisational Citizenship Behaviour During Covid-19 Pandemic among IT Employees in Tamil Nadu

T Sunitha^{1*} and Anitha U²

¹Assistant Professor, Department of Business Administration, PS.PT. MGR Government Arts and Science College, Nagapattinam, (Affiliated to Annamalai University), Tamil Nadu, India.

²Ph.D Research Scholar, Department of Business Administration, Annamalai University, Annamalai Nagar, Tamil Nadu, India.

Received: 22 Jan 2024

Revised: 09 Feb 2024

Accepted: 06 May 2024

*Address for Correspondence

T Sunitha

Assistant Professor,
Department of Business Administration,
PS.PT. MGR Government Arts and Science College,
Nagapattinam, (Affiliated to Annamalai University),
Tamil Nadu, India.
Email: sunitha.au@gmail.com



This is an Open Access Journal / article distributed under the terms of the **Creative Commons Attribution License** (CC BY-NC-ND 3.0) which permits unrestricted use, distribution, and reproduction in any medium, provided the original work is properly cited. All rights reserved.

ABSTRACT

The COVID-19 pandemic has triggered profound changes in the way organizations operate, with a significant impact on the work environment and employee behavior. This research paper examines the effects of the work environment on Organizational Citizenship Behavior (OCB) among IT employees in Tamil Nadu, India, during the COVID-19 pandemic. OCB, encompassing discretionary actions that contribute positively to the organization, plays a crucial role in organizational success. The study's focus is on investigating the altered work environment's influence on IT employees' engagement in OCB. By conducting a quantitative analysis, this research delves into the relationship between the work environment and various facets of OCB. A cross-sectional survey was administered to IT employees, collecting data on work environment and OCB dimensions. The findings of the study shed light on the complex interplay between the pandemic-induced work environment changes and OCB engagement. The analysis reveals noteworthy insights into how remote work have had an effect on IT employees' willingness to engage in OCB. The study also underscores the importance of supportive work environments in fostering positive employee behaviors, even in the face of unprecedented challenges. This research contributes to the existing literature by empirically highlighting the effects of the altered work environment on OCB during the COVID-19 pandemic. The findings underscore the significance of



**Sunitha and Anitha**

crafting strategies that mitigate the negative impact of the pandemic-induced work environment changes, thereby enhancing OCB and promoting organizational resilience.

Keywords: OCB, IT employees, work environment, employee behavior

INTRODUCTION

In the wake of the unprecedented COVID-19 pandemic, organizations across the globe have undergone significant transformations in their operations, strategies, and workforce management practices. This pandemic has brought about a paradigm shift in the way work is conducted, particularly within the Information Technology (IT) sector, where remote work and virtual collaboration have become the new norm. The dynamic nature of the pandemic has not only posed challenges to business continuity but has also cast a spotlight on the intricate relationship between the work environment and employee behavior. Organizational Citizenship Behavior (OCB), a concept rooted in the realm of organizational psychology, has garnered considerable attention due to its profound impact on the efficiency and effectiveness of organizations. OCB encompasses discretionary actions that go beyond formal job responsibilities and contribute positively to the overall work environment and organizational climate. These behaviors, ranging from helping colleagues to engaging in innovative problem-solving, have been linked to enhanced team cohesion, reduced turnover rates, and improved organizational performance. Against this backdrop, this research embarks on a journey to delve into the intricate interplay between the work environment and OCB among IT employees in Tamil Nadu, India, during the tumultuous times of the COVID-19 pandemic. The study aims to scrutinize how the challenging work environment imposed by the pandemic has influenced IT employees' engagement in OCB, ultimately contributing to a deeper understanding of the dynamics between external stressors and employee behavior. In the subsequent sections, this paper will elucidate the theoretical underpinnings of OCB and the work environment, review relevant literature, outline the research methodology employed, present and discuss the findings, and conclude with implications for both academia and organizational practice.

RESEARCH RATIONALE

The significance of this study lies in its potential to unearth valuable insights into the adverse effects of the altered work environment on employee behavior, specifically focusing on OCB during the COVID-19 pandemic. While existing literature has extensively explored the relationship between work environment and OCB, the unprecedented circumstances brought forth by the pandemic necessitate a fresh examination. By concentrating on the IT sector, which has been at the forefront of adopting remote work practices, this study can contribute empirically grounded knowledge that may aid organizations in devising strategies to foster OCB even in times of crisis.

RESEARCH OBJECTIVES

The objectives of this research include:

1. Investigating the impact of work environment on OCB during COVID -19 Pandemic period.
2. To Identifying influence of work environment on different facets of OCB.

REVIEW OF LITERATURE

Smith, J., & Johnson, A. (2018) explored the relationship between the work environment and organizational citizenship behavior (OCB). The authors found that a positive work environment characterized by supportive management, clear communication, and opportunities for employee development significantly correlated with



**Sunitha and Anitha**

higher engagement in OCB. The findings emphasized the importance of cultivating a conducive work environment to promote desirable employee behaviors. **Brown, L., & Williams, R. (2019)** revealed that while remote work increased flexibility, it also led to reduced spontaneous interactions among employees, potentially impacting OCB engagement. The findings underscore the need for organizations to address these challenges to maintain a positive work environment and foster OCB. **Chen, Q., & Wang, Y. (2020)** investigated the mediating role of job satisfaction in the relationship between the work environment and OCB. The authors found that a positive work environment positively influenced job satisfaction, which in turn enhanced engagement in OCB. These findings highlight the importance of considering job satisfaction as a mechanism through which the work environment impacts employee behavior. **Gupta, R., & Sharma, S. (2017)** found that a supportive work environment played a crucial role in encouraging employees to engage in OCB even in challenging circumstances. The study provides insights into the relevance of work environment factors during times of uncertainty. **Lee, S., & Park, E. (2016)** found that open and transparent communication channels facilitated the exchange of help and support, leading to higher engagement in OCB. The findings emphasize the significance of effective communication as a key determinant of employee behavior. **Malhotra, D., & Kapoor, M. (2019)** examined the relationship between job insecurity and OCB within the IT industry. The research revealed that increased job insecurity was associated with decreased engagement in OCB over time. The findings suggest that addressing job insecurity and providing stability in the work environment could positively impact employee behavior. **Patel, V., & Shah, R. (2020)** investigated the role of civic virtue in promoting OCB within the work environment. Civic virtue, characterized by active participation in organizational activities, was found to significantly contribute to engagement in OCB. The findings underscore the importance of fostering a sense of belonging and participation in the workplace to encourage positive behaviors. **Ramanathan, S., & Kumar, R. (2017)** explored the relationship between work-life balance and OCB among IT professionals. The research indicated that employees who perceived a healthy work-life balance were more likely to engage in OCB. The findings suggest that maintaining a balanced work environment that respects personal time contributes to positive employee behaviors. **Yang, H., & Wu, Y. (2019)** emphasized the significance of cultivating a fair and just work environment to promote positive behaviors.

RESEARCH METHODOLOGY

The primary objective of this study was to investigate the detrimental effects of the work environment on Organizational Citizenship Behavior (OCB) among IT employees in Tamil Nadu during the COVID-19 pandemic. Descriptive research design was adopted for this study, which includes surveys and fact finding enquires with adequate interpretation. Primary data was collected using convenience sampling method with the help of google form questionnaire. A total of 390 respondents were surveyed in Tamil Nadu. The Chi-square test, One-way ANOVA test and correlation analysis were applied to identify the objective of the study.

DATA ANALYSIS

To examine the altered work environment's influence on OCB engagement, this research aimed to contribute insights into the complex interplay between external stressors and employee behavior within the unique context of a global crisis.

Altered Work Environment and OCB Engagement

The analysis of the data collected through a cross-sectional survey revealed noteworthy insights into the relationship between the work environment and OCB among IT employees. The COVID-19 pandemic has led to significant changes in the traditional work landscape, with remote work becoming a prominent practice. While remote work offers flexibility, it also presents challenges related to isolation, communication barriers, and blurred work-life boundaries. These challenges were found to influence employees' willingness to engage in OCB. The dimensions of OCB, including altruism, conscientiousness, sportsmanship, courtesy, and civic virtue, were examined in relation to specific aspects of the altered work environment. Altruism, involving voluntary assistance to colleagues, exhibited a



**Sunitha and Anitha**

decline, possibly due to the reduced opportunities for spontaneous interactions in a remote work setting. Similarly, the conscientiousness dimension, characterized by going beyond job requirements, showed variations, suggesting that the lack of face-to-face supervision might impact this behavior. From the above table the p value less than 0.001 indicates that there is a significant difference among the level of work environment of IT employees. The level of work environment of employees is not equally distributed. Based on the percentage, majority of employees belongs to moderate level (46%).

Different alphabet among different level of work environment denotes significant at 1% level using Duncan Multiple Range Test (DMRT)

The ANOVA analysis aimed to explore significant differences in Organizational Citizenship Behavior (OCB) dimensions based on different levels of the work environment among IT employees in Tamil Nadu during the COVID-19 pandemic. From the above table, the mean value 4.27 indicates that the respondents who highly favor work from home are high influence on altruism factor compared to those in a low and moderate work environment. This indicates that employees in a supportive work environment were more likely to engage in altruistic behaviors, providing voluntary assistance to colleagues. Based on Duncan Multiple Range Test (DMRT), there is a significant difference among low, medium and high level work environment at 1 percent level. The respondents in a high work environment displayed a higher mean score ($M = 4.57$) compared to those in a low work environment for conscientiousness factor. The p value indicates that there is a significant difference among level of work environment and conscientiousness factor. The mean value 3.83 indicates that the respondents in low work environment are high influence on sportsmanship factor of OCB compared to moderate and high work environment. KuldeepKaur (2021) highlighted the importance of participation and job involvement are required by the individuals to acquire the Organizational Citizen behavior. Similarly, for the OCB dimension of "courtesy" and "civic virtue", the respondents in a high work environment displayed a higher mean value compared to those in a low work environment. Based on Duncan Multiple Range Test (DMRT), there is a significant difference among level of work environment and courtesy and civic virtue factor. These findings suggest that the work environment significantly influences employees' engagement in the dimensions of OCB. In the context of the COVID-19 pandemic, the supportive or challenging work environment seems to play a role in shaping employee behavior.

Correlation analysis was used to examine the relative effects of work environment and Organizational Citizenship Behaviour factors. The result of correlation analysis is presented in the above table. 3. It is observed from the table.3 that work environment is positively correlated with altruism, conscientiousness, courtesy, and civic virtue factors, which indicates that supportive work environment in facilitating positive employee behaviors. MohamedMousa_Hiba K._Massoud_Rami M._Ayoubi (2020) found that workplace happiness positively affects employees' organizational citizenship behavior. However, the work environment is negatively correlated with the sportsmanship factor, because the reduced frequency of face-to-face interactions and the shift to virtual communication seemed to influence employees' willingness to provide voluntary assistance to colleagues leading to negative influence on Sportsmanship dimension of OCB. The p value infers that the altered work environment and OCB factors is significant at 1 percent level. Yang, H., & Wu, Y. (2019) emphasized the significance of cultivating a fair and just work environment to promote positive behaviors. The finding suggest that a supportive work environment may positively influence employees' engagement in certain dimensions of OCB, namely altruism, conscientiousness, courtesy, and civic virtue factor. While the effect on sportsmanship was not as pronounced, there is still a trend indicating the potential impact of the work environment. It's important to consider individual differences, work-related stressors, and other factors that may contribute to the observed variations in OCB engagement.

FINDINGS

The research study aimed to investigate the effects of the work environment on Organizational Citizenship Behavior (OCB) among IT employees in Tamil Nadu during the COVID-19 pandemic. The analysis of the data collected from a cross-sectional survey provided insightful findings that illuminate the complex relationship between the altered work environment and employee behavior. The study revealed that the effects of the altered work environment during the pandemic extend to the engagement in OCB among IT employees. The reduced frequency of personal



**Sunitha and Anitha**

interactions and the challenges of remote communication have potentially led to highly favor the four dimensions of OCB leaving only one dimension to be moderately favorable of OCB facets (i.e. sportsmanship). However, it is essential to recognize that the observed changes might not solely result from the remote work environment; other factors, such as absence of physical presence of peer group, job uncertainty and personal stressors induced by the pandemic, may also contribute. These findings emphasize the significance of a supportive work environment in facilitating positive employee behaviors, even in the face of external disruptions. As organizations continue to navigate the pandemic and its aftermath, strategies that address the challenges associated with remote work and promote effective communication become crucial to maintaining OCB engagement.

Impact of Remote Work environment on OCB dimensions

The findings indicated that the altered work environment, characterized by the widespread adoption of remote work due to the pandemic, had a notable impact on the dimensions of OCB. Employees experiencing a high level of remote work engagement reported significantly higher levels of altruism, Conscientiousness, civic virtue, and courtesy compared to those with limited remote work opportunities. The reduced frequency of face-to-face interactions and the shift to virtual communication seemed to influence employees' willingness to provide voluntary assistance to colleagues leading to moderate influence on Sportsmanship dimension of OCB

SUGGESTIONS

Based on the findings of this study, several actionable suggestions can be proposed for organizations aiming to create positive work environment for the altered work environment on OCB engagement during the COVID-19 pandemic:

- **Foster Virtual Interaction Platforms:** Organizations should invest in virtual platforms that facilitate spontaneous interactions among remote employees. Regular team meetings, virtual coffee breaks, and online collaboration tools can help bridge the communication gap and encourage altruistic behaviors.
- **Recognize and Reward Altruism:** Recognizing and rewarding altruistic behaviors can incentivize employees to provide voluntary assistance to their colleagues. Employee recognition programs that highlight altruism can contribute to a culture of mutual support and engagement.
- **Promote Virtual Team Building:** Organizations can design virtual team-building activities and events to foster a sense of belonging and civic virtue among remote employees. Online workshops, virtual team challenges, and collaborative projects can encourage employees to actively participate in organizational activities thereby encouraging the spirit of sportsmanship during WFH.
- **Regular check-ins, mentorship programs, and access to resources for managing stress** can contribute to maintaining positive employee behavior.

LIMITATIONS AND FUTURE DIRECTIONS

While this study offers valuable insights, it is important to acknowledge its limitations. The cross-sectional design restricts the ability to establish causal relationships between the work environment changes and OCB engagement. Future research could adopt longitudinal designs to capture the dynamics over time. Additionally, the study focused on the IT sector in Tamil Nadu, limiting the generalizability of the findings to other sectors and regions.

CONCLUSION

In conclusion, this research contributes to the existing literature by empirically highlighting the effects of the altered work environment on OCB among IT employees during the COVID-19 pandemic. The study underscores the importance of considering external stressors and challenges in understanding employee behavior. This research study unveils valuable insights into the positive effects of the altered work environment on Organizational Citizenship Behavior (OCB) among IT employees during the COVID-19 pandemic. The findings highlight the importance of addressing the challenges posed by remote work and communication barriers to promote positive employee behaviors. By implementing the suggested strategies, organizations can foster a supportive work environment and enhance OCB engagement, contributing to organizational resilience and success in unprecedented





Sunitha and Anitha

times. As organizations continue to navigate these unprecedented times, creating a supportive work environment remains a critical strategy for fostering positive employee behaviors and maintaining organizational resilience.

REFERENCES

1. Adams, J. S. (1963). Towards an understanding of inequity. *Journal of Abnormal and Social Psychology*, 67(5), 422-436.
2. Bakker, A. B., & Demerouti, E. (2007). The job demands-resources model: State of the art. *Journal of Managerial Psychology*, 22(3), 309-328.
3. Brown, L., & Williams, R. (2019). Remote Work and OCB: A Comparative Study Before and After COVID-19. *International Journal of Human Resource Management*, 35(5), 721-735.
4. Byrne, Z. S., & Hochwarter, W. A. (2008). Perceived organizational support and performance: Relationships across levels of organizational cynicism. *Journal of Managerial Psychology*, 23(2), 187-205.
5. Chen, Q., & Wang, Y. (2020). The Mediating Role of Job Satisfaction in the Relationship between Work Environment and OCB. *Journal of Applied Psychology*, 48(2), 187-203.
6. George, J. M. (1991). State or trait: Effects of positive mood on prosocial behaviors at work. *Journal of Applied Psychology*, 76(3), 299-307.
7. Greenberg, J. (1990). Organizational justice: Yesterday, today, and tomorrow. *Journal of Management*, 16(2), 399-432.
8. Gupta, R., & Sharma, S. (2017). Organizational Citizenship Behavior During Uncertain Times: A Study of IT Sector. *International Journal of Management Research*, 29(4), 521-536.
9. Lee, C., & Allen, N. J. (2002). Organizational citizenship behavior and workplace deviance: The role of affect and cognitions. *Journal of Applied Psychology*, 87(1), 131-142.
10. Lee, S., & Park, E. (2016). The Role of Communication Patterns in Influencing OCB. *Journal of Communication in Organizations*, 39(1), 112-128.
11. Malhotra, D., & Kapoor, M. (2019). Job Insecurity and OCB: A Longitudinal Study in the IT Industry. *Journal of Organizational Behavior*, 41(6), 721-738.
12. Nair, S., & Rao, K. (2018). Impact of Leadership Styles on OCB: A Comparative Study of IT Employees. *Leadership & Management in Technology*, 37(2), 201-215.
13. Patel, V., & Shah, R. (2020). Role of Civic Virtue in Promoting OCB: A Cross-Sectional Analysis. *Journal of Applied Organizational Psychology*, 45(3), 312-326.
14. Podsakoff, P. M., MacKenzie, S. B., Paine, J. B., & Bachrach, D. G. (2000). Organizational citizenship behaviors: A critical review of the theoretical and empirical literature and suggestions for future research. *Journal of Management*, 26(3), 513-563.
15. Podsakoff, P. M., Whiting, S. W., Podsakoff, N. P., & Blume, B. D. (2009). Individual-and organizational-level consequences of organizational citizenship behaviors: A meta-analysis. *Journal of Applied Psychology*, 94(1), 122-141.
16. Ramanathan, S., & Kumar, R. (2017). Work-Life Balance and OCB: A Study of IT Professionals. *Journal of Work and Family*, 32(4), 489-503.
17. Smith, C. A., Organ, D. W., & Near, J. P. (1983). Organizational citizenship behavior: Its nature and antecedents. *Journal of Applied Psychology*, 68(4), 653-663.
18. Smith, J., & Johnson, A. (2018). The Impact of Work Environment on Organizational Citizenship Behavior: A Review. *Journal of Organizational Psychology*, 42(3), 215-230.
19. Van Dyne, L., & LePine, J. A. (1998). Helping and voice extra-role behaviors: Evidence of construct and predictive validity. *Academy of Management Journal*, 41(1), 108-119.
20. Yang, H., & Wu, Y. (2019). The Impact of Perceived Fairness on OCB: A Study of IT Employees. *Employee Relations*, 41(2), 234-248.





Sunitha and Anitha

Table 1. Chi-square test for goodness of fit of equality of level of work environment of employees

Level of Job Description	Frequency	Percent	Chi-square value	P value
Low	109	28	26.723	< 0.001**
Moderate	178	46		
High	103	26		
Total	390	100		

Note: ** denotes significant at 1% level

Table 2. ANOVA for significant difference among level of Work Environment of IT Employees with respect to OCB Factors.

Factors of OCB	Work Environment	N	Mean	Std. Dev.	f- value	Sig.
ALTRUISM	Low	109	3.92	0.835 ^a	7.228	0.001**
	Moderate	178	4.09	0.576 ^b		
	High	103	4.27	0.611 ^c		
CONSCIENTIOUSNESS	Low	109	3.89	0.811 ^a	35.336	<0.001**
	Moderate	178	4.17	0.525 ^b		
	High	103	4.57	0.402 ^c		
SPORTSMANSHIP	Low	109	3.83	0.868 ^a	7.545	0.001**
	Moderate	178	3.31	1.119 ^{bc}		
	High	103	3.50	1.227 ^c		
COURTESY	Low	109	4.05	0.911 ^{ab}	9.441	<0.001**
	Moderate	178	4.22	0.547 ^{ab}		
	High	103	4.45	0.552 ^c		
CIVIC VIRTUE	Low	109	3.21	0.887 ^a	22.463	<0.001**
	Moderate	178	3.63	0.773 ^b		
	High	103	3.93	0.694 ^c		

Note:1. ** denotes significant at 1% level

Table 3. Relationship between Work Environment and OCB Factors

OCB Factors	Pearson Correlation of Work Environment
ALTRUISM	0.236**
CONSCIENTIOUSNESS	0.436**
SPORTSMANSHIP	-0.155**
COURTESY	0.321**
CIVIC VIRTUE	0.411**

Note: ** denotes significant at 1% level





Anti-Urolithiatic Potential of Nandukkal Parpam against Calcium Oxalate Stone Induced Renal Cell Injury using NRK-52E Cell Lines

Gayathri Gunalan^{1*}, Rajendra Kumar A², Durga A³, Sathiyarajeswaran P⁴ and Muthu Kumar NJ⁵

¹Research Officer [Biochemistry]-S II, Department of Biochemistry, Siddha Regional Research Institute [Central Council for Research in Siddha, Ministry of Ayush, Govt. of India], Puducherry - 605013.

²Research Officer [Siddha]-S III, Department of Clinical Research, Central Council for Research in Siddha Headquarters, [Ministry of Ayush, Govt. of India], Chennai- 600047.

³Senior Research Fellow [Biochemistry], Department of Biochemistry, Siddha Regional Research Institute [Central Council for Research in Siddha, Ministry of Ayush, Govt. of India], Puducherry - 605013.

⁴Assistant Director [Siddha]-S IV & I/c, Department of Clinical Research, Siddha Regional Research Institute [Central Council for Research in Siddha, Ministry of Ayush, Govt. of India], Puducherry - 605013.

⁵Director General, Central Council for Research in Siddha Headquarters, [Ministry of Ayush, Govt. of India], Chennai- 600047.

Received: 22 Jan 2024

Revised: 09 Feb 2024

Accepted: 15 May 2024

*Address for Correspondence

Gayathri Gunalan

Research Officer [Biochemistry]-S II,

Department of Biochemistry,

Siddha Regional Research Institute

[Central Council for Research in Siddha, Ministry of Ayush, Govt. of India],

Puducherry, India.

Email: ggsrri16@gmail.com



This is an Open Access Journal / article distributed under the terms of the **Creative Commons Attribution License** (CC BY-NC-ND 3.0) which permits unrestricted use, distribution, and reproduction in any medium, provided the original work is properly cited. All rights reserved.

ABSTRACT

Nandukkal Parpam[NP] is classical herbo mineral formulation of Siddha system of medicine. It is used for the treatment of various diseases including renal diseases, urinary disorders, musculo-skeletal diseases, etc. As the experimental evidence for its therapeutic indications are scanty, the present study was aimed at to evaluate the anti-urolithiatic potential of NP against calcium oxalate induced renal cell injury using NRK-52E cell lines. The purpose of the current investigation was to assess the anti-urolithiatic capability of NP by inhibiting the crystallization of calcium oxalate and also shielding renal tubular epithelial cells from oxalate induced cell injury. The inhibition of crystallization was studied using the nucleation and aggregation assay. The cytoprotective efficacy against oxalate-induced damage was evaluated by means of LDH assay and MTT assay. NP substantially prevented the calcium oxalate [CaOx] crystallization in a concentration dependent manner. It was shown to be safe and did not exhibit any noticeable cytotoxicity for NRK-52E cells until the maximum dose of 500µg. After exposing NRK-52E

75693



Gayathri Gunalan *et al.*,

cells to oxalate crystals, NP shielded the cells from injury. It inhibited the development and retention of crystals and also improves renal cell viability which was observed through reduced LDH leakage. Based on the experimental results, NP was found to be a potent anti-urolithiatic formulation that protects the renal cells from oxalate-induced injury by inhibiting CaOx crystallization and preventing tubular retention of crystals. Further extensive research is required to elucidate the molecular mechanisms involved in the anti-urolithiatic action of NP.

Keywords: Nandukkal, Siddha, Kalladaippu, Kidney stones, Urolithiasis

INTRODUCTION

Urolithiasis is the third most prevalent disease of the urinary system that affects about 11% population in India[1-3], affects about 12% of the world's population, with a recurrence rate of 70–81% in men and 47–60% in women [4]. It is characterized by the development of calculi anywhere throughout the urinary tract, including the kidneys, ureters, bladder, and urethra[5]. Its Symptoms include colicky pain, vomiting, dysuria, haematuria, pyuria and oliguria[6]. Complication of urolithiasis can lead to acute or chronic renal failure, pyelonephritis, pyonephritis and pyonephritic abscess which might proceed to life threatening situations and even fatal [7]. Urinary calculi form as a result of the urine being oversaturated with the substances that cause stones, which causes crystallisation, crystal nucleation, crystal aggregation, and crystal growth before adhering to the renal tubules [8]. Depending on their chemical composition, stones can have different types such as calcium oxalate monohydrate, calcium oxalate dihydrate, basic calcium phosphate (brushite), magnesium ammonium phosphate (struvite), uric acid, and cystine stones [9]. More than 80% of stones are composed of calcium oxalate (CaOx)[10,11]. The CaOx stones occurs in two forms viz. calcium oxalate monohydrate (COM) and Calcium oxalate dehydrate (COD). COM is the more stable one and it has high affinity for renal tubular cells and it is the more frequent observed form clinically[8,12]. The most common causes of stone formation are poor urine flow, urinary tract foreign bodies, microbial infections, oxalates and calcium rich diets, vitamin abnormalities like hypovitaminosis A and hypervitaminosis D, and metabolic diseases like hyperthyroidism, cystinuria, gout, intestinal dysfunction, etc. Additionally, an imbalance between promoters and inhibitors might result in the production of stones[13].

For the management of urinary calculi, a variety of surgical techniques are available, including Shock Wave Lithotripsy (SWL), Ureteroscopic Lithotripsy (URS), Digital Endoscopy, Percutaneous Nephrolithotomy (PNL), and robotic surgery. But most of these methods have a number of downsides as well [14]. Although there are a number of allopathic treatments available, traditional medicines are gaining importance because of their safety, low risk of adverse effects, and comparative superior effectiveness in removing stones and reducing the chance of recurrence [15]. Stone formation dates back to the traditional eras. One of the world's indigenous traditional medical systems is the siddha system. Its history dates from BC 5000 to BC 2000. A line of 18 Siddhars from the land of Tamil, including Agasthiyar and Thirumoolar, created this historic traditional medical method [16]. The Siddha medicinal system has a formulation called Nandukkal Parpam (NP) and this mostly prescribed for kidney problems, particularly kidney stones/calculi. As per Siddha Formulary, NP has been given for various therapeutic purposes including urinary obstruction (*Neeradaippu*), renal calculi (*Kalladaippu*), prostate obstruction of the urethra (*Sadhaiyadaippu*), and oliguria/anuria (*Neerkattu*) [17]. In another Siddha literature namely *Kalnandu soothiram*, it was mentioned that Nandukkal has been used to cure a variety of illnesses, including fevers of various kinds, musculoskeletal problems, mental disorders, gastrointestinal disorders, ophthalmological disorders, and venereal diseases [18]. NP is usually prescribed along with variety of adjuvants viz. water, tender coconut, decoction of *A. longifolia* L. *Nees* or *A. lanata* L. juice based on the required therapeutic effects [17]. Although it has a strong traditional literature background and widely used among Siddha Physicians, the scientific data reported to establish the anti-urolithiatic activity of this drug are scanty. Hence, the present study was aimed to investigate and validate the *in vitro* anti urolithiatic potential of NP against calcium oxalate stones induced renal cell injury using NRK-52E cell lines. The study's findings may



Gayathri Gunalan *et al.*,

also provide insight on the cellular mechanisms by which NP inhibits or reduces the calcium oxalate stones and thereby exerts its curative effects.

METHODS AND MATERIALS

Chemicals

The Siddha drug, NP was purchased from IMPCOPS, Chennai (Batch No.SII-185). Cell culture chemicals like Dulbecco's Modified Eagle's Medium (DMEM), 1X Phosphate - Buffered Saline (PBS), Fetal Bovine Serum (FBS), Antibiotic-Antimycotic Solution (100x) and Trypsin-EDTA solution were purchased from Sigma-Aldrich (St. Louis, MO, USA). Fine chemicals like 3-(4,5-dimethylthiazol-2-yl)-2,5-diphenyltetrazolium bromide (MTT), Dimethyl sulphoxide (DMSO), cell culture grade, Nicotinamide Adenine Dinucleotide Hydrogen (NADH) were procured from HiMedia Laboratories private limited (Mumbai, India). Sodium oxalate, Sodium pyruvate, Calcium chloride were of Sisco Research Laboratories Private Limited [Maharashtra, India] make. All other the chemicals and reagents used were of analytical grade.

Nucleation Assay

In vitro anti-urolithiatic activity of NP was evaluated by nucleation assay following the method described by Mandal *et al* (2017) [19]. 5mM calcium chloride and 7.5mM sodium oxalate solution were prepared in the buffer containing 50mM Tris and 150mM sodium chloride [pH-6.5]. Stock solutions of NP (test) and Cystone (standard) were made at the concentration of 10mg/ml. About 1ml of calcium chloride solution was mixed with different concentration of NP ranging from 200-1000 µg /ml. In control set instead of test sample, 1ml of distilled water was added. Crystallization process was initiated by adding 1ml of sodium oxalate solution into the above mixture. Finally, the absorbance was read at 620nm after incubating samples at 37°C for 30 min.

Percentage inhibition of nucleation was calculated as follows:

$$\text{Percentage inhibition} = \left[\frac{C - S}{C} \right] \times 100$$

Where, C = turbidity of control

S = turbidity of sample

Aggregation assay

The inhibitory activity of NP against CaOx crystal aggregation was studied by following the method described by the Bawariet *al* (2018) [20]. Equal volume of 50mM calcium chloride and 50mM sodium oxalate were combined together, and then heated to 60°C in a water bath for 1 hour, followed by incubation at 37°C. Calcium chloride crystals were dried and its solution was prepared in a buffer containing 0.05M Tris-HCl and 0.5M NaCl (pH-6.5). 1ml of various concentration of NP was mixed with 3ml of CaOx crystal solution and incubated at 37°C for 30 min. Absorbance of the reaction mixture was measured at 620nm in a Microprocessor based Double beam UV-Visible Spectrophotometer (IgeneLabserve, India). Percentage of aggregation was calculated as follows:

$$\% \text{ Inhibition} = [1 - OD \text{ Test} / OD \text{ Control}] \times 100,$$

Cell culture

NRK-52E cells (Normal rat kidney epithelial cells) were procured from NCCS, Pune (India). The cells were maintained in the Dulbecco's Modified Eagle's Medium supplemented with 10% FBS and Antibiotic-Antimycotic Solution (100x) at 37°C with 5% CO₂.

Cytoprotective effect of NP against oxalate-induced injury

NRK-52E cells were first trypsinized and then seeded in a 24-well plate with a seeding density of 1×10⁵ cells per well. The plate was then incubated overnight to allow cell attachment. 600 µg/ml of oxalate solution was added to each well and the cells were incubated for 24 hours in the presence/absence of 100–500 µg/ml of NP. Cells controls [positive and negative control groups] were also maintained in the same way. Cell viability was determined by MTT





Gayathri Gunalan et al.,

assay and cytoprotection of NP against oxalate-induced cell injury was monitored in the medium using lactate dehydrogenase (LDH) leakage assay.

Cytotoxicity Assay

The effect of NP on cell viability of NRK-5E cells was assessed by MTT [3-[4,5-dimethylthiazole-2-yl]-2,5-biphenyl tetrazolium bromide] assay [21]. To explore the cytotoxicity of NP towards NRK-52E cells, cells were treated with various concentration of NP ranging from 100, 200,300,400 and 500 µg/ml and the same were prepared by serial dilution. The cells were then incubated for 24 hours at 37°C with 5% CO₂. After incubation, the growth medium was removed from each well. 0.5 mg/mL of MTT solution was added to each well and incubated again for 4 h at 37°C. DMSO was used to solubilize the dye and the absorbance measurement was made at 570 nm using ERBA plate reader.

LDH leakage assay

Cytoprotective property of NP against oxalate-induced injury was assessed by evaluating LDH leakage[22]. After the drug treatment period, the growth medium was used for LDH leakage assay. About 1.5ml of culture media was transferred to micro centrifuge tube and centrifuged at 16,000 g for 20min. Then 20µl of supernatant was mixed with the 200 µl of reagent containing 2.5mM sodium pyruvate and 0.2mM NADH. Decrease in absorbance at 340nm was measured using microplate reader for 3min. The LDH activity (U/L) was determined by calculating the change in absorbance per min.

Statistical analysis

All the values were expressed as mean ± SD. Data analysis was done by one-way analysis of variance (ANOVA) followed by Duncan's multiple range test (DMRT). P<0.05 was set as statistical significance."

RESULTS

Nucleation Assay

The effect of NP on the nucleation of calcium oxalate crystals was shown in Figure 1. In comparison to the control, the percentage of inhibition demonstrated by NP at 100µg/ml was 6.06%, and at 200, 300, 400, and 500µg/ml, the inhibition was nearly consistent within the range of 11.68% - 34.84%. The IC 50 value of NP w.r.t inhibition of CaOx crystal nucleation was found to be 717.56 µg/ml whereas for the standard drug cystone, it was 577.36 µg/ml.

Aggregation assay

Figure 2 shows the effect of NP on aggregation of CaOx crystals. From the figure, it was evident that a substantial decrease in CaOx crystal aggregation was seen at 500µg/ml of NP and the percentage decrease in aggregation was found to be 37.06 %. But for 500µg/ml of cystone, it was 58.04 %. This shows that the study drug was able to decrease the growth and aggregation of CaOx crystals. The IC 50 value of NP w.r.t crystal aggregation was 674.58 µg/ml and for cystone it was 430.73 µg/ml. The reduction in number and size of the aggregates of CaOx crystals were apparently visible in the microscopic images relative to the control as shown in figure 2.

Cytotoxicity assay/MTT assay

The effect of various concentrations of NP in NRK-52E cell lines was assessed using MTT assay and the results were presented in Table.1. The IC₅₀ value of NP was found to be 906.16µg/ml. Even at highest concentration NP did not show any notable toxicity and thus found to be safe.

Cytoprotective effect of NP against oxalate induced Injury

NP significantly prevented oxalate-induced damage in NRK-52E cells when examined using the MTT test. Figure 4 illustrates how the oxalate significantly damaged renal tubular epithelial cells, reducing their viability to 42%. NP considerably raised the percentage of viable renal epithelial cells and prevented damage in a concentration-



**Gayathri Gunalan et al.,**

dependent manner. As the concentration of NP increased, the percentage of viable cells also increased. At the maximum tested concentration of 500 µg/ml, NP has significantly increased the cell viability to 71% even in the presence of oxalate [$P < 0.0001$]. At all the tested concentrations of NP, the results were statistically significant when compared with the oxalate alone cells group and cell control group. Figure 5 shows the effect of NP on LDH leakage due to oxalate induced NRK52E cells damage. It was evident that oxalate only treated cells are highly damaged and the LDH level was found to maximum of 60U/L. In the presence of NP, the LDH leakage was much prevented and it was found to range from 50U/L to 28U/L in dose dependent fashion. This kind of cytoprotectivity is statistically significant [$P < 0.0001$] when compared with the cell control and oxalate alone cell group. Increased LDH activity can be correlated with increased cell damage. CaOx crystals has caused significant damage to renal cells resulted in a rise in LDH activity and reduced cell viability (Figure 6).

DISCUSSION

Urolithiasis is one of the most prevalent renal diseases. Though many stone removal procedures are available currently, the high rate of recurrence which is about 50% at a follow up period of 5 years emphasizes the importance of prevention [7]. Limitations in the success rate of chemical drugs are due to the involvement of multiple biochemical pathways in its pathogenesis. Thus there is a need for better treatment modality which has various targets such as antioxidant, anti-inflammatory, antispasmodic activities, etc.[23]. COM is the most thermodynamically stable and more frequent urinary calculi when compared to other types of stones. Various studies have revealed that COM crystals causes renal cell injury via the production of free radicals [24,25]. This injury triggers and promotes the crystal nucleation, aggregation and stone development further [26]. Due to increased production of reactive oxygen species (ROS), oxidative stress was created leading to decrease in cell viability and finally to cell death via either apoptosis or necrosis [8]. This further causes variety of changes in the normal architecture of renal tubular epithelial cells. It also alters the membrane integrity and facilitates the adherence and retention of COM crystals further. Thus an imbalance between ROS and the antioxidants in renal epithelial cells is a critical step in the pathogenesis of urolithiasis[27]. Nandukkal parpam, a herbo-mineral siddha formulation commonly prescribed for various diseases including urinary disorders, gastrointestinal disorders, venereal diseases. It has many pharmacological activities like antioxidant, anti-inflammatory, anti-urolithiatic activity, etc. In our earlier publication, the invitro free radical scavenging activity of nandukkal parpam was elaborated using various invitro models [28]. Hence, the present study aimed at to investigate the anti-urolithiatic activity of NP using NRK-52E cells to demonstrate its preventive action on COM induced renal cell injury. Nucleation plays a vital role in CaOx urolithiatic pathogenesis. It is a thermodynamically driven event which makes the dissolved solute in a supersaturated solution to crystallize spontaneously [29]. Nandukkal Parpam has inhibited 34.84% of nucleation of CaOx crystals at 500 µg/ml when compared to the standard cystone which inhibits 43.30% at 500 µg/ml concentration. The inhibitory activity shows that NP has prevented the fusion of free calcium and oxalate ions by complexing with them. Similar observation was demonstrated by various researchers [30].

CaOx polymorphism plays a key role in urolithiasis. Being a thermodynamically stable form, COM tends to aggregate into large crystals and adhere strongly to renal epithelial tissues leading to cell injury. NP prevents the aggregation of CaOx crystals significantly by 37.06% at 500 µg/ml dose with a IC 50 value of 674.58 µg/ml whereas cystone prevents the aggregation by 58.04% at 500 µg/ml(IC 50 : 430.73 µg/ml). Prevention of aggregation plays an important role in the treatment of urolithiasis. As the size of the crystals decreases, the tendency to pass out spontaneously through urine increases. Hence crystal growth is very much crucial for urolithiasis management. NP exhibited significant inhibitory activity towards crystal aggregation and thereby created a scientific evidence for the usage of the traditional Siddha medicine. By preventing the aggregation, NP also reduces the crystal retention and thereby protects the renal cell from damage. Accumulation of CaOx crystals in renal epithelial cells leads to disruption in ROS and antioxidant equilibrium and proceeds to oxidative damage of involved cells. Mitochondria and the enzyme, NADPH Oxidase are the major source of reactive oxygen species in renal cells [31,32]. It also activates the renin angiotensin system which in turn activates the NADPH oxidase and enhances oxidative stress



**Gayathri Gunalan et al.,**

further [33] All these chemical reactions disrupt the membrane integrity and leads to cell death. As the cell integrity decreases, LDH leakage increases. This is evident from Figure 4, 5 and 6. In untreated control cells, due to higher concentration of oxalates, LDH activity was maximum of about 60U/L. As the concentration of NP increases, the cell damage was prevented even in the presence of oxalates and thus observed decrease in LDH activity of about 28% at 500 µg/ml concentration of NP. This cytoprotective activity is dose dependent and it increases with the concentration of NP. It was also evident with the results of MTT assay in which NP presence increases the cell viability (Table 1). The IC 50 value of NP was found to be 906.16 µg/ml. As the concentration of NP increases, cell viability also increased when compared with the control cells and oxalate alone cell group. This kind of cytoprotective effect may be due to the antioxidant property of NP which was already proven in our earlier publication [28]. Thus by preventing the nucleation, aggregation and retention of CaOx crystals, NP decreases the formation of urolithiatic stones. Even if formed, in small sizes it eliminates by eliciting its antioxidant potential and thus prevents the renal tubular epithelial cells from CaOx induced cell injury.

CONCLUSION

From the present study, it was confirmed that Nandukkal Parpam, a herbo-mineral Siddha formulation has significant anti-urolithiatic activity against CaOx stones. It prevents the CaOx crystal formation which is a key event in urolithiasis. Besides, it also increases the cell viability by preventing the renal cells (NRK-52E) from oxalate induced injury through its antioxidant nature. Thus the present study validates the usage of NP for urolithiasis through various scientific methods. Further detailed studies are required to elucidate the cellular mechanisms involved in the anti-urolithiatic activity of NP. This paves way for the safe, economical, patient friendly and traditional way of urolithiasis management.

REFERENCES

1. Leye A, Jaeger P, Robertson W, Unwin R. Renal stone disease. *Medicine* 2007; 35:415-9.
2. Worcester EM, Coe FL. Nephrolithiasis. *Prim Care* 2008; 35:369-91, vii.
3. Lulat SI, Yadav YC, Balaraman R, Maheshwari R. Antiurolithiatic effect of lithocare against ethylene glycol-induced urolithiasis in Wistar rats. *Indian J Pharmacol* 2016; 48:78-82.
4. Joy JM, Prathyusha S, Mohanalakshmi S, Praveen Kumar AVS, Ashok Kumar CK. Potent herbal wealth with litholytic activity: a review. *IJDD* 2012; 2:66-75.
5. Vijaya T, Kumar MS, Ramarao NV, Babu AN, Ramarao N. Urolithiasis and its causes- short review. *J Phytopharmacol* 2013; 2:1-6.
6. Tiwari A, Soni V, Londhe V, Bhandarkar A, Bandawane D, Nipate S. An overview on potent indigenous herbs for urinary tract infirmity: urolithiasis. *Asian J Pharm Clin Res* 2012; 5:7-12.
7. Hussain M, Rizvi SA, Askari H, Sultan G, Lal M, Ali B, Naqvi SA. Management of stone disease: 17 years' experience of a stone clinic in a developing country. *J Pak Med Assoc.* 2009; 59:843-846.
8. Aggarwal KP, Narula S, Kakkar M, Tandon C. Nephrolithiasis: molecular mechanism of renal stone formation and the critical role played by modulators. *Biomed Res Int* 2013; 13:292-953.
9. Nagal A, Singla RK. Herbal resources with antiurolithiatic effects: a review. *Indo Global J Pharm Sci* 2013; 3:6-14.
10. Ghelani H, Chapala M, Jadav P. Diuretic and antiurolithiatic activities of an ethanolic extract of *Acoruscalamus* L. rhizome in experimental animal models. *J Tradit Complement Med* 2016; 6:431-6.
11. Bhagavathula AS, Mahmoud AI-Khatib AJ, Elnour AA, Al Kalbani NM, Shehab A. *Ammivisnagain* treatment of urolithiasis and hypertriglyceridemia. *Pharmacognosy Res* 2014; 7:3 97-400.
12. Basavaraj DR, Biyani CS, Browning AJ, Cartledge JJ. The role of urinary kidney stone inhibitors and promoters in the pathogenesis of calcium containing renal stones. *EAU-EBU update series.* 2007;5[3]:126-36.





Gayathri Gunalan et al.,

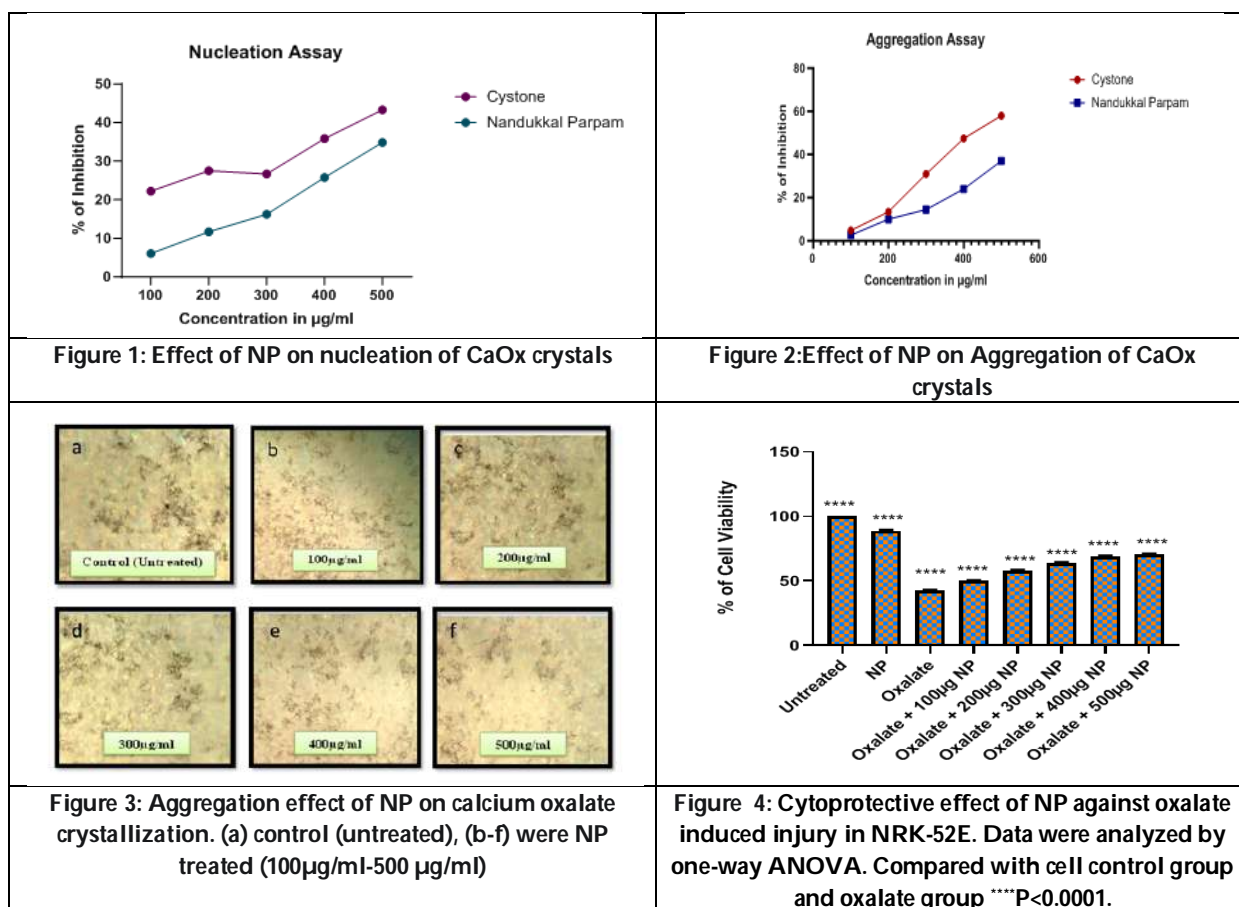
13. Vijaya T, Kumar MS, Ramarao NV, Babu AN, Ramarao N. Urolithiasis and its causes- short review. J Phytopharmacol 2013; 2:1-6.
14. Rosa M, Usai P, Miano R, Kim FJ, Agrò EF, Bove P, et al. Recent findings and new technologies in nephrolithiasis: a review of the recent literature. BMC Urol 2013; 13:1-11.
15. Alok S, Jain SK, Verma A, Kumar M, Sabharwal M. Pathophysiology of kidney, gall bladder and urinary stones treatment with herbal and allopathic medicine: a review. Asian Pac J Trop Dis 2013;3: 496-504.
16. Thiagarajan. *GunapadamThathu - Jeevavaguppu*, II edition, Directorate of Indian Medicine and Homeopathy, 1968; pp:557-558.
17. Siddha Formulary of India, Vol I [2011], Govt. of India, Ministry of Health and Family welfare, Dept. of AYUSH, New Delhi.
18. ArunaiNambiraj, N.; Panicker, T.M.R.; Seethalakshmi, S.; Chinnama Abraham.; Paul Korath, M. and Jagadeesa, K. Prophylactic effect of 'Nandukkal Parpam' [A Siddha combination drug] on ethylene glycol induced calcium oxalate microlithiasis in the kidneys of wistar rats. Bombay Hosp J, 2002; 44[3]:402-405.
19. Mandal. B.; Swati Madan S.; Ahmad.**In vitro Inhibition of Calcium Oxalate Nucleation by Extract-based Fractions of Aerial Parts and Roots of *Aervalanata*[Linn.]Juss. ex Schult.** Indian J Pharm Sci,2017; 79[6]:957-964.
20. SwetaBawari,;ArchanaNegiSah,; DeveshTewari. Antiurolithiatic Activity of *Daucuscarota*: An in vitro Study. Pharmacogn J, 2018; 10[5]:880-884.
21. Ahmed SA, Al-Shanon AF, Al-Saffar AZ, Tawang A, Al-Obaidi JR. Antiproliferative and cell cycle arrest potentials of 3-O-acetyl-11-keto- β -boswellic acid against MCF-7 cells in vitro. J Genet EngBiotechnol. 2023; 21[1]:75.
22. Goyal PK, Verma SK, Sharma AK. Antiurolithiatic Potential of Neeri against Calcium-Oxalate Stones by Crystallization Inhibition, Free Radicals Scavenging, and NRK-52E Cell Protection from Oxalate Injury. Pharmacogn Mag, 2017; 13: S549-S554.
23. Khan A, Bashir S, Khan SR, Gilani AH. Antiurolithic activity of *Origanumvulgare* is mediated through multiple pathways. BMC Complement Altern Med. 2011; 11:96.
24. Aihara K, Byer KJ, Khan SR. Calcium phosphate-induced renal epithelial injury and stone formation: involvement of reactive oxygen species. Kidney Int. 2003; 64:1283-1291.
25. Escobar C, Byer KJ, Khaskheli H, Khan SR. Apatite induced renal epithelial injury: insight into the pathogenesis of kidney stones. J Urol. 2008; 180:379-387.
26. Byer K, Khan SR. Citrate provides protection against oxalate and calcium oxalate crystal induced oxidative damage to renal epithelium. J Urol. 2005; 173:640-646.
27. Ghodasara J, Pawar A, Deshmukh C, Kuchekar B. Inhibitory effect of rutin and curcuminon experimentally-induced calcium oxalate urolithiasis in rats. Pharmacognosy Res 2010; 2:388-92.
28. GayathriGunalan, A. Durga, A. Archana and A. Rajendra Kumar. *In vitro* free radical scavenging activity of *Nandukkal Parpam*: A herbo-mineral Siddha formulation. Ann. Phytomed, 2023; 12[1]:247-250. <http://dx.doi.org/10.54085/ap.2023.12.1.101>.
29. Butterweck V, Khan SR. Herbal medicines in the management of urolithiasis: alternative or complementary? Planta Med. 2009; 75:1095-1103.
30. Bawari S, Sah AN, Tewari D. Antiurolithiatic Activity of *Daucuscarota*: An *in vitro* Study. Pharmacog J. 2018;10[5]:880-4.
31. Umekawa T, Byer K, Uemura H, Khan SR. Diphenyleneiodium[DPI] reduces oxalate ion- and calcium oxalate monohydrate and brushite crystal-induced upregulation of MCP-1 in NRK 52E cells. Nephrol Dial Transplant 2005; 20:870-8.
32. Olugbami JO, Gbadegesin MA, Odunola OA. *In vitro* free radical scavenging and antioxidant properties of ethanol extract of *Terminalia glaucescens*. Pharmacognosy Res 2015; 7:49-56.
33. Umekawa T, Hatanaka Y, Kurita T, Khan SR. Effect of angiotensin II receptor blockage on osteopontin expression and calcium oxalate crystal deposition in rat kidneys. J Am SocNephrol 2004; 15:635-44.





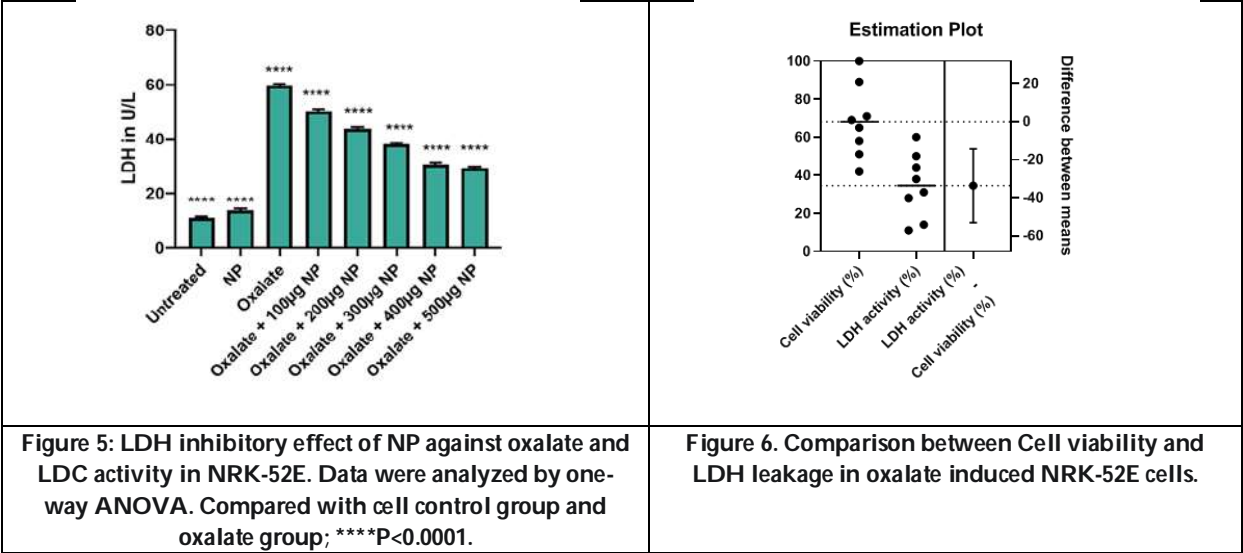
Table 1: Cytotoxicity of NP on NRK-52E cells.

Concentration in $\mu\text{g/ml}$	% Cell viability
200	82.89 \pm 1.68
400	75.13 \pm 0.57
600	62.41 \pm 0.80
800	54.02 \pm 0.76
1000	43.57 \pm 0.98
IC50	906.16 $\mu\text{g/ml}$





Gayathri Gunalan et al.,





A Comprehensive Case Study on Complete Trisomy 9 and Mosaicism Trisomy 16 Rescue: Report of Two Rare Cases and Assessment of Phenotypic-Genetic Association

Sujithra Appavu^{1,2}, Aruni Wilson Santhosh Kumar^{3,4*}, Flora Bai^{1,2}, Vinoth Appavu⁵ and Chirayu Padhiar⁶

¹Department of Biotechnology, Sathyabama Institute of Science and Technology, Chennai, Tamil Nadu, India.

²Department of Cytogenetics, Life Cell International Private Limited, Chennai, Tamil Nadu, India.

³Vice Chancellor, Amity University, Mumbai, Maharashtra, India.

⁴Musculoskeletal Disease Research Centre, Loma Linda Veterans Affairs, United States of America.

⁵Associate professor, Department of Emergency Medicine, Thanjavur Medical College, Thanjavur, Tamil Nadu, India.

⁶Department of Biologics, Senior Medical Director, Life Cell International Private Limited, Chennai, Tamil Nadu, India.

Received: 22 Jan 2024

Revised: 09 Feb 2024

Accepted: 30 May 2024

*Address for Correspondence

Aruni Wilson Santhosh Kumar

Vice Chancellor,

Amity University,

Mumbai, Maharashtra, India.

Musculoskeletal Disease Research Centre,

Loma Linda Veterans Affairs,

United States of America.

Email: drwilsonaruni@hotmail.com



This is an Open Access Journal / article distributed under the terms of the **Creative Commons Attribution License** (CC BY-NC-ND 3.0) which permits unrestricted use, distribution, and reproduction in any medium, provided the original work is properly cited. All rights reserved.

ABSTRACT

The study aimed to enhance and describe clinicians' understanding of the disorders and unravel their genetic intricacies achieved from prenatal screening. Two maternal cases were investigated in this study. Case 1 involved a 31-year-old pregnant woman, and Case 2 involved another 29-year-old pregnant woman of undisclosed gestational age. The prenatal investigation explored two cases presenting Case 1 where a range of tests such as ultrasound examination, biochemical analysis, quantitative fluorescence-polymerase chain reaction (QF PCR), and conventional karyotyping, showed complete trisomy 9(T 9), while Case 2 exhibited features of trisomy 16(T 16) rescue mosaicism and prenatal screening was performed utilizing Conventional karyotyping, Whole Chromosome Painting (WCP), Short Tandem Repeat, and Chromosomal Microarray analysis. Trisomy 9 case exhibited multisystem malformations with high risk for trisomy 21 in 1:817 and Tetralogy of Fallot which further confirmed complete Trisomy

75702



Sujithra Appavu *et al.*,

9 by conventional karyotyping. Case 2 had more than three allele traces on chromosome 16. Foetal sample submitted for CMA study noted trisomy 16 rescue led to a mosaic of two distinct cell lines and this case study was initially studied via conventional karyotyping presenting with uncertainty (46,X?). WCP probes indicated negative and the complex interplay between rescue trisomy 16 and UPD mechanisms providing valuable insights into dynamic processes influencing chromosomal stability. Clinical history highlights significant indicators such as single umbilical artery, echogenic small bowel loops, and a decline in growth velocity. Additionally, presence of normal liquor and a noted high-resistance umbilical artery Doppler flow pattern further contributes intricate diagnostic picture, ultimately resulting in termination of pregnancy.

Keywords: Aneuploidy; Complete Trisomy 9; Conventional Karyotyping; Prenatal diagnosis; Trisomy 16 rescue mosaic syndrome; uniparental-disomy;

INTRODUCTION

The clinical relevance of trisomy in general is defined as a genetic condition that attributes to an extra chromosomal copy. In other words, an individual with trisomy cases presents with 47 chromosomes instead of 46. Trisomy pregnancies in particular results in live births but majority cases end prematurely with miscarriage [1]. Both T 9 and T 16 are relatively rare chromosomal abnormalities. Both these trisomy cases and its prevalence vary however upon considering the general trisomy presentation on a global scale the presented case study is less commonly reported in clinical literature [2]. Also, the overall prevalence of trisomy cases influenced majorly by factors like maternal age, parental genetic factors, genetic carrier status, non-disjunction during the time of cell division and maternal health status and other environmental and unknown factors [3]. Clinical evidence revealed that the earliest documented report of trisomy 9 mosaicism dates back to 1973, highlighting its historical obscurity in the field of prenatal diagnostics [4]. This condition's rarity extends to its global prevalence, with live births resulting from trisomy 9 conceptions being exceedingly scarce. Only a mere 0.1% of trisomy 9 conceptions lead to live births [5], and likewise when considering trisomy 16 is estimated in about 1.5% of pregnancy cases that are clinically recognized. The prevalence of trisomy 16 varies among genders and is much more commonly expressed in the males. In mosaic trisomy 16, however, a larger proportion of female fetuses exist. However, even among these live-born cases, the prognosis remains grim, with survival times ranging from mere minutes to, in the best-case scenario, nine months after birth [6]. Live-born foetuses with complete trisomy 9 typically exhibit a mosaic phenotype, adding to the complexity of its diagnosis. Notably, trisomy 9 does not exhibit gender bias, affecting both male and female foetuses equally. Both trisomy 9 and trisomy 16 are chromosomal abnormalities resulting from meiosis I nondisjunction, but they involve different chromosomes (9 and 16, respectively) [1]. Nondisjunction referred to in this scenario is a condition in which there is a failure of homologous chromosomes to disjoin correctly during meiosis.

This results in the production of gametes containing extra or missing chromosome count than the normal. Consequently, the individual may develop a trisomal or monosomal syndrome. Mosaic trisomy 16 (MT 16) arises as a result of a complex phenomenon known as trisomy rescue, the underlying causes of which remain enigmatic. The presence of aneuploidy itself contributes to chromosomal instability due to abnormalities in cell cycle progression or cell proliferation. In the case of mosaic trisomy 16, this condition evolves through the postzygotic loss of one copy of chromosome 16 [7]. The pregnancy cases of MT16 usually starts with complete extra chromosome 16 during the egg cell formation, a natural yet unexpected error occurs resulting in the separation of chromosomes that further results in the separation of extra chromosome 16 in egg cell [8]. This phenomenon could be termed as uniparental disomy (UPD), wherein both members of the chromosomal pair being inherited by one parent whereas the other parent's chromosome for that pair is missing. This UPD condition however rarely occurs during spermatogenesis [9]. Following the conception phase, there are typically three chromosome 16s—usually two inherited one from the



**Sujithra Appavu et al.,**

mother and one from the father. In post-conception phase, a remarkable natural mechanism attempts to rectify this anomaly, resulting in a partial correction. This corrective process, known as trisomy correction or trisomy rescue (Fig.1), strives to restore normal chromosomal balance [10]. This intricate interplay of genetic events sheds light on the dynamic and finely tuned processes that govern chromosomal inheritance, offering insight into the mechanisms underlying MT16. Notably, maternal uniparental disomy is a distinctive feature observed in approximately one-third of mosaic trisomy 16 cases. UPD represents an alternate mechanism contributing to disruptions in human gene expression, potentially leading to human diseases. Prenatal screening and diagnostic tests can provide more information about the chromosomal health of the fetus, helping parents make informed decisions about their pregnancy. Genetic counselling is often recommended for couples with concerns about the risk of chromosomal abnormality. Firstly, it is an exceedingly rare pregnancy condition, often unfamiliar among many medical practitioners [11]. Secondly, the likelihood for fetal survival in utero was reported to be quite a challenge thus rendering the condition elusive [12]. Consequently, considering complete T9 on a broader prenatal screening might not be included in the roster of potential diagnoses due to its rarity in trisomy prevalence [13]. Nonetheless, the precise identification of fetuses afflicted by T9 remains pivotal owing to the dire prognosis. Both trisomy conditions in particular are essential due to their extreme rarity, limited medical awareness, low survival rates, and mosaic phenotype. This condition, with its complex clinical manifestations and genetic implications, necessitates a profound understanding for timely identification, informed decision-making by expectant parents, and improved medical care. Additionally, its historical obscurity emphasizes the need for comprehensive exploration and discussion in the medical community. Foetuses afflicted by complete trisomy 9 exhibit a panoply of anomalies that could readily be discerned during prenatal ultrasound evaluation. These anomalies primarily affect cardiovascular, musculoskeletal, craniofacial, and even genitourinary systems. However, certain findings may be subtle, eluding from routine ultrasound investigations [14]. From our understanding so far from literature investigations clearly represent that the clinical characteristics of the diverse systems affected by T9 and T16 syndrome holds paramount significance despite the lack in diverse clinical case studies. This paper strives to shed some limelight and providing insights from the achieved prenatal outcomes from both these case studies.

METHODS

Case Description

Prenatal screening and diagnosis are pivotal components of maternal and foetal healthcare, aiming to ensure the well-being of both the expectant mother and the developing foetus. Among the spectrum of chromosomal anomalies, trisomy 47, + 9, otherwise termed trisomy 9 syndrome holds significant concern due to its potential to profoundly influence the outcome of a pregnancy. Case 2 is a 29-year-old female with remarkable pregnancy findings during ultrasonography was identified; the test results further revealed a single umbilical artery, echogenic small bowel loops, and non-homogeneous placenta. The chromosomal status determined from the amniotic fluid cells at 24 weeks and 6 days of gestation and prenatal samples were analysed using a chromosomal microarray (CMA). CMA analysis revealed that all chromosomes, including sex, are normal, confirming a diploid pattern (Normal copy set = 2 sets) except for chromosome 16, which has several allele tracks (more than 3).

Patient clinical history

Maternal Age: 31 Years (case 1); 29 Years (case 2)

Gestational Age: At the time of assessment, the patient was precisely at 12.3 weeks into her pregnancy, marking the beginning of the second trimester. For case 2, amniocentesis was conducted at 17.4 weeks of gestation, calculated based on the last menstrual period (LMP).

Cytogenetic Analysis Method:

All the Amniotic fluid samples inoculated into the Amniomax culture medium were incubated at 37 °C with 5 % CO₂ and cultured for 10 to 15 days to karyotyping and were subjected as per standard protocol. Amniotic fluid sample culture medium inoculated Cells were monitored daily (24 hours) for their growth conditions. During the harvest,





Colcemid was used to stop the cell division. Fixative therapy was administered after hypotonic treatment. The chromosomes were prepared by the conventional method, and subjected to GTG banding for both cases. In this study, ultrasonographic evaluation were done. Along with the ultrasonographic findings, the assessment of biomarkers plays a vital role. Conventional karyotyping investigation was performed for both the case studies.

RESULTS & DISCUSSION

Overall Impression observed from clinical history: Based on the patient's clinical history, they have been diagnosed with both Tetralogy of Fallot and amenorrhea for the past 7 months and Intermediate risk trisomy 21(1:817). The forthcoming subsection provides detailed outcomes achieved from trisomy-9 case.

Ultrasonographic Outcomes of Case 1

At 20 weeks of gestation, a comprehensive sonographic evaluation was conducted, revealing the following Findings For case 1, the fetal Crown-Rump Length (CRL) measuring 51 mm, aligned seamlessly with the expected gestational age (Fig. 2). This observation indicated healthy growth and development at this crucial stage of pregnancy. Normal nuchal translucency measurement of 2.33 mm was recorded for case 1, falling within the expected range for this stage of pregnancy. The assessment of the ductus venosus revealed normalcy, indicating healthy blood flow in the fetal circulatory system. A left pleural effusion, as detected in the ultrasound examination, raised concerns about fetal well-being. Pleural effusion, the accumulation of fluid in the fetal chest cavity, can have several underlying causes, including chromosomal abnormalities. It necessitates further investigation and monitoring. Furthermore, Case 1, diagnosed with complete trisomy 9, revealed a potential cardiac manifestation with findings aligning with 'Tetralogy of Fallot' (TOF) with abnormal cardiac angle or extracardiac defects This congenital heart defect was characterized via sonographic findings confirming abnormalities such as ventricular septal defect (VSD), overriding aorta, pulmonary stenosis, and right ventricular hypertrophy. For case 2 ultrasonography findings showed features like a single umbilical artery, echogenic small bowel loops, and a drop in growth velocity. Additionally, the evaluation of amniotic fluid (liquor) and the Doppler flow pattern in the umbilical artery provides further insights into the fetal condition, particularly growth and vascular dynamics. In Trisomy 16 cases, the unborn baby can have one of a few outcomes.

Biochemical Markers for Case 1

In conjunction with sonographic findings, the assessment of biochemical markers played a crucial role in the evaluation: PAPP-A (Pregnancy-associated plasma protein-A): The PAPP-A level was measured at 2.87 mIU/mL, slightly above the median (1.08 MoM). The free β hCG level was recorded at 15.2 ng/mL, with a notably reduced value of 0.34 MoM. A decreased free β hCG level can be indicative of an elevated risk for chromosomal abnormalities, necessitating further investigation. The findings collectively showcased the intricate processes of prenatal screening and diagnosis in the Indian context, where culturally sensitive and informed decision-making is paramount. In such cases, the collaboration between medical expertise and personalized care assumes a profound significance in maternal and fetal healthcare. In our case, we observed a distinctive triphasic waveform in the ductus venosus flow, which displayed no abnormalities. It is noteworthy that a similar case report can be found in Reference [15]. However, it's important to acknowledge that the literature does contain descriptions of abnormal reverse ductus venosus flow in fetuses with trisomy 9 [16]. In the case presented here, our observations primarily centered around cardiovascular, musculoskeletal, genitourinary, and central nervous system malformations. Trisomy 9 has a notably strong association with central nervous system abnormalities, with particular emphasis on conditions like Dandy-Walker malformation. Cardiac malformations have been reported to occur in a substantial percentage of trisomy 9 cases, ranging from 75-80% [4]. The biochemical findings provided certain key insights on the complexity of trisomy 9 syndrome and emphasized the importance of thorough prenatal assessments and diagnostic evaluations in cases of suspected chromosomal anomalies.



**Prenatal Genetic Screening for Case 1**

The subsequent GTG banding conventional karyotyping (Fig.2) revealed a chromosomal makeup of 47 +9 employing 20 cells across two primary cultures. Upon receiving the karyotype results, the couple made the difficult decision to terminate the pregnancy. Regrettably, they opted not to pursue a pathological anatomy analysis. This decision signifies the emotional and complex choices individuals must make when faced with such challenging prenatal diagnoses. Fig.3 the QF PCR analysis for chromosome-specific markers indicates a normal complement of 13, 18, 21 and sex chromosomes.

Prenatal genetic screening for case 2

Case 2, karyotyping (Fig.4) was performed, and the chromosome analysis revealed a seemingly normal chromosome complement. Further investigation or additional testing may be warranted to elucidate the nature of this uncertainty and provide a more detailed characterization of the chromosomal composition. From the chromosomal analysis via karyotyping, Fig 4. presented with conventional karyotype with GTG banding. In a total of 20 cells originating from two primary cultures, the karyotype exhibited of cultured amniocytes revealed a normal chromosome complement. 46,X? [30]. Short Tandem Repeat (STR) profile of the fetus (Fig 4.) showed findings that specifically highlighted that the chromosome 16 markers. The presence of three allele peaks indicates a notable aberration in the chromosomal composition. The trisomic condition is visually represented by the three distinct peaks, indicating the presence of an additional copy of chromosome 16 in certain cells. This is characteristic of mosaic trisomy 16. The Chromosomal Microarray (CMA) Allele tracks are depicted in Fig.4. Revealed a more detailed view of chromosome 16. The presence of multiple tracks on chromosome 16 signifies genetic complexity, with more than the expected two tracks.

This aligns with the mosaic trisomy 16 condition, indicating the coexistence of cell lines with different chromosomal compositions. The tracks provide a visual representation of the mosaic nature of the trisomy, showcasing the variability in chromosomal content within the analysed sample. Which according to the literature is said to be trisomy 16 rescue resulting in a mosaic of two different cell lines in the fetal sample submitted for CMA analysis. This pattern seen in this fetus is very unusual and rare and as per medical literature, only one report has been published on trisomy 18 rescue. Based on the available literature this was classified as Likely Pathogenic. Trisomy 16 rescue occurs due to very low-level mosaicism of two different diploid cell lines contributing to the multiple allele tracks. However, Fig.4 Whole Chromosome Painting (WCP) probes labelled with FITC, Rhodamine, and Aqua were utilized. These probes facilitates in depth assessment of chromosomes from interphase or metaphase cells, thereby enabling in identification of numerical as well as structural chromosomal aberrations with greater specificity and sensitivity. The analysis revealed that the WCP probes were negative for any abnormality as detected by probes for chromosome 16 (Fig 4.). This suggests that based on the tested probes, there were no apparent abnormalities or chromosomal aberrations involving chromosome 16 in the analysed sample.

CONCLUSION

In this study, we presented two compelling cases involving prenatal screening and diagnosis, focusing on trisomy 9 syndrome (Case 1) and mosaic trisomy 16 rescue (Case 2). These cases underscore the complexities and challenges in prenatal care, emphasizing the importance of integrating various diagnostic tools for a comprehensive evaluation. The thorough analysis of Case 1 revealed a chromosomal anomaly identified as trisomy 9 syndrome. The clinical assessment, ultrasonographic findings, and biochemical markers collectively contributed to a high-risk profile for trisomy 47,+9. Specific sonographic markers, such as the presence of pleural effusion, raised concerns about potential chromosomal abnormalities. Furthermore, the karyotype investigation confirmed the presence of an extra chromosome 9 in the fetal cells (47,+9). The decision to terminate the pregnancy was made following amniocentesis results, highlighting the emotional and complex choices individuals face in such challenging situations. Case 2 presented unique challenges in the karyotyping analysis. Initially indicating a seemingly normal chromosome complement, closer examination revealed uncertainty concerning the sex chromosomes (46, X? [30]). This uncertainty underscores the intricacies involved in chromosomal analysis and the need for further investigation to clarify the



**Sujithra Appavu et al.,**

nature of the chromosomal composition. In contrast, Whole Chromosome Painting (WCP) probes were negative for abnormalities involving chromosome 16, highlighting the importance of employing multiple diagnostic approaches. Case 2 further demonstrated the clear impact of chromosomally defective pregnancies on the decision of the parents to terminate the pregnancy. Both these case studies underscored the significance of early detection, thorough prenatal assessments, and genetic counseling in cases of suspected chromosomal abnormalities.

REFERENCES

1. M. Krivega, & Z. Storchova, "Consequences of trisomy syndromes-21 and beyond". *Trends in Genetics*, Vol. 39(3), pp. 172-174, 2023.
2. T. V. Bihunyak, Y. I. Bondarenko, O. O. Kulyanda, S. M. Charnosh, A. S. Sverstiuk, & K. O. Bihuniak, "Chromosomal Diseases In The Human Pathology," *International Journal of Medicine and Medical Research*, Vol. 6(1), pp. 50-60, 2020.
3. A. R. Victor, "Empirical Studies on the Evaluation of Current Embryo Selection Techniques in Human in-vitro Fertilization". University of Kent, United Kingdom, 2022.
4. W.D. Schwendemann, S.A. Contag, J.R. Wax, R. C. Miller, W. J. Polzin, P. P. Koty, & W. J. Watson, "Sonographic Findings in Trisomy 9". *J Ultrasound Med*; Vol. 28(1), pp. 39-42, 2009
5. A. A. Armstrong, S. L. Gaw, & L. D. Platt, "Mosaic Trisomies 8, 9, and 16. In Obstetric Imaging: Fetal Diagnosis and Care," *Elsevier*, pp. 617-620, 2018.
6. G. A. Machin, & J. A. Crolla, "Chromosome constitution of 500 infants dying during the perinatal period: With an appendix concerning other genetic disorders among these infants". *Humangenetik*, Vol. 23, pp. 183-198, 1974.
7. L. Zhou, H. Li, C. Xu, X. Xu, Z. Zheng, & S. Tang, "Characteristics and mechanisms of mosaicism in prenatal diagnosis cases by application of SNP array". *Molecular Cytogenetics*, Vol. 16(1), p. 13, 2023.
8. S. R., Kim, E. J. Choi, Y. J. Kim, T. Y. Kim, & Y. J. Lee, "Prenatally Diagnosed Rare Trisomy 16 Mosaicism in Human Amniotic Fluid Cells in the Second Trimester: A Case Report". *Development & Reproduction*, Vol. 22(2), p. 199, 2018.
9. C. Robberecht, T. Voet, G.E. Utine, A. Schinzel, N. de Leeuw, J. P. Fryns, & J. Vermeesch, "Meiotic errors followed by two parallel postzygotic trisomy rescue events are a frequent cause of constitutional segmental mosaicism". *Mol Cytogenet* Vol. 5, p. 19, 2012.
10. G. Coticchio, A. Barrie, C. Lagalla, A. Borini, S. Fishel, D. Griffin, & A. Campbell, "Plasticity of the human preimplantation embryo: developmental dogmas, variations on themes and self-correction". *Human reproduction update*, Vol 27(5), pp. 848-865, 2021.
11. A.Sallam, "A Qualitative Approach to Understanding the Attitudes of Maternal Fetal Medicine Specialists Regarding Prenatal Diagnosis, Disability and Termination," PhD diss., Yale University, 2021.
12. J. Roberts, "The visualised foetus: A cultural and political analysis of ultrasound imagery". Routledge, 2016.
13. Xu, M. Li, J. Peng, Y. Zhang, H. Li, G. Zheng, & D. Wang, "Case report: A case report and literature review of complete trisomy 9". *Frontiers in Genetics*, 14, 2023.
14. W. Sepulveda, I. Rojas, J. A. Robert, C. Schnapp, & J. L. Alcalde, "Prenatal detection of velamentous insertion of the umbilical cord: a prospective color Doppler ultrasound study". *Ultrasound in obstetrics & gynecology*, Vol. 21(6), pp. 564-569, 2003.
15. N. Bijok, J. Fiskari, R. R. Gustafson, & V. Alopaeus, "Chip scale modelling of the kraft pulping process by considering the heterogeneous nature of the lignocellulosic feedstock," *Chemical Engineering Research and Design*, Vol. 193, pp. 13-27, 2023.
16. C. Murta, A. Moron, M. Ávila, L. França, & P. Vargas, (2000). Reverse flow in the umbilical vein in a case of trisomy 9. *Ultrasound in Obstetrics and Gynecology: The Official Journal of the International Society of Ultrasound in Obstetrics and Gynecology*, Vol. 16(6), pp. 575-577.



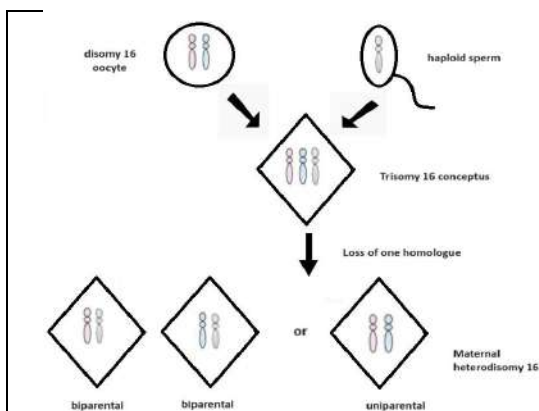
Sujithra Appavu *et al.*,

Fig 1. Trisomy Rescue Mechanism. The Above Illustration Indicates the Loss in one Homologue from the Trisomy Conceptus Attributing to Upd Among 1/3rd of The Cases. The Example Presented in this Case for Trisomy 16 Conceptus.



Fig. 2: Ultrasonographic Assessment (Right) and Karyotype of Fetus (Left) for Case Study on Complete T9 Viewed at 20th Gestational Week: Findings Present Agenesis of Cerebellar Vermis, Cranial Deformity, Nuchal Fold Change, Cardiomegaly, Multicystic Right and Left Kidney with Pyelectasis, Nuchal Fold Change and Severe Oligohydramnios. Conventional Karyotyping Revealed 47,X?,+9 (Right). Chromosome Analysis of Cultured Amniocytes Indicating The Presence of an Additional Copy of Chromosome 9, Suggestive of Trisomy 9

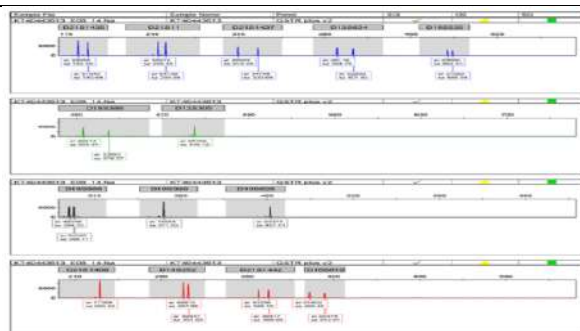


Fig. 3: Electrophoretogram : Case 1 Showed Electrophoretogram Analysis for Chromosome-Specific Markers Indicates a Normal Complement of 13, 18, 21 and Sex Chromosomes.

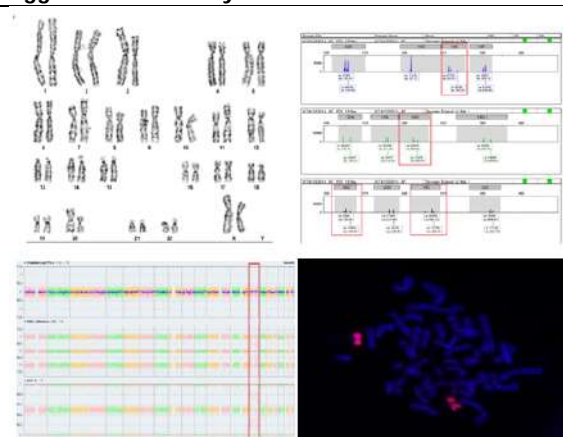


Fig 4 Prenatal Screening of Trisomy 16 Mosaic Rescue Case. Upper Right Presents 46,X? Chromosome Analysis of Cultured Amniocytes Revealed Normal Chromosome Complement; Upper Left Reported Str-Profile of the Fetus Showing Three Allele Peaks for Chromosome 16 Markers; Lower Left Image Presented Cma- Allele Tracks Showing Multiple Tracks on Chromosome 16 & Lower Right Showed Wcp Analysis on Case 2. Negative For Any Abnormality as Detected by Wcp Probes for Chromosome 16.





Recognizing the Consequences of Polycystic Ovarian Syndrome on Health - Related Quality of Life for use in Diagnostics

Janvika Varma¹, Aparna Pandey² and Urjitsinh Zala^{3*}

¹Research Scholar, Faculty of Science and Humanities, Department of Biochemistry, Sankalchand Patel University, Gujarat, India.

²Associate Professor, Faculty of Science and Humanities, Department of Biochemistry, Sankalchand Patel University, Gujarat, India.

³Assistant Professor, Department of Medical Laboratory Technology, ITM Vocational University, Vadodara, Gujarat, India.

Received: 02 Feb 2024

Revised: 09 Mar 2024

Accepted: 26 Apr 2024

*Address for Correspondence

Urjitsinh Zala

Assistant Professor,
Department of Medical Laboratory Technology,
ITM Vocational University,
Vadodara, Gujarat, India.
Email: urjit77.uz@gmail.com



This is an Open Access Journal / article distributed under the terms of the **Creative Commons Attribution License** (CC BY-NC-ND 3.0) which permits unrestricted use, distribution, and reproduction in any medium, provided the original work is properly cited. All rights reserved.

ABSTRACT

PCOS is not only a physical condition, but it also has significant psychological implications. Women with PCOS are more likely to experience anxiety, depression, and poor quality of life compared to women without the disorder. This report investigates the relationship between various factors and Poly-cystic Ovary Syndrome (PCOS) based on a survey conducted among patients diagnosed with PCOS and a control group. The factors examined include age, education level, occupation, marital status and PCOS duration. The results indicate potential correlations and provide valuable insights for understanding the impact of these factors on PCOS. The findings reveal that PCOS is more prevalent in younger age groups, particularly among women aged 23-33, aligning with previous research on the diagnosis of PCOS in women of reproductive age. Education level shows a possible association with PCOS, as a higher proportion of patients have completed college or hold a university degree compared to the control group. Occupation-wise, a significant portion of individuals with PCOS are engaged in full-time employment, while unemployment seems to have a lesser impact on PCOS occurrence. Marital status shows a higher prevalence of PCOS among married individuals, indicating potential hormonal and stress-related factors associated with reproductive health. The duration of PCOS varies, with a majority of patients living with the condition for 1 to 5 years. The findings suggest that education level, occupation, marital status, and personal connections may influence the occurrence and understanding of PCOS. Future research should



**Janvika Varma et al.,**

aim to further exploring these correlations and develop targeted interventions to address the unique needs of different age groups affected by PCOS.

Keywords: Poly-cystic Ovary Syndrome, Psychological implications, Life Quality, Women's health

INTRODUCTION

A complicated endocrine condition called poly-cystic ovary syndrome (PCOS) affects women across the world that are of reproductive age. A variety of clinical, hormonal, and metabolic characteristics, such as irregular menstrual periods, hyperandrogenism, insulin resistance, and ovarian dysfunction resulting in ovarian cyst development, define it. PCOS affects between 5% and 20% of women globally, however the precise prevalence is uncertain because it depends on the diagnostic criteria and population being investigated [1]. PCOS is not only a physical condition, but it also has significant psychological implications. In contrast to women without the condition, women with PCOS are more prone to experiencing depression, anxiety, and a poor quality of life. The psychological impact of PCOS can be severe, affecting relationships, social functioning, and overall well-being. According to studies, women experiencing PCOS are more likely to experience feelings of sadness or anxiety than women lacking the condition. They are additionally inclined to report having low self-esteem, body dissatisfaction, and lower sexual satisfaction [2]. The psychological impact of PCOS may be attributed to several factors. First off, PCOS's physical symptoms, such as obesity gain, sexual orientation, and acne, can make people feel self-conscious and low on self-worth. Second, PCOS-related hormonal abnormalities can have an impact on mood and emotional control. For example, high levels of androgen may lead to irritability and aggression, while low levels of estrogen can lead to feelings of depression and anxiety [3]. The impact of PCOS on fertility and reproductive function can be a significant source of stress for women with the disorder. Many women who suffer from PCOS battle with infertility and may need medical help to get pregnant. This can lead to feelings of isolation, anxiety, and depression. The purpose of the current study is to assess how PCOS affects women's quality of life in terms of their health and to shed light on the factors that influence this impact. The analysis was done by HRQoL. The HRQoL questionnaire is a useful tool for evaluating the impact of PCOS on the quality of life of affected individuals. The questionnaire takes into account various aspects of daily life that may be affected by PCOS, such as the ability to perform daily activities, social interactions, and emotional well-being. The researchers seek to obtain a thorough knowledge of PCOS by looking at how it affects these many facets of life. They also believe that doing so will help them design therapies that will enhance the health of those who are affected.

METHOD

Subjects

Researchers frequently carry out investigations to better understand the causes behind PCOS. One such study, which seeks to ascertain how PCOS affects impacted people's health-related quality of life (HRQoL), was carried out in Vadodara, India. The study recruited a total of 140 participants, including 110 PCOS subjects and 30 healthy individuals as a control group. The participants were selected from a broad range of age groups, between 14 to 40 years. In order to be included in the study, the participants must meet the Rotterdam criteria for PCOS, which require the presence of at least two of the following signs: medical and/or biochemical traits of poly-cystic ovaries, excess androgen, and ovulatory dysfunction. The participants were then asked to complete a questionnaire on their HRQoL. The data was collected over a period of three to five months, from July 2021 to November 2021, in collaboration with the Government Primary and Tertiary Health Care facility located in Vadodara city. The participants' emotional, mental, physical, and interpersonal wellness will be evaluated by way of a questionnaire on their HRQoL.





Questionnaire

The researchers plan to collect data using the self-report consuming and exercise examination (EEE) / health related quality of life questionnaire (HRQoL) (Çelik & Köse, 2021a). The EEE questionnaire is a well-established tool for assessing the impact of consuming and exercise patterns on various aspects of psychological, physical, and behavioural function over time. The HRQoL questionnaire will be incorporated within the EEE and was used to evaluate the impact of PCOS on the health-related quality of life of participants. The HRQoL questionnaire comprises 27 questions that assess 6 different factors. These factors include year of birth (3 questions), geographic origin (4 questions), marital status (5 questions), occupation (6 questions), education (6 questions) and duration of PCOS symptoms (3 questions). These questions are used to evaluate the physical, psychological, and social well-being of the participants. The data collected from the HRQoL questionnaire was analyzed and plotted generated through software to identify trends and patterns in the responses. The researchers used this data to identify potential areas of concern and develop targeted interventions to address these issues. The findings of this study contributed significantly to our understanding of how PCOS affects the quality of life of those who are affected and indirectly influenced the creation of strategies that would help these people achieve better health outcomes. The questions are listed here were used in the form for the present study (Table 1).

RESULTS AND DISCUSSION

Correlation of age with PCOS

Women of age to conceive are susceptible to the complicated hormonal condition known as polycystic ovarian syndrome (PCOS). While age itself is not a direct cause of PCOS, there may be a correlation between age and the manifestation and severity of PCOS symptoms. The participants of the current study are divided into three age groups based on their birth of year: 33 to 43; 23 to 33 and below 23 (Figure 1). In the patient group, the largest number of individuals fell into the 23-33 age range, with 52 participants, followed by the 33-43 age range, with 23 participants. The lowest number of patients was in the below 23 age range, with 25 participants. Conversely, in the control group, the distribution differed, with the maximum number of individuals falling into the 23-33 age range (35 %), followed by the below 23 age range (35 %). The smallest number of individuals in the control group was in the 33-43 age range, with 30 %. The distribution of age ranges suggests that PCOS is more prevalent in the younger age groups, particularly among those aged 23-33. This finding aligns with existing research indicating that PCOS is commonly diagnosed in women of reproductive age. The higher number of patients in the 23-33 age range may be attributed to the age at which PCOS symptoms typically manifest, leading individuals to seek medical attention and receive a diagnosis. In contrast, the control group exhibits a more even distribution across the age ranges, with no clear dominance in any category. This result suggests that PCOS may have a more significant impact on younger individuals compared to the general population. These results highlight the significance of early PCOS discovery, awareness, and management in women of reproductive age.

To fully understand how aging affects PCOS and to provide focused therapies that cater to the particular needs of the many age groups afflicted by this disorder, more study is required. PCOS can be diagnosed at any age after puberty. However, it is often diagnosed during a woman's reproductive years, typically between the ages of 15 to 30. Similar results observed in current study as shown in Figure 1. The diagnostic criteria for PCOS include clinical and/or laboratory evidence of menstrual irregularities, elevated androgen levels, and poly-cystic ovaries on ultrasound. An overview of poly-cystic ovarian syndrome (PCOS) in older women is given in the other paper is goes through PCOS symptoms, diagnostic standards, and long-term health hazards related to the illness. The report also summarizes the information that is currently known on PCOS's effects on patients' long-term health risks when they have reached reproductive age [4]. Although women with PCOS are more likely to have cardio-metabolic risk factors, the research contends that there is presently insufficient proof to conclude that older women with PCOS have higher rates of cardiovascular morbidity and death [5]. Uncertainty surrounds the average age of menopause in PCOS patients, however the anti-mullerian hormone (AMH) level may be a useful indicator of age-related ovulatory performance in PCOS patients with an-ovulatory cycles. The paper suggests that extensive prospective cohort studies should be



**Janvika Varma et al.,**

performed to explain morbidity and mortality in aging women having PCOS [4]. Teenage girls and young women with PCOS have hormonal abnormalities during their reproductive years, which can result in irregular periods, acne, weight gain, and excessive hair growth. Additionally, it increases the chance of developing type 2 diabetes, high blood pressure, and heart disease, as well as issues with fertility. PCOS is a frequent health issue that affects up to 22% of women overall and 5%–10% of various ethnic groupings. One in 15 women throughout the world is affected by this diverse endocrine condition [6].

Impact of geographic origin

The impact of geographic origin, such as urban, rural, inter-state, or tribal, on the prevalence of PCOS is not well-established and can vary among different populations. A combination of hormonal, environmental, and genetic variables affects PCOS. While several research have investigated the relationship between PCOS and geographical characteristics, it is crucial to interpret the results with caution and take into account the limits of the data at hand. Based on the self-answered questionnaire, we have determined the prevalence rate of PCOS in our study. Additionally, it is observed that the incidence rate in urban areas is higher than in rural areas. According to the poll, just 20–25% of individuals in rural areas were aware of PCOS, while 70–80% of girls in urban areas were. The geographic origin of individuals participated in current study is presented in Figure 2. One noteworthy finding from our research is that the frequency is lower in rural populations than in urban ones. Nonetheless, the fact that there are relatively fewer PCOS cases in rural areas may be the result of low or nonexistent exposure to pollution, junk food, and other endocrine disruptors, as well as lack of awareness. Additionally, girls in rural areas are less likely to rely on labour-saving appliances or automobiles for transportation, which helps them, maintain a healthy body mass index [7]. Limited data is available regarding the prevalence of PCOS in tribal communities. The lack of reports or studies may be due to several factors, including limited access to healthcare services, lower awareness of PCOS, cultural differences. Sometimes, such communities do not have a single reported/registered PCOS case as specific genetic and environmental factors are unique to these communities. Future studies are required to understand the prevalence and influence of PCOS within tribal populations. It is crucial to note that individual observations or subjective experiences may not accurately reflect the overall frequency of PCOS in specific geographic groups.

PCOS is a multifaceted condition, and multiple factors contribute to its development and prevalence. Large-scale, well-designed studies that account for various demographic, genetic, environmental, and lifestyle factors are necessary to establish a more thorough knowledge of the connection between geographic origin and PCOS. According to residency and race/ethnicity, the study estimates the prevalence of poly-cystic ovarian syndrome (PCOS) using data from other international studies. The prevalence of PCOS in the United States, the United Kingdom, Spain, Greece, Australia, and Mexico has been determined using the NIH's diagnostic criteria [8] (Wolf et al., 2018). To assess whether there is a substantial variation in the prevalence of PCOS among regions, racial or ethnic groups, the available data is unconvincing. This paper highlights the challenges in diagnosing PCOS, including the lack of universally used guidelines and evaluation methods with varying sensitivity [8] (Wolf et al., 2018). This article discusses about how poly-cystic ovarian syndrome (PCOS) manifests differently depending on ethnicity and race. Women of all races and ethnic origins can develop PCOS, a common endocrine condition. According to the report, two gene loci that were first discovered in Han Chinese women and then confirmed in women with European heritage. It is possible that PCOS is an old evolutionary feature, according to this [9]. The paper also highlights that PCOS phenotypic expression varies among different ethnic and racial groups. Women from North and South America, Europe, Asia, and the Middle East have been found to have different PCOS phenotype [10] [11]. For instance, although Hispanic women are more susceptible to metabolic syndrome (MetS) and type 2 diabetes mellitus (T2DM), women of African origin with PCOS are more likely to have risk factors for hypertension and cardiovascular disease (CVD) [12]. The author does point out that in younger populations; there could not be much variation in these reproductive or metabolic characteristics. Additionally, they explain how significantly ethnic variances in PCOS are determined by a person's genetic origin. Numerous potential areas have been found by genome-wide association studies, although it is still unclear how much these regions contribute to PCOS. This indicates that more study is necessary to determine the genetic and environmental variables that influence the occurrence and manifestation of PCOS in various racial and ethnic groups [13].



Janvika Varma *et al.*,**Correlation of education level with PCOS cases**

This report investigates the relationship between education level and the prevalence of PCOS. A sample of individuals, comprising both patients diagnosed with PCOS and a control group, was surveyed. The participants were classified into five education categories: Complete College, University Degree, Some College, Completed High School, and Primary School or less (results shown in table 2). The results were analyzed to determine the distribution of education levels among the surveyed individuals. The findings shed light on the potential impact of education on PCOS and provide valuable insights for future research and healthcare interventions. The results indicate that the distribution of education levels varies between the PCOS patients and the control group. Among the patients, the majority (45 %) completed college, while 18 % had a university degree. In comparison, the control group had 40% of individuals who completed college and only 10% with a university degree. The higher proportion of individuals with higher education levels among PCOS patients suggests a possible association between education and PCOS. It is noteworthy that the distribution of education levels in the control group was relatively similar across all categories, indicating a more evenly distributed educational background. In contrast, the PCOS patients showed a higher percentage of individuals with higher education levels. This observation could be due to a range of factors, including awareness and access to health-seeking behaviours or the influence of socioeconomic factors. It's crucial to take into account the limitations of this study though, the population as a whole might not be adequately represented by the sample size, and the results may be influenced by selection bias or other confounding variables not accounted for in this analysis. Additionally, the data presented here only provides a snapshot of the relationship between education and PCOS and does not establish causation or the direction of the relationship.

According to the study, women who had poor socioeconomic status (SES) as children are more likely to acquire PCOS. Even after accounting for age, BMI, waist circumference, and usage of oral contraceptives, the correlation between low SES and PCOS remained statistically significant. Additionally, the author discovered that PCOS was more common in women who had high personal education but poor parental education [14]. Only those who were obese, though, were statistically significant for the connection. According to the study, PCOS may develop as a result of long-term exposure to low SES. To fully comprehend the underlying processes driving this connection, more study is necessary [15]. A different author sought to determine how an educational program affected teenage girls' understanding of PCOS. In a research on the prevalence and knowledge of PCOS among female scientific students at various public universities in Quetta, all respondents, or 100% of them, had heard of the condition [16]. 96 female students participated in the study, which used a quasi-experimental research approach. An interviewing questionnaire and a knowledge evaluation instrument were used to gather the data. Most of the students had accurate understanding of the diagnosis, etiology, risk factors, complications, and treatment of PCOS after the educational session. In comparison to their pretest values, the post-test mean scores were much higher following the educational program. The study found that the educational program was successful in raising adolescent girls' awareness of PCOS [17].

Impact of occupation on PCOS

Occupation can have an impact on PCOS (Poly-cystic Ovary Syndrome) in various ways. The occupations were categorized in 5 major groups: employed- part-time and full-time, unemployed, homemaker and student (Figure 3). The patient group has a lower percentage of individuals who are unemployed compared to the control group. This suggests that unemployment may have a lesser impact on the occurrence of PCOS. The second lowest percentage of individuals was observed in the part-time employed group. The data suggests that 29% of the patients with PCOS are employed full-time. This indicates that a significant portion of individuals with PCOS were engaged in full-time employment. Among the patients with PCOS, 28% were home makers. The data indicates that 26% of the patients with PCOS are students. Here are some factors related to occupation that can influence PCOS. It is important to remember that different people might experience different effects, and not all individuals in the same occupation will have the same experience. PCOS is a result of several contributing factors, including diabetes, being obese, other hormonal imbalances [18, 19]. Expecting employment, insufficient judgment abilities, plus a lack of social interaction are all associated with a development of stressful conditions [19]. (Tsai & Liu, 2012). Employed women are more likely to develop PCOS than homemakers, since tension as either an indicator or a trigger of PCOS risk variables [20].





The study on the occupation ability of PCOS as compared to control was investigated by Kujanpaa et. al., (2022) [21]. Identifying PCOS-positive and PCOS-negative women in the Northern Finland Birth Cohort in 1966, assessing their self-rated work capacity and potential confounders at age 46, extracting incidence rate ratios (IRRs) for disability and unemployment days during a prospective 2-year follow-up, evaluating hazard ratios (HRs) for disability retirement between 16 and 52 years of age from national registers, and computing incidence rate ratios (IRRs) for PCOS-positive and PCOS-negative [21]. Women with PCOS judged their health as poorer and were more likely to be obese at age 46 than women without PCOS. Compared to women without PCOS, those with PCOS were also more likely to be on disability leave or jobless. In models adjusted for health and socioeconomic characteristics, the afflicted women accrued an extra month's worth of disability and unemployed days on average over the course of the two-year follow-up period, which corresponded to an approximately 25% greater risk for both conditions [22]. Finally, compared to non-PCOS women, the study discovered a two-fold increased cumulative risk for disability retirement by age 52 [21].

Association of marital status with PCOS

The survey data analyzed the association between marital status and PCOS. The participants were classified into four categories: Married/Common, Single, Separated, and Divorced (Figure 4). The count of individuals in each marital status category was recorded for both the PCOS group and the control group. The following discussion explores the observed results and their implications. Most individuals with PCOS in the survey (52%) were married. Lower percentage of individuals (45 %) found in control group (without PCOS). This recommends that a significant number of the PCOS individuals are in a committed relationship. The higher prevalence of PCOS among married individuals may be attributed to various factors, including hormonal changes associated with reproductive health, stress, and access to healthcare. Approximately 36% of the participants with PCOS were single. Similar observation was found in a control group with 35% of individuals. This indicates that a considerable number of individuals with PCOS are not currently in a committed relationship. The prevalence of PCOS among single individuals suggests that marital status may not be a determining factor in the progress or presence of PCOS. Other factors, such as genetics, hormonal imbalances, and lifestyle factors, may play more significant roles in PCOS occurrence among single individuals [23]. A small proportion (8%) of the surveyed individuals with PCOS reported being separated. However, the insufficient sample volume of this group necessitates caution in interpreting this finding. Whereas, 20 % of participants were found to be separated in control group. Only 4% of the individuals with PCOS in the survey reported being divorced. The small number of divorced individuals limits the conclusions that can be drawn from this finding. It is hard to conclude a strong association between divorce and PCOS based on this limited sample size.

Future studies with a larger and more diverse sample are needed to explore this relationship further. Based studies indicate that infertility might be a greater concern for infertile women than PCOS, although the condition may have detrimental impacts on several facets that affect individuals. Moreover, PCOS will not be the only factor affecting infertile female social support along with satisfaction in marriage [24]. The contradicting results were observed in another study. The study presented a cross-tabulation of marital status in both normal and PCOS groups. The normal group had 30 married and 20 unmarried females, while the PCOS group had 14 married and 36 unmarried females. The study found a correlation between marital status and PCOS, with a higher percentage of unmarried females in the PCOS group [25]. In the other research, infertile women with and without polycystic ovarian syndrome (PCOS) had their marital satisfaction and social support levels evaluated and compared. Between July and September 2015, the study was carried out at the Royan Institute, a referral reproductive clinic in Tehran, Iran. There were 150 infertile women with PCOS and 150 infertile women without PCOS in total. The Multidimensional Scale of Perceived Social Support (MSPSS) and the ENRICH Marital contentment Scale were used, respectively, to measure social support and marital contentment. The study's findings revealed that when it comes to social support and marital happiness, infertile women with or without PCOS do not significantly vary from each other. According to the study's findings, infertility could possibly be more significant for infertile women than PCOS, despite the possibility that PCOS may have detrimental impacts on several elements of suffering individuals [26] (Navid et al., 2018). There were notable distinctions among married and single PCOS patients concerning overall health ($P < 0.001$), physical wellness ($P < 0.027$), responsibilities resulting from medical conditions ($P < 0.006$), a part restrictions resulting from psychological



Janvika Varma *et al.*,

issues ($P < 0.002$), distress ($P < 0.001$), functioning in society ($P < 0.001$), energy/fatigue, along with psychological state [27].

PCOS duration of the patient group

The survey data includes the duration of PCOS among the patient group. The distribution of PCOS duration is represented in figure 5. Approximately 26% of the patients with PCOS in the survey reported having the condition for less than 1 year. This suggests that a significant proportion of individuals with PCOS are relatively new to the diagnosis. The majority, about 67%, of the patients with PCOS in the survey reported having PCOS for a duration ranging from 1 to 5 years. This indicates that a significant number of individuals have been living with PCOS for a moderate duration. Only 7% of the patients reported having PCOS for more than 5 years. This suggests that a smaller proportion of individuals with PCOS have been dealing with the condition for an extended period. A study published by Moran *et al.* (2010) [28] investigated the duration of PCOS among a large cohort of women. They found that 33% of the participants had been diagnosed with PCOS within the past year, indicating a relatively recent diagnosis. This finding is consistent with the 26% of patients in the survey reporting PCOS duration of less than 1 year [28] (Moran *et al.*, 2010). PCOS was identified in 77.1% in subjects, including an average age population ranging from eighteen to twenty years during the period of assessment [29]. Additionally, a study by Trent *et al.* (2003) [30] published in *Fertility and Sterility* examined the duration of PCOS in a population of women seeking fertility treatment. They reported that 57% of the women had been diagnosed with PCOS for less than 5 years, which is comparable to the 67% of patients in the survey reporting a PCOS duration of 1 to 5 years [31].

CONCLUSION

This report presents the findings from a survey investigating the correlation of age, education level, occupation, marital status and PCOS duration with the prevalence and understanding of Polycystic Ovary Syndrome (PCOS). The results highlight several key correlations and provide valuable insights into the impact of these factors on PCOS. The distribution of age groups among the participants suggests that PCOS is more prevalent in younger age groups, aligning with previous research indicating that PCOS is commonly diagnosed in women of reproductive age. The education level of individuals with PCOS shows a possible association, with a higher proportion having completed college or holding a university degree compared to the control group. Occupation-wise, a significant number of individuals with PCOS are employed full-time, indicating potential implications of occupational factors on PCOS occurrence. Marital status reveals a higher prevalence of PCOS among married individuals, possibly linked to hormonal changes associated with reproductive health, stress, and access to healthcare. The duration of PCOS varies among patients, with a considerable proportion being relatively new to the diagnosis, while others have been living with the condition for a moderate duration. In conclusion, this study provides valuable insights into the correlation between age, education level, occupation, marital status and PCOS duration with the prevalence and understanding of PCOS. The findings emphasize the importance of early detection, awareness, and management of PCOS, particularly among younger individuals. Further research is needed to comprehensively explore these correlations and develop targeted interventions to address the unique needs of different age groups affected by PCOS.

REFERENCES

1. Ndefo, U. A., Eaton, A., & Green, M. R. (2013). Polycystic ovary syndrome: a review of treatment options with a focus on pharmacological approaches. *P & T: A Peer-Reviewed Journal for Formulary Management*, 38(6), 336–355. <http://www.ncbi.nlm.nih.gov/pubmed/23946629>
2. Sadeghi HM, Adeli I, Calina D, Docea AO, Mousavi T, Daniali M, Nikfar S, Tsatsakis A, Abdollahi M. Polycystic Ovary Syndrome: A Comprehensive Review of Pathogenesis, Management, and Drug Repurposing. *International Journal of Molecular Sciences*. 2022;23(2):583.





Janvika Varma et al.,

3. Tabassum F, Jyoti C, Sinha HH, Dhar K, Akhtar MS. Impact of polycystic ovary syndrome on quality of life of women in correlation to age, basal metabolic index, education and marriage. PLOS ONE. 2021;16(3).
4. Çelik Özlem, Köse MF. An overview of polycystic ovary syndrome in aging women. Journal of the Turkish-German Gynecological Association. 2021;22(4):326-33.
5. Helvaci N, Yildiz BO. Polycystic ovary syndrome and aging: Health implications after menopause. Maturitas. 2020;139:12-9.
6. Mohamed HAA. Effect of educational program on the level of knowledge regarding polycystic ovarian syndrome among adolescent girls. Journal of Nursing Education and Practice. 2016;6(10).
7. Vidya Bharathi R, Swetha S, Neerajaa J, Varsha Madhavica J, Janani DM, Rekha S, S. R, B. U. An epidemiological survey: Effect of predisposing factors for PCOS in Indian urban and rural population. Middle East Fertility Society Journal. 2017;22(4):313-6.
8. Wolf W, Wattick R, Kinkade O, Olfert M. Geographical Prevalence of Polycystic Ovary Syndrome as Determined by Region and Race/Ethnicity. International Journal of Environmental Research and Public Health. 2018;15(11):2589.
9. Rosenfield RL, Ehrmann DA. The Pathogenesis of Polycystic Ovary Syndrome (PCOS): The Hypothesis of PCOS as Functional Ovarian Hyperandrogenism Revisited. Endocrine Reviews. 2016;37(5):467-20.
10. VanHise K, Wang ET, Norris K, Azziz R, Pisarska MD, Chan JL. Racial and ethnic disparities in polycystic ovary syndrome. Fertility and Sterility. 2023;119(3):348-54.
11. Chiaffarino F, Cipriani S, Dalmartello M, Ricci E, Esposito G, Fedele F, La Vecchia C, Negri E, Parazzini F. Prevalence of polycystic ovary syndrome in European countries and USA: A systematic review and meta-analysis. European Journal of Obstetrics & Gynecology and Reproductive Biology. 2022;279:159-70.
12. Wijeyaratne CN, Dilini Udayangani S, Balen AH. Ethnic-specific polycystic ovary syndrome: epidemiology, significance and implications. Expert Review of Endocrinology & Metabolism. 2013;8(1):71-9.
13. Dumesic DA, Oberfield SE, Stener-Victorin E, Marshall JC, Laven JS, Legro RS. Scientific Statement on the Diagnostic Criteria, Epidemiology, Pathophysiology, and Molecular Genetics of Polycystic Ovary Syndrome. Endocrine Reviews. 2015;36(5):487-25.
14. Rubin KH, Andersen MS, Abrahamsen B, Grintborg D. Socioeconomic status in Danish women with polycystic ovary syndrome: A register-based cohort study. Acta Obstetrica et Gynecologica Scandinavica. 2018;98(4):440-5.
15. Merkin SS, Azziz R, Seeman T, Calderon-Margalit R, Daviglius M, Kiefe C, Matthews K, Sternfeld B, Siscovick D. Socioeconomic Status and Polycystic Ovary Syndrome. Journal of Women. 2011;20(3):413-9.
16. Haq, Noman & Khan, Zarmina & Riaz, Sohail & Nasim, Aqeel & Shahwani, Razzaq & Tahir, Maria. Prevalence and Knowledge of Polycystic Ovary Syndrome (PCOS) Among Female Science Students of Different Public Universities of Quetta, Pakistan. "Imperial Journal of Interdisciplinary Research (IJIR). 2017;. 3: 385-392.
17. Mohamed HAA. Effect of educational program on the level of knowledge regarding polycystic ovarian syndrome among adolescent girls. Journal of Nursing Education and Practice. 2016;6(10).
18. M M. The Relationship between Job Stress and Musculoskeletal Disorders among Midwives. Ergonomics International Journal. 2023;7(3).
19. Tsai Y-C, Liu C-H. Factors and symptoms associated with work stress and health-promoting lifestyles among hospital staff: a pilot study in Taiwan. BMC Health Services Research. 2012;12(1).
20. Arefi MF, Pajohideh Z, Teimori-Boghsani G, Babaei-Pouya A. Is the Risk of Polycystic Ovary Syndrome among Working Women Higher and Vice Versa? The Open Public Health Journal. 2022;15(1).
21. Kujanpää L, Arffman RK, Vaaramo E, Rossi H-R, Laitinen J, Morin-Papunen L, Tapanainen J, Ala-Mursula L, Piltonen TT. Women with polycystic ovary syndrome have poorer work ability and higher disability retirement rate at midlife: a Northern Finland Birth Cohort 1966 study. European Journal of Endocrinology. 2022;187(3):479-88.
22. Karjula S, Morin-Papunen L, Auvinen J, Ruokonen A, Puukka K, Franks S, Järvelin M-R, Tapanainen JS, Jokelainen J, Miettunen J, Piltonen TT. Psychological Distress Is More Prevalent in Fertile Age and Premenopausal Women With PCOS Symptoms: 15-Year Follow-Up. The Journal of Clinical Endocrinology & Metabolism. 2017;102(6):1861-9.





Janvika Varma et al.,

23. De Leo V, Musacchio MC, Cappelli V, Massaro MG, Morgante G, Petraglia F. Genetic, hormonal and metabolic aspects of PCOS: an update. *Reproductive Biology and Endocrinology*. 2016;14(1).
24. Bagheri Lankarani N. Marital satisfaction and social support in infertile women with and without polycystic ovary syndrome seeking assisted reproduction. 2017;.
25. Manzoor I, Bacha R, Gilani SA. Sonographic association of polycystic ovaries with intraovarian arterial pulsatility and resistive index. *Gynecological Endocrinology*. 2019;35(10):851-3.
26. Navid B, Mohammadi M, Sasannejad R, Aliakbari Dehkordi M, Maroufizadeh S, Hafezi M, Omani-Samani R. Marital satisfaction and social support in infertile women with and without polycystic ovary syndrome. *Middle East Fertility Society Journal*. 2018;23(4):450-5.
27. Tabassum F, Jyoti C, Sinha HH, Dhar K, Akhtar MS. Impact of polycystic ovary syndrome on quality of life of women in correlation to age, basal metabolic index, education and marriage. *PLOS ONE*. 2021;16(3).
28. Moran LJ, Misso ML, Wild RA, Norman RJ. Impaired glucose tolerance, type 2 diabetes and metabolic syndrome in polycystic ovary syndrome: a systematic review and meta-analysis. *Human Reproduction Update*. 2010;16(4):347-63.
29. Tiwari A, Mathur A. Prevalence of polycystic ovary syndromes (PCOS) in adolescent girls and young women: A questionnaire-based study. *Indian Journal of Obstetrics and Gynecology Research*. 2023;10(3):330-4.
30. Trent ME, Rich M, Austin S, Gordon CM. Fertility Concerns and Sexual Behavior in Adolescent Girls with Polycystic Ovary Syndrome. *Journal of Pediatric and Adolescent Gynecology*. 2003;16(1):33-7.
31. Mohamed HAA. Effect of educational program on the level of knowledge regarding polycystic ovarian syndrome among adolescent girls. *Journal of Nursing Education and Practice*. 2016;6(10).

Table 1: List of questions included in survey form

Sankalchand Patel University, Visnagar	
Questionnaire form for PCOS Patients	
1) Registration No:	
2) Patient's Name:	
3) DEMOGRAPHIC AND OTHER VARIABLES OF PATIENTS WITH PCOS	
Variable	
Year of birth:	
1	1980 to 1990
2	1990 to 2000s
3	2000s to 2021
Geographic Origin:	
1	Urban Patients
2	Rural Patients
3	Inter-state Patients
4	Tribal Patients
Marital Status:	
1	Married/Common
2	Single
3	Separated
4	Divorced





Janvika Varma et al.,

Occupations:	
1	Employed full-time
2	Employed part-time
3	Unemployed: a) Looking for job b) Not looking for job
4	Home maker
5	Students
Education (the highest level):	
1	Primary School or less
2	Completed High School
3	Some College
4	Complete College
5	Some University
6	University Degree
Duration of PCOS Symptoms	
1	Less than 1 years
2	1-5 years
3	> 5 years

Table 2: Level of education in surveyed individuals.

Education	Patients	Control
Complete College	45	40
University Degree	18	10
Some College	17	20
Completed High School	17	15
Primary School or less	3	15

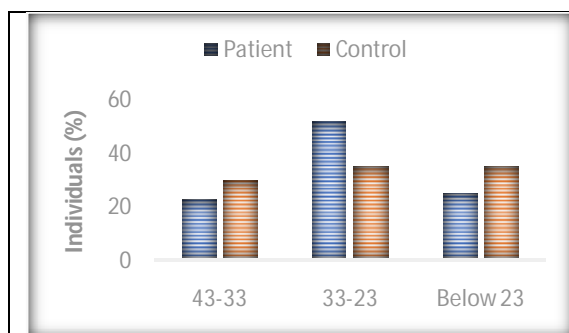


Figure 1: Age of the individuals participated in study.

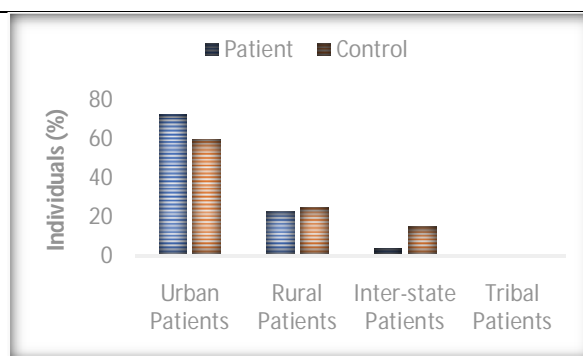


Figure 2: The geographic origin of the individuals



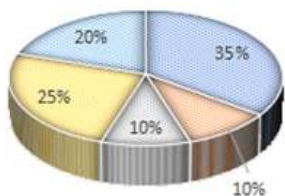


Figure 3: Analysis of occupation impact with PCOS (B)

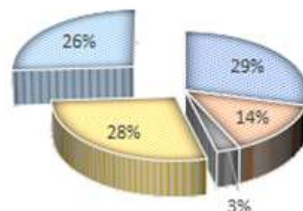


Figure 3: without PCOS (A).

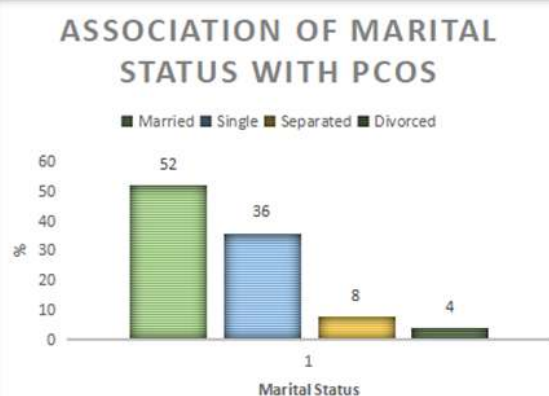


Figure 4: Analysis of Association of marital status with PCOS

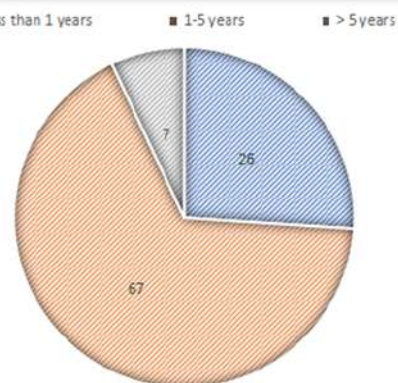


Figure 5: Duration of PCOS symptoms in percentage.





Chemistry and Bioactivity of *Crocus sativus* L. As an Active Ingredient of Cosmetics and Pharmaceuticals

Ruchi Kohli¹, Amit Mittal² and Anu Mittal^{1*}

¹Assistant Professor, Department of Chemistry, Guru Nanak Dev University College, Punjab, India.

²Professor, Department of Pharmaceutical Chemistry, Lovely Professional University, Punjab, India.

Received: 30 Jan 2024

Revised: 09 Feb 2024

Accepted: 26 Apr 2024

*Address for Correspondence

Anu Mittal

Assistant Professor,
Department of Chemistry,
Guru Nanak Dev University College,
Punjab, India.
Email: anuchem.patti@gndu.ac.in



This is an Open Access Journal / article distributed under the terms of the **Creative Commons Attribution License** (CC BY-NC-ND 3.0) which permits unrestricted use, distribution, and reproduction in any medium, provided the original work is properly cited. All rights reserved.

ABSTRACT

This review explores the pharmacological and cosmetic properties of *Crocus Sativus* L. (saffron) which is crucial to harness its potential for developing effective medications and skincare products. The bioactive components of plant (crocin, crocetin, picrocrocin, safranal) are discussed with focus on their structure, properties, synthetic pathways, and methods of extraction of bioactive compounds from saffron. The research work offers valuable insights on the practical applications and effectiveness of saffron in cosmetics as astringent, antioxidant, anti-inflammatory and in herbal medicine as neuroprotective, anticonvulsant, antidepressant, anticarcinogenic, antidiabetic, antihypertensive, antimutagenic agent. Future prospects involve need for more refined research to explore neuroprotective action or risk factors of using saffron for brain related disorders, the incorporation of saffron extract in drug formulations, its genetic improvement and to understand the exact mechanism of action of bioactive components of saffron.

Keywords: *crocus sativus*, saffron, antioxidant, crocin, safranal, crocetin, anticancer

INTRODUCTION

Saffron, the ancient, blooming perennial plant botanically classified as *Crocus Sativus* L., belonging to Iridaceae family, derives its nomenclature from French word Safran. This term traces its roots to the latin word Safranum, itself derived from Arabic word za'faran signifying the colour "Yellow" [1,2]. Around 80% of the global saffron production emanates from Iran, with additional cultivation observed in other countries such as china, Pakistan, France, Greece, Switzerland, Spain, India and Italy [3]. India accounts for a mere 5% of the World's total saffron production, with the districts of Pulwama and Budgam districts in J&K contributing a substantial 90% of country's saffron output. Nearly

75720



**Ruchi Kohli et al.,**

36000 flowers yield 1 pound of stigmas while the dried counterparts from roughly 70000 flowers result in 500 g pristine saffron. Valued at \$ 40-50 per gram saffron stands as the preeminent spice globally, often acclaimed as “red gold” or the “golden condiment” [4,5]. Saffron commands high price because of its short blooming season (~ 3 weeks in the fall) necessitating manual harvesting. The cultivation of *Crocus sativus* is labour intensive and time-consuming. *Crocus sativus* is the most researched species responsible for producing saffron and its associated health benefits. Featured in medicinal plant catalogs and European pharmacopoeias, saffron contributed to myriad compound formulations spanning 16th to 20th centuries. The plant's medicinal and pharmaceutical significance waned with the emergence of synthetic drugs from chemical synthesis. Nonetheless, contemporary endeavours aim to reaffirm saffron's recognized bioactivity, sparking renewed interest. This review mainly outlines the major phytochemicals in *Crocus sativus*, their extraction techniques and wide range of bioactivities as an active ingredient in cosmetics and pharmaceuticals.

DISCUSSIONS

About the plant

The botanical classification and common names of *Crocus Sativus* are described in table 1 and 2 respectively [6]. The stemless and triploid nature of *C. Sativus* renders it sterile [7]. It is a herb with circular corm beneath the soil measuring 3-5 cm in diameter. The plant propagates by corms vegetatively. Exhibiting 6-8 grass like leaves it develops short sprinkle roots at the corm's base and the perimeter, culminating in the emergence of light purple coloured flower as the first visible feature of the plant [8]. The homogeneous violet hue of the three sepals and petals renders them indistinguishable. There are three stamens with filaments twice as long as the anthers. A slender, light yellow style emerges from the flower's central ovary, culminating in three vibrant red stigmas measuring 2-3 cm. These stigmas, founts of saffron, are manually harvested -25-30 mm each-from every flower [9]. The cultivation and production of saffron face challenges as the plant thrives in arid deserts yet demands substantial water. The irrigation in such desolate regions is costly and droughts result in crop losses.

Chemical composition of *Crocus Sativus* L. and important apocarotenoids

Many researches focus on analyzing the composition of saffron and identifying its active phytochemicals. Over 150 volatile and non-volatile compounds have been found in saffron, from which less than 50 have been identified [11]. Terpenoids and terpene alcohols are the main volatile components, including safranal which possesses therapeutic applications. A variety of volatile components such as 4,4-dimethyl-2-cyclopenten-1-one, Alpha-Pinene, 1-carboxaldehyde-5,5-dimethyl-2-methylene-3-cyclohexene, eucarvone, heptanal, alpha-Isophorone, hexadecanoic acid, tetradecanoic acid, 10,13-octadecadienoic acid, methyl ester, 4,8,12,16-tetramethylheptadecan-4-olide and other components in low quantities have been determined with ultrasound-assisted extraction (UAE) along with dispersive liquid liquid microextraction (DILLME) technique coupled with gas chromatography mass spectrometry (GCeMS) technique, only a small fraction out of several volatile compounds occurring in saffron contribute to the overall aroma. Safranal, 4-ketoisophorone and dihydrooxophorone have been reported to be the most prevailing aroma active compounds of Iranian saffron as analyzed by GCeMS olfactometry [12, 13]. On the other hand, non-volatile constituents include picrocrocin, crocetin, and crocin responsible for saffron's bitter taste, aroma and distinctive colour respectively [14]. Stigma of the saffron contains bioactive compounds including anthocyanins, flavonoids, pigments, volatile fragrant essences, and vitamins including minerals, vitamins, carbohydrates, in addition to primary phytochemicals picrocrocin, phenol, delphinidin, safranal, kaempferol, crocetin with strong bioactivity and antioxidant potential [15]. The quality of saffron is decided by a variety of factors including chemical profile, concentration of major components, climate, soil composition, geographic location, genetic traits, cultivation conditions, and processing and storage methods [16]. Researches on saffron stability depict temperature and humidity has an impact on the degradation of active components of saffron. Proximate analysis of primary chemical components of saffron is depicted in table 3 [5]. The concentration of each component varies with soil fertility, cultivation origin, and growing conditions. Saffron's whole flower and spice bio residues have low fat and high minerals and carbohydrate content. Whereas, stamens have high lipids and proteins content and low carbohydrate



**Ruchi Kohli et al.,**

content. The four major bioactive compounds in saffron are crocin (dicarboxylic acid ester), crocetin (a natural carotenoid dicarboxylic acid), picrocrocin (iridoid glycoside precursor of safranal) and safranal

Crocin

Systematic (IUPAC) name: 8, 8-diapo-8, 8-carotenoic acid.

It is most important water-soluble carotenoid compound (approx. 80%) responsible for red color of saffron. It is 8,8-diapocarotene-8,8-dioic acid and with chemical formula: $C_{44}H_{70}O_{28}$ and molecular weight of 976.96 g/mol, it consists of a central zeaxanthin molecule with two glucose molecules attached to it [17]. It is dicarboxylic acid ester of the polyene carotenoid crocetin, which makes up 10% of the dry weight of saffron. The chemical structure of crocin contains central crocetin molecule, which is flanked by two units of gentiobiose, a disaccharide of glucose. It is a symmetrical molecule with a long, flexible carbon chain that contains conjugated double bonds. Contrary to safranal, crocins (crocin-1 or a-crocin or digentiobioside crocetin, crocin-2 or tricrocin or gentioglucoside crocetin, crocin-3 or gentiobioside crocetin, crocin-4 or glucoside crocetin, crocin-5 or diglucoside crocetin) are stable under ambient conditions. α -Crocins or Crocin 1 directly crystallized at a melting point of 186 °C and isolated in pure form.

Crocetin

It is 8,8'-diapocarotenedioic acid. It is a dicarboxylic acid with chemical formula $C_{20}H_{24}O_4$ formed by hydrolysis of crocin and is a derivative of carotenoid zeaxanthin. The oxidative degradation of zeaxanthin precursor leads to crocetins (α -crocetin or crocetin I, crocetin II, β -crocetin, g-crocetin); which after breaking, produce crocetin. It is composed of central cyclohexene ring, with two carboxylic acid groups attached to it. It has conjugated double bonds, responsible for its bright color and gives distinctive aroma of saffron. Its melting point is 285° C and a molecular weight of 328.4 g/mol [18].

Picrocrocin

Chemically it is 4-(β -D-glucopyranosyloxy)-2, 6,6-trimethylcyclohex-1-ene-1- carboxaldehyde. It is the second most abundant component (approximately 1% to 13% of saffron's dry matter), responsible for the bitter flavour of saffron. The molecule with chemical formula of $C_{16}H_{26}O_7$ and molecular weight of 330.37 g/mol, is an iridoid glycoside responsible for bitter taste of saffron [3]. It is formed by hydrolysis of a glucose molecule from its precursor safranal. Chemical structure of picrocrocin is composed of crocetin molecule linked to a molecule of glucose. The crocetin unit in picrocrocin is composed of eight isoprene units, arranged in a unique pattern of alternating double and single bonds. The glucose moiety in picrocrocin is a six-carbon sugar molecule attached to crocetin unit through an ether bond. The presence of glucose unit makes picrocrocin hydrophilic and soluble in water. It is a precursor of saffron aroma components (safranal and HTCC: 4-hydroxy-2,6,6-trimethyl-1-cyclohexen-1- carboxaldehyde).

Safranal

Chemically it is 2,6,6-trimethyl-1,3-cyclohexadiene-1-carboxaldehyde. It is a monoterpene aldehyde and aglycon of picrocrocin having molecular formula $C_{10}H_{14}O$, has molecular weight of 150. 21 g/mol and is the main terpenoid compound of the saffron's distilled essential oil, responsible for the aroma of saffron [19]. It is formed by oxidative degradation (de-glucosylation) of picrocrocin. Its chemical structure consists of a monocyclic ring system with a conjugated aldehyde group (CHO) and an isopropyl side chain. In some samples, up to 70% of the total volatile fraction of saffron is proposed to be in the form of safranal. The Safranal represents approximately 30 to 70% of essential oil and 0.001 to 0.006% of dry matter

METHODS OF OBTAINING APOCAROTENOIDS FROM SAFFRON

A number of hypotheses have been proposed on the methods of obtaining apocarotenoids from saffron. The first theory proposes protocrocin (glycosyl derivative of zeaxanthin) has oxidase enzyme which degrades it into two molecules of picrocrocin and one molecule of crocin [20]. Moreover, safranal is detected in minimum level in fresh stigmas of saffron. Fallahi et al. suggested another pathway in which saffron apocarotenoids are formed by cleavage of carotenoid (zeaxanthin and β carotene) by dioxygenases. Cleavage leads to crocetin and hydroxyl- β -cyclocitral. Afterwards, glucosylation by glycosyltransferases, hydroxyl - β -cyclocitral forms picrocrocin, crocetin forms crocin.



**Ruchi Kohli et al.,**

Finally, safranal is produced by hydrolysis of picrocrocin [21]. The hypothesis proposed by Sereshti et al. is also consistent with that suggested by Fallahi et al. zeaxanthin is cleaved by *Crocus sativus* Zeaxanthin cleavage deoxygenase to form crocetin dialdehyde and hydroxyl- β -cyclocitral (HTCC). HTCC follows two pathways: 1. by action of heat it forms safranal directly, releasing H^+ and OH^- . 2. It converts to picrocrocin by the action of UDPG-glucosyltransferase [22]

Conventional and novel techniques for extraction of bioactive compounds of *Crocus Sativa* L.

The extraction of bioactive compounds of saffron is crucial for their utilization in food, pharmaceutical and cosmetic industries. To extract bioactive compounds from saffron, there is a need for an economically and environmentally viable method. It is challenging to extract, isolate and characterize these elements as they are sensitive to temperature, light and humidity [23]. The traditional methods (steam distillation, hydro distillation, maceration, soxhlet and solvent extraction) of saffron extraction are costly, time consuming, employ large volumes of organic solvents, challenging to achieve high purity extracts, result in low yield and sometimes breakdown heat sensitive bioactive compounds [24]. However, modern extraction techniques such as ultrasound assisted extraction, microwave assisted extraction, high hydrostatic pressure extraction, pulsed electric field extraction, enzyme assisted extraction have reduced extraction time, increased yield of bioactive compounds and minimized the use of organic solvents and heat exposure and efficiently extract bioactive components of saffron [25,26]. The choice of extraction technique depends on factors like the type of bioactive compound, the desired yield and the cost effectiveness of the extraction process. Figure 6 shows various conventional and novel methods for extraction of bioactive compounds of saffron.

Cosmetology uses of saffron

Saffron cherished for its cosmetic purposes since ancient times, plays pivotal role in conventional Iranian and Greek medicine. Renowned for enhancing the skin tone and healing erysipelas, it effectively manages psoriasis. In traditional Greek medicine, saffron not only refresh facial skin but also treat skin diseases, acne, wounds. Saffron imparts eternal youthful properties making body younger and radiant. Rich in compounds such as crocin, safranal and picrocrocin, saffron unfolds a spectrum of cosmetic potential. Crocin serves as anti-dark spot and antioxidant, safranal as perfume, while combined action of safranal, crocin and Crocetin exhibits anti-UV, anti-inflammatory and pigmentary actions. Additionally, presence of vitamin C, zinc and flavonoids imparts face toning properties, crocin, crocetin and kaempferol contribute to anti-wrinkle benefits. Saffron's inclusion in herbal cosmetics is attributed to its astringent activity, making it valuable asset in pursuit of skincare excellence.

Anti-UV Agent

Saffron rich in carotenoids like crocin, crocetin and zeaxanthin, possess antioxidant properties that may shield the skin from the detrimental effects of free radicals and UV radiation. Saffron lotion, potentially superior to homosalate, acts as an effective sunscreen, diminishing sunburn, wrinkles, dryness, sagging, skin ageing and also provide natural radiance. Numerous studies indicate photoprotective effects of these carotenoids [27,28].

Reduce hyperpigmentation

Saffron formulations exhibit skin lightening effects, reduce hyperpigmentation and exert anti rhythmic effect on human skin. Crocin in saffron suppresses synthesis of excess melanin. While its antioxidant and antiinflammatory attributes aid in diminishing dark spots by inhibiting tyrosinase activity[29].

Anti-Aging Effect and Diseases of the Skin

Basil leaves and saffron diminish imperfections like acne. Saffron soaked strands in olive oil or virgin coconut oil etc serve to exfoliate and promote blood circulation. A formulation containing 3% C. Sativus is anticipated to decrease the expression of inflammatory markers including TNF and interleukin, rendering it efficacious for melanoma treatment [30].



**Ruchi Kohli et al.,****Perfumery**

Red gold saffron is most ancient perfume ingredient. Employed in ancient Greece, Rome and Egypt, it served as single note perfume as well as in complex blends. Its aromatic essence adorned temples and is a valued addition to both feminine and masculine fragrances [31].

As natural pigment in cosmetics

Various plant pigments like chlorophyll from green leaves, curcumin, carotenoids from pepper have been employed for centuries to colour the cosmetics and food. The high cost of saffron limited its application in cosmetics; nonetheless it serves as a substitute to tetrazine and turmeric in scenarios where the latter is susceptible to light induced fading [32].

Face Toner

Pistil of *C. sativus* function as potent face toner as it contains Vitamin C, Zinc and flavonoids which treat facial skin [33]. Vitamin C treats hyper pigmentation, Zinc aids in transportation of vitamin A through retinol binding protein, while Flavonoids serve as depigmenting and skin brightening agents, inhibiting tyrosinase activity during melanogenesis [34].

Pharmacological activities of saffron

Saffron, highlighted in the ancient prescriptions of Unani, Ayurveda, Chinese and homeopathic medicines boasts promoting therapeutic potential for health promotion and disease management. Various parts of Saffron specifically leaf, corn, stigma, tepals contain bioactive compounds that modulate physiological and biological processes, leading to health benefits. Additionally, saffron has longstanding medicinal roles in Ayurvedic, Tibetan, Persian and Chinese medicine as digestive aid, anticonvulsant, anticancer and antidepressant [4,5]

Treating sexual dysfunction

saffron exhibits remarkable sexual enhancement effects, with Persian saffron historically employed for its aphrodisiac properties dating back to Cleopatra times. Recognized as a natural aphrodisiac, saffron positively influences sexual performance and fertility in both men and women. Its usage results in improvement of erectile dysfunction and intercourse satisfaction in men [35]. Notably safe and effective, saffron proves beneficial in ameliorating fluoxetine induced sexual dysfunction in women in domains of arousal, lubrication and pain. Due to the above-mentioned health benefits, it is also called "love spice". Saffron significantly improves period symptoms, prevents polycystic ovarian syndrome and serves as a remedy for menstrual pain and menopausal problems.

Antidepressant

Depression a widespread affliction affecting 11.6% of the global population is predicted to be second leading cause of overall disability by 2020[36]. The petals and stigmas of saffron are equally effective in treating mild to moderate depression by inhibiting certain brain neurotransmitters like serotonin [37].

Anticarcinogenic

The potential anti tumor and anti-cancer properties of saffron and its components (particularly carotenoids) have been explored in various studies. Combining saffron extract with synthetic compounds like sodium selenite and sodium arsenite shows a synergistic effect in preventing cancer through chemotherapy [38]. Botsoglou demonstrated saffron's dose-dependent inhibitory effects on cancer cells [39]. Administering saffron prior to anti-tumor drug treatment, reduced the cellular DNA damage [40]. Numerous studies show saffron to suppress cancer cell growth, inhibit proliferation and migration and downregulate metalloproteinases and urokinases, impacting various types of cancer. Crocin and crocetin exhibits strong anticancer effect by altering gene expression and inhibiting cellular production. Saffron's interaction with topoisomerase II suggests its potential in combating free radicals [41]. Researchers propose saffron as potential treatment for a variety of cancers such as gastric, skin, colorectal, breast, hepatic, cervical, ovarian, prostate, lungs, pancreatic and leukaemia etc [42].



**Ruchi Kohli et al.,****Anti inflammatory and analgesic effects**

saffron tinctures and extracts are employed for treating abscesses, wounds, fever, lower back pain, along with exhibiting anti-inflammatory and analgesic effects for both acute and chronic pain. Anti-inflammatory properties stem from antioxidant chemicals (such as crocin, crocetin, kaempferol, quercetin) inhibiting roduction of proinflammatory cytokines in animal models. Similarly, Vosooghi S. et al. discovered that Saffron extracts can boost White blood cell count, neutrophil count, platelet count and eosinophil number in ovalbumin-sensitized rat's blood [43]. Hydroethanolic saffron extracts demonstrate protective effects against ischemia and acute kidney disorders in rats. The anti-inflammatory properties of saffron arise from its component's alkaloids, tannins, saponins, anthocyanins and flavonoids.

Healing of second-degree burns

A study reported greater efficacy of saffron extract cream over silver Sulphur diazine in treating heat induced burns. Saffron significantly enhances re-epithelialization of burn wounds as compared to other treatments [44].

Effects on Eyes

Recent researches indicate saffron and its primary components possess neuroprotective effect. Its extract diminishes eye diseases like eye inflammation, retinal degeneration, cataracts, light mediated photoreceptor cell death and improve retinal function and blood circulation [45]. Crocin inhibits pro-inflammatory responses in retinal cell while crocetin prevented retinal degeneration. Saffron safeguards photoreceptors from light induced damage , improved visual function in age related muscular edema and retinitis pigmentosa [46].

Effects on blood glucose and insulin resistance

Both *in vitro* and *in Vivo* studies coupled with clinical trials substantiate therapeutic potential of saffron and its constituents as antidiabetic, hypolipidemic antihypertensive effect, metabolic syndrome, obesity and managing diabetes mellitus. Crocin improved insulin sensitivity and serum glycemic profiles in diabetic animal models, alongside favorable modifications in lipid profile [47, 48]

Effects on cholesterol levels

Saffron, rich in riboflavin and thiamine, is one of the best cardiovascular supplement. Flavonoids particularly lycopene found in saffron provide heart disease protection. The crocetin of saffron regulates cholesterol, promoting optimal levels and reducing the risks of heart attack. Further crocin inhibit pancreatic and gastric lipase activity resulting in low lipid absorption [49].

Effects on gastrointestinal and Genitourinary system

Saffron is believed to possess certain positive qualities related to gastrointestinal and genital systems, particularly in terms of stimulating stomach, decreasing appetite, jaundice and liver enlargement, antifatulent and regulating intestinal activity [50]. It aids in treatment of amenorrhea, aphrodisiac, impotency, emmenagogue, promoting mensuration and even having abortive properties and also treating conditions like hemorrhoids and prolapsed anus.

Antioxidant

The potential antioxidant activity of saffron is chiefly attributed to its unique carotenoid crocin. The synergistic effect of bioactive components (crocin, safranal, flavonoids, dimethylcrocetin) are responsible for remarkable antioxidant activity, with crocin effectively neutralizing free radicals and protecting cells against oxidative stress and is helpful in addressing neurogenerative disorders. The antioxidant and lipid lowering potential improves insulin resistance [51]. Saffron surpasses other spices in total polar phenols and antioxidant activity. Crocin and safranal capture free radicals while crocetin efficiently combats lipid peroxidation. These compounds show promise in treating cardiovascular and psychological issues and prevent cancer. Saffron extracts counteract oxidative stress in various organs and its main constituent crocin protects against continuous restraint stress. Aqueous saffron extracts hinder reactive oxygen species and intracellular signals, boosting cell viability and inhibiting apoptotic pathway [52].



**Ruchi Kohli et al.,****Effects on nervous system**

Saffron and its bioactive components exhibit anxiolytic, antidepressant, neuroprotective and memory enhancing effects in both preclinical and clinical studies, hence could be employed in development of drugs for nervous system disorders and treatment of mental disorders such as depression and dementia. Researches reveal saffron prevents 6-hydroxydopamine induced parkinsonism and therapeutic potential of crocetin fights severe neurological disorders and neuronal death in rats [53].

Conclusions and future perspectives

Crocus Sativus (saffron) holds significant importance in pharmaceuticals and cosmetics and has been subject of extensive phytochemical and biochemical studies by the researchers. The phytochemicals (crocin, crocetin, picrocrocin, safranal) extracted from saffron using both conventional and novel technologies possess wide range of activities like antioxidant, antidepressant, anticarcinogenic, anti-inflammatory etc. There is a need to explore further the potential neuroprotective action or risk factors of using *C. sativus* for brain related disorders. It would provide a novel lead compound in the formation of drugs used in the management of brain-related diseases. Medicinal properties make it useful in production of drugs, herbal medicines and also a valuable ingredient in many cosmetic products. There is need to put efforts on genetic improvement of saffron for more number and larger size flowers and creating a germplasm bank and searching better cultivation techniques as the high labour costs and low returns of saffron limits its widespread use. Further research is needed to understand the exact mechanism of action of bioactive components of saffron at molecular level. The increased knowledge of active phytochemicals of saffron could lead to innovative ideas in the realm of natural medicine in the near future.

REFERENCES

1. Baba SA, Malik AH, Wani ZA, Mohiuddin T, Shah Z, Abbas N, Ashraf N. Phytochemical analysis and antioxidant activity of different tissue of *Crocus sativus* and oxidative stress alleviating potential of saffron extract in plants, bacteria and yeast. *S Afr J Bot* 2015; 99: 80.
2. Jan S, Wani AA, Kamili AN, Kashtwari M. Distribution, chemical composition and medicinal importance of saffron (*Crocus sativus* L.). *Afr J Plant Sci* 2014; 8: 537.
3. Pitsikas, N. Constituents of saffron (*Crocus sativus* L.) as potential candidates for the treatment of Anxiety disorders and schizophrenia. *Molecules* 2016; 21: 303.
4. Gohari AR, Saeidnia S, Mahmoodabadi MK. An overview on saffron, phytochemicals, and medicinal Properties. *Pharmacogn Rev* 2013; 7: 61.
5. Abu-Izneid TA, Rauf A, Khalil AA, Olatunde A, Khalid A, Alhumaydhi FA. Nutritional and health beneficial properties of saffron (*Crocus sativus* L.) : a comprehensive review. *Crit Rev Food Sci Nutr* 2022. DOI: 10.1080/10408398.2020.1857682
6. Sidiq S, Shrivastava P. Antimicrobial, antioxidant, and anticancer activities of saffron (*Crocus sativus*): a review. *JETIR* 2020; 7: 41.
7. Ahrazem O, Moraga AR, Nebauer SG, Molina RV, Gomez LG. Saffron: Its photochemistry, Developmental Processes, and biotechnological prospects. *J Agric Food Chem*, <http://dx.doi.org/10.1021/acs.jafc.5b03194>
8. Anjum N, Pal A, Tripathi YC. Phytochemistry and Pharmacology of Saffron, the most precious natural source of colour, flavour and medicine. *SMU Medical Journal* 2015; 2: 335.
9. Khan NT, Jameel N. *Biomed J Sci Tech Res* 2020; 28: 21916.
10. Srivastava R, Ahmed H, Dixit RK, Dharamveer, Saraf SA. *Crocus sativus* L.: A comprehensive review. *Pharmacogn Rev* 2010; 4: 200.
11. Yang W, Qiu X, Wu Q, Chang FE, Zhou T, Zhou M, Pei. Active constituents of saffron (*Crocus sativus* L.) and their prospects in treating neurodegenerative diseases (Review). *Exp Ther Med* 2023; 25: 235.
12. Sereshti H, Heidari R, Samadi S. Determination of volatile components of saffron by optimised ultrasound-assisted extraction in tandem with dispersive liquid-liquid microextraction followed by gas chromatography-mass spectrometry. *Food chem* 2014; 143: 499.





Ruchi Kohli et al.,

13. Amanpour A, Sonmezdag AS, Kelebek H, Selli S. GC-MS-olfactometric characterization of the most aroma-active components in a representative aromatic extract from Iranian saffron (*Crocus sativus* L.). *Food Chem* 2015; 182: 251.
14. Bagur MJ, Salinas GLA, Monreal AMJ, Chaouqi S, Llorens S, Tome MM, Alonso GL. Saffron: An old Medicinal Plant and a potential Novel Functional Food. *Molecules* 2018; 23: 30.
15. Cardone L, Castronuovo D, Perniola M, Cicco N, Candido V. Saffron (*Crocus sativus* L.), the king of spices: An overview. *Sci Hortic* 2020; 272: 109560.
16. Liu J, Chen N, Yang J, Yang B, Ouyang Z, Wu C, Yuan Y, Wang W, Chen M. An integrated approach combining HPLC, GC/MS, NIRS, and chemometrics for the geographical discrimination and commercial categorization of saffron. *Food Chem* 2018; 253: 284.
17. Shahi T, Assadpour E, Jafari SM. Main chemical compounds and pharmacological activities of stigmas and tepals of 'red gold'; saffron. *Trends Food Sci* 2016; 58: 69.
18. Bhat ZS, Jaladi N, Khajuria RK, Shah ZH, Arumugam N. Comparative analysis of Bioactive N-Alkylamides Produced by Tissue Culture Raised versus Field Plantlets of *Spilanthes Ciliata* using LC-Q-TOF (HRMS). *J Chromatogr B Anal Technol Biomed Life Sci* 2016; 1017: 195.
19. Maggi L, Carmona M, Zalacain A, Kanakis CD, Anastasaki E, Tarantilis PA et al. Changes in saffron volatile profile according to its storage time. *Food Res Int* 2010; 43: 1329.
20. Sosa RA, -Moorillon GVN, -Velasco CEO, -Cruz ARN, -Carranza PH, -Perez, TSC. Detection of saffron's main bioactive compounds and their relationship with commercial Quality. *Foods* 2022; 11: 3245.
21. Fallahi HR, Aghhavan-Shajari M, Sahabi H, Behdani MA, Sayyari-Zohan, MH, Vatandoost S. Influence of Some Pre and Post-Harvest Practices on Quality of Saffron Stigmata. *Sci Hortic (Amst)* 2021; 278: 109846.
22. Sereshti H, Ataolahi S, Aliakbarzadeh G, Zarre S, Poursorkh Z. Evaluation of storage time effect on saffron chemical profile using gas chromatography and spectrophotometry techniques coupled with chemometrics. *J Food Sci Technol* 2018; 55: 1350.
23. Gallego R, Montero L, Cifuentes A, Ibáñez E, Herrero M. Green extraction of bioactive compounds from microalgae. *J Anal Test* 2018; 2: 109.
24. Heydari S, Haghighyegh GH. Extraction and microextraction techniques for the determination of compounds from saffron. *Can Chem Trans* 2014; 2: 221.
25. Dey A, Neogi S. Oxygen scavengers for food packaging applications: A review. *Trends Food Sci*. 2019; 90: 26.
26. Sarfarazi M, Jafari SM, Rajabzadeh G, Feizi J. Development of an environmentally-friendly solvent-free extraction of saffron bioactives using subcritical water. *LWT* 2019; 114: 108428.
27. Roniawati I, Putriana NA, Putri AN, Nuraini YA. Review: Bioactivities of saffron as an active ingredient in cosmetics. *Indo J pharm* 2021; 3: 74.
28. Gabros A, Trevor AN, Patrick MZ. *Sunscreens And Photoprotection*. StatPearls Publishing 2020.
29. Das I, Das S, Saha T. Saffron suppresses oxidative stress in DMBA-induced skin carcinoma: A histopathological study. *Acta Histochem* 2010; 112: 317.
30. Xing HG, Li Z, Huachen W, Hong DC. Efficacy and safety of innovative cosmaceuticals. *Clin Dermatol* 2008; 26: 367.
31. Mzabri I, Addi M, Berrichi A. Traditional and modern uses of saffron (*Crocus Sativus*). *Cosmetics* 2019; 6: 63.
32. Colledge, MAR. 'Parthians', Translated to Persian by M. Rajabnia; Hirmand: Tehran, Iran 2005, 1.
33. Salvi A, Prima M. Kelayakan Sediaan Penyegar (face toner) Putik Bunga Saffron (*Crocus Sativus*) Sebagai Kosmetik Tradisional Perawatan Kulit Wajah. *Jurnal Tata Rias dan Kecantikan* 2021; 3:1.
34. Telang PS. Vitamin C in dermatology. *Indian Dermatol Online J* 2013; 4: 143.
35. Lahmass I, Khoudri MEL, Ouahhoudi S, Lahmass M, Khoulati A, Benyoussef S. et al. Biological effects and pharmacological activities of saffron of *Crocus sativus*. *Arabian Journal of medicinal and aromatic plants* 2021; 7: 254.
36. Suganya K, Preethi PS, Suganya M, Nanthini RUA, *Int J Pharm Pharm Sci* 2016; 6: 7.
37. Khazdair MR, Anaigoudari A, Hashemzahi M, Mohebbati R. Neuroprotective potency of some spice herbs, a literature review. *J Tradit Complement Med* 2018; 9: 98.





Ruchi Kohli et al.,

38. Abdullaev F. Biological properties and medicinal use of saffron (*Crocus Sativus* L.). *Acta Hort (ISHS)* 2006; 739: 339.
39. Botsoglou NA, Florou PP, Nikolakakis I, Giannenas I, Dotas V, Botsoglou EN, Aggelopoulos S. Effect of dietary saffron (*Crocus Sativus* L.) on the oxidative stability of egg yolk. *Br Poult Sci* 2005; 46: 701.
40. Riverón NL. et al. The combination of natural and synthetic agents: a new pharmacological approach in cancer chemoprevention. *Procedures Western Pharmacol Society* 2002; 45: 74.
41. Festuccia C, Mancini A, Gravina GL. et al. Antitumor effects of saffron-derived carotenoids in prostate cancer cell models. *Biomed Res Int* 2014; Article ID 135048
42. Bhandari PR. *Crocus Sativus* L. (saffron) for cancer chemoprevention: A mini review. *J Tradit Complement Med* 2015; 5: 81.
43. Vosooghi S, Mahmoudabady M, Neemati A, Aghababa H. Preventive effects of hydroalcoholic extract of saffron on haematological parameters of experimental asthmatic rats. *Avicenna J Phytomed* 2013; 3: 279.
44. Khorasani G, Hosseinimehr SJ, Zamani P, Ghasemi M, Ahmadi A. The effect of saffron (*Crocus sativus*) extract for healing of second-degree burn wounds in rats. *Keio J Med* 2008; 57: 190.
45. -Albarral JAF, Ramirez AI, de Hoz R. et al. Neuroprotective and anti-inflammatory effects of a hydrophilic saffron extract in a model of glaucoma. *Int J Mol Sci* 2019; 20: 4110.
46. Sepahi S, Azam AG, Hossieni SM, Mohajeri SA, Khodaverdi E. Pharmacological effects of saffron and its constituents in ocular disorders from in vitro studies to clinical trials: A Systematic Review. *Curr Neuropharmacol* 2021; 19: 392.
47. Sani A, Tajik A, Seiedi SS et al. A review on the anti-diabetic potential of saffron. *Nutr. Metab. Insights.* 2022; 15: doi: 10.1177/11786388221095223.
48. Jazani AM, Karimi A, Azgomi RND. The potential role of saffron (*Crocus Sativus* L.) and its components in oxidative stress in diabetes mellitus: A systematic review. *Clin Nutr ESPEN* 2022; 48: 148.
49. Kamalipour M, Akhondzadeh S. Cardiovascular effects of Saffron: An Evidence-Based Review. *J Tehran heart Cent.* 2011; 6: 59.
50. Khorasany AR, Hosseinzadeh H. Therapeutic effects of saffron (*Crocus sativus* L.) in digestive disorders: A review. *Iran J Basic Med Sci.* 2016; 19: 455.
51. Rahmani AH, Khan AA, Aldebasi YH. Saffron (*Crocus sativus*) and its active Ingredients: Role in the Prevention and Treatment of Disease. *Pharmacogn J* 2017; 9: 873.
52. Madan K, Sanju N. In –vitro evaluation of antioxidant, anti-elastase, anti-collagenase, anti-hyaluronidase activities of safranin and determination of its sun protection factor in skin photoaging. *Bioorg Chem* 2018; 77: 159.
53. Maqbool Z, Arshad MS, Ali A, Aziz A, Khalid W, Afzal MF, Bangar SP, Addi M, Hano C, Lorenzo JM. Potential role of phytochemical extract from saffron in development of functional foods and protection of Brain-related disorders. *Oxid Med Cell Longev* 2022; Article ID 6480590.

Table 1: Botanical nomenclature of *Crocus Sativus* L.[10]

Division	EmbryophytaSiphanogama
Kingdom	Plantae
Subdivision	Angiospermae
Class	Monocotyledonae
Order	AsparagalesEpigynae
Family	Iridaceae
Subfamily	Crocoideae
Genus	Crocus
Species	C. Sativus





Ruchi Kohli et al.,

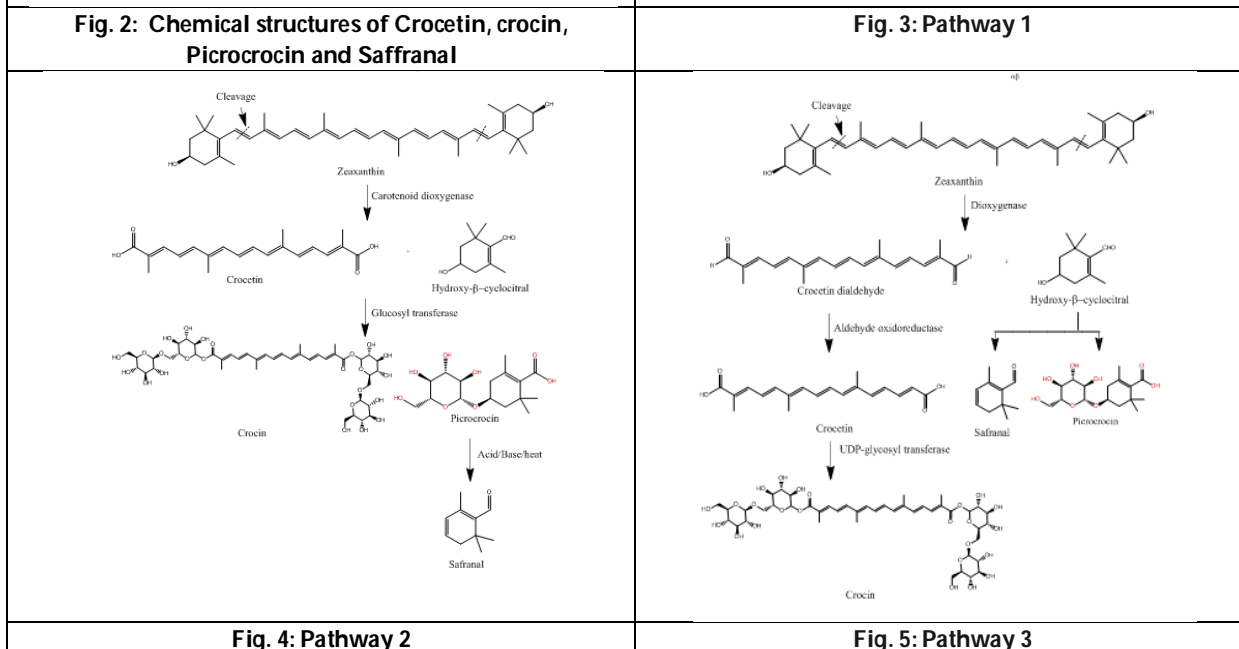
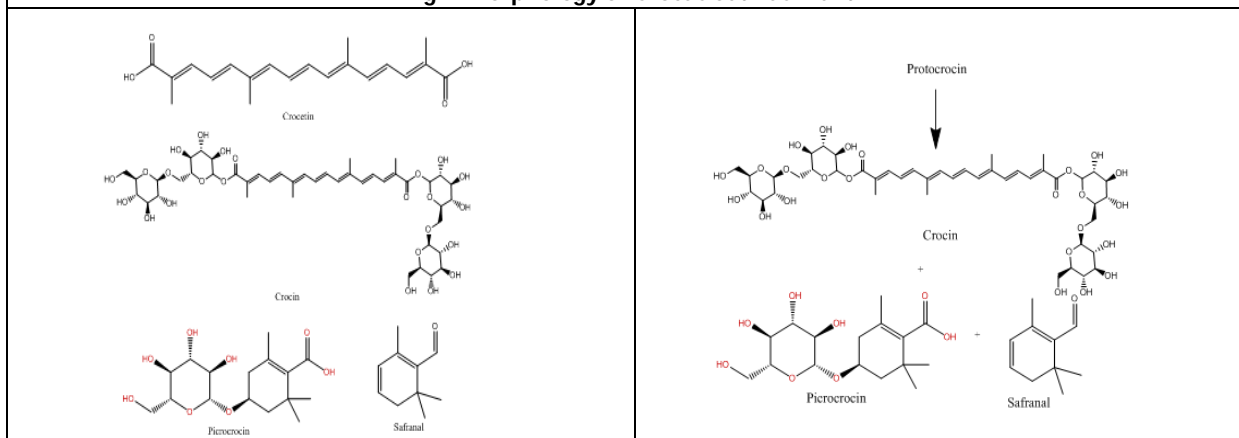
Table 2: Popular *Crocus Sativus* names in different languages.

Language	Name
Hindi	Kesar
English	Saffron
Bengali	Jafran, kumkum
Tamil	Kumkumappoo
Telugu	KumkumaPuvvu
Kannada	Kesarada
Malayalam	Kunkumapoovu
Arabic	Za'faran
Persian	Za'feran
Turkish	Zaffran
Spanish	Azafran
French	Safran
Italian	Zafferano
German	Safran
Dutch	Saffraan
Portuguese	Acafrao
Sanskrit	Rakta, Balhik, Asrugvar, kumkum, Shonit, Ghusrun, Agneeshekhar, Kashmir, Rudhir, kashmiraj

Table 3: Proximate analysis of chemical constituents of *Crocus Sativus L.*

Chemical constituent	Amount	Chemical constituent	Amount
Moisture	10-14%	Crude protein	12-14%
Ash	6-7%	Crude fiber	4-5%
Crude fat	5-8%	Amino acid	Concentration(mg/100g)
Nitrogen free extract	52-63%	Aspartic acid	0.040-0.048
a) Reducing sugar	20%	Glutamic acid	0.017-0.036
b) Gumsand dextrans	9-10%	Threonine	0.019-0.026
c) Starch	6-7%	Serine	0.016-0.023
d) Pentoses	6-7%	Alanine	0.13-0.17
Minerals		Proline	0.057-0.080
a) Phosphorous	3270 µg/g	Leucine	0.017-0.020
b) Magnesium	1300-1350 µg/g	Valine	0.022-0.037
c) Calcium	862-1070 µg/g	Isoleucine	0.012-0.019
d) Iron	92-110 µg/g	Glycine	0.007-0.016
e) Potassium	10.70-14.86 mg/g	Lysine	0.026-0.027
f) Sodium	42-100 µg/g	Histidine	0.0120.019
		Arginine	0.007-0.012
		Tyrosinase	0.008-0.011
		Phenylalanine	0.012-0.030
Fatty Acids	Concentration	Vitamins	Concentration
Palmitic acid	16.2g/100g	Vitamin A	27µg
LInoleic acid	28.5g/100g	Vitamin B1	0.115mg
Linolenic acid	21.0g/100g	Vitamin B2	5-13µg
Stearic acid	-	Vitamin B6	1.01mg
Oleic acid	-	Vitamin C	80mg
Arachidonic acid	-		



**Fig 1: Morphology of Crocus Sativus Plant**



Ruchi Kohli et al.,

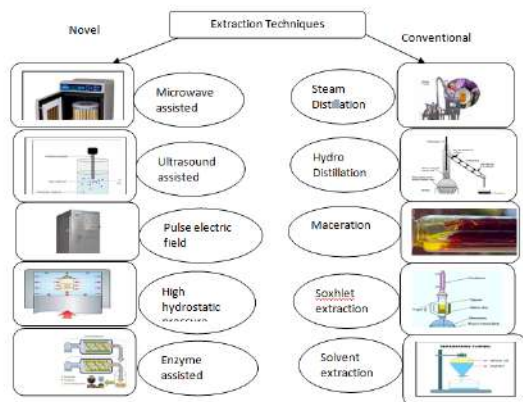


Fig 6: Conventional and Novel extraction methods used to extract bioactive compounds from Saffron.

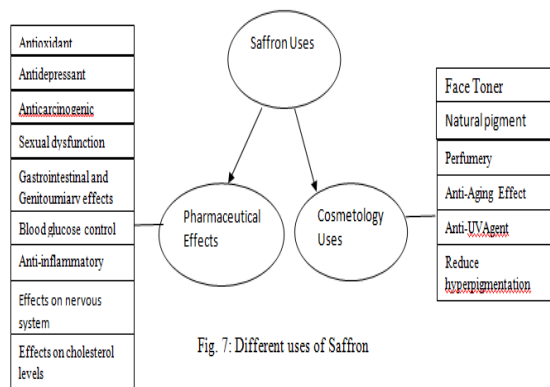


Fig. 7: Different uses of Saffron





Phytochemical Characterization of Commercial Varieties of *Melia dubia* Cav. - A Bio Prospective Approach for Sustainable Utility and Conservation

Mahalakshmi. R¹ and S. Uma Gowrie^{2*}

¹Research Scholar, Department of Plant Biology and Plant Biotechnology, Ethiraj College for Women (Autonomous), Affiliated to the University of Madras, Chennai, Tamil Nadu, India.

²Research Supervisor, Department of Plant Biology and Plant Biotechnology, Principal and Secretary in Ethiraj College for Women (Autonomous), Affiliated to the University of Madras, Chennai, Tamil Nadu, India.

Received: 17 Jan 2024

Revised: 09 Feb 2024

Accepted: 26 Apr 2024

*Address for Correspondence

S. Uma Gowrie

Research Supervisor,
Department of Plant Biology and Plant Biotechnology,
Principal and Secretary
Ethiraj College for Women (Autonomous),
Affiliated to the University of Madras,
Chennai-600 008, Tamil Nadu, India.
Email: umasezhian@gmail.com



This is an Open Access Journal / article distributed under the terms of the **Creative Commons Attribution License** (CC BY-NC-ND 3.0) which permits unrestricted use, distribution, and reproduction in any medium, provided the original work is properly cited. All rights reserved.

ABSTRACT

Melia dubia Cav. (syn. *Melia composita*) and *Melia azedarach* L. are two important tree species belonging to Mahogany family (Meliaceae) noted for pharmacological importance in Indian System of Traditional Medicine. *Melia dubia* Cav. is a money-spinning tree with several end uses and as a source of pulp with the trade name 'Malabar Neem'. The tree species are the potential resources of bio-constituents with numerous pharmaceutical properties. Limonoids are the predominant group of secondary metabolites in the tree species. The objective of the study is to analyze the potent phytoconstituents from the leaf samples of *Melia dubia* Cav. (**FRI/MD/232-Varsha and FRI/MD/349-Shashi**) raised in pot culture for which the seeds were procured from Forest Research Institute (FRI), Dehradun, Uttarakhand, India in comparison with *Melia azedarach* L. Qualitative and quantitative phytochemical analysis, separation, characterization methods such as UV-Vis spectrophotometer, FTIR, TLC, GC-MS analysis and *in vitro* bioassays had indicated the maximum amount of terpenoids in *Melia dubia* Cav. commercial varieties which is on par with *Melia azedarach* L. Further, the bioactive compounds from GC-MS analysis were screened for anthelmintic, antiviral properties and the specific limonoid was tend to act as a novel anthelmintic and antiviral agent which was proved through *in silico* molecular docking. The present study had revealed that there was no significant variation between *Melia dubia* Cav. commercial varieties



**Mahalakshmi and Uma Gowrie**

and *Melia azedarach* L. with respect to phytoconstituents. In the present study, the bioprospecting of the leaf samples of the commercial varieties have been reported for the first time. The promotion of plantation with these *Melia dubia* Cav. superior varieties and *Melia azedarach* L. can be a promising raw material or resources for pharmaceutical industries for sustainable utility and serve as an agro forestry model for generating the socio-economic status of farmers.

Keywords: *Melia dubia* Cav, *Melia azedarach* L., phytoconstituents, limonoids, melianone, sustainable utility, conservation.

INTRODUCTION

Melia dubia Cav., (Family: Meliaceae), is a dicotyledonous, deciduous, perennial multipurpose tree species growing upto 25m in height [1]. In India, the tree species is widely distributed in Sikkim, Himalayas, North Bengal, Upper Assam, Northern Circars, Deccan, Western Ghats and also in countries like Sri Lanka, Malaysia, Africa, USA, Mexico, Central America, Caribbean, Japan, Southern Europe, Australia, China and many Pacific islands [2]. The tree grows well in sandy loam, red and lateritic soil with an annual rainfall of above 800mm[3]. *Melia dubia* Cav. could be one such very important indigenous tree which is adaptive to a wide agroclimatic conditions of India [4]. The various plant parts serves as a ware house of pharmacological importance due to its potent phytochemicals such as alkaloids, carbohydrates, steroids, tannins, flavonoids, saponins, glycosides, terpenoids, phenols possessing antineoplastic, antidiabetic, antifungal, antibacterial, anti-leprosy, antiviral, anthelmintic, anti-oxidant properties and many more [5,6]. Limonoids are the major group of bioactive compounds reported in this tree species which possess antifeedant and cytotoxic or growth inhibiting property to different kinds of insect species namely *Spodoptera littoralis* and *Helicoverpa armigera*. *Melia azedarach* and *Melia dubia* have similar pharmacological profile but with different morphological characteristics (roots, fruits, leaves, seeds, bark and flowers) [7]. Different parts of *Melia* species possess essential pharmacological activities such as anti-inflammatory, hepatoprotective, analgesic, anticancer, anti-microbial, antifeedant, anti-diabetic, anti-larvicidal properties and the seeds are particularly used to treat infertility problems. *Melia dubia* Cav. is a promising versatile tree species which is found to be very much suitable for agroforestry due to its industrial uses as a source of pulp, biomass and plywood. This tree species has got attention among peasants due to its characteristic features such as fast growth, stem erectness without any branches, non-susceptible to insect attack, less shade effect, and farmer's friendly due to its low maintenance cost and increased income. Recent works in tree improvement has broaden the market of *Melia dubia* Cav. timber by converting it into special plywood products such as shuttering grade plywood, laminated veneer lumber (LVL), compreg, marine grade plywood and many more [8]. The commercial varieties of *Melia dubia* Cav. recently released are yet to be explored for its pharmacological properties apart from its end uses. Hence, the objective and purpose of the present study is to compare the pharmacological properties of the varieties of *Melia dubia* Cav. with that of *Melia azedarach* L. The novelty of the present research work is to analyze the potential phytoconstituents from the leaf samples of the tree species of *Melia dubia* Cav. (FRI/MD/232-Varsha and FRI/MD/349-Shashi) raised in pot culture for sustainable utility and conservation.

MATERIALS AND METHODS

Sample collection and authentication

Leaf samples of the commercial varieties of *Melia dubia* Cav. (FRI/MD/232-VARSHA and FRI/MD/349- SHASHI) were collected from the pot culture for which the seeds were procured from Forest Research Institute (FRI), Dehradun, Uttarakhand, India in comparison with the wild species, *Melia azedarach* L. which was collected at Perambur (Lat N 13° 7' 13.9206", Long E 80° 14' 42.7218") Chennai and was authenticated from Department of Botany, Madras Christian College, Chennai, Tamil Nadu, India (Figure 1 & Figure 2).



**Mahalakshmi and Uma Gowrie****Crude extract preparation**

The collected leaf samples were dried using shade dry method, powdered and stored in air tight containers for further studies. Extraction was carried out using cold percolation method by using different solvents of variable polarity namely, petroleum ether, ethyl acetate, acetone, methanol and aqueous (1:10 w/v) for about 48 hours and filtered using Whatman No. 1 filter paper. The resultant filtrate was used for the experimental work [9].

Qualitative phytochemical screening

The preliminary qualitative phytochemical analysis was carried out for both the commercial varieties of *Melia dubia* Cav. and the wild sp., *Melia azedarach* L. using standard procedures [10,11].

Quantitative phytochemical analysis

Using standard protocols, the primary and secondary metabolites namely total soluble sugars [12], proteins [13], lipids [14], alkaloids [15], phenols, flavonoids [16], tannins [17] and terpenoids [18] were quantified with their standards.

Antibacterial assay

Antibacterial activity of the promising extracts (methanol and aqueous) at different concentrations of the leaf samples were assayed against *Escherichia coli*, *Bacillus cereus* and *Bacillus subtilis* which were collected from Department of Microbiology, Ethiraj College for Women (Autonomous), Chennai, Tamil Nadu. Agar well diffusion method was followed [19,20]. Plates were maintained in triplicates.

Antioxidant assay

Antioxidant activity of the leaf sample extracts were determined on the basis of the scavenging activity of the stable 2, 2-diphenyl-2-picrylhydrazyl (DPPH) free radical method with slight modification. Different concentrations of methanol extract were prepared (100 – 500 $\mu\text{g mL}^{-1}$). Ascorbic acid was used as standard. Per cent inhibition and IC_{50} values were calculated using UV-Vis Spectrophotometer (UV 1650PC Shimadzu)[21].

Ultra Violet-Visible Spectrophotometer (UV-Vis) analysis and Fourier Transform Infrared Spectrophotometer (FT-IR) analysis

Methanol and aqueous leaf sample extracts were analyzed for the presence of secondary metabolites using a UV-Vis Spectrophotometer (UV-1650PC Shimadzu) with a range between 400-800 nm [22]. 10 mg of the dried powder of the leaf sample extracts (methanol and aqueous) were ground with KBr salt using a mortar and pestle and compressed into a thin pellet. FTIR-Shimadzu, IR affinity 1, Japan equipped with DLaTGS detector with a scan range of 400 to 4000 cm^{-1} with a resolution of 4 cm^{-1} and a mirror speed of 2.8 mm sec^{-1} was used. The infrared spectra were recorded at 4000-500 cm^{-1} [23,24].

Thin Layer Chromatography analysis (TLC)

TLC analysis was carried out using Kieselgel 60 F₂₅₄ TLC sheets for the methanol extracts of the leaf samples to detect the presence of terpenoids with the developing solvent system, Chloroform: Methanol (7:3) and visualized in iodine vapour chamber [25].

Gas Chromatography Mass Spectrometry (GC-MS) analysis

GC-MS analysis of methanol extract of the leaf samples were carried out in Vellore Institute of Technology, Sophisticated Instrumentation Facility (SIF), Chemistry Division, School of Advanced Sciences, Vellore, Tamil Nadu using Clarus 680 GC employed with fused silica column, packed with Elite-5MS (5% biphenyl 95%dimethylpolysiloxane, 30 m \times 0.25 mm ID \times 250 μm df) with helium as carrier gas and 1 ml/min flow rate was maintained. The spectrum was compared with the database of known components in GC-MS NIST (2008) library.





Mahalakshmi and Uma Gowrie

In silico molecular docking

In silico analysis through molecular docking confirms the functional role of the specific bioactive compound. *Melia dubia* Cav.-Shashi with promising bioactivities were taken for *in silico* docking to study its pharmacological activities (anthelmintic and antiviral property). The target molecules were retrieved from Protein Data Bank (PDB) (<http://www.rcsb.org/pdb/>). The bioactive compound details were obtained from Pub Chem database. The bioactive compounds were docked against the target protein using Molecule software, an online, integrated drug discovery platform. Docking results represented the interaction or binding affinity between the target and ligand molecules [9].

RESULTS**Qualitative phytochemical screening**

The phytochemical analysis carried out using the crude extracts of the leaf samples indicated the presence of wide range of phytochemicals. The methanol and aqueous extracts of the commercial varieties, Varsha and Shashi revealed a broad spectrum of potent primary and secondary metabolites such as alkaloids, phenols, glycosides, terpenoids, flavonoids, tannins and carbohydrates. Maximum presence of terpenoids were observed in the *Melia* leaf extracts (Figure 3). However, the petroleum ether extract revealed the presence of saponins. Similar results were obtained in the methanol and aqueous extracts of the *Melia azedarach* L. (Table 1). The results were in the order of **methanol extract > aqueous extract > ethyl acetate extract > acetone extract > petroleum ether extract**.

CVV denotes Commercial variety Varsha; CVS denotes Commercial variety Shashi; MEAZ denotes *Melia azedarach* L.

Quantification studies

Since the qualitative phytochemical analysis revealed the presence of carbohydrates, proteins, lipids, phenols, alkaloids, flavonoids, terpenoids and tannins in the leaf samples of *Melia dubia* Cav. and *Melia azedarach* L., these phytoconstituents were quantified with their respective standards (glucose, BSA, cholesterol, gallic acid and tannic acid). Maximum amount of terpenoids in both the commercial varieties of *Melia dubia* Cav. (Varsha- 75.44 ± 0.28 mg/g and Shashi- 76.25 ± 0.45 mg/g) and in *Melia azedarach* L. (71.24 ± 0.33 mg/g) were observed. The results obtained were of the following order, **Terpenoids > Phenols > Flavonoids > Alkaloids > Proteins > Tannins > Total Soluble Sugars > Lipids**. It was revealed that no remarkable variations were found among the leaf extracts of commercial varieties of *Melia dubia* Cav. and the wild sp. *Melia azedarach* L. (Figure 4).

Antibacterial assay

Methanol extract of *Melia dubia* Cav., commercial varieties (Varsha and Shashi) and *Melia azedarach* L. at $100 \mu\text{g mL}^{-1}$ showed maximum zone of inhibition of 15.45 ± 0.23 mm, 16.33 ± 0.21 mm, 13.32 ± 0.25 mm against *Bacillus cereus*. **There were no marked variations** among the leaf extracts of commercial varieties of *Melia dubia* Cav. and the wild sp. *Melia azedarach* L. (Figure 5).

Antioxidant assay

Antioxidant activity carried out at different concentrations (100 – $500 \mu\text{g mL}^{-1}$) of methanol and aqueous extracts of the leaf samples revealed inhibition of free radicals in a dose dependant manner. Antioxidant potential of the samples are determined based on the IC_{50} value. The IC_{50} value is the measure of the extract concentration that is required for 50 % inhibition. Lesser IC_{50} value denotes the higher antioxidant potential of the sample extracts. Promising results were obtained in $500 \mu\text{g mL}^{-1}$ concentration of the leaf extracts. Methanol extract of Varsha showed maximum per cent inhibition of 66.34 ± 0.45 with IC_{50} value of $164.2 \mu\text{g mL}^{-1}$, followed by Shashi of 67.89 ± 0.56 with IC_{50} value of $151.3 \mu\text{g mL}^{-1}$ and *Melia azedarach* L. showed 64.47 ± 0.77 per cent inhibition with IC_{50} value of $182.6 \mu\text{g mL}^{-1}$. Standard ascorbic acid had a per cent inhibition of 90 ± 1.5 at $500 \mu\text{g mL}^{-1}$ with IC_{50} value of $149.1 \mu\text{g mL}^{-1}$ (Figure 6).



**Mahalakshmi and Uma Gowrie****Ultra Violet-Visible Spectrophotometer (UV-Vis) analysis**

UV-Visible spectrophotometer analysis revealed several peak values, where the methanol extract of Varsha, Shashi and *Melia azedarach* L. showed promising peaks at 668.50 nm, 656.00 nm, 614.50 nm, 536.00 nm, 465.50 nm, 460.00 nm, 446.00 nm, 431.50 nm and 431.50 nm. An aqueous extract of Shashi indicated peaks at 399.00 nm, 389.00 nm, 378.50 nm, 369 nm, 231.00 nm and 219.50 nm (Figure 7). All these peak values represent the characteristics of terpenoids in the *Melia* leaf extracts.

Fourier Transform Infrared Spectrophotometer (FTIR) analysis

FTIR analysis of the of the leaf sample extracts revealed the varied distribution of functional groups within the organic fractions and provides a basis for a comparison of compositional differences between the *Melia dubia* Cav. commercial varieties and *Melia azedarach* L. Methanol and aqueous leaf extract of Varsha, Shashi and *Melia azedarach* L. showed different functional groups such as alkyl halides, aliphatic amines, sulfate, carboxylic acid, aromatics, amines, alkanes, 1°,2°amines- amides, alcohols, phenols and benzamide, alkynes, aromatics, aliphatic amines, 1° amines, isocyanate, alkanes, alcohol, phenols and aldehydes (Figure 8). The presence of all these functional groups in the leaf extracts strongly depicts the characteristics of terpenoids in the *Melia* leaf extracts.

Thin Layer Chromatography (TLC) analysis

Methanol extract of the commercial varieties of *Melia dubia* Cav., Varsha, Shashi and *Melia azedarach* L. using the solvent system Chloroform: Methanol (7:3), showed pale brownish colour with R_f values of 0.48, 0.55 and 0.43 respectively indicating the presence of terpenoids (Figure 9).

Gas Chromatography Mass Spectrometry (GC-MS) analysis

GC-MS spectrum of the leaf samples of *Melia dubia* Cav. commercial varieties and *Melia azedarach* L. indicated the presence of various bioactive compounds which includes terpenoids (limonoids), phenols, primary metabolites, flavonoids and small functional groups (Figure 10). However, **Melianone** with a peak area per cent of 82.4 was found to be in abundant in the commercial variety of *Melia dubia* Cav., Shashi followed by Varsha (79.1) and *Melia azedarach* L. (76.7). Further, there was not much variations in the presence of bioactive compounds between the commercial varieties and *Melia azedarach* L. (Tables 2).

In silico molecular docking

Since Melianone was found to be predominant in *Melia dubia* Cav., Shashi, it was subjected to *in silico* molecular docking. With respect to anthelmintic property with the target molecule, the *Cysticercus* gene, larval tapeworm (3MND), the docking analysis of Melianone from Shashi showed docking scores of -6.7, -6.4, -6.3 and -6.2 kcal/mol. Docking analysis of the standard albendazole indicated docking scores of -6.8, -6.7, -6.5 and -6.3 kcal/mol. With respect to antiviral property with the target molecule, Flavi virus gene (DENV) Dengue virus (5XAJ), the docking analysis of Melianone from Shashi showed docking scores of -6.7, -6.5, -6.4 and -6.1 kcal/mol. Docking analysis of the standard acetaminophen indicated docking scores of -6.9, -6.7, -6.4 and -6.2 kcal/mol (Figure 11). The leaf samples of Shashi revealed prominent binding affinity against the target molecules on par with the standard drugs (Albendazole and Acetaminophen). Thus, docking results are clear evidence for the commercial variety of *Melia dubia* Cav. having anthelmintic and antiviral properties confirming its pharmacological value.

DISCUSSION

Melia dubia Cav. is one of the short rotation money spinning tree species known as 'Malabar Neem' improving the socio-economic status of the farmers. In spite of its end uses, the pharmacological importance of various parts of the tree species which is not much explored in the commercial varieties. Different parts of the tree species are found to be with ample number of phytochemical components. Leaves are considered to be a warehouse of primary and secondary metabolites such as total soluble sugars, proteins, lipids, alkaloids, phenols, flavonoids, tannins and terpenoids. Certain terpenes have well characterized functions in plant growth (or) development and so can be



**Mahalakshmi and Uma Gowrie**

considered primary rather than secondary metabolites. For ex; The gibberellins, an important group of plant hormones are diterpenes with growth-regulating functions, originate from triterpenes. Terpenes are toxins and feeding deterrents to many herbivorous insects and mammals; thus, they appear to play important defensive roles in the plant kingdom. Among the non-volatile terpene anti herbivore compounds are the limonoids, a group of triterpenes (C_{30}) well known as bitter substances. The most powerful deterrent to insect feeding known as Azadirachtin [26]. Terpenoids or terpenes are involved in several metabolic pathways in the treatment of human diseases. These are classified as monoterpenes (C_{10}), sesquiterpenes (C_{15}), diterpenes (C_{20}), and sesterterpenes (C_{25}). They also exhibit biological activities against inflammation, malaria, cancer and several communicable diseases[27]. Qualitative and quantitative analysis of phytochemicals between the *Melia dubia* Cav. commercial varieties and *Melia azedarach* L. was not found to have variations in distribution of plant metabolites.

However, terpenoids were abundantly present in the leaf extracts. Terpenoids inhibit the nucleic acids, cytoplasmic membrane and energy metabolism resulting in potent antibacterial activity. Reactive oxygen species are formed by exogenous and endogenous chemicals or metabolic processes in the human body resulting in cell death and damage of healthy tissue. Leaves of *Melia dubia* Cav. commercial varieties are observed to be a potent antioxidant due to the presence of terpenoids (limonoids) [28]. Chromatographic and characterization studies such as UV-Vis, FTIR, TLC and GC-MS analysis revealed the presence of various secondary metabolites especially terpenoids in the *Melia dubia* Cav. commercial varieties and *Melia azedarach* L. which are responsible for the promising antibacterial, antioxidant, antiviral and anthelmintic activities. Different functional groups may be attributed to the existence of variety of potential phytochemicals. Major bioactive limonoids in the *Melia* sp. include **Melianone, Melianol, Meliacin, Meliacarpin, Meliartenin and Meliantriol**[29]. However, **Melianone** was found abundantly present in Shashi followed by Varsha and then *Melia azedarach* L. indicating the presence of bioactive compounds with a varied area per cent distribution. It is a need of the hour to produce a novel drug using medicinal plant or tree species. *In silico* molecular docking confirmed the functional role of a melianone from *Melia dubia* Cav. Mcule, an integrated drug discovery online platform. Melianone docked against the target protein molecules revealed promising anthelmintic and antiviral properties of the through maximum binding affinity or docking scores. More negative values are an indication of higher binding affinity. Rigid docking method which was followed where the bond angles, bond lengths were not modified at any stage of the analysis [9]. *Melia* species are related to its limonoids (melianone) possessing a C-secoskeleton ring reported as being the most active resulting in the suppression of disease target genes [34]. Promising binding affinities against the disease targets confirmed that *Melia dubia* Cav. commercial varieties are enriched with terpenoids (limonoids) which are of pharmacological value. Novelty and significant findings of the present study includes,

1. First report on the bioprospecting of the leaf samples of the recently released commercial varieties of *Melia dubia* Cav. in comparison with *Melia azedarach* L.
2. It provides a scientific validation to the primary and secondary phytoconstituents with its pharmaceutical properties in *Melia dubia* Cav. commercial varieties.
3. These leaf samples can be recommended for pharmaceutical industries for the development of novel drugs with clinical trials.

CONCLUSION

The study has revealed that in addition to the end uses of the commercial varieties of *Melia dubia* Cav., its leaf samples are found to be the potential resources of phytoconstituents which can be extensively used in pharmaceutical industries. Thus, the promotion of extensive plantation using the superior commercial varieties of *Melia dubia* Cav. will be a suitable agro forestry model for generating livelihoods to the farmers in addition to its commercial end uses.





ACKNOWLEDGEMENT

The authors thank Principal & Secretary, Ethiraj College for Women (Autonomous), Ethiraj Centre for Research, Innovation & Creativity (ECRIC), Head, Former and Present, Faculty members and supporting staff of the Department of Plant Biology and Plant Biotechnology, Ethiraj College for Women (Autonomous), Chennai- 600 008, Tamil Nadu, India for their valuable support, encouragement throughout the entire period of research. We would like to thank Dr. Ashok Kumar, Scientist 'G', Division of Genetics and Tree Propagation, Forest Research Institute (FRI), Dehradun, Uttarakhand for extending their facility in seed procurement for my research work. We would also like to express our sincere thanks for the facilities extended by the Central Instrumentation Centre of Ethiraj College for Women (Autonomous) and Sophisticated Instrumentation Facility (SIF) Laboratory, School of Advanced Sciences, Chemistry Division, Vellore Institute of Technology (VIT), Vellore, Tamil Nadu, India.

CONFLICTS OF INTERESTS

The authors declared that they had no conflicts of interests.

REFERENCES

1. Warriar RR. *Melia dubia* Cav., Institute of forest genetics and tree breeding (Indian council of forestry research and education);2011.
2. Hasegawa M, Matsumura J, Kusano R, Tsushima S, Sasaki Y. Acoustoelastic effect in *Melia azedarach* for nondestructive stress measurement. *Constr Build Mater* 2010; 24(9):1713-1717.
3. Anand B, Devagiri GM, Maruti G, Vasudev HS, Khaple AK. Effects of Pre-sowing Seed Treatments on Germination and Seedling Growth Performance of *Melia dubia* Cav: An important Multipurpose Tree. *J. Life Sci* 2012; 1:59-63.
4. Parthiban KT, Bharathi AK, Seenivasan R, Kamala K, Rao MG. Integrating *Melia dubia* in agroforestry farms as an alternate pulpwood species. *Asia-Pacific Agroforestry Newsletter* 2009; 34:3-4.
5. Sharma R, Arya V. A Review on Fruits Having Anti-Diabetic Potential. *J. Chem. Pharm. Res* 2011; 3:204-212.
6. Valentina P, Ilango K, Kiruthiga B, Parimala M.J. Preliminary phytochemical analysis and biological screening of extracts of leaves of *Melia dubia* Cav. *International Journal of Research in Ayurveda and Pharmacy* 2013;4(3):417-419.
7. Yadav R, Pednekar A, Rewachandani Y. A comprehensive review on Meliaceae family. *World journal of Pharmaceutical Sciences* 2015; 3(4):2321-3320.
8. Mohanty B N. *Melia Dubia* plantation for Integration of Agroforestry and Plywood industries. 2015; 16(1).
9. Valli SA, Gowrie SU. A study on the bioactive potential of fresh and dried sprouts of *Cocos nucifera* L. in vitro and *in silico* approach. *International Journal of Pharmacy and Pharmaceutical sciences* 2017; 9(3):0975-1491.
10. Raaman N. *Phytochemical techniques*. 1st ed. New India Publication Agency, New Delhi, 2006. pp 19-24.
11. Harborne JB. *Textbook of Phytochemical Methods. A Guide to Modern Techniques of Plant Analysis*. 5th ed. Chapman and Hall Ltd, London, 1998 21-72.
12. Hedge JE, Hofreiter BT. In: *Carbohydrate Chemistry*, 17 (Eds. Whistler R.L. and Be Miller, J.N.), Academic Press, New York; 1962.
13. Lowry OH, Rosebrough NJ, Farr AL, Randall RJ. Protein measurement with the Folin phenol reagent. *J Biol Chem* 1951; 193(1):265-75.
14. Folch J, Lees M, Stanley G.H.S. A Simple method for the isolation and purification of total lipides from animal tissues. *J Biol Chem* 1957; 226(1):497-509.
15. John B, Sulaiman CT, George S, Reddy VRK. Spectrophotometric estimation of total alkaloids in selected *Justicia* species. *International Journal of Pharmacy and Pharmaceutical Sciences* 2014; 6(5): 0975-1491.





Mahalakshmi and Uma Gowrie

16. Kamtekar S, Keer V, Pati V. Estimation of Phenolic content, Flavonoid content, Antioxidant and Alpha amylase Inhibitory Activity of Marketed Poly herbal Formulation. Journal of Applied Pharmaceutical Science 2014; 4 (09):061-065
17. Saranya VTK, Gowrie S. Pharmacological studies: Antibacterial, antioxidant, and anti-inflammatory efficacy of Casuarina equisetifolia root extracts. Asian Journal of Pharmaceutical and Clinical Research 2018; 11(8):270
18. Ferguson NM. A Textbook of pharmacognosy, Journal of Pharmacy and Pharmacology: An International Journal of Pharmaceutical Science, 1956; 9(1).
19. Perez C, Pauli M, Bazerque P. An antibiotic assay by agar-well diffusion method. Acta Biologica et MedecineExperimentaalis 1990; 15:113-115.
20. Chathurdevi G, Gowrie S. Endophytic fungi isolated from medical plant—A promising source of potential bioactive metabolites. Int. J. Curr. Pharm. Res 2016; 8, 50–56.
21. Brand-Williams W, Cuvelier ME, Berset C. Use of a free radical method to evaluate antioxidant activity-lebensm.-wiss. U.-technol 1995; 28:25-30.
22. Kalaichelvi K, Dhivya SM. Screening of phytoconstituents, UV-VIS spectrum and FTIR analysis of *Micrococcamercurialis* L. Benth, International Journal of Herbal Medicine 2017; 10(3):462-466.
23. Coates J. Interpretation of infrared spectra, a practical approach. Encyclopedia of analytical chemistry 2000; 12, 10815-10837.
24. Bose P, Gowrie S. Assessment of bioactive metabolites from the root endophyte isolated from *Casuarina junghuhniana* Miq. Asian Journal of Pharmaceutical and Clinical Research 2017; 10(4):137.
25. Kristanti H, Tunjung SAW. Detection of alkaloid, flavonoid and terpenoid compounds in bread tree (*Artocarpus communis*) leaves and pulps. Journal of KnE life sciences 2015; 2(2):129-133.
26. Taiz L, Zeiger E, Moller MI, Murphy A. Plant physiology and development. 6th ed. A41-a417, 2015.
27. Wang KA, Lim CS, Mohamad K, Morita H, Hirasawa Y, Takeya K *et al*. Phytochemical characterization of *Melia dubia* for their biological properties. Bioorg. Med. Chem 2007; 15, 5997.
28. Huang M, Abel C, Sohrvalli R, Petri J, Haupt I, Cosmano J *et al*. Variation of herbivore-induced volatile terpene among Arabidopsis ecotypes depends on allelic differences and subcellular targeting of two terpene synthases TPS02 and TPS03. Plant Physiol 2010; 153:1293–1310.
29. Wallia, S., Saha, S., Rana, V.S. (2014). Plant-Derived Pesticides as an Alternative to Pest Management and Sustainable Agricultural Production: Prospects, Applications and Challenges. Advances in Plant Biopesticides. D. Singh ed. 2014.
30. Scapinello, J., Oliveira, J.V., Chiaradia, A.L., Tomazelli, O., Niero, R., Magro, J.D. (2014). Insecticidal and growth inhibiting action of the supercritical extracts of *Melia azedarach* on *Spodoptera frugiperda*, Revista Brasileira de Engenharia Agrícola e Ambiental, 866–872.

Table 1: Phytochemical screening of leaf extracts of *Melia dubia* Cav. commercial varieties and *Melia azedarach* L. using different solvents

S. No	Phytoconstituents	Petroleum ether			Ethyl acetate			Acetone			Methanol			Aqueous		
		CV V	C VS	ME AZ	CV V	C VS	ME AZ	CV V	C VS	ME AZ	CV V	C VS	ME AZ	CV V	C VS	ME AZ
1.	Alkaloids: Mayer's test	-	-	-	-	-	-	-	-	-	-	-	-	-	-	-
	Dragendroff's test	+	+	+	+	+	+	+	+	+	+	+	+	++	++	++
2.	Phenols: Ferric chloride test	-	-	-	-	-	-	-	-	-	++	++	+	++	++	+



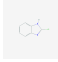








Mahalakshmi and Uma Gowrie

	Lead acetate test	+	+	+	+	+	+	+	+	+	++	++	++	++	++	++
3.	Glycosides	–	–	–	–	–	–	–	–	–	+	+	+	+	+	+
4.	Terpenoids	+	+	+	+	+	+	+	+	+	++	++	++	++	++	++
5.	Flavonoids	+	+	+	+	+	+	+	+	+	++	++	++	++	++	++
6.	Tannins	+	+	+	+	+	+	+	+	+	+	+	+	+	+	+
7.	Carbohydrates	–	–	–	–	–	–	–	–	–	+	+	+	+	+	+
8.	Proteins and amino acids	–	–	–	–	–	–	–	–	–	+	+	+	+	+	+
9.	Lipids	–	–	–	–	–	–	–	–	–	+	+	+	+	+	+
10.	Saponins	+	+	+	–	–	–	–	–	–	–	–	–	–	–	–

+ indicates Presence, ++ indicates Strong presence, - indicates Absence





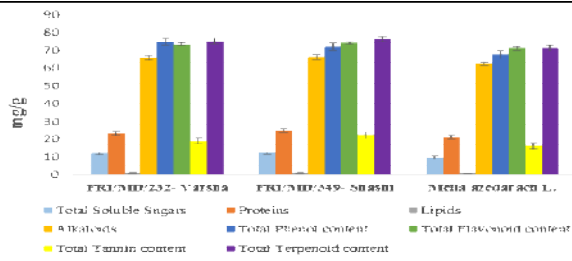
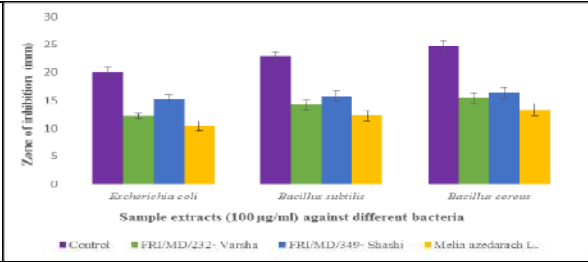
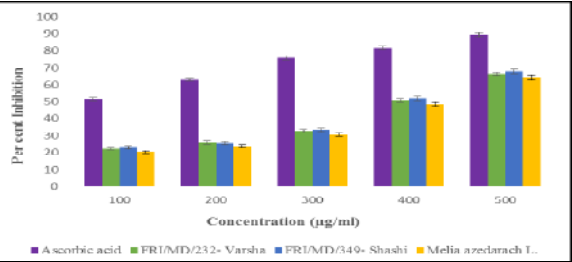
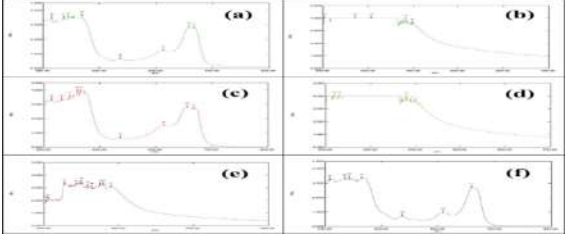
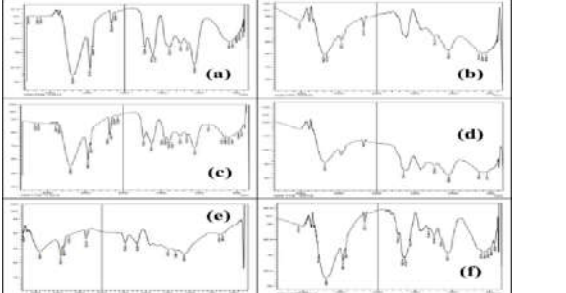
Table 2: GC-MS analysis of methanol extract of *Melia dubia* Cav.- Shashi

S.No	Compound Name	Retention Time	Molecular weight	Molecular formula	Peak area %	Molecular structure	Biological activities (PubChem, NIST & ChEBI)
1.	2-Chlorobenzimidazole	6.238	152.58	C ₇ H ₅ ClN ₂	55.23		Strong pesticidal, anti-microbial, anti-inflammatory and anticancer agent
2.	1-Octadecyne	18.325	250.5	C ₁₈ H ₃₄	43.06		Potent antimicrobial agent and an antioxidant
3.	Heptacosanoic acid, methyl ester	19.170	424.7	C ₂₈ H ₅₆ O ₂	43.11		Anti-microbial agent
4.	Tetradecanoic acid, 12-methyl-, methyl ester	19.235	256.42	C ₁₆ H ₃₂ O ₂	73.99		Possess larvicidal and repellent activity
5.	N-Hexadecanoic acid	20.090	256.42	C ₁₆ H ₃₂ O ₂	43.04		Exhibit anti-inflammatory, antioxidant, hypocholesterolemicnematicidal, pesticidal, anti-androgenic, hemolytic properties.
6.	Oleic acid	21.506	282.5	C ₁₈ H ₃₄ O ₂	44.05		Has anti-inflammatory antiandrogenic, anticancer, insectifuge and antimicrobial properties
7.	E-2-Octadecadecen-1-ol	21.806	268.5	C ₁₈ H ₃₆ O	45.11		Pesticidal agent





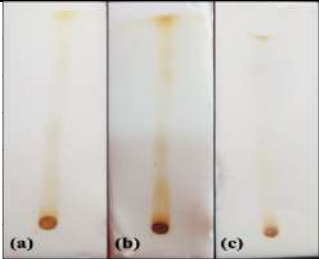
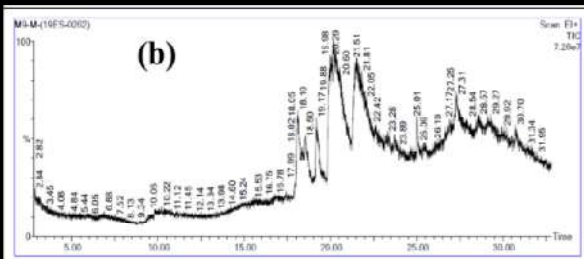
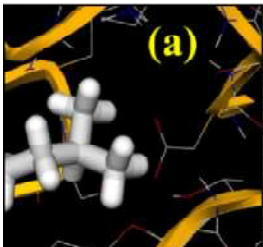
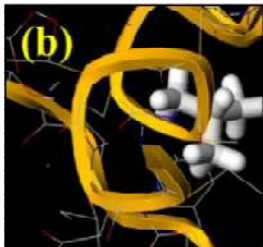
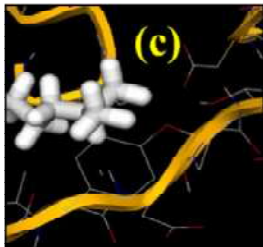
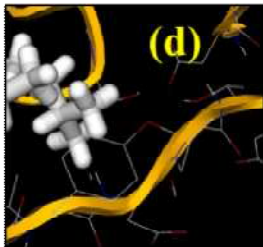
Mahalakshmi and Uma Gowrie

8.	Melianone	217.12	470.7	$C_{30}H_{46}O_4$	82.40		Strong antioxidant, anti-inflammatory, pesticidal antimicrobial, anticancer properties
<div>   </div>							
Figure 1: (a) Luxuriant growth of commercial varieties of <i>Melia dubia</i> Cav.-(FRI/MD/232- Varsha and FRI/MD/349- Shashi) and (b) Leaf sample of <i>Melia azedarach</i> L.				Figure 2: Leaves of commercial varieties of <i>Melia dubia</i> Cav.			
							
Figure 3: Phytochemical analysis of <i>Melia</i> leaf extracts- Terpenoids				Figure 4: Quantitative analysis of the leaf samples of <i>Melia dubia</i> Cav. commercial varieties and <i>Melia azedarach</i> L.			
							
Figure 5: Antibacterial activity of methanol leaf extract (100 µg ml ⁻¹) of <i>Melia dubia</i> Cav. commercial varieties and <i>Melia azedarach</i> L. against different bacteria				Figure 6: Antioxidant activity of methanol leaf extract of <i>Melia dubia</i> Cav. commercial varieties and <i>Melia azedarach</i> L.			
							
Figure 7: UV-Visible spectrum of leaf extracts of <i>Melia dubia</i> Cav. commercial varieties and <i>Melia azedarach</i> L.				Figure 8: FTIR spectrum of leaf extracts of <i>Melia dubia</i> Cav. commercial varieties and <i>Melia azedarach</i> L. (a) &			





Mahalakshmi and Uma Gowrie

(a) & (b) Methanol and aqueous extract of Varsha(c)& (d) Methanol and aqueous extract of Shashi (e) & (f) Methanol and aqueous extract of <i>Melia azedarach</i> L.	(b) Methanol and aqueous extract of Varsha (c) & (d) Methanol and aqueous extract of Shashi (e) & (f) Methanol and aqueous extract of <i>Melia azedarach</i> L.
	
Figure 9: TLC analysis of methanol leaf extracts of terpenoids (a) Varsha (b) Shashi (c) <i>Melia azedarach</i> L.	Figure 10: GC-MS analysis of methanol leaf extracts - Shashi
	  
Figure 11: Illustration of <i>in silico</i> molecular docking (a) & (b) Albendazole and Melianone docked against Cysticercus gene (larval tapeworm) (c) & (d) Acetaminophen and Melianone docked against Flavi virus gene (DENV) Dengue	





Partial Replacement of Copper Slag as a Fine Aggregate - A Review

Dindod Rutika^{1*} and Sharma Ankita²

¹Student, Department of M.Tech (Transportation) - Civil Engineering, Parul University Waghodia, Vadodara, Gujarat, India.

²Faculty, Department of M.Tech (Transportation) - Civil Engineering, Parul University Waghodia, Vadodara, Gujarat, India.

Received: 21 Jan 2024

Revised: 19 Feb 2024

Accepted: 26 Apr 2024

*Address for Correspondence

Dindod Rutika

Student,

Department of M.Tech (Transportation) - Civil Engineering, P

arul University Waghodia,

Vadodara, Gujarat, India.

Email: 2203032110001@paruluniversity.ac.in



This is an Open Access Journal / article distributed under the terms of the **Creative Commons Attribution License** (CC BY-NC-ND 3.0) which permits unrestricted use, distribution, and reproduction in any medium, provided the original work is properly cited. All rights reserved.

ABSTRACT

The main focus of this paper is on the partial replacement of traditional fine aggregate with copper slag in concrete mixtures. It reviews existing research on this topic and presents a comprehensive analysis of the influence of copper slag as a replacement material on the compressive strength, tensile strength, and durability of concrete. By examining the relevant literature, this paper provides a thorough understanding of the benefits and limitations associated with the incorporation of copper slag in concrete. This review paper not only aims to inform researchers, engineers, and practitioners about the potential of copper slag in the construction industry but also underscores the need for sustainable and eco-friendly alternatives to conventional construction materials. It serves as a valuable resource for those seeking insights into the utilization of copper slag as a fine aggregate replacement and its impact on the performance of concrete structures.

Keywords: Copper slag, fine aggregate, concrete, partial replacement, mechanical properties, durability, construction materials, and sustainability.

INTRODUCTION

Copper slag is a byproduct resulting from the extraction and refining of copper ore. This industrial waste material is generated during the process of smelting copper at high temperatures. Over the years, copper slag has gained attention and importance as a versatile material with numerous potential applications across various industries, including construction, engineering, and environmental sectors. Copper slag exhibits distinctive properties that make it a subject of growing interest. Its chemical composition comprises various oxides, such as iron, silica, alumina,



**Dindod Rutika and Sharma Ankita**

calcium oxide, and magnesium oxide, along with traces of heavy metals and other impurities. This unique composition contributes to its diverse properties, which include high hardness, durability, and resistance to abrasion. In the past, copper slag was predominantly considered as waste material and was often disposed of in landfills, leading to environmental concerns. However, in recent years, its potential as a sustainable resource has become increasingly recognized. Researchers and industries have explored innovative ways to reutilize copper slag, turning it from waste into a valuable raw material with numerous applications. One prominent application of copper slag is in the construction and civil engineering sectors, where it is commonly employed as a partial replacement for conventional fine aggregates in concrete production. This utilization not only reduces the environmental impact by recycling an otherwise discarded material but also enhances the mechanical and durability properties of concrete. Copper slag in concrete mixtures has shown promising results, with improved compressive strength, tensile strength, and resistance to harsh environmental conditions. Beyond construction, copper slag finds application in areas such as abrasives for surface preparation, the manufacturing of roofing granules, and even as a component in soil stabilization and road construction. Its versatility, combined with its sustainable attributes, positions copper slag as a material of significant interest in today's quest for eco-friendly and cost-effective solutions across various industries. In this introduction to copper slag, we will delve further into its properties, production processes, and the various applications that have emerged as a result of ongoing research and development. This paper aims to provide a comprehensive overview of copper slag, shedding light on its potential to contribute to a more sustainable and efficient industrial landscape.

Copper Slag Valuable Industrial Properties

1. **Hardness:** Copper slag is known for its high hardness, which makes it an excellent material for abrasive blasting. It is often used for cleaning, surface preparation, and rust or paint removal in industrial settings.
2. **Durability:** The durability of copper slag is a significant advantage, particularly in construction. When used as a partial replacement for fine aggregate in concrete, it can enhance the concrete's resistance to wear and abrasion.
3. **Chemical Composition:** Copper slag typically consists of oxides, including iron oxide, silica (silicon dioxide), alumina (aluminum oxide), calcium oxide, and magnesium oxide. The specific chemical composition may vary depending on the source and production process.
4. **Granular Texture:** It usually has a granular texture, which makes it suitable for use as a coarse or fine aggregate in concrete mixes. The particle size distribution can be controlled to meet specific requirements in construction applications.
5. **Density:** Copper slag has a density that is generally higher than that of natural aggregates, which can contribute to the improved density and strength of concrete when used as a partial replacement.
6. **Color:** Copper slag typically has a dark color, which may vary from black to deep brown, depending on the source and impurities present.
7. **Low Absorption:** Copper slag tends to have low water absorption, which can be advantageous in concrete production, as it helps reduce the overall water demand of the mix.
8. **Angular Shape:** The particles of copper slag are often angular, which can contribute to better interlocking within concrete mixes, leading to enhanced mechanical properties.
9. **Chemical Inertness:** Copper slag is generally chemically inert, meaning it does not react with most chemicals commonly found in construction and industrial environments, making it a stable material in various applications.
10. **High Melting Point:** Copper slag results from the smelting of copper ore at high temperatures, which imparts it with a high melting point and resistance to thermal degradation.
11. **Non-Porous:** It is non-porous, which means that it is less likely to absorb moisture, preventing potential deterioration due to freeze-thaw cycles in concrete applications.



**Dindod Rutika and Sharma Ankita****Environmentally Sustainable**

The use of copper slag as a recycled material is environmentally friendly as it helps in reducing the disposal of industrial waste and conserving natural resources. It's important to note that the specific properties of copper slag can vary depending on the source and production process. Therefore, understanding the properties of a particular batch of copper slag is crucial when using it in specific applications. These properties make copper slag a versatile material with potential applications in construction, abrasives, and other industrial fields. The aim of using copper slag as a partial replacement for fine aggregate in concrete is multifaceted and involves several objectives, including:

- **Sustainability:** The primary aim is to promote sustainability in construction by reducing the environmental impact. By reusing a waste material like copper slag, we can lower the demand for natural sand and gravel, which are finite resources. This helps in conserving natural resources and reducing the environmental footprint associated with mining and quarrying.
- **Waste Reduction:** Another key aim is to address the issue of industrial waste management. Copper slag is a byproduct of the copper extraction and refining process. Utilizing it in construction reduces the amount of waste material that would otherwise end up in landfills, minimizing environmental pollution.
- **Improved Mechanical Properties:** Incorporating copper slag in concrete aims to enhance the mechanical properties of the resulting material. Copper slag, due to its hardness and angular shape, can contribute to increased compressive strength, flexural strength, and abrasion resistance in concrete. This is particularly important in applications where durable and strong concrete is required, such as in roads, pavements, and industrial flooring.
- **Economic Benefits:** By partially replacing fine aggregate with copper slag, there can be economic advantages. In some cases, copper slag may be more cost-effective than natural aggregates, leading to potential cost savings in concrete production.
- **Enhanced Durability:** Copper slag can contribute to improved durability of concrete due to its low water absorption and resistance to chemical attacks. This is beneficial in applications exposed to aggressive environments, such as marine structures or structures subjected to chemical exposure.
- **Improved Workability:** Depending on the particle size distribution and properties of the copper slag used, it can contribute to improved workability in concrete mixes, making it easier to handle and place during construction.
- **Reduced Environmental Impact:** The production of concrete is associated with a significant carbon footprint. By using copper slag as a replacement for fine aggregate, we can reduce the carbon emissions associated with concrete production. Additionally, the use of copper slag in concrete can lower the demand for river sand, which can help protect river ecosystems and prevent illegal sand mining.
- **Research and Development:** Using copper slag in concrete provides an avenue for ongoing research and development. Engineers and researchers aim to optimize the proportion of copper slag in concrete mixes, ensuring that it meets specific performance and sustainability goals. In summary, the aim of using copper slag as a partial replacement for fine aggregate in concrete is to create a more sustainable, durable, and cost-effective construction material while also addressing waste management and environmental concerns. This approach aligns with the broader goal of promoting eco-friendly practices in the construction industry.

METHODOLOGY-RELATED WORK

M. Pavan Kumaret al., (2015) [3] in their study the current construction industry faces a challenge of replacing natural resources in the production of cement and sand. This study addresses this issue by exploring the use of industrial by-products, namely Copper slag and Ground Granulated BlastFurnace Slag (GGBS), derived from the manufacturing processes of copper and iron. The incorporation of these materials not only lowers construction costs but also contributes to environmental sustainability by utilizing materials that are typically considered waste. The research focuses on optimizing a concrete mix with a grade of M25 by partially replacing cement with GGBS and sand with



**Dindod Rutika and Sharma Ankita**

Copper Slag. Various replacement percentages are considered: for cement, 0% (without GGBS), 5%, 10%, 15%, and 20%, and for sand, 0% (without copper slag), 10%, 20%, 30%, and 40%. An experimental study is conducted to assess the workability and strength characteristics of the resulting concrete. The properties of the concrete are evaluated through compressive, flexural, and split tensile strength tests, comparing the performance of the mixtures with GGBS and Copper slag replacements to conventional concrete. The study aims to provide insights into the mechanical behavior of the concrete mix with these advanced mineral admixtures, offering a potential solution to both cost reduction and environmental impact in construction practices. M. V. Patil et al., (2015) [5] in their research copper slag, a by-product from the copper smelting and refining process, was examined in this study as a partial replacement for sand in concrete. Six sets of concrete mixtures were created, incorporating varying proportions of copper slag, ranging from 0% to 100%. The experimental procedure involved testing concrete specimens at different curing periods (7, 28, 56 days) to assess compressive strength. The findings revealed that the addition of copper slag to sand, in percentages from 0% to 100%, resulted in increased compressive strength and flexural strength of the concrete. This improvement is attributed to the high toughness of copper slag, suggesting its potential as a beneficial and effective partial replacement for sand in concrete mixes. Zine Kiran Sambhaji et al., (2016) [8] this study explores the use of copper slag, an industrial byproduct from copper manufacturing, as a substitute for fine aggregate in M25 grade concrete. Approximately 26.6 million tons of copper slag are generated in the copper industry worldwide.

The objective is to promote the utilization of this byproduct in construction materials. Various concrete mixtures were prepared with different proportions of copper slag, ranging from 0% to 100%, and tested for strength, workability, and durability. The results indicate that 50% copper slag and 50% sand (CS+50%S) provide an optimal proportion for use as a replacement material in concrete. This mixture exhibits High-Performance Concrete (HPC) characteristics. Additionally, a 30% replacement of copper slag in the concrete mix also demonstrates HPC characteristics. The study concludes that, based on test results surpassing the control mix, it is feasible to fully replace fine aggregate with copper slag (100% CS) in concrete. The flexibility in proportion allows for customization based on specific construction requirements. Arivalagan. Set al., (2013) [9] The research focuses on waste management strategies, particularly the partial replacement of sand with Copper Slag in mortar and concrete due to the scarcity of fine aggregate. Copper slag, a byproduct from sterlite industries, is explored as a potential replacement for sand. Various concrete mixtures with different percentages of copper slag (ranging from 0% to 100%) were tested for compressive strength, split tensile strength, and flexural strength after a 28-day curing period. The highest compressive strength achieved was 35.11MPa at 40% replacement, compared to the control mix at 30MPa. The study concludes that using copper slag as a fine aggregate in concrete significantly enhances compressive, split tensile, and flexural strength, as well as energy absorption characteristics.

PRODUCTION OF COPPER SLAG

Copper slag is a by-product generated during the smelting and refining of copper ore. It is typically produced in copper mines and metallurgical operations. Here's an overview of the production of copper slag

- **Copper Ore Mining:** The process begins with the extraction of copper ore from mines. Copper ore contains various minerals, including copper, along with impurities and gangue materials.
- **Crushing and Grinding:** The mined copper ore is usually crushed and ground into smaller particles to facilitate the extraction of copper minerals. This process involves the use of crushers and mills.
- **Concentration:** After crushing and grinding, the copper-bearing minerals are separated from the gangue materials through a process called concentration. This often involves froth flotation, where chemicals and air bubbles are used to separate the copper minerals from other minerals in the ore.
- **Smelting:** The concentrated copper ore is then subjected to high-temperature smelting in a furnace. During smelting, the copper concentrates are heated to separate the copper from the impurities. This process generates liquid copper and a slag that is rich in non-copper minerals.
- **Slag Separation:** The molten slag, which is less dense than the copper, rises to the top and is separated from the copper. This slag is typically removed from the surface of the copper and allowed to cool.
- **Solidification:** The separated slag is then allowed to cool and solidify. As it cools, it forms a glassy or



**Dindod Rutika and Sharma Ankita**

granulated material, depending on the cooling process used.

- **Processing:** Depending on the specific operation and its environmental regulations, the copper slag may undergo further processing or treatment to reduce its environmental impact or recover additional metals.

Copper slag can be used in various applications, including as an abrasive material for sandblasting, in the construction industry for making cement and concrete, and as an aggregate in road construction. It is important to manage copper slag responsibly to minimize its environmental impact and potential health risks associated with its use. Regulations and practices for handling and disposing of copper slag may vary by location and jurisdiction.

USES OF COPPER SLAG

- **Sandblasting Abrasive:** Copper slag is often used as an abrasive material in sandblasting operations. It is an effective abrasive due to its hardness, angular shape, and high density. It can remove rust, paint, and other surface contaminants from various materials.
- **Construction and Concrete:** Copper slag can be used as a partial replacement for sand in concrete and cement applications. When used in concrete, it can improve its strength, durability, and resistance to corrosion. The slag can also be used as a fine or coarse aggregate in concrete mixtures.
- **Road Construction:** In road construction, copper slag can be used as an aggregate in asphalt mixes and road bases. It provides stability and improves the wear resistance of the road surface.
- **Tile and Ceramic Industry:** Copper slag can be used as a raw material in the production of ceramic tiles and bricks. It helps in reducing the firing temperature required for these products.
- **Water Filtration:** Copper slag can be utilized in water filtration processes. It can remove contaminants and impurities from water, making it suitable for industrial and environmental applications.
- **Roofing Granules:** Copper slag can be processed into granules and used as roofing granules for shingles. These granules provide color and protection to the roofing material.
- **Ship Ballast:** In some cases, copper slag has been used as ship ballast, helping to maintain stability in marine vessels.
- **Landscaping and Abrasive Blasting:** Copper slag can be used in landscaping projects, as well as for abrasive blasting in various industries, such as metal cleaning and paint removal.
- **Wastewater Treatment:** Copper slag can aid in wastewater treatment processes, helping to remove heavy metals and contaminants from wastewater.

Soil Stabilization

It can be used for soil stabilization in construction projects to enhance the load-bearing capacity of the soil. It's important to note that the suitability of copper slag for a particular application depends on its specific characteristics, such as particle size, shape, and chemical composition. Additionally, local regulations and environmental considerations should be taken into account when using copper slag, as it may contain trace elements and impurities that need to be managed properly to prevent environmental contamination. While copper slag has several advantages, it also has some disadvantages and potential drawbacks, including:

- **Environmental Concerns:** Copper slag may contain trace elements and impurities, including heavy metals, which can be a concern for the environment if not properly managed. Disposing of copper slag without appropriate measures can lead to soil and water contamination.
- **Health Risks:** The dust generated during the handling and processing of copper slag can pose health risks to workers if inhaled. Adequate safety precautions and personal protective equipment are necessary when working with copper slag.
- **Variable Quality:** The quality and properties of copper slag can vary depending on its source and production methods. Inconsistent quality can lead to difficulties in achieving desired results in various applications.
- **Abrasiveness:** While its abrasive properties are advantageous for some applications, the high abrasiveness of



**Dindod Rutika and Sharma Ankita**

copper slag can be damaging to certain surfaces or materials, requiring careful selection of abrasive materials for specific jobs.

- **Containment and Handling Costs:** Proper containment and handling of copper slag are essential to prevent environmental and health issues. Managing and disposing of copper slag can incur additional costs for businesses.
- **Limited Availability:** The availability of copper slag is limited to areas near copper smelting and refining operations, which may not be readily accessible in all regions.
- **Not Suitable for All Applications:** Copper slag is not suitable for all applications. Its use should be carefully considered and evaluated for compatibility with specific project requirements and environmental regulations.
- **Regulatory Compliance:** Compliance with environmental and safety regulations may require additional measures and costs when using copper slag in various applications.
- **Alternative Materials:** In some cases, alternative materials may be more suitable or cost-effective for specific applications, making copper slag less competitive in those contexts. It's essential to understand these disadvantages and take appropriate precautions when using copper slag in various applications to mitigate potential risks and ensure responsible and safe utilization. Additionally, local regulations and environmental considerations must be followed to manage copper slag effectively. This review is about to partial replacement of copper slag as a fine aggregate. Many other papers are studied by author to know the results.

TESTING METHODS FOR HARDENED CONCRETE WITH COPPER SLAG REPLACEMENT

Methods of Testing for Both hardened concrete and partial replacement with copper slag as a fine aggregate.

- **Improved Strength:** Partial replacement of fine aggregate with copper slag can lead to improved compressive and flexural strength in concrete, enhancing its structural performance.
- **Enhanced Durability:** Concrete incorporating copper slag as a partial replacement for fine aggregate tends to exhibit improved resistance to chemical attacks, corrosion, and abrasion.
- **Reduction in Environmental Impact:** Using copper slag as a fine aggregate replacement in concrete helps reduce the demand for natural sand, promoting resource conservation and sustainable construction practices.
- **Reduced Carbon Footprint:** The use of copper slag can lead to a reduction in the carbon footprint of concrete production, as it often requires less energy compared to natural sand.
- **Improved Workability:** Concrete containing copper slag may exhibit good workability, making it easier to handle and place during construction.
- **Cost Savings:** Copper slag is often more cost-effective than natural sand, which can lead to cost savings in concrete production.
- **Enhanced Aesthetics:** Copper slag can provide a unique texture and color to concrete, which may be desirable for architectural and decorative purposes.
- **Regulatory Compliance:** Ensure that the use of copper slag in concrete complies with local regulations and standards to address any potential environmental or safety concerns.
- **Optimal Mix Design:** To achieve the desired concrete properties, it's important to conduct appropriate mix design tests when using copper slag as a replacement for fine aggregate.
- **Quality Control:** Quality control measures should be in place to ensure consistent and reliable results when using copper slag in concrete production.
- **Health and Safety:** Protect workers from potential health hazards by implementing safety measures, such as dust control, when handling and processing copper slag.
- **Optimal Percentage:** The percentage of copper slag used as a replacement for fine aggregate should be carefully determined based on the specific concrete requirements and project goals.
- **Research and Testing:** Consider conducting research and testing to evaluate the performance of concrete with copper slag under local conditions and in accordance with applicable standards.
- **Long-Term Performance:** Assess the long-term durability and performance of concrete containing copper slag to ensure it meets the project's requirements and remains structurally sound over time.



**Dindod Rutika and Sharma Ankita**

- **Environmental Impact Assessment:** Evaluate the environmental impact of sourcing and using copper slag, taking into account transportation, production, and disposal considerations.
- **Cost-Benefit Analysis:** Conduct a cost-benefit analysis to determine the economic advantages of using copper slag as a fine aggregate replacement in concrete.

When using copper slag as a partial replacement for fine aggregate in concrete, it's essential to strike a balance between achieving the desired performance improvements and ensuring compliance with local regulations and safety standards. Proper mix design and quality control are critical to the success of such applications.

CONCLUSION

The partial replacement of copper slag as a fine aggregate in concrete presents a promising solution to address the challenges associated with traditional fine aggregates. While it offers advantages in terms of strength, durability, and environmental sustainability, its successful implementation requires careful consideration of mix design, regulatory compliance, safety, and long-term performance. Further research and practical applications are essential to harness the full potential of copper slag in the construction industry. This review paper underscores the importance of responsible and informed use of copper slag in concrete to meet the growing demand for sustainable and eco-friendly construction practices.

REFERENCES

1. Vikas Dhanger and Jitendra Chouhan, "Study on Utilization of Copper Slag in Sustainable Construction of Rigid Pavements" (International Research Journal of Engineering and Technology, 2019).
2. Jayapal Naganur and Chethan B. A. "Effect of Copper Slag as a Partial Replacement of Fine Aggregate on the Properties of Cement Concrete" (International Journal of Research (IJR), Karnataka, 2014).
3. M. Pavan Kumar and Y. Mahesh, "The Behaviour of Concrete by Partial Replacement of Fine Aggregate with Copper Slag and Cement with GGBS- An Experimental Study" (IOSR Journal of Mechanical and Civil Engineering – (IOSR-JMCE), 2015).
4. Tamil Selvi P*, Lakshmi Narayani P and Ramya G "Experimental Study on Concrete Using Copper Slag as Replacement Material of Fine Aggregate" Civil & Environmental Engineering Research Article; 4:5; 2014.
5. M. V. PATIL "Properties and Effects Of Copper Slag In Concrete" International Journal of Advances in Mechanical and Civil Engineering; Volume-2, Issue-2; 2015.
6. IRC:SP:121-2018- Page No – (20-24).
7. I.S. 10262: 2019.
8. Zine Kiran Sambhaji¹, Prof. Pankaj B. Autade² "Effect of Copper Slag As A Fine Aggregate on Properties of Concrete" IRJET; Volume: 03 Issue: 06; 2016.
9. Arivalagan.S, Experimental Study on the Flexural Behavior of Reinforced Concrete Beams as Replacement of Copper Slag as Fine Aggregate, Journal Of Civil Engineering And Urbanism Volume 3 (2013).
10. Khanzadi, M and Behnood, A. 2009 "Mechanical properties of high-strength concrete incorporating copper slag as coarse aggregate", "Construction and Building Materials, Vol. 23, 2183–2188.
11. Madhavi, T.Ch. 2014. Copper slag in concrete as replacement material. International Journal of Civil engineering and technology (IJCET). Vol.5, Issue, 3, pp.327-332.





Dynamics of Tracking the Glucose- Insulin Interaction Inside the Body of Diabetes Patient's within the Context of Various Fractional Derivatives

T.Saradhadevi^{1*}, A.Kalavathi² and R.Baranitha²

¹Research Scholar, Department of Mathematics, Sri GVG Visalakshi College for Women, Udumalpet, Tiruppur, (Affiliated to Bharathiar University, Coimbatore), Tamil Nadu, India.

²Assistant Professor, Department of Mathematics, Sri GVG Visalakshi College for Women, Udumalpet, Tiruppur, (Affiliated to Bharathiar University, Coimbatore), Tamil Nadu, India.

Received: 29 Jan 2024

Revised: 09 Feb 2024

Accepted: 27 Apr 2024

*Address for Correspondence

T.Saradhadevi

Research Scholar,
Department of Mathematics,
Sri GVG Visalakshi College for Women,
Udumalpet, Tiruppur,
(Affiliated to Bharathiar University, Coimbatore),
Tamil Nadu, India.
Email: search2saradha@gmail.com



This is an Open Access Journal / article distributed under the terms of the **Creative Commons Attribution License** (CC BY-NC-ND 3.0) which permits unrestricted use, distribution, and reproduction in any medium, provided the original work is properly cited. All rights reserved.

ABSTRACT

This paper proposes a fractional variable-order model of glucose-insulin interaction in the sense of Liouville-Caputo, Caputo-Fabrizio and Atangana -Baleanu fractional derivatives. To establish the equilibrium point and test the stability of the fractional model. Existence and Uniqueness of fractional solutions have been demonstrated by using Lipschitz condition. Numerical simulations have been performed by means of Liouville-Caputo, Caputo-Fabrizio and Atangana -Baleanu sense and graphical results using various values of the fractional order parameter for the dynamics of the model are presented.

Keywords: Fractional variable-order model, Lipschitz condition, Liouville-Caputo, Caputo-Fabrizio, Atangana-Baleanu

INTRODUCTION

People of all ages are affected by the metabolic disorder known as diabetes mellitus (DM), or simply diabetes. Now, diabetes has become an epidemic and is associated with serious side effects like blindness, retinopathy, nephropathy, and peripheral neuropathy. Every year, the number of people with diabetes worldwide rises. Numerous





Saradhadevi et al.,

mathematicians modeled the interactions between insulin and glucose within the human body. Such models are commonly restricted to ordinary differential equations. The minimal model, which is used to interpret the results of the intravenous glucose tolerance test (IVGT), is the most commonly used model in the study of diabetes. A three-compartment minimal model was developed in 1981 by Bergman et al.[1] in order to analyze and quantify insulin sensitivity and pancreatic responsiveness to the glucose tolerance of human subjects. De Gstateatano and A. Arino[2] modified the minimal model by incorporating the insulin dynamics. There are three state variables in their updated model. The plasma glucose concentration is represented by $G(t)$, the insulin concentration is represented by $I(t)$, and the insulin-excitabile tissue glucose up take activity is described by $X(t)$, an auxiliary function. Differential equations of integer order are generalized to form fractional differential equations. Only the fractional derivatives of Caputo-Fabrizio (CF)[3] and Atangana-Baleanu (AB)[4] have non-singular kernels; the kernels of Riemann-Liouville and Caputo exhibit singularity. Fractional calculus has been used by numerous mathematicians and researchers to simulate real-world issues [5–15], especially in the field of medicine [16–26]. In view of the above, this study is motivated by the application of the variable- order fractional derivative in Liouville-Caputo, Caputo-Fabrizio and Atangana-Baleanu sense to understand the dynamic behaviour of glucose-insulin interaction model. The present paper is organized as follows: Section 2, gives the necessary preliminary information for the fractional model. Section 3 describes the classical version of glucose-insulin interaction model and its corresponding fractional order model. Section 4 is for finding the equilibrium points and checks the stability of the proposed fractional model. Section 5 presents the existence and uniqueness of fractional solutions. Numerical results and simulations for the proposed fractional model are discussed in Section 6. Section 7, summarizes all obtained results of the work.

PRELIMINARIES

This section provides some basic definitions of fractional calculus which are used in subsequent sections.

Definition 2.1: The Liouville–Caputo (LC) fractional derivative with variable-order $\alpha(t)$ is defined as [32]

$${}^{LC}_0 D_t^{\alpha(t)} f(t) = \frac{1}{\Gamma(1-\alpha(t))} \int_0^t (t-u)^{-\alpha(t)} f(u) du, \quad 0 < \alpha(t) \leq 1$$

Definition 2.2: The Caputo–Fabrizio (CF) derivative with variable-order $\alpha(t)$ in Liouville–Caputo sense is defined as follows

$${}^{CF}_0 D_t^{\alpha(t)} f(t) = \frac{(2-\alpha(t))M(\alpha(t))}{2(1-\alpha(t))} \int_0^t \exp\left[\frac{-\alpha(t)}{(1-\alpha(t))}\right] (t-u) f'(u) du, \quad 0 < \alpha(t) < 1$$

where $M(\alpha(t)) = \frac{2}{2-\alpha(t)}$ is a normalization function.

Definition 2.3: The Atangana–Baleanu (AB) fractional derivative with variable-order $\alpha(t)$ in Liouville–Caputo sense is defined as follows

$${}^{AB}_0 D_t^{\alpha(t)} f(t) = \frac{B(\alpha(t))}{(1-\alpha(t))} \int_0^t E_{\alpha(t)}\left[\frac{-\alpha(t)}{(1-\alpha(t))}\right] (t-u)^{\alpha(t)} f'(u) du, \quad 0 < \alpha(t) \leq 1$$

where $B(\alpha(t)) = 1 - \alpha(t) + \frac{\alpha(t)}{\Gamma(\alpha(t))}$ is a normalization function.

Remark: When $\alpha(t)$ is a constant, then we retrieve the constant order fractional derivative in Liouville-Caputo, Caputo-Fabrizio and Atangana-Baleanu sense.

Model formulation in Classical and Fractional Sense

Classical model of Glucose-Insulin interaction inside the body of diabetes patients

Many Mathematical models are used to analyse glucose-insulin interaction of diabetic patients. A simplified regulation model of glucose insulin interaction given in [31] is considered here. The model formulation as in [31] is

$$\frac{dG}{dt} = -s_1 G(t) - s_2 G(t)I(t) + s_1 G_b; \quad G(0) = G_0$$





$$\begin{aligned}\frac{dX}{dt} &= -s_2X(t) + s_3I(t) - s_3I_b ; X(0) = X_0 \\ \frac{dI}{dt} &= s_4G(t) - s_5I(t) + s_5I_b ; I(0) = I_0\end{aligned}\quad (1)$$

where the plasma glucose concentration is referred to as $G(t)$, generalized insulin variable for the remote compartment is represented as $X(t)$, and the plasma insulin concentration is denoted as $I(t)$. To explain the spread of the disease in a particular population, G_b indicates the basal blood glucose concentration, I_b represents the basal blood insulin concentration, s_1 signifies the glucose clearance rate that is not influenced by insulin, s_2 is the rate at which active insulin is cleared, s_3 reflects the independent increase of insulin in the ability of glucose uptake in tissues per unit of insulin concentration I_b , s_4 indicates the rate at which pancreatic β -cells release insulin after a glucose injection with glucose concentration G_b , and s_5 is the decay rate for insulin in plasma when pancreatic β -cells release insulin.

Fractional version of the classical model

The fractional model of the system (1) is obtained by replacing the classical derivative by the operator $\frac{d^{\alpha(t)}f(t)}{dt}$

$$\begin{aligned}\frac{d^{\alpha(t)}G(t)}{dt} &= -s_1^{\alpha(t)}G(t) - s_2^{\alpha(t)}G(t)I(t) + s_1^{\alpha(t)}G_b ; G(0) = G_0 \\ \frac{d^{\alpha(t)}X(t)}{dt} &= -s_2^{\alpha(t)}X(t) + s_3^{\alpha(t)}I(t) - s_3^{\alpha(t)}I_b ; X(0) = X_0 \\ \frac{d^{\alpha(t)}I(t)}{dt} &= s_4^{\alpha(t)}G(t) - s_5^{\alpha(t)}I(t) + s_5^{\alpha(t)}I_b ; I(0) = I_0\end{aligned}\quad (2)$$

The equilibria of the above fractional-order model can be obtained from $\frac{d^{\alpha(t)}G(t)}{dt}=0$, $\frac{d^{\alpha(t)}X(t)}{dt}=0$ and $\frac{d^{\alpha(t)}I(t)}{dt}=0$.

It was observed that the system (1) has two equilibria, namely the disease free equilibrium (E_{df}) and the endemic equilibrium (E_{end}). The disease free equilibrium point of model (2) is $E_{df} = (G_b, 0, 0)$ and the endemic equilibrium is $E_{end} = (G^*, X^*, I^*)$

$$\begin{aligned}\text{where } G^* &= \frac{s_1^{\alpha(t)}G_b}{s_1^{\alpha(t)}G(t) + s_2^{\alpha(t)}I^*}, \quad X^* = \frac{-s_3^{\alpha(t)}(I^* - s_3^{\alpha(t)}I_b)}{s_2^{\alpha(t)}}, \\ I^* &= \frac{-[s_1^{\alpha(t)}s_2^{\alpha(t)} - s_2^{\alpha(t)}s_5^{\alpha(t)}I_b] \pm \sqrt{[s_1^{\alpha(t)}s_2^{\alpha(t)} - s_2^{\alpha(t)}s_5^{\alpha(t)}I_b]^2 + 4(s_2^{\alpha(t)}s_5^{\alpha(t)})(s_1^{\alpha(t)}s_5^{\alpha(t)}I_b + s_1^{\alpha(t)}s_4^{\alpha(t)}G_b)}}{2(s_2^{\alpha(t)}s_5^{\alpha(t)})}\end{aligned}$$

The jacobian matrix corresponding to disease free equilibrium point and endemic equilibrium point is given by

$$\begin{aligned}J_{df} &= \begin{bmatrix} -s_1^{\alpha(t)} & 0 & -s_2^{\alpha(t)}G \\ 0 & -s_2^{\alpha(t)} & 0 \\ 0 & 0 & -s_5^{\alpha(t)} \end{bmatrix} \text{ and} \\ J_{end} &= \begin{bmatrix} -s_1^{\alpha(t)} - s_2^{\alpha(t)}I^* & 0 & -s_2^{\alpha(t)}G^* \\ 0 & -s_2^{\alpha(t)} & s_3^{\alpha(t)} \\ 0 & 0 & -s_2^{\alpha(t)}s_4^{\alpha(t)}G^* - s_1^{\alpha(t)}s_5^{\alpha(t)} - s_2^{\alpha(t)}s_5^{\alpha(t)}I^* \end{bmatrix}\end{aligned}$$

The eigen values of the above jacobian matrix J_{df} and J_{end} are obtained by using the characteristic equation

$\text{Det}(J - \lambda I) = 0$. For disease free equilibrium point the eigen values are $\lambda_1 = -s_1^{\alpha(t)}$, $\lambda_2 = -s_2^{\alpha(t)}$, $\lambda_3 = -s_5^{\alpha(t)}$ and for endemic case $\lambda_1 = -s_1^{\alpha(t)} - s_2^{\alpha(t)}I^*$, $\lambda_2 = -s_2^{\alpha(t)}$, $\lambda_3 = -[s_2^{\alpha(t)}s_4^{\alpha(t)}G^* + s_1^{\alpha(t)}s_5^{\alpha(t)} + s_2^{\alpha(t)}s_5^{\alpha(t)}I^*]$

In both cases, the eigen values are negative, hence the system (2) is locally asymptotically stable at (E_{df}) and (E_{end}).

Existence and Uniqueness of Fractional solutions

Existence and Uniqueness of Fractional solutions by the Liouville-Caputo model

In this section, we establish the existence and uniqueness of solutions of the Liouville-Caputo model.

Let us construct the system (2) as

$$\begin{aligned}{}^{LC}_0D_t^{\alpha(t)}[G(t)] &= F_1(t, G) = -s_1^{\alpha(t)}G(t) - s_2^{\alpha(t)}G(t)I(t) + s_1^{\alpha(t)}G_b \\ {}^{LC}_0D_t^{\alpha(t)}[X(t)] &= F_2(t, X) = -s_2^{\alpha(t)}X(t) + s_3^{\alpha(t)}I(t) - s_3^{\alpha(t)}I_b\end{aligned}\quad (3)$$





$${}^L C_0^{\alpha(t)} D_t^{\alpha(t)} [I(t)] = F_3(t, I) = s_4^{\alpha(t)} G(t) - s_5^{\alpha(t)} I(t) + s_5^{\alpha(t)} I_b$$

By using Liouville-Caputo fractional integral operator to the above system, we get

$$G(t) - G(0) = \frac{1}{\Gamma(\alpha(t))} \int_0^t (t-k)^{\alpha(t)-1} F_1(K, G(t)) dk$$

$$X(t) - X(0) = \frac{1}{\Gamma(\alpha(t))} \int_0^t (t-k)^{\alpha(t)-1} F_2(K, X(t)) dk$$

$$I(t) - I(0) = \frac{1}{\Gamma(\alpha(t))} \int_0^t (t-k)^{\alpha(t)-1} F_3(K, I(t)) dk$$

We will show that the kernel F_i for $i = 1, 2, 3$ follows the Lipschitz condition and contraction.

Theorem 4.1.1:

The kernel $F_i(K, G)$ for $i = 1, 2, 3$ satisfies Lipschitz condition and contraction if the following inequality $0 \leq r_i < 1$ holds.

Proof:

Consider two functions G and \bar{G}

$$\begin{aligned} \|F_1(t, G) - F_1(t, \bar{G})\| &= \left\| -s_1^{\alpha(t)} G - s_2^{\alpha(t)} GI + s_1^{\alpha(t)} \bar{G} + s_2^{\alpha(t)} \bar{G}I + s_1^{\alpha(t)} G_b - s_1^{\alpha(t)} \bar{G}_b \right\| \\ &\leq s_1^{\alpha(t)} \|G - \bar{G}\| + s_2^{\alpha(t)} \|I\| \|G - \bar{G}\| \\ &\leq [s_1^{\alpha(t)} + s_2^{\alpha(t)} u_3] \|G - \bar{G}\| \\ &\leq r_1 \|G - \bar{G}\| \end{aligned} \quad (4)$$

where $\|G(t)\| \leq u_1$, $\|X(t)\| \leq u_2$, $\|I(t)\| \leq u_3$ and $r_1 = s_1^{\alpha(t)} + s_2^{\alpha(t)} u_3$ are positive constants. As a result, the Lipschitz condition is met for r_1 and if $0 \leq r_1 < 1$, then r_1 follows contraction. Similarly, it can be exhibited and demonstrated in the other equations as follows

$$\|F_2(t, X) - F_2(t, \bar{X})\| \leq r_2 \|X - \bar{X}\|$$

$$\|F_3(t, I) - F_3(t, \bar{I})\| \leq r_3 \|I - \bar{I}\|$$

Therefore F_i satisfies Lipschitz condition. Also, if $0 \leq r_i < 1$, then the kernels follows contractions.

From system (3), the recurrent form can be written as follows

$$\Phi_{1n} = G_n(t) - G_{n-1}(t) = \frac{1}{\Gamma(\alpha(t))} \int_0^t (t-k)^{\alpha(t)-1} [F_1(K, G_{n-1}) - F_1(K, G_{n-2})] dk$$

$$\Phi_{2n} = X_n(t) - X_{n-1}(t) = \frac{1}{\Gamma(\alpha(t))} \int_0^t (t-k)^{\alpha(t)-1} [F_2(K, X_{n-1}) - F_2(K, X_{n-2})] dk$$

$$\Phi_{3n} = I_n(t) - I_{n-1}(t) = \frac{1}{\Gamma(\alpha(t))} \int_0^t (t-k)^{\alpha(t)-1} [F_3(K, I_{n-1}) - F_3(K, I_{n-2})] dk$$

Using the initial conditions $G(t) = G(0)$, $X(t) = X(0)$, $I(t) = I(0)$ for the above equation and taking norm, we get

$$\begin{aligned} \|\Phi_{1n}(t)\| &= \|G_n(t) - G_{n-1}(t)\| = \left\| \frac{1}{\Gamma(\alpha(t))} \int_0^t (t-k)^{\alpha(t)-1} [F_1(K, G_{n-1}) - F_1(K, G_{n-2})] dk \right\| \\ &\leq \frac{1}{\Gamma(\alpha(t))} \int_0^t \|(t-k)^{\alpha(t)-1} [F_1(K, G_{n-1}) - F_1(K, G_{n-2})]\| dk \end{aligned}$$

Now using Lipschitz condition in the above equation, we obtain

$$\|\Phi_{1n}(t)\| \leq \frac{r_1}{\Gamma(\alpha(t))} \int_0^t \|\Phi_{1(n-1)}(k)\| dk$$





Similarly,

$$\begin{aligned}\|\Phi_{2n}(t)\| &\leq \frac{r_2}{\Gamma(\alpha(t))} \int_0^t \|\Phi_{2(n-1)}(k)\| dk \\ \|\Phi_{3n}(t)\| &\leq \frac{r_3}{\Gamma(\alpha(t))} \int_0^t \|\Phi_{3(n-1)}(k)\| dk\end{aligned}\quad (5)$$

which implies that it can be written as

$$G_n(t) = \sum_{i=1}^n \Phi_{1i}(t); X_n(t) = \sum_{i=1}^n \Phi_{2i}(t); I_n(t) = \sum_{i=1}^n \Phi_{3i}(t)$$

Theorem 4.1.2:

The Liouville-Caputo model (3) has system of solutions if there exists $t > 1$ such that $\frac{r_i t}{\Gamma(\alpha(t))} \leq 1$ for $i=1,2,3$

Proof:

Consider,

$$\|\Phi_{1n}(t)\| \leq \frac{r_1}{\Gamma(\alpha(t))} \int_0^t \|\Phi_{1(n-1)}(k)\| dk$$

Replacing n by $n-1$ in the above inequality

$$\begin{aligned}\|\Phi_{1(n-1)}(t)\| &\leq \frac{r_1}{\Gamma(\alpha(t))} \int_0^t \|\Phi_{1(n-2)}(k)\| dk \\ &\leq \left[\frac{r_1}{\Gamma(\alpha(t))} \right]^2 \int_0^t \|\Phi_{1(n-2)}(k)\| dk\end{aligned}$$

Again, replacing n by $n-2$ in the given inequality

$$\|\Phi_{1(n-2)}(t)\| \leq \left[\frac{r_1}{\Gamma(\alpha(t))} \right]^3 \int_0^t \|\Phi_{1(n-3)}(k)\| dk$$

On substituting in this way and use the initial condition

We obtain

$$\|\Phi_{1n}(t)\| \leq \|G_n(0)\| \left[\frac{r_1 t}{\Gamma(\alpha(t))} \right]^n$$

Similarly, we get

$$\|\Phi_{2n}(t)\| \leq \|X_n(0)\| \left[\frac{r_2 t}{\Gamma(\alpha(t))} \right]^n$$

$$\|\Phi_{3n}(t)\| \leq \|I_n(0)\| \left[\frac{r_3 t}{\Gamma(\alpha(t))} \right]^n$$

This result proved the existence and continuity of solutions.

To show that $G(t)$, $X(t)$, $I(t)$ are the solutions of (3), we consider the following equations

$$\begin{aligned}G(t) - G(0) &= G_n(t) - R_{1n}(t) \\ X(t) - X(0) &= X_n(t) - R_{2n}(t) \\ I(t) - I(0) &= I_n(t) - R_{3n}(t)\end{aligned}\quad (6)$$

$$\|R_{1n}(t)\| = \left\| \frac{1}{\Gamma(\alpha(t))} \int_0^t [F_1(K, G_n) - F_1(K, G_{n-1})] dk \right\|$$

$$\leq \frac{1}{\Gamma(\alpha(t))} \int_0^t \| [F_1(K, G_n) - F_1(K, G_{n-1})] \| dk$$

$$\leq \frac{1}{\Gamma(\alpha(t))} r_1 \|G_n - G_{n-1}\| t$$

Applying the above process recursively,

$$\|R_{1n}(t)\| = \left[\frac{r_1 t}{\Gamma(\alpha(t))} \right]^{n+1} \cdot M$$

where M is the Lipschitz constant





Saradhadevi et al.,

when $n \rightarrow \infty$, $\|R_{1n}(t)\| \rightarrow 0$
 similarly we prove for
 $\|R_{2n}(t)\| \rightarrow 0, \|R_{3n}(t)\| \rightarrow 0$ as $n \rightarrow \infty$
 Hence the proof.

Theorem 4.1.3:

If the condition $\left[1 - \frac{r_i t}{\Gamma(\alpha(t))}\right] \geq 0$, for $i = 1, 2, 3$ holds then Caputo model have unique solution

Proof:

To establish the uniqueness for a solution of the system (3), consider the different set of solutions for the system (3), say \bar{G}, \bar{X} and \bar{I} . Then as an outcome of the first equation of (3), we write

$$G(t) - \bar{G}(t) = \frac{1}{\Gamma(\alpha(t))} \int_0^t [F_1(K, G) - F_1(K, \bar{G})] dk$$

Using the norm of above equation

$$\|G(t) - \bar{G}(t)\| = \left\| \frac{1}{\Gamma(\alpha(t))} \int_0^t [F_1(K, G) - F_1(K, \bar{G})] dk \right\|$$

Now by applying Lipschitz condition

$$\|G(t) - \bar{G}(t)\| = \frac{1}{\Gamma(\alpha(t))} r_1 t \|G(t) - \bar{G}(t)\|$$

Consequently

$$\|G(t) - \bar{G}(t)\| - \frac{1}{\Gamma(\alpha(t))} r_1 t \|G(t) - \bar{G}(t)\| \leq 0$$

$$\|G(t) - \bar{G}(t)\| \left[1 - \frac{1}{\Gamma(\alpha(t))} r_1 t\right] \leq 0 \quad (7)$$

Since $\left[1 - \frac{1}{\Gamma(\alpha(t))} r_1 t\right] > 0$, equation (7) becomes the form

$$\|G(t) - \bar{G}(t)\| = 0$$

$$\text{i.e., } G(t) = \bar{G}(t)$$

similarly we prove

$$X(t) = \bar{X}(t) \text{ and } I(t) = \bar{I}(t)$$

Hence the theorem is proved

Existence and Uniqueness of Fractional solutions by the Caputo-Fabrizio model

Let us construct the system (2) in the sense of Caputo-Fabrizio, we have

$$\begin{aligned} {}^{CF}D_t^{\alpha(t)}[G(t)] &= F_1(t, G) = -s_1^{\alpha(t)} G(t) - s_2^{\alpha(t)} G(t)I(t) + s_1^{\alpha(t)} G_b \\ {}^{CF}D_t^{\alpha(t)}[X(t)] &= F_2(t, X) = -s_2^{\alpha(t)} X(t) + s_3^{\alpha(t)} I(t) - s_3^{\alpha(t)} I_b \end{aligned} \quad (8)$$

$${}^{CF}D_t^{\alpha(t)}[I(t)] = F_3(t, I) = s_4^{\alpha(t)} G(t) - s_5^{\alpha(t)} I(t) + s_5^{\alpha(t)} I_b$$

The Caputo-Fabrizio integral form of the above system is

$$\begin{aligned} G(t) - G(0) &= \frac{1 - \alpha(t)}{M(\alpha(t))} F_1(t, G) + \frac{\alpha(t)}{M(\alpha(t))} \int_0^t F_1(\tau, G) d\tau \\ X(t) - X(0) &= \frac{1 - \alpha(t)}{M(\alpha(t))} F_2(t, X) + \frac{\alpha(t)}{M(\alpha(t))} \int_0^t F_2(\tau, X) d\tau \\ I(t) - I(0) &= \frac{1 - \alpha(t)}{M(\alpha(t))} F_3(t, I) + \frac{\alpha(t)}{M(\alpha(t))} \int_0^t F_3(\tau, I) d\tau \end{aligned} \quad (9)$$

Here we have to prove the kernel F_i for $i = 1, 2, 3$ follows the Lipschitz condition and a contraction



**Theorem 4.2.1:**

The kernel $F_i(t, G)$, for $i = 1, 2, 3$ satisfies the Lipschitz condition and a contraction if the following inequality $0 \leq \rho_i < 1$ holds.

Proof:

This theorem is proved as similar as theorem 4.1.1

The recurrent form of (9) for the first equation is

$$\psi_{1n} = G_n(t) - G_{n-1}(t) \\ = \frac{1 - \alpha(t)}{M(\alpha(t))} [F_1(t, G_{n-1}) - F_1(t, G_{n-2})] + \frac{\alpha(t)}{M(\alpha(t))} \int_0^t [F_1(\tau, G_{n-1}) - F_1(\tau, G_{n-2})] d\tau$$

Similarly ψ_{2n} and ψ_{3n} are also be derived

Using the initial condition and taking norm, we get

$$\|\psi_{1n}\| \leq \frac{1 - \alpha(t)}{M(\alpha(t))} \| [F_1(t, G_{n-1}) - F_1(t, G_{n-2})] \| + \frac{\alpha(t)}{M(\alpha(t))} \int_0^t \| [F_1(\tau, G_{n-1}) - F_1(\tau, G_{n-2})] \| d\tau$$

Since ρ_1 satisfies Lipschitz condition

$$\|\psi_{1n}(t)\| \leq \frac{1 - \alpha(t)}{M(\alpha(t))} \rho_1 \| [\psi_{1(n-1)}(t)] \| + \frac{\alpha(t)}{M(\alpha(t))} \rho_1 \int_0^t \|\psi_{1(n-1)}(\tau)\| d\tau \quad (10)$$

Similarly $\|\psi_{2n}(t)\|$ and $\|\psi_{3n}(t)\|$ can also be obtained.

Therefore,

$$G_n(t) = \sum_{i=1}^n \psi_{1i}(t), X_n(t) = \sum_{i=1}^n \psi_{2i}(t), I_n(t) = \sum_{i=1}^n \psi_{3i}(t)$$

Theorem 4.2.2:

The Caputo Fabrizio fractional derivative model (8) has system of solutions if there exists $v > 1$ such that

$$\left[\frac{1 - \alpha(t)}{M(\alpha(t))} \rho_i + \frac{\alpha(t)}{M(\alpha(t))} \rho_i v \right] \leq 1, \text{ for } i=1,2,3$$

Proof:

Operating (10) recursively and using the initial conditions we have

$$\|\psi_{1n}(t)\| \leq \|G_n(0)\| \left[\frac{1 - \alpha(t)}{M(\alpha(t))} \rho_1 + \frac{\alpha(t)}{M(\alpha(t))} \rho_1 v \right]^n$$

Similarly we have for $\|\psi_{2n}(t)\|$ and $\|\psi_{3n}(t)\|$, this result proved the existence and continuity of solution.

To show that $G(t)$, $X(t)$ and $I(t)$ are solutions of (8)

Consider

$$G(t) - G(0) = G_n(t) - D_{1n}(t)$$

$$X(t) - X(0) = X_n(t) - D_{2n}(t)$$

$$I(t) - I(0) = I_n(t) - D_{3n}(t)$$

Now

$$\|D_{1n}(t)\| \leq \frac{1 - \alpha(t)}{M(\alpha(t))} \| [F_1(t, G_n) - F_1(t, G_{n-1})] \| + \frac{\alpha(t)}{M(\alpha(t))} \int_0^t \| [F_1(\tau, G_n) - F_1(\tau, G_{n-1})] \| d\tau \\ \leq \frac{1 - \alpha(t)}{M(\alpha(t))} \rho_1 \| G_n - G_{n-1} \| + \frac{\alpha(t)}{M(\alpha(t))} \rho_1 \| G_n - G_{n-1} \| v \\ \leq \left[\frac{1 - \alpha(t)}{M(\alpha(t))} \rho_1 + \frac{\alpha(t)}{M(\alpha(t))} \rho_1 v \right] \| G_n - G_{n-1} \|$$

Applying the above process recursively

$$\|D_{1n}(t)\| \leq \left[\frac{1 - \alpha(t)}{M(\alpha(t))} \rho_1 + \frac{\alpha(t)}{M(\alpha(t))} \rho_1 v \right]^{n+1} S$$

where S is the Lipschitz constant

when $n \rightarrow \infty$, $\|D_{1n}\| \rightarrow 0$





Similarly we prove for $\|D_{2n}\| \rightarrow 0$, $\|D_{3n}\| \rightarrow 0$ as $n \rightarrow \infty$
Hence the proof

Theorem 4.2.3:

If the condition $\left[1 - \left[\frac{1-\alpha(t)}{M(\alpha(t))}\rho_i + \frac{\alpha(t)}{M(\alpha(t))}\rho_i v\right]\right] \geq 0$, for $i=1,2,3$, holds then the Caputo-Fabrizio fractional derivative model have unique solutions.

Proof:

Suppose the system (8) has another solution \bar{G}, \bar{X} and \bar{I} then

$$G(t) - \bar{G}(t) = \frac{1-\alpha(t)}{M(\alpha(t))} [F_1(t, G) - F_1(t, \bar{G})] + \frac{\alpha(t)}{M(\alpha(t))} \int_0^t [F_1(\tau, G) - F_1(\tau, \bar{G})] d\tau$$

Using norm and applying Lipschitz condition

$$\|G(t) - \bar{G}(t)\| \leq \left[\frac{1-\alpha(t)}{M(\alpha(t))}\rho_1 + \frac{\alpha(t)}{M(\alpha(t))}\rho_1 v\right] \|G(t) - \bar{G}(t)\|$$

Consequently we have

$$\|G(t) - \bar{G}(t)\| \left[1 - \left[\frac{1-\alpha(t)}{M(\alpha(t))}\rho_1 + \frac{\alpha(t)}{M(\alpha(t))}\rho_1 v\right]\right] \leq 0$$

Since $\left[1 - \left[\frac{1-\alpha(t)}{M(\alpha(t))}\rho_i + \frac{\alpha(t)}{M(\alpha(t))}\rho_i v\right]\right] > 0$, we have

$$\|G(t) - \bar{G}(t)\| = 0$$

i.e., $G(t) = \bar{G}(t)$

Similarly we prove

$$X(t) = \bar{X}(t) \text{ and } I(t) = \bar{I}(t)$$

Hence the proof

Existence and Uniqueness of solutions for the Atangana-Baleanu fractional model

Let us construct (2) in Atangana-Baleanu fractional derivative in Caputo sense

$$\begin{aligned} {}^{AB}_0 D_t^{\alpha(t)} [G(t)] &= F_1(t, G) = -s_1^{\alpha(t)} G(t) - s_2^{\alpha(t)} G(t) I(t) + s_1^{\alpha(t)} G_b \\ {}^{AB}_0 D_t^{\alpha(t)} [X(t)] &= F_2(t, X) = -s_2^{\alpha(t)} X(t) + s_3^{\alpha(t)} I(t) - s_3^{\alpha(t)} I_b \end{aligned} \quad (11)$$

$${}^{AB}_0 D_t^{\alpha(t)} [I(t)] = F_3(t, I) = s_4^{\alpha(t)} G(t) - s_5^{\alpha(t)} I(t) + s_5^{\alpha(t)} I_b$$

The Atangana-Baleanu integral form of the above system is

$$\begin{aligned} G(t) - G(0) &= \frac{1-\alpha(t)}{AB(\alpha(t))} F_1(t, G) + \frac{\alpha(t)}{AB(\alpha(t)) \Gamma(\alpha(t))} \int_0^t (t-\gamma)^{\alpha(t)-1} F_1(\gamma, G) d\gamma \\ X(t) - X(0) &= \frac{1-\alpha(t)}{AB(\alpha(t))} F_2(t, X) + \frac{\alpha(t)}{AB(\alpha(t)) \Gamma(\alpha(t))} \int_0^t (t-\gamma)^{\alpha(t)-1} F_2(\gamma, X) d\gamma \\ I(t) - I(0) &= \frac{1-\alpha(t)}{AB(\alpha(t))} F_3(t, I) + \frac{\alpha(t)}{AB(\alpha(t)) \Gamma(\alpha(t))} \int_0^t (t-\gamma)^{\alpha(t)-1} F_3(\gamma, I) d\gamma \end{aligned} \quad (12)$$

Now to prove the kernel F_i for $i = 1, 2, 3$ follows the Lipschitz condition and contraction.

Theorem 4.3.1:

The kernel $F_i(\gamma, G)$, for $i = 1, 2, 3$ satisfies the Lipschitz condition and contraction if $0 \leq \delta_i < 1$ holds.

Proof:

The proof is similar to the proof of 4.1.1

Now the recurrent form of (12) is

$$\begin{aligned} \theta_{1n} &= G_n(t) - G_{n-1}(t) \\ &= \frac{1-\alpha(t)}{AB(\alpha(t))} [F_1(t, G_{n-1}) - F_1(t, G_{n-2})] + \frac{\alpha(t)}{AB(\alpha(t)) \Gamma(\alpha(t))} \int_0^t (t-\gamma)^{\alpha(t)-1} [F_1(\gamma, G_{n-1}) - F_1(\gamma, G_{n-2})] d\gamma \end{aligned}$$





Similarly θ_{2n}, θ_{3n} are also be derived.

Using the initial condition and taking norm, we get

$$\|\theta_{1n}\| \leq \frac{1-\alpha(t)}{AB(\alpha(t))} \| [F_1(t, G_{n-1}) - F_1(t, G_{n-2})] \| + \frac{\alpha(t)}{AB(\alpha(t)) \Gamma(\alpha(t))} \int_0^t (t-\gamma)^{\alpha(t)-1} \| [F_1(\gamma, G_{n-1}) - F_1(\gamma, G_{n-2})] \| d\gamma$$

Since δ_1 satisfies Lipschitz condition

$$\|\theta_{1n}\| \leq \frac{1-\alpha(t)}{AB(\alpha(t))} \delta_1 \|\theta_{1(n-1)}\| + \frac{\alpha(t)}{AB(\alpha(t)) \Gamma(\alpha(t))} \delta_1 \int_0^t (t-\gamma)^{\alpha(t)-1} \|\theta_{1(n-1)}(\gamma)\| d\gamma$$

Similarly for $\|\theta_{2n}\|, \|\theta_{3n}\|$

which implies that it can be written as

$$G_n(t) = \sum_{i=1}^n \theta_{1i}(t), X_n(t) = \sum_{i=1}^n \theta_{2i}(t), I_n(t) = \sum_{i=1}^n \theta_{3i}(t) \quad (13)$$

Theorem 4.3.2:

The Atangana-Baleanu derivative model (11) have system of solutions, if there exists $\mu > 1$ such that

$$\left[\frac{1-\alpha(t)}{AB(\alpha(t))} \delta_i + \frac{\alpha(t)}{AB(\alpha(t)) \Gamma(\alpha(t))} \delta_i \mu \right] \leq 1 \text{ for } i = 1, 2, 3.$$

Proof:

Consider,

$$\|\theta_{1n}\| \leq \|G_n(0)\| \left[\frac{1-\alpha(t)}{AB(\alpha(t))} \delta_i + \frac{\alpha(t)}{AB(\alpha(t)) \Gamma(\alpha(t))} \delta_i \mu \right]^n$$

Similarly $\|\theta_{2n}\|$ and $\|\theta_{3n}\|$ can also be obtained

These results proved the existence and continuity of solution.

Now to show that $G(t), X(t)$ and $I(t)$ are solutions of (11)

Consider

$$G(t) - G(0) = G_n(t) - E_{1n}(t)$$

$$X(t) - X(0) = X_n(t) - E_{2n}(t)$$

$$I(t) - I(0) = I_n(t) - E_{3n}(t)$$

Now

$$\begin{aligned} \|E_{1n}(t)\| &\leq \frac{1-\alpha(t)}{AB(\alpha(t))} \| [F_1(t, G_n) - F_1(t, G_{n-1})] \| + \frac{\alpha(t)}{AB(\alpha(t)) \Gamma(\alpha(t))} \int_0^t (t-\gamma)^{\alpha(t)-1} \| [F_1(\gamma, G_n) - F_1(\gamma, G_{n-1})] \| d\gamma \\ &\leq \frac{1-\alpha(t)}{AB(\alpha(t))} \delta_1 \|G_n - G_{n-1}\| + \frac{\alpha(t)}{AB(\alpha(t)) \Gamma(\alpha(t))} \delta_1 \|G_n - G_{n-1}\| \mu \\ &\leq \left[\frac{1-\alpha(t)}{AB(\alpha(t))} \delta_1 + \frac{\alpha(t)}{AB(\alpha(t)) \Gamma(\alpha(t))} \delta_1 \mu \right] \|G_n - G_{n-1}\| \end{aligned}$$

Applying the above process recursively

$$\|E_{1n}(t)\| \leq \left[\frac{1-\alpha(t)}{AB(\alpha(t))} \delta_1 + \frac{\alpha(t)}{AB(\alpha(t)) \Gamma(\alpha(t))} \delta_1 \mu \right]^{n+1} W$$

where W is the Lipschitz constant

when $n \rightarrow \infty, \|E_{1n}\| \rightarrow 0$

Similarly we prove for $\|E_{2n}\| \rightarrow 0, \|E_{3n}\| \rightarrow 0$ as $n \rightarrow \infty$

Hence the proof.

Theorem 4.3.3:

If the condition $\left[1 - \left[\frac{1-\alpha(t)}{AB(\alpha(t))} \delta_i + \frac{\alpha(t)}{AB(\alpha(t)) \Gamma(\alpha(t))} \delta_i \mu \right] \right] \geq 0$ For $i=1,2,3$, holds then the Atangana-Baleanu fractional derivative model have unique solutions.

Proof:

Suppose the system (16) has another solution \bar{G}, \bar{X} and \bar{I} then

$$G(t) - \bar{G}(t) = \frac{1-\alpha(t)}{AB(\alpha(t))} [F_1(t, G) - F_1(t, \bar{G})] + \frac{\alpha(t)}{AB(\alpha(t)) \Gamma(\alpha(t))} \int_0^t (t-\gamma)^{\alpha(t)-1} [F_1(\gamma, G) - F_1(\gamma, \bar{G})] d\gamma$$





Using norm and apply Lipschitz condition

$$\|G(t) - \bar{G}(t)\| \leq \left[\frac{1-\alpha(t)}{AB(\alpha(t))} \delta_1 + \frac{\alpha(t)}{AB(\alpha(t)) \Gamma(\alpha(t))} \delta_1 \mu \right] \|G(t) - \bar{G}(t)\|$$

Consequently we have

$$\|G(t) - \bar{G}(t)\| \left[1 - \left[\frac{1-\alpha(t)}{AB(\alpha(t))} \delta_1 + \frac{\alpha(t)}{AB(\alpha(t)) \Gamma(\alpha(t))} \delta_1 \mu \right] \right] \leq 0$$

Since $\left[1 - \left[\frac{1-\alpha(t)}{AB(\alpha(t))} \delta_1 + \frac{\alpha(t)}{AB(\alpha(t)) \Gamma(\alpha(t))} \delta_1 \mu \right] \right] > 0$, we have

$$\|G(t) - \bar{G}(t)\| = 0$$

i.e. $G(t) = \bar{G}(t)$

Similarly we prove

$$X(t) = \bar{X}(t) \text{ and } I(t) = \bar{I}(t)$$

Hence the proof

Numerical results and simulations

In this section, Numerical results and Simulations are obtained by considering the Numerical scheme[32] given in the sense of Liouville-Caputo, Caputo-Fabrizio and Atangana –Baleanu fractional derivatives.

Let us consider our fractional model as

$${}_0^*D_t^\alpha u(t) = f(t, u(t))$$

Where * denotes LC, CF and AB terms and $u(t) = (G(t), X(t), I(t))$.

Now we use the numerical scheme [32] represented for Liouville-Caputo (14), Caputo-Fabrizio(15) and Atangana-Baleanu(16) fractional derivatives in (2)

$$u_{n+1}(t) = u(0) + \frac{1}{\Gamma(\alpha(t))} \sum_{m=0}^n \left(\frac{h^{\alpha(t)} f(t_m, u_m)}{\alpha(t)(\alpha(t)+1)} ((n-m+2+2\alpha) - \frac{h^{\alpha(t)} f(t_{m-1}, u_{m-1})}{\alpha(t)(\alpha(t)+1)}) \right. \\ \left. ((n+1-m)^{\alpha(t)+1} - (n-m)^{\alpha(t)}(n-m+1+\alpha(t))) \right) \quad (14)$$

$$(u_{n+1}) = (u_n) + \left[\frac{(2-\alpha(t))(1-\alpha(t))}{2} + \frac{3h}{4} \alpha(t)(2-\alpha(t)) \right] f(t_n, u_n) - \left[\frac{(2-\alpha(t))(1-\alpha(t))}{2} + \frac{h}{4} \alpha(t)(2-\alpha(t)) \right] f(t_{n-1}, u_{n-1}) \quad (15)$$

$$u_{n+1}(t) = u(0) + \frac{\Gamma(\alpha(t))(1-\alpha(t))}{\Gamma(\alpha(t))(1-\alpha(t)) + \alpha(t)} f(t_n, u_n) \\ + \frac{1}{(\alpha(t)+1)((1-\alpha(t))\Gamma(\alpha(t)) + \alpha(t))} \sum_{m=0}^n \left(h^{\alpha(t)} f(t_m, u_m) ((n+1-m)^{\alpha(t)}(n-m+2+\alpha(t)) - (n-m)^{\alpha(t)}(n-m+2+2\alpha(t)) - h^{\alpha(t)} f(t_{m-1}, u_{m-1}) ((n+1-m)^{\alpha(t)+1} - (n-m+1+\alpha(t))) \right) \quad (16)$$

the numerical simulation and graphical results of the fractional model (2) is obtained by applying the above numerical scheme and using MATLAB R2023a.

Figure [1-3] indicates different Plasma Glucose concentration $-G(t)$, Insulin Action- $X(t)$ and Plasma Insulin Concentration- $I(t)$ for different α fractional orders $\alpha = 0.75$, $\alpha = 0.85$, $\alpha = 0.95$, and $\alpha = 1$ in Liouville-Caputo sense. The graphical results shows that the plasma glucose concentration level for normal persons are immediately uptake and it becomes stable within our considered time; however for diabetic patients, these levels decreases progressively. When it comes to insulin action, glucose will be rapidly diluted by insulin for normal person, but for diabetes patients, glucose will be diluted slowly by insulin action and will remain in the patient's body. For healthy individuals, the level of plasma insulin concentration will be falling and eventually get stabilized; however, for those with diabetes, the level of plasma insulin will be rising quickly and remains constant over time. Figure [5-6] indicates $G(t)$, $X(t)$ and $I(t)$ for fractional orders $\alpha = 0.75$, $\alpha = 0.85$, $\alpha = 0.95$, and $\alpha = 1$ in Caputo-Fabrizio derivative. It





shows that when the value of α decreases, the concentration of plasma glucose rises and eventually becomes stable for normal persons, in the case of diabetic patients, the plasma glucose concentration decreases, when α decreases. For normal persons, the Insulin action $[X(t)]$ rises in proportion to an increase in α ; whereas in diabetic patients, the increasing value of α makes Insulin action process slowly and it makes undiluted glucose to remain in patient's body. When α increases, the concentration of plasma insulin $[I(t)]$ becomes stable faster for normal persons. However, in patients with diabetes, the concentration of plasma insulin reaches its maximum and stays constant. Figure[7-9] represents $G(t)$, $X(t)$ and $I(t)$ for fractional orders $\alpha = 0.75$, $\alpha = 0.85$, $\alpha = 0.95$, and $\alpha = 1$ using Atangana – Baleanu derivative. When α rises, the concentration of Plasma Glucose $[G(t)]$ rises quickly and stabilizes for normal persons; whereas, the level of $G(t)$ gradually drops for diabetic patients. In healthy individuals, the Insulin action $[X(t)]$ rapidly decreases as α increases and in diabetic patients, $X(t)$ eventually decreases and stays constant as α increases. When α increases, the concentration of plasma insulin $[I(t)]$ decreases and stabilizes quickly for normal persons. For patients with diabetes, $I(t)$ increases quickly and reaches a constant value within our considered time. The graphical results of Liouville-Caputo, Caputo-Fabrizio and Atangana-Baleanu derivatives are compared for different fractional orders $\alpha=0.82$, $\alpha=0.96$, $\alpha=1$ and illustrated in figure[10-12]. Figure 10 shows that for normal persons, the level of $G(t)$ rises quickly with increasing time and becomes stable in all cases of LC, CF, and ABC.

When compared to LC and CF, the AB operator rapidly decreases in the case of $X(t)$. However, $I(t)$ falls and then stays constant for all derivatives of LC, CF, and AB. For diabetic patient-1, figure 11 indicates that, the level of $G(t)$ falls down rapidly and it remains constant in all cases of LC, CF and AB. However, the level of $X(t)$ decreases and it becomes stable within our considered time. In case of $I(t)$, the LC, CF and AB quickly rises and constant after time. Figure 12 depicts that for diabetic patient-2, the level of $G(t)$ and $X(t)$ decreases eventually and constant over time in all cases of LC, CF and AB; Whereas, the level of $I(t)$ increases rapidly and it stays constant by using all the three operators. The above discussion shows that AB gives more appropriate and reliable results when compared to LC and CF. Figure[13-21] predicts $G(t)$, $X(t)$ and $I(t)$ for both Normal persons and Diabetes Patients in cases of LC, CF and AB at $\alpha(t) = 0.7 + (0.1)\sin(\frac{t}{50})$, $\alpha(t) = 1/(1 + \exp(-t))$ and $\alpha(t) = \tanh(t + 1)$ respectively. The simulation result shows that the rises and falling of glucose-insulin levels are almost the same as of non-integer order but they are variable dependent. Compared to LC and CF, AB provides more appropriate and reliable results, according to the above graphical results. With these studies, the diabetes patients can be treated properly with suitable input values of insulin to normalize glucose level.

CONCLUSION

In this work, we presented the dynamics of the model, Glucose –Insulin interaction inside the body of diabetes patients in the framework of fractional calculus. We applied three fractional operators, Liouville-Caputo, Caputo-Fabrizio, and the Atangana-Baleanu to the fractional model of Glucose-Insulin interaction. Initially, the classical model given in [31] is formulated in Fractional sense. Equilibrium points for the given model have been calculated and discussed the stability of the proposed model. The existence and Uniqueness of solutions in fractional order cases are proved. Numerical simulation was performed and the graphical results are obtained at different fractional values are illustrated in number of graphs at different fractional values. The given derivative and algorithm work very well to understand the dynamics of the given model. The idea of this research has provided some important outcomes for diabetes medical practitioners and their related complications.

REFERENCES

1. Bergman, R.N., Phillips, L.S., Cobelli, C. (1981). Physiologic evaluation of factors controlling glucose tolerance in man: measurement of insulin sensitivity and beta-cell glucose sensitivity from the response to intravenous glucose. J. Clin. Invest, 68(6), 1456–1467





2. De Gaetano, A., Arino, O.(2000). Mathematical modelling of the intravenous glucose tolerance test. *J.Math. Biol.*,40(2), 136–168.
3. Caputo M, Fabrizio M.(2015) A new definition of fractional derivative without singular kernel. *ProgrFract Differ Appl* ,(2):1–13.
4. Atangana A, Baleanu D. (2016) New fractional derivatives with nonlocal and non-singular kernel: theory and application to heat transfer model. *Thermal Science* ,20(2):757–63.
5. Owolabi KM.(2017). Mathematical modelling and analysis of two-component system with Caputo fractional derivative order. *Chaos Solitons Fract*,103:544–54.
6. Owolabi KM. (2017). Robust and adaptive techniques for numerical simulation of nonlinear partial differential equations of fractional order. *Commun Nonlinear Sci Numer Simul*,44:304–17.
7. Guo YM, Zhao Y, Zhou YM, Xiao ZB, Yang XJ. (2017). On the local fractional LWR model in fractal traffic flows in the entropy condition. *Math Methods Appl Sci*.40(17),6127–32.
8. Kumar S, Kumar A, Baleanu D.(2016). Two analytical methods for time-fractional nonlinear coupled Boussinesq-Burger's equations arise in propagation of shallow water waves. *Nonlinear Dyn*,1:1–17.
9. Atangana A, Aguilar JFG.(2018). Decolonisation of fractional calculus rules: breaking commutativity and associativity to capture more natural phenomena, *EurPhys J Plus*, 133:1–23.
10. Zhao D, Singh J, Kumar D, Rathore S, Yang XJ. (2017). An efficient computational technique for local fractional heat conduction equations in fractal media. *J Nonlinear Sci Appl*,10(4):1478–86.
11. Kumar D, Singh J, Baleanu D. (2018). Analysis of regularized long-wave equation associated with a new fractional operator with Mittag-Leffler type kernel. *Physica A* 2018;492:155–67. J.E.Solís-Pérez et al. / *Chaos, Solitons and Fractals*, 114, 175–185.
12. Atangana A.(2018). Non validity of index law in fractional calculus: a fractional differential operator with Markovian and non-Markovian properties. *Physica A* ,505:688–706.
13. Hristov J.(2017). Derivation of the fractional Dodson equation and beyond: transient diffusion with a non-singular memory and exponentially fading-out diffusivity. *ProgrFract Differ Appl*,3(4):1–16.
14. Singh J, Kumar D, Baleanu D, Rathore S.(2018). An efficient numerical algorithm for the fractional drinfeldsokolovwilson equation. *Appl Math Comput*,335:12–24.
15. Hristov J.(2017) The non-linear Dodson diffusion equation: approximate solutions and beyond with formalistic fractionalization. *Math Nat Sci*.1(1),1–17.
16. Singh J, Kumar D, Hammouch Z, Atangana A.(2018) A fractional epidemiological model for computer viruses pertaining to a new fractional derivative. *Appl Math Comput* ,316:504–15.
17. Baskonus HM, Mekkaoui T, Hammouch Z, Bulut H.(2015). Active control of a chaotic fractional order economic system. *Entropy*.17(8),5771–83.
18. Yao JJ, Kumar A, Kumar S.(2015). A fractional model to describe the Brownian motion of particles and its analytical solution. *AdvMechEng* ,7(12):1–11.
19. Ghanbari B. (2018) A new generalized exponential rational function method to find exact special solutions for the resonance nonlinear Schrödinger equation. *EurPhys J Plus*.133(4),1–18.
20. Owolabi KM, Atangana A.(2017). Numerical simulation of non-integer order system in subdiffusive, diffusive, and superdiffusive scenarios. *J Comput Nonlinear Dyn*,12(3):1–7.
21. Yavuz M, Bonyah E.(2019) New approaches to the fractional dynamics of schistosomiasis disease model. *PhysA* ,525:373–93.
22. Kumar D, Singh J, Al Qurashi M, Baleanu D.(2019) A new fractional SIRS-SI malaria disease model with application of vaccines, antimalarial drugs, and spraying. *Adv Differ Equ* ,(1):278.
23. Ullah S, Khan MA, Farooq M, Hammouch Z, Baleanu D. (2019). A fractional model for the dynamics of tuberculosis infection using Caputo-Fabrizio derivative. *Discrete Contin Dyn Syst Ser S* ,11–27.
24. Yusuf A, Qureshi S, Inc M, Aliyu AI, Baleanu D, Shaikh AA.(2018). Two-strain epidemic model involving fractional derivative with Mittag-Leffler kernel. *Chaos* ,28(12):123121
25. Qureshi S, Yusuf A. (2019). Fractional derivatives applied to MSEIR problems: Comparative Study with real world data. *EurPhys J Plus* ,134(4):171.





Saradhadevi et al.,

26. Qureshi S, Atangana A.(2019). Mathematical analysis of dengue fever outbreak by novel fractional operators with field data. PhysA ,526:121127.
27. Bas E, Acay B, Ozarslan. (2019).R. Fractional models with singular and non-singular kernels for energy efficient buildings. Chaos ,29(2):023110.
28. Diethelm K.(2013) A fractional calculus based model for the simulation of an outbreak of dengue Fever. Nonlinear Dyn,71(4):613–19.
29. Owolabi KM, Pindza E. (2019). Modeling and simulation of nonlinear dynamical system in the frame of nonlocal and non-singular derivatives. Chaos Solitons Fractals,127:146–57.
30. Qureshi S, Yusuf A, Shaikh AA, Inc M.(2019). Transmission dynamics of varicella zoster virus modeled by classical and novel fractional operators using real statistical data. Phys.534:122149.
31. Sonia Akter, Md.SirajulIslam,Md.Haider Ali Biswas.(2020). Mathematical model Applied to Monitoring the Glucose-Insulin Interaction inside the Body of Diabetes Patients.GANIT journal of BandladeshMathematical Society.
32. J.E.Solis-Perez,J.E. Gomez-Aguilar ,A.Atangana. (2018).Novel numerical method for solving variable-order fractional differential equations with power, exponential and Mittag-Leffler laws. Chaos,Solitons and Fractals 114.175-185.

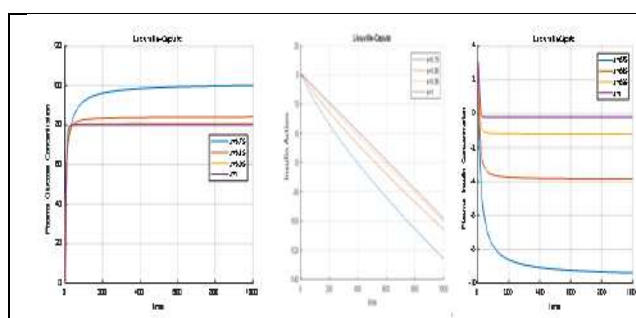


Figure 1: Glucose-insulin regulatory system for normal person, with different parameters $s_1 = 0.2$, $s_2 = 0.00123$, $s_3 = 6.92 \times 10^{-6}$, $s_4 = 0.0249$, $s_5 = 0.2769$, $G_b = 80$, $I_b = 7$ in Liouville-Caputo sense

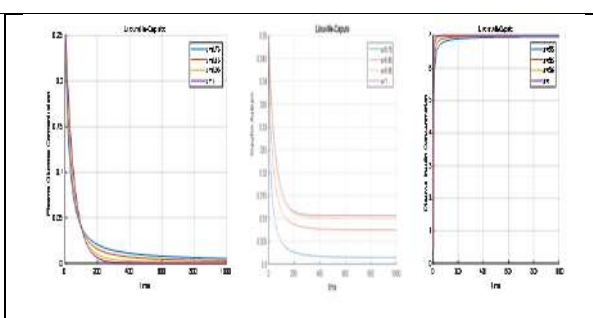


Figure 2: Glucose-Insulin regulatory system for diabetes patient 1, with different parameters $s_1 = 0$, $s_2 = 0.0027$, $s_3 = 5.3 \times 10^{-6}$, $s_4 = 0.0042$, $s_5 = 0.264$, $G_b = 80$, $I_b = 7$ in Liouville-Caputo sense.

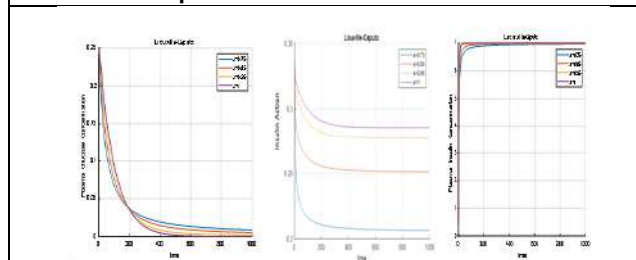


Figure 3: Glucose-Insulin regulatory system for diabetes patient 2, with different parameters $s_1 = 0$, $s_2 = 0.00142$, $s_3 = 115.94 \times 10^{-6}$, $s_4 = 0.0046$, $s_5 = 0.2814$, $G_b = 80$, $I_b = 7$ in Liouville Caputo sense

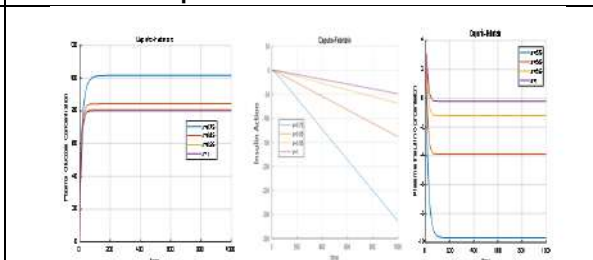


Figure 4: Glucose-insulin regulatory system for normal person, with different parameters $s_1 = 0.2$, $s_2 = 0.00123$, $s_3 = 6.92 \times 10^{-6}$, $s_4 = 0.0249$, $s_5 = 0.2769$, $G_b = 80$, $I_b = 7$ using Caputo-Fabrizio derivative





Saradhadevi et al.,

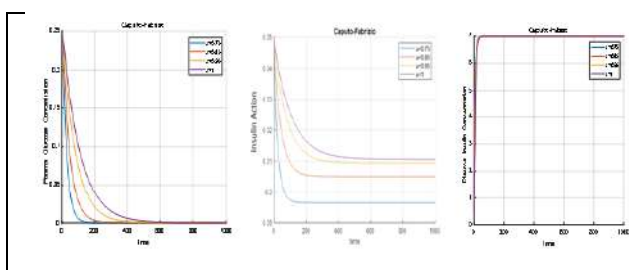


Figure 5 :Glucose-Insulin regulatory system for diabetes patient 1,with different parameters $s_1 = 0$, $s_2=0.0027, s_3=5.3 \times 10^{-6}, s_4= 0.0042, s_5=0.264, G_b=80, I_b=7$ using Caputo-Fabrizio derivative.

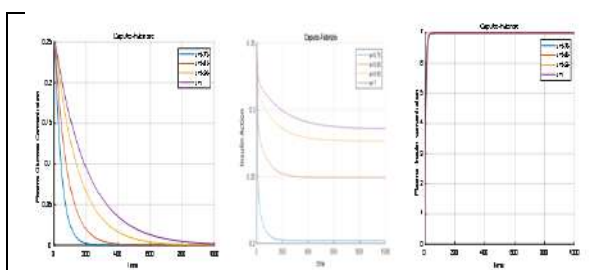


Figure 6:Glucose-Insulin regulatory system for diabetes patient 2,with different parameters $s_1 = 0$, $s_2=0.00142, s_3=115.94 \times 10^{-6}, s_4= 0.0046, s_5=0.2814, G_b=80, I_b=7$ using Caputo-Fabrizio derivative

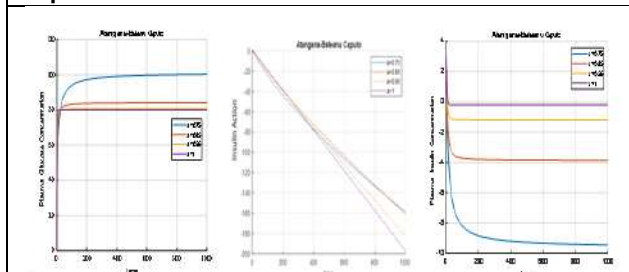


Figure 7: Glucose-insulin regulatory system for normal person, with different parameters $s_1 = 0.2$, $s_2=0.00123, s_3=6.92 \times 10^{-6}, s_4= 0.0249, s_5=0.2769, G_b=80, I_b=7$ using Atangana-Baleanu operator

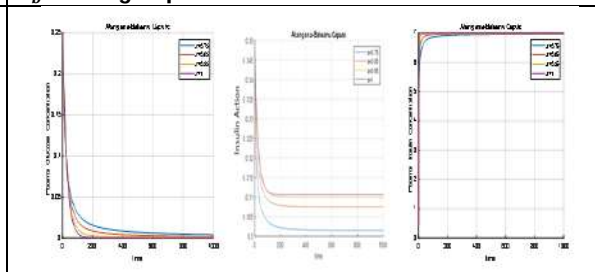


Figure 8 :Glucose-Insulin regulatory system for diabetes patient 1,with different parameters $s_1 = 0$, $s_2=0.0027, s_3=5.3 \times 10^{-6}, s_4= 0.0042, s_5=0.264, G_b=80, I_b=7$ using Atangana-Baleanu operator

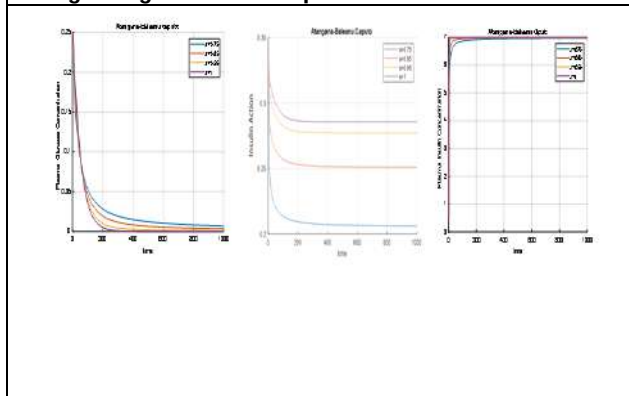


Figure 9:Glucose-Insulin regulatory system for diabetes patient 2,with different parameters $s_1 = 0$, $s_2=0.00142, s_3=115.94 \times 10^{-6}, s_4= 0.0046, s_5=0.2814, G_b=80, I_b=7$ using Atangana-Baleanu operator.

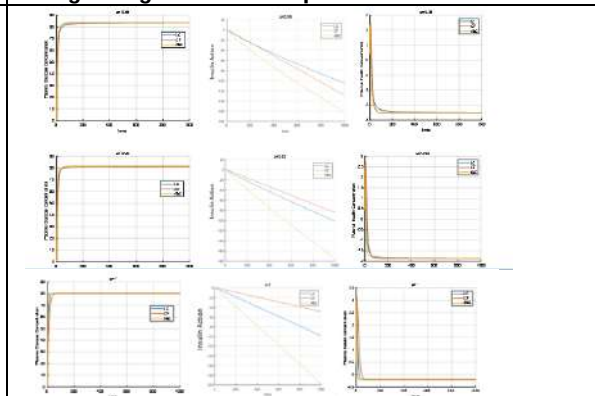


Figure 10:Comparison graph of Glucose-Insulin regulatory system(2) of normal persons at $\alpha=0.82, \alpha=0.96, \alpha=1$ for Liouville-Caputo, Caputo-Fabrizio and Atangana-Baleanu derivatives.



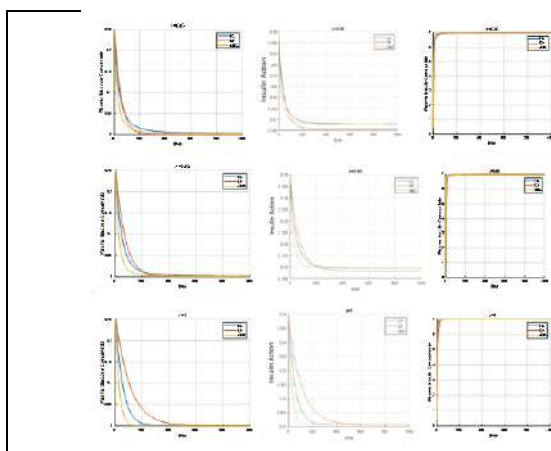


Figure 11: Comparison graph of Glucose-Insulin regulatory system(2) of Diabetes Patient -1 at $\alpha=0.82, \alpha=0.96, \alpha=1$ for Caputo, Caputo-Fabrizio and Atangana-Baleanu derivatives

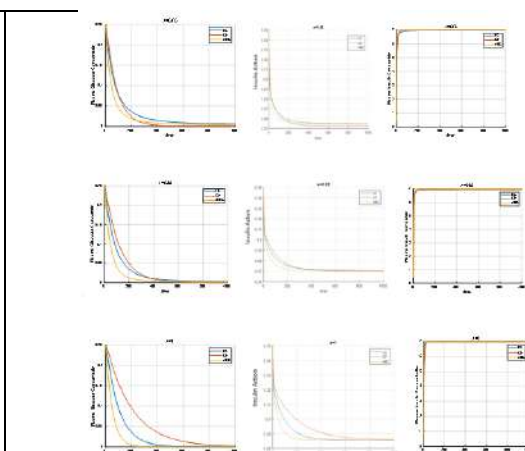


Figure 12: Comparison graph of Glucose-Insulin regulatory system(2) of Diabetes Patient -2 at $\alpha=0.82, \alpha=0.96, \alpha=1$ for Caputo, Caputo-Fabrizio and Atangana-Baleanu derivatives

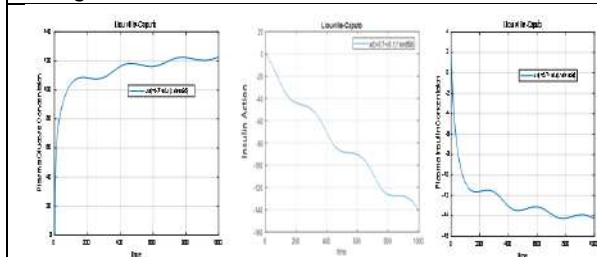


Figure 13: Numerical simulation obtained for normal person at $\alpha(t) = 0.7 + (0.1)\sin(\frac{t}{50})$ in Liouville-Caputo sense.

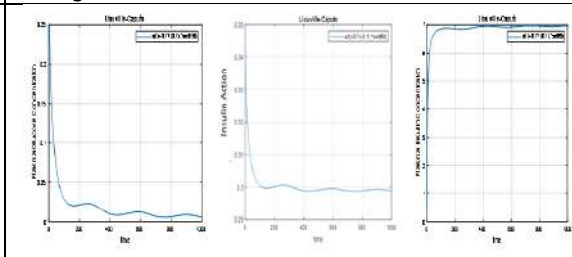


Figure 14: Numerical simulation obtained for Diabetes Patient-1 at $\alpha(t) = 0.7 + (0.1)\sin(\frac{t}{50})$ in Liouville-Caputo sense.

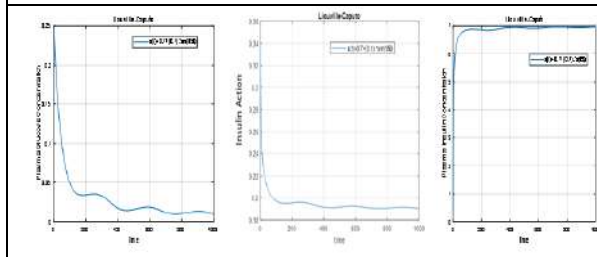


Figure 15: Numerical simulation obtained for Diabetes Patient-2 at $\alpha(t) = 0.7 + (0.1)\sin(\frac{t}{50})$ in Liouville-Caputo sense.

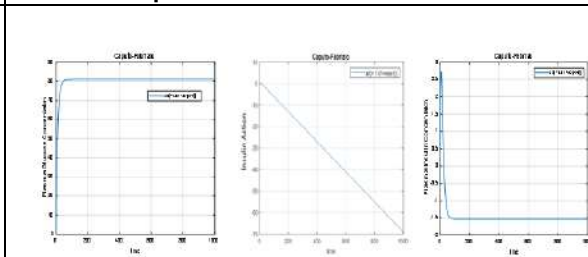


Figure 16: Numerical simulation obtained for normal person at $\alpha(t) = 1/(1 + \exp(-t))$ in Caputo-Fabrizio sense.





Saradhadevi et al.,

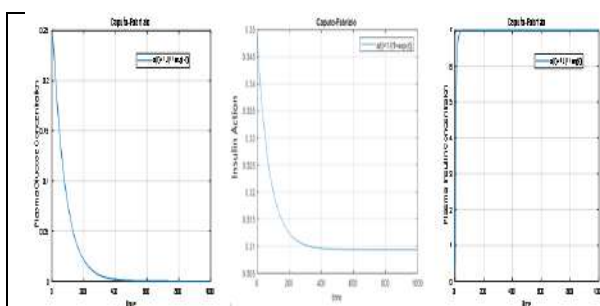


Figure 17: Numerical simulation obtained for Diabetes Patient -1 at $\alpha(t) = 1/(1 + \exp(-t))$ in Caputo-Fabrizio sense

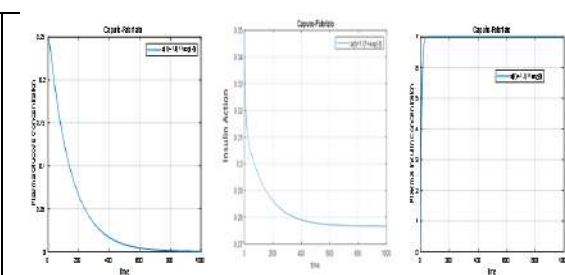


Figure 18: Numerical simulation obtained for Diabetes Patient -2 at $\alpha(t) = 1/(1 + \exp(-t))$ in Caputo-Fabrizio sense

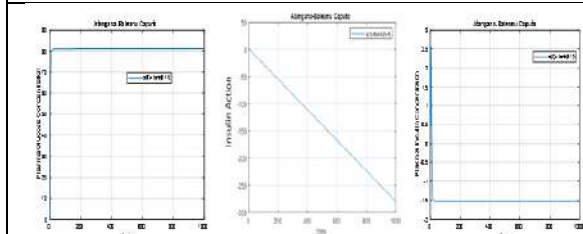


Figure 19: Numerical simulation obtained for normal person at $\alpha(t) = \tanh(t + 1)$ using Atangana-Baleanu Caputo derivative.

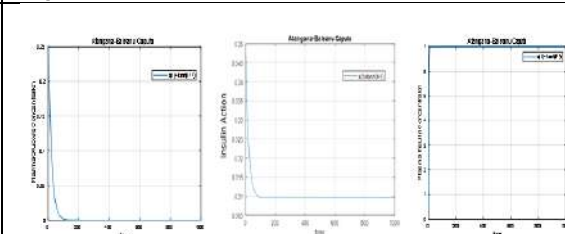


Figure 20: Numerical simulation obtained for Diabetes Patient -1 at $\alpha(t) = \tanh(t + 1)$ using Atangana-Baleanu Caputo derivative.

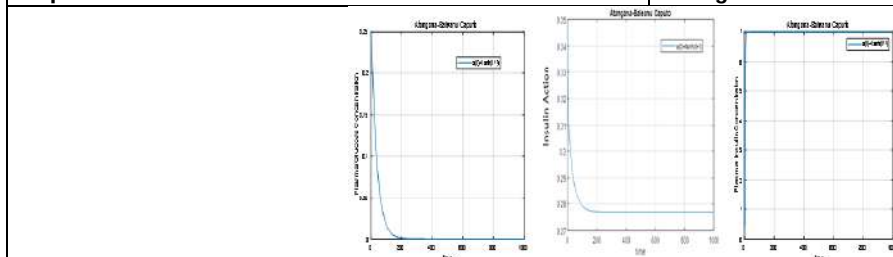


Figure 21: Numerical simulation obtained for Diabetes Patient -2 at $\alpha(t) = \tanh(t + 1)$ using Atangana-Baleanu Caputo derivative.





***In vitro* Anticancer Activity of *Permoterma reticulatum* on Human Skin Cancer Cell Line SK-MEL-28 (Skin Melanoma)**

Ritesh Tiwari¹, Ritu Jain¹, Naveen Gupta², Dharmendra Singh Rajpoot³ and Ajay Kumar Shukla^{4*}

¹Ph.D Research Scholar, Department of Pharmacy, Madhyanchal Professional University, Bhopal, Madhya Pradesh, India.

²Principal, Department of Pharmacy, Institute of Pharmacy, Madhyanchal Professional University, Bhopal, Madhya Pradesh, India.

³Associate Professor, Department of Pharmacy, Madhyanchal Professional University, Bhopal, Madhya Pradesh, India.

⁴Assistant Professor, Department of Pharmacy, Dr. Rammanohar Lohia Avadh University Ayodhya, Uttar Pradesh, India.

Received: 30 Jan 2024

Revised: 09 Feb 2024

Accepted: 27 Apr 2024

***Address for Correspondence**

Ajay Kumar Shukla

Assistant Professor,

Department of Pharmacy,

Dr. Rammanohar Lohia Avadh University Ayodhya,

Uttar Pradesh, India.

Email: ashukla1007@gmail.com



This is an Open Access Journal / article distributed under the terms of the **Creative Commons Attribution License** (CC BY-NC-ND 3.0) which permits unrestricted use, distribution, and reproduction in any medium, provided the original work is properly cited. All rights reserved.

ABSTRACT

Permoterma reticulatum is one of the traditional plants with well-known medicinal qualities that is frequently prescribed to treat a wide range of ailments. Around the world, non-toxic plant-based products are being used for conventional medical purposes, and developing nations rely on herbal medicines to meet their basic healthcare needs. The purpose of this work is to investigate anticancer activity of *Permoterma reticulatum* the hydroalcoholic extract (PRHE), using MTT assays on the human skin cancer cell line SK-MEL-28 (skin melanoma). When the concentration of PRHE was increased from 25 to 400g/ml, the percentage of inhibition of the human skin cancer cell line SK-MEL-28 (skin melanoma) by PRHE and conventional medicines was found to be 55.83% and 92.65%, respectively. This indicates that the PRHE activated a cell arrest mechanism and slowed the development of cancer cells.

Keywords: MTT assay, *Permoterma reticulatum*, human skin cancer cell line SK-MEL-28 (skin melanoma), IC₅₀ value, cytotoxic activity.





INTRODUCTION

Roughly 75% of skin cancer-related deaths worldwide are attributed to malignant melanoma, a very aggressive kind of the disease. Recent years have seen an increase in the incidence of this malignancy [1]. The process by which melanoma advances to a metastatic stage is complex and involves a number of biochemical pathways, including cell cycle disruption, apoptosis evasion, abnormalities in extracellular matrix adhesion, and cell motility and invasion [2]. Regrettably, serious side effects are linked to the restricted availability of chemotherapeutic drugs for the treatment of malignant melanoma [3]. Natural chemicals are seen as a possible alternative in cancer therapy because of their various chemical structures and pharmacological processes. However, because many anticancer medications are associated with hematological problems and chemotherapeutic resistance, there is still a pressing need to create drugs with low toxicity in normal tissues and anti-metastatic efficacy [4, 5, 6]. Since ancient times, lichens have been used in traditional medicine, and they are now a popular choice for complementary therapies around the globe. Researchers have studied lichens' secondary metabolites over the past century because they show a range of biological activity. In Malaysia's mountainous regions, lichen diversity is higher. It has been observed that the secondary metabolites of these lichens exhibit a wide range of biological activities, including antimicrobial, antiviral, antiprotozoal, enzyme inhibitory, insecticidal, antitermite, cytotoxic, antioxidant, wound healing, antiherbivore, analgesic, and anti-inflammatory qualities. Even while lichens produce a wide range of bioactive chemicals, their low natural concentrations prevent many of their potential applications from being realized. The antibacterial activity of four Parmotrema species (Parmotrema praesorediosum, P. rampoddense, P. tinctorum, and P. reticulatum) was investigated in the present study [7, 8, 9, 10]. Antibacterial drugs derived from natural sources are less harmful to humans and cause fewer adverse effects, mimicking the actions of the body's natural defenses.

Usnic acid is a yellow pigment and derivative of dibenzofuran that is formed in the upper cortex of several species of lichens, and it is an integral part of their products. Pneumococcus, Streptococcus, and Mycobacterium tuberculosis are only a few of the Gram-positive bacteria that can be effectively combated using usnic acid [11]. Many phenolic chemicals, including anthraquinones, xanthenes, dibenzofuranes, depsides, and depsidones, are produced by lichens and have been shown to have important biological properties like antioxidant, antiviral, antifungal, and anticancer properties. Numerous in vitro and in vivo investigations have demonstrated the potential of lichen metabolites as anticancer drugs, however clinical studies are still pending [12]. It was discovered that lichen extracts made by ethanol and methanol extraction contained sizable levels of flavonoids. The purpose of this work is to examine the anti-inflammatory properties of P. reticulatum extracts on different in vivo mouse models as well as the in vitro antibacterial activity of the extracts against gram-positive and gram-negative bacteria [13]. Because lichen extracts include phenolic and flavonoid content, prior research has shown their potential as a natural source of antioxidants [13]. The presence of flavonoids and usnic acid in P. reticulatum's acetone extract may have contributed to the plant's notable anti-inflammatory properties [14]. Many phytoconstituents, including artemisinin, lupeol, curcumin, quercetin, brazilin, catechin, ursolic acid, β -sitosterol, and myricetin, are undergoing clinical trials or pharmacokinetic development. More than 60% of anticancer medications are derived from plants or their synthetic derivatives. On the other hand, little is known about the remaining chemicals, which suggests that more research is necessary [15]. Since the structural diversity of phytochemicals found in plants makes them an important source of new cytotoxic drugs, more than 3000 plants have been identified to have anticancer effects globally. Although research on the cytotoxicity of African plant extracts against cancer cells is still lacking, it has been established how important traditional African plants are for the prevention and treatment of diseases, including cancer [16]. Hence, this study aims to investigate the in vitro cytotoxicity of P. reticulatum against the human skin cancer cell line SK-MEL-28 (skin melanoma).

MATERIAL AND METHODS

Plant collection and preparation



**Ritesh Tiwari et al.,**

Plant material was collected locally from amarkantak region of Madhya Pradesh., India. Identified and authenticated was done by plants materials are verified by Pharmacognosist, Dr. Sandeep Kumar Singh, at the Central Ayurvedic Research Institute in Jhansi, Uttar Pradesh, with accession numbers CARI/H/13282021, Botanical Survey of India, Central Regional Centre, Prayagraj, U.P.

Extraction of plant material

Plant material of *P. reticulatum* was extracted by using cold maceration method; plant samples were collected, washed, rinsed and dried properly. Powder form of plant sample was extracted with hydroalcoholic solvent (30:70) and allows standing for 4-5 days each. The extract was filtered using filter paper to remove all unextractable matter, including cellular materials and other constituents that are insoluble in the extraction solvent. Extract was transferred to beaker and evaporated; excessive moisture was removed and extract was collected in air tight container. Qualitative analysis of extracts of different solvents was carried out to find out the presence of various phytoconstituents [17]. Extraction yield of all extracts were calculated using the following equation below:

$$\text{Percentage Yield} = \frac{\text{Actual yield}}{\text{Theoretical yield}} \times 100$$

Qualitative Phytochemical Estimation of Extracts [Kokate et al., 2010].

Phytochemical Estimation of extracts was determined using standard techniques such as alkaloids, flavonoids, tannins, phenol, saponins and glycosides etc.

In-vitro anti cancer cell study**Cell culture**

We obtained the human skin cancer cell line SK-MEL-28 (skin melanoma) from Pune, India's National Centre for Cell Science (NCCS). The experimental cells were maintained at 37 °C in a 5% CO₂ incubator and grown in Minimum Essential Medium (MEM, GIBCO), which was additionally supplemented with 4.5 gm/L of glucose, 2 mM/L of glutamine, and 5% of foetal bovine serum (FBS for growth media).

Cell plating and MTT assay

Test chemicals' *in-vitro* inhibitory effects on cell growth were assessed using minor modifications to the Mosmann MTT assay methodology. Human skin cancer cell line SK-MEL-28 (skin melanoma) from T-25 flasks were maintained in 96-well tissue culture plates at a density of 5 x 10³ cells/well in the growth medium and cultivated at 37°C in the presence of 5% CO₂. The supernatant growth media was removed from each well and reconstituted with 100 μ l of dimethyl sulfoxide to solubilize the coloured formazan material. Each well received 20 μ l of fresh MTT (5 mg/ml in PBS) before being incubated for 24 hours at 37°C. The absorbance OD was recorded at 570 nm on an ELISA reader following a 30-minute incubation time [18, 19].

$$\% \text{ of cell viability} = (\text{OD of test} / \text{OD of control}) \times 100.$$

Data interpretation

Lower absorbance values than those of the control cells are a sign that the rate of cell growth has slowed down. On the other hand, a higher absorption rate indicates increased cell proliferation. Occasionally, a surge in proliferation may be offset by a decrease in cell mortality; signs of cell death may include morphological changes.

RESULTS

P. reticulatum were taken and removed throughout the extraction process. It was discovered that the extract had a yield of 8.1%.



**Ritesh Tiwari et al.,****Phytochemical screening test**

According to research, PRHE has the best potential for bioactivity of any extract when it comes to glycosides, alkaloids, glycosides, phenolic compounds, tannins, saponins, flavonoids, and proteins. Hence, PRHE chose us for additional research. Results are shown in below Table 1.

The PRHE natural material was tested for anticancer activities using the MTT test technique. Measurements of cell viability and proliferation are prerequisites for in vitro experiments designed to assess a cell population's response to external stimuli. In cell growth investigations, radioactive thymidine incorporated into cellular DNA has been used. The MTT assay method lowers cell metabolic activity and, to a lesser amount, the activities of dehydrogenase enzymes to produce dipping equivalents such as NADH and NADPH. The MTT cell proliferation assay method allows for both growth rate and the reduction in cell viability that occurs when apoptosis is caused by metabolic processes.

Effect of PRHE on human skin cancer cell line SK-MEL-28 (skin melanoma)

Table 2 displays the results of the MTT cell growth inhibition assay performed for PRHE of medicinal herb composition at various concentration dosages of 25, 50, 100, 200, and 400 g/ml. Inhibition of Caco-2 cancer cell growth caused by the composition of a herbal extract and a standard sample was compared in Fig. 1. Using the MTT test method, the IC₅₀ value for PRHE was discovered to be 102.75µg/ml. The tetrazolium salt reduction is a reproducible and dependable technique for evaluating cell growth. Utilizing the 3-(4, 5Dimethylthiazol-2-yl)-2, 5-diphenyltetrazolium bromide (MTT) assay technique, the test extract's impact on cellular viability and proliferation was assessed. Enzymes that dehydrogenase produce NADH and NADPH when they reduce tetrazolium, which indicates that the cell is metabolically active. As shown in Figure 1, formazan forms purple crystals that are not very soluble in water. Both the formazan concentration and the product's color intensity at 570 nm were measured using dimethyl sulfoxide (DMSO). This matched the number of surviving cells in the culture perfectly. Based on untreated cells (basal), which had a 100% viability control, the results were expressed as a percentage of viability (log). The percentage of inhibition of the human skin cancer cell line SK-MEL-28 (skin melanoma) by PRHE and conventional medicines was determined to be 66.83 and 82.65%, respectively, when the concentration of PRHE increased from 25 to 400g/ml. This indicates that the PRHE activated a cell arrest mechanism and slowed the development of cancer cells [19, 20].

DISCUSSION

Plants, herbs, and ethnobotanicals have benefited humans from the beginning of time and are still utilized to treat and enhance health in many countries today. Because they are less hazardous, herbal medications are becoming more and more popular around the world. Modern medicine is based on natural ingredients and plants, which also have a big influence on how commercial drugs are developed. Using cancer cell lines, the in-vitro MTT screening method was used to assess PRHE's anticancer potential. The MTT test analyzes reagent color change and evaluates cell viability using colorimetry. The activity of mitochondrial dehydrogenases controls the cytotoxicity of live cells.

Investigations of anticancer activities were carried out in this work. The conventional drug and PRHE both demonstrated evidence of reducing the growth of the human skin cancer cell line SK-MEL-28 (skin melanoma) by 55.83% and 92.65%, respectively, according to the MTT assay method. Primarily investigated in vitro, plant phenolic compounds have demonstrated inhibition of cell growth at various cell cycle phases (G1, S, and G2) through both direct and indirect mechanisms, including down regulating cyclins and cdks and acting as prooxidants to enhance the expression of p21, p27, and p53 genes. Pharmaceutical companies will be able to create an ecologically friendly medication for the treatment of cancer patients thanks to the research findings. There could be a large variety of bioactive substances in *P. reticulatum*. All of these appear to be promising bioactive substances that have the ability to halt the growth of specific cancer cells. In particular, they stop the growth of tumor cells, such as the human skin cancer cell line SK-MEL-28 (skin melanoma). The anticancer impact of TPFHE might stem from its capacity to initiate apoptosis. *P. reticulatum* inhibits the proliferation of the human skin cancer cell line SK-MEL-28 (skin melanoma). It



**Ritesh Tiwari et al.,**

implied that TPFHE contained phytochemicals called polyphenolic substances. It is necessary to conduct more research on these bioactive polyphenolic components. Most of the secondary metabolites found in herbal plants have been employed by all medical systems to treat a wide range of illnesses, such as diabetes, cancer, arthritis, and others. As long as this pattern continues, phytoconstituents will continue to be the best practical source for anticancer medication compositions. The cytotoxicity potential of the whole-plant hydroalcoholic extract of *P. reticulatum* was assessed in this work using MTT assays. The *P. reticulatum* of hydroalcoholic extract showed a very good% of cell inhibition with increasing concentration of the bioactive component of the test material, based on the results of those assays.

CONCLUSION

We conclude that using in vitro research lessens the need for animal-based clinical trials. It facilitates the rapid evaluation of a larger variety of substances with less effort. The MTT assay on human skin cancer cell line SK-MEL-28 (skin melanoma) examination, according to research, demonstrated the PRHE's possibly powerful and unique anticancer action. In general, the findings suggest that this native tree may be used as a novel chemotherapeutic drug to treat skin cancer. This finding may open the door for new directions in cancer research and plant-based cancer therapies that avoid the negative effects of chemotherapy, greater chemical dosages, and chemotherapeutic agents.

REFERENCE

1. Hussein MR, Haemel AK, Wood GS. Apoptosis and melanoma: Molecular mechanisms. J Pathol. 2003; 199:275–288.
2. Soengas MS, Lowe SW. Apoptosis and melanoma chemoresistance. Oncogene. 2003; 22:3138–3151.
3. Senderowicz AM. Novel small molecule cyclin-dependent kinases modulators in human clinical trials. Cancer Biol Ther. 2003;2(4 Suppl 1):S84–S95.
4. Gordaliza M: Natural products as leads to anticancer drugs. Clin Transl Oncol 9(12): 767-76, 2007.
5. Hanikoglu A, Hanikoglu F, Ozben T: Natural product inhibitors of histone deacetylases as new anticancer agents. Curr Protein Pept Sci 19(3): 333-340, 2018.
6. Tan BL, Norhaizan ME: Manilkara zapota (L.) P. Royen leaf water extract triggered apoptosis and activated caspase-dependent pathway in HT-29 human colorectal cancer cell line. Biomed Pharmacother 110: 748-757, 2019.
7. Bombuwala K, Subramaniam V, DeSilva KS, Karunaratne V, Adikaram NKB, Herath HMTB, "Antitermite and antifungal activity of Usnic acid and Atranorin", Ceylon Journal of Sciences: Physical Sciences 1, no. 6, 8-12 (1999).
8. Kumar SVP, Kekuda PTR, Vinayaka KS, Sudharshan SJ, Mallikarjun N, Swathi D. "Studies on antibacterial, anthelmintic and antioxidant of a macrolichen Parmotrema pseudotinctorum (des. Abb.) Hale (Parmeliaceae) from Bhadra Wildlife Sanctuary, Karnataka", International Journal of Pharmtech Research 2, no. 2,1207-1214 (2010).
9. Mitrovic T, Stamenkovic S, Cvetkovic V, Nikolic M, Tosic S, Stojicic D."Lichens as source of versatile bioactive compounds", Biologica Nyssana 1, no. 2, 1-6 (2011).
10. Barreto RSS, Albuquerque-Junior RLC, Pereira-Filho RS, Quintans JSS, Barreto AS, De Santana JM, Santana-Filho VJ, M. R. V. Santos RV, R. L. Bonjardim, A. S. S. Araujo and L. J. Quintas-Junior, "Evaluation of woundhealing activity of atranorin, a lichen secondary metabolite, on rodents", Brazilian Journal of Pharmacognosy 2, no. 23, 310-319 (2013).
11. Cansaran D, Kahya D, Yurdakulola E, Atakol O. Identification and quantitation of usnic acid from the lichen Usnea species of Anatolia and antimicrobial activity. J Biosci. 2006; 61:773–6.
12. Solárová Z, Liskova A, Samec M, Kubatka P, Büsselberg D, Solár P. Anticancer Potential of Lichens Secondary Metabolites. Biomolecules 2020, 10, 87:1-31.





Ritesh Tiwari et al.,

13. Sharma BC, Kalikotay S. Screening of antioxidant activity of lichens Parmotrema reticulatum and Usnea sp. from Darjeeling hills, India. IOSR Journal of Pharmacy 2012; 2(6):54-60.
14. Jain AP, Bhandarkar S, Rai G, Yadav AK, Lodhi S. Evaluation of Parmotrema reticulatum Taylor for Antibacterial and Antiinflammatory Activities. Indian J Pharm Sci. 2016; 78(1): 94–102.
14. Mazumder K, Biswas B, Raja IM, Fukase K. A Review of Cytotoxic Plants of the Indian Subcontinent and a Broad-Spectrum Analysis of Their Bioactive Compounds. Molecules 2020, 25, 1904:1-40.
15. Mbele, M.; Hull, R.; Dlamini, Z. African medicinal plants and their derivatives: Current efforts towards potential anti-cancer drugs. Exp. Mol. Pathol. 2017, 103, 121–134.
16. Kokate CK, Purohit AP, Gokhale SB. Pharmacognosy. 45th ed. Pune: Nirali Prakashan; 2010. p. 6.19.
17. Sugathakumari N. Mohan, Achuthan S. Hemanthakumar, Thankappan S. Preetha. Evaluation of Inhibition of Proliferation of SK-Mel-28 Cell Lines by Acmeilla ciliata (Kunth) Cass. Cell Biomass. International Journal of Pharmaceutical Sciences and Drug Research, 2022; 14(2):181-188.
18. Daveri E, Valacchi G, Romagnoli R, Maellaro E, Maioli E. Antiproliferative Effect of Rottlerin on Sk-Mel-28 Melanoma Cells. Evid Based Complement Alternat Med. 2015; 2015: 545838.
19. Canga, I.; Vita, P.; Oliveira, A.I.; Castro, M.Á.; Pinho, C. In Vitro Cytotoxic Activity of African Plants: A Review. Molecules 2022, 27, 4989:1-18.

Table 1: Results of phytochemical screening test of Hydroalcoholic Extract

Test for Alkaloids		
1.	Mayer's Test	+
2.	Hager's Test	+
Test for steroids		
1.	Salkowski Test	-
2.	Libermann-Burchard's Test	-
Test for Flavonoids		
1.	Lead Acetate Test	+
2.	Alkaline Reagent Test	+
3.	Shinoda Test	+
Test for Tannins and Phenolic Compounds		
1.	FeCl ₃ Test	+
2.	Lead Acetate Test	+
3.	Gelatine Test	+
Test for Saponins		
1.	Froth Test	+
Test for Glycosides		
1.	Legal's Test	+
2.	Keller Killani Test	+
3.	Borntrager's Test	+

+ = Components present



Ritesh Tiwari *et al.*,

Table 2: Dose Response of Test sample on human skin cancer cell line SK-MEL-28 (skin melanoma)

Concentration (ug/ml)	% Cell Survival of STD	% Cell Inhibition of STD	% Cell Survival of PRHE	% Cell Inhibition of PRHE
0	0	0	0	0
25	78.23	21.77	93.13	6.87
50	46.18	53.82	86.06	13.94
100	28.23	71.77	71.27	28.73
200	21.96	78.04	55.34	44.66
400	7.35	92.65	44.17	55.83

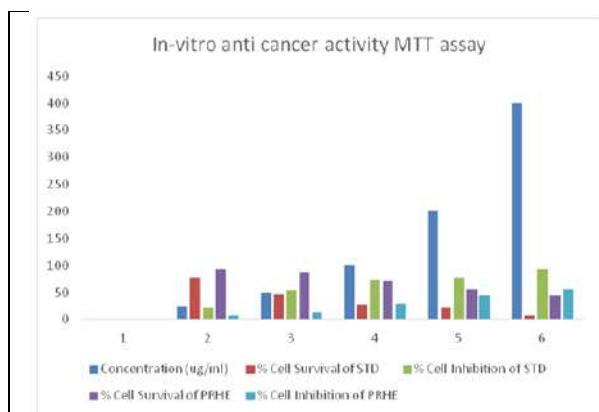


Figure 1: Effect of PRHE on human skin cancer cell line SK-MEL-28 (skin melanoma) growth inhibition

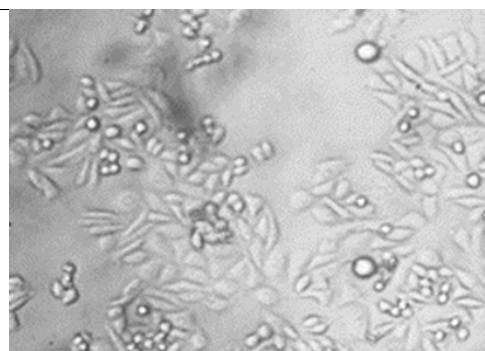


Figure 3: Images of human skin cancer cell line SK-MEL-28 (skin melanoma) Before treated cell lines

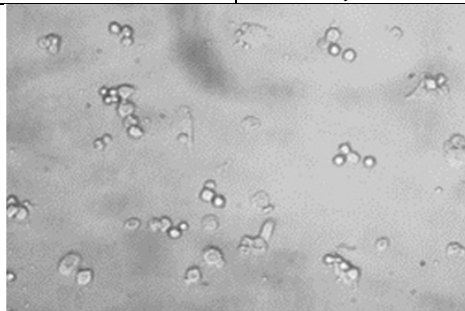


Figure 3: Images of human skin cancer cell line SK-MEL-28 After treated cell lines at 400 µg/ml





Advancements in Brain Tumor Detection and Classification: Integrating Machine Learning and Medical Imaging Techniques

R. Saranya*

Assistant Professor, Department of Computer Science with Data Analytics, PSG College of Arts and Science, (Affiliated to Bharathiar University) Coimbatore, Tamil Nadu, India.

Received: 22 Jan 2024

Revised: 09 Feb 2024

Accepted: 27 Apr 2024

*Address for Correspondence

R. Saranya

Assistant Professor,

Department of Computer Science with Data Analytics,

PSG College of Arts and Science, (Affiliated to Bharathiar University)

Coimbatore, Tamil Nadu, India.

Email: saranya_r@psgcas.ac.in>



This is an Open Access Journal / article distributed under the terms of the **Creative Commons Attribution License** (CC BY-NC-ND 3.0) which permits unrestricted use, distribution, and reproduction in any medium, provided the original work is properly cited. All rights reserved.

ABSTRACT

The primary objective of this study is to develop an efficient method for early detection of abnormal brain cell growth and malignant brain tumours through the analysis of Magnetic Resonance Image (MRI). The focus is on improving diagnostic capabilities to reduce mortality rates associated with these conditions. In pursuit of our objective, we employed a Convolutional Neural Network (CNN) model, leveraging its deep learning capabilities for accurate analysis of MRI images. The model was trained and evaluated using a dataset comprising 3000 MRI images, and its performance was assessed based on the metric of accuracy. Our investigation reveals that the proposed CNN model outperforms alternative models in the identification of brain tumours. By analyzing the dataset, our CNN achieved exceptional results, attaining an accuracy rate of 93%. This suggests that the CNN's ability to discern aberrant brain cell growth in MRI images is highly promising for early and precise detection. In automatic detection of brain tumor images different convolutional algorithm is introduced. In this proposed method, CNN algorithm is introduced which provided effective results compared to other algorithms. In conclusion, our study demonstrates the effectiveness of a Convolutional Neural Network in detecting abnormal brain cell growth and malignant tumours from MRI images. The proposed method is compared with existing SVM method. The proposed method obtained accuracy of 93% compared to SVM. This proposed method underscores the potential of this model as a valuable tool in early diagnosis. Early detection is crucial for timely intervention and treatment, which can significantly contribute to minimizing mortality rates associated with brain-related illnesses. Further research and validation are warranted to ascertain the robustness and generalizability of the proposed CNN model in diverse clinical settings.

Keywords: Brain Tumor, Machine Learning, Segmentation, CNN algorithm, MRI, Validation.





INTRODUCTION

A brain tumour develops when brain cells proliferate excessively and indecorously. Excessive cell proliferation leads the creation of a mass or lump, which can impair normal brain function and put strain on surrounding tissues. These abnormal growths may be benign or malignant, and they have the potential to spread to other parts of the body. Benign tumours typically grow slowly and have well-defined borders. They do not infiltrate the surrounding tissues or spread throughout the body. Malignant tumours, on the other hand, are more aggressive and can invade neighbouring tissues before spreading to other sections of the brain or even the body via blood. Brain tumour symptoms can differ widely depending on their size [1], location, and whether they impact specific parts of the brain. Common symptoms include vomiting, dizziness, fatigue, and changes in mood or behaviour. A medical history evaluation, neurological assessment, imaging tools (such as MRI or CT scans), and sometimes a biopsy can be used to evaluate the kind and grade of the tumour [2]. Treatment options for brain tumors can include surgery to remove the tumor, targeted therapies, and other innovative approaches, depending on the specific characteristics of the tumor and the overall health of the patient. Because brain tumors can have serious implications for a person's health and quality of life, early detection, accurate diagnosis, and appropriate treatment are crucial. If someone is experiencing persistent or worsening neurological symptoms, it's important for them to seek medical attention promptly. The brain is a highly complex organ that controls various bodily functions and processes [3]. Tumors that develop within the brain can disrupt its normal functioning and potentially lead to a range of neurological symptoms, depending on their size, location, and type. Brain tumors are classified based on several factors, including their cell type, location, and behavior. Some common types of brain tumors include gliomas, meningiomas, pituitary adenomas, and medullo blastomas, among others. Gliomas are one of the most common types and arise from glial cells, which provide support and protection to nerve cells in the brain [4]. Brain tumor symptoms can exhibit considerable variation and might encompass persistent headaches, seizures, alterations in vision, challenges with balance and coordination, shifts in cognitive abilities, and changes in personality [5].

The precise manifestations can differ based on the tumor's location, size, and impact on surrounding brain structures. Diagnosis typically involves a combination of medical history assessment, neurological exams, and medical imaging techniques such as MRI scans. If a brain tumor is suspected, a biopsy might be performed to determine its type and grade [6]. Treatment options for brain tumors include surgery, radiation therapy, and chemotherapy, often used in combination. Benign tumors might be removed through surgery, while malignant tumors may require a more comprehensive approach involving various treatments. Brain tumors pose significant medical challenges due to their complexity and potential impact on crucial brain functions. The research study titled "Design and Implementation of Brain Tumor Detection Using a Machine Learning Approach [7]," conducted by G. Hemanth, M. Janardhan, and L. Sujihelen, introduces an innovative method for automated segmentation. This method harnesses the power of Convolutional Neural Networks (CNNs) with small 3x3 kernels. What makes this approach unique is its capability to simultaneously perform both segmentation and classification using a single technique. In contrast to conventional Neural Networks (NNs), which are commonly used for such tasks, CNNs are employed. The distinguishing feature of CNNs is their layered architecture, which significantly enhances the accuracy of classifying outcomes. On-going research aims to better understand the underlying causes of brain tumors, improve early detection methods, and develop more targeted and effective treatment approaches to enhance patient outcomes and quality of life. Early diagnosis, advances in medical technology, and multidisciplinary medical care have led to improved prognosis and treatment options for individuals diagnosed with brain tumours.

METHODOLOGY

Convolutional Neural Network (CNN) is a machine learning algorithm used for brain tumor detection. CNN is used for tasks that involve image recognition, pattern detection, and feature extraction. Here's a breakdown of how CNNs work in detecting the tumor in the brain



**Saranya****Convolutional Layers**

CNN algorithm start with convolutional layers, which is used for the application of filters to the MRI input image. These filters scan the image pixel by pixel, learning to detect various features of the image. In brain tumor detection, these filters might capture specific patterns indicative of tumours.

Pooling Layers

The VGG-16 algorithm is a convolutional neural network (CNN) architecture built for image classification applications. Its sophisticated design and strong performance on a wide range of visual recognition tasks have helped it acquire prominence. The VGG-16 algorithm has been developed for the critical problem of detection using medical imaging data, such as magnetic resonance imaging (MRI) scans, in this context.

Flattening

The result from first two layers is then converted into a 1D vector. This vector is then fed into fully connected layers.

Fully Connected Layers

Fully linked layers process flattened features and make decisions using acquired patterns. In the context of brain tumour identification, these layers can evaluate complicated correlations between various characteristics to determine whether or not a tumour is present. [8].

Output Layer

The final layer of the CNN produces the classification results. For brain tumor detection, it might output whether a tumor is detected or not, along with the probability scores.

Training

Classify the dataset into three categories: training, validation, and verification. The training set updates the model's parameters, the validation set monitors the model's performance during training, and the test set evaluates the model's overall performance. Feed the training photographs into the model, and then calculate the loss [9]. Using the particular optimisation algorithm, back propagate the loss through the network to update the weights and biases. This method should be performed for numerous epochs (iterations over the full training dataset). The success of the CNN model in brain tumour verification is that it correctly detects tumours in the brain. This is especially useful when analysing medical photos, when discovering tiny patterns can be difficult. It is vital to remember that CNNs are not a replacement for medical professionals, but rather a valuable tool that can help discover tumours as early as possible. They can assist doctors in making more accurate assessments by identifying potential areas of concern in medical pictures, resulting in faster and more informed patient care decisions. Figure 1. represents the proposed method.

Data Collection

Collect a dataset of brain MRI scans or other relevant medical images that include both images with tumor and images without tumor (normal cases).

Data Preprocessing

Preprocess the images to ensure consistent quality and format. This might involve resizing, rescaling intensity values, and potentially applying noise reduction techniques.

Data Annotation

Annotate the images to create ground truth labels indicating the presence and location of tumors in the images. Expert radiologists often perform this task.





Saranya

Feature Extraction

Extract relevant features from the images that can help discriminate between tumor and non-tumor regions. In the case of medical images, these features might include texture, shape, and intensity information.

Model Selection

The process of Model Selection involves the careful choice of a suitable machine learning model. Convolutional Neural Networks (CNNs) are frequently employed for image analysis tasks owing to their capacity to autonomously learn significant features from the data [10].

Data Splitting

It requires dividing the dataset into several separate subsets: training, validation, and test sets. The training set's objective is to help the model learn, whereas the validation set is used to fine-tune hyperparameters. Finally, the test set is critical for measuring the model's overall performance and efficacy.

Model Training

Train the chosen model using the training set. The model learns to map the extracted features to the tumor classification.

Clinical Integration

Validate the model's performance in a clinical setting, possibly involving collaboration with medical professionals to ensure the model's accuracy aligns with clinical figure requirements.

Deployment

Once the model has proven to be reliable and safe, it can be used in the actual world. This may entail incorporating it into a medical imaging system or interface used by radiologists or physicians. It is vital to note that the methodology may differ depending on the specifics of the situation, accessible data, and breakthroughs in the field. Collaboration among medical professionals, computer scientists, and machine learning experts is required to develop accurate and trustworthy methods for brain tumour identification. Furthermore, ethical concerns and patient data protection must be carefully considered during the procedure.

Dataset Collection

For our brain tumor detection research, we curated a dataset from publicly accessible online data. The dataset consists of MRI images, which is considered the most effective technique for detecting brain tumors. This dataset comprises types of brain tumor scans, including Meningioma tumor, healthy samples, Pituitary tumor, Glioma tumor. In total, our dataset contains 3264 MRI images. To visualize the distribution of these images based on the various forms of brain tumor, we provided a breakdown. In this dataset there will be different types of tumor so that there will be correct accuracy which will be given by CNN model. Availability of a significant number of samples for each tumor type ensures that the models can learn to distinguish between differentiates between brain tumor types. Figure 2.shows the input image.

DATA PREPROCESSING

Preprocessing is an important stage to preparing data for training the model. In our case, the MRI images are brought from a patient data but are of low quality and lacked clarity. To make them suitable for further processing and analysis, we applied various preprocessing techniques. One of the essential steps in preprocessing was normalization [11]. By normalizing the MRI images, we ensured that their pixel values were scaled to a standardized range, typically between 0 and 1. This step helps in reducing the impact of varying pixel intensities and ensures consistency across the dataset. Moreover, to address the issue of blurriness and improve the image quality, we employed Gaussian and Laplacian filters. The Gaussian filter was used to smoothen the images by reducing noise and creating





Saranya

a more uniform appearance. This filtering process helps in enhancing image features and reducing the influence of small artifacts or disturbances. Additionally, the Laplacian filter was applied to sharpen the images and emphasize the edges and boundaries of brain structures [12]. This step further aid in enhancing the relevant features in the MR images, making them more distinct and easier to analyze. By employing these preprocessing techniques, we aimed to rich the overall quality of the MRI scans, making them more suitable for training machine learning models for brain tumor detection [13]. Improved image clarity and reduced noise contribute to better model performance and more accurate tumor classification[14].Figure3. represents the preprocessed which can be given as an input for the detecting the tumor in the brain.

Data division and Augmentation

Given that our dataset was relatively small, consisting of only 3264 MR images, it presented a challenge for training deep neural networks effectively. This network generally works on more number of datasets to achieve good results and avoid over fitting [15]. To mitigate this limitation and enhance the model's learning capacity, we employed these techniques. Data augmentation is a process of improving the quality of the original images. This approach helps to create new and diverse samples, making the training process more robust and preventing the model from memorizing the limited data [16].We divided our dataset as 3 subsets: 70% for training, 15% for testing, and 20% for validation. For data augmentation, we applied several transformations to the MRI images:

Mirroring

We created mirror images of the original MR images to introduce more variations in the dataset.

Rotation

By rotating the images, we simulated different angles from which the MRI scans could be taken, further enriching the dataset.

Width and Height Shifting

We shifted the images horizontally and vertically to simulate slight changes in the positioning of the brain structures within the scans [17].

Zooming

Zooming in and out of the images allowed us to create different scales and perspectives, adding more diversity to the dataset. By augmenting the data in this manner, we effectively increased the effective size of our dataset, making it more suitable for training images. The dataset helped to improve the model generalization enabling to perform better on data [18].

Validation Process

In our study, selecting an appropriate validation procedure for the dataset of 3264 scan images was crucial to give accurate estimation of the deep learning model's performance [19]. We opted for the holdout validation process, a commonly used method known for producing better results. This validation technique includes dividing the MRI scans into two categories as training dataset and a testing dataset. This division enables the CNN model for better training and facilitates evaluation of its performance. Specifically, 70% of the dataset used for training period while the remaining 20% for validation period and 10% for testing During training phase, CNN model is trained using it to learn and optimize its parameters. According to the CNN model performance we can calculate how the model is good performing. Training the model with more 80% of the dataset is very important for the model to learn about the different types of images.





RESULTS AND DISCUSSION

In this section, the performance of the proposed method has been evaluated based on the experimental results. The problem was experimented on 3000 brain images taken from kaggle dataset. The experiments have been done on Hp Pavilion dv5 with Intel® Core™ 2 Duo CPU @ 2.00GHz with 3 GB RAM running on Microsoft Windows 10 platform. The performance of the proposed method is evaluated using following performance metrics.

Performance metrics

In our evaluation of the CNN model and analysis of model performance is took into account several key metrics. The metrics are helpful to find how well the models are being performed. The main metrics is accuracy.

Accuracy

Accuracy was a fundamental metrics is used to evaluate how the CNN model is good in working in a binary classification task like brain tumor detection. It measures the proportion of prediction made by CNN model out of the number of samples in the dataset [20].

Accuracy calculation

Accuracy = $\frac{\text{True positives} + \text{True negatives}}{\text{True positives} + \text{True negatives} + \text{False positives} + \text{False negative}}$. True Positives (TP) denote the number of tumour cases correctly predicted as tumours by the model. True Negatives (TN) are the number of non-tumor patients that are appropriately identified as such. False Positives (FP) refer to instances in which non-tumor cases are incorrectly categorised as tumours, resulting in a Type I mistake. Similarly, False Negatives (FN) identify the occasions where tumour patients are incorrectly categorised as non-tumors, which constitutes a Type II error. The precision of this model provides us with a clear grasp of how well it performs in brain tumour and non-tumor cases. A high accuracy score indicates that the model is providing more accurate detection.

Machine learning model

The VGG-16 algorithm is a convolutional neural network (CNN) architecture built for image classification applications. Its sophisticated design and strong performance on a wide range of visual recognition tasks have helped it acquire prominence. The VGG-16 algorithm has been developed for the critical problem of detection using medical imaging data, such as magnetic resonance imaging (MRI) scans, in this context. Brain tumor detection is a critical application in the field of medical imaging, as early and accurate diagnosis plays a pivotal role in patient treatment and prognosis. The VGG-16 algorithm's ability to learn intricate features from images, coupled with its adaptability, makes it suitable for this task. The algorithm's architecture consists of multiple convolutional layers organized into five blocks, each followed by max-pooling layers. These layers are responsible for progressively learning hierarchical features from the input images. By leveraging the rich set of features extracted from the images, the algorithm can discern patterns indicative of the presence of brain tumors. The VGG-16 algorithm's versatility allows researchers and practitioners to fine-tune its pre-trained weights on medical imaging datasets containing brain MRI scans. This process involves adapting the network's architecture to accommodate the specific characteristics of the medical images, such as their dimensions and channel information. Furthermore, the fully connected layers of the algorithm are customized to output the desired classification, such as identifying whether an MRI scan indicates the presence of a brain tumor or not which show in Figure 4. The proposed method is compared with existing SVM method. The SVM method achieves only 84 % but the proposed attains the accuracy of 93% which is shown in Figure 5. This shows that the proposed method works better compared to existing method. By training the algorithm on a substantial dataset of labelled brain MRI scans, it can learn to distinguish between normal brain tissue and abnormal regions indicative of tumors. This learned knowledge enables the algorithm to subsequently analyze new, unseen MRI scans and provide predictions about the likelihood of a brain tumor's presence. In summary, the adaptation of the VGG-16 algorithm for brain tumor detection showcases the intersection of deep learning, medical imaging, and computer-aided diagnosis. This programme has the potential to help medical practitioners make accurate and quick diagnoses, leading to better patient care and results. However, it is vital to





Saranya

stress that the algorithm's use in clinical settings requires extensive testing and coordination with physicians to ensure its safety and reliability.

CONCLUSION

Detecting the tumor earlier is important for reducing global mortality rates. However, due to their complex form and structure, accurately detecting brain tumors remains challenging. MR images play a significant role for identifying tumor as soon for affected peoples. In this paper, we utilized many of the MRI scans and developed CNN architecture for early tumor identification, which yielded promising results that is 93% of accuracy. Deep learning model have is important for classification and detection. One limitation was the lengthy training process due to the CNN's layers and limited GPU capacity, but this was improved after upgrading our GPU system. For future work, incorporating individual patient information from various sources could enhance brain cancer identification accuracy

REFERENCES

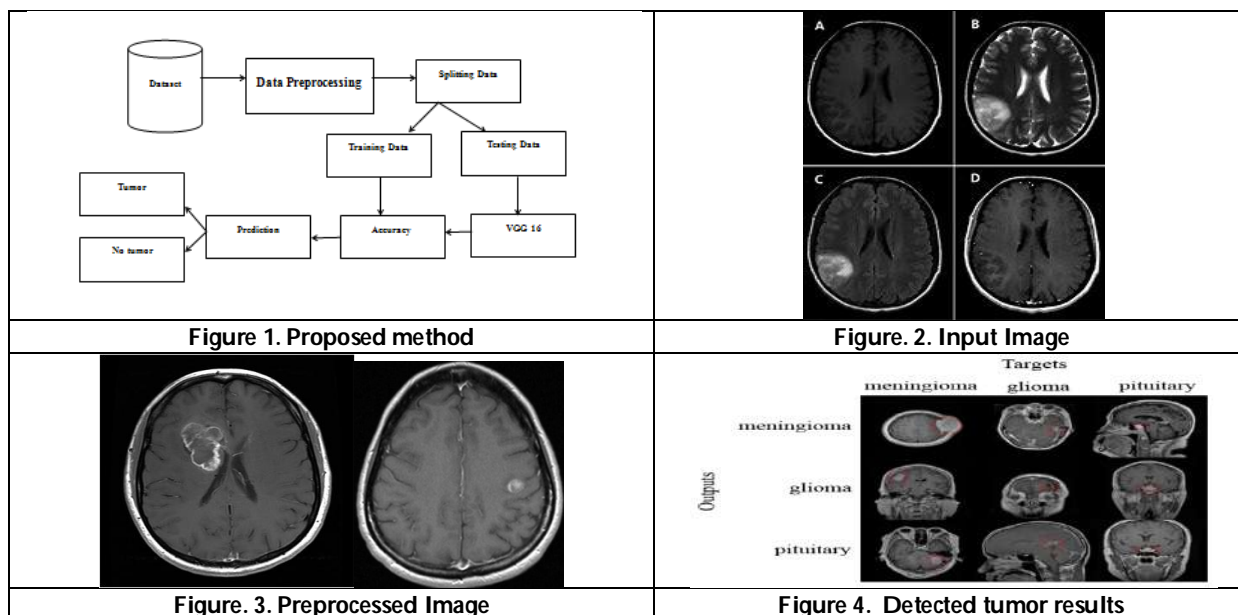
1. Akram, F., Liu, D., Zhao, P., Kryvinska, N., Abbas, S., and Rizwan, M "Trustworthy intrusion detection in e-healthcare systems", *Frontiers in public health*, 9, 2021. <https://doi.org/10.3389/fpubh.2021.788347>.
2. Alanazi, M. F., Ali, M. U., Hussain, S. J., Zafar, A., Mohatram, M., Irfan, M., et al, "Brain tumor/mass classification framework using magnetic-resonance-imaging-based isolated and developed transfer deep-learning model", *Sensors* 22, 372, 2022. DOI: 10.3390/s22010372.
3. Ali, T. M., Nawaz, A., Rehman, A. U., Ahmad, R. Z., Javed, A. R., Gadekallu, T. R., et al., "A sequential machine learning-cum-attention mechanism for effective segmentation of brain tumor", *Frontiers in Oncology*. 12, 873268, 2022. <https://doi.org/10.3389/fonc.2022.873268>.
4. Alrashedy, H. H. N., Almansour, A. F., Ibrahim, D. M., and Hammoudeh, M. A. A. (2022), "Braingan: brain mri image generation and classification framework using gan architectures and CNN models", *Sensors* 22, 4297. DOI: 10.3390/s22114297.
5. Alsaif, H., Guesmi, R., Alshammari, B. M., Hamrouni, T., Guesmi, T., Alzamil, A., et al., "A novel data augmentation-based brain tumor detection using convolutional neural network", *Applied Sciences*. 12, 3773, 2022. <https://doi.org/10.3390/app12083773>.
6. N. Abiwinanda, M. Hanif, S. T. Hesaputra, A. Handayani and T. R. Mengko, "Brain tumor classification using convolutional neural network", In *World congress on medical physics and biomedical engineering* 2018, pp. 183-189, 2019. DOI : <https://dx.doi.org/10.13005/bpj/1511>
7. W. Ayadi, W. Elhamzi, I. Charfi and M. Atri, "Deep CNN for brain tumor classification", *Neural Processing Letters*, vol. 53, no. 1, pp. 671-700, 2021. <https://doi.org/10.1007/s11063-020-10398-2>.
8. S. Kollem, K. R. L. Reddy and D. S. Rao, "Denoising and segmentation of MR images using fourth-order non-linear adaptive PDE and new convergent clustering", *International Journal of Imaging Systems and Technology*, vol. 29, no. 3, pp. 195-209, 2019. <https://doi.org/10.1002/ima.22302>
9. Al-Galal S.A.Y., Alshaikhli I.F.T., Abdulrazzaq M.M. MRI brain tumor medical images analysis using deep learning techniques: A systematic review. *Health Technol.* 2021;11:267–282. DOI:10.1007/s12553-020-00514-6.
10. Rahman M.L., Reza A.W., Shabuj S.I. An internet of things-based automatic brain tumor detection system. *Indones. J. Electr. Eng. Comput. Sci.* 2022;25:214–222, pp214-222. DOI: <http://doi.org/10.11591/ijeecs.v25.i1.pp504-510>.
11. Ayadi W., Elhamzi W., Charfi I., Atri M. Deep CNN for Brain Tumor Classification. *Neural Process. Lett.* 2021;53:671–700. <https://doi.org/10.1007/s11063-020-10398-2>.
12. Liu J., Li M., Wang J., Wu F., Liu T., Pan Y. A survey of MRI-based brain tumor segmentation methods. *Tsinghua Sci. Technol.* 2014;19:578–595. DOI: 10.1109/TST.2014.6961028.





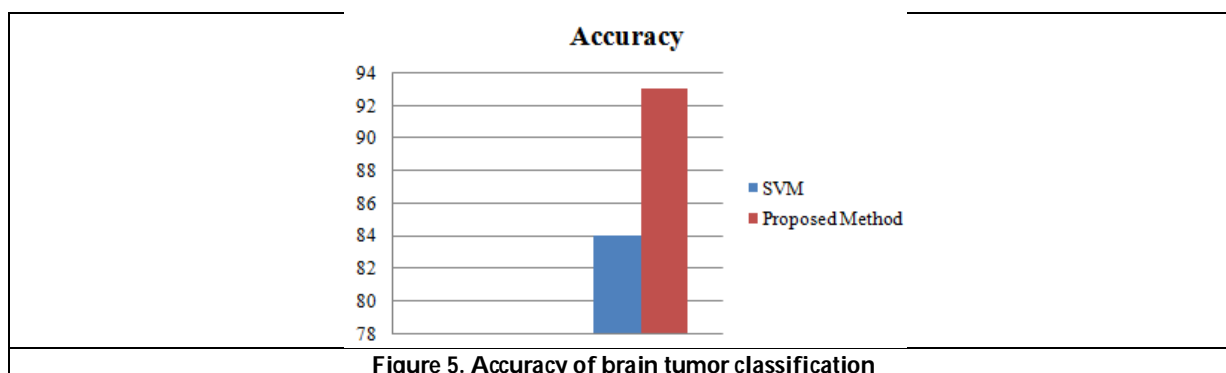
Saranya

13. Yang Y., Yan L.F., Zhang X., Han Y., Nan H.Y., Hu Y.C., Hu B., Yan S.L., Zhang J., Cheng D.L., et al. Glioma Grading on Conventional MR Images: A Deep Learning Study With Transfer Learning. *Front. Neurosci.* 2018;12:804. <https://doi.org/10.3389/fnins.2018.00804>.
14. Nazir M., Shakil S., Khurshid K. Role of deep learning in brain tumor detection and classification (2015 to 2020): A review. *Comput. Med. Imaging Graph.* 2021;91:101940, DOI: 10.1016/j.compmedimag.2021.101940
15. El-Kenawy E.S.M., Mirjalili S., Abdelhamid A.A., Ibrahim A., Khodadadi N., Eid M.M. Meta-Heuristic Optimization and Keystroke Dynamics for Authentication of SmartphoneUsers. *Mathematics.* 2022;10:2912. <https://doi.org/10.3390/math10162912>
16. El-kenawy E.S.M., Albalawi F., Ward S.A., Ghoneim S.S.M., Eid M.M., Abdelhamid A.A., Bailek N., Ibrahim A. Feature Selection and Classification of Transformer Faults Based on Novel Meta-Heuristic Algorithm. *Mathematics.* 2022;10:3144, <https://doi.org/10.3390/math10173144>.
17. El-Kenawy E.S.M., Mirjalili S., Alassery F., Zhang Y.D., Eid M.M., El-Mashad S.Y., Aloyaydi B.A., Ibrahim A., Abdelhamid A.A. Novel Meta-Heuristic Algorithm for Feature Selection, Unconstrained Functions and Engineering Problems. *IEEE Access.* 2022;10:40536–40555. DOI: 10.1109/ACCESS.2022.3166901
18. Ibrahim A., Mirjalili S., El-Said M., Ghoneim S.S.M., Al-Harathi M.M., Ibrahim T.F., El-Kenawy E.S.M. Wind Speed Ensemble Forecasting Based on Deep Learning Using Adaptive Dynamic Optimization Algorithm. *IEEE Access.* 2021;9:125787–12580, DOI:10.1109/ACCESS.2021.3111408.
19. El-kenawy E.S.M., Abutarboush H.F., Mohamed A.W., Ibrahim A. Advance Artificial Intelligence Technique for Designing Double T-shaped Monopole Antenna. *Comput. Mater. Contin.* 2021;69:2983–2995. <https://doi.org/10.32604/cmc.2021.019114>.
20. Samee N.A., El-Kenawy E.S.M., Atteia G., Jamjoom M.M., Ibrahim A., Abdelhamid A.A., El-Attar N.E., Gaber T., Slowik A., Shams M.Y. Metaheuristic Optimization Through Deep Learning Classification of COVID-19 in Chest X-Ray Images. *Comput.Mater.Contin.* 2022;73:4193–4210, <https://doi.org/10.32604/cmc.2022.031147>.





Saranya





A Clinical Study of “Gunja Taila Nasya” and “Dashmoola Shrit Ksheera Shirodhara

Madhu^{1*} and Gyan Prakash Sharma²

¹MD Scholar, Department of Panchakarma, Post Graduate Institute of Ayurveda, (Affiliated to Dr. Sarvepalli Radhakrishnan Rajasthan Ayurveda University) Jodhpur, Rajasthan, India.

²Associate Professor, Department of Panchakarma, Post Graduate Institute of Ayurveda, (Affiliated to Dr. Sarvepalli Radhakrishnan Rajasthan Ayurveda University) Jodhpur, Rajasthan, India.

Received: 22 Jan 2024

Revised: 09 Feb 2024

Accepted: 27 Apr 2024

*Address for Correspondence

Madhu

MD Scholar,

Department of Panchakarma,

Post Graduate Institute of Ayurveda,

(Affiliated to Dr. Sarvepalli Radhakrishnan Rajasthan Ayurveda University)

Jodhpur, Rajasthan, India.

Email: madhu17beniwal@gmail.com



This is an Open Access Journal / article distributed under the terms of the **Creative Commons Attribution License** (CC BY-NC-ND 3.0) which permits unrestricted use, distribution, and reproduction in any medium, provided the original work is properly cited. All rights reserved.

ABSTRACT

Ardhambhedaka is a condition classified under *Urdhawajatrugata Roga* in *Ayurvedic* medicine. It derives its name from the hallmark symptom of severe, lasting pain affecting one side of the head, with recurring episodes occurring every fifteen days, or monthly intervals. The signs and symptoms of *Ardhambhedaka* bear similarities to migraine headaches in modern medicine. The available contemporary treatment including NSAIDs, triptans, antidepressants and anticonvulsants has drawbacks like drug dependence, medication withdrawal syndrome, and chances of developing chronic headache. Present study *Gunja Taila Nasya Karma* and *Dashmoola shrit ksheera Shirodhara* was done on 30 patients of *Ardhambhedaka* (Migraine), who were divided into two groups by using Lottery Randomization Method. It was done on the basis of various scales i.e. VAS Score, MIDAS and Subjective Parameter. The VAS Score declined by 8.36 ± 1.50 to 2.36 ± 1.65 , 7.60 ± 1.40 to 4.13 ± 1.55 and MIDAS Score 31.50 ± 10.96 to 11.43 ± 5.46 , 0.87 ± 11.56 to 17.87 ± 8.71 in Group A and B respectively. *Gunja Taila Nasya* and *Dashmoola Shrit Ksheera Shirodhara* were found to be effective treatments for *Ardhambhedaka* but clinically *Gunja Taila Nasya* was more effective.

Keywords: *Ardhambhedaka*, *Panchkarma*, *Migraine*, *Nasya karma*, *Ayurveda*, *Shirodhara*





INTRODUCTION

The human body is recognized to contain 107 *Marmas*, with "Shirah" being designated as the primary *Marma* (vital point)^[1]. "Shirah" holds a special status as the "Uttamanga" or most important component among all the bodily structures, serving as the sanctuary for *Prana* (life force) and all sensory faculties (*Indriyas*)^[2]. Among the various disorders associated with the head mentioned in *Ayurvedic* texts, "Ardhavybhedaka Roga" is one such condition, classified under the category of "Shirorogas"^[3]. *Acharya Chakrapani*, the commentator of *Charaka Samhita*, provided a clarification for the term *Ardhavybhedaka*, stating it as "Ardha Mastaka Vedana"^[4]. According to *Acharya Charaka*^[5] and *Madhava*^[6], it is considered a *Vata* or *Vata-Kaphaja* disease. According to *Acharya Sushruta*, it is classified as a *Tridoshaja* disease^[7]. According to *Acharya Vagbhatta*, it is categorized as a *Vataja* disease^[8]. *Ardhavybhedaka* is correlated with Migraine on the basis of sign and symptoms. The word migraine is derived from the Greek word Hemi-Crania, meaning "half of the head" because the pain of migraine often occurs on one side (Megrim means hemicranial). Pain also sometimes spreads to affect the entire head. Migraine is a complex neurological disorder that manifests with recurrent headaches, nausea, vomiting, photophobia or phonophobia. There may or may not be a neurological accompaniment in the form of an aura^[9]. *Aacharya's* explained that all the *Panchkarma* procedures are indicated for *Ardhavybhedaka*. However, *Nasya karma* and *Shirodhara* plays a vital role in disintegrating the pathology of the disease. *Panchakarma* aims to address the root causes of the disease and enhance overall well-being.

AIMS AND OBJECTIVES

1. To evaluate the effect of *Nasya* in management of *Ardhavybhedaka*.
2. To evaluate the effect of *Shirodhara* in management of *Ardhavybhedaka*.

MATERIALS & METHODS

Ethical Clearance and CTRI Registration: The Clinical study was started after the approval of Institutional ethics committee IEC No. DSRRAU/UPGIAS&R/ IEC/20-21/403 and the Research work have been registered in Clinical Trial Registry of India CTRI/2022/09/045891. The Drug was prepared in the pharmacy of DSRRU, Jodhpur, Rajasthan.

Selection of Patients

All patients fulfilling the inclusion criteria were selected from the OPD of *Panchkarma* Department, PGIA Jodhpur, irrespective of their sex, caste, religion, occupation and economic status. Patients were included in the study after taking a written consent. All details of the patients were recorded and maintained in the specially prepared proforma [CRF-Clinical Registration Format].

Sampling method: Lottery Randomization Method

Group A: *Gunja Taila Nasya (Shirovirechan Nasya)* was given for 7 days followed by a gap of 7 days, two sitting was given in 15 Patients and total days in completion of *Nasya Karma* were 28 days.

DOSE: 4-4 *bindu* each nostril. [Standardization of *Bindu*: 1 *Bindu* = 0.5 ml]

Group B: *Dashmoola shrit ksheera Shirodhara* in 15 patients for 14 days.

DOSE: 1.5 liter medicated *ksheera*.

Inclusion Criteria

1. Diagnosed and confirmed cases of *Ardhavybhedaka* (Migraine) according to CRF.
2. Patients between the age group of 16-45 years of either sex, religion, occupation.
3. Clinically Fit for *Nasya Karma* and *Shirodhara*.
4. Patients willing to give written consent.



**Madhu and Gyan Prakash Sharma****Exclusion Criteria**

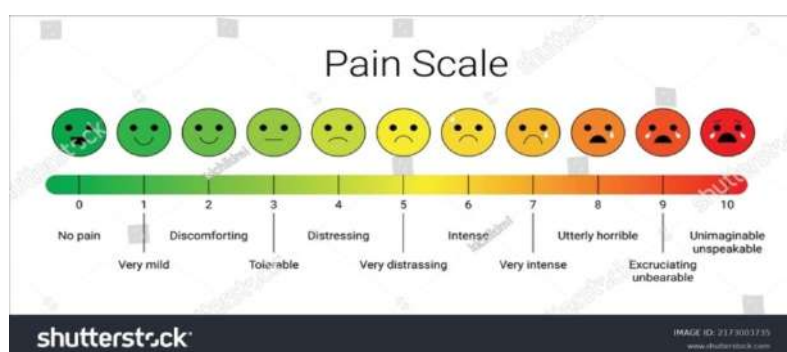
1. Patients who were suffering from secondary headaches like meningitis, brain tumour, encephalitis, cervical spondylitis, sinus, refractive errors & glaucoma.
2. Patients who were suffering from chronic disease like hypertension, COPD, renal disease etc.
3. Pregnant and lactating women.
4. A Patient of *Ardhavybhedaka* who was taking other treatment was excluded.
5. *Nasya* and *Shirodhara Ayogya*.

Withdrawal Criteria

1. If any adverse effect noted which require immediate medical intervention.
2. Patient not willing to continue the treatment.
3. Any other acute illness.

ASSESSMENT CRITERIA

Assessment of the Therapy was carried out before treatment and after treatment. It was done on the basis of various scales i.e. VAS Score, MIDAS and Subjective Parameter.

Visual Analogue Score (VAS)**MIDAS (Migraine Disability Assessment Test)**

Questionnaire was put together to help you measure the impact your headaches have on your life. The information on this questionnaire is also helpful for your primary care provider to determine the level of pain and disability caused by your headaches and to find the best treatment for you.





The Migraine Disability Assessment Test

The MIDAS (Migraine Disability Assessment) questionnaire was put together to help you measure the impact your headaches have on your life. The information on this questionnaire is also helpful for your primary care provider to determine the level of pain and disability caused by your headaches and to find the best treatment for you.

INSTRUCTIONS

Please answer the following questions about ALL of the headaches you have had over the last 3 months. Select your answer in the box next to each question. Select zero if you did not have the activity in the last 3 months. Please take the completed form to your healthcare professional.

- On how many days in the last 3 months did you miss work or school because of your headaches?
- How many days in the last 3 months was your productivity at work or school reduced by half or more because of your headaches? (Do not include days you counted in question 1 where you missed work or school.)
- On how many days in the last 3 months did you not do household work (such as housework, home repairs and maintenance, shopping, caring for children and relatives) because of your headaches?
- How many days in the last 3 months was your productivity in household work reduced by half or more because of your headaches? (Do not include days you counted in question 3 where you did not do household work.)
- On how many days in the last 3 months did you miss family, social or leisure activities because of your headaches?

Total (Questions 1-5)

What your Physician will need to know about your headache:

- On how many days in the last 3 months did you have a headache? (If a headache lasted more than 1 day, count each day.)
- On a scale of 0 - 10, on average how painful were these headaches? (where 0=no pain at all, and 10=pain as bad as it can be.)

Scoring: After you have filled out this questionnaire, add the total number of days from questions 1-5 (ignore A and B).

MIDAS Grade	Definition	MIDAS Score
I	Little or No Disability	0-5
II	Mild Disability	6-10
III	Moderate Disability	11-20
IV	Severe Disability	21+

If Your MIDAS Score is 6 or more, please discuss this with your doctor.

© Innovative Medical Research, 1997
© 2007, AstraZeneca Pharmaceuticals, LP. All Rights reserved.

Subjective Parameters

Based on symptoms of disease that is Intensity of Headache, Painless interval, Duration of Headache (hours/ days), Nausea, Vomiting, Photophobia, Phonophobia, Vertigo and Visual disturbance.

OBSERVATIONS AND RESULTS

In the clinical study, 30 individuals who had been clinically diagnosed and confirmed to have *Ardhavabhedaka* (Migraine) were enrolled based on the Case Report Format (CRF). Among these 30 patients, one patient discontinued the treatment. **Demographic data** shows that maximum numbers of patients were from Age group of 36-45 years 43.33% (17) out of which Females were 60% (18), Hindus 100% (30), Married 63.33% (19), Rural Habitat 60% (18), Graduate 43.33% (13), Housewife 26.67% (8), Socio-economic status- Middle class 63.33% (19), Family history- Nothing significant 76.67% (23), Treatment history- No History 50% (15), Normal General Appearance 60% (18), Mixed Diet 53.33% (16), *Vishamagni* 30% (9), *Madhyama Kosta* 50% (15), Normal bowel habit 56.67% (17), *Madhyama Sharir* 43.33% (13), *Vata-Kapha Sharir Prakriti* 50% (15), *Rajasika Mansika prakriti* 63.33% (19), *Samyaka Nidra* 66.67% (20), No addiction 36.67% (11), *Madhyama Sara* 73.33% (22), *Madhyama Samhana* 73.33% (22), *Madhyama Pramana* 73.33% (22), *Pravara Satmya* 46.67% (14), *Madhyama Satva* 53.33% (16), *Madhyama Abhyavaharan Shakti* 46.67% (14), *Madhyama Jarana Shakti* 56.67% (17), *Madhyama Vyayama Shakti* 76.67% (23), *Madhyama Vaya* 56.67% (17) observed.

Data Related to Disease

A maximum number of patient's i.e. 50% (15) patients were having chronicity within 1 year, 53.33% (16) were having sudden onset of disease, 53.33% (16) were having moderate severity of disease, 90% (27) were having unilateral side of headache, 50% (15) had no such Menstrual association, 66.67% (20) were having severe MIDAS Scale observed.





Madhu and Gyan Prakash Sharma

Group A and Group B showed statistically significant result in all the parameters like VAS Score, Intensity of headache, Painless Interval, Duration of Headache, Nausea, Vomitting, Photophobia, Phonophobia, Vertigo, Visual Disturbance and MIDAS Score.

Mann Whitney U Test is carried out for comparison between Group A and Group B. From above table, we can observe that, P-Value for all parameters is less than 0.05. Hence, we can conclude that, there is significant difference between Group A and Group B. Further, we can observe that, mean rank for Group A is greater than Group B. Hence, we can conclude that, effect observed in Group A is better than Group B.

Overall efficacy of therapies in Group A and Group B

In Group A, 35.71% of patients showed marked improvement, 57.14% of patients showed moderate improvement and 7.14% of patients showed mild improvement. In Group B, 86.67% of patients showed mild improvement, 13.33% of patients showed moderate improvement and 0% of patients was have no changes.

DISCUSSION

A scientific correlation between *Ardhambhedaka* and Migraine can be established based on their shared cardinal feature of unilateral headache and paroxysmal episodes. It can be concluded that *Vata* is the predominant *Dosha* involved in *Ardhambhedaka*. Probable Mode of Action of *Gunja Taila*: Components of *Gunja Taila* - *Tila taila* (Sesame oil), *Bhringraj* (*Eclipta alba*), *Kanji* and *Gunja* (*Abrus precatorius*). Maximum contents of this oil have *Madhura* - *Katu* - *Tikta* - *Kashaya rasa*, *Laghu*, *Ruksha guna*, *Ushna veerya*, *Katu Vipaka* and *Kapha*- *Vata Shamaka* property. *Tila taila* had been proven Analgesic, Anti-Oxidant properties and as per *Ayurveda* classics effects on - *Daurbalya*, *Pakalighata*, *Puyameha*, *Sirahsula*, *Sula*, *Vatavikara*, *Vrana*. *Bhringraj* (*Eclipta alba*) had been proven Hepato-protective, Anti-Inflammatory, Antiviral properties and as per *Ayurveda* classics effects on - *Sirah sula*, *Pandu*, *Kamla*, *Svasa-Kasa*, *Netra roga*. *Gunja* (*Abrus precatorius*) had been proven CNS Depressant, Analgesic, Anti-Muscarinic, Anti-Spasmodic properties and as per *Ayurveda* classics effects on - *Darunaka*, *Krimi danta*, *Visarpa*, *Shoola*, *Kaphavatahara*. *Kanji* has *Rochaka*, *Pachaka*, *Agnideepana*, *Shoolanashaka*, *Ajirana nashak*, *Kostha Suddhikar* properties. Probable mode of action of *Nasya Karma*: A drug administered nasally travels to the *Sringataka Marma* and spreads within the cranial circulation (*Murdha*), eventually reaching a pivotal point where the pathways of the *Netra* (eyes), *Kshotra* (ear), *Kantha* (throat), and *Siramukhas* (blood vessels converge). It effectively eliminates the unhealthy *Doshas* from the *Urdhavajatru* (upper neck area), akin to how *Munja* grass is cleanly separated from its stem. *Abhyanga*: The *Ayurvedic* texts suggest gentle massage on specific areas including the frontal, temporal, maxillary, mastoid, and neck regions before and after *Nasya*. There is a *Marma* point called *Manya* located on either side of the trachea in the neck, which is believed to correspond to the carotid sinuses. The procedures, postures, and practices associated with *Nasya Karma* play a vital role in drug absorption and transportation. *Swedana*: Massage can stimulate blood circulation, promoting vasodilation (*Sroto Vispharana*) and lymphatic flow in the targeted area, thereby potentially improving the distribution and absorption of the medication. Second, local fomentation, which involves applying warm compresses or heat, may induce a hypno-analgesic effect by diverting stimuli.

During the drug absorption process from the nasal cavity, the initial step involves traversing the mucus layer. While small and uncharged particles can easily move through this barrier, larger and charged particles might encounter difficulties in crossing it. The olfactory nerve functions as a chemoreceptor. This nerve is connected to the limbic system and hypothalamus through the olfactory pathway. These brain regions play a role in regulating endocrine secretions. Stimulating the hypothalamus electrically in animals can trigger secretions from the anterior pituitary. Consequently, drugs administered through this pathway stimulate higher brain centers, influencing the regulation of both the endocrine and nervous systems. Keeping the head in a lower position and retaining the medicine in the nasopharynx, as well as employing massage and local fomentation techniques. Probable Mode of Action of *Dashmoola Shrit Ksheera*: Among the ten ingredients in *Dashmoola*, 50% (5 *Dravyas*) possess *Vata-Kapha Shamak* properties, 40% (4 *Dravyas*) have *Tridosaghna* properties, and 10% (1 *Dravya*) exhibits *Vata-Pitta Shamak* properties. This signifies that all the constituents in *Dashmoola* (100%) possess *Vata Shamak* properties, and 90% (9 *Dravyas*) have



**Madhu and Gyan Prakash Sharma**

Vata-Kapha Shamak properties. Consequently, it becomes a potent compound for pacifying *Vata Dosha*, *Vata-Kapha Dosha*, and *Tridosha* in general. Considering that *Ardhavybedaka* is primarily a *Vata*-dominant condition (*Vata-kapha-Ch.* or *Tridosha* Su.), there is a strong possibility that the treatment could disrupt the pathogenesis (*Samprapti vighatna*) of *Ardhavybedaka Roga*. Milk possesses the qualities of *Madhura Rasa*, *Snigdha*, *Guru*, *Mridu*, and *Sandra Guna* which collectively help pacify *Vata* and *Pitta Doshas*. Additionally, milk shares similar properties with *Ojas*(immunity), making it a promoter of *Ojas* in the body. Probable mode of action of *Shirodhara*: According to *Acharya Charaka*, the head, also known as *Uttamanga*, is the foundation for all the sense faculties or *Indriya*^[10]. Due to this fact *Shirodhara* provides strength to *prana*, *Udana* & *Vyana Vayu*, *Sadhaka Pitta*, *Tarpaka Kapha* and *indriyas* which are vitiated in case of psychological disorders. According to *Yoga Sutra*, in *Shirodhara* patient is made to lie down in supine position as in *shavasana*. This position itself is used for relaxation in yogic science. Effect of *Shirodhara* on *Marma*: *Shirodhara* makes the patient concentrate on *Sthapni*, *Utshepa*, *Avarta*, *Shankha* and *Apanga Marma* area by which the stability arrives in the function. Hypothesis for the Possible Mechanisms of *Shirodhara*'s Effects: In *Shirodhara*, *Dhara* is poured continuously over the forehead of patient in a specific manner from a specific height and for a specific period of time. Every substance located at a specific height has Potential Energy (P.E. = mgh) and this energy is turned into Kinetic Energy when the substance falls from that height. This is the "Law of Conservation of Energy" ^[11,12]. Thus it can be concluded that P.E.= K.E i.e. $mgh = \frac{1}{2} mv^2$. It is evident from the preceding explanation that when anything falls from a given height, it generates momentum, that momentum may induce a change in voltage and stimulate nerve impulse creation or accentuate nerve impulse conduction.

This is most likely why the medication is administered for 45 minutes to an hour during *Shirodhara*. *Shirodhara* creates a continual pressure and vibration that is intensified by the hollow sinus in the frontal bone. The vibration is subsequently carried inwards via the cerebrospinal fluid (CSF) fluid medium. This vibration, along with a bearable amount of temperature, may stimulate the functioning of the thalamus and the basal forebrain, bringing the levels of serotonin and catecholamine back to normal. Pressure has an influence on impulse conduction as well. When a nerve is subjected to extended pressure, impulse conduction is disrupted and a portion of the body relaxes. *Shirodhara* is a method that employs extended and continuous pressure to trickle medicinal liquid over the forehead to calm the mind and alleviate stress by controlling nerve progression/stimulation^[13]. Acetylcholine in small dosages lowers blood pressure, resulting in reduced activity of the central nervous system and mental tranquillity^[14]. Serotonin (5-hydroxytryptamine, 5-HT) is a neurotransmitter in the brain that has an enormous influence over many brain functions. It is synthesized, from the amino acid L-tryptophan, in brain neurons and stored in vesicles. *Shirodhara* bring a calming effect because after completion of procedure patient feel relax and sleepy^[15]. So it may say that one of the mechanisms of action of *Shirodhara* is by raising the level of Serotonin. These hypotheses suggest a multifaceted approach to *Shirodhara*'s effects, potentially involving energy conversion, momentum, neurotransmitter modulation, and nerve stimulation.

CONCLUSION

Gunja Taila Nasya and *Dashmoola Shrit Ksheera Shirodhara* were found to be effective treatments for *Ardhavybedaka* but clinically *Gunja Taila Nasya* was more effective. Moreover, both therapies were determined to be safe and cost-effective.

LIMITATIONS OF THE STUDY

The inclusion of both self-assessment and observer-based rating scales in the study creates the potential for scoring errors. Sample size of the study was small and time Period for clinical trial was of short duration.





REFERENCES

1. Sushruta Samhita of Maharsi Sushruta edited by Ayurveda Tattva Sandipika by Kaviraja Ambikadutta Shastri, Chaukhambha Sanskrit Sansthan, Part I (Reprint 2012) Sharira sthana chapter 6/9
2. Charaka Samhita by Agnivesha, Revised by Charaka and Dridhabala 'Vidyotini' Hindi commentary Part I (Reprint year 2012) Chaukhambha Bharati Academy, Varanasi, by Prof. Kashinath Shastri and Dr. Gorakhnath Chaturvedi, Sutra sthana chapter 17/12
3. Charaka Samhita of Agnivesha Revised by Charaka and Dridhabala, 'Vidyotini' Hindi commentary by Pt. Kasinath sastri and Dr. Gorakha Nath Chaturvedi, Chaukhambha Bharati Academy, Varanasi, Part II, (Reprint year 2012), Shidhi sthana chapter 9/74-78
4. Agniveesha, Charaka Samhita with Ayurveda Dipika Sanskrita Commentary by Chakrapani, Revised by Acharya Charaka & Dradhabala, Chaukhambha Publication, New Delhi, Re-print 2014, Sutra Sthana chap. 7/16, page –49
5. Agniveesha, Charaka Samhita with Ayurveda Dipika Sanskrita Commentary by Chakrapani, Revised by Acharya Charaka & Dradhabala, Chaukhambha Publication, New Delhi, Re-print 2014, Sidhdhi Sthana chap. 9/75, page –721
6. Madhavakar, Madhava Nidana with Madhukosh commentary by Shri Vijayrakshita and Shri Kanthadatta, chap. 60 Shiro roga nidana / 1 madhukosha commentary, page – 475
7. Sushruta, Sushruta Samhita with the Nibandh sangraha sanskrita commentary by Dalhanacharya, Chaukhambha Surbharti Publication, Varanasi, 2014, Uttar tantra chap. 25/16 page – 655
8. Vagbhatta, Ashtang Hridayam with Nirmala hindi commentary by Dr. Brahmanand Tripathi, Chaukhambha Sanskrit Pratishthan, Delhi, Re – print 2011, Uttar Sthan chap. 23/7, page - 1050
9. API Textbook of Medicine By YP Munjal, Volume 1, 10th Edition, Jaypee Brothers Medical Publishers P. Ltd. Page No. 24
10. Agniveesha, Charaka Samhita with Ayurveda Dipika Sanskrita Commentary by Chakrapani, Revised by Acharya Charaka & Dradhabala, Chaukhambha Publication, New Delhi, Re-print 2014, Sutra Sthana chap. 17/3, page –332
11. Giles, R. (1964). Mathematical Foundations of Thermodynamics, Macmillan, New York, pp. 2, 97.
12. Landsberg, P.T. (1978). Thermodynamics and Statistical Mechanics, Oxford University Press, Oxford UK, ISBN 0-19-851142-6, p. 79.
13. Sahu A. K., Sharma A. K., A Clinical Study on Anidra And It's Management With Shirodhara and Mansyadi Kwatha. Journal of Ayurveda. 2009,3.
14. Singh O. P.,Singh L.,Kumar A. A Clinical Study to evaluate the role of Akshitarpana, Shirodhara and an Ayurvedic Compound in Childhood Computer Vision Syndrome. IJRAP 2011, 2 (3) 708-714.
15. Young SN (2007). "How to increase serotonin in the human brain without drugs". Rev. Psychiatr. Neurosci. 32(6): 394–99. Kajaria Divya et. al : An Appraisal of the Mechanism of Action of Shirodhara Annals of Ayurvedic Medicine Vol-2 Issue-3 July-Sep. 2013 117.



Table 1. Effect of *Gunja Taila Nasya* and *Dashmoola Shrit Ksheera Shirodhara* on symptoms of *Ardhavybedaka* (Migraine)

Symptoms	GROUP A				GROUP B			
	Mean Score \pm SD		P-Value	% Change	Mean Score \pm SD		P-Value	% Change
	0 Day	28 Day			0 Day	28 Day		
VAS Score	8.36 \pm 1.50	2.36 \pm 1.65	0.000	71.79%	7.60 \pm 1.40	4.13 \pm 1.55	0.000	45.61%
Intensity of Headache	3.14 \pm 0.95	0.93 \pm 0.73	0.000	70.45%	2.87 \pm 0.99	1.93 \pm 0.80	0.001	32.56%
Painless interval (In days)	3.00 \pm 0.78	1.14 \pm 0.86	0.001	61.90%	2.67 \pm 0.98	1.73 \pm 0.96	0.001	35.00%
Duration of Headache	3.14 \pm 0.86	1.14 \pm 0.77	0.000	63.64%	3.00 \pm 0.85	2.07 \pm 0.80	0.002	31.11%
Frequency of Nausea	1.86 \pm 1.10	0.86 \pm 0.77	0.003	53.85%	1.87 \pm 1.19	1.13 \pm 0.83	0.002	39.29%
Frequency of Vomiting	1.50 \pm 1.29	0.29 \pm 0.61	0.015	80.95%	1.47 \pm 1.19	0.80 \pm 0.86	0.014	45.45%
Photophobia	2.93 \pm 1.00	1.29 \pm 0.61	0.001	56.10%	2.33 \pm 0.98	1.27 \pm 0.88	0.000	45.71%
Phonophobia	1.79 \pm 0.89	0.57 \pm 0.76	0.001	68.00%	1.20 \pm 0.77	0.80 \pm 0.68	0.033	33.33%
Vertigo	1.36 \pm 1.15	0.43 \pm 0.51	0.009	68.42%	1.20 \pm 1.21	0.60 \pm 0.91	0.006	50.00%
Visual Disturbance	0.50 \pm 0.76	0.14 \pm 0.36	0.025	71.43%	0.87 \pm 1.06	0.60 \pm 0.74	0.047	30.77%
MIDAS Score	31.50 \pm 10.96	11.43 \pm 5.46	0.000	63.72%	30.87 \pm 11.56	17.87 \pm 8.71	0.000	42.12%



Table 2. Inter-group comparison in 30 Patients of *Ardhavybhedaka* (Migraine)

Variable	Group	Mean Rank	Sum of Ranks	Mann-Whitney U	P-Value
VAS Score	Group A	21.82	305.50	9.5	0.000
	Group B	8.63	129.50		
Intensity of Headache	Group A	21.00	294.00	21.0	0.000
	Group B	9.40	141.00		
Painless interval (In Days)	Group A	19.54	273.50	41.5	0.003
	Group B	10.77	161.50		
Duration of Headache	Group A	20.11	281.50	33.5	0.001
	Group B	10.23	153.50		
Nausea	Group A	16.43	230.00	85.0	0.034
	Group B	13.67	205.00		
Vomiting	Group A	16.46	230.50	84.5	0.033
	Group B	13.63	204.50		
Photophobia	Group A	18.61	260.50	54.5	0.013
	Group B	11.63	174.50		
Phonophobia	Group A	19.25	269.50	45.5	0.005
	Group B	11.03	165.50		
Vertigo	Group A	16.43	230.00	85.0	0.035
	Group B	13.67	205.00		
Visual Disturbance	Group A	16.00	224.00	91.0	0.043
	Group B	14.07	211.00		
MIDAS Score	Group A	19.00	266.00	49.0	0.014
	Group B	11.27	169.00		





***Nigella sativa*: A Botanical Marvel for Modern Neurological Disorders and Beyond**

Deepak Solanki¹, Seema Mehdi^{2*}, K L Krishna, Tamsheel Roohi Fatima¹, Mohini Milmlile¹, Lenisha Sequeira¹

¹Post Graduate Student, Department of Pharmacology, JSS College of Pharmacy, (Affiliated to JSS Academy of Higher Education & Research) Mysore, Karnataka, India.

²Lecturer, Department of Pharmacology, JSS College of Pharmacy, (Affiliated to JSS Academy of Higher Education & Research) Mysore, Karnataka, India.

³Associate Professor and Head, Department of Pharmacology, JSS College of Pharmacy, (Affiliated to JSS Academy of Higher Education & Research) Mysore, Karnataka, India.

Received: 22 Jan 2024

Revised: 09 Feb 2024

Accepted: 27 Apr 2024

***Address for Correspondence**

Seema Mehdi

Lecturer,

Department of Pharmacology,

JSS College of Pharmacy,

(Affiliated to JSS Academy of Higher Education & Research)

Mysore, Karnataka, India.

Email: seemamehdi@jssuni.edu.in



This is an Open Access Journal / article distributed under the terms of the **Creative Commons Attribution License** (CC BY-NC-ND 3.0) which permits unrestricted use, distribution, and reproduction in any medium, provided the original work is properly cited. All rights reserved.

ABSTRACT

Nigella sativa (NS) is frequently referred to as a "remarkable botanical specimen" owing to its extensive range of biological and pharmacological functions. It possesses anti-inflammatory, antioxidant, antibacterial, anti-apoptotic, anti-mutagenic, and anti-carcinogenic properties. Substantiated evidence suggests that *N. sativa* may contribute to the treatment of neurodegenerative diseases, as well as ailments such as cough, fever, diarrhea, and eczema. Historically, it has been employed for managing conditions like hyperglycemia, hypertension, allergies, and gastrointestinal distress. The abundant presence of antioxidants in NS has led to its widespread utilization as a medicinal herb. Scientific investigations have demonstrated the efficacy of oil extracted from NS seeds in the treatment of cerebral hypoperfusion and restoration of spatial memory. Moreover, increased scopolamine levels in NS have been found to alleviate acetylcholine levels and oxidative stress in mouse brains, thereby enhancing learning and memory. The neuroprotective properties of NS and its component thymoquinone (TQ) have been examined in both human and animal models of various neurological disorders, including Alzheimer's disease, epilepsy, and neurotoxicity. For centuries, the seeds and oil derived from the *Nigella sativa* (NS) plant have been utilized in traditional medicine worldwide. Consequently, the primary aim is to explore the potential





Deepak Solanki et al.,

antidepressant effects of this plant. Animal studies have demonstrated the protective effects of NS against damage to the brain, kidneys, lungs, heart, and liver.

Keywords: *Nigella Sativa*, Parkinson's Disease, Alzheimer's disease, Multiple Sclerosis, Epilepsy.

INTRODUCTION

Depression is a prevalent mental disorder that afflicts a significant number of individuals. Globally, about 5% of adults experience depression.(1)Depression is a mental health disorder characterized by persistent feelings of sadness, hopelessness, and a lack of interest or pleasure in activities.“Depression” comes from the Latin word *depressio*, meaning to press down.(2)Depression affects more women than males. Approximately 50% more women worldwide suffer from depression.The effective management and treatment of depression necessitate the involvement of proficient specialists in the field of mental health, including psychiatrists and psychologists. Mental illnesses, such as depression, exhibit considerable frequency, not only in developing nations but also in more advanced societies.(3) Moreover, they are notably prevalent among military personnel.(4)One estimation suggests that the population of individuals residing in the United States who have experienced significant depression amounts to approximately 17.3 million. (5)Depression constitutes a notable mood disorder that can manifest in diverse manifestations, exerting a significant influence on the overall burden that society's health endures due to depression.(6)(7) Various therapeutic medications are currently used to treat depression; however, their clinical applications are limited due to significant side effects such as impaired psychomotor function, potentiation of other central depressive drugs, and the potential for dependency.(8) Consequently, there is ongoing global research to discover novel herbal remedies for depression. While numerous plant-based treatments have been employed historically, many herbal medicines remain unexplored.(9) This review study was conducted on experimental animals to evaluate the effectiveness of NS as a treatment for stress-induced depression and to gain a deeper understanding of the underlying mechanisms involved.

***Nigella Sativa* and its Historical Significance in Traditional Medicine**

NS possesses antioxidant properties, and scientific investigations have demonstrated its ability to alleviate oxidative stress, a condition that can potentially result in ischemia. Additionally, this plant extract shields erythrocytes against lipid peroxidation and ameliorates the augmented osmotic features induced by hydrogen peroxide. The effects of this extract on neurological conditions such as epilepsy and mental disorders like bipolar disorder have been subject to thorough examination. Notably, *N. Sativa* has been observed to have a substantial impact on mood disorders.(10)

Nigella sativa (NS), commonly referred to as Black Seed, is a flowering plant belonging to the Ranunculaceae family. It is widely recognized for its therapeutic properties and finds usage in various regions across the globe. The plant's seeds have a rich history of being employed for both medicinal and culinary purposes due to their versatile nature. One notable historical context is ancient Egypt, where archaeological findings, including black seeds discovered in the tomb of King Tutankhamun, point to the plant's valued status in ancient Egyptian culture. This early use underscores the enduring importance of NS in traditional healing practices.(11) Islamic literature praises its effectiveness as a form of medical treatment. *Nigella sativa* (NS), a medicinal plant, is native to Western Asia, Eastern Europe, and the Middle East. In Arabic, NS seeds are known as "Al-Habba Al-Sauda" and "Al-Habba Al-Barakah," while in English, they are commonly referred to as "black seed" or "dark cumin".

There have been indications for a considerable period that NS seeds are used as a remedy for a wide range of ailments in several Asian countries, including some in the Middle East. This plant holds significant importance in Islamic nations due to its diverse applications. Furthermore, the renowned book "Canon of Medicine," written by Avicenna, highlights the potential of NS seeds in enhancing physical vitality while alleviating feelings of fatigue and depression.(12)(13) Beyond that, NS has found its place in Ayurvedic texts, the traditional system of medicine in India, as well as in other Asian healing traditions.(14) Its historical use is not limited to a specific region, as the plant's seeds have been recognized for their therapeutic properties by ancient Greek and Roman figures such as Hippocrates





Deepak Solanki et al.,

and Dioscorides. Throughout the Middle East and various African cultures, NS has been a staple in traditional medicinal practices. Its applications range from addressing digestive and respiratory issues to serving as a general tonic for overall well-being. The plant's versatility and historical significance in diverse cultures highlight its enduring reputation as a medicinal herb.⁽¹⁵⁾ In recent times, the historical uses of NS have attracted scientific attention. Modern research has explored its potential anti-inflammatory, antioxidant, and immune-modulating properties. While historical and cultural contexts have long valued black seed for its health benefits, ongoing scientific investigations aim to provide a deeper understanding of its efficacy and mechanisms of action. As with any herbal remedy, it is advisable for individuals to consult healthcare professionals before incorporating NS into their wellness routines. This collaborative approach ensures a balanced perspective that combines traditional wisdom with contemporary scientific insights.⁽¹⁶⁾ The growing interest in herbal remedies and natural supplements as complementary approaches to conventional treatments for mental health conditions, coupled with NS's historical importance, contributes to the relevance of the review. Scientific exploration of NS and its potential neuroprotective and mood-regulating properties adds to the rationale. Depression, a prevalent global health concern with varying treatment responses, prompts the need to investigate alternative therapies⁽¹⁷⁾. The review aims to critically evaluate existing scientific studies on NS oleoresin and depression, identify potential mechanisms of action, and inform future research and clinical practices. By addressing gaps in knowledge, the review seeks to contribute to a holistic understanding of mental health interventions, offering insights for researchers, healthcare professionals, and individuals seeking evidence-based information on the effects of NS oleoresin on depression

NIGELLA SATIVABOTANICAL FEATURES AND ITS CHEMICAL CONSTITUENTS

NS is an herb belonging to the Ranunculaceae family, and it holds significant importance as a constituent in various medicinal preparations. NS is a perennial flowering plant capable of attaining heights ranging from 20 to 90 centimetres. Its leaves are finely divided, featuring leaf segments that are slender and somewhat curved. Additionally, the plant's blossoms consist of five to ten petals and are often characterized by delicate shades such as yellow, white, pink, light blue, or pastel purple. The natural fruit of this herb is a large capsule that has undergone inflation and comprises three to seven fused follicles. Each follicle contains multiple seeds within. ⁽¹⁷⁾⁽¹⁸⁾ The seeds exhibit the characteristics of being minute, dicotyledonous, trigonous, angular, and regucose-tubercular, measuring 2-3.5mm in length and 1-2mm in width. Their outer surface is black, while the inner portion appears white. They possess a mild fragrance and a bitter taste. Examining the seed's epidermis through a transverse section under a microscope reveals a single layer of oval-shaped cells with thick walls. The exterior of these cells is covered by a papillose cuticle, and upon closer observation, a dark brown substance can be observed within them. ⁽¹⁹⁾ After the epidermis, there is a layer of cells with thick walls and rectangular enlargements, exhibiting a rosy chestnut colour.

This layer is succeeded by two to four layers of parenchymatous cells with thick walls and tangential extensions. Following this, there is a layer known as the pigment layer, composed of inward pigment cells. These cells possess a nearly columnar shape and thick walls, extending either in a rectangular or stretched-out form. The endosperm, on the other hand, consists of cells with thin walls, assuming either a rectangular or polygonal shape. The arrangement of these cells within the endosperm can vary. When observed under a microscope, powdered seeds display dark parenchymatous cells and oil globules.⁽²⁰⁾⁽²¹⁾ Several different active compounds are extracted from the combinations of dark seeds and subsequently published. Some examples of these components include thymoquinone (TQ), thymohydroquinone (THQ), thymoquinone (DQ), p-cymene (7%-15%), carvacrol (6%-12%), 4-terpineol (2%-7%), t-anethole (1%-4%), sesquiterpene-longifolene (1%-8%), -pinene (1%-8%). Additionally, the seeds contain two distinct types of alkaloids: those with a pyrazole ring and those with an indazole ring. Among these alkaloids, nigericin and nigellidine can be found in the plant's seeds. The NS seeds also contain saponin, which has been hypothesized to possess anticancer properties. Furthermore, the seeds contain the pentacyclic triterpene alpha-hederin.⁽²²⁾ NS seeds can exhibit high levels of protein (26.7%), fat (28.5%), carbohydrates (24.9%), crude fiber (8.4%), and total ash (4.8%). Moreover, the seeds are rich in a wide variety of essential vitamins and minerals, including copper, phosphorus, zinc, iron, and others. Chemical substances such as nigellone, avenasterol-5-ene, avenasterol-7-ene, campesterol, obtusifoliol, cholesterol, citrostadienol, cycloeucalenol, stigmastanol, gramisterol, lophenol, obtusifoliol, stigmasterol-7-ene, -amyrin, butyrospermol, cycloartenol, 24-methylene-cyclo, and 3-O-[-D-

75793

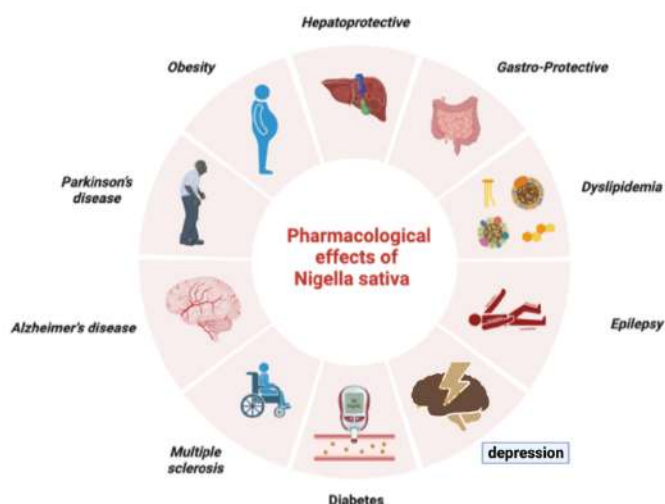




Deepak Solanki et al.,

xylopyranosyl (1.3)- L-rhamnopyranosyl(1.2)—L-arabino-pyranosyl] -28-O-[β -L-rhamnopyranosyl. The structure is represented by [β -D-glucopyranosyl (1.6)—Dgluco-pyranosyl]. Additionally, bitter principles, tannin, resin, protein, reducing sugar, glycosidal saponin, hederagenin, melanin, melanthigenin, hederagenin glycoside, melanthigenin glycoside, and hederagenin glycoside are all constituents of the bitter principle. Other compounds found include 3-O-[β -D-xylopyranosyl (1.2) (1.2) - α -L-rhamnopyranosyl-(1.2) - β -D-glucopyranosyl] 11-methoxy-16, 23-dihydroxy-28-methyl-olean-12-enoate. (23) The incorporation of biochemical methodologies into the investigation of *N. Sativa* has yielded definitive evidence regarding the existence of a diverse array of organic constituents. Among these substances, a noteworthy category is comprised of the volatile phytochemicals derived from the essential oil of *N. Sativa*. Within this group, various compounds such as TQ, thymol, thymoquinone, carvacrol, 4-terpineol, p-cymene, -pinene, -pinene, and t-anethole can be classified. TQ, similar to numerous other compounds, exhibits a broad spectrum of pharmacological activities. The extract of *N. Sativa* may contain alkaloids such as Nigellimine, nigellimine-N-oxide, nigericin, and nigellone. Another alkaloid, nigellimine, can also be found. Additionally, the essential oil present in *N. Sativa* encompasses a variety of nutrients including proteins, saturated and unsaturated free fatty acids, vitamins, and minerals. (24)(25)

PHARMACOLOGICAL EFFECTS OF NIGELLA SATIVA



Parkinson's disease

Parkinson's disease is characterized as a neurodegenerative condition marked by the gradual degeneration of neurons within the basal ganglia of the brain, which play a crucial role in coordinating movement.(26) Although the existing pharmacological treatments effectively alleviate the symptoms of Parkinson's disease, they are accompanied by a substantial array of adverse effects. (27)(28)(29)In certain cases, the therapy of Parkinson's disease might benefit from the use of natural herbal items. Recent studies have looked at whether or not *N. Sativa* would be able to slow or stop the progression of Parkinson's disease. Effects of a NS seed extract on chemical parameters as well as a chlorpromazine-induced experimental animal model of catalepsy were investigated, amongst other things (TBARS, GSH, Nitrite, and Total Protein). The severity of the cataleptic symptomatology diminished to a great degree.(30)(31) Furthermore, it was observed in a rat model of early Parkinson's disease that thymoquinone alleviated the associated behavioural and cellular impairments, along with the oxidative stress indicators. Thymoquinone's capacity to reverse the condition was demonstrated. Rats with unilateral intrastriatal 6-hydroxydopamine (6-OHDA) lesions were orally administered thymoquinone (5 and 10 mg/Kg, three times daily) for a duration of one week. The study was limited to a week. Prior treatment with thymoquinone significantly enhanced turning behaviour, reduced MDA levels, and prevented neuronal death in the substantia nigra. These findings provided support for the concept that TQ possesses neuroprotective properties in neurodegenerative conditions such as Parkinson's disease. (32)



**Deepak Solanki et al.,**

In an animal model utilized to study Parkinson's disease, certain data indicated that an ethanolic extract derived from the seeds of *Nigella Sativa* (EENS) demonstrated potential in safeguarding neurons against the neurotoxic effects induced by chlorpromazine (CPZ). Animals were subjected to intraperitoneal administration of chlorpromazine at a dosage of 3 milligrams per kilogram, resulting in the manifestation of cataleptic symptoms. This dosage is commonly employed to simulate Parkinson's disease in experimental models. Notably, when the ethanolic extract of NS was administered at specified doses of 200 and 400 mg/kg, a significant reduction in the extent of catalepsy was observed in the group treated with CPZ. In stark contrast to the CPZ-treated group, the administration of EENS at doses of 200 and 400 mg/kg resulted in a substantial decrease in lipid peroxidation and a reversal of the elevated nitrite levels. Furthermore, the concentration of glutathione (GSH) in rats administered with EENS (both 200 and 400 mg/kg) was markedly elevated compared to rats treated solely with CPZ. (33) A study was conducted to investigate the muscle rigidity induced by the drug perphenazine in adult male mice. The findings were then compared to those obtained from the administration of orally consumed *N. Sativa* hydroalcoholic seed extract. Mice that received *N. Sativa* extract at a dosage of 100 mg/kg displayed a notable improvement in their muscle stiffness score after 40 minutes. Conversely, mice given *N. Sativa* extract at a dosage of 50 mg/kg did not exhibit a significant distinction from the control group, which received water. Furthermore, in comparison to the control group, the *N. Sativa* group administered at a dosage of 200 mg/kg displayed a statistically significant enhancement in both the initial and final scores for muscle stiffness. (34)(35)

Alzheimer's disease

Alzheimer's dementia (AD) is a neurodegenerative disorder characterized by the progressive atrophy and reduction in size of the brain, as well as the abnormal formation of cortical senile plaques resulting from the aggregation of the 4.2-kD amyloid beta peptide (Ab). In order to conduct this study, hippocampal neurons were cultivated in vitro, and the researchers examined the potential protective effects of thymoquinone (TQ) in contrast to the cell death induced by Ab1-42.(36)(37) The researchers observed an increase in the amount of cell death in hippocampal cell cultures following the administration of Ab, and this increase was found to be dependent on the dosage.(33,34) In spite of being subjected to TQ at concentrations of 0.1, 1.0, 10.5, and 100 nM, there was no discernible difference in the percentage of hippocampal neurons that survived. However, when TQ was administered in concert with Ab1-42, there was a considerable improvement in the number of cells that survived. Ab1-42 was shown to produce an increase in ROS generation as well as a putative depolarization of the mitochondrial membrane. TQ was found to be effective in inhibiting both of these effects. In addition to this, TQ inhibited the recycling of synaptic vesicles, partially restored spontaneous firing, and decreased the amount of aggregation of the Ab1-42 protein.(38)(39)

Furthermore, the neuroprotective efficacy of thymoquinone (TQ) was assessed in the rat hippocampus at an oral dosage of 5 mg/kg/day. It demonstrated significant effectiveness in mitigating neuronal damage induced by acute forebrain ischemia. Comparatively, ischemic rats displayed marked oxidative damage characterized by a substantial reduction in catalase and superoxide dismutase (SOD) activity, as well as glutathione (GSH) levels within the hippocampal tissue, as opposed to the control group.(40) Notably, TQ therapy resulted in a significantly lower loss of hippocampal cells compared to the number lost due to ischemia alone, suggesting that TQ pre-treatment significantly reduced the extent of cellular death. TQ pre-treatment corresponded with elevated levels of glutathione (GSH), increased catalase (CAT) and superoxide dismutase (SOD) activity, and decreased levels of malondialdehyde (MDA).(41) Both thymohydroquinone (THQ) and thymoquinone (TQ) exhibited the ability to impede lipid oxidation in the hippocampal homogenate induced by iron-ascorbate.(42)(43)

Multiple sclerosis

Multiple sclerosis (MS), an immune-mediated disorder characterized by the demyelination of nerve fibers, affects younger individuals with greater frequency compared to older individuals due to the heightened vulnerability of their central nervous systems (CNS). Multiple sclerosis represents one of the main contributors to adult disability. Consequently, this chronic, progressive, and potentially debilitating illness will have notable social and economic repercussions.(44) Due to its antioxidant properties, NS has been frequently employed in the management of neurological disorders, including Parkinson's disease and Alzheimer's disease.(45,46) The biological activity of the





plant stems from the constituents present in the essential oil derived from the seeds of the NS plant. Previous research conducted on rats with Experimental Autoimmune Encephalomyelitis (EAE) demonstrated that treatment with *N. Sativa* effectively inhibited the production of reactive oxygen species (ROS) induced by EAE. This inhibitory effect was observed through a reduction in the levels of malondialdehyde (MDA) in the brain and spinal cord tissues, as well as a decrease in brain nitric oxide (NO) levels. Furthermore, Mohamed et al. discovered that thymoquinone treatment contributed to the alleviation of EAE, potentially attributed to an elevation in glutathione levels.(47)(48) In terms of histological observations, the cerebellum of the EAE group displayed focal degeneration of Purkinje cells, accompanied by a decrease in lymphocytic infiltration in the meninges of the cerebellar folia. These changes were consistent across both groups. The peripheral cerebellar medulla exhibited indications of diffuse gliosis in the molecular layer and minimal aggregation of mononuclear cells around blood vessels, while the central cerebellar medulla exhibited severe astrogliosis (characterized by astrocyte hyperplasia and hypertrophy) and the formation of axonal spheroids. Notably, both the "EAE + *N. Sativa*" and "*N. Sativa* + EAE" groups did not exhibit any signs of inflammatory cell infiltration in the meninges or perivascular mononuclear cell aggregation in the cerebellar medullary region. This observation was consistent in both groups. Conversely, reactive astrogliosis in the cerebellar medulla was significantly reduced in the group that received both EAE and *N. Sativa*, and it was markedly diminished in the group that received both *N. Sativa* and EAE. (49)(50)(51)

Epilepsy

An aqueous extract of *Nigella sativa* (NS) seed pods underwent evaluation regarding its potential efficacy as an anticonvulsant through both laboratory and clinical studies. The results demonstrated that the ingestion of NS extract led to reduced locomotor activity, impaired motor coordination, and increased sleep duration.(52) In another study, a model of epilepsy was induced in animals using pilocarpine, allowing the mice to develop chronic epilepsy over a period of 22 days. The animals were orally administered *Nigella sativa* oil (NSO) (4 ml/kg) once a day for a total of 21 days. The effects on oxidative stress, excitability, and seizure induction were examined in male Wistar albino rats with epilepsy. The findings indicated that NSO exhibited anti-convulsant properties and possessed significant antioxidant capabilities.(53) The present study aimed to investigate the efficacy of oil derived from NS in counteracting the alterations in amino acid neurotransmitters associated with epilepsy, specifically induced by intravenous injection of pilocarpine at a dose of 380 mg/kg. The oil was administered to the experimental subjects as a placebo. Upon administration of pilocarpine, the levels of GABA, aspartate, taurine, glycine, and glutamate exhibited an increase in the cortex. However, in the hippocampus, levels of glycine and taurine declined. It was observed that the high dosage of NS oil (4 ml/kg) did not alleviate the negative effects caused by pilocarpine injection.(54) In a rat model of seizures induced by pentylenetetrazole (PTZ) at a dose of 40 mg/kg body weight, the effects of an aqueous seed extract from NS were evaluated.(55) The NS extract hindered the animals' coordination abilities, reduced their locomotor activity, and increased the duration of their sleeping periods (52–55).

As compared to the control animals that served as the baseline, those pre-treated with NS extract demonstrated increased resistance to convulsions. Furthermore, NS treatment led to a decrease in the severity score and extended the time between seizures. Notably, NS successfully inhibited the effects of picrotoxin, a GABA_A antagonist, as well as delayed the onset of seizures. In the context of kindling seizures induced in mice by PTZ at a dose of 35 mg/kg intraperitoneally, the antioxidant and anticonvulsant effects of NS oil were investigated. Compared to mice treated with valproate and PTZ, mice administered NS oil at a dose of 12 ml/kg orally exhibited significantly lower seizure scores and were protected against the seizure-inducing actions and mortality caused by PTZ. Additionally, the NS oil substantially enhanced the levels of GSH while drastically reducing the levels of MDA, as compared to the PTZ group.(56) A randomized, double-blind, and controlled clinical trial was conducted to compare the effects of an aqueous NS extract dosage with a placebo in reducing the occurrence of epileptic seizures in children under the age of 13 diagnosed with epilepsy. The dosage of the NS extract was 40 mg/kg. Twenty children were randomly assigned to receive either the extract or placebo three times a day for a total duration of fourteen days. The administration of NS extract significantly reduced the number of seizures experienced by each patient. (57)



**ALS (Amyotrophic lateral sclerosis)**

Chronic inflammation has been associated with a multitude of ailments, encompassing conditions such as cancer, diabetes, cardiovascular disease, Alzheimer's disease, and epilepsy. Amyotrophic lateral sclerosis (ALS), rheumatoid arthritis (RA), and asthma are the medical conditions under consideration. (58) All of these factors contribute to a progressive and irreversible harm to cells and/or neurons. Furthermore, chronic inflammation has been associated with a multitude of viral ailments. Consequently, the crucial role played by the anti-inflammatory properties exhibited by various *N. sativa* samples and TQ may serve as promising reservoirs for the advancement of a novel innovation in anti-inflammatory medication, aimed at addressing a wide range of disorders. (59)(60)

ANTIOXIDANT PROPERTIES**Overview of Antioxidants in *Nigella Sativa***

Oxidative stress results from imbalance between reactive oxygen species (ROS) and antioxidant capacity which is in turn related to the pathogenesis of several human diseases. Antioxidants are compounds that help neutralize harmful free radicals in the body, which can contribute to oxidative stress and various health issues. (61) *Nigella sativa* is believed to possess antioxidant properties due to their high content of phenolic compounds by reducing the production of reactive oxygen species (ROS) and malondialdehyde (MDA). (62) Oxidative stress poses a significant threat to the nervous system, inducing various neuronal injuries through the production of reactive oxygen species (ROS). These injuries involve destructive processes such as lipid degradation in the cellular membrane, DNA cleavage, cell membrane lipid peroxidation, and protein oxidation. Concurrently, ROS can disrupt mitochondrial respiration, exacerbating cellular damage. Maintaining an oxidant-antioxidant balance is crucial, with endogenous antioxidant enzymes, including catalase (CAT), arylesterase, paraoxonase, and thiol, playing a vital role in mitigating oxidative stress. Monitoring their levels in serum or tissue is essential for understanding this balance. Notably, *Nigella sativa*, enriched with antioxidants like thymoquinone, has demonstrated neuroprotective effects by alleviating oxidative stress in the brain. (63) *Nigella sativa* (NS) is rich in thymoquinone (TQ), functioning as a potent free radical scavenger. NS exhibits the ability to enhance the production and activity of antioxidant enzymes, including superoxide dismutase (SOD), catalase (CAT), glutathione peroxidase (GPx), and glutathione S transferase (GSH-ST). Compared to synthetic antioxidants like BHA and BHT, NS oil (NSO) demonstrates higher antioxidant potential and superior anti-radical activity against DPPH radicals. (64) The diverse antioxidant compounds in NS extract, such as TQ, carvacrol, t-anethole, and 4-terpineol, contribute to its effectiveness. TQ, with its robust antioxidant properties, indirectly suppresses reactive oxygen species production and inhibits lipid peroxidation.

NS serves as a free radical scavenger, enhancing both non-enzymatic (GSH and vitamin C) and enzymatic (SOD, CAT, GPX, and GST) components of the antioxidant system. It restores elevated levels of malondialdehyde (MDA) and conjugated diene to normal levels. NSO and TQ exhibit non-enzymatic inhibition of lipid peroxidation in liposomes. Antioxidant assessments reveal that NS extracts containing TQ are three times more potent than TQ alone, highlighting a synergistic effect. In vitro tests demonstrate the remarkable ability of NSO compounds, including quinone, carvacrol, and 4-terpineol, to neutralize free radicals by connecting them.

Flavanol glycosides and aglycones present in NS contribute to its antioxidant and antiradical effects. Clinical trials further validate the antioxidant properties of NS. Additionally, TQ is identified as a mitochondria-targeted antioxidant, replenished through a reduction in the centre of mitochondrial complex III in the respiratory chain. (65) *Nigella sativa* (NS) exhibits diverse antioxidant properties attributed to its bioactive compounds. Thymoquinone (TQ), a key component, acts as a potent free radical scavenger, reducing oxidative stress. NS is rich in flavonoids and phenolic compounds, known for neutralizing free radicals and protecting against oxidative damage. Vitamin E in NS contributes to safeguarding cell membranes. Studies suggest NS may enhance superoxide dismutase (SOD) activity, reinforcing its antioxidant defences. The antioxidant-rich NS has been linked to reduced oxidative stress in various tissues. TQ is recognized as the active component responsible for NS's medicinal effects, including radical scavenging and inhibiting 5-lipoxygenase products during inflammation. The anti-toxic effects of NS are directly linked to its potent antioxidant activity, countering oxidative stress-induced lipid uptake in cells. Overall, NS's antioxidant-rich composition underscores its potential health benefits by mitigating oxidative damage and supporting cellular well-being. (66)



**Scientific Evidence and Studies**

Numerous studies confirm *Nigella Sativa*'s (NS) antioxidant prowess, demonstrated by its ability to diminish reactive oxygen species (ROS) and malondialdehyde (MDA) production. The high thymoquinone content in NS acts as an effective free radical scavenger, augmenting the production and activity of crucial antioxidant enzymes like superoxide dismutase (SOD), catalase (CAT), glutathione peroxidase (GPx), and glutathione S transferase (GSH-ST). Essential *Nigella sativa* seed oil, analysed through TLC screening methods, revealed radical scavenging properties in thymoquinone, carvacrol, tanethole, and 4 terpineol. These constituents, along with the essential oil, exhibited variable antioxidant activity in nonspecific hydrogen atom or electron-donating assays. Furthermore, they proved effective as radical hydroxyl scavengers in liposome non-enzymatic lipid peroxidation and deoxyribose degradation tests, emphasizing NS's diverse and potent antioxidant capabilities.(66) Clinical trials investigating *Nigella sativa* (NS) supplementation yield conflicting results regarding oxidative stress and antioxidant activity parameters. Some studies demonstrate a significant reduction in malondialdehyde (MDA), nitric oxide (NO), and superoxide dismutase (SOD) levels compared to controls.(67) However, others find no significant changes in MDA, glutathione peroxidase (GPx), or total antioxidant capacity (TAC). In preclinical studies involving rats and various stress-inducing agents, NS consistently decreases MDA levels. The variation in MDA response to NS may be attributed to factors like supplementation duration, cellular conditions, and disease types or severity.

Notably, SOD levels consistently increase with NS supplementation, as evidenced in both clinical and preclinical studies involving oxidative stress-inducing agents. The increased SOD levels suggest that NS may primarily mitigate free radicals by enhancing SOD activity and converting superoxide anions into less harmful by-products, thus potentially alleviating cellular damage and disease progression exacerbated by oxidative stress. The NS was also proven to improve the non-enzymatic antioxidant system through direct scavenging of carbon-centered radicals and hydroxyl radicals. Interestingly, in this meta-analysis, the effect of NS supplementation on TAC was not significant, suggesting that although the effect of NS is beneficial for increasing enzymatic antioxidants such as SOD, the overall effect of NS on the TAC might not be beneficial.(61) In a series of in vitro tests, *Nigella sativa* (NS) essential oil demonstrated antioxidant activity, functioning as a donating agent in the DPPH assay and exhibiting hydroxyl radical scavenging properties in both non-enzymatic lipid peroxidation and the deoxyribose test. Recent studies revealed that NS essential oil (NSO) and thymoquinone (TQ) reversed cyclophosphamide-induced dysregulation in lipid profiles. In vivo experiments further confirmed antioxidant effects, with TQ administration increasing quinone reductase and glutathione transferase activities. NSO or TQ administration in sensitized guinea pigs inhibited reactive oxygen species generation and elevated antioxidant enzymes SOD and glutathione levels.

TQ, known for its dual pro-oxidant and antioxidant activities, exhibited antioxidant effects by scavenging superoxide, hydroxyl radicals, and singlet molecular oxygen. Its potent antioxidant potential was associated with its redox properties and unhindered access to subcellular compartments, reducing toxicity in various conditions such as nephrotic syndrome, gentamicin-induced nephrotoxicity, and cyclosporine A-induced injury in rat hearts. Experimental studies consistently support the antioxidant prowess of NS and its constituents, emphasizing their potential therapeutic benefits.(66)(68) Numerous experimental studies have investigated the effects of *Nigella sativa* oil, powder, or its primary active component, thymoquinone (TQ), in animal disease models. Findings consistently demonstrate that both *Nigella sativa* oil and TQ enhance antioxidant enzyme activity while reducing inflammatory and oxidative stress factors. These effects are attributed to the inhibition of lipoxygenase and cyclooxygenase pathways in arachidonate metabolism, which is crucial for the generation of inflammatory mediators. The pro-oxidant or antioxidant nature of TQ is context-dependent, influenced by its reduction to semiquinone or thymohydroquinone. Thymohydroquinone exhibits antioxidant properties, while semiquinone can act as a pro-oxidant, generating reactive oxygen species (ROS). Notably, TQ effectively suppresses elevated lipid peroxidation levels, as evidenced by reduced malondialdehyde (MDA) levels, highlighting its robust antioxidant potential. The authors also report TQ's ability to scavenge free radicals by inhibiting nitric oxide (NO) production through the suppression of inducible nitric oxide synthase (iNOS).(61)





NEUROPROTECTIVE EFFECTS

Studies on Neurological Disorders

Neurological disorders, such as Alzheimer's Disease (AD), Parkinson's Disease (PD), Anxiety, Depression, Encephalomyelitis, Epilepsy, Ischemia, and Traumatic Brain Injury (TBI), impose significant health burdens. Thymoquinone (TQ), a prominent compound found in *Nigella sativa*, exhibits therapeutic potential in mitigating these disorders through its anti-inflammatory and antioxidant properties. In Alzheimer's Disease, the accumulation of beta-amyloid ($A\beta$) leads to neuronal damage and cognitive decline. TQ counteracts AD progression by suppressing proinflammatory molecules (ROS, TNF, IL-1b, IL-6), reducing hippocampal inflammation, and protecting against $A\beta$ -induced neurotoxicity. TQ's antioxidant impact is evident in the inhibition of ROS formation, preventing oxidative stress-related damage and improving synaptic vesicle recycling. In vivo studies corroborate TQ's neuroprotective role, decreasing hippocampal neuron loss and attenuating oxidative stress. Parkinson's Disease, characterized by dopaminergic system degeneration, involves oxidative stress and inflammation. TQ's antioxidant prowess inhibits free radical formation, protecting against oxidative damage and preserving mitochondrial function. TQ shields mesencephalic dopaminergic neurons, reducing lactate dehydrogenase release and maintaining mitochondrial membrane potential. Additionally, TQ safeguards against α -SN-oligomers-induced synaptic toxicity, lowers astrocyte stimulation, and alleviates catalepsy induced by oxidative stress. (69) Anxiety disorders, driven by GABAergic pathways and nitric oxide-cyclic guanosine monophosphate (NO-cGMP), find relief with TQ. TQ demonstrates anxiolytic effects by increasing GABA levels in unstressed conditions and elevating GABA content while reducing plasma nitrite in stressed conditions. These effects suggest TQ's role in modulating neurotransmitters associated with anxiety. Major depressive disorder involves inflammatory parameters, and TQ displays neuroprotective effects against lipopolysaccharide (LPS)-induced depression-like behaviour, attenuating IL-6, TNF- α , and CRP levels. Encephalomyelitis, a model for multiple sclerosis, is characterized by oxidative stress.

TQ improves EAE symptoms by ameliorating oxidative stress, reducing tail weakness, paralysis, and inflammation, and increasing spinal cord glutathione levels. In epilepsy, TQ protects against glutamate-induced cellular toxicity by reducing ROS production, inhibiting apoptosis, and modulating GABA receptors. TQ's anticonvulsant activity involves opioid kappa receptors, highlighting its multifaceted impact on epileptic pathogenesis. Ischemia-induced brain damage involves oxidative stress and inflammatory responses. TQ's neuroprotective effects encompass reduced MDA levels, inhibited neuronal cell death, and modulation of iNOS-induced NO production, mitigating the peroxynitrite radical's harmful effects. TQ activates nuclear erythroid 2-related proteins and heme-oxygenase-1, pivotal in preventing cell death, inflammation, apoptosis, and autophagy after ischemia. Traumatic Brain Injury induces complex damage, including oxidative stress and inflammation. TQ ameliorates neural cell damage post-TBI by decreasing MDA levels, exhibiting neuroprotective effects in mitochondrial membranes and neuronal nuclei. (70) In conclusion, TQ from *Nigella sativa* emerges as a promising therapeutic agent for various neurological disorders due to its versatile mechanisms. It counteracts neuroinflammation, reduces oxidative stress, and exhibits neuroprotective effects in diverse neurological conditions. Experimental evidence from in vitro and in vivo studies underscores TQ's potential in ameliorating Alzheimer's, Parkinson's, anxiety, depression, encephalomyelitis, epilepsy, ischemia, and traumatic brain injury, offering hope for innovative therapeutic interventions in neurological health.

Role of Thymoquinone (TQ)

Thymoquinone (TQ), the principal active component in *Nigella sativa* seeds, possesses unique attributes with a molecular weight of 164.204 g/mol, and its lipophilic nature allows efficient penetration through the blood-brain barrier. Functioning as a potent antioxidant, TQ acts as a free radical scavenger, normalizing nitric oxide (NO) levels, enhancing antioxidant enzyme activities, and decreasing MDA levels, particularly benefiting brain regions responsible for memory. (71) Furthermore, TQ exhibits robust anti-inflammatory effects by downregulating key mediators and pathways, contributing to overall neuroprotection. It modulates immune responses, enhances T-cell-mediated immunity, and suppresses B-cell-mediated immune responses. TQ also demonstrates anticonvulsant effects, primarily through interaction with gamma-aminobutyric acid (GABA) receptors, presenting itself as a potential adjuvant therapy alongside conventional anticonvulsant drugs. Additionally, TQ showcases anti-apoptotic



**Deepak Solanki et al.,**

activity, suggesting a role in preventing or reducing programmed cell death associated with neurodegenerative conditions. It serves as a protective shield against neurotoxic substances, preserving mitochondrial function and reversing neurotoxic effects caused by various agents. Influencing neurotransmitter levels and activity, TQ is crucial for maintaining healthy brain function. Moreover, TQ exhibits antidepressant effects by influencing plasma and brain tryptophan concentrations and modulating cytokine production, with limited data suggesting anxiolytic effects. Studies also hint at TQ's cognitive-enhancing effects, showcasing its potential as a natural intervention for memory disorders. TQ emerges as a multifaceted compound with significant therapeutic potential in neurological health, holding promise for diverse neurological conditions and warranting further research.(61)(72)(73)

MOLECULAR PATHOGENESIS OF DEPRESSION

Gamma-aminobutyric acid (GABA) serves as the principal inhibitory neurotransmitter, contrasting with the role of excitatory neurotransmitters. Although inhibitory neurotransmission is crucial for proper brain functioning, the population of GABA neurons is relatively small in comparison to glutamate neurons. Despite this disparity, GABA neurons are extensively distributed throughout the brain and fulfil significant functions in numerous processes, including the regulation of motivation, anxiety, and the reward system. Consequently, they constitute an indispensable element in the endeavour to alleviate symptoms associated with major depressive disorder. (74) Numerous investigations have demonstrated a correlation between dysfunctions in the GABA neurotransmission system and Major Depressive Disorder (MDD). A comprehensive meta-analysis of magnetic resonance spectroscopy studies revealed that individuals afflicted with MDD exhibit diminished levels of GABA within their brain regions compared to baseline healthy controls.(28)(75) Conversely, there was no variance between patients with depression that had gone into remission and healthy controls.(76) Researchers led by Mann and his colleagues found that patients suffering from major depressive disorder had lower amounts of the neurotransmitter GABA in their cerebrospinal fluid (CSF) than healthy controls did.(77,78)The prefrontal cortices (PFCs) of depressed persons have been found in many autopsies to possess unusually low quantities of GABA synthase & glutamic acid decarboxylase. The GABA_A receptor mediators $\alpha 2/\alpha 3$ are responsible for the antidepressant effect that is produced by the activation of the GABA system. This lends credence to the idea that a disruption in the delicate balance maintained by the GABA and glutamate systems lies at the heart of the depressive condition. It has been proven that depressive-like behaviour may be induced in a mouse model that lacks the GABA_A receptor by changing the quantities of potential GABA candidates in the brain.(79)(80)

NIGELLA SATIVA, THYMOQUINONE AND DEPRESSION

Recent reports indicate that depression does not involve only inappropriate endocrine functions of monoamines. Several monoamine neurotransmitters, especially dopamine, serotonin, and norepinephrine, are important in regulating the HPA axis. Various hormonal abnormalities such as cortisol, growth hormone (GH), or changes in thyroid hormone levels indicate endocrine dysfunction, particularly of the hypothalamic-pituitary-adrenal (HPA) axis. Experimental studies have examined different types of stress and their effects on the HPA axis in different situations. (31)Experimental studies in rats have shown that although there are different types of stressors, often distinguished between 'social stress' and 'physical stress', both types unbalance the central dopaminergic ligand, but impair the HPA axis. but through different pathways such as Increased cyclin kinase from the hypothalamus, ACTH from the pituitary, and glucocorticoids the from adrenal cortex. A focus on disrupted neural plasticity is likely owing to a lack of neurotrophic factors, excess glucocorticoids and glutamate, activation of microglial cells, and increased production of pro-inflammatory cytokines.(51) Diabetes and insulin resistance are linked to changes in brain imaging, depression, and an increase in the prevalence of age-related cognitive decline.(81)Antidepressants are associated with symptoms such as the delayed onset of action, side effects, and drug-diet interactions.(82) Chemical and synthetic drugs used to treat depression disrupt therapeutic alliances because of their numerous side effects and high prices. As a result, there is a need to focus on these concerns and improve current treatment options.(79) Tricyclic antidepressants such as selective serotonin reuptake inhibitors (SSRIs), and selective serotonin and norepinephrine reuptake inhibitors are more effective than placebo in treating severe depressive disorder, according to evidence from several randomised controlled studies. However, it should be remembered that the pharmaceutical sector funds the majority of studies. It is also well-documented evidence that serotonergic-norepinephrinergic



**Deepak Solanki et al.,**

mirtazapine is effective. It is at least as successful as other tricyclic antidepressants or SSRIs, even though it is not very effective.(83)For patients with severe or long-term depression, a multifaceted tiered care model of treatment with amitriptyline, imipramine, or fluoxetine, along with integrated pharmacotherapy programs, has been demonstrated to be effective in treating depression as a standalone therapy. In general, there is strong evidence that SSRIs are better tolerated than tricyclic antidepressants, making them the preferred first-line drugs for depression.Hence, interventions that only employ monoamine reuptake inhibitors may not be sufficient in completely reversing the behavioural and biochemical changes observed in individuals suffering from depression.(84) Behaviour encompasses a range of actions that can be influenced by various factors, such as infections, disruptions in the immune system, and an excess of pro-inflammatory cytokines. There are notable similarities between the symptoms associated with depression and the behaviours associated with illness. Common symptoms of depression include anorexia, loss of appetite, insomnia, fatigue, malaise, anxiety, and cognitive impairments. Depression is generally characterized by a combination of these symptoms.(67) In animal studies, researchers have assessed detrimental behaviours through different behavioural measures, including open field, raised plus maze, and forced swimming tests, among others. By administering ethanolic extract of *Nigella Sativa* at doses of 100, 200, and 400 mg/kg, researchers observed significant anti-anxiety and antidepressant effects in these tests.

Bacterial toxins have the potential to impact immune system functioning and result in behavioural manifestations of nervousness or depression. Lipopolysaccharide (LPS), a highly toxic endotoxin produced by bacteria, stimulates excessive production of inflammatory cytokines in the body, thereby eliciting sickness symptoms. It is believed that the plant's anti-inflammatory and antioxidant properties are responsible for the ability of NS's hydro-alcoholic extract to mitigate LPS-induced sickness behaviours in rats. The extract was administered at doses of 100, 200, and 400 mg/kg.Emerging research findings suggest that toxic heavy metals might contribute to the onset of depression symptoms. Mercury, in particular, exerts detrimental effects primarily on the digestive tract, kidneys, and heart. Given that mercuric chloride induced feelings of anxiety and depression in Wistar rats, the researchers aimed to investigate whether NS oil at a dosage of 2 ml/kg/day could alleviate these side effects. Rats in the study were subjected to mercuric chloride administration for a duration of three weeks, which led to the induction of anxiety and depression-like behaviours (74,75).The detrimental effects of mercuric chloride on the behavioural functions of rats were reversed after rats were given a treatment consisting of 2 mL of NS oil per kilogram of body weight for a period of four weeks. This was demonstrated by an increase in the number of line crossings, open arm time, and swimming time during the forced swimming test. It's possible that the antioxidant qualities of NS oil are what led to the improvement in the individuals' behavioural performance. Thymoquinone (TQ), derived from NS, is renowned for its noteworthy anti-inflammatory and antioxidant properties. TQ not only exhibits potent antioxidant activity but also possesses attributes that effectively combat infections, toxicity, diabetes, hypertension, and safeguard the liver.

However, the limited solubility and bioavailability of TQ have hindered its widespread utilization in research. To address this issue, TQ solid lipid nanoparticles, abbreviated as TQSLN, are currently being developed and employed. The production of the monoamine neurotransmitter serotonin (5-HT), which possesses antidepressant properties, occurs in the brain through the conversion of the amino acid tryptophan via a process called tryptophan conversion (TRP). Another potential pathway for the degradation of TRP is the kynurenine (KYN) pathway. In the presence of inflammatory mediators such as interferon gamma, the first enzyme in this pathway, indoleamine-2,3-dioxygenase (IDO), becomes activated. This activation represents the initial step in the indoleamine pathway (IFN-). Consequently, increased IDO activity is associated with lower 5-HT concentrations and higher KYN concentrations. Recent studies have also established a link between the KYN pathway and depression. In a study conducted by Alam et al., the antidepressant effects of orally administered TQSLN at a dosage of 20 milligrams per kilogram were investigated using a rat model subjected to prolonged forced-swim stress. The results of this study revealed that the antidepressant effects of TQSLN were accompanied by altered levels of brain-derived neurotrophic factor (BDNF), as well as decreased levels of tumour necrosis factor-alpha and interleukin-6 in the hippocampus tissue of the rats. Furthermore, TQSLN treatment successfully reduced IDO activity in stressed rats. It was observed that an increased 5-HT to TRP ratio in the hippocampus corresponded to lower IDO activity. Additionally, separate research demonstrated that TQSLN had a calming effect on rats exposed to lipopolysaccharide (LPS), as evidenced by a



**Deepak Solanki et al.,**

significant decrease in immobility time. The rats treated with TQSLN exhibited decreased immobility time and increased swimming and climbing times, indicative of improved performance in the forced swimming test. TQSLN treatment resulted in elevated levels of BDNF and the 5-HT to TRP ratio in the hippocampus, along with a decrease in the KYN to TRP ratio and the expression of TNF- α , IL-6, and NF- κ B. These alterations, coupled with the enhanced behavioural performance of TQSLN-treated rats, collectively highlight the positive effects of TQSLN administration. (85) Reserpine is one of the antihypertensive drugs that has been linked to an increased risk of developing depression in patients. Samad et al. showed in a second study that administering TQ to rats at dosages of 10 and 20 mg/kg reduced the inflammation and oxidative damage in the rats' hippocampi, which in turn eased the anxiety and depression that had been produced by reserpine. Diabetes mellitus, which is a metabolic disease, represents a significant danger to the health of a sizeable portion of the world's population. Depression in diabetics is a common complication of the disease diabetes mellitus. TQ (10 and 20 mg/kg) was able to reduce depression in type 2 diabetic rats. This was accomplished by reducing the levels of IL-1 and TNF- α as well as oxidative stress. (70,78) Concanavalin A (Con A), a plant mitogen that is a member of the legume lectin family, is known to trigger a powerful immune activation [77]. When rats were given this poison, it was discovered that they developed signs of disease as a result of being exposed to it. According to the findings of study conducted by Nazir and colleagues, the anti-inflammatory activity of TQ may protect mice from the anxiety and depression caused by a dosage of Con A equal to 10 mg/kg.

Anxiolytic effects of TQ (2.5 and 5 mg/kg/day) were also investigated in the setting of arsenic poisoning-induced damage to the hippocampus in rats. The fact that pre-treatment with 5 mg/kg of TQ improved behavioural performance in behaviour tests, increased glutathione & SOD activity, and reduced levels of lipid peroxidation (LPO), tumour necrosis factor alpha (TNF- α), and interferon (IFN- α) in rat hippocampal tissue, as described by Firdaus et al., demonstrates the antidepressant effects of both NS and TQ. NS seeds have been used traditionally for medical purposes for a very long time, namely for the purpose of promoting a sense of well-being, increasing one's level of energy, and assisting in recovery from feelings of despair and fatigue. Both the forced swimming test as well as the open field test have been employed in recent research to investigate how the effects of thymoquinone and the hydro-alcoholic extract of NS on depression-like behaviour brought on by lipopolysaccharide in rats. All groups were subjected to the forced swimming test, including the saline-only controls, the lipopolysaccharide 100 g/kg intraperitoneal two-hours-prior-to-test active controls, and the treatment groups (which received varying doses of NS extract or thymoquinone before lipopolysaccharide).

Following each session, the time spent sitting still was recorded. In each of the three trials, the lipopolysaccharide group had a longer period of immobility compared to the control group that only received saline. However, the amount of time spent immobile was shorter in the groups that were pre-treated with thymoquinone and NS extract rather than in the active control group. The number of peripheral crossings in the open-field test was lower in the animal's pre-treatment with thymoquinone or NS extract, however greater in the animals serving as active controls. The number of peripheral crossings was higher in the active controls than in the passive controls. In addition, the number of central crossings in the lipopolysaccharide group was lower than in the saline control group, whereas the number of central crossings in the NS extract and thymoquinone treatment animals was more than in the active control group. This finding was uncovered by comparing the lipopolysaccharide group to the saline controls. (8) According to the results, the hydroalcoholic extract of *N. Sativa* & its active component, thymoquinone, may protect rats against depression-like behaviours brought on by lipopolysaccharide. In light of the encouraging findings from animal research demonstrating the antidepressant and anxiety-relieving benefits of NS seed, a randomized, placebo-controlled clinical study of NS seed was carried out on young, healthy teenage human volunteers at a boarding school. (7,9,77) Anxiety and depression levels were evaluated at the beginning of the study as well as after the participants had taken 500 mg once daily of either a placebo (Group A) or NS seed (Group B) for four weeks (Group B). Although there was no statistically significant difference in the results for measuring mood and anxiety between groups A & B, Variation within Group B was Statistically Significant, but there was none within group A. This was due to the fact that group B included more participants. According to the authors of the study, taking a supplement containing NS seed helped enhance both the participants' mood and their level of anxiety. (86)





CONCLUSION

In the realm of combating and treating depression, no medication has thus far emerged as unequivocally superior to others. To address this gap, several neuroprotective compounds, including nutraceuticals, have undergone investigation to explore their potential advantages. Based on the evidence presented in this context, it is plausible that NS/TQ could be beneficial in impeding the onset and progression of depression. Further preclinical research and the translation of these findings into clinical practice necessitate extensive long-term studies involving a substantial population of individuals undergoing treatment for depression. This course of action is warranted due to the compounds' safety profiles and the promising results obtained from preclinical investigations conducted in vitro and in vivo. In particular, a comprehensive study is needed to ascertain the full extent of NS's effectiveness. However, no research has been conducted to compare NS with its individual compounds, despite TQ exhibiting superior neuroprotective effects. Considering the current contradictory nature of studies on brain bioavailability and passage through the blood-brain barrier, it is crucial to elucidate the pharmacokinetics of these drugs. Furthermore, it is imperative to undertake a significant amount of additional preclinical research to identify potential interactions between NS/TQ and other medications, elucidate the effects over an extended period, and ultimately verify and evaluate the efficacy of NS/TQ across different stages of AD.

REFERENCES

1. Depressive disorder (depression) [Internet]. [cited 2024 Jan 17]. Available from: <https://www.who.int/news-room/fact-sheets/detail/depression>
2. What Is Depression? [Internet]. [cited 2024 Jan 17]. Available from: <https://www.psychiatry.org/443/patients-families/depression/what-is-depression>
3. Mehdi S, Manohar K, Shariff A, Kinattingal N, Wani SUD, Alshehri S, et al. Omega-3 Fatty Acids Supplementation in the Treatment of Depression: An Observational Study. *Journal of Personalized Medicine*. 2023 Feb;13(2):224.
4. Depression (major depressive disorder) - Symptoms and causes - Mayo Clinic [Internet]. [cited 2023 Jan 12]. Available from: <https://www.mayoclinic.org/diseases-conditions/depression/symptoms-causes/syc-20356007>
5. Insel TR. Assessing the economic costs of serious mental illness. *Am J Psychiatry*. 2008 Jun;165(6):663–5.
6. Moitra M, Santomauro D, Collins PY, Vos T, Whiteford H, Saxena S, et al. The global gap in treatment coverage for major depressive disorder in 84 countries from 2000–2019: A systematic review and Bayesian meta-regression analysis. *PLOS Medicine*. 2022 Feb 15;19(2):e1003901.
7. Major Depression - National Institute of Mental Health (NIMH) [Internet]. [cited 2024 Jan 17]. Available from: <https://www.nimh.nih.gov/health/statistics/major-depression>
8. Basavaraju SM, Mudhol S, Peddha MS, Ud Din Wani S, Krishna KL, Mehdi S, et al. Nanoemulsion-based piperine to enhance bioavailability for the treatment of LPS-induced depression-like behaviour in mice. *Neuroscience Letters*. 2023 Sep 25;814:137441.
9. Karrouri R, Hammani Z, Benjelloun R, Otheman Y. Major depressive disorder: Validated treatments and future challenges. *World J Clin Cases*. 2021 Nov 6;9(31):9350–67.
10. Leong XF, Rais Mustafa M, Jaarin K. Nigella sativa and Its Protective Role in Oxidative Stress and Hypertension. *Evid Based Complement Alternat Med*. 2013;2013:120732.
11. Hannan MA, Rahman MA, Sohag AAM, Uddin MJ, Dash R, Sikder MH, et al. Black Cumin (*Nigella sativa* L.): A Comprehensive Review on Phytochemistry, Health Benefits, Molecular Pharmacology, and Safety. *Nutrients*. 2021 May 24;13(6):1784.
12. Salem A, Bamosa A, Alam M, Alshuraim S, Alyalak H, Alagga A, et al. Effect of Nigella sativa on general health and immune system in young healthy volunteers: a randomized, placebo-controlled, double-blinded clinical trial. *F1000Research* [Internet]. 2021 [cited 2024 Jan 17];10. Available from: <https://www.ncbi.nlm.nih.gov/pmc/articles/PMC10600512/>





Deepak Solanki et al.,

13. (PDF) An updated knowledge of Black seed (*Nigella sativa* Linn): Review of phytochemical constituents and pharmacological properties [Internet]. [cited 2024 Jan 17]. Available from: https://www.researchgate.net/publication/344464257_An_updated_knowledge_of_Black_seed_Nigella_sativa_Linn_Review_of_phytochemical_constituents_and_pharmacological_properties
14. (PDF) *Nigella sativa*: Phytochemistry, Pharmacology and its Therapeutic Potential [Internet]. [cited 2024 Jan 17]. Available from: https://www.researchgate.net/publication/334681183_Nigella_sativa_Phytochemistry_Pharmacology_and_its_Therapeutic_Potential
15. Ur Rehman M. *Nigella sativa*: Monograph. journal of pharmacognosy and phytochemistry. 2015 Oct 22;4:103–6.
16. Malik P, Akhtar J, Kumar P, Ali A. Traditional and modern usage of *Nigella sativa* L. (Black cumin). *Annals of Phytomedicine: An International Journal*. 2022 Dec 30;11:255–65.
17. Salehi B, Quispe C, Imran M, Ul-Haq I, Živković J, Abu-Reidah IM, et al. *Nigella* Plants - Traditional Uses, Bioactive Phytoconstituents, Preclinical and Clinical Studies. *Front Pharmacol*. 2021;12:625386.
18. Tiwari P, Jena S, Satpathy S, Sahu P. *Nigella sativa*: Phytochemistry, Pharmacology and its Therapeutic Potential. *Research Journal of Pharmacy and Technology*. 2019 Jul 25;12:3111–6.
19. Black cumin | Description, Plant, Seeds, Spice, Medicine, Uses, & Facts | Britannica [Internet]. 2023 [cited 2024 Jan 18]. Available from: <https://www.britannica.com/plant/black-cumin>
20. Morphological features of *Nigella sativa*, vegetative and reproductive | Download Scientific Diagram [Internet]. [cited 2023 Jan 12]. Available from: https://www.researchgate.net/figure/Morphological-features-of-Nigella-sativa-vegetative-and-reproductive_fig1_307877302 - Yahoo India Search Results [Internet]. [cited 2024 Jan 18].
21. El-Morsy MH, Osman HES. Morphological Characters of *Nigella sativa*. In: Fawzy Ramadan M, editor. *Black cumin (Nigella sativa) seeds: Chemistry, Technology, Functionality, and Applications* [Internet]. Cham: Springer International Publishing; 2021 [cited 2024 Jan 18]. p. 23–9. (Food Bioactive Ingredients). Available from: http://link.springer.com/10.1007/978-3-030-48798-0_3
22. Akram Khan M, Afzal M. Chemical composition of *Nigella sativa* Linn: Part 2 Recent advances. *Inflammopharmacology*. 2016 Jun;24(2–3):67–79.
23. Cheikh-Rouhou S, Besbes S, Hentati B, Blecker C, Deroanne C, Attia H. *Nigella sativa* L.: Chemical composition and physicochemical characteristics of lipid fraction. *Food Chemistry*. 2007 Jan 1;101(2):673–81.
24. Beheshti F, Norouzi F, Abareschi A, Anaeigoudari A, Hosseini M. Acute Administration of *Nigella sativa* Showed Anxiolytic and Anti- Depression Effects in Rats. *CNF*. 2019 Jan 16;14(5):422–31.
25. Kazemi M. Phytochemical Composition, Antioxidant, Anti-inflammatory and Antimicrobial Activity of *Nigella sativa* L. Essential Oil. *Journal of Essential Oil Bearing Plants*. 2014 Sep 3;17(5):1002–11.
26. Sahyadri M, Nadiga APR, Mehdi S, Mruthunjaya K, Nayak PG, Parihar VK, et al. Mitochondria–lysosome crosstalk in GBA1-associated Parkinson’s disease. *3 Biotech*. 2022 Sep;12(9):230.
27. Balakrishnan R, Azam S, Cho DY, Su-Kim I, Choi DK. Natural Phytochemicals as Novel Therapeutic Strategies to Prevent and Treat Parkinson’s Disease: Current Knowledge and Future Perspectives. *Oxid Med Cell Longev*. 2021;2021:6680935.
28. Beheshti F, Khazaei M, Hosseini M. Neuropharmacological effects of *Nigella sativa*. *Avicenna J Phytomed*. 2016;6(1):104–16.
29. DeMaagd G, Philip A. Parkinson’s Disease and Its Management: Part 1: Disease Entity, Risk Factors, Pathophysiology, Clinical Presentation, and Diagnosis. *P T*. 2015 Aug;40(8):504–32.
30. Cleveland Clinic [Internet]. [cited 2024 Jan 18]. Parkinson’s Disease: What It Is, Causes, Symptoms & Treatment. Available from: <https://my.clevelandclinic.org/health/diseases/8525-parkinsons-disease-overview>
31. Mohtashami R, Fallah Huseini H, Heydari M, Amini M, Sadeqhi Z, Ghaznavi H, et al. Efficacy and safety of honey based formulation of *Nigella sativa* seed oil in functional dyspepsia: A double blind randomized controlled clinical trial. *Journal of Ethnopharmacology*. 2015 Dec;175:147–52.



**Deepak Solanki et al.,**

32. Kooti W, Hasanzadeh-Noohi Z, Sharafi-Ahvazi N, Asadi-Samani M, Ashtary-Larky D. Phytochemistry, pharmacology, and therapeutic uses of black seed (*Nigella sativa*). *Chin J Nat Med*. 2016 Oct;14(10):732–45.
33. Khazdair MR. The Protective Effects of *Nigella sativa* and Its Constituents on Induced Neurotoxicity. *J Toxicol*. 2015;2015:841823.
34. Rabiei Z, Solati K, Amini-Khoei H. Phytotherapy in treatment of Parkinson's disease: a review. *Pharm Biol*. 2019 Dec;57(1):355–62.
35. (PDF) Thymoquinone in autoimmune diseases: Therapeutic potential and molecular mechanisms [Internet]. [cited 2024 Jan 18]. Available from: https://www.researchgate.net/publication/347906988_Thymoquinone_in_autoimmune_diseases_Therapeutic_potential_and_molecular_mechanisms
36. Singh SK, Srivastav S, Yadav AK, Srikrishna S, Perry G. Overview of Alzheimer's Disease and Some Therapeutic Approaches Targeting A β by Using Several Synthetic and Herbal Compounds. *Oxid Med Cell Longev*. 2016;2016:7361613.
37. Rathmann KL, Conner CS. Alzheimer's disease: clinical features, pathogenesis, and treatment. *Drug Intell Clin Pharm*. 1984 Sep;18(9):684–91.
38. Murphy MP, LeVine H. Alzheimer's disease and the amyloid-beta peptide. *J Alzheimers Dis*. 2010;19(1):311–23.
39. Yiannopoulou KG, Papageorgiou SG. Current and Future Treatments in Alzheimer Disease: An Update. *J Cent Nerv Syst Dis*. 2020;12:1179573520907397.
40. Breijyeh Z, Karaman R. Comprehensive Review on Alzheimer's Disease: Causes and Treatment. *Molecules*. 2020 Dec 8;25(24):5789.
41. Nadiga Et Al A. Zebrafish (*Danio rerio*): An Alternative Model Organism for Central Nervous System Disorders Screening. *Egyptian Journal of Aquatic Biology and Fisheries*. 2022;26(4):1355–79.
42. Ramesh M, Govindaraju T. Multipronged diagnostic and therapeutic strategies for Alzheimer's disease. *Chem Sci*. 2022 Nov 30;13(46):13657–89.
43. Kumar A, Sidhu J, Goyal A, Tsao JW. Alzheimer Disease. In: StatPearls [Internet]. Treasure Island (FL): StatPearls Publishing; 2023 [cited 2024 Jan 18]. Available from: <http://www.ncbi.nlm.nih.gov/books/NBK499922/>
44. Reich DS, Lucchinetti CF, Calabresi PA. Multiple Sclerosis. *N Engl J Med*. 2018 Jan 11;378(2):169–80.
45. Häusler D, Weber MS. Vitamin D Supplementation in Central Nervous System Demyelinating Disease—Enough Is Enough. *Int J Mol Sci*. 2019 Jan 8;20(1):218.
46. Kuhlmann T, Antel J. Multiple sclerosis: 2023 update. *Free Neuropathol*. 2023 Jan;4:4–3.
47. Compston A, Coles A. Multiple sclerosis. *The Lancet*. 2008 Oct 25;372(9648):1502–17.
48. Immune-Mediated Disease and MS | National MS Society [Internet]. [cited 2024 Jan 18]. Available from: <https://www.nationalmssociety.org/What-is-MS/Definition-of-MS/Immune-mediated-disease>
49. Future I of M (US) C on MSCS and S for the, Joy JE, Richard B. Johnston J. Clinical and Biological Features. In: Multiple Sclerosis: Current Status and Strategies for the Future [Internet]. National Academies Press (US); 2001 [cited 2024 Jan 18]. Available from: <https://www.ncbi.nlm.nih.gov/books/NBK222386/>
50. Pirko I, Noseworthy JH. Demyelinating Disorders of the Central Nervous System. *Textbook of Clinical Neurology*. 2007;1103–33.
51. Rae-Grant A, Day GS, Marrie RA, Rabinstein A, Cree BAC, Gronseth GS, et al. Practice guideline recommendations summary: Disease-modifying therapies for adults with multiple sclerosis: Report of the Guideline Development, Dissemination, and Implementation Subcommittee of the American Academy of Neurology. *Neurology*. 2018 Apr 24;90(17):777–88.
52. Hosseinzadeh H, Parvardeh S. Anticonvulsant effects of thymoquinone, the major constituent of *Nigella sativa* seeds, in mice. *Phytomedicine*. 2004 Jan;11(1):56–64.
53. Tiruppur Venkatachallam SK, Pattekhani H, Divakar S, Kadimi US. Chemical composition of *Nigella sativa* L. seed extracts obtained by supercritical carbon dioxide. *J Food Sci Technol*. 2010 Dec;47(6):598–605.
54. Ezz HSA, Khadrawy YA, Noor NA. The neuroprotective effect of curcumin and *Nigella sativa* oil against oxidative stress in the pilocarpine model of epilepsy: a comparison with valproate. *Neurochem Res*. 2011 Nov;36(11):2195–204.





Deepak Solanki et al.,

55. Aqueous extract of Piper betle L. leaf and Areca catechu L. nut protects against pentylentetrazole-induced seizures and positively modulates cognitive function in adult Zebrafish | Advances in Traditional Medicine [Internet]. [cited 2024 Jan 19]. Available from: <https://link.springer.com/article/10.1007/s13596-022-00664-0>
56. Seghatoleslam M, Alipour F, Shafieian R, Hassanzadeh Z, Edalatmanesh M, Sadeghnia HR, et al. The effects of *Nigella sativa* on neural damage after pentylentetrazole induced seizures in rats. Journal of Traditional and Complementary Medicine. 2015 Aug 1:6.
57. Tavakoli-Rouzbehani OM, Abbasnezhad M, Kheirouri S, Alizadeh M. Efficacy of *nigella sativa* oil on endothelial function and atherogenic indices in patients with coronary artery diseases: A randomized, double-blind, placebo-control clinical trial. Phytother Res. 2022 Dec;36(12):4516–26.
58. Pahwa R, Goyal A, Jialal I. Chronic Inflammation. In: StatPearls [Internet]. Treasure Island (FL): StatPearls Publishing; 2023 [cited 2024 Jan 18]. Available from: <http://www.ncbi.nlm.nih.gov/books/NBK493173/>
59. Bensiamour-Touati K, Kacimi G, Haffaf EM, Berdja S, Aouichat-Bouguerra S. In Vivo Subacute Toxicity and Antidiabetic Effect of Aqueous Extract of *Nigella sativa*. Evidence-Based Complementary and Alternative Medicine. 2017;2017:1–13.
60. Amyotrophic lateral sclerosis: a clinical review - PMC [Internet]. [cited 2024 Jan 18]. Available from: <https://www.ncbi.nlm.nih.gov/pmc/articles/PMC7540334/>
61. M M, A F, Sn F, N HE, M K. Effect of *Nigella sativa* L. supplementation on inflammatory and oxidative stress indicators: A systematic review and meta-analysis of controlled clinical trials. Complementary therapies in medicine [Internet]. 2020 Nov [cited 2024 Jan 18];54. Available from: <https://pubmed.ncbi.nlm.nih.gov/33183658/>
62. Gueffai A, Gonzalez-Serrano DJ, Christodoulou MC, Orellana-Palacios JC, Ortega MLS, Ouldoumna A, et al. Phenolics from Defatted Black Cumin Seeds (*Nigella sativa* L.): Ultrasound-Assisted Extraction Optimization, Comparison, and Antioxidant Activity. Biomolecules. 2022 Sep 16;12(9):1311.
63. Effects of *Nigella sativa* on apoptosis and GABA A receptor density in cerebral cortical and hippocampal neurons in pentylentetrazol induced kindling in rats | Request PDF [Internet]. [cited 2024 Jan 18]. Available from: https://www.researchgate.net/publication/310475030_Effects_of_Nigella_sativa_on_apoptosis_and_GABA_A_receptor_density_in_cerebral_cortical_and_hippocampal_neurons_in_pentylentetrazol_induced_kindling_in_rats
64. Tavakkoli A, Hosseinzadeh H. Chapter 21 - *Nigella sativa* L. and thymoquinone as neuroprotective antioxidants. In: Martin CR, Preedy VR, editors. Oxidative Stress and Dietary Antioxidants in Neurological Diseases [Internet]. Academic Press; 2020 [cited 2024 Jan 18]. p. 325–41. Available from: <https://www.sciencedirect.com/science/article/pii/B9780128177808000219>
65. Ardiana M, Pikir BS, Santoso A, Hermawan HO, Al-Farabi MJ. Effect of *Nigella sativa* Supplementation on Oxidative Stress and Antioxidant Parameters: A Meta-Analysis of Randomized Controlled Trials. The Scientific World Journal. 2020 May 6;2020:e2390706.
66. Phytochemical Profile and Antioxidant Activity of *Nigella sativa* L Growing in Morocco [Internet]. [cited 2024 Jan 18]. Available from: <https://www.hindawi.com/journals/tswj/2021/6623609/>
67. Healthcare | Free Full-Text | Analysis of Antidepressants Utilization for Patients Visiting Psychiatric Out-Patient Clinic in a Tertiary Care Hospital [Internet]. [cited 2024 Jan 19]. Available from: <https://www.mdpi.com/2227-9032/10/10/2081>
68. Burits M, Bucar F. Antioxidant activity of *Nigella sativa* essential oil. Phytother Res. 2000 Aug;14(5):323–8.
69. A Review on Possible Therapeutic Effect of *Nigella sativa* and Thymoquinone in Neurodegenerative Diseases - PubMed [Internet]. [cited 2024 Jan 18]. Available from: <https://pubmed.ncbi.nlm.nih.gov/29962349/>
70. Pottoo FH, Ibrahim AM, Alammari A, Alsinan R, Aleid M, Alshehhi A, et al. Thymoquinone: Review of Its Potential in the Treatment of Neurological Diseases. Pharmaceuticals (Basel). 2022 Mar 27;15(4):408.
71. Patel RR Victor Preedy, Vinood, editor. Ancient and Traditional Foods, Plants, Herbs and Spices used in Cardiovascular Health and Disease. Boca Raton: CRC Press; 2023. 396 p.
72. Pharmaceuticals | Free Full-Text | Thymoquinone: Review of Its Potential in the Treatment of Neurological Diseases [Internet]. [cited 2024 Jan 18]. Available from: <https://www.mdpi.com/1424-8247/15/4/408>



**Deepak Solanki et al.,**

73. Javidi S, Razavi BM, Hosseinzadeh H. A review of Neuropharmacology Effects of *Nigella sativa* and Its Main Component, Thymoquinone. *Phytother Res*. 2016 Aug;30(8):1219–29.
74. Raza M, Alghasham AA, Alorainy MS, El-Hadiyah TM. Potentiation of Valproate-induced Anticonvulsant Response by *Nigella sativa* Seed Constituents: The Role of GABA Receptors. *Int J Health Sci (Qassim)*. 2008 Jan;2(1):15–25.
75. Seeds of *N. sativa* (A). Chemical structure of thymoquinone (B). | Download Scientific Diagram [Internet]. [cited 2024 Jan 18]. Available from: https://www.researchgate.net/figure/Seeds-of-N-sativa-A-Chemical-structure-of-thymoquinone-B_fig2_263130220
76. Kiralan M, Özkan G, Bayrak A, Ramadan MF. Physicochemical properties and stability of black cumin (*Nigella sativa*) seed oil as affected by different extraction methods. *Industrial Crops and Products*. 2014 Jun 1;57:52–8.
77. The molecular neurobiology of depression | Nature [Internet]. [cited 2024 Jan 18]. Available from: <https://www.nature.com/articles/nature07455>
78. Brigitta B. Pathophysiology of depression and mechanisms of treatment. *Dialogues Clin Neurosci*. 2002 Mar;4(1):7–20.
79. Lang UE, Borgwardt S. Molecular mechanisms of depression: perspectives on new treatment strategies. *Cell Physiol Biochem*. 2013;31(6):761–77.
80. Wu C, Sun D. GABA receptors in brain development, function, and injury. *Metab Brain Dis*. 2015 Apr;30(2):367–79.
81. *Nigella sativa* L. seeds modulate mood, anxiety and cognition in healthy adolescent males - PubMed [Internet]. [cited 2024 Jan 18]. Available from: <https://pubmed.ncbi.nlm.nih.gov/24412554/>
82. Pramod BR, Mehdi S, Undela K, Kishor M, Rao PV, Krishna KL. Lifestyle and substance use-an important cause for treatment-resistant depression and major depressive disorders. *Drug Invent Today*. 2019;11:284–90.
83. Ahmad A, Husain A, Mujeeb M, Khan SA, Najmi AK, Siddique NA, et al. A review on therapeutic potential of *Nigella sativa*: A miracle herb. *Asian Pac J Trop Biomed*. 2013 May;3(5):337–52.
84. Yimer EM, Tuem KB, Karim A, Ur-Rehman N, Anwar F. *Nigella sativa* L. (Black Cumin): A Promising Natural Remedy for Wide Range of Illnesses. *Evid Based Complement Alternat Med*. 2019;2019:1528635.
85. Tavakkoli A, Mahdian V, Razavi BM, Hosseinzadeh H. Review on Clinical Trials of Black Seed (*Nigella sativa*) and Its Active Constituent, Thymoquinone. *J Pharmacopuncture*. 2017 Sep;20(3):179–93.
86. Bin Sayeed MS, Shams T, Fahim Hossain S, Rahman MR, Mostofa A, Fahim Kadir M, et al. *Nigella sativa* L. seeds modulate mood, anxiety and cognition in healthy adolescent males. *J Ethnopharmacol*. 2014 Feb 27;152(1):156–62.





Digital Comparator using Complementary Metal Oxide Semiconductor Technology

Rajendra Prasad Madepogu^{1*}, Ravi Kishore.G² and Prakash Jogi³

¹Professor, Department of Electronics and Communication Engineering, Vidya Jyothi Institute of Technology, (Affiliated to Jawaharlal Nehru Technological University), Hyderabad, Telangana, India.

²Associate Professor, Department of Electronics and Communication Engineering, Vidya Jyothi Institute of Technology, (Affiliated to Jawaharlal Nehru Technological University), Hyderabad, Telangana, India.

³Assistant Professor, Department of Electronics and Communication Engineering, Vidya Jyothi Institute of Technology, (Affiliated to Jawaharlal Nehru Technological University), Hyderabad, Telangana, India.

Received: 22 Jan 2024

Revised: 09 Feb 2024

Accepted: 27 Apr 2024

*Address for Correspondence

Rajendra Prasad Madepogu

Professor,

Department of Electronics and Communication Engineering,

Vidya Jyothi Institute of Technology,

(Affiliated to Jawaharlal Nehru Technological University),

Hyderabad, Telangana, India.

Email: sudhay@mrec.ac.in



This is an Open Access Journal / article distributed under the terms of the **Creative Commons Attribution License** (CC BY-NC-ND 3.0) which permits unrestricted use, distribution, and reproduction in any medium, provided the original work is properly cited. All rights reserved.

ABSTRACT

A 2-bit comparator using CMOS technology is proposed in this paper. The delay and power of 2-bit comparator are examined in this research. This paper determines that CMOS technology forefronts by reducing the number of transistors which have less capacitances and increased speed when compared with other techniques. In this paper, comparison is made with the simulation results that prove that CMOS logic design is preferable with reduced delay and power. The proposed work is simulated using Synopsys tool called HSPICE, and the results are observed for different voltages. The proposed model delay and power dissipation results are minimum at 1.50 ns, maximum at 1.53 ns and minimum at 131.64 μ W, maximum at 2003.6 μ W. The transistor count in the proposed comparator is 102 and simulation is done by utilising HSPICE, which is the leading tool and the results are provided in the results section.

Keywords: Comparator, 1-bit Comparator, 2-bit Comparator, CMOS, CNTFET, GNRFT, Delay, Power Dissipation





INTRODUCTION

An electronic device known as a magnitude comparator or digital comparator [1], [2] compares two numbers as binary inputs and indicates whether the first value is larger than, less than, or equal to the second number. Comparators are mostly utilised in central processing units (CPUs) and micro-controllers (MCUs). A comparator has two inputs that are to be compared and produces the output that has three conditions based on the inputs provided to the circuit. Also, comparators have applications like sorting algorithms, biometric verifications, image, signal processing and priority encoding [3]-[5]. Comparator has two inputs of any number of bits with three outputs. Based on the inputs applied to the comparator, the outputs are obtained by comparing the values assigned to the inputs. The three possible outcomes for a comparator are greater than, equal to and less than [6]. This research paper is a basic survey on advanced system of 2 bit comparator. This paper provides information about an electronic apparatus known as comparator. A comparator has a capability of accepting two inputs, and obtaining three outputs based on the comparison between the two inputs provided. This article is presented as: literature survey in second section, logic gates and 1-bit comparator in third section, proposed design in fourth section, simulation results in section five and finally conclusion part in section six.

LITERATURE SURVEY

Digital 1-bit comparator has dual inputs A and B and each of 1-bit have three outputs and that produces outputs based on the comparison between the inputs. The functioning of comparator is realized by analysing the truth table and it is designed with 2 NOT gates, 2 AND gates, and one XNOR gate and simulated on HSPICE. 1-bit comparator is designed by using CMOS logic, as CMOS logic has better noise immunity and CMOS logic is better in terms of power and area [7]. 2-bit comparator is a block with two inputs, each of 2 bits with three outputs. Output for different combinations of inputs can be analysed [8]. 2-bit comparator is designed by using NOT, AND, XNOR and OR gates. CMOS based 2-bit comparator with two inputs; each of 2 bits is designed and simulated using CMOS technology [8]. In order to do the comparison of two 2-bit inputs, we follow a series of steps. Consider the inputs $A=A_2, A_1$ and $B=B_2, B_1$. To check if A is greater than B or vice-versa, then primarily compare MSB of both the inputs applied. If MSB of the two inputs are not same, that means if A_2 is greater than B_2 then the resultant output will be $A>B$ and $A<B$ in vice versa. If MSB of the applied two inputs are equal, then move for next successive bit, in order to compare the other bit of the two inputs. If the LSB bits are also equal, in such case the resultant output will be A equal to B [9].

LOGIC GATES AND 1-BIT COMPARATOR

CMOS INVERTER

CMOS NOT gate is having one input and single output and the input combinations are binary values 0s and 1s [10]. The output is exact complement of the input A that is $A\text{-bar}$ as shown in below figure.

CMOS AND gate

CMOS 2-input AND gate is having two inputs and single output [10]. The entire transistor count is 6 and they are 3 PMOS transistors and 3 NMOS transistors. The output for input binary values 11 is high and remaining conditions are low as shown in below table. CMOS 3-inputs AND gate is having three inputs and single output [10]. The entire transistor count is 8 and they are 4 PMOS transistors and 4 NMOS transistors. The output for input binary values 111 is high and remaining conditions are low as shown in below table.



**CMOS 3-input OR gate**

CMOS 3-inputs OR gate is having three inputs and single output [10]. The entire transistor count is 8 and they are 4 PMOS transistors and 4 NMOS transistors. The output for input values 000 is low and remaining conditions are high as shown in below table.

CMOS EX-NOR gate

CMOS 2-inputs EX-NOR gate is having two inputs and single output [10]. The entire transistor count is 14 and they are 7 PMOS transistors and 7 NMOS transistors. The output for input binary values 00 & 11 is high and remaining conditions are low as shown in below table.

CMOS 1-Bit Comparator

The 1-bit comparator is having two inputs and three outputs. The entire transistor count is 30. The output for input binary values 00 & 11 is high i.e. ($A=B$) and remaining conditions for the input binary values 01 is high i.e. ($A<B$) and input binary values for the 10 is high i.e. ($A>B$) [10] as shown in below table.

The equations for the outputs are

$$Y_0 = A'B' + AB \quad (1)$$

$$Y_1 = AB' \quad (2)$$

$$Y_2 = A'B \quad (3)$$

PROPOSED 2-BIT COMPARATOR

Proposed comparator is 2-bit comparator. In this, we have given two inputs with 2-bit each. The outputs are equal to (Y_0), greater than (Y_1) and less than (Y_2). If anyone of the output is true, then other outputs become false.

The equations for 2-bit comparator are shown in (4), (5) and (6)

$$Y_0 = (A_2 \text{ AND } B_2') + (A_1 \text{ AND } B_2' \text{ AND } B_1') + (A_2 \text{ AND } A_1 \text{ AND } B_1') \quad (4)$$

$$Y_1 = (A_1 \text{ EX-NOR } B_1). (A_2 \text{ EX-NOR } B_2) \quad (5)$$

$$Y_2 = (A_2' \text{ AND } B_2) + (A_2' \text{ AND } A_1' \text{ AND } B_1) + (A_1' \text{ AND } B_2 \text{ AND } B_1) \quad (6)$$

The diagram of 2-bit comparator is designed using 4 NOT gates, seven AND gates, two OR gates and two EX-NOR gates, through which output is obtained based on the comparison. The AND gates as two inputs and three inputs with one output. The OR gates with three inputs and one output. EX-NOR gates with two inputs and one output.

- The first AND gate inputs are A_2, B_2' , the obtained output is given to 3 to 1 OR gate.
- The second AND gate inputs are A_2, A_1, B_1' , the obtained output is given to 3 to 1 OR gate.
- The third AND gate inputs are A_1, B_2', B_1' , the obtained output is given to 3 to 1 OR gate.
- The first EX-NOR gate inputs are A_2, B_2 , the obtained output is given to 2 to 1 AND gate.
- The second EX-NOR gate inputs are A_1, B_1 , the obtained output is given to 2 to 1 AND gate.
- The fourth AND gate inputs are A_2', B_2 , the obtained output is given to 3 to 1 OR gate.
- The fifth AND gate inputs are A_2', A_1', B_1 , the obtained output is given to 3 to 1 OR gate.
- The sixth AND gate inputs are A_1', B_2, B_1 , the obtained output is given to 3 to 1 OR gate.
- Outputs of first three AND gates are given to 3 input OR gate, that provides the output Y_0 , i.e. A greater than B. Outputs of two EX-NOR gates are given to 2 input AND gate, that provides the output Y_1 , i.e. A equal to B.

Outputs of other three AND gates are given to 3 input OR gate, that provides the output Y_2 , i.e. A less than B.

The table 7 represents the 2-bit inputs as (A_2, A_1), (B_2, B_1) and three outputs (Y_0, Y_1, Y_2). We have given all possible combinations and by analysis, we got the three outputs that are considered as Y_0, Y_1 and Y_2 respectively.

RESULTS

Simulations are performed on HSPICE tool of Synopsys Company under 32 nano metre BSIM 4 model card libraries. The transistor dimensions are considered as length of PMOS, NMOS are 32 nm and width of PMOS, NMOS are 3200 nm and 1600 nm. The below Figure provides the results of HSPICE simulations of the input and output of 2-bit





Rajendra Prasad Madepogu et al.,

comparator. In this circuit, inputs are considered as A1, B1, A2 and B2 and outputs obtained are Y0, Y1 and Y2, based on the values provided to the inputs.

- When the inputs A1 is 1, A2 is 1, B1 is 1 and B2 is 1, outputs Y1 (A equal to B) becomes 1 and Y0, Y2 are zeros.
- When the inputs A1 is 1, A2 is 0, B1 is 1 and B2 is 1, outputs Y2(A less than B) becomes 1 and Y0, Y1 are zeros.
- When the inputs A1 is 0, A2 is 1, B1 is 0 and B2 is 0, outputs Y0(A greater than B) becomes 1 and Y1, Y2 are zeros.
- When the inputs A1 is 0, A2 is 0, B1 is 0 and B2 is 0, outputs Y1 (A equal to B) becomes 1 and Y0, Y2 are zeros.

The simulation waveform that is shown in the Fig. displays results with four different input combinations that can be verified using the table 7. By analysing Figs 9 & 10, it can be observed that with the variations in the voltage at different values, power dissipation alters for 2 bit comparator. Also, the variations in the delay are observed at different voltage values for 2 bit comparator. The Table provides the comparison of 2-bit comparator with different voltage values, those results in power dissipation in micro-Watts and delay in nano-seconds. Total count of the transistors utilised is 102 for proposed 2-bit comparator. It is observed from the table that as the voltage values increases, there is an increment in power dissipation and as the voltage value increases, there is decrement in delay. The minimum delay is 1.5091 ns and maximum delay is 1.5377ns. The minimum power is 131.64 μ W, and maximum power is 2003.6 μ W for 2-bit comparator as mentioned in table.

CONCLUSION

Analysis is done in order to propose the architecture of 2-bit comparator for optimizing power and delay values. 2-bit comparator is designed with transistor count of 102 and with decreased power dissipation and delay measures. CMOS is a very well-known technology to design 2-bit comparator. The table provided above displays the comparison between transistor count used and along with power dissipation and delay for seven distinct voltage levels. The proposed work is simulated using Synopsys tool called HSPICE, and the results are observed for different voltages. The proposed model delay and power dissipation results are minimum at 1.50 ns, maximum at 1.53 ns and minimum at 131.64 μ W, maximum at 2003.6 μ W. Hence, it is derived that the proposed model, power dissipation and delay of CMOS 2-bit comparator logic is examined. Further scope of the work is to design comparator by using CNTFET or GNRFT technologies.

REFERENCES

1. M. Ercegovic, T. Lang, J. Moreno, *Introduction to Digital Systems*, John Wiley and Sons, 1999.
2. N. Weste, D. Harris, *CMOS VLSI design: A Circuits and Systems Perspective*, 4th Edition, Addison Wesley, 2011.
3. Malti Bansal, Jasmeet Singh, *Qualitative Analysis of 2-bit CMOS Magnitude Comparator and GDI Magnitude Comparator using FinFET Technology (18nm)*, pp. 1323-1327, 2020.
4. H. J. R. Liu and H. Yao, *High-Performance VLSI Signal Processing Innovative Architectures and Algorithms*, vol. 2. Piscataway, NJ: IEEE Press, 1998.
5. Y. Sheng and W. Wang, "Design and implementation of compression algorithm comparator for digital image processing on component," in *Proc. 9th Int. Conf. Young Comput. Science*, pp. 1337–1341, 2008.
6. C.-H. Huang, J.-S. Wang, "High-performance and power-efficient CMOS comparators," *IEEE Journal of Solid-state Circuits*, vol. 38, no. 2, pp.254–262, Feb. 2003.
7. C. Efstathiou, K. Dimolikas, C. Papaioannou and Y. Tsiatouhas, "Low Power and High Speed Static CMOS Digital Magnitude Comparators", *IEEE International Conference on Electronics, Circuits and Systems (ICECS)*, Vol. 6, No.8, pp.
8. Akash Gupta, Manohar Khatri, Sachin Kumar Rajput, Anu Mehra and Shikha Bathla, "Design of Low Power magnitude comparator," *IEEE*, pp.754-758, 2017.





9. Pranay Singh and Pramod Kumar Jain, "Design and Analysis of Low Power, High Speed 4- Bit Magnitude Comparator, " *International conference on recent innovations in electrical, electronics & communication engineering - (ICRIEECE)*, pp.1680-1683, 2018.
10. M. Morris Mano and Michael D. Ciletti, " *Digital Design* ", 5th Edition, Pearson Education, 2011.

Truth Table 1

A	\bar{A}
0	1
1	0

Truth Table 2

A	B	Y
0	0	0
0	1	0
1	0	0
1	1	1

Truth Table 3

Input (A)	Input (B)	Input (C)	Output (Y)
A=0	B=0	C=0	Y=0
A=0	B=0	C=1	Y=0
A=0	B=1	C=0	Y=0
A=0	B=1	C=1	Y=0
A=1	B=0	C=0	Y=0
A=1	B=0	C=1	Y=0
A=1	B=1	C=0	Y=0
A=1	B=1	C=1	Y=1

Truth Table 4

Input (A)	Input (B)	Input (C)	Output (Y)
A=0	B=0	C=0	Y=0
A=0	B=0	C=1	Y=1
A=0	B=1	C=0	Y=1
A=0	B=1	C=1	Y=1
A=1	B=0	C=0	Y=1
A=1	B=0	C=1	Y=1
A=1	B=1	C=0	Y=1
A=1	B=1	C=1	Y=1

Truth Table 5

Input (A)	Input (B)	Output (Y)
A=0	B=0	Y=1
A=0	B=1	Y=0





Rajendra Prasad Madepogu et al.,

A=1	B=0	Y=0
A=1	B=1	Y=1

Truth Table 6

Input (A)	Input (B)	Output (Y0)	Output (Y1)	Output (Y2)
A=0	B=0	Y0=1	Y1=0	Y2=0
A=0	B=1	Y0=0	Y1=0	Y2=1
A=1	B=0	Y0=0	Y1=1	Y2=0
A=1	B=1	Y0=1	Y1=0	Y2=0

Truth Table 7

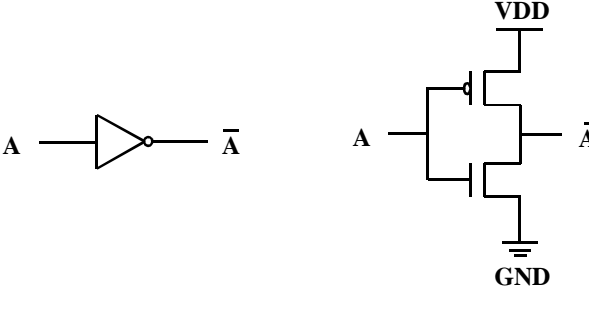
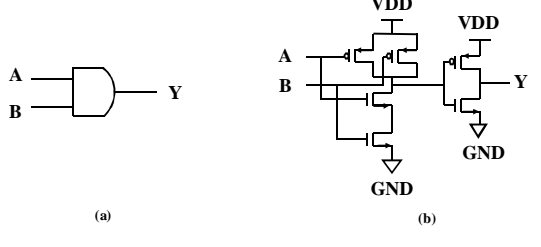
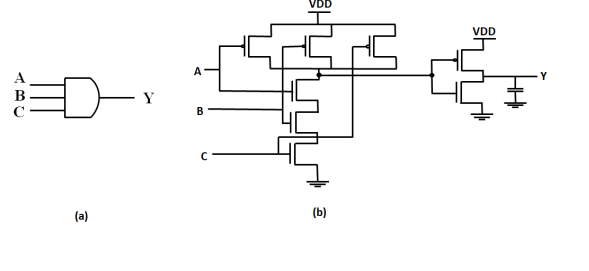
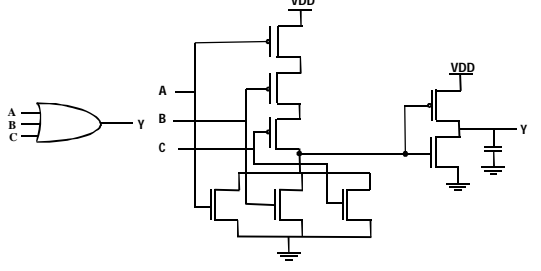
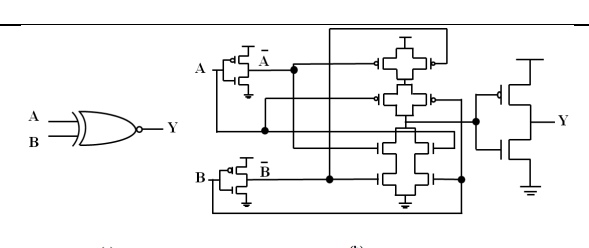
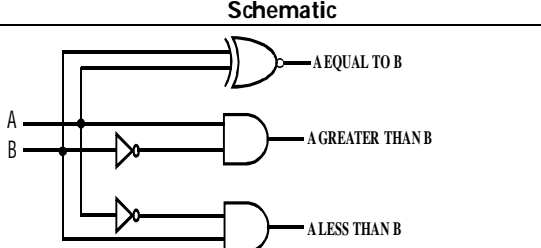
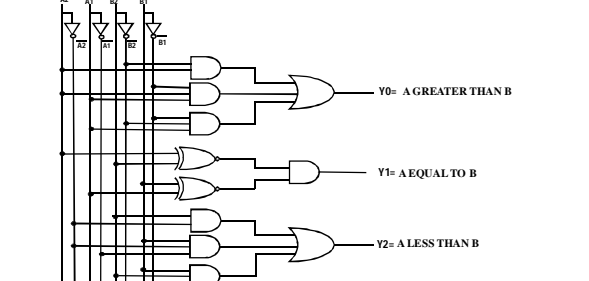
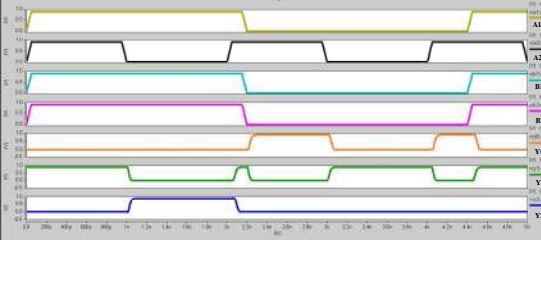
Input (A2)	Input (A1)	Input (B2)	Input (B1)	Output (Y0)	Output (Y1)	Output (Y2)
A2=0	A1=0	B2=0	B1=0	Y0=0	Y1=1	Y2=0
A2=0	A1=0	B2=0	B1=1	Y0=0	Y1=0	Y2=1
A2=0	A1=0	B2=1	B1=0	Y0=0	Y1=0	Y2=1
A2=0	A1=0	B2=1	B1=1	Y0=0	Y1=0	Y2=1
A2=0	A1=1	B2=0	B1=0	Y0=1	Y1=0	Y2=0
A2=0	A1=1	B2=0	B1=1	Y0=0	Y1=1	Y2=0
A2=0	A1=1	B2=1	B1=0	Y0=0	Y1=0	Y2=1
A2=0	A1=1	B2=1	B1=1	Y0=0	Y1=0	Y2=1
A2=1	A1=0	B2=0	B1=0	Y0=1	Y1=0	Y2=0
A2=1	A1=0	B2=0	B1=1	Y0=1	Y1=0	Y2=0
A2=1	A1=0	B2=1	B1=0	Y0=0	Y1=1	Y2=0
A2=1	A1=0	B2=1	B1=1	Y0=0	Y1=0	Y2=1
A2=1	A1=1	B2=0	B1=0	Y0=1	Y1=0	Y2=0
A2=1	A1=1	B2=0	B1=1	Y0=1	Y1=0	Y2=0
A2=1	A1=1	B2=1	B1=0	Y0=1	Y1=0	Y2=0
A2=1	A1=1	B2=1	B1=1	Y0=0	Y1=1	Y2=0

Table 8: The Comparison of 2-Bit Comparator

Combinational Circuit	Technology	Transistor Count	Voltage (V)	Power Dissipation (μ W)	Delay (ns)
2-Bit Comparator	CMOS 32nm	102	0.9	131.64	1.5377
2-Bit Comparator	CMOS 32nm	102	1	183.37	1.5277
2-Bit Comparator	CMOS 32nm	102	1.1	266.78	1.5212
2-Bit Comparator	CMOS 32nm	102	1.2	406.90	1.5168
2-Bit Comparator	CMOS 32nm	102	1.3	652.04	1.5133
2-Bit Comparator	CMOS 32nm	102	1.4	1113.5	1.5111
2-Bit Comparator	CMOS 32nm	102	1.5	2003.6	1.5091



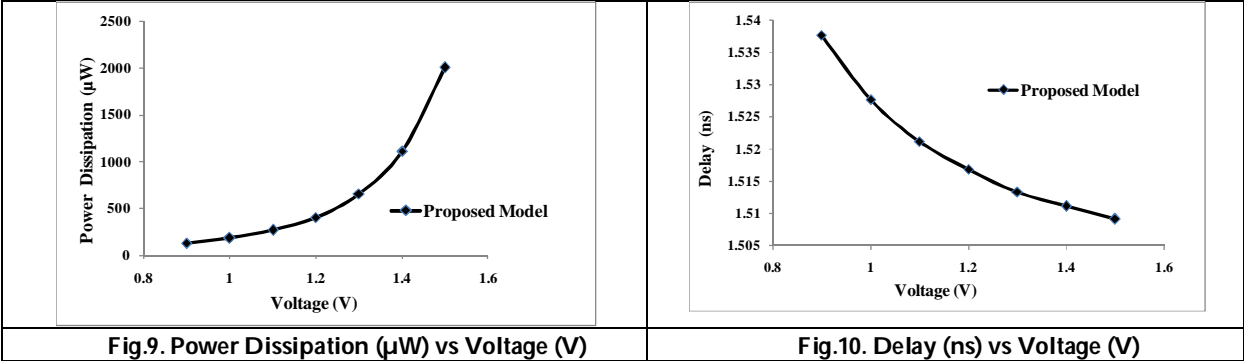


 <p>(a) (b)</p>	 <p>(a) (b)</p>
<p>Fig.1 (a) Inverter symbol (b) inverter schematic</p>	<p>Fig.2 (a) AND symbol (b) AND Schematic</p>
 <p>(a) (b)</p>	 <p>(a) (b)</p>
<p>Fig.3 (a) 3-Input AND symbol (b) 3-Input AND Schematic</p>	<p>Fig.4 (a) 3-Input OR symbol (b) 3-Input OR Schematic</p>
 <p>(a) (b)</p>	
<p>Fig.5 (a) XNOR symbol (b) XNOR Schematic</p>	<p>Fig 6: 1-bit comparator logic diagram</p>
	
<p>Fig.7.2-bit Comparator logic diagram</p>	<p>Fig.8.2-bit Comparator waveform</p>





Rajendra Prasad Madepogu et al.,





***In vitro* Anti-Fungal and Anti-Bacterial Activity of *Abutilon indicum* (Linn.) Flower Extract**

Meenakshi Sundari T^{1*}, Saravanakumar A², Sangeetha S³ and K. Supriya⁴

¹Associate Professor, Department of Pharmacognosy, Vellalar College of Pharmacy, Thindal, Erode - 638012, (Affiliated to Tamil Nadu Dr. M.G.R. Medical University, Chennai) Tamil Nadu, India.

²Professor and Principal, Department of Biotechnology, Vellalar College of Pharmacy, Maruthi Nagar, Thindal, Erode -638012, (Affiliated to Tamil Nadu Dr. M.G.R. Medical University, Chennai), Tamil Nadu, India.

³Associate Professor, Department of Pharmaceutical Chemistry, Vellalar College of Pharmacy, Maruthi Nagar, Thindal, Erode -638012, (Affiliated to Tamil Nadu Dr. M.G.R. Medical University, Chennai), Tamil Nadu, India.

⁴UG Student, Department of Pharmacy, Vellalar College of Pharmacy, Thindal, Erode -638012, (Affiliated to Tamil Nadu Dr. M.G.R. Medical University, Chennai) Tamil Nadu, India.

Received: 22 Jan 2024

Revised: 07 Feb 2024

Accepted: 03 May 2024

***Address for Correspondence**

Meenakshi Sundari T

Associate Professor,

Department of Pharmacognosy,

Vellalar College of Pharmacy, Thindal, Erode -638012,

(Affiliated to Tamil Nadu Dr. M.G.R. Medical University, Chennai)

Tamil Nadu, India.

Email: jaimeenakshi2513@gmail.com



This is an Open Access Journal / article distributed under the terms of the **Creative Commons Attribution License** (CC BY-NC-ND 3.0) which permits unrestricted use, distribution, and reproduction in any medium, provided the original work is properly cited. All rights reserved.

ABSTRACT

This study aimed to determine the antibacterial and antifungal activity of ethanolic extracts of *Abutilon indicum* against bacterial and fungal species. Both antifungal and antibacterial behaviours were examined using the disc diffusion method. An ethanolic extract of *Abutilon indicum* Linn flower extract has significant antibacterial and antifungal activity against various species. The flower extract contains flavonoids, tannins, terpenoids, and alkaloids as secondary metabolites, which have significant antibacterial and antifungal properties. These flowers of *Abutilon indicum* are utilised to enhance semen production and in Siddha medicine. The antimicrobial activity of the plant materials is attributed to the presence of secondary products in the plant. The results were examined using the conventional antimicrobial drugs chloramphenicol for bacteria and fluconazole for fungus. Plant extracts inhibited growth in a dose-dependent manner.





Keywords: *Abutilon indicum*, Antibacterial activity, Antifungal activity, Inhibition, Disc Diffusion Method.

INTRODUCTION

Nature is widely utilized as a source of medicine and many synthetic medications have been developed by isolating compounds found in nature. Natural products deserve more research because they can be employed as medications to cure human diseases. These treatments would be highly effective against infections and would have few if any, adverse side effects [1]. According to the World Health Organization, 55 million people died worldwide in 2011, with infectious diseases accounting for one-third of all deaths. Most naturally existing and synthetically generated bioflavonoids have antibacterial and antifungal activities. The antibacterial activity is a significant attribute for providing sufficient defence against microorganisms[2]. Drugs made from plants consume up to 25% of the total, but in rapidly emerging countries like India and China, this number rises to as high as 80%. India is one of the world's most medico-culturally diversified countries, with a long and ancient history of using plants for medicinal purposes [3]. *Abutilon indicum*, a member of the Malvaceae family, is used medicinally and goes by the names Thuthi and Atibala. This plant grows erect, woody, and shrubby in tropical and subtropical nations and exists worldwide. For thousands of years, plants have been utilized as medicine. In our traditional medical system, the *Abutilon indicum* (Linn.) plant deals with various deficiencies in the body. A member of the Malvaceae family, *Abutilon indicum* (Linn.) is generally known as the English "country mallow" owing to its use as a medicinal herb[4]. Herbal or plant products contain flavonoids, phenolic compounds, terpenoids, and other elements that assist reduced blood glucose levels. *Abutilon indicum* is a tiny shrub native to tropical and subtropical regions frequently decoratively cultivated in Karnataka, Tamil Nadu. It is an erect, branching shrub that grows to 0.5–1 m in height.

Almost every part of Atibala has medicinal properties and is traditionally used to cure various diseases[5]. The plant roots are demulcent and diuretic, making them beneficial when treating chest and urethritis. This extract made from the roots is used to cure fevers and has been discovered to be effective in treating haematuria and leprosy. In addition to reducing body pain, the leaves can cure ulcers[6]. The leaf decoction internally treats toothache, sore gums, and bladder inflammation. The bark has many medicinal purposes, including those of a diuretic, a fever reducer, and an anthelmintic. The seeds are a common ingredient in remedies for various gastrointestinal issues, including piles, laxatives, expectorants, chronic cystitis, gleet, and gonorrhoea. The plant's leaves include steroids, saponins, sugars, and flavonoids. Gallic acid can be found in the plant's roots. In addition to asparagine, mucilaginous compounds can be found throughout the plant [7]. The primary types of chemicals are saponins, flavonoids, alkaloids, hexoses, a combination of n-alkanes (C22–C34), and alkanol. Betasitosterols, vanillic acid, Para-coumaric acid, caffeic acid, fumaric acid, Para-hydroxybenzoic, galatonic, para-beta-D-glycosyloxybenzoic, and amino acids are some of the main compounds reported in the plant. In addition to alpha-pinene, caryophyllene oxide, Endemol, borneol, geraniol, geranyl acetate element, alpha-cineole, and a few other minor compounds, *Abutilon indicum* includes essential oils [8]. The plant's seed oil contains cis-12, 13-epoxy oleic (vernolic) acid, 9, 10-methylene-octadec-9-enoic (sterculic) acid, and 8,9-methylene-heptadec-8-enoic (malvalic) acid[9]. This research aimed to examine the antimicrobial and antifungal properties of *Abutilon indicum* Linn, a traditional medicine used to treat symptoms caused by micro-organisms.

MATERIALS AND METHODS

The disease-free *Abutilon indicum* flowers were harvested freshly from the Erode district of Tamil Nadu. Because if selected the dark and calm place for drying the flowers. Then plant materials are frequently assessed for fungal growth. In addition, dried plant material was ground into a powder using an electric blender and sieved through a





40 mesh detector to achieve a uniform size. Further, to maintain plant material was kept at 4°C in an airtight container [10].

PREPARATION OF EXTRACT

A coarse powder was prepared from the air-dried flower *Abutilon indicum*. The soxhlet extraction has been used to extract ethanol from the dried powder flower. This extract was strained using muslin, and then the filter was evaporated under decreased pressure and vacuum dried.

IN-VITRO ANT BACTERIAL ACTIVITY

Selection of Microorganism

To investigate the performance of these compounds against antibacterial and anti-fungi, we collected a variety of microorganisms from the Department of Microbiology at Vellalar College of Pharmacy, Erode. It includes *Escherichia coli*, *Streptococcus pyogenes*, *Candida albicans*, and *Aspergillus Niger*.

Antibacterial Activity Using the Disc Diffusion Method

Extracts of the leaves were tested for their antibacterial activity directed at the chosen bacterial strains. Each sterile cotton swab was filled with 20 ml of nutritional agar solution that had been sterilised. Then, a sterile cork borer with 150 µl of each ethanol was used to make a 0.5 cm well in the medium [11, 12]. After incubating the plants for 24-48 hours, the extracts were separated into individual wells at 37 °C. These findings were examined during the incubation period, while the measurement associated with each well in the diameter of the incubation period using the disc diffusion method, as shown in Fig. 1. As an examination, conventional antibacterial including chloramphenicol, were utilized in the incubation zone, as stated in Table 1.

Antifungal Activity Using the Disc Diffusion Method

The leaf extracts have been tested for antifungal activity to identify fungus strains. Each sterile cotton swab received 20 ml of nutritional agar medium prepared in a sterile environment. Then, a sterile cork borer containing 150 µl of each ethanol was used to create a 0.5 cm deep well in the medium. The extracts were placed into separate wells after incubating the plants at 37 °C for 24-48 hours [13]. Following incubation, the outcome was evaluated, and the diameter of the incubation region around each well was recorded. The standard antifungal fluconazole was utilized as a control, as shown in Table 2.

RESULTS AND DISCUSSION

The present study was performed to measure the antibacterial and antifungal activity from ethanolic flower extracts with *Abutilon indicum* examined at different concentration (10 µl/ml, 20 µl/ml, 30 µl/ml, 40 µl/ml) within two pathogenic strains of bacteria (*Escherichia coli*, *Streptococcus pyogenes*) and two fungal strains (*Candida albicans*, *Aspergillus niger*). The antibacterial and antifungal activity of ethanolic extracts was investigated in terms of bacterial growth inhibition zone [14]. When tested for antibacterial and antifungal activities, extract concentration (µl/ml) increased linearly with efficacy, in addition to traditional antibiotics that include chloramphenicol for bacteria and fluconazole for fungus [15]. The results reveal that *Abutilon indicum* flower extracts have significant antifungal activity against *Aspergillus niger*.

CONCLUSION

The present investigation aims to examine the anti-bacterial and anti-fungal activity of *Abutilon indicum* methanolic flower extract using a zone of inhibition assay. These findings are displayed in Tables 1 and 2. The ethanolic extracts evaluated in this investigation exhibited varying inhibitory zones against the identified bacterial and fungal pathogens. In this work, the ethanolic extract of *Abutilon indicum* flower exhibited significant anti-bacterial activities.



**Meenakshi Sundari et al.,**

The extract showed zones of inhibition of 22 ± 0.43 and 21 ± 0.70 on nutritional agar medium plates against *Staphylococcus pyrogens* and *E. coli*, respectively. According to the conventional Chloramphenicol discs, which had inhibition zones of 15 ± 0.1 and 17 ± 0.1 , respectively, this activity was significantly higher. An excellent anti-fungal effect was observed in the ethanolic extract of the *Abutilon indicum* flower. On nutrient agar medium plates, it inhibited *Candida albicans* and *Aspergillus niger* with zones of inhibition of 20 ± 0.35 and 22 ± 0.38 , respectively. The standard ketoconazole disc had zones of inhibition of 12 ± 0.5 and 14 ± 0.5 , respectively. Therefore, *Abutilonindicum* flower extracts are very effective against bacteria and fungi.

REFERENCES

1. Krisanapun C, Peungvicha P, Temsiririrkkul R, Wongkrajang Y. Aqueous extract of *Abutilon indicum* Sweet inhibits glucose absorption and stimulates insulin secretion in rodents. *Nutrition research*. 2009, 29(8), pp.579-87.
2. Nelluri NR, Kumar P, Agarwal NK, Gouda TS, Setty SR. Phytochemical and pharmacological evaluation of leaves of *Abutilon indicum*. *Indian Journal of Traditional Knowledge*. 2003, 2(1), pp.79-83.
3. Raut S, Bandawane D. PHARMACOGNOSTIC AND PHARMACOLOGICAL ASPECT OF *ABUTILON INDICUM* LINN: A REVIEW. *World journal of pharmaceutical research*. 2017, 7(3), pp.286-301.
4. Porchezian E, Ansari SH. Effect of liquid extract from fresh *Abutilon indicum* leaves and *Allium cepa* bulbs on paracetamol and carbontetrachloride induced hepatotoxicity. *Die Pharmazie*. 2000, 55(9), pp.702-703.
5. Roshan S, Ali S, Khan A, Tazneem B, Purohit MG. PHCOG MAG.: Research Article Wound Healing activity of *Abutilon Indicum*. *Phcog Mag*. 2008, 4(15), pp.85-88.
6. Kuo PC, Yang ML, Wu PL, Shih HN, Thang TD, Dung NX, Wu TS. Chemical constituents from *Abutilon indicum*. *Journal of Asian natural products research*. 2008, 10(7), pp.689-693.
7. Pandey DP, Rather MA, Nautiyal DP, Bachheti RK. Phytochemical analysis of *Abutilon indicum*. *Int J Chem Tech Res*. 2011, 23(2), pp.642-645.
8. Suryawanshi VS, Umate SR. A Review on Phytochemical Constituents of *Abutilon indicum* (Link) Sweet-An Important Medicinal Plant in Ayurveda. *Plantae Scientia*. 2020, 3(3), pp.15-19.
9. Abdul MM, Sarker AA, Saiful IM, Muniruddin A. Cytotoxic and antimicrobial activity of the crude extract of *Abutilon indicum*. *International Journal of Pharmacognosy and Phytochemical Research*. 2010, 2(1), pp.1-4.
10. Musheerul H, Marifatul HS, Huma H, RA M, Sri S, Akhtar R, Muhammad Z. Study of *Abutilon theophrasti* Stem Extract for its Antibacterial Activity. *Research Journal of Chemistry and Environment*. 2021, 25(3), pp.14-16.
11. Gonelimali FD, Lin J, Miao W, Xuan J, Charles F, Chen M, Hatab SR. Antimicrobial properties and mechanism of action of some plant extracts against food pathogens and spoilage microorganisms. *Frontiers in microbiology*. 2018, 9(1), pp.1639.
12. Balouiri M, Sadiki M, Ibensouda S.K. Methods for in vitro evaluating antimicrobial activity: A review. *Journal of pharmaceutical analysis*. 2016, 6(2), pp.71-79.
13. Saranya D, Sekar J, Raj GA. Phytochemical analyses, antibacterial and antifungal activity of leaves from *Abutilon indicum* (L.) Sweet. *J. Chem. Pharm. Res*. 2015, 7(12), pp.524-530.
14. Shanmugapriya S, Anuradha, R. Efficacy of *Abutilon indicum* L. against Bacterial and Fungal Species. *Int. J. Curr. Microbiol. App. Sci*. 2015, 4(12), pp.402-407.
15. ChumbhaleDeshraj S, Chaudhari SR, Upasani CD. Antibacterial and antifungal activity of stem bark of *abutilon indicum* (linn.) Sweet. *Int. J. Pharm. Res. Dev*. 2015, 7(1), pp.23-27.





Meenakshi Sundari et al.,

Table 1. Displays the Antibacterial Activity

S. No	Microorganisms Test mm	Standard drug (Chloramphenicol) (10µg/ml)	Zone of inhibition in mm			
			10 mg	20 mg	30 mg	40 mg
1.	<i>E.coli</i>	15±0.1	17±0.18	19±0.42	20±0.45	22±0.43
2.	<i>S. pyogenes</i>	17±0.1	17±0.32	18±0.49	19±0.56	21±0.70

Table 2. Shows the Antifungal Activity

S. No	Microorganisms Test mm	Standard drug (Fluconazole) (10µg/ml)	Zone of inhibition in mm			
			10 mg	20 mg	30 mg	40 mg
1.	<i>C. albicans</i>	12±0.5	15±0.25	17±0.32	18±0.49	20±0.35
2.	<i>Aspergillus niger</i>	14±0.5	13±0.27	12±0.36	17±0.43	22±0.38

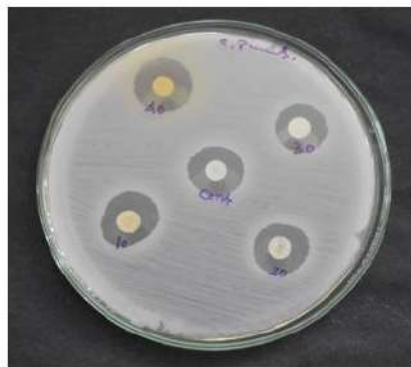
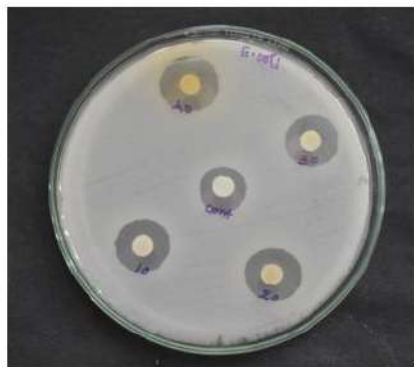


Figure 1. Depicts the Disc Diffusion Method





Supportive Model for Improving the Service Quality in the Secondary Education

Pankaj Mohindru^{1*} and Kamaljit Singh²

¹Assistant Professor, Department of Electronics and Communication Engineering, Punjabi University, Patiala, Punjab, India.

²Research Scholar, Department of University School of Applied Management, Punjabi University, Patiala, Punjab, India.

Received: 22 Jan 2024

Revised: 09 Feb 2024

Accepted: 04 May 2024

*Address for Correspondence

Pankaj Mohindru

Assistant Professor,
Department of Electronics and Communication Engineering,
Punjabi University,
Patiala, Punjab, India.
Email: arseamict@gmail.com



This is an Open Access Journal / article distributed under the terms of the **Creative Commons Attribution License** (CC BY-NC-ND 3.0) which permits unrestricted use, distribution, and reproduction in any medium, provided the original work is properly cited. All rights reserved.

ABSTRACT

To improve the service quality in Secondary Education the model of the researcher revolves around Learning, Enthusiasm, Organization, Group Interaction, Service Quality, Individual Relationship, Elaboration, and Exam & Assignment, which are Co-related with each other and service quality merely depends upon Reliability, responsiveness, Assurance, Empathy and Tangibility of the Lecturer and Student. The researcher's main target is to develop a supportive model that will improve the Service Quality in Secondary Education, which plays a key role in the education sector. It will lead the students toward the future they have dreamed of in their childhood. This study is conducted by the use of Primary as well as Secondary Data. The evolution of end-user computing has led to a consciousness of the necessity to estimate the quality of services provided by the information systems function. There are so many companies inside and outside the country, which are working to enhance the service quality of Digital education. The service quality of Digital Education is improving day by day with the passage of time and with the development of technology. It can also reduce the fee structure and everyone can learn with a go service quality in Digital Education. As we know there are many flaws in the old teaching system but with the help of Digital Education, it can be covered in the future. It will also help in Rural areas. As we know the world is becoming digital day by day and with the help of Digital Education and good service quality children who don't have the necessary environment for the same can also study. Online education has since surfaced the way for an educational change in the way teachers teach and how students learn. This study will give advantage to academic researchers, educators, application developers and policymakers.



**Pankaj Mohindru and Kamaljit Singh**

Keywords: Supportive Model, Service Quality, Digital Education, Enthusiasm, Organization, Group Interaction, and Student Satisfaction.

INTRODUCTION

Service Quality always plays an essential and energetic role to achieve the success in the Secondary education sector. In the present Era the evolution of end-user computing and the importance on excellence in a firm's products and facilities has driven Information Systems (IS) managers to evaluate the quality of IS facility provided to its users. Several researches and government reports at official level has acknowledged the same and given approvals for its enhancement. As we know technology is continuously changing day by day so the expectations of students are also increasing towards the service quality of education. There are so many private institutes which are providing digital education, but mostly private institutes are not having the necessary and improved equipment for this. Schools and other educational institutes are continuously working towards the student satisfaction with the improvement in the service quality in Digital Education. Secondary education segment is facing pressure to increase the quality in education. Presently, educational institutions are increasing their effort on constant development and focus on student fulfilment. Students are having numerous options to choose after Secondary Education to earn a degree. According to the Raubinger et.al (The Development of Secondary Education. New York: Macmillan, 1969)- there are seven cardinal principles of Secondary Education, which are Health, Command of Fundamental Process, Worthy Home Membership, Vocation, Civic Education, Worthy use of leisure and Ethical Character. These seven purposes do not "suggest that the procedure of education can be distributed into separated fields" (Raubinger, Rowe, Piper, West, 106). Therefore, all of the seven ideologies are interrelated. In order for these ideologies to be successful the student must have enthusiasm to follow these and an ethical character that will allow this learning to take place.

In Indian context some independent accreditation bodies plays a dynamic role in providing quality certification to the secondary education institutions. The study of service quality in secondary education is significant and essential to the institutions to deliver information on the success of education tactics and enhancement programs. There is a hectic competition after the globalization flourish growth of secondary education in India. The evaluation of the schools through service quality in education provided by them helps students to select their avenue of education. Even though, there are numerous studies on service quality in several service segments, only a few studies are related to the service quality of Secondary education. The previous researches on the service quality of Digital Education are not covering all features; hence, the present study tries to fill the research gap. Presently, it is the phase to look more holistically at how quality aspects must be united, integrated, and modified through the institution — including but not limited to a course-level focus — to purposely design the student learning practise to address existing and developing desires. Online education desires to be mission-aligned as well as integrated with quality assurance — not as a distinct activity but through courses, programs and pathways, and institutional goals for student learning. Nevertheless, of the way an education is distributed, stakeholders expect and deserve quality. This point was highlighted throughout the Summit by Dr. Heather F. Perfetti, President, Middle States Commission: "You now see the phrase 'regardless of modality' throughout our standards, and institutions are leveraging their work with QM as one mechanism to show the tie back to meeting accreditation standards." (Dr. Deb Adair, QM Executive Director January 2022).

RATIONALE OF THE STUDY

Digital education will be beneficial to academic institutes and other education provider organizations. Academic institutions can manage their activities systematically and easily with the help of digital education. With the help of effective and newest Information technology capable devices and through interactive-audio-visual teaching contents they can transfer the knowledge equally and easily from educator to every student (RampraveshGond et al, March 2017). It will give them the benefits over other academic institutes which are unable to provide service quality in





digital education. Educators can teach their students more effectively and easily with the help of digital education. Online they can update their time table of teaching, holiday's information, events and other activities anytime from anywhere. Teachers also can check the progress of their student online. Beneficiary contents related to the courses of the students can be updated by them easily. They can teach difficult subjects to students easily and clearly with digital education tools (RampraveshGond et al, March 2017). A standard quality in teaching is needed to educate the students better. In education sector Punjab is having an important place. There are thousands of Senior Secondary Schools in Punjab having lacs of students enrolled across different fields (DPI Secondary Education Mohali). Information technology has changed many sectors of every field but it is in the beginning phase of acceptance in the education sector. So, it is important to enhance the service quality of digital education and take it to the next level. Government has to support experienced and right digital technology providers having better service quality for the development of digital education sector. Many private and government players are developing new techniques to enhance the service quality of digital education in India. Establishment of these techniques and tools in education will lower the expenditure of education and enhance the teaching & learning skills. More importance should be given to these private and government players to increase and improve the service quality of digital education.

A digital education start-up, Byju's, has raised US\$ 50 million from the Chan Zuckerberg Initiative, founded by Facebook founder Mark Zuckerberg for the development of digital education in India. Tata Trusts part of the Tata Group and Khan Academy are starting web based free learning portal to deliver no cost digital education in India. The Cisco Systems planning to speculate 100 million US Dollars in India to enhance digital education. It will help to introduce six new labs, which will be capable to facilitate to coach approximately 2,50,000 students by year 2020.

LITERATURE REVIEW

Blended learning is a combination of numerous delivery methods, such as collaboration software, online courses and information management practices. Self-paced learning, live learning and face-to-face classrooms are the parts of the blended learning (PurnimaValiathan, 2002). Technology growth in internet has the probability to renovate the old structure of education. Initiative of delivery of e-learning by internet created opportunities in the business and in education sector. E-learning allowed the educational institutions geographical reach, to establish themselves as international educational providers. E-learning will provide universities a new formed competition, with complete benefits of their traditional, already establish standings. Students can take profits as they can absorb education outside the lecture hall and become self-directed independent learners (Singh, G. et al. 2005). Lane Fischer et al. (2015) examined the difference in conclusions between the students that learn using open educational resources (OER) and those who did not. The learners who learn by using OER done better than that pupil who learn without OER. The students who have given the paper by using e-learning tools done better than those who given the exam without using e-learning tools. They examined that the usage of e-learning tools possibly has the adverse effect on the students who completely depend on e-learning tools (Tomas Moravec et al., 2015).

The two main key difficulties confronted by Indian Schools viz., inadequate infrastructure and poor quality teaching can be solved by digital intervention. Many companies are proposing digital learning solutions (DLS) for schools (Sugant et al 2016). IT tools that are useful in E-education discussed by Dr. Jayesh M. Patel (2017) are Moodle, Twitter, Blogger, Diigo, PREZI, Wikispaces etc. The usage of this technology is very useful for the students and it also satisfied the child centred approach. Digitization has transformed our education system but without dropping the old traditional classroom learning. Digital education is the mixture of both features; classroom learning and online learning techniques. Digitization is the right technique to decrease the frivolous usage of paper and there are also many more benefits of digitization (Dr. Umesh Kumari 2019). Dr. Ajay Kumar (2019) claimed that Digital Education is required in this competitive world because the participation of Innovation and Technology is surplus in every area and it is changing quickly from the last few years. Service is defined as "the work, activity and benefits that create consumer fulfilment" (Duque Oliva, 2005, p. 2). Additional theories claim that services have two essential characteristics, intangibility, no differentiation between production and delivery, and the inseparability of production and consumption. Furthermore, one of the note worthy unique characteristics between tangible products and



**Pankaj Mohindru and Kamaljit Singh**

services is that they cause dissimilarities in determining the quality of service. Therefore, one cannot evaluate services and tangible products in the identical method. The renowned characteristics are intangibility, heterogeneity, and inseparability (Parasuraman, Zeithaml, & Berry, 1985). Observed Service Quality is subjective because it is estimated by customers based on their observations. It can also be described as an assertiveness regarding the superiority of one service that is composed of manifold dimensions (Duque Oliva, 2005; Colmenares&Saavedra, 2007). As a revolution, online education is compressed by the identical elementary factors as in-person education, though the old-style learning atmosphere has not been precisely designed for the online student. Those of you aware with Quality Matters (QM) are also possibly to be familiar with the QM “Quality Pie” — the elements disturbing the student learning experience in the online classroom. These factors, which need to be purposely designed for online students, with course design, course delivery (teaching), course content, learning technologies, institutional infrastructure, faculty preparation and support, and student preparation and support. QM tools were initially established to precisely address the course design aspect because it was believed both critical to online learner success and because, at the time, most online courses were being established by faculty who comprehensibly lacked course design proficiency. It was the place where a quality intervention was utmost expected to have an impression. As proficiency in course design became more approximately accessible in the field, QM began creating tools and services to address other factors(Dr. Deb Adair, QM Executive Director January 2022).

Scope of the study

The scope of this study is restricted to the Senior Secondary Schools of the Punjab State. Senior Secondary education acts as a link between primary and higher education and a significant stage towards planning for vocational and professional education. In this phase of education student's general education came to an end and at this step they have to make selections of the courses for the upcoming studies of their curiosity. There are over almost 5000 (Table 1) such schools in the whole state that becomes the population for the study. The whole Punjab is divided into four regions (Fig: 1) named as Majha, Doaba, Malwa and Pothohar. Data has been collected from 450 schools from these 4 regions has been taken under study.

Population of the study

There are more than 5000 Senior Secondary Schools in Punjab and out of which about 4000-4500 Sr. Sec. Schools are using digital education for learning and teaching purpose. The number of schools correspondingly from all the four parts of the state of Punjab and collected the data. The sampling method and justification is given in the upcoming section.

Sampling method & its justification

The sample size of 450 schools almost 10% of the population has been taken to collect valuable information. Stratified convenience sampling method was used in the research. One teacher (approx. 450 in totality) and two students (approx. 900) Out of the selected schools were surveyed for the research on service quality of digital education.

Two separate questionnaires were created separately for teachers as well as students to gather the primary data. The questionnaire for teachers consisted of 59 questions and that for students consisted of 69 questions. According to Hair et al., a minimum eight to ten times data points of the number of items are needed to do factor analysis (2010). After submitting 450 questionnaires, received roughly 440 of which 10 had missing or unbalanced information. The survey had a 97.6% response rate. For students also the researcher was able to collect about 865 responses with response rate of 96.11 %. The stratification was carried out as follows:

Demographic Profile of the Respondents

The general profile of the responders is covered in this section. These questions were posed as a questionnaire to the respondents, and they provided their responses concerning the preferences from which these tables were created. About 950 samples for students and 450 for teachers were taken in the data collection, of which 85 responses of students and 10 for faculty were excluded due to inaccuracies. As a result, 865 samples left for students and 440 of that of teachers. This sample is a good demonstrative of state of Punjab as the sample is collected from nearly all areas of Punjab and is acceptable to undertake factor analysis as well as SEM (Hair et. al.2020).



**Pankaj Mohindru and Kamaljit Singh****Age Education of Respondents**

The important component of the study is the age of the respondents. The respondents to the survey who were 17 years of age made up the majority, which is nearly 43% of the responders (Fig 6.2). The 18 years age is the next important segment. These were generally students of class 11th and 12th who responded to the survey. As far as the faculty survey was concerned the extreme number of respondents was from the age group of 30 to 35 years. Others were ready to accept the survey and the young teachers could not understand the significance of the study so they did not respond properly.

Gender of Respondents

The gender breakdown of the responders is concealed in the next table. Consequently, it is particularly evident from table 6.3 that, out of 865 student respondents, 346 respondents are female. Likewise in the case of faculty respondents also it was established that very few female teachers responded. The female respondents of the study were mostly from urban schools as the rural teachers hesitated to respond to the survey.

Type of school of Respondents

Another crucial element of the study is the respondents' level of education. The types of school the respondents are studying are shown in table 6.4. The majority of respondents both faculty and students were from private school. Very few government school students and faculty are undertaking online education. The respondents who are undertaking digital education from government school are mostly urban people. Students of rural government schools do not have much idea about online education also. As expected, the trends are quite advanced in case of private schools. Majority of the private schools are in urban areas and are laying a lot of stress on digital education.

Area of school of Respondents

The next important aspect of the study is the area of school of the respondents. Most of the faculty members who responded to the survey were from the urban schools where as semi urban school faculty were second in the order. The situation was bit different in case of students where almost 50 per cent respondents were from the semi urban school and about 30 per cent from the urban area. This indicates the interest levels of the school teachers and students towards electronic education as well as studies promoting them. Faculty from the rural areas generally avoided talking to the researcher and the ones who responded were also not very proactive.

Type of Subject of Respondents

The next significant feature of the respondent's profile is subject of the respondents. The four different domain areas were taken i.e., arts, commerce, medical and non-medical to ask from the students. The results of the study are given in table no 6.6. It can be seen that maximum students as well as faculty engaged in digital education are from medical or non-medical line. Commerce students are next significant group of students who are using electronic education.

RESULTS

This objective intends to develop a research model that can help in understanding of the relationship between service quality of digital education and other factors like learning enthusiasm etc with improved service quality. Since service quality is a second order construct which is a combination of reliability responsiveness, assurance, empathy and tangibility we use the structural equation modelling tool to determine relationships. This model is prepared by collecting data from the students studying in the school (all private, government and government aided schools) of Punjab that are using digital education methods to study. Before applying the confirmatory factor analysis i.e. SEM, the data was subjected to exploratory factor analysis to check whether the constructs coverage appropriately or not. The results of the factor analysis show that there were no signs of multi co-linearity in the constructs so the researcher proceed with the CFA. Based on the literature review the following research model is suggested:





Research Model

The following section shows the pictorial representation of the research model. Based on intense literature review and hypothesis the researcher is able to finalise the model. In this model service quality is taken up as second order construct that is measured by reliability, responsiveness, assurance, empathy and tangibility. The remaining constructs are taken as first order.

Testing of Normality

The Skewness-Kurtosis method was used to test the univariate normality of the variables (Hair, et al., 2010; Byrne, 2010). All of these were computed using the SPSS version (software package for social sciences). All of the computed values were found to be within the recommended range. As shown in table 4.14, the value of skewness was less than three, and the value of kurtosis was less than eight. Kline (2011); West, Finch, and Curran (1995).

Structural equation modeling analysis

The analysis moment structures (AMOS) statistical software and the structural equation modelling (SEM) technique were used to evaluate the hypothesis given in the research model (Figure 4.1), and a two-stage method was used to test the theoretical relationships (Anderson and Garbing, 1922; Schumacker and Lomax, 2010). All the constructs of the model were first measured and then structurally modeled.

Measurement model: Confirmatory factor analysis

The present study used maximum likelihood approach to estimate the model's parameters in and confirmatory analysis (CFA) was used to determine the reliability and validity of the obtained data. The variance-covariance matrices formed the background of all analyses (Hair et al., 2010). The convergent and discriminant validity of the measuring model were evaluated using standardized loadings, as shown in Table 7.3. The Table 7.3 also includes the obtained Cronbach's alpha, average variance extracted (AVE), and composite reliability (CR) values. All of the standardized values are greater than .662, and the t-values show significance at the 0.001 level. Cronbach's Alpha, composite reliability, and average variance extracted (AVE), as recommended by Hair et al., (2010) can be used to validate construct reliability, convergent validity, and discriminant validity. In Table 7.3, all Cronbach's Alpha values are significantly higher than the 0.02 (Nunnally, 1962) threshold level and CR values ranging from 0.606 to 0.958 exceeded the 0.60 i.e., above the threshold level, indicating that the scale was reliable (Hair et al., 2010). The AVE values range from 0.617 (RS) to 0.747 (AS), all of which are greater than 0.05 i.e. threshold value, Hair et al. (2010). Furthermore, all of the squared AVE values in Table 7.3 are greater than inter-correlation estimates for other related constructs, indicating that the measurement model has high discriminant validity (Fornell and Larcker, 1981). The independent variables were also looked for multi-collinearity. The variance expansion factors (VIF) for all independent variables were less than the threshold value of 5.0. (Belsley, Kuh, and Welsch, 1960)

Model Fitness

To ensure the model's fitness, all significant and required fit indexes were evaluated (Hair et al., 2010, Kline, 2010). Purifications and reassessments were carried out because two major indices, GFI and CFI, were unable to meet the threshold values ensuring a good fit between the data and the proposed model (Anderson and Gerbing, 1988; Bagozzi and Yi, 2012; Byrne, 2010). This is an iterative procedure that improves model fitness by using various criteria such as standardized regression weights (factor loadings), modification indices, and standardized covariance matrix (Byrne, 2010; Hair et al., 2010).

Structural model and hypotheses testing

The structural model's results are strikingly similar to those of the measurement model, according to the same criteria used in the measurement model to determine the goodness of fit of the suggested model. This demonstrates how well the data fits the model. GFI = 0.952, AGFI = 0.225, CFI = 0.936, NFI = 0.915, RMR = 0.065, and RMSEA = 0.066 all fell within the threshold values: GFI = 0.915, AGFI = 0.255, CFI = 0.959, NFI = 0.933, RMR = 0.062, and RMSEA = 0.063. When it came to path coefficient analysis, the model's various causal links proved significant. Table 7.5 depicts the research model's hypotheses outcomes and path coefficients, as well as the path analysis results.



**Pankaj Mohindru and Kamaljit Singh**

Pertaining to the path analysis the coefficient of the first order path analysis were found to be LN ($\beta = 0.515$, $p < 0.001$), OR ($\beta = 0.386$, $p < 0.001$), EN ($\beta = 0.216$, $p < 0.001$), GI ($\beta = 0.228$, $p < 0.001$), IR ($\beta = 0.296$, $p < 0.001$), EL ($\beta = 0.226$, $p < 0.001$), EA ($\beta = 0.326$, $p < 0.001$) all have a statistically significant relationship with BI to adopt mobile payments. The result of second path coefficients have also found to be significant RE ($\beta = 0.436$, $p < 0.001$), RS ($\beta = 0.368$, $p < 0.001$), AS ($\beta = 0.208$, $p < 0.001$), EMP ($\beta = 0.206$, $p < 0.001$), T ($\beta = 0.310$, $p < 0.001$).

DISCUSSION

The result of the structural equation modelling highlighted certain very significant results that helped the researcher to achieve the objective of the research. The most important factor that emerged from the analysis is learning. With highest beta value ($\beta = 0.515$) this emerged to most important concern for students. The second important construct that emerged out of the study was organization with $\beta = 0.386$. This means how the knowledge material is construct and made easy for student to understand. Basically, if the student find the online learning difficult to understand than he/ she will not be able to use and gain knowledge from it. The next significant construct was examination and assignments with $\beta = 0.326$. Indian students give a lot of importance to the assignment work and more importantly exams. If the online education does not help those getting good marks, the facility is of no use to the students. The next important construct as per their significance were individual relation with $\beta = 0.296$, Group interaction with $\beta = 0.228$, elaboration with $\beta = 0.226$, and enthusiasm with $\beta = 0.216$. The students are very serious about their personal query handling as well as the teachers inviting them for group discussion. This motivates them and brings them in limelight. Besides the coefficients of second order path analysis, where the construct service quality was measured as second order construct. This was done using five constructs i.e., reliability, responsiveness, tangibility, assurance and empathy. As far as the results of second order path coefficients are concerned, the maximum significant factor proved to be Reliability with $\beta = 0.436$. This means that the students expect that the information provide by students, school website and all different sources should be accurate and trust worthy. The next important factor that contributes to service quality is responsiveness with $\beta = 0.368$. This means that the teachers and school staff should be quick in their problem solving and should provide quick solutions to their problem. The next important construct is Tangible with $\beta = 0.310$ which means school should have all the latest all infrastructure and facilities so that the online education can be used effectively. The last two important constructs are assurance with $\beta = 0.208$ and empathy with $\beta = 0.206$. This means that although the students lay importance on assurance and empathy while taking up online education but their significance is less.

REFERENCES

1. J.B.Arbaugh (2000). Virtual Classroom versus Physical Classroom: An Exploratory Study of Class Discussion Patterns and Student Learning in an Asynchronous Internet-Based MBA Course. Article in Journal of Management Education, Vol. 24 No.2, April 2000 213-233.
2. ShikhaDua, Ms SeemaWadhawan, Ms Sweetly Gupta (2016). Issues, Trends & Challenges of Digital Education: An Empowering innovative classroom model for learning. International Journal of Science Technology and Management. Vol. No.5, Issue No. 05. ISSN 2394-1537
3. Jayesh M. Patel (2017). Web based tools of technology in future teaching learning strategies. international education. E-ISSN No: 2454-9916, Volume 3, Issue 2
4. Dr. Ajay Kumar (2019). Digitalization of educational system in India. International Journal of Applied Research. SP4: 04-06. ISSN 2394-7500
5. Dr.RanjuBala (2019). Digitization in Higher Education. International Journal of Applied Research. SP4: 297-299
6. Dr.UmeshKumari (2019). Digital education: Scope and challenge. International Journal of Applied Research. SP4:01-03





Pankaj Mohindru and Kamaljit Singh

7. Dr. Vijay Laxmi and Neelam (2019). Digitization of Higher Education. International Journal of Applied Research. SP4: 197-199
8. Lane Fischer, John Hilton III, T. Jared Robinson, David A. Wiley (2015). A multi-institutional study of the impact of open textbook adoption on the learning outcomes of postsecondary students. 27:159-172
9. Long Pham et al (2019). Does e-learning service quality influence e-learning student satisfaction and loyalty? Evidence from Vietnam. International Journal of Educational Technology in Higher Education, volume 16, Article number: 7 (2019)
10. Aderonkelfeoma Folorunsho (2016) . Young Children's Engagement and Interactions with Digital and Non-Digital Activities: A Case Study
11. R Surgant et al (2016). Impact of Information Dimension on Service Quality of Digital Learning Solutions in Schools. Review of Integrative Business and Economics Research, Vol. 5, no. 1, pp.152-167, January 2016
12. Navkiran Kaur (2019). Digitization of Education in 21st Century. International Journal of Applied Research. SP4: 20-22
13. Tagreed Kattoua, Prof. Musa Al-Lozi, Dr. Ala'aldin Alrowwad (2016)- A Review of Literature on E-Learning Systems in Higher Education. ISSN:2229- 6247
14. Ravinder Kaur (2019). Digitization of Indian Education: A hope or hype. International Journal of Applied Research. SP4:01-03
15. Purnima Valiathan (2002). Blended Learning Models. old. astd.org/LC/2002/ 0802_valiathan.htm
16. Singh, G.; O'Donoghue, J.; and Worton, H., A Study Into The Effects Of e-learning On Higher Education, Journal of University Teaching & Learning Practice, 2(1), 2005.
17. Jinal Jani et al (2015). Digital India: A need of Hours. Volume 5, Issue 8, August 2015.
18. <https://www.sciencepubco.com/index.php/ijet/article/view/26759/13755>
19. <http://www.babushahi.com/pae2017/constituencies.php>
20. <https://www.digitaldoughnut.com/articles/2018/september/5-ways-in-which-digital-education-is-changing-the>
21. <https://e-learningindustry.com/digital-education-is-transforming-teaching-methods-7-ways>
22. <https://en.wikipedia.org/wiki/Education>
23. <https://www.ncbi.nlm.nih.gov/pmc/articles/PMC1764819/>
24. <https://pdfs.semanticscholar.org/5443/6f2ce08a83fb5f14f523e79b65b8a2c2f708.pdf>
25. researchgate.net/publication/309242990_A_Review_of_Literature_on_E-Learning_Systems_in_Higher_Education
26. <http://educomp.com/content/story-digital-education>
27. <https://economictimes.indiatimes.com/industry/services/education/digital-india-indian-education-system-has-a-great-opportunity/articleshow/46200490.cms>
28. http://timesofindia.indiatimes.com/articleshow/94987904.cms?utm_source=contentofinterest&utm_medium=text&utm_campaign=cppst

Table 1: Schools population for the study

Regions of Punjab	Count of Senior Secondary Schools
Doaba	991
Majha	994
Malwa	2717
Poah	425
Grand Total	5127

Table 2: Table showing sampling Distribution

S no.	Regions of Punjab	Data points for faculty	Data points for students
1	HOSHIARPUR	30	60
2	JALANDHAR	30	60





Pankaj Mohindru and Kamaljit Singh

3	KAPURTHALA	30	60
4	S.B.S. NAGAR	30	60
5	AMRITSAR	30	60
6	GURDASPUR	30	60
7	PATHANKOT	30	60
8	TARN TARAN	30	60
9	BARNALA	30	60
10	PATIALA	30	60
11	SANGRUR	30	60
12	LUDHIANA	30	60
13	FATEHGARH SAHIB	30	60
14	ROOPNAGAR	30	60
15	SAS NAGAR	30	60
TOTAL		450	900

Table 3: Age of the respondents

Age of the student respondents				
	16 years	17 years	18 years	Above 18 years
Student	180	379	242	64

Age of the Faculty respondents				
	25-30 Years	30-35 years	35-40 years	Above 40 years
Faculty	48	228	93	71

Table 4: Gender of the respondents

Gender of the respondents		
	Male	Female
Faculty	298	152
Student	519	346

Table 5: Type of school of Respondents

Type of school of Respondents			
	Government	Government aided	Private
Faculty	89	117	234
Student	140	288	437

Table 6: Area of school of Respondents

Area of school of Respondents			
	Urban	Rural	Semi Urban
Faculty	255	71	114
Student	230	189	446

Table 7: Type of Subject of Respondents

Type of Subject of Respondents				
	Arts	Commerce	Medical	Non – medical
Faculty	29	97	178	146
Student	94	156	320	295





Pankaj Mohindru and Kamaljit Singh

Table 8: Assessment of Normality

	Mean	Std. Deviation	Skewness	Kurtosis
RE1	3.668	.6666	.666	-.061
RE2	3.665	.6656	.655	.101
RE3	3.635	.6656	.666	.366
RE2	3.566	.6636	-.603	.635
RE5	3.556	.6568	-.566	.516
RE6	3.565	.6683	-.566	.366
RE6	3.655	.6666	.615	.156
RS1	3.660	.6506	.666	.050
RS2	3.665	.6655	.366	.105
RS3	3.655	.5655	-.666	.063
RS2	3.665	.5036	-.606	-.056
RS5	3.606	.5161	-.553	.055
RS6	3.526	.5336	-.650	.366
AS1	3.561	.5106	-.563	.110
AS2	3.635	.6265	-.366	.136
AS3	3.666	.6616	.566	.066
AS2	3.661	.6206	-.556	.153
AS5	3.666	.6565	.656	.666
AS6	3.626	.5355	-.365	.061
AS6	3.606	.6660	-.301	.056
LN1	3.666	.5566	-.353	.061
LN2	3.630	.5653	.165	-.660
LN3	3.666	.6508	-.666	-.666
LN2	3.668	.6666	.666	-.061
EMP1	3.665	.6656	.655	.101
EMP2	3.635	.6656	.666	.366
EMP3	3.566	.6636	-.603	.635
EMP2	3.556	.6568	-.566	.516
EMP5	3.565	.6683	-.566	.366
T1	3.655	.6666	.615	.156
T2	3.660	.6506	.666	.050
T3	3.665	.6655	.366	.105
T2	3.655	.5655	-.666	.063
T5	3.665	.5036	-.606	-.056
T6	3.606	.5161	-.553	.055
EN1	3.526	.5336	-.650	.366
EN2	3.561	.5106	-.563	.110
EN3	3.635	.6265	-.366	.136
EN2	3.666	.6616	.566	.066
OR1	3.661	.6206	-.556	.153
OR2	3.666	.6565	.656	.666
OR3	3.626	.5355	-.365	.061
OR2	3.606	.6660	-.301	.056
G11	3.666	.5566	-.353	.061
G12	3.630	.5653	.165	-.660
G13	3.666	.6508	-.666	-.666





Pankaj Mohindru and Kamaljit Singh

GI2	3.668	.6666	.666	-.061
IR1	3.665	.6656	.655	.101
IR2	3.635	.6656	.666	.366
IR3	3.566	.6636	-.603	.635
IR2	3.556	.6568	-.566	.516
EL1	3.565	.6683	-.566	.366
EL2	3.655	.6664	.615	.156
EL3	3.668	.6466	.664	-.061
EL2	3.665	.6656	.654	.101
EA1	3.635	.6656	.666	.366
EA2	3.566	.6636	-.603	.635
EA3	3.556	.6548	-.566	.516
EA2	3.565	.6683	-.566	.366
EA5	3.655	.6466	.615	.156

Table 9: Standardized loadings, Cronbach's alpha values, CR and AVE

Constructs	Items	Standardized loadings	Cronbach's Alpha	Composite Reliability (CR)	Average Variance Extracted (AVE)
Reliability (RE)	RE1	0.616	0.903	0.606	0.662
	RE2	0.81			
	RE3	0.859			
	RE4	0.665			
	RE5	0.866			
	RE6	0.651			
Responsiveness (RS)	RS1	0.805	.817	0.824	0.617
	RS2	0.626			
	RS3	0.616			
	RS4	0.851			
	RS5	0.62			
	RS6	0.652			
Assurance (AS)	AS1	0.688	.946	0.958	0.747
	AS2	0.665			
	AS3	0.816			
	AS4	0.635			
	AS5	0.255			
	AS6	0.616			
	AS7	0.613			
Learning (LN)	LN1	0.665	.837	0.874	0.660
	LN2	0.806			
	LN3	0.661			
	LN4	0.803			
Empathy (EMP)	EMP1	0.832	.857	0.808	0.639
	EMP2	0.622			
	EMP3	0.829			
	EMP4				
	EMP5	0.616			
Tangibles (T)	T1	0.81			
	T2	0.859			





Pankaj Mohindru and Kamaljit Singh

	T3	0.665	.843	0.824	0.638
	T4	0.866			
	T5	0.651			
	T6	0.865			
Enthusiasm (EN)	EN1	0.805	.783	0.740	0.645
	EN2	0.626			
	EN3	0.616			
	EN4	0.851			
Organization (OR)	OR1	0.62	.819	0.845	0.617
	OR2	0.652			
	OR3	0.688			
	OR4	0.665			
Group Interaction (GI)	GI1	0.816	.944	0.917	0.722
	GI2	0.635			
	GI3	0.255			
	GI4	0.616			
Individual Relation (IR)	IR1	0.613	.844	0.874	0.661
	IR2	0.665			
	IR3	0.806			
	IR4	0.661			
Elaboration (EL)	EL1	0.803	.852	0.898	0.679
	EL2	0.832			
	EL3	0.622			
	EL4	0.829			
Examination and assignments (EA)	EA1	.784	.824	0.829	0.533
	EA2	0.616			
	EA3	0.81			
	EA4	0.859			
	EA5	0.665			
Improved Service quality (ISQ)	ISQ1	.645	0.826	0.674	0.521
	ISQ2	0.616			
	ISQ3	0.81			

Table 10: Discriminant Validity

RE	RS	AS	LN	EMP	T	EN	OR	GI	IR	EL	EA	ISQ
RS	0.622											
AS	0.665** *	0.621										
LN	0.526** *	0.566** *	0.639									
EMP	0.666** *	0.630** *	0.636** *	0.666								
T	0.696** *	0.625** *	0.535** *	0.361** *	0.656							
EN	0.621** *	0.525** *	0.632** *	0.566** *	0.635** *	0.636						





Pankaj Mohindru and Kamaljit Singh

OR	0.626** *	0.562** *	0.613** *	0.556** *	0.665** *	0.515* *	0.62					
GI	0.569** *	0.656** *	0.512** *	0.663** *	0.659** *	0.569* *	0.665* *	0.622				
IR	.612***	.622***	.526***	.689***	.622***	.656**	.682**	.626***	.632** *			
EL	0.659** *	0.569** *	0.665** *	0.525** *	0.632** *	0.566* *	0.659* *	0.569** *	0.665* *	0.612		
EA	0.621** *	0.525** *	0.632** *	0.566** *	0.659** *	0.569* *	0.665* *	0.659** *	0.569* *	0.665** *	0.615	
ISQ	0.659** *	0.569** *	0.665** *	0.659** *	0.569** *	0.665* *	0.632* *	0.566** *	0.659* *	0.569** *	0.665* *	0.62 9

Note: Factor Correlation Matrix with squared roots of AVE on the diagonal

Table 11 :Path Coefficients and result of the analysis

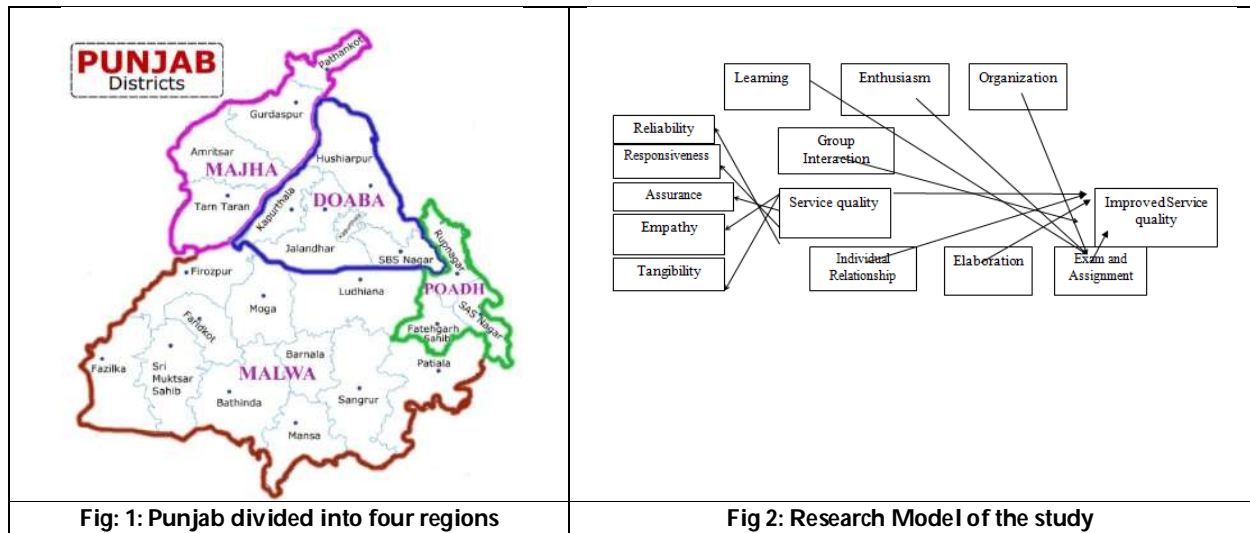
Hypotheses	Path	Standardized direct Effect	Critical Ratio	Result
H1	ISQ \leftarrow LN	0.515	5.612***	Accepted
H2	ISQ \leftarrow OR	0.386	11.590***	Accepted
H3	ISQ \leftarrow EN	0.216	13.590***	Accepted
H2	ISQ \leftarrow GI	0.228	3.668***	Accepted
H5	ISQ \leftarrow IR	0.296	12.622***	Accepted
H6	ISQ \leftarrow EL	0.226	12.013***	Accepted
H7	ISQ \leftarrow EA	0.326	6.632***	Accepted
Second order path coefficients				
H8	SQ \leftarrow RE	0.436	16.190***	Accepted
H9	SQ \leftarrow RS	0.368	8.638***	Accepted
H10	SQ \leftarrow AS	0.208	8.638***	Accepted
H11	SQ \leftarrow EMP	0.206	16.190***	Accepted





Pankaj Mohindru and Kamaljit Singh

H12	SQ ← T	0.310	8.638***	Accepted
-----	--------	-------	----------	----------

Notes: * $p < 0.001$, ** $p < 0.001$, *** $p < 0.001$ 



Comparative Analysis of Proposed Deep Learning based Vehicle Detection Model for Low Light Intensity Conditions

Pramod Kumar Vishwakarma^{1*} and Nitin Jain²

¹Ph.D. Research Scholar, Department of Computer Science and Engineering, Chandigarh University, Gharuan, Mohali, Punjab-140413, India.

²Professor, Department of Computer Science and Engineering, Chandigarh University, Gharuan, Mohali, Punjab-140413, India.

Received: 22 Jan 2024

Revised: 09 Feb 2024

Accepted: 06 May 2024

*Address for Correspondence

Pramod Kumar Vishwakarma

Ph.D. Research Scholar,
Department of Computer Science and Engineering,
Chandigarh University, Gharuan,
Mohali, Punjab-140413, India.
Email: pramod.v1201@gmail.com



This is an Open Access Journal / article distributed under the terms of the **Creative Commons Attribution License** (CC BY-NC-ND 3.0) which permits unrestricted use, distribution, and reproduction in any medium, provided the original work is properly cited. All rights reserved.

ABSTRACT

Most object detection models cannot fulfill great execution under evening and other lacking enlightenment conditions, which may be since of the grouping of enlightening lists and run of the process labeling appears. Open enlightening files assembled for protest discovery are for the most part captured with satisfactory encompassing lighting. In any case, their labeling appears commonly center on clear objects and neglect murky and blocked objects. Hence, the location execution levels of routine vehicle location strategies are confined in evening conditions without satisfactory brightening. At the point when objects include few pixels and the nearness of basic components is uncommon, ordinary convolutional neural systems (CNNs) may involvement the sick impacts of veritable information incident since of the not too bad number of convolutional assignments. This review presents answers for information assortment and the labeling show of evening information to deal with different kinds of circumstances, remembering for vehicle detection. Besides, the review proposes an explicitly upgraded framework dependent on the quicker area-based CNN model. The framework has a handling velocity of 16 edges each second for 500×375 -pixel images, and it accomplished a mean normal accuracy (Guide) of 0.8497 in our approval section including metropolitan evening and amazingly deficient lighting conditions. The trial results showed that our proposed strategies can accomplish high detection execution in different evening time conditions, for example, metropolitan evening time conditions with deficient brightening, and very dim conditions with almost no lighting. The proposed framework beats unique techniques that have a Guide worth of around 0.2.





Keywords: Deep learning, Object detection, Object tracking, YOLOv8, Vehicle detection, Model, CNN.

INTRODUCTION

Highway control and intelligent activity executives rely heavily on vehicle detection and estimations in highway watching video situations. An enormous data set of activity video footage has been acquired for examination thanks to the well-known foundation of activity surveillance cameras. A more distant, off-street surface can be considered for the main part at a high survey point. From this vantage position, the vehicle's question measure varies dramatically, and the finding precision of a little object far from the road is minimal. It is critical to effectively manage the over difficulties and help implement them, regardless of mind-boggling camera scenarios. Using the results of vehicle detection for vehicle counting and tracking of multi-object, this paper focuses on the aforementioned challenges and proposes a reasonable course of action. Currently, there is a wall separating the fields of deep learning and conventional machine vision when it comes to object detection in vehicles that rely on visual cues. Traditional methods of machine vision isolate a vehicle from an appropriate background image by tracking its motion. There are three main methods that fall under this category [1]: using foundation deduction [2], consistent video frame contrast [3], and optical stream [4]. By comparing the pixel intensities of two consecutive video frames, the video frame differentiation technique determines the contrast. Other than, the moving forefront district is isolated by the edge [3]. By utilizing this strategy and suppressing commotion, the ending of the vehicle can likewise be distinguished [5]. At the point when the establishment picture within the video is settled, the foundation data is utilized to build up the establishment model [5]. Then, at that point, each outline picture is contrasted and the foundation model, and the moving object can likewise be fragmented.

The optical stream method is capable of locating the motion region of a video. The generation of the optical stream field incorporates both the velocity and direction of motion of each individual pixel [4]. Methods that rely on vehicle characteristics for detection purposes, including the Speeded Up Robust Features (SURF) and the Scale Invariant Feature Transform (Channel) techniques, have been utilised frequently. To complete tasks like vehicle detection and layout, for instance, 3D models have been employed [6]. Vehicles are categorized into three groups: cars, buses, and motorcycles, based on the connection bends of 3D ridges on their exteriors [7]. When applied to the problem of object identification in vehicles, deep convolutional networks (CNNs) have shown astonishing results. CNNs have the ability to perform tasks that are connected to machine learning, such as case, arrangement, and bounding box relapse, and they are also extremely capable of learning information about pictures [8]. One can usually classify the detection method into two broad groups. The two-stage methodology makes an up-and-comer box of the object by means of different calculations and a while later characterizes the protest by a convolutional neural arrange. The one-stage procedure doesn't make an up-and-comer box be that as it may straightforwardly changes over the situating issue of the object-bounding confine to a relapse issue for handling.

Locale CNN (R-CNN) [9] uses particular region search [10] within the picture as part of the two-stage approach. It takes a lot of time to prepare the deeper plan of the organization and uses up some of the capacity notice, and the picture contribution to the convolutional network should be of a fixed size. You Just Have to Look Once (Fair Go For It) [13] and Single Shot Multibox Detector (SSD) [12] are two of the most prominent one-stage approaches. SSD utilises the Multibox [14], Locale Proposition Network (RPN), and multi-scale representation techniques in order to place the object with greater precision. Additionally, it makes use of a preset set of anchor boxes that have varied angle proportions. The Just do it [13] network divides the image into an appropriate amount of matrices, in contrast to SSD. Predicting objects with their centers of mass inside the system is the responsibility of each lattice. The BN (Cluster Standardization) layer was added to YOLOv2 [15], which speeds up network intermingling by standardizing the contributions of each layer. For every one of the ten categories, YOLOv2 uses a multi-scale preparation method to pick a different image size at random. In order to find objects in vehicles, we use the YOLOv3 [16] network. Following in the footsteps of YOLOv2, YOLOv3 makes use of calculated relapse for the object class. As



**Pramod Kumar Vishwakarma and Nitin Jain**

a two-class cross-entropy misfortune approach, categorization misfortune may handle various title concerns for the same object. In addition, the container certainty is relapsed using important relapse to find out if the IOU of the inferred box and the genuine box is more than 0.5. In the event that multiple need boxes satisfy the requirement, the one with the largest amount of time remaining on the IOU will be taken. Foreseeing the object in the image, YOLOv3 employs three distinct scales in the final protest figure. Methods for detecting vehicles using vision have produced abundant results. To identify the difference in two images with a short time frame slack, the Multivariate Adjustment Detection (Distracted) method [20] was employed in [19] between sections of the Bangalore, India, highway. A modified image that incorporates the moving cars is used to measure the vehicle thickness of the road. The authors of [21] locate the histogram of the edge steepness by applying the Canny edge calculation [22] to a road image; they use the Koramangala road in Bangalore, MG as an example. After that, a closed vehicle model is determined by the steepness, and the k-implies calculation is used to divide the insights regarding the steepness of the edge into three distinct portions. In order to eliminate obstructions caused by improvements in the scene, a shading model was created using a difference-based methodology to identify and eliminate vehicle shadow zones [23]. The elimination of the shadow zone has the potential to considerably improve the effectiveness of the vehicle detecting system.

In [23], highways were the sites of the examination. In order to build a finder for vehicle detection, which was tested using Indian vehicle photos, the authors of [24] used the Accumulate and Haar-like properties. Whatever the case may be, the over approach fails to differentiate between different types of vehicles when used for vehicle detection. Furthermore, without illumination, it is difficult to eliminate the vehicle's edge or identify it while it is in motion, leading to certain problems with poor vehicle recognition accuracy and impacting the detection findings for additional use [19, 20]. Another fundamental ITS task is the development of advanced vehicle object identification applications, such as multi-object tracking [26]. When it comes to introducing objects, the majority of multi-object tracking methods use either Detection Based Tracking or Sans detection tracking. The foundation displaying technique is initially utilised by the Detection Based Tracking method in order to recognise moving objects inside video frames for the purpose of tracking. While the DFT technique is required to introduce the next item, it is unable to handle the expansion or takeoff of existing objects. A Number of Concerns Both the intra-frame object comparability and the related between-frame object issue must be taken into account in the subsequent calculation. Normalised cross-correlation (NCC) can be used to determine the resemblance of items inside a frame. The Bhattacharyya distance is utilised, for instance, in [27], in order to ascertain the distance of the shading histogram that links the objects together. It is important to ensure that a query can only occur on a single pathway, and that a single pathway can only compare to a single object when there is a relationship between objects that are spread across multiple frames. Rejection at the detection level or avoidance at the direction level can handle this problem at the moment. Although it is sluggish, [28] used SIFT feature foci for object tracking to address the problems caused by the size and brightness fluctuations of moving objects. According to [29], this study suggests using the Circle include point detection calculation. Sphere outperforms SIFT in terms of extracting feature centres and does it at a far faster rate. To summarise, it seems that research on deep convolutional organise techniques has surpassed that on ordinary tactics for vehicle object identification. The number of publicly available datasets including scenes of explicit activity is decreasing. Convolutional neural networks are prone to scalability issues, which renders small item finding inaccurate.

PROPOSED MODEL

Used dataset

The image in the dataset is taken from a video of highway inspections (Fig. 4). With its 12-meter height, adjustable field of vision, and lack of a fixed placement, the highway checking camera was installed on the side of the road. The photographs taken from this vantage point depict the lengthiest stretch of highway and feature vehicles whose sizes are blown away. All told, the images in the collection come from 23 separate observation cameras set up in various environments with varying degrees of illumination. The automobiles are categorized into three distinct groups in this dataset. A text archive containing the item classification's numerical code and the bounding box's normalized



**Pramod Kumar Vishwakarma and Nitin Jain**

facilitate worth stores the mark record. Remember that we made the tiny things in the surrounding street area more clear; this is how the dataset incorporates objects of vehicles that have been massively resized. The number of features in an example that is far from the camera is much lower than in one that is close to it. The detection accuracy of small vehicle objects can be improved with the use of clarified events of varying sizes. Separate sets, designated as "preparation" and "test," make up this dataset. In general, there are 5.15 elucidated illustrations in every picture. Potentially applicable in many different countries, including India, our dataset has the potential to be a comprehensive vehicle focus set. Our dataset offers a plethora of high-quality images, proper lighting, and detailed descriptions, in contrast to the existing vehicle datasets. We divided up the road surface area so that subsequent vehicle detection could make an accurate contribution. A picture without revolution is created for the erased road surface by constructing a square shape around a basis. A quarter of the handled image is the near-to-removed space of the road surface, and the other four-fifths of the image are the near-to-proximal space of the road surface; these two regions are defined in relation to the beginning of the arrange hub. In order to fix the problem where the car in the picture could be split in half using the previous method, the close to proximal and near to far off regions cross-over by 100 pixels. We examine the near-to-proximal and near-to-removed regions' pixel upsides segment by segment. You can't see the road surface location in the segment's image if all of the pixel values are zero. In this case, the segment is deleted. Distant regions and proximal spaces of the street surface are the saved regions after the not-street surface regions are banished.

Vehicle detection using deep learning

The YOLOv8 model is made up of different types of layers that work together to understand images and find objects within them. These layers include convolutional layers, bottleneck layers, spatial pyramid pooling, upsample layers, concatenation layers, and a detection layer. Each type of layer has its own specific job in helping the model learn about images and spot objects. The model's architecture, shown in Table 2, details how these layers are arranged. Convolutional layers are like the building blocks, helping the model see different parts of the image. They start by transforming the input image to help the model recognize features better. As the model goes deeper, these layers keep doubling the information it understands while also paying attention to different details in the image. The bottleneck layer is another important part of this model. It's used multiple times and helps the model become smarter while keeping the calculations it needs to do under control. Think of it like a smart way to handle lots of information efficiently. The spatial pyramid pooling layer helps the model understand the size of objects in the picture. It combines information from different parts of the image to make sure it doesn't miss objects that might be big or small. Layers like up sample and concatenation are like tools that help the model see more details. They increase the sharpness of what the model understands and allow it to combine different pieces of information from various parts of the image. This is really helpful for finding objects that might be different sizes or in different parts of the picture. Finally, the detection layer is responsible for the actual job of finding objects. It figures out what objects are in the image and where they are located. It looks at different sizes and shapes of objects to make sure it finds them accurately. The way YOLOv8 is designed helps it do a great job of finding objects in pictures of all sizes and shapes. It's really good at doing this quickly, which makes it perfect for tasks where you need to spot things in real-time, like in video or live camera feeds.

DESIGN OF THE MODEL

Using the detected car box placements of the two areas, we want to return to the original image and verify the object's placement. Potentially invaluable is the location and categorization data gleaned from object tracking utilising the vehicle object detection method. The vehicle detection method disregards the specific characteristics and state of the vehicle since the data given above is sufficient for an automobile inspection.

Tracking of Multi-object

This section demonstrates the process of pursuing various objects based on the object confine identified in the "Vehicle detection utilising YOLOv3" section. Here, we extract the features of the recognised automobiles using the Sphere computation, and we get excellent results. When it comes to coordination with expenses and computing execution, the Sphere calculation seems to be preferable. As an alternative to the graphic representation



**Pramod Kumar Vishwakarma and Nitin Jain**

computations used by Sift and SURF, this calculation might be a fantastic choice. To identify feature centres, the Circle calculation employs the Features from Sped up Fragment Test (Quick). Then, it employs the Harris administrator to carry out corner detection. The Short computation is used to calculate the descriptor after the include focuses have been obtained. The system of coordinates is constructed with an extra point as the centre of the circle and the origin of the point position as the x-axis. So, the attribute point identifier is revolution consistent, and the coordinate framework can be swiveled by the picture's rotation. Changing the picture point also allows for the proposal of a dependable point. Once the parallel feature point descriptor is obtained, the highlight centres are coordinated with the help of the XOR operation, which improves the coordination with efficacy.

Analysis of Trajectory

This segment illustrates the analysis of the directions that moving objects are going in as well as the counting of various data pertaining to object traffic. It is possible to travel in either direction on the bulk of the highways, and the streets are separated from one another by disconnection borders. In accordance with the heading of the vehicle tracking direction, we are able to identify the path that the vehicle takes on the planet facilitate framework and indicate its direction of movement as either towards or away from the camera's position (with A and B, respectively). As a detection line for the purpose of vehicle characterisation measurements, a straight line is inserted into the picture of the activity scene. On the top edge of the traffic image, at the halfway point, you can see where the recognition line is positioned. Counting the road activity stream that occurs within both directions at the same time is being done. It is at the point in time when the direction of the item passes the detection line that the information pertaining to the object is recorded. At the end, it is possible to retrieve the total number of items in a particular time period that are organised in a variety of methods and classes.

Framework Using YOLOv8

The eighth version of the YOLO model family is YOLOv8. The YOLO models can identify every object in a picture with just one forward pass; the name comes from the fact that they only look at the image once. One key difference amongst the YOLO models was how they framed the current job. In order to avoid classification issues, the authors of the research rethought the object identification task as a regression problem: how to predict the coordinates of the bounding box. Big datasets like COCO and ImageNet are used to pre-train YOLO models. They may play both the role of student and master at the same time because of this. They are able to learn new courses very rapidly and give quite accurate predictions on the classes they have been instructed on (master ability). In addition to being able to train quickly, YOLO models may achieve great accuracy with relatively modest model sizes. They are more approachable for developers like us since they can be taught on single GPUs. As of early 2023, the most recent version of these YOLO models is YOLOv8. Its predecessors were significantly altered, and it now features anchor-free detection, C3 convolutions, and mosaic augmentation, among other changes. The YOLOv8 model was developed and is maintained by the Ultralytics team; it is an open-source SOTA model. Sharing, modifying, and distributing the program is made possible by the GNU General Public License, which is part of the distribution. There is a thriving and constantly expanding YOLOv8 community. The Ultralytics team is responsible for writing and maintaining YOLOv8. The original developer of YOLO models was computer scientist Joseph Redmon. Using Darknet Architecture, he went through three versions of YOLO, the most recent of which was YOLOv3. With some small tweaks and some PyTorch shadowing, Glenn Jocher renamed YOLOv3 to YOLOv5. Next, YOLOv8 was built by modifying the architecture of YOLOv5. On January 10th, 2023, YOLOv8 was formally launched. It is currently still in the midst of development.

Comparison of YOLOv8 and YOLOv5.

Two major modifications have occurred:

1. Detection Without Anchors
2. Enhancements with Mosaics

Let's take a close look at these modifications one by one:





Pramod Kumar Vishwakarma and Nitin Jain

Detection Without Anchors

First, we need to grasp the concept of anchor boxes in order to grasp anchor-free detection. One of the biggest issues with object detection was fixed with anchor boxes. A grid cell containing the middle of an item is assigned to it before anchor boxes. Building bounding boxes and assigning them to certain classes becomes very complicated if the centers of two objects are identical. One way to look at anchor boxes is as generic forms. Think about a scenario where we have two boxes that serve as anchors: Box 1 and Box 2. Anchor Boxes enhanced training by raising mAP in most cases. These were already part of earlier YOLO models. There are a number of reasons why YOLOv8's architecture deviates from Anchor Boxes: One problem is that the model isn't flexible enough to suit fresh data because it was trained with prebuilt anchors. Second, irregularities can't be accurately mapped using polygon anchor boxes since there aren't enough of them.

Enhancement of Mosaic Data

A lot of picture enhancements are done to training images by YOLOv8. Data mosaicing is one kind of augmentation. A straightforward method of augmentation known as mosaic data augmentation involves feeding the model input that is a composite of four separate photos. Because of this, the model is able to learn real-world objects even when partially obscured or from diverse angles. Mosaic Data Augmentation was deactivated for the past 10 epochs because it was found to decrease performance.

YOLOv8 life cycle Mathematically

The YOLO(You Only Look Once) object detection algorithm, including YOLOv8, involves several mathematical components and steps in its lifecycle as described below.

Input Data

The input image is usually a 3D tensor with the following dimensions: (H, W, C), where H is the height of the image, W is its width, and C represents the number of colour channels (commonly 3 in RGB images). YOLOv8 then uses this information to create an output image.

Anchor Boxes

YOLOv8 anticipates bounding boxes of varying sizes and aspect ratios using anchor boxes. The dataset provides the parameters for these anchor boxes, which are provided in advance as width and height pairs (w_i , h_i).

Grid Cells

We use a structure made up of cells to partition the input image. Everything inside the borders of a given grid cell is subject to its own set of predictions. The design of the network dictates the diagonal and horizontal numbers of grid cells.

Convolutional Neural Network (CNN):

YOLOv8 employs a deep CNN architecture to process the input image and extract features. Convolutional layers, down-sampling layers (such as strided convolution or max-pooling), and feature extraction modules make up the architecture.

$$Z_i = \text{Convi}(Z_{i-1})$$

where (Z_i) represents the feature map produced by the (i th) convolutional layer, and (Convi) denotes the convolutional operation.

Predictions

For each grid cell, Class probabilities and bounding boxes are predicted using YOLOv8. For any prediction involving a bounding box, there are four numbers that reflect its dimensions and centre: (x), (y), (w), and (h), as well as a confidence score (Con_f) indicating the confidence that an object is present within the box. Class probabilities ($P(\text{Class}_i)$) represent the likelihood of the object belonging to a particular class (i).





Pramod Kumar Vishwakarma and Nitin Jain

Prediction = (x, y, w, h, Con_f, P(Class1), P(Class2),, P(Classn))

Non-Maximum Suppression (NMS)

To filter out redundant bounding box predictions, YOLOv8 uses Non-Maximum Suppression. This involves:

- Discarding boxes with low confidence scores ($Con_f < confidence_threshold$).
- Suppressing overlapping boxes by keeping the one with the highest confidence score.

The NMS algorithm computes the Intersection over Union (IoU) between bounding boxes and removes boxes with IoU above a certain threshold.

IoU = Area of Intersection/Area of Union

Evaluation Metrics

- Intersection over Union (IoU): The overlap between the predicted bounding boxes and the ground truth bounding boxes is measure by the IoU.

Precision and Recall

The F1 score is derived from two metrics: recall, which evaluates the proportion of actual positives to the total number of positive predictions, and accuracy, which counts the proportion of true positives to all anticipated positives.

F1 Score

The F1 Score combines recall and precision into a single number by taking their balanced average. It helps to measure how well a model finds relevant items (precision) and captures all relevant items (recall) at the same time.

$$F_1 = 2 \cdot \frac{precision \cdot recall}{precision + recall} \quad (1)$$

$$precision = \frac{TP}{TP + FP} \quad (2)$$

$$recall = \frac{TP}{TP + FN} \quad (3)$$

MAP (Mean Average Precision): The Mean Average Precision, or MAP, is a statistic that takes into account the average accuracy across precision-recall curves for different types of objects.

One of the most common metrics utilised in the field of object recognition and information retrieval is known as Mean Average Precision (mAP). This metric is particularly useful for assessing the effectiveness of models in identifying numerous classes or categories. Calculated by taking the average of the Average Precision (AP) values that were calculated independently for each class or category that was included in the dataset, it is expressed as a percentage.

$$mAP = 1/N \sum_{i=1}^N AP_i ;$$

Where N represent the total number of classes of object



**Pramod Kumar Vishwakarma and Nitin Jain**

RESULTS AND DISCUSSION

The processes that were utilised to test the methods that were outlined in the "Methods" section are described in full below. For the purpose of our testing, we utilised the preexisting collection of vehicle objects that is located in the "Vehicle dataset" area. In order to capture three separate scenes, our inquiry made use of high-quality highway recordings, as can be shown in Figures 4 and 5.

Vehicle tracking and counting

In the aftermath of the acquisition of the object box, we carried out an investigation into the direction of the vehicle and tracked it using the Circle feature point coordinating mechanism. The comparison Sphere expected position was generated inside the study whenever the coordinating with point of each object achieved a value larger than ten. For the purpose of counting, we determined the direction of travel of the vehicle by utilizing the detection line, taking into consideration the procedure that resulted in the development of the following direction. The emphasis of our investigation was on three other films that come from the same era as the scene described in the "Network planning and vehicle detection" section, but each of these films has a different number of frames.

CONCLUSION

Our results included an assessment of our framework's evening detecting hones. Images captured under the artificial illumination of city nightlights can still be processed by our system. No matter how dim the lighting is, the system can still make out the general shapes of objects as if they were completely illuminated, even in very low light. Things with few pixels, items with a haze, and objects that are blocked seem to be the focus of our labeling. The results show that our creative approach to deal with include extraction outperforms conventional methods [7,8], which rely heavily on the illumination from car headlights and taillights, in very dim lighting. Systems with simple paths, such as ResNet101 [2], also have decent night detection performance, as we discovered. Our framework made use of ResNet101 to extract features. During the night, frameworks that use networks with alternate courses as feature extractors may accurately identify partially transparent and somewhat small objects. Interestingly, the ResNet101 framework needed roughly twice as much processing time as the VGG16 framework for images with a 500×375 pixel dimension. In order to achieve continuous detection with a system that has somewhat limited processing capability, the picture size should be reduced for implanted frameworks. Objects that are obstructed, tiny, or hazy, especially in extremely dark environments, are the focus of our review, which also includes advanced labeling methods and frameworks. Even on the exhibition levels, we saw significant simplification and improvements. According to the testing results, whether it's dark outside or there isn't enough light, the models trained with our evening data sets—which were identified by our shows—seem to differentiate between small, obscured objects. In settings that were extremely dim, with almost no brightening or lighting that was incredibly powerless, our methods provided detection execution levels that were worthy of praise. The levels of detection execution achieved by the techniques that were proposed were higher than those achieved by the initial tactics. During the process of handling images at a resolution of 500×375 pixels, the Guide values increased from around 0.2 to 0.8497, achieving a frame rate of 16 frames per second. The visual correlation of the yield photographs provided both an external and an emotional confirmation of this conclusion. The technique that we have suggested is capable of accurately identifying automobiles in a variety of urban evening settings, including those that are extremely dim. In the work that we planned to do in the future, we anticipated working on the implementation of our system by employing several standardization methodologies that were optional. We anticipated that we would be able to zero in on the photographs that were taken under extremely bright lighting conditions. In particular for the data we collected during the evening hours, we advised that suitable measurements be encouraged in order to appropriately quantify the model exhibition for enclosing items.





REFERENCES

1. Abdullah Asım Yılmaz, Iman Askerzade, Mehmet Serdar Guzel, Gazi Erkan Bostanci, "A Vehicle Detection Approach using Deep Learning Methodologies", 2018
2. Sumeyra Tas, Ozgen Sari, Yaser Dalveren, Senol Pazar, Ali Kara and Mohammad Derawi, "Deep Learning-Based Vehicle Classification for Low Quality Images", MDPI, 2022
3. Vijayaraghavan, M. Laavanya, "Vehicle Classification and Detection using Deep Learning", IJEAT, 2019
4. Janak Trivedi, Mandalapu Sarada Devi, Dave Dhara "Vehicle Classification Using the Convolution Neural Network Approach", 2021
5. Ruchi Patel, Dr. N. M. Patel, Dr. U. K. Jaliya, "Vehicle Detection, Classification and Tracking Using Deep Learning", 2020
6. Patel Parin, Gayatri Pandi, "Vehicle Detection in Traffic Monitoring with Machine Learning", 2018
7. Trivedi, Mandalapu Sarada Devi, Dave Dhara, "Vehicle Classification Using the Convolution Neural Network Approach", Series Transport, 2021
8. Yidan Chen¹ and Zhenjin Li, "An Effective Approach of Vehicle Detection Using Deep Learning", Hindawi, 2022
9. Stephen Karungaru, Lyu Dongyang, and Kenji Terada, "Vehicle Detection and Type Classification Based on CNN-SVM", 2021
10. Mukesh Prasad, Chih-Ling Liu, Dong-Lin Li, Chandan Jha, Chin-Teng Lin¹, "Multi-view Vehicle Detection based on Part Model with Active Learning", 2018
11. Neriman Yaras, "Vehicle Type Classification with Deep Learning", İZMİR, 2020
12. Hadi Ghahremannezhad, Mohammad O. Faruque, Chengjun Liu, "Vehicle Classification in Video Using Deep Learning", 2019
13. V. Vijayaraghavan, M. Laavanya, "Vehicle Classification and Detection using Deep Learning", IJEAT, 2019
14. Watcharin Maungmai, Chaiwat Nuthong, "Vehicle Classification with Deep Learning", IEEE, 2019
15. Syeda Aneeba Najeeb, Rana Hammad Raza, Adeel Yusuf¹ and Zamra Sultan, "Fine-Grained Vehicle Classification in Urban Traffic Scenes using Deep Learning", 2018
16. Ahmad Arinaldi, Jaka Arya Pradana, Arlan Arventa Gurusinga, "Detection and Classification of Vehicles for Traffic Video Analytics", 2018
17. Mrs. Sujatha D Badiger, Dr. M. uttarakumari, "Vehicle Classification Using Machine Learning Algorithms Based on the Vehicular Acoustic Signature", ISSN, 2019
18. Sathyanarayana N. And Anand M. Narasimhamurthy, "Vehicle Type Classification Using Hybrid Features and a Deep Neural Network", 2022
19. Adami Fatima Zohra, Salmi Kamilia, Abbas Faycal, Saadi Souad, "Detection and Classification of Vehicles Using Deep Learning", IJCST, 2018
20. Preetha Jagannathan, Sujatha Rajkumar, Jaroslav Frnda, Parameshchari Bidare Divakarachari, and Prabu Subramani, "Moving Vehicle Detection and Classification Using Gaussian Mixture Model and Ensemble Deep Learning Technique", 2021
21. Ioan Păvăloia, Anca Ignat, "Iris Image Classification Using SIFT Features", 2019
22. Ryfial Azhara, Desmin Tuwohingidea, Dasrit Kamudia, Sarimuddina, Nanik Suciati, "Batik Image Classification Using SIFT Feature Extraction, Bag of Features and Support Vector Machine", 2015
23. Dimitrios Tsourounis, Dimitris Kastaniotis, Christos Theoharatos, Andreas Kazantzidis and George Economou, "SIFT-CNN: When Convolutional Neural Networks Meet Dense SIFT Descriptors for Image and Sequence Classification", MDPI, 2022
24. V. Sowmya, R. Radha², "Efficiency - Optimized Approach - Vehicle Classification Features Transfer Learning and Data Augmentation Utilizing Deep Convolutional Neural Networks" 2020
25. Andrzej Bułak, Bogusław Cyganek, Michał Koziarski, Bogdan Kwolek, Bogusław Olborski¹, Zbigniew Antosz, Jakub Swadzba and Piotr Sitkowski, "Classification of Histopathological Images using Scale-Invariant Feature Transform", 2022





Pramod Kumar Vishwakarma and Nitin Jain

26. Mrs. D. HEMA, "Object Detection and Learning Via Feature Descriptors", 2021
27. Varsha Devi Sachdeva, Junaid Baber, Maheen Bakhtyar, Ihsan Ullah, Waheed Noor, Abdul Basit2, "Performance Evaluation of SIFT and Convolutional Neural Network for Image Retrieval", IJACSA, 2017
28. Lingxi Xie, Qi Tian, Jingdong Wang, and Bo Zhang "Image Classification with Max-Sift Descriptors"
29. Neriman YARAŞ, "Vehicle Type Classification with Deep Learning", İZMİR, 2020
30. Ghaith Al-refai, Hisham Elmoaqet and Mutaz Ryalat, "In-Vehicle Data for Predicting Road Conditions and Driving Style Using Machine Learning", MDPI, 2022
31. Seda Kul, Ahmet Sayar, Süleyman Eken "A Concise Review on Vehicle Detection and Classification", 2017
32. Ahmad Bahaa Ahmad, Hakim Saibi, Abdelkader Nasreddine Belkacem and Takeshi Tsuji, "Vehicle Auto-Classification Using Machine Learning Algorithms Based on Seismic Fingerprinting", MDPI, 2022
33. Hansi Liu "Vehicle Verification Using Deep Learning for Connected Vehicle Sharing Systems", 2019
34. Rune Prytz, "Machine learning methods for vehicle predictive maintenance using off-board and on-board data"
35. Faiza T, Shayini R, "A Novel Deep Learning Architecture for Vehicle Make and Model Recognition: A Review", IJCRT, 2022
36. Sipan Masoud Mustafa "Vehicle Detection and Tracking Using Machine Learning Techniques", Nicosia, 2019

Table 1. YOLOv8 Model Architecture

Layer	Type	Feature Maps	K/S/P
1	Conv	3 → 16	3x3 / 2 / 1
2	Conv	16 → 32	3x3 / 2 / 1
3	C2f (Bottleneck)	32 → 32	Various
4	Conv	32 → 64	3x3 / 2 / 1
5	C2f (Bottleneck)	64 → 64	Various
6	Conv	64 → 128	3x3 / 2 / 1
7	C2f (Bottleneck)	128 → 128	Various
8	Conv	128 → 256	3x3 / 2 / 1
9	C2f (Bottleneck)	256 → 256	Various
10	SPPF	256 → 128	Various
11	Upsample	-	2.0 Scale
12	Concat	-	-
13	C2f (Bottleneck)	384 → 128	Various
14	Upsample	-	2.0 Scale
15	Concat	-	-
16	C2f (Bottleneck)	192 → 64	Various
17	Conv	64 → 64	3x3 / 2 / 1
18	Concat	-	-
19	C2f (Bottleneck)	192 → 128	Various
20	Conv	128 → 128	3x3 / 2 / 1
21	Concat	-	-
22	C2f (Bottleneck)	384 → 256	Various
23	Detect	Various	Various

Table 2: The aggregate count of vehicles identified through various methodologies

Video Names	Video Frames	Vehicle category	Total number of vehicles					
			Proposed method		Input imagedetection method		Number of Vehicles in Video	
			Remoteare a	Proximalare a	Remoteare a	Proximalare a	Remoteare a	Proximalare a
Video 1	10000	Car	9,728	11,510	693	8,616	9,840	11,550
		Bus	1062	569	72	379	1,082	580





Pramod Kumar Vishwakarma and Nitin Jain

		Motorcycl e	11,701	7,390	40,040	3,703	11,792	8,471
Video 2	10000	Car	6,890	5,515	1,192	3,356	6,914	5,654
		Bus	594	874	102	295	607	882
		Motorcycl e	9,097	7,509	3,122	2,738	9,169	7,731
Video 3	10000	Car	5,804	4,136	1,024	1,188	5,834	4,352
		Bus	755	316	126	195	783	329
		Motorcycl e	9,708	7,900	3,231	3,266	9,726	8,007

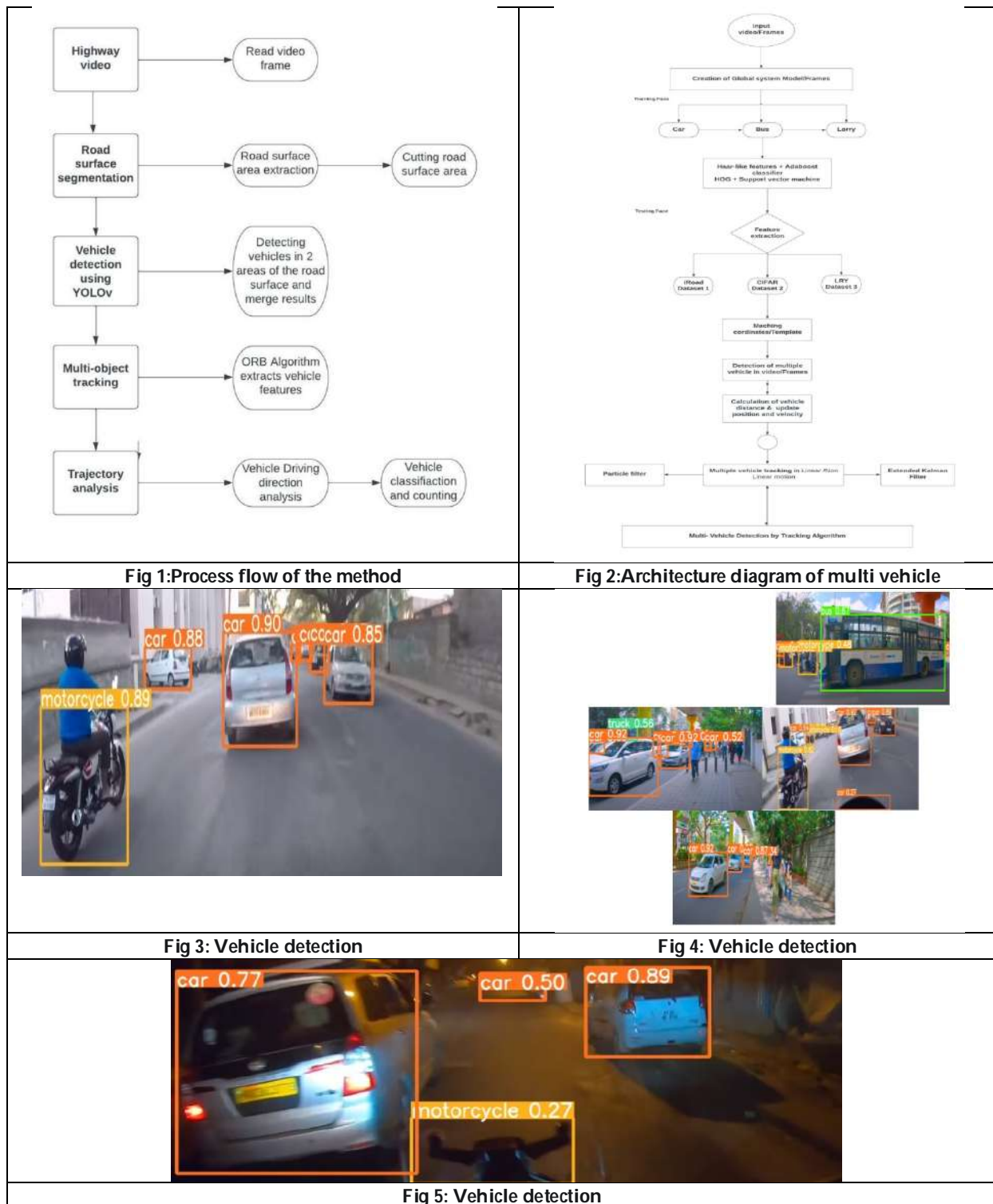
Table 3: The real vehicle numbers are compared using a variety of methodologies

	Vehicle Category	Remote Area		Proximal Area		Average Percentage	
		Proposed method	Input-image detection method	Proposed Method	Input-image detection method	Proposed method	Input-image detection method
Number of Vehicles in Video	Car	99.26%	11.58%	99.39%	43.54%	99.175%	30.06%
	Bus	98.94%	22.08%	98.05%	63.86%	98.995%	42.97%
	Motorcycle	99.11%	18.21%	98.61%	80.99%	98.56%	49.6%
Over all correct Percentage		98.64%	31.96%	98.82%	72.80%	98.976%	48.86%

Table 4: Performance of the proposed model

Images	Box (P)	R	mAP50	mAP 50-95	Mask (P)	R	mAP50	mAP50-95
25000	0.962	0.94	0.967	0.934	0.961	0.96	0.947	0.941
25000	0.971	0.97	0.979	0.955	0.951	0.97	0.969	0.953
25000	0.952	0.97	0.985	0.985	0.972	0.96	0.975	0.981
25000	0.961	0.98	0.975	0.956	0.951	0.97	0.975	0.946
25000	0.984	0.98	0.961	0.985	0.983	0.98	0.981	0.985







Oxidative Stress; A Contributing Factor for Emergence of Polycystic Ovary Syndrome

Ankita Dudhal¹, Aniket Narayanakar² and Sonali Nipate^{3*}

¹Assistant Professor, Department of Pharmacology, D. Y. Patil College of Pharmacy, Akurdi, (Affiliated to Savitribai Phule Pune University) Pune, Maharashtra, India.

²Assistant Professor, Department of Pharmacology, Dr. Ashok Gujar College of Pharmacy, Solapur, (Affiliated to Dr. Babasaheb Ambedkar Marathwada University) Maharashtra, India.

³Associate Professor, Department of Pharmacology, Modern College of Pharmacy, Nigdi, (Affiliated to Savitribai Phule Pune University) Pune, Maharashtra, India.

Received: 22 Jan 2024

Revised: 09 Feb 2024

Accepted: 06 May 2024

*Address for Correspondence

Sonali Nipate

Associate Professor,
Department of Pharmacology,
Modern College of Pharmacy,
Nigdi, (Affiliated to Savitribai Phule Pune University)
Pune, Maharashtra, India.
Email: sonynipate@rediffmail.com



This is an Open Access Journal / article distributed under the terms of the **Creative Commons Attribution License** (CC BY-NC-ND 3.0) which permits unrestricted use, distribution, and reproduction in any medium, provided the original work is properly cited. All rights reserved.

ABSTRACT

Hyperandrogenism and persistent anovulation are two hallmarks of the complex endocrine condition known as polycystic ovarian syndrome (PCOS). Patients with PCOS exhibit a wide range of symptoms, making diagnosis challenging. Ultrasonographic follicle examination and hormonal assessment of androgen level are part of the diagnostic workup. Insulin resistance is unique to PCOS-afflicted obese women. It is now known that oxidative stress is a major factor in the pathophysiology of numerous illnesses, including PCOS. Even though extremely intricate antioxidant enzymatic and non-enzymatic systems regulate the formation and propagation of intracellular reactive oxygen species (ROS), knowing the mechanisms underlying oxidative stress is crucial for developing PCOS prevention and treatment plans. This article examines the research on the connection between oxidative stress and PCOS development.

Keywords: Oxidative stress, PCOS, herbal drugs against PCOS





INTRODUCTION

The medical condition known as PCOS, or polycystic ovarian syndrome, is diverse and is typified by persistent anovulation and hyperandrogenism. A PCOS patient may exhibit a wide range of symptoms, including weight gain, infertility, excessive hair growth, irregular or skipped menstrual cycles, and acne. PCOS is a low-grade inflammatory illness that affects 5–10% of premenopausal women globally. It is associated with hormone imbalance, which can lead to problems with female infertility. According to data from the World Health Organization (WHO), 116 million women worldwide (3.4%) may be afflicted with PCOS. There is a dearth of information regarding PCOS prevalence in India. Twenty percent of Indian women are thought to have PCOS. Hyperandrogenism, which causes excessive facial hair growth, acne, anovulation, and numerous ovarian cyst formation, is one of the main clinical characteristics of PCOS. Numerous investigations noted notable fluctuations in oxidative stress markers within the pathophysiology of PCOS. Oxygen free radicals that are produced in excess cause clinical characteristics associated with PCOS. (1). PCOS arises from the interplay of various environmental and heritable factors. Genetic or environmental factors may be the underlying cause of the congenital conditions leading to aberrant theca cell androgenic function. Insulin-resistant hyperinsulinism, which might have an acquired or congenital foundation, is the main postnatal cause. In the past few years, research on genetics and epigenetics has significantly advanced our understanding of the specifics. Because ovarian androgenic function tests can demonstrate farnesol-induced generation of reactive oxygen species (FOH) in the great majority of cases (87%) it is a key component in the etiology of PCOS. Generalized ovarian steroid hyper-responsiveness to LH, as demonstrated by an off-label gonadotropin releasing hormone agonist (GnRHag) or human chorionic gonadotropin (hCG) test, is a characteristic shared by two-thirds of FOH patients. (5). It is suggested that genes involved in folliculogenesis should also be taken into consideration as potential candidates for the aetiology of PCOS due to the discovery of anomalies in the early, gonadotrophin-independent phases of ovarian follicle formation. Few case-control studies have been published to date, nonetheless, with sufficient power to either confirm or rule out the candidate genes analyzed as important aetiological determinants. Numerous studies have been published in the literature that have shown connections between polymorphisms in genes related to steroidogenesis and the production or function of insulin. (6). As Women are more susceptible to a variety of illnesses and disorders due to oxidative stress, which also disrupts their hormone cycles. This article focuses on the relationship between oxidative stress and PCOS, as well as antioxidants that are sold as herbal medications.

Role of Oxidative stress

Increased reactive oxygen species (ROS) and insufficient endogenous and exogenous antioxidant production or availability inside the body are the main causes of oxidative stress. The balance of antioxidants is upset. Free radicals cause harm to cells and can even be fatal. Thus, OS may result from a drop in antioxidant defense systems as well as an increase in oxidants (free radicals or reactive species). Increased reactive oxygen species (ROS) are linked to a number of reproductive conditions, including endometriosis, polycystic ovarian syndrome (PCOS), and preeclampsia (7).

Physiological role of ROS in the ovary

Through signaling, reactive oxygen species (ROS) control a number of ovarian physiological processes, including meiosis, ovulation, corpus luteum maintenance, and regression, as well as oocyte growth and fertilization (Fig. 3). •OH and $1O_2$ are two of these regulatory ROS that can only reside in distinct areas and have relatively limited diffusion distances. Furthermore, $O_2\bullet^-$'s volatility and its incapacity to permeate through membranes restrict its potential as a signaling molecule. H_2O_2 molecules, on the other hand, are essential messengers in signaling pathways because of their low reactivity, high selectivity, high diffusivity, and good membrane permeability. One of the most important things the ovary does is ovulate, which is a similar process to inflammation. Increased secretion of the luteinizing hormone before ovulation leads to increased inflammatory precursors in the ovary, which results in excessive ROS production. The increased ROS are involved in cumulus expansion, progesterone production, the expression of preovulatory genes, and the activation of signals contributing to ovulation.





Ankita Dudhal et al.,

Oxidative stress and reproduction in women with PCOS

Another crucial intraovarian regulation of folliculogenesis is oxidative metabolism. A group of follicles start to grow and develop in the ovary every month, but only one of them becomes the dominant follicle (9). Antioxidants impede this process, which is regulated by an increase in ROS, and they also aid in the advancement of meiosis II. ROS impacts the course of meiosis II, reduces DNA damage and gonadotropin secretion, and prevents the synthesis of ATP (10). It is one of the states with elevated OS, which causes disruptions in the luteal and ovarian follicular phases of the cycle (9). ROS and MDA levels were shown to be elevated in the follicular fluid of women with PCOS. It decreased TAC, which was directly associated with reduced oocyte maturation and fertilization rates, poor embryo quality, and lower pregnancy rates. Also, AGEs affect the ovarian cells directly in women with PCOS. It was investigated that PCO ovaries displayed an increased concentration of AGE deposition in granulosa, theca, and ovarian endothelial cells (7).

Pathological role of ROS in ovarian diseases

ROS are essential for ovarian physiological function; however, excessive ROS levels can induce the development of ovarian diseases (Fig 4). Increased ROS production owing to factors such as aging and drinking, beyond the antioxidant capacity can induce OS and lead to the oxidative damage of lipids, proteins, and DNA. Excessive ROS production can directly affect the target of signalling pathways and also induce abnormal results by interacting with intermediate reaction steps as second messengers. This oxidative damage and the abnormal signalling pathways finally manifest in age-related ovarian dysfunction, ovarian cancer, PCOS, and ovarian endometriosis.

Reactive oxygen species ROS and PCOS

One of the most prevalent complicated endocrine disorders and a significant contributor to anovulatory infertility is PCOS. Although the pathophysiology is still poorly understood, ROS are recognized to be crucial. For a variety of factors, the OS in PCOS patients is more robust than in healthy individuals. IR plays a key role in the etiology of PCOS and is intimately linked to obesity, hyperandrogenism, and ovulatory dysfunction. In individuals with IR, hyperglycemia increases the generation of reactive oxygen species (ROS) through the NADPH oxidase p47(phox) component. Leukocytes are more susceptible to hyperglycemia and OS is exacerbated by hyperandrogenemia. Another important factor in the generation of ROS in obese people is NADPH oxidase. Increased fatty acid levels in adipocytes cause NADPH oxidase activation, which raises OS. The increased ROS through these mechanisms can promote the development of PCOS. OS reduces the sensitivity of skeletal muscle to insulin, resulting in the development of IR. Additionally, OS impairs glucose uptake in muscle and adipose tissue and induces pancreatic β -cell dysfunction. Elevated OS exacerbates PCOS progression by increasing the size of mature adipocyte, inducing obesity-promoting preadipocyte proliferation and adipocyte differentiation. These associations suggest that ROS play a crucial role in the pathogenesis of PCOS, thereby providing a novel perspective into the treatment of PCOS patients: the inhibition of ROS production through antioxidant therapy to alleviate PCOS symptoms.

ROS and ovarian endometriosis

Ovarian endometriosis is the most common lesion of endometriosis, which causes not only severe menstrual pain but also infertility. The monthly conception rate in healthy women is 15–20% compared with 2–10% in women with endometriosis. OS plays a vital role in endometriosis-related infertility. In patients with ovarian endometriosis, endometriotic tissue causes increased expression of OS markers in the surrounding normal ovarian cortex, suggesting that OS was occurring. (11).

Herbal drug available in market against PCOS

Antioxidant supplementation is being investigated as a possible treatment for reproductive diseases linked to infertility and may be useful in reducing the generation of reactive oxygen species (ROS) (2009). Antioxidants fall into two categories: primary, enzymatic, and natural, and secondary, non-enzymatic, and synthetic. Antioxidants that are enzymatic include GPX, catalase, and SOD. Vitamin E, vitamin C, beta carotene, lutein, α -lipoic acid, selenium, lycopene, taurine, L-carnitine, coenzyme Q10, and others are examples of non-enzymatic antioxidants.¹¹ In eukaryotes, there are three different kinds of SOD: extracellular SOD (EC-SOD), manganese SOD





Ankita Dudhal et al.,

(Mn-SOD), and copper/zinc SOD (Cu/Zn - SOD). Antioxidants can be obtained from foods or supplements (non-enzymatic) or produced endogenously (12).

Watermelon seed (*Citrullus lanatus*)

Citrullus lanatus seed extracts possess anti-oxidant activities and the potency of anti-oxidant activities depends on the type of extract. Recent studies have shown that many dietary polyphenolic constituents derived from plants are more effective antioxidants.

Licorice (*Glycyrrhiza glabra*)

Glycyrrhiza glabra is a member of the Fabaceae family. It mostly consists of 2-9% glycyrrhizin, glycyrrhizin acid, carbohydrates, amino acids, flavonoids, and isoflavonoids. The main phytoestrogens in liquorice are glabridin, glabrene, liquiritigenin, isoliquiritin, and liquiritin. *Glycyrrhiza*'s flavonoids have an anti-androgenic impact because they interact with estrogenic receptors and have estrogenic activity. Furthermore, flavonoids have the ability to aid in the release of insulin, which lowers blood sugar and helps treat PCOS. *Panax ginseng* is known as "the king of herbs" and has been used for more than 2000 years. The saponins found in ginseng are the active molecules responsible for its useful therapeutic activity, and they include major ginsenosides, namely ginsenoside. *P. ginseng* can stimulate the growth of estrogen receptor (ER)-positive (p) cells in vitro. Ginsenoside Rb1 and Rg1 can stimulate ERs with estrogen-like activity (13).

Cinnamon (*Cinnamomum verum*)

The Lauraceae family of herbaceous plants includes the cinnamon plant. Sri Lanka and tropical Southern India are home to cinnamon plants. Cinnamon is said to behave as an insulin sensitizer by numerous research. Several flavonoids and polyphenols found in cinnamon have antioxidant and free radical scavenging properties [23]. According to certain research, the cinnamon extract's Type-A polymers and procyanidine polyphenols improve insulin signaling at the post-receptor level, boost PI3 kinase activity, and improve the GLUT4 glucose transporter to increase the absorption of glucose.

Aloe (*Kumari mussbar*)

Biological source: Dried latex of leaves of various species of aloes, mainly *Aloe barbadensis*.

Family: *Liliaceae*.

Part(s) used: Leaves and juice.

Aloe vera has been discovered to have "antimicrobial", "anti-carcinogenic", "anti-viral", "immunomodulatory", "anti-oxidant", "anti-inflammatory", "skin protecting", and "wound healing" qualities, in addition to managing PCOS and being antidiabetogenic. *Aloe vera* is a *Liliaceae* plant that contains secondary metabolites such as anthraquinone derivatives, flavonoids, phytosterols, polyphenols and other nutrients. Aloe emodin and barbaloin are the major constituents of *Aloe vera*.

Ashwagandha (*Withania root, ashwagandha, and clustered wintercherry*)

Biological source: Dried roots and stem bases of *Withania somnifera* Dunal.

Family: *Solanaceae*.

Part(s) used: Ashwagandha powder, roots, barks, leaves, fruits, and seeds.

One such ayurvedic herb that has historically been recognized as a potent adaptogen is ashwagandha powder. Adaptogen herbs assist the body in harmonizing hormone levels, which may therefore lessen stress and PCOS symptoms.

Shatavari (*Asparagus Satmuli*)

Biological source: Dried tuberous roots of *Asparagus racemosus* Wild.

Family: *Liliaceae*.

Part of use: Dried roots.



**Ankita Dudhal et al.,**

PCOS is brought on by a hormonal imbalance in a woman's body, as was previously described. According to various research studies, when women take 5 gms of shatavari, their hormones are balanced. Shatavari naturally boosts antioxidant levels in a woman's body, improves menstruation, and decreases fertility (8). It helps in promoting normal development of ovarian follicles, regulates menstrual cycle and revitalizes the female reproductive system mainly due to its phytoestrogen (natural plant based estrogen). It also helps in combating the hyperinsulinemia [6]. (14).

Fenugreek (*Trigonella foenum-graecum* L)

Asia cultivates fenugreek, or *Trigonella foenum-graecum* L., an annual plant used historically as a spice crop. Ten to twenty aromatic yellow seeds can be found in its crust. Fenugreek reduces insulin resistance in PCOS-affected women and possesses anti-diabetic and cholesterol-lowering properties. Soluble fibers included in fenugreek extracts lower blood sugar levels by limiting the enzymatic breakdown and absorption of carbs, which in turn lowers postprandial glucose levels. Fenugreek inhibits alpha-amylase and sucrose while promoting insulin synthesis and release from beta-pancreatic cells, resulting in hypoglycemic effects. Hassanzadeh et al. looked into how fenugreek seed extract affected PCOS-affected women's insulin resistance (15).

CONCLUSION

Oxidative stress occurs due to the increased reactive oxygen species (ROS) and the insufficient production or availability of endogenous and exogenous antioxidants in the body. Herbal Drugs containing high amount of antioxidants can be used as treatment against PCOS as role of oxidative stress is crucial in female reproductive health. Herbal drugs mentioned in the review are already in use and available in market.

ACKNOWLEDGEMENT

I would like to thank Mrs. Sonali Nipate mam for continuous guidance and support and I am also thankful to Mr. Aniket Narayankar sir for his contribution in the review.

Conflict of Interest -We declare no competing or conflict of interest

REFERENCES

1. Moore M. Discover the impact of oxidative stress on female reproduction | HHC [Internet]. *Life Science product* / Helvetica Health Care. (2022) [cited 2023 Oct 16]. Available from: <https://www.h-h-c.com/the-effects-of-oxidative-stress-on-female-reproduction/>
2. Manokaran K, Bhat P, Nayak D, Baskaran R, Paramasivam P, Ahmed SF, et al. Oxidative stress and female reproductive disorder: A review. *Asian Pac J Reprod.* (2022)May 1;11(3):107–16. <https://doi.org/10.4103/2305-0500.346088>.
3. Fertility Coaching and counseling - DIFFERENCE BETWEEN PCO AND PCOS Ovarian cysts | Facebook [Internet]. [cited 2023 Oct 16]. Available from: <https://www.facebook.com/fertilitysupportafrica/photos/a.347450265995638/671518043588857/>
4. ResearchGate [Internet]. [cited 2023 Oct 16]. Percentage of women with physician-confirmed PCOS versus women without... Available from: https://www.researchgate.net/figure/Percentage-of-women-with-physician-confirmed-PCOS-versus-women-without-PCOS-among-users_fig3_349760149
5. Rosenfield RL. Current concepts of polycystic ovary syndrome pathogenesis. *Curr Opin Pediatr.* (2020) Oct;32(5):698–706.doi: 10.1097/MOP.0000000000000945.





Ankita Dudhal et al.,

6. Franks S, McCarthy MI, Hardy K. Development of polycystic ovary syndrome: involvement of genetic and environmental factors. *Int J Androl.* (2006);29(1):278–85. DOI: 10.1111/j.1365-2605.2005.00623.
7. Rudnicka E, Duszewska AM, Kucharski M, Tyczyński P, Smolarczyk R. OXIDATIVE STRESS AND REPRODUCTIVE FUNCTION: Oxidative stress in polycystic ovary syndrome. *Reproduction.* (2022) Dec 1;164(6):F145–54. DOI: 10.1530/REP-22-0152
8. SUGINO N. Reactive oxygen species in ovarian physiology. *Reprod Med Biol.*(2005) Mar 7;4(1):31–44. DOI: 10.1007/BF03016135
9. Agarwal A, Aponte-Mellado A, Premkumar BJ, Shaman A, Gupta S. The effects of oxidative stress on female reproduction: a review. *Reprod Biol Endocrinol.* (2012) Jun 29;10(1):49. DOI: 10.1186/1477-7827-10-49
10. Behrman HR, Kodaman PH, Preston SL, Gao S. Oxidative stress and the ovary. *J Soc Gynecol Investig.*(2001);8(1 Suppl Proceedings):S40-42. DOI: 10.1016/s1071-5576(00)00106-4
11. Liang J, Gao Y, Feng Z, Zhang B, Na Z, Li D. Reactive oxygen species and ovarian diseases: Antioxidant strategies. *Redox Biol.*(2023)Mar 7;62:102659. doi: 10.1016/j.redox.2023.102659
12. Panti AA, Shehu CE, Saidu Y, Tunau KA, Nwobodo EI, Jimoh A, et al. Oxidative stress and outcome of antioxidant supplementation in patients with polycystic ovarian syndrome (PCOS). *Int J Reprod Contracept Obstet Gynecol.* (2018) Apr 28;7(5):1667. DOI: <https://doi.org/10.18203/2320-1770.ijrcog20181892>
13. Lakshmi JN, Babu AN, Kiran SSM, Nori LP, Hassan N, Ashames A, et al. Herbs as a Source for the Treatment of Polycystic Ovarian Syndrome: A Systematic Review. *Biotech Basel Switz.* (2023)Jan 3;12(1):4. DOI: 10.3390/biotech12010004
14. Pachiappan S, Matheswaran S, Pushkalai P, Muthusamy G. Medicinal plants for polycystic ovary syndrome: A review of phytomedicine research. *Int J Herb Med.* (2017); 5(2): 78-80 Received: 14-01-2017 Accepted: 15-02-2017
15. Ashkar F, Rezaei S, Salahshoornezhad S, Vahid F, Gholamalizadeh M, Dahka SM, et al. The Role of medicinal herbs in treatment of insulin resistance in patients with Polycystic Ovary Syndrome: A literature review. *Biomol Concepts.* (2020) Mar 26;11(1):57–75.DOI: 10.1515/bmc-2020-0005.

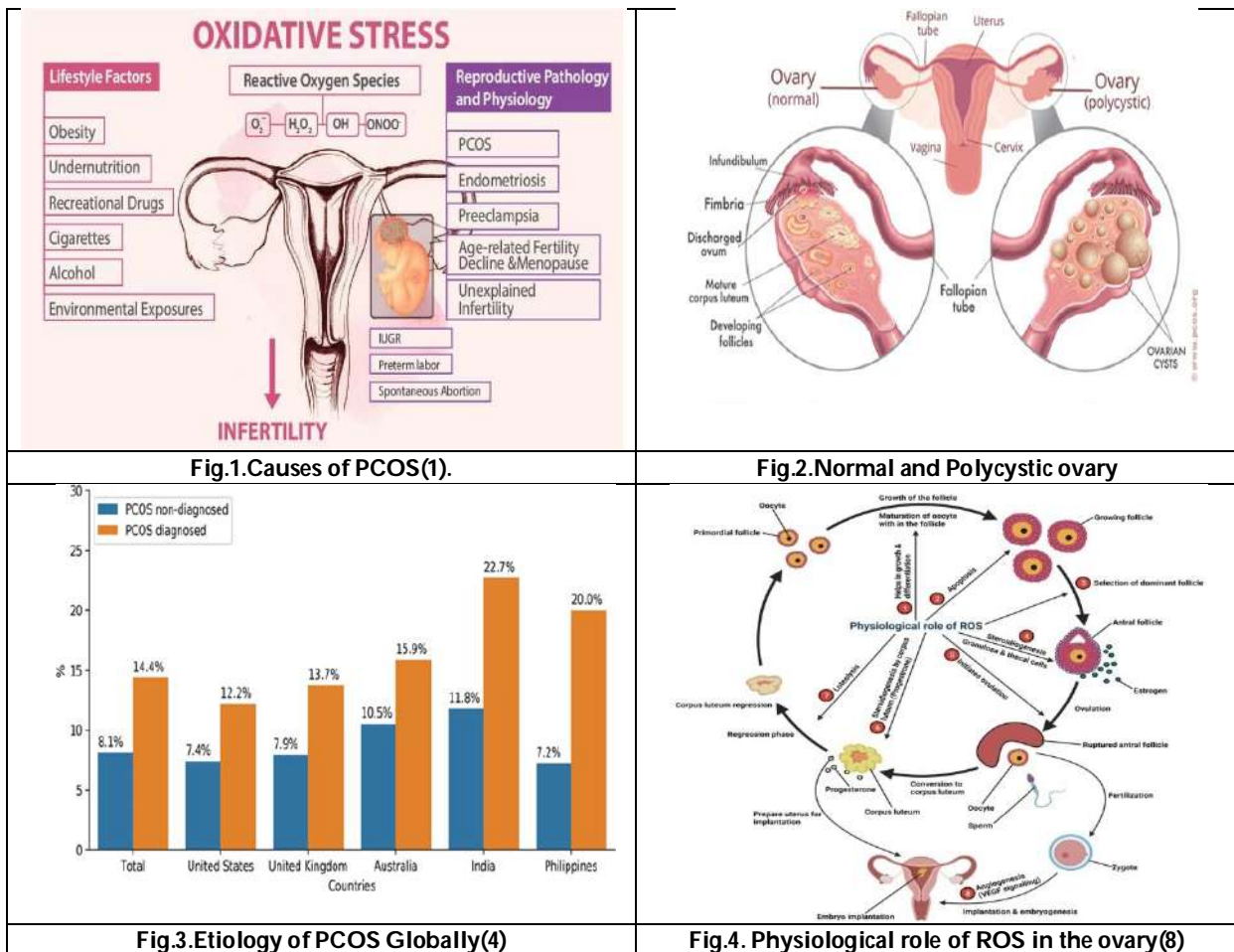
Table 1. Herbal drug and role in women health

Herbal Drug	Role in women health
Citrullus lanatus seed	Anti-apoptosis, anti-aging, anti- carcinogen, anti-inflammation, anti-atherosclerosis, cardiovascular protection and improvement of endothelial function
Glycyrrhiza glabra	a potent anti-androgen and helps the body to maintain biosynthesis and the release of estrogen
Panax ginseng	estrogen-like activity
Cinnamon	inhibit the glycogen synthesis, and enhance glycogen synthesis and hypoglycemic effects.
Aloe	reversion of estrous cyclicity and improved steroidogenic activity.
Ashwagandha	assist the body in harmonizing hormone levels,
Shatavari	improves menstruation
Fenugreek	hypoglycemic effects





Ankita Dudhal et al.,





Comparative Evaluation of Effectiveness of Conventional Desensitizing Agents and Diode Laser in Treatment of Dentinal Hypersensitivity using Scanning Electron Microscopy

Mukund V.Singh¹, Indrani Roy^{2*}, Aparna Palekar³, Basawaraj Biradar⁴ and Nihar Bhandari⁵

¹Associate Professor, Department of Conservative Density and Endodontics, Rural Dental College Pravara Institute of Medical Sciences (Deemed to be University), Loni, Maharashtra, India.

²III MDS PG Student, Department of Conservative Density and Endodontics, Rural Dental College Pravara Institute of Medical Sciences (Deemed to be University), Loni, Maharashtra, India.

³Professor & HoD, Department of Conservative Density and Endodontics, Rural Dental College Pravara Institute of Medical Sciences (Deemed to be University), Loni, Maharashtra, India.

⁴Professor, Department of Conservative Density and Endodontics, Rural Dental College Pravara Institute of Medical Sciences (Deemed to be University), Loni, Maharashtra, India.

⁵PG Student, Department of Conservative Density and Endodontics, Rural Dental College Pravara Institute of Medical Sciences (Deemed to be University), Loni, Maharashtra, India.

Received: 22 Jan 2024

Revised: 09 Feb 2024

Accepted: 27 Apr 2024

*Address for Correspondence

Indrani Roy

III MDS PG Student,

Department of Conservative Density and Endodontics,

Rural Dental College Pravara Institute of Medical Sciences (Deemed to be University),

Loni, Maharashtra, India.

Email: indrani.roy98@gmail.com



This is an Open Access Journal / article distributed under the terms of the **Creative Commons Attribution License** (CC BY-NC-ND 3.0) which permits unrestricted use, distribution, and reproduction in any medium, provided the original work is properly cited. All rights reserved.

ABSTRACT

To Evaluate & Compare The Effectiveness Of A Diode Laser, Calcium Sodium Phosphosilicate (Novamin) & Arginine Calcium Carbonate (ACC) In Occluding Dentinal Tubules. This in vitro study included 10 teeth with intact root surfaces unaltered by extraction procedure for specimen preparation. Each tooth was disinfected, air dried and cut into 4 sections. Total 40 sections were prepared ,which were acid etched. They were divided into 4 groups- Saline (Control), Novamin, Arginine Calcium Carbonate & Diode laser. In diode laser group, specimens were lased with 980 nm diode laser at 0.5 W/PW (62.2J /cm²) in a NC (non-contact) mode for 30 seconds. Specimens were evaluated under Scanning Electron Microscope (SEM) at 10kv– 20kv under x 2000, x5000 magnification for surface characteristics and patency of dentinal tubules. Total number of tubules visible, open, completely and partially occluded were recorded and compared. Although, it was observed that all the three agents were able to obtain dentine tubule occlusion, there was statistically significant difference in the percentage of tubule occlusion in the dentine discs treated by Diode laser compared to the toothpastes. Diode laser was most effective in treating dentinal hypersensitivity.





Keywords: Dentinal hypersensitivity, lasers, novamin, arginine calcium carbonate.

INTRODUCTION

Dentinal hypersensitivity is characterized as acute, non-spontaneous, short or long lasting pain originating from exposure of dentin to thermal, chemical, mechanical or osmotic stimuli that cannot be attributed to any other dental pathology.^[2] Dentinal hypersensitivity is a common occurrence and is often one of the main reasons why patients seek dental treatment. The reported prevalence of DH varies from 4% - 57%.^[3]

MATERIAL & METHODOLOGY

The present in vitro SEM study was undertaken at Department of Conservative Dentistry & Endodontics, Rural Dental College, Loni, Maharashtra, India. The study was conducted during the period from January 2023 to June 2023. Teeth with intact root surfaces and unaltered by extraction procedure were included for specimen preparation. Teeth treated previously with desensitizing therapy, cracked teeth with defective restorations were excluded. Teeth which had undergone root canal therapy or with any apical lesion, caries, roughness of root surfaces, developmental anomalies such as concrescence, fusion were also excluded.

Preparation of the specimen

Ten selected freshly extracted teeth were cleaned of gross debris and stored in 10% formalin solution. Teeth were ground with carbide bur to remove outer enamel layer and polished with 600 grit SiC paper. Teeth were then sectioned with a carborundum disc attached to a straight hand piece (KAVO EWL type 4415, KAVO®, West Germany). A total of 40 dentin samples of 2 mm thickness were obtained in both longitudinal and transverse section. The dentin specimens were placed in an ultrasonic cleaner (SONICER®, Yoshida Dental Mfg Co Ltd, Osaka, Japan) with distilled water for 30 seconds. Later, the specimens were etched with 37% phosphoric acid for a period of two minutes and then rinsed in distilled water. The prepared samples were randomly assigned to 4 groups

Saline group: 10 specimens were treated with saline and they served as control group.

Novamin (SHY-NM) group: 10 specimens were treated with Novamin.

Diode Laser group

10 specimens were lased with 980 nm Diode Laser (Epic X, Biolase) at 0.5 W/PW (62.2 J/cm²) in noncontact mode for 30 seconds.

Arginine Calcium Carbonate/ACC (Colgate sensitive pro-relief) Group: 10 specimens were treated with ACC. Half of the samples from each group were randomly selected to be subjected to acid challenge by 6% citric acid. All of the samples were sputter coated with layer of gold/ palladium followed by SEM analysis.

Scanning electron microscope analysis

The analysis of specimens under SEM (Carl Zeiss NTS Ltd., Baden-Wurttemberg, Germany) micrographs was carried out by an expert to evaluate occlusion of dentinal tubules. SEM test samples were evaluated at 10-20KV and under x2000, x5000 magnification for surface characteristics and patency or occlusion of dentinal tubules. Test samples were examined by low voltage SEM to determine the effect of the abovementioned agents and diode laser on dentin tubule occlusion. The total number of tubules open, completely and partially occluded tubules was counted in each photograph. All the specimens were scanned for determining occlusion of tubules using following criteria. The tubules were considered completely occluded when they show either complete penetration of the crystal or complete



**Mukund V.Singh et al.,**

obliteration of the canals by the reaction products. The tubules were considered partially occluded when there is a central opening in the canal with circumferential closure of the tubule or more than 50% reduction in the diameter of the tubule. The percentage of tubules blocked was calculated as: Number of tubules blocked x100/total number of tubules.

RESULTS

Percentages of completely occluded tubules and comparison of efficacy of laser & desensitizing toothpastes in occluding tubules by One-Way ANOVA.

Evaluation of occlusion of tubules

DISCUSSION

According to Morris et al., it was observed that in-vivo studies of DH, a very powerful placebo effect has been noted, particularly when dealing with small number of subjects and eligible teeth. Hence, the in- vitro examination of products using a reproducible model such as the dentin discs makes it a feasible model to understand occluding, and thus, desensitising properties of potential desensitising agents.^[5] Diode laser leads to increase in mitochondrial ATP through bio-stimulation, increases pain threshold of free nerve ending, provide analgesic effect by increase in endorphins. It also inhibits cyclooxygenase enzyme which causes conversion of arachidonic acid into prostaglandin which in turn increases the pain transmission by glutamate or substance P. There is also formation of secondary dentin by odontoblast due to bio-stimulation.^[11] The active ingredient of Novamin is a bioactive glass, Ca^{2+} and PO_4^{3-} from Novamin along with mineral ions from saliva are able to form a calcium phosphate (Ca-P) layer onto dentine surfaces or into tubules resulting in physical tubule occlusion.^[14] The mechanism of action of ACC was explained by Kleinberg, who suggested that the combination of arginine and calcium carbonate forms a positively charged complex which readily binds to the negatively charged dentine surface and within the dentinal tubules. In addition, the alkaline pH of the ACC is sufficient to facilitate the deposition of Ca^{+2} and PO_4 ions from saliva and/or dentinal fluid to form plugs that seal the open tubules. Among the test products, Diode laser was the most resistant to acid challenge, followed by Novamin and then ACC. This provides evidence of the potential of laser to be used as a sustainable tubule occluding agent to relieve DH.^[18] SEM investigation was selected for this study because it is a non-destructive approach for surface analysis. It also provides high-resolution, 3D images and topographical information.

CONCLUSION

In the present study, the tubules treated with the desensitising agents revealed tubule occlusion while most of the tubules in the control group were found to be open with some of them occluded with a smear layer. Although, it was observed that all the three agents were able to obtain dentine tubule occlusion, there was statistically significant difference in the percentage of tubule occlusion in the dentine discs treated by Diode laser compared to the toothpastes.

REFERENCES

1. Holland GR, Narhi MN, Addy M, Gangarosa L, Orchardson R. Guidelines for the design and conduct of clinical trials on dentine hypersensitivity. J Clin Periodontol 1997;24:808– 813.
2. Rees JS, Addy M. A cross-sectional study of dentine hypersensitivity. J Clin Periodontol 2002;29:997–1003.
3. Irwin CR, McCusker P. Prevalence of dentine hypersensitivity in a general dental population. J Ir Dent Assoc 1997;43:7–9.
4. Bissada NF. Symptomatology and clinical features of hypersensitive teeth. Arch Oral Biol 1994;39:31S–32S.
5. Brannstrom M. Sensitivity of dentine. Oral Surg Oral Med Oral Pathol 1966;21:517–526.





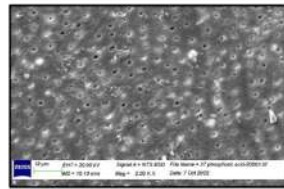
Mukund V.Singh et al.,

6. Absi EG, Addy M, Adams D. Dentine hypersensitivity: a study of the patency of dentinal tubules in sensitive and non-sensitive cervical dentine. *J Clin Periodontol* 1987;14:280–284.
7. Parolia A, Kundabala M, Mohan M. Management of dentinal hypersensitivity: a review. *J Calif Dent Assoc* 2011;39:167–179.
8. Roësing CK, Fiorini T, Liberman DN, Cavagni J. Dentine hyper- sensitivity: analysis of self-care products. *Braz Oral Res* 2009;23:56–63.
9. Burwell AK, Litkowski LJ, Greenspan DC. Calcium sodium phosphosilicate (NovaMin): remineralization potential. *Adv Dent Res* 2009;21:35–39.
10. Rajesh KS, Hedge S, Arun Kumar MS, Shetty DG. Evaluation of the efficacy of a 5% calcium sodium phosphosilicate (Nov- amin®) containing dentifrice for the relief of dentinal hyper- sensitivity: a clinical study. *Indian J Dent Res* 2012;23:363– 367.
11. Kumar RV, Shubhashini N, Seshan H, Kranti K. A clinical trial comparing a stannous fluoride based dentifrice and a strontium chloride based dentifrice in alleviating dentinal hypersensitivity. *J Int Oral Health*. 2010;2:37-50.
12. Birang R, Yagini J. Comparative evaluation of dentine surface changes following Nd:YAG laser irradiation by SEM. *Dent Res J*. 2006;3(2):01-07.
13. Gupta G, Gupta P, Gupta R. Iontophoresis and dentistry. *Indian J Dent Sci*. 2010;2:27-31.
14. Pashley DH, O' Meara JA, Kepler EE, Galloway SE, Thompson SM, Stewart FP. Dentin permeability. Effects of desensitizing dentrifices invitro. *J Periodontol*. 1984;55:522- 25.
15. McBride MA, Gilpatrick RO. The effectiveness of sodium fluoride iontophoresis in patients with sensitive teeth. *Quintessence Int*. 1991;22(8):637-40.
16. Hashim NT, Gasmalla BG, Sabahelkheir AH, Awooda AM. Effect of the clinical application of the diode laser (810 nm) in the treatment of dentine hypersensitivity. *BMC Res Notes*. 2014;7(1):31.
17. Ladalardo TC, Pinheiro A, Campos RA, Brugnera junior A, Zanin F, Albernaz PL. Laser therapy in the treatment of dentine hypersensitivity. *Braz Dent J*. 2004;15(2):144- 50.
18. Sicilia A, Cuesta – Frechoso S, Suarez A, Pordomingo A, De Juan P. Immediate efficacy of the diode laser application in the treatment of dentine hypersensitivity in periodontal maintenance patients: a randomised clinical trial. *J Clin Periodontol*. 2009;36(8):650-60.
19. Yilmaz H.G, Yilmaz B, Cengiz E. Long term effect of diode laser irradiation compared to sodium fluoride varnish in the treatment of dentine hypersensitivity in periodontal maintenance patients: A randomised controlled clinical study. *Photomed Laser Surg*. 2011;29(11):721-25.
20. Mittal R, Singla MG, Sood A, Dua A, Sodhi PS. Clinical evaluation of middle power output 810 nm GaAlAs Diode Laser for treating severe dentin hypersensitivity: A randomised clinical trial. *Int J Laser Dent*. 2014;4(1):20-25.
21. Lopes AO, Eduardo C, Correa Aranha AC. Clinical evaluation of low power laser and a desensitizing agent on dentin hypersensitivity. *Lasers Med Sci*. 2015;30(2):823-29.
22. Umana M, Heysselaer D, Tielemans M, Compere P. Dentinal tubules sealing by means of diode lasers (810 and 980 nm): A preliminary invitro study. *Photomed laser Surg*. 2013;31(7):307-14.
23. Nandkumar A, Iyer VH. In vitro analysis comparing efficacy of lasers and desensitizing agents on dentin tubule occlusion: a scanning electron microscope study. *Int J Laser Dent*. 2014;4(1):01-07.

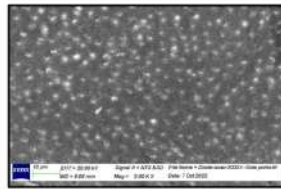
Table 1

Group	Mean no. of open tubules	Mean no. of occluded tubules	% of completely occluded tubules
Diode laser group	158	147.2	93.16%
Novamin group	161.4	130.2	80.66%
ACC group	152.4	99.6	65.42%
Saline group	150	20.3	13.53%



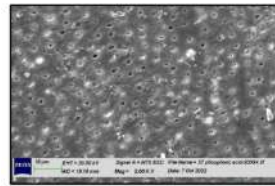


Pre-treatment

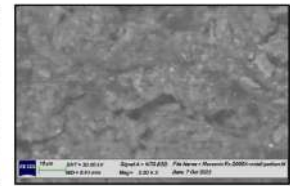


Post-treatment

Fig 1: Diode Laser Group

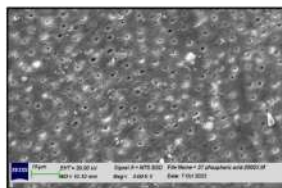


Pre-treatment

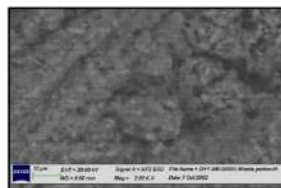


Post-treatment

Fig 2: Novamin Group

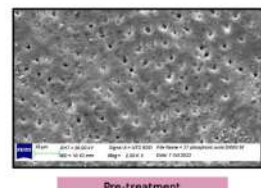


Pre-treatment

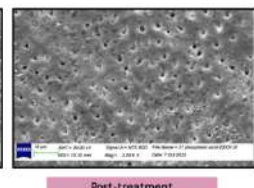


Post-treatment

Fig 3: Arginine Calcium Carbonate (ACC) Group



Pre-treatment



Post-treatment

Fig 4: Saline Group



Fig 5: Evaluation of occlusion of tubules





An M/M/1 Retrial Queue with Recurrent Customers, Non-Persistent Customers and Server Vacation

S.Pazhani Bala Murugan^{1*} and P.Madhangi²

¹Associate Professor, Department of Mathematics, Annamalai University, Annamalai Nagar, Tamil Nadu, India.

²Guest Lecturer, Government Arts and Science College, Manalmedu -Mayiladuthurai, (Affiliated with Bharathidasan University, Tiruchirappalli), Tamil Nadu, India

Received: 03 Jan 2024

Revised: 10 Apr 2024

Accepted: 10 May 2024

*Address for Correspondence

S.Pazhani Bala Murugan

Associate Professor,

Department of Mathematics,

Annamalai University, Annamalai Nagar,

Tamil Nadu, India.

Email: spbm1966@gmail.com



This is an Open Access Journal / article distributed under the terms of the **Creative Commons Attribution License** (CC BY-NC-ND 3.0) which permits unrestricted use, distribution, and reproduction in any medium, provided the original work is properly cited. All rights reserved.

ABSTRACT

In this article, we examine an M/M/1 Retrial Queue with Recurrent Customers, Non- Persistent Customers and Server Vacation. In this model, retrial times, vacation times and all service times are assumed to have an exponential distribution. We obtain the probability generating function for the number of customers in the system. We also compute the average number of customers in the system. Some of the special cases are discussed. To calibrate the model's stability some numerical examples are illustrated.

Keywords: Retrial Queue, Recurrent customers, Non-Persistent Customers, Server vacation and Steady-state equations.

MSC 2010 No.:60K25, 68M20, 90B22

INTRODUCTION

In this paper, an M/M/1 retrial queueing model with recurrent customers, non-persistent Customers and server vacation is taken. Retrial queues are characterized by the phenomenon that arriving customers who find the server busy join the retrial group (called orbit) to repeat their request for service after some random time. Retrial queueing systems have been widely used to model many practical problems in telephone switching systems, telecommunication networks, and computers competing to gain service from a central processing unit. For re cent





Pazhani Bala Murugan and Madhangi

bibliographies on retrial queues, see [1,3,7]. Boxma and Cohen[2] studied an M/G/1 queue in which there is a fixed number of permanent customers present who rejoin the queue on their completion of service. This system with permanent customers in the retrial context was analyzed by Farahmand [8]. Moreno[13] discussed an M/G/1 retrial queue with recurrent customers and general retrial times. When a primary customer finds a server busy, the customer becomes unsatisfied and may quit the system permanently without receiving service. The retrial queueing model with non-persistent customers studied by Krishnamoorthy et al., [12] and Kasturi Ramanath et al., [11]. Queues with vacations have been studied extensively in the past: a comprehensive survey can be found in Teghem[18] and Doshi[6]. The Organization of the paper is as follows: The model under consideration is described in section 2. In section 3, we analyze the model by deriving the system steady state equations. Using the equations the probability generating function of queue length are obtained in section 4. In section 5, the operating characteristics exhibited. In section 6, numerical examples are exhibited.

MODEL DESCRIPTION

We consider an M/M/1 retrial queue with transit (also called ordinary) customers and a fixed number K ($K \geq 1$) of recurrent (also called permanent) customers. After service completion, recurrent customers always return to the retrial group and transit customers leave the system forever. Transit customers arrive according to a Poisson process with rate λ . If a transit customer finds the server free on his arrival, he occupies the server, otherwise, he enters the retrial group with probability γ or leave the system forever with probability $(1-\gamma)$, in accordance with an FCFS discipline. We will assume that only the transit customers at the head of the orbit is allowed for access to the server. Successive inter-retrial times of any transit customer follow an exponential distribution with rate α . The service times for the transit customers are exponentially distributed with rate μ_1 .

There is a fixed number K of permanent customers in the system. After having received service, recurrent customers immediately return to the retrial group in accordance with an FCFS discipline. We will assume that only the recurrent customer at the head of orbit is allowed for access to the server. Successive inter-retrial times of any recurrent customer follow an exponential distribution with rate α . The service times for the recurrent customers are exponentially distributed with rate μ_2 . After each service completion, the next customers to be served is determined by a competition between the primary customers retrial time of transit customers and recurrent customers. After completion of service there is no transit customers in the orbit the server takes the vacation of random length. At the end of vacation, if the server finds no transit customer in the orbit, he immediately take another vacation and continuous in this manner until he finds atleast one transit customer upon return from the vacation. The vacation times are exponentially distributed with parameter β . The inter arrival times, retrial times, service times and vacation times are mutually independent.

MODEL ANALYSIS

Let $O(t)$ be the number of customers in the orbit at time t and $C(t)$ denotes the server state at time t .

$$C(t) = \begin{cases} 0 & \text{if the server is idle (or) free (or) uncopied} \\ 1 & \text{if the server is busy with transit customers} \\ 2 & \text{if the server is busy with recurrent customers} \\ 3 & \text{if the server is on vacation} \end{cases}$$

We observe that $\{(O(t), C(t)): t \geq 0\}$ is a continuous Markov chain.

We define the following limiting probabilities for our subsequent analysis of the queueing model.

$$P_{0,n} = \lim_{t \rightarrow \infty} \{C(t) = 0, O(t) = n\}, \quad n \geq k+1$$

$$P_{1,n} = \lim_{t \rightarrow \infty} \{C(t) = 1, O(t) = n\}, \quad n \geq k$$

$$P_{2,n} = \lim_{t \rightarrow \infty} \{C(t) = 2, O(t) = n\}, \quad n \geq k$$

$$P_{3,n} = \lim_{t \rightarrow \infty} \{C(t) = 3, O(t) = n\}, \quad n \geq k$$





Pazhani Bala Murugan and Madhangi

The system has the following set of steady state equations:

$$(\lambda + \alpha + \beta)P_{0,n} = \mu_1 P_{1,n} + \mu_2 P_{2,n-1} + \theta P_{3,n}; n \geq k + 1 \quad (1)$$

$$(\lambda\gamma + \mu_1)P_{1,k} = \alpha P_{0,k+1} \quad (2)$$

$$(\lambda\gamma + \mu_1)P_{1,n} = \lambda P_{0,n} + \lambda\gamma P_{1,n-1} + \alpha P_{0,n+1}; n \geq k + 1 \quad (3)$$

$$(\lambda\gamma + \mu_2)P_{2,k} = \beta P_{0,k+1}; \quad (4)$$

$$(\lambda\gamma + \mu_2)P_{2,n} = \beta P_{0,n+1} + \lambda\gamma P_{2,n-1}; n \geq k + 1 \quad (5)$$

$$\lambda\gamma P_{3,k} = q\mu_1 P_{1,k} \quad (6)$$

$$(\lambda\gamma + \theta)P_{3,n} = \lambda\gamma P_{3,n-1}; n \geq k + 1 \quad (7)$$

4. PROBABILITY GENERATING FUNCTIONS OF QUEUE LENGTH

We define the following probability generating functions:

$$P_0(z) = \sum_{n=k+1}^{\infty} P_{0,n} z^n, P_1(z) = \sum_{n=k}^{\infty} P_{1,n} z^n \quad (8)$$

$$P_2(z) = \sum_{n=k}^{\infty} P_{2,n} z^n, P_3(z) = \sum_{n=k}^{\infty} P_{3,n} z^n \quad (9)$$

$$(\lambda + \alpha + \beta)P_0(z) = \mu_1 P_1(z) + \mu_2 z P_2(z) + \theta P_3(z) - (\lambda\gamma + \theta)P_{3,k} z^k \quad (9)$$

$$(\lambda\gamma - \lambda\gamma z + \mu_1)P_1(z) = (\lambda + \alpha z^{-1}) P_0(z) \quad (10)$$

$$(\lambda\gamma - \lambda\gamma z + \mu_2)P_2(z) = \beta z^{-1} P_0(z) \quad (11)$$

$$(\lambda\gamma - \lambda\gamma z + \theta)P_3(z) = (\lambda\gamma + \theta)P_{3,k} z^k \quad (12)$$

applying (8) into equations (1)-(7), we get

substituting equations (10), (11) and (12) in (9), we get

$$P_0(z) = \frac{-(\lambda\gamma + \theta)P_{3,k} z^k (\lambda\gamma - \lambda\gamma z + \mu_1)(\lambda\gamma - \lambda\gamma z + \mu_2)\lambda\gamma(1-z)}{(1-z)z^{-1}(\lambda\gamma - \lambda\gamma z + \theta) \left[(\lambda + \alpha + \beta)\lambda\gamma z [\lambda\gamma(1-z) + \mu_1 + \mu_2] - (\lambda z + \alpha)\lambda\gamma\mu_1 - \beta\lambda\gamma\mu_2 z - \alpha\mu_1\mu_2 \right]} \quad (13)$$

Substituting (13) in (10), we get

$$P_1(z) = \frac{-(\lambda\gamma + \theta)P_{3,k} z^k (\lambda + \alpha z^{-1})(\lambda\gamma - \lambda\gamma z + \mu_2)\lambda\gamma(1-z)}{(1-z)z^{-1}(\lambda\gamma - \lambda\gamma z + \theta) \left[(\lambda + \alpha + \beta)\lambda\gamma z [\lambda\gamma(1-z) + \mu_1 + \mu_2] - (\lambda z + \alpha)\lambda\gamma\mu_1 - \beta\lambda\gamma\mu_2 z - \alpha\mu_1\mu_2 \right]} \quad (14)$$

Substituting (13) in (11), we get

$$P_2(z) = \frac{-(\lambda\gamma + \theta)P_{3,k} z^k \beta z^{-1} (\lambda\gamma - \lambda\gamma z + \mu_1)\lambda\gamma(1-z)}{(1-z)z^{-1}(\lambda\gamma - \lambda\gamma z + \theta) \left[(\lambda + \alpha + \beta)\lambda\gamma z [\lambda\gamma(1-z) + \mu_1 + \mu_2] - (\lambda z + \alpha)\lambda\gamma\mu_1 - \beta\lambda\gamma\mu_2 z - \alpha\mu_1\mu_2 \right]} \quad (15)$$

From (12), we get

$$P_3(z) = \frac{-(\lambda\gamma + \theta)P_{3,k} z^k}{(\lambda\gamma - \lambda\gamma z + \theta)} \quad (16)$$

Let us define $P(z) = P_0(z) + z(P_1(z) + P_2(z) + P_3(z))$ as the probability generating function for number of customers in the system irrespective of the server state.

Substituting equations (13), (14), (15) and (16) in the above equation we get,

$$P(z) = \frac{\left[\begin{array}{l} (\lambda + \alpha + \beta)(\lambda\gamma - \lambda\gamma z + \mu_1 + \mu_2)\lambda\gamma z \\ - \lambda\gamma\mu_1(\lambda z + \alpha) - \lambda\gamma\mu_2\beta z - \alpha\mu_1\mu_2 \\ - \lambda\gamma z[(\lambda\gamma - \lambda\gamma z)(\lambda\gamma - \lambda\gamma z + \mu_1 + \mu_2) \\ + \mu_1\mu_2 + (\lambda\gamma - \lambda\gamma z)(\lambda + \alpha + \beta) \\ + (\lambda z + \alpha)\mu_2 + \beta\mu_1] \end{array} \right]}{(\lambda\gamma - \lambda\gamma z + \theta) \left[\begin{array}{l} (\lambda + \alpha + \beta)\lambda\gamma z [\lambda\gamma(1-z) \\ + \mu_1 + \mu_2] - (\lambda z + \alpha)\lambda\gamma\mu_1 \\ - \beta\lambda\gamma\mu_2 z - \alpha\mu_1\mu_2 \end{array} \right]} (\lambda\gamma + \theta)P_{3,k} \quad (17)$$





Pazhani Bala Murugan and Madhangai

Applying the normalizing condition $P(1)=1$, in equation (17), we get

$$P_{3,k} = \left(\frac{1}{1 + \frac{\lambda\gamma}{\theta}} \right) \left(\frac{1}{1 + \frac{\lambda\gamma}{\alpha}} \right) \left[1 - \frac{\lambda\gamma}{\mu_1} \left(1 + \frac{\lambda}{\alpha} + \frac{\beta\mu_1}{\alpha\mu_2} \right) \right] \quad (18)$$

Which implies that the utilisation factor is $\rho = \frac{\lambda\gamma}{\mu_1} \left(1 + \frac{\lambda}{\alpha} + \frac{\beta\mu_1}{\alpha\mu_2} \right)$ and the steady state condition is therefore

$$\frac{\lambda\gamma}{\mu_1} \left(1 + \frac{\lambda}{\alpha} + \frac{\beta\mu_1}{\alpha\mu_2} \right) \leq 1 \quad (19)$$

Particular cases

1. If $\theta \rightarrow \infty$ then the present model will be remodeled as an M/M/1 retrial queue with recurrent customers and non-persistent customers.
2. If $\theta \rightarrow \infty$ and $\theta \rightarrow \infty$, then the present model will be remodeled as an M/M/1 queue with recurrent customers and non-persistent customers.
3. If $\theta \rightarrow \infty$ and $\theta \rightarrow \infty$ and $k=0$ then the present model will be remodeled as an M/M/1 queue with non-persistent customers.
4. If $k=0$, then the present model will be remodeled as an M/M/1 retrial queue with non-persistent customers and server vacation.
5. If $k=0, \gamma=1$, and $\theta \rightarrow \infty$, then the present model will be remodeled as an M/M/1 retrial queue.

OPERATING CHARACTERISTICS

Let L_s denote the mean number of customers in the system.

The Probability generating function for the number of customers in the system is

$$P(z) = \frac{N(z)}{D(z)} (\lambda\gamma + \theta) P_{3,k}$$

$$N(z) = \begin{bmatrix} (\lambda + \alpha + \beta)(\lambda\gamma - \lambda\gamma z + \mu_1 + \mu_2)\lambda\gamma z \\ -\lambda\gamma\mu_1(\lambda z + \alpha) - \lambda\gamma\mu_2\beta z - \alpha\mu_1\mu_2 \\ -\lambda\gamma z[(\lambda\gamma - \lambda\gamma z)(\lambda\gamma - \lambda\gamma z + \mu_1 + \mu_2) \\ + \mu_1\mu_2 + (\lambda\gamma - \lambda\gamma z)(\lambda + \alpha + \beta) \\ + (\lambda z + \alpha)\mu_2 + \beta\mu_1] \end{bmatrix}$$

$$D(z) = (\lambda\gamma - \lambda\gamma z + \theta) \begin{bmatrix} (\lambda + \alpha + \beta)\lambda\gamma z[\lambda\gamma(1 - z)] \\ + \mu_1 + \mu_2 - (\lambda z + \alpha)\lambda\gamma\mu_1 \\ - \beta\lambda\gamma\mu_2 z - \alpha\mu_1\mu_2 \end{bmatrix}$$

$$P_{3,k} = \left(\frac{1}{1 + \frac{\lambda\gamma}{\theta}} \right) \left(\frac{1}{1 + \frac{\lambda\gamma}{\alpha}} \right) \left[1 - \frac{\lambda\gamma}{\mu_1} \left(1 + \frac{\lambda}{\alpha} + \frac{\beta\mu_1}{\alpha\mu_2} \right) \right]$$

Differentiating with respect to z

$$P'(z) = \frac{D(z)N'(z) - D'(z)N(z)}{[D(z)]^2} (\lambda\gamma + \theta) P_{3,k}$$

$$N'(z) = \begin{bmatrix} (\lambda + \alpha + \beta)(\lambda\gamma - \lambda\gamma z + \mu_1 + \mu_2)\lambda\gamma z \\ -\lambda\gamma\mu_1(\lambda z + \alpha) - \lambda\gamma\mu_2\beta z - \alpha\mu_1\mu_2 \\ -\lambda\gamma z[(\lambda\gamma - \lambda\gamma z)(\lambda\gamma - \lambda\gamma z + \mu_1 + \mu_2) \\ + \mu_1\mu_2 + (\lambda\gamma - \lambda\gamma z)(\lambda + \alpha + \beta) \\ + (\lambda z + \alpha)\mu_2 + \beta\mu_1] \end{bmatrix}$$





Mukund V.Singh et al.,

$$N'(z) = \begin{bmatrix} (\lambda + \alpha + \beta)(\lambda\gamma - \lambda\gamma z + \mu_1 + \mu_2)\lambda\gamma \\ -(\lambda + \alpha + \beta)\lambda\gamma z^2 - \lambda\gamma\mu_1 - \lambda\gamma\mu_2\beta \\ -\lambda\gamma(\lambda\gamma - \lambda\gamma z)(\lambda\gamma - \lambda\gamma z + \mu_1 + \mu_2) \\ +\lambda^2\gamma^2 z(\lambda\gamma - \lambda\gamma z + \mu_1 + \mu_2) \\ +\lambda^2\gamma^2 z(\lambda\gamma - \lambda\gamma z) - \lambda\gamma\mu_1\mu_2 \\ -\lambda\gamma(\lambda\gamma - \lambda\gamma z)(\lambda + \alpha + \beta) \\ +\lambda^2\gamma^2 z(\lambda + \alpha + \beta) + \lambda^2\gamma z(\lambda\gamma - \lambda\gamma z) \\ -\lambda\gamma(\lambda z + \alpha)\mu_2 - \lambda^2\gamma z\mu_2 - \lambda\gamma\beta\mu_1 \end{bmatrix}$$

$$D(z) = (\lambda\gamma - \lambda\gamma z + \theta) \begin{bmatrix} (\lambda + \alpha + \beta)\lambda\gamma z[\lambda\gamma(1 - z)] \\ +\mu_1 + \mu_2] - (\lambda z + \alpha)\lambda\gamma\mu_1 \\ -\beta\lambda\gamma\mu_2 z - \alpha\mu_1\mu_2 \end{bmatrix}$$

$$D'(z) = \begin{bmatrix} -\lambda\gamma[(\lambda + \alpha + \beta)(\lambda - \lambda z + \mu_1 + \mu_2)\lambda\gamma z] \\ +(\lambda\gamma - \lambda\gamma z + \theta)(\lambda + \alpha + \beta)\lambda\gamma z \\ +(\lambda\gamma - \lambda\gamma z + \theta)(\lambda + \alpha + \beta) \\ (\lambda\gamma - \lambda\gamma z + \mu_1 + \mu_2)\lambda\gamma \\ -\lambda^2\gamma\mu_1(\lambda\gamma - \lambda\gamma z + \theta) \\ +\lambda^2\gamma^2\mu_1(\lambda z + \alpha) \\ -(\lambda\gamma - \lambda\gamma z + \theta)\lambda\gamma\mu_2\beta z \\ +\lambda^2\gamma^2\mu_2\beta z + \lambda\gamma\alpha\mu_1\mu_2 \end{bmatrix}$$

At $z=1$

$$L_s = P(1) = \frac{D(1)N'(1) - D'(1)N(1)}{[D(1)]^2} P_{3,k}$$

$$N(1) = (\lambda + \alpha + \beta)(\mu_1 + \mu_2)\lambda\gamma$$

$$-\lambda\gamma\mu_1(\lambda + \alpha) - \lambda\gamma\mu_2\beta - \alpha\mu_1\mu_2$$

$$-\lambda\gamma\mu_1\mu_2 - \lambda\gamma(\lambda + \alpha)\mu_2 + \lambda\gamma\beta\mu_1$$

$$N'(1) = (\lambda + \alpha + \beta)[(\mu_1 + \mu_2)\lambda\gamma - \lambda\gamma + \lambda^2\gamma^2] + \lambda^2\gamma^2\mu_1[\lambda^2 + \lambda\gamma - \mu_2 - \beta] + \lambda\gamma\mu_2 - [\beta + \lambda\gamma - (\lambda + \alpha) - \lambda]$$

$$D(1) = \theta(\lambda + \alpha + \beta)(\mu_1 + \mu_2)\lambda\gamma - \lambda\gamma\mu_1(\lambda + \alpha)\theta - \theta\lambda\gamma\mu_2\beta - \beta\alpha\mu_1\mu_2$$

$$D'(1) = \begin{pmatrix} (\lambda + \alpha + \beta) \\ [(\mu_1 + \mu_2)\lambda^2\gamma^2 + \theta\lambda\gamma + \theta(\mu_1 + \mu_2)] \\ +\lambda\gamma\mu_1[\lambda\gamma(\lambda + \alpha) - \theta\lambda + \alpha\mu_2] \\ +\lambda\gamma\mu_2\beta[\lambda\gamma - \theta] \end{pmatrix}$$

NUMERICAL RESULTS

The curved graph constructed in Figure 2 and the values tabulated in the Table 1 are obtained by setting the fixed values $\mu_1=1$, $\alpha=1$, $\beta=0.3$, $k=1$, $\theta=1$, $\lambda=0.1$, $t=0.1$, $t=0.3$ and varying the values of λ from 1 to 2 incremented with 0.2 and extending the values of μ_2 from 1.5 to 1.9 in steps of 0.2. We observed that as λ rises L_s also rises which shows the stability of the model.





Mukund V.Singh et al.,

The curved graph constructed in Figure 3 and the values tabulated in the Table 2 are obtained by setting the fixed values $\mu_1=1$, $\mu_2=1.5$, $\alpha=1$, $k=1$, $\theta=1$, $\rho=0.1$, $\tau=0.1$, $t=0.3$ and varying the values of λ from 1 to 2 incremented with 0.2 and extending the values of β from 0.3 to 0.9 in steps of 0.3. We observed that as λ rises L_s also rises which shows the stability of the model.

The curved graph constructed in Figure 4 and the values tabulated in the Table 3 are obtained by setting the fixed values $\mu_1=1$, $\mu_2=1.5$, $\beta=0.3$, $k=1$, $\theta=1$, $\rho=0.1$, $\tau=0.1$, $t=0.3$ and varying the values of λ from 1 to 2 incremented with 0.2 and extending the values of α from 1 to 2 in steps of 0.5. We observed that as λ rises L_s also rises which shows the stability of the model.

The curved graph constructed in Figure 5 and the values tabulated in the Table 4 are obtained by setting the fixed $\mu_2=1.5$, $\alpha=1$, $\beta=0.3$, $k=1$, $\theta=1$, $\rho=0.1$, $\tau=0.1$, $t=0.3$ and varying the values of λ from 1 to 2 incremented with 0.2 and extending the values of μ_1 from 3 to 7 in steps of 2. We observed that as λ rises L_s also rises which shows the stability of the model.

CONCLUSION

In this paper, An M/M/1 retrial queue with recurrent customers, non-persistent customers and server vacation is evaluated. We obtained the PGF for the number of customers and the mean number of customers in the system. We also derived the performance measures. We obtained some particular cases. We illustrate some numerical results.

REFERENCES

1. J.R.Artalijo, "Accessible bibliography on retrial queues", Mathematical and computer Modelling 30(1999) 1-6.
2. O.J Boxma, J.W.Cohen, "The M/G/1 queue with permanent customers" IEEE Journal on selected Areas in communication 9(2)(1991) 179-184.
3. O.J.Boxma, S.Schlegel and U.Yechiali, "M/G/1 queue with waiting server timer and vacations", American Mathematical Society Translations, 2(207), pp.25-35 (2002).
4. V.M.Chandrasekaran, K.Indhira, M.C.Saravananarajan and P.Rajadurai, "A survey on working vacation queueing models", International Journal of Pure and Applied Mathematics, 106(6), pp.33-41 (2016).
5. Cohen J.W., "The single server queue", North-Holland, Amsterdam, (1969).
6. Doshi B.T., "Queueing systems with vacations-A survey", Queueing Systems, 1(1986), 29-66.
7. G.I.Falin, J.G.C.Templeton, "Retrial Queues", Chapman and Hall, London, 1997.
8. K.Farahmand, "Single line queue with repeated demands" Queueing Systems 6(1990) 223-228.
9. K.Farahmand, "Single line queue with recurrent demands", Queueing Systems 22(1996) 425-435.
10. R.Kalyanaraman and S.Pazhani Bala Murugan.S, "A single server queue with additional optional service in batches and server vacation", Vol.2 56(2008), 2765-2776.
11. Kasturi Ramanath and Kalidass K., "An M/G/1 Retrial Queue with Non-Persistent Customers, a Second Optional Service and Different Vacation Policies, Applied Mathematical Sciences, 4(40) (2010), 1967 - 1974.
12. Krishnamorthy A., Deepak T.G. and Joshua V.C., "An M/G/1 retrial queue with non-persistent customers and orbital search", Stochastic Analysis and Applications, 23(2005), 975-997.
13. Moreno P., "An M/G/1 retrial queue with recurrent customers and general retrial times", Applied Mathematics and Computation, Vol.159(2004), 651-666.
14. Pazhani Bala Murugan S. and Madhangi P, "Analysis of a Morkovian retrial queue with feedback, recurrent customers and server vacation" Indian Journal of Natural Science 80(14) (2022-23), 63735-63759, (Web of Science Indexed).
15. Pazhani Bala Murugan S. and Madhangi P, "Analysis of a Morkovian retrial queue with recurrent customers, switch over time and server vacation" European Chemical Bulletin 12(special issue 13), (2023) 620-631, Scopus Indexed





Pazhani Bala Murugan and Madhangi

16. Senthil Kumar M. and Arumuganathan R., "Performance analysis of an M/G/1 retrial queue with non-persistent calls, two phases of heterogeneous service and different vacation policies", Int. J. of Open Problems in Comp. Sci. and Math., 2(2)(2009),196-214.
17. Shan Gao and Jinting Wang, "Performance and reliability analysis of an M/G/1-G retrial queue with orbital search and non-persistent customers", European Journal of Operational Research, 236(2014), 561-572.
18. J.Teghem, "Control of the service process in queueing system". Eur.J.Oper. Res., Vol.23(1986), 141-158.

Table 1: L_s with turn over of λ

λ	$\mu_2=1.5$	$\mu_2=1.7$	$\mu_2=1.9$
1.0	4.8143	4.5814	4.3986
1.2	5.6674	5.3903	5.1731
1.4	6.7691	6.4321	6.1687
1.6	8.2758	7.8518	7.5214
1.8	10.4975	9.9345	9.4977
2.0	14.1457	13.3292	12.7003

Table 2: L_s with turn over of λ

λ	$\beta=0.3$	$\beta=0.6$	$\beta=0.9$
1.0	4.5498	5.2590	6.0084
1.2	5.3249	6.1555	7.0471
1.4	6.3425	7.3602	8.4776
1.6	7.7599	9.0859	10.5880
1.8	9.8873	11.7744	14.0149
2.0	13.4373	16.5236	20.4972

Table 3: L_s with turn over of λ

λ	$\alpha=1$	$\alpha=1.5$	$\alpha=2$
1.0	4.8143	3.7425	3.2430
1.2	5.6674	4.2438	3.6044
1.4	6.7691	4.8442	4.0226
1.6	8.2758	5.5873	4.5179
1.8	10.4975	6.5434	5.1202
2.0	14.1457	7.8339	5.8759

Table 4: L_s with turn over of λ

λ	$\mu_1=3$	$\mu_1=5$	$\mu_1=7$
1.0	2.2870	1.9132	1.7596
1.2	2.4745	2.0379	1.8611
1.4	2.6660	2.1541	1.9503
1.6	2.8665	2.2635	2.0284
1.8	3.0823	2.3684	2.0964
2.0	3.2198	2.4712	2.1559





Pazhani Bala Murugan and Madhangi

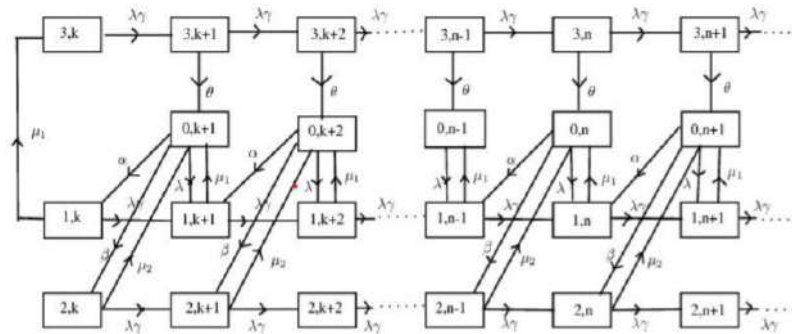
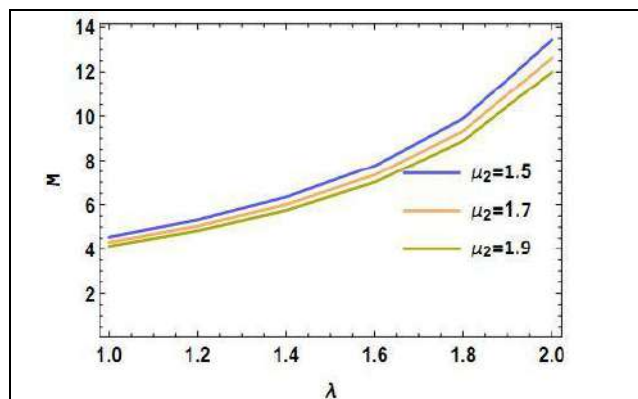
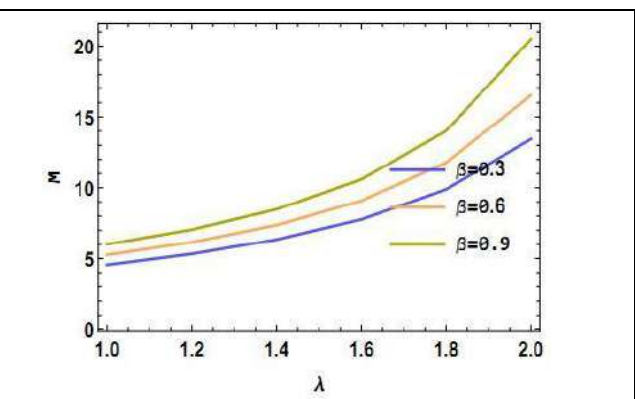
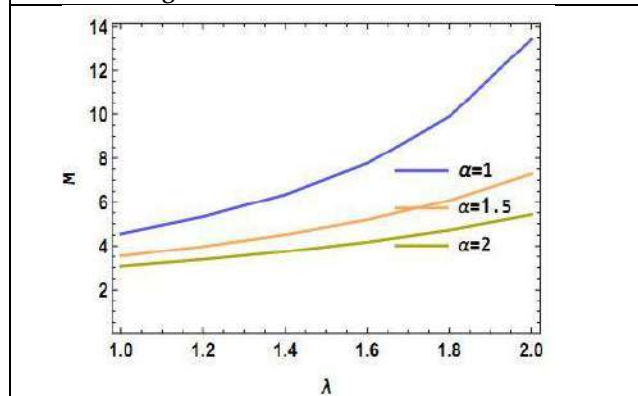
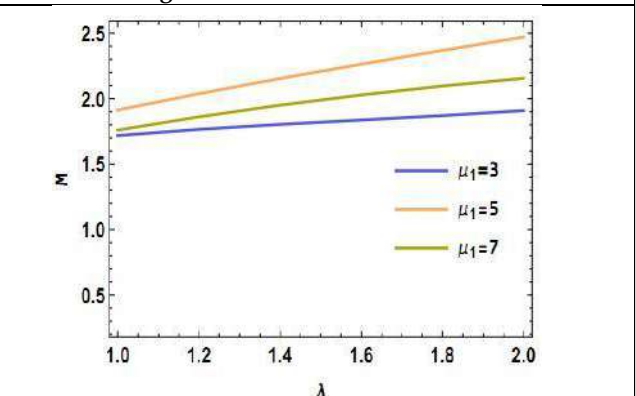


Figure 1: Transition state diagram of the model.

Figure 2: L_s with turn over ofFigure 3: L_s with turn over ofFigure 4: L_s with turn over ofFigure 5: L_s with turn over of



Alienation and Hybridization in Rohinton Mistry's Short Story, *Lend Me Your Light*

C. Shahin Banu^{1*}, M.Renuga², N.Vadivu¹ and G. Saratha Lakshmi¹

¹Assistant Professor, Department of English, Sona College of Technology, Salem, (Affiliated to Anna University) Chennai, Tamil Nadu, India.

²Professor, Department of English, Sona College of Technology, Salem, (Affiliated to Anna University) Chennai, Tamil Nadu, India.

Received: 22 Jan 2024

Revised: 09 Feb 2024

Accepted: 15 May 2024

*Address for Correspondence

C. Shahin Banu

Assistant Professor,
Department of English,
Sona College of Technology,
Salem, (Affiliated to Anna University)
Chennai, Tamil Nadu, India.
Email: shahin@sonatech.ac.in



This is an Open Access Journal / article distributed under the terms of the **Creative Commons Attribution License** (CC BY-NC-ND 3.0) which permits unrestricted use, distribution, and reproduction in any medium, provided the original work is properly cited. All rights reserved.

ABSTRACT

Alienation is an emotional isolation, which forms the subject of many psychological, sociological, literary and philosophical studies. Alienation arises as innate significance of existential dilemma both in intrinsic and extrinsic terms. The alienated protagonists struggle to face displacement in Rohinton Mistry's short story *Lend me Your Light*. Alienation in its diverse forms has been dealt with in the existentialistic literature. Alienation is the consequence of loss of identity. The displacement and search for identity is a prominent theme in modern fiction. The postcolonial term Hybridity displays a combination of two or more cultures and the culturally hybrid person is supposed to live with a new community. Mistry's characters are alienated from native and also live in different culture of Hybridization. The aim of the paper is to analyse the alienation and Hybridization in Mistry's Short Story *Lend me Your Light*.

Keywords: Alienation, isolation, existential dilemma, displacement, Hybridity

INTRODUCTION

Mistry starts the story "Lend me your Light" with an epigraph from Rabindranath Tagore's Gitanjali. "Lend me your Light" is a story of alienation and displacement. Tagore's verse analyses the diasporic writers' sense of guilt for leaving their homeland. Main characters of this story are Jamshed, Percy and Kersi. Kersi tries to cope with migration and his responses varies from the experience as "destructive, agonizing, and painful" (Frank: 18-19) to the



**Shahin Banu et al.,**

experience of migration. Rohinton Mistry has incorporated various themes such as loneliness, immigrant life, cultural encounter, identity crisis, tradition and modernity, etc. "Lend me your Light" describes the mental agony of characters during immigration. Jamshed, Percy and his brother Kersi are intimate friends. Jamshed goes to the United States and Kersi to Canada. Life in different countries changes the attitudes of characters towards cultural differences. Sten P. Moslund says,

It seems that we are witnessing a massive international and transnational defeat of gravity, an immense uprooting of origin and belonging, an immense displacement of borders, with all the clashes, meetings, [...] reshaping the cultural landscapes of the world's countries and cities (2).

Confusion arises in characters whether the new identity can be accepted or rejected to lead a life in a diaspora situation. Vinoth. M. says, "Relationship in life matters and means a lot for every individual in a family, society and cultural group. When we explore a relationship that gives meaning to our life, helps us to elevate and encourage us to do things that we cannot do is "Mentorship" (2022). Ajay Hebles describes, "Jamshed who scornful of his native India, leaves for the Promised land of America, and Percy, who adamantly stays in India to help villagers in their fight against exploitation, the story finds its focus in Kersi, the narrator, who comes to represent the struggle between the two extreme positions" (20). Jamshed thinks that India is full of corruption and crime. As he is unable to get a better position in India, he migrates to the United States. He feels that "Ghaties" 179 (TFB 176) a member of lower caste in India, get preference in India. He Says, "In particular version of reality we inherited, ghatis were always flooding places, they never just went there. Ghatis were flooding the banks, desecrating the sanctity of institutions, and taking up all the covered jobs. Ghati is even flooding the colleges and Universities, a thing unheard of whenever you turned, the bloody Ghatis were flooding the place" (TFB 176).

Jamshed "the young Parsi male striving for happiness and individual liberation (moksha) through emigration to North America" (Somacarrea-Inigo 80). He adapts in multicultural America where money enables him to assimilate to capitalist America. Nilufer E. Bharucha describes the Parsees as "an assimilative people who have over the centuries perfected the difficult art of being both global and local at one and at the same time something that the rest of the world is beginning to talk about only recently" (42).

Similarly in Amitav Ghosh's *The Shadow Lines*, the narrator's cousin ignores her Indianness and wants to get adapted into the host country. Percy does not prefer to move to foreign countries instead he commits himself to challenging social injustice in India. He believes that corruption and crime can be removed. He practices solidarity towards his fellow human beings. For Jamshed, capitalism overrides ethnic as well as caste differences in America. Percy lives in India and works towards improving the social status within India. These two characters, Jamshed and Percy want to erase differences in their lives but they design their way of living differently. For Jamshed money and capitalism constitutes sameness, but for Percy humanity is the central bond between individuals. Mistry emphasizes the value of humanity which is very essential for every individual. Jamshed and Percy arise for two extreme points of view concerning their concept of migration. Kersi relinquishes his dream to return to his homeland and stays as a young writer. He holds his emotions that is mentally and physically for home land and foreign. His literary work occupies the between native and foreign. He observes life in a dual perspective of double identity in culture, loyalty and even language. Jamshed persistently values the quality of the West so finds imperfection with his homeland. Kersi feels guilt for leaving his homeland and struggles to hold the contradictions of his own cultural hybridity. This cultural hybridity and the distorting of the boundaries of ethnic and religious identity are realities of minority existence and being a Parsi. The story depicts an everlasting struggle between community identity and dissolution of boundaries. The coping process of self-examination and personal adaptation takes its own ground on the basis of an identity that results from the interaction of memory and present experience, leading to an uncertain consciousness. Mistry expertly reveals the anxiety arising among Parsi individuals both in Indian society, where they are often excluded by the predominant Hindu and Muslim populations, and in Western nations. Mistry's character Kersi runs behind rats with his cricket bat in "One Sunday", and he plucks white hairs from his father's head in "Of White Hairs and Cricket", he migrates to Canada in "Lend me your Light". He is caught between two worlds Bombay





Shahin Banu et al.,

which he left and Canada which he adopted. Kersi's migration results in alienation and he has a guilty feeling towards the culture he left in Bombay. He makes an effort to recover the culture he has left in Bombay. Lakshmi, G. Saratha says, "Accepting changes in life can be scary in the beginning but allowing the fear to stop you growing, evolving and progressing is all the more devastating" (2021).

Mistry shows that Kersi finds it difficult to adapt himself to the new environment. He brings the intertextual reference to Greek Mythology by taking recourse to TS Eliot's, *The Waste Land*, section III. Kersi suffers from conjunctivitis (eye disease) like the blind seer Tiresias in mythological character. He says, "I, Tiresias, blind and throbbing between two lives, the one in Bombay and the one to come in Toronto" (180 TFB). Mythological character Tiresias is a man of the in-between, the world and underworld who has received the gift of prophecy as compensation for the blindness. He is a man of both sexes as well as moving between the world and the underworld. God endows him the ability to see the future. In the waste land, Tiresias, speaks, "I, Tiresias, though blind, throbbing between two lives, old man with wrinkled female breasts, can see the violent hour, the evening hour that strives home ward, and brings the sailor home from sea, III western" (29).

According to C.P. Ravichandra, Kersi on the other hand, merely suffers from his hybridity in the mundane, post religious sphere of the diaspora. He cannot make out the sailor coming home i.e. Ulysses, whom Tiresias in Eliot's poem speaks of, for he himself is on an odyssey, i.e. Sentenced to wander the earth in search of a home Kersi's failure to perceive the sailor is a failure to evaluate his situation in Canada as someone who is essentially homeless (20). Kersi's comparison to Tiresias shows his failure, and he suffers from his hybridity in the diaspora situation.

Mistry's *Lend me Your Light* is related to Nathaniel Hawthorne American novelist and short story writer, whose works are the theme of alienation. Alienation is emotional isolation or dissociation from others. In Hawthorne's novels and short stories, characters are consistently alienated and experience isolation from society like Mistry's character Kersi. He is isolated from their loved ones both physically and psychologically. Vadivu N. states, "Terrible sense of desolation influences the psychological condition of a person who has to face the situation with hope" (2021).

Mistry highlights the common man's issues such as family and ethical values, diasporic consciousness in his stories. He wishes to preserve the culture and tradition of Parsi. He brings out the immigrant's nostalgia and alienation of Parsis in India. He makes an emphatic claim for a balanced attitude towards identity construction in multicultural Canada. The hues and cries of human life are shown without any paradoxes in these short stories. All these stories address the social issues and dilemmas faced by individuals. The short story collection deals with entirely different thematic perceptions highlighting the modern issues and trends of Indian mindset and differs a lot from his novels. Beena Kamalani says about Mistry's works, "I had never met such people in fiction before. How was it possible that now that world, a world I had come to see as lost, or at least gone from me, was here now, mine to savor, to remember and to treasure?" (2013).

Mistry's writings are "concerned with the politics of migrancy and with the tension between the migrant's geographical distance from India and his continuing political responsibility towards that nation" (Herbert 32). Mistry's light imagery in this story does not only allude to James Herd's moral darkness juxtaposed to Percy's qualities as light brings but also to highlight its concern with vision and seeing. Mistry's characters renew the past and try to recreate the lost identities by a deep perception of an "in between-space", the experience of hybridization. Mistry points out that the title "*Lend Me Your Light*" is not only a demand for humanism and solidarity but also a will to truth. Mistry conveys that though the Parsis feel the sense of racial discrimination, but they are proud of India and their ethnic identity.

REFERENCES

1. Barry, Herbert, and Erich Lindemann. "Critical Ages for Maternal Bereavement in Psychoneuroses." *Psychosomatic Medicine*, vol. 22, no. 3, 1960, pp. 166–181.



**Shahin Banu et al.,**

3. doi:10.1097/00006842-196005000-00002.
4. Frank, S. (2008). *Migration and Literature*. New York: Palgrave Macmillan.
5. Kamalani, Beena. "'Lend Me Your Light': Rohinton Mistry and the Art of Storytelling." *World Literature Today*, vol. 87, no. 1, Jan.-Feb. 2013, pp. 53. *Gale Literature Resource Center*, link.gale.com/apps/doc/A324206631/LitRC?u=anon~d3ee9f25&sid=googleScholar&xid=1eacc43b. Accessed 15 Feb. 2024.
6. Lakshmi, G. Saratha. *Emergence of Autonomous Self through Predicaments in The Select Novels of Shashi Deshpande*, 2021, Periyar University, Ph.D. Dissertation.
7. Mistry, Rohinton. *Tales from Firozsha Bagh*. Penguin Books Canada Limited, London. 1987.
8. Moslund, S. P. (2010). *Migration Literature and Hybridity*. London: Palgrave Macmillan.
9. Ross, R. L. (1999). Seeking and Maintaining Balance: Rohinton Mistry's Fiction. *World Literature Today*, 73(2), 239–244. <https://doi.org/10.2307/40154686>
10. Vadivu N. *Transcultural Turn of the dislocated self in the select Novels of Chitra Banerjee Divakaruni's*, 2021, Periyar University, Ph.D. Dissertation.
11. Vinoth. M. *Inculcating cultural values through mentor (-ship) in Louise Erdrich Tracks*, Bhavaveen, <https://telugujournalbhavaveena.blogspot.com/>
12. <https://drive.google.com/file/d/1YEOYryawJAVorghkYQPIUGkmE0uQ8Z7n/view>





Design and Evaluation of Novel Hydrogel Formulation of *Tridax procumbens*

Pallavi Dhekale¹, Poonam Taru², Reshma Todkari¹ and Renuka Sawale^{1*}

¹Assistant Professor, Department of Pharmaceutical Chemistry, KJEl's Trinity College of Pharmacy, Pune (Affiliated to Dr. Babasaheb Ambedkar Technological University), Maharashtra, India.

²Assistant Professor, Department of Pharmacognosy, Vishwakarma University Pune, Maharashtra, India.

Received: 08 Feb 2024

Revised: 11 Mar 2024

Accepted: 10 May 2024

*Address for Correspondence

Renuka Sawale

Assistant Professor,
Department of Pharmaceutical Chemistry,
KJEl's Trinity College of Pharmacy, Pune
(Affiliated to Dr. Babasaheb Ambedkar Technological University),
Maharashtra, India.



This is an Open Access Journal / article distributed under the terms of the **Creative Commons Attribution License** (CC BY-NC-ND 3.0) which permits unrestricted use, distribution, and reproduction in any medium, provided the original work is properly cited. All rights reserved.

ABSTRACT

Herbal medicine has grown in relevance on a global scale for both medical and financial reasons. The use of herbal medications has grown, but in both industrialized and developing nations, there are significant questions about their efficacy, safety, and quality. Patients are becoming more compliant with herbal medicines because they don't have the usual adverse effects of allopathic medications. The goal of the current study is to create and assess a herbal gel that contains leaf extract from *Tridax*. Carbapol 940, propylene glycol, methyl and propyl parabens, *Tridax procumbens* leaf extract, and the necessary quantity of distilled water were used to create the gel formulation. Tri-ethanolamine was added drop by drop to maintain the pH of the skin. The formulations' physicochemical characteristics, such as pH, spreadability, and viscosity, were ascertained. Given that allopathic treatments have adverse effects, herbal remedies are thought to be safer than allopathic ones. Preparing the extract and their formulations for improved absorption and penetration of the active moiety into the systemic circulation is one strategy for ensuring its life.

Keywords: *Tridaxprocumbens*, leaf extract, guar gum, hydrogel.

INTRODUCTION

: Since the beginning of time, medicinal plants have been a key source of cures for illnesses affecting humans. It is understandable that 1.42 billion people, or one-fourth of the world's population, rely on traditional medicine to treat a variety of illnesses. Eco-friendly and bio friendly plant-based products have received a lot of attention lately as potential treatments and preventative measures for many human illnesses [1]. It is known that the majority of people





Pallavi Dhekale *et al.*,

on the planet have used traditional medicine, especially plant-based medicines, for their primary medical needs.¹ Indian flora contains a wide range of plants with therapeutic qualities. These plants can be used to discover efficient substitutes for manufactured medications. Plants are essential for treating a wide range of human illnesses, and because herbal therapies don't have the common side effects. There are two traditional lines of treatment for rheumatoid arthritis in the allopathic medical system, both of which have drawbacks [1]. Therefore, using tried-and-true Ayurvedic herbal medication compositions would be the better course of action [2]. Therefore, research into these medications and their efficient formulation is necessary for improved patient acceptance [4,5,6,7,8] Herbal-based remedies have long been used in India to treat and cure a wide range of illnesses. Additionally, a wide range of prescriptions for medical conditions like wound healing, inflammation, skin infections, leprosy, diarrhea, scabies, venereal illness, ulcers, snake bites, etc. are included in Indian folk medicine. For a variety of skin conditions, about 80% of the world's population still uses traditional medicine [29]. Herbal remedies for wound care include debridement, disinfecting, and creating a moist atmosphere to promote the creation of an environment that is conducive to the body's natural healing process. One of the top research topics in the world is the study of medicinal plants. The application of topical antibiotic therapy is a crucial approach to wound care.³⁰ Medicinal herbs have been utilized extensively and with great success to promote wound healing in folk medicine.⁹ This has spurred numerous studies that seek to confirm the assertions and identify probable mechanisms explaining these herbs' ability for promoting wound healing and eradicating infections [31]. Transdermal medication delivery is the term used to describe the administration of drugs through the skin in order to create a systemic impact. Transdermal drug delivery systems (TDDS) offer a way to maintain medication release while lowering the dosage and thereby lowering the negative effects of oral therapy [10]. Semisolids come in a variety of dose forms, each with special qualities.

MATERIAL AND METHODS

Method of extraction: Decoction method was used for extraction [15].

- 1) Wash the leaves with water to remove dust and soil particles.
- 2) Leaves were boiled in water for 15 min, then cooling, straining and passing through filter paper to produce the required volume

Method for preparation of hydrogels [15-16]: For the preparation of hydrogel weight 0.3 gm gaur gum in beaker, then add 3 gm of glycerin for avoid lumping stir it and mix well, add 45ml of demineralized water and mix. Gel like appearance was obtained then add 7.5 ml of 4% borax solution in to the gel. Keep the solution 1 hr. undisturbed condition for formation of cross linking hydrogel.

Evaluation test [17,18,19,21]

A) Homogeneity: Once the gels had been added in the container, their appearance and the presence of any aggregates were visually inspected to test for homogeneity.

B) pH measurement

A digital pH meter was used to measure the pH of several gel formulations. After precisely weighing 2.5 gm of gel, it was mixed with 25 ml of distilled water and kept for two hours. Three separate measurements of each formulation's pH were made, and the average results are shown. Using a pH meter, the dispersions' pH was determined

C) Spreadability: Concentric circles of different radius were drawn on graph paper and a glass plate was fixed onto it. 5gms of gel was placed on the center of the lower plate. Another glass plate of 100±5 gm was placed gently on the gel and the spread diameter was recorded after 1 minute of each addition

D) Sensitivity test: Ten healthy male and female volunteers underwent a skin irritancy test. 100 mg of gel was administered over a 2 cm region, and any lesions or irritation/redness were checked for.

E) Antimicrobial study (Zone of inhibition): The antibacterial activity of *Tridax procumbens* from its different gel formulations. The antibacterial activity was determined by measuring the zone of inhibition.





Pallavi Dhekale et al.,

RESULTS AND DISCUSSION

Characterization of polymer: [22,23,24,25] Colour and appearance: Colour and appearance of the polymer is checked and is as mentioned below in table.

Physico-chemical evaluation of *Tridax procumbens* leaf [26] Different Physico-chemical evaluation tests of *Tridax procumbens* leaf extract were done and results of the tests are as mentioned below in table

Preliminary phyto-chemical screening [25,26,27] Different preliminary phyto-chemical screening tests are done and results of the tests are as mentioned below in table

Evaluation of Hydrogel Formulation [28,29,20]

Physical Evaluation: The formulation showed good homogeneity with absence of lumps and grittiness.

pH Determination: [21]: pH of formulation = 6.7

The pH of the formulation is 6.7 which is considered as acceptable to avoid the risk of irritation upon application to the skin.

Spread ability: Table no. 5: Spread ability test of hydrogel

Skin irritation: Formulation passed the skin irritation test when applied to the volunteers.

Antimicrobial study: Zone of inhibition [30, 31] Antibacterial activity was determined by measuring the zone of inhibition. The result from the formulation was satisfactory and the greatest activity was observed in formulation.

The range of zone of inhibition for the *staphylococcus aureus* bacteria is 23 and the *Escherichia coli* bacteria is 31.

CONCLUSION

It was found that *Tridax procumbens* gel formulations containing gelling agents, like guar gum, have adequate antifungal, physicochemical, and rheological properties. All of the generated gel's Colour, homogeneity, consistency, spreadability, and pH value were found to be satisfactory. The following parameters were verified to be within the acceptable limits and produced positive results. It is feasible to draw the conclusion that the formulation showed enhanced drug release research outcomes in terms of spreadability, uniformity, and homogeneity. Promising antibacterial effectiveness against *E. coli* was demonstrated by the gel. Therefore, the generated mixture was thought to have the potential to be used as a topical treatment for bacterial infections of the skin. Delivery needs to be improved continuously, not just for hydrophobic substances but also for more sensitive molecules like proteins, antibodies, or nucleic acids, which are damaged by interactions with the hydrogel delivery vehicle. If these problems could be resolved, there would be a significant rise in the possibility for hydrogel-based drug delivery to properly distribute next-generation drugs at the appropriate rate and location throughout the body.

REFERENCES

1. M. Blumenthal, A. Goldberg, & J. Brinckmann, "Herbal medicine. Expanded commission E monographs", MA: Integrative Medicine, 2020 <https://doi.org/10.7326/0003-4819-133-6-200009190-00031>
2. Chen, J., Zhu, H., Zhu, Y., Zhao, C., Wang, S., Zheng, Y., & Wang, H. "Injectable self-healing hydrogel with siRNA delivery property for sustained STING silencing and enhanced therapy of intervertebral disc degeneration. *Bioactive materials*", 2022, 9, pp.29-43. <https://doi.org/10.1016/j.bioactmat.2021.08.003>
3. S. H. Aswathy, U. Narendrakumar, & I. Manjubala, Commercial hydrogels for biomedical applications. *Heliyon*, 2020, 6(4), e03719. <https://doi.org/10.1016/j.heliyon.2020.e03719>
4. S.C.Pang, S. F. Chin, S. H. Tay, & F. M. Tcheng, "Starch-maleate- polyvinyl alcohol hydrogels with controllable swelling behaviors. *Carbohydrate Polymers*" 2011, 84(1), pp 424-429. <https://doi.org/10.5402/2012/723686>





Pallavi Dhekale et al.,

5. S. Jain, N. Jain, A. Tiwari, N. Balekar, & D. K. Jain. "Simple evaluation of wound healing activity of polyherbal formulation of roots of *Ageratum conyzoides* Linn". Asian Journal of Research in Chemistry, 2009, 2(2), pp. 135-138.
6. S. Agrawal, D. Mohale, & G. S. Talele, "Pharmacological activities of *Tridax procumbens* (Asteraceae). Medicinal Plants" International Journal of Phytomedicines and Related Industries, 2010, 2(2), pp. 73-78.
7. S. Shaik, M. R. Kummara, S. Poluru, C. Allu, J. Gooty, M., C. R. Kashayi, "A green approach to synthesize silver nanoparticles in starch-co-poly (acrylamide) hydrogels by *tridax procumbens* leaf extract and their antibacterial activity. International Journal of Carbohydrate Chemistry, 2013.
8. D. S. Arora, & Kaur, G. J.. Antibacterial activity of some Indian medicinal plants. Journal of natural medicines, 2007, 61, pp. 313-317.
9. R. P. Samy, & S. Ignacimuthu, "Antibacterial activity of some folklore medicinal plants used by tribals in Western Ghats of India." Journal of Ethnopharmacology, 2000, 69(1), pp. 63-71.
10. O. Wichterle, & Lim, D. (1960). "Hydrophilic gels for biological use. Nature, 185(4706), pp. 117-118.
11. M. Sarangi, & S. Padhi, "Novel herbal drug delivery system: An overview" Archives of Medicine and Health Sciences, 2018, 6(1), pp. 171-171. DOI: 10.4103/amhs.amhs_88_17
12. N. K. Kashyap., N. Kumar, & M. R. Kumar, "Hydrogels for 28 pharmaceutical and biomedical applications. Critical Reviews™ in Therapeutic Drug Carrier Systems" 22(2).
13. E. M. Ahmed, F. S. Aggor, A. M. Awad, & A. T. El-Aref, "An innovative method for preparation of nanometal hydroxide superabsorbent hydrogel" Carbohydrate polymers, 2013, 91(2), pp. 693-698.
14. Ali, A., & S. Ahmed, Recent advances in edible polymer based hydrogels as a sustainable alternative to conventional polymers. Journal of agricultural and food chemistry, 2018, 66(27), pp. 6940-6967.
15. A. L. Udupa, D. R. Kulkarni, & S. L. Udupa, "Effect of *Tridax procumbens* extracts on wound healing. International Journal of Pharmacognosy" 1995, 33(1), pp. 37-40.
16. Tiwari, U., Rastogi, B., Singh, P., Saraf, D. K., & Vyas, S. P. "Immunomodulatory effects of aqueous extract of *Tridax procumbens* in experimental animals" Journal of Ethnopharmacology, 2014, 92(1), pp. 113-119.
17. Thuille, N., Fille, M., & Nagl, M, Bactericidal activity of herbal extracts. International journal of hygiene and environmental health, 2003, 206(3), pp. 217-221.
18. Brandl, F., Kastner, F., Gschwind, R. M., Blunk, T., Teßmar, J., & Göpferich, A. Hydrogel-based drug delivery systems: Comparison of drug diffusivity and release kinetics. Journal of Controlled Release, 2010, 142(2), pp. 221-228.
19. Hamidi, M., Azadi, A., & Rafiei, P. Hydrogel nanoparticles in drug delivery. Advanced drug delivery reviews, 2008, 60(15), pp. 1638-1649.
20. Koehler, J., Brandl, F. P., & Göpferich, A. M. Hydrogel wound dressings for bioactive treatment of acute and chronic wounds. European Polymer Journal, "2018, 100, 1-11.
21. Kumar, T. P., & Eswaraiah, M. C Formulation and evaluation of topical hydrogel containing antifungal drug. Pharm. Pharmacol. Int. J, 2020, 8, pp. 249-254.
22. Devi, V. K., Jain, N., & Valli, K. S. "Importance of novel drug delivery systems in herbal medicines" Pharmacognosy reviews, 2010, 4(7), pp. 27.
23. Onaciu, A., Munteanu, R. A., Moldovan, A. I., Moldovan, C. S., & Berindan Neagoe, I Hydrogels based drug delivery synthesis, characterization and administration. Pharmaceutics, 2019, 11(9), pp. 432.
24. Raj, R. Review On Hydrogel Based Transdermal Patches: A Novel Approach For Effective Drug Delivery. 2021, pp. 29
25. Duwa, R., Emami, F., Lee, S., Jeong, J. H., & Yook, S. "Polymeric and lipid-based drug delivery systems for treatment of glioblastoma multiforme." Journal of Industrial and Engineering Chemistry, 2019, 79, pp. 261-273.
26. Singh, A., Sharma, P. K., Garg, V. K., & Garg, G. "Hydrogels: a review. Int. J. Pharm. Sci. Rev. Res, 2010, 4(2), pp. 97-105.
27. Vigata, M., Meinert, C., Huttmacher, D. W., & Bock, N., Hydrogels as drug delivery systems: A review of current characterization and evaluation techniques. Pharmaceutics, 2020, 12(12), pp. 1188.
28. G Tahir, F., Ganji, F., & M Ahooyi, T. Injectable thermosensitive chitosan/glycerophosphate-based hydrogels for tissue engineering and drug delivery applications: a review. Recent patents on drug delivery & formulation, 2015, 9(2), pp. 107-120





Pallavi Dhekale et al.,

29. Rokade, P., Rokade, D., &Dhekale, P. Extraction and antimicrobial activity of *Cestrum nocturnum*. *Int. J. Adv. Res*, 2018, 6, pp. 739-741.
30. Shinde, M., Sawant, A., Dhekale, P., & Sharma, A. Effect of different extracts of *Psidiumguajava* leaves on antibacterial and antifungal activity. *World J Pharmaceut Res*, 2018, 7(13), pp. 523-528.
31. Sawant, A., Shinde, M., &Dhekale, P. Combination extract of *Calendula officinalis* and *Psidium gujava* on antibacterial and antifungal activity. *International Journal of Current Advanced Research*, 2018, 7, pp. 12787-90.

Table 1. Method for preparation of hydrogels

Sr. no.	Name of ingredients	Qty.	Uses
1	Tridaxprocumbens extract	1 gm	Antimicrobial agent, natural wound healer
2	Gaur gum	0.3 gm	Suspending agent, Binding agent, Emulsifying agent
3	Glycerol	3 gm	Prevent the lump formation
4	4 % Borax solution	7.5 ml	Cross linking agent, buffering agent
5	Water	q.s.	Solvent

Table 2: Colour and appearance of polymers

Test	Result
Colour	White
Appearance	Powder

Table no.3: Physico-chemical evaluation of *Tridax procumbens* leaf

Sr. no.	Test	Result			
1	Description	Green			
2	Determination of moisture	0.3 mg			
3	Total ash value	11%			
4	Acid insoluble ash value	3.8%			
5	Water insoluble ash value	2.9%			

Table 4. Preliminary phyto-chemical screening

Sr. No.	Test	Result
1	Tests for carbohydrates	(+)ve
2	Test for steroid	(+)ve
3	Test for alkaloids	(+)ve
4	Test for saponins	(+)ve
5	Test for flavonoids	(+)ve
6	Test for Tannins and Phenolic compounds	(+)ve

Table no. 5: Spread ability test of hydrogel

Sr. no.	Initial diameter	Diameter after spreading
1	0.7cm	4.4cm
2	0.6cm	4.9cm
3	0.8cm	4.8cm
	Mean	4.7cm


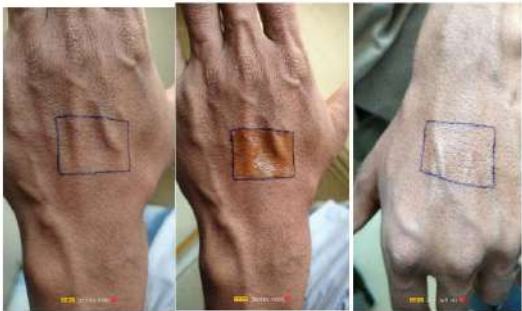
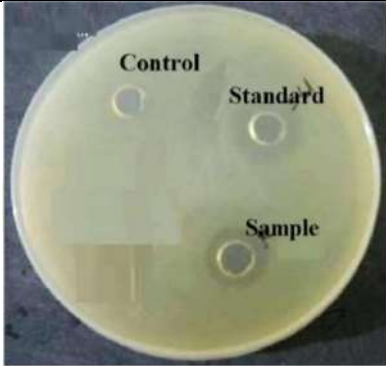
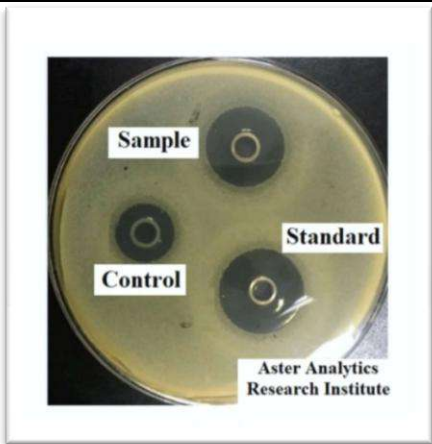




Pallavi Dhekale et al.,

Table 6. The range of zone of inhibition for the *staphylococcus aureus* bacteria is 23 and the *Escherichia colibacteria* is 31.

Sample ID	Conc.Of stock slolution	Zone of inhibition (mm)	
		<i>Staphylococcus aureus</i>	<i>Escherichia coli</i>
R1	50mg/ml	23	31
Std.	0.5mg/ml	46	38

	 <p>Skin before applied skin after application</p>
<p>Fig no 1: Spreadability test</p>	<p>Fig No 2. Skin irritation test</p>
	 <p>Aster Analytics Research Institute</p>
<p>Fig. 3. Antibacterial activity (<i>Escherichia coli</i>)</p>	<p>Fig. 9. antibacterial activity (<i>Staphylococcus aureus</i>)</p>





Microplastics Serve as a Vector for Heavy Metals in *Euthynnus affinis* Collected from South-east coast of Bay of Bengal and An Assessment of Public Health and Well-Being.

Yasmeen Ali Rafi¹, Kuppusamy Elumalai² and Deepalakshmi Balakrishnan³

¹Ph.D Research Scholar, Department of Zoology, Government Arts College for Men, Nandanam, (Affiliated to University of Madras) Chennai, Tamil Nadu, India.

²Assistant Professor, Department of Zoology, Government Arts College for Men, Nandanam, (Affiliated to University of Madras) Chennai, Tamil Nadu, India.

³Research Assistant, Department of Research and Development, Sree Balaji Medical College and Hospital, (Affiliated to Bharat Institute of Higher Education and Research) Chennai, Tamil Nadu, India.

Received: 20 Jan 2024

Revised: 09 Feb 2024

Accepted: 14 May 2024

*Address for Correspondence

Yasmeen Ali Rafi

Ph.D Research Scholar,

Department of Zoology,

Government Arts College for Men,

Nandanam, (Affiliated to University of Madras)

Chennai, Tamil Nadu, India.

Email: yasmeenphd4@gmail.com



This is an Open Access Journal / article distributed under the terms of the **Creative Commons Attribution License** (CC BY-NC-ND 3.0) which permits unrestricted use, distribution, and reproduction in any medium, provided the original work is properly cited. All rights reserved.

ABSTRACT

Microplastics (MPs) (< 5 mm) accumulate in the ocean as a result of the mechanical, thermal, and biological degradation of dumped plastics, causing an alarming rise in marine pollution. Marine organisms unintentionally consume these plastics, either directly or through the food chain. In this investigation, MPs and heavy metals were found in frequently consumed Mackerel tuna (*Euthynnus affinis*) that was harvested from the fish market at Edward Elliot's Beach on the southeast coast of the Bay of Bengal. An alkaline KOH digestion was used to discover MPs in the muscle tissue of 100 tuna fish. A total of 55 fish had MPs detected in their bodies, wherein 530 particles have been separated, with an average of 9.6 ± 0.6 MPs per fish. Two different morphology of MPs were recovered from the fish with the fragments dominating in abundance than fibres which belong to the category of Nylon (Polyamide) polymers. Numerous heavy metals that are adherent to the MPs have been detected by XRD (X-ray diffractometer), which affirmed the presence of Cd, Hg, Ba and Te. Values <1 obtained in the Hazard Index (HI) and Carcinogenic Risk (CR) show that consuming Mackerel tuna does not cause any carcinogenic and non-carcinogenic risk to the consumers.

Keywords: Microplastics, Heavy metals, Fish, Bay of Bengal, Polymers.





Yasmeen Ali Rafi et al.,

INTRODUCTION

Massive amounts of plastic garbage have been produced due to the world's population growth [1]. Ineffective disposal techniques cause these plastics to enter the ocean which results in marine plastic pollution [2]. The natural weathering and breakdown of big plastic trash produces microscopic plastic particles called microplastics (MPs), which are less than 5 mm in diameter into the environment [3, 4]. Plastics collect a wide range of environmental toxins when they are discharged into the environment. Recent investigations have demonstrated that MPs have a propensity towards heavy metals, which are omnipresent contaminants in the marine ecosystem. Numerous heavy metals are included in the MPs matrix of polymers as chemical by-products or operational additions [5]. It has been documented that these metals bioaccumulate on MPs in both terrestrial and aquatic habitats [6]. The MPs found across the North Atlantic subtropical gyre to the beaches of Western Europe encompassed heavy metals [7,8]. Therefore, MPs provide a pathway for environmental heavy metals to infiltrate living things. In addition to aquatic creatures, human beings are also susceptible to bioaccumulating these toxic metals [9]. The amount of metals and MPs found inside the edible parts of benthic and pelagic fish species was extensively studied by researchers near the northeast Persian Gulf. Groupers had the most elevated quantities of Se, Ni, Zn, and Cr, whereas barracudas had greater proportions of As, Fe, V, and Hg [10]. In a study, it has been proven that Zn, Cu, Mn, Cr, Fe, and Hg are present in polymers, such as polyethylene, polyamide, and polypropylene [11]. Thus, consuming MPs via fish allots a route for the entry of metals into living things [9]. The current study offers novel details about the existence of MPs along with heavy metals in the edible tissue taken from Mackerel tuna (*Euthynnus affinis*) netted from the Bay of Bengal.

MATERIALS AND METHODS

The sample was taken at Edward Elliot's beach, with latitudes 12.999529 °N and longitude 80.272411° E situated along the Bay of Bengal. This location features a lengthy strip of outlets with a wide selection of food and beverage choices, as well as tourist activities in proximity to the ocean which contributes to huge dumping of plastic wastes near the seashore. In December 2023, 100 fresh fish of *Euthynnus affinis* were gathered from fish market vendors along the shoreline. The fish were carried to the lab in cold packaging filled with ice. To prevent samples from deteriorating, all laboratory samples are kept in deep freezers at -20°C. The samples were thawed, photographed and their characteristic features were recorded (Fig.1). To concentrate only on the edible part of the muscles, the fish were eviscerated and the other parts were discarded. After homogenizing 10 g of muscle with a motor and pestle, the muscle is dissolved in 200 ml of 20% (w/v) KOH. The samples are incubated inside the immersion bath at 60°C for 42–48 hours. The resulting solution was filtered using 180 mm diameter Whatman Quantitative filter paper, Grade 589/3, which has pores with a size of less than 2µm and a thickness of 160µm [12].

Analysis of MPs and Heavy metals

Under a 200x binocular microscope magnification, MPs in the filter paper were visually distinguished and recognized by taking into account their physical attributes, including form, colour, size, and texture [13]. To determine the composition of the polymer, the separated MPs were further subjected to Fourier transform infrared spectroscopy with attenuated total reflectance (FTIR-ATR) analysis. Heavy metals accumulated within the confines of the same MPs are then analysed using an X-ray diffractometer (XRD) [14].

Human health risk assessment

The average quantity of metal discovered in the muscle tissue of fish is estimated, and the daily consumption of 50 g and 100g of fish for children and adults has been taken into consideration for calculating toxic metal exposure [15]. The following formulas were used to calculate Estimated Daily Intake (EDI), Target Hazard Quotient (THQ), Hazard index (HI), and Carcinogenic risk (CR).

$$EDI = FIR \times C/BW$$





Yasmeen Ali Rafi et al.,

Where, BW is the body weight, presuming 60 kg for adults and 15 kg for children inhabitants, C indicates the amount of metal in mg/kg and FIR represents food intake rate (g/person/day) [15]. The fish intake rate per day, measured on a wet weight basis, was 59.91 g for adults and 52.9 g for children [16].

$$THQ = [(Efr \times ED \times FIR \times C) / RfD \times BW \times AT] \times 10^{-3}$$

$$HI = \sum THQs$$

Where, Efr is the exposure frequency (365 days/year), ED is the exposure duration (70 years), RfD is the reference dose of the metal and AT is the average time for non-carcinogens (365 days/year × number of exposure years) [17]. Individuals exposed to HI levels > 1 may be at substantial risk of developing various diseases (non-carcinogenic), whereas < 1 imply no danger at all [18].

$$TR = [(Efr \times ED \times FIR \times C \times CSf_0) / (BW \times AT)] \times 10^{-3}$$

Where, CSf₀(mg/kg/day) is used to quantify the oral carcinogenic potency slopes factor of a certain carcinogen (USEPA, 2011) [19].

RESULTS

In a total of 100 fish, 53 males and 47 females were segregated separately. The fish was measured to have a mean length of 11 ± 2 cm and a mean forked length of 9.5 ± 0.5 cm. Each fish weighed approximately 380 ± 20 g, with an average Gastro-Intestinal Tract weight of 0.009 ± 0.005 g. The fish is renowned for its widespread shoaling behaviour in the pelagic niche of the ocean and for being an intense carnivore. MPs from the ocean can reach *Euthynnus affinis* by unintentional direct consumption or indirectly via the food chain as it has wide gastronomic variability [20]. The MPs would have accumulated in the muscles after translocating through the circulation from the GIT [21]. It was found that 55 out of 100 fish (55%) had MPs in their muscles, which accounted for over 530 particles that were detected. Each fish had a maximum of 9.6 ± 0.6 particles with a density of $0.85\text{--}0.99\text{ cm}^{-3}$, isolated from the edible part. Two different morphologies of MPs like fragments and fibres with varying percentages were obtained from the filter paper (Fig.2). Fragments (62.26%) were found to be prevalent among the MPs gathered (Fig.3 A, B), with yellow (36.79%) and Black (25.47%) colour variances and fibres (Fig.3 C) appeared in a lower percentage (37.74%), with blue fibres (19.82%) and red fibres (17.92%) accounting for the smallest ranges of MPs in the sample.

Following the MPs picture collection, Fourier transform infrared spectroscopy with attenuated total reflectance (FTIR-ATR Model: JASCO FT/IR-4X) was used to evaluate the probable particles. The distinct polymer in the separated plastic particles was identified as Polyamide by the peaks that emerged in the infrared spectra acquired between 600 cm^{-1} and 3000 cm^{-1} (Fig.4). The peaks occurred at different wave numbers such as 691.4 cm^{-1} , 1030.6 cm^{-1} , 1459.3 cm^{-1} , 1559.9 cm^{-1} , 2851.4 cm^{-1} depicts C=O bend, C-O stretching, CH₂ bending, N-H bending and C-H stretching, which confirmed the presence of Polyamide polymer, which is classified as nylon [22,23]. Peaks from X-ray diffractometer (XRD- SMARTLAB 9 KW, RIKAGU, JAPAN) with two theta values of 22.73 (111), 27.81 (211), and 33.8 (211) verified the presence of cadmium (Cd), mercury (Hg), and barium (Ba) (Fig.5). On MPs, a trace amount of the uncommon element tellurium is also detected, with two theta values of 29.343 (001) [24]. The enormously found MPs, like fragments, had higher concentrations of heavy metals (84%) which indicates that the interaction between their vast surface area and heavy metals is sufficient to transport them in large quantities. In contrast, fibres revealed a smaller amount (16%) of the heavy metals that were identified. Therefore, van der Waal forces, electrostatic interactions, physical and chemical adsorption may all have an impact on MPs' ability to transmit heavy metals through their vector effect. Heavy metal content in MPs confirms that they are the ideal carrier for transporting heavy metals via the adsorption process.





Yasmeen Ali Rafi et al.,

Evaluation of carcinogenic and non-carcinogenic risk

Utilizing EDI, THQ, HI, and CR values, the possible risk to consumer's health caused by heavy metals in the consumable muscle sections of the studied species was evaluated (Table 1). The EDI values were found to be lower than the FAO/WHO and USEPA's acceptable range for adults and children who consume a fish meal of 100 and 50 g per day. As a result, neither adults nor children were at possibility for health problems from it. THQ readings were found to be less than one, which did not represent a health risk to consumers. For adults, HI values were found to be 0.4493 mg/kg, and for Children, it is 0.9826 mg/kg, which is also <1, signifying non-carcinogenic risk to the people. The results show that the Mean CR values for adults and children were 0.0001707 and 0.000150, less than 1, indicating that one -three meals/week does not increase the risk of cancer in the future.

CONCLUSION AND DISCUSSION

The current investigation confirmed that the edible portion of *Euthynnus affinis*, which was collected from Besant Nagar Beach consisted of heavy metals adhered to MPs. In muscle tissue, MPs were present in the following order of occurrence: Yellow fragment > Black fragment > Blue fibre > Red fibre. Numerous studies have indicated that MPs serve as an ideal channel for carrying different heavy metals. This was confirmed through XRD analysis, which showed that tellurium (Te), barium (Ba), mercury (Hg), and cadmium (Cd) were all present in the polyamide polymer. There were different concentrations of these heavy metals on MPs: Te (0.02 mg/kg), Ba (0.58 mg/kg), Hg (0.03 mg/kg), and Cd (0.45 mg/kg). Compared to fibres, fragments exhibited a higher quantity of heavy metals on their surface. Therefore, it is clear from this work that heavy metals are adsorbed on the MPs' and that is facilitated by the fragments' large surface area. Additionally, the potential health risks associated with ingesting this fish were also evaluated where, the HI and CR values suggested that the intake of *Euthynnus affinis* is non-carcinogenic in detected levels. To reduce the pollution caused by plastics, one of the key study areas is understanding the number, dispersion, and conduct of MPs in the marine realm. Examining how MPs and heavy metals interact inside marine creatures' organ systems and how this affects metabolism is a crucial subject, which needs intense investigation. Long-term, comparative monitoring studies that assess how MPs and heavy metals affect different organisms across a range of habitats also need to be conducted.

ACKNOWLEDGEMENTS

The authors express their profound gratitude to the principal of Nandanam College for generously giving research opportunities and offering extensive laboratory assistance, which greatly contributed to the success of the study.

REFERENCES

1. North EJ, Halden RU. Plastics and environmental health: the road ahead. Rev. Environ. Health. 2013 Apr 1;28(1):1-8.
2. Gallo F, Fossi C, Weber R, Santillo D, Sousa J, Ingram I, Nadal A, Romano D. Marine Litter Plastics and Microplastics and Their Toxic Chemicals Components. Analysis of Nanoplastics and Microplastics in Food. 2020 Dec 2;159.
3. Hartmann NB, Huffer T, Thompson RC, Hasselov M, Verschoor A, Daugaard AE, Rist S, Karlsson T, Brennholt N, Cole M, Herrling MP. Are we speaking the same language? Recommendations for a definition and categorization framework for plastic debris.
4. Fendall LS, Sewell MA. Contributing to marine pollution by washing your face: microplastics in facial cleansers. Mar. Pollut. Bull. 2009 Aug 1;58(8):1225-8.
5. Turner A, Holmes L, Thompson RC, Fisher AS. Metals and marine microplastics: Adsorption from the environment versus addition during manufacture, exemplified with lead. Water Res. 2020 Apr 15;173:115577.
6. Liu S, Shi J, Wang J, Dai Y, Li H, Li J, Liu X, Chen X, Wang Z, Zhang P. Interactions between microplastics and heavy metals in aquatic environments: a review. Front. microbiol. 2021 Apr 22;12:652520.





Yasmeen Ali Rafi et al.,

7. Prunier J, Maurice L, Perez E, Gigault J, Wickmann AC, Davranche M, Ter Halle A. Trace metals in polyethylene debris from the North Atlantic subtropical gyre. *Environ. Pollut.* 2019 Feb 1;245:371-9.
8. Turner A, Wallerstein C, Arnold R. Identification, origin and characteristics of bio-bead microplastics from beaches in western Europe. *Sci. Total Environ.* 2019 May 10;664:938-47.
9. Naqash N, Prakash S, Kapoor D, Singh R. Interaction of freshwater microplastics with biota and heavy metals: a review. *Environ. Chem. Lett.* 2020 Nov;18(6):1813-24.
10. Akhbarizadeh R, Moore F, Keshavarzi B. Investigating a probable relationship between microplastics and potentially toxic elements in fish muscles from northeast of Persian Gulf. *Environ. Pollut.* 2018 Jan 1;232:154-63.
11. Selvam S, Manisha A, Roy PD, Venkatramanan S, Chung SY, Muthukumar P, Jesuraja K, Elgorban AM, Ahmed B, Elzain HE. Microplastics and trace metals in fish species of the Gulf of Mannar (Indian Ocean) and evaluation of human health. *Environ. Pollut.* 2021 Dec 15;291:118089.
12. Karami A, Golieskardi A, Choo CK, Romano N, Ho YB, Salamatinia B. A high-performance protocol for extraction of microplastics in fish. *Sci. Total Environ.* 2017 Feb 1;578:485-94.
13. Dekiff JH, Remy D, Klasmeier J, Fries E. Occurrence and spatial distribution of microplastics in sediments from Norderney. *Environ. Pollut.* 2014 Mar 1;186:248-56.
14. Attaelmanan AG, Aslam H, Ali T, Dronjak L. Mapping of heavy metal contamination associated with microplastics marine debris-A case study: Dubai, UAE. *Sci. Total Environ.* 2023 Sep 15;891:164370.
15. Copat C, Arena G, Fiore M, Ledda C, Fallico R, Sciacca S, Ferrante M. Heavy metals concentrations in fish and shellfish from eastern Mediterranean Sea: consumption advisories. *Food and chemical toxicology.* 2013 Mar 1;53:33-7.
16. USEPA. 2008. Integrated Risk Information System. United States Environmental Protection Agency, Washington, DC, USA. Accessed on 25 May 2020.
17. USEPA. 2011. USEPA Regional Screening Level (RSL) Summary Table: November 2011.
18. Fakhri Y, Mohseni-Bandpei A, Oliveri Conti G, Keramati H, Zandsalimi Y, Amanidaz N, Hosseini Pouya R, Moradi B, Bahmani Z, RasouliAmirhajeloo L, Baninameh Z. Health risk assessment induced by chloroform content of the drinking water in Iran: systematic review. *Toxin Rev.* 2017 Oct 2;36(4):342-51.
19. USEPA. 2011. USEPA Regional Screening Level (RSL) Summary Table: November 2011.
20. Rohit P, Chellappan A, Abdussamad EM, Joshi KK, Koya KP, Sivadas M, Ghosh S, Margaret MuthuRathinam A, Kemparaju S, Dhokia HK, Prakasan D. Fishery and bionomics of the little tuna, *Euthynnus affinis* (Cantor, 1849) exploited from Indian waters. *Indian J. Fish.* 2012;59(3):37-46.
21. Makhdoumi P, Hossini H, Pirsahab M. A review of microplastic pollution in commercial fish for human consumption. *Rev. Environ. Health.* 2023 Mar 28;38(1):97-109.
22. Jung MR, Horgen FD, Orski SV, Rodriguez V, Beers KL, Balazs GH, Jones TT, Work TM, Brignac KC, Royer SJ, Hyrenbach KD. Validation of ATR FT-IR to identify polymers of plastic marine debris, including those ingested by marine organisms. *Mar. Pollut. Bull.* 2018 Feb 1;127:704-16.
23. Verleye GA, Roeges NP, De Moor MO. Easy identification of plastics and rubbers. iSmithersRapra Publishing; 2001.
24. Krämer V, Brandt G. Structure of cadmium tellurate (IV), CdTeO₃. *Acta Crystallographica Section C: Crystal Structure Communications.* 1985 Aug 15;41(8):1152-4.

Table 1: Types and Concentration of Heavy Metals With EDI, RfD, and THQ Values.

S.No	Type of heavy metal	Concentration of heavy metal (mg/kg) of sample	Estimated Daily Intake (EDI) (mg/kg)	Reference Dose of metal (RfD) (mg/kg)	Total Hazard Quotient (THQ) (mg/kg)
1	Cadmium (Cd)	0.45	Adult- 0.00449	1× 10 ⁻³	0.4493
			Children-0.01587		0.5871





Yasmeen Ali Rafi et al.,

2	Mercury (Hg)	0.03	Adult- 0.00059	3×10^{-4}	0.0998
			Children-0.00105		0.3522
3	Barium (Ba)	0.58	Adult- 0.00579	7×10^{-2}	0.0082
			Children-0.02045		0.0292
4	Tellurium (Te)	0.02	Adult- 0.00019	5×10^{-3}	0.0039
			Children-0.00070		0.0141

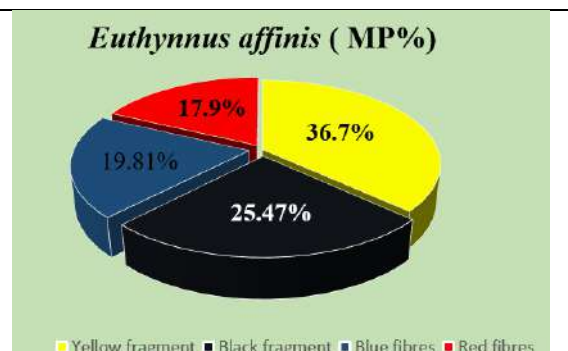
Fig.1. Mackerel tuna (*Euthynnus affinis*)

Fig.2. Pie chart showing different colour and morphology of MPs collected.

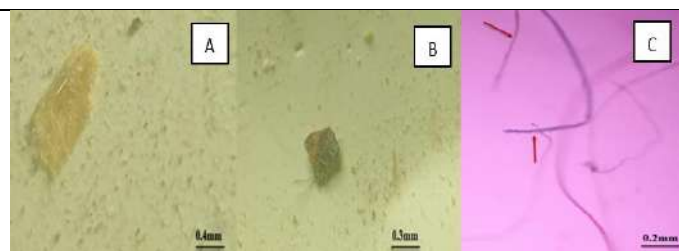


Fig.3. Represents MPs under microscopic view, A) Yellow fragments and B) Black fragments, C) Red and blue fibres.

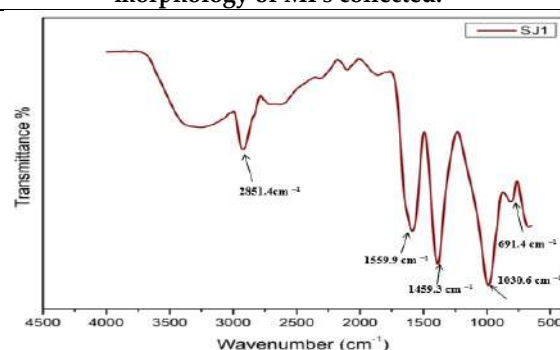


Fig.4. FTIR-ATR spectra depicting characteristic peaks of Nylon (Polyamide) polymer.

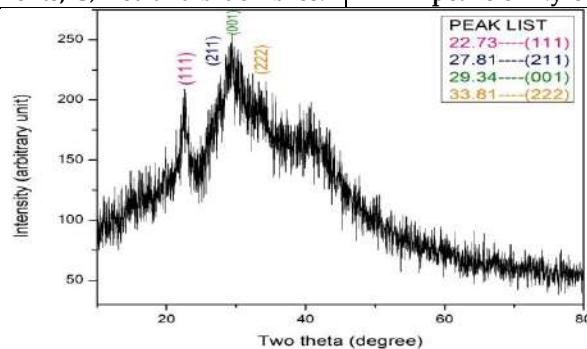


Fig.5. It represents XRD peaks corresponding to heavy metals with two theta values of 22.73 (Cd), 27.81 (Hg), 33.8 (Ba), 29.34 (Te).





A Study on Nano Semi Generalized B - Closed Sets in Nano Topological Spaces

K. Kavipriya^{1*} and T. Indira²

¹Research Scholar, PG and Research Department of Mathematics, Seethalakshmi Ramaswami College (Affiliated to Bharathidasan University) Tiruchirappalli, Tamil Nadu, India.

²Associate Professor, Department of Mathematics, Seethalakshmi Ramaswami College (Affiliated to Bharathidasan University) Tiruchirappalli, Tamil Nadu, India.

Received: 22 Jan 2024

Revised: 09 Feb 2024

Accepted: 11 May 2024

*Address for Correspondence

K. Kavipriya

Research Scholar, PG and Research
Department of Mathematics,
Seethalakshmi Ramaswami College
(Affiliated to Bharathidasan University) Tiruchirappalli,
Tamil Nadu, India.
Email: kavipriyakannan1512@gmail.com



This is an Open Access Journal / article distributed under the terms of the **Creative Commons Attribution License** (CC BY-NC-ND 3.0) which permits unrestricted use, distribution, and reproduction in any medium, provided the original work is properly cited. All rights reserved.

ABSTRACT

The objective of this study is to define a new class of nano closed set in nano topological spaces, namely nano semi generalized b closed set (abbreviated Nsgb-closed). Its characteristics are investigated. The attributes of Nsgb-interior and Nsgb-closure are examined using the new set.

Keywords: Nano Topology, Nsgb-closed, Nsgb-open, Nsgb-interior and Nsgb-closure

AMS Subject Classification: 54A05

INTRODUCTION

Lellis Thivagar [7] developed a new type of topology called nano topology in 2013 and described new types of closed sets such as nano closed, nano semi closed and so on. Bhuvaneshwari and Ezhilarasi [1] investigated nano semi generalized and nano generalized semi closed sets in 2014. Parimala and Indirani [5] defined Nano b-open set in 2016. Lalitha and Franciana Shalini [4] coined $N\hat{g}$ -closed set in 2017. The present study is to define and study the traits of a new nano closed set namely Nano semi generalized b-closed set (Nsgb-closed). To define and examine the properties of the interior and closure of this nano closed set.





PRELIMINARIES

Definition 2.1: [7] Let U indicate a non-empty set of finite elements referred as the Universe, and R signify an equivalence relation on U referred as the Indiscernibility relation. Then U is partitioned into distinct equivalence classes. The elements in one's equivalence class are perceived to be indistinguishable. The **Approximation space** is denoted by the pair (U, R) . Let $S \subseteq U$. Then

- The **Lower Approximation** of S ($L_R(S)$) is the set of all elements with respect to R which can be certain categorized as S with respect to R where $R(S)$ is the equivalence class determined by s in S .

$$L_R(S) = \bigcup_{s \in U} \{R(s) : R(s) \subseteq S\}$$

- The **Upper Approximation** of S ($U_R(S)$) is the set of all elements with respect to R which can be possibly categorized as S with respect to R .

$$U_R(S) = \bigcup_{s \in U} \{R(s) : R(s) \cap S \neq \emptyset\}$$

- The **Boundary Region** of S ($B_R(S)$) is the set of all elements with respect of R which can be labeled neither as S nor as not- S with respect to R .

$$B_R(S) = U_R(S) - L_R(S).$$

Definition 2.2: [7] Let R be an equivalence relation on the universe U and $S \subseteq U$ and $\tau_R(S) = \{U, \emptyset, L_R(S), U_R(S), B_R(S)\}$ must satisfy the following axioms.

- U and $\emptyset \in \tau_R(S)$
- The arbitrary union of the elements of $\tau_R(S) \in \tau_R(S)$.
- The finite intersection of the elements of $\tau_R(S) \in \tau_R(S)$.

Then $\tau_R(S)$ is known as **Nano topology** on U with respect to S . The pair $(U, \tau_R(S))$ is known as the Nano topological space. The elements in $\tau_R(S)$ are the nano open sets and its complements are the nano closed sets of U .

Definition 2.3: [7] The set $B = \{U, L_R(S), B_R(S)\}$ is the **basis** for $\tau_R(S)$.

Definition 2.4: [7] Let E be any subset of U then

The union of all nano open subsets of U contained in E is stated as the **Nano interior of E** ($Nint(E)$). $Nint(E) = \bigcup \{\text{nano open subsets of } U \subseteq E\}$. Thus $Nint(E) \subseteq E$.

The intersection of all nano closed subsets of U containing E is stated as the **Nano closure of E** ($Ncl(E)$). $Ncl(E) = \bigcap \{\text{nano closed subsets of } U \supseteq E\}$. Thus $E \subseteq Ncl(E)$

Definition 2.5: Let $E \subseteq U$ in $(U, \tau_R(S))$. Then

1. **Nano semi closed (Ns-closed)** [7]: if $Nint(Ncl(E)) \subseteq E$
2. **Nano pre closed (Np-closed)** [7]: if $Ncl(Nint(E)) \subseteq E$
3. **Nano regular closed (Nr-closed)** [3]: if $Ncl(Nint(E)) = E$
4. **Nano α -closed ($N\alpha$ -closed)** [7]: if $Ncl(Nint(Ncl(E))) \subseteq E$
5. **Nano b- closed (Nb -closed)** [5]: if $Nint(Ncl(E)) \cap Ncl(Nint(E)) \subseteq E$
6. **Nano \hat{g} - closed ($N\hat{g}$ -closed)** [4]: if $Ncl(E) \subseteq K$, whenever $E \subseteq K$, where K is nano semi open in U
7. **Nano semi generalized closed (Nsg-closed)** [1]: if $Ns-cl(E) \subseteq K$, whenever $E \subseteq K$, where K is nano semi open in U
8. **Nano generalized semi closed (Ngs-closed)** [1]: if $Ns-cl(E) \subseteq K$, whenever $E \subseteq K$, where K is nano open in U
9. **Nano regular generalized closed (Nrg-closed)** [3]: if $Nr-cl(E) \subseteq K$, whenever $E \subseteq K$, where K is nano regular open in U .
10. **Nano generalized pre regular closed (Ngpr-closed)** [6]: if $Np-cl(E) \subseteq K$, whenever $E \subseteq K$, where K is nano regular open in U .
11. **Nano generalized closed (Ng- closed)** [2]: if $Ncl(E) \subseteq K$, whenever $E \subseteq K$, where K is nano open in U .





Kavipriya and Indira

NANO SEMI GENERALIZED B-CLOSED SET (NSGB-CLOSED)

Definition 3.1: A subset E of $(U, \tau_R(S))$ is **Nsgb-closed** if $Nb-cl(E) \subseteq K$, whenever $E \subseteq K$, where K is nano semi open in U . A subset E of $(U, \tau_R(S))$ is **Nsgb-open** if the complement $U - E$ is Nsgb-closed.

Example 3.2: Let $U = \{m, n, o, p\}$, $S = \{n, p\} \subseteq U$, $U/R = \{\{m\}, \{n\}, \{o, p\}\}$, $\tau_R(S) = \{U, \phi, \{n\}, \{n, o, p\}, \{o, p\}\}$

Nsgb-closed = $\{U, \phi, \{m\}, \{n\}, \{o\}, \{p\}, \{m, n\}, \{m, o\}, \{m, p\}, \{o, p\}, \{m, n, o\}, \{m, n, p\}, \{m, o, p\}\}$

Nsgb-open = $\{\phi, U, \{n, o, p\}, \{m, o, p\}, \{m, n, p\}, \{m, n, o\}, \{o, p\}, \{n, p\}, \{n, o\}, \{m, n\}, \{p\}, \{o\}, \{n\}\}$

Theorem 3.3: Nano closed implies Nsgb-closed.

Proof: Let E be a nano closed set in U . So that $Ncl(E) = E$. Let $E \subseteq K$, where K is Ns-open in U . Then $E = Ncl(E) \subseteq K$. Since $Nb-cl(E) \subseteq Ncl(E)$. Then $Nb-cl(E) \subseteq K$, whenever $E \subseteq K$, where K is Ns-open in U . Therefore E is Nsgb-closed in U .

Theorem 3.4: Ns-closed, Np-closed, Nr-closed, $N\alpha$ -closed implies Nsgb-closed.

The proof follows from the fact that $Nb-cl(E) \subseteq Ns-cl(E)$, $Np-cl(E)$, $Nr-cl(E)$, $N\alpha-cl(E)$ resp.

Example 3.5: From example 3.2, we have

Nano closed = $\{U, \phi, \{m, o, p\}, \{m\}, \{m, n\}\}$.

Ns-closed = $\{U, \phi, \{m\}, \{n\}, \{m, n\}, \{o, p\}, \{m, o, p\}\}$

Np-closed = $\{U, \phi, \{m\}, \{o\}, \{p\}, \{m, n\}, \{m, o\}, \{m, p\}, \{m, n, o\}, \{m, n, p\}, \{m, o, p\}\}$

Nr-closed = $\{U, \phi, \{m, n\}, \{m, o, p\}\}$,

$N\alpha$ -closed = $\{U, \phi, \{m\}, \{m, n\}, \{m, o, p\}\}$

Nsgb-closed = $\{U, \phi, \{m\}, \{n\}, \{o\}, \{p\}, \{m, n\}, \{m, o\}, \{m, p\}, \{o, p\}, \{m, n, o\}, \{m, n, p\}, \{m, o, p\}\}$.

Here the subset $\{o\}$ is Nsgb-closed but not Nano-closed, not Ns-closed. The subset $\{o, p\}$ is Nsgb-closed but not Np-closed, not Nr-closed, not $N\alpha$ -closed. Thus the converse need not be true.

Theorem 3.6: Nano b-closed implies Nsgb-closed.

Proof: Let E be a Nb-closed set in U . So that $Nb-cl(E) = E$. Let $E \subseteq K$, where K is Ns-open in U . Then $E = Nb-cl(E) \subseteq K$. Then $Nb-cl(E) \subseteq K$, whenever $E \subseteq K$, where K is Ns-open in U . Therefore E is Nsgb-closed in U .

Example 3.7:

Let $U = \{m, n, o, p, q, r\}$, $S = \{m, n, o\}$, $U/R = \{\{m\}, \{n, r\}, \{o\}, \{p\}, \{q\}\}$, $\tau_R(S) = \{U, \phi, \{m, o\}, \{m, n, o, r\}, \{n, r\}\}$,

Nano b-closed = $\{U, \phi, \{m\}, \{n\}, \{o\}, \{p\}, \{q\}, \{r\}, \{m, n\}, \{m, o\}, \{m, p\}, \{m, q\}, \{m, r\}, \{n, o\}, \{n, p\}, \{n, q\}, \{n, r\}, \{o, p\}, \{o, q\}, \{o, r\}, \{p, q\}, \{p, r\}, \{q, r\}, \{m, n, p\}, \{m, n, q\}, \{m, o, p\}, \{m, o, q\}, \{m, p, q\}, \{m, p, r\}, \{m, q, r\}, \{n, o, p\}, \{n, o, q\}, \{n, p, q\}, \{n, p, r\}, \{n, q, r\}, \{o, p, q\}, \{o, p, r\}, \{o, q, r\}, \{p, q, r\}, \{m, n, p, q\}, \{m, o, p, q\}, \{m, p, q, r\}, \{n, o, p, q\}, \{n, p, q, r\}, \{o, p, q, r\}, \{m, n, o, p, q\}, \{m, n, p, q, r\}, \{m, o, p, q, r\}, \{n, o, p, q, r\}\}$

Nsgb-closed = $\{U, \phi, \{m\}, \{n\}, \{o\}, \{p\}, \{q\}, \{r\}, \{m, n\}, \{m, o\}, \{m, p\}, \{m, q\}, \{m, r\}, \{n, o\}, \{n, p\}, \{n, q\}, \{n, r\}, \{o, p\}, \{o, q\}, \{o, r\}, \{p, q\}, \{p, r\}, \{q, r\}, \{m, n, p\}, \{m, n, q\}, \{m, o, p\}, \{m, o, q\}, \{m, p, q\}, \{m, p, r\}, \{m, q, r\}, \{n, o, p\}, \{n, o, q\}, \{n, p, q\}, \{n, p, r\}, \{n, q, r\}, \{o, p, q\}, \{o, p, r\}, \{o, q, r\}, \{p, q, r\}, \{m, n, o, p\}, \{m, n, o, q\}, \{m, n, p, q\}, \{m, n, p, r\}, \{m, n, q, r\}, \{m, o, p, q\}, \{m, o, q, r\}, \{m, p, q, r\}, \{n, o, p, q\}, \{n, o, p, r\}, \{n, p, q, r\}, \{o, p, q, r\}, \{m, n, o, p, q\}, \{m, n, o, p, r\}, \{m, n, o, q, r\}, \{m, n, p, q, r\}, \{m, o, p, q, r\}, \{n, o, p, q, r\}\}$.

Here the subsets $\{m, n, o, p\}$, $\{m, n, o, q\}$, $\{m, n, p, r\}$, $\{m, n, q, r\}$, $\{m, o, q, r\}$, $\{n, o, p, r\}$, $\{n, o, q, r\}$, $\{m, n, o, p, r\}$, $\{m, n, o, q, r\}$ Nsgb-closed but not Nb-closed.

Theorem 3.8: Nano \hat{g} -closed implies Nsgb-closed.

Proof: Let E be a $\hat{N}g$ -closed set in U and $E \subseteq K$, where K is Ns-open in U . Then $Ncl(E) \subseteq K$, whenever $E \subseteq K$, where K is Ns-open in U . Since $Nb-cl(E) \subseteq Ncl(E)$, then $Nb-cl(E) \subseteq K$, whenever $E \subseteq K$, where K is Ns-open in U . Therefore E is Nsgb-closed in U .





Kavipriya and Indira

Theorem 3.9: Nsg-closed implies Nsgb-closed.

Proof: Let E be a Nsg-closed set in U and $E \subseteq K$, where K is Ns-open in U . Then $Ns-cl(E) \subseteq K$, whenever $E \subseteq K$, where K is Ns-open in U . Since $Nb-cl(E) \subseteq Ns-cl(E)$, then $Nb-cl(E) \subseteq K$, whenever $E \subseteq K$, where K is Ns-open in U . Therefore E is Nsgb-closed in U .

Example 3.10: Let $U = \{m, n, o, p\}$, $S = \{m, n\} \subseteq U$, $U/R = \{\{m, n\}, \{o, p\}\}$, $\tau_R(S) = \{U, \emptyset, \{m, n\}\}$,

$N\hat{g}$ -closed = $\{U, \emptyset, \{o, p\}, \{m, o, p\}, \{n, o, p\}\}$,

Nsg-closed = $\{U, \emptyset, \{o\}, \{p\}, \{o, p\}, \{m, o, p\}, \{n, o, p\}\}$

Nsgb-closed = $\{U, \emptyset, \{m\}, \{n\}, \{o\}, \{p\}, \{m, o\}, \{m, p\}, \{n, o\}, \{n, p\}, \{o, p\}, \{m, o, p\}, \{n, o, p\}\}$.

Here the subsets $\{m\}$, $\{n\}$, $\{m, p\}$, $\{n, p\}$ are Nsgb-closed but not $N\hat{g}$ -closed, not Nsg-closed. Thus the converse need not be true.

Theorem 3.11: Nsgb-closed set ϕ Ngs-closed set.

Proof: Let $U = \{m, n, o, p\}$, $S = \{o, p\}$, $U/R = \{\{m, n\}, \{o, p\}\}$, $\tau_R(S) = \{U, \emptyset, \{o, p\}\}$,

Nsgb-closed = $\{U, \emptyset, \{m\}, \{n\}, \{o\}, \{p\}, \{m, n\}, \{m, o\}, \{m, p\}, \{n, o\}, \{n, p\}, \{m, n, o\}, \{m, n, p\}\}$,

Ngs-closed = $\{U, \emptyset, \{m\}, \{n\}, \{m, n\}, \{m, o\}, \{m, p\}, \{n, o\}, \{n, p\}, \{m, n, o\}, \{m, n, p\}, \{m, o, p\}, \{n, o, p\}\}$. Here the subsets $\{o\}$, $\{p\}$ are Nsgb-closed but not Ngs-closed. The subsets $\{m, o, p\}$, $\{n, o, p\}$ are Ngs-closed but not Nsgb-closed. Thus the sets Nsgb-closed and Ngs-closed are independent.

Theorem 3.12: Nsgb closed set ϕ Nrg-closed set

Theorem 3.13: Nsgb-closed set ϕ Ngpr-closed set.

Proof: From example 3.2, Nsgb-closed = $\{U, \emptyset, \{m\}, \{n\}, \{o\}, \{p\}, \{m, n\}, \{m, o\}, \{m, p\}, \{o, p\}, \{m, n, o\}, \{m, n, p\}, \{m, o, p\}\}$, Nrg-closed = $\{U, \emptyset, \{m\}, \{m, n\}, \{m, o\}, \{m, p\}, \{n, o\}, \{n, p\}, \{m, n, o\}, \{m, n, p\}, \{m, o, p\}, \{n, o, p\}\}$, Ngpr-closed = $\{U, \emptyset, \{m\}, \{o\}, \{p\}, \{m, n\}, \{m, o\}, \{m, p\}, \{n, o\}, \{n, p\}, \{m, n, o\}, \{m, n, p\}, \{m, o, p\}, \{n, o, p\}\}$

Here the subset $\{n\}$ is Nsgb-closed but not Nrg-closed and Ngpr-closed. The subset $\{n, o\}$ is Nrg-closed and Ngpr-closed but not Nsgb-closed. Thus the sets Nsgb-closed and Nrg-closed, Nsgb-closed and Ngpr-closed are independent.

Theorem 3.14: Nsgb-closed set ϕ Ng-closed set.

Proof: Let $U = \{m, n, o, p\}$, $S = \{o\}$, $U/R = \{\{m, n\}, \{o, p\}\}$, $\tau_R(S) = \{U, \emptyset, \{o, p\}\}$,

Nsgb-closed = $\{U, \emptyset, \{m\}, \{n\}, \{o\}, \{p\}, \{m, n\}, \{m, o\}, \{m, p\}, \{n, o\}, \{n, p\}, \{m, n, o\}, \{m, n, p\}\}$,

Ng-closed = $\{U, \emptyset, \{m\}, \{n\}, \{m, n\}, \{m, o\}, \{m, p\}, \{n, o\}, \{n, p\}, \{m, n, o\}, \{m, n, p\}, \{m, o, p\}, \{n, o, p\}\}$. Here the subsets $\{o\}$, $\{p\}$ are Nsgb-closed but not Ng-closed. The subsets $\{m, o, p\}$, $\{n, o, p\}$ are Ng-closed but not Nsgb-closed. Thus the sets Nsgb-closed and Ng-closed are independent.

Theorem 3.15: The union of Nsgb-closed sets not necessarily be Nsgb-closed.

Proof: From the example 3.2, let $E = \{n\}$, $F = \{p\}$ then $E \cup F = \{n, p\}$ is not a Nsgb-closed set. Thus $E \cup F$ not necessarily be Nsgb-closed.

Theorem 3.16: The intersection of Nsgb-closed sets is Nsgb-closed.

Proof: Assume E and F are two Nsgb-closed sets in $(U, \tau_R(S))$. To Prove: $E \cap F$ is Nsgb-closed. Let $E \cap F \subseteq K$. Let K be a Ns-open set in U . Then $Nb-cl(E) \subseteq K$ and $Nb-cl(F) \subseteq K$, whenever $E \subseteq K$ and $F \subseteq K$, where K is Ns-open. Now $Nb-cl(E) \cap Nb-cl(F) \subseteq K$. Since $Nb-cl(E) \cap Nb-cl(F) = Nb-cl(E \cap F)$ implies $Nb-cl(E \cap F) \subseteq K$. Thus, $Nb-cl(E \cap F) \subseteq K$, whenever $E \cap F \subseteq K$, where K is Ns-open in U . Therefore $E \cap F$ is Nsgb-closed.

T

heorem 3.17: If E is Nsgb-closed set of $(U, \tau_R(S))$ then there is no non-empty Ns-closed set in $Nb-cl(E) - E$.

Proof: Given E is Nsgb-closed. Then $Nb-cl(E) \subseteq K$, whenever $E \subseteq K$, K is Ns-open in U . To Prove: $Nb-cl(E) - E$ doesn't contain any non-empty Ns-closed set. Suppose A be a non-empty Ns-closed set is in $Nb-cl(E) - E$. ie., $A \subseteq Nb-cl(E) - E$, $A \neq \emptyset$. $\Rightarrow A \subseteq Nb-cl(E) \cap E^c$. Then $A \subseteq Nb-cl(E)$ and $A \subseteq E^c \rightarrow (1)$. Now consider $A \subseteq E^c$, then $E \subseteq A^c$ where A^c





Kavipriya and Indira

is non-empty Ns-open. Since E is Nsgb-closed, $Nb-cl(E) \subseteq A^c$, A^c is non-empty Ns-open. Then $A \subseteq (Nb-cl(E))^c \rightarrow$ (2). From (1) and (2), $A \subseteq Nb-cl(E)$ and $A \subseteq (Nb-cl(E))^c \Rightarrow A \subseteq Nb-cl(E) \cap (Nb-cl(E))^c = \emptyset \Rightarrow A \subseteq \emptyset$. Therefore $A = \emptyset$, which is a contradiction.

Theorem 3.18: For a Nsgb-closed set E in $(U, \tau_R(S))$, E is Nb-closed iff $Nb-cl(E) - E$ is Ns-closed.

Proof: *Necessary Part:* Let a Nsgb-closed set be E . *To Prove:* $Nb-cl(E) - E$ is Ns-closed. Assume E is Nb-closed. Then $E = Nb-cl(E)$ implies $Nb-cl(E) - E = \emptyset$, where \emptyset is Ns-closed. Thus $Nb-cl(E) - E$ is Ns-closed.

Sufficient Part: Let $Nb-cl(E) - E$ is Ns-closed. *To Prove:* E is Nb-closed. By theorem 3.17, $Nb-cl(E) - E = \emptyset$. Then $Nb-cl(E) = E$. Thus, E is Nb-closed.

Theorem 3.19: Let E be both Ns-open and Nsgb-closed in $(U, \tau_R(S))$ then E is Nb-closed.

Proof: Given E is Ns-open and Nsgb-closed. Then by definition, $Nb-cl(E) \subseteq E \rightarrow$ (1) whenever $E \subseteq E$, E is Ns-open in U . But always any set is contained in its Nb-closure, then $E \subseteq Nb-cl(E) \rightarrow$ (2). From (1) and (2), $E = Nb-cl(E)$. Thus E is Nb-closed.

Theorem 3.20: In $(U, \tau_R(S))$ the intersection of a Nsgb-closed set E and a Nb-closed set B containing E is always a Nsgb-closed set.

Proof: Given E is Nsgb-closed. Then $Nb-cl(E) \subseteq K$, whenever $E \subseteq K$, where K is Ns-open in U . Given $E \subseteq B$, where B is Nb-closed. Since $E \subseteq B \Rightarrow E \cap B = E \subseteq K$ implies $E \cap B \subseteq K$. Now $Nb-cl(E \cap B) = Nb-cl(E) \subseteq K$ implies $Nb-cl(E \cap B) \subseteq K$, whenever $E \cap B \subseteq K$, K is Ns-open. Thus $E \cap B$ is Nsgb-closed.

Theorem 3.21: If E is a Nsgb-closed set and $E \subseteq B \subseteq Nb-cl(E)$, then B is Nsgb-closed set.

Proof: Given E is Nsgb-closed \rightarrow (1) and $E \subseteq B \subseteq Nb-cl(E) \rightarrow$ (2). From (1), $Nb-cl(E) \subseteq K$, whenever $E \subseteq K$, K is Ns-open. Then (2) becomes $E \subseteq B \subseteq Nb-cl(E) \subseteq K \Rightarrow B \subseteq K$. As given $B \subseteq Nb-cl(E)$ implies $Nb-cl(E)$ is the Nb-closed set containing B . But $Nb-cl(B)$ is the smallest Nb-closed set containing B . So $B \subseteq Nb-cl(B) \subseteq Nb-cl(E) \subseteq K$. Hence $Nb-cl(B) \subseteq K$, whenever $B \subseteq K$, K is Ns-open. Thus B is Nsgb-closed.

Theorem 3.22: For s in U , the set $U - \{s\}$ is Nsgb-closed or Ns-open.

Proof: Let $s \in U$. Suppose $U - \{s\}$ is not Ns-open in U . *To Prove:* $U - \{s\}$ is Nsgb-closed. $U - \{s\} \subset U$, here U is the only Ns-open set containing $U - \{s\}$. Now $Nb-cl(U - \{s\}) \subseteq U$. This implies $Nb-cl(U - \{s\}) \subseteq U$, whenever $U - \{s\} \subseteq U$, U is Ns-open. Thus $U - \{s\}$ is Nsgb-closed.

Theorem 3.23: If $B \subseteq E \subseteq U$, B is Nsgb-closed set relative to E and E is both Ns-open and Nsgb-closed subset of U , then B is Nsgb-closed set relative to U .

Proof: Assume $B \subseteq E$, where E is Ns-open in U . *Claim:* $Nb-cl(B) \subseteq E$. Given E is Ns-open in U and since $E \subseteq E$ implies $E \cap E = E$ says E is Ns-open in E . Since B is Nsgb-closed relative to E then $Nb-cl(B) \cap E \subseteq E$, whenever $B \subseteq E$, E is Ns-open in E . Also given E is Nsgb-closed and Ns-open in U then $Nb-cl(E) \subseteq E \rightarrow$ (1) whenever $E \subseteq E$, E is Ns-open in U . Here $B \subseteq E$ then $Nb-cl(B) \subseteq Nb-cl(E) \subseteq E$ (by (1)) \rightarrow (2). $Nb-cl(E) \subseteq E$ and $Nb-cl(B) \cap E = Nb-cl(B)$. Then (2) becomes $Nb-cl(B) \cap E \subseteq Nb-cl(E) \cap E = E$. Thus $Nb-cl(B) \cap E \subseteq E$, whenever $B \subseteq E$, E is Ns-open in U . Thus $Nb-cl(B) \subseteq E$, whenever $B \subseteq E$, E is Ns-open in U . Therefore B is Nsgb-closed relative to U .

Theorem 3.24: Let $E \subseteq V \subseteq U$ and if E is Nsgb-closed in U then E is Nsgb-closed relative to V .

Proof: Given $E \subseteq V \subseteq U$ and E is Nsgb-closed in U . Let $E \subseteq K$, K be Ns-open in V such that $K = H \cap V$, where H is Ns-open in U . Then $E \subseteq H \cap V$, where $H \cap V$ is Ns-open in V . Thus $E \subseteq H$ and $E \subseteq V$. Since E is Nsgb-closed in U , $Nb-cl(E) \subseteq H$. Then $Nb-cl(E) \cap V \subseteq H \cap V = K$. Thus $Nb-cl(E) \cap V \subseteq K$, whenever $E \subseteq K$, K is Ns-open in V . Hence E is Nsgb-closed relative to V .

Nsgb- Open

- A subset E^c is Nsgb-open if E is Nsgb-closed.
- Each Nano open set is Nsgb-open set.





Kavipriya and Indira

Theorem 3.25: The union of Nsgb-open sets is Nsgb-open.

Proof: Assume E, F are Nsgb-open sets in U . To Prove: $E \cup F$ is Nsgb-open. Since the subsets E, F are Nsgb-open then $U - E, U - F$ are Nsgb-closed. By theorem 3.16, intersection of Nsgb-closed sets is Nsgb-closed. Then $(U - E) \cap (U - F) = U - (E \cup F)$ is Nsgb-closed and hence its complement $E \cup F$ is Nsgb-open in U .

Theorem 3.26: The intersection of Nsgb-open sets not necessarily Nsgb-open.

Example: From example 3.2, let $E = \{m, o, p\}$, $F = \{m, n\}$ then $E \cap F = \{m\}$ is not a Nsgb-open set. Thus intersection not necessarily be Nsgb-open.

Theorem 3.27: For $E \subseteq U$, E is Nsgb-open iff $F \subseteq \text{Nb-int}(E)$ whenever F is Ns-closed and $F \subseteq E$.

Proof: Necessary Part: Let E be Nsgb-open. Suppose $F \subseteq E$, where F is Ns-closed. Then $U - E$ is Nsgb-closed and $U - E \subseteq U - F$, where $U - F$ is Ns-open. By definition, $\text{Nb-cl}(U - E) \subseteq U - F$ this implies $U - \text{Nb-int}(E) \subseteq U - F$. Hence $F \subseteq \text{Nb-int}(E)$.

Sufficient Part: Assume $F \subseteq \text{Nb-int}(E)$, F is Ns-closed and $F \subseteq E$. To Prove: E is Nsgb-open. It is enough to prove $U - E$ is Nsgb-closed. Let $U - E \subseteq K$, K is Ns-open. Then $U - K \subseteq E$ and $U - K$ is Ns-closed. By the hypothesis, $U - K \subseteq \text{Nb-int}(E) \Rightarrow U - \text{Nb-int}(E) \subseteq K \Rightarrow \text{Nb-cl}(U - E) \subseteq K$. Thus $\text{Nb-cl}(U - E) \subseteq K$, whenever $U - E \subseteq K$, K is Ns-open. This shows $U - E$ is Nsgb-closed. Hence E is Nsgb-open.

This gives the definition of **Nsgb-open set**, a subset E of $(U, \tau_R(S))$ is Nsgb-open if $F \subseteq E$, where F is Ns-closed then $F \subseteq \text{Nb-int}(E)$.

Theorem 3.28: Each Nano open is Nsgb-open.

Proof: Let E be Nano open in U . Then $E = \text{Nint}(E)$ and $E \subseteq \text{Ncl}(E)$. Let $F \subseteq E$, where F is Ns-closed in U implies $F \subseteq \text{Nint}(E)$ and since $\text{Nint}(E) \subseteq \text{Nb-int}(E)$ gives $F \subseteq \text{Nb-int}(E)$. Thus $F \subseteq \text{Nb-int}(E)$ whenever $F \subseteq E$ where F is Ns-closed in U . Therefore E is Nsgb-open. But not each Nsgb-open is Nano open that can be seen through the example 3.2.

Theorem 3.29: A subset E is Nsgb-closed then $\text{Nb-cl}(E) - E$ is Nsgb-open.

Proof: Let E be Nsgb-closed. To Prove: $\text{Nb-cl}(E) - E$ is Nsgb-open. Let F be a Ns-closed set with $F \subseteq \text{Nb-cl}(E) - E$. By theorem 3.17, $F = \emptyset$. $\Rightarrow F \subseteq \text{Nb-int}(\text{Nb-cl}(E) - E)$. Thus $\text{Nb-cl}(E) - E$ is Nsgb-open.

Theorem 3.30: If $\text{Nb-int}(E) \subseteq B \subseteq E$ and if E is Nsgb-open then B is Nsgb-open.

Proof: Let $\text{Nb-int}(E) \subseteq B \subseteq E$. Then $E^c \subseteq B^c \subseteq \text{Nb-cl}(E^c)$, where E^c is Nsgb-closed. By theorem 3.21, B^c is Nsgb-closed. Thus B is Nsgb-open.

NSGB- CLOSURE AND NSGB- INTERIOR

Definition 4.1: Let $E \subseteq U$ in $(U, \tau_R(S))$.

- i) **Nsgb-interior of E** ($\text{Nsgb-int}(E)$) is stated as the union of all Nsgb-open sets contained in E .
ie., $\text{Nsgb-int}(E) = \cup \{B: B \text{ is Nsgb-open in } U \text{ such that } B \subseteq E\} \Rightarrow \text{Nsgb-int}(E) \subseteq E$
 - ii) **Nsgb-closure of E** ($\text{Nsgb-cl}(E)$) is stated as the intersection of all Nsgb-closed sets containing E .
ie., $\text{Nsgb-cl}(E) = \cap \{B: B \text{ is Nsgb-closed in } U \text{ such that } E \subseteq B\} \Rightarrow E \subseteq \text{Nsgb-cl}(E)$
- $\text{Nsgb-int}(E)$ is the largest Nsgb-open subset in U contained in E .
➤ $\text{Nsgb-cl}(E)$ is the smallest Nsgb-closed subset in U containing E .

From example 3.2, let $E = \{n, o\}$ then $\text{Nsgb-int}(E) = \{n, o\}$, $\text{Nsgb-cl}(E) = \{m, n, o\}$.

Theorem 4.2: With respect to S , let the nano topological space $(U, \tau_R(S))$ where $S \subseteq U$. Let $E \subseteq U$, then

- i) $[\text{Nsgb-int}(E)]^c = \text{Nsgb-cl}(E^c)$
- ii) $[\text{Nsgb-cl}(E)]^c = \text{Nsgb-int}(E^c)$

Proof:

- i) $[\text{Nsgb-int}(E)]^c = [\cup \{B: B \text{ is Nsgb-open, } B \subseteq E\}]^c = \cap \{B^c: B^c \text{ is Nsgb-closed, } E^c \subseteq B^c\} = \text{Nsgb-cl}(E^c)$
- ii) $[\text{Nsgb-cl}(E)]^c = [\cap \{B: B \text{ is Nsgb-closed, } E \subseteq B\}]^c = \cup \{B^c: B^c \text{ is Nsgb-open, } B^c \subseteq E^c\} = \text{Nsgb-int}(E^c)$





Kavipriya and Indira

Taking complements, (i) and (ii) becomes

$$\text{i) } \text{Nsgb-int}(E) = [\text{Nsgb-cl}(E^c)]^c$$

$$\text{ii) } \text{Nsgb-cl}(E) = [\text{Nsgb-int}(E^c)]^c$$

Theorem 4.3: For $E, F \subseteq U$ in $(U, \tau_R(S))$

1. $E \subseteq \text{Nsgb-cl}(E)$
2. E is Nsgb-closed iff $\text{Nsgb-cl}(E) = E$
3. $\text{Nsgb-cl}(\emptyset) = \emptyset$ and $\text{Nsgb-cl}(U) = U$
4. $E \subseteq F \Rightarrow \text{Nsgb-cl}(E) \subseteq \text{Nsgb-cl}(F)$
5. $\text{Nsgb-cl}(E) \subseteq \text{Nsgb-cl}(\text{Nsgb-cl}(E))$
6. If $E \subseteq F$, where F is any Nsgb-closed set then $\text{Nsgb-cl}(E) \subseteq F$.

Proof:

To Prove (1): By the definition of Nsgb-closure of E , it is evident that $E \subseteq \text{Nsgb-cl}(E)$.

To Prove (2): Let E be Nsgb-closed. Then E is the smallest Nsgb-closed set containing itself. Thus, $\text{Nsgb-cl}(E) = E$.

Conversely, let $\text{Nsgb-cl}(E) = E$. Since $\text{Nsgb-cl}(E)$ is the Nsgb-closed set, then E is Nsgb-closed.

To Prove (3): Since \emptyset and U are Nsgb-closed, then by (2), $\text{Nsgb-cl}(\emptyset) = \emptyset$ and $\text{Nsgb-cl}(U) = U$.

To Prove (4): Let $E, F \subseteq U$, such that $E \subseteq F$. By definition of Nsgb-closure, $\text{Nsgb-cl}(F) = \cap \{J : F \subseteq J, J \text{ are Nsgb-closed in } U\}$. If $F \subseteq J \in \text{Nsgb-closed sets of } U$, then $\text{Nsgb-cl}(F) \subseteq J$, for some J is Nsgb-closed in U . Since $E \subseteq F \Rightarrow E \subseteq F \subseteq J$. Also $\text{Nsgb-cl}(F) \subseteq J$. Then $\text{Nsgb-cl}(E) \subseteq \cap \{J : F \subseteq J, J \in \text{Nsgb-closed sets of } U\} = \text{Nsgb-cl}(F)$. Thus $\text{Nsgb-cl}(E) \subseteq \text{Nsgb-cl}(F)$.

To Prove (5): WKT: $E \subseteq \text{Nsgb-cl}(E) \Rightarrow \text{Nsgb-cl}(E) \subseteq \text{Nsgb-cl}(\text{Nsgb-cl}(E))$.

But if given E is Nsgb-closed then $\text{Nsgb-cl}(E) = \text{Nsgb-cl}(\text{Nsgb-cl}(E))$

To Prove (6): Let $E \subseteq F$, where F is Nsgb-closed. Since $\text{Nsgb-cl}(E)$ is the intersection of all Nsgb-closed sets containing E then $\text{Nsgb-cl}(E)$ is contained in each Nsgb-closed sets containing E . Here in particular $E \subseteq F$, implies $\text{Nsgb-cl}(E) \subseteq F$.

Theorem 4.4: For $I, J \subseteq U$ in $(U, \tau_R(S))$

- i) $\text{Nsgb-cl}(I) \cup \text{Nsgb-cl}(J) \subseteq \text{Nsgb-cl}(I \cup J)$
- ii) $\text{Nsgb-cl}(I \cap J) \subseteq \text{Nsgb-cl}(I) \cap \text{Nsgb-cl}(J)$

Proof:

To Prove (i): Let $I \subseteq I \cup J$ and $J \subseteq I \cup J$. By (4) of Theorem 4.3, $\text{Nsgb-cl}(I) \subseteq \text{Nsgb-cl}(I \cup J)$ and $\text{Nsgb-cl}(J) \subseteq \text{Nsgb-cl}(I \cup J)$. Hence $\text{Nsgb-cl}(I) \cup \text{Nsgb-cl}(J) \subseteq \text{Nsgb-cl}(I \cup J)$.

To Prove (ii): Let $I \cap J \subseteq I$ and $I \cap J \subseteq J$. By (4) of theorem 4.3, $\text{Nsgb-cl}(I \cap J) \subseteq \text{Nsgb-cl}(I)$ and $\text{Nsgb-cl}(I \cap J) \subseteq \text{Nsgb-cl}(J)$. Hence $\text{Nsgb-cl}(I \cap J) \subseteq \text{Nsgb-cl}(I) \cap \text{Nsgb-cl}(J)$.

Theorem 4.5: For $E, F \subseteq U$ in $(U, \tau_R(S))$

1. $\text{Nsgb-int}(E) \subseteq E$
2. E is Nsgb-open iff $\text{Nsgb-int}(E) = E$
3. $\text{Nsgb-int}(\emptyset) = \emptyset$ and $\text{Nsgb-int}(U) = U$
4. $E \subseteq F \Rightarrow \text{Nsgb-int}(E) \subseteq \text{Nsgb-int}(F)$
5. $\text{Nsgb-int}(\text{Nsgb-int}(E)) \subseteq \text{Nsgb-int}(E)$
6. If $E \subseteq F$, where F is any Nsgb-open set, then $F \subseteq \text{Nsgb-int}(E)$

Proof:

To prove (1): By the definition of Nsgb-interior of E , it is evident that $\text{Nsgb-int}(E) \subseteq E$.





Kavipriya and Indira

To Prove (2): WKT: E be Nsgb-open iff $U-E$ is Nsgb-closed. As given E is Nsgb-open then $U-E$ is Nsgb-closed. Since $U-E$ is Nsgb-closed, by theorem 4.3(2), $\text{Nsgb-cl}(U-E) = U-E \Rightarrow U-\text{Nsgb-cl}(U-E) = E$. Since $U - \text{Nsgb-cl}(U-E) = \text{Nsgb-int}(E)$, then $\text{Nsgb-int}(E) = E$. Conversely, let $\text{Nsgb-int}(E) = E$. Since $\text{Nsgb-int}(E)$ is Nsgb-open, then E is Nsgb-open.

To Prove (3): Since \emptyset and U are Nsgb-open, using (2), $\text{Nsgb-int}(\emptyset) = \emptyset$ and $\text{Nsgb-int}(U) = U$.

To Prove (4): Given $E \subseteq F \Rightarrow U-F \subseteq U-E$. By (4) of theorem 4.3, $\text{Nsgb-cl}(U-F) \subseteq \text{Nsgb-cl}(U-E)$ then $U-\text{Nsgb-cl}(U-E) \subseteq U-\text{Nsgb-cl}(U-F)$. By theorem 4.2, $\text{Nsgb-int}(E) \subseteq \text{Nsgb-int}(F)$.

To Prove (5): WKT: $\text{Nsgb-int}(E) \subseteq E \Rightarrow \text{Nsgb-int}(\text{Nsgb-int}(E)) \subseteq \text{Nsgb-int}(E)$. But if given E is Nsgb-open then $\text{Nsgb-int}(\text{Nsgb-int}(E)) = E$.

To Prove (6): Let $F \subseteq E$, where F is Nsgb-open. By (4), $\text{Nsgb-int}(B) \subseteq \text{Nsgb-int}(E)$. Since F is Nsgb-open then by (2), $\text{Nsgb-int}(F) = F$. Hence $F \subseteq \text{Nsgb-int}(E)$.

Theorem 4.6: For a subset E in U , then

i) $\text{Nsgb-cl}(E) \subseteq \text{Ncl}(E)$

ii) $\text{Nint}(E) \subseteq \text{Nsgb-int}(E)$.

Proof:

i) WKT: $E \subseteq \text{Ncl}(E)$, $\text{Ncl}(E)$ is a nano closed set. Let $B = \text{Ncl}(E)$. Since each nano closed is Nsgb-closed. This says B is Nsgb-closed. Now $E \subseteq B$, where B is Nsgb-closed. By (6) of theorem 4.3, $\text{Nsgb-cl}(E) \subseteq B$. Therefore, $\text{Nsgb-cl}(E) \subseteq \text{Ncl}(E)$.

ii) WKT: $\text{Nint}(E) \subseteq E$, $\text{Nint}(E)$ is a nano open set. Let $B = \text{Nint}(E)$. Since each nano open set is Nsgb-open set. This says B is Nsgb-open. Now $B \subseteq E$, where B is Nsgb-open. By (6) of theorem 4.5, $B \subseteq \text{Nsgb-int}(E)$. Therefore, $\text{Nint}(E) \subseteq \text{Nsgb-int}(E)$.

Theorem 4.7: For a subset E in U , $\text{Nsgb-int}(E) \subseteq \text{Nsgb-cl}(E)$.

Proof: Let $E \subseteq U$. WKT: $\text{Nsgb-int}(E) \subseteq E$ and $E \subseteq \text{Nsgb-cl}(E)$. This implies $\text{Nsgb-int}(E) \subseteq E \subseteq \text{Nsgb-cl}(E)$. Thus $\text{Nsgb-int}(E) \subseteq \text{Nsgb-cl}(E)$.

Remark 4.8: If E is both Nsgb-open and Nsgb-closed then $\text{Nsgb-int}(E) = \text{Nsgb-cl}(E) = E$.

Theorem 4.9: For $I, J \subseteq U$ in $(U, \tau_R(S))$

$\text{Nsgb-int}(I) \cup \text{Nsgb-int}(J) \subseteq \text{Nsgb-int}(I \cup J)$

$\text{Nsgb-int}(I \cap J) \subseteq \text{Nsgb-int}(I) \cap \text{Nsgb-int}(J)$

Proof: To Prove (i): Let $I \subseteq I \cup J$ and $J \subseteq I \cup J$. By (4) of Theorem 4.5, $\text{Nsgb-int}(I) \subseteq \text{Nsgb-int}(I \cup J)$ and $\text{Nsgb-int}(J) \subseteq \text{Nsgb-int}(I \cup J)$. $\text{Nsgb-int}(I) \cup \text{Nsgb-int}(J) \subseteq \text{Nsgb-int}(I \cup J)$

To Prove (ii): Let $I \cap J \subseteq I$ and $I \cap J \subseteq J$. By (4) of theorem 4.5, $\text{Nsgb-int}(I \cap J) \subseteq \text{Nsgb-int}(I)$ and $\text{Nsgb-int}(I \cap J) \subseteq \text{Nsgb-int}(J)$. Then $\text{Nsgb-int}(I \cap J) \subseteq \text{Nsgb-int}(I) \cap \text{Nsgb-int}(J)$.

CONCLUSION

This paper defined Nsgb-closed and Nsgb-open set, Nsgb-interior and Nsgb-closure and their properties are investigated. Further the study can be extended to define continuous map, homeomorphisms, connectedness and compactness based on this new set. Real life applications can be given using nano topology with its basis.

REFERENCES

1. Bhuvaneswari, K., and A. Ezhilarasi. "On nano semi-generalized and nano generalized-semi closed sets in nano topological spaces." *International Journal of Mathematics and Computer Applications Research* 4, no. 3 (2014): 117-124.



**Kavipriya and Indira**

- <http://www.tjprc.org/publishpapers/2-45-1402625257-Maths%20-%20IJMCAR%20-On%20Nano%20Semigeneralised%20and%20-%20K.BHUVANESWARI.pdf>
2. Bhuvaneswari, K., and K. Mythili Gnanapriya. "Nano Generalized closed sets in nano topological space." *International Journal of Scientific and Research Publications* 4, no. 5 (2014): 1-3. <https://www.ijsrp.org/research-paper-0514/ijsrp-p2984.pdf>
 3. Devi, P. Sulochana, and K. Bhuvaneswari. "On nano regular generalized and nano generalized regular closed sets in nano topological spaces." *International Journal of Engineering Trends and Technology (IJETT)* 8, no. 13 (2014): 386-390. <https://ijettjournal.org/assets/volume/volume-13/number-8/IJETT-V13P277.pdf>
 4. Lalitha, R., and A. Francina Shalini. "On Nano generalized Λ -closed and open sets in Nano topological spaces." *International Journal of Applied Research* 3, no. 5 (2017): 368-371. <https://www.allresearchjournal.com/archives/?year=2017&vol=3&issue=5&part=F&ArticleId=3702>
 5. Parimala, M., C. Indirani, and S. Jafari. "On nano b-open sets in nano topological spaces." *Jordan Journal of Mathematics and Statistics* 9, no. 3 (2016): 173-184. <http://repository.yu.edu.jo/bitstream/123456789/753/1/657460.pdf>
 6. Parvathy, C. R., and S. Praveena. "On nano generalized pre regular closed sets in nano topological spaces." *IOSR Journal of Mathematics (IOSR-JM)* 13, no. 2 (2017): 56-60. <https://www.iosrjournals.org/iosr-jm/papers/Vol13-issue2/Version-3/J1302035660.pdf>
 7. Thivagar, M. Lellis, and Carmel Richard. "On nano forms of weakly open sets." *International journal of mathematics and Statistics Invention* 1, no. 1 (2013): 31-37. <https://ijmsi.org/Papers/Version.1/E0111031037.pdf>





Optimization of Economic Order Quantity (EOQ) Model in Terms of Trigonal Fuzzy Numbers with Linear Regression Analysis

K. Kalaiaarasi^{1,*} and S. Swathi²

¹Assistant Professor, PG and Research Department of Mathematics, Cauvery College for Women (Autonomous), (Affiliated to Bharathidasan University), Tiruchirappalli, Tamil Nadu, India. D. Sc (Mathematics) Research Fellow, Srinivas University, Mangaluru, Karnataka, India.

²Ph. D Research Scholar, PG and Research Department of Mathematics, Cauvery College for Women (Autonomous), (Affiliated to Bharathidasan University), Tiruchirappalli, Tamil Nadu, India.

Received: 22 Jan 2024

Revised: 09 Feb 2024

Accepted: 14 May 2024

*Address for Correspondence

K. Kalaiaarasi

Assistant Professor,

PG and Research

Department of Mathematics,

Cauvery College for Women (Autonomous),

(Affiliated to Bharathidasan University),

Tiruchirappalli, Tamil Nadu, India.

D. Sc (Mathematics) Research Fellow,

Srinivas University, Mangaluru, Karnataka, India.

Email: kkalaiarasi.maths@cauverycollege.ac.in



This is an Open Access Journal / article distributed under the terms of the **Creative Commons Attribution License** (CC BY-NC-ND 3.0) which permits unrestricted use, distribution, and reproduction in any medium, provided the original work is properly cited. All rights reserved.

ABSTRACT

This research advances the Economic Order Quantity (EOQ) model by introducing Trigonal Fuzzy Numbers to effectively manage uncertainties in inventory systems. Trigonal Fuzzy Numbers, known for their flexibility in handling uncertainties through arithmetic operations, are incorporated into key parameters such as demand, ordering cost, and holding cost. The objective is to minimize the total cost, including ordering cost, holding cost, and setup cost, utilizing the Kuhn-Tucker optimization method. The defuzzification is performed using Centroid method. The research navigates the complexity of Trigonal Fuzzy Numbers and provides a numerical example to demonstrate the practical application of the proposed methodology. The results showcase the impact of fuzziness on optimal order quantities and costs, offering decision-makers a realistic perspective for enhanced inventory management. Linear regression is employed as a tool for visualizing the relationships among actual and predicted fuzzy total costs and their connection with the optimal Economic Order Quantity. This work contributes to the theoretical foundations of fuzzy inventory modelling and provides an innovative solution for addressing uncertainties in supply chain optimization.





Keywords: Inventory model, Total cost, Trigonal Fuzzy Number, Kuhn – Tucker method, Centroid method, Linear Regression.

INTRODUCTION

Inventory management stands as a cornerstone in the realm of supply chain optimization, wielding a profound impact on operational efficiency, financial health, and overall organizational success. Central to the science of inventory control is the concept of Economic Order Quantity (EOQ), a model introduced by Harris in 1913. The EOQ model strives to strike a balance between ordering and holding costs, providing a foundation for determining the optimal order quantity that minimizes the total cost of inventory. While the EOQ model has proven instrumental over the years, its traditional formulations assume a world of precision and determinism, a stark contrast to the real-world complexities characterized by uncertainties, fluctuations, and dynamic parameters. In this context, the quest to enhance the EOQ model to accommodate the intricacies of contemporary supply chains has led researchers to explore alternative methodologies, with a particular focus on fuzzy logic and innovative fuzzy number systems. The traditional EOQ model revolves around crisp and well-defined values for parameters such as demand, ordering costs, and holding costs. However, the introduction of uncertainty into these parameters necessitates a departure from crisp values to models that can capture the inherent imprecision and vagueness. Fuzzy logic provides a natural avenue for such modelling, allowing for the representation of uncertainties through linguistic variables and fuzzy sets. Zhang and Zhang (2022) and Sahoo et al. (2021) are among the pioneers who embraced fuzzy logic in inventory modelling. Their work laid the groundwork for introducing imprecision into the decision-making process, enabling a more realistic representation of the uncertainties associated with demand patterns and supply chain dynamics. Yet, within the realm of fuzzy logic, the exploration of novel fuzzy number systems has gained prominence.

Trigonal Fuzzy Numbers, introduced by Kalaiaarasi and Swathi (2023), have emerged as a particularly promising avenue. Unlike traditional fuzzy numbers that operate in a linear fashion, Trigonal Fuzzy Numbers allow for more flexible and nuanced handling of uncertainties through arithmetic operations. This inherent flexibility presents an exciting opportunity to enhance the EOQ model further. Moreover, optimization techniques play a pivotal role in refining inventory models. Traditional EOQ optimization often relies on calculus-based methods. However, for scenarios involving both equality and inequality constraints, the Kuhn-Tucker (KT) method, an extension of the Lagrange multiplier method, emerges as a robust tool. Nayak et al. (2024) have demonstrated the effectiveness of the KT method in solving constrained optimization problems, offering a valuable addition to the inventory management toolkit. This research endeavours to push the boundaries of conventional EOQ modelling by integrating Trigonal Fuzzy Numbers and leveraging optimization techniques like the KT method. The subsequent sections will delve into an extensive literature review, tracing the evolution of inventory models, the application of fuzzy logic, and the potential benefits and challenges associated with the integration of Trigonal Fuzzy Numbers into the EOQ framework. Through this exploration, the aim is to contribute to the arsenal of tools available for modern inventory management, providing solutions that resonate with the uncertainties inherent in contemporary supply chain ecosystems. Additionally, linear regression is employed as a tool for visualizing the relationships among actual and predicted fuzzy total costs and their connection with the optimal Economic Order Quantity, adding a layer of analytical depth to the research.

METHODOLOGY

Trigonal Fuzzy Numbers: Representation and Membership Function

A Trigonal Fuzzy Number A_{30g} is represented as a sequence of values $(a_1, a_2, a_3, \dots, a_{30})$, where each a_i corresponds to the membership degree for a specific interval. The membership function $\mu_{A(x)}$ can be expressed as follows:

$$\mu_{A(x)} = \begin{cases} 0, & \text{for } x < a_1, \end{cases}$$





Kalaiarasi and Swathi

$$\begin{aligned}
 &(x - a_1) / (a_2 - a_1), && \text{for } a_1 \leq x < a_2, \\
 &&& (a_3 - x) / (a_3 - a_2), && \text{for } a_2 \leq x < a_3, \\
 &&& 0, && \text{for } x < a_3, \\
 &(x - a_3) / (a_4 - a_3), && \text{for } a_3 \leq x < a_4, \\
 &(a_5 - x) / (a_5 - a_4), && \text{for } a_4 \leq x < a_5, \\
 &&& 0, && \text{for } x < a_5, \\
 &(x - a_5) / (a_6 - a_5), && \text{for } a_5 \leq x < a_6, \\
 &(a_7 - x) / (a_7 - a_6), && \text{for } a_6 \leq x < a_7, \\
 &&& \dots \\
 &&& 0, && \text{for } x < a_{29}, \\
 &(x - a_{29}) / (a_{30} - a_{29}), && \text{for } a_{29} \leq x < a_{30}, \\
 &&& 0, && \text{for } x \geq a_{30}
 \end{aligned}$$

This function elegantly captures the gradual shift in membership degrees as x moves through the intervals defined by a_1 to a_{30} .

Arithmetical Operations Under the Function Principle

Let A_{30g} and B_{30g} be two Trigonal Fuzzy Numbers defined as $A_{30g} = (a_1, a_2, \dots, a_{30})$ and $B_{30g} = (b_1, b_2, \dots, b_{30})$.

Addition of Trigonal Fuzzy Numbers

$$\begin{aligned}
 C_{30g} &= A_{30g} \oplus B_{30g} = (c_1, c_2, \dots, c_{30}) \\
 c_i &= a_i + b_i \text{ for } i = 1 \text{ to } 30
 \end{aligned}$$

Subtraction of Trigonal Fuzzy Numbers: $C_{30g} = A_{30g} \ominus B_{30g} = (c_1, c_2, \dots, c_{30})$

$$c_i = a_i - b_i \text{ for } i = 1 \text{ to } 30$$

Multiplication of Trigonal Fuzzy Numbers: $C_{30g} = (D_{30g}) \otimes B_{30g} = (c_1, c_2, \dots, c_{30})$

$$c_i = a_i \times b_i \text{ for } i = 1 \text{ to } 30$$

Division of trigonal Fuzzy Numbers: $C_{30g} = A_{30g} \oslash B_{30g} = (c_1, c_2, \dots, c_{30})$

$$c_i = \frac{a_i}{b_i} \text{ for } i = 1 \text{ to } 30$$

Kuhn-Tucker (KT) method: Optimization Technique for Constrained Problems

The Kuhn-Tucker (KT) method, also known as the Karush-Kuhn-Tucker (KKT) method, is an optimization technique used to solve constrained optimization problems. It is an extension of the Lagrange multiplier method and is particularly useful for problems with both equality and inequality constraints.

Assume the situation is given by

Minimize $x = f(y)$

Subject to $g_i(y) \geq 0, i = 1, 2, \dots, n$

Constraints on non-negativity $y \geq 0$, if any, it will include in the n constraints.

Using nonnegative surplus variables, the inequality constraints can be converted into equations. Let P_i^2 be the surplus quantity added to the i^{th} constraints $g_i(y) \geq 0$.

Let $\theta = (\theta_1, \theta_2, \dots, \theta_n), g(y) = (g_1(y), g_2(y), \dots, g_n(y))$ & $P_2 = (P_1^2, P_2^2, P_n^2)$

The Kuhn – Tucker conditions require k and h to be the minimization problem's stable endpoints.

$$\begin{cases} \theta \leq 0 \\ \nabla f(y) - \theta \nabla g(y) = 0, \\ \theta_i g_i(y) = 0, \quad i = 1, 2, \dots, n \\ g_i(y) \geq 0, \quad i = 1, 2, \dots, n \end{cases}$$





Kalaiarasi and Swathi

Centroid method for trigonal fuzzy number: Calculation of Center of Mass for Fuzzy Numbers

The centroid method for trigonal fuzzy numbers involves calculating the center of mass for a given fuzzy number, represented as A_{30} in this context. The center of mass, denoted as $C(A)$, is determined by taking the average of the membership degrees associated with the intervals defined by the trigonal fuzzy number. Mathematically, it is expressed as:

$$C(A) = \frac{1}{3} \sum_{i=1}^{30} a_i$$

Alternatively, the formula can be written as:

$$C(A) = \frac{a_1 + a_2 + a_3 + a_4 + a_5 + a_6 + a_7 + a_8 + a_9 + a_{10} + a_{11} + a_{12} + a_{13} + a_{14} + a_{15} + a_{16} + a_{17} + a_{18} + a_{19} + a_{20} + a_{21} + a_{22} + a_{23} + a_{24} + a_{25} + a_{26} + a_{27} + a_{28} + a_{29} + a_{30}}{3}$$

This calculation provides a representative value for the fuzzy number's center of mass, enhancing interpretability and facilitating decision-making in the context of trigonal fuzzy numbers.

Notations

P: Ordering cost per order.

Q: Economic Order Quantity.

R: Holding cost per unit per time period.

S: Setup cost per order.

Decision Variable:

Economic Order Quantity (Q): The variable to be optimized.

EOQ Model Formulation: Balancing Costs for Efficient Inventory Management

In the Economic Order Quantity (EOQ) model, the primary objective is to minimize the total cost, denoted as Z , by considering three fundamental components: ordering cost ($P/Q * R$), holding cost ($Q/2 * S$), and setup cost ($Q/2 * S$). The ordering cost is determined by dividing the ordering cost per order (P) by the economic order quantity (Q) and multiplying it by the holding cost per unit per time period (R). Holding cost arises from maintaining inventory and is calculated by dividing the economic order quantity (Q) by 2 (to find the average inventory level) and then multiplying it by the setup cost per order (S). Setup cost, associated with initiating or resuming production, is similarly computed. The overarching objective is to find the optimal economic order quantity (Q) that minimizes the collective impact of these costs, striking a balance between ordering, holding, and setup expenses for efficient inventory management.

The mathematical expression for the total cost (Z) is defined as:

$$Z = \frac{P}{Q} \times R + \frac{Q}{2} \times S$$

To determine the optimal economic order quantity, the derivative of Z with respect to Q is calculated:

$$\frac{dZ}{dQ} = -\frac{PR}{Q^2} + \frac{S}{2} = 0$$

$$\text{Setting } \frac{dZ}{dQ} = 0$$

$$\frac{PR}{Q^2} = \frac{S}{2}$$

Solving for Q

$$Q^2 = \frac{2PR}{S}$$

The optimal economic order quantity (EOQ) is represented by the expression

$$Q = \sqrt{\frac{2PR}{S}}$$





Kalaifarasi and Swathi

This expression signifies the calculated EOQ, representing the quantity at which ordering costs and holding costs are balanced, thereby minimizing the collective impact of ordering, holding, and setup expenses for efficient inventory management.

Optimization of Trigonal Fuzzy Inventory model

In the Trigonal Fuzzy Inventory model, the variables

$\tilde{P} = (P_1, P_2, P_3, \dots, P_{30})$, $\tilde{Q} = (Q_1, Q_2, Q_3, \dots, Q_{30})$, $\tilde{R} = (R_1, R_2, R_3, \dots, R_{30})$, $\tilde{S} = (S_1, S_2, S_3, \dots, S_{30})$ are introduced as fuzzy numbers. These fuzzy parameters allow for a more flexible and realistic representation of uncertainties and imprecisions in the inventory model.

The fuzzy total cost \tilde{Z}_i is formulated as

$$\tilde{Z}_i = \frac{\tilde{P}_i}{\tilde{Q}_i} \times \tilde{R}_i + \frac{\tilde{Q}_i}{2} \times \tilde{S}_i$$

This equation captures the fuzzy nature of the parameters and reflects the ordering cost, holding cost, and setup cost within the inventory model. To obtain a crisp value for the fuzzy total cost \tilde{Z}_i , the defuzzification process is employed, utilizing the centroid method. The centroid method calculates the center of mass of the fuzzy numbers \tilde{Z}_i to provide a single representative value \tilde{Z}_i , making the overall cost more interpretable.

$$\tilde{Z} = \frac{1}{3}(\tilde{Z}_i), i = 1, 2, 3, \dots, 30$$

Where,

$$\tilde{Z}_i = \frac{\tilde{P}_i}{\tilde{Q}_i} \times \tilde{R}_i + \frac{\tilde{Q}_i}{2} \times \tilde{S}_i$$

$$\tilde{Z} = \frac{1}{3} \left[\frac{\tilde{P}_i}{\tilde{Q}_i} \times \tilde{R}_i + \frac{\tilde{Q}_i}{2} \times \tilde{S}_i \right]$$

The partial derivative of \tilde{Z} with respect to \tilde{Q}_i is expressed as

$$\frac{\partial \tilde{Z}}{\partial \tilde{Q}_i} = \frac{1}{3} \left(-\frac{\tilde{P}_i \times \tilde{R}_i}{\tilde{Q}_i^2} + \frac{1}{2} \times \tilde{S}_i \right)$$

This derivative represents the rate of change of the total cost with respect to the fuzzy order quantity \tilde{Q}_i and is crucial in identifying optimal values.

By setting $\frac{\partial \tilde{Z}}{\partial \tilde{Q}_i} = 0$, the equation

$$-\frac{\tilde{P}_i \times \tilde{R}_i}{\tilde{Q}_i^2} + \frac{1}{2} \times \tilde{S}_i = 0 \text{ is derived.}$$

This step is essential in finding critical points where the derivative equals zero, indicating potential locations for minimum or maximum values.

Solving for \tilde{Q}_i^2

$$\tilde{Q}_i^2 = \frac{2 \times \tilde{P}_i \times \tilde{R}_i}{\tilde{S}_i}$$

This equation provides a relationship between the fuzzy order quantity \tilde{Q}_i , ordering cost \tilde{P}_i , demand rate \tilde{R}_i , and setup cost \tilde{S}_i .

Solving for \tilde{Q}_i

$$\tilde{Q}_i = \sqrt{\frac{2 \times \tilde{P}_i \times \tilde{R}_i}{\tilde{S}_i}}$$

This expression provides a defuzzified value for the optimal order quantity \tilde{Q}_i , considering the fuzzy nature of the parameters in the trigonal fuzzy inventory model.

Numerical Example**Economic Order Quantity (EOQ) Analysis**

The economic order quantity (Q) for the crisp case, given $P = 4$, $R = 9$, $S = 16$





Kalaifarasi and Swathi

$$Q = \sqrt{\frac{2PR}{S}}$$

$$Q = \sqrt{\frac{2 \times 4 \times 9}{16}}$$

$$Q = \sqrt{\frac{72}{16}}$$

$$Q = \sqrt{4.5}$$

Resulting in $Q \approx 2.12$

Substituting the calculated Q along with $P = 4$, $R = 9$, $S = 16$ into the expression for total cost (Z),

$$Z = \frac{P}{Q} \times R + \frac{Q}{2} \times S$$

$$Z = \frac{4}{2.12} \times 9 + \frac{2.12}{2} \times 16$$

$$Z \approx 8.49 \times 9 + 1.06 \times 16$$

$$Z \approx 76.41 + 16.96$$

The total cost is computed as $Z \approx 93.37$

This represents the balance between ordering and holding costs, optimizing inventory management for the given deterministic parameters.

Fuzzy Case: Trigonal Fuzzy Numbers

The fuzzy case introduces trigonal fuzzy numbers P_i, R_i, S_i , capturing uncertainties.

$$\tilde{P}_i = \begin{bmatrix} 2.9, 3.1, 3.1, 3.2, 3.2, 3.3, 3.4, 3.5, 3.5, 3.6, \\ 3.7, 3.8, 3.8, 3.9, 3.9, 4.0, 4.0, 4.2, 4.5, 4.7, \\ 4.9, 5.2, 5.5, 5.8, 6.0, 6.3, 6.6, 6.8, 7.0, 7.3, 7.6 \end{bmatrix}$$

$$\tilde{R}_i = \begin{bmatrix} 7.1, 7.3, 7.6, 7.8, 8.0, 8.3, 8.5, 8.7, 8.9, 9.1, \\ 9.3, 9.5, 9.7, 9.9, 10.0, 10.2, 10.4, 10.6, 10.8, 11.0, \\ 11.2, 11.4, 11.6, 11.8, 12.0, 12.2, 12.4, 12.6, 12.8, 13.0 \end{bmatrix}$$

$$\tilde{S}_i = \begin{bmatrix} 13.6, 13.8, 14.0, 14.2, 14.4, 14.6, 14.8, 15.0, 15.2, 15.4, \\ 15.6, 15.8, 16.0, 16.2, 16.4, 16.6, 16.8, 17.0, 17.2, 17.4, \\ 17.6, 17.8, 18.0, 18.2, 18.4, 18.6, 18.8, 19.0, 19.2, 19.4 \end{bmatrix}$$

The fuzzy order quantity \tilde{Q}_i is calculated for 30 different scenarios ($i=1,2,3,\dots,30$) using the formula $\tilde{Q}_i = \sqrt{\frac{2 \times \tilde{P}_i \times \tilde{R}_i}{\tilde{S}_i}}$

$$\tilde{Q}_i \approx \begin{bmatrix} 1.893, 1.905, 1.923, 1.939, 1.956, 1.975, 1.994, 2.014, 2.034, 2.054, \\ 2.073, 2.092, 2.110, 2.128, 2.146, 2.163, 2.179, 2.195, 2.211, 2.226, \\ 2.242, 2.257, 2.271, 2.286, 2.300, 2.314, 2.328, 2.341, 2.355, 2.368 \end{bmatrix}$$

These values provide a range of potential order quantities considering the fuzziness in parameters.

Corresponding fuzzy total costs \tilde{Z}_i are then determined for each scenario ($i=1,2,3,\dots,30$) using the formula

$$\tilde{Z}_i = \frac{\tilde{P}_i}{\tilde{Q}_i} \times \tilde{R}_i + \frac{\tilde{Q}_i}{2} \times \tilde{S}_i$$

$$\tilde{Z}_i \approx \begin{bmatrix} 2.767, 2.752, 2.738, 2.724, 2.710, 2.696, 2.681, 2.667, 2.653, 2.639, \\ 2.624, 2.610, 2.596, 2.582, 2.567, 2.553, 2.539, 2.525, 2.511, 2.496, \\ 2.482, 2.468, 2.453, 2.439, 2.425, 2.411, 2.396, 2.382, 2.368, 2.353, 2.339 \end{bmatrix}$$

These fuzzy total costs represent the impact of uncertainties on the overall cost, providing a more realistic view of the potential outcomes.

For the fuzzy case, after considering the fuzzy parameters, the calculated fuzzy order quantity is approximately $\tilde{Q}_i \approx 2.102$ and $\tilde{Z}_i \approx 23.25139$. This scenario demonstrates the influence of fuzziness on the order quantity and total cost, showcasing the flexibility of the fuzzy model in capturing uncertainties for more realistic decision-making in inventory management.



**Kalaiaarasi and Swathi****Linear regression**

Linear regression visualization serves as a powerful analytical tool, offering insights into the intricate relationships between variables within a predictive model. In this specific case, the utilization of a 3D surface plot enhances our understanding by visually portraying the interconnections among actual fuzzy total cost, predicted fuzzy total cost, and the optimal Economic Order Quantity (EOQ), denoted as Q^* .

The provided data showcases matrices representing the actual fuzzy total cost and the corresponding predictions:

Actual Fuzzy Total Cost:

```
[[ 9.16045817 9.80881188 9.47944112]
 [12.45346535 13.52363184 12.63506173]
 [17.31356209 18.08311688 17.99836066]
 [25.95576923 27.76019417 26.75717703]
 [52.80940594 55.12815534 54.808]]
```

Predicted Fuzzy Total Cost

```
[ 9.16045817 12.45346535 17.31356209 25.95576923 52.80940594]
```

The 3D surface plot serves as a comprehensive visual representation, illustrating the correlations among actual and predicted fuzzy total costs and their relationship with the optimal EOQ. Each point on the surface plot corresponds to a specific combination of actual and predicted fuzzy total cost values. The depth of the plot is indicative of the associated optimal EOQ. Notably, the surface plot aligns with the mathematical plane $Z = X + Y$. This alignment signifies a close match between the predicted and actual fuzzy total costs. The alignment with $Z = X + Y$ suggests that the fuzzy linear regression model excels in predicting fuzzy total cost. It indicates a robust performance in capturing the relationships within the given data. As one navigates along the surface, exploring different points, the plot reveals how changes in actual and predicted fuzzy total costs are associated with variations in the optimal EOQ. This interactive exploration contributes to a nuanced understanding of the system dynamics. The 3D surface plot, as a visual tool, facilitates a profound comprehension of the model's performance and the intricate interplay between different variables. It offers valuable insights into the accuracy of fuzzy linear regression predictions and their implications for optimizing EOQ, contributing to a more thorough analysis of the system under consideration.

CONCLUSION

This research presents a pioneering approach to optimize the EOQ model by integrating Trigonal Fuzzy Numbers, showcasing a sophisticated and flexible method to handle uncertainties in inventory management. Through the application of the Kuhn-Tucker optimization method, the model gains robustness, proving effective in scenarios featuring both equality and inequality constraints. Despite the inherent complexity of Trigonal Fuzzy Numbers, this research demonstrates their efficacy in capturing nuanced uncertainties, providing decision-makers with a more realistic representation of the dynamic supply chain environment. The numerical example vividly illustrates the practical implementation of the proposed methodology, emphasizing the substantial impact of fuzziness on order quantities and total costs. The defuzzification process, particularly employing the centroid method, adds interpretability to the fuzzy total cost, aiding decision-making in real-world scenarios. By calculating the center of mass of the fuzzy numbers, the centroid method yields a single representative value for the fuzzy total cost, enhancing overall interpretability and facilitating optimal decision-making. Moreover, the incorporation of linear regression visualization serves as a powerful analytical tool, offering insights into the intricate relationships between variables within a predictive model. The 3D surface plot provides a comprehensive visual representation, illustrating the correlations among actual and predicted fuzzy total costs and their relationship with the optimal EOQ. This interactive exploration contributes to a nuanced understanding of the system dynamics.





Kalaiaarasi and Swathi

Future Work

This research contributes significantly to the understanding of fuzzy inventory models and their applications in contemporary supply chain ecosystems. As industries navigate increasingly uncertain and dynamic conditions, the integration of Trigonal Fuzzy Numbers emerges as a promising avenue for refining inventory management strategies. The proposed approach not only enriches theoretical foundations but also equips practitioners with a valuable tool for making informed decisions amidst uncertainties. Future research directions could explore the broader application of this methodology across diverse industry contexts and assess its performance under varying degrees of uncertainty. This work lays a solid foundation for advancing inventory management methodologies and sets the stage for continued innovations in the field.

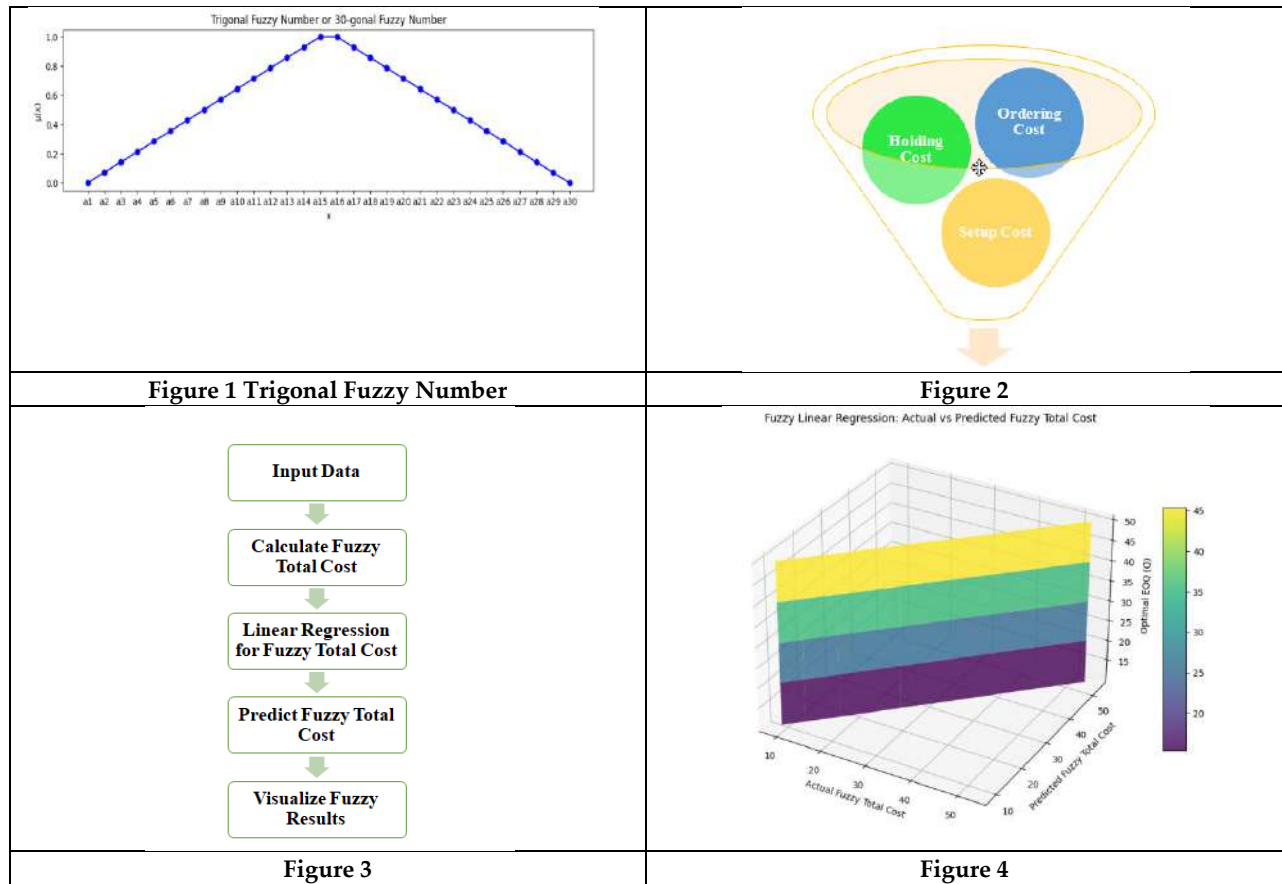
REFERENCES

1. Das, K., & Islam, S. (2024). A deterministic multi-item inventory model with quadratic demand under neutrosophic and Pythagorean hesitant fuzzy programming approach. *Results in Control and Optimization*, 14, 100367.
2. Garg, H., Sugapriya, C., Rajeswari, S., Nagarajan, D., & Alburaikan, A. (2024). A model for returnable container inventory with restoring strategy using triangular fuzzy numbers. *Soft Computing*, 1-12.
3. Nayak, D. K., Paikray, S. K., & Sahoo, A. K. (2024). Profit maximization inventory model for non-instantaneous deteriorating items with imprecise costs. In *Modeling and Applications in Operations Research* (pp. 123-138). CRC Press.
4. Sugapriya, C., Saranyaa, P., Nagarajan, D., & Pamucar, D. (2024). Triangular intuitionistic fuzzy number-based backorder and lost sale in production, remanufacturing, and inspection process. *Expert Systems with Applications*, 240, 122261.
5. Venugopal, R., Veeramani, C., & Edalatpanah, S. A. (2024). Enhancing daily stock trading with a novel fuzzy indicator: Performance analysis using Z-number based fuzzy TOPSIS method. *Results in Control and Optimization*, 14, 100365.
6. Kalaiaarasi, K., & Swathi, S. (2023). Arithmetic Operations of Trigonal Fuzzy Numbers Using Alpha Cuts: A Flexible Approach to Handling Uncertainty. *Indian Journal of Science and Technology*, 16(47), 4585-4593. <https://doi.org/10.17485/IJST/v16i47.2654>
7. Shunmugapriya, S., Sundhari, V., & Kalaiaarasi, K. (2023). The Optimization Machine Learning Approach Of Sensitive Analysis Of Fuzzy Inventory Germination Of Plants Generates One-Year-Old-Seeds And Two-Year-Old-Seeds With Fuzzy Inventory. *Journal of Survey in Fisheries Sciences*, 344-355.
8. Hao, Z., Zhang, H., & Zhang, Y. (2023). Stock Portfolio Management by Using Fuzzy Ensemble Deep Reinforcement Learning Algorithm. *Journal of Risk and Financial Management*, 16(3), 201.
9. Kumar, P., Dutta, D., & Kumar, P. (2022). Fuzzy inventory model without shortage using trapezoidal fuzzy number with sensitivity analysis. *Authorea Preprints*.
10. Malik, A. K., & Garg, H. (2021). An improved fuzzy inventory model under two warehouses. *Journal of Artificial Intelligence and Systems*, 3(1), 115-129.
11. Zhang, L., & Zhang, H. (2022). A fuzzy logic-based approach to inventory control in a supply chain. *International Journal of Production Economics*, 241, 107998.
12. Sahoo, A. K., Nayak, D. K., & Panigrahi, R. (2021). A fuzzy inventory model with partial backordering under inflationary conditions. *Computers, Materials & Continua*, 67(2), 1603-1617.
13. Xu, Z., & Xie, N. (2020). A novel fuzzy inventory model with imperfect items and variable lead time. *International Journal of Production Research*, 58(7), 2115-2131.
14. Manogaran, G., & Lopez, D. (2017). A survey of big data architectures and machine learning algorithms in healthcare. *Journal of King Saud University-Computer and Information Sciences and Engineering*.
15. Abbasi, B., & Saghaei, A. (2015). A fuzzy EOQ model with partial backordering for deteriorating items under inflation and time value of money. *International Journal of Production Economics*, 164, 1-13.





Kalaiaarasi and Swathi





Reinventing Identities: A Study in Chitra Banerjee Divakaruni's Novel

N.Vadivu^{1*}, G.Saratha Lakshmi¹ and C.Shahin Banu²

¹Assistant Professor (Senior Grade), Department of English, Sona College of Technology, Salem, (Affiliated to Anna University) Chennai, Tamil Nadu, India.

²Assistant Professor, Sona College of Technology, Salem, (Affiliated to Anna University) Chennai, Tamil Nadu, India.

Received: 22 Jan 2024

Revised: 09 Feb 2024

Accepted: 11 May 2024

*Address for Correspondence

N.Vadivu

Assistant Professor (Senior Grade),
Department of English, Sona College of Technology,
Salem, (Affiliated to Anna University)
Chennai, Tamil Nadu, India.
Email: vadivun@sonatech.ac.in



This is an Open Access Journal / article distributed under the terms of the **Creative Commons Attribution License** (CC BY-NC-ND 3.0) which permits unrestricted use, distribution, and reproduction in any medium, provided the original work is properly cited. All rights reserved.

ABSTRACT

This paper intends to explore the portrayal of diasporic identity in Chitra Banerjee Divakaruni's *Oleander Girl*. Postcolonial literature is venturing into diasporic dynamism to a large extent. Though life is moving on with the progression of technology, age-old stereotypical roles of women are still being expected by the society. Modern women are vigorous to throw away their traditional bondage and fetters. They are predominantly wedged in the process of reformulating and rediscovering their own roles, position and liaison within the societal earth. The struggle of woman's adherence and rejection to the tradition forms the nexus of modern Diasporic life. This cultural grapple continues even after their migration. Divakaruni traces the message of identity crises in the novel *Oleander Girl*. Her novels depict the portraits of modern Indian women who are torn between their historical past and progressive present. She highlights diasporic women protagonists, living in two cultures, their delineation, isolation, expulsion, mental trauma, and dislocation at the plane of diasporic consciousness.

Keywords: quintessence, transformation, inherited identity, tradition, diaspora, postcolonial

INTRODUCTION

Divakaruni poignantly brings out the feminist aspect of *Korobi* in the novel *Oleander Girl*. She is a young orphan, who loses her protective grandfather, and has support of none other than her own valour. She stands by her decision in seek for her father. She is neither afraid of breaking her engagement nor vexed about the remarks of the people. She just desires to pursue her heart. Divakaruni makes her protagonist confront the hegemonic power through the affirmation of her willpower. In spite of acknowledging the hardship on her way she decides to give up all her solace and even forgo her love to trace her identity. She tells:





Vadivu et al.,

I need to find him, talk to him. I need to know who he is. And he can finally tell me about my mother – the things that no one else knows. My mother, in love. Won't that be wonderful, Rajat? Then I will know who I really am, too. But how will I find him? I don't even have his name. And America is such a big country (OG 67).

Even when Korobi is informed that itinerating to America and hiring a detective there would “cost a lot” as she would “have to pay him in dollars” (OG 71), she remains strong-minded. Korobi with bemused emotions manages to persuade everyone and with the blessings of her grandmother undertakes a journey to the other end of the globe braving all perils. She pledges that she will return back to India and wed Rajat. Her mother Anu lived masked identities as she couldn't go against her father. She travelled oceans to pursue her dreams and even had a live in relationship with Rob. But Korobi a headstrong person follows her own inner voice. She emerges as the quintessence of audacity, thereby invalidating all gender assumptions. Divakaruni herself validates that perhaps what distinguishes her characters are their courage and spirit and a certain stubbornness which enables them to keep going even when facing a setback. I think this developed organically as I wrote, but also it came out of a desire to portray women as powerful and intelligent forces in the world. Korobi's upbringing parallels the upbringing of the mythical princess afolk tale that has been employed by Divakaruni as a literary device to express the contradiction that exists between reality and fiction. Her quest for her father shatters numerous illusions about herself just similar to the princess's quest for life which is traumatized by the callous realities of the world. Korobi walks with the remembrance of family values and vows of India, but when required she adjusts, assimilates and accepts the American way of living. Her experience of migration in search of her own identity presents her in a 'in-between' prospective of Diaspora. Her journey to find her father makes her throw all the redundant burdens she used to carry as part of her personality being completely an Indian. Her attitude is neither western nor modern, but it is her liability in fixing her stance in her family and at home. Divakaruni as a true feminist places her priorities above the hassles of the patriarchal outlook of the society. Divakaruni delineates the challenges faced by Korobi as an immigrant poignantly. The author unfolds a series of hardships Korobi goes through and empowers her with the courage and determination to fight against all the odds. She slowly acquires the survival skills of an immigrant to sustain her hunt for her father in New York. Multifaceted oppressions make women apart, but women thrust to confront the hostility of sexism and racism which degrades her around the globe. Korobi's life as an immigrant takes a different turn as she tries to adjust to the American way of living. After an unsuccessful trip to Boston, she plans her travel to California in search of her father. When she realises that she doesn't have enough funds for her travel, Mr. Desai suggests her to approach Rajat for money. But she is determined not to ask money from Rajat. Divakaruni gives a strong voice to Korobi as she says, “I'll get the money,” I say with jaunty rashness, though I have no idea how. I know this much, though: I'm not going to ask Rajat” (OG 172). Korobi's feminine sensibility is exhibited by Divakaruni when she sells her thick black hair to raise money for her trip to California trip. Divakaruni presents her as an independent and assertive woman who takes decisions independently according to her requirements in America. Ranajit Guha points out, however,

that often strength can be found in the difficult experiences of an immigrant if she can “mobilize the past as a fund of energies and resources... to clear a path which has the future with all its potentiality on its horizon. A difficult path opened up by the tragic disjunction of [her] past and present” (158).

From a receptive and docile woman, she transmogrifies into a courageous, tough and independent woman, geared up to face all challenges in life. The resolution to “release Rajat from the engagement” (OG 79) is again an intrepid gesture that not only emphasizes her idiosyncrasy of spirit but also her non-conformity to the stereotype. She says to Rajat, “I'm so confounded. All the things I was so glad for, my family, my legacy they're just half-valid. The other portion of me-I know nothing about it. Then again, actually all this time my dad was alive, and in America” (66). She exhibits sovereignty over her life. She finally does something that proves that she has right over her own life and can take decisions for herself. The search for the roots implies her feminist quest for self-actualisation as her identity remains fragmented. Korobi which means 'Oleander' in fact symbolises power underneath a delicate veneer. This inner vigour helps her to accomplish self-actualisation.





Vadivu et al.,

Divakaruni harmoniously weaves the story of Seema who gets inspired by the feminist mindset of Korobi. She narrates how Seema walks out of her wedded life refusing to suffer in silence the tyranny of her husband. As a young immigrant woman, she is disillusioned by her life in America. Korobi's guts and determination influences Seema to cut her hair and sell her jewellery to return back to her mother's place in India for her delivery. She doesn't want to stay with Mitra who isn't much concerned about her. The changing identity of Korobi inspires Seema to move her identity from a devoted wife to a dedicated mother who doesn't trust her husband's care at the decisive stage of her life. She prefers to reside with her mother so that she can deliver the child safely. Brah has rightly situated this idea of the diaspora from the angle of not individual exile but from the angle of a collective and shared community relationship by sharing the solidarity of being exile and diaspora. The diaspora communities set their parameters of existence by the collective discourses and share this solidarity with each other as a new kind of shared experience, which they endured through their journey. Brah identifies this shared solidarity in his words and says, "

They lead to a confluence of narratives that point to the one journey lived and re-lived, reproduced, partially or entirely repeated, as each diaspora and diasporic community goes through this journey and registers its parameters into the collective discourse" (183).

Divakaruni convincingly projects Korobi's process of acculturation and sense of hybrid identity. Korobi is fairly secure in the company of Vic, Mr. Desai's nephew though he is an alien to her. As she is not aware of her father's second name, the issue becomes quite complex. She narrows down her search to three gentlemen with Rob as their first name. She tells lie after lie so as to meet men named Rob. It hurts her feelings, but it doesn't dissuade her from continuing her search. Vic's appreciative word of Korobi's daring act holds her back to her womanly sensibility and true identity. She draws strength from Vic who consoles her when she goes through the terrible phase of life in search of her alterity. Women in diaspora often find that they are a member of multiple cultures simultaneously. Abraham aptly asserts that this is a complex balancing act for women in diaspora and remarks,

As an ethnic minority, South Asian immigrant women... have to cope with semi permeable boundaries that allow them... to partially internalize the norms and values of the dominant culture while being simultaneously excluded by the dominant group from total membership in that culture. (198)

Vic is fascinated by the way in which Korobi handles her life. Her feminist ways charm him and he tells her how she can seek her own identity. He says, "You need to look away from someone else's past into your own future. You think if you learn who your father and mother were; it'll teach you who you are? But you are someone already. You'd see if you weren't so busy focusing elsewhere" (OG 217).

Divakaruni brings in a twist in the story through Vic's confession of his love and admiration for her. He offers Korobi a job and requests her to stay with him in California as she can earn her own money. This unexpected proposal tempts her. She realises that she can "become a new Korobi" in America (OG 218). Her assimilation into the American culture and the thought that a financially empowered woman can earn her own money prompts her to think about the occasion. Divakaruni influentially projects Korobi's process of acculturation and her sagacity of hybrid identity. As an immigrant woman she feels she can acquire a new identity in America. Minh-ha comments upon the dilemma that immigrants experience, "The search for an identity is...usually a search for that lost, pure, true, real, genuine, original, authentic self, often situated within a process of elimination of all that is considered other, superfluous, fake, corrupted, or Westernized" (415). She realizes that life with Vic will undeniably be appealing. Caught in the whirlpool of cultural clashes of freedom in America and conservative lifestyle in India, she is in a total dilemma. America is thus, presented as the land of opportunity and success, where immigrants can gradually abandon their hybrid condition by Divakaruni. There is a clash of identities within Korobi to make a choice between the life in India with Rajat and life with Vic in America. Divakaruni creates characters who persevere on their 'difference' by re-inventing their own identities and negotiating their transnational cosmopolitan identities.





Vadivu et al.,

Korobi discerns about her mother's student life in USA with the help of her mother's friend Meera Anand. She discovers that her father is an African- American. Korobi shares this news with her grandmother. She tells her that when she looks at her self in the mirror, she sees her skin, hair everything differently. Divakaruni elucidates the impact of this revelation on her. Her new identity is that she is half-black. Her alterity is she is the daughter of Rob Lacey, an African American father. During her meeting with her actual father, she discerns about his life with Anu, her mother. From a state of idyllic ignorance, she moves towards an appalling revelation that enlightens her. Her mission brings her in confrontation with a stark reality that makes her cynical about the cultural values of her society. Korobi comes to know of another resentful unacceptable truth about her life that her mother and father were never married; that she was born out of their wedlock. She is unable to comprehend this fact. She feels awfully shameful about herself. Her father tells her that Anu had promised Bimal Roy that she will never marry against her father's wish. To keep up her promise Anu didn't agree for marriage despite his repetitive requests. Korobi realises that it is the prejudices of her austere caste system that narrows the traditional outlook of the society that jeopardizes human relationships for she says, 'I'm not sure the city will love me back. That it will accept the secrets I'm carrying' (OG 270). Her parents' marriage was barred basically due to the racial and religious prejudices.

Korobi becomes disillusioned about her otherness and her alterity. She comments, "Some kinds of success are worse than failure. It would have been better not, to have found my father than to live with this profound shame" (OG 246).

The Bose family's refusal of her new identity as an illegitimate child does not upset her. She determines to pursue her studies. Her grandmother is amazed by her transformation. Her trans-cultural experience transforms her into an empowered woman. Though she gets frequent calls from her father and Vic inviting her to reside in America, she makes up her mind to stay in her own country. She says, "I can't deny that America's siren song had pulled at me. But I came back, of my own choice. Surely that counts for something. I love my mother. But I am not her. My journey has taught me that" (OG 280).

Korobi is too strong a woman to heed to the temptations. She is vividly clear about her mission America which is to ascertain her discrepancy and not to settle there. She combats her temptations and demonstrates to be unlike her mother Anu. She says, "I'm Korobi, Oleander, capable of surviving drought and frost and the loss of love" (OG 274-275). This might and self-determination in her inner psyche helps her to attain self-actualization at the end. Her transcultural expedition from ignorance opens up her chase for identity which makes her a bold, convinced and conscientious woman as her name suggests. In the narrative it is Korobi who finally resolves all conflicts and qualms by striking poise between tradition and modernity. Korobi, faithful to her name, is an Oleander Girl who is not only fine-looking but also resolute. In an interview to Debby DeRosa, regarding the particular flower Oleander and its importance in the novel, Divakaruni says:

The oleander seemed to be the perfect symbol for the book on many levels. It is ambiguous, positive and negative, beautiful and dangerous --and hardy, capable of protecting itself. It is central to the mystery of the protagonist Korobi's mother Anu, because Anu (dying at childbirth) chooses to name her daughter after this complicated flower. A question that drives the novel is why Anu chooses to name her daughter Korobi after this flower. Why not Rose or Jasmine or Lily, as is more common? It is also a flower that grows in both India and America, connecting the two worlds through which the novel and our protagonist travels.

Korobi's transcultural expedition gives her revelation and makes her more poised in the Eastern as well as the Western world. As Banu, C. Shahin says, "Terrible sense of desolation influences the psychological condition of a person who has to face the situation with hope" (2021). The cultural clashes Korobi experiences in America make her tough as a woman. As Bhabha says the hybrid identity is situated within this third space, as 'lubricant' (56) in the juxtaposition of cultures. The hybrids approach is with their inherent acquaintance of 'transculturation' in and their





Vadivu et al.,

skill to transverse, negotiate and mediate affinity and difference within a dynamic of exchange and inclusion in both the cultures. To translate, Bhabha aspires that it is in this space that we will find those words with which we can speak of “ourselves and others”. And by probing this ‘Third Space’, we may evade the politics of schism and emerge as the “others of ourselves”. His analysis, which is chiefly based on the Lacanian conceptualization of mimicry as camouflage focuses on colonial ambivalence. Chandra Talpade Mohanty, an outstanding postcolonial women's activist in her paper “Under Western Eyes: Feminist Scholarship and Colonial Discourses” *Feminist Review*, discourses about the assertive women's activist approach of the west. She rebukes the interpretation of the Third World Ladies by Western women's activists. Divakaruni has portrayed Korobi as a women's activist who tends to follow what her heart utters and takes decisions herself without worrying about the consequences that she will confront. The traditional Bengali culture forms the foundation of Korobi's brought up and the broad-minded American culture makes her understand the intentions of her grandfather to protect the women of his family by binding them with his prospects. Korobi says, “I feel a twinge, I can't deny that America's alarm melody had pulled at me. Be that as it may, I returned, voluntarily. Clearly that means something. I love my mom. In any case, I am not her. My excursion has instructed me that” (280). In the words of Richard Slimbach, “Our willingness to transcend the character, and totally develop their potential identities. Impacted by both the cultures, Korobi empowers herself and confronts the obstacles. In this manner, she rediscovers herself as a resilient woman. Dislocation today is ascribed and substantiated as the distinctive feature of humanity and not just a feature of the Diasporas alone.

REFERENCES

1. Divakaruni, Chitra Banerjee. *Oleander Girl*. Penguin books India. 2013. Print. 2.
2. ----“Interview with the author of *Oleander Girl*” DeRosa, Debby. March 28, 2013. Web. 25th
3. Jan 2014
4. Abraham, Margaret. “Introduction”. *Speaking The Unspeakable: Marital Violence*
5. *Among South Asian Immigrants In The United States*, Rutgers UP, New Jersey, 2000. p. 8.
6. Banu, C. Shahin. *Excruciation and Endurance in the Select works of Rohinton Mistry*. 2021, Periyar University. Ph.D. dissertation.
7. Bhabha, Homi. *The Location of Culture*. London: Routledge, 1994, pp.53-54.
8. Brah, A. *Cartographies of Diaspora: Contesting Identities*. London: Routledge. 1996,
9. p.183.
10. Guha, Ranajit. “The Migrant's Time.” *Postcolonial Studies*. 1.2 (1998): 155-160. Print.
11. Lakshmi G .Saratha. *Emergence of Autonomous Self through Predicaments in the Select Novels of Shashi Deshpande*. 2021, Periyar University. Ph.D. dissertation.
12. Minh-ha, Trinh. “Not You/Like You: Postcolonial Women and the Interlocking Questions of Identity and Difference.” In *Dangerous Liaisons: Gender, Nation and Postcolonial Perspectives*. Eds. A. McClintock, A. Mufti, and E. Shohat. Minneapolis: U of Minnesota, 1989, p. 415-19. Print.
13. Mohanty, Chandra Talpade. “Under Western Eyes: Feminist Scholarship and Colonial Discourses.” *Feminist Review*, No.30 (1988): 61-88. JSTOR 10 July 2013. <http://www.jstor.org/stable/1395054>
14. Slimbach, R. *The Transcultural Journey*. *Frontiers: The Interdisciplinary Journal of Study Abroad*, Vol 11, no.1, 2005, pp. 204-230.





A Stochastic Model for Length Biased Uma Distribution with Properties and its Applications

M. Sakthivel^{1*} and P. Pandiyan²

¹Research Scholar, Department of Statistics, Annamalai University, Annamalai Nagar, Chidambaram, Tamil Nadu-608002, India.

²Professor, Department of Statistics, Annamalai University, Annamalai Nagar, Chidambaram, Tamil Nadu-608002, India.

Received: 22 Jan 2024

Revised: 09 Feb 2024

Accepted: 15 May 2024

*Address for Correspondence

M. Sakthivel

Research Scholar,
Department of Statistics,
Annamalai University, Annamalai Nagar,
Chidambaram, Tamil Nadu-608002, India.
Email: velstat98@gmail.com



This is an Open Access Journal / article distributed under the terms of the **Creative Commons Attribution License** (CC BY-NC-ND 3.0) which permits unrestricted use, distribution, and reproduction in any medium, provided the original work is properly cited. All rights reserved.

ABSTRACT

The application of statistical analysis is one of the most important applications in health research. Cancer studies mostly require special statistical considerations in order to find the appropriate model for fitting the survival data. Existing classical distributions rarely fit such data well, and some additional parameters are being added to the basic model. In this paper, we introduce new one-parameter continuous probability distributions with applications to two real-life datasets. The proposed distribution is obtained by using a weighted model and is referred to as the length biased Uma distribution. This distribution is a generalization of the baseline distribution, which is the Uma distribution. We studied the nature of distribution with the help of its mathematical and statistical properties. These are density functions, distribution functions, moments, moment-generating functions, survival functions, hazard rate functions, entropies, and Bonferroni and Lorenz curves. The probability density function of order statistics for this distribution is also obtained. We perform classical estimation of parameters by using the technique of maximum likelihood estimation. The application of the model to two real data sets that describe the survival of some cancer patients is finally presented and compared to the fit attained by some other well-known distributions.

Keywords: Length biased Model, Reliability Analysis, Statistical Properties, Entropies, Order Statistics, Likelihood Ratio, Estimation of the Parameter.





INTRODUCTION

Medical scientists are mostly interested in studying the survival of patients with cancer in their applied research. Many statistical distributions have been extensively utilized for analyzing time-to-event data, also referred to as survival of reliability data, in different areas of applicability, including the medical field. These studies are most often requiring special statistical attention and adjustment in the context of finding and choosing the appropriate model that accurately determines and estimates the survival data and yields reliable results and valid inferences. The concepts of size biased sampling and weighted distribution pertaining to observational studies and surveys of research related to forestry, ecology, bio-medicine, reliability, and several other areas have been widely studied in the literature. Adding extra parameter to an existing distribution brings the classical distribution in a more flexible situation and the distribution becomes useful for data analysis purpose. As a result, weighted distributions arise naturally generated from a stochastic process and are recorded with some weighted function. When the weight function depends on the length of the unit of interest, the resulting distribution is called length biased. Rao identified various situations that can be modeled by weighted distribution. An investigator records an observation by nature according to a certain stochastic model. The observation will not have the original distribution unless every observation is given an equal chance of being recorded. Suppose that the original observation X has $f(x)$ as the probability density function pdf (which may be probability density when X is continuous) and that the probability of recording the observation x is $0 \leq w(x) \leq 1$, then the pdf $f_w(x)$, the observation is

$$f_w(x) = \frac{w(x)f(x)}{\omega}, x > 0$$

Where ω is the normalizing factor obtained to make the total probability equal to unity. With an arbitrary non-negative weight function $w(x)$ which may exceed unity, where $w(x) = x$ or $x^\alpha, \alpha > 0$ when $\alpha = 1$, are called distributions with arbitrary $w(x)$ of is a special case. The weighted distribution with $w(x) = x$ is called the (length biased) or sized biased distribution. When the probability of observing a positive-valued random variable is proportional to the value of the variable the resultant is length biased distribution. Weighted distribution was firstly introduced by Fisher (1934)¹³ developed a new concept of distribution the weighted distribution, to model the ascertainment bias. The concept of weighted functions was first introduced by Rao (1965)²⁹ on discrete distributions arising out of ascertainment, then identified various situations that can be modelled by weighted distributions. A sampling plan that gives unequal probabilities to the various units by Patil and Rao (1977)²⁵ a weighted distributions a survey of their applications. Patil and Rao (1978)²⁶ weighted distributions and size-biased sampling with application to wildlife populations and human families. We study the properties of the weighted distributions in comparison with those of the original distributions for positive-valued random variables. Such random variables and distributions arise naturally in life testing, reliability, and economics. Blumenthal (1971)⁷ proportional sampling in life length studies. Cox (1969)⁹ some sampling problems in technology. Schaeffer (1972)³³ size-biased sampling.

Mahfoud and patil (1982)²¹ on weighted distributions. Gupta (1986)¹⁵ relations for reliability measures under length-biased sampling. Kochar and Gupta (1987)¹⁸ some result on weighted distributions for positive-valued random variables, the weighted distributions have compared with the original distributions with the partial orderings of probability distributions. Also find out finally moments of the weighted distribution have been obtained. Oluyede (1999)²⁴ on inequalities and selection of experiments for length biased distribution occurs naturally for some sampling plans in reliability, and survival analysis. Also, length biased distributions are proved for monotone hazard functions and mean residual life functions. Finally, entropy measures are also investigated. Blumenthal (1967)⁸ and Schaeffer (1972)³³ the sampling mechanism selects units with probability proportional to some measure of the unit, the relating distribution is called a size biased. Size biased and length biased distributions have been used in etiological studies Simon (1980). Cnaan (1985)¹⁰ on survival models with two phases and length biased sampling. Recently, different authors have reviewed and studied the various length biased probability models illustrated and their applications in different fields. Ahmad, A., et al. (2016)⁴, Length-biased weighted Lomax distribution: statistical properties and application. Ahad and Ahmad (2018)² discussed the Characterization and estimation of the length biased Nakagami distribution. Al-Omari and Alsmairam (2019)³ obtained the Length-biased Suja distribution and Its





Sakthivel and Pandiyan

application. Rather and Subramanian(2019)³¹ discussed the length-biased erlang-truncated exponential distribution with life time data. Ekhsosuehi et al (2020)¹² presented The Weibull length biased exponential distribution. Klinjan and Aryuyuen(2021)¹⁷ the author discussed by the length-biased power Garima distribution and its application to model lifetime data. Ben Ghorbal(2022)⁵ introduced the On Properties of Length-Biased Exponential Model. Mustafa, A., and Khan, M. I. (2022)²³ The length-biased power hazard rate distribution: Some properties and applications. Benchettah et al (2023)⁶ discussed the on composite length-biased exponential-Pareto distribution: Properties, simulation, and application in actuarial science. Mathew, J. (2023)²² obtained the Generalization of Length Biased Weighted Generalized Uniform Distribution and Its Applications. Salama, M. M., et al. (2023)³⁴ have been discussed by The Length-Biased Weighted Exponentiated Inverted Exponential Distribution: Properties and Estimation. Rather, A. A. (2023)³² discussed the Length Biased Weighted New Quasi Lindley Distribution: Statistical Properties and Applications. In this research, we adopt the idea of proposing a new one parameter distribution. The proposed distribution is such that length biases the Uma distribution. The Uma distribution introduced by Rama Shanker (2022)³⁶ is a newly proposed one-parameter lifetime model for various medical science applications. The present paper is to discuss some properties of the length-biased Uma distribution. The proposed length-biased Uma distribution focuses on exploring the adaptability to describe the survival time by analyzing some cancer datasets. These include the shape of the density, distribution, survival, hazard rate functions, the moments, the moment-generating function, harmonic mean, likelihood ratio, some associated measures, and the limiting distributions of order statistics. Maximum likelihood estimators of the model parameter are derived. Further, the efficient fitting of data with the length-biased Uma distribution is also shown over the other well-known classical distributions. All computations throughout this paper were performed using the statistical programming language R.

LENGTH BIASED UMA DISTRIBUTION

In this section, we define the probability density function (pdf) and cumulative distribution function (cdf) of the length biased Uma distribution.

A new one parameter life time distribution name as Uma distribution. The probability density function (pdf) of the Uma distribution is given by

$$f(x; \theta) = \frac{\theta^4}{\theta^3 + \theta^2 + 6} (1 + x + x^3) e^{-\theta x} \quad ; x > 0, \theta > 0 \quad (1)$$

And cumulative distribution function of the Uma distribution is given by

$$F(x; \theta) = 1 - \left[1 + \frac{\theta x (\theta^2 x^2 + 3\theta x + \theta^2 + 6)}{\theta^3 + \theta^2 + 6} \right] e^{-\theta x} \quad ; x > 0, \theta > 0 \quad (2)$$

We have considered a random variable x with a probability density function $f(x)$. Let $w(x)$ be a non-negative weight function. Denote a new probability density function.

$$f_w(x) = \frac{w(x)f(x)}{E[w(x)]} \quad ; x > 0$$

Where $w(x)$ be the non-negative weight function and $E[w(x)] = \int w(x)f(x)dx < \infty$

and corresponding random variable by X_w , which is called the weighted random variable corresponding to x . When $w(x) = x^c$, $c > 0$, we say that X_w size-biased of order c . such a selection procedure is called size-biased sampling of order c . when $c = 1, 2$, X_w is simply called size-biased (or length biased) and has a probability density function

$$f_w(x) = \frac{xf(x)}{E(X)} \quad ; x > 0$$

Gupta (1986)¹⁵ has obtained some relations between the reliability measures of the original distribution and those of the length biased distribution.

The weighted distribution is obtained by applying the weighted function as $w(x) = x^c$, in weights we use $c = 1$, $w(x) = x$ to the Uma distribution in order to obtain the length biased Uma distribution. The probability density function of the length biased Uma distribution given by





Sakthivel and Pandiyan

$$f_w(x; \theta) = \frac{x f(x; \theta)}{E(X)} \quad ; x > 0, \theta > 0, \alpha > 0 \quad (3)$$

Where,

$$E(X) = \int_0^{\infty} x f(x; \theta) dx$$

After simplification we get, gamma function is given by

$$\Gamma(Z) = \int_0^{\infty} t^{Z-1} e^{-t} dt$$

$$E(X) = \left[\frac{\theta^3 + 2\theta^2 + 24}{(\theta^3 + \theta^2 + 6)\theta} \right] \quad (4)$$

Substituting the value of equation (1) and (4) in equation (3), we get the probability density function (pdf) of length biased Uma distribution.

$$f_w(x; \theta) = \frac{\theta^5}{(\theta^3 + 2\theta^2 + 24)} x(1 + x + x^3)e^{-\theta x} \quad ; x > 0, \theta > 0, \quad (5)$$

After simplification, using a lower incomplete gamma function is given by

$$\gamma((z+1), \theta x) = \int_0^{\theta x} t^{(z+1)-1} e^{-t} dt$$

We will get cumulative distribution function (cdf) of weighted Uma distribution is given by

$$F_w(x; \theta) = \int_0^x f_w(x; \theta) dx$$

$$= \int_0^x \frac{\theta^5}{(\theta^3 + 2\theta^2 + 24)} x(1 + x + x^3)e^{-\theta x} dx$$

$$= \frac{\theta^5}{(\theta^3 + 2\theta^2 + 24)} \int_0^x x(1 + x + x^3)e^{-\theta x} dx$$

Put $\theta x = t$, $x = \frac{t}{\theta}$, $dx = \frac{1}{\theta} dt$

When $x \rightarrow 0$, $t \rightarrow 0$ and $x \rightarrow x$, $t \rightarrow \theta x$

$$= \frac{\theta^5}{(\theta^3 + 2\theta^2 + 24)} \int_0^{\theta x} \frac{t}{\theta} \left(1 + \frac{t}{\theta} + \left(\frac{t}{\theta} \right)^3 \right) e^{-t} \frac{1}{\theta} dt$$

Solving integral, we obtain

$$F_l(x; \theta) = \frac{(\theta^3 \gamma(2, \theta x) + \theta^2 \gamma(3, \theta x) + \gamma(5, \theta x))}{(\theta^3 + 2\theta^2 + 24)} \quad ; x > 0, \theta > 0 \quad (6)$$

RELIABILITY ANALYSIS

In this section, we will discuss the reliability function, hazard function, reverse hazard function, cumulative hazard function, Odds rate, Mills ratio, and Mean Residual function for the proposed length biased Uma distribution.

Reliability function

The reliability or survival function, (x) , is the probability of an item that will survive after a time x . using, the reliability function of the length biased Uma distribution is given by

$$S(x) = 1 - F(x)$$

$$S(x) = 1 - \frac{(\theta^3 \gamma(2, \theta x) + \theta^2 \gamma(3, \theta x) + \gamma(5, \theta x))}{(\theta^3 + 2\theta^2 + 24)}$$

Hazard function

The hazard function is also known as hazard rate of length biased Uma distribution is given by

$$h(x) = \frac{f(x)}{1 - F(x)}$$

$$h(x) = \frac{\theta^5}{(\theta^3 + 2\theta^2 + 24) - (\theta^3 \gamma(2, \theta x) + \theta^2 \gamma(3, \theta x) + \gamma(5, \theta x))} x(1 + x + x^3)e^{-\theta x}$$





Sakthivel and Pandiyan

Revers hazard rate

Revers hazard rate function of length biased Uma distribution is given by

$$h_r(x) = \frac{f(x)}{F(x)}$$

$$h_r(x) = \frac{\theta^5}{(\theta^3\gamma(2, \theta x) + \theta^2\gamma(3, \theta x) + \gamma(5, \theta x))} x(1 + x + x^3)e^{-\theta x}$$

Cumulative hazard function

Cumulative hazard function of length biased Uma distribution is given by

$$H(x) = -\ln(1 - F(x))$$

$$H(x) = \ln\left(\frac{(\theta^3\gamma(2, \theta x) + \theta^2\gamma(3, \theta x) + \gamma(5, \theta x))}{(\theta^3 + 2\theta^2 + 24)} - 1\right)$$

Odds rate function

Odds rate function of length biased Uma distribution is given by

$$O(x) = \frac{F(x)}{1 - F(x)}$$

$$O(x) = \frac{(\theta^3\gamma(2, \theta x) + \theta^2\gamma(3, \theta x) + \gamma(5, \theta x))}{(\theta^3 + 2\theta^2 + 24) - (\theta^3\gamma(2, \theta x) + \theta^2\gamma(3, \theta x) + \gamma(5, \theta x))}$$

Mills Ratio

Mills Ratio of length biased Uma distribution is given by

$$\text{Mills Ratio} = \frac{1}{h_r(x)}$$

$$= \frac{1}{h_r(x; \theta, \delta)}$$

$$h_r(x; \theta, \delta) = \left(\frac{(\theta^3\gamma(2, \theta x) + \theta^2\gamma(3, \theta x) + \gamma(5, \theta x))}{\theta^5 x (1 + x + x^3)e^{-\theta x}} \right)$$

Mean Residual function

Mean Residual function of length biased Uma distribution is given by

$$M(x) = \frac{1}{S(x)} \int_x^\infty t f(t) dt - x$$

$$M(x) = 1 - \frac{(\theta^3\gamma(2, \theta x) + \theta^2\gamma(3, \theta x) + \gamma(5, \theta x))}{(\theta^3 + 2\theta^2 + 24)}$$

$$\times \int_x^\infty t \frac{\theta^5}{(\theta^3 + 2\theta^2 + 24)} t(1 + t + t^3)e^{-\theta t} dt - x$$

$$\text{Put } \theta t = x, \quad t = \frac{x}{\theta}, \quad dt = \frac{1}{\theta} dx$$

When $x \rightarrow 0, t \rightarrow 0$ and $x \rightarrow x, t \rightarrow \theta x$

Solving integral, we obtain

$$M(x) = \frac{(\theta^3\Gamma(3, \theta x) + \theta^2\Gamma(4, \theta x) + \Gamma(6, \theta x))}{(\theta^3 + 2\theta^2 + 24) - (\theta^3\gamma(2, \theta x) + \theta^2\gamma(3, \theta x) + \gamma(5, \theta x))} - x$$

STATISTICAL PROPERTIES

In this section, we derived the structural properties of length biased Uma distribution.

Moments

Let X_w denoted the random variable following length biased Uma distribution then r^{th} order moments $E(X^r)$ is obtained a

$$E(X_w^r) = \mu_r' = \int_0^\infty x^r f_w(x; \theta, \delta) dx$$





Sakthivel and Pandiyan

$$\int_0^x x^r \frac{\theta^5}{(\theta^3 + 2\theta^2 + 24)} x(1+x+x^3)e^{-\theta x} dx$$

$$= \frac{\theta^5}{(\theta^3 + 2\theta^2 + 24)} \int_0^\infty x^{r+1} (1+x+x^3)e^{-\theta x} dx$$

Put $\theta x = t$, $x = \frac{t}{\theta}$, $dx = \frac{1}{\theta} dt$

$$= \frac{\theta^5}{(\theta^3 + 2\theta^2 + 24)} \int_0^\infty \left(\frac{t}{\theta}\right)^{r+1} \left(1 + \frac{t}{\theta} + \left(\frac{t}{\theta}\right)^3\right) e^{-t} \frac{1}{\theta} dt$$

Solving integral, we obtain

$$E(X_w^r) = \mu'_r = \frac{[\theta^3 \Gamma(r+2) + \theta^2 \Gamma(r+3) + \Gamma(r+5)]}{\theta^r (\theta^3 + 2\theta^2 + 24)}$$

Putting $r = 1, 2, 3, 4$ in equation (7), the mean of length biased Uma distribution is obtained as

$$\mu'_1 = \frac{[2\theta^3 + 6\theta^2 + 120]}{\theta (\theta^3 + 2\theta^2 + 24)}$$

$$\mu'_2 = \frac{[6\theta^3 + 24\theta^2 + 720]}{\theta^2 (\theta^3 + 2\theta^2 + 24)}$$

$$\mu'_3 = \frac{[24\theta^3 + 120\theta^2 + 5040]}{\theta^3 (\theta^3 + 2\theta^2 + 24)}$$

$$\mu'_4 = \frac{[120\theta^3 + 720\theta^2 + 40320]}{\theta^4 (\theta^3 + 2\theta^2 + 24)}$$

$$\text{Variance} = \mu'_2 - (\mu'_1)^2$$

$$\sigma^2 = \frac{[6\theta^3 + 24\theta^2 + 720]}{\theta^2 (\theta^3 + 2\theta^2 + 24)} - \left(\frac{[2\theta^3 + 6\theta^2 + 120]}{\theta (\theta^3 + 2\theta^2 + 24)}\right)^2$$

$$\sigma^2 = \frac{2\theta^6 + 2844\theta^5 + 518352\theta^4 + 864\theta^3 + 2016\theta^2 + 17280}{\theta^2 (\theta^3 + 2\theta^2 + 24)^2}$$

Standard Deviation

$$S.D(\sigma) = \frac{\sqrt{2\theta^6 + 2844\theta^5 + 518352\theta^4 + 864\theta^3 + 2016\theta^2 + 17280}}{\theta (\theta^3 + 2\theta^2 + 24)}$$

Coefficient of Variation

$$C.V\left(\frac{\sigma}{\mu}\right) = \frac{\sqrt{2\theta^6 + 2844\theta^5 + 518352\theta^4 + 864\theta^3 + 2016\theta^2 + 17280}}{[2\theta^3 + 6\theta^2 + 120]}$$

Dispersion

$$\text{Dispersion} = \frac{\sigma^2}{\mu}$$

$$= \frac{2\theta^6 + 2844\theta^5 + 518352\theta^4 + 864\theta^3 + 2016\theta^2 + 17280}{\theta (\theta^3 + 2\theta^2 + 24)(2\theta^3 + 6\theta^2 + 120)}$$

Harmonic Mean

The Harmonic mean of the length biased Uma distribution is defined as

$$H.M = E\left[\frac{1}{x}\right] = \int_0^\infty \frac{1}{x} f_l(x; \theta) dx$$

$$H.M = \int_0^\infty \frac{1}{x} \frac{\theta^5}{(\theta^3 + 2\theta^2 + 24)} x(1+x+x^3)e^{-\theta x} dx$$

$$H.M = \frac{\theta^5}{(\theta^3 + 2\theta^2 + 24)} \int_0^\infty x^{-1} x(1+x+x^3)e^{-\theta x} dx$$





Sakthivel and Pandiyan

$$H.M = \frac{\theta^5}{(\theta^3 + 2\theta^2 + 24)} \int_0^\infty x^{1-1} (1+x+x^3) e^{-\theta x} dx$$

$$H.M = \frac{\theta^5}{(\theta^3 + 2\theta^2 + 24)} \left(\int_0^\infty e^{-\theta x} dx + \int_0^\infty x e^{-\theta x} dx + \int_0^\infty x^3 e^{-\theta x} dx \right)$$

$$H.M = \frac{\theta^5}{(\theta^3 + 2\theta^2 + 24)} \left(\frac{1}{\theta} + \frac{1!}{\theta^2} + \frac{3!}{\theta^4} \right)$$

$$H.M = \frac{\theta(\theta^3 + \theta^2 + 2)}{(\theta^3 + 2\theta^2 + 24)}$$

Moment Generating function and Characteristic function

Let X_w follows length biased Uma distribution then the moment generating function (mgf) of X is obtained as

$$M_{X_l}(t) = E(e^{tx}) = \int_0^\infty e^{tx} f_l(x; \theta) dx$$

Using Taylor's series

$$M_{X_l}(t) = \int_0^\infty \left[1 + tx + \frac{(tx)^2}{2!} + \dots \right] f_l(x; \theta) dx$$

$$M_{X_l}(t) = \int_0^\infty \sum_{j=0}^\infty \frac{t^j}{j!} x^j f_l(x; \theta) dx$$

$$M_{X_l}(t) = \sum_{j=0}^\infty \frac{t^j}{j!} \int_0^\infty x^j f_l(x; \theta) dx$$

$$M_{X_l}(t) = \sum_{j=0}^\infty \frac{t^j}{j!} E(X_l^j)$$

$$M_{X_l}(t) = \sum_{j=0}^\infty \frac{t^j}{j!} \frac{[\theta^3 \Gamma(j+2) + \theta^2 \Gamma(j+3) + \Gamma(j+5)]}{\theta^j (\theta^3 + 2\theta^2 + 24)}$$

$$M_{X_l}(t) = \frac{1}{(\theta^3 + 2\theta^2 + 24)} \sum_{j=0}^\infty \frac{t^j}{j!} [\theta^3 \Gamma(j+2) + \theta^2 \Gamma(j+3) + \Gamma(j+5)] \quad (8)$$

Similarly, we can get the characteristic function of length biased Uma distribution can be obtained as

$$\phi_{X_l}(t) = M_{X_w}(it)$$

$$\phi_{X_l}(t) = \sum_{j=0}^\infty \frac{(it)^j}{j!} \mu_j$$

$$\phi_{X_l}(t) = \sum_{j=0}^\infty \frac{(it)^j}{j!} \frac{[\theta^3 \Gamma(j+2) + \theta^2 \Gamma(j+3) + \Gamma(j+5)]}{\theta^j (\theta^3 + 2\theta^2 + 24)}$$

$$\phi_{X_l}(t) = \frac{1}{(\theta^3 + 2\theta^2 + 24)} \sum_{j=0}^\infty \frac{(it)^j}{j!} [\theta^3 \Gamma(j+2) + \theta^2 \Gamma(j+3) + \Gamma(j+5)] \quad (9)$$

MEAN DEVIATION

Let X be a random variable from length biased Uma distribution with mean μ . Then the deviation from mean is defined as

$$D(\mu) = E(|X - \mu|)$$

$$D(\mu) = \int_0^\infty |X - \mu| f_l(x; \theta) dx$$

$$D(\mu) = \int_0^\mu (\mu - x) f_l(x; \theta) dx + \int_\mu^\infty (x - \mu) f_l(x; \theta) dx$$

$$D(\mu) = \mu \int_0^\mu f_l(x; \theta) dx - \int_0^\mu x f_l(x; \theta) dx + \int_\mu^\infty x f_l(x; \theta) dx - \int_\mu^\infty \mu f_l(x; \theta) dx$$

$$D(\mu) = \mu F(\mu) - \int_0^\mu x f_l(x; \theta) dx - \mu[1 - F(\mu)] + \int_\mu^\infty x f_l(x; \theta) dx$$





Sakthivel and Pandiyan

$$D(\mu) = 2\mu F(\mu) - 2 \int_0^\mu x f_l(x; \theta) dx$$

Now,

$$\int_0^\mu x f_l(x; \theta) dx = \int_0^\mu x \frac{\theta^5}{(\theta^3 + 2\theta^2 + 24)} x(1 + x + x^3)e^{-\theta x} dx$$

$$\text{Put } \theta x = t, \quad x = \frac{t}{\theta}, \quad dx = \frac{1}{\theta} dt$$

When $\mu \rightarrow 0, t \rightarrow 0$ and $\mu \rightarrow \mu, t \rightarrow \theta\mu$

Solving integral, we obtain

$$D(\mu) = \frac{2\mu (\theta^3\gamma(2, \theta\mu) + \theta^2\gamma(3, \theta\mu) + \gamma(5, \theta\mu))}{(\theta^3 + 2\theta^2 + 24)} - \frac{2(\theta^3\gamma(3, \theta\mu) + \theta^2\gamma(4, \theta\mu) + \gamma(6, \theta\mu))}{(\theta^3 + 2\theta^2 + 24)}$$

MEAN DEVIATION FROM MEDIAN

Let X be a random variable from length biased Uma distribution with median M . Then the mean deviation from median is defined as

$$D(M) = E(|X - M|)$$

$$D(M) = \int_0^\infty |X - M| f_l(x; \theta, \delta) dx$$

$$D(M) = \int_0^M (M - x) f_l(x; \theta, \delta) dx + \int_M^\infty (x - M) f_l(x; \theta, \delta) dx$$

$$D(M) = MF(M) - \int_0^M x f_l(x; \theta, \delta) dx - M[1 - F(M)] + \int_M^\infty x f_l(x; \theta, \delta) dx$$

$$D(M) = \mu - 2 \int_0^M x f_l(x; \theta, \delta) dx$$

Now,

$$\int_0^M x f_l(x; \theta) dx = \int_0^M x \frac{\theta^5}{(\theta^3 + 2\theta^2 + 24)} x(1 + x + x^3)e^{-\theta x} dx = \frac{\theta^5}{(\theta^3 + 2\theta^2 + 24)} \int_0^M x^2(1 + x + x^3)e^{-\theta x} dx$$

$$\text{Put } \theta x = t, \quad x = \frac{t}{\theta}, \quad dx = \frac{1}{\theta} dt$$

When $M \rightarrow 0, t \rightarrow 0$ and $M \rightarrow M, t \rightarrow \theta M$

Solving integral, we obtain

$$D(M) = \mu - \frac{2[\theta^3\gamma(3, \theta M) + \theta^2\gamma(4, \theta M) + \gamma(6, \theta M)]}{\theta(\theta^3 + 2\theta^2 + 24)}$$

ORDER STATISTICS

In this section, we derived the distributions of order statistics from the length biased Uma distribution.

Let $X_{(1)}, X_{(2)}, X_{(3)}, \dots, X_{(n)}$ be the order statistics of the random sample $X_1, X_2, X_3, \dots, X_n$ selected from length biased Uma distribution. Then the probability density function of the k^{th} order statistics $X_{(k)}$ is defined as.

$$f_{X_{(k)}}(x) = \frac{n!}{(r-1)!(n-k)!} f_X(x) [F_X(x)]^{k-1} [1 - F_X(x)]^{n-k} \quad (10)$$

Inserting equation (5) and (7) in equation (9), the probability density function of k^{th} order statistics $X_{(k)}$ of the length biased Uma distribution is given by

$$f_{X_{(k)}}(x) = \frac{n!}{(n-1)!(n-k)!} \left[\frac{(\theta^3\gamma(2, \theta x) + \theta^2\gamma(3, \theta x) + \gamma(5, \theta x))}{(\theta^3 + 2\theta^2 + 24)} \right]^{k-1} \times \left[1 - \frac{(\theta^3\gamma(2, \theta x) + \theta^2\gamma(3, \theta x) + \gamma(5, \theta x))}{(\theta^3 + 2\theta^2 + 24)} \right]^{n-k} \times \frac{\theta^5}{(\theta^3 + 2\theta^2 + 24)} x(1 + x + x^3)e^{-\theta x}$$

The distribution of the minimum first order statistics $X_{(1)} = \min(X_1, X_2, X_3, \dots, X_n)$ and the largest order statistics $X_{(n)} = \max(X_1, X_2, X_3, \dots, X_n)$ can be computed by replacing k in the previous equation by 1 and n , so we get.

$$f_{X_{(1)}}(x) = \frac{n\theta^5}{(\theta^3 + 2\theta^2 + 24)} x(1 + x + x^3)e^{-\theta x} \times \left[1 - \frac{(\theta^3\gamma(2, \theta x) + \theta^2\gamma(3, \theta x) + \gamma(5, \theta x))}{(\theta^3 + 2\theta^2 + 24)} \right]^{n-1}$$





$$f_{X(n)}(x) = \frac{n \theta^5}{(\theta^3 + 2\theta^2 + 24)} x (1 + x + x^3) e^{-\theta x} \times \left[\frac{(\theta^3 \gamma(2, \theta x) + \theta^2 \gamma(3, \theta x) + \gamma(5, \theta x))}{(\theta^3 + 2\theta^2 + 24)} \right]^{n-1}$$

Quantile function

The quantile function of a distribution with cumulative distribution function $F_l(x; \theta)$ is defined by $q = F_l(x_q; \theta)$, where $0 < q < 1$. Thus, the quantile function of length biased Uma distribution is the real solution of the equation.

$$1 - q = 1 - \frac{(\theta^3 \gamma(2, \theta x) + \theta^2 \gamma(3, \theta x) + \gamma(5, \theta x))}{(\theta^3 + 2\theta^2 + 24)}$$

LIKELIHOOD RATIO TEST

In this section, we derive the likelihood ratio test from the length biased Uma distribution.

Let $x_1, x_2, x_3, \dots, x_n$ be a random sample from the length biased Uma distribution.

To testing the hypothesis, we have the null and alternative hypothesis.

$$H_0: f(x) = f(x; \theta) \quad \text{against} \quad H_1: f(x) = f_l(x; \theta)$$

In test whether the random sample of size n comes from the Uma distribution or length biased Uma distribution, the following test statistics is used.

$$\begin{aligned} \Delta &= \frac{L_1}{L_2} = \prod_{i=1}^n \frac{f_l(x_i; \theta)}{f(x_i, \theta)} \\ \Delta &= \prod_{i=1}^n \left(\frac{\frac{\theta^5}{(\theta^3 + 2\theta^2 + 24)} x_i (1 + x_i + x_i^3) e^{-\theta x_i}}{\frac{\theta^4}{\theta^3 + \theta^2 + 6} (1 + x_i + x_i^3) e^{-\theta x_i}} \right) \\ \Delta &= \prod_{i=1}^n \frac{\theta^5}{(\theta^3 + 2\theta^2 + 24)} x_i (1 + x_i + x_i^3) e^{-\theta x_i} \times \frac{\theta^3 + \theta^2 + 6}{\theta^4 (1 + x_i + x_i^3) e^{-\theta x_i}} \\ \Delta &= \prod_{i=1}^n \left(\frac{\theta(\theta^3 + \theta^2 + 6)}{(\theta^3 + 2\theta^2 + 24)} x_i \right) \\ \Delta &= \frac{L_1}{L_2} \left(\frac{\theta(\theta^3 + \theta^2 + 6)}{(\theta^3 + 2\theta^2 + 24)} \right)^n \prod_{i=1}^n x_i \end{aligned}$$

We have rejected the null hypothesis if

$$\Delta = \left(\frac{\theta(\theta^3 + \theta^2 + 6)}{(\theta^3 + 2\theta^2 + 24)} \right)^n \prod_{i=1}^n x_i > k$$

Equivalently, we also reject null hypothesis, where

$$\begin{aligned} \Delta^* &= \prod_{i=1}^n x_i > k \left(\frac{\theta(\theta^3 + \theta^2 + 6)}{(\theta^3 + 2\theta^2 + 24)} \right)^n \\ \Delta^* &= \prod_{i=1}^n x_i > k^* \text{ where } k^* = k \left(\frac{\theta(\theta^3 + \theta^2 + 6)}{(\theta^3 + 2\theta^2 + 24)} \right)^n \end{aligned}$$

for large sample size n , $2 \log \Delta$ is distribution as chi-square variates with one degree of freedom. Thus, we rejected the null hypothesis, when the probability value is given by $p(\Delta^* > \alpha^*)$, where $\alpha^* = \prod_{i=1}^n x_i$ is less than level of significance and $\prod_{i=1}^n x_i$ is the observed value of the statistics Δ^* .

BONFERRONI AND LORENZ CURVES AND GINI INDEX

The Bonferroni and Lorenz curve is a powerful tool in the analysis of distributions and has applications in many fields, such as economies, insurance, income, reliability, and medicine. The Bonferroni and Lorenz curves for a X be the random variable of a unit and $f(x)$ be the probability density function of x . $f(x)dx$ will be represented by the probability that a unit selected at random is defined as

$$B(p) = \frac{1}{p\mu_1} \int_0^q x f_l(x; \theta) dx$$





Sakthivel and Pandiyan

And

$$L(p) = \frac{1}{\mu_1} \int_0^q x f_1(x; \theta) dx$$

Where,

$$\mu_1' = \frac{[2\theta^3 + 6\theta^2 + 120]}{\theta(\theta^3 + 2\theta^2 + 24)}$$

and

$$q = F^{-1}p$$

$$B(p) = \frac{1}{p \frac{[2\theta^3 + 6\theta^2 + 120]}{\theta(\theta^3 + 2\theta^2 + 24)}} \int_0^q x \frac{\theta^5}{(\theta^3 + 2\theta^2 + 24)} x(1 + x + x^3) e^{-\theta x} dx$$

$$B(p) = \frac{\theta^6}{p[2\theta^3 + 6\theta^2 + 120]} \int_0^q x^2 (1 + x + x^3) e^{-\theta x} dx$$

Put $\theta x = t$, $x = \frac{t}{\theta}$, $dx = \frac{1}{\theta} dt$

When $x \rightarrow 0$, $t \rightarrow 0$ and $x \rightarrow q$, $t \rightarrow \theta q$

$$B(p) = \frac{\theta^6}{p[2\theta^3 + 6\theta^2 + 120]} \int_0^{\theta q} \left(\frac{t}{\theta}\right)^2 \left(1 + \frac{t}{\theta} + \left(\frac{t}{\theta}\right)^3\right) e^{-t} \frac{1}{\theta} dt$$

Solving integral, we obtain

$$B(p) = \frac{(\theta^3 \gamma(3, \theta q) + \theta^2 \gamma(4, \theta q) + \gamma(5, \theta q))}{p[2\theta^3 + 6\theta^2 + 120]}$$

$$L(p) = pB(p)$$

$$L(p) = \frac{(\theta^3 \gamma(3, \theta q) + \theta^2 \gamma(4, \theta q) + \gamma(5, \theta q))}{[2\theta^3 + 6\theta^2 + 120]}$$

Gini Index

The information in the Lorenz Curve is often summarized in a single measure called the Gini index (proposed in a 1912 paper by the Italian statistician Corrado Gini. It is often used as a gauge of economic inequality, measuring income distribution. The Gini index is defined as

Therefore, the Gini index is for length biased Uma distribution

$$G = 1 - 2 \int_0^1 L(p) dp$$

$$G = 1 - 2 \int_0^1 \frac{(\theta^3 \gamma(3, \theta q) + \theta^2 \gamma(4, \theta q) + \gamma(5, \theta q))}{[2\theta^3 + 6\theta^2 + 120]} dp$$

Solving integral, we obtain

$$G = 1 - 2 \frac{(\theta^3 \gamma(3, \theta q) + \theta^2 \gamma(4, \theta q) + \gamma(5, \theta q))}{[2\theta^3 + 6\theta^2 + 120]}$$

STOCHASTIC ORDERING

Stochastic ordering is an important tool in finance and reliability to assess the comparative performance of the models. Let X and Y be two random variables with pdf, cdf, and reliability functions $f(x)$, $f(y)$, $F(x)$, $F(y)$. $S(x) = 1 - F(x)$ and $F(y)$.

- 1- Likelihood ratio order ($X \leq_{LR} Y$) if $\frac{f_{X_i}(x)}{f_{Y_i}(x)}$ decreases in x
- 2- Stochastic order ($X \leq_{ST} Y$) if $F_{X_i}(x) \geq F_{Y_i}(x)$ for all x
- 3- Hazard rate order ($X \leq_{HR} Y$) if $h_{X_i}(x) \geq h_{Y_i}(x)$ for all x
- 4- Mean residual life order ($X \leq_{MRL} Y$) if $MRL_{X_i}(X) \leq MRL_{Y_i}(X)$ for all x

Show that length biased Uma distribution satisfies the strongest ordering (likelihood ratio ordering)

Assume that X and Y are two independent Random variables with probability distribution function $f_{i_x}(x; \theta)$ and $f_{i_y}(x; \lambda)$. If $\theta < \lambda$, then





Sakthivel and Pandiyan

$$\Lambda = \frac{f_{lx}(x; \theta)}{f_{ly}(x; \lambda)}$$

$$\Lambda = \left(\frac{\frac{\theta^5}{(\theta^3 + 2\theta^2 + 24)} x(1 + x + x^3) e^{-\theta x}}{\frac{\lambda^5}{(\lambda^3 + 2\lambda^2 + 24)} x(1 + x + x^3) e^{-\lambda x}} \right)$$

$$\Lambda = \frac{\theta^5}{(\theta^3 + 2\theta^2 + 24)} x(1 + x + x^3) e^{-\theta x} \times \frac{(\lambda^3 + 2\lambda^2 + 24)}{\lambda^5 x (1 + x + x^3)} e^{\lambda x}$$

$$\Lambda = \left(\frac{\theta^5 (\lambda^3 + 2\lambda^2 + 24)}{\lambda^5 (\theta^3 + 2\theta^2 + 24)} \right) \times \left(\frac{(x + x^2 + x^4)}{(x + x^2 + x^4)} \right) e^{-(\theta - \lambda)x}$$

Therefore,

$$\log[\Lambda] = \log \left(\frac{\theta^5 (\lambda^3 + 2\lambda^2 + 24)}{\lambda^5 (\theta^3 + 2\theta^2 + 24)} \right) + \log(x + x^2 + x^4) - \log(x + x^2 + x^4) - (\theta - \lambda)x$$

Differentiating with respect to x, we get.

$$\frac{\partial \log[\Lambda]}{\partial x} = \left(\frac{1 + 2x + 4x^3}{x(1 + x + x^3)} \right) - \left(\frac{1 + 2x + 4x^3}{x(1 + x + x^3)} \right) + (\lambda - \theta)$$

Hence, $\frac{\partial \log[\Lambda]}{\partial x} < 0$ if $\theta < \lambda$. Thus $X \leq_{LRO} Y$, $X \leq_{HRO} Y$, and $X \leq_{SO} Y$

ENTROPIES

It is well known that entropy and information can be considered measures of uncertainty or the randomness of a probability distribution. It is applied in many fields, such as engineering, finance, information theory, and biomedicine. The entropy functionals for probability distribution were derived on the basis of a variational definition of uncertainty measure.

Shannon Entropy

Shannon entropy of the random variable X such that length biased Uma distribution is defined as

$$S_p = - \int_0^\infty f(x) \log f(x) dx$$

$$S_p = - \int_0^\infty f_l(x; \theta) \log f_l(x; \theta) dx$$

$$S_p = - \int_0^\infty \frac{\frac{\theta^5}{(\theta^3 + 2\theta^2 + 24)} x(1 + x + x^3) e^{-\theta x}}{\log \left(\frac{\theta^5}{(\theta^3 + 2\theta^2 + 24)} x(1 + x + x^3) e^{-\theta x} \right)} dx$$

9.2 Rényi Entropy

Entropy is defined as a random variable X is a measure of the variation of the uncertainty. It is used in many fields, such as engineering, statistical mechanics, finance, information theory, biomedicine, and economics. The entropy measure is the Rényi of order which is defined as

$$R_\beta = \frac{1}{1 - \beta} \log \left(\int_0^\infty f_l^\beta(x; \theta) dx \right)$$

Where, $\beta > 0$ and $\beta \neq 1$

$$R_\beta = \frac{1}{1 - \beta} \log \left(\frac{\theta^5}{(\theta^3 + 2\theta^2 + 24)} x(1 + x + x^3) e^{-\theta x} dx \right)^\beta$$

$$= \frac{1}{1 - \beta} \log \left(\frac{\theta^5}{(\theta^3 + 2\theta^2 + 24)} \right)^\beta \int_0^\infty x^\beta (1 + x + x^3)^\beta e^{-\theta x} dx \quad (11)$$

Using Binomial expansion in equation (11), we get

$$(1 + x + x^3)^\beta = \sum_{i=0}^\beta \binom{\beta}{i} 1^{\beta-i} (x + x^3)^i$$





$$\begin{aligned}
 (x + x^3)^i &= \sum_{j=0}^i \binom{i}{j} x^{i-j} x^{3j} \\
 &= \sum_{i=0}^{\beta} \binom{\beta}{i} \sum_{j=0}^i \binom{i}{j} x^{i-j+3j}
 \end{aligned} \tag{12}$$

Substituting equation (12) in (11) we get,

$$\begin{aligned}
 R_{\beta} &= \frac{1}{1-\beta} \log \left(\frac{\theta^5}{(\theta^3 + 2\theta^2 + 24)} \right)^{\beta} \sum_{i=0}^{\beta} \sum_{j=0}^i \binom{\beta}{i} \binom{i}{j} \int_0^{\infty} x^{\beta} x^{i+2j} e^{-\theta \beta x} dx \\
 R_{\beta} &= \frac{1}{1-\beta} \log \left(\frac{\theta^5}{(\theta^3 + 2\theta^2 + 24)} \right)^{\beta} \sum_{i=0}^{\beta} \sum_{j=0}^i \binom{\beta}{i} \binom{i}{j} \frac{\Gamma(\beta + i + 2j + 1)}{(\theta \beta)^{\beta + i - j + 3j + 1}} \\
 R_{\beta} &= \frac{1}{1-\beta} \log \left(\frac{\theta^5}{(\theta^3 + 2\theta^2 + 24)} \right)^{\beta} \sum_{i=0}^{\beta} \sum_{j=0}^i \binom{\beta}{i} \binom{i}{j} \left(\frac{1}{\theta \beta} \right)^{\beta + i + 2j + 1} \Gamma(\beta + i + 2j + 1)
 \end{aligned}$$

Tsallis Entropy

The Boltzmann-Gibbs (B-G) statistical properties initiated by Tsallis have received a great deal of attention. This generalization of (B-G) statistics was first proposed by introducing the mathematical expression of Tsallis entropy (Tsallis, (1988) for continuous random variables, which is defined as

$$S_{\lambda} = \frac{1}{\lambda - 1} \left(1 - \int_0^{\infty} f_l^{\lambda}(x; \theta) dx \right)$$

Where, $\lambda > 0$ and $\lambda \neq 1$

$$\begin{aligned}
 S_{\lambda} &= \frac{1}{\lambda - 1} \left(1 - \int_0^{\infty} \left(\frac{\theta^5}{(\theta^3 + 2\theta^2 + 24)} x(1 + x + x^3) e^{-\theta x} dx \right)^{\lambda} dx \right) \\
 S_{\lambda} &= \frac{1}{\lambda - 1} \left(1 - \left(\frac{\theta^5}{(\theta^3 + 2\theta^2 + 24)} \right)^{\lambda} \int_0^{\infty} x^{\lambda} (1 + x + x^3)^{\lambda} e^{-\lambda \theta x} dx \right)
 \end{aligned} \tag{13}$$

Using Binomial expansion in equation (13), we get

$$= \sum_{i=0}^{\beta} \binom{\beta}{i} \sum_{j=0}^i \binom{i}{j} x^{i-j+3j} \tag{14}$$

Substituting equation (12) in (13) we get,

$$\begin{aligned}
 S_{\lambda} &= \frac{1}{\lambda - 1} \left(1 - \left(\frac{\theta^5}{(\theta^3 + 2\theta^2 + 24)} \right)^{\lambda} \sum_{i=0}^{\lambda} \sum_{j=0}^i \binom{\lambda}{i} \binom{i}{j} \int_0^{\infty} x^{\lambda} x^{i+2j} e^{-\theta \lambda x} dx \right) \\
 S_{\lambda} &= \frac{1}{\lambda - 1} \left(1 - \left(\frac{\theta^5}{(\theta^3 + 2\theta^2 + 24)} \right)^{\lambda} \sum_{i=0}^{\lambda} \sum_{j=0}^i \binom{\lambda}{i} \binom{i}{j} \int_0^{\infty} x^{(\lambda + i + 2j + 1) - 1} e^{-\theta \lambda x} dx \right) \\
 S_{\lambda} &= \frac{1}{\lambda - 1} \left(1 - \left(\frac{\theta^5}{(\theta^3 + 2\theta^2 + 24)} \right)^{\lambda} \sum_{i=0}^{\lambda} \sum_{j=0}^i \binom{\lambda}{i} \binom{i}{j} \frac{\Gamma(\lambda + i + 2j + 1)}{(\theta \lambda)^{\lambda + i + 2j + 1}} \right) \\
 S_{\lambda} &= \frac{1}{\lambda - 1} \left(1 - \left(\frac{\theta^5}{(\theta^3 + 2\theta^2 + 24)} \right)^{\lambda} \sum_{i=0}^{\lambda} \sum_{j=0}^i \binom{\lambda}{i} \binom{i}{j} \left(\frac{1}{\theta \lambda} \right)^{\lambda + i + 2j + 1} \Gamma(\delta \lambda + i + 2j + 1) \right)
 \end{aligned}$$

ESTIMATIONS OF PARAMETER

In this section, the maximum likelihood estimates and Fisher's information matrix of the length biased Uma distribution parameter is given.



**Maximum Likelihood estimation (MLE) and Fisher's Information Matrix**

Consider $x_1, x_2, x_3, \dots, x_n$ be a random sample of size n from the length biased Uma distribution with parameter θ the likelihood function, which is defined as

$$L(x; \theta) = \prod_{i=1}^n f_i(x_i; \theta)$$

$$L(x; \theta) = \prod_{i=1}^n \frac{\theta^5}{(\theta^3 + 2\theta^2 + 24)} x_i (1 + x_i + x_i^3) e^{-\theta x_i}$$

$$L(x; \theta) = \left(\frac{\theta^5}{(\theta^3 + 2\theta^2 + 24)} \right)^n \prod_{i=1}^n x_i (1 + x_i + x_i^3) e^{-\theta x_i}$$

The log-likelihood function is given by

$$\log L = n(5) \log \theta - n \log[\theta^3 + 2\theta^2 + 24] + \sum_{i=1}^n \log(x_i (1 + x_i + x_i^3) e^{-\theta x_i})$$

$$\log L = n(5) \log \theta - n \log[\theta^3 + 2\theta^2 + 24] + \sum_{i=1}^n \log x_i + \sum_{i=1}^n \log(1 + x_i + x_i^3) - \theta \sum_{i=1}^n x_i \quad (15)$$

The maximum likelihood estimation of θ can be obtained by differentiating equation (15) with respect to θ

$$\frac{\partial \log L}{\partial \theta} = \frac{n5}{\theta} - n \left(\frac{\theta(3\theta + 4)}{(\theta^3 + 2\theta^2 + 24)} \right) - \sum_{i=1}^n x_i = 0 \quad (16)$$

The equation (13) gives the maximum likelihood estimation of the parameters for the length biased Uma distribution. However, the equation cannot be solved analytically, thus we solved numerically using R programming with data set.

To obtain confidence interval we use the asymptotic normality results. We have that if $\hat{\lambda} = (\hat{\theta})$ denotes the MLE of $\lambda = (\theta)$ we can state the results as follows:

$$\sqrt{n}(\hat{\lambda} - \lambda) \rightarrow N_2(0, I^{-1}(\lambda))$$

Where $I(\lambda)$ is Fisher's Information Matrix. i.e.,

$$I(\lambda) = -\frac{1}{n} \left(E \left(\frac{\partial^2 \log L}{\partial \theta^2} \right) \right)$$

Where

$$E \left(\frac{\partial^2 \log L}{\partial \theta^2} \right) = -\frac{n(5)}{\theta^2} + n \left(\frac{3\theta^4 + 8\theta^3 + 8\theta^2 - 144\theta - 96}{(\theta^3 + 2\theta^2 + 24)^2} \right)$$

Since λ being unknown, we estimate $I^{-1}(\lambda)$ by $I^{-1}(\hat{\lambda})$ and this can be used to obtain asymptotic confidence interval for θ .

APPLICATIONS

Dat set 1: This data consists of the life time (in years) of 40-blood cancer (leukemia) patients from one of ministry of health hospitals in Saudi Arabia reported in (25). This actual data is

0.315	0.496	0.616	1.145	1.208	1.263	1.414	2.025	2.036	2.162
2.211	2.370	2.532	2.693	2.805	2.910	2.912	3.192	3.263	3.348
3.427	3.499	3.534	3.767	3.751	3.858	3.986	4.049	4.244	4.323
4.381	4.392	4.397	4.647	4.753	4.929	4.973	5.074	5.381	

Data set 2: The data under consideration are the life times of 20 leukemia patients who were treated by a certain drug (20). The data are

1.013	1.034	1.109	1.226	1.509	1.533	1.563	1.716	1.929	1.965	2.061	2.344	2.546
-------	-------	-------	-------	-------	-------	-------	-------	-------	-------	-------	-------	-------





2.626	2.778	2.951	3.413	4.118	5.136
-------	-------	-------	-------	-------	-------

To compare to the goodness of fit of the fitted distribution, the following criteria: Akaike Information Criteria (AIC), Bayesian Information Criteria (BIC), Akaike Information Criteria Corrected (AICC) and $-2 \log L$.

AIC, BIC, AICC and $-2 \log L$ can be evaluated by using the formula as follows.

$$AIC = 2k - 2 \log L, \quad BIC = k \log n - 2 \log L \text{ and } AICC = AIC + \frac{2k(k+1)}{(n-k-1)}$$

Where, k = number of parameters, n sample size and $-2 \log L$ is the maximized value of loglikelihood function.

From table 1 and 2, it can be clearly observed and seen from the results that the length biased Uma distribution have the lesser AIC, BIC, AICC, $-2 \log L$, and values as compared to the Uma, Aradhana, Ishita, Akshaya, Shanker, Rama, Exponential, Lindley, Akash distributions, which indicates that the length biased Uma distribution better fits than the Uma, Aradhana, Ishita, Akshaya, Shanker, Rama, Exponential, Lindley, Akash distributions. Hence, it can be concluded that the length biased Uma distribution leads to a better fit over the other distributions.

CONCLUSIONS

Choosing a suitable model for fitting survival data has been a major concern among researchers. One of the most popular distributions for real-time data is the Uma distribution. In this paper, the Uma distribution is extended to provide a new distribution called the length biased Uma distribution to model life-time data. We propose the cdf and pdf of the length biased Uma distribution in Section 2. We have considered the mathematical and statistical properties of the derived distribution. From the graphs drawn from pdf and cdf-derived distributions. The hazard rate function, survival function, and their graphs for the new distribution are given in Section 3. The expressions for finding the mean and median are given in sections 5 and 6. The expression for its r^{th} moments of derived distribution is given in 4. We have also derived the entropy and the pdf of its r^{th} order statistics in 11 and 7. The use of statistical distributions in medical research is critical and can have a significant impact on the general public's health, particularly for cancer patients. thus, the applications of this distribution to certain real data sets that describe the survival of some cancer patients provide a demonstration of the utility of this distribution. The method of maximum likelihood estimation to estimate its parameters is discussed in Section 12. Moreover, the derived distribution is applied to two real data sets and compared with the other well-known distribution in Section 13. Results show that the length biased Uma distribution provides a better fit than other well-known distributions.

REFERENCES

1. Al-Saiary ZA, Bakoban RA. The Topp-Leono generalized inverted exponential distribution with real data application. *Entropy*.2020;22(10):1144.
2. Ahad, S. M., & Ahmad, S. P. (2018). Characterization and estimation of the length biased Nakagami distribution. *Pakistan Journal of Statistics and Operation Research*, 697-715.
3. Al-Omari, A. I., & Alsmairam, I. K. (2019). Length-biased Suja distribution and Its application. *Journal of Applied Probability and Statistics*, 14(3), 95-116.
4. Ahmad, A., Ahmad, S. P., & Ahmed, A. (2016). Length-biased weighted Lomax distribution: statistical properties and application. *Pakistan Journal of Statistics and Operation Research*, 245-255.
5. Ben Ghorbal, A. (2022). On Properties of Length-Biased Exponential Model. *Mathematical Problems in Engineering*, 2022.
6. Benchettah, M. H., Zeghdoudi, H., & Raman, V. (2023). On composite length-biased exponential-Pareto distribution: Properties, simulation, and application in actuarial science. *Frontiers in Applied Mathematics and Statistics*, 9, 1137036.
7. Bekker, A., Roux, J. J. J., & Mosteit, P. J. (2000). A generalization of the compound Rayleigh distribution: using a Bayesian method on cancer survival times. *Communications in Statistics-Theory and Methods*, 29(7), 1419-1433.





Sakthivel and Pandiyan

8. Blumenthal, S. (1967). Proportional sampling in life length studies. *Technometrics*, 9(2), 205-218.
9. Cox, D. (1969). Some sampling problems in technology», *New Developments in Survey Sampling* (NL Johnson et H. Smith, eds.).
10. Cnaan, A. (1985). Survival models with two phases and length biased sampling. *Communications in Statistics-Theory and Methods*, 14(4), 861-886.
11. David, H. A. (1970). Order Statistics, Wiley & Sons, New York.
12. Ekhsosuehi, N., Kenneth, G. E., & Kevin, U. K. (2020). The Weibull length biased exponential distribution: Statistical properties and applications. *Journal of Statistical and Econometric Methods*, 9(4), 15-30.
13. Fisher, R. A. (1934). The effect of methods of ascertainment upon the estimation of frequencies. *Annals of eugenics*, 6(1), 13-25.
14. Gupta, R. C., & Kirmani, S. N. U. A. (1990). The role of weighted distributions in stochastic modeling. *Communications in Statistics-Theory and methods*, 19(9), 3147-3162.
15. Gupta, R. C., & Keating, J. P. (1986). Relations for reliability measures under length biased sampling. *Scandinavian Journal of Statistics*, 49-56.
16. J. F Lawless, Statistical Models and methods for lifetime data, 2nd ed., vol. 362. New York, USA: John Wiley & Sons, 2003.
17. Klinjan, K., & Aryuyuen, S. (2021). The length-biased power Garima distribution and its application to model lifetime data. *Songklanakarin Journal of Science & Technology*, 43(3).
18. Kochar, S. C., & Gupta, R. P. (1987). Some results on weighted distributions for positive-valued random variables. *Probability in the Engineering and Informational Sciences*, 1(4), 417-423.
19. Kirmani, S. N. U. A., & Alam, S. N. (1974). On goodness of fit tests based on spacings. *Sankhyā: The Indian Journal of Statistics, Series A*, 197-203.
20. Mansour, M., Yousof, H. M., Shehata, W. A., & Ibrahim, M. (2020). A new two parameter Burr XII distribution: properties, copula, different estimation methods and modeling acute bone cancer data. *Journal of Nonlinear Science and Applications*, 13(5), 223-238.
21. Mahfoud, M. and Patil, GP (1982), On Weighted Distributions. *Statistics and Probability*, 479-492.
22. Mathew, J. (2023). Generalization Of Length Biased Weighted Generalized Uniform Distribution And Its Applications. *Reliability: Theory & Applications*, 18(2 (73)), 565-578.
23. Mustafa, A., & Khan, M. I. (2022). The length-biased power hazard rate distribution: Some properties and applications. *Statistics in Transition new series*, 23(2), 1-16.
24. Oluyede, B. O. (1999). On inequalities and selection of experiments for length biased distributions. *Probability in the Engineering and Informational Sciences*, 13(2), 169-185.
25. Patil, G.P. & Rao, C.R. (1977). Weighted distribution: A survey of their application. In P.R. Krishnaiah(ed.), *Applications of Statistics*. Amsterdam: North Holland Publishing Company, pp. 383-405.
26. Patil, G. P., & Rao, C. R. (1978). Weighted distributions and size-biased sampling with applications to wildlife populations and human families. *Biometrics*, 179-189.
27. Rényi, A. (1961). On measures of entropy and information. In *Proceedings of the Twelfth Berkeley Symposium on Mathematical Statistics and Probability, Volume 1: Contributions to the Theory of Statistics* Vol. 4, pp. 547-562. University of California Press.
28. R Core Team, R: A Language and Environment for Statistical Computing. R Foundation for Statistical Computing, Vienna, Austria, 2021.
29. Rao, C. R. (1965). On discrete distributions arising out of methods of ascertainment. *Sankhyā: The Indian Journal of Statistics, Series A*, 311-324.
30. Rather, A. A., & Subramanian, C. (2018). Length biased Sushila distribution. *Universal Review*, 7(XII), 1010-1023.
31. Rather, A. A., & Subramanian, C. (2019). The length-biased erlang-truncated exponential distribution with life time data. *Journal of information and Computational Science*, 9(8), 340-355.
32. Rather, A. A. (2023). Length Biased Weighted New Quasi Lindley Distribution: Statistical Properties and Applications. In *G Families of Probability Distributions* (pp. 288-301). CRC Press.
33. Schaeffer, R.L. (1972). Size-biased sampling. *Technometrics* 14: 635-644





Sakthivel and Pandiyan

34. Salama, M. M., El-Sherpieny, E. S. A., & Abd-elaziz, A. E. A. (2023). The Length-Biased Weighted Exponentiated Inverted Exponential Distribution: Properties and Estimation. *Computational Journal of Mathematical and Statistical Sciences*, 2(2), 181-196.
35. Tsallis, C. (1988). Possible generalization of Boltzmann-Gibbs statistics. *Journal of statistical physics*, 52, 479-487.
36. Rama Shanker (2022). Uma distribution properties and application. *Biometrics & Biostatistics International Journal*, vol 11, (5), 165-169.
37. Wang, Q. A. (2008). Probability distribution and entropy as a measure of uncertainty. *Journal of Physics A: Mathematical and Theoretical*, 41(6), 065004.

Table 1; MLEs AIC,BIC,AICC, and $-2\log L$ of the fitted distribution for the given data set 1

Distribution	ML Estimates	$-2\log L$	AIC	BIC	AICC
Length Biased Uma	$\hat{\theta} = 1.42222284(0.9686643)$	139.2556	141.2556	142.9192	141.3608
Weighted Uma	$\hat{\theta} = 1.4798000(0.2452669)$ $\hat{\delta} = 1.1654482(0.6472984)$	139.1868	143.1868	146.514	143.5111
Uma	$\hat{\theta} = 1.05464889(0.07842196)$	144.4455	146.4455	148.109	146.5507
Aradhana	$\hat{\theta} = 0.75060122(0.07108124)$	149.4283	151.4283	153.0918	151.5335
Ishita	$\hat{\theta} = 0.80668240(0.06521656)$	147.9967	149.9967	151.6603	150.1019
Akshaya	$\hat{\theta} = 0.98152890(0.07981806)$	144.7945	146.7945	148.458	146.8997
Shanker	$\hat{\theta} = 0.54972161(0.05806214)$	144.7945	155.9545	157.6181	156.0597
Rama	$\hat{\theta} = 1.10146523(0.08055189)$	143.3158	145.3158	147.1023	145.4210
Exponential	$\hat{\theta} = 0.31893857(0.05107054)$	167.1353	169.1353	170.7988	169.0405
Lindley	$\hat{\theta} = 0.2577071(0.06161721)$	156.5028	158.5028	160.1664	158.6080
Akash	$\hat{\theta} = 0.80168363(0.07120997)$	149.0561	151.0561	152.7196	151.1613

Table 2; MLEs AIC,BIC,AICC, and $-2\log L$ of the fitted distribution for the given data set 2

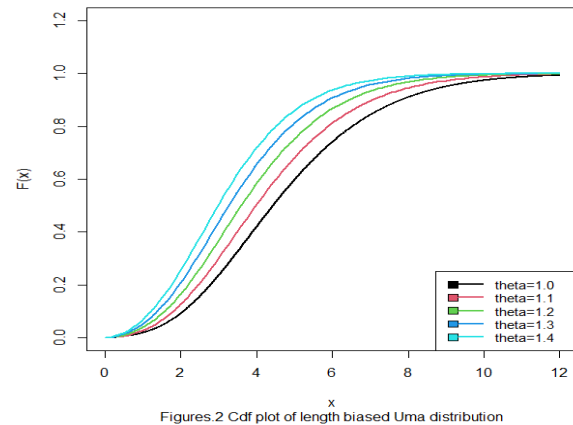
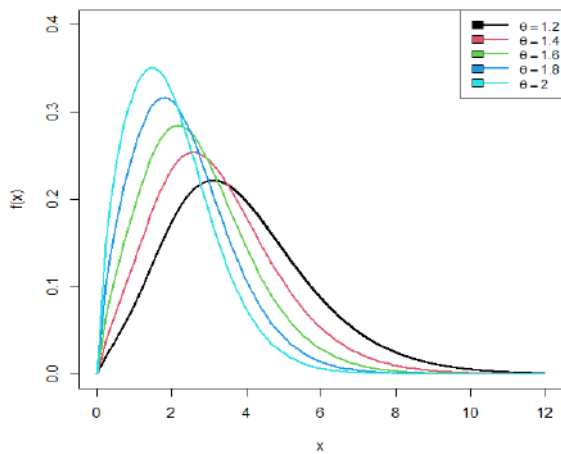
Distribution	ML Estimates	$-2\log L$	AIC	BIC	AICC
Length Biased Uma	$\hat{\theta} = 1.8420800(0.1783061)$	52.09955	56.09955	57.98843	56.8054
Weighted Uma	$\hat{\theta} = 2.8413084(0.7386713)$ $\hat{\delta} = 3.1011464(1.5087565)$	55.1066	57.1066	58.05104	57.3418
Uma	$\hat{\theta} = 1.3223930(0.1406723)$	61.67133	63.67133	64.61577	63.8935
Aradhana	$\hat{\theta} = 0.985545(0.135948)$	60.60053	62.60053	63.54497	62.82275
Ishita	$\hat{\theta} = 0.9975990(0.1134076)$	62.74297	64.74297	65.68741	64.9651
Akshaya	$\hat{\theta} = 1.2738546(0.1506672)$	58.05546	60.05546	60.9999	60.2776
Shanker	$\hat{\theta} = 0.7124395(0.10777871)$	63.08856	65.08856	66.033	65.3107



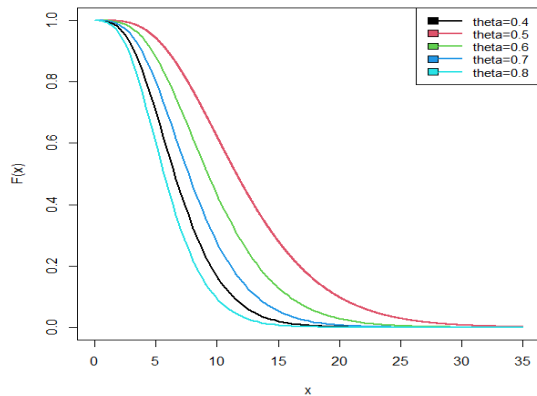


Sakthivel and Pandiyan

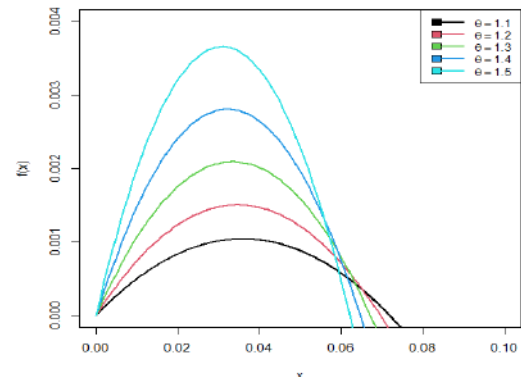
Rama	$\hat{\theta} = 1.3784229(0.1415338)$	62.41991	64.41991	65.36435	64.6421
Exponential	$\hat{\theta} = 0.4463246(0.1023934)$	68.65501	70.65501	71.59945	70.8772
Lindley	$\hat{\theta} = 0.7076860(0.1200725)$	64.02158	66.02158	66.96602	66.2438
Akash	$\hat{\theta} = 0.0297001(0.1317933)$	62.69158	64.69158	65.63602	64.9138



Figures.2 Cdf plot of length biased Uma distribution



Figures.3 survival function of length biased Uma distribution



Figures.4 Hazard function of length biased Uma distribution





Phytosomes as Novel Drug Delivery System for Herbal Extract and Phytoconstituents

Pratiksha S. Waghmare^{1*}, Rutuja Titkare¹ and T.A. Sande²

¹M.Pharm, Department of Pharmaceutics, PES Modern College of Pharmacy, Moshi (for Ladies), (Affiliated to Savitribai Phule Pune University), Pune, Maharashtra, India.

²Assistant Professor, Department of Pharmaceutics, PES Modern College of Pharmacy, Moshi (for Ladies), (Affiliated to Savitribai Phule Pune University), Pune, Maharashtra, India.

Received: 22 Jan 2024

Revised: 09 Feb 2024

Accepted: 15 May 2024

*Address for Correspondence

Pratiksha S. Waghmare

M.Pharm,

Department of Pharmaceutics,

PES Modern College of Pharmacy, Moshi (for Ladies),

(Affiliated to Savitribai Phule Pune University),

Pune, Maharashtra, India.

Email: Pratiksha.waghmare2904@gmail.com



This is an Open Access Journal / article distributed under the terms of the **Creative Commons Attribution License** (CC BY-NC-ND 3.0) which permits unrestricted use, distribution, and reproduction in any medium, provided the original work is properly cited. All rights reserved.

ABSTRACT

Plant-based medications have been used traditionally for a very long time.[3]In the kingdom of plants, there are between 300,000 and 400,000 higher species. Only 5-15% of this plant variety has been reported to have pharmacological effects, and approximately 150-200 species are commonly used in western medicine, with plants accounting for one-fourth of all prescribed medicines globally.[4] Furthermore, the crystalline nature of some phytochemicals can make dissolution difficult, limiting absorption and bioavailability. These challenges necessitate the development of novel strategies to increase the bioavailability of phyto-constituents in order to maximize their therapeutic benefits

Keywords: The term “phyto” means plant and “some” means cell-like. Compared to traditional herbal extracts, phytosomes are more efficiently absorbed, utilized, and yield superior results.

INTRODUCTION

Phytosomes are novel drug delivery system used for herbal extract or phytoconstituents. Phytosomes are delivery systems that are structurally related to liposomes But differ from Nano liposomes based on an appropriate stoichiometric ratio that active compounds are chemically bound to the carrier structure, for example through H bonds which enhances the storage and digestive stability of the system.[1,2]Throughout history, natural products was discovered and used for both the treatment and prevention of various diseases. Examples of these products





Pratiksha S. Waghmare et al.,

include the Indian Ayurveda, Egyptian "Ebers Papyrus," Chinese Material Medicine, , and many more. The use of herbal medicine has been recorded for more than 5,000 years. Plant-based medications have been used traditionally for a very long time.[3]In the kingdom of plants, there are between 300,000 and 400,000 higher species. Only 5-15% of this plant variety has been reported to have pharmacological effects, and approximately 150-200 species are commonly used in western medicine, with plants accounting for one-fourth of all prescribed medicines globally.[4] Herbal medicines are gaining popularity due to their capability to treat a wide range of diseases with fewer adverse reactions and higher therapeutic value. As new analysis methods evolved into readily accessible in the early 19th century, scientists developed the ability to extract, identify, and adapt the active ingredients from natural products (plants, algae, fungi, and microorganisms), resulting in the transition of raw materials to synthetic pharmaceuticals.[5]Herbal medicine indicates some challenges. Poor aqueous solubility, low permeability across biological barriers, rapid metabolism, and substantial first-pass metabolism in the liver and gastrointestinal tract were the main obstacles. Furthermore, the crystalline nature of some phytochemicals can make dissolution difficult, limiting absorption and bioavailability. These challenges necessitate the development of novel strategies to increase the bioavailability of phyto-constituents in order to maximize their therapeutic benefits.[6]To overcome the challenges listed above, we can convert herbal medications into novel drug delivery systems such as Phytosomes. The Phytosome technology, developed by the Italian company Indena S.P.A., significantly improves the bioavailability of selected phyto-medicines through the incorporation of phospholipids that into standardized extracts and thus significantly improving absorption and utilization.[7] Phytosomes are a composition of naturally occurring active ingredients and phospholipid that can be applied topically or orally. They increase the absorption of plant extracts or extracted active compounds. The term "phyto" means plant and "some" means cell-like. Compared to traditional herbal extracts, phytosomes are more efficiently absorbed, utilized, and yield superior results. They are cell-like structures created by the stoichiometric reaction between phospholipids and standardized compounds or polyphenolic compounds in a non-polar solvent. Because of scientific breakthroughs, the phytosomes are now widely used in pharmaceuticals, cosmeceutical, and nutraceutical sectors to prepare a wide range of formulations, including emulsions, solutions, gels, lotions, and creams.[8]

PHYTOSOMES AS NOVEL VESICULAR DRUG DELIVERY SYSTEM

Novel vesicular drug delivery systems aim to deliver the drug at a rate determined by the body's need during the treatment period, while also directing the active entity to the site of action. To achieve targeted and controlled delivery of drugs, a number of novel vesicular drug delivery methods with various routes of administration were developed.[9] Targeted drug delivery is an approach of transporting the therapeutic agent to the tissues of interest while decreasing the relative concentration of therapeutic agent in remaining tissues which enhances the efficacy of treatment and minimizes the side effects. Drug targeting refers to the transporting drugs to receptors, organs, or any other particular region of the body to which the entire drug is to be delivered.[10] Some example of vesicular drug delivery system for herbal drugs: Aquasomes, Cryptosomes, Discosomes, Emulosomes, Enzymosomes, Ethosomes, Erythrosomes, Genosomes, Homosomes, Phytosomes, Protosomes, Ufsomes, Virosomes.[11]

BACKGROUND ON PHOSPHOLIPID COMPLEX TECHNOLOGY

Phytosomes are typically created by combining active biological plant-based compounds with phospholipids, such as PC, PS, and PE, at particular stoichiometric ratios under controlled conditions. Soon after mixing, aprotic solvents such as ethyl acetate, methylene chloride, dioxane, and acetone are evaporated below a constant a vacuum condition to completely isolate the complex, implying that the phytoconstituents will be incorporated into the phytosomes lipids vesicles.[12] Phosphatidylcholine is a bi-functional substance with a lipophilic phosphatidyl moiety and a hydrophilic choline moiety. The phosphatidylcholine molecules choline head is specifically attached these particular compounds, while the lipid soluble phosphatidyl part, which consists of the body and tail, eventually envelopes the choline, bound material. As a result, the phytoconstituents form a lipid consistent molecular complex with phospholipids, known as the phyto-phospholipid complex.[13]A small microsphere develops. Because of the gastroprotective characteristic of phosphatidylcholine, the phytosome technology creates a small cell that protects the plant extract or its active constituent from degradation by gastric secretions and gut bacteria.[14]



Pratiksha S. Waghmare *et al.*,

THE COMPOSITION OF PHYTOSOMES

By docking the active polar component to a phospholipid, which is an essential component of the membrane, molecules can be stabilized through hydrogen bonding. Phosphatidylcholine, which is utilized in phytosomes, has a micelle structure similar to that of a cell membrane. Components of Formulation: Plant-derived active substances can interact with phospholipids to produce phyto-phospholipid complexes. Phospholipids, phyto-active compounds, solvents, and consequently the ratio quantitative relationship involved in the formulation of phytosomes all that is required for the production of phytosomes.[15,16]



Phospholipids

Plant seeds and egg yolks are the two most common natural sources of phospholipid. Commercial phospholipids are those made in an industrial setting. Based on the structure of their backbone, phospholipids are categorized as either sphingomyelins or glycerophospholipids.[17] Phospholipids such as phosphatidylcholine, phosphatidylethanolamine, phosphatidylserine, phosphatidic acid, phosphatidylinositol, and phosphatidylglycerol are the main phospholipids used for producing complexes with a hydrophilic head group and two hydrophobic hydrocarbon chains. Phosphatidyl choline is the phospholipid that is usually used in the creation of phospholipid complexes. Because of its amphipathic characteristics, phosphatidyl choline has a moderate solubility in lipid and aqueous conditions, which is one of its benefits.[18] Moreover, phosphatidyl choline has a low-toxic and an elevated biocompatibility due to their essential function in cell membranes. Phosphatidyl choline molecules have been shown to have hepatoprotective properties and to produce positive clinical outcomes when used to treat liver diseases like hepatitis, fatty liver, and hepatocirrhosis. Phospholipids are utilized as a vehicle-creating component in the production of phytosomes.[19]

Photoactive components

Researchers typically choose phyto-active constituents not so much for their *in vivo* activities as for their notable *in vitro* pharmacological effects. Most of these compounds are flavonoids. Water-based flavonoids, such as quercetin, catechin, and silibinin, are found in plants and prefer the aqueous phase where they cannot pass through biological membranes. As lipophilic flavonoids, rutin and curcumin cannot dissolve in aqueous gastrointestinal fluids. Phytosome complexes improve the water solubility of hydrophilic flavonoids and the membrane penetrability of lipophilic flavonoids in the aqueous phase. Furthermore, by assembling into complexes, flavonoids can be shielded from outside influences like hydrolysis, photolysis, and oxidation.[20]

Solvents

Several researchers have used a variety of solvents as a catalyst to form phytosome complexes. Protic solutions such as ethanol have largely replaced the aromatic hydrocarbons, halogen derivatives, methylene chloride, ethyl acetate, and cyclic ethers that were previously used to create phytophospholipid complexes. In fact, phospholipid complexes have been successfully formed recently using protic solvents like ethanol and methanol. Phospholipids and polyphenols can rationally interact with these solvents. Numerous varieties of solvents have been effectively investigated. Due to its low damage and reduced residue, ethanol is a popular and useful solvent. When the phytosomes interact with a solvent having a lower dielectric constant like water or a buffer solution some liposomal drug combinations become effective. The supercritical fluid (SCF) method is currently employed to regulate the material of interest's morphology, size, and shape. One of the SCF technologies, the supercritical antisolvent





Pratiksha S. Waghmare *et al.*,

technique (SAS), is becoming more and more popular as a viable way to produce micronic and submicronic particles with regulated sizes and size distributions. To lessen the solute's solubility in the solvent, an anti-solvent (often CO₂) is used at supercritical temperatures.[21]

SELECTION OF HERBAL PLANT

The idea of preparing medicinal plants for experimentation or to prepare the extract requires timely and appropriate plant collection, expert validation, sufficient drying, and grinding. When appropriate, the bioactive compound is then extracted, fractionated, and isolated. It also includes figuring out how much and what kind of bioactive compounds are present.[24] Herbal plant have pharmacological properties and therapeutic activities such as antioxidants, astringent, anti-irritant, antimicrobial, hepato- and photo-protective qualities, as well as moisturizing and anti-aging effects. Because of these characteristics, they enhance the body's pharmacological and pharmacokinetic profiles and have a healing, softening, rejuvenating, and sunscreen effect on the skin.[25] One can choose herbal plant based on their nature, availability, estimation technique, stability, and efficiency of produced formulation should according to previous studies, after thoroughly reviewing the literature on herbs and correlating the activity of herbal compounds depending on chemical categories such as flavonoids, monoterpenes, polyphenols, indols, and organosulfides.[26]

TECHNIQUES FOR MAKING PHYTOSOMES

The structures of phytosomes, which are made of soybean lecithin and standardized extracts that contain phytochemicals or polyphenolic compounds, are strikingly similar to those of human cells. Extracts or particular active ingredients are typically complexed in dietary phospholipids using solvent evaporation/anti-solvent precipitation methods with alcoholic or organic solvents; however, super critical fluids have also been employed recently.[27]

Commonly used method

1. Solvent Evaporation Technique:
2. Anti-solvent preparation method:
3. Rotary evaporation technique
4. Either injection method :

Solvent evaporation method

The phytosome can be developed employing the solvent evaporation method. Phospholipid is dissolved in organic solvent, such as methanol, ethanol, chloroform, using continuous stirring at. The phospholipid solution is mixed with the active phytoconstituent after it has been dissolved in polar or non-polar solvent. After two hours of stirring, the clear mixture is evaporated under vacuum and left there for a whole night. The remaining material, a powder, and sealed are gathered together. The resulting powder is collected as a phytophospholipid complex or phytosomes.[28]

Anti-solvent precipitation technique(salting out method)

Particular amount of extracts of plants and phospholipid dissolved in dichloromethane in round bottom flask. The mixture is then refluxed for two hours at a temperature not to exceed 60°C. The mixture condenses to Hexane is carefully added and stirred continuously, and the precipitate should filter, collect, and kept in desiccators for the entire night. In a mortar and pestle, crushed dry Precipitate and sieved into meshes. The powdered complex should be stored in an amber-colored container made from glass at room temperature during storage.[29]

Rotary evaporation technique

In a rotary circular bottom flask, the specific volume of plant material and phospholipid were dissolved in solvent, then stirred continuously and reflux for 3 hours at a temperature not exceeding 40-60°C. Then placed in rotary evaporator A thin film of the sample was collected, to which n-hexane was applied and a magnetic stirrer was used to





Pratiksha S. Waghmare *et al.*,

constantly stir the mixture. The precipitate was extracted and deposited at room temperature in an amber-colored glass bottle.[30]

The ether-injection technique

this method combines the aqueous phase of extracted herbs with lipids dissolved into an organic solvent. Diethyl ether-soluble phospholipids are gradually added, drop by drop, to an aqueous solution containing the phytoconstituents that are encapsulated. When the solvent is subsequently removed, it causes the development of cellular vesicles, which results in complex formation. Concentration affects Phytosome structure; at lower concentrations, amphiphiles in the mono state are formed; at higher concentrations, however, a range of structures with various May forms, such as spherical, cylindrical, disc, cubic, or hexagonal vesicles, etc.[31]

NOVEL METHODS

Conventional techniques have a number of drawbacks, such as time consuming, multistep procedures, and challenging the extraction process. Materials of interest can have their structure, dimensions, and shape can altered using supercritical fluid techniques. High product purity, control over crystal polymorphism, the ability to handle thermolabile materials, a single-step method, and sustainable technology are additional advantages. While the rapid growth of supercritical solutions (RESS) utilizes a supercritical fluid (usually CO₂) as a solvent, methods is use as anti-solvent to limit the ability of the solute to dissolve in the solvent. [32]

1. **Gas anti-solvents technique (GAS),**
2. **Supercritical antisolvent technique (SAS),**
3. **Solution enhanced dispersion by supercritical fluids (SEDS)**

Gas anti-solvents technique (GAS)

In this method where an organic solvent is first used to partially dissolve a solid sample in a vessel. After that, the solution is pressurized with a dense gas or supercritical fluid, which causes the solid to precipitate as a fine granule. It is not necessary for the CO₂ gas used as an anti-solvent to be supercritical. To accomplish uniform mixing, it is injected into the solution within an enclosed chamber, preferably at the bottom. Solutes precipitate because the dissolution of CO₂ gas limits the solubilisation efficacy of organic solvents. In order to get rid of any remaining solvent, the particles are rinsed with more anti-solvent. In this event that occurs, the solutes may solubilize and compromise the stability of the product throughout the compression stage. When compared with the solvent anti-solvent technique, the gas anti-solvent technique provides superior outcomes when scaled up to industrial levels. [33]

Supercritical anti-solvent precipitation (SAS)

In this method Sub micrometre-sized particles with a narrow size distribution are produced when the pressure in the SAS is decreased, and eliminating of the solvent from the gas phase. The supercritical condition of CO₂ is a requirement. Both the solution and the CO₂ are pumped from above into an enclosed chamber. Compared to GAS, this strategy has been shown to be effective on a large scale.[34]

Solution enhanced dispersion by supercritical fluids (SEDS)

Researchers have been far more interested in supercritical fluid (SCF) technology in recent years than in conventional pharmaceutical manufacturing techniques because of SCFs' favorable environmental effects and promising economic prospects. The solution-enhanced dispersion by supercritical fluids (SEDS) process is one of the most effective ways to create pharmaceutical drug and products and biomaterials at any measure, from micro- to nanoscale levels, out of all the SCF-assisted generation of particles techniques. The resulting small sized molecules from the SEDS process have improved physical characteristics, such as increased bioavailability because of their large surface area.[35]





Pratiksha S. Waghmare *et al.*,

PHYTOSOMES CONTAINING DOSAGE FORMS

While topical and oral administration of phytosome preparations are viable, it is crucial to investigate the dosage forms' disintegration and dissolving times in order to optimise the bioavailability of the formulation. Here are a few dosage forms for phytosomes.[36]

Hard gelatin capsules

There are hard gelatin capsules containing the Phytosome complex available; however, the amount of powder that may be filled is limited by the capsules' low density. Direct volumetric filling without precompression is an option, and piston tamp capsule loading allows for a higher powder content. Pre-compression could speed up the disintegration process. To achieve effective product development, Indena suggests closely monitoring parameters and developing the ideal production process with an initial dry granulation procedure.[37]

Soft gelatin capsules

Using vegetable or semi-synthetic oils, the Phytosome complex may be utilized in oily vehicles to produce suspensions for soft gelatin capsules. For best results, some researchers advise employing a granulometry of 100% <200 µm. However, not all Phytosome complexes function in the same way when placed in soft gelatin capsules and distributed in oily media, therefore initial feasibility studies are required to ascertain the most effective technique.[37]

Tablets

Dry granulation is the most effective approach for manufacturing tablets with higher unitary dosages and adequate technical and biological properties. Direct compression is appropriate for low uniform dosages because to the Phytosome complex's restricted flow capacity, possible adhesion, and low visual density. To optimize mechanical qualities, dilute the Phytosome complex in 60-70% excipients. Wet granulation should be avoided since water and heat have a negative impact on the phospholipid complex's stability.[37]

Topical dosage form

The Phytosome complex can be used topically by distributing it in a tiny quantity of lipid stage and incorporating it into an emulsion at low temperatures. Topical treatments contain primary lipid solvents that can dissolve these complexes. The complex can alternatively be disseminated in the liquid phase and added to the final formulation at a lower temperature alongside a tiny amount of lipids.[37]

PHYTOSOMES ARE SUPERIOR THAN HERBAL EXTRACTS

The use of phytosomal technology as a therapeutic carrier dates back to 1989. The increased reliability and significance of herbal extracts in bio evaluation and in-vitro studies can be explained by their many phytosomal benefits. Their metabolism is more effective to that of traditional herbal extracts from the past.[17, 38]

Phytosomal technology developments offer several benefits, including:

Increased bioavailability

For improved absorption, the hydrophilic herbal extract can pass through the intestinal lumen due to the phytophospholipid complex. When in phospholipids complex with their lipophilic heads, the bioavailability of secondary metabolites is significantly increased.[39]

Minimal risk profile

According to published data, the toxicological effects are minimal, and the small-scale manufacturing.

High entrapment effectiveness

the biological marker its produces forms nano cellular vesicles around bonding with soya lipids, and drug distribution can be specified. Additionally, there is no production of toxic metabolites. [40]





Pratiksha S. Waghmare *et al.*,

Drug delivery through the transdermal rout

Herbal phytosomes can also be used in transdermal drug delivery to enhance the drug's diffusion through the skin because they serve as a precursor for the delivery of a wide variety of drugs, including peptides and protein.[41]

Safety and synergy

Phosphatidylcholine, which is utilized in complexation and is a crucial component of the cell membrane, is one of the approved additives used in the phytosome formulation, guaranteeing its safety and security. Since phosphatidylcholine has hepatoprotective properties of its own, a synergistic effect has been seen when complexing with hepatoprotective medications. In stressful environmental conditions, the synergistic benefits of protecting the skin from endogenous or exogenous toxins are clearly visible. Because of the improved absorption of the active ingredient, the phytosome concept ensures a longer duration of action at low dose with a low risk profile.[42]

Biodegradable

The phosphatidylcholine used in the formulation of phytosomes functions as a vehicle and is an essential component of the cell membrane, ensuring that drug frame-up is not obstructed during formulation manufacturing. [43]

Economic efficacy

With this technology, phytoconstituents can be delivered affordably. The cellular vesicular system is obedient and available for additional immediate development. It is relatively simple to produce because making phytosomes doesn't require a sophisticated technological investment or sophisticated practical speculation. [44]

PRE-FORMULATION STUDIES

Phytochemical Analysis

For plant extracts, an extensive phytochemical analysis should be performing Alkaloids, glycosides, terpenoids, phenolics, lignans, steroids, aliphatic compounds, polysaccharides, essential oils, and fatty acids were subjected to chemical testing.[45]

Organoleptic Properties

Color, odor, and appearance are among the organoleptic characteristics that are examined in the plant drug sample.[46]

Boiling Point

Applying a melting point apparatus, a capillary method is used to determine the melting point of plant extract. [46]

The solubility of plant extract

Plant extract saturation solubility in basic and acidic pH values is determined.[47]

Transition temperature

Differential scanning calorimetry (DSC) is used to ascertain the transition temperature of the vesicular lipid system.[47]

The phyto component of phytosomes standard calibration curve:

Accurately measured phytosomes were transferred individually into four separate volumetric flasks and dissolved in different organic solvents. The volume was then adjusted to the desired level. The stock solution should be in concentration. A UV-visible spectrophotometer is used to measure the solution absorbance at a specific wavelength. A calibration curve is produced by projecting the graph of absorbance versus concentration.[47]





Pratiksha S. Waghmare et al.,

EVALUATION TEST FOR PHYTOSOMES**Physical compatibility test**

The solubility and physical compatibility studies serve as the primary foundation for the selection of medications and phospholipids used to prepare phytosomes. Pre-formulation studies were conducted to evaluate drug-phospholipid compatibility and interactions using potential formulation phospholipids or polymers.[48]

Differential Scanning Calorimetry Studies

Thermogram of plant extract or phytoconstituent is obtained using Differential scanning calorimeter using aluminum pans. The dry samples of drugs were separately weighed, fixed in aluminum pans hermetically and warmed at an examining rate between 30°C to 300°C. The ideal environment was provided by cleansing nitrogen stream at the rate as required. [49]

FT-IR Spectroscopy

FT-IR range of the drugs using the FT-IR Spectrophotometer by the KBr pellet method. The active component is separately blended with IR grade KBr in the proportion of ratio and the active is also mixed with excipients to check compatibility. Each blend is compacted in the form of a pellet by applying 10 tons of pressure in a hydraulic press. The pellets were scanned over a wavenumber range of in the Fourier Transform Infrared instrument and spectral analysis was done. Software used for the data analysis.[50]

Solubility Determination

Plant extract saturation solubility is evaluated in acidic, phosphate buffers and organic solvents. The amount of drug measurement is added separately of each media in screw-capped tubes. In order to facilitate the solubilisation, a vortex mixture was employed. After a 48-hour period, of aliquots was extracted from every sample using Whatman filter paper utilizing a UV Visible Spectrophotometer and absorbance is determined.[51]

Partition coefficient

The oil and aqueous phases are required to calculate the partition coefficient. Water is used in the aqueous phase and N-octanol in the oil phase. Exactly measured solvent and water were added to the separating funnel, and the mixture was shaken constantly for two hours until equilibrium was reached. And drug was added. The assembly is then allowed to remain in place for the entire night. For a 24-hour period, the oil and water phases were separated, and the drug content of each was determined by measuring the absorbance at a specific wavelength in a UV spectrophotometer.[51]

Determination of %

Yield Assurance of % yield of phytosomes of curcumin was calculated by the accompanying equation

$$(\%) \text{ Yield} = \frac{\text{Practical yield}}{\text{Theoretical yield}} \times 100$$

Theoretical yield[51]

X-ray diffraction (XRD)

XRD analysis can be used to study the structure of crystalline materials, including atomic arrangement, crystalline size, and flaws. Results obtained with an X-Ray diffractometer using graphite monochromatic at a count rate. At the moment, X-ray diffraction is a helpful method for examining the microstructure of both crystalline and some amorphous materials. X-ray diffraction is typically performed on the active components or ingredients of phytophospholipid complexes, PCs, and their physical mixes.[36]

Vesicle size and Zeta potential

Using a computerized evaluation system and photon correlation spectroscopy (PCS), dynamic light scattering (DLS) can be used to measure the particle size and zeta potential. The stability of colloidal dispersions is influenced by the strength of electrostatic repulsion between similarly charged particles, which is indicated by the magnitude of zeta



Pratiksha S. Waghmare *et al.*,

potential. The SPC phosphate group is present in a pH-neutral water environment, phytosomes are negatively charged. High absolute ZP values have been proposed as a partial indicator of physical stability to ensure the formation of a high energy barrier against globule rupture.[52]

H-NMR

The ¹H-NMR signal from the atoms present in the complex's formation changes significantly in nonpolar solvents, and the signals unique to each individual a compound are not summated. It is necessary to broaden the signals coming from the flavonoid protons to indicate that the proton cannot be relieved. Within phospholipids, all the signals broaden, and the singlet that corresponds to choline's N-(CH₃)₃ shifts upward. New broad bands appear when the sample is heated to 60°; these bands mostly match to the flavonoid moiety's resonance.[53]

C-NMR

All of the flavonoid carbons are readily apparent in the ¹³C-NMR spectra of (+)-catechin and its stoichiometric complex with distearoylphosphatidylcholine, especially when recorded in C₆D₆ at room temperature. While most of the resonances of the chain of fatty acids maintain their initial sharp line form, the signals corresponding to the glycerol and choline portion of the lipid are broadened and some are shifted. All of the signals associated with the flavonoid moieties reappear upon heating. They are still very broad and partially overlap.[54]

Entrapment efficiency

Using the ultra-centrifugation technique, the drug entrapment efficiency is determined by weighing a specific amount of phyto-phospholipid complex equal to the amount of herbal drug encapsulated and adding it to phosphate buffer. The mixture is then stirred for a specified time period on the magnetic stirrer and allowed to stand. The transparent solution is then removed and centrifuged. The supernatant is then filtered through Whatman filter paper, and absorbance is then determined by utilizing UV or HPLC. [55]

The drug entrapment % is calculated by using the following formula

$$\text{Entrapment Efficiency \%} = \frac{\text{Weight of extract in complex}}{\text{Weight of total extract taken}} \times 100$$

$$\text{Drug loading (\%)} = \frac{\text{Weight of the entrapped drug}}{\text{Weight of the Formulation}} \times 100$$

In vitro and in vivo evaluation models

The biologically active phytoconstituents in the phytosomes are expected to have therapeutic action, which determines the model for in vitro and in vivo evaluations. For example, the antioxidant and free radical scavenging capabilities of the phytosomes can be used to evaluate the in-vitro antihepatotoxic activity. The effect of prepared phytosomes on animals against hepatotoxicity can be investigated for evaluating antihepatotoxic activity in vivo. The in vivo safety evaluation methodology is described by skin sensitization and tolerability studies of Phytosome.[56]

ADVANTAGES OF PHYTOSOMES

Phytosomes provide the following benefits.

1. The drug's entrapment efficiency is immense and specified due to the conjugation with phospholipids resulting in vesicles. [57][25]
2. The highest absorption of small components has resulted in a reduction of the dose requirement. [58]
3. Using phytosomes to deliver the herbal medication need not compromise nutritional safety of the extract of herbs.[59]





Pratiksha S. Waghmare et al.,

4. The drug has been proven to be delivered correctly to the appropriate tissues.
5. In phytosome formulation significantly increase in the drug bioavailability takes place. [60]
6. When creating phytosomes, there are no issues with drug entrapment. Phosphatidylcholine molecules and the herbal phytoconstituents form new chemical bonds in phytosomes, which results in a good stability profile. [61]
7. Phytosomes show a noticeably higher clinical benefit. [62]
8. In addition to serving as a carrier and skin-nourishing agent or in topical preparation phosphatidylcholine is utilized in the formulation of phytosomes. [63]

DISADVANTAGE OF PHYTOSOMES

1. A phytosome may quickly eliminate the phytoconstituent in terms of all benefits. [58]
2. The main restriction on phytosomes is to be the phytoconstituent leaching off some, which decreased the predicted concentration of the drug.[59]

PROBLEMS IN PRODUCTION OF PHYTOSOME AS DRUG PRODUCTS:[72]-[74]

Although phytosome production has many benefits, there are certain drawbacks as well. Due to inadequate natural product regulations in India, plant-derived products may be sometimes of low quality or ineffective. Consequently, trade is down, and prescriptions are not given as commonly.

1. Low yield of the plant material used, among other obstacles
2. If the extract contains any cytotoxic ingredients,
3. restricted sample bioavailability,
4. Defects in the botanical classification and application of herbal plants.
5. The degree to which plant extracts dissolve in water and other solvents
6. Using over-the-counter medications,
7. Using plants that trigger allergic reactions because they contain volatile components or pollen.
8. Using conventional medicines without permission.

CURRENT DEVELOPMENTS IN PHYTOSOME

- Sonam Sharma et al. Development, Characterization, and Evaluation of Hepatoprotective Effect of *Abutilon indicum* and *Piper longum* Phytosomes. Using a proprietary method developed by Indena, phytosomes emerged. The following factors were used in the characterization process: high performance thin liquid chromatography, differential scanning calorimetry, scanning electron microscopy, percentage yield, entrapment efficiency, and particle size determination. The combined extract has demonstrated hepatoprotective activity; however, the phytosomal preparation, when used at a lower dose than the combined extract, has a stronger hepatoprotective effect on CCl₄-induced liver damage in rat. [75]
- Sawant Rutuja et al. formed the phytosomal antifungal gel composition of *Azadirachta indica*, or neem. The neem phytosomal gel formulation was created with the goals of enhancing patient compliance, reducing doses for therapy, and getting away with the adverse effects of first pass metabolism. Due to their large macromolecules and poor lipid solubility, several herbal plants extract exhibit strong in-vitro activity but low absorption and permeation through the skin. Thin film hydration method was used to produce the phytosome. Particle size, entrapment effectiveness, drug content, zeta potential SEM, and FTIR were used to characterize the phytosome. Additionally, the optimized phytosome complex was prepared as gels using different polymers at different concentrations, and the Franz diffusion cell was used to evaluate the phytosome complex's homogeneity, pH, drug content, and in vitro and ex vivo permeation.[76]
- Anju Singh et al. Development And Evaluation Of Anti-Diabetic Activity Of Phytosomes For Better Therapeutic Effect Of Extract. By using extracts of *Swertia chirayita* and *Zizyphus mauritiana*. Hyperglycemia, a common metabolic abnormality linked to diabetes, is caused by insufficient insulin synthesis or errors in insulin action. The extracts of *Swertia chirayita* and *Zizyphus mauritiana*, two prominent medicinal plants, have been used for type 2 diabetes. A study confirmed the glucose tolerance



**Pratiksha S. Waghmare et al.,**

activity of phytosomes containing these extracts, which controlled blood glucose levels and showed sustained release activity best, fitted with the Korsmeyer model. In vivo glucose test tolerance tests showed that phytosomes prevented blood glucose level increases after 60 minutes. However, they did not show better anti-diabetic activity in streptozotocin-induced models.[77]

- Andi Dian Permana et al. work on Propolis phytosomal nanocarriers have been delivered using *Apis mellifera*, a plant recognized for its antioxidant and photoprotective qualities. It has been discovered that these nanocarriers improve skin retention and dissolution behavior in biorelevant media. Using ethanol for propolis extraction, phytosomes are made using phospholipid L- α -Phosphatidylcholine, and Fourier transform infrared (FTIR) spectroscopy. As indicated by the SPF values, the phytosomes have been found to improve the propolis compounds' dissolution, penetrability, and skin retention. They may also have the ability to absorb UVA and UVB radiation. Propolis delivery methods that show promise for treating organ damage, oxidative stress, and skin aging are present in this work.[78]
- Nabil A. Alhakamy et al. Quercetin phytosomes functionalized with scorpion venom for the treatment of breast cancer maximizing the response surface in vitro and anticancer activity against MCF-7 cells. Reflux and anti-solvent precipitation were used to prepare QRT-PHM-SV formulations, following the previously described procedure with minor adjustments. The QRT-SV phytosomes were created and optimized in this study through the use of the experimental design. The prepared formulations possessed a high zeta potential and were Nano scale in size. When compared to the plain formula and QRT, the optimized QRT-SV phytosomes demonstrated that the administration of the QRT formula significantly increased the expression of the mRNAs for caspase, Bax, Bcl-2, and p53. When compared to the basic formula and QRT alone, the QRT formula significantly decreased TNF- and NF-B activity in terms of inflammatory indicators. Overall, the research showed that the optimized QRT formulation that was created could be a potentially effective in breast cancer treatment.[79]
- El-Batal et al. Silymarin Nanocrystal and Phytosome Preparation and Characterization with Gamma Irradiation Stability Investigation Examine how silymarin is made by dissolving it in various solvents (acetone, acetonitrile, ethanol, and methanol) to create nanocrystals, then combining silymarin with lecithin to create phytosomes. and ascertained the phytosome's or crystal's drug content, dissolution, and other physicochemical characteristics. However, the impact of gamma irradiation has been assessed. Utilizing TEM and SEM, crystal morphology was determined. XRD, DSC, and FT-IR Characterized solid state Using DLS, the size of the particles was ascertained and the produced nanocrystals and phytosomes' in vitro drug release was assessed. Both phytosomes and nanocrystals have the potential to be effective methods for improving silymarin's qualities and for providing a prolonged release after radiation therapy.[80]
- N. Allam et al. present study on Curcumin phytosomes has been developed into soft gels using a solvent evaporation method to increase curcumin content. Thirteen different formulations were developed using oils, hydrophilic vehicles, and bioactive surfactants. TEM analysis showed good stability and a spherical structure of the phytosomes in complex formulations. Stability studies showed a stable curcumin dissolution pattern in hydrophilic vehicle formulations. Soft gelatin capsules offer advantages over hard gelatin capsules due to their ability to increase drug loading and bioavailability through different bioactive excipients. However, careful selection of excipients is crucial to avoid salting out phenomena due to the differences in solubility of active herbal drugs in different excipients.[81]
- Bui Thanh Tung et al. studied Hepatoprotective effect of Phytosome Curcumin against paracetamol-induced liver toxicity in mice as *Curcuma longa*, a plant with curcumin, has been studied for its pharmacological effects, but its low bioavailability makes it limited in clinical use. A phytosome curcumin formulation was developed and tested on its hepatoprotective effect on paracetamol-induced liver damage in mice. The study found that phytosome curcumin had a stronger hepatoprotective effect compared to curcumin-free curcumin. It effectively suppressed paracetamol-induced liver injury by reducing lipid peroxidation levels and enhancing enzymatic antioxidant activities. This suggests that phytosome curcumin has strong antioxidant activity and potential hepatoprotective effects.[82]





REFERENCES

1. Gaikwad AR, Ahire KD, Gosavi AA, Salunkhe KS, Khalkar A. Gaikwad Abhijeet R. Phytosome as a novel drug delivery system for bioavailability enhancement of Phytoconstituents and its applications: A Review. *Journal of Drug Delivery and Therapeutics*. 2021;11(3):138–52. doi:10.22270/jddt.v11i3.4847
2. Singh D. Phytosomes: An advanced drug delivery system for Herbal Drug. *Global Journal of Pharmacy & Pharmaceutical Sciences*. 2018;6(1). doi:10.19080/gjpps.2018.06.555679
3. Amal Ali Elkordy, Rita Rushdi Haj-Ahmad, Amani S. Awaad, and Randa Mohammed Zaki, An overview on natural product drug formulations from conventional medicines to nanomedicines: past, present and future *Journal of Drug Delivery Science and Technology*, 63(102459). ISSN 1773- 2247
4. Sadaf Mushtaq, Bilal Haider Abbasi, Bushra Uzair , Rashda Abbasi, NATURAL PRODUCTS AS RESERVOIRS OF NOVEL THERAPEUTIC AGENTS EXCL *Journal* 2018;17:420-451 – ISSN 1611-2156
5. Aman Dekebo, Introductory Chapter: Plant Extracts DOI: Pande Shital, Dhawale Shashikant , "Phytosome: A Key Strategy to Improve Bioavailability of Phyto-constituents in Drug Delivery" *Eur. Chem. Bull.* 2023,12(issue 8),8740-8759 DOI: 10.48047/ecb/2023.12.8.712
6. Shukla Ajay, Pandey Vikas, Shukla Rajesh, Bhatnagar Punit, and Jain Suchit, Herbosomes: A Current Concept of Herbal Drug Technology An Overview *Journal of Medical Pharmaceutical and Allied Sciences* (2012) 01; 39-56
7. Anupama Singha, Vikas Anand Saharanb, Manjeet Singha, and Anil Bhandaria, Phytosome: Drug Delivery System for Polyphenolic Phytoconstituents *Iranian Journal of Pharmaceutical Sciences Autumn* 2011; 7(4): 209-219 *ijps.sums.ac.ir*
8. K. Charana Sriya, Dividevara Sai, and P. Ravi Sankar Phytosomes: A Novel Approach for Herbal Phytochemicals for Enhancing the Bioavailability *Int. J. Pharm. Sci. Rev. Res.*, 60(2) ISSN 0976 – 044X
9. Kareparamban J, Nikam P, Jadhav A, Kadam v, Phytosome: A novel revolution in herbal drugs, *International journal of research in pharmacy and chemistry*, 2, 2012, 299-310.
10. Gupta S, Singh RP, Lokwani P, Yadav S, Gupta SK, Vesicular system as a targeted drug delivery system: An overview, *International Journal of Pharmaceutical Technology*, 3, 2011, 987-1021.
11. Waleed S. Alharbi , Fahad A. Almughem , Alshaimaa M. Almeahmady , Somayah J. Jarallah , Wijdan K. Alsharif , Nouf M. Alzahrani and Abdullah A. Alshehri, Review Phytosomes as an Emerging Nanotechnology Platform for the Topical Delivery of Bioactive Phytochemicals *Pharmaceutics* 2021, 13, 1475. <https://doi.org/10.3390/pharmaceutics13091475>
12. Sanjib Bhattacharya, Phytosomes: The New Technology for Enhancement of Bioavailability of Botanicals and Nutraceuticals *International Journal of Health Research*, September 2009; 2(3): 225-232
13. Bombardelli E. Phytosome: new cosmetic delivery system. *Boll Chim Farm* 1991; 130 (11): 431-38
14. Pavan M Patel, Chirag M Modi, Harshad B Patel, Urvesh D Patel, Divya M. Ramchandani, Harsh R Patel, and Bhulesh V Paidia Phytosome: An Emerging Technique for Improving Herbal Drug Delivery *The Journal of Phytopharmacology* 2023; 12(1):51-58 ISSN 2320-480X
15. Hou Z, Wei H, Wang Q, Sun Q, Zhou C, Zhan C, Zhang Q. New method to prepare mitomycin C loaded nanoparticles with high drug entrapment efficiency. *Nanoscale Res. Lett.* 2009;4(7):732- 737.
16. Sudhir Kumar, Ashish Baldi, and Dinesh Kumar Sharma Phytosomes: A Modernistic Approach for Novel Herbal Drug Delivery - Enhancing Bioavailability and Revealing Endless Frontier of Phytopharmaceuticals *J Develop Drugs* 9:2. doi: 10.4172/2329-6631. 1000195
17. Singh RP, Gangadharappa HV, Mruthunjaya K. Phytosome loaded novel herbal drug delivery system: A review. *Int. Res. J. Pharm.* 2016;7(6):15-21.
18. Drescher S, van Hoogevest P. The Phospholipid Research Center: Current Research in Phospholipids and Their Use in Drug Delivery. *Pharmaceutics*. 2020 Dec 18;12(12):1235. doi: 10.3390/pharmaceutics12121235. PMID: 33353254; PMCID: PMC7766331.
19. Jasemi, S.V.; Khazaei, H.; Aneva, I.Y.; Farzaei, M.H.; Echeverría, J. Medicinal Plants and Phytochemicals for the Treatment of Pulmonary Hypertension. *Front. Pharmacol.* 2020, 11.





Pratiksha S. Waghmare et al.,

20. Gabetta B, Fuzzati N, Griffini A, Lolla E, Pace R. Characterization of proanthocyanidins from grape seeds. *Fitoter.* 2000;71(2):162-75
21. Basnet P, Basnet NS. Curcumin: an anti-inflammatory molecule from a curry spice on the path to cancer treatment. *Molecules.* 2011;16(6):4567-98
22. Nimbalkar CK, Hatware K. Phytosomes: Novel drug delivery system, *Indian J Drugs.* 2017;5(1):16-36
23. Azwanida N. A review on the extraction methods use in medicinal plants, principle, strength and limitation. *Medicinal and Aromatic Plants.* 2015;4(196):2167-0412.1000196
24. Harshal Ashok Pawar, and Bhagyashree Dilip Bhangale, Phytosome as a Novel Biomedicine: A Microencapsulated Drug Delivery System *J Bioanal Biomed* 2015, 7:1 DOI: 10.4172/1948-593X.1000116
25. Abubakar AR, Haque M. Preparation of Medicinal Plants: Basic Extraction and Fractionation Procedures for Experimental Purposes. *J Pharm Bioallied Sci.* 2020 Jan-Mar;12(1):1-10. doi: 10.4103/jpbs.JPBS_175_19. Epub 2020 Jan 29. PMID: 32801594; PMCID: PMC7398001.
26. Patil MS, Patil SB, Chittam KP, Wagh RD, Phytosomes: novel approach in herbal medicines, *Asian J Pharm Sci Res* 2, 1-9, 2012.
27. Zhao X, Shi C, Zhou X, Lin T, Gong Y, Yin M, Fang J. Preparation of a nanoscale dihydromyricetin-phospholipid complex to improve the bioavailability: in vitro and in vivo evaluations. *Eur. J. Pharm. Sci.* 2019;138:104-113
28. Azeez NA, Deepa VS, Sivapriya V. Phytosomes: emergent promising nano vesicular drug delivery system for targeted tumor therapy. *Adv. Nat. Sci.: Nanosci. Nanotechnol.* 2018; 9(3):33-37.
29. Khan J, Alexander A, Ajazuddin, Saraf S, Saraf S. Recent advances and future prospects of phyto-phospholipid complexation technique for improving pharmacokinetic profile of plant actives. *J Control Release.* 2013 May 28;168(1):50-60.
30. Pandita A, Sharma P. Pharmacosomes: an emerging novel vesicular drug delivery system for poorly soluble synthetic and herbal drugs. *ISRN Pharm.* 2013 Sep 9; 2013:348186. doi: 10.1155/2013/348186. PMID: 24106615; PMCID: PMC3782844.
31. Li J, Wang X, Zhang T, Wang C, Huang Z, Luo X, Deng Y. A review on phospholipids and their main applications in drug delivery systems. *Asian J. Pharm. Sci.* 2015; 10(2):81-98.
32. Nadia Esfandiari, Seyed Ali Sajadian, CO₂ utilization as gas antisolvent for the pharmaceutical micro and nanoparticle production: A review, *Arabian Journal of Chemistry*, Volume 15, Issue 10, 2022, 104164, ISSN 1878-5352,
33. Sheth P, Sandhu H. Amorphous solid dispersion using supercritical fluid technology. In: Shah N, Sandhu H, Choi DS, Chokshi H, Malick AW, editor. *Amorphous Solid Dispersions*. New York: Springer; 2014
34. Saroha K, Waliyan P, Pahwa R, Pal S, Singh I, Kumar M. Phytosomes: A Promising Strategy for Enhanced Therapeutic Benefits of Phytochemicals. *Int. j. res. pharm.* 2020; 11(1): 3157- 3163.
35. Dr. Rupal Dubey, Khushboo Mehandole, Dr. Bhaskar Gupta, and Anamika Marry David phytosomes: an innovative approach to enhance the bioavailability and therapeutic efficacy of herbal extract 2023 *JETIR* September 2023, Volume 10, Issue 9 *JETIR*2309414.
36. Vipin k Agrawal, Amresh Gupta, Shashank Chaturvedi Improvement in bioavailability of class-iii drug: phytolipid delivery system *International Journal of Pharmacy and Pharmaceutical Sciences* ISSN- 0975-1491
37. D.K. Sanghi, Rakesh Tiwle. Herbal Drugs an Emerging Tool for Novel Drug Delivery Systems. *Research J. Pharm. and Tech.* 6(9): September 2013; Page 962-966.
38. Bombardelli E, Curri SB, Del NP, Tubaro A, Gariboldi P. Complexes between phospholipids and vegetal derivatives of biological interest. 1989;60:1-9.
39. Agarwal A, Kharb V, Saharan VA. Process optimization, characterization and evaluation of resveratrol-phospholipid complexes using box-behnken statistical design. *Int Curr Pharm J.* 2014;3(7):301-8.
40. Das MK, Kalita B. Design and evaluation of phytophospholipid complexes (Phytosomes) of rutin for transdermal application. *J Appl Pharma Sci.* 2014; 4(10):051-57.
41. Kidd P, Head K. A review of the bioavailability and clinical efficacy of milk thistle phytosome: a silybin-phosphatidylcholine complex (Siliphos). *Altern Med Rev.* 2005 Sep;10(3):193-203. PMID: 16164374.





Pratiksha S. Waghmare et al.,

42. Salazar J, Muller RH, Moschwitz JP. Combinative particle size reduction technologies for the production of drug nanocrystals. *J Pharma*. 2014; pp:1-11.
43. Pandey S. Phytosomes: Technical revolution in phytomedicine. *Inter J Pharm Tech Res*. 2010; 2:627-31.
44. Deivasigamani Senthil Kumar, Karthikeyan Deivasigamani and Biswabara Roy Development and Optimization of Phytosome for Enhancement of Therapeutic Potential of Epiyangambin in *Tinospora cordifolia* Extract Identified by GC–MS and Docking Analysis *Pharmacognosy Magazine* 19(2) 371–384, 2023
45. Parul A. Itadwar, And Prashant K. Puranik Novel Umbelliferone Phytosomes: Development And Optimization Using Experimental Design Approach And Evaluation Of Photo-Protective And Antioxidant Activity *International Journal of Pharmacy and Pharmaceutical Sciences* ISSN- 0975-1491 Vol 9, Issue 1, 2017
46. Baljeet Kaur, Anamika Saxena , Kirti Roy , Manoj Bhardwaj, and Manoj Bisht Development And In-Vitro Evaluation Of Phytosomes Containing Herbal Extract Of *Centella Asiatica* For Antiulcer And Antioxidant Activity *Journal of Advanced Scientific Research* 2023; 14 (03): 29-44 ISSN 0976-9595.
47. Rasaie S, Ghanbarzadeh S, Mohammadi M, Hamishehkar H. Nano phytosomes of quercetin: a promising formulation for fortification of food products with antioxidants. *Pharmaceutical sciences*. 2014; 20: 96-101.
48. Li Y, Wu H, Jia M, Cui F, Lin J, Yang X, Wang Y, Dai L, Hou Z. Therapeutic effect of folate-targeted and pegylated phytosomes loaded with a Mitomycin C - soybean phosphatidylcholine complex. *Mol. Pharmaceutics*. 2014; 11:3017–3026.
49. Bhattacharyya SS, Paul S, De A, Das D, Samadder A, Boujedaini N, Khuda-Bukhs AR. Poly (lactide-co glycolide) acid nanoencapsulation of a synthetic coumarin: Cytotoxicity and bio-distribution in mice, in cancer cell line and interaction with calf thymus DNA as target. *Toxicology and Applied Pharmacology*. 2011; 253:270–281.
50. Bhavesh Shah, S. B. Puranik, and Raghuchandan H. S. Preparation and Evaluation of Curcumin Phytosomes *IJPPR* March 2020 Vol.:17, Issue:4
51. Delgi U., Urbino S. D. Tolerability and cutaneous sensitization study in healthy volunteers after topical application of the product glycyrrhetic acid-Phytosome® ointment. Unpublished data submitted by CTFA, 2004, 36: 2
52. Valenzuela A, Aspillaga M, Vial S, Guerra R. Selectivity of silymarin on the increase of the glutathione content in different tissues of the rat. *Planta Med*. 1989 Oct;55(5):420-2. doi: 10.1055/s-2006-962056. PMID: 2813578.
53. Anwana U. Ubong-Isaac, Eghianruwa A. Queensley , and Akpan J. Enomfon Herbosomes in the Delivery of Phytotherapeutics and Nutraceuticals: Concepts, Applications and Future Perspective *Covenant Journal of Physical and Life Sciences (CJPL)* Vol. 3 No 2. December, 2015.
54. Wang SB, Chen AZ, Weng LJ, Chen MY, Xie XL. Effect of drug-loading methods on drug load, encapsulation efficiency and release properties of alginate/poly-L-arginine/chitosan ternary complex microcapsules. *Macromol. Biosci*. 2004; 4:27–30.
55. Hou Z, Li Y, Huang Y, Zhou C, Lin J, Wang Y, Cui F, Zhou S, Jia M, Ye S, Zhang Q. Phytosomes loaded with mitomycin C–Soybean phosphatidylcholine complex developed for drug delivery. *Mol. Pharmaceutics*. 2013; 10: 90–101
56. Varde N, Mehta N, Thakor N, Shah V, and Upadhyay U (2012) Phytosomes: a potential phospholipid nanoparticulate carrier for the bioavailability enhancement of herbal extracts. *International journal of comprehensive pharmacy* 10: 1-7.
57. Saha S, Sarma A, Saikia P, Chakrabarty T (2013) Phytosome: A Brief Overview. *Scholars Academic Journal of Pharmacy* 2: 12-20
58. Barani M, Sangiovanni E, Angarano M, Rajizadeh MA, Mehrabani M, Piazza S, Gangadharappa HV, Pardakhty A, Mehrbani M, Dell'Agli M, Nematollahi MH. Phytosomes as Innovative Delivery Systems for Phytochemicals: A Comprehensive Review of Literature. *Int J Nanomedicine*. 2021 Oct 15;16: 6983-7022. doi: 10.2147/IJN.S318416. PMID: 34703224; PMCID: PMC8527653.
59. GMM Maghraby El, A.C.Williams, B.W.Barry: Oestradiol skin delivery from ltradeformable liposome: refinement of surfactant concentration. *Int. J. Pharm* 2000; 196: 63-74.
60. Fry, D. W. White J. C., Goldman I. D. Rapid secretion of low molecular weight solutes from liposomes without dilution .*Anal. Biochem* 1978; 90: 809-815.





Pratiksha S. Waghmare et al.,

61. Maryana W, Rachmawati H, Mudhakir D. Formation of phytosome containing silymarin using thin layer hydration technique aimed for oral delivery. *Mater Today Proc Asian J Pharm.sci and cli.Res*2016;3:857-8.
62. Mazumder A, Dwivedi A, du Preez JL, du Plessis J. In vitro wound healing and cytotoxic effects of sinigrin-phytosome complex. *IntJPharm* 2016;498(1-2):284.
63. Mao JT, Xue B, Fan S, Neis P, Qualls C, Massie L, Fiehn O. Leucoselect Phytosome Modulates Serum Eicosapentaenoic Acid, Docosahexaenoic Acid, and Prostaglandin E3 in a Phase I Lung Cancer Chemoprevention Study. *Cancer Prev Res (Phila)*. 2021 Jun; 14(6):619-626. doi: 10.1158/1940-6207.CAPR-20-0585. Epub 2021 Mar 11. PMID: 33707173; PMCID: PMC8225569.
64. Naik SR, Panda VS. Hepatoprotective effect of Ginkgoselect Phytosome in rifampicin induced liver injury in rats: evidence of antioxidant activity. *Fitoterapia*. 2008 Sep; 79(6):439-45. doi: 10.1016/j.fitote.2008.02.013. Epub 2008 Jun 5. PMID: 18534776.
65. Jyoti Vaish Phytosomal Nanotechnology Platform for Various Formulations of Glycyrrhiza glabra Human Journals Research Article December 2022 Vol.:26, Issue:1
66. Tawheed Amin, and Suman Vikas Bhat A Review on Phytosome Technology as a Novel Approach to Improve The Bioavailability of Nutraceuticals *International Journal of Advancements in Research & Technology*, Volume 1, Issue3, August-2012 1 ISSN 2278-7763
67. Belcaro G, Ledda A, Hu S, Cesarone MR, Feragalli B, Dugall M. Greenselect phytosome for borderline metabolic syndrome. *Evid Based Complement Alternat Med*. 2013;2013: 869061. doi: 10.1155/2013/869061. Epub 2013 Nov 14. PMID: 24348726; PMCID: PMC3848081.
68. Loguercio C, Festi D. Silybin and the liver: from basic research to clinical practice. *World J Gastroenterol*. 2011 May 14; 17(18):2288-301. doi: 10.3748/wjg.v17.i18.2288. PMID: 21633595; PMCID: PMC3098397.
69. Tassell MC, Kingston R, Gilroy D, Lehane M, Furey A. Hawthorn (*Crataegus* spp.) in the treatment of cardiovascular disease. *Pharmacogn Rev*. 2010 Jan;4(7):32-41. doi: 10.4103/0973-7847.65324. PMID: 22228939; PMCID: PMC3249900.
70. Magrone T, Pugliese V, Fontana S, Jirillo E. Human use of Leucoselect® Phytosome® with special reference to inflammatory-allergic pathologies in frail elderly patients. *Curr Pharm Des*. 2014;20(6):1011-9. doi: 10.2174/138161282006140220144411. PMID: 23701566.
71. Nooreen Z, Rai VK, Yadav NP. Phytopharmaceuticals: a new class of drug in India. *Ann Phytomed*. 2018;7(1):27-37
72. Barkat MA, Das SS, Beg S, Ahmad FJ. Nanotechnologybased phytotherapeutics: current status and challenges. In: Beg S, Barkat M, Ahmad F (eds) *Nanophytoedicine*. Springer, Singapore 2020. pp. 1-7.
73. Alharbi WS, Almughem FA, Almeshmady AM, Jarallah SJ, Alsharif WK, Alzahrani NM, Alshehri AA. Phytosomes as an emerging nanotechnology platform for the topical delivery of bioactive phytochemicals. *Pharmaceutics*. 2021;13(9):1475.
74. Raveesha Peeriga, Parimala Kolli and Lakshmana Rao Atmakuri PHYTOSOMES TECHNOLOGYIJRPC 2023, 13(1), 1-6 ISSN: 2231-2781.
75. Sonam Sharma, and Alakh Niranjana Sahu Development, Characterization, and Evaluation of Hepatoprotective Effect of Abutilon indicum and Piper longum Phytosomes *Phcog Res* 2016;8:29-36.
76. Rutuja Sawant and Sheela Yadav Formulation And Evaluation Of A Phytosomal Gel Containing Azadirachta Indica Extract- Phospholipid Complex *World Journal Of Pharmacy And Pharmaceutical Sciences* Volume 11, Issue 4, 1751-1768 Research Article Issn 2278 – 4357.
77. Anju Singh, Rakhi Mishra, Avishikta Ray, Surabhi Tripathy, Satkar Prasad, Reenu Yadav Development And Evaluation Of Anti Diabetic Activity Of Phytosomes For Better Therapeutic Effect Of Extract *Journal of Pharmaceutical Negative Results* Volume 14 .
78. Andi Dian Permana, Rifka Nurul Utami, Aaron J. Courtenay, Marianti A. Manggau, Ryan F. Donnelly, Latifah Rahman, Phytosomal nanocarriers as platforms for improved delivery of natural antioxidant and photoprotective compounds in propolis: An approach for enhanced both dissolution behaviour in biorelevant media and skin retention profiles, *Journal of Photochemistry and Photobiology B: Biology*, Volume 205, 2020, 111846, ISSN 1011-1344,



Pratiksha S. Waghmare *et al.*,

79. Alhakamy, N.A.; Fahmy, U.A.; Eldin, S.M.B.; Ahmed, O.A.A.; Aldawsari, H.M.; Okbazghi, S.Z.; Alfaleh, M.A.; Abdulaal, W.H.; Alamoudi, A.J.; Mady, F.M. Scorpion Venom-Functionalized Quercetin Phytosomes for Breast Cancer Management: In Vitro Response Surface Optimization and Anticancer Activity against MCF-7 Cells. *Polymers* 2022, 14, 93
80. Ahmed Ibrahim El-Batal, Shahira F Elmenshaw, Ahmed M Abdelhaleem Ali, Enas Goodha Eldbaiky Preparation and Characterization of Silymarin Nanocrystals and Phytosomes with Investigation of their Stability using Gamma Irradiation *Indian Journal of Pharmaceutical Education and Research* Vol 52
81. Ahmed N. Allam, Ibrahim A. Komeil And Ossama Y. Abdallah Curcumin phytosomal soft gel formulation: Development, optimization and physicochemical characterization *Acta Pharm.* 65 (2015) 285–297
82. Bui Thanh Tung, Nguyen Thanh Hai, and Phan Ke Son Hepatoprotective effect of Phytosome Curcumin against paracetamol-induced liver toxicity in mice *Braz. J. Pharm. Sci.* 2017;53(1):e16136
83. Giori, Andrea; Franceschi, Federico Phospholipid complexes of olive fruits or leaves extracts having improved bioavailability *International Publication Number* WO 2007/118631 A1
84. Bombardelli, Ezio Via Ripamonti, Patri, Gian Franco Via Ripamonti, Pozzi, Roberto Via Ripamonti, Complexes of saponins with phospholipids and pharmaceutical and cosmetic compositions containing them. EP 0 283 713 B1
85. Bombardelli, Ezio Via Ripamonti, Mustich, Giuseppe Via Ripamonti, Bilobalide derivatives, their applications and formulations containing them. EP 0 441 279 A1
86. Bombardelli, Ezio Via Ripamonti, Patri, Gianfranco via Ripamonti Pozzi, Roberto via Ripamonti, Complexes of neolignane derivatives with phospholipids, the use thereof and pharmaceutical and cosmetic formulations containing them. EP 0 464 297 A1
87. Gabetta; Ezio Bombardelli; Giorgio Pifferi, complexes of flavanolignans with phospholipids, preparation thereof and associated pharmaceutical compositions Patent Number: 4,764,508
88. Ezio Bombardelli; Paolo Morazzoni, PHOSPHOLIPID COMPLEXES OF PROANTHOCYANDIN A2 AS ANTIATHEROSCLEROTIC AGENTS US 6,429,202 B1
89. Paolo Morazzoni, Orlando Petrini, Andrew Scholey, David Kennedy, USE OF A GINKGO COMPLEXES FOR THE ENHANCEMENT OF COGNITIVE FUNCTIONS AND THE ALLEVIATION OF MENTAL FATIGUE Patent No.: US 8,591,965 B2
90. Giori Andrea Franceschi federico Phospholipid complex of curcumin having improved bioavailability WO 2007/101551 A2
91. Ezio Bombardelli; Gian F. Patri, Complex compounds of bioflavonoids with phospholipids, their preparation and use, and pharmaceutical and cosmetic compositions containing them US 5043323
92. Ceteris Holding B.V., Amsterdam (Olanda) Succursale Di Lugano Composition for treatment of dyslipidemia and inflammation US 2017/0014374 A1

Table 1-composition of phytosome with examples

Components	Examples
Phospholipids	Soyaphosphatidylcholine, dipalmitoylphosphatidylcholine, egg phosphatidyl choline, distearylphosphatidylcholine[18,19]
Solvent	acetone, Dioxane, methylene chloride [21]
Non solvent	Aliphatic hydrocarbons or n-hexane[21]
Alcohol	Ethanol, methanol [22]
Colours and dye	Rhodamine 6G, DHPE-rhodamine, fluorescein, 6 carboxy fluorescence[23]





Pratiksha S. Waghmare et al.,

Table 2: Formulation of Herbal Phytosomes[64]-[71]

Phytosomes	Phytoconstituent complexed with PC	Uses
Leucoselect phytosome	Procyanidolic oligomers (PCOs) from grape seeds	It functions as a comprehensive antioxidant and is a suitable choice for young persons Also effective for the eyes, lungs, diabetes, varicose veins, and heart disease prevention.
Siliphos TM milk thistle phytosome	Silybin from silymarin	Mostly used for the liver or skin support,
Ginkgoselect phytosome	24 % ginkgo flavono glycosides from Ginkgo biloba	Good choice for old patients, Provide Protects to brain and vascular lining
Glycyrrhiza phytosome	18-beta glycyrrhetic acid	They have more potential for the management of retinal blood vessel problems and venous insufficiency and show Anti-inflammatory Activity
Mirtoselect phytosome	Anthocyanosides from an extract of Bilberry	These improve capillary tone, reduce abnormal blood vessel permeability & are potent antioxidants.
Greenselect phytosome	Epigallocatechin 3-O-gallate from camelia sinensis (Green tea)	Show good effect for protection against cancer and damage to cholesterol, work as Systemic antioxidant.
Silybin phytosome	Silybin from silymarin (milk thistle)	it is mostly used product, if the liver or skin needs additional antioxidant protection
Hawthorn phytosome	Flavonoids	More effective in heart disease
Oleaselect phytosome	Polyphenols from olive oil	it inhibit harmful oxidation of LDL cholesterol as potent antioxidant , and also have anti-inflammatory activity.
Lymphaselect phytosome	A standardized extract of	Used for chronic venous melilotus officinalis, insufficiency of the lower limbs, and Indicated for venous disorders.
Sabalselect phytosome	An extract of saw palmet to berries through supercritical CO ₂ (carbon dioxide) extraction	Beneficial for non-cancerous prostate enlargement, It delivers fatty acids, alcohols and sterols that benefit prostate health.

Table -3 Patents on Phytosomes with Patent Number

Sr.no.	Patent no.	Title	Innovation
1	WO 2007/118631 A1	Phospholipid complexes of olive fruits or leaves extracts having improved bioavailability	The current invention applies to novel phospholipid complexes of olive fruit or leaf extracts with increased bioavailability.[83]
2	EP0283713A2	Complexes of saponins with phospholipids and pharmaceutical and cosmetic compositions containing them.	The invention relates to triterpene saponin complexes, which complexed with fat, phytosterols, and phospholipids, as well as a method of making them. Some of these substances can affect the cardiovascular, neurological, and endocrine systems.[84]
3	EP 0 441 279 A1	Bilobalide derivatives, their applications and formulations containing them	The development and implementation of complexes containing natural or synthesized phospholipids and bilobalide, a sesquiterpene isolated from Ginkgo biloba leaves, for medicinal purposes are covered by the invention. The method outlined in the patent illustrates Ginkgo biloba's potential as a medicinal ingredient.[85]



Pratiksha S. Waghmare *et al.*,

4	EP 0 464 297 A1	Complexes of neolignane derivatives with phospholipids, the use thereof and pharmaceutical and cosmetic formulations containing them.	The present invention concerns the complexation of extracts with phospholipids from <i>Krameria triandra</i> Ruiz et Pav and other <i>Eupomatia</i> plants, along with certain phenolic compounds constituents of that group that are of neo-lignane or norneolignane nature; the methods for making these extracts and complexes and pharmaceutical compositions which include them. [86]
5	US 4764508	Complexes of flavanolignans with phospholipids, preparation thereof and associated pharmaceutical compositions	Innovation regarding to new compounds that are lipophilic complexes of phospholipids and silybin, silidianin, and silicristin, as well as the unconventional techniques used to produce these complexes. Flavanolignans can be utilized to treat acute and chronic liver diseases of toxic, metabolic, infectious, or degenerative origin. The new compounds absorb more readily in the gastrointestinal system and produce greater amounts in plasma compared to particular flavanolignans. [87]
6	US 6,429,202 B1	Phospholipid complexes of proanthocyanidin a2 as antiatherosclerotic agents	The current invention concerns the use of proanthocyanidin A2 phospholipid complexes or extracts that are enriched in proanthocyanidin A2 in the formulation of medications for the prevention and treatment of atherosclerosis, myocardial infarction, and cerebral infarction. [88]
7	US 8,591,965 B2	Use of a ginkgo complexes for the enhancement of cognitive functions and the alleviation of mental fatigue	The present invention relates to a novel use of a Ginkgo complex for the enhancement of cognitive function and mental fatigue functions. [89]
8	WO 2007/101551 A2	Phospholipid complex of curcumin having improved bioavailability	It has found that the phospholipid complexes of curcumin provide higher systemic levels of parent agent than unformulated curcumin can be prepared in protic solvents. [90]
9	US 5043323	Complex compounds of bioflavonoids with phospholipids, their preparation and use, and pharmaceutical and cosmetic compositions containing them	This invention is relating to complex compounds combining flavonoids with phospholipids, to a process for their preparation and to pharmaceutical and cosmetic compositions containing them. [91]
10	US 2017/0014374 A1	Composition for treatment of dyslipidemia and inflammation	Innovation related to combination of phytosomes three herbal plants curcumin, green tea, and and combination. For the treatment of dyslipidemia and inflammation. [92]





Crafting Harmony: A Panoptic Review on Types of Mixture Design and it's Pragmatic Outline

Vaishnavi Bhosale^{1*}, Pooja Munjal¹, Chaitali Dongaonkar², Shashikant Dhole³, Bhagyashree Parande², Nikita Kapale¹ and Pooja Ghule⁴

¹Student, Department of Pharmaceutics, PES Modern College of Pharmacy (for Ladies), Moshi, (Affiliated to Savitribai Phule Pune University) Pune, Maharashtra, India.

²Assistant Professor, Department of Pharmaceutics, PES Modern College of Pharmacy (for Ladies), Moshi, (Affiliated to Savitribai Phule Pune University) Pune, Maharashtra, India.

³Principal, Department of Pharmaceutics, PES Modern College of Pharmacy (for Ladies), Moshi, (Affiliated to Savitribai Phule Pune University) Pune, Maharashtra, India.

⁴Student, Department of Pharmaceutics, MET Institute of Pharmacy, Nashik, (Affiliated to Savitribai Phule Pune University) Pune, Maharashtra, India.

Received: 22 Jan 2024

Revised: 09 Feb 2024

Accepted: 17 May 2024

*Address for Correspondence

Vaishnavi Bhosale

Student,

Department of Pharmaceutics,

PES Modern College of Pharmacy (for Ladies),

Moshi, (Affiliated to Savitribai Phule Pune University)

Pune, Maharashtra, India.

Email: vaishnavibhosle4@gmail.com



This is an Open Access Journal / article distributed under the terms of the **Creative Commons Attribution License** (CC BY-NC-ND 3.0) which permits unrestricted use, distribution, and reproduction in any medium, provided the original work is properly cited. All rights reserved.

ABSTRACT

Mixture design, a powerful statistical methodology, plays a pivotal role in optimizing formulations and processes in pharmaceutical development. This review provides a comprehensive examination of various types of mixture designs and their applications within the pharmaceutical context. Types of mixture design such as Simple Centroid Design, D-Optimal Design, Simple Lattice Design, and Axial Design. The application of these mixture designs in pharmaceutical development is elucidated, emphasizing their roles in optimizing drug formulations, dosage forms, and manufacturing processes. By creating models that link the process's inputs and outputs, knowledge is acquired. Through the work of significant contributors, the development of the QbD approach and the statistical tool kit for its application, this review demonstrates the fundamentals of quality theory. Therefore, the goal of this review is to give a general overview of the principles of Mixture designs and how they are used in the creation of pharmaceuticals.





Vaishnavi Bhosale et al.,

Keywords: Mixture Design Geometry, Simple Centroid Design, D-Optimal Design, Simple Lattice Design, and Axial Design.

INTRODUCTION

Specialized response surface experiments are known as mixture experimental designs or MEDs. This method involves factors (x) being a mixture of components and responses (y) being a function of the amounts of each ingredient or component. The mole ratio, weight, volume, and other measures are typically used to determine the proportionate amounts of each component. The most crucial thing to remember while creating a mixture is that the ratios of every ingredient should add up to one. This restriction prevents the factor levels from being selected independently since they are dependent on the q-1 component levels. It is mathematically expressed in the following equation: [1]

$$0 \leq X_i \leq 1; \sum_{i=1}^q X_i = 1 \quad \dots (1)$$

Mixture experiments most naturally occur when studying the composition of material and the effect of the material composition on one or more responses of interest.

SIGNIFICANCE OF MIXTURE DESIGN

Mixture designs are specialized experimental designs that provide precise data when the response is influenced by the relative quantities of the components. Every run needs to add up to the same amount, and every component needs to be recorded in the same units of measurement. Using a small number of experimental runs, these designs help provide the most information possible. [2]

RATIONAL OF MIXTURE DESIGN

1. Optimization of Formulations

By using mixture designs, scientists can methodically investigate various component combinations inside a mixture in order to determine its ideal formulation. This is important in sectors where product efficacy and safety depend on the proper ingredient blend, such as medications and cosmetics.[3]

2. Resource Efficiency

By concentrating on the most illuminating experimental runs, mixture designs allow researchers to manage resources more effectively. A fractional factorial or other optimized design can be utilized to gather useful information with fewer experiments, as opposed to trying every conceivable combination.[3]

3. Comprehending Component Interactions:

Mixture studies promote comprehension of the ways in which the relative amounts of various components interact and impact the response variable. Gaining understanding of the fundamental mechanisms and processes controlling the system can be accomplished with the use of this information.[4]

4. Handling Constraints:

Combination designs are created to handle restrictions brought about by the total number of elements in a combination, ensuring that the experiment's circumstances are both realistic and workable. This is especially important in scenarios where the sum of the parts of the mixture must equal a certain quantity, like 100%.

5. Statistical Efficiency:

Reliability of estimates is achieved with minimal testing thanks to the statistical efficiency of mixture designs. Deliberately choosing combinations that produce the greatest amount of system information is how this is accomplished.

6. Relationships Not Well Represented by Traditional Experimental Designs:

In contrast, mixture models provide a more realistic picture of the underlying system by capturing nonlinear relationships between component proportions and the response variable.



Vaishnavi Bhosale *et al.*,

MIXTURE DESIGN GEOMETRY

Cuboidal shapes define the 2^k factorial design spaces. A 2^3 factorial design is defined by a true cube. Mixture design spaces, because of the sum to one constraint, are described by simplex shapes of dimension $q-1$ (there are q mixture factors). Simplex Regions for triangle simplex and tetrahedron simplex as shown in Fig. 1

TYPES OF MIXTURE DESIGN

There are several types of mixture design

Simplex Centroid Design

Using a simplex centroid design, the formulation variables were optimized. Three parameters were assessed in this design by varying their concentrations. Concurrently while maintaining a steady state of total focus. The design of a simplex centroid for a three-component system (A, B, C, and D) is shown as an equilateral triangle in a two-dimensional area. [5, 6] The statistical analysis of the Simplex Centroid Design batches was done using Design-Expert software. To study the influence of each factor on response and behavior of the system within the designed space, response surface plots were generated. [7]

Simplex Lattice Design

Henry Scheffe has presented a new statistical technique for examining the characteristics of multi-component systems as a function of composition. [8] An invaluable new technique for examining blend characteristics across a broad compositional range is the lattice method. For systems consisting of four or more components, it is quite beneficial. Precise mapping of responses across broad compositional ranges, and sometimes beyond domains of direct interest, should improve the efficacy of experiments by identifying effects that might otherwise remain unnoticed. [8] An invaluable new technique for examining blend characteristics across a broad compositional range is the lattice method. For systems consisting of four or more components, it is quite beneficial. Precise mapping of responses across broad compositional ranges, and sometimes beyond domains of direct interest, should improve the efficacy of experiments by identifying effects that might otherwise remain unnoticed.

The two main components of the method are as follows:

1. Attributes or responses are measured at lattice composition points; and
2. The responses are then represented by polynomial equations that have a unique correlation to the lattice points. [8]

Extrem Vertices Design

The design of extreme vertices is a method for carrying out experiments with mixes when they are subject to constraints from multiple elements. The amount of the factor space that would arise if the factor levels were limited to just 0% to 100% is decreased by the restrictions that have been placed. The process involves choosing the vertices and different centroids of the generated hyper-polyhedron as the design of coming up with a special set of therapy combos. This choice is driven by the urge to investigate both the factor space's center and its boundaries. [9] Researchers examine the response surface of a dependent variable (denoted as y) in mixed experiments, such as the quantity of light produced by a particular size flare in candles. The relationship between this response surface and Q factors ($q \geq 3$), is examined. The proportion X_i of the entire mixture is used to represent each Q factor (or component).

In particular:

$$\sum_{i=1}^q x_i = 1 \text{ and } 0 \leq a_i \leq X_i \leq b_i \leq 1 \quad \dots (2)$$

When x is subject to limits set by the researcher or the physical context, and $i = 1, q$ and the parameters a_i and b_i . For $i = 1, \dots, q$, Scheffe introduced mixed experiments with the cases $a_i = 0$ and $b_i = 1$.

The $\{q, m\}$ simplex lattice design, according to him, is a design that fills the factor space uniformly. The values of each factor are evenly spaced and range from 0 to 1, so that the total of all the factors $\sum_{i=1}^q x_i$ equals 1.

For example, observations at positions (1, 0, 0), (0, 1, 0), (0, 0, 1), (0.5, 0.5, 0), (0.5, 0, 0.5), and (0, 0.5, 0.5) are part of a full $\{3, 2\}$ lattice. These points can be seen as a two-dimensional simplex in Figure 4 and as an illustration in Figure 3 of the plane $x_1 + x_2 + x_3 = 1$ in the first octant. [9]



**Vaishnavi Bhosale et al.,**

As an extension since the case that will be detailed later comprises four factors, a {4, 3} lattice is depicted in Figure 5 as a three-dimensional simplex (tetrahedron). The q -dimensional factor space typically simplifies to a polyhedron of dimension $(q - 1)$. It's crucial to remember that simplex lattice designs and other language and notation used in mixture experiments offer an organized method for examining the connections between various mixture components and how they affect the dependent variable.

Optimal Design

D-optimal, A-optimal, and IV-optimal designs are differentiated by the Design Expert program. The algorithm selects points that minimize the volume of the confidence ellipsoid of the coefficients; A-optimal design minimizes the average variance of the polynomial coefficients; D-optimality is desired for the factorial and screening designs to discover the most important variables. The integrated variance criteria is used in the "IV" or "I" optimal design. [11]

D- and I-optimal designs for mixture trials where the constituents are assumed to be continuous over the resulting design space and are linearly constrained. [11] The D-optimal technique has an advantage over other approaches in that it requires fewer runs, which lowers the expense of experimenting. D-optimal is typically utilized in the culinary, pharmaceutical, and cosmeceutical industries for product development. [1]

CONCLUSION

In summary, this review underscores the importance of mixture design geometries, with a specific emphasis on optimal simple centroid, simple lattice, and axial designs in the context of pharmaceutical optimization. These sophisticated design frameworks offer valuable tools for the methodical exploration and enhancement of pharmaceutical mixtures, ensuring the efficiency of drug formulation and development. By utilizing these mixture design geometries, scientists in the pharmaceutical sector can streamline experimentation, pinpoint optimal formulations, and improve drug efficacy. As the demand for personalized medicine and innovative drug delivery systems rises, the application of mixture design geometries is positioned to play a crucial role in expediting pharmaceutical development, ultimately contributing to the provision of Safer, more efficient, and patient-centric therapeutic solutions

ABBREVIATIONS

QbD = Quality by Design

MEDs = Mixture Experimental Designs

HPMC = Hydroxy Propyl Methyl Cellulose

CaO = Calcium Oxide

CaCl₂ = Calcium Chloride

DS = Drug Substance

SMEDDS = Self-Microemulsifying Drug Delivery System

ATV = Atrovastatin

DOE = Design of Experiments

VCO = Virgin Coconut Oil

REFERENCES

1. Kayaroganam P. Response Surface Methodology-Research Advances and Applications. IntechOpen; 2023.
2. Beg S. Mixture designs and their applications in pharmaceutical product development. Design of Experiments for Pharmaceutical Product Development: Volume I: Basics and Fundamental Principles. 2021:87-96.
3. Anderson M, Whitcomb P. Find the optimal formulation for mixtures. Stat-Ease Inc, Minneapolis. 2002.





Vaishnavi Bhosale et al.,

4. Mancenido MV, Pan R, Montgomery DC, Anderson-Cook CM. Comparing D-optimal designs with common mixture experimental designs for logistic regression. *Chemometrics and Intelligent Laboratory Systems*. 2019 Apr 15;187:11-8.
5. L. Lachman, H. Lieberman, J. Kaning. *Theory and Practice of Industrial Pharmacy*, 3rd edition Lei & Feiberger, Philadelphia, Pa, USA, 3rd edition, 1970.
6. Patel MB, Shaikh F, Patel V, Surti NI. Application of simplex centroid design in formulation and optimization of floating matrix tablets of metformin. *Journal of Applied Pharmaceutical Science*. 2017 Apr 30;7:023-30.
7. Madgulkar AR, Bhalekar MR, Padalkar RR, Shaikh MY. Optimization of carboxymethyl-xyloglucan-based tramadol matrix tablets using simplex centroid mixture design. *Journal of pharmaceuticals*. 2013;2013. <https://doi.org/10.1155/2013/396468>
8. Gorman JW, Hinman JE. Simplex lattice designs for multicomponent systems. *Technometrics*. 1962 Nov 1:463-87.
9. McLean RA, Anderson VL. Extreme vertices design of mixture experiments. *Technometrics*. 1966 Aug 1:447-54. <http://dx.doi.org/10.1080/00401706.1966.10490377>
10. Jeirani Z, Jan BM, Ali BS, Noor IM, Hwa SC, Saphanuchart W. The optimal mixture design of experiments: Alternative method in optimizing the aqueous phase composition of a microemulsion. *Chemometrics and Intelligent Laboratory Systems*. 2012 Mar 15; 112:1-7. <https://doi.org/10.1016/j.chemolab.2011.10.008>.
11. Coetzer R, Haines LM. The construction of D-and I-optimal designs for mixture experiments with linear constraints on the components. *Chemometrics and Intelligent Laboratory Systems*. 2017 Dec 15;171:112-24. <https://doi.org/10.1016/j.chemolab.2017.10.007>
12. Azevedo S, Cunha LM, Mahajan PV, Fonseca SC. Application of simplex lattice design for development of moisture absorber for oyster mushrooms. *Procedia food science*. 2011 Jan 1;1:184-9. <https://doi.org/10.1016/j.profoo.2011.09.029>
13. Désiré A, Paillard B, Bougaret J, Baron M, Couarraze G. Extruder scale-up assessment in the process of extrusion-spheronization: comparison of radial and axial systems by a design of experiments approach. *Drug development and industrial pharmacy*. 2013 Feb 1;39(2):176-85. <https://doi.org/10.3109/03639045.2012.665458>
14. Yeom DW, Song YS, Kim SR, Lee SG, Kang MH, Lee S, Choi YW. Development and optimization of a self-microemulsifying drug delivery system for atorvastatin calcium by using D-optimal mixture design. *International Journal of nanomedicine*. 2015 Jun 5:3865-78. <https://doi.org/10.2147/IJN.S83520>
15. Maher PG, Fenelon MA, Zhou Y, Kamrul Haque M, Roos YH. Optimization of β -casein stabilized nanoemulsions using experimental mixture design. *Journal of food science*. 2011 Oct;76(8):C1108-17. <https://doi.org/10.1111/j.1750-3841.2011.02343.x>
16. Yeom DW, Song YS, Kim SR, Lee SG, Kang MH, Lee S, Choi YW. Development and optimization of a self-microemulsifying drug delivery system for atorvastatin calcium by using D-optimal mixture design. *International Journal of nanomedicine*. 2015 Jun 5:3865-78.
17. Yeom DW, Song YS, Kim SR, Lee SG, Kang MH, Lee S, Choi YW. Development and optimization of a self-microemulsifying drug delivery system for atorvastatin calcium by using D-optimal mixture design. *International Journal of nanomedicine*. 2015 Jun 5:3865-78. <https://doi.org/10.1080/10717544.2023.2173337>

Table 1: Types of simplex shapes

SR. NO.	Q=X (X=2,3,4)	SIMPLEX SHAPE
1.	q=2	Straight line
2.	q=3	Triangle
3.	q=4	Tetrahedron





Vaishnavi Bhosale et al.,

Table 2: Examples of Mixture Design Type

SR. NO.	MIXTURE DESIGN TYPE	INDEPENDENT VARIABLE	DEPENDANT VARIABLE	CONCLUSION
1.	Simplex Centroid Design	HPMC K15 M and κ - Carrageenan, sodium bicarbonate	Floating lag time (sec) (Flag) Drug released after 1 hour (%) Time required for 90% (t90)	It was conclude that the drug's release pattern is more flexible when kappa carrageenan and HPMC K 15 M are combined. Nevertheless, adding more kappa carrageenan is not a good idea because it will speed up the drug's release from the formulation and impede its regulated release by making it more hydrated.
2	Simplex Centroid Design	Carboxymethyl xyloglucan , HPMC K100M , and dicalcium phosphate	percent of drug release at 2 nd hour and at 8 th hour	The current study's achieved matrix kinetics and sustained drug release suggest that the hydrophilic matrix tablet made with carboxymethyl xyloglucan and HPMC-K100M can be used to effectively sustain drug release for up to 8 to 12 hours at a time.
3	Simplex lattice design	CaO, CaCl ₂ and sorbitol	Moisture content	The ultimate moisture content of the mixed absorber was most significantly impacted by the CaCl ₂ . The mass fractions of calcium oxide, calcium chloride, and sorbitol in the optimized desiccant mixture were 0.50, 0.26, and 0.24, respectively.
4	Axial system	DS concentration, DS solubility, Extrusion system, Spheronization time, Extrusion scale	Extrusion rate (g/s), Extrusion yield(%), Pellet Size, Pellet Size Dispersion, Elongation, Usable Yield (%), Solidity, Pycnometric Density(g/cm), Friability, Diametral Crushing Force (N), Tween 80 (min)	In light of the findings, the axial system emerges as the most effective and straightforward method to scale up, requiring no modifications to the formulation or process, when compared to the lab scale. Through various design analyses, the design of experiments technique made it possible to analyze crucial parameters and their interactions on the various responses, as well as to discover the extrusion system that is most efficient.
5.	D-Optimal Design	Capmul MCM, Tween 20 , and Tetra glycol	Mean droplet size and percentage of drug released in 15 minutes	Using the response surface methodology-based statistical optimization tool, d-optimal mixture design, we were able to produce an optimum ATV loaded SMEDDS formulation in this study. Comparing the optimized ATV-loaded SMEDDS formulation to the ATV suspension, the rats demonstrated excellent in vitro dissolving and in vivo oral





Vaishnavi Bhosale et al.,

				bioavailability. The formulation contained 7.16% Capmul MCM (oil; X1), 48.25% Tween 20 (surfactant; X2), and 44.59% Tetra glycol (co surfactant; X3).
--	--	--	--	---

Table 3: Application of Mixture Design

SR. NO.	DESIGN	FORMULATION VARIABLE	OUTCOMES	REFERENCES
1.	Mixture Design	β -casein (2.5%, 5%, 7.5%, and 10% w/w), lactose (0% to 20% w/w), and trehalose (0% to 20% w/w)	A successful application of Mixture Design of Experiments (DOE) enabled the prediction of both glass transition and rheological properties, crucial for the formulation of a continuous phase tailored for nanoemulsions.	[15]
2.	D-optimal Mixture Design	VCO (10–20%, w/w), Tween 80 : Pluronic PF68 (10–15%, w/w), xanthan gum (0.5–1.0%, w/w) and water (64.008–79.291)	The permeability test results indicated that, when applied for 8 hours, copper peptide in aqueous solution, with or without a penetration enhancer, exhibited negligible transport through the cellulose acetate membrane. However, the incorporation of nanoemulsion notably enhanced the permeability of copper peptide, leading to a significant increase of $21.89 \pm 0.53\%$ in active matter release after an 8-hour application.	[16]
3.	Mixture Design	Concentrations of thyme oil (10% and 25%), labrasol (40% and 70%), and transcutol (20% and 40%)	The itraconazole and thyme oil-based self-nanoemulsifying drug delivery systems could offer an effective defense against oral diseases caused by microbial infections.	[17]

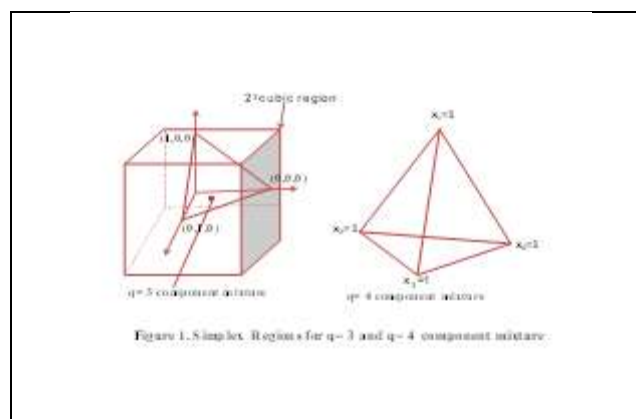


Fig. 1 Simplex Regions for q=3 and q=4 component mixture Simplex Regions for triangle simplex and tetrahedron simplex as shown in Fig. 1

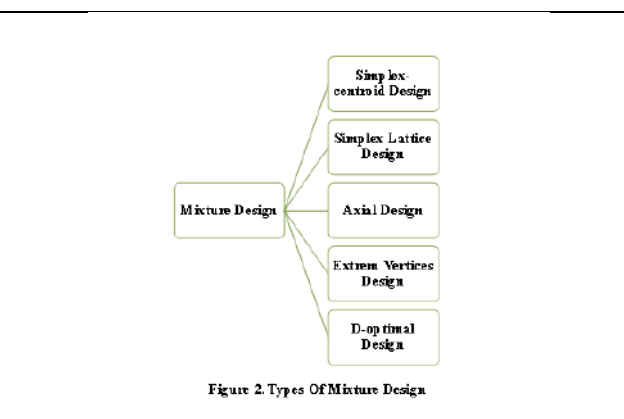
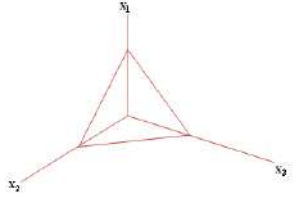
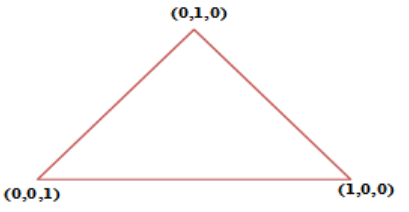
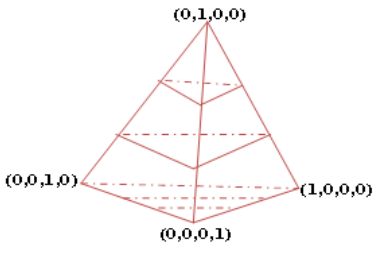


Fig. 2 Types of Mixture Design





Vaishnavi Bhosale et al.,

 <p>Figure 3. $[x_1 + x_2 + x_3 = 1]$ plane</p>	 <p>Fig. 4 $[3, 2]$ lattice</p>
<p>Fig. 3 $[x_1 + x_2 + x_3 = 1]$ plane For example, observations at positions $(1, 0, 0)$, $(0, 1, 0)$, $(0, 0, 1)$, $(0.5, 0.5, 0)$, $(0.5, 0, 0.5)$, and $(0, 0.5, 0.5)$ are part of a full $\{3, 2\}$ lattice. These points can be seen as a two-dimensional simplex in Figure 4 and as an illustration in Figure 3 of the plane $x_1 + x_2 + x_3 = 1$ in the first octant . [9]</p>	
 <p>Figure 5. $[4,3]$ lattice</p>	
<p>Fig. 5 $[4, 3]$ lattice[As an extension, since the case that will be detailed later comprises four factors, a $\{4, 3\}$ lattice is depicted in Figure 5 as a three-dimensional simplex (tetrahedron).] [9]</p>	





Teachers' Perception on the Role of Occupational Therapy in School Settings: A Cross-Sectional Study from Alahsa City, Saudi Arabia

Senthil Vadivel^{1*}, Talal Alshammari², Christopher Amalraj V³, Arun Vijay Subbarayalu⁴, Raju Suresh Kumar⁵, Suresh Melamalai¹, Hussain Albagshi⁶, Ahmad Alonizan⁶, Mohammed Aldakhil⁶, Redha Snyhr⁶

¹Lecturer, Department of Occupational Therapy, College of Applied Medical Sciences, King Saud bin Abdulaziz University for Health Sciences, Al Ahsa, Kingdom of Saudi Arabia.

²Teaching Assistant, Department of Occupational Therapy, College of Applied Medical Sciences, King Saud bin Abdulaziz University for Health Sciences, Al Ahsa, Kingdom of Saudi Arabia.

³Professor, Vice Deanship for Development and Community Partnership, College of Medicine, Imam Abdulrahman Bin Faisal University, Dammam, Saudi Arabia.

⁴Assistant Professor, Deanship of Quality and Academic Accreditation and Department of Physical Therapy, Imam Abdulrahman Bin Faisal University, Post Box: 1982, Dammam-31441, Saudi Arabia.

⁵Assistant Professor, Department of Basic Sciences, College of Science and Health Professions, King Saud bin Abdulaziz University for Health Sciences, Jeddah, Kingdom of Saudi Arabia.

⁶Internship Student, Department of Occupational Therapy, College of Applied Medical Sciences, King Saud bin Abdulaziz University for Health Sciences, Al Ahsa, Kingdom of Saudi Arabia.

Received: 22 Jan 2024

Revised: 09 Feb 2024

Accepted: 18 May 2024

*Address for Correspondence

Senthil Vadivel

Lecturer,

Department of Occupational Therapy,

College of Applied Medical Sciences,

King Saud bin Abdulaziz University for Health Sciences,

Al Ahsa, Kingdom of Saudi Arabia.

Email: senthilvadivelpalanichamy@yahoo.co.in



This is an Open Access Journal / article distributed under the terms of the **Creative Commons Attribution License** (CC BY-NC-ND 3.0) which permits unrestricted use, distribution, and reproduction in any medium, provided the original work is properly cited. All rights reserved.

ABSTRACT

Understanding the role of occupational therapy (OT) is essential for all professionals, including teachers, in order to help people engage in meaningful activities and enhance their general well-being. Despite its significance, little is known about the level of teachers' awareness regarding occupational therapy's role in Al Ahsa City schools. This study aimed to measure teachers' awareness of occupational therapy and highlight its importance in the school context. A cross-sectional study design was adopted. Three hundred seventy-seven teachers from public and private schools were invited to participate in an online survey using a semi-structured tool, including both closed-ended and open-ended items, to collect quantitative data on teachers' knowledge and understanding of occupational therapy roles. The results showed inadequate teachers' awareness of the role of occupational therapy. Most participants had only

75949



Senthil Vadivel *et al.*,

learned about the term “OT” through the survey, suggesting a significant gap in their understanding of the contribution of occupational therapy in the school environment. No statistically significant differences in awareness were found between male and female participants and between public and private/international school teachers. The study concluded a significant gap in knowledge and awareness about occupational therapy between teachers in public and private/international schools in Al Ahsa City, Saudi Arabia. There is an urgent need to provide school teachers with education and awareness of the role of occupational therapy by encouraging collaboration between teachers and occupational therapists, thereby increasing their awareness and understanding of the potential benefits for students, such as improved academic performance, better behavior, and social skills. This, in turn, can create a supportive and inclusive learning environment that promotes students' overall well-being.

Keywords: Occupational therapy, Awareness, Knowledge, Teachers, Al Ahsa, Schools

INTRODUCTION

Occupational therapy (OT) is the therapeutic use of activities of daily living (occupations) with groups or individuals to improve or increase engagement in habits, routines, roles, and rituals in school, family, community, workplace, and other contexts [1]. The goal of occupational therapists (OTs) is to promote independence as much as possible. Particularly for children with sensory and motor disabilities, occupational therapists motivate them to engage in worthwhile activities and provide a range of common academic, social, recreational, self-sufficient living, and occupational assistance [2]. Education is one of the key performance areas according to the Occupational Therapy Practice Framework: Domain and Process, Fourth Edition (OTPF-4), which is defined as the activities required for learning and participation in the classroom. Because OTs focus on a range of occupations (e.g., education, social interaction, play, leisure, career, and daily activities), they are in a unique position to make a significant contribution to school services [2]. An earlier study also emphasizes the value of occupational therapists collaborating with other professionals in educational settings to promote school engagement and a well-rounded education for all children [3]. When at-risk youth were compared with a control group, traditional vocational handwriting instruction was found to improve test scores [4]. As evidenced by the World Federation of Occupational Therapy (WFOT) publication on the topic in 2016, this has helped fuel growing interest in school-based occupational therapy (SBOT) around the world. According to WFOT, the work of occupational therapists in schools should be professionally and educationally relevant, with a focus on promoting student engagement, optimization and overall well-being.

However, policymakers appear to lack a clear understanding of what constitutes occupational therapy school services, as they routinely include them in legislation along with physiotherapy and speech therapy. If someone knows what an occupational therapist does, it is typically because a family member or close relative has received occupational therapy, directly provided services, or had a close personal relationship with them [5]. Through their roles as therapists, mediators, teachers, collaborators and supporters, occupational therapists play a critical role in creating an enabling environment (directly and indirectly) [5]. As such, OTs working in schools have recognized the need to move from a form of direct, one-on-one care to more group and classroom-based care. By providing necessary instruction to teachers and parents, OT's primary contribution is to improve children's success in the classroom [6]. The contribution of OTs in schools is diverse. By assessing children's abilities and resources, OTs are able to find solutions that can reduce or eliminate learning difficulties. These principles are consistent with the American Occupational Therapy Association (AOTA) Recommendations for School-Based Occupational Therapy Practice, which emphasize the use of expertise to assist children in preparing for and actively participating in important educational and developmental activities in a school environment [7]. Further, Transition is one of the occupational therapy services that helps students adapt to their new environment. Transition services are often offered in schools, providing a modified environment to help children and their families ease the transition.



**Senthil Vadivel et al.,**

Therefore, this service is crucial during the intervention phase for students with disabilities. Not only does it prepare students for academic success in kindergarten, preschool, and high school, but it also helps children develop social skills and activities of daily living (ADL), which are important for transition planning. Additionally, this program helps children and families adapt to new environments [8]. According to the World Federation of Occupational Therapists (WFOT), occupational therapists (OTs) should be employed in education to support and promote full participation and well-being by utilizing their skills and identifying ways to reduce participation limits and learning activity limitations among students. England's Code of Practice for special educational needs and disabilities suggests joint commissioning as a method for integrating OT services into schools [9]. Occupational adaptation is an important process to understand as we learn more about humans as workers. Scientists advocate for a better understanding of this process in certain settings, such as academic settings.

In meeting everyday expectations and role demands and interacting with the academic environment, academic educators continually demonstrate occupational adaptability. However, little is known about this process [10]. Regarding the role of occupational therapy in schools, teachers are the first to raise public awareness of the need for occupational therapy in schools [1-2]. Teachers also advised occupational therapists to make their responsibilities at school clear to both themselves and other students. An earlier study also indicated that teachers voiced that occupational therapist should continue to support and educate them about children with special needs by demonstrating and modeling more of the recommended occupational treatments, programs and work to promote students' sensory and motor functions [11]. Even though OTs work in a multidisciplinary team with other healthcare professionals to rehabilitate patients, their role is much limited in school environment in Saudi Arabian context. Despite studies conducted on uncovering the perceptions of the various professionals about Occupational Therapy in Saudi Arabia[12-13], none of the studies have focused on school teachers in Saudi Arabia. Thus, this study is the first to examine the perception of occupational therapy roles among teachers in urban Al-Ahsa schools in Saudi Arabia, with a two-fold aim: (i) school teachers' awareness and knowledge of the role of occupational therapy and its scope and the type of students who benefit from it, and (ii) whether there is a relationship between gender and teachers' perceptions of the role of occupational therapy, its scope and the type of students who benefit from it.

MATERIALS AND METHODS

Study Design

A cross sectional study design was adopted to ascertain the teachers' perception about the role of occupational therapy in School settings with a specific reference to Al Ahsa, Saudi Arabia.

Study Setting and participants

All full-time teachers, both male and female, belonging to the public and private schools, Alahsa Saudi Arabia formed the population of the study. Those teachers who were in their training phase and other administrative staff are excluded. The study received ethical clearance from the Institutional Review Board (IRB) of King Abdullah International Medical Research Center (KAIMRC) (study number NRA22A/033/09).

Sampling methods

Since the authors could not accurately predict the total number of teachers employed in public and private schools, Alahsa Saudi Arabia, the required sample size was calculated based on the formula for estimating the sample size for an infinite population. i.e., $Z^2 \times p \times (1-p) / C^2$ [Z score for 95% confidence level = 1.96; p = percentage of population assumed as 50% or 0.50 and c = confidence interval or margin of error = 0.05 or 5%]. With a 95% confidence interval and a 5% margin of error, the expected sample size is 385. Accordingly, 400 questionnaires were distributed among the teachers; however, this study received responses from 377 samples who volunteered to participate, demonstrating a response rate of 94%. A snowball sampling technique was adopted where the questionnaire was distributed to teachers who, in turn, circulated it among their peers for participation. On scrutiny of the filled survey



**Senthil Vadivel et al.,**

forms, 35 survey forms are incomplete and are excluded. Finally, 352 completed questionnaires were considered for analysis.

Instrumentation

The questionnaire utilized in this research was a structured validated tool developed and adopted by Raghuram et al. (2021) [14]. The questionnaire was translated into both English and Arabic and content validation was carried out through English and Arabic language Expert teachers, as well as the co-investigator. The questionnaire consisted of three sections that included demographic data, employment status, and teacher's awareness and knowledge of occupational therapy. It comprised of both closed (multiple-choice questions and binary questions with yes/no options) and open-ended questions.

Data Collection Procedure

Data were collected via email using an online survey questionnaire created using Google Forms. Permission was obtained from the General Directorate of Education in Al Ahsa to distribute the questionnaire link to teachers via email. All participants are required to complete the informed consent form before completing the questionnaire. Participants were given a specific time frame to complete the questionnaire and data were collected and analyzed between December 2022 and June 2023.

Data Analysis

The statistical software program SPSS version 24.0 was used to perform the analysis. Descriptive statistics such as frequencies and percentages were used to represent participants' awareness of occupational therapy. In addition, chi-square statistics were applied to examine the association between gender and school type (private/public) in terms of teachers' awareness of the role of occupational therapy, the location where they can receive the services, and the type of students who can benefit from them.

RESULTS**Baseline characteristics of the participants:**

The majority (45.7%) of participating teachers were 41-50 years of age, while only 17 (4.8%) participants exceeded 61 years old. Of the participants, 249 (70.7%) subjects were males, and the others were females. The mean duration of the work experience was 15.82 ± 8.24 years. It was found that the majority of participants had a bachelor's degree (96%), worked at a public school (88.6%), and had full-time employment (88.6%). Other characteristics of participants are shown in Table 1. From Table 2, it was observed that there was no significant difference between both gender concerning teachers' awareness and knowledge about the role of occupational therapy ($p > 0.05$). It was found that the majority of participants had similar views on the role of occupational therapy. Moreover, it is inferred that there was a significant difference between both groups of participants in terms of knowledge about OT ($p < 0.001$) with most participants (75%) from private/international schools having this knowledge, while 48.8% of participants from public schools had such knowledge. Furthermore, the majority (62.5%) of private/international school participants had become familiar with the term OT through social media, while only 48.1% of public-school participants had acquired this knowledge through this survey. Also, there were significant differences between both groups regarding the role of OT ($p = 0.03$) where both groups differently perceived the role of OTs in performing all written functions, including treating those who cannot engage in daily activities due to injury, illness, or other conditions as well as managing injured patients through mobility and exercise, manual treatments, education, and counselling and treat patients who are taking medications for illness. Further, there is difference in the perception of participants from other groups concerning their knowledge about nature of academic program where OTs needs to qualify after schooling. Other data as regarding awareness about the role of OT showed no significant differences between both groups of participants. From Table 3, it was revealed that both genders had insignificant differences in awareness of the extent of OT practice and the type of students who would benefit from occupational therapy ($p > 0.05$). In addition, it was found that after this survey, despite insignificant differences ($p = 0.25$), the majority of participants showed interest in gaining much more knowledge about occupational therapy (women = 78.6% vs. men = 82.7%).



**Senthil Vadivel et al.,**

Regarding the extent of OT practice, there are significant differences between both groups ($p < 0.001$), with 50% of participants from private/international schools and 38.5% from public schools, considering all selected locations, including government organizations/institutions / Hospitals, Non-Governmental Organizations (NGOs), Acute Hospitals and Nursing Homes, Rehabilitation Centers/Clinics/De-addiction Centers, Mental Health Facilities, Special Schools/Regular Schools, Community Based Rehabilitation Centers (CBR), Social Agencies, etc. Disaster Management, Projects, Hospice Care, Chronic Patient Care Centers. Industries can offer occupational therapy. Furthermore, there was no significant difference between the opinions of participants from both schools regarding the type of students who would benefit from occupational therapy ($p > 0.05$); However, after this survey, the majority of participants had more knowledge about occupational therapy (87.5% vs. 80.8%; $p = 0.21$)

DISCUSSION

The results of this research indicate that there is insufficient knowledge about the role of occupational therapy among teachers in schools in Al Ahsa city. Although most participants had a bachelor's degree (96%) and years of teaching experience, the study found that most participants had only learned about the term OT through the survey. This suggests a need for greater education and awareness of the role of occupational therapy in schools. Interestingly, the study found no significant differences between male and female participants in their awareness of the extent of occupational therapy practice ($p = 0.24$) or the type of students who would benefit from this therapy ($p = 0.17$) [Table 3]. This suggests that gender may not be a significant factor in determining occupational therapy awareness in this context. However, the study found that the majority of participants gained more knowledge about occupational therapy after completing the survey. This suggests the potential for educational interventions to improve knowledge and understanding of the role of occupational therapy in educational settings [15]. To further strengthen the role of occupational therapy in schools, it is important to address the barriers that may prevent teachers from referring students to occupational therapy services. This may include increasing awareness and recognition of the role of occupational therapy, improving referral pathways and providing appropriate resources and support [16].

Several studies have highlighted the potential benefits of occupational therapy in school settings. A systematic review by Missiuna et al. found that occupational therapy interventions in schools can improve children's participation in school activities and academic performance [17]. Another study by Pfeiffer et al. found that occupational therapy can also be effective in promoting positive behavior and social skills in children with behavioral and emotional disorders [18]. A recent report suggested greater involvement of occupational therapists in educational settings, increasing the importance of OT Professional and its benefits would increase role in supporting children's mental health [19]. In addition, the American Occupational Therapy Association (AOTA) has developed guidelines for occupational therapy in schools that emphasize the importance of responding to each student's individual needs and working with teachers, parents, and other professionals to ensure successful participation to promote school activities [20-21]. Further, the results of this study show that there are significant differences in knowledge and awareness about occupational therapy (OT) between participating teachers from private/international schools and those from public schools. Participants from private/international schools were more likely to have knowledge of occupational therapy and to be familiar with the term occupational therapy through social media channels. This may be due to differences in access to information and resources between public and private schools [22]. However, in-depth research is needed to determine the causes of differences in knowledge and awareness of occupational therapy between public and private/intranational school participants. This may include examining differences in access to information and resources, as well as differences in training and professional development opportunities for teachers and staff in public schools compared to those in private/intranational school [3]. Interestingly, while it was also found that there were no significant differences between the two groups in their understanding of the written functions of OT, there were no significant differences in their awareness of the overall role of OT. This suggests that both groups may have a similar understanding of the general principles of OT. The study also found that there were no significant differences between the two groups in



**Senthil Vadivel et al.,**

their awareness of which types of students would benefit from occupational therapy. This suggests that both groups may have similar understandings of the potential benefits of OT for students with different needs, and it is consistent with the results of previous studies [22-23]. It is important to remember that the majority of participants reported gaining more knowledge about occupational therapy after completing the survey. This illustrates the potential of educational interventions to raise awareness and increase knowledge about occupational therapy offerings in schools, regardless of the type of school. Several studies have highlighted the potential benefits of occupational therapy in school settings, including improving students' academic performance, behavior, and social skills [17-18]. According to an earlier study, children who struggle with sensory integration and processing issues can perform better in school and participate more when there is a sensory integration intervention with OT consulting in their educational setting [24].

LIMITATIONS

This study has some limitations. First, the study sample was limited to teachers in schools in Al Ahsa city and may not be representative of all Saudi Arabian teachers. Second, self-reported data may be susceptible to social desirability bias and may not fully reflect participants' actual knowledge and awareness. Third, the underlying reasons for the differences in participants' knowledge and awareness of occupational therapy between public and private/international schools were not thoroughly examined due to the cross-sectional nature of the study.

RECOMMENDATIONS

Further research is needed to examine the reasons for the differences in knowledge and awareness of occupational therapy between public and private/international school participants. Because the study did not examine how teachers' increased knowledge and awareness of occupational therapy impacts student outcomes, future work should focus on examining these effects. The authors emphasized the urgent need to develop targeted educational interventions for teachers and staff in public schools to increase their understanding and awareness of the role of occupational therapy in Saudi schools. Additionally, promote collaboration and communication between occupational therapists, teachers, and other professionals in the school environment to promote the successful participation of all students in school activities. Promote the use of social media and other accessible health-related channels to promote greater knowledge of the role of occupational therapy in schools among teachers and staff in public schools in Saudi Arabia.

CONCLUSION

The results of this study appear to indicate that there are significant gaps in knowledge and awareness about occupational therapy between teachers in public and private/international schools in Al Ahsa city, Saudi Arabia. Teachers from private/international schools were more likely to have knowledge of occupational therapy and had become familiar with the term 'occupational therapy' through social media channels. However, both groups had the same ideas about the overall function of occupational therapy and the type of students who would benefit from occupational therapy. The study highlights the need for improved education and awareness of the role of occupational therapy in schools, particularly among public school teachers. Educational interventions aimed at improving school teachers' knowledge and awareness of occupational therapy can help increase their understanding of the potential benefits of occupational therapy for students, resulting in all students successfully participating in school activities and achieving their academic goals so that their performance, behavior and social skills improve.



Senthil Vadivel *et al.*,

ACKNOWLEDGEMENT

The authors thank the assistant professor. Raguram, Head of Department, Faculty of Occupational Therapy, Sri Ramachandra Institute of Higher Education and Research, Chennai, India, for allowing us to use his previous research survey questionnaire in our study. Authors also thank the research coordinator of the study, assistant professor Dr. Mohammad Al Mohaini, Department of Basic Sciences, College of Applied Medical Sciences, KSAU-HS, Al Ahsa, for his unwavering support and guidance from the beginning of the study to the end.

REFERENCE

1. Occupational Therapy Practice Framework: Domain and Process—Fourth Edition. Am J Occup Ther. 2020; Vol. 74(Supplement_2): 7412410010p1–7412410010p87. doi: <https://doi.org/10.5014/ajot.2020.74S2001>
2. Vadivel S, Mani P, Al Anezi N, Al Subaie MH, Al Mulhim AF, Al Mulhim MK, Al Yemeni OA. Knowledge and awareness about occupational therapy among healthcare professionals in Al-Ahsa. World Journal of Biology Pharmacy and Health Sciences. 2021;8(1):008-12.
3. Kaelin V, Ray-Kaesler S, Moiola S, Kocher Stalder C, Santinelli L, Echsel A et al. Occupational Therapy Practice in Mainstream Schools: Results from an Online Survey in Switzerland. Occupational Therapy International. 2019; 2019:1-9.
4. Benson J. School-Based Occupational Therapy Practice: Perceptions and Realities of Current Practice and the Role of Occupation. Journal of Occupational Therapy, Schools, & Early Intervention. 2013;6(2):165-178.
5. Jacobs-Nzuzi Khuabi L, Swart E, Soeker M. A Service User Perspective Informing the Role of Occupational Therapy in School Transition Practice for High School Learners with TBI: An African Perspective. Occupational Therapy International. 2019;2019:1-15.
6. Campbell WN, Missiuna CA, Rivard LM, Pollock NA. “Support for everyone”: Experiences of occupational therapists delivering a new model of school-based service. Canadian Journal of Occupational Therapy. 2012;79(1):51-9.
7. Chow J, Pickens N. Measuring the Efficacy of Occupational Therapy in End-of-Life Care: A Scoping Review. 2022.
8. Salazar Rivera J, Boyle C. The Differing Tiers of School-Based Occupational Therapy Support: A Pilot Study of Schools in England. Journal of Occupational Therapy, Schools, & Early Intervention. 2020;13(3):264-282.
9. O'Donoghue C, O'Leary J, Lynch H. Occupational Therapy Services in School-Based Practice: A Pediatric Occupational Therapy Perspective from Ireland. Occupational Therapy International. 2021; 2021:1-11.
10. Cabatan M, Grajo L, Sana E. Occupational adaptation as a lived experience: The case of Filipino occupational therapy academic educators. Journal of Occupational Science. 2020;27(4):510-524.
11. Fairbairn M, Davidson I. Teachers' Perceptions of the Role and Effectiveness of Occupational Therapists in Schools. Canadian Journal of Occupational Therapy. 1993;60(4):185-191.
12. Hassan IzzeddinSarsak. Arab healthcare professionals' knowledge and perception of occupational therapy. Sarsak Bulletin of Faculty of Physical Therapy, 2022; 27 (40): 1-6. <https://doi.org/10.1186/s43161-022-00098-4>
13. Hassan IzzeddinSarsak. Perceptions of the Occupational Therapy Profession Among Medical and Health Science Students in Saudi Arabia. Annals of International Occupational Therapy. 2020;3(2):78-83.
14. Raghuram P, Sundaresan T, Loganathan S, Achshal S. AWARENESS AND KNOWLEDGE OF OCCUPATIONAL THERAPY AMONG MAINSTREAM SCHOOL TEACHERS IN NORTH CHENNAI. Journal of Emerging Technologies and Innovative Research [Internet]. 2021;8(12). Available from: <https://www.jetir.org/papers/JETIR2112445.pdf>
15. Seoane-Martín, M.E, Rodríguez-Martínez, M.C. Potential. Role of Occupational Therapist Intervention in Elementary School for Children with Additional Support Needs: A Systematic Review. Children. 2023; 10: 1291. <https://doi.org/10.3390/children10081291>





Senthil Vadivel et al.,

16. von Zweck C, Naidoo D, Govender P, Ledgerd R. Current Practice in Occupational Therapy for COVID-19 and post-COVID-19 Conditions. *Occup Ther Int.* 2023; 2023:5886581. doi: 10.1155/2023/5886581. PMID: 37250066; PMCID: PMC10219768.
17. Guidelines for Occupational Therapy Services in Early Intervention and Schools. *Am J Occup Ther.* 2017 Nov/Dec;71(Supplement_2):7112410010p1-7112410010p10. doi: 10.5014/ajot.2017.716S01. PMID: 29308998.
18. Missiuna CA, Pollock NA, Levac DE, Campbell WN, Whalen SD, Bennett SM, Hecimovich CA, Gaines BR, Cairney J, Russell DJ. Partnering for change: An innovative school-based occupational therapy service delivery model for children with developmental coordination disorder. *Canadian Journal of Occupational Therapy.* 2012;79(1):41-50.
19. Pfirman N, Rivera C, Saffer A. Health Promotion and Wellness for All Students: School-Based Occupational Therapy as a Preventive Approach. *Am J Occup Ther.* 2023; 1;77(2):7702090010. doi: 10.5014/ajot.2023.050242. PMID: 36996456
20. Spencer B, Sherman L, Nielsen S, Thormodson K. Effectiveness of occupational therapy interventions for students with mental illness transitioning to higher education: A systematic review. *Occupational therapy in mental health.* 2018;34(2):151-64.
21. Susan M. Cahill; Stephanie Beisbier. Occupational Therapy Practice Guidelines for Children and Youth Ages 5–21 Years. *The American Journal of Occupational Therapy,* 2020; 74(4): 7404397010p1–7404397010p48. <https://doi.org/10.5014/ajot.2020.744001>
22. Jeryl D. Benson, Kimberly A. Szucs & J. J. Mejasic (2016) Teachers' perceptions of the role of occupational therapist in schools, *Journal of Occupational Therapy, Schools, & Early Intervention.* 9; 3: 290-301, DOI: 10.1080/19411243.2016.1183158
23. Edick, Jennifer, "Elementary Teachers' Perceptions of the Value of Collaboration with School-Based Occupational Therapists" (2021). *Occupational Therapy Doctorate Capstone Projects.* 73. <https://encompass.eku.edu/otdcapstones/73>
24. Whiting CC, Schoen SA, Niemeyer L. A Sensory Integration Intervention in the School Setting to Support Performance and Participation: A Multiple-Baseline Study. *Am J Occup Ther.* 2023;77(2):7702205060. doi: 10.5014/ajot.2023.050135. PMID: 37053435.

Table 1: Baseline characteristics of enrolled participants

Age group	Mean ± SD	Level of Education	N (%)
20-30 years	39 (11.1%)	Bachelor's degree	338 (96%)
31-40 years	92 (26.1%)	Master's degree & PhD	14 (4%)
41-50 years	161 (45.7%)	Type of school	
51-60 years	43 (12.2%)	Private / International	40 (11.4%)
≥ 61 years	17 (4.8%)	Public	312 (88.6%)
Sex		Currently served age groups	
Male	249 (70.7%)	High school	100 (28.4%)
Female	103 (29.3%)	Lower Primary	37 (10.5%)
Experience (years)	15.82 ± 8.24	Middle school	120 (34.1%)
Type of employment		Upper Primary	95 (27%)
Full time	312 (88.6%)		
Part-time	40 (11.4%)		





Table 2: Association between gender concerning the teachers' awareness and knowledge about the role of occupational therapy.

Variables of teacher's awareness and knowledge on Occupational therapy	Female (n= 103)	Male (n= 249)	p-value	Private/international (n= 40)	Public (n=312)	p-value
Do you know about Occupational Therapy?						
Yes	47 (45.6%)	126 (50.6%)	0.23 ^{ns}	30 (75%)	143 (45.8%)	< 0.001 ^{***}
No	56 (54.4%)	123 (49.4%)		10 (25%)	169 (54.2%)	
When did you get familiar with the term "Occupational Therapy						
During my education	10 (9.7%)	23 (9.2%)	0.95 ^{ns}	4 (10%)	29 (9.3%)	0.01*
Social media	41 (39.8%)	106 (42.6%)		25 (62.5%)	122 (39.1%)	
Through this survey	48 (46.6%)	111 (44.6%)		9 (22.5%)	150 (48.1%)	
At the work	3 (2.9%)	8 (3.2%)		1 (2.5%)	10 (3.2%)	
Other	1 (1%)	1 (0.40%)		1 (2.5%)	1 (0.30%)	
Have you ever referred a person for Occupational Therapy						
Yes	19 (18.4%)	40 (16.1%)	0.34 ^{ns}	2 (5%)	57 (18.3%)	0.02*
No	84 (81.6%)	209 (83.9%)		38 (95%)	255 (81.7%)	
What do you think an Occupational Therapist will do?						
Treat those who cannot engage in in daily activities due to injury, illness, or other conditions and assist them in acquiring, regaining, maintaining, and developing the abilities necessary for both daily living and employment.	16 (15.5%)	64 (25.7%)	0.17 ^{ns}	11 (27.5%)	69 (22.1%)	0.03*
Treatment options for patients who are injured, ill, or incapacitated including mobility exercises manual treatments, education, and counselling. OTs help patients manage their pain and avoid illness, maintaining their health and that of all age groups.	14 (13.6%)	23 (9.2%)		3 (7.5%)	34 (11%)	
Treat people who are ill, with medicines.	16 (15.5%)	35 (14.1%)		0(0)	51 (16.3%)	
All of above.	57 (55.4%)	127 (51%)		26 (65%)	158 (50.6%)	
Do you think an Occupational Therapist can work in School?						
Yes	37 (35.9%)	74 (29.7%)	0.15 ^{ns}	11 (27.5%)	100 (32.1%)	0.34 ^{ns}
No	66 (64.1%)	175 (70.3%)		29 (62.5%)	212 (67.9%)	



Senthil Vadivel *et al.*,

Have you worked with an Occupational Therapist before?						
Yes	4 (3.9%)	9 (3.6%)	0.55 ^{ns}	2 (5%)	11 (3.5%)	0.44 ^{ns}
No	99 (97.1%)	240 (97.4%)		38 (39%)	301 (96.5%)	
What is the course/program is opt for an Occupational Therapist, after schooling						
Diploma in occupational therapy or Allied Health Sciences	22 (21.4%)	43 (17.3%)	0.66 ^{ns}	5 (12.5%)	60 (19.2%)	0.01*
Bachelor in occupational therapy or Allied Health Sciences	51 (49.5%)	130 (52.2%)		15 (37.5%)	166 (53.2%)	
Master in occupational therapy or Allied Health Sciences	30 (29.1%)	76 (30.5%)		20 (50%)	86 (27.6%)	
What is the duration of the Occupational Therapy Course/program?						
2.5 years	15 (14.6%)	36 (14.5%)	0.63 ^{ns}	4 (10%)	47 (15.1%)	0.11 ^{ns}
3 years	15 (14.6%)	27 (10.8%)		4 (10%)	38 (12.2%)	
4.5 years	59 (57.3%)	141 (56.6%)		20 (50%)	180 (57.6%)	
5 years	14 (13.5%)	45 (18.1%)		12 (30%)	47 (15.1%)	
Identify the location where colleges are there to offer Occupational Therapy courses/program in the kingdom of Saudi Arabia?						
Mecca region	9 (8.7%)	20 (8%)	0.68 ^{ns}	2 (5%)	27 (8.6%)	0.06 ^{ns}
Riyadh region	24 (23.3%)	47 (18.9%)		13 (32.5%)	58 (18.6%)	
Eastern region	22 (21.4%)	49 (19.7%)		3 (7.5%)	68 (21.8%)	
All the above	48 (46.6%)	133 (53.4%)		22 (55%)	159 (51%)	

ns-no significance ($p > 0.05$); * and *** Significance ($p < 0.05$, $p < 0.001$).

Table 3: Association between gender concerning teachers' awareness about the scope of OT practice and type of students who will benefit from occupational therapy

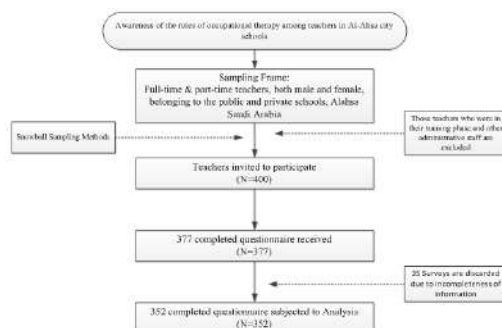
Variables of teacher's awareness about the scope of OT practice and type of students who will benefit from occupational therapy	Female (n= 103)	Male (n=249)	p-value	Private/International (n= 40)	Public (n=312)	p-value
Where do Occupational Therapists provide services (Scope of work)						
Government organizations / Institutions / Hospitals / Projects	8 (7.8%)	21 (8.4%)	0.24 ^{ns}	1 (2.5%)	28 (8.9%)	< 0.001***
Non-Government Organizations (NGOs)	5 (4.9%)	8 (3.2%)		0 (0)	13 (4.2%)	
Acute care hospitals and nursing homes are examples of private industries.	4 (3.9%)	15 (6%)		0 (0)	19 (6.1%)	
Rehabilitation centers / Clinics / De-Addiction Centers, Mental Health	14 (13.6%)	26 (10.4%)		3 (7.5%)	37 (11.9%)	



Senthil Vadivel *et al.*,

Setups etc.						
Special schools/ Mainstream Schools	10 (9.7%)	23 (9.2%)		10 (25%)	23 (7.4%)	
Community-Based Rehabilitation (CBR), Social Agencies, and Disaster Management	2 (1.9%)	1 (0.40%)		0 (0)	3 (1%)	
Projects Hospice care, Chronic care centers	8 (7.8%)	32 (12.9%)		4 (10%)	36 (11.5%)	
Industries	9 (8.7%)	7 (2.9%)		0 (0)	16 (5.1%)	
Private Practices	5 (4.9%)	14 (5.6%)		2 (5%)	17 (5.4%)	
All of the Above	38 (36.8%)	102 (41%)		20 (50%)	120 (38.5%)	
In your opinion what type of students will be benefitted from Occupational Therapy						
Children having handwriting, reading, and calculating problems	9 (8.7%)	12 (4.9%)	0.17 ^{ns}	1 (2.5%)	20 (6.4%)	0.79 ^{ns}
Children who are under stress/ Depression, low self-esteem, and other issues with mental health	7 (6.8%)	17 (6.8%)		3 (7.5%)	21 (6.7%)	
Children who are having maladaptive behavior, self-injurious and other behavioral problems	8 (7.8%)	18 (7.2%)		2 (5%)	24 (7.7%)	
Children who are having attention deficits and hyperactivity behavior problems	2 (1.9%)	14 (5.6%)		2 (5%)	14 (4.5%)	
Children who have speech and hearing deficit	2 (1.9%)	12 (4.8%)		1 (2.5%)	13 (4.2%)	
Children who have sensory problems	1 (1%)	5 (2%)		0 (0)	6 (1.9%)	
Children who have Autistic features	2 (1.9%)	3 (1.2%)		1 (2.5%)	4 (1.3%)	
Children who have poor social communication skills	7 (6.8%)	3 (1.2%)		0 (0)	10 (3.2%)	
All of the Above	65 (63.2%)	165 (66.3%)		30 (75%)	200 (64.1%)	
After the survey would you like to get more knowledge about Occupational Therapy						
Yes	81 (78.6%)	206 (82.7%)	0.25 ^{ns}	35 (87.5%)	252 (80.8%)	0.25 ^{ns}
No	22 (21.4%)	43 (17.3%)		5 (12.5%)	60 (19.2%)	

ns- no significance ($p > 0.05$), ***Significance ($p < 0.001$).

**Senthil Vadivel et al.,****Figure-1: Flow Chart showing the study methodology**



Optimizing Resilience and Goal Achievement – A Psychological Study Od Shashi Deshpande's Select Novels

G.Saratha Lakshmi*,

Assistant Professor, Department of Humanities and Languages, Sona College of Technology, Salem,
Tamil Nadu. India.

Received: 15 Feb 2024

Revised: 12 Apr 2024

Accepted: 22 May 2024

*Address for Correspondence

G.Saratha Lakshmi

Assistant Professor,
Department of Humanities and Languages,
Sona College of Technology,
Salem, Tamil Nadu. India.
Email: saratha@sonatech.ac.in



This is an Open Access Journal / article distributed under the terms of the **Creative Commons Attribution License** (CC BY-NC-ND 3.0) which permits unrestricted use, distribution, and reproduction in any medium, provided the original work is properly cited. All rights reserved.

ABSTRACT

Simon de Beauvoir statement, 'one is not born a woman one becomes one,' has a special relevance to India where conventions, religious and social taboos dictate and inhibit woman's individuality. Femininity as a cultural construct inscribes the society's view about women. ShashiDeshpande bares the subtle processes of oppression and gender differentiations operative within the institution of the family and the male centered Indian society at large. As a writer she presents feministic critiques of the patriarchal Indian society. Her art lies in selecting situations with which most Indian women can identify. ShashiDeshpande never encourages women to sacrifice their entire self for the sake of their domestic bonds. She wants them to break the shackles of the bond and enjoy the breeze of freedom, self- reliance, and financial independence.

Keywords :Regeneration, Psychology, Circumscription, Concentration, Patriarchy, Effacement, Liberation, Vigorous, Affirmations, Identity, Prejudice.

INTRODUCTION

Indian mythology depicts women as of epitome of sacrifice surrender and effacement. The heroic failures of the female ensure the victory of the males. On the contrary Deshpande very interestingly manipulates the Indian myths to create a space for women to challenge the traditions of subservience and circumscription. Women in India have been suppressed and oppressed in the name of the sugar coated words like familial bonds, motherhood, and divinity of women. Women need not be worshipped as goddesses and then burnt into ashes in the name of pathi-bhakthi. Women should emerge from the ashes in to the goddess of fire and burn the injustice against them. They don't want



**Saratha Lakshmi**

to be the epitome of sacrifice anymore. Sumi's interpretation of Sairandhri's psychology is completely new and modern which exhibits her longing for an independent life.

'Don't you think this was something she (Sairandhri) had often wanted, to be herself, to sleep alone, to be free, for a while of her five husbands? ... To have the pleasure, the liberty of being alone, her own mistress, not to have to share her bed night with a husband – yes she must have longed for it' (85-86).

Through a reorientation of the myth ShashiDeshpande suggests that a married woman may desire to enjoy an independent existence occasionally. Sumi in *A MATTER OF TIME* was never oppressed or dominated either by her husband or her father. She marries the man of her choice and challenged patriarchy. When her husband chooses to leave his family life, she never begs him to return to the family life nor dumbly accepts to pathetic condition. Immediately, she begins to build herself and her daughters and finally emerges as a woman of confident. Sumi's eldest daughter Aru discards the concept of marriage and decides to become a self-aware confident and autonomous woman. Patriarchy could not control the central female characters in the novel *A Matter of time*.

Though Gopal's desertion tumbled up the normal life of the family Sumi and her daughters gradually recovers with vigorous desire to succeed in life. They never accept inferior and pitiable position.

'The three girls have changed in themselves, too. Aru's reserve has turned in to secretiveness. She goes out a great deal, more than she did before and it is obvious that this has nothing to do with college and her studies. In fact, she has nothing to do with college or her studies. In fact, she resigned from the student council, something she had taken very seriously until now. Charu has become wholly single minded and dogged, the intensity of her pursuit of a seat in a medical college frightening. Nothing else seems to exist for her, apart from her evening classes and her books when she is at home. And though Seema belying Sumi fears, looks the most untouched, she keeps a look from her mother and sisters, following Kalyani about even holding her sari end' (59).

Deshpande's concentration was on four major issues that are indispensable for the existential affirmation of women: education, financial independence, control over her sexuality and the moral choice. She never expects a brave new world, but she insists upon the space for women to exist. If women are not allowed to affirm their existence, they will record their protest by challenging the stereotyped images of women like Mira, Urmil, Kalyani, Sumi and Aru. The success of a country or the entire human race is closely linked with woman's degeneration and regeneration. It is only a matter of time when the logic of woman's liberation has to be enforced to avoid complete social disruption. In all her novels ShashiDeshpande represents the contemporary modern women's struggle to define and attain an autonomous selfhood. As Banu.C.Shahin says, "Pain and disappointment are part of life which no one can avoid or escape and experiencing something which is not in our plan should not be considered as failure or indicators of an unorganized life" (2021). Her female protagonists are at great pain to free themselves from stultifying traditional constraints. Her concern is mainly to explore the root cause of the fragmentation and to find out what happens to the heroines in the process of achieving individuality and existential affirmations.

The identity of women is minimized in family and their separated identity is attached with their husbands and sons respectively. As Vadivu.N.says, "Dislocation today is ascribed and substantiated as the distinctive feature of humanity and not just a feature of diaspora alone." (2021) Women are threatened by the social stigma of safety and protection. There are certain social taboos prevailing in the society that completely doom the individuality of women. Women in Indian society are denied of the possibility of existential affirmation. But ShashiDeshpande's women characters have strength of their own. In spite of challenges and hostilities, they remain unraveled and unrushed. For example, Urmila in 'The Binding Vine' is dare enough to declare I am not going to





Saratha Lakshmi

break. With great courage and dauntless confidence, not only the protagonists but most of the female characters achieve self-identity and affirm existence.

According to Marxist feminist theory unfair prejudice within the society must be abolished. A social system in which all the members of the society have equal rights and power must be established. 'Religion is the opiate of masses' is the famous quote used by Karl Marx. According to this theory people rely on their beliefs as pain killers. The rulers practice those beliefs in a way that fulfill their desires. Same is the case in the patriarchal system. By quoting the traditional stories of Sita and Draupadi, women are cheated by the patriarchal system. We can see Urmi as an advocate of Marxist feminist theory when she tries getting justice to the lower class poor girl Kalpana. According to Kalpana's mother Sakuntai women are supposed to lead a submissive life. When her daughter Kalpana is raped instead fighting for justice she prefers to hide the issue. Instead of getting justice she scolds her daughter for being bold. The female characters in 'A Matter of Time' like Kalyani, Sumi, Charu and Aru are perfect examples of women who never bother about the conventional ideas of patriarchal system and fight against the traditional life imposed upon them by the society.

REFERENCES

- Alexander, J (2018). "Women Protagonists in the Select Fictional Writings of ShashiDeshpande and ManjuKapur A study."
- Anuradha Roy, Patterns of Feminist Consciousness in Indian Women Writers (New Delhi: Prestige Books, 1999), pp. 29-32.
- Banu, C. Shalin. "Excruciation and Endurance in the select works of RohintonMistry. 2021, PeriarUniversity. Phd dissertation.
- Barch G.D. 'Feminine in India's Literature' Indian Book Chronicle June 1995; pp 17-18.
- Beauvoir de Simon (1988), The Second Sex, Picador Classic Edition, London: Pen
- Daya, Shari. "Embodying modernity: reading narratives of Indian women's sexual autonomy and violation." Gender, Place & Culture 16.1 (2009): 97-110.
- Deshpande, Shashi (2003), 'Why I am a Feminist', Writing from the Margin and
- UntouchaGeorge, Rosemary M., and Rosemary Marangoly George. The politics of home: Postcolonial relocations and twentieth-century fiction. Cambridge University Press, 1996.
- Gopal, Priyamvada. The Indian bility. Rowman & Littlefield, 1997.
- Fludernik, Monika. "Carceral topography: Spatiality, liminality and corporality in the literary prison." Textual Practice 13.1 (1999): 43-77.
- Jackson, Elizabeth. Feminism and contemporary Indian women's writing. Springer, 2010.
- Jain, Jasbir. Indigenous roots of feminism: Culture, subjectivity and agency. SAGE Publications India, 2011.
- Manohar, D. Murali. Indian English Women's Fiction: A Study of Marriage, Career and Divorce. Atlantic Publishers & Dist, 2007.
- Martin, Nancy M. "Mirabai comes to America: the translation and transformation of a Saint." The Journal of Hindu Studies 3.1 (2010): 12-35.
- Vadivu, N. 'Transcultural turn of the dislocated self in The select novels of Chitra Banerjee Divakaruni, 2021, Periar University. Ph.d dissertation.





K- Algebra on Pentapartitioned Neutrosophic Sets

R.Radha^{1*} and R. K. Gayathri Devi²

¹Assistant Professor, Department of Science and Humanities, Karpagam College of Engineering, Coimbatore, (Affiliated to Anna University, Chennai), Tamil Nadu, India.

²Assistant Professor and Head, Department of Mathematics, Bishop Ambrose College, (Affiliated to Bharathiar University) Coimbatore, Tamil Nadu, India.

Received: 19 Oct 2023

Revised: 12 Mar 2024

Accepted: 24 May 2024

*Address for Correspondence

R.Radha

Assistant Professor,
Department of Science and Humanities,
Karpagam College of Engineering, Coimbatore,
(Affiliated to Anna University, Chennai),
Tamil Nadu, India.
Email: r.radha@kce.ac.in



This is an Open Access Journal / article distributed under the terms of the **Creative Commons Attribution License** (CC BY-NC-ND 3.0) which permits unrestricted use, distribution, and reproduction in any medium, provided the original work is properly cited. All rights reserved.

ABSTRACT

A Pentapartitioned neutrosophic set (PNS) is a powerful structure where we have five components Truth, Falsity, Ignorance, Contradiction and unknown. And also it generalizes the concept of fuzzy, intuitionistic and neutrosophic set. In this paper we have proposed the concept of K-algebras on Pentapartitioned neutrosophic set, level subset of PNS and studied some of the results.

Keywords: Pentapartitioned Neutrosophic Set (PNS), K-algebras, Pentapartitioned Neutrosophic K-algebra

INTRODUCTION

Dar and Akram [12] proposed a novel logical algebra known as K-algebra. The algebraic structure of a group G which K-algebra was built on should have a right identity element and satisfy the properties of non-commutative and non-associative. Furthermore this group G is of the type where each non-identity element is not of order 2 and K-algebra was built by adjoining the induced binary operation on G [11,12,13]. Zadeh's [25] fuzzy set theory was a powerful framework which deals the concept of uncertainty, imprecision and also it represented by membership function which lies in a unit interval of $[0,1]$. Fuzzy K-algebra was introduced by Akram et.al [2,3,5] and also they established this in a wide-reaching way through other researchers. When fuzzy set was broadened, a new set called Intuitionistic fuzzy set which was introduced by Atanasov [9] in 1983. It has an additional degree called the degree of nonmembership. Intuitionistic fuzzy K-subalgebras was proposed by Akram et al. [4,6]. Intuitionistic Fuzzy Ideals of BCK-Algebras was proposed by Y.B.Jun, K.H.Kim[14]





Radha and Gayathri Devi

Neutrosophic set which is a generalization of fuzzy set and intuitionistic fuzzy set was introduced by Smarandache[20] in 1998. Akram et al.[8] studied K-algebras on single valued neutrosophic sets and also discussed homomorphisms between the single valued neutrosophic K-subalgebras. Belnap[10] introduced the concept of five valued logic that is the information are represented by five components T,F,None,Both which denotes true, false, neither true nor false, both true and false and unknown respectively. Based on this concept Smarandache proposed five numerical valued neutrosophic logic where indeterminacy is splitted into three terms known as Contradiction(C) and Unknown(U) and unknown(G). The concept of Pentapartitioned Neutrosophic Pythagorean Sets was introduced by R. Radha and A. Stanis Arul Mary. Fuzzy K-algebra was introduced by Akram et.al [2,3,5] and also they established this in a wide-reaching way through other researchers. The concept of Quadripartitioned Neutrosophic Pythagorean sets and K- algebra on the respective set was initiated by R. Radha and A. Stanis Arul Mary. In this paper, we extend the concepts to Pentapartitioned Neutrosophic Pythagorean Sets. Rama Malik and Surpathi Pranamik [22] introduced pentapartitioned neutrosophic set and its properties.

Neutrosophic set which is a generalization of fuzzy set and intuitionistic fuzzy set was introduced by Smarandache[23] in 1998. In addition to membership and non membership function neutrosophic set has one more extra component called indeterminacy membership function. Also all the values of these three components lies in the real standard or non-standard subset of unit interval $] -0, 1+ [$ where $-0 = 0 - \epsilon$, $1+ = 1 + \epsilon$, ϵ is an infinitesimal number. Algebraic structures applied in Neutrosophic set theory[7] and it has immense applications in different disciplines. A. A. A. Agboola, B. Davvaz[1] presented the introduction to neutrosophic BCI/BCK algebras. Smarandache and Wang et al. [21] introduced single-valued neutrosophic set which plays a vital place in many real life problems and it takes the values from the subset of $[0,1]$. Akram et al.[8] studied K-algebras on single valued neutrosophic sets and also discussed homomorphisms between the single valued neutrosophic K-subalgebras. Belnap[10] introduced the concept of five valued logic that is the information are represented by five components T,F,None,Both which denotes true,false, neither true nor false, both true and false and unknown respectively. Based on this concept Smarandache proposed five numerical valued neutrosophic logic where indeterminacy is splitted into three terms known as Contradiction(C) and Unknown(U) and unknown(G). RajashiChatterjee, et al[19] introduced Quadripartitioned Single Valued Neutrosophic(QSVN) set in which we have four components T,C,U and F respectively and also it lies in the real unit interval of $[0,1]$. R. Radha and A. Stanis Arul Mary [15-18] introduced the concept of Pentapartitioned neutrosophic Pythagorean Sets and topological space. The concept of heptapartitioned neutrosophic sets was introduced by us. The Quadripartitioned Neutrosophic Pythagorean set on K- algebra has been initiated by us. In this paper, we have studied the concept of Pentapartitioned Neutrosophic K-algebra and discussed some of its properties.

Preliminaries

Definition 2.1[12] Let (G, \cdot, \odot, e) be a group in which each non-identity element is not of order 2. Then a K-algebra is a structure $K = (G, \cdot, \odot, e)$ on a group G in which induced binary operation $\odot: G \times G \rightarrow G$ is defined by $\odot(x, y) = xy^{-1}$ and satisfies the following axioms:

- (i) $(x \odot y) \odot (x \odot z) = (x \odot ((e \odot z) \odot (e \odot y))) \odot x$,
- (ii) $x \odot (x \odot y) = (x \odot (e \odot y)) \odot x$,
- (iii) $x \odot x = e$,
- (iv) $x \odot e = x$,
- (v) $e \odot x = x^{-1}$, for all $x, y, z \in G$.

Definition 2.2[8] A single-valued neutrosophic set $A = (T_A, I_A, F_A)$ in a K-algebra K is called a single-valued neutrosophic K-subalgebra of K if it satisfies the following conditions:

- (i) $T_A(s \odot t) \geq \min\{T_A(s), T_A(t)\}$,
 - (ii) $I_A(s \odot t) \geq \min\{I_A(s), I_A(t)\}$,
 - (iii) $F_A(s \odot t) \leq \max\{F_A(s), F_A(t)\}$, for all $s, t \in G$.
- Note that $T_A(e) \geq T_A(s)$, $I_A(e) \geq I_A(s)$, $F_A(e) \leq F_A(s)$, for all $s \in G$.





Radha and Gayathri Devi

Definition 2.3[22]

Let P be a non-empty set. A Pentapartitioned Neutrosophic set $PNS A$ over P characterizes each element p in P by a truth-membership function T_A , a contradiction membership function C_A , an ignorance membership function G_A , unknown membership function U_A and a falsity membership function F_A , such that for each $p \in P$,

$$0 \leq T_A + C_A + U_A + G_A + F_A \leq 5$$
Pentapartitioned Neutrosophic K-subalgebra**Definition 3.1**

A Pentapartitioned Neutrosophic set $M = (A1_M, A2_M, A3_M, A4_M, A5_M)$ in a K -algebra K is called a Pentapartitioned neutrosophic K -subalgebra of K if it satisfies the following conditions.

(i) $A1_M(e) \geq A1_M(u)$, $A2_M(e) \geq A2_M(u)$, $A3_M(e) \leq A3_M(u)$, $A4_M(e) \leq A4_M(u)$ and $A5_M(e) \leq A5_M(u)$ for all $u \in G$.

(ii) $A1_M(u \odot v) \geq \min \{A1_M(u), A1_M(v)\}$

(iii) $A2_M(u \odot v) \geq \min \{A2_M(u), A2_M(v)\}$

(iv) $A3_M(u \odot v) \leq \min \{A3_M(u), A3_M(v)\}$

(v) $A4_M(u \odot v) \leq \min \{A4_M(u), A4_M(v)\}$

(vi) $A5_M(u \odot v) \leq \min \{A5_M(u), A5_M(v)\}$

Example 3.1

Let $M = (A1_M, A2_M, A3_M, A4_M, A5_M)$ is the cyclic group of order five in a K -algebra $K = (G, \cdot, \odot, e)$. The Cayley's table for \odot is given as follows.

\odot	E	g	g^2	g^3	g^4
E	E	g^4	g^3	g^2	G
G	G	e	g^4	g^3	g^2
g^2	g^2	g	e	g^4	g^3
g^3	g^3	g^2	g	E	g^4
g^4	g^4	g^3	g^2	G	E

We define a PNP set in K -algebra as follows.

$A1_M(e) = 0.5$, $A2_M(e) = 0.4$, $A3_M(e) = 0.1$, $A4_M(e) = 0.3$, $A5_M(e) = 0.2$,

$A1_M(u) = 0.1$, $A2_M(u) = 0.2$, $A3_M(u) = 0.4$, $A4_M(u) = 0.5$, $A5_M(u) = 0.3$

for all $u \neq e \in G$. Clearly it shows that $M = (A1_M, A2_M, A3_M, A4_M, A5_M)$ is a PNP K -algebras of K .

Proposition 3.1

If $M = (A1_M, A2_M, A3_M, A4_M, A5_M)$ denotes a Pentapartitioned neutrosophic K -algebras of K then,

a) $(\forall u, v \in G), (A1_M(u \odot v) = A1_M(v) \Rightarrow A1_M(u) = A1_M(e))$
 $(\forall u, v \in G), (A1_M(u) = A1_M(e) \Rightarrow A1_M(u \odot v) \geq A1_M(v))$

b) $(\forall u, v \in G), (A2_M(u \odot v) = A2_M(v) \Rightarrow A2_M(u) = A2_M(e))$
 $(\forall u, v \in G), (A2_M(u) = A2_M(e) \Rightarrow A2_M(u \odot v) \geq A2_M(v))$

c) $(\forall u, v \in G), (A3_M(u \odot v) = A3_M(v) \Rightarrow A3_M(u) = A3_M(e))$
 $(\forall u, v \in G), (A3_M(u) = A3_M(e) \Rightarrow A3_M(u \odot v) \leq A3_M(v))$

d) $(\forall u, v \in G), (A4_M(u \odot v) = A4_M(v) \Rightarrow A4_M(u) = A4_M(e))$
 $(\forall u, v \in G), (A4_M(u) = A4_M(e) \Rightarrow A4_M(u \odot v) \geq A4_M(v))$

e) $(\forall u, v \in G), (A5_M(u \odot v) = A5_M(v) \Rightarrow A5_M(u) = A5_M(e))$





Radha and Gayathri Devi

$$(\forall u, v \in G), (A5_M(u) = A5_M(v) \Rightarrow A5_M(u \odot v) \geq A5_M(v))$$

Proof :

We only prove (a) and (c). (b) (d) and (e) proved in a similar way.

(a) First we assume that $A1_M(u \odot v) = A1_M(v) \forall u, v \in G$. Put $v = e$ and by Definition we get $A1_M(u) = A1_M(u \odot e) = A1_M(e)$. Let for $u, v \in G$ be such that $A1_M(u) = A1_M(e)$ then, $A1_M(u \odot v) \geq \min\{A1_M(u), A1_M(v)\} = \min\{A1_M(e), A1_M(v)\} = A1_M(v)$.

Now to prove (c) consider that $A3_M(u \odot v) = A3_M(v) \forall u, v \in G$. Put $v = e$ and by Definition, we have $A3_M(u) = A3_M(u \odot e) = A3_M(e)$. Let for $u, v \in G$ be such that $A3_M(u) = A3_M(e)$ then, $A3_M(u \odot v) \leq \max\{A3_M(u), A3_M(v)\} = \max\{A3_M(e), A3_M(v)\} = A3_M(v)$. Hence the proof.

Definition 3.2

Let $M = (A1_M, A2_M, A3_M, A4_M, A5_M)$ be a Pentapartitioned neutrosophic set in a K-algebra of K and let $(\lambda, \mu, \vartheta, \xi, \varphi) \in [0,1] \times [0,1] \times [0,1] \times [0,1] \times [0,1]$ with $\lambda + \mu + \vartheta + \xi + \varphi \leq 5$. Then the sets,

$$M_{(\lambda, \mu, \vartheta, \xi, \varphi)} = \{u \in G | A1_M(u) \geq \lambda, A2_M(u) \geq \mu, A3_M(u) \leq \vartheta, A4_M(u) \leq \xi, A5_M(u) \leq \varphi\},$$

$M_{(\lambda, \mu, \vartheta, \xi, \varphi)} = U(A1_M, \lambda) \cap U'(A2_M, \mu) \cap L(A3_M, \vartheta) \cap L'(A4_M, \xi) \cap L''(A5_M, \varphi)$ are called $(\lambda, \mu, \vartheta, \xi, \varphi)$ level subsets of Pentapartitioned neutrosophic set M.

And also the set $M_{(\lambda, \mu, \vartheta, \xi, \varphi)} = \{u \in G | A1_M(u) > \lambda, A2_M(u) > \mu, A3_M(u) < \vartheta, A4_M(u) < \xi, A5_M(u) < \varphi\}$ is known as strong $(\lambda, \mu, \vartheta, \xi, \varphi)$ level subset of M.

Note: The set of all $(\lambda, \mu, \vartheta, \xi, \varphi) \in Im(A1_M) \times Im(A2_M) \times Im(A3_M) \times Im(A4_M) \times Im(A5_M)$ is known as image of M = $(A1_M, A2_M, A3_M, A4_M, A5_M)$

Proposition 3.2

If $M = (A1_M, A2_M, A3_M, A4_M, A5_M)$ is a Pentapartitioned neutrosophic K-algebra of K then the level subsets,

$$U(A1_M, \lambda) = \{u \in G | A1_M(u) \geq \lambda\}, U'(A2_M, \mu) = \{u \in G | A2_M(u) \geq \mu\},$$

$$L(A3_M, \vartheta) = \{u \in G | A3_M(u) \leq \vartheta\}, L'(A4_M, \xi) = \{u \in G | A4_M(u) \leq \xi\} \text{ and } L''(A5_M, \varphi) = \{u \in G | A5_M(u) \leq \varphi\}$$

are K-subalgebras of K for every $(\lambda, \mu, \vartheta, \xi, \varphi) \in Im(A1_M) \times Im(A2_M) \times Im(A3_M) \times Im(A4_M) \times Im(A5_M) \subseteq$

$[0,1]$ where $m(A1_M), Im(A2_M), Im(A3_M), Im(A4_M)$ and $Im(A5_M)$ are sets of values

$A1(M), A2(M), A3(M), A4(M)$ and $A5(M)$ respectively.

Proof :

Let $M = (A1_M, A2_M, A3_M, A4_M, A5_M)$ be a Pentapartitioned neutrosophic set in a K-algebra of K and $(\lambda, \mu, \vartheta, \xi, \varphi) \in Im(A1_M) \times Im(A2_M) \times Im(A3_M) \times Im(A4_M) \times Im(A5_M)$ be such that $U(A1_M, \lambda) \neq \emptyset, U'(A2_M, \mu) \neq \emptyset, L(A3_M, \vartheta) \neq \emptyset, L'(A4_M, \xi) \neq \emptyset$ and $L''(A5_M, \varphi) \neq \emptyset$. We have to show that U, U', L, L' and L'' are level

K-subalgebras. Let for $u, v \in U(A1_M, \lambda)$, $A1_M(u) \geq \lambda$ and $A1_M(v) \geq \lambda$. By definition, we get $A1_M(u \odot v) \geq \min\{A1_M(u), A1_M(v)\} \geq \lambda$. It shows that $u \odot v \in U(A1_M, \lambda)$. Hence $U(A1_M, \lambda)$ is a level K-subalgebra of K. Similarly we can prove for $U'(A2_M, \mu), L(A3_M, \vartheta), L'(A4_M, \xi)$ and $L''(A5_M, \varphi)$.

Theorem 3.1

Let $M = (A1_M, A2_M, A3_M, A4_M, A5_M)$ be a Pentapartitioned neutrosophic set in a K-algebra of K. Then $M = (A1_M, A2_M, A3_M, A4_M, A5_M)$ is a Pentapartitioned neutrosophic K-sub algebra of K if and only if $M_{(\lambda, \mu, \vartheta, \xi, \varphi)}$ is a K-subalgebra of K for every $(\lambda, \mu, \vartheta, \xi, \varphi) \in Im(A1_M) \times Im(A2_M) \times Im(A3_M) \times Im(A4_M) \times Im(A5_M)$ with $\lambda + \mu + \vartheta + \xi + \varphi \leq 5$.

Proof:

First assume that $M_{(\lambda, \mu, \vartheta, \xi, \varphi)}$ is a K-subalgebra of K. If the conditions in Definition 3.1 fails then there exist $s, t \in G$ such that,

$$A1_M(s \odot t) < \min\{A1_M(s), A1_M(t)\}$$

$$A2_M(s \odot t) < \min\{A2_M(s), A2_M(t)\}$$

$$A3_M(s \odot t) > \max\{A3_M(s), A3_M(t)\}$$

$$A4_M(s \odot t) > \max\{A4_M(s), A4_M(t)\}$$





Radha and Gayathri Devi

$$A5_M(s \odot t) > \max\{A5_M(s), A5_M(t)\}$$

$$\text{Now let } \lambda_1 = \frac{1}{2}(A1_M(s \odot t) + \min\{A1_M(s), A1_M(t)\}),$$

$$\mu_1 = \frac{1}{2}(A2_M(s \odot t) + \min\{A2_M(s), A2_M(t)\}),$$

$$\vartheta_1 = \frac{1}{2}(A3_M(s \odot t) + \max\{A3_M(s), A3_M(t)\}),$$

$$\xi_1 = \frac{1}{2}(A4_M(s \odot t) + \max\{A4_M(s), A4_M(t)\})$$

$$\varphi_1 = \frac{1}{2}(A5_M(s \odot t) + \max\{A5_M(s), A5_M(t)\})$$

Now we have,

$$A1_M(s \odot t) < \lambda_1 < \min\{A1_M(s), A1_M(t)\}$$

$$A2_M(s \odot t) < \mu_1 < \min\{A2_M(s), A2_M(t)\}$$

$$A3_M(s \odot t) > \vartheta_1 > \max\{A3_M(s), A3_M(t)\}$$

$$A4_M(s \odot t) > \xi_1 > \max\{A4_M(s), A4_M(t)\}$$

$$A5_M(s \odot t) > \varphi_1 > \max\{A5_M(s), A5_M(t)\}$$

This implies that $s, t \in X_{(\lambda, \mu, \vartheta, \xi, \varphi)}$ and $s \odot t \notin X_{(\lambda, \mu, \vartheta, \xi, \varphi)}$ which is a contradiction. This proves that the conditions of Definition 3.1 is true. Hence $M = (A1_M, A2_M, A3_M, A4_M, A5_M)$ is a Pentapartitioned neutrosophic K-sub algebra of K.

Now assume that $M = (A1_M, A2_M, A3_M, A4_M, A5_M)$ be a Pentapartitioned neutrosophic K-subalgebra of K. Let for $(\lambda, \mu, \vartheta, \xi, \varphi) \in \text{Im}(A1_M) \times \text{Im}(A2_M) \times \text{Im}(A3_M) \times \text{Im}(A4_M) \times \text{Im}(A5_M)$ with $\lambda + \mu + \vartheta + \xi + \varphi \leq 5$ such that $M_{(\lambda, \mu, \vartheta, \xi, \varphi)} \neq \emptyset$. Let $u, v \in M_{(\lambda, \mu, \vartheta, \xi, \varphi)}$ be such that,

$$A1_M(u) \geq \lambda, A1_M(v) \geq \lambda',$$

$$A2_M(u) \geq \mu, A2_M(v) \geq \mu',$$

$$A3_M(u) \leq \vartheta, A3_M(v) \leq \vartheta',$$

$$A4_M(u) \leq \xi, A4_M(v) \leq \xi',$$

$$A5_M(u) \leq \varphi, A5_M(v) \leq \varphi'$$

Now assume that $\lambda \leq \lambda', \mu \leq \mu', \vartheta \geq \vartheta', \xi \geq \xi'$ and $\varphi \geq \varphi'$. It follows from Definition 3.1 that,

$$A1_M(u \odot v) \geq \lambda = \min\{A1_M(u), A1_M(v)\},$$

$$A2_M(u \odot v) \geq \mu = \min\{A2_M(u), A2_M(v)\},$$

$$A3_M(u \odot v) \leq \vartheta = \max\{A3_M(u), A3_M(v)\},$$

$$A4_M(u \odot v) \leq \xi = \max\{A4_M(u), A4_M(v)\}$$

$$A5_M(u \odot v) \leq \varphi = \max\{A5_M(u), A5_M(v)\}$$

This shows that $u \odot v \in M_{(\lambda, \mu, \vartheta, \xi, \varphi)}$. Hence $M_{(\lambda, \mu, \vartheta, \xi, \varphi)}$ is a K-subalgebra of K.

Theorem 3.2

Let $M = (A1_M, A2_M, A3_M, A4_M, A5_M)$ be a Pentapartitioned neutrosophic K-subalgebra and $(\lambda_1, \mu_1, \vartheta_1, \xi_1, \varphi_1), (\lambda_2, \mu_2, \vartheta_2, \xi_2, \varphi_2) \in \text{Im}(A1_M) \times \text{Im}(A2_M) \times \text{Im}(A3_M) \times \text{Im}(A4_M) \times \text{Im}(A5_M)$ with $\lambda_i + \mu_i + \vartheta_i + \xi_i + \varphi_i \leq 5$ for $i = 1, 2$. Then $M_{(\lambda_1, \mu_1, \vartheta_1, \xi_1, \varphi_1)} = M_{(\lambda_2, \mu_2, \vartheta_2, \xi_2, \varphi_2)}$ if $(\lambda_1, \mu_1, \vartheta_1, \xi_1, \varphi_1) = (\lambda_2, \mu_2, \vartheta_2, \xi_2, \varphi_2)$.

Proof:

When $(\lambda_1, \mu_1, \vartheta_1, \xi_1, \varphi_1) = (\lambda_2, \mu_2, \vartheta_2, \xi_2, \varphi_2)$ then the result is obvious for $M_{(\lambda_1, \mu_1, \vartheta_1, \xi_1, \varphi_1)} = M_{(\lambda_2, \mu_2, \vartheta_2, \xi_2, \varphi_2)}$. Conversely assume that $M_{(\lambda_1, \mu_1, \vartheta_1, \xi_1, \varphi_1)} = M_{(\lambda_2, \mu_2, \vartheta_2, \xi_2, \varphi_2)}$. Since $(\lambda_1, \mu_1, \vartheta_1, \xi_1, \varphi_1) \in \text{Im}(A1_M) \times \text{Im}(A2_M) \times \text{Im}(A3_M) \times \text{Im}(A4_M) \times \text{Im}(A5_M)$ there exists $u \in G$ such that $A1_M(u) = \lambda_1, A2_M(u) = \mu_1, A3_M(u) = \vartheta_1, A4_M(u) = \xi_1$

and $A5_M(u) = \varphi_1$. This implies that $u \in X_{(\lambda_1, \mu_1, \vartheta_1, \xi_1, \varphi_1)} = X_{(\lambda_2, \mu_2, \vartheta_2, \xi_2, \varphi_2)}$.

Hence $\lambda_1 = A1_M(u) \geq \lambda_2, \mu_1 = A2_M(u) \geq \mu_2, \vartheta_1 = A3_M(u) \leq \vartheta_2, \xi_1 = A4_M(u) \leq \xi_2$ and $\varphi_1 = A5_M(u) \leq \varphi_2$. Also $(\lambda_2, \mu_2, \vartheta_2, \xi_2, \varphi_2) \in \text{Im}(A1_M) \times \text{Im}(A2_M) \times \text{Im}(A3_M) \times \text{Im}(A4_M) \times \text{Im}(A5_M)$ there exists $v \in G$ such that $A1_M(v) = \lambda_2, A2_M(v) = \mu_2$





Radha and Gayathri Devi

$A3_M(v) = \vartheta_2$, $A4_M(v) = \xi_2$, $A5_M(v) = \varphi_2$ and . This implies that $v \in X_{(\lambda_2, \mu_2, \vartheta_2, \xi_2, \varphi_2)} = X_{(\lambda_1, \mu_1, \vartheta_1, \xi_1, \varphi_1)}$. Hence $\lambda_2 = A1_M(v) \geq \lambda_1$, $\mu_2 = A2_M(v) \geq \mu_1$, $\vartheta_2 = A3_M(v) \leq \vartheta_1$, $\xi_2 = A4_M(v) \leq \xi_1$ and $\varphi_2 = A5_M(v) \leq \varphi_1$. Hence $(\lambda_1, \mu_1, \vartheta_1, \xi_1, \varphi_1) = (\lambda_2, \mu_2, \vartheta_2, \xi_2, \varphi_2)$.

Theorem 3.3

Let I be a K-subalgebra of K-algebra K . Then there exists a Pentapartitioned neutrosophic K-subalgebra $M = (A1_M, A2_M, A3_M, A4_M, A5_M)$ of K-algebra K such that $M = (A1_M, A2_M, A3_M, A4_M, A5_M) = I$ for some $\lambda, \mu \in (0,1]$ and $\vartheta, \xi, \varphi \in [0,1]$

Proof :

Let $M = (A1_M, A2_M, A3_M, A4_M, A5_M)$ be a Pentapartitioned neutrosophic set in K-algebra K given by,

$$\begin{aligned} A1_M(u) &= \begin{cases} \lambda \in (0,1], & \text{if } u \in I \\ 0, & \text{otherwise} \end{cases} \\ A2_M(u) &= \begin{cases} \mu \in (0,1], & \text{if } u \in I \\ 0, & \text{otherwise} \end{cases} \\ A3_M(u) &= \begin{cases} \vartheta \in [0,1), & \text{if } u \in I \\ 0, & \text{otherwise} \end{cases} \\ A4_M(u) &= \begin{cases} \xi \in [0,1), & \text{if } u \in I \\ 0, & \text{otherwise} \end{cases} \\ A5_M(u) &= \begin{cases} \varphi \in [0,1), & \text{if } u \in I \\ 0, & \text{otherwise} \end{cases} \end{aligned}$$

Let $u, v \in G$. If $u, v \in I$ then $u \odot v \in I$ and so,

$$\begin{aligned} A1_M(u \odot v) &\geq \min\{A1_M(u), A1_M(v)\}, \\ A2_M(u \odot v) &\geq \min\{A2_M(u), A2_M(v)\}, \\ A3_M(u \odot v) &\leq \max\{A3_M(u), A3_M(v)\}, \\ A4_M(u \odot v) &\leq \max\{A4_M(u), A4_M(v)\}, \\ A5_M(u \odot v) &\leq \max\{A5_M(u), A5_M(v)\} \end{aligned}$$

Suppose $u \notin I$ or $v \notin I$ then,

$$\begin{aligned} A1_M(u) &= 0 \text{ or } A1_M(v) = 0, A2_M(u) = 0 \text{ or } A2_M(v) = 0, A3_M(u) = 0 \text{ or } A3_M(v) = 0, \\ A4_M(u) &= 0 \text{ or } A4_M(v) = 0 \text{ and } A5_M(u) = 0 \text{ or } A5_M(v) = 0 \end{aligned}$$

It implies that,

$$\begin{aligned} A1_M(u \odot v) &\geq \min\{A1_M(u), A1_M(v)\}, \\ A2_M(u \odot v) &\geq \min\{A2_M(u), A2_M(v)\}, \\ A3_M(u \odot v) &\leq \max\{A3_M(u), A3_M(v)\}, \\ A4_M(u \odot v) &\leq \max\{A4_M(u), A4_M(v)\}, \\ A5_M(u \odot v) &\leq \max\{A5_M(u), A5_M(v)\} \end{aligned}$$

Hence $M = (A1_M, A2_M, A3_M, A4_M, A5_M)$ is a Pentapartitioned neutrosophic K-subalgebra of K .

Consequently $X_{(\lambda, \mu, \vartheta, \xi, \varphi)} = I$

Theorem 3.4

Let K be a K-algebra. Let a chain of K-subalgebras: $X_0 \subset X_1 \subset X_2 \subset \dots \subset X_n = G$. Then the level K-subalgebras of the pentapartitioned neutrosophic K-subalgebra remains same as the K-subalgebras of this chain.

CONCLUSIONS

Need of algebra in today's life is more important since it plays a vital role without even recognizing it. Algebraic thinking helps us to solve the real-world problems in a logical way. Recently K-algebra applied in fuzzy set, intuitionistic fuzzy set and single valued neutrosophic set which helps us to extend the concept to K-algebra on





Radha and Gayathri Devi

Pentapartitioned neutrosophic sets. In this paper we have studied K-algebras on Pentapartitioned single valued neutrosophic sets and studied some of the results. This section is not mandatory, but can be added to the manuscript if the discussion is unusually long or complex.

Funding: "This research received no external funding"

Conflicts of Interest: "The authors declare no conflict of interest."

REFERENCES

1. A. A. A. Agboola, B. Davvaz, Introduction to neutrosophic BCI/BCKalgebras, International Journal of Mathematics and Mathematical Sciences, Article ID 370267, (2015) 1-6.
2. M. Akram, K. H. Dar, Generalized fuzzy K-algebras, VDM Verlag Dr. Miller, 2010, ISBN-13: 978-363927095.
3. M. Akram, K. H. Dar, Y. B. Jun, E. H. Roh, Fuzzy structures of $K(G)$ algebra, Southeast Asian Bulletin of Mathematics, 31 (2007), 625-637.
4. M. Akram, K. H. Dar, B.L.Meng, K. P. Shum, Interval-valued intuitionistic fuzzy ideals of K-algebras, Wseas Transactions on Mathematics, ISSN: 1109-2769, Issue 9, Vol.7,(2008)
5. M. Akram, K. H. Dar, P. K. Shum, Interval-valued (α, β) -fuzzy K-algebras, Applied Soft Computing, 11 (2011), 1213-1222.
6. M. Akram, B. Davvaz, F. Feng, Intuitionistic fuzzy soft K-algebras, Mathematics in Computer Science, 7 (2013), 353-365.
7. M.Akram, H.Gulzar, Smarandache, Neutrosophic Soft Topological K-Algebras, Neutrosophic Sets and Systems, Vol.25(2019), 104-124
8. M.Akram, H.Gulzar, K. P. Shum, Certain notions of single-valued neutrosophic K-algebras, Italian Journal Of Pure And Applied Mathematics – N.42–2019 (271–289)
9. K Atanassov (1986) Intuitionistic Fuzzy Sets, Fuzzy Sets and Systems.20, 87-96.
10. N D Belnap Jr. (1977) A useful four valued logic, Modern Uses of Multiple Valued Logic, 9–37.
11. K.H. Dar, M. Akram, Characterization of a $K(G)$ -algebra by self maps, Southeast Asian Bulletin of Mathematics, 28 (2004), 601-610.
12. K.H. Dar, M. Akram, On a K-algebra built on a group, Southeast Asian Bulletin of Mathematics, 29 (2005), 41-49.
13. K.H. Dar, M. Akram, On K-homomorphisms of K-algebras, International Mathematical Forum, 46 (2007), 2283-2293.
14. Y.B.Jun, K.H.Kim, Intuitionistic Fuzzy Ideals of BCK-Algebras, Internat.J.Math.&Math.Sci, Vol.24, No.12(2000) 839-849.
15. R. Radha , A. Stanis Arul Mary, PentapartitionedNeutrosophic Pythagorean sets, International Research Journal on Advanced Science Hub, volume3,025 February2021,62-68.
16. R. Radha , A.. Stanis Arul Mary, PentapartitionedNeutrosophic Pythagorean soft sets, International Research Journal of Mathematics in Engineering Technology and Science,volume3,Issue2,906-913
17. R. Radha ,A. Stanis Arul Mary, HeptapartitionedNeutrosophic sets, International Journal of creative research thoughts,volume9,Issue2,222-230
18. R. Radha , A..Stanis Arul Mary, K- algebra on PentapartitionedNeutrosophicpythagorean sets AIP Proceedings (Accepted)
19. R. Radha , A.Stanis Arul Mary, Neutrosophic Pythagorean Soft Set, Neutrosophic sets and systems,volume42,62-78.
20. R. Radha, A. Stanis Arul Mary. PentapartitionedNeutrosophicpythagorean Lie algebra,(Accepted)
21. R. Radha, A.Stanis Arul Mary, Improved Correlation Coefficients of Pentapartitionedneutrosophic Pythagorean sets using MADM,(Communicated)
22. Rama Malik, SurpatiPranamik, PentapartitionedNeutrosophic sets and its properties, Neutrosophic sets and systems,vol36, 2020





Radha and Gayathri Devi

23. F Smarandache (1999), A Unifying Field in Logics. Neutrosophy: Neutrosophic Probability, Set and Logic, American Research Press, Rehoboth.
24. H Wang , F Smarandache, YQ Zhang, R Sunderraman(2010) Single valued neutrosophic sets, MultispaceMultistruct 4:410-413.
25. L A Zadeh(1965), Fuzzy sets, Inf. Control 8, 338-353.





Heart Disease Prediction using Machine Learning and Multi Agent Systems

Chandanita Thakur¹, Shibakali Gupta and Somsubhra Gupta³

¹Research Scholar, Department of Computer Science and Engineering, Swami Vivekananda University, Barrackpore, West Bengal, India.

²Assistant Professor, Department of Computer Science and Engineering, University Institute of Technology, Burdwan, West Bengal, India.

³Professor and Dean of Science, Department of Computer Science and Engineering Swami Vivekananda University, Barrackpore, West Bengal, India.

Received: 28 May 2024

Revised: 1 Jun 2024

Accepted: 03 Jun 2024

*Address for Correspondence

Chandanita Thakur

Research Scholar,

Department of Computer Science and Engineering,

Swami Vivekananda University,

Barrackpore, West Bengal, India.

Email: thakur.chandanita@gmail.com



This is an Open Access Journal / article distributed under the terms of the **Creative Commons Attribution License** (CC BY-NC-ND 3.0) which permits unrestricted use, distribution, and reproduction in any medium, provided the original work is properly cited. All rights reserved.

ABSTRACT

Early detection of Heart disease can prevent the death rate. Early detection depends on the analysis and prediction of the assortment of different parameters responsible for that disease. Health care industries have already accumulated enormous data. Scientists and researchers have paid their best attention to extract insights from the medical data by using Data Mining or Machine Learning. Different Machine Learning Techniques have helped Medical Science to achieve different levels of accuracy. There are different Machine Learning Algorithms to achieve accuracy but implementation of Multi Agent approach incorporated with Machine Learning Algorithm is an innovative approach in the field of Artificial Intelligence. To improve accuracy, the present research work has used a hybrid dataset which is a combination of five standard datasets. Objective of the present paper is to apply a Multi Agent System with Machine Learning Algorithm and Execution of Machine Learning Algorithm using Intelligent Agent. The present paper concentrates on Twenty Six different machine learning Algorithms applied on Heart Disease dataset for flawless prediction of Heart Disease, its Accuracy, Balance Accuracy, ROC-AUC, F1-Score etc. The present paper attempts to predict heart disease using "Twenty Six" different Machine Learning Algorithms implemented by Agent and predicted Heart Disease with 93.8% accuracy. The paper also concentrates on development of the Multi Agent System and training it with the Best fit (Among Twenty-Six Machine Learning Algorithms) Algorithm. Agents in the newly created Multi Agent System have predicted the possibility of heart disease with an Accuracy of 96.8% approximately. The



**Chandanita Thakur et al.,**

complete work has been implemented using Python (Jupyter Notebook). Implementation of Multi Agent System with Machine Learning Algorithm is the novelty of the present research work which can explore a new era in the Field of Artificial Intelligence.

Keywords: Multi Agent System(MAS), Agent ,Machine Learning Algorithms, Accuracy, Heart Disease

INTRODUCTION

There are several works in the literature of Machine Learning where the Heart Disease detection Accuracy is predicted. Several authors have used a maximum four to five Machine Learning algorithms for prediction of accuracy of Heart Disease. But Multi Agent System is not been implemented using python for prediction and improvement of accuracy along with Machine Learning Algorithms. Intelligent Agent is not used to implement each Machine Learning algorithm using python. Almost all the previous literatures have worked on a standard dataset. But different datasets can also be shuffled and merged to achieve better accuracy. To meet the above mentioned gap in literature the present work has merged five different datasets to accomplish higher accuracy. An Additional essence of this research work is introduction of Intelligent Agents and creation of Multi Agent System. The present research work creates and trains Intelligent Agents. Twenty Six different Machine Learning algorithms got executed by using Agent and predicts the algorithm with maximum accuracy(93.8%).The present paper also creates Multi Agent System trained with the Best fit(Among Twenty Six Machine Learning Algorithms) Algorithms for a Hybrid Data set. All the Agents should be Trained and Tested. They all will be able to Predict the possibility of heart disease with higher Accuracy of 96.8%.This paper is a complete implementation of Machine Learning Algorithm using an Intelligent Agent and Multi Agent System for prediction of accuracy of Heart disease using Python(Jupyter Notebook).

STATE OF ART REVIEW

PROBLEM STATEMENT

The present work has used Twenty Six different Machine Learning Algorithms. for prediction of Heart disease by using Hybrid dataset (for Heart disease). Accuracy, Balance Accuracy, ROC-AUC,F1-Score is calculated and compared for all Twenty Six Algorithms. Multi Agent System is developed and Multiple Agents are trained with the best fit Algorithm. It is tested that the trained Agents can predict the heart disease with almost the same accuracy.

METHODOLOGY

Data Collection

In order to perform an Heart Disease prediction, the proposed method has adapted the High Dimensional dataset. At first, the heart disease data is created from five different datasets and used for analysis. This Heart Disease dataset has been presented by integrating various datasets already available individually but not combined before. Hence, the integration makes it the largest heart disease dataset accessible for clinical research purposes.

The five datasets employed for its curation are provided below

- Cleveland – 323
- Hungarian – 304
- Long beach VA – 280
- Stalog (heart) – 290
- Switzerland – 143



**Chandanita Thakur et al.,**

The Heart Disease dataset (mixture of Hungarian, Cleveland, Stalog, long beach VA, Switzerland datasets) comprised a total of 1280 records of patients from Hungary, UK, US, and Switzerland. It encompasses 11 features. These datasets are collected together to make clinical diagnosis accurately.

Preparing the Data(Refer Figure 1-10)

Data preparation involves checking for Null values, making data scalable, selection of features, making correlation matrix etc.

1. **Data Preparation**-Data preparation is a very important consideration in Machine Learning. To check for Null values `df.isnull().sum()` function is used. It returns the number of Null values in the dataset. The present hybrid dataset is free from Null values. This is all about cleaning data and removing outliers from data. The present data is free from Null values.
2. **Scalability check**-To make the dataset Scalable, `StandardScaler()` function is used. `StandardScaler()` function converts values from higher order to lower order. Conversion of values from higher to lower order reduces the possibility of error. Code and output of Conversion of Higher order values to Lower order is given below
3. **Feature Selection** - It is required to select only those features that are non-correlated among themselves and highly dependent on target variables. Main intention of the feature selection method is to remove non-informative or redundant predictors from the model and to retain most useful features in order to predict the target variables. Feature selection is done by ANOVA f-test. The result of feature selection is given below (both values and plotting).
4. **Dependency of all the parameters together on heart disease**- How each and every individual parameter of the dataset is responsible for heart disease is altogether represented graphically. From the graph given below it is clear that heart disease is dependent on age. Heart disease possibility is more in Middle ages. There is a high possibility of having heart disease around the age of 50-60. Heart disease is not much dependent on Gender etc. In addition, a bar graph for individual features is presented in Figure. 5 to provides a comprehensive view of the empirical outcomes. It is also found that the possibility of heart disease is more at the age of 50-60 from the experimented plot given below.
5. **Correlation matrix**-A statistical method called correlation matrix is used to establish the relationship between two variables in this Hybrid dataset. It is best utilized for variables that explore linear relationships among one another. This matrix is a table in which every cell contains a correlation coefficient, where 1 is considered as a strong relationship between variables, 0 as a neutral relationship and -1 as a not strong relationship. From the diagram below, it is clear that Target is dependent on ST slope because Target-ST slope value is positive. Target is less dependent on Cholesterol because Target-cholesterol value is negative.

Choosing a Model

A machine learning model determines the output generated after running a machine learning algorithm on the collected data. It is important to choose a model which is relevant to the task at hand. The present work creates two different type of models. In first category, every model is separately trained with Twenty seven different algorithms by using Agent and all algorithms are separately passed in agent model. In second category, Multi Agent model is developed and implemented the best fit algorithm among Twenty Six algorithms.

Training the Model

Training is the most important step in machine learning. In training, prepared data needs to be passed to a machine learning model to find patterns and make predictions. It results in the model learning from the data so that it can accomplish the task set. Over time, with training, the model gets better at predicting. Here the dataset is splitted into two segments. One is training the model and another one is testing. 70-80 percent of data can be kept for training and 20-30 percent for testing. The present work has used 67% data for training and the rest 33% of data for testing.





Evaluating the Model

This phase checks the performance of the model which is done by testing the performance of the model on previously unseen data. The hybrid data was already splitted and the Model was tested with testing data(33%).Twenty Six different Machine Learning algorithms got tested and predicted by using Agent and predicts Accuracy,BalanceAccuracy,ROC-AUC,F1-Score.Those scores of all the algorithm is given below Graphical Representation of Accuracy of different Algorithms are given below.

Parameter Tuning

Once the model is created and evaluated this phase is an attempt to check whether the accuracy can be improved in any way. This is done by tuning the parameters present in the model. The present work has developed a Multi Agent System where agents have trained the Hybrid data and executed RandomForestClassifier() Algorithm (the best algorithm among twenty six algorithms tested before) with almost same accuracy.

Making Predictions

Multiple Agents have been created and trained with RandomForestClassifier() as it is proved as the best accurate algorithm for the present dataset. Newly trained Multi Agent System is able to detect the possibility of heart disease with almost the same accuracy.

RESULT

The present work has used Twenty Six different Machine Learning Algorithms for prediction of Heart disease by using Hybrid dataset(for Heart disease). Accuracy, Balance Accuracy,ROC-AUC,F1-Score is calculated and compared for all Twenty Six Algorithms. RandomForestClassifier() have been proved as the best for accurate prediction of Heart Disease with 93.8% of accuracy. RandomForestClassifier() Implemented with Multi Agent System is developed to make the prediction more accurately. Predicted accuracy using Multi Agent System is around 96.8%.

CONCLUSION

The uniqueness of this up to the minute research work is incorporation of the Multi Agent System with machine learning Algorithm which is a rare example in the field of data Science. Execution of Machine learning algorithm with the help of intelligent agent can bring a new age in the field of Data science. Social contribution of this paper is early detection of Heart disease using the Multi Agent System. Multi Agent System is applied with Machine Learning Algorithm for analysis of Heart Disease. This innovative work manifests future Scientists and Researchers in two ways. The first one is use of Hybrid dataset i.e. blending of five different standard dataset to improve accuracy of prediction and another one is implementation of Multi Agent System in Machine Learning Algorithm using Jupyter Notebook.RandomForestClassifier() has been proved as the best for diagnosis of heart disease with 93.8% accuracy where as by using Multiagent model, RandomForestClassifier() only has produced accuracy of 96.8 %. Hybrid dataset Implementation and incorporation of Multi Agent System using Machine Learning Algorithm to achieve highest level of accuracy is the novelty of the present research work which can explore a new era in the Field of Artificial Intelligence .This research work can be extended by implementing Multi Agent System by Artificial neural Network to achieve more accuracy for Heart Disease Prediction.

REFERENCES

1. Islam Daoud Suliman,D. Vasumathi,“Prediction of Heart Disease Using Machine Learning Algorithms”,IEEE,23November,2023,10.1109/ICCCNT56998.2023.10308096,https://ieeexplore.ieee.org/xpl/conhome/10306338/proceeding, doi.org/10.1109/ICCCNT56998.2023.10308096





Chandanita Thakur et al.,

2. Chintan Bhatt, Parth Patel, Tarang Ghetia "Effective Heart Disease Prediction Using Machine Learning Techniques" <https://doi.org/10.3390/a16020088>, <https://www.mdpi.com/1999-4893/16/2/88>
3. Ochin Sharma, "Prediction and Analysis of Heart Attack using Various Machine Learning Algorithms", IEEE, 03 April, 2023, <https://doi.org/10.1109/AISC56616.2023.10085460>
4. Niloy Biswas, Md Mamun Ali, Md Abdur Rahaman, Minhajul Islam, Md. Rajib Mia, "Machine Learning-Based Model to Predict Heart Disease in Early Stage Employing Different Feature Selection Techniques", BioMed Research, Volume 2023, ArticleID-6864343, [Int.https://doi.org/10.1155/2023/6864343](https://doi.org/10.1155/2023/6864343)
5. Dhanunjaya Rao, B. Amani Rama Padma Priya, B. Venkata Sai Sowmyal, T. Chandrasekhar, "Machine Learning Algorithms For Prediction Of Heart Disease", International Research Journal of Modernization in Engineering Technology and Science, e-ISSN: 2582-5208, DOI : <https://www.doi.org/10.56726/IRJMETS35616>
6. Nadikatla Chandrasekhar et al., "Enhancing Heart Disease Prediction Accuracy through Machine Learning Techniques and Optimization", 2023, <https://doi.org/10.3390/pr11041210>
7. Huating Sun, Jianan Pan, "Heart Disease Prediction Using Machine Learning Algorithms with Self-Measurable Physical Condition Indicators", Journal of Data Analysis and Information Processing, 2023, ISSN Online: 2327-7203, doi.org/10.4236/jdaip.2023.111001
8. Md. Imam Hossain, Mehadi Hassan Maruf, Md Asikur Rahman Khan, "Heart disease prediction using distinct artificial intelligence techniques: performance analysis and comparison", Springer Link, 12 June 2023, <https://doi.org/10.1007/s42044-023-00148-7>
9. G. Harinadha Babu, Gunda Jayasree, Chattu Ashika, Vajja Ahalya, Katta Asha Niroopa, "Heart Disease Prediction System Using Random Forest Technique" <https://doi.org/10.22214/ijraset.2023.48764>
10. Neha Nandal, Rohit Tanwar, "Machine learning-based heart attack prediction: A symptomatic heart attack prediction method and exploratory analysis", This article is included in the Computational Modelling and Numerical Aspects in Engineering collection, <https://doi.org/f1000research.com/articles/11-1126>
11. Paras Negi, Manoj Kumar Bisht, "Analysis and Prediction of Heart Attack using Machine Learning Models", IEEE, 28, March, 2023, doi.org/10.1109/ICCCS55188.2022.1
12. Janaraniani N, Lipika Goel, Rohit Tanwar, "Heart Attack Prediction using Machine Learning", IEEE, 21-23 September 2022, <https://doi.org/10.1109/ICIRCA54612.2022.9985736>
13. Chaimaa Boukhatem, Heba Yahia Youssef, Ali Bou Nassif, "Heart Disease Prediction Using Machine Learning", IEEE, 18 March, 2022, <https://doi.org/10.1109/ASET53988.2022.9734880>
14. P. Chinnasamy, "Machine learning based cardiovascular disease prediction", IEEE, 21-23 September 2022, <https://doi.org/10.1109/ICIRCA54612.2022.9985736>
15. Sumaira Ahmed, Salahuddin Shaikh, Farwa Ikram, "Prediction of Cardiovascular Disease on Self-Augmented Datasets of Heart Patients Using Multiple Machine Learning Models", Volume 2022 | Article ID 3730303 <https://doi.org/10.1155/2022/3730303>
16. Victor Chang, Vallabhanent Rupa Bhavani, Ariel Qianwen Xu, "An artificial intelligence model for heart disease detection using machine learning algorithms", Science Direct, Volume, 2, Nov 2022, <https://doi.org/10.1016/j.health.2022.100016>
17. Mihir Patel, Rahul Patange, Chaitanya Patil, "Predicting Heart Disease Using Machine Learning Algorithms", IRJET, Volume: 09 Issue: 04 Apr 2022, e-ISSN: 2395-0056, p-ISSN: 2395-0072
18. Jian Yang, Jinhan Guan, "A Heart Disease Prediction Model Based on Feature Optimization and Smote-Xgboost Algorithm" <https://doi.org/10.3390/info13100475>
19. Pinaki Ghosh, Umesh Kumar Lilhore, Sarita Simaiya, Atul Garg, "Prediction of the Risk of Heart Attack Using Machine Learning Techniques", Springer, Singapore, 12 October 2022, pp 613–621, https://doi.org/10.1007/978-981-19-4687-5_47
20. Harshit Jindal, Sarthak Agaewal, Rishabh Khera, Rachna Jain, Preeti Nagrath, "Heart disease prediction using machine learning algorithms" IOP Conf. Series: Materials Science and Engineering, <https://doi.org/10.1088/1757-899X/1022/1/012072>
21. Apurv Garg, Bhartendu Sharma, Rijwan Khan, "Heart disease prediction using machine learning techniques", IOP Conf. Series: Materials Science and Engineering, doi.org/10.1088/1757-899X/1022/1/012046



Chandanita Thakur *et al.*,

22. Elwahsh H, "A new smart healthcare framework for real-time heart disease detection based on deep and machine learning", doi.org/10.1088/1757-899X/1022/1/012046

Table 1: State of Review

Ref No	Disease	Algorithm Used	Accuracy%	Year	Dataset
[1]	Cardiac	KNN, DT, NB, LR, RF	LR -96.6	2023	Cleveland Dataset
[2]	Cardio vascular	RF, DT, MP, XGB	MLP-87.28	2023	70000 instances of Kaggle
[3]	Heart attack	Data Mining, ML	Paper not available	2023	Paper not available
[4]	Heart	LR, SVM, DT	LR -96.6	2023	UCI
[5]	Heart	DT, GB, LR, SVM, RF	86.7	2023	Cleveland Dataset
[6]	Heart	RF, KNN, LR, NB, GB, AdaB	93.44	2023	Cleveland Dataset
[7]	Heart	LR, NN, SVM, DT, RF	RF-82.18	2023	Cleveland dataset from UCI ML
[8]	Heart	LR, NN, SVM, DT, RF	RF-90	2023	Data have been collected from hospitals, diagnostic centers and clinic centers in Bangladesh
[9]	Heart	DT, NB, LR, SVM, RF	86.7	2023	Realtime
[10]	Heart Attack	XGB, LR	XGB-94, LR-92	2022	UCL
[11]	Heart attack	SVM, KNN	NA	2022	NA
[12]	Heart attack	NB, DT, WARM	DT-99.5	2022	Raw Clinical
[13]	Heart	MLP, SVM, RF, NB	91.67	2022	NA
[14]	Cardiovascular	SVM	NA	2022	NA
[15]	Heart failure	LR, KNN, MNB, ET, RF, DT, GBC, DT LGBM, HGBC and XGB	RF-87.03	2022	NA
[16]	Heart	LR, RF	RF-83	2022	NA
[17]	Heart	LR, SVM, KNN	KNN-83 SVM-92.1 DT-89.6 LR-92	2022	NA
[18]	Heart	LR, SVM, and KNN,	93.44	2022	NA
[19]	Heart attack	Paper not available	Paper not available	2021	Paper not available
[20]	Cardiovascular	NB, KNN, LR	87.5	2021	UCI
[21]	Heart	KNN, RF	KNN-86.885 RF-81.967	2021	Paper not available
[22]	Heart (CVD)	SGD(SHDML framework)	NA	2021	NA





```
In [12]: from sklearn.preprocessing import StandardScaler
scaler = StandardScaler()
X_train = pd.DataFrame(scaler.fit_transform(X_train), columns = X.columns)
X_test = pd.DataFrame(scaler.transform(X_test), columns = X.columns)
```

	age	sex	chest pain type	resting bp s	cholesterol	fasting blood sugar	resting ecg	max heart rate	exercise angina	oldpeak	ST slope
0	0.006170	0.55581	0.83251	-0.570451	0.486889	-0.524865	-0.786977	-0.073524	-0.774866	0.066381	0.622932
1	0.688184	0.55581	0.83251	-0.137068	-2.051882	1.906232	0.361779	-0.300240	1.206563	0.158118	2.249121
2	0.003989	0.55581	-0.237023	-0.137068	0.200988	-0.524865	-0.786977	0.213241	-0.774866	0.786974	0.622932
3	-0.714033	0.55581	0.83251	0.520750	0.154101	-0.524865	-0.786977	-1.524501	1.206563	0.516882	0.622932
4	0.041007	0.55581	-1.354257	3.170354	0.713592	-0.524865	*5.510535	2.052265	-0.774866	-0.028513	-0.984256

Fig 1. Original Higher order values

```
Feature age: 59.662016
Feature sex: 75.065709
Feature chest pain type: 255.706824
Feature resting bp s: 6.793919
Feature cholesterol: 45.409481
Feature fasting blood sugar: 41.903455
Feature resting ecg: 8.855108
Feature max heart rate: 186.245664
Feature exercise angina: 232.343071
Feature oldpeak: 142.495132
Feature ST slope: 337.877510
```

Fig 2. Lower order values

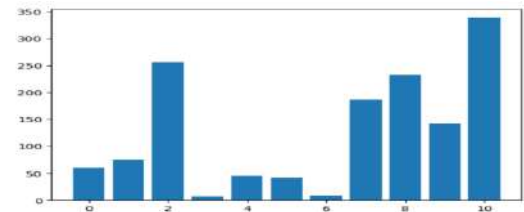


Fig 3. Feature Selection: ANOVA f-Test

```
In [10]: import matplotlib.pyplot as plt
plt.subplot(11,1,1)
plt.plot(range(0,df.shape[0]),df.iloc[:,0],label="age")
plt.legend()
```

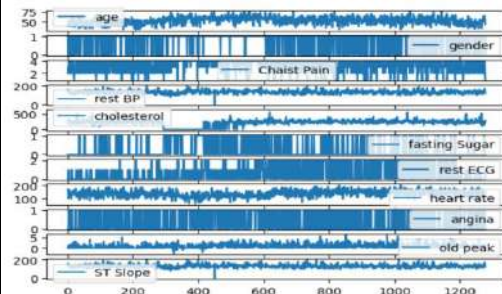


Fig 4. How each and every individual parameter of dataset is responsible for Heart attack is represented graphically

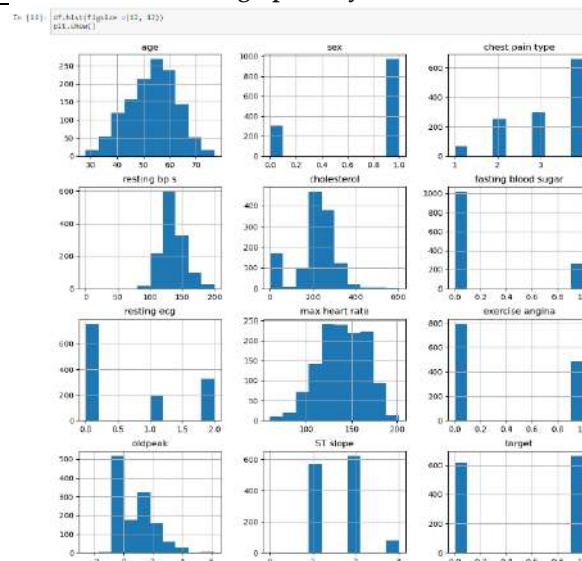


Fig 5. Bar graph for individual features to provide a comprehensive view of the empirical outcomes.



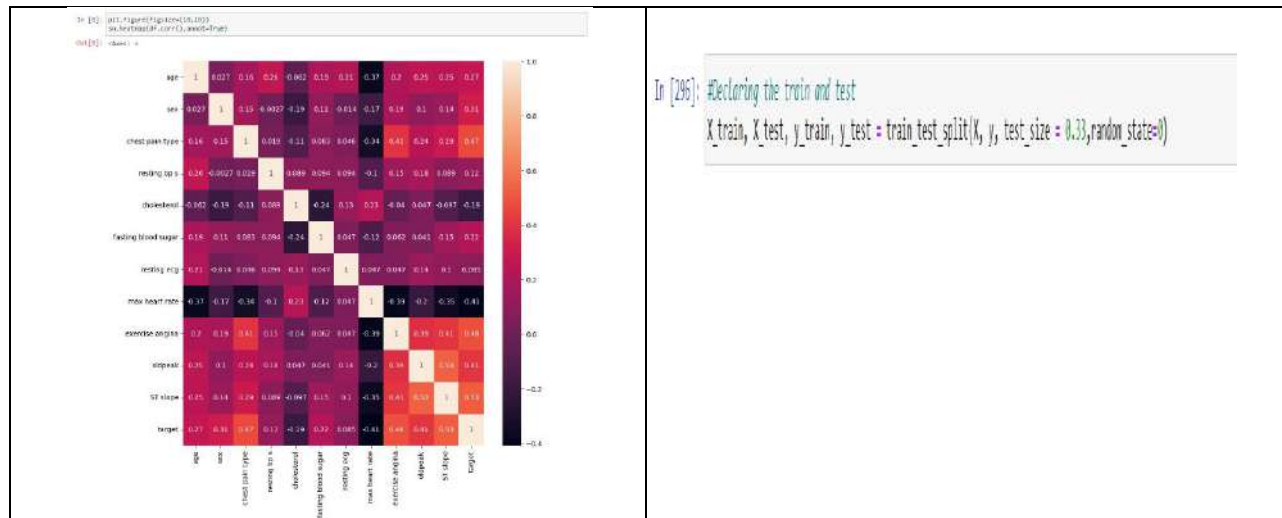


Fig 6. Correlation Matrix

In [295]: #Declaring the train and test
X_train, X_test, y_train, y_test = train_test_split(X, y, test_size = 0.33, random_state=0)

Fig 7. Model Training

In [464]: import pandas as pd
db={ "Model": "LabelPropagation", "Accuracy": accuracy, "Balance Accuracy": bsa, "ROC AUC": roc, "F1-Score": score_Label_Propag }
result_df=result_df.append(db, ignore_index=True)
result_df

Out[464]:

	Model	Accuracy	Balance Accuracy	ROC AUC	F1-Score
0	Logistic Regr.	0.853428	0.853571	0.853428	0.853428
1	SVC	0.922795	0.922795	0.922795	0.924350
2	RF	0.938534	0.938435	0.938435	0.938534
3	DT	0.872340	0.873647	0.873647	0.872340
4	GNB	0.855792	0.856225	0.856225	0.855792
5	knn	0.867612	0.867017	0.867017	0.867612
6	sgdc	0.834515	0.835089	0.835089	0.834515
7	perceptron	0.735225	0.731941	0.731941	0.735225
8	lsvc	0.853428	0.853571	0.853428	0.853428
9	NuSVC	0.862884	0.861330	0.861330	0.862884
10	QuadraticDiscriminantAnalysis	0.843972	0.844290	0.844290	0.843972
11	NeuralCentroid	0.853428	0.853052	0.853052	0.850000
12	CalibratedClassifierCV	0.853428	0.853762	0.853762	0.853428
13	BernoulliNB	0.848700	0.848645	0.848645	0.848700
14	PassiveAggressiveClassifier	0.782506	0.782725	0.782725	0.782506
15	RidgeClassifierCV	0.851064	0.851299	0.851299	0.851064
16	RidgeClassifier	0.851064	0.851299	0.851299	0.851064
17	LinearDiscriminantAnalysis	0.851064	0.851299	0.851299	0.851064
18	AdaBoostClassifier	0.851064	0.851180	0.851180	0.851064
19	BaggingClassifier	0.878433	0.880475	0.880475	0.878433
20	ExtraTreesClassifier	0.935170	0.935481	0.935481	0.935170
21	LOGITClassifier	0.921986	0.922335	0.922335	0.921986
22	XGBClassifier	0.931442	0.931236	0.931236	0.931442
23	LabelSpreading	0.912530	0.912463	0.912463	0.912530
24	LabelPropagation	0.912530	0.912463	0.912463	0.912530
25	DummyClassifier	0.500995	0.500900	0.500900	0.500995
26	LabelPropagation	0.500995	0.500900	0.500900	0.912530

Fig 8. Accuracy ,Balance Accuracy,ROC-AUC,F1-Score is calculated for all the algorithms used to predict Heart disease.



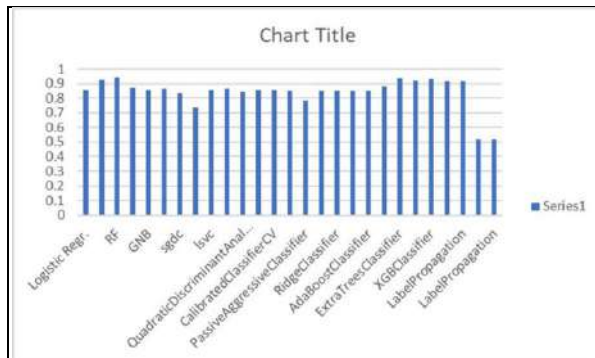
Chandanita Thakur *et al.*,

Fig 9. Graphical Representation of Accuracy of different Algorithms are given below

```
class Agent1:
    def __init__(self):
        self.model = RandomForestClassifier(n_estimators=20,criterion='gini')

    def train(self, X, y):
        self.model.fit(X, y)
    def predict(self, X):
        return self.model.predict(X)

# Define Agent 2
class Agent2:
    def __init__(self):
        self.model = RandomForestClassifier()
    def train(self, X, y):
        self.model.fit(X, y)
    def predict(self, X):
        return self.model.predict(X)

# Train and predict using agents
agent1 = Agent1()
agent2 = Agent2()

# Train Agent 1
agent1.train(x_train, y_train)
# Get predictions from Agent 1
predictions_agent1 = agent1.predict(X_test)
# Train Agent 2
agent2.train(x_train, y_train)
# Get predictions from Agent 2
predictions_agent2 = agent2.predict(X_test)
print("Agent1 accuracy=",accuracy_score(y_test, predictions_agent1))
print("Agent2 accuracy=",accuracy_score(y_test, predictions_agent2))

Agent1 accuracy= 0.96875
Agent2 accuracy= 0.96484375
```

Fig 10. Random Forest Classifier() is implemented to train and test Multiple Agents :Produced accuracy approximately same





Impact of Row Planting Teff Technology Adoption on Small Holder Farmers' Income in Dendi and Ejere Districts of West Shewa Zone, Ethiopia

Aman Rikitu¹, Arif Abraham², Amsalu Kaba², Dabesa Wagari² and B. Chandra Sekhar Singh^{3*}

¹Assistant Professor, Department of Agriculture Economics, School of Agriculture Economics and Rural Development, Ambo University, Ethiopia, East Africa.

²Lecturer, Department of Agriculture Business and Value Chain Management, School of Agriculture Economics and Rural Development, Ambo University, Ethiopia, East Africa.

³Assistant Professor, Department of Plant Science, School of Agriculture, Ambo University, Ethiopia, East Africa.

Received: 19 Mar 2024

Revised: 09 May 2024

Accepted: 03 Jun 2024

*Address for Correspondence

B. Chandra Sekhar Singh
Assistant Professor,
Department of Plant Science,
School of Agriculture,
Ambo University, Ethiopia, East Africa.
Email: singhsekhar960@gmail.com



This is an Open Access Journal / article distributed under the terms of the **Creative Commons Attribution License** (CC BY-NC-ND 3.0) which permits unrestricted use, distribution, and reproduction in any medium, provided the original work is properly cited. All rights reserved.

ABSTRACT

Ethiopia continues to be among the world's poorest countries despite substantial economic progress. This is because to the country's high population growth, poor rural infrastructure, and antiquated agricultural techniques. Teff row planting technology is one of the emerging technologies in this nation that farmers are attempting to use. Thus, the purpose of this study was to investigate how the technology of teff-row planting affected the income of smallholder farmers in the Oromia regional state's West Shewa zone. Data from 352 sample households, both qualitative and quantitative, were used in the study. For data analysis, the study used econometrics (PSM) and descriptive statistics. The adoption of teff-row-planting technology by farm households was positively and significantly impacted by improved seed, training, chemical fertilizer, and the number of oxen, as indicated by the Probit-part of the PSM-model. However, the distance from the closest market had a negative and significant impact on farm households. The PSM's average treatment impact indicates that there is a significant income gap between those who use this technology and those who do not. The average increase in adopter household income, according to the impact study of the PSM-outcome, is 945.10 ETB. As a result, in order to increase the overall impact, relevant organizations like the government, NGOs, and society should take the appropriate action based on the listed important criteria.



Aman Rikitu *et al.*,**Keywords:** Adopters, Household, Probit, PSM-technology, row planting, Smallholder farmers

INTRODUCTION

Ethiopia's economy is heavily reliant on agricultural production and other industries. Crop production makes up 27.4% of the entire agricultural contribution, while agriculture alone accounts for 34.9% of the GDP (NBE, 2018). (NPC, 2016). The main sources of food and income for more than 80% of Ethiopians are agriculture and cattle (FAO, 2017). More than 83.9% of export revenue comes from this sector (Matoussa *et al.*, 2013), and it provides 70% of the raw materials needed for secondary activities (MoFED, 2010). Ethiopia has one of the lowest rates of income inequality in the world and the lowest in Africa, despite its enormous relevance (EE, 2020). Cereals are Ethiopia's main food crops in terms of both area covered and production volume. They contribute 87.48 percent of grain production and account for 95% of agricultural production, making them the second-largest contributor to the country's agricultural sector's economic contribution (CSA, 2017). Cereal production accounts for more than 80.0% of agricultural land and employs 60.0% of the labour force in rural areas (FAO, 2020). One of the cereal crops that constitutes the most significant economic crop for 43% of Ethiopia's smallholder farmers is teff, which accounts for 21% of all grain production and around 32% of the country's yearly average (Birrara, 2017). Furthermore, teff is Ethiopia's second-most significant cash crop after coffee, bringing in roughly \$500 million USD annually for nearby farmers (Minten *et al.*, 2013). Teff grains are comparable to wheat and rice in terms of nutrition, containing 357 kcal per 100 grams (Cheng *et al.*, 2017). Nutritionists and food scientists around the world are becoming more interested in teff research because of its high protein and amino acid content, low glycemic index, gluten-free nature, and suitability for patients with type 2 diabetes (FAO, 2015). Although the total amount of teff produced has doubled between 2003-2004 and 2015-2016, yields are still lower than those of maize and experience significant losses (between 25-30% before and after harvest). This lowers the amount of grain that is available to consumers by as much as 50%. Additionally, although the yields of teff are very high, which attracts some growers to the crop as a cash crop, the crop's labour-intensive character and high production costs also indicate the need for fertilizer (ATA, 2013 a). However, despite the relatively high cost structure, production has been rising annually at a rate of about 11% because of land expansion and yield increases; also, significant latent demand has led to price hikes. Ethiopia's central and northwest highlands have historically been the country's primary teff-producing regions.

The Oromia region is the nation's most significant teff-producing region; according to estimates, it accounts for up to 48% of the nation's overall production (Ibrahim *et al.*, 2018). Teff leads all cereal crops in the Oromia region, accounting for 29.46 percent of the total area planted, according to the CSA data for the 2018-19 crop year. During the production year, 2.57 million small holders produced 2.56 million tons of teff on an area of 1.43 million hectares, yielding 1.79 t/ha (CSA, 2019). One of the Oromia region's teff-producing zones is West Shewa. Throughout 2019 and 2020, 0.29 million small-holder farmers in this zone cultivated teff on 0.161 million hectares, with a total production of 0.166 million tons. According to Minten (2013) the average productivity was recorded at 1.029 t/ha. Teff production's agronomic methods haven't altered all that much throughout time, which has slowed the growth of teff productivity. Teff is sown almost entirely by disseminating due of its small seed size. One of the primary causes of Ethiopia's low teff yields is thought to be the traditional sowing technique (Berhane *et al.*, 2011). Because of challenges with weeding and hoeing, as well as inconsistent seed dispersal, high-speed manual seeding may yield low production. By decreasing seed rate, expanding the distance between seedlings, enhancing weeding, and improving nutrient uptake, row planting technology can raise yield and productivity levels (Chauhan, 2014). Without taking into account row planting technology, the study by Berihun *et al.*, 2014; Zeng *et al.*, 2015; Tigist, 2017 concentrated on better seed types and chemical fertilizer. Despite this, a modest number of studies have been conducted in Ethiopia on the factors that affect the income of smallholders who plant teff in its raw form. It is the most significant crop in terms of economic impact on income and the reduction of rural poverty. Nonetheless, there is a paucity of scientific data about the extent to which the income of smallholder farmers is impacted by the row planting technique of teff production (Fekadu, 2020). Accordingly, the study areas have a high potential for teff production, and households have been using the row planting technology for teff production for a long time (from



Aman Rikitu *et al.*,

2003 until now). However, there are few well-documented comparative analysis studies available on the factors influencing smallholder households' adoption of this technology and the results that they get. Furthermore, nothing is known about how raw teff planting technology affects smallholder farmers' earnings in the research region. Therefore, by identifying factors that affect and the impact of adopting raw planting teff technology on the income of smallholder farmers in the research region, this study aims to close the information gap on the impact of teff raw planting technology on smallholder farmers' income.

METHODOLOGY

Description of the study area

The study was conducted in the West Shawa zone of Ethiopia's Oromia National Regional State, namely in the Dendi and Ejere district. Dendi was located 83 kilometers from the West Shawa zone's administrative hub, Ambo Town, and 83 kilometers from Addis Ababa. The district currently consists of two administrative cities and 22 rural kebeles. Ginchi serves as Dendi's administrative hub; other settlements include Olonkomi and Ehud Gebeya. South West borders Dendi on the south; Ambo borders it on the west; Jaldu borders it on the north; and Ejere borders it on the east. Situated in the West Shoa Zone of Oromia Regional State, the district capital of Ejere is located 50 kilometers west of Addis. Its borders are as follows: the Southwest Shoa Zone to the south, Dendi district to the west, Jeldu district to the northwest, Meta Robi to the north, Adda Berga district to the northeast, and Walmara district to the east (DEWAO, 2015). Its approximate area is 592.19 square kilometers. Both districts are renowned for having excellent agriculture and livestock production potential. The majority of a household's consumption and income generating comes from crop cultivation. Teff, wheat, barley, and maize are among the cereal crops that are commonly produced in the region; the main crops that are planted are pulses like chickpeas, haricot beans, and faba beans. In addition, the region produces sweet potatoes, onions, potatoes, tomatoes, peppers, and cabbage. The majority of crops grown are annuals, and rain-fed agriculture primarily uses animal labour. In addition to crops, raising livestock is another source of food and revenue. Furthermore, it serves as the source of traction power and transpiration. In the research region, farmers maintain a sizable population of livestock (cattle, sheep, donkeys, and horses) for a variety of uses (DEWAO, 2015).

Data collection

Using checklists and structured questionnaires, the study gathered information about raw planting teff from adopter and non-adopter families. Sixteen seasoned enumerators received training on how to gather information using in-person interviews and formal questionnaires. To augment the survey results, other techniques included focus groups, key informant interviews, and observations.

Sampling technique and sample size determination

Eight rural kebeles in total four in each of the two districts were chosen at random for the first stage. Populations in the eight kebeles that were chosen for the second stage were divided into adopter and non-adopter groups based on teff row planting. Ultimately, 332 sample households-166 adopter and 166 non-adopters were proportionate to the size identified in the third step. As a result, 332 sample homes both adopter and non-adopter of raw planting technology-will get a structured questionnaire about teff output. The sample sizes of the heads of households in this study were calculated using the sample size determination formula developed by Kothari (2004).

$$n = \frac{Z^2 qpN}{e^2(N-1) + Z^2 qp} \dots \dots \dots (1)$$

$$\frac{(1.96)^2(0.55)(0.45) 3200}{(0.05)^2(3199) + (1.96)^2(0.55)(0.45)} = 332$$

Where: n=sample size; N= size of total population from which the sample is drawn; Z=95% confidence interval under normal curve (1.96); e=acceptable error term (0.05) and P and q are estimates of the proportion of population to be sampled (P=0.45 and p + q=1). Five percent (5%) of error term (e=0.05) will be used to take representative data for this study.



Aman Rikitu *et al.*,

DATA ANALYSIS

Descriptive analysis

The study used descriptive statistics such as mean, standard deviation, percentages, and frequency to compare and contrast sample units based on desired characteristics, drawing important conclusions.

Econometrics model specification

Adoption model specification

Farmers' decisions to use the teff row planting technology were examined using a dichotomous variable model. In the econometric literature, the linear probability model (LPM), logit, and probit are frequently utilized to estimate binary response variable models for binary choice models (Gujarati, 2009). The dependent variable, or response, is binary or dichotomous, with two possible values: 1 in the case that the household is using row planting technology for teff production, and 0 in the other case. Qualitative response models are necessary for this kind of relationship's estimation. In contrast to regression models, which have a quantitative dependent variable, this indicates that the dependent regressor is qualitative in character. According to (Gujarati, 2009), logit or probit models are frequently used to analyse determinant studies for a small number of dependent variables, and the outcomes are comparable. While the logistic function has somewhat flatter tails than the probit function, the normal curve under the logit function approaches the axes more quickly. Other than that, the logit and probit models are similar. In contrast, Caliendo and Kopeing (2005) imply that the probit model was chosen for this investigation even though both models produced outputs that were similar.

Probit model

Probit model is used when the dependent variable is binary (takes on two values, usually 0 or 1), and it need to model the probability of one outcome occurring. To use this model four key elements are very crucial. These key elements are:

1. Dependent Variable: A binary variable representing a yes/no choice or the presence/absence of an outcome.
2. Independent Variables: Explanatory variables that potentially influence the probability of the outcome occurring.
3. Latent Variable: An unobserved continuous variable that determines the probability of the observed binary outcome.
4. Cumulative Distribution Function (CDF): The probit model uses the standard normal CDF (Φ) to link the latent variable to the observed binary outcome.

Model specification

1. The Latent Variable

$$y^* = \beta_0 + \beta_1 x_1 + \beta_2 x_2 + \dots + \beta_k x_k + \varepsilon \dots \dots \dots (2)$$

Y^* is the latent variable (not directly observed).

β_0 is the intercept.

$\beta_1, \beta_2, \dots, \beta_k$ are the coefficients of the independent variables.

x_1, x_2, \dots, x_k are the independent variables.

ε is the error term, assumed to be normally distributed with mean 0 and variance 1.

2. Link the Latent Variable to the Observed Binary Outcome:

$$Y = 1 \text{ if } Y^* > 0 \quad (3)$$

$$Y = 0 \text{ if } Y^* \leq 0 \quad (4)$$

This means the probability of $Y = 1$ is equal to the probability that Y^* is positive.





3. Specify the Probability Model:

$$P(Y = 1) = \Phi(\beta_0 + \beta_1\chi_1 + \beta_2\chi_2 + \dots + \beta_k\chi_k) \dots \dots \dots (5)$$

Φ is the standard normal CDF.

Interpretation

The coefficients ($\beta_1, \beta_2, \dots, \beta_k$) represent the change in the latent variable associated with a one-unit change in the corresponding independent variable. In probit model it is difficult to interpret the coefficient as probability directly. Therefore, for the interpretation this study used marginal effects to assess the change in probability for a given change in an independent variable.

Matching methods of propensity score estimation

The study uses propensity score matching (PSM) to distinguish between households with and without the program Caliendo and Kopeinig (2005) in order to investigate the effect of teff raw planting adoption technology on the revenue of smallholder farmers. By establishing a statistical comparison group and matching individual data, the PSM technique ensures consistent estimated raw planting teff impact while accounting for sample selection bias and self-selection. The technique finds and pairs adopter homes with non-adopter households based on observable traits (X_i). Propensity scores are derived using a binary probit estimation raw planting technology adoption of teff in order to achieve this. In order to create the PSM framework, let Y_i be the household i 's outcome variable. Then, Y_{1i} and Y_{0i} represent household outcomes with and without the adoption of raw teff production planting, respectively. A dummy variable I_i indicates whether or not household I has adopted the raw planting technique for teff production; if the family has adopted, $I_i = 1$, and if not, $I_i = 0$. The following describes how raw teff planting affects household I 's results:

$$Y_1 = Y_{1i} - Y_{0i} \dots \dots \dots (6)$$

Where $\Delta_i Y_{ii}$ is denotes the change in the outcome variable of household i , resulting from adoption to raw planting teff. A household cannot be both ways, therefore, at any time, either Y_{1i} (adopter household) or Y_{0i} (non-adopter household) is observed for that household. Two means are common in the impact analysis framework, the average treatment effect and the average treatment effect on the treated (ATT).

According to the guide line steps in propensity score matching prepared by (Garden Nelson *et al.*, 2018) the following steps was followed. To estimates the effect of Average Treatment Effect of raw planting technology of teff production on the outcomes of the whole population without regards to raw planting teff would be obtained by averaging the impact across all the individuals in the population.

$$ATE = E(Y_1 - Y_0) \dots \dots \dots (7)$$

Where $E(Y_1 - Y_0)$ is represents the average (or expected value).

On the other hand, the average treatment effect on the treated (ATT), this measures the impact of the program on those individuals who participated:

$$ATT = E(Y_1 - Y_0 | D = 1) \dots \dots \dots (8)$$

Also using the fact that the average of a difference is the difference of the averages, the ATT can be rewritten as:

$$ATT = E(Y_1 | D = 1) - E(Y_0 | D = 1) \dots \dots \dots (9)$$

This answers the question, how much did household adoption in the raw planting teff production benefit compared to what they would have experienced without adoption of raw planting teff production. Data on $E(Y_1 | D = 1)$ are available from the adopter. An evaluator's classic problem is to find $E(Y_0 | D = 1)$. So, the difference between $E(Y_1 | D = 1) - E(Y_0 | D = 1)$ cannot be observed for the same household. Due to this problem, one has to choose a proper substitute for it in order to estimate ATT. The possible solution for this is to use the mean outcome of the comparison individuals, $E(Y_0 | D = 0)$ as a substitute to the counterfactual mean for those being treated, $E(Y_0 | D = 1)$ after correcting the difference between treated and untreated households arising from selection effect. In non-experimental studies, one has to introduce some identifying assumptions to solve the selection problem. The following are two assumptions to solve the selection problem Caliendo and Kopeinig (2005).





Aman Rikitu et al.,

RESULTS AND DISCUSSION

Under this chapter the study discusses the results of descriptive statistics, inferential statistics and econometrics model. Accordingly, the entire variables used in the econometrics model were divided in to two such as dummy variables and continuous variables for chi-square test and t-test comparisons. Finally, the entire variable tested using econometrics model was checked and all the significant variables were analyzed and discussed.

Descriptive Statistics of Dummy Variables by teff row plantation adoption

Table 2 demonstrates that of the 291 male-headed households, 148 (50.86%) adopted the technology of teff row plantations, while 143 (49.14%) did not. The results also showed that, out of the 293 homes with extension access, 149 (or 50.85%) adopted row planting teff technique, while 144 (or 49.15%) did not. The results also showed that, out of the 222 households that used enhanced seed, 134 (60.36%) adopted row planting teff technique, whereas 88 (39.64%) did not. In terms of enhanced seed, the ch2 result in **Table 3** demonstrated a statistically significant difference (at a 1% significance level) between row plantation adopters and non-adopters. Of the 219 households that were sampled for pesticide use, 120 (54.79%) adopted row plantation teff technology, while 99 (45.21%) did not. The chi2 result indicates that there is a statistically significant difference in the use of pesticides between those who embrace teff row plantation technology and those who do not.

Descriptive statistics of continuous variable

According to Table 3, the average age of the heads of households using the teff row planting technology is 44.83 years, with a standard deviation of 0.843, whereas the average age of the households using the non-teff row planting technology is 46.824 years, with a standard deviation of 0.824. While non-adopter households had an average educational level of 2.64 with a standard deviation of 0.262, adopter households using teff row planting technique had an average education level of 3.24 with a standard deviation of 0.281. Teff row plantation adopter and non-adopter families had average family sizes of 6.28 and 5.81, respectively, with a significant difference in family size between the two groups at the 1 percent significance level. As a result, larger family sizes were shown to be more adoptive than smaller ones. This suggests that, as row plantations require a greater labour force, larger families employed family members to work on their teff plantations. Farm households that plant teff rows have an average distance of 2.32 hours, with a standard deviation of 0.123, from the closest market. In contrast, households that do not utilize this technology have an average distance of 2.62 hours, with a standard deviation of 0.142. The results of the t-test indicate that, when it comes to the farm household's distance from the closest market, there is a statistically significant difference between those who use the teff row planting technology and those who do not, at a 10% significance level. Table 3's results indicate that, for households that have adopted teff row planting technology, the average income from teff production is 66133.39 Birr with a standard deviation of 3760.814, whereas income from non-adopter households' teff production is 49009.78 with a standard deviation of 3147.834. At a 1% significance level, the t-test result demonstrates a statistically significant difference between adopters and non-adopters of teff row planting. This table's result also reveals that families that adopted teff row planting technique used an average of 780.62 ETB with a standard deviation of 79.155, whereas those that adopted teff row planting technology used an average of 1272.76 with a standard deviation of 2.6.285. The results of the t-test indicate that there is a statistically significant difference in the amount of herbicide used by families using teff row plantation technique compared to those that do not. The data presented in Table xxx indicates that farmers who use teff row planting technique have an average of 1.28 oxen with a standard deviation of 0.079, whereas those who do not use the technology have an average of 1.02 oxen with a standard deviation of 0.061. According to the t-test result, there is a significant difference in the number of oxen between those who embrace the teff row planting technology and those who do not.

Outcome of the econometric model

The adoption of teff row plantation technology is addressed by the probit regression model. If a sampled home in the study region adopted a teff row plantation, they were assigned a score of 1, otherwise a score of 0. The adoption of teff row plantation technique is significantly influenced by the number of oxen, fertilizer, improved seed, distance,



**Aman Rikitu et al.,**

and training, according to the results of the probit Regression model shown in **Table 4**. The variables for the study were chosen based on prior knowledge, empirical study results, and theoretical justifications. With less than 1 percent probability level, one of the 14 explanatory factors included in the analysis was determined to have a highly significant impact on the adoption of teff row plantation technology. This is an enhanced seed that has a beneficial impact on the dependent variable. At a probability level of less than five, the remaining four significant variables were deemed significant at a level of 10. These included the number of oxen, training received, fertilizer use, and the household's distance from the closest market. **Table 4** results show that, at a 1 percent significant level, better seed has a substantial impact on farm families' adoption of teff row planting technology. Teff row planting methodology makes sense for homes that have easy access to better seed. The results of the marginal effect of enhanced seed indicate that the likelihood of adopting teff row planting technology increases by 36.6 percent with access to improved seed. Teff row plantations are used by households that have access to enhanced seed since they have less information about the practice than households that do not employ this technology. The study's findings indicate a significant correlation between the use of teff row planter technology and the availability of enhanced seed. The findings of this investigation are consistent with those of the (Kidanemariam *et al.*, 2012) study. **Table 4's** conclusion demonstrates that, at a 10% significance level, a household's distance from the farmer training centre has a negative impact on the adoption of teff row plantation technology. The results of the marginal effect demonstrate that the adoption of teff row plantation technique fell by 3.7% for every hour that farm households' distance from the farmer training centre increased. This suggests that a farmer who lives close to the farmer training centre will have easier access to up-to-date knowledge and will be able to use this technology with more ease.

The findings are based on the research of Adunea and Fekadu (2019). **Table 4's** results showed that, at the five percent significance level, fertilizer use had a favourable and substantial impact on farm families' adoption of teff row planting technique. According to the results of the marginal impact, farmers are 0.2 percent more likely to use the teff row plantation method if they have access to fertilizer. This finding indicates a high correlation between fertilizer consumption and teff row plantation method. According to evidence gathered from focus groups and key informant interviews, farmers with access to fertilizer employed teff row planting technique to protect their finances and resources. This outcome was consistent with the research conducted by Vandercastelen *et al.*, (2013). The results shown in **Table 5** indicate that, at a five percent significance level, training in farm production has a favourable and substantial impact on teff row plantation technology. The likelihood that teff row plantation technology will be adopted has increased by 14.1% when farm households have access to training, according to the marginal effect result. Apart from the results of the model, the data gathered from focus groups and key informant interviews indicates that teff row planting technology and training are positively correlated. This suggests that receiving instruction in agricultural activities and teff row plantation technology have a substantial favourable association Fekadu and Adunea, (2020). **Table 5's** findings indicate a positive correlation between the quantity of oxen and the technology used in teff row plantations. The study's findings demonstrate that, at a 10% significance level, the quantity of oxen has a favourable and significant impact on teff row plantation technology. According to the marginal effect result, for every additional ox, there is a 6.4% increase in the probability of using teff-row plantation technology. According to the information gathered from the focus group discussion and key informant interviews, farmers in the research area prepare rows using oxen. The outcome matched the research conducted by Musa *et al.*, (2017).

Impact analysis's propensity score matching (PSM) outcome

The influence on farm income was calculated in this section using the PSM technique and a binary dependent variable (teff row plantation technology). **Figure 1** demonstrates the high level of agreement between the propensity score match control group and the bath treated group. After matching, the kernel density indicates that the density is very high, roughly at 0.7. a propensity score histogram that is employed to verify the performance or validity of the propensity score matching estimation by validating the common support or overlap criterion. Assuming that the qualities are observed, the chance of taking part in any intervention falls between 0 and 1. (Caliendo and Kopeinig 2005). To determine whether matching is successful in making the distributions appear more similar, the propensity score distributions for the treated and untreated groups must be visually evaluated while the overlap condition is



**Aman Rikitu et al.,**

being observed (Bryson *et al.*, 2002). The propensity score histogram, which is used to evaluate the degree of overlap between the treatment and control groups, is shown in **Figure 2**. The two groups have sufficient similarities or mutual support, as demonstrated by the graph below. The result recognized a significant overlap in the shared support region. Figure 3 illustrates the significant overlap in the distribution of propensity scores between those who received treatment and those who did not in both groups. Furthermore, the results indicated that certain individuals are not within the shared support network. In addition, there are people who receive treatment (on support) and people who do not (off support). According to the results, there was a significant level of overlap between the propensity scores of the household head farmers who were adopters and those who were not. Thankfully, it is evident that the top half of the graph represents the treated or adopter groups, while the lower half represents the untreated and non-adopter groups. The frequent areas of support along the x-axis are displayed along with the score densities on the y-axis. Ten household heads (six from treatment houses and four from control households) whose propensity scores fell beyond the zone of common support were thus excluded from the study as a result of this constraint. Thus, it seems that the 322 houses that were part of the observations were sufficient to predict the impact of teff row plantation technology on the households under investigation. We computed the distribution of the projected propensity scores matching utilizing kernel density for both the adopters (treatment) and non-adopters (control) groups to see if there was a shared support. **Figure 3** presents the results graphically. The propensity score of the non-adopters (control) group is represented by the long line (left upper and right below line); the propensity score of the adopters (treated) group is represented by the short line (left below and right upper line). The figure shows the total sample household head as represented by the normal line (the middle line). The distribution of estimated propensity scores, expressed using kernel density, for adopter and non-adopter households before and after the common support condition was imposed are shown in **Figures 2 and 3**, respectively. The majority of participant families have propensity scores of approximately 25000, whereas the majority of non-participating households have propensity scores of approximately 0.7, as illustrated in these figures.

Average treatment effect

The impact component of this study focuses on determining the average treatment effect on the treated (ATT) teff row planting technology. The counterfactual means of the treated must be replaced with the mean outcome of the untreated, as it is not possible to quantify this effect using before and after data due to the lack of baseline data (Caliendo and Kopeinig, 2005). It accounts for sample selection bias caused by observable differences between the comparison and treatment groups. Every individual observation in the treatment group is matched with an identical observation from the control group that has similar observable qualities to establish a statistical comparison group, which takes self-selection into account. **Table 5** indicates that there is a significant difference between those who have adopted teff row planting technology and those who have not. The main objective of the study was to determine how adopting the teff row planting technology will affect households' income. **Table 5** shows that sample homes that adopted the teff row planting technology had an average income of 65603.15 ETB, compared to non-adopters who only get 64657.95 ETB. Adopter household income has increased by an average of 945.10Birr, according to the impact analysis of the PSM outcome, which takes into consideration pre-intervention disparities between adopters and non-adopters of this technology. PSM results show that the technology of teff row planting has a significant effect on wheat productivity.

CONCLUSIONS

In Ethiopia, cereals make up 87.48% of grain production and 95% of all agricultural output. They are the country's main food crops. For 43% of small-holder farmers, teffa cereal crop that accounts for 21% of total grain production and 32% of average annual production is the most significant economic crop. The second-most significant cash crop, teff brings roughly \$500 million USD annually for nearby farmers. People with type 2 diabetes can benefit from it because of its low glycemic index, high protein content, and amino acid content. It is also gluten-free. With 48% of the country's teff produced there, Ethiopia's Oromia region is the main producer. By covering 1.43 million hectares and yielding 2.56 million tons with a yield of 1.79 t/ha from 2.57 million smallholders, teff accounted for 29.46



**Aman Rikitu et al.,**

percent of all cereal crop land in 2018-19. Ethiopia's teff production has been declining as a result of the traditional broadcasting seeding techniques, which are difficult to hoe and weed and give low yields due to small seeds. The implementation of row planting technology has the potential to enhance productivity and yield levels through many means such as lowered seed rate, increased spacing between seedlings, enhanced weed control, reduced competition, and enhanced branching and nutrient uptake. The planning and execution of technology-related activities must take into account the obstacles to the application of agricultural technology in order to address the problems with teff production in the research region. Therefore, policy makers and planners of new technology need to have a full awareness of farmers' requirements and capacity for adopting teff row planting in order to build technology that will work for farmers. The results of the study showed that the application of teff row planting greatly boosted adopters' productivity, revenue, and food security; for these reasons, it is desirable to encourage the adoption of this row planting technique. Improved seed, training, fertilizer, number of oxen, and distance from the closest market are all highly significant variables, according to the results of the econometrics model. As a result, in order to increase household production and income, relevant parties like policymakers, NGOs, and the general public should focus on the aforementioned factors. The significance of the seeded machine is further demonstrated by the qualitative data in addition to the quantitative results. Because planting teff in a row requires a lot of labour, as indicated by the qualitative data, it is advised that technological innovators be pushed to develop a seeded machine for farmers to reduce their cost of production. In order to successfully promote, adopt, and scale up effective agronomic practices and extension, farmers should be contacted and given awards for improving household row planting techniques that will boost teff yield. To guarantee food security, policymakers should create more effective farmer education programs and offer more practical teff cultivation machinery. Therefore, increasing the adoption of technology by including the previously described steps may result in a rise in both the number of users and the area of crops planted using row planting technology. Consequently, accelerating the pace of technology adoption would unavoidably result in notable and long-lasting gains in productivity and revenue for teff.

DATA AVAILABILITY

Data is available in the manuscript

CONFLICT OF INTEREST

The authors don't have any possible conflicts of interest

ACKNOWLEDGEMENT

The authors would like to thank Dendi and Ejere Agricultural Office for providing research data facilities to this study.

REFERENCES

1. ATA (2013a)., "Results of 2012., New Tef Technologies Demonstration Trials Draft Report VF".
2. Berihun K., Bihon K., and Kibrom A., (2014). Adoption and Impact of Agricultural Technologies on Farm Income: Evidence from Southern Tigray, Northern Ethiopia. *International Journal of Food and Agricultural Economics*, 2(4), 91-106.
3. Berhane, G., Z. Paulos, and K. Tafere., (2011). Foodgrain Consumption and Calorie Intake Patterns in Ethiopia. Ethiopia Strategy Support Paper (ESSP) II Working Paper 23. Addis Ababa, Ethiopia: International Food Policy Research Institute (IFPRI)
4. Birrara E., (2017) Teff production and marketing in Ethiopia. *A Journal of Radix International Educational and Research Consortium*, 6(4), 2250-3994
5. Bryson, A., Dorsett, R. & S, P. (2002). The use of propensity score matching in the evaluation of labour market policies, working paper no. 4, department for work and pensions.





Aman Rikitu et al.,

6. Caliendo, M. and Kopeinig, S. (2005). Some Practical Guidance for the Implementation of Propensity Score Matching: Discussion Paper No. 1588. University of Cologne.
7. Chauhan, H.S, S.K.A, Anuruddhika, S.W., Manoja, D.K., Sakinda, and B.W. Upali. (2014). Effect of rice establishment methods on weedy rice infestation and grain yield of cultivated rice (O. Sativa L.) In Sri Lanka Crop Prot.55.
8. Cheng A, Mayes S, Dalle G, Demissew S, Massawe F (2017) Diversifying crops for food and nutrition security - A case of teff. Biol Rev Camb Philos Soc, 92(1): 188-98.
9. CSA (2017) Agricultural sample survey 2016/2017 (2009 E.C).Volume I report on area and production of major crops (private peasant holdings, meher season), Addis Ababa
10. Dinku A (2019), Assessment of constraints and opportunities in small-scale beef cattle fattening business: Evidence from the West Hararghe Zone of Ethiopia. Int J Vet Sci Res 5(2): 058-068. DOI: <http://dx.doi.org/10.17352/ijvsr.000042>
11. DEWAO (Ejere District Agriculture Office). (2015). Annual Report of the District. Ejere, West Shoa zone, Ethiopia.
12. Ethiopia Economy (2020) , CIA World Factbook. https://theodora.Com/wfbcurrent/Ethiopia/ethiopia_economy.html.
13. Ethiopia, CSA (Central Statistical Agency). (2020). Agricultural Sample Survey 2019/2020. Area and Production of Major Crops. (Private Peasant Holdings, Meher Season). Addis Ababa: CSA
14. FAO,2017.EmergencesituationreportethiopiaEthiopia%C2%A0_%20FAO%20in%20Emergencies.html
15. FAO, (2020).Land use [online]. Rome. (cited September 2020). <http://www.fao.org/faostat/en/#data/RL>.
16. Fekadu Adamu NegussieFA (2020) Impact of row planting teff technology adoption on the income of smallholder farmers: The case of Hidabu Abote District, North Shoa Zone of Oromia Region, Ethiopia. Int J Agric Sc Food Technol 6(2): 195-203.DOI: <https://dx.doi.org/10.17352/2455-815X.000074>
17. Gerald Nelson, Jessica Bogard, Keith Lividini, Joanne Arsenault, Malcolm Riley, Timothy B. Sulser, Daniel Mason-D' Croz, Brendan Power, David Gustafson, Mario Herrero, Keith Wiebe, Karen Cooper, Roseline Remans and Mark Rose grant, (2018) Nature Sustainability 1:773-781 | www.nature.com/natsustain
18. Gujarati, D. N., Boston: McGraw-Hill (2009) "Basic Econometrics", 5th ed.
19. Ibrahim WH, Mekdim DR, Guush B, Bart M, Alemayehu ST (2018) Teff and its role in the agricultural and food economy: The economics of teff: Exploring ethiopia's biggest cash crop. International Food Policy Research Institute Washington, DC. Chapter 2.
20. Kidanemariam, A., Gebrekidan, H., Mamo, T., Kibret, K., et al. (2012) Impact of Altitude and Land Use Type on Some Physical and Chemical Properties of Acidic Soils in Tsegede Highlands, Northern Ethiopia. Open Journal of Soil Science, 2, 223-233. <http://dx.doi.org/10.4236/ojss.2012.23027>
21. Kothari, C.R. (2004) Sample Size Determination. Research Methodology. New Age International Publications.1, 74-81.
22. Matousa, P., Todob, Y., and Mojoc, D. (2013). Roles of extension and ethno-religious networks in acceptance of resource-conserving agriculture among Ethiopian farmers. International Journal of Agricultural Sustainability 11(4), 301-316.
23. Minten B, Tamru S, Engida E, Kuma T (2013) Ethiopia's value chain on the move: the case of teff. ESSP Working Paper series, 52, 1-26
24. MoFED. (2010). Growth and Transformational Plan GTP 2010-2015. Ministry of Finance and Economic Development. Addis Ababa.
25. National Bank of Ethiopia, (2018): Annual Report on Economic performance.
26. NPC. (2016). Federal Democratic Republic of Ethiopia Growth and Transformation Plan II (GTP II) (2015/16-2019/20) ; I: National Planning Commission May, 2016 AddisAbaba.http://dagethiopia.org/new/images/DAG_DOCS/GTP2_English_Translation_Final_June_21_2016.pdf.
27. Tigist M.(2017). Productivity and household welfare impact of technology adoption: Micro-level evidence from rural Ethiopia, United Nations University working paper (007).





Aman Rikitu et al.,

28. Vandecasteele, J., M. Dereje Regassa, B. Minten, and A. S. Taffesse. (2013). Scaling-Up Adoption of Improved Technologies: The Impact of the Promotion of Row Planting on Farmers' Teff Yields in Ethiopia. ESSP II Working Paper 60. Addis Ababa, Ethiopia: International Food Policy Research Institute.
29. Zeng, D., J. Alwang, G.W. Norton, B. Shiferaw, M. Jaleta and C. Yirga, (2015). Ex-Post Impacts of Improved Maize Varieties on Poverty in Rural Ethiopia. *Agricultural Economics* 46 (4), 515-526

Table 1: Sample size by districts, kebeles, adopter and non-adopter

	District	Sample		Sample taken		
	Kebele	Adopter	Non-adopter	Adopter	Non-adopter	Total
Dendi	Wamurasa Ko	167	226	20	20	40
	Faji Qalila	379	418	32	30	62
	Loqloqa	100	112	14	16	30
	Warga	195	251	22	22	44
	Talbo	109	119	15	16	31
Ejere	Hora	199	189	22	21	43
	Amaro	291	307	29	30	59
	Indode	66	77	12	13	25
	Total	1488	1712	166	166	332

Source: Dendi and Ejere Agricultural Office (2021)

Table 2. Descriptive and inferential result of dummy variables used for the study

Teff row plantation					
	adopters		Non-adopters		
Variables	No.	%	No.	%	χ^2 -value
Female	13	41.94	18	58.06	0.8924
Male	148	50.86	143	49.14	
Access to extension	149	50.85	144	49.15	0.9474
Irrigation water	46	3.49	40	46.51	0.5711
Improved seed	134	60.36	88	39.64	30.6915***
Pesticide	120	54.79	99	45.21	6.2953***
Seeder	44	55.00	36	45.00	1.0645
Cooperative	30	57.69	22	42.31	1.4678

Note: *** showed 1% significance level

Table 3: Descriptive statistics for continuous variables

Teff row plantation technology					
	adopters		Non-adopters		
Variables	mean	Stand. error	mean	Stand. error	t-test
Age	44.83	0.843	46	0.824	0.984
Education	3.23	0.281	2.64	0.262	-1.534
Family S.	6.28	0.199	5.81	0.209	1.611**
own land	1.04	0.033	1.08	0.046	0.673
Yield	7.64	0.991	7.36	0.962	-0.201
distance	2.32	0.123	2.62	0.142	1.550*
Income teff	66133.39	3760.814	49009.78	3147.834	-3.491***





Aman Rikitu et al.,

Fertilizer	5781.24	389.421	6503.60	561.503	1.057
Herbicide	780.62	79.155	1272.76	206.285	2.233***
N of oxen	2.28	0.079	1.02	0.061	-2.639***

Note: *** showed 1% significance level

Table 4: Probit model result of the study

Variables	Coefficient	Standard errs.	P> z	Dy/dx
sex	0.311	0.279	0.266	0.109
age	0.002	0.008	0.807	0.001
Education level	0.005	0.023	0.825	0.001
Family size	-0.055	0.035	0.116	-0.026
Own land	-0.090	0.149	0.544	-0.037
Access to extension	-0.033	0.291	0.908	-0.038
irrigation	-0.030	0.177	0.863	-0.004
Improved seed	0.9729	0.177	0.000***	0.366
distance	-0.089	0.051	0.079*	-0.037
training	0.3448	0.176	0.051**	0.141
seeder	0.1170	0.195	0.550	0.046
fertilizer	0.005	0.003	0.024**	0.002
Number of oxen	0.162	0.089	0.069*	0.064
Credit amount	0.000	0.003	0.460	0.004
cons	-0.684	0.545	0.210	-

Note: ***, ** and * shows 1%, 5% and 10% percent significance level

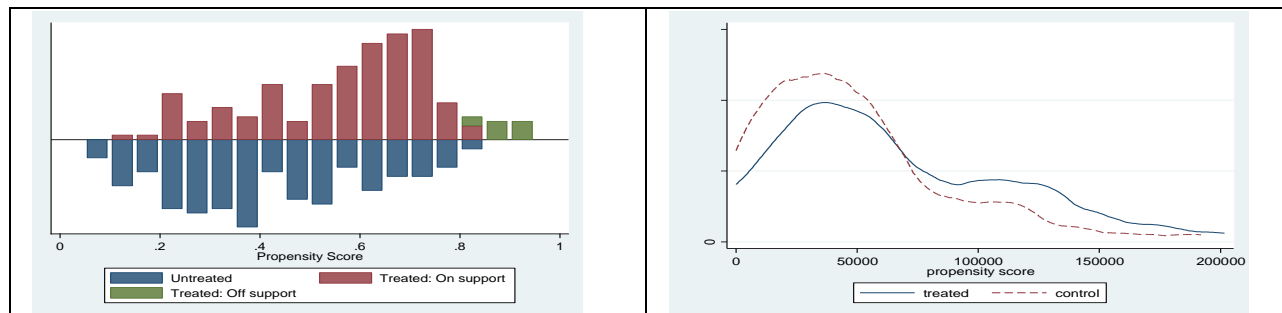


Figure 1. Propensity score

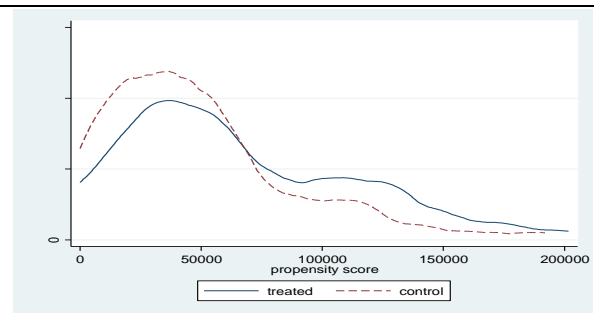


Figure: 2. Kernel density before matching

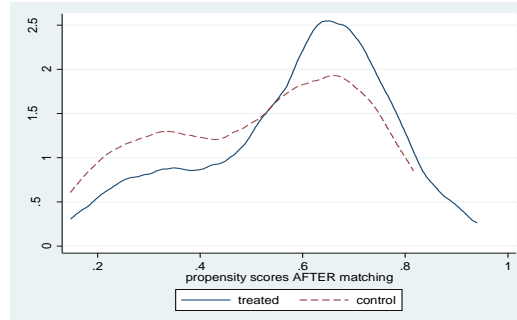


Figure 3. kernel density after matching





Bioanalytical Method Development and Validation of Lacidipine in Human Plasma by LC-MS/MS

K.E. Pravallika¹, T.Gurumurthy^{2*} and P.Ravi¹

¹Assistant Professor, Department of Pharmaceutical Analysis, Acharya Nagarjuna University College of Pharmaceutical Sciences, Guntur, Andhra Pradesh, India.

²Assistant Professor, Department of Pharmaceutical Analysis, Creative Educational Society's College of Pharmacy, Kurnool, Andhra Pradesh, India.

Received: 30 Dec 2023

Revised: 09 Jan 2024

Accepted: 27 Mar 2024

*Address for Correspondence

T.Gurumurthy

Assistant Professor,

Department of Pharmaceutical Analysis,

Creative Educational Society's College of Pharmacy,

Kurnool, Andhra Pradesh, India.

Email: gurumurthy.telugu@gmail.com



This is an Open Access Journal / article distributed under the terms of the **Creative Commons Attribution License** (CC BY-NC-ND 3.0) which permits unrestricted use, distribution, and reproduction in any medium, provided the original work is properly cited. All rights reserved.

ABSTRACT

A high performance liquid chromatography mass spectrometric method for the estimation of Lacidipine, in human plasma, was developed and validated using carbamazepine as internal standard (IS). Sample preparation was accomplished by Solid - Phase extraction technique. The reconstituted samples were chromatographed on Zorbax XDB - Phenyl, 75 X 4.6 mm, 5 μ m (make: Agilent) column using a mobile phase consisting of HPLC Grade Acetonitrile : 5 mM Ammonium acetate buffer (80 : 20 v/v). There was a flow of 1 ml/min. The method was validated over a concentration range of 0.2052 ng / mL to 12.5026 ng / mL of Lacidipine with the detection of lacidipine m/z - 456.20 (parent) and 354.20 (product) and internal standard carbamazepine m/z - 237.10 (parent) and 194.10 (product) in positive ion mode. The results of the study showed that the proposed LC MS method is simple, rapid, precise and accurate, which is useful for the estimation of Lacidipine in bulk fluids and biological plasma sample analyte with accuracy and reproducibility.

Keywords: LCMS/MS, Biological research, Validation, Lacidipine, Carbamazepine

INTRODUCTION

Lacidipine (LAC) is a calcium channel blocker used to reduce blood pressure in hypertension. It has good hydrophobic interactions that give high distribution of drug in the lipophilic membrane. Chemically, it is (E)-4-[2-[3-(1, 1-dimethylethoxy)-3-oxo-1-propenyl] phenyl]-1, 4-dihydro-2, 6-dimethyl-3,5 pyridine di-carboxylic acid diethyl



**Pravallika et al.,**

ester that contains dihydropyridine ring responsible for antihypertensive activity. It is the most commonly used antihypertensive drug as it has high vascular selectivity, tolerability and large dose acceptability with negative inotropic effects. In spite of anti-hypertensive activity, it shows anti-atherosclerotic, antibacterial and antioxidant effects such as Vitamin E. It has such an important role in treating the life-threatening cardiovascular disorders. The various formulations are available in the market pertaining to this drug. In order to assess the pharmacokinetic parameters, toxicological properties and to estimate the exact concentration of LAC, various analytical techniques are employed for the estimation of LAC in pharmaceutical dosage forms, biological matrices and for the physical characterization of LAC. Here these methods are described to give a clear glance for the future scientists to develop few more easily adoptable methods

MATERIALS AND METHODS

Chemicals and solvents: Lacidipine & carbamazepine were purchased from Hetero Labs, Hyderabad (India). acetonitrile and methanol J.T. BAKER. Buffer was purchased from Merck and hplc grade water was obtained from the Milli-Q water system. The remaining compounds were all of analytic quality.

LC-MS/MS Instrument & Software

High performance liquid chromatography system manufactured by Shimadzu. Which consist of PDA detector, Quaternary solvent manager, sample manager, column heating compartment was used for assay determination of lacidipine. HPLC instrument was controlled by software Analyst 1.4.2. A Thermo Hypersil BDS C18 75 x 3.5 mm, column with particle size of 3.0 μm was used as stationary phase for chromatographic separation. Sartorius semi micro analytical balance was used for all weighing, Thermo pH meter was used for buffer pH adjustment, and sonicator used to dissolve the solutions. The electro spray ionisation (ESI) interface of a triple quadrupole mass spectrometer API 4000 operating in the positive ion mode was used to ionise the analyte and detect the IS.

Preparation of standard solutions & (QC) samples

Weighed accurately, about 10 mg of Lacidipine working standard and transferred to a 10 mL clean glass volumetric flask, dissolved in 1 % formic acid in methanol and made up the volume with the same to produce a solution of 1.000 mg / mL. Corrected the above concentration of lacidipine solution accounting for its potency and the actual amount weighed. The stock solution was stored in refrigerator at 2 – 8 °C and used for maximum of three days. Stock solution was prepared under monochromatic light.

Sample Preparation

500 μL of the plasma sample was pipetted into polypropylene pre labeled RIA vials, 50 μL (4.0301 ng / mL of Carbamazepine) Internal standard spiking solution Experimental Chapter – 4 67 Division of Pharmaceutical Analysis & Quality Assurance, CPR, RIPER was added, except in blank plasma samples where 50 μL diluent was added to it. Then 500 μL of extraction buffer was added to it and vortexed. The following sample processing steps were followed.

Oasis HLB, 30 mg / 1CC SPE cartridges were taken (Make: Waters)

(New cartridge for each sample) ↓

Conditioned the cartridges with 1.0 mL Methanol, followed by 1.0 mL of extraction buffer and 1.0 mL of Milli - Q - Water ↓

Whole sample was applied which was already prepared in RIA vials ↓

(Completely dried the cartridges) ↓

Cartridges were washed, after applying maximum pressure when the sample gets down, with 1.0 mL of extraction buffer and followed by 2 mL Milli - Q - Water. ↓

Then sample was eluted with 2.0 mL of dichloromethane and evaporated in steam of nitrogen at 40°C until dryness.

↓

The residue was reconstituted with 0.50 mL of mobile Phase, transferred into auto sampler vials.





RESULTS AND DISCUSSION

System Suitability Test

System suitability was performed by injecting 6 consecutive injections of Lacidipine at middle concentration (12.0092 ng / mL) of calibration range and Carbamazepine at working concentration (0.8060 ng / mL).

Linearity

A regression equation with a weighting factor of 1 / (concentration ratio) 2 of drug to IS concentration was judged to produce the best fit for the concentration - detector response relationship for lacidipine in human plasma. The representative calibration curve for regression analysis is illustrated in Figure 10. The results were presented in Table 23

Precision and Accuracy

To assess precision and accuracy of the developed analytical method, 5 distinct concentrations (QC's) in the range of CC were prepared, processed and evaluated using 6 replications per Q.C concentrations.

Recovery

Processed 24 blank plasma samples. Prepared each 6 sets of recovery comparison samples by reconstituting with 0.2500 mL of final recovery dilutions of quality control samples (LQC, MQC 2 and HQC) and internal standard, representing 100 % extraction and injected. The recovery comparison samples of lacidipine were compared against extracted samples of LQC, MQC 2 and HQC of PA batch - V. The recovery comparison samples of internal standard were compared against the response of internal standard in MQC 2 level (25 - 30).

Stability Experiments

As part of the method validation, the stability study was assessed. The following stability test was created to gauge how easily Solriamfetol might decompose under certain conditions

Freeze - thaw Stability

The stability of lacidipine in human plasma was determined during three freeze-thaw cycles. Six replicates, each of LQC (0.6101 ng / mL) and HQC (10.7717 ng / mL) were analysed after three freeze - thaw cycles. The freeze - thaw quality control samples were quantified against the freshly spiked calibration curve standards of concentration range equivalent to that used for the calculation of precision and accuracy, refer, Table 35a. The results were presented in Table 35b

Bench Top Stability

Bench Top Stability of lacidipine using six sets each of LQC (0.6101 ng / mL) and HQC (10.7717 ng / mL) was determined at 6 hours. The quality control samples were quantified against the freshly spiked calibration curve standards 35a. The results were presented in Table 35c

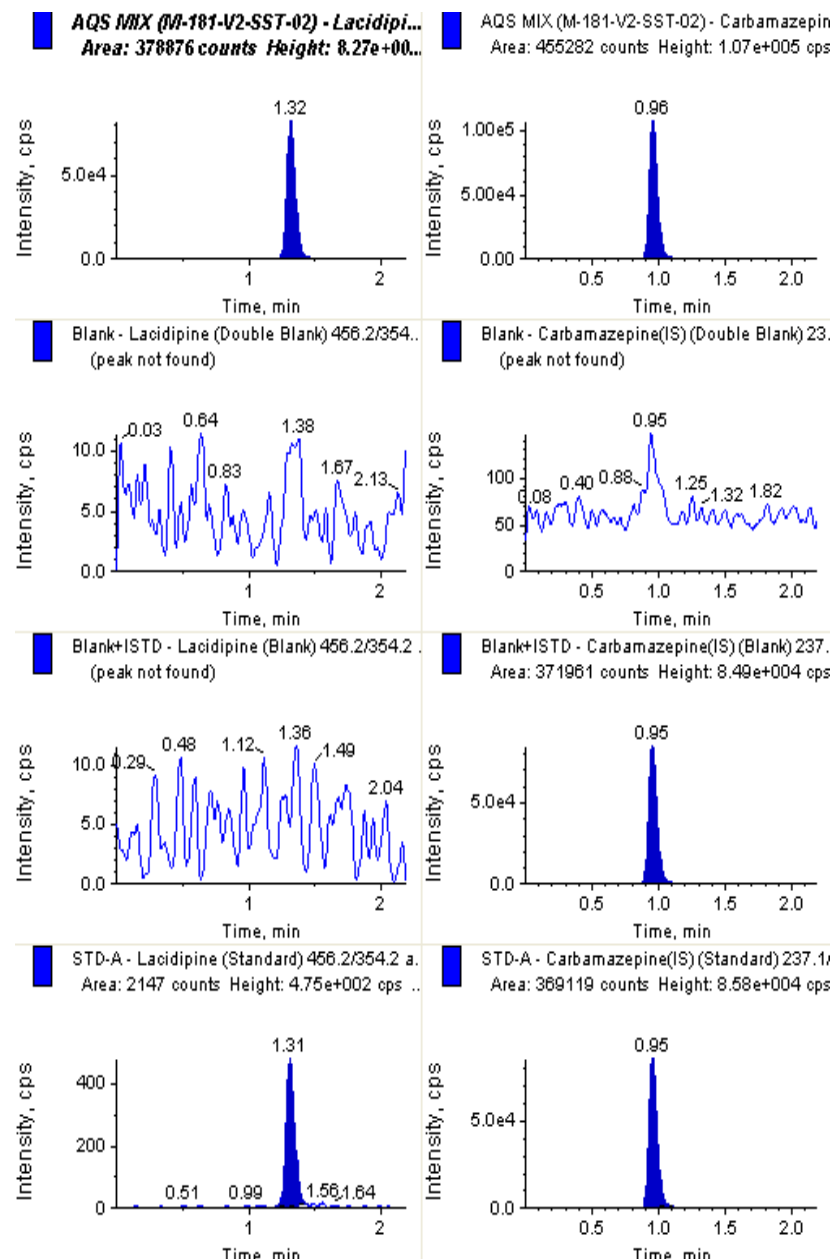
Wet - Extract Stability

In assessing the wet extract stability, six sets of QC samples (LQC (0.6101 ng / mL) and HQC (10.7717 ng / mL)) were processed and placed in the room temperature (20 ± 5 °C). These samples were injected after a period of 35 hours and were quantified against freshly spiked calibration curve standards of concentration range equivalent to that used for calculation of precision and accuracy,





Pravallika et al.,



CONCLUSION

The results of selectivity, matrix effect, sensitivity, linearity, precision and accuracy, stabilities, recovery and dilution integrity presented in this report are within the acceptance range for bioanalytical batch acceptance criteria, USFDA acceptance range as per 'Guidance for Industry - Bioanalytical Method Validation (May 2001)' given by CDER. This analytical method is valid for the estimation of lacidipine, in human plasma over a range of 0.2052 ng / mL to 12.5026 ng / mL with the detection of lacidipine m/z -456.20 (parent) and 354.20 (product) and internal standard carbamazepine m/z - 237.10 (parent) and 194.10 (product) in positive ion mode. In summary, we have developed and validated a specific and reproducible LC-MS/MS assay to quantify lacidipine in human plasma in negative ion mode.





Pravallika et al.,

REFERENCES

1. Ramakrishna N. V. S., Vishwottam K. N., Puran S., Manoj S., Santosh, M., Koteswara M., 2004, Journal of Mass Spectrometry, 39, 824 - 832.
2. Baranda Ana B., Mueller Claudia A., Alonso Rosa M., Jiménez Rosa M., Weinmann, Wolfgang., Therapeutic Drug Monitoring, February 2005, Vol27, Issue 1, 44 - 52.
3. Gannu Ramesh., Yamsani Vamshi Vishnu., Palem Chinna Reddy., Yamsani Shraavan Kumar and Yamsani Madhusudan Rao., Analytica Chimica Acta, Vol 632, Issue 2, 26 January 2009, 278 - 283.
4. S. Braggio., S. Sartori., F. Angeri., M. Pellegatti., Journal of Chromatography B: Biomedical Sciences and Applications, Vol 669, Issue 2, 21, July 1995, 383 - 389.
5. María J. Nozal., José L. Bernal., Juan J. Jiménez., María T. Martín., Francisco J. Diez, Journal of Chromatography A, Vol 1024, Issues 1 - 2, 23 January 2004, 115 - 122.
6. Shantha Kumar P.T., Nagaraju P.T., U.Siva Kumar., International Journal of Pharmaceutical Sciences Review and Research, Vol5, Issue 3, Nov - Dec 2010, Article - 003, 14 - 17. Bibliography Chapter - 7
7. Nagaraju P.T., K.P. Channabasavaraj., Shantha Kumar P.T., International Journal of Pharm Tech Research, Vol. 3, No.1, Jan - Mar 2011, 18 - 23.
8. Fortuna A., Sousa J., Alves G., Falcão A., Soares-da-Silva P., Anal Bioanal Chem. 2010 Jun, 397(4), 1605 - 15.
9. K. Srinivasa Rao., Nikhil Belorkar., Journal of Advanced Pharmaceutical Research, 2010, 1, 36- 47.
10. Kelmann R. G., Kuminek G., Teixeira H. F., Koester L. S., Chromatographia Wiesbaden, 2007, Vol 66, Number 5 - 6, 427 - 430.
11. B. Jovic., M. Zecevic., A. Protic., L. Zivanovic., P. Dzodic., Chromatographia, 2009, 70(9 - 10), 1343 - 1351.

Table 1. Within Batch Precision and Accuracy for Sensitivity of Lacidipine

S.No	Conc. (ng / mL)
	LLOQ
	0.2052
1	0.1926
2	0.1864
3	0.1883
4	0.1858
5	0.1963
6	0.1947
AVERAGE	0.19068
S.D	0.004455
C.V. %	2.34
% NOMINAL	92.93

Table 2: Freeze Thaw Stability (Three Cycles) of Lacidipine

	Concentration (ng / mL)	
	LQC	HQC
QC	0.6101	10.7717
55	0.5615	9.7098
56	0.5328	11.0278
57	0.5836	10.8883
58	0.5521	10.0744
59	0.5530	9.8803
60	0.5670	10.1197





Pravallika et al.,

Mean	0.55833	10.28338
S.D	0.016987	0.544430
C.V. %	3.04	5.29
% Nominal	91.52	95.47
N	6	6

Table 3 Auto sampler Stability Data of Lacidipine for 6 hours

	Concentration (ng / mL)	
	LQC	HQC
QC	0.6101	10.7717
61	0.5721	10.9944
62	0.5209	10.1252
63	0.5567	10.0246
64	0.5793	10.4095
65	0.5647	9.6657
66	0.5362	11.2259
Mean	0.55498	10.40755
S.D	0.022343	0.598466
C.V. %	4.03	5.75
% Nominal	90.97	96.62

Table 4: Recovery of Lacidipine in human plasma

	LQC Response		MQC 2 Response		HQC Response	
	Extracted QC	Unextracted QC	Extracted QC	Unextracted QC	Extracted QC	Unextracted QC
REC QC	LQC (25 - 30)	LQC (1 - 6)	MQC 2 (25 - 30)	MQC 2 (1 - 6)	HQC (25 - 30)	HQC (1 - 6)
1	19918	22286	203085	230395	340221	383760
2	19500	22247	202068	228547	340295	382581
3	20431	21781	200707	222361	352407	384100
4	19286	22506	213319	230378	345645	383086
5	21335	22128	233685	230795	370148	383120
6	21514	22460	211419	227107	368818	385848
Mean	20330.7	22234.7	210713.8	228263.8	352922.3	383749.2
S.D	934.95	262.44	12393.91	3214.97	13589.66	1160.05
C.V. %	4.60	1.18	5.88	1.41	3.85	0.30
N	6	6	6	6	6	6
% Recovery	91.44		92.31		91.97	





Decision Making Method to Assess the Most Affected Diseases among the People in the Particular Area using Fuzzy Soft Matrices

R.Hema* and S.Prabha

Assistant Professor, Department of Mathematics, A.V.V.M Sri Pushpam College (Autonomous) Poondi, Thanjavur, (Affiliated to Bharathidasan University, Tiruchirappalli), Tamil Nadu, India

Received: 04 Feb 2024

Revised: 12 Apr 2024

Accepted: 23 May 2024

*Address for Correspondence

R.Hema

Assistant Professor,
Department of Mathematics,
A.V.V.M Sri Pushpam College (Autonomous)
Poondi, Thanjavur,
(Affiliated to Bharathidasan University, Tiruchirappalli),
Tamil Nadu, India.



This is an Open Access Journal / article distributed under the terms of the **Creative Commons Attribution License** (CC BY-NC-ND 3.0) which permits unrestricted use, distribution, and reproduction in any medium, provided the original work is properly cited. All rights reserved.

ABSTRACT

In recent days non-communicable diseases play an important role in morality. The failure of awareness about NCD increases the risk level of the disease. The analysis of the procedure is to maintain and control the diseases and this control is established by several methods using fuzzy soft analysis. Here, we use the method of the fuzzy soft matrix to find out the people highly affected by diseases in a particular place using the Decision-Making Analysis Method. We first generalize the product of two fuzzy soft matrices. Two or more Fuzzy Soft Matrices in different types of sets can be manipulated in Health Care procedures and applied to a Decision-Making problem. Then we can use the algorithm with the product of Fuzzy Soft Matrix to deal with such problems.

Keywords: Fuzzy Set, Fuzzy Soft Set, Fuzzy Soft Matrix, Decision Making

INTRODUCTION

In our real-world scenarios, we frequently encounter mathematical problems involving uncertainty, particularly in fields such as Environmental Sciences, Economics, and Medicine. Classical methods often fall short due to the insufficiency and incompleteness of the available data. To address this uncertainty, Zadeh introduced the fuzzy set theory in 1965. Subsequently, Molodtsov proposed the innovative Soft Set theory to handle uncertainties effectively. Cagman then defined the Soft Matrix as a representation of the Soft Set.





Hema and Prabha

Maji later combined the Fuzzy Set and Soft Set to form the concept of Fuzzy Soft Set, which was further revised and improved by Ahamad and Kharal based on Maji's work. The use of matrices are widespread in various fields of science and engineering, and they are particularly well-suited for addressing problems involving uncertainty. While classical matrix methods may not suffice for tackling uncertainty, Fuzzy Soft Matrices, derived from Fuzzy Soft Sets, provide a promising alternative. This approach was initiated by Yong Yang and Chenli Ji to address decision-making problems through the use of Fuzzy Soft Matrices. To manage and control non-communicable diseases (NCDs), various methods, including fuzzy analysis, have been employed. This research employs the method of fuzzy soft matrices to identify highly affected individuals in specific locations using a Decision-Making Analysis approach. We generalize the multiplication of two fuzzy soft matrices and apply it to healthcare procedures. Multiple Fuzzy Soft Matrices from different types of sets can be manipulated in healthcare procedures and utilized in decision-making problems. The algorithm involving the product of Fuzzy Soft Matrices is employed to address these challenges.

The history of these mathematical approaches reveals a progression from the introduction of soft set theory by Molodstov in 1999 to the development of fuzzy soft decision-making algorithms by Maji in 2001. Further advancements were made by Roy and Maji in 2007, followed by the work of Ahamed and Tharal in 2009, the definition of soft matrices by Cagman in 2010, and the proposal of a weighted fuzzy soft set by Feng in the same year. Yong's successful application of the notion of fuzzy soft matrices in certain decision-making problems in 2011 and the extensions made by Neog, Bora, and Sut in 2012 further enriched this field of study. New results on fuzzy soft matrices have been explored by Seyyed Hossein Jafari Petroudi, Zahra Nabati, and Alireza Yaghobi. The application of fuzzy soft matrices in medical diagnosis has also been demonstrated by Lavanya M and Akila S. The research project culminates in an algorithm that offers a comprehensive solution to problems involving Fuzzy Soft Matrices.

Algorithm

Step 1: Begin by acquiring two fuzzy soft matrices, denoted as $A^{(1)}$ & $B^{(1)}$, each being $n \times n$ matrices.

Take a fuzzy soft matrix X_1 with $n \times 1$, $n=1,2,\dots,r$.

Multiply $A^{(1)} \times X_1 = Y_{11}$ (say),

Multiply $B^{(1)} \times X_1 = Z_{12}$ (say)

$Y_{11} \cup Z_{12} = \{y_{ij} + z_{ij} - y_{ij}z_{ij}\} = R_{11} = R^{(1)}$ (say)

Step 2: Extend the procedure by obtaining two additional fuzzy soft matrices, labeled as $A^{(2)}$ & $B^{(2)}$, also in the format of $n \times n$ matrices.

Take a fuzzy soft matrix X_2 with $n \times 1$, $n=1,2,\dots,r$.

Multiply $A^{(2)} \times X_2 = Y_{21}$ (say),

Multiply $B^{(2)} \times X_2 = Z_{22}$ (say)

$Y_{21} \cup Z_{22} = R_{21} = R^{(2)}$ (say).

Step 3: Repeat the same process iteratively to generate a total of n pairs of matrices, resulting in $R^{(3)}$, $R^{(4)}$, and so forth up to $R^{(n)}$

Step 4: Introduce a single fuzzy soft weight matrix W , which is an $n \times n$ matrix.

Step 5: Construct the matrix S_{ij} by utilizing the previously derived $R^{(1)}$, $R^{(2)}$, ..., $R^{(n)}$

Step 6: Combine the fuzzy soft matrix S_{ij} with the weight matrix W through an addition process.

$U_i = \min \{1, S_{ij} + W_{ij}\}$

We get the fuzzy soft matrix U_1 .

Step 7: Select the high value related to diseases and give the ranking.





Hema and Prabha

Step 8: Select the most preference group and also find the most preference person in a group

Procedure

Here we have selected the four most common prevalence diseases viz., Diabetes, Cancer, Blood Pressure, and Cardiac Vascular Disease. They are notoriously known as “silent killers”.

We chose the persons in a group who were affected by Frequent urination, Increased thirst, unexplained weight loss, and blurred vision symptoms. Consider group A ⁽¹¹⁾ have set of four male persons {P₁, P₂, P₃, P₄} with the set of 4 symptoms {S₁, S₂, S₃, S₄} related to diabetes. B ⁽¹¹⁾ have set of 4 female persons {P₁, P₂, P₃, P₄} with the set of 4 symptoms

{S₁, S₂, S₃, S₄} related to diabetes.

S₁- Frequent urination

S₂-Increased thirst

S₃- Unexplained weight loss

S₄- blurred vision

To give the membership grade using linguistic variables for the symptoms to realize the person in days

Symptom in days	Linguistic variable	Fuzzy Number
0 - 9 -	very Low -	0,0.1
10 - 19 -	low -	0.2-0.4
20 - 29 -	medium -	0.5,0.6
30 - 39 -	high -	0.7,0.8
Above 40 -	very high -	0.9,1

First, we construct a Fuzzy Soft Set (F₁, E₁) for male persons

$$(F_1, E_1) = \{ F(P_1) = (S_1, 0.8) (S_2, 0.2) (S_3, 0.05) (S_4, 0.7) \}$$

$$F(P_2) = (S_1, 0.7) (S_2, 0.5) (S_3, 0.6) (S_4, 0.3)$$

$$F(P_3) = (S_1, 0.03) (S_2, 0.7) (S_3, 0.4) (S_4, 0.2)$$

$$F(P_4) = (S_1, 0.6) (S_2, 0.2) (S_3, 0.4) (S_4, 0.9) \}$$

we construct Fuzzy Soft Set (G₁, H₁) for female persons

$$(G_1, H_1) = \{ G(P_1) = (S_1, 0.5) (S_2, 0.7) (S_3, 0.8) (S_4, 0.7) \}$$

$$G(P_2) = (S_1, 0.9) (S_2, 0.3) (S_3, 0.5) (S_4, 0.8)$$

$$G(P_3) = (S_1, 0.8) (S_2, 0.6) (S_3, 0.4) (S_4, 0.3)$$

$$G(P_4) = (S_1, 0.7) (S_2, 0.3) (S_3, 0.9) (S_4, 0.6) \}$$

Thus, the person-symptom fuzzy soft matrix A¹¹, B¹¹

$$A^{(11)} = \begin{pmatrix} 0.8 & 0.2 & 0.5 & 0.7 \\ 0.7 & 0.5 & 0.6 & 0.3 \\ 0.3 & 0.7 & 0.4 & 0.2 \\ 0.6 & 0.2 & 0.4 & 0.9 \end{pmatrix} \quad B^{(11)} = \begin{pmatrix} 0.5 & 0.7 & 0.8 & 0.7 \\ 0.9 & 0.3 & 0.5 & 0.8 \\ 0.8 & 0.6 & 0.4 & 0.3 \\ 0.7 & 0.3 & 0.9 & 0.6 \end{pmatrix}$$





Hema and Prabha

Symptom -related to the occurrence of disease fuzzy soft set $(C_1, D_1) =$

$$F(S_1) = (d_1, 0.7)$$

$$F(S_2) = (d_1, 0.5)$$

$$F(S_3) = (d_1, 0.8)$$

$$F(S_4) = (d_1, 0.4)$$

And symptom - occurrence of disease fuzzy soft column matrix $X_1 =$

$$\begin{pmatrix} 0.7 \\ 0.5 \\ 0.8 \\ 0.4 \end{pmatrix}$$

$$A^{(1)}X_1 = \begin{pmatrix} 0.8 & 0.2 & 0.5 & 0.7 \\ 0.7 & 0.5 & 0.6 & 0.3 \\ 0.3 & 0.7 & 0.4 & 0.2 \\ 0.1 & 0.2 & 0.4 & 0.9 \end{pmatrix} \begin{pmatrix} 0.7 \\ 0.5 \\ 0.8 \\ 0.4 \end{pmatrix} \quad B^{(1)}X_1 = \begin{pmatrix} 0.5 & 0.7 & 0.8 & 0.7 \\ 0.9 & 0.3 & 0.5 & 0.8 \\ 0.8 & 0.6 & 0.4 & 0.3 \\ 0.7 & 0.3 & 0.9 & 0.6 \end{pmatrix} \begin{pmatrix} 0.7 \\ 0.5 \\ 0.8 \\ 0.4 \end{pmatrix}$$

$$|Y_{11} \cup Z_{12} = \begin{pmatrix} 0.56 \\ 0.49 \\ 0.35 \\ 0.42 \end{pmatrix} \cup \begin{pmatrix} 0.64 \\ 0.63 \\ 0.56 \\ 0.72 \end{pmatrix} = \begin{pmatrix} .8416 \\ .9534 \\ .714 \\ .8376 \end{pmatrix} = \begin{pmatrix} 0.2515 \\ 0.2849 \\ 0.2134 \\ 0.2503 \end{pmatrix} = R_{11} = R^{(1)}$$

In this set of persons, they realize A lump or mass, changes in bowel or bladder habits, changes in skin, and pain. Consider group A_{21} have set of four male persons $\{P_1, P_2, P_3, P_4\}$ with the set of 4 symptoms $\{S_1, S_2, S_3, S_4\}$ related to Cancer. B_{21} have set of 4 female persons $\{P_1, P_2, P_3, P_4\}$ with the set of 4 symptoms $\{S_1, S_2, S_3, S_4\}$ related to Cancer.

S_1	-	A lump or mass
S_2	-	changes in bowel or bladder habits
S_3	-	changes in skin
S_4	-	pain.

To give the membership grade using linguistic variables for the symptoms to realize the person in days

Symptom in days	Linguistic variable	Fuzzy Number
0 -9	- very Low	- 0,0.1
10 -19	- low	- 0.2-0.4
20 -29	- medium	- 0.5,0.6
30 - 39	- high	- 0.7,0.8
Above 40	- very high	- 0.9,1

First, we construct Fuzzy Soft Sets

$$(F_2, E_2) = \{F(P_1) = (S_1, 0.7) (S_2, 0.3) (S_3, 0.5) (S_4, 0.1)$$

$$F(P_2) = (S_1, 0.2) (S_2, 0.9) (S_3, 0.6) (S_4, 0.3)$$

$$F(P_3) = (S_1, 0.9) (S_2, 0.4) (S_3, 0.7) (S_4, 0.9)$$

$$F(P_4) = (S_1, 0.8) (S_2, 0.5) (S_3, 0.1) (S_4, 0.7)\}$$

$$(G_2, H_2) = \{G(P_1) = (S_1, 0.5) (S_2, 0.9) (S_3, 0.7) (S_4, 0.3)$$

$$G(P_2) = (S_1, 0.9) (S_2, 0.8) (S_3, 0.4) (S_4, 0.6)$$

$$G(P_3) = (S_1, 0.5) (S_2, 0.6) (S_3, 0.3) (S_4, 0.8)$$

$$G(P_4) = (S_1, 0.3) (S_2, 0.7) (S_3, 0.8) (S_4, 0.9)\}$$





Hema and Prabha

Thus the person-symptom fuzzy soft matrix A^{21}, B^{21}

$$A^{(21)} = \begin{pmatrix} 0.7 & 0.3 & 0.5 & 0.1 \\ 0.2 & 0.9 & 0.6 & 0.3 \\ 0.8 & 0.4 & 0.7 & 0.9 \\ 0.9 & 0.5 & 0.1 & 0.7 \end{pmatrix} \quad B^{(21)} = \begin{pmatrix} 0.5 & 0.9 & 0.7 & 0.3 \\ 0.9 & 0.8 & 0.4 & 0.6 \\ 0.5 & 0.6 & 0.3 & 0.8 \\ 0.3 & 0.7 & 0.8 & 0.9 \end{pmatrix}$$

symptoms -Occurrence of Cancer Fuzzy Soft Set $(C_2, D_2) =$

$$F(S_1) = (d_2, 0.5)$$

$$F(S_2) = (d_2, 0.8)$$

$$F(S_3) = (d_2, 0.4)$$

$$F(S_4) = (d_2, 0.3)$$

$$\text{And symptom - Occurrence of Cancer Fuzzy Soft column matrix } X_2 = \begin{pmatrix} 0.5 \\ 0.8 \\ 0.4 \\ 0.3 \end{pmatrix}$$

$$A^{(21)}X_2 = \begin{pmatrix} 0.7 & 0.3 & 0.5 & 0.1 \\ 0.2 & 0.9 & 0.6 & 0.3 \\ 0.8 & 0.4 & 0.7 & 0.9 \\ 0.9 & 0.5 & 0.1 & 0.7 \end{pmatrix} \begin{pmatrix} 0.5 \\ 0.8 \\ 0.4 \\ 0.3 \end{pmatrix} \quad B^{(21)}X_2 = \begin{pmatrix} 0.5 & 0.9 & 0.7 & 0.3 \\ 0.9 & 0.8 & 0.4 & 0.6 \\ 0.5 & 0.6 & 0.3 & 0.8 \\ 0.3 & 0.7 & 0.8 & 0.9 \end{pmatrix} \begin{pmatrix} 0.5 \\ 0.8 \\ 0.4 \\ 0.3 \end{pmatrix}$$

$$Y_{21} \cup Z_{22} = \begin{pmatrix} 0.35 \\ 0.72 \\ 0.40 \\ 0.45 \end{pmatrix} \cup \begin{pmatrix} 0.72 \\ 0.64 \\ 0.48 \\ 0.56 \end{pmatrix} = \begin{pmatrix} 0.818 \\ 0.8992 \\ 0.688 \\ 0.758 \end{pmatrix} = \begin{pmatrix} 0.2586 \\ 0.2843 \\ 0.2175 \\ 0.2396 \end{pmatrix} = R_{21} = R^{(2)}$$

We select a group of persons who were affected by Dizziness, Nose bleeds, agitation, Headache.

Consider group A^{31} have set of male persons $\{P_1, P_2, P_3, P_4\}$ with the set of 4 symptoms

$\{S_1, S_2, S_3, S_4\}$ related to High Blood Pressure . B^{31} have set of 4 female persons

$\{P_1, P_2, P_3, P_4\}$ with the set of 4 symptoms $\{S_1, S_2, S_3, S_4\}$ related to High Blood Pressure .

S_1	-	Dizziness
S_2	-	Nose bleeds
S_3	-	Agitation
S_4	-	Headache

To give the membership grade using linguistic variables for the symptoms to realize the person in days

Symptom in days	Linguistic variable	Fuzzy Number
0 - 9	very Low	0,0.1
10-19	low	0.2-0.4
20-29	medium	0.5,0.6
30- 39	high	0.7,0.8
Above 40	very high	0.9,1

First, we construct Fuzzy Soft Sets

$$(F_3, E_3) = \{F(P_1) = (S_1, 0.5) (S_2, 0.7) (S_3, 0.9) (S_4, 0.2)$$

$$F(P_2) = (S_1, 0.2) (S_2, 0.9) (S_3, 0.3) (S_4, 0.8)$$

$$F(P_3) = (S_1, 0.9) (S_2, 0.1) (S_3, 0.5) (S_4, 0.4)$$

$$F(P_4) = (S_1, 0.6) (S_2, 0.4) (S_3, 0.8) (S_4, 0.6)\}$$





Hema and Prabha

$$(G_3, H_3) = \{G(P_1) = (S_1, 0.6) (S_2, 0.4) (S_3, 0.5) (S_4, 0.8)$$

$$G(P_2) = (S_1, 0.7) (S_2, 0.8) (S_3, 0.4) (S_4, 0.6)$$

$$G(P_3) = (S_1, 0.3) (S_2, 0.5) (S_3, 0.9) (S_4, 0.7)$$

$$G(P_4) = (S_1, 0.4) (S_2, 0.2) (S_3, 0.7) (S_4, 0.6)\}$$

Thus the person - symptom Fuzzy Soft Matrix $A^{(31)}$, $B^{(31)}$

$$A^{(31)} = \begin{pmatrix} 0.5 & 0.7 & 0.9 & 0.2 \\ 0.2 & 0.9 & 0.3 & 0.8 \\ 0.9 & 0.1 & 0.5 & 0.4 \\ 0.6 & 0.4 & 0.8 & 0.6 \end{pmatrix} \quad B^{(31)} = \begin{pmatrix} 0.6 & 0.4 & 0.5 & 0.8 \\ 0.7 & 0.8 & 0.4 & 0.6 \\ 0.3 & 0.5 & 0.9 & 0.7 \\ 0.4 & 0.2 & 0.7 & 0.6 \end{pmatrix}$$

Symptom - Occurrence of High Blood Pressure Fuzzy Soft Set $(C_3, D_3) =$

$$F(S_1) = (d_3, 0.7)$$

$$F(S_2) = (d_3, 0.5)$$

$$F(S_3) = (d_3, 0.8)$$

$$F(S_4) = (d_3, 0.3)$$

Symptom - Occurrence of High Blood Pressure Fuzzy Soft column matrix $X_3 =$

$$X_3 = \begin{pmatrix} 0.7 \\ 0.5 \\ 0.8 \\ 0.3 \end{pmatrix}$$

$$A^{(31)} X_3 = \begin{pmatrix} 0.5 & 0.7 & 0.9 & 0.2 \\ 0.2 & 0.9 & 0.3 & 0.8 \\ 0.9 & 0.1 & 0.5 & 0.4 \\ 0.6 & 0.4 & 0.8 & 0.6 \end{pmatrix} \begin{pmatrix} 0.7 \\ 0.5 \\ 0.8 \\ 0.3 \end{pmatrix} \quad B^{(31)} X_3 = \begin{pmatrix} 0.6 & 0.4 & 0.5 & 0.8 \\ 0.7 & 0.8 & 0.4 & 0.6 \\ 0.3 & 0.5 & 0.9 & 0.7 \\ 0.4 & 0.2 & 0.7 & 0.6 \end{pmatrix} \begin{pmatrix} 0.7 \\ 0.5 \\ 0.8 \\ 0.3 \end{pmatrix}$$

$$Y_{31} \cup Z_{32} = \begin{pmatrix} 0.72 \\ 0.45 \\ 0.63 \\ 0.64 \end{pmatrix} \cup \begin{pmatrix} 0.42 \\ 0.49 \\ 0.72 \\ 0.56 \end{pmatrix} = \begin{pmatrix} 0.8376 \\ 0.7195 \\ 0.8964 \\ 0.8416 \end{pmatrix} = \begin{pmatrix} 0.2542 \\ 0.2185 \\ 0.2720 \\ 0.2554 \end{pmatrix} = R_{31} = R^{(3)}$$

In this fourth set of persons, they realize chest pain, shortness of breath, palpitations, sweating

Consider group $A^{(41)}$ have set of four male persons $\{P_1, P_2, P_3, P_4\}$ with the set of 4 symptoms $\{S_1, S_2, S_3, S_4\}$ related to the CVD. $B^{(41)}$ have set of 4 female persons $\{P_1, P_2, P_3, P_4\}$ with the set of 4 symptoms $\{S_1, S_2, S_3, S_4\}$ related to the CVD.

- S_1 - Chest pain
- S_2 - Shortness of breath
- S_3 - Palpitations
- S_4 - Sweating

To give the membership grade using linguistic variables for the symptoms to realize the person in days

Symptom in days	Linguistic variable	Fuzzy Number
0-9	Very Low	0,0.1
10-19	low	0.2-0.4
20-29	medium	0.5,0.6
30- 39	high	0.7,0.8
Above 40	very high	0.9,1





Hema and Prabha

First, we construct Fuzzy Soft Sets

$$(F_4, E_4) = \{F(P_1) = (S_1, 0.7) (S_2, 0.3) (S_3, 0.1) (S_4, 0.8)$$

$$F(P_2) = (S_1, 0.2) (S_2, 0.5) (S_3, 0.3) (S_4, 0.4)$$

$$F(P_3) = (S_1, 0.9) (S_2, 0.1) (S_3, 0.2) (S_4, 0.4)$$

$$F(P_4) = (S_1, 0.3) (S_2, 0.6) (S_3, 0.2) (S_4, 0.5)\}$$

$$(G_4, H_4) = \{G(P_1) = (S_1, 0.4) (S_2, 0.3) (S_3, 0.5) (S_4, 0.4)$$

$$G(P_2) = (S_1, 0.5) (S_2, 0.4) (S_3, 0.6) (S_4, 0.3)$$

$$G(P_3) = (S_1, 0.6) (S_2, 0.5) (S_3, 0.4) (S_4, 0.7)$$

$$G(P_4) = (S_1, 0.9) (S_2, 0.3) (S_3, 0.5) (S_4, 0.2)\}$$

Thus, the person-symptom fuzzy soft matrix $A^{(41)}$, $B^{(41)}$

$$A^{(41)} = \begin{pmatrix} 0.7 & 0.3 & 0.1 & 0.8 \\ 0.2 & 0.5 & 0.3 & 0.4 \\ 0.5 & 0.1 & 0.2 & 0.4 \\ 0.3 & 0.6 & 0.2 & 0.5 \end{pmatrix} \quad B^{(41)} = \begin{pmatrix} 0.4 & 0.3 & 0.5 & 0.4 \\ 0.5 & 0.4 & 0.6 & 0.3 \\ 0.6 & 0.5 & 0.4 & 0.7 \\ 0.9 & 0.3 & 0.5 & 0.2 \end{pmatrix}$$

Symptom – Occurrence of CVD Fuzzy Soft Set $(C_4, D_4) =$

$$F(S_1) = (d_4, 0.5)$$

$$F(S_2) = (d_4, 0.8)$$

$$F(S_3) = (d_4, 0.9)$$

$$F(S_4) = (d_4, 0.7)$$

$$\text{symptom - Occurrence of CVD Fuzzy Soft column matrix } X_4 = \begin{pmatrix} 0.5 \\ 0.8 \\ 0.9 \\ 0.7 \end{pmatrix}$$

$$A^{(41)} X_4 = \begin{pmatrix} 0.7 & 0.3 & 0.1 & 0.8 \\ 0.2 & 0.5 & 0.3 & 0.4 \\ 0.5 & 0.1 & 0.2 & 0.4 \\ 0.3 & 0.6 & 0.2 & 0.5 \end{pmatrix} \begin{pmatrix} 0.5 \\ 0.8 \\ 0.9 \\ 0.7 \end{pmatrix} \quad B^{(41)} X_4 = \begin{pmatrix} 0.4 & 0.3 & 0.5 & 0.4 \\ 0.5 & 0.4 & 0.6 & 0.3 \\ 0.6 & 0.5 & 0.4 & 0.7 \\ 0.9 & 0.3 & 0.5 & 0.2 \end{pmatrix} \begin{pmatrix} 0.5 \\ 0.8 \\ 0.9 \\ 0.7 \end{pmatrix}$$

$$Y_{41} \cup Z_{42} = \begin{pmatrix} 0.56 \\ 0.40 \\ 0.28 \\ 0.48 \end{pmatrix} \cup \begin{pmatrix} 0.45 \\ 0.54 \\ 0.49 \\ 0.45 \end{pmatrix} = \begin{pmatrix} 0.758 \\ 0.724 \\ 0.6328 \\ 0.714 \end{pmatrix} = \begin{pmatrix} 0.2680 \\ 0.2559 \\ 0.2205 \\ 0.2524 \end{pmatrix} = R_{41} = R^{(4)}$$

Health care analyze the test for those symptoms related

Lab Test	Normal range	Abnormal Range
Systolic blood pressure	<120mmHg	≥140mmHg





Hema and Prabha

Diastolic blood pressure	<80mmHg	≥90mmHg
BUN	7-20 mg/dL	> 20mg/dL
Creatine	0.6-1.2 mg/dL	>1.2 mg/dL
Fasting blood sugar	70-99mg/dL	126 mg/dL or higher
OGTT	95mg/dL or lower	200 mg/dL or higher
A1C	4.8-6.4%	6.5% or higher
Tumor markers	Low	High
Enzymes	Low	High
Blood cells	Normal	Low

Echo-cardiogram may show abnormalities such as heart muscle thickening or heart valve problems. Using this data with linguistic variables to give the membership grade of abnormal level

Linguistic variable Fuzzy Number

very Low	-	0,0.1
low	-	0.2-0.4
Medium	-	0.5,0.6
high	-	0.7,0.8
very high	-	0.9,1

The Person - Test result in Fuzzy Soft Set

$(F, E) = \{F(P_1) = (t_1, 0.7) (t_2, 0.6) (t_3, 0.5) (t_4, 0.6)$

$F(P_2) = (t_1, 0.5) (t_2, 0.6) (t_3, 0.3) (t_4, 0.6)$

$F(P_3) = (t_1, 0.7) (t_2, 0.5) (t_3, 0.6) (t_4, 0.2)$

$F(P_4) = (t_1, 0.6) (t_2, 0.5) (t_3, 0.7) (t_4, 0.4)\}$

Thus, the Person-Test result Fuzzy Soft Matrix W

$$\begin{pmatrix} 0.7 & 0.6 & 0.5 & 0.6 \\ 0.5 & 0.6 & 0.3 & 0.6 \\ 0.7 & 0.5 & 0.6 & 0.2 \\ 0.6 & 0.5 & 0.7 & 0.4 \end{pmatrix}$$

Finally, the four groups of persons affected by four types of disease combined with symptoms and the lab test,

$$S_{ij} + W = \begin{pmatrix} 0.2515 & 0.2586 & 0.2542 & 0.2680 \\ 0.2849 & 0.2843 & 0.2185 & 0.2559 \\ 0.2134 & 0.2175 & 0.2720 & 0.2205 \\ 0.2503 & 0.2396 & 0.2554 & 0.2524 \end{pmatrix} + \begin{pmatrix} 0.7 & 0.6 & 0.5 & 0.6 \\ 0.5 & 0.6 & 0.3 & 0.6 \\ 0.7 & 0.5 & 0.6 & 0.2 \\ 0.6 & 0.5 & 0.7 & 0.4 \end{pmatrix}$$

Finally, to obtain which type of disease affected person mostly live in that place





Hema and Prabha

$$U_1 = \begin{matrix} & \text{Diabetes} & \text{Cancer} & \text{High BP} & \text{CVD} \\ \begin{pmatrix} 0.9515 & 0.8586 & 0.7542 & 0.8680 \\ 0.7849 & 0.8843 & 0.5185 & 0.8559 \\ 0.9134 & 0.7175 & 0.8720 & 0.4205 \\ 0.8503 & 0.7396 & 0.9554 & 0.6524 \end{pmatrix} & = & \begin{pmatrix} 0.9515 \\ 0.7849 \\ 0.9134 \\ 0.8503 \end{pmatrix} & \begin{matrix} 1 \\ 4 \\ 2 \\ 3 \end{matrix} \\ \begin{matrix} 0.8750 & 0.8 & 0.7750 & 0.6992 \\ 1 & 2 & 3 & 4 \end{matrix} & & & \end{matrix}$$

CONCLUSIONS

The leading cause of mortality worldwide claims a staggering 17.9 million lives annually on a global scale, Research conducted by the Indian Council of Medical Research and Registrar General of India reveals that India bears a significant burden, accounting for approximately 60% of the world's heart disease cases. Hypertension has also seen a substantial rise in India, with an estimated 25.3% of adults aged 18 and above affected, a notable increase from 0.64 million in 1996 to 1.4 million in 2019. Additionally, the prevalence of diabetes in India is a growing concern, with approximately 101 million people living with diabetes and an additional 136 million individuals in the pre-diabetes stage, as reported by a recent study conducted by the Madras Diabetes Research Foundation and the Indian Council of Medical Research. Moreover, the projected number of new cancer cases in India for 2022 indicates that one in nine individuals is at risk of developing cancer during their lifetime. Identifying individuals most affected by diabetes involves selecting those with the highest cumulative data values within each respective column. In the provided matrix, the selection process designates the individual with the highest value in the first column as the most affected. This procedure can be applied to the preferences for disease analysis among individuals in a specific location for various health conditions.

REFERENCES

1. A.R. Roy, P.K Maji, "A Fuzzy soft set theoretic approach to decision making problems". *J Comput Appl Math* 203(2), 2007
2. D.Molodstov, 'Soft set theory-First result', *Comput Math Appl* 27,1999
3. N.Cagman, S.Enginoglu, "Fuzzy soft matrix theory and its application in decision making", *Iranian Journal of fuzzy systems*, 2012
4. Adlassing, K.P., "Fuzzy set theory in medical diagnosis", *IEEE Transaction Systems Man Cybernetics*, 16(2), pp260-265, 1986
5. Tridiv Jyoti Neog, Manoj Bora, Dusmanta Kumar sut, "On Fuzzy Soft Matrix Theory", *International Journal of Mathematical Archive*, 2012
6. Y.Yang, C.Ji, "Fuzzy soft matrices and their applications", In: *International conference on artificial intelligence and computational intelligence*, Springer; pp 618- 627, 2011
7. P.K.Maji, A.R. Roy, R.Biswas, "An application of soft sets in a Decision making problems", *Computers and Mathematics with Applications*, 44, 1077-1083, 2002
8. T.M.Basu, N.K.Mahapatra, S.K.Mondal, "Different Types of Matrices in Fuzzy Soft Set Theory and Their Application in Decision Making Problems", *Engineering Science and Technology*, 2(3), 389 -398, 2012
9. V. Renukadevi, G. Sangeetha, (2016) "A novel approach to decision making via fuzzy soft sets", *Turkish Journal of Fuzzy Systems*, 7, 41 – 54, 2016.
10. N. Sarala, S. Rajkumari, "Application of intuitionistic Fuzzy soft matrices in decision making problem by using medical diagnosis", *IOSR Journal of Mathematics*, 2007





Prediction Model for Identifying the Impact of Business Innovation in Service Industries

R.Subalakshmi^{1*} and D.Ramya²

¹Assistant Professor, Department of Computer Applications, PSG College of Arts and Science, (Affiliated to Bharathiar University) Coimbatore, Tamil Nadu, India.

²Assistant Professor, Department of Statistics, PSG College of Arts and Science, (Affiliated to Bharathiar University) Coimbatore, Tamil Nadu, India.

Received: 22 Jan 2024

Revised: 09 Feb 2024

Accepted: 03 May 2024

*Address for Correspondence

R.Subalakshmi

Assistant Professor,

Department of Computer Applications,

PSG College of Arts and Science,

(Affiliated to Bharathiar University)

Coimbatore, Tamil Nadu, India.

Email: subalakshmi@psgcas.ac.in



This is an Open Access Journal / article distributed under the terms of the **Creative Commons Attribution License** (CC BY-NC-ND 3.0) which permits unrestricted use, distribution, and reproduction in any medium, provided the original work is properly cited. All rights reserved.

ABSTRACT

The aim of this research is to assess how business analytics influences innovation, contributing to enhanced performance and the development of new products. Given the intense competition in global service industries, close monitoring of both business performance and innovation in new products becomes imperative. The study employed an exploratory quantitative environmental scan method to examine the event and gather relevant data. In a data-centric environment, structural equation modeling (SEM) is often engaged to improve the analysis of data acquired from exploratory quantitative research. Business analytics is conventionally divided into descriptive, predictive, and prescriptive categories. In the context of this study, descriptive analysis draws on business innovation trends to provide insights into current situations. Predictive analytics utilizes statistical SEM models to precisely predict future events, while prescriptive analytics examines decision outcomes to determine necessary actions. Consequently, the analysis indicates a notable positive impact of innovation on firm performance. Research findings indicate that increased innovation in products, processes, and distribution channels can positively influence business performance.

Keywords: Innovation, Modelling, Prediction, Printing Industry, Analytics





INTRODUCTION

This study specifically addresses innovations in the printing industry related to its business performance as well as product innovations and technical knowledge in the printing sector. It is always acceptable that printing is an integral part of any job in service industry, engineering and any other profitable aspect. The printing industry is a publishing industry from small printing process to large printing process. Generally, products in this industry include business cards, flyers, letterheads, books, brochures, posters, cards, information sheets, etc. In printing industry the journals printed using offset, digital and web printing processes. However, the printing industry often faces challenges such as digital competition, declining profits in the printing industry, and technology investment. To meet these challenges and ensure that every printing company should be able to make an impact in terms of innovation. Innovation is also important so that businesses can compete and consolidate innovation. This article attempts to use some statistical techniques to evaluate the industry's performance with respect to innovation. The use of statistical methods and data analysis techniques to gain insights and improve strategic decisions confines to analytics in business. Organizations use effective business tools to support decision-making. Firstly, descriptive analytics furnishes insights into past events by examining pre-existing information through aggregation methods to identify designs and trends within the data. Secondly, predictive analytics aids in anticipating forthcoming events likely to occur. In projecting future outcomes based on historical data, the study employs prescriptive analysis through data mining and statistical modeling. Prescriptive analytics focuses on generating actionable insights rather than merely observing data. Decision-making relies on both descriptive and predictive information to achieve its objectives. Structural Equation Modeling (SEM) represents an enhanced version of the general linear model (GLM), allowing researchers to construct models based on regression equations. These models are typically specific to investigating relationships among various dependent and independent factors.

Advantages of employing SEM include

- Reduction of error variance in estimated parameters within SEM.
- Incorporation of observed variables and latent variables in SEM.
- Establishment of a unique framework for estimating linear models using SEM.
- Provision of both a general model fit test and a separate test for parameter estimation.
- Simultaneous comparison of regression coefficients, error estimates, mean, and variance.

REVIEW OF LITERATURE

The researcher presents significant insights into Structural Equation Modeling (SEM) in their study, focusing on statistical modeling as outlined by Hair et al. (2006 and 1998). According to the researcher, these models play a crucial role in estimating multiple interrelated dependencies, representing correlated hidden concepts and contributing to the estimation of measurement errors. Yu-Kai (2009) elaborates that the ultimate objective of SEM is to model a set of dependent variables linked to a group of unobserved components and measured by observable variables. The study delves into key functional aspects, offering a more detailed perspective. From a research standpoint, Bennett, Levis, and Robinson (2010) categorize analyses into descriptive, predictive, and prescriptive, aligning with INFORMS, encompassing various methods such as statistical techniques, modeling, neural network predictions, and forecasting. Holsapple et al. (2014) emphasize a data-centric culture that underscores reliable behavioral patterns and principles based on analytical decision-making. Similarly, Kiron et al. (2013) and others characterize a data-driven culture as pivotal for organizational improvement. This definition aligns with the complexities of morals, principles, norms, and indicators defining how an organization conducts business, consistent with organizational culture literature. Schein (1990) suggests that the practice of distinguishing organizations from one another is essential. Various researchers have documented the concept of a data-centered culture, highlighting the value of information necessity for industries. In organizations, the data-centric aspect is developed to gain a competitive advantage in Business Analytics (BA). Operational decisions in organizations increasingly prioritize





data-driven insights, a sentiment promoted by Davenport et al. (2001), Kiron and Shockley (2011), and Kiron et al. (2013).

OBJECTIVES OF THE RESEARCH

- Evaluate the operational impact of innovations within the printing industry.
- Recognize the factors influencing the introduction of new products.
- Investigate effectiveness using exploratory quantitative approaches.
- Evaluate the alignment of all dimensions with recommended values and demonstrate the suitability of the structural model.

Design of Research Problem

This research approach uses descriptive quantitative models to show the relationship between exogenous and endogenous variables. Figure 2 provides this classification. Within this investigation, Figure 3 has been devised to delineate the firm performance outcomes linked to innovation. A series of inquiries, measured on a 5-point Likert scale, was formulated to gather data. Input from 150 customers, specifically those engaged in printing-related tasks, was sought. To structure the study comprehensively, the analysis was conducted employing structural equation modeling.

DATA ANALYSIS AND INTERPRETATION

Use the collected samples to determine the suitability of the model by SEM analysis. The model was tested with AMOS version 16. SEM can be used to assess causal relationships between variables and confirm model fit. SEM also determines goodness of data to the proposed model. Models are evaluated using the relationship between chi-square values and resultant df (χ^2/df), RMSEA, GFI, IFI, TLI, CFI, AGFI, and PGFI. In Figure 4, a relationship among the variables is shown. Table 2 focuses on evaluating the normality of the data. The skewness values in the table suggest that the majority of variables have values less than 2.58, indicating a normal distribution. However, some variables exhibit ratios greater than 2.58, signifying a departure from normal distribution. Furthermore, the multivariate normality test value of 6.702 (>2.58) indicates that the multivariate data does not conform to a normal distribution. It's important to note that for mathematical modeling, particularly when employing multiple regression, the absence of normality in the dependent variable may not be a critical consideration. Table 3 shows the results for the standardized and unstandardized coefficients and associated test statistics, where the coefficients represent the change in the dependent variable per unit change in the independent variable. The values in the table indicate innovation gives an optimistic impact on the success of the firm. This means that innovation helps to identify the rate of change in business.

Hypotheses

H0 (Null Hypothesis): The planned model exhibits the best fit.

H1 (Alternative Hypothesis): The planned model does not exhibit the best fit.

Evaluation of the null hypothesis (H0) involves testing whether the innovation performance of the firm yields a chi-square value of 22.864 with 19 degrees of freedom and a probability greater than 0.05 ($p > 0.05$). These results suggest that the data fits the planned model adequately, as evidenced by CMIN/DF values below 5. Thus, it can be inferred that the proposed structure is suitable. Table 5 reveals a p-value of 0.243 (greater than 0.05), indicating a well-fitting model. Notably, the Goodness of Fit Index (GFI) is 0.968, and the Adjusted Goodness of Fit Index (AGFI) is 0.925 (>0.9), both considered favorable. The Normal Fit Index (NFI) is 0.964, and the Comparative Fit Index (CFI) is 0.99, suggesting a strong model fit. The Root Mean Square Residual (RMR) is 0.079, and the approximate Root Mean Square Error of Approximation (RMSEA) is 0.037 (<0.08), further supporting a satisfactory fit. Additionally, the RFI, IFI, and TLI scores all exceed 0.9, indicating an excellent model fit.





Subalakshmi and Ramya

CONCLUSION

This research is to determine business performance through innovation, to find a model for launching new products. Descriptive analysis provides evidence of this. Using predictive analytics in SEM models helps foretell performance of business according to financial insights, customer insights, business process insights, and employability insights. Enterprise performance can be enhanced through innovation, manifested by way of product innovation, process innovation, and sales innovation. The findings suggest that fostering innovation and measuring business performance will enable the print industry to compete with digital, increase profits and make meaningful technology investments.

FUTURE WORK

Business performance factors can be studied in a transnational setting. Moreover, the research can also be applied in the future to the service industry functioning globally, which will help in identifying relevant business insights.

REFERENCES

1. Chen, Hsiu-chin & Chiang, Roger & Storey, Veda. (2012). "Business Intelligence and Analytics: From Big Data to Big Impact". MIS Quarterly. 36. 1165-1188.
2. Davenport, T. H., Harris, J. G., De Long, D. W., & Jacobson, A. L., (2001) "Data toknowledge to results: building an analytic capability". California Management Review, 43(2), 117–138.
3. Davenport, T. Harr., (2013). "Analytics 3.0". Harvard Business Review, 91(12), 64–72.
4. Hair Jr., J. F., Anderson, R. E., Tatham, R. L., & Black, W. C. (1998). "Multivariate Data Analysis", NJ: Prentice Hall.
5. Hair, J., Black, W., Babin, B., Anderson, R., & Tatham, R. (2006). "Multivariate Data Analysis" NJ: Pearson Prentice Hall.
6. Hair, J. F., Ringle, C. M., & Sarstedt, M. (2013). "Partial least squares structural equation modelling: Rigorous applications, better results and higher acceptance. Long Range Planning", 46(1-2), 1-12.
7. Holsapple, Clyde & Lee-Post, Anita & Pakath, Ram. (2014). "A Unified Foundation for Business Analytics". Decision Support Systems. 64.
8. Kiron, David & Ferguson, R.B. & Prentice, Pamela. (2013). "From value to vision: Reimagining the possible with data analytics". MIT Sloan Management Review: Spring Research Report. 1-19.
9. Michael J. Mortenson, Neil F. Doherty, Stewart Robinson (2015), "Operational research from Taylorism to Terabytes: A research agenda for the analytics age", European Journal of Operational Research, Volume 241, Issue 3, Pages 583-595.
10. Robinson, A., Levis, J., & Bennett, G., (2010). "INFORMS to officially join analytics movement". OR/MS Today, 37(5), 59
11. Huang, Y. (2009). "The Effect Of Airline Service Quality On Passengers' Behavioural Intentions Using Servqual Scores: A Taiwan Case Study". Journal of the Eastern Asia Society for Transportation Studies, 427-427.





Subalakshmi and Ramya

Table 1. Relationship among variables in the Structural Equation Modelling

Observed, endogenous variables	Observed, exogenous variables	Unobserved, exogenous variables
<ul style="list-style-type: none"> BP - Business Performance FI - Financial Insight CI - Customer Insight BPI - Business Process Insight LEA - Learning of Employment Ability 	<ul style="list-style-type: none"> INNOVATION PDI - Product Innovation PCI - Process Innovation DI - Distribution Innovation 	<ul style="list-style-type: none"> e1 - error of business performance e2 - error of FI e3 - error of CI e4 - error of BPI e5 - error of LEA e6 - error of Innovation

Table 2: Assessment of normality of SEM

Variable	min	max	skew	r.r.	kurtosis	r.r.
DI	1.000	5.000	-.693	-3.467	-.562	-1.405
PCI	1.000	5.000	-.737	-3.683	-.471	-1.178
PDI	1.000	5.000	-.350	-1.750	-.698	-1.745
CI	1.000	5.000	.768	3.842	-.305	-.762
FI	1.000	5.000	.735	3.674	-.305	-.762
LEA	1.000	5.000	.616	3.078	-.616	-1.539
BPI	1.000	5.000	.905	4.525	-.069	-.172
Innovation	1.000	5.000	-.552	-2.759	-.899	-2.248
BP	1.000	5.000	-.293	-1.464	-.916	-2.291
Multivariate					15.401	6.702

Table 3: Unstandardized (B) and Standardised (Beta) coefficients of SEM

	Unstandardized Coefficients (B)	S.E. of B	Standardised Coefficients Beta	t-value	P-value	Remarks
Innovation <-- PDI	.200	.076	0.175	2.619	.009	**
Innovation <-- PCI	.283	.082	0.246	3.469	***	***
Innovation <-- DI	.542	.074	0.502	7.345	***	***
BP <-- Innovation	.178	.073	0.188	2.445	.014	*
BP <-- BPI	.012	.124	0.011	1.099	.021	*
BP <-- LEA	.183	.099	0.177	1.850	.044	*
BP <-- FI	-.056	.121	-0.044	-.461	.645	-
BP <-- CI	.174	.101	0.171	1.730	.034	*

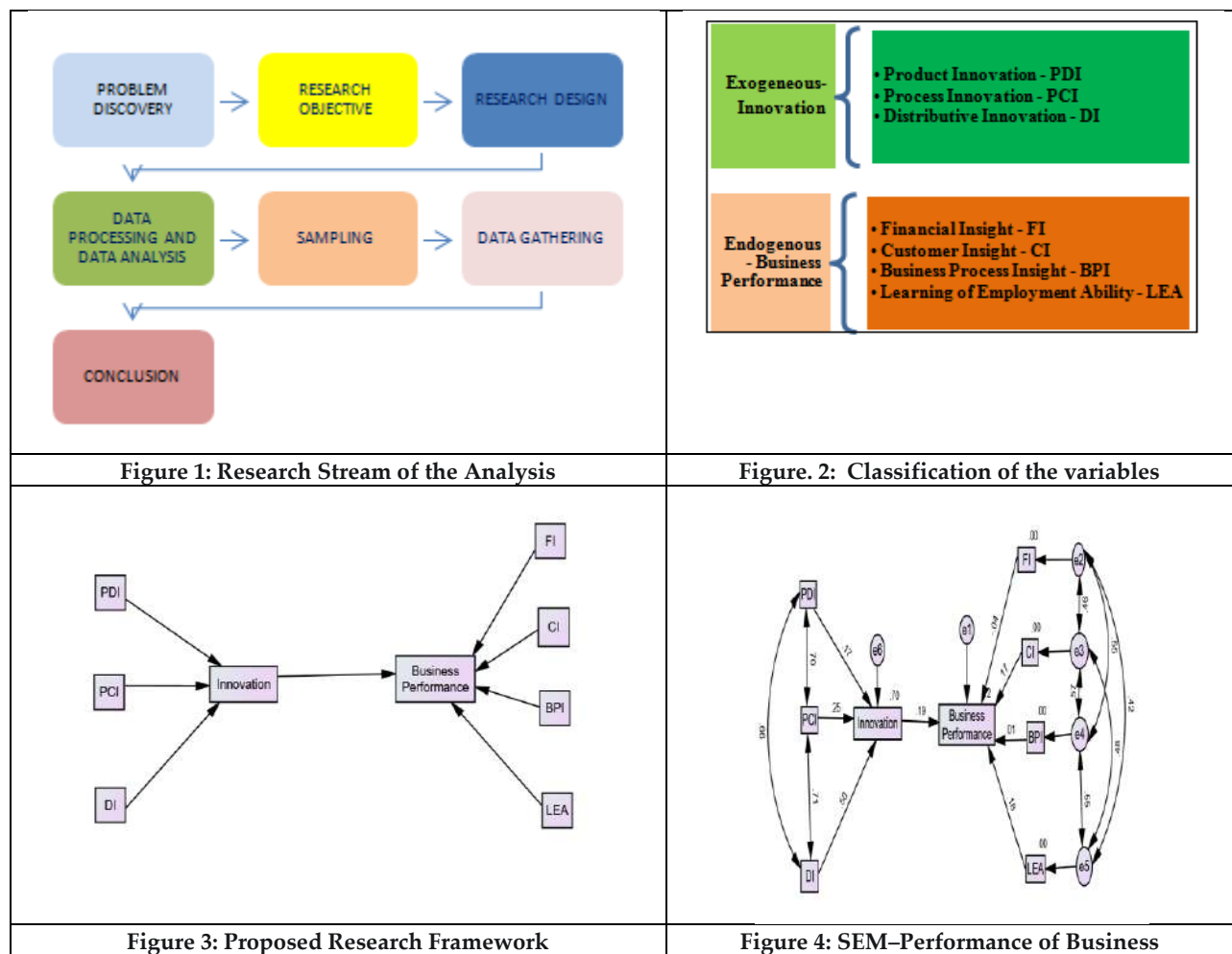




Subalakshmi and Ramya

Table 4: Summary of Model Fit

Model	NP	PAR	CMIN	DF	P	CMIN/DF
Default model	26	22.864	19	.243	1.203	
Saturated model	45	.000	0			
Independence model	9	628.261	36	.000	17.452	





A Study of Technology Skills among Secondary Level Students in Relation to their Personality Traits

Ashish Choudhary^{1*} and Mool Raj Sharma²

¹Research Scholar, Department of Educational Studies, Central University of Jammu, Jammu & Kashmir, India.

²Professor, MIER College of Education (Autonomous), Jammu, Jammu & Kashmir, India.

Received: 20 Jan 2024

Revised: 09 Feb 2024

Accepted: 15 May 2024

*Address for Correspondence

Ashish Choudhary

Research Scholar,

Department of Educational Studies,

Central University of Jammu,

Jammu & Kashmir, India.

Email: ashishchoudhary4081@gmail.com



This is an Open Access Journal / article distributed under the terms of the **Creative Commons Attribution License** (CC BY-NC-ND 3.0) which permits unrestricted use, distribution, and reproduction in any medium, provided the original work is properly cited. All rights reserved.

ABSTRACT

Technology is becoming an important part in today's life as everything is digitalizing in India. In the field of education, technology is being used to deliver content and to help student to visualize the concepts and explore more about concepts taught in the class. In India, many programmes have been initiated by the government in secondary schools like provision of computer labs, internet, smart board, now the provision of online classes. So, it is important that every student should have knowledge of technology skills as it is need of the hour for competing in the new technological era. Today, the world is becoming more and more competitive and quality of performance is the key factor for one's progress. There are factors such as technology skills, academic achievement, personality traits, emotional, cultural and intellectual which influence the success and failure of students. The aim of the present study was to develop a better understanding of the secondary level students' personality traits and its relation with technology skills. Simple random sampling technique was used. The sample consisted of 208 secondary level students, studying in 9th and 10th class of Jammu district. Self- devised Technology Skill Scale was used for assessing level of technology skills among students. Scale for Introversion and Extroversion Dimension was used to know about personality traits of students. Percentage, Mean, and ANOVA were used to analyse the data. The findings of the study clearly revealed that 27% of the students have basic skills and 47% students have intermediate skills and rest of students i.e. about 26 % exhibits advanced technology skills among secondary level students. Further, No significant difference was found in technology skills score of secondary level students in relation to their personality traits (Introversion, Ambivert and Extroversion). It was also found that there exists significant difference in technology skills score of secondary level students with respect to their type of school (Government and Private), Gender



**Ashish Choudhary and Mool Raj Sharma**

(Male and Female) and Family Income (low, Average and High). The study also revealed that there exists significant interactional effect of type of school, gender and family income on technology skills scores of secondary level students.

Keywords: Technology Skills, Secondary Students and Personality Traits.

INTRODUCTION

Today, there is no any field of activity where technology is not being used. We apply technology in almost everything we do in our daily lives. On society the impact of technology is so huge and it also plays a very important role in the field of education too (Ananthula, 2015). With the development of technology, India has witnessed an enhanced online education over a period of few years. In the past few years, So many working professional and students have joined different e-learning platforms to enhance their skills. Mostly rural areas of India lag in educational facilities and still they are struggling with outdated teaching methods, shortage of teachers, lack of teaching resources, inadequate student- teacher ratio, for providing them same level of quality education as urban students are taking, digital education is a good option (Ramananda, 2020). Various workforces will need to adapt new technology skills, the danger of not learning technology skills is that children will only become passive consumers of technology (Beckingham, 2019). The Government of India, especially its Ministry of Human Resource Development, has introduced several initiatives related to ICT in its school system. Computer labs, National E-library, Smart Schools, and Swayam courses from class 9th onwards, use of blended learning, collaborative learning in classroom are some of the examples of these initiatives. In secondary schools children's should be provided opportunities to learn advanced technology skills that will help in widen their prospects as adults. Students should be encouraged to develop technology skills from the very young age. It is important for all the secondary level students of 21st century to have the knowledge of these basic technology skills in order to compete in the today's working world. Technology skills have also been classified as technology in the classroom: Search the web, Connect through social media, Collaborate with other students online, Video conferencing and sharing videos, Blogging, Use a Tablet/Mobile/ laptop, E-Mail Management Skills, File Management, Web site Design Skills, Downloading Software from the Web Knowledge - including e-Books, Installing Computer Software onto a Computer System, Computer Related Storage Devices Knowledge, Educational Copyright Knowledge, Computer Security Knowledge (Turner, 2005). Secondary level students' are in adolescent stage of development, where the personality and its components are growing, clashing, watching, imitating, demanding, giving, receiving, sharing. So, at this stage adolescent develops various traits of personality. It is the most important stage in the student's life, it bridges between the general information of the mind and personality of the students.

Personality is defined as the totality of all the activities that can be discovered by long period of observation so that reliable information can be obtained about personality. It also refers the way of individual feelings, thoughts, behaviours and social adjustments among individuals that influence one's expectations, values, perception and attitudes (Nadeem, 2017). The investigator reviewed so many literature on personality and found that various studies has been conducted with different traits of personality like openness, conscientiousness, extraversion, introversion, agreeableness and neuroticism, psychoticism many more and also found some studies on introversion and extroversion trait of personality and its relationship with English as second language proficiency (Zafar, Khan and Meenakshi, 2018), Relationship between introversion/Extroversion personality trait and proficiency in ESL writing skills (Qanwal and Ghani, 2019), Influence of extroversion and introversion on decision making ability (Khalil, 2016). There is conviction that the individual differences of personality in general and the Introversion and Extraversion dimension in particular reflects what an individual will do. Thus the investigator created interest in knowing about introversion and extroversion personality trait of secondary level students. Our personality traits help us to make important life choices: the kind of environment we want to live in, work we want to do and even the type of person we want to work with them. Our different combination of genes contributes to build our personality and we cannot



**Ashish Choudhary and Mool Raj Sharma**

change it. Instead of trying to change our personality, students should try to use that energy towards learning and developing new skills that will help us to achieve the goals of life (Onuka, 2018). Our personality is uniquely ours - whether they tend toward extroversion, introversion, or ambiversion. There is nothing wrong with any one of these personality traits. They are just ways to describe how we get our energy and relate to the world. MacCutcheon concludes we all utilize both sides of the spectrum in various circumstances. In order to be most successful in the world, it is important to develop skills to exercise both ends introversion and extroversion, which in-turn boost up our energies and prepare us for future trends to achieve our goals (Muza, Muhammad and Aliero, 2020). Research evidence seems to indicate that students had not appropriate familiarity with technology skills. Level of technology skills to use computer, internet was at moderate level and mobile skills to assess and download information was at high level (Kadir, 2013, Minikutty and Raj, 2015 and Babajide, 2019). Studies revealed significant difference between male and female technology skills (Umar and Jalil, 2012 and Raja and Sridharan, 2019), Studies showed that difference in technology skills level among government and private school students (Ananthula, 2015), Research evidence seems to indicate significant relationship between academic achievement and personality traits (Martey and Larbi, 2016 and Suvarna and Bhat, 2016). Studies also revealed that there was a significant relationship between personality traits and all digital literacy skills (Ahmed and Rasheed, 2020).

NEED AND SIGNIFICANCE

Traditionally technologies are not so much used in our educational field, but today we are witnessing a revolution based on technologies. In developing countries like India, where technology plays a very important role in all the fields of life, it is important to integrate technology in education sector also. The application of technology has become a critical part of the learning processes for both students and teachers inside and outside the classroom settings. As technology is very important component in today's life, it becomes imperative to study the factors that influence the technology skills of the students. Secondary level is an important stage of education. This is the adolescence stage of one's life. These are the years before entering the bigger and serious part of education that is career. It is extremely important to focus during these years. These years of school life are very much vulnerable to problems of various kinds and the personality traits of students are affected to greater extent. The findings of the study may prove beneficial for students, teachers, administrators, policymakers and for parents.

OBJECTIVES OF THE STUDY

1. To study the technology skills among secondary level students.
2. To study the difference in scores obtained on technology skills with respect to the personality traits (introversion, ambivert and extroversion) of secondary level students.
3. To study the interactional effect of type of school, gender and family income in scores obtained on technology skills of secondary level students.

HYPOTHESES OF THE STUDY

1. There is no significant difference in scores obtained on technology skills of secondary level students with respect to type of school (Government and Private) they are studying in.
2. There is no significant difference in scores obtained on technology skills with respect to the personality traits (introversion, ambivert and extroversion) of secondary level students.
3. There is no significant difference in scores obtained on technology skills of secondary level students with respect to their gender (Male and Female)
4. There is no significant difference in scores obtained on technology skills of secondary level students with respect to their family income (Low, Average and High).
5. There is no significant interactional effect of type of school, gender and family income in scores obtained on technology skills of secondary level students.





Ashish Choudhary and Mool Raj Sharma

RESEARCH METHODOLOGY

Descriptive Survey Method has been employed for gathering information from secondary level students in the present investigation. Simple random sampling technique has been used for selecting 208 secondary level students from Jammu district. *Technology Skill Scale* was used for knowing the level of technology skills among secondary level students and *Scale for Introversion – Extraversion Dimension* (SIED) by Sanjay Vohra, (1993) used to know about the personality traits (Introversion, Ambivert and Extraversion) of secondary level students.

RESULTS AND INTERPRETATION

Objective 1: To study technology skills among secondary level students.

Table 1 depicts that the students who have scores range between 0-36 have basic skills, and between 37-52 have intermediate skills and the scores range between 53-60 have advanced level skills. So, near about 27% of the students have basic skills and 47% students have intermediate skills and rest of students i.e. about 26 % exhibits advanced technology skills on the scale used for the present study. The data has been presented diagrammatically in Figure 1.

Objective 2: To study the difference in scores obtained on technology skills with respect to the personality traits (introversion, ambivert and extroversion) of secondary level students.

Ho1: There is no significant difference in scores obtained on technology skills with respect to the personality traits (introversion, ambivert and extroversion) of secondary level students. Table 2 shows the calculated F-ratio for the technology skills and personality traits is 1.71. The calculated value is less than the table value 3.35 (.05 level) and 5.49 (.01 level) against 2 and 27 df, which is not significant. Therefore, the **hypothesis 5** "There is no significant difference in scores obtained on technology skills of secondary level students with respect to their personality traits (introversion, ambivert and extroversion)" is accepted. It means that a personality trait (introversion, ambivert and extroversion) does not effect technology skills scores of secondary level students.

Objective 3: To study the interactional effect of type of school, gender and family income in scores obtained on technology skills of secondary level students.

For achieving this objective, following hypotheses Ho2, Ho3, Ho4 and Ho5 were tested by using Analysis of variance (ANOVA) by the investigator and hypothesis wise results are given in following Table 3.

Ho 2: There is no significant difference in scores obtained on technology skills of secondary level students with respect to type of school (Government and Private) they are studying in.

Ho 3: There is no significant difference in scores obtained on technology skills of secondary level students with respect to their gender (Male and Female).

Ho 4: There is no significant difference in scores obtained on technology skills of secondary level students with respect to their family income (Low, Average and High).

Ho5: There is no significant interactional effect of type of school, gender and family income in scores obtained on technology skills of secondary level students.

Table 3 shows the interactional effect of type of school, gender and family income in scores obtained on technology skills of secondary level students. F-ratio for the main effect of 'A' i.e., type of school is 46.6 as shown in Table 3. Which is significant at 0.01 level of significance as it is greater than the table value i.e. 1.86 (0.05 level) and 2.40 (0.01 level) against 1 and 60 df. Therefore, the **hypothesis 2** "There is no significant difference in scores obtained on technology skills of secondary level students with respect to type of school (Government and Private) they are studying in" is rejected. It means that the type of school (Government and Private) influenced the technology skills scores of secondary level students. Tables 4 revealed the mean score of government secondary level students is 33.3 and mean score of private secondary level students is 46.1 respectively, which means private school students have high technology skills scores than government secondary school students. The F-ratio for the main effect 'B' i.e., gender (Male and Female) is 4.1 as shown in Table 3. Which is significant at 0.01 level of significance as it is greater than the table value 1.86 (0.05 level) and 2.40 (0.01 level) against 1 and 60 df. Therefore **hypothesis 3** "There is no





Ashish Choudhary and Mool Raj Sharma

significant difference in scores obtained on technology skills of secondary level students with respect to their gender (Male and Female)" is rejected. It means that the gender (male and female) influenced the technology skills scores of secondary level students. Table 5 revealed that the mean score of male is 39.9 and mean score of female secondary level students is 39.5 respectively, which means male students have high technology skills scores than female secondary level students. The F-ratio for the main effect 'C' i.e., family income (low, average and high) is 7.2 as shown in Table 3. Which is significant at .01 level of significance as it is greater than the table value 1.81 (0.05 level and 2.32 (0.01 level) against 2 and 60 df. Therefore **hypothesis 4** "There is no significant difference in scores obtained on technology skills of secondary level students with respect to their family income (Low, Average and High)" is rejected. It means that the level of family income (low, average and high) effect the technology skills scores of secondary level students. Table 6 reveals that the mean scores of low family income students is 42.8, mean scores of average family income students is 46.7 and mean score of high family income students secondary level students is 49.5 respectively, which means students' who have high family income have high technology skills scores than average and low family income secondary level students. Further, the F- ratio for the interactional effect A×B×C (type of school, gender and family income) is 5.9 as shown in Table 3. Which is significant at 0.01 level of significance as it is greater than the table value 1.81 (0.05 level) and 2.32 (0.01 level) against 2 and 60 df. It shows that there is significant interactional effect of type of school, gender and family income on technology skills scores of secondary level students. Therefore **hypothesis 5** "There is no significant interactional effect of type of school, gender and family income in scores obtained on technology skills of secondary level students" is rejected. It means that the interactional effect of type of school, gender and family income collectively effect the technology skills scores of secondary level students.

DISCUSSION AND CONCLUSIONS

1. The knowledge of technology skill is not now an activity for the few but for everyone. Findings indicated that most of students have not an adequate level of technology skill, which is a similar result as found by Robabi and Arbabisarjou (2015) and Babajide (2019) that students have not satisfactory knowledge of computer literacy.
2. It is also found from the study that there is no significant difference of technology skills scores of introversion, ambivert and extroversion students.
3. It was also concluded from the findings that there is significant difference in technology skills scores of male and female, government and private secondary school students. Boys had high level of technology skills scores than secondary school girls; private school students also have high technology skills scores than government secondary school students, the possible reasons behind better technology skills among private secondary school students are good infrastructure, facilities, smart classrooms, well equipped computer labs. This is similar with results reported by Ananthula (2015), who found significant difference between level of computer awareness on the basis of gender (boys and girls) and type of school (government and private) as well.
4. There was also significant difference in technology skills scores of students who had low, average and high level of family income. The students who had high level of family income have high level of technology skills scores than students who had average and low level of family income, this may be due to availability of technology tools like mobile, laptop, computer, internet. Also significant difference has been found to exist in triple interaction i.e. type of school, gender and family income collectively on technology skills scores of secondary level students.

EDUCATIONAL IMPLICATIONS

On the basis of discussion and conclusions of the study, the following educational implications were suggested by the investigator for students, teachers, schools and policymakers.

For students: As everything is digitalizing in today's world it the need of every student to familiarize with technology. The result of the present study helps the students to know how much they are capable for working in today's digital world and how much they are ready for future trends. The knowledge about high level of technology



**Ashish Choudhary and Mool Raj Sharma**

skills helps the students to choose their career accordingly and knowing about personality traits helps the students to take their decisions about choosing the subjects for higher education and make themselves to be competent for future work area.

For teachers: Teachers' should provide more time to students to assess computer labs, who have low and average level of technology skills. The teachers should use and integrate technology in teaching learning process in order to bridge the digital divide in today's technological age, Video graphics and text material, smart board with internet in every classroom, digital libraries, search and download content and soon should be available regarding the curriculum of the students. The teachers' should provide guidance to students in choosing their subjects for their professional career, according to the personality traits of the students' introversion, ambivert and extroversion. It was found that secondary level girls have low technology skills. For improving the technology skills of girls, the school teachers' should organize the workshop regarding the awareness of technology uses in the present era and motivate the girls for using technology in their day to day life activities and improve their technology skills.

For administrator: The school administration should organize career counselling for students, according to their level of technology skills, so that they can make best choice according to their technology skills level after matriculation. Proper infrastructure and facilities should be provided by schools and awareness programme about the use of technology. So that students who have low and intermediate level of technology skills can develop them. The government school administration should take steps to empower the technology awareness among the students, who were studying in government schools as government school students have low technology skills. The results also showed that students who have low level of family income have low level of technology skills. The school administration should provide proper infrastructure and facilities in school so that every student can assess the computer labs. Various activities should be organized by the secondary schools for the childrens' who have some personality related problems.

For policymakers: Results of the study helps the policy makers to know about the level of technology skills among secondary level students and choosing the more appropriate policy for improving or advancing the technology skills so that they can ready for future trends. Curriculum should also reframed and include activities like debates, seminars, symposium, cultural activities, quiz etc for students that will help them in developing a good and balanced personality traits. Grants should be sanctioned specially for the government schools because government school students have low technology skill as compared to private schools, for improving their infrastructure. Scholarship should be provided to economically disadvantage students so that they can buy their own computer, laptops, smartphone etc. as it was found in the present study that students from low economic status have low level of technology skills.

REFERENCES

1. Ahmed, S., & Rasheed, T. (2020). Relationship between personality traits and digital literacy skills: a study of university librarians. *Digital Library Perspectives*, 36(2), 326-350. Retrieved June 25, 2020 from Relationship between personality traits and digital literacy skills: a study of university librarians | Emerald Insight
2. Ananthula, R. (2015). Computer awareness among secondary school students – A study. *IJARIIIE-ISSN(O)-2395-4396*, 1(3), 264-267. Retrieved December 2, 2019 from http://ijariie.com/Adm_in UploadPdf/Computer_Awareness_among_Secondary_School_Students_%E2%80%93_A_Study_ijariie1234_volu me_1_13_ page_264_267.pdf
3. Babajide, R.H. (2019). Computer awareness level among junior secondary school students in Ijebu north local government Ogun state. Retrieved April 1, 2020 from <https://www.academia.edu/41262606/>





Ashish Choudhary and Mool Raj Sharma

4. Beckingham, K. (March, 8, 2019). *Why are technology skills so important to today's students*. Retrieved January 20, 2020 from <https://edtechnology.co.uk/comments/why-are-tech-skills-so-important-to-todays-students/#:~:text=Students%20who%20are%20developing%20tech,to%20flourish%20in%20today's%20society.>
5. Kadir, K. H. A. (2013). *Level of ICT skills among secondary school students*. Technology, Education and Science International Conference. Retrieved March 9, 2020 from https://www.academia.edu/7675254/Level_of_ICT_Skills_Among_Secondary_School_Students_A_Preliminary_Survey
6. Khalil, R. (2016). Influence on extroversion and introversion on decision making ability. *International Journal of Research and Medical Sciences*, 4(5), 1534-1538. Retrieved October 10, 2020 from <https://www.msjonline.org/index.php/ijrms/article/view/756>
7. Martey, E. M., & Aborakwa-Larbi, K. (2016). Assessing the impact of personality traits on academic performance. *International Journal of Research in Engineering, IT and Social Sciences*, 6(3), 1-17. Retrieved February 29, 2020 from http://www.indusedu.org/pdfs/IJREISS/IJREISS_442_53047.pdf
8. Minikutty, & Raj, S. (2015). ICT literacy: A study among higher secondary school students. *Paripex - Indian Journal of Research*, 4(4), 4-6. Retrieved March 1, 2020 from https://www.worldwidejournals.com/paripex/recent_issues_pdf/2015/April/April_2015_1429011883_102.pdf
9. Muza, S. H., Muhammad, S., & Aliero, H. S. (2020). Extroversion, Introversion and students academic performance of senior secondary schools. *International Journal of Advanced Academic Research*, 6(4), 1-12. Retrieved November 3, 2020 from <https://www.ijaar.org/articles/v6n4/ahe/ijaar-ahe-v6n4-apr20-p21.pdf>
10. Nadeem, N.A. (2017). Study of personality characteristics scientific temper vocational preferences and academic achievement of rural and urban secondary school students. (Doctoral dissertation, Central University of Kashmir, Jammu and Kashmir). Retrieved March 8, 2020 from <https://shodhganga.inflibnet.ac.in/handle/10603/220343>
11. Onuka, A. O. U. (2018). Student's computer skills and students achievement in senior secondary school biology in Ogun state, Nigeria. *International Journal of Computer Applications*, 179(24), 33-38. Retrieved December 1, 2019 from <https://www.ijcaonline.org/archives/volume179/number24/29082-2018916435>
12. Qanwal, S. & Ghani, M. (2019). Relationship between introversion/ extroversion personality trait and proficiency in ESL writing skills. *International Journal of English Linguistics*, 9(4), 107-118. Retrieved January 5, 2021 from https://www.researchgate.net/publication/334216269_Relationship_Between_IntroversionExtroversion_Personality_Trait_and_Proficiency_in_ESL_Writing_Skills
13. Raja, P., & Sridharan, K. (2019). A study on higher secondary students' awareness towards utilization of computer. *International Journal of Innovative Research in Science, Engineering and Technology*, 8(3), 2104-2106. Retrieved January 5, 2020 from https://www.ijirset.com/upload/2019/march/60_A%20STUDY.pdf
14. Ramananda. (2020, January 19). Budget 2020: Why technology and digital education initiatives are key to bridge India's skill gap (Blog Post). Retrieved from <https://yourstory.com/2020/01/budget-2020-government-technology-digital-education>
15. Robabi, H., & Arbabisarjou, A. (2015). Computer literacy among students of Zahedan University of medical sciences. *Global Journal of Health Science*, 7(4), 136-142. Retrieved January 2, 2020 from <https://pubmed.ncbi.nlm.nih.gov/25946919/>
16. Suvarna, V. D., & Bhat, H. S. G. (2016). A study on academic achievement and personality of secondary school students. *Research in Pedagogy*, 1(6), 99-108. Retrieved December 2, 2019 from <http://research.rs/wp-content/uploads/2016/06/10-Suvarna-Ganesha-Bhata.pdf>
17. Turner, I. (2005). 20 Technology skills every educator should have. *The Journal Transforming Education Through Technology*, 1-10. Retrieved January 7, 2020 from <https://thejournal.com/Articles/2005/06/01/20-Technology-Skills-Every-Educator-Should-Have.aspx?Page=1>
18. Umar, I. N., & Jalil, N. A. (2012). ICT skills, practices and barriers of its use among secondary school students. *Procedia - Social and Behavioral Sciences*, 46, 5672-5676. Retrieved December 13, 2019 from https://www.researchgate.net/publication/271609705_ICT_Skills_Practices_and_Barriers_of_Its_Use_Among_Secondary_School_Students





Ashish Choudhary and Mool Raj Sharma

19. Zafar, S., Khan, Z., & Meenakshi, K. (2017). Extroversion-introversion tendencies and their relationship with ESL proficiency. *Pertanika Journal of Social Science and Humanities*, 25(2), 687-703. Retrieved December 22, 2020 from https://www.researchgate.net/publication/317762565_Extraversion-introversion_tendencies_and_their_relationship_with_ESL_proficiency_A_study_of_Chinese_students_in_Vellore_India

Table 1: Level of Technology Skill of Students (N=208)

Raw Scores Range	Skill Level	Frequency (N)	Percentage (%)
0-36	Basic skills	56	26.92%
37-52	Intermediate skills	98	47.12%
53-60	Advanced skills	54	25.96%

Table 2: ANOVA Table for difference between technology skills and personality traits.

	Sum of Squares	DF	Mean Square	F	Sig.
Between Groups	495.2	2	247.6		
Within Groups	3920	27	145.2	1.71	Not Significant

Table 3: Summary of three way ANOVA (2×2×3) factorial design

Sources of variations	SS	df	MS	F-ratio	Significance
A (Type of school)	10976.6	1	10976.6	46.6	Significant**
B (Gender)	960.7	1	960.7	4.1	Significant**
C (Family income)	3406.4	2	1703.2	7.2	Significant**
A×B	136.1	1	136.1	0.6	Not significant
B×C	877.3	2	438.65	1.9	Significant*
A×C	3369.45	2	1684.7	7.1	Significant**
A×B×C	2805.7	2	1402.8	5.9	Significant**
Within	14134.9	60	235.6		
Total	36667.15				

**Significant at .01 level

Table 4: Mean difference between government and private secondary level students' technology skills score

Type of school	Mean Value
Government	33.3
Private	46.1

Table 5: Mean difference between Male and Female secondary level students' technology skills score

Gender	Mean Value
Male	39.9
Female	39.5

Table 6: Mean difference between Low, Average and High family income students' technology skills score

Family Income	Mean Value
Low	42.8
Average	46.7
High	49.5





Ashish Choudhary and Mool Raj Sharma

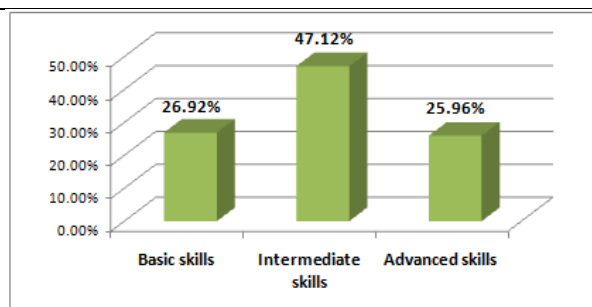


Figure 1: percentage wise distribution of students according to their technology skill levels

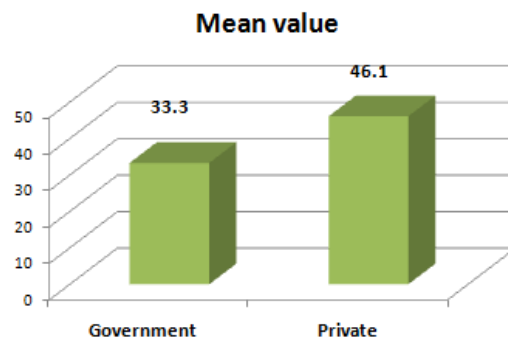


Figure 2: Type of school wise mean value of technology skills score of secondary level students

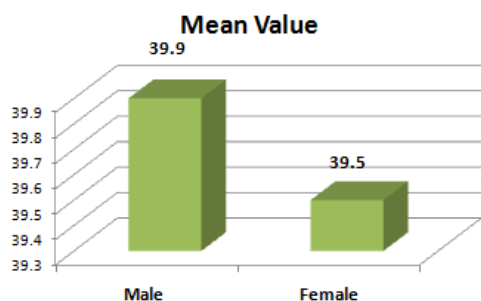


Figure 3: Gender wise mean value of technology skills score of secondary level students

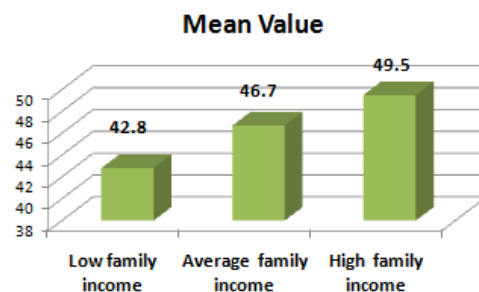


Figure 4: Family income wise mean value of technology skills score of secondary level students.





Phytochemical and Antibacterial Activity of Medicinal Plant *Strychnos nux-vomica*, L Loganiaceae

C. Sathya^{1*} and M.N. Abubacker²

¹Assistant Professor, Department of Botany, Bishop Heber College, (Affiliated to Bharathidasan University) Tiruchirappalli, Tamil Nadu, India.

²Associate Professor, Department of Biotechnology, National College, (Affiliated to Bharathidasan University) Tiruchirappalli, Tamil Nadu, India.

Received: 20 Jan 2024

Revised: 09 Feb 2024

Accepted: 14 May 2024

*Address for Correspondence

C. Sathya

Assistant Professor,
Department of Botany,
Bishop Heber College,
(Affiliated to Bharathidasan University)
Tiruchirappalli, Tamil Nadu, India.
Email: sathyasana22@gmail.com



This is an Open Access Journal / article distributed under the terms of the **Creative Commons Attribution License** (CC BY-NC-ND 3.0) which permits unrestricted use, distribution, and reproduction in any medium, provided the original work is properly cited. All rights reserved.

ABSTRACT

Medicinal plant was *Strychnos nux - vomica*, L. Loganiaceae was screened for its phyto chemical compounds by HPTLC technique which revealed the presence of alkaloids, flavonoid, saponins and steroids, Antibacterial activity was tested against *Bacillus subtilis* NCBT 012, *Staphylococcus aureus* NCBT051 (Gram +), *Escherichia coli* NCBT048 (Gram-) bacteria using ethanolic leaf extract. Maximum antibacterial activity was noticed in *E. coli*, followed by *P.aeruginosa* and *S.aureus*.

Keywords: Antibacterial activity, alkaloids, Disc Diffusion method, phytochemical analysis, *Strychnos - nuxvomica*

INTRODUCTION

Strychnos nux - vomica, L. (*Loganiaceae*), a tropical medicinal plant (Gamble, 2016), the seeds are used as toxic, stimulant treatment of paralysis and nervous disorders, seeds are added to beverages to make them intoxicating effect (Umrao sing et al. 1990) This medicinal plant has been utilized traditionally in many Countries of the world where limited access to formal health cares are limited (Adewole and Carton – Martius, 2006). The remedies and health approaches are free from side effects is an important aspects of drug obtained from the medicinal plants. (Abubacker et al 2018, Mahoud fathi



**Sathya and Abubacker**

et.al.2022).These are about 3000 medicinal plants have been recognized in India, 70%. of rural Populations are dependent on the traditional system of Ayurveda medicine. To Promote Indian herbal drugs there is a need to evaluate the therapeutic properties of the drugs as per WHO guidelines (Dubly et. al. 2004).There are reports of using root extract (Mahalingam 2011), flower extract (Glad Maheshet al 2015) and seed extract (Louds Magdalin Joy and Reginld appavoo 2015) of *S. nux-vomica* for antibacterial screening. The Present work evaluates the phytochemical and antibacterial activity of leaf ethanolic extract of this plant.

MATERIALS AND METHODS

Plant material

The plant *S.nux -vomica*, L. Loganiaceae (Fig-1) were collected from the green house Bishop Heber College, Tiruchirapalli, Tamil Nadu, India, which were, washed initially with 2%. Naclsolution followed by sterile distilled Water, air dried under sterile condition and finally powdered and used for the experimental work.

Bacterial Culture

The Clinical isolates of bacterial cultures tested in this work *Bacillus subtilis* NCBT 012 *Escherichia coli* NCBT 003, *Pseudomonas aeruginosa* NCBT 048 and *Staphylococcus aureus* NCBT 051 were maintained in immobilized condition in Nutrient. gelatin medium of gelatin 15g, Nutrient broth 100ml with pH 7.2 (Harrigan and Mc Cance 1969) Microbiology laboratory in the PG and Research Department of Biotechnology, National College, Tiruchirapalli, TamilNadu, India.

Preparation of leaf extract

Hundred grams of shade dried *S. nux -vomica* leaf powder was extracted with ethanol 1 litre of Solvent for 18 hours by conditions hot percolation using soxlet apparatus. After Completion of extraction the extract was dried and concentrated by vacuum distillation, the greenish brown residues obtained was stored in desicator for further phytochemical analysis using HPTLC (Harborne et al.1984) Hundred mg of extracted residue was then dissolved in ethanol and centrifuged at 3000 rpm 5min. Transferred the supernatant into 5ml volumetric flask and made up to the mark with ethanol. This solution was used as test solution for HPTLC analysis (Patel et. al 2010) 5 µl of this solution was loaded as band in was 10x10 cm silica gel 60F254 TLC Plate 0.2 mm thickness (Merck KGaA, Darm Stadt, Germany) Hamilton syringe using Hamilton syringe and CAMAG LINOMAT 5 instrument developing chamber with respective mobile phase. The developed plate was dried by hot air to evaporate solvents plate from the plate and the plate was dried by hot air to evaporate solvents from the plate and the plate was kept in photo - documentation Chamber CAMAG REPROSTAR 3 and the images were captured at white light. Than the plate was fixed for Scanning at 366nm and 500nm, the peaks display were noted in Densitogram.

Antibacterial assay

Disc Diffusion Method

Antibiogram was conducted by disc diffusion method (Banck et al 1966, NCCLS 1993) using standard disc as positive control. The surface of media were inoculated with bacterial strains from a pure nutrient broth culture. The test extract was loaded in the plain bio-discs (Hi media) and were placed on the bacterial inoculated media. After 48 hrs of incubation at a specific temperature ($32 \pm 1^\circ\text{C}$) for *B. subtilis* and ($37 \pm 1^\circ\text{C}$) for *E.coli*, *P. aeruginosa* and *S. aureus*. The culture plates were examined and the diameter of inhibition zones were measured in mm. Standard antibiotic disc Amikacin (30µg) was used as positive Control in this study.





DISCUSSION

PHYTOCHEMICAL ANALYSIS:

Plants are a major source of medicine with a biological deliberations like antibacterial and antifungal activities. Almost 25% of conventional drugs are used in primary health care of majority of world population (Ekor 2014). Phytochemical analysis conducted from the leaf ethanolic extract of *S. nux-vomica* by HPTLC method revealed the presence of alkaloids, flavonoids, steroids, and saponins. HPTLC technique is an excellent method with respect to selectivity and sensitivity in the detection of compounds (Patel et, al.2010, a). These phytochemicals are reported to have many biological and therapeutic properties (Narender et, al 2012, Vishnu et, al 2013., Patel, et.al 2010,b)(Benedec et, al 2013., Charalampus et.al 2013)and based on the earlier work the cumulative effect of phytochemicals of *S. nux-vomica* leaf ethanolic extract was tested and it seems to be a potential antibacterial compound of plant origin.

Antibacterial activity

Antibacterial screening study revealed that the ethanolic leaf extract showed maximum 20.07 ± 0.20 mm inhibition against *E.coli* at 100 μ g/ml concentration, the positive control Amikacin showed 28.0 ± 0.10 mm zone of inhibition at 30 μ g/disc contraction which is followed by 16.0 ± 0.15 mm for *P.aeruginosa*, 14.0 ± 0.10 mm for *B.subtilis* and *S.aureus* at 100 μ g/ml concentration of leaf extract. Mahalingam et.al (2011), stated good antibacterial activity of ethylacetate and n-butanol root extract *S. nux-vomica*, the zone of inhibition ranged from 13-16mm against *E.coli*, *S. aureus*, and *Klebsiella sp* of Londs magdalen joy and Reginald Appavoo (2015) also antibacterial activity of *S. nux-vomica* seed extract for *E.coli* and *klebsiella sp*. of Glad Mahesh et, al (2015) studied the flower extract of *S.nux-vomica* and stated antibacterial activity. The present work is yet another evidence and confirmed antibacterial activity of *S.nux- vomica* leaf ethanolic extract.

RESULTS

Phytochemical analysis by HPTLC:

Medicinal plants are natural resources yielding valuable herbal product, which are often used in the treatment of various Ailments in the traditional health care system. *S .nux- vomica* leaf extract were screened for secondary metabolites using HPTLC analysis which revealed the pressure of alkaloids, flavonoid, saponins and sterols. Bright yellow coloured zone were present in sample at Rf value for 0.10 to 0.23 represent alkaloid 1 and 0.23 to 0.30 for alkaloids in the densitogram. Bluish green coloured Zone with Rf value 0.37 to 0.43 in the densitogram represent flavonoids, Green Coloured zone at Rf value 0.11 to 0.18 represent steroid 1, and 0.67 to 0.87 refers to steroid 2 greyish green coloured zone in sample at different Rf values representsaponins 1 to 5, Rf 0.21 to 0.32 saponin 2, 0.32 to 0.40 saponin3, 0.61 to 0.70 saponin 4 and 0.50 to 0.61 represent saponin 5 .

Antibacterial Assay

The antibiogram revealed that maximum antibacterial activity was against *E. coli*, which is followed by *P. aeuroginosa*, *B. subtilis*, and *S. aureus*. For *E. coli* 12.0 ± 00.5 , 16.0 ± 0.10 and 20.0 ± 0.20 mm zone of inhibitions were noticed for 25, 50 and 100 μ g/ml concentration respectively against 28.0 ± 0.10 mm for Amikacin 30 μ g/ml as a positive control. Whereas for both *B.subtilis* and *S. aureus* 10.0 ± 0.10 , 12.0 ± 0.15 14.0 ± 0.10 mm zone of inhibition was seen for 25,50 and 100 μ g/ml concentration respectively and for Alkaline control 32.0 ± 0.05 for *B.subtilis* and 24.0 ± 0.05 for *S. aureus* zone of inhibition was found. *P.aeruginosa* have shown 10.0 ± 0.10 , 14.0 ± 0.15 , and 16.0 ± 0.15 mm zone of inhibition was noticed for 25, 50, and 100 μ g/ml concentration respectively and for amikacin control, 30.0 ± 0.10 mm zone of inhibition was noticed.





Sathya and Abubacker

CONCLUSION

The potential of leaf extract of *S. nux-vomica* medicinal plants for developing antibacterial drugs is promising and it can lead to contributing and vital role in phytomedicines for both Gram-positive and Gram-negative time bacteria. Plant-based antibacterial drugs have lesser side effects than synthetic drugs and to conclude that the leaf ethanolic extract of *S.nux-vomica* could be used as antibacterial drugs, further studies in this will explore the other potential uses of thin medicinal plants.

ACKNOWLEDGMENT

Author C. Sathya wish to thank the head, PG ad research department of Botany Bishop Heber College, Tiruchirapalli, and the principal for providing the infrastructure facilities and encouragement to carry over their research work.

REFERENCES

1. Abubacker, M. N., Gurunathan, S., Ganapathy, G., & Prince, M.. Survey of some Ethanol medicine used by the tribal population in Nilgiri Hills, South India. American Journal of Ethnomedicine, 2018;5, 1-7.
2. Adewole, S. O., & Caxton Martins, E. A.. Morphological changes and Hypoglycemic effect of Annona muricata L. (Annonaceae) leaf aqueous extract as pancreatic -B- cells of streptozotocin treated diabetic rats. African Journal of Biomedical Research, 2006; 9, 173-187.
3. Bauck, A. W., Kirby, W. M., Sheris, J. C., & Turek, M.. Antibiotic sensibility testing by a standardized single disc method. Annals of Clinical Pathology, (1996);45, 149-158.
4. Benedec, D., Vlase, L., Oniga, I., Mot, A. C., Damian, G., & Hangann, O. Polyphenolic composition, antioxidant and antibacterial activities for two Romanian subspecies of Achillea distans, wouldst. Et. Kit. Ex wild. Molecules, 2013;18, 8725-8739.
5. Cheralampos, P., Konstantina, L., Olga, K. M., Pangiotiz, Z., & Vassikia, K. S. Antioxidant capacity of selected plant extracts and their essential oil. Antioxidants, 2013;2, 11-22.
6. Dubey, N. K., Rajesh Kumar, & Pramila Tripathi. Global promotion of herbal medicine: Indian opportunity. Current Science, 2004;86, 1-10.
7. Gamble, J. S. (2016). Flora of the Presidency of Madras. Neeraj Publishing House.
8. Harrigan, W. F., & Mccance, M. E. (1969). Laboratory methods in microbiology. Academic Press.
9. Londs Magdaline Joy, A., & Reginald Appavoo, M. A. Antibacterial and antifungal activity of Strychnos nux-vomica seed extract. Journal of Chemical and Pharmaceutical Research, 2015;7, 1495-1499.
10. Mahalingam, R., Bharathidasan, V., Ambikapathy, A., & Panerselvam. Antibacterial activity of Strychnos nux-vomica root extract. Asian Journal of Plant Science and Research, 2011; 1, 86-90.
11. Mahmoud Fathi, Maryam Ghane, & Leila Pishkar. Phytochemical Composition, Antibacterial, and Antibiofilm Activity of Malva sylvestris Against Human Pathogenic Bacteria. Jundishapur Journal of Natural Pharmaceutical Products, 2022; 17(1).
12. Narender, P. O., Ganga, R., Sambasiva, E., Mallikarjuna, T., & Praneeth, V. S. Quantification of phytochemical constituents and in vitro antioxidant activity of Mesua ferrea leaves. Asian Pacific Journal of Tropical Biomedicine, 2012; 2, 539-542.
13. NCCLS. Performance standards for antimicrobial disc susceptibility tests. NCCLS Publications. 1993
14. Patel, M. R., Patel, R. B., Parikh, J. R., & Patel, B. G. HPTLC method for estimation of Tazarotene in tropical gel formation and in vitro study. Analytical Methods, 2010;2, 275-281.
15. Patel, R. B., Patel, M. R., Bhari, K. K., & Patel, B. G. Development and validation of an HPTLC method for determination of olanzapine in the formulation. Journal of AOAC International, 2010; 93, 811-819.
16. Ekor, M. The growing use of herbal medicines; Issues relating to adverse reactions and challenges in





Sathya and Abubacker

- monitoring safety. *Frontiers in Pharmacology*, 2014; 4, 177.
17. Patel, R. B., Patel, M. R., Bhatt, K. K., & Patel, B. G. Development and validation of HPTLC method for estimation of Carbamazepine in Formulation and its In vitro release. *Chromatography Research International*, 2010.
 18. Umarao Singh, Wadhwan, A. M., & Johri, B. M. Dictionary of economic plants in India. Indian Council of Agricultural Research. 1990
 19. Vishnu, R., Nisha, R., Jamuna, S., & Paulsamy, S. (20). Quantification of total phenolics and flavonoids and evaluation of In vitro antioxidant properties of ethanolic leaf extract of *Tarenna asiatica* – an endemic medicinal plant species of Maruthamalai Hills, Western Ghats, Tamil Nadu. *Journal of Research in Plant Science*, 2, 196-204.
 20. Glad Mahesh, M. L., Magdalin Joy, A. L., Ratchagan, K., & Sundaramurthy, A. Antibacterial and antioxidant activity of *Strychnos nux-vomica* flower extract. *Journal of Chemical and Pharmaceutical Research*, 2015; 7, 748-752.
 21. Harborne, J. B. *Phytochemical methods: A guide to modern techniques of plant analysis*. Chapman and Hall. 1984.

Table 1: Antibacterial sensitivity studies of ethanolic by extract of *S.nux-vomica* against *B. subtilis*, *E. coli*, *P. aeruginosa*, and *S.aureus* results are presented

Organism/Antibiotic disc	Concentration µg/ml	Zone of inhibition(mm) Time 48 hr
<i>B.subtilis</i> NCBT 012Amikacin (control)	25	10.0±0.10
	50	12.0±0.15
	100	14.0±0.10
	30	32.0±0.05
<i>E.coli</i> NCBT 003 Amikacin (control)	25	12.0±0.05
	50	16.0±0.10
	100	20.00±0.20
	30	28.0±0.10
<i>P.Aeruginosa</i> NCBT 048 Amikacin (control)	25	10.0±10.0
	50	14.0±0.15
	100	16.0±0.15
	30	30.0 ± 0.10
<i>Aureus</i> NCBT 051 Amikacin (control)	25	10.0 ± 0.10
	50	12.0 ± 0.05
	100	14.0 ± 0.10
	30	24.0 ± 0.05





Sathya and Abubacker



Figure:1

PLATE - 2: EXTRACTION OF PLANT MATERIALS



Figure:2

PLATE - 3: ANTIBACTERIAL ACTIVITY IN PLANT MATERIAL WITH EXTRACTION SOLVENT



Figure:3

PLATE - 4: ANTIBACTERIAL ACTIVITY IN PLANT MATERIAL WITH EXTRACTION SOLVENT

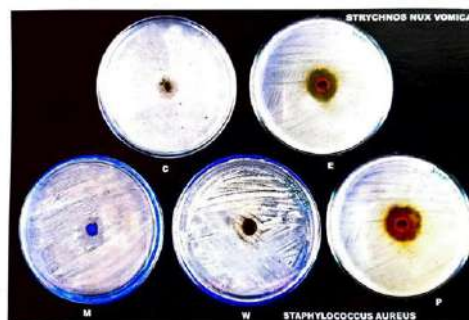


Figure:4

PLATE - 5: ANTIFUNGAL ACTIVITY IN PLANT MATERIAL WITH EXTRACTION SOLVENT



Figure:5

PLATE - 7: THIN LAYER CHROMATOGRAPHY TECHNIQUE SEPARATION OF ALKALOIDS FROM STRYCHNOS NUX VOMICA



Figure:6





Sathya and Abubacker

PLATE - 8: SODIUM DODECYL SULPHATE –POLY ACRYLAMIDE GEL
ELECTROPHORESIS [SDS – PAGE]

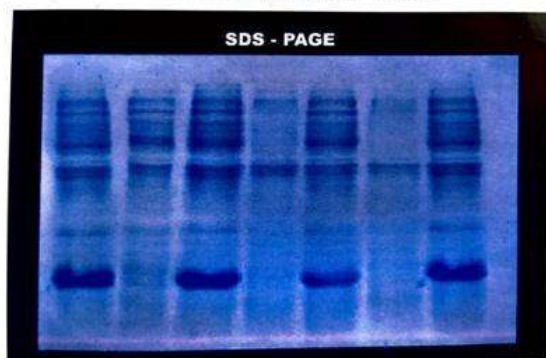


Figure:7





An M/G/1 Retrial Queue with Recurrent Customers, General Retrial Times, Switchover Time and Working Vacation

S.Pazhani Bala Murugan¹ and A. Jeba Pauline Veronica^{2*}

¹Associate Professor, Department of Mathematics, Annamalai University, Annamalainagar, Cuddalore, Tamil Nadu, India.

²Research Scholar, Department of Mathematics, Annamalai University, Annamalainagar, Cuddalore, Tamil Nadu, India.

Received: 20 Jan 2024

Revised: 09 Feb 2024

Accepted: 14 May 2024

*Address for Correspondence

A. Jeba Pauline Veronica

Research Scholar,

Department of Mathematics,

Annamalai University,

Annamalainagar, Cuddalore,

Tamil Nadu, India.

Email: ajpv2519@gmail.com



This is an Open Access Journal / article distributed under the terms of the **Creative Commons Attribution License** (CC BY-NC-ND 3.0) which permits unrestricted use, distribution, and reproduction in any medium, provided the original work is properly cited. All rights reserved.

ABSTRACT

An M/G/1 retrial queue with recurrent customers, general retrial times, switch overtime with working vacation is get into the contemplation of this work. We consider two types of customers; recurrent and transit customers. All service times and retrial times for transit customers follow general distribution, retrial time for recurrent customers and working vacation time are assumed to have an exponential distribution, also service time of the recurrent customers follows and general distribution and switch overtime to the working vacation of server follows an exponential distribution. The PGF and the mean of number of customers in an imperceptible waiting area are get by the effective action of supplementary variable technique. As a matter of interest, some special cases are furnished.

Keywords: Retrial queue, Recurrent customer, Transit customer, Working vacation, Switchover time, Supplementary variable technique, Probability generating function, Waiting time, Idle State.

MSC 2010 No.:60k25, 90B22.

INTRODUCTION

For the last few years, there has been extensive research into retrial queue in the field of queuing theory. *Retrial queues* are distinguished by the fact that an arriving customer discovers, a server is busy when it arrives, it is





Pazhani Bala Murugan and Jeba Pauline Veronica

requested to leave or decides to leave the service zone and enters to an invisible place to the server, known as an *orbit*. Continuing to follow some random period, the customer makes many efforts to obtain service. This request is independent of the other customers in the orbit. In the analysis of telephone and other communication systems, these models with repeated attempts appear often. One could visit [6,7,21] to allow a more detailed examination of the retrial queues. Boxma OJ, Cohen JW[14] investigated an $M/G/1$ queue with specific number of recurrent customers, who rejoin the queue after completing their service (Basically in Stochastic Process, a state is considered to be *recurrent* if, whenever we leave it, we will return to it with probability one. Instead, *transient* if the probability of return is less than one.). Farahmand[9] examined the idea of recurrent customers in the retrial queue, examining two cases: the constant case, in which the call-up rate of each customer is independent of the number of customers in orbit, and the inconstant case, in which the call-up rate drops as, in orbit the number of customers rises. Moreno [12] investigated an $M/G/1$ retrial queue with a specific number K recurrent customers ($K = 1,2,3,\dots$) which are return to orbit immediately after service; once the service complete, transit customers who exit the system will never return. Vacation queueing model was introduced as a development of the classical queueing theory in the 1970's. In this, the server may be unavailable for some timeframe for number of reasons, such as: searching for restoration, starting to work at some other queues, checking for new work, or merely by taking a break from their work, these are regular traits of many communication systems. So, this timeframe is known as *vacation* (the server is inaccessible to the primary customers). In addition, vacation strategy deliberated by Servi and Finn [18], a new vacation tactic known as Working Vacation was developed (WV). During a time period of WV , the server offers customers a lower rate of service than during the Usual Busy(UB) period. Moreover, suppose there is a customer in the service zone when completion of the Working Vacation(WV) period, the server can end the vacation and access to its UB period while servicing, known as *vacation interruption*. Wu and Takagi [20] investigated $M/G/1/MWV$. For the recent development on $M/G/1$ retrial queue with vacation policy, one could see: the retrial queue with vacation was established in [10], the $M/G/1$ retrial queue with MWV was investigated in [15], $M/G/1$ retrial queue with single working vacation in [16]. Moreover, [5] provide a complete investigation of WV period. Here we present, characterisation of the model, steady state probabilities, some special cases and then conclusion.

MODEL DESCRIPTION

In this article we investigate on an $M/G/1$ retrial queue, retrial time follows general with WV period. We examine a retrial queue with single server and customers of two types: one is transit (also known as usual) customers and another on is specific number of $T(>1)$ recurrent (commonly known as permanent) customers. Recurrent customers usually back to the retrial group (orbit) once service is completed and whereas transit customers depart the system permanently. In accordance with the Poisson process the transit customers arrive with rate λ . When server is on off work and the transit customer finds it then he occupy it and leaves after completion of his service; otherwise, he enters the orbit by FCFS discipline. Suppose that at the head of the orbit only the transit customer has access to the server. For any transit customer, the successive inter-retrial times we have an arbitrary probability distribution function $R(\zeta)$, in which its corresponding probability density function(pdf) $r(\zeta)$ and Laplace-Stieltjes Transform(LST) $R^*(s)$ in WV period. Also in UB , following $S(\zeta)$, $s(\zeta)$ and $S^*(s)$ are distribution function, pdf and LST on inter-retrial times of any transit customer respectively. When the orbit remain only $T(>0)$ recurrent customers when the service is finished, the server takes a vacation, and the duration of the vacation period is exponentially distributed with rate η : If there are customers in the system at the end of a vacation, the server will begin a fresh hectic(busy) period. Otherwise, he waits for a customer. Such a vacation policy is called a single working vacation. When server ready to switchover time to the WV , server waits for some arbitrary time period which follows an exponential distribution with rate α . In WV period the service times of the transit customers are *i.i.d* with a probability distribution function $H_{v_1}(\zeta)$, a pdf $h_{v_1}(\zeta)$, a LST $H_{v_1}^*(s)$. Similarly, in UB period we have $H_{u_1}(\zeta)$, $h_{u_1}(\zeta)$ and $H_{u_1}^*(s)$. The system has set number of T recurrent customers. After have been served, he straight away go back to the orbit according to FCFS discipline. We infer that at the head of the orbit the recurrent customer only approach to the server. Subsequent interretrial times of recurrent customers is exponentially distributed with parameter γ having a finite mean $1/\gamma$. This is also for WV period. In WV period the service times of the specific





Pazhani Bala Murugan and Jeba Pauline Veronica

number T of recurrent customers are *i.i.d* with a probability distribution function $H_{v_2}(\zeta)$, a pdf $h_{v_2}(\zeta)$, a LST $H_{v_2}^*(s)$. Similarly, in UB period we have $H_{u_2}(\zeta)$, $h_{u_2}(\zeta)$ and $H_{u_2}^*(s)$. We assume that interarrival times, retrial times, working vacation times and service times are mutually independent. It is evident from this description that the formation of our retrial queue can be understood as, an oscillating between the periods of an idle and busy period along with WV period of the server. The customer who has to be served next is decided by a vying between two exponentially distributed rates (λ and γ) and general retrial time of transit customers (i.e., foremost customer in the orbit if any transit customer or if any recurrent customer or if any fresh arrival rivalry for service). Which are the primary distinction between waiting queue (classic) in the absence of retrials. The prime objective of our paper is to providing influence of the WV period on class of customers (recurrent and transit customers) with switchover time to the working vacation.

MODEL ANALYSIS

Following Subsequent random variables are used in this model.

- $O(\tau)$ - Size of the orbit at time " τ ."
- $R^0(\tau)$ - The remaining retrial time of transit customer in WV period at the head of the orbit at τ .
- $H_{v1}^0(\tau), H_{v2}^0(\tau)$ - The remaining service time of transit and recurrent customers in WV period at time τ .
- $S^0(\tau)$ - The remaining retrial time of transit customer in UB period at time τ .
- $H_{u1}^0(\tau), H_{u2}^0(\tau)$ - The remaining service time of transit and recurrent customers in UB period at time τ .

$$\phi(\tau) = \begin{cases} 0 & \text{if the server is not occupied in } WV \text{ period at time } \tau \\ 1 & \text{if the server is occupied by transit customer in } WV \text{ period at time } \tau \\ 2 & \text{if the server is occupied by recurrent customer in } WV \text{ period at time } \tau \\ 3 & \text{if the server is not occupied in } UB \text{ period at time } \tau \\ 4 & \text{if the server is occupied by transit customer in } UB \text{ period at time } \tau \\ 5 & \text{if the server is occupied by recurrent customer in } UB \text{ period at time } \tau. \end{cases}$$

where, $\phi(\tau)$ denotes states of the server at " τ ."

Now, the supplementary variables $H_{v1}^0(\tau), H_{v2}^0(\tau), H_{u1}^0(\tau), H_{u2}^0(\tau), R^0(\tau)$ and $S^0(\tau)$ are introduced to generate bivariate Markov Process $\{(\phi(\tau), O(\tau)); \tau \geq 0\}$.

Where $S(\tau) = R^0(\tau)$ if $\phi(\tau) = 0$; $H_{v1}^0(\tau)$ if $\phi(\tau) = 1$; $H_{v2}^0(\tau)$ if $\phi(\tau) = 2$;
 $S^0(\tau)$ if $\phi(\tau) = 3$; $H_{u1}^0(\tau)$ if $\phi(\tau) = 4$; $H_{u2}^0(\tau)$ if $\phi(\tau) = 5$.

Following are the limiting probabilities

$$\begin{aligned} V_{0,T} &= \lim_{\tau \rightarrow \infty} \Pr\{O(\tau) = T, \phi(\tau) = 0\} \\ V_{0,m} &= \lim_{\tau \rightarrow \infty} \Pr\{O(\tau) = m, \phi(\tau) = 0, \zeta < R^0(\tau) \leq \zeta + d\zeta; \tau \geq 0, \zeta \geq 0, m \geq T + 1 \\ V_{1,m} &= \lim_{\tau \rightarrow \infty} \Pr\{O(\tau) = m, \phi(\tau) = 1, \zeta < H_{v1}^0(\tau) \leq \zeta + d\zeta; \tau \geq 0, \zeta \geq 0, m \geq T \\ V_{2,m} &= \lim_{\tau \rightarrow \infty} \Pr\{O(\tau) = m, \phi(\tau) = 2, \zeta < H_{v2}^0(\tau) \leq \zeta + d\zeta; \tau \geq 0, \zeta \geq 0, m \geq T + 1 \\ U_{0,T} &= \lim_{\tau \rightarrow \infty} \Pr\{O(\tau) = T, \phi(\tau) = 3\} \\ U_{0,m} &= \lim_{\tau \rightarrow \infty} \Pr\{O(\tau) = m, \phi(\tau) = 3, \zeta < S^0(\tau) \leq \zeta + d\zeta; \tau \geq 0, \zeta \geq 0, m \geq T + 1 \\ U_{1,m} &= \lim_{\tau \rightarrow \infty} \Pr\{O(\tau) = m, \phi(\tau) = 4, \zeta < H_{u1}^0(\tau) \leq \zeta + d\zeta; \tau \geq 0, \zeta \geq 0, m \geq T \\ U_{2,m} &= \lim_{\tau \rightarrow \infty} \Pr\{O(\tau) = m, \phi(\tau) = 5, \zeta < H_{u2}^0(\tau) \leq \zeta + d\zeta; \tau \geq 0, \zeta \geq 0, m \geq T + 1 \end{aligned}$$

For $i = 0, 1, 2$ we define following LST and PGF of WV period and UB period,

$$\begin{aligned} V_{i,m}^*(\theta) &= \int_0^\infty e^{-\theta\zeta} V_{i,m}(\zeta) d\zeta, U_{i,m}^*(\theta) = \int_0^\infty e^{-\theta\zeta} U_{i,m}(\zeta) d\zeta, \\ V_{i,m}^*(0) &= \int_0^\infty V_{i,m}(\zeta) d\zeta, U_{i,m}^*(0) = \int_0^\infty U_{i,m}(\zeta) d\zeta, \\ V_i^*(\ell, \theta) &= \sum_{m=T+1}^\infty V_{i,m}^*(\theta) \ell^m, U_i^*(\ell, \theta) = \sum_{m=T+1}^\infty U_{i,m}^*(\theta) \ell^m, \\ V_i^*(\ell, 0) &= \sum_{m=T+1}^\infty V_{i,m}^*(0) \ell^m, U_i^*(\ell, 0) = \sum_{m=T+1}^\infty U_{i,m}^*(0) \ell^m, \end{aligned}$$





Pazhani Bala Murugan and Jeba Pauline Veronica

$$V_i(\ell, 0) = \sum_{m=T+1}^{\infty} V_{i,m}(0)\ell^m, U_i(\ell, 0) = \sum_{m=T+1}^{\infty} U_{i,m}(0)\ell^m.$$

For $i = 1, 2$ LST of service times in WV period and UB period are,

$$H_{vi}^*(\theta) = \int_0^{\infty} e^{-\theta\zeta} s_{vi}(\zeta) d\zeta, H_{ui}^*(\theta) = \int_0^{\infty} e^{-\theta\zeta} s_{ui}(\zeta) d\zeta$$

LST of retrial time of transit customers in WV period and UB period are,

$$R^*(\theta) = \int_0^{\infty} e^{-\theta\zeta} r(\zeta) d\zeta, S^*(\theta) = \int_0^{\infty} e^{-\theta\zeta} s(\zeta) d\zeta$$

Then the system of steady state equations are illustrated by the following differential difference equations:

$$\sigma V_{0,T} = \alpha U_{0,T} + V_{1,T}(0) + V_{2,T-1}(0) \quad (1)$$

$$-\frac{d}{d\zeta} V_{0,m}(\zeta) = -\sigma V_{0,m}(\zeta) + V_{1,m}(0)r(\zeta) + V_{2,m-1}(0)r(\zeta), m \geq T+1 \quad (2)$$

$$-\frac{d}{d\zeta} V_{1,T}(\zeta) = -(\lambda + \eta)V_{1,T}(\zeta) + V_{0,T+1}(0)h_{v1}(\zeta) + \lambda V_{0,T}h_{v1}(\zeta) \quad (3)$$

$$-\frac{d}{d\zeta} V_{1,m}(\zeta) = -(\lambda + \eta)V_{1,m}(\zeta) + V_{0,m+1}(0)h_{v1}(\zeta) + \lambda V_{1,m-1}(\zeta) + \lambda h_{v1}(\zeta) \int_0^{\infty} V_{0,m}(\zeta) d\zeta, m \geq T+1 \quad (4)$$

$$-\frac{d}{d\zeta} V_{2,T-1}(\zeta) = -(\lambda + \eta)V_{2,T-1}(\zeta) + \gamma V_{0,T}h_{v2}(\zeta) \quad (5)$$

$$-\frac{d}{d\zeta} V_{2,m}(\zeta) = -(\lambda + \eta)V_{2,m}(\zeta) + \lambda V_{2,m-1}(\zeta) + \gamma h_{v2}(\zeta) \int_0^{\infty} V_{0,m+1}(\zeta) d\zeta, m \geq T \quad (6)$$

$$(\lambda + \gamma + \alpha)U_{0,T} = \eta V_{0,T} + U_{1,T}(0) + U_{2,T-1}(0) \quad (7)$$

$$-\frac{d}{d\zeta} U_{0,m}(\zeta) = -(\lambda + \gamma)U_{0,m}(\zeta) + U_{1,m}(0)s(\zeta) + \lambda U_{2,m-1}(\zeta)s(\zeta) + \eta s(\zeta) \int_0^{\infty} U_{0,m}(\zeta) d\zeta, m \geq T+1 \quad (8)$$

$$-\frac{d}{d\zeta} U_{1,T}(\zeta) = -\lambda U_{1,T}(\zeta) + U_{0,T+1}(0)h_{u1}(\zeta) + \lambda U_{0,T}(\zeta)h_{u1}(\zeta) + \lambda h_{u1}(\zeta) \int_0^{\infty} U_{1,T}(\zeta) d\zeta \quad (9)$$

$$-\frac{d}{d\zeta} U_{1,m}(\zeta) = -\lambda U_{1,m}(\zeta) + U_{0,m+1}(0)h_{u1}(\zeta) + \lambda U_{1,m-1}(\zeta) + \lambda h_{u1}(\zeta) \int_0^{\infty} U_{0,m}(\zeta) d\zeta + \eta h_{u1}(\zeta) \int_0^{\infty} V_{1,m}(\zeta) d\zeta, m \geq T+1 \quad (10)$$

$$-\frac{d}{d\zeta} U_{2,T-1}(\zeta) = -\lambda U_{2,T-1}(\zeta) + \gamma U_{0,T}(\zeta)h_{u2}(\zeta) + \eta h_{u2}(\zeta) \int_0^{\infty} V_{2,T-1}(\zeta) d\zeta \quad (11)$$

$$-\frac{d}{d\zeta} U_{2,m}(\zeta) = -\lambda U_{2,m}(\zeta) + \lambda U_{2,m-1}(0) + \gamma h_{u2}(\zeta) \int_0^{\infty} U_{0,m+1}(\zeta) d\zeta + \eta h_{u2}(\zeta) \int_0^{\infty} V_{2,m}(\zeta) d\zeta, m \geq T \quad (12)$$

Taking the LST from (2) to (6) and from (8) to (12) on both sides, we have following results

$$\theta V_{0,m}^*(\theta) - V_{0,m}(0) = \sigma V_{0,m}^*(\theta) - V_{1,m}(0)R^*(\theta) - V_{2,m-1}(0)R^*(\theta), m \geq T+1 \quad (13)$$

$$\theta V_{1,T}^*(\theta) - V_{1,T}(0) = (\lambda + \eta)V_{1,T}^*(\theta) - V_{0,T+1}(0)H_{v1}^*(\theta) - \lambda V_{0,T}(0)H_{v1}^*(\theta) \quad (14)$$

$$\theta V_{1,m}^*(\theta) - V_{1,m}(0) = (\lambda + \eta)V_{1,m}^*(\theta) - \lambda V_{1,m-1}^*(\theta) - V_{0,m+1}(0)H_{v1}^*(\theta) - \lambda V_{0,m}^*(0)H_{v1}^*(\theta), m \geq T+1 \quad (15)$$

$$\theta V_{2,T-1}^*(\theta) - V_{2,T-1}(0) = (\lambda + \eta)V_{2,T-1}^*(\theta) - \gamma V_{0,T}H_{v2}^*(\theta) \quad (16)$$

$$\theta V_{2,m}^*(\theta) - V_{2,m}(0) = (\lambda + \eta)V_{2,m}^*(\theta) - \lambda V_{2,m-1}^*(\theta) - \gamma V_{0,m+1}^*(0)H_{v2}^*(\theta), m \geq T \quad (17)$$

$$\theta U_{0,m}^*(\theta) - V_{0,m}(0) = (\lambda + \gamma)U_{0,m}^*(\theta) - V_{1,m}(0)S^*(\theta) - V_{2,m-1}(0)S^*(\theta) - \eta V_{0,m}^*(0)S^*(\theta), m \geq T+1 \quad (18)$$

$$\theta U_{1,T}^*(\theta) - U_{1,T}(0) = \lambda U_{1,T}^*(\theta) - U_{0,T+1}(0)H_{u1}^*(\theta) - \eta V_{1,T}^*(0)H_{u1}^*(\theta) - \lambda U_{0,T}H_{u1}^*(\theta) \quad (19)$$

$$\theta U_{1,m}^*(\theta) - U_{1,m}(0) = \lambda U_{1,m}^*(\theta) - \lambda U_{1,m-1}^*(\theta) - U_{0,m+1}(0)H_{u1}^*(\theta) - \eta V_{1,m}^*(\theta)H_{u1}^*(\theta) - \lambda U_{0,m}^*(0)H_{u1}^*(\theta), m \geq T+1 \quad (20)$$

$$\theta U_{2,T-1}^*(\theta) - U_{2,T-1}(0) = \lambda U_{2,T-1}^*(\theta) - \gamma U_{0,T}^*(0)H_{u2}^*(\theta) - \eta V_{2,T-1}^*(0)H_{u2}^*(\theta) \quad (21)$$

$$\theta U_{2,m}^*(\theta) - U_{2,m}(0) = \lambda U_{2,m}^*(\theta) - \lambda U_{2,m-1}^*(\theta) - \gamma U_{0,m+1}^*(0)H_{u2}^*(\theta) - \eta V_{2,m}^*(0)H_{u2}^*(\theta), m \geq T \quad (22)$$





Pazhani Bala Murugan and Jeba Pauline Veronica

In (13) take a summation over m from $T + 1$ to ∞ then multiply with ℓ^m and result,

$$(\theta - \sigma)V_0^*(\ell, \theta) = V_0(\ell, \theta) - R^*(\theta)[\ell V_1(\ell, 0) + \ell V_2(\ell, 0) - [V_{1,T}(0) + V_{2,T-1}(0)]\ell^T] \quad (23)$$

In (15) take a summation over m from $T + 1$ to ∞ then multiply with ℓ^m and combine this result with (14),

$$[\theta - (\lambda_\ell + \eta)]V_1^*(\ell, \theta) = V_1(\ell, 0) - H_{v1}^*(\theta)\left[\frac{V_0(\ell, 0)}{\ell} + \lambda V_0^*(\ell, 0) + \lambda V_{0,T}\ell^T\right] \quad (24)$$

In (17) take a summation over m from T to ∞ then multiply with ℓ^m and combine this result with (16),

$$[\theta - (\lambda_\ell + \eta)]V_2^*(\ell, \theta) = V_2(\ell, 0) - \frac{\gamma H_{v2}^*(\theta)}{\ell}[V_0^*(\ell, 0) + V_{0,T}\ell^T] \quad (25)$$

Placing $\theta = \sigma$ in (23), result

$$V_0(\ell, \theta) = R^*(\sigma)[V_1(\ell, 0) + \ell V_2(\ell, 0) - \ell^T[V_{1,T}(0) + V_{2,T-1}(0)]] \quad (26)$$

Placing $\theta = 0$ in (23) and sub., (26) in (23), results

$$V_0^*(\ell, 0) = \frac{1}{\sigma}[1 - R^*(\sigma)][V_1(\ell, 0) + \ell V_2(\ell, 0) - \ell^T[V_{1,T}(0) + V_{2,T-1}(0)]] \quad (27)$$

Placing $\theta = \lambda_\ell + \eta$ in (24), result

$$V_1(\ell, 0) = H_{v1}^*(\lambda_\ell + \eta)\left[\frac{V_0(\ell, 0)}{\ell} + \lambda V_0^*(\ell, 0) + \lambda V_{0,T}\ell^T\right] \quad (28)$$

Placing $\theta = 0$ in (24), and sub., (28) in (24), result

$$V_1^*(\ell, 0) = \frac{1 - H_{v1}^*(\lambda_\ell + \eta)}{\lambda_\ell + \eta}\left[\frac{V_0(\ell, 0)}{\ell} + \lambda V_0^*(\ell, 0) + \lambda V_{0,T}\ell^T\right] \quad (29)$$

Placing $\theta = \lambda_\ell + \eta$ in (25), results

$$V_2(\ell, 0) = \frac{\gamma H_{v2}^*(\lambda_\ell + \eta)}{\ell}[V_0^*(\ell, 0) + V_{0,T}\ell^T] \quad (30)$$

Placing $\theta = 0$ in (25) and sub., (30) in (25), results

$$V_2^*(\ell, 0) = \frac{\gamma[1 - H_{v2}^*(\lambda_\ell + \eta)]}{\ell(\lambda_\ell + \eta)}[V_0^*(\ell, 0) + V_{0,T}\ell^T] \quad (31)$$

where, $\sigma = \lambda + \gamma + \eta$ and $\lambda_\ell = \lambda - \lambda\ell$.

Sub., (27) and (30) in (26), results

$$V_2(\ell, 0) = \frac{\ell^T \sigma R^*(\sigma)[\lambda H_{v1}^*(\lambda_\ell + \eta) + \gamma H_{v2}^*(\lambda_\ell + \eta)]V_{0,T} - [V_{1,T}(0) + V_{2,T-1}(0)]}{\ell \sigma - H_{v1}^*(\lambda_\ell + \eta)[\lambda \ell + (\lambda - \lambda \ell + \gamma + \eta)R^*(\sigma)] - \gamma \ell [1 - R^*(\sigma)]H_{v2}^*(\lambda_\ell + \eta)} \quad (32)$$

Let, $f(\ell) = \ell \sigma - H_{v1}^*(\lambda_\ell + \eta)[\lambda \ell + (\lambda - \lambda \ell + \gamma + \eta)R^*(\sigma)] - \gamma \ell [1 - R^*(\sigma)]H_{v2}^*(\lambda_\ell + \eta)$

For $\ell = 0$ and $\ell = 1$ we obtain $f(0) < 0$ and $f(1) > 0 \Rightarrow \exists$ a real root $\ell_1 \in (0, 1)$ such that $f(\ell_1) = 0$.

At $\ell = \ell_1$ in (32) is converted into

$$[V_{1,T}(0) + V_{2,T-1}(0)] = [\lambda H_{v1}^*(\lambda - \lambda \ell_1 + \eta) + \gamma H_{v2}^*(\lambda - \lambda \ell_1 + \eta)]V_{0,T} = \chi_{\ell_1} V_{0,T} \quad (33)$$

Displace using (33) in (32),

$$V_0(\ell, 0) = \frac{\ell^{T+1} \sigma R^*(\sigma) V_{0,T}}{Z_1(\ell)} [[\lambda H_{v1}^*(\lambda_\ell + \eta) + \gamma H_{v2}^*(\lambda_\ell + \eta)] - \chi_{\ell_1}] \quad (34)$$

By solving (26) to (31) we get followings results for WV period,

$$V_1(\ell, 0) = \frac{\ell^T V_{0,T} H_{v1}^*(\lambda_\ell + \eta)}{Z_1(\ell)} [\sigma [\lambda \ell + \gamma H_{v2}^*(\lambda_\ell + \eta) R^*(\sigma)] - [\lambda \ell + (\lambda_\ell + \gamma + \eta) R^*(\sigma)] \chi_{\ell_1}] \quad (35)$$

$$V_2(\ell, 0) = \frac{\gamma \ell^{T-1} V_{0,T} H_{v2}^*(\lambda_\ell + \eta)}{Z_1(\ell)} [\sigma [\ell - H_{v1}^*(\lambda_\ell + \eta) R^*(\sigma)] - \ell [1 - R^*(\sigma)] \chi_{\ell_1}] \quad (36)$$

$$V_0^*(\ell, 0) = \frac{\ell^{T+1} [1 - R^*(\sigma)] V_{0,T}}{Z_1(\ell)} [[\lambda H_{v1}^*(\lambda_\ell + \eta) + \gamma H_{v2}^*(\lambda_\ell + \eta)] - \chi_{\ell_1}] \quad (37)$$

$$= \frac{V_0(\ell) \ell^T}{Z_v(\ell)} V_{0,T}$$

$$V_1^*(\ell, 0) = \frac{\ell^T V_{0,T} [1 - H_{v1}^*(\lambda_\ell + \eta)]}{(\lambda_\ell + \eta) Z_1(\ell)} [\sigma [\lambda \ell + \gamma H_{v2}^*(\lambda_\ell + \eta) R^*(\sigma)] - [\lambda \ell + (\lambda_\ell + \gamma + \eta) R^*(\sigma)] \chi_{\ell_1}] \quad (38)$$

$$= \frac{V_1(\ell) \ell^T}{Z_v(\ell)} V_{0,T}$$





Pazhani Bala Murugan and Jeba Pauline Veronica

$$V_2^*(\ell, 0) = \frac{\gamma \ell^{T-1} V_{0,T} [1 - H_{v2}^*(\lambda_\ell + \eta)]}{(\lambda_\ell + \eta) Z_1(\ell)} [\sigma[\ell - H_{v1}^*(\lambda_\ell + \eta) R^*(\sigma)] - \ell[1 - R^*(\sigma)] \chi_{\ell_1}]$$

(39)

$$= \frac{V_0(\ell) \ell^T}{Z_v(\ell)} V_{0,T}$$

where,

$$Z_1(\ell) = \ell\sigma - H_{v1}^*(\lambda_\ell + \eta)[\lambda\ell + (\lambda - \lambda\ell + \gamma + \eta)R^*(\sigma)] - \gamma\ell[1 - R^*(\sigma)]H_{v2}^*(\lambda_\ell + \eta)$$

$$\text{and } Z_v(\ell) = (\lambda_\ell + \eta)Z_1(\ell)$$

In (18) take a summation over m from $T+1$ to ∞ then multiply with ℓ^m and result,

$$[\theta - (\lambda + \gamma)]U_0^*(\ell, \theta) = U_0(\ell, 0) - S^*(\theta)[\eta V_0^*(\ell, \theta) + U_1(\ell, 0) + \ell U_2(\ell, 0) - \ell^T [V_{1,T}(0) + V_{2,T-1}(0)]]$$

(40)

In (20) take a summation over m from $T+1$ to ∞ then multiply with ℓ^m and combine this result with (19),

$$[\theta - \lambda_\ell]U_1^*(\ell, \theta) = U_1(\ell, 0) - H_{u1}^*(\theta)[\eta V_1^*(\ell, \theta) + \frac{V_0(\ell, 0)}{\ell} + \lambda U_0^*(\ell, 0) + \lambda U_{0,T} \ell^T]$$

(41)

In (22) take a summation over m from T to ∞ then multiply with ℓ^m and combine this result with (21),

$$[\theta - \lambda_\ell]U_2^*(\ell, \theta) = U_2(\ell, 0) - H_{v2}^*(\theta)[\eta V_2^*(\ell, 0) + \frac{\gamma}{\ell} V_0^*(\ell, 0) + \gamma U_{0,T} \ell^{T-1}]$$

(42)

Placing $\theta = \lambda + \gamma$ in (37), result

$$U_0(\ell, \theta) = S^*(\lambda + \gamma) [\eta V_0^*(\ell, 0) + V_1(\ell, 0) + \ell V_2(\ell, 0) - \ell^T [U_{1,T}(0) + U_{2,T-1}(0)]]$$

(43)

Placing $\theta = 0$ in (37) and sub., (40) in (37), results

$$U_0^*(\ell, 0) = \frac{1 - S^*(\lambda + \gamma)}{\lambda + \gamma} [\eta V_0^*(\ell, 0) + V_1(\ell, 0) + \ell V_2(\ell, 0) - \ell^T [U_{1,T}(0) + U_{2,T-1}(0)]]$$

(44)

Placing $\theta = \lambda_\ell$ in (38), result

$$U_1(\ell, 0) = H_{u1}^*(\lambda_\ell) [\eta V_1^*(\ell, 0) + \frac{U_0(\ell, 0)}{\ell} + \lambda U_0^*(\ell, 0) + \lambda U_{0,T} \ell^T] \quad (45)$$

Placing $\theta = 0$ in (38) and sub., (42) in (38), results

$$U_1^*(\ell, 0) = \frac{1 - H_{u1}^*(\lambda_\ell)}{\lambda_\ell} [\eta V_1^*(\ell, 0) + \frac{U_0(\ell, 0)}{\ell} + \lambda U_0^*(\ell, 0) + \lambda U_{0,T} \ell^T] \quad (46)$$

Placing $\theta = \lambda_\ell$ in (39), results

$$U_2(\ell, 0) = H_{u2}^*(\lambda_\ell) [\eta V_2^*(\ell, 0) + \frac{\gamma}{\ell} U_0^*(\ell, 0) + \gamma U_{0,T} \ell^{T-1}] \quad (47)$$

Placing $\theta = 0$ in (39) and sub., (44) in (39), results

$$U_2^*(\ell, 0) = \frac{1 - H_{v2}^*(\lambda_\ell)}{\lambda_\ell} [\eta V_2^*(\ell, 0) + \frac{\gamma}{\ell} U_0^*(\ell, 0) + \gamma U_{0,T} \ell^{T-1}] \quad (48)$$

Solving (43) to (48), we get following results for UB period

$$U_0(\ell, 0) = \frac{(\lambda + \gamma) \ell^{S^*(\lambda + \gamma)}}{Z_2(\ell)} \left\{ \eta V_0^*(\ell, 0) + H_{u1}^*(\lambda_\ell) \eta V_1^*(\ell, 0) + H_{u2}^*(\lambda_\ell) \eta V_2^*(\ell, 0) + [\lambda H_{u1}^*(\lambda_\ell) + \gamma H_{u2}^*(\lambda_\ell)] U_{0,T} \ell^T - \lambda + \gamma U_{0,T} + \lambda + \gamma - \chi \ell^{1V_0, T} \ell^{T-1} \right\} \quad (49)$$

$$U_1(\ell, 0) = \frac{H_{u1}^*(\lambda_\ell)}{Z_2(\ell)} \{ [\lambda\ell + (\lambda_\ell + \gamma) S^*(\lambda + \gamma)] \eta V_0^*(\ell, 0) + [\ell(\lambda + \gamma) + \gamma\ell[1 - S^*(\lambda + \gamma)] H_{u2}^*(\lambda_\ell)] \eta V_1^*(\ell, 0) + \ell H_{u2}^*(\lambda_\ell) [\lambda\ell + \gamma S^*(\lambda + \gamma)] \eta V_2^*(\ell, 0) - ((\lambda + \gamma) U_{0,T} + (\lambda + \gamma - \chi_{\ell_1}) U_{0,T}) \ell^T [\lambda\ell + \lambda\ell + \gamma S^* \lambda + \gamma + \ell T U_{0,T} \ell + \gamma \lambda\ell + \gamma H_{u2}^* \lambda\ell S^* \lambda + \gamma] \} \quad (50)$$

$$U_2(\ell, 0) = \frac{H_{u2}^*(\lambda_\ell)}{Z_2(\ell)} \{ \gamma[1 - S^*(\lambda + \gamma)] \eta V_0^*(\ell, 0) + \gamma[1 - S^*(\lambda + \gamma)] H_{u1}^*(\lambda_\ell) \eta V_1^*(\ell, 0) + [\ell(\lambda + \gamma) - [\lambda\ell + \lambda - \lambda\ell + \gamma S^* \lambda + \gamma H_{u1}^* \lambda\ell \eta V_2^* \ell, 0 - \gamma 1 - S^* \lambda + \gamma \lambda + \gamma U_{0,T} + \lambda + \gamma - \chi \ell^{1V_0, T} \ell^{T-1} U_{0,T} - S^* \lambda + \gamma H_{u2}^* \lambda\ell] \} \quad (51)$$





$$U_0^*(\ell, 0) = \frac{\ell[1-S^*(\lambda+\gamma)]}{Z_2(\ell)} \left\{ \eta V_0^*(\ell, 0) + H_{u1}^*(\lambda_\ell) \eta V_1^*(\ell, 0) + H_{u2}^*(\lambda_\ell) \eta V_2^*(\ell, 0) + [\lambda H_{u1}^*(\lambda_\ell) + \gamma H_{u2}^*(\lambda_\ell)] U_{0,T} \ell^T - (\lambda + \gamma) U_{0,T} + (\lambda + \gamma - \chi_{\ell_1}) V_{0,T} \right\} \ell^T \quad (52)$$

$$U_1^*(\ell, 0) = \frac{1-H_{u1}^*(\lambda_\ell)}{\lambda_\ell Z_2(\ell)} \left\{ [\lambda \ell + (\lambda_\ell + \gamma) S^*(\lambda + \gamma)] \eta V_0^*(\ell, 0) + [\ell(\lambda + \gamma) + \gamma \ell[1 - S^*(\lambda + \gamma)] H_{u2}^*(\lambda_\ell)] \eta V_1^*(\ell, 0) + \ell H_{u2}^*(\lambda_\ell) \lambda \ell + \lambda \ell + \gamma S^*(\lambda + \gamma) \eta V_2^*(\ell, 0) - \lambda + \gamma U_{0,T} + \lambda + \gamma - \chi_{\ell_1} 1 U_{0,T} \ell^T + \lambda \ell + \gamma S^*(\lambda + \gamma) \ell T U_{0,T} \ell + \gamma \lambda \ell + \gamma H_{u2}^*(\lambda_\ell) S^*(\lambda + \gamma) \right\} \quad (53)$$

$$U_2^*(\ell, 0) = \frac{1-H_{u2}^*(\lambda_\ell)}{\lambda_\ell Z_2(\ell)} \left\{ \gamma[1 - S^*(\lambda + \gamma)] \eta V_0^*(\ell, 0) + \gamma[1 - S^*(\lambda + \gamma)] H_{u1}^*(\lambda_\ell) \eta V_1^*(\ell, 0) + [\ell(\lambda + \gamma) - [\lambda \ell + \lambda - \lambda \ell + \gamma S^*(\lambda + \gamma) \eta V_2^*(\ell, 0) - \gamma 1 - S^*(\lambda + \gamma) \ell T U_{0,T} \ell + \lambda \ell + \gamma H_{u2}^*(\lambda_\ell) S^*(\lambda + \gamma)]] \right\} \quad (54)$$

where,

$Z_2(\ell) = (\lambda + \gamma) \ell - H_{u1}^*(\lambda_\ell) [\lambda \ell + (\lambda - \lambda \ell + \gamma) S^*(\lambda + \gamma)] - \gamma \ell H_{u2}^*(\lambda_\ell) [1 - S^*(\lambda + \gamma)]$ and take $Z_u(\ell) = \lambda_\ell Z_2(\ell)$.

When server is on *WV* period, we define the PGF for the no., of customers in the orbit as,

$$U_v(\ell) = V_0^*(\ell, 0) + V_1^*(\ell, 0) + V_2^*(\ell, 0) + V_{0,T} \ell^T$$

where, $V_0^*(\ell, 0), V_1^*(\ell, 0), V_2^*(\ell, 0)$ are found in (37) to (39).

When server is on *UB* period, we define the PGF for the no., of customers in the orbit as,

$$U_u(\ell) = U_0^*(\ell, 0) + U_1^*(\ell, 0) + U_2^*(\ell, 0) + U_{0,T} \ell^T$$

where, $U_0^*(\ell, 0), U_1^*(\ell, 0), U_2^*(\ell, 0)$ are found in (52) to (54).

Define, PGF for no., of customers in the orbit as, $U(\ell) = U_v(\ell) + U_u(\ell)$.

Make use of normalizing condition $U(1) = 1$, we get idle probability $V_{0,T}$ of *WV* period as,

$$V_{0,T} = \left\{ \frac{\sigma - \chi_{\ell_1}}{\eta} - \frac{1}{2\lambda Z_v(1) Z_2(1)} \left\{ 2 \left\{ \frac{\eta}{Z_v(1)} [Z_v(1) [Q_0'(1) + (T+1) Q_0(1)] - Z_v'(1) Q_0(1)] + \frac{\eta}{Z_v(1)} [Z_v(1) [Q_1'(1) + T Q_1(1)] - Z_v'(1) Q_1(1)] + \frac{\eta}{Z_v(1)} [Z_v(1) [Q_2'(1) + (T-1) Q_2(1)] - Z_v'(1) Q_2(1)] - Z_v(1) T (\lambda + \gamma - \chi_{\ell_1}) \right\} \right\} [-1 - S^*(\lambda + \gamma)] + \lambda H_{u1}^*(\lambda_\ell) [\lambda + \gamma S^*(\lambda + \gamma)] + \lambda \gamma H_{u2}^*(\lambda_\ell) [1 - S^*(\lambda + \gamma)] \right\} + \eta Q_0(1) \left\{ -2\lambda [1 - S^*(\lambda + \gamma)] + 2\lambda^2 H_{u1}^*(\lambda_\ell) [1 - S^*(\lambda + \gamma)] - \lambda^2 H_{u1}^*(\lambda_\ell) [\lambda + \gamma S^*(\lambda + \gamma)] - \lambda^2 \gamma H_{u2}^*(\lambda_\ell) [1 - S^*(\lambda + \gamma)] \right\} + \eta Q_1(1) \left\{ -2\lambda [1 - S^*(\lambda + \gamma)] + 2\lambda H_{u1}^*(\lambda_\ell) [\lambda [1 - S^*(\lambda + \gamma)] + [\lambda + \gamma S^*(\lambda + \gamma)]] - \lambda^2 H_{u1}^*(\lambda_\ell) [\lambda + \gamma S^*(\lambda + \gamma)] - \lambda^2 \gamma H_{u2}^*(\lambda_\ell) [1 - S^*(\lambda + \gamma)] \right\} + \eta Q_2(1) \left\{ -4\lambda [1 - S^*(\lambda + \gamma)] + 2\lambda H_{u1}^*(\lambda_\ell) [\lambda [1 - S^*(\lambda + \gamma)] + [\lambda + \gamma S^*(\lambda + \gamma)]] + 2\lambda (\lambda + \gamma) H_{u2}^*(\lambda_\ell) - \lambda^2 H_{u1}^*(\lambda_\ell) [\lambda + \gamma S^*(\lambda + \gamma)] - \lambda^2 \gamma H_{u2}^*(\lambda_\ell) [1 - S^*(\lambda + \gamma)] \right\} + \frac{2Z_v(1) (\lambda + \gamma) S^*(\lambda + \gamma) (\lambda + \gamma + \eta - \chi_{\ell_1}) [1 - \gamma H_{u2}^*(\lambda_\ell)]}{\alpha} - Z_v(1) (\lambda + \gamma - \chi_{\ell_1}) \left\{ -2\lambda [1 - S^*(\lambda + \gamma)] + 2\lambda^2 H_{u1}^*(\lambda_\ell) [1 - S^*(\lambda + \gamma)] - \lambda^2 H_{u1}^*(\lambda_\ell) [\lambda + \gamma S^*(\lambda + \gamma)] - \lambda^2 \gamma H_{u2}^*(\lambda_\ell) [1 - S^*(\lambda + \gamma)] \right\} \right\}^{-1} \quad (55)$$

where,

$$Z_v(1) = \eta \{ \sigma - H_{v1}^*(\eta) [\lambda + (\gamma + \eta) R^*(\sigma)] - \gamma H_{v2}^*(\eta) [1 - R^*(\sigma)] \} \quad \dots\dots\dots(i)$$

$$Z_v'(1) = -\lambda \{ \sigma - H_{v1}^*(\eta) [\lambda + (\gamma + \eta) R^*(\sigma)] - \gamma H_{v2}^*(\eta) [1 - R^*(\sigma)] \} + \eta \{ \sigma - \lambda H_{v1}^*(\eta) [1 - R^*(\sigma)] - \gamma H_{v2}^*(\eta) [1 - R^*(\sigma)] + \lambda H_{v1}^*(\eta) \times [\lambda + (\gamma + \eta) R^*(\sigma)] + \lambda \gamma H_{v2}^*(\eta) [1 - R^*(\sigma)] \} \dots\dots\dots(ii)$$

$$Z_2'(1) = (\lambda + \gamma) S^*(\lambda + \gamma) \left\{ 1 - \left[\frac{\lambda E(H_{u1}) [\lambda + \gamma S^*(\lambda + \gamma)]}{(\lambda + \gamma) S^*(\lambda + \gamma)} + \frac{\lambda \gamma E(H_{u2}) [1 - S^*(\lambda + \gamma)]}{(\lambda + \gamma) S^*(\lambda + \gamma)} \right] \right\} = (\lambda + \gamma) S^*(\lambda + \gamma) (1 - \rho)$$

where, ρ is the mean service time and the stability condition in system is obtained from (55).

$$V_0(1) = \eta [1 - R^*(\sigma)] [\lambda H_{v1}^*(\eta) + \gamma H_{v2}^*(\eta)] - \chi_{\ell_1} \quad \dots\dots\dots(iii)$$





Pazhani Bala Murugan and Jeba Pauline Veronica

$$\begin{aligned}
 V_1(1) &= [1 - H_{v1}^*(\eta)] [\sigma[\lambda + \gamma H_{v2}^*(\eta) R^*(\sigma)] - [\lambda + (\gamma + \eta) R^*(\sigma)] \chi_{\ell_1}] \\
 V_2(1) &= \gamma [1 - H_{v2}^*(\eta)] [\sigma[1 - H_{v1}^*(\eta) R^*(\sigma)] - [1 - R^*(\sigma)] \chi_{\ell_1}] \\
 V_0'(1) &= -\lambda [1 - R^*(\sigma)] \left[[\lambda H_{v1}^*(\eta) + \gamma H_{v2}^*(\eta)] - \chi_{\ell_1} + \eta [\lambda H_{v1}'^*(\eta) + \gamma H_{v2}'^*(\eta)] \right] \\
 V_1'(1) &= \lambda H_{v1}'^*(\eta) [\sigma[\lambda + \gamma H_{v2}^*(\eta) R^*(\sigma)] - [\lambda + (\gamma + \eta) R^*(\sigma)] \chi_{\ell_1}] \\
 &\quad + \lambda [1 - H_{v1}^*(\eta)] \left[\sigma[1 - \gamma R^*(\sigma) H_{v2}'^*(\eta)] - \chi_{\ell_1} [1 - R^*(\sigma)] \right] \\
 V_2'(1) &= \lambda \gamma H_{v2}'^*(\eta) [\sigma[1 - H_{v1}^*(\eta) R^*(\sigma)] - \chi_{\ell_1} [1 - R^*(\sigma)]] + \gamma [1 - H_{v2}^*(\eta)] \left[\sigma[1 + \lambda H_{v1}'^*(\eta) R^*(\sigma)] - \chi_{\ell_1} [1 - R^*(\sigma)] \right]
 \end{aligned}$$

and also, we can get idle probability $U_{0,T}$ of UB period from (7).

SPECIAL CASES

1. If there is no vacation i.e., $\eta \rightarrow \infty$, the server does not wait after the completion of the service then the present model will be remodelled as [12].
2. If there is no recurrent customers i.e., $T = 0$ and the server does not wait after the completion of the service then the present model will be remodelled as [16].
3. If there is no vacation and no retrial, i.e., $T = 0$ and $\lim_{\gamma \rightarrow 0}$ also the server does not wait after the completion of the service then the present model will be remodelled as [14].

CONCLUSION

In this paper, an $M/G/1$ retrial queue with recurrent customers, general retrial times, switchover time and working vacation is evaluated. We obtain the PGF for the number of customers and the mean number of customers in the orbit. We worked out the waiting time distributions. We also derive the performance measures. We perform some special cases.

ACKNOWLEDGMENT

We express our sincere thanks to the team of peer-reviewers and editors of the journal to bring this article in the present enriched form.

Competing Interests

The authors declare that they have no competing interests.

Authors Contributions

All the authors contributed significantly in writing this article. The authors read and approved the final manuscript.

REFERENCES

1. ArtalejoJR: Accessible bibliography on retrial queue. Math. Comput. Modell., 1999;30:1-6.
2. ArtalejoJR and FalinG: Standard and retrial queueing systems: A Comparative analysis. Rev. Math. Comput., 2002;15:101-129.
3. ArtalejoJR, JoshuaVC, and KrishnamoorthyA: An $M/G/1$ retrial queue with orbital search by server: In Advances in Stochastic Modelling, eds., New Jersey: Notable Publications 2002;41-54.
4. BoxmaOJ, SchlegelS and YechialiU: $M/G/1$ queue with waiting server timer and vacations. American Mathematical Society Translations 2002;2(207):25-35.





Pazhani Bala Murugan and Jeba Pauline Veronica

5. Chandrasekaran VM, Indhira K, Saravanarajan MC and Rajadurai P: A survey on working vacation queueing models, International Journal of Pure and Applied Mathematics 2016;106(6):33-41.
6. Falin GI: A Survey on Retrial Queues. Queueing Systems Theory and Applications 1990;7:127-168.
7. Falin GI and Templeton JGC: Retrial queues, Chapman and Hall, London; 1997.
8. Gomez-CorralA: Stochastic analysis of a single server retrial queue with general retrial time, Naval Res. Log., 1999;46:561-581.
9. FarahmandK: Single line queue with recurrent repeated demands. Queueing Systems 1996;22:425-435.
10. KalyanaramanR and Pazhani Bala MuruganS: A single server retrial queue with vacation. J.Appl.Math.and Informatics 2008;26(3-4):721-732.
11. MedhiJ: Stochastic Models in Queueing Theory. Second Edition;2003.
12. MorenoP: An M/G/1 retrial queue with recurrent customers and general retrial times. Applied Mathematics and Computation 2004;159:651-666.
13. Naishuo Tian, Xinqiu Zhao and Kaiyu Wang: The M/M/1 queue with single working vacation. International journal of Information and Management sciences 2008;19(14): 621-634.
14. Boxma OJ, Cohen JW: The M/G/1 queue with permanent customers. IEEE Journal on Selected Areas in Communications 1991;9(2):179-184.
15. Pazhani Bala MuruganS and SanthiK: An M/G/1 retrial queue with multiple working vacation. International Journal of Mathematics and its Applications 2016;4(2-D):35-48.
16. Pazhani Bala MuruganS and SanthiK: An M/G/1 retrial queue with single working vacation. Appl.Appl.Math., 2017;12(1):1-22.
17. Rajadurai P: A study on M/G/1 retrial queueing system with three different types of customers under working vacation policy. Int. J. Mathematical Modelling and Numerical Optimisation 2018;8(4):393-417.
18. ServiL and FinnS: M/M/1 queue with working vacations (M/M/1/WV). Perform. Eval, 2002;50:41-52.
19. TakineT and HasegawaT: A note on M/G/1 vacation system with waiting time limits. Kyoto University Adv. Appl. Prob., 1990;22:513-518.
20. Wu D and Takagi H: M/G/1 queue with multiple working vacations. Perform. Eval, 2006;63:654-681.
21. Yang T and Templeton JGC: A Survey on Retrial Queues, Queue. Syst., 1987;2:201-233.





Cultural Development and Scientific Ingenuity: Sultan Zain-ul-Abidin's Enduring Legacy in Kashmir

Sarfraz Ahmad Rather^{1*} and R. Rajeshwari²

¹Research Scholar, Department of History, Annamalai University, Chidambaram, Cuddalore, Tamil Nadu, India.

²Assistant Professor, Department of History, Thanthai Periyar Government Arts and Science College (Autonomous), (Affiliated To Bharathidasan University) Tiruchirapalli, Tamil Nadu, India.

Received: 20 Jan 2024

Revised: 09 Feb 2024

Accepted: 30 May 2024

*Address for Correspondence

Sarfraz Ahmad Rather

Research Scholar,

Department of History,

Annamalai University,

Chidambaram, Cuddalore,

Tamil Nadu, India.

Email: sarfrazahmad4030@gmail.com



This is an Open Access Journal / article distributed under the terms of the **Creative Commons Attribution License** (CC BY-NC-ND 3.0) which permits unrestricted use, distribution, and reproduction in any medium, provided the original work is properly cited. All rights reserved.

ABSTRACT

Sultan Zain-ul-Abidin's reign in Kashmir marked a period of profound cultural development intertwined with scientific innovation. It is truly noteworthy that the cultural legacy he established and bequeathed still persists to this day. This paper delves into the multifaceted aspects of Zain-ul-Abidin's rule, highlighting his pivotal role in shaping the region's cultural landscape while fostering scientific advancements. Under his patronage, Kashmir experienced a renaissance in various cultural domains, including art, architecture, calligraphy, music, dance, and cuisine. Additionally, Sultan Zain-ul-Abidin's support laid the groundwork for scientific inquiry, particularly in the fields of herbal medicine, pharmacology, and culinary sciences. This paper explores how Zain-ul-Abidin's inclusive policies and visionary leadership contributed to the vibrancy and resilience of Kashmir's cultural heritage, intertwining creativity with scientific progress to forge an enduring legacy that continues to shape the region's identity.

Keywords: Zain-ul-Abidin, literature, Kashmiri Wazawan, Culture, Art and architecture, Culinary, Development, Healthcare





INTRODUCTION

Zain-ul-Abidin ruled Kashmir for fifty years (1420–1470) as the eighth Sultan of the region. Undoubtedly, among all the Sultans who ruled Kashmir, Zain-ul-Abidin stood as the supreme figure. A period of nearly fifty years passed under his benevolent rule, bringing peace and prosperity to his subjects. Despite the passage of almost five centuries, he gained a halo in the public imagination that still surrounds his name. Indeed, his subjects continued to refer to him as Budshah (the Great King). The reign of Sultan Zain-ul-Abidin heralded a golden era in Kashmir, marked by unparalleled cultural and scientific advancements. His court became a hub for numerous literary luminaries, where his generous sponsorship and progressive linguistic policy favored Persian, Sanskrit, and Kashmiri equally. This era witnessed a flourishing of original works and translations, with scholars like Pandit Nottasoma, Yodha Bhatta, and Avatara Bhatta making significant contributions. In the historical context of Kashmir, the culinary landscape during Zain-ul-Abidin's period stands as a testament to the region's rich cultural fusion. This era marked a significant culinary evolution with the introduction of diverse dishes from Persia and Central Asia. The distinctive "Kashmiri Wazawan," renowned for its unique taste, emerged during this time, reflecting a culinary amalgamation. The social classes, including the ascetics, Ulama, and Sufis, all indulged in varying degrees of gastronomic delight. The staple food, rice, played a crucial role, leading to both culinary abundance and occasional famines. Beyond food, the period witnessed a parallel development in attire, with Sultan Zain-ul-Abidin's reign contributing to a flourishing sartorial culture characterized by intricate designs and vibrant colors. Beyond cultural achievements, Sultan Zain-ul-Abidin's reign is notable for advancements in medical science and the treatment of diseases, underscoring his legacy of fostering both cultural and scientific ingenuity in Kashmir.

METHODOLOGY

This historical investigation adopted a descriptive approach. Following an extensive examination, information was gathered from both primary and secondary sources, encompassing books, scholarly articles, journals, and encyclopedias. Examining the noteworthy achievements of Sultan Zain-ul-Abidin throughout his leadership, he unveils his pivotal contribution to transforming the Kashmir region into a flourishing and prosperous area.

Objectives of the Study

- To highlight the Sultan Zain-ul-Abidin's status as a supreme figure among all the rulers of Kashmir.
- To examine Zain-ul-Abidin's patronage and humanistic outlook in literature.
- To examine the architectural contributions of Zain-ul-Abidin in medieval Kashmir.
- To explore how he supported renowned artists and contributed to the flourishing sartorial culture of the era.
- To examine the specific cultural developments that took place during Zain-ul-Abidin's reign in Kashmir.
- To highlight Sultan Zain-ul-Abidin's impact on Kashmir's scientific and medical advancements

DISCUSSION AND RESULTS

LITERATURE

The reign of Zain-ul-Abidin was a golden age for literary activities. Zain-ul-Abidin decorated his court with a huge number of literary luminaries and generously sponsored the development of learning. His broad humanistic perspective was evident not only in literary endeavors but also across various domains. Zain-ul-Abidin implemented an enlightened language policy, equally endorsing Persian, Sanskrit, and Kashmiri.

Persian

During Sultan Zain ul Abidin's reign, his court attracted a notable influx of Persian scholars from various cultural hubs. Among them were the Maulana brothers, Mir Muhammad Rumi and Ahmad Rumi, experts in diverse fields, who migrated from Rum to settle in Kashmir. Enjoying the Sultan's patronage, they received considerable favors.



**Sarfaraz Ahmad Rather and Rajeshwari**

Other luminaries, including Qazi Jamal, Maulana Kabir, Sayyid Muhammad Luristani, and Sayyid Muhammad Sistani, graced the court with their intellect and eloquence in subtle speech and versification. Qazi Jamal assumed the prestigious role of high Qazi in Kashmir, while Maulana Kabir served as the Sultan's tutor and later played a pivotal role in overseeing the renowned Nowshahr Institute of Higher Learning. The court's distinguished poets, Maulana Fatehi and others, contributed outstanding Persian poetry, serving as poet laureates. Sultan Zain ul Abidin, himself a scholar, wrote fine pieces of prose and poetry in Persian. A few verses, preserved in the Persian chronicles, remain the only remnants of the diwan compiled by Zain-ul-Abidin under the pen name "Qutb." Notably, the Sultan excelled in versification, as evidenced by his two prose works—one on gunpowder and fireworks and another, "Shikayat," expressing his distress over his sons' misdeeds. Moreover, the court's literary achievements extended to the translation of significant Sanskrit works into Persian, including the Mahabharata, Kalhana's Rajatarangini, Vrishatkathasara, Hatakesvara Samhita, and the Puranas, contributing to the high literary development of Persian writing during this period [1].

Sanskrit

Since ancient times, the cultural history of Kashmir has deeply intertwined with Sanskrit learning, boasting renowned centers of education comparable to Nalanda and Takshashila. The region boasted a rich literary tradition and was revered as the abode of the Goddess of Learning, Saraswati. However, with the advent of Muslim rule, royal patronage for Sanskrit declined, posing a threat to the tradition. During the reign of Sultan Zain-ul-Abidin, a pivotal shift occurred as he extended generous patronage to Sanskrit learning, reviving the old tradition that suffered during previous regimes. Noteworthy scholars, including Jonaraja, Srivara, Pandit Notthasoma, Avatar Bhatta, Yodha Bhatta, and Narahari, flourished under his support. Jonaraja, the Sultan's court poet, played a crucial role in the revival, producing significant works such as the Rajatarangini, a historical masterpiece in the classical Sanskrit style. Srivara, another luminary under Zain-ul-Abidin's patronage, was a versatile scholar proficient in Hindu religion, philosophy, and Persian. He wrote the Jaina-Rajatarangini, a chronicle of kings in the Kavya style, which is his notable work. Other scholars like Pandit Notthasoma, Narahari, and Sriva contributed to various fields, including medicine, literature, and musicology. Despite Zain-ul-Abidin's reign, Sanskrit continued to serve as an official language alongside the gradually rising Persian. The bilingual tradition persisted, with official documents issued in both Sanskrit and Persian. Zain-ul-Abidin himself was proficient in both languages, reflecting the cultural synthesis that characterized his era. The period under Sultan Zain-ul-Abidin emerged as a renaissance for Sanskrit learning, challenging the narrative of a complete decline during Muslim rule in Kashmir [2].

Kashmiri

The Kashmiri language and literature experienced a momentous stage of development under Sultan Zain-ul-Abidin's patronage. Recognized as a medium of instruction in higher education, Kashmiri became a vehicle for translating popular works originally composed in Sanskrit and Persian. This era witnessed the creation of noteworthy original works, with prominent figures such as Pandit Nottasoma, Yodha Bhatta, and Avatara Bhatta flourishing in the Sultan's court. Nottasoma, a distinguished poet, penned a biography of Zain-ul-Abidin in the form of a Kashmiri poem titled Jainaclarita. Yodha Bhatta, also a poet, contributed Jainaprakasa, a historical drama portraying the Sultan's rule. Avatara Bhatta, a student of Salhana Acharya, authored Jainavilas, incorporating Zain-ul-Abidin's teachings. Unfortunately, none of these works survives today, except for Avatara Bhatta's Banasurkatha, composed in the twenty-sixth year of the Sultan's reign (1446 A.D.). This masterpiece, revolving around the Puranic mythology of Usha and Anirudha's love and the ensuing conflict between Lord Krishna and Banasura, stands as a testament to the evolving Kashmiri language during that period. The literary achievements of this period, marked by translation, original creation, and linguistic evolution, contribute significantly to the cultural legacy of Sultan Zain-ul-Abidin's era [3].

Patronage of Painting

Sultan Zain-ul-Abidin was a patron of the art of painting, and the leading artist in his court was Mulla Jamil Hafiz. Mulla Jamil Hafiz displayed exceptional proficiency in his craft, producing twelve different renditions of a single theme. The Sultan, recognizing his artistic brilliance, generously rewarded him. Zain-ul-Abidin, known for his liberal



**Sarfaraz Ahmad Rather and Rajeshwari**

outlook, permitted the depiction of various human and animal figures in paintings, including the popular trend of portrait painting. Haji Khan preserved a portrait of the Sultan for solace after his father's demise. The art of painting extended to the creation of diverse patterns on cloth, featuring circular designs, platforms, and depictions of both men and the goddess Durga. The surviving specimens of paintings from that era are found on the ceilings of the Madani mosque and the tiles of Zain-ul-Abidin's tomb. The mosque's ceiling is adorned with small, thin pieces of wood arranged in various geometrical forms and painted in different colors, although these colors have faded over time. Particularly noteworthy are the painted tiles adorning the walls of Madani's tomb [4]. These are the patterns represent various types of flower-combinations, geometrical patterns, and animal figures. The colours generally used are red, blue, indigo, yellow, light, and dark green, brown and reddish- brown. One of the tiles, which of donkeys and lions[5]. The renowned instance was discovered by Nicholls, an archaeologist from the Archaeological Survey of India; however, it no longer exists. The portrayal of the creature's physical attributes closely resembled that of a leopard and was skillfully performed. The neck of it changed to resemble a human trunk. A fox observed silently amidst the flower and cloud formations. The beast measured approximately four feet in length and assumed a distinctly heraldic posture. Nicholls made the survey and found that the chest, shoulders, and head of the human were already missing. The creature's tail terminated in a dragon-like visage. The picture had a blue backdrop, a red trunk for the man, a yellow body with light green patches for the leopard, reddish-brown heads for the dragon and the fox, and flowers of various colors. The representation was truly distinctive and held considerable importance in certain aspects. First, it was positively un-Islamic, and its portrayal on the tomb of a distinguished Muslim saint is perhaps the only example of its kind in the whole range of Indian-Islamic architecture. Secondly, the cloud forms are peculiar to the Chinese and Persian influences on Kashmiri art. These were, however, used later by the Mughals in Fatehpur Sikri, Sikandar, and the Red Fort. Thirdly, the use of a dragon also perhaps represents Chinese influence [6].

Art of Calligraphy

The Arabic writing style can look very beautiful, and this flexibility led to a tradition of using it for art. People didn't just use it in books but also in buildings as a form of decoration. Zain-ul-Abidin really liked calligraphy and brought skilled writers from Samargand and Balkh. He even gave them land in the Pargana of Phag for their support. The state sent one of the scribes to Mecca to copy a famous Quran commentary called Kashshaf. The state covered his travel expenses and provided for his family while he was away. The Zainalank stone slab, the entrance of Madan's mosque, and the graves of Zain-ul-Abidin's queen, Makhumah khatun, among others, still preserve some examples of this calligraphy [7].

The Devotion of Zain-ul-Abidin for Architecture

In the context of architecture, Zain-ul-Abidin is known as the Shah Jahan of Kashmir. He was a great builder. But the irony of fate is that only his mother's tomb and the mosque of Madani have survived. All the other structures are in a dilapidated condition. He founded a new town of Naushahr, which is today a part of Srinagar, as his capital. He embellished it with magnificent houses for his officers, courtiers, and intelligent individuals. But the most impressive architecture he built there was a wooden palace with twelve floors, each holding fifty rooms, halls, and corridors. It was topped by a golden dome, and its large hallways were covered with glass. Besides Naushahr, significant towns and buildings may be found in places like Zinapor, Zainagir, Zainagam, Zainakundal, and Zainkot. He built wonderful buildings in all these locations. An expansive palace with a beautiful garden was constructed at Zainagir. Zain-ul-Abiden completed the construction of Jamia Masjid in Srinagar, which was initiated by Sikandar. Similarly, Ali Shah, like his brother, also constructed a bridge and named it Zaina Kadal after himself[8]. He also built a swinging bridge in the town. He built rest houses for himself in important villages and cities where he stayed. When he went on his tours and he travelled much over his dominions the people were not subjected to any hardship on that account. In addition, inns were built for tourists on the main roadways. Villages were gifted with funds for their maintenance, and food was supplied free [9]. Zain-ul-Abidin was undoubtedly the greatest and the most prolific builder during the medieval period in Kashmir.



**Sarfaraz Ahmad Rather and Rajeshwari****Revival of Music and Dance**

Sultan Zain-ul-Abidin reintroduced music after it was banned by Sikandar. Zain-ul-Abidin was a big lover of music and other fine arts. He always gave musicians large sums of money. Hearing of the Sultan's generosity and love of music, a large number of talented musicians from all over the world came to Kashmir. Khorasan's Mulla Udi was one such artist. Another master was Mulla Jamal, a remarkable expert in vocal music [10] Srivara, the writer of the 'Zaina Rajatarangini,' was also a talented musician who often entertained the king, and the latter would always reward him for his fine performances. When the Raja of Gwalior learned of the Sultan's fondness for music, he sent him a collection of standard books on Indian music, including the 'Sangitachudamani.' Gwalior, being a hub of musical art, later took pride in its connections with Tan Sen. Zain-ul-Abidin largely attributed the elevation of music in Kashmir to a pinnacle of excellence. Besides being an aficionado of music himself, he spent his evenings with singers and dancers. Under Sultan Zain-ul-Abidin's rule, Kashmir saw a fusion of traditional musical practices into a new form, blending the indigenous folk music of Kashmir with influences from Persia, Central Asia, Turkey, and India. This resulted in the creation of a new genre known as Kashmiri 'Sufiana Mousiqui,' considered the classical music of Kashmir [11] Sikandar's Puritanism had ruined the art of drama and dancing, which the Sultan revived. At the invitation of Sultan Zain-ul-Abidin, many male and female actors and dancers came to Kashmir, and the king organized special festivals for their performances. Srivara vividly portrays a grand performance held during the spring festival, which was graced by the Sultan's presence. These festive events took place in different parts of the valley, including Anantnag, Bijbehara, Pampore, Baramulla, and various other locations[12].

Food and Drinks

The food and drinks of the period were important and fascinating. The dishes during this period are characterized by an extreme variety and richness of taste. The contemporary literature gives a long list of various dishes cooked and consumed by the aristocracy [13]. All people, with the exception of a small group of ascetics, namely, the Rishis, were very fond of the tastiest dishes. Even the Ulama and Sufis were far more fond of rich dishes than the common people. The Ulama were notorious for their gluttony and gigantic appetite for delicious foods, while the kitchens of the Sufis represented the index of almost all the rich dishes of the period. The higher classes arranged feasts that featured a wide variety of dishes. However, the dishes of the common masses suffered from a lack of taste and variety. They took frugal meals in order to maintain their bodies and income in line with their economic position. During Sultan Zain-ul-Abidin's rule in Kashmir, there was a noteworthy development in the realm of food and drinks. This period witnessed a significant culinary evolution with the introduction of diverse dishes from Persia and Central Asia, contributing to the rich and unique Kashmiri Wazawan cuisine. The staple food, rice, played a crucial role, leading to both culinary abundance and occasional famines. The distinctive "Kashmiri Wazawan," renowned for its special taste, emerged during this time, reflecting a culinary amalgamation. The culinary landscape of Kashmir flourished with various varieties of Palavs, including Zarad Palav, Surkh Palav, Siyah Palav, Turush Palav, and Shola Palav. The introduction of wheat, maize, and barley as secondary foods added diversity to the diet. The continuous use of water nuts by the people living around lakes, especially in the Kamraz district, contributed to the unique culinary heritage of the region. Overall, Sultan Zain-ul-Abidin's era left an indelible mark on Kashmir's food culture, influencing its tastes and traditions for centuries to come [14].

Dress and Ornaments

The traditional attire of Kashmir holds significant historical importance, evolving over time. Before the period of Harsha (1089–1101), historical records by Kalhana suggest that people did not have a specific headdress, leaving their hair loose. Harsha later introduced the turban and short court influenced by Mohammadans, potentially reflecting the attire during the Sultanate's foundation. The arrival of Sufi saints and Muslim theologians from Persia and Central Asia brought new clothing styles to Kashmir, including the long robe and round turban, laying the groundwork for the Pheran, the contemporary Kashmiri dress. During the rule of Sultan Zain-ul-Abidin in Kashmir, there was a notable development in the realm of clothing. Known for his patronage of the arts and culture, Sultan Zain-ul-Abidin fostered an environment that encouraged artistic expression, including in the domain of attire. The dress of the people of Kashmir during the period was influenced by the climatic conditions, availability of raw materials, foreign influences, the influence of the two communities (the Hindus and the Muslims) on each other,



**Sarfraz Ahmad Rather and Rajeshwari**

religious considerations, and last but not least, economic considerations.[15]. The culture of Kashmir has had a profound impact on foreigners since the time of its early rulers. The geographical features of Kashmir are renowned. The Mughals and Sultans contributed to enhancing the jewelry designs of the valley. Sultan Zain-ul-Abidin's royal attire and ornaments adorned with various colored threads gained him fame. Earing, nose drops, and bangles were used by various women [16]. Elaborate and finely embroidered garments became popular, showcasing intricate patterns and vibrant colors. Fabrics such as silk and wool were favored, and skilled artisans excelled in the creation of exquisite shawls and robes. The sartorial elegance of this period not only served as a means of personal expression but also underscored the cultural richness and prosperity of Kashmir under his rule[17].

Scientific Renaissance in Kashmir

During Sultan Zain-ul-Abidin's reign, Kashmir experienced a profound scientific renaissance that left an indelible mark on the region's history. The Sultan's patronage of traditional healers like Hakims and Vaidas led to significant advancements in herbal medicine. Under his support, these healers engaged in systematic collection, identification, and utilization of medicinal plants, laying the groundwork for early pharmacological studies. This scientific inquiry into herbal remedies not only improved healthcare but also contributed to the understanding of bioactive compounds in plants. The establishment of dispensaries providing free medical care further democratized access to healthcare, marking an early form of public health system development in Kashmir. Sultan Zain-ul-Abidin's visionary approach fostered a cross-cultural exchange of medical practices by inviting Hakims from India and Central Asia, enriching the local medical system and reflecting a scientific openness to diverse healing traditions. Beyond healthcare, Sultan Zain-ul-Abidin's reign witnessed a flourishing of scientific endeavors across various domains. His inclusive policies created an environment where scientific and cultural innovations thrived, leading to a renaissance in Kashmir's intellectual landscape. This era saw significant advancements in areas such as literature, arts, architecture, and technological innovation [18].

CONCLUSION

Sultan Zain-ul-Abidin's reign in Kashmir not only brought about a flourishing of cultural arts but also catalyzed scientific advancements, thus shaping the region's identity in profound ways. His multifaceted patronage of art, architecture, calligraphy, music, dance, and culinary arts left an indelible mark on the region's cultural heritage. His passion for the arts transformed Kashmir into a vibrant cultural center, and his support for painting, calligraphy, and architectural endeavors created a legacy that continues to influence Kashmiri artistic traditions. The Sultan's influence extended to the culinary landscape, introducing diverse dishes from Persia and Central Asia and his patronage fostered a holistic renaissance in Kashmir, nurturing advancements in health, culture, and scientific inquiry. His contributions have left an enduring legacy that continues to shape the cultural identity of Kashmir, making him one of the greatest and most revered rulers in its history.

REFERENCES

1. Haidar Malik, Tarikh-i-Kashmir, Bhavna Prakashan, Delhi, 1991, pp. 46-47.
2. Khawaja Nizamuddin, Tabaqat-i-Akbari, Vol. III, Royal Asiatic society of Bengal, Calcutta, 1939, pp. 658-659.
3. N.K. Zutshi, Sultan Zain-ul-Abidin of Kashmir, An Age of Enlightenment, Nupur Prakashan, Lucknow, 1976, p.191.
4. Ibid., p. 195.
5. R.C. Kak, Ancient Monuments of Kashmir, the Indian Society, London, 1933, p. 93.
6. Archaeological Survey of India Annual Report 1906-7.
7. N.K. Zutshi, op. cit., p. 196.
8. Zain ul Abideen's love for Education and Buildings - Asnaav.





Sarfaraz Ahmad Rather and Rajeshwari

9. Mohibul Hasan, Kashmir under Sultans, Iran Society, Culcutta, 1959, pp. 94-95.
10. P.M.K. Bamzai, Culture and Political History of Kashmir, Vol. II, M.D Publications Pvt Ltd, New Delhi, 1994, p. 333.
11. N.K. Zutshi, op. cit., pp. 197-198.
12. G.M.D Sofi, Kashir, Being a History of Kashmir, Vol. II, University Of Punjab, Lahore, 1948, p. 27.
13. M. L Saqi, Kuliyat-i-Sheikh-ul-Alam, A collection of the sayings of Shaikh Nooru'd-Din, Srinagar, 1979, p. 90.
14. Anonymous, Thafat-ul-Ahbab, MSS NO. 551, Research Library Srinagar, pp. 282-283.
15. Tariq Ahmad Sheikh, Composite Culture of Kashmir: A Reflection of Social Customs and Practices, International Journal for Innovative Research in Multidisciplinary Field, Vol. 3, Issue - 7, 2017, p. 36.
16. P N K Bamzai, Cultural and Political History of Kashmir, op. cit., p. 523.
17. Francisco Pelsaert, Jahangir's India, W. Heffer & Sons Ltd., Cambridge, 1925, pp. 33-35.
18. Mehrdin, Nadia, et al. "The Glorious Reign of Sultan Zain-Ul-Abidin Bud Shah (A Great Muslim Ruler Of Kashmir 1420-1470 AD)." Journal of Positive School Psychology, 2023, pp. 2050-2056.





Survey Study of “Kaal Bhojanam Aarogyakaranama” in Relation to Agni

Nisha Jakhar¹, Rajesh Kumar Sharma² and Dinesh Chandra Sharma³

¹MD Scholar, Department of Kriya Sharir, Post Graduate Institute of Ayurveda, (Affiliated to Dr. Sarvepalli Radhakrishnan Rajasthan Ayurveda University) Jodhpur, Rajasthan, India.

²HoD and Professor, Department of Kriya Sharir, Post Graduate Institute of Ayurveda, (Affiliated to Dr. Sarvepalli Radhakrishnan Rajasthan Ayurveda University) Jodhpur, Rajasthan, India.

³Associate Professor, Department of Kriya Sharir, Post Graduate Institute of Ayurveda, (Affiliated to Dr. Sarvepalli Radhakrishnan Rajasthan Ayurveda University) Jodhpur, Rajasthan, India.

Received: 20 Jan 2024

Revised: 09 Feb 2024

Accepted: 14 May 2024

*Address for Correspondence

Nisha Jakhar

MD Scholar,

Department of Kriya Sharir,

Post Graduate Institute of Ayurveda,

(Affiliated to Dr. Sarvepalli Radhakrishnan Rajasthan Ayurveda University)

Jodhpur, Rajasthan, India.

Email: nishajakhar1994@gmail.com



This is an Open Access Journal / article distributed under the terms of the **Creative Commons Attribution License** (CC BY-NC-ND 3.0) which permits unrestricted use, distribution, and reproduction in any medium, provided the original work is properly cited. All rights reserved.

ABSTRACT

Ahara (Diet) is one of the *Trayopasthambha* described in *Ayurveda* and is crucial for existence, where everyone's lives revolve around food. It provides us with the vitality and nutrients we need to live a healthy, and active life. Since metabolic problems are caused by persons who skip meals and eat at inappropriate times, due to their busy life more common in youngsters. A Study on 100 volunteers taking food on time and not taking food on time on the basis of self-developed survey proforma. Out of 100 volunteers, 73% volunteers having *Samagni*, 18% volunteers having *Vishamagni*, 5% volunteers having *Mandagni* and 4% volunteers having *Tikshnagni*. *Agni* plays a pivotal role in maintaining good health of a human being. Out of 100 volunteers, Maximum number of volunteers 73% volunteers having *Samagni* and their health status was excellent.

Keywords: *Ayurveda, Ahara, Kaal Bhojana, Aarogya, Agni, Dosha*

INTRODUCTION

Ahara (Diet) plays an important role in maintaining a good energy level among human beings. The purpose of *Ayurveda* science is to maintain the health of the healthy and cure disease of diseased. In *Ayurveda* health is a state where *Dosha, Agni, Dhatus*, waste products, all physiological functions should be in homeostatic state and soul,



**Nisha Jakhar et al.,**

senses and mind should be in a state of total wellbeing [1]. In this era of modernization, the society is conscious enough about “what to eat”? but least about “how to eat” and “when to eat”? In *Ayurvedic* text importance of *Anna* (food) and time when to eat is explained. Food is the vital breath of living beings (that is why) the people rush to the food. Complexion, cheerfulness, good voice, life, imagination, happiness, contentment, corpulence, strength, intellect-all these are dependent on food. The worldly activities done for livelihood, the *Vedic* ones for attainment of heaven and those for emancipation also depend on food [2]. Proper time for meals is always after the digestion of previous meals - i.e. ‘*Kaal Bhojanam*’, which is most Important for the health [3]. The man who uses wholesome diet and behaviour, moves cautiously, is unattached to sensual pleasures, donates, observes equality, is truthful, forbearing and devoted to the persons of authority becomes free from diseases. One who is endowed with excellent intellect, speech and action leading to happy consequence submissive mind, clear understanding, knowledge, penance and continued effort in *yoga*, does not fall a victim to diseases [4]. All the classics, including *Vedas*, have mentioned two *Kaals* for meals, viz. *Sanya Kaal* and *Pratah Kaal*. *Sushruta* had indicated two *Kaals* for *Samagni*, while only one for *Durbala Agni*. Thus, *Kaal* is a dependent factor on the condition of *Agni*. It can be evaluated from the symptoms of *Jirna Ahara*. Proper quality and quantity of food intake in right time may be one of the secrets of good health. Time has a major role in digestion, absorption and metabolism. If person fails to take food according to physiological rhythm of hunger than such timing will greatly affect the body, resulting in less energy to work and letter may lead to various kind of life style disorders especially digestive disorder (*Agnimandya*). The ideal time for taking food is: Take food after passing faeces and urine. The sense organs are clear. The body is feeling light. Belching is pure. Heart/chest is clear. *Vata* is moving downwards (in the normal way). Desire for food. fatigue is relieved and abdomen is loose (soft) that is the ideal best time for food [5]. In this present era human is earning wealth and not paying attention towards health due to hectic schedule and life style people not taking food on time and not following the rule of taking food on time and proper nutrients of food. To make the life *Sukhayu* and *Dirghayu*. *Acharya Charaka* mention the importance of *kaal Bhojana*. Observing many troublesome diseases caused by irregular dieting, the wise should eat wholesome, measured and timely food with self-restraint.⁶ Food taken in right quantity at right time (*kaal Bhojana*) is also important. *Acharya charaka* has stated that the food taken in right quantity certainly provides strength, complexion, happiness and longevity to the person without disturbing the normalcy. Individual should consume the right quantity of food at right time that helps to maintain proper digestive power. This work highlights the importance of right time for food intake. Food which is taken timely will digest properly and maintains homeostasis of body.

MATERIAL AND METHOD

LITERARY REVIEW

References will be collected from classical *Ayurvedic* texts as well as from previous research works, research articles, from internet and modern science literatures, *Ayush* research portal, Google scholar etc.

Selection of volunteer

A Study on 100 volunteers taking food on time and not taking food on time on the basis of self-assessed questionnaire was selected from jodhpur and surrounding areas.

ELIGIBILITY CRITERIA

Inclusion Criteria

Volunteers of age group 20-40 years will be taken.

Volunteers of either gender will be taken.

Volunteers should fulfil the criteria and willing for survey.





Nisha Jakhar et al.,

Exclusion Criteria

Volunteers having any type of systemic disease like diabetes, hypertension, cardiac disorder, GIT disorders like gastritis, IBS etc. Person who is not willing to participate in the study.

AIMS AND OBJECTIVE

- Present research work has been undertaken with following objectives.
- Brief study about the *Ahara* mentioned in *Ayurvedic* texts.
- To study role of *Kaal Bhojanam Aarogyakaranam* in maintaining the healthy lifestyle.
- To study role of *Kaal Bhojanam Aarogyakaranam* in relation to *Agni*.
- Assessment of *Agni* on the basis of questionnaire.
- Assessment of *Kaal Bhojana* on the basis of questionnaire.
- Literature review of *Ahara* mentioned in *Ayurvedic* and modern text in relation to *Agni*.
- To make public aware about the hazards of not taking food on time.

OBSERVATION AND RESULT

Out of the 100 apparently volunteers studied in this survey, a maximum of 64% of volunteers belonged to the age group 26-30 years. Minimum volunteers 8% were found from the age group 36-40 years. Maximum number of volunteers i.e., 60 % were males whereas 40 % were females. 78 % of volunteers were Hindu whereas 22 % were Muslim. 65 % of volunteers were vegetarian and 35 % were mixed. Maximum of 62% of volunteers are student, 17 % of volunteers are service, 10 % of volunteers are labour, 7 % volunteers are housewife and minimum 4% volunteers are businessman . 37% of volunteers were married while 63 % were unmarried. 84% of volunteers were from middle class, 6% were from upper class and only 10% were from lower class. 85 % of volunteers were urban dwellers, while 15 % were rural dwellers. The living style is much changed in urban areas than in rural. The environmental factors, the working atmosphere and living conditions all contribute to this. 61% of volunteers belonged to the *VP Prakriti*. 30 % of volunteers are *VK Prakriti*, 9 % of volunteers are *PK Prakriti* .Maximum of 73% of volunteers belonged to the *Samagni*, 18% belonged to *Vishamagni*, 5 % volunteers are *Mandagni* and minimum 4 % are belonged to *Tikshanagni* .

QUESTIONNAIRE BASED DISCUSSION**Do you take morning food in between 9Am to 12Pm?**

Among 100 Volunteers , 90 % Volunteers were taken morning food between 9AM to 12 PM and 10 % Volunteers were not taken morning food between 9AM to 12 PM .Because *Agni* performs well in second *Prahara* of the day i.e. 9 AM to 12 PM, that's why those who taken the food between the second *Prahara* of the day their health status was excellent.

Do you take dinner in between 7 Pm to 8 Pm?

Among 100 Volunteers , 52 % Volunteers were taken evening food between 7 PM to 8 PM and 48 % Volunteers were not taken evening food between 7 PM to 8 PM .Because *Agni* performs well in first *Prahara* of the night i.e. 6 PM to 9 PM, that's why those who taken the food between the first *Prahara* of the night their health status was excellent.

Do you take food after urination and defecation?

Among 100 Volunteers ,70 % Volunteers were taken food after urination and defecation and 30 % volunteers were not taken food after urination and defecation.Because when food is taken while you have the urge of urination and defecation, *Acharya Charaka* says that it's *Sarvadhātu Pradushak* and also *Vata Vivardhaka* that ultimately cause the *Ajirna*.



**Nisha Jakhar et al.,****Do you take food when your belching is pure?**

Among 100 volunteers, 62% were given food when their belching was pure, while 38% were given food when their belching was not pure. Because pure belching indicates the *Jirna Ahara*, while impure belching indicates the *Ajirna*, when you take the food on the *Ajirna Ahara*, the first *Ahara* is *Prinit Rasa Upsarjita* by *Uttar Ahara*, which causes *Sarva Dosha Prakopa*.

Do you take food when you feel hunger?

Among 100 Volunteer, 89% Volunteer were taken food after they feel hungry and 11% volunteer taken food without considering whether they are hungry or not. Because if one takes food before the digestion of the previous meal, the digestive product of the previous food i.e. undigested *Ahara Rasa* of food taken afterwards it provokes all the *Doshas*. It also altered the *Jatharagni* because of formation of *Ama*.

Do you feel active after taking food?

Among 100 volunteers, 60% feel active after taking food, while 40% don't feel active after having the food.

Can you understand all types of taste?

Among 100 volunteers, 95% volunteers had sense for all kind of taste while 5% volunteers had no sense of taste.

Do you have a sense of touch?

Among 100 volunteers, 97% volunteers had sense of touch while 3% volunteers had no sense of touch.

Can you differentiate between good and bad smell?

Among 100 volunteers, 93% volunteers were able to differentiate between good and bad smell while 7% volunteers were not able to differentiate between good and bad smell.

Do you hear properly without using any ear aids?

Among 100 volunteers, 92% volunteers were able to hear without any ear aid while 8% volunteers were not able to hear clearly or without hearing aid.

Do you see near or distant objects without using spectacles?

Among 100 volunteers, 46% volunteers were able to see without spectacles while 54% volunteers were not able to see without spectacles.

Does your body feel light before taking food?

Among 100 volunteers, 89% feel light after taking food, while 11% don't feel light after having the food.

Do you feel lightness in epigastric region?

Among 100 volunteers, 85% feel lightness in epigastric region after taking food, while 15% don't feel lightness in epigastric region after having the food. Because according to *Ayurveda*, those who divided their *Kukshi* into three parts—one part for *Ahara*, a second part for *Dravya* and a third part for *Dosha Gati*— These rules of *Samyak Ahara* is the main factors behind the lightness in the epigastric region after having food.

Do you feel abdominal laxity?

Among 100 volunteers, 60% abdominal laxity after taking food, while 40% don't feel abdominal laxity after having the food. Because according to *Ayurveda*, those who divided their *Kukshi* into three parts—one part for *Ahara*, a second part for *Dravya* and a third part for *Dosha Gati*— These rules of *Samyak Ahara* is the main factors behind the lightness in the epigastric region & abdominal laxity after having food.





Nisha Jakhar et al.,

Do you feel interest in taking food?

Among 100 volunteers, 97% interest in taking food, while 7% don't take interest in taking the food. Because according to *Ayurveda*, if you are not taking *Ahara* with full concentration and interest, *Ahara* will not be situated firmly in *Aamashya* and will not develop *Avasad*, while those who take interest in *Ahara* will not have this type of complication.

CONCLUSION

The relationship between *Kaal Bhojana* and *Agni* was:

The assessment is done by self-developed questionnaire which is based on the classical texts. For this study 100 volunteers were selected and the assessment were done by filling the self -developed survey proforma. The study was drugless and based on observation (Survey study). Among 100 Volunteers , 90 % Volunteers were taken morning food between 9AM to 12 PM and 10 % Volunteers were not taken morning food between 9AM to 12 PM. Because *Agni* performs well in second *Prahara* of the day i.e. 9 AM to 12 PM, that's why those who taken the food between the second *Prahara* of the day their health status was excellent. Among 100 Volunteers, 52 % Volunteers were taken evening food between 7 PM to 8 PM and 48 % Volunteers were not taken evening food between 7 PM to 8 PM. Because *Agni* performs well in first *Prahara* of the night i.e. 6 PM to 9 PM, that's why those who taken the food between the first *Prahara* of the night their health status was excellent. *Agni* plays a pivotal role in maintaining good health of a human being. *Agni* not only performs functioning of digestion but also contributes to the strength, luster, *Oja*, *Teja* and *Prana* (life energy). *Samagni* resembles healthy physical and mental status while vitiated *Agni* (*Mandagni*) resulted diseased condition. *Ajirana*, *Aam dosa*, *Alasak*, *Aamvisha*, *Shokajatisar*, *Visuchika*, *Urustambh* and *Ghrhniroga* etc. are diseases related to *Agni*. The good conduction of *Ahara* and *Vihara* along with *Ayurveda* remedies help to manage diseases of *Agni*. Out of 100 volunteers, 73% volunteers having *Samagni* and their health status was excellent, 18% volunteers having *Vishamagni* , 5% volunteers having *Mandagni* and a minimum of 4% volunteers having *Tikshnagni* and the health status of all of them was average. That's why we can conclude that volunteers who had *Samagni* and also had taken food on time (*Kaal Bhojana*), their health status was excellent (*Aarogya*).

REFERENCES

1. Sushruta Samhita by Ambikadutt Sastri chapter 15 verse 11, by chouxhambha Sanskrit Prakasana Varanasi.
2. Brahmanand Tripathi. Sutra Sthana Chapter 27 verse 349-351 Charaka Samhita with Ayurveda Dipika Commentary. Reprint edition. Varanasi: Chaukhamba Orientalia.
3. Brahmanand Tripathi. Sutra Sthana Chapter 25 verse 40 Charaka Samhita with Ayurveda Dipika Commentary. Reprint edition. Varanasi: Chaukhamba Orientalia.
4. Brahmanand Tripathi. Sharir Sthana Chapter 2 verse 46-47 Charaka Samhita with Ayurveda Dipika Commentary. Reprint edition. Varanasi: Chaukhamba Orientalia.
5. Sushruta uttar tantra chapter 64 verse 86, by chouxhambha Sanskrit Prakasana Varanasi.
6. Brahmanand Tripathi. Nidan sthana Chapter 6 verse 11 Charaka Samhita with Ayurveda Dipika Commentary. Reprint edition. Varanasi: Chaukhamba Orientalia

(Que.1) Do you take morning food in between 9 AM to 12 PM ?

LUNCH TIME	NO. OF VOLUNTEERS		PERCENTAGE
9 AM-12 PM	YES	90	90%
	NO	10	10%
	TOTAL	100	100%





Nisha Jakhar et al.,

(Que.2) Do you take dinner in between 7 PM to 8 PM ?

DINNER TIME	NO. OF VOLUNTEERS		PERCENTAGE
7 PM-8 PM	YES	52	52 %
	NO	48	48 %
	TOTAL	100	100%

(Que.3) Do you take food after urination and defecation ?

FOOD INTAKE AFTER URINATION AND DEFECACTION	NO. OF VOLUNTEERS		PERCENTAGE
	YES	70	70%
	NO	30	30%
	TOTAL	100	100%

Que.4) Do you take food when your belching's are pure ?

FOOD INTAKE WHEN BELCHING'S PURE	NO. OF VOLUNTEERS		PERCENTAGE
	YES	62	62 %
	NO	38	38 %
	TOTAL	100	100 %

(Que .5) Do you take food when you feel hunger ?

FOOD INTAKE WHEN FEEL HUNGER	NO. OF VOLUNTEERS		PERCENTAGE
	YES	89	89 %
	NO	11	11 %
	TOTAL	100	100 %

Que.6) Do you feel active after taking food ?

FEEL ACTIVE AFTER TAKING FOOD	NO. OF VOLUNTEERS		PERCENTAGE
	YES	60	60 %
	NO	40	40 %
	TOTAL	100	100 %

(Que.7) Can you understand all types of taste ?

UNDERSTAND ALL TYPES OF TASTE	NO. OF VOLUNTEERS		PERCENTAGE
	YES	95	95 %
	NO	5	5 %
	TOTAL	100	100 %

(Que. 8) Do you have a sense of touch ?

SENSE OF TOUCH	NO. OF VOLUNTEERS		PERCENTAGE
	YES	97	97 %
	NO	3	3 %
	TOTAL	100	100 %





Nisha Jakhar et al.,

(Que.9) Can you differentiate between good and bad smell?

DIFFERENTIATE BETWEEN GOOD AND BAD SMELL	NO. OF VOLUNTEERS		PERCENTAGE
	YES	93	93 %
	NO	7	7 %
	TOTAL	100	100 %

(Que.10) Do you hear properly without using any ear aids ?

HEAR PROPERLY WITHOUT USING ANY EAR AIDS	NO. OF VOLUNTEERS		PERCENTAGE
	YES	92	92 %
	NO	8	8 %
	TOTAL	100	100 %

(Que.11) Do you see near or distant objects without using spectacles ?

DIFFERENTIATE BETWEEN GOOD AND BAD SMELL	NO. OF VOLUNTEERS		PERCENTAGE
	YES	46	46 %
	NO	54	54 %
	TOTAL	100	100 %

(Que.12) Does your body feel light before taking food ?

BODY FEEL LIGHT BEFORE TAKING FOOD	NO. OF VOLUNTEERS		PERCENTAGE
	YES	89	89 %
	NO	11	11 %
	TOTAL	100	100 %

(Que.13) Do you feel lightness in epigastric region ?

FEEL LIGHTNESS IN EPIGASTRIC REGION	NO. OF VOLUNTEERS		PERCENTAGE
	YES	85	85 %
	NO	15	15 %
	TOTAL	100	100 %

(Que.14) Do you feel abdominal laxity ?

FEEL ABDOMINAL LAXITY	NO. OF VOLUNTEERS		PERCENTAGE
	YES	60	60 %
	NO	40	40 %
	TOTAL	100	100 %

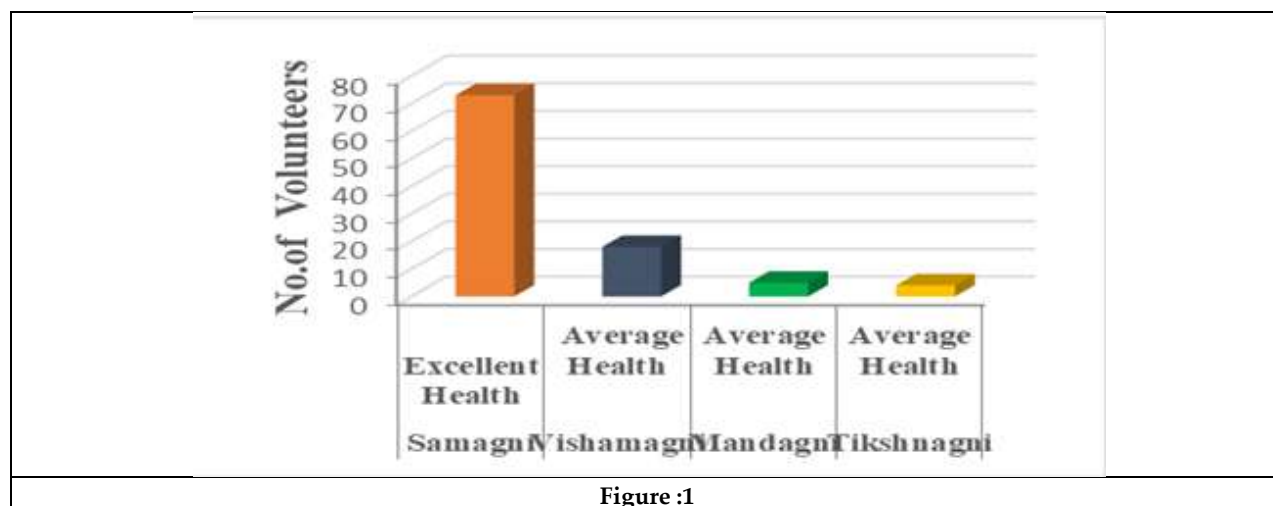
(Que.15) Do you feel interest in taking food ?

FEEL INTERESTED IN TAKING FOOD	NO. OF VOLUNTEERS		PERCENTAGE
	YES	93	93 %
	NO	7	7 %
	TOTAL	100	100 %



Nisha Jakhar *et al.*,**Concluded Result**

<i>Agni</i>	No. of Volunteers	Health Status
<i>Samagni</i>	73	Excellent
<i>Vishamagni</i>	18	Average
<i>Mandagni</i>	5	Average
<i>Tikshnagni</i>	4	Average





***In silico* Exploration for Anti Snake Venom Natural Compounds Targeting Phospholipase**

Lurdhu mary.Kunduri¹, Srikala kamireddy^{2*}, Dr.CH K V L S N Anjana Male³, A.G.N.Harshitha Devi⁴, Kota.Sandhya⁴, Potturi.Bhuvaneswari⁴, D.Veeresh⁴, D.Jayasri⁴, B.Lakshmi Deepika⁴

¹Assistant Professor, Department of Pharmaceutical Analysis, Vignans Foundation for Science, Technology and Research, (Affiliated to Vignan Deemed to be University) Guntur, Andhra Pradesh, India.

²Associate Professor, Department of Pharmaceutics, Nirmala College of Pharmacy Mangalagiri, (Affiliated to Acharya Nagarjuna University) Andhra Pradesh, India.

³Professor, Department of Pharmaceutical Chemistry, NIMS Institute of Pharmacy, Jaipur, Rajasthan, India.

⁴Student, Department of Pharm D, Nirmala College of Pharmacy Mangalagiri, (Affiliated to Acharya Nagarjuna University) Andhra Pradesh, India.

Received: 22 Jan 2024

Revised: 09 Feb 2024

Accepted: 14 May 2024

***Address for Correspondence**

Srikala Kamireddy

Associate Professor,

Department of Pharmaceutics,

Nirmala College of Pharmacy Mangalagiri,

(Affiliated to Acharya Nagarjuna University)

Andhra Pradesh, India.

Email: srikalamadhu@gmail.com



This is an Open Access Journal / article distributed under the terms of the **Creative Commons Attribution License** (CC BY-NC-ND 3.0) which permits unrestricted use, distribution, and reproduction in any medium, provided the original work is properly cited. All rights reserved.

ABSTRACT

The main objective for the current *In silico* exploration is for anti-snake venom natural compounds targeting PLA2. We found some reported natural compounds with PLA2 bioactivity had been selected for virtual screening. Compounds were chosen according to the molecular diversity, representing various categories of chemical structures in the natural compounds, including 16 compounds. Molecular docking simulations were done with the **iGEMDOCK**. Top compounds with better binding energy and interaction profiles were analyzed and the best 3 compounds Aristolochic acid Gallo catechin acid and Quercetin were also evaluated through the pharmacophore mapping to know the pharmacophore features through **SWISSADME**. But Aristolochic acid and Quercetin interacted with critical amino acid residues H1S48 and ASP49 and were similar to the co-crystallized ligands. Therefore, these compounds could be further explored as hit compounds for optimization to development as Phospholipase A2 inhibitors.





Lurdhu mary.Kunduri et al.,

Keywords: PLA2, ASV,SVPLA2,ASP49,H1S48.

INTRODUCTION

India accounts for more snake bites globally due to its tropical location and agriculture-oriented economy where the majority of people work in the fields and are prone to the risk of snake bites. It is a controllable well-being risk that inhabitants of rural areas in tropical and subtropical regions often encounter. Despite snake bites being a potentially fatal ancient ophidian occurrence, snake bite infestation was added to WHO's list of ignored tropical illnesses in 2009. Snake infestation is a major medical issue, particularly in areas where snakes are numerous. A significant proportion of snake bites in India are triggered by the four most frequently encountered species include *Naja Naja* (commonly known as the Spectacled Cobra), *Bangarus Caeruleus* (often referred to as the ubiquitous Krait), *Daboia Russell* (scientifically known as Russells Viper), and *Echis Carinatus* (commonly known as the Saw-scaled Viper). Snake venom has a high concentration of phospholipase A2 (PLA2) enzymes with a wide range of functions. Additional consequences of snake venom phospholipase A2 (svPLA2) include cardiac toxicity, myotoxicity, pre (or) post-synaptic, neurotoxicity, edema hemolysis, low blood pressure, convulsion, platelet aggregation inhibition, and anticoagulation therapy. (2)

GRAPHICAL ABSTRACT

MATERIALS AND METHODOLOGY

The methodology outlines a systematic approach for virtual screening, selection, and evaluation of natural compounds that have the potential to target and inhibit PLA2 enzymes.

A more detailed breakdown of the steps involved:

Data Collection

- **Snake Venom PLA2 Structures**

The first stage involves the collection of 3D structures pertaining to diverse snake venom phospholipase A2 enzymes. These structures can be obtained from reputable protein structure databases like the Protein Data Bank (PDB).

- **Natural Compounds Library**

A library of natural compounds known for their anti-inflammatory, antioxidant, or enzyme-inhibitory properties is compiled. These compounds can be sourced from phytochemical databases, existing literature, or natural product databases.

Preparation of Protein and Ligand Structures:

- **Protein Preparation:** In this step, the crystallographic structures of PLA2 enzymes are retrieved. To prepare the protein for docking, water molecules, cofactors, and other heteroatoms are removed. Hydrogen atoms are introduced into the protein structure, and charges are subsequently allocated. The energy of the protein structure is minimized to achieve a stable conformation suitable for further analysis.
- **Ligand Preparation:** The 3D structures of natural compounds are retrieved from relevant sources. To ensure accurate results, 2D structures are converted into 3D conformations. Charges are assigned to the ligand structures, and energy minimization is performed to optimize their structures.

Molecular docking

- Molecular docking is a computational technique used to identify the optimal alignment between two molecules.



**Lurdhu mary.Kunduri et al.,**

- Docking is a computational technique used to anticipate the optimal positioning of a ligand inside an active site, resulting in the formation of a stable complex.
- Determining the accurate relative orientation of the "key" required to unlock the "lock". • The protein may be conceptualised as the "lock" and the ligand as the "key".

TYPES OF DOCKING

One kind of docking is protein-protein docking, where both molecules involved are often treated as rigid structures. The concept of 6 degrees of freedom refers to the six independent variables that define the position and orientation of an object in three-dimensional space. The search space and the energetics of potential binding confirmation pertain to the exploration of possible molecular configurations and the associated energy considerations in the context of molecular binding. Protein-ligand docking is a computational method used to predict the binding interactions between a protein and a ligand molecule. The ligand exhibits flexibility, but the receptor remains stiff. The flexible ligand was transformed into stiff pieces that were interconnected by one or more hinges, or alternatively, the conformational space was explored by molecular dynamics simulations. Utilizing molecular docking software such as

- Virtual screening of compounds done using the **PYRX** software
- Molecular Docking simulations were done with **IGEMDOCK** software
- Pharmacophore features predictions with the **ZINCPharmer** Web Tool
- ADME assessment with the **SWISS ADME** web server.

It is to define the binding site on the PLA2 enzyme, the active site residues and potential binding pockets are carefully considered. Virtual docking experiments are then conducted for each natural compound within the library against the PLA2 enzyme structures. These experiments generate binding poses and calculate binding affinity scores, providing insights into the compounds' potential to interact with the target protein.

Phospholipase A2 (PLA₂s)

In numerous species, including bacteria, plants, invertebrates like spider insects, and human tissues in snake venom, PLA₂s enzymes are frequently present. The category of secreted phospholipases, referred to as PLA₂s, include lipids that are either unbound or possess aspartate amino acid residues at position 49 (Asp49). These PLA₂s have the ability to facilitate the hydrolysis of the sn-2 acyl link in phospholipids and are present in many cellular types. The toxins BaPLA₂I and BaPLA₂, which belong to the group of PLA₂s isolated from snake venom, provide two examples of isolated PLA₂s that exhibit a diverse range of remarkable biological effects whether acting alone or in combination.

PLA₂ IS THE MOST WIDELY FOUND VENOM COMPONENT PRESENT ACROSS VARIOUS VENOMOUS SNAKE SPECIES**CHARACTERISTICS OF THE MAIN FAMILIES OF SNAKE VENOM TOXINS**

Snake venoms contain a diverse array of components, including proteins, peptides, and enzymes that have evolved for various purposes, such as immobilizing prey, digesting prey, and defending against predators. These components can be broadly categorized into several main families:

Neurotoxins

- **Characteristics:** These are venom components that target the nervous system. They often act by blocking neurotransmission at neuromuscular junctions.
- **Effects:** Paralysis, muscle weakness, respiratory failure.
- **Examples:** Alpha-neurotoxins (found in elapids like cobras and coral snakes), beta-neurotoxins (found in elapids), and presynaptic neurotoxins (found in vipers and pit vipers).



**Lurdhu mary.Kunduri et al.,****Hemorrhagins**

- **Characteristics:** Hemorrhagins are responsible for promoting bleeding by degrading capillary walls and interfering with blood clotting mechanisms.
- **Effects:** Hemorrhage, excessive bleeding.
- **Examples:** Metalloproteases found in vipers and pit vipers.

3. Myotoxins:

- **Characteristics:** These components are associated with muscle damage and necrosis. They often cause pain and swelling at the bite site.
- **Effects:** Muscle necrosis, myoglobinuria (presence of myoglobin in urine), local tissue damage.
- **Examples:** Various myotoxins found in vipers and pit vipers.

Cytotoxins

- **Characteristics:** Cytotoxins damage and disrupt cell membranes, leading to cell death and inflammation.
- **Effects:** Local tissue damage, inflammation.
- **Examples:** Phospholipase A2 enzymes.

Procoagulants and Anticoagulants

- **Characteristics:** Procoagulants promote blood clotting, while anticoagulants inhibit it. Some snake venoms contain both types.
- **Effects:** Disturbance in blood clotting mechanisms, leading to either clot formation (procoagulants) or bleeding (anticoagulants).
- **Examples:** Various coagulation factors and serine proteases.

Cardiotoxins

- **Characteristics:** Cardiotoxins affect the cardiovascular system, often causing heart irregularities and decreased blood pressure.
- **Effects:** Cardiac arrhythmias, hypotension.
- **Examples:** Found in some elapids like kraits.

Dendrotoxins

- **Characteristics:** These are specific neurotoxins found in the venom of mambas, targeting voltage-gated potassium channels in nerve cells.
- **Effects:** Paralysis, neurological dysfunction.

Postsynaptic Neurotoxins

- **Characteristics:** These neurotoxins affect the neuromuscular junction, leading to paralysis.
- **Effects:** Muscle paralysis, respiratory failure.
- **Examples:** Found in some vipers and pit vipers.

Enzymes

- **Characteristics:** Enzymes in snake venom serve various purposes, including facilitating the actions of other venom components. Phospholipase A2 (PLA2) is a common example, which degrades cell membranes and promotes inflammation.

These families of snake venom components can vary in composition and effects between snake species. Understanding these venom components is crucial for developing effective antivenom and improving our knowledge of snakebite treatment and prevention.



Lurdhu mary.Kunduri *et al.*,**PHOSPHOLIPASE A2 (PLA2)****Characteristics**

PLA2 enzymes are a diverse family of proteins found in snake venom. They are responsible for catalyzing the hydrolysis of phospholipids, which are essential components of cell membranes. PLA2 enzymes come in various isoforms, each with unique properties and effects.

Mechanism

PLA2 enzymes target the sn-2 position of phospholipids, cleaving the fatty acid chains from the glycerol backbone. This enzymatic activity results in the release of arachidonic acid, a precursor for inflammatory eicosanoids like prostaglandins and leukotrienes. Lipid mediators are of paramount importance in the process of inflammation, since they have the potential to induce both localized tissue damage and systemic consequences.

Effects: The effects of snake venom PLA2 enzymes can be broadly categorized into:

- **Cytotoxic PLA2:** Disrupt cell membranes, leading to cellular damage and inflammation.
- **Neurotoxic PLA2:** Target the nervous system, causing paralysis.
- **Myotoxic PLA2:** Damage muscle tissues, leading to muscle necrosis and myoglobinuria.

Examples

Different snake species produce PLA2 enzymes with distinct properties. For example, the cobra produces a neurotoxic PLA2, while the viper's venom contains myotoxic PLA2 enzymes.

Mechanism of Action (MOA) of PLA2 Inhibitors:

- PLA2 inhibitors work by disrupting the enzymatic activity of snake venom PLA2 enzymes. They can achieve this through various mechanisms, including:
- Competitive inhibition, where they bind to the active site of PLA2 and block its access to phospholipid substrates.
- Non-competitive inhibition, where they interact with allosteric sites on the enzyme, altering its conformation and reducing its catalytic activity.
- By inhibiting PLA2, these compounds help mitigate the effects of snake envenomation, such as local tissue damage, inflammation, and systemic toxicity.

Side Effects of PLA2 Inhibitors:

The side effects of PLA2 inhibitors can include allergic reactions in some individuals. Additionally, these inhibitors may interact with other medications, leading to potential drug-drug interactions.

STRUCTURAL FEATURES & ACTIVE SITE OF SNAKE VENOM PLA2 PROTEIN

The primary structure of snake venom PLA2 enzymes consists of approximately 120-140 amino acids, forming an α -helical bundle. At the active site, a calcium ion is coordinated by specific amino acid residues, notably in a calcium-binding loop. This calcium ion plays a crucial role in the catalytic mechanism, aiding in the hydrolysis of phospholipids. The hydrophobic channel at the active site accommodates the sn-2 fatty acid chains of phospholipids during hydrolysis. The specific structural features of snake venom PLA2 proteins can vary among different snake species, contributing to their distinct properties and effects.

The structure of the unconstrained phospholipase A2 (PLA2) with Protein Data Bank (PDB) identifier 1FB2.

The protein exhibits many secondary structural components, including α -helices (H1, H2, and H3), short helices (SH1, SH2, and SH3), and two β strands that contribute to the formation of the β -wing.



**Lurdhu mary.Kunduri et al.,****Critical Active Site residues**

The amino acid residues identified in the sequence are Leucine 2, Leucine 3, Phenylalanine 5, Glycine 6, Isoleucine 9, Alanine 18, Isoleucine 19, Tryptophan 22, Serine 23, Cysteine 29, Glycine 30, Cysteine 45, Histidine 48, Aspartic Acid 49, and Phenylalanine 106.

These are the compounds that are mainly selected based on the molecular diversity of active PLA2.

Scoring and Prioritization

The docking results are analyzed, with a focus on binding affinities, intermolecular interactions, and binding poses. Based on these findings, natural compounds are prioritized. The compounds demonstrating strong binding affinities and forming key interactions with active site residues are moved to the forefront.

Molecular Dynamics Simulations

Molecular dynamics simulations are used to enhance comprehension of the stability and dynamics exhibited by ligand-receptor complexes. These simulations allow researchers to observe the interactions between the ligand and PLA2 over a specified time period, providing critical insights into the dynamic behavior of the complexes.

Analysis and Visualization

The results of the molecular dynamics simulations are carefully analyzed. The stability of the ligand-receptor complexes, any conformational changes, and the nature of interactions are scrutinized. Visualizations are generated to illustrate binding interactions, including Hydrogen bonding, hydrophobic interactions, and π - π stacking interactions are three significant non-covalent forces that play crucial roles in many biological and chemical processes using molecular visualization tools.

Hit Compound Selection

Building on the molecular docking and dynamics results, the most promising natural compounds are identified. These compounds exhibit robust and stable interactions with PLA2 enzymes. Additionally, they display potential for inhibiting PLA2 enzymatic activity, effectively preventing the hydrolysis of phospholipids and mitigating venom-induced inflammation. The pharmacokinetic properties of the selected hit compounds are predicted. This assessment provides valuable insights into the pharmacokinetics and safety of the compounds.

In Silico Toxicity Assessment

An *in silico* toxicity assessment is performed to evaluate the safety profile of the selected compounds. This step is crucial for identifying any potential adverse effects that may arise from these compounds.

**ARISTOLOCHIC ACIDGALLOCATHECHIN QUERCETIN
GALLOCATECHIN**

Gallocatechin is a flavonoid found in various plant sources, particularly in tea, with recognized antioxidant and anti-inflammatory properties. Understanding the pharmacophore features and binding mechanisms of Gallocatechin is paramount for unlocking its therapeutic potential. The pharmacophore features of Gallocatechin encompass:

Hydroxyl Groups

Gallocatechin is rich in hydroxyl (-OH) groups, which serve as both hydrogen bond donors and acceptors. These groups enable Gallocatechin to engage in critical interactions with polar residues in the active sites of target proteins.

Aromatic Rings

Gallocatechin contains aromatic ring structures, which can participate in π - π stacking interactions with aromatic amino acid residues within the binding pockets of target proteins. These interactions enhance its binding affinity and inhibitory potential. To gain insights into the binding mechanisms of Gallocatechin, molecular docking studies were conducted. Gallocatechin forms hydrogen bonds with crucial polar residues in the active sites of target proteins. These interactions are fundamental for its ability to inhibit enzymatic activities related to oxidative stress and



**Lurdhu mary.Kunduri et al.,**

inflammation. The aromatic rings of Gallocatechin engage in π - π stacking interactions with aromatic amino acid residues in the binding sites of target proteins. These interactions contribute significantly to its binding affinity and therapeutic potential.

QUERCETIN

Hydroxyl and Carbonyl Groups

Quercetin contains multiple hydroxyl (-OH) and carbonyl (C=O) groups, which serve as hydrogen bond donors and acceptors. These functional groups can engage in crucial interactions with polar residues in target proteins.

Aromatic Rings

The presence of multiple aromatic rings allows Quercetin to participate in π - π stacking interactions with aromatic amino acid residues within the active sites of proteins.

Protein Targets

Receptors relevant to the biological activities of Quercetin were selected as docking targets, including enzymes involved in inflammation, oxidative stress, and cancer pathways.

ARISTOLOCHIC ACID

Aristolochic Acid is a bioactive compound with a notorious reputation due to its nephrotoxic and carcinogenic properties. However, it also holds potential therapeutic applications. This article aims to uncover the pharmacophore features of Aristolochic Acid and its interaction with target proteins through molecular docking.

The pharmacophore features of Aristolochic Acid include:

- **Aromatic Moiety:** Aristolochic Acid contains an aromatic ring system, which may facilitate π - π stacking interaction with aromatic residues in target proteins.
- **Hydrogen Bonding Donor/Acceptor:** It possesses hydrogen bonding functionalities, allowing it to engage in hydrogen bond interactions with polar residues in the active site of target proteins.
- Molecular docking studies revealed detailed binding modes of Aristolochic Acid with its target proteins.

Key observations include

- Aristolochic Acid forms hydrogen bonds with critical residues within the active site of its target proteins. These interactions are crucial for its pharmacological effects.
- The aromatic rings in Aristolochic Acid can engage in π - π stacking interaction with aromatic residues in the binding pockets of its protein targets, contributing to its binding affinity and activity

Reported Anti PLA2 compounds

RESULTS AND DISCUSSION

The compounds which are the least binding energy have more stability. Aristolochic acid, Gallocatechin, and Quercetin show good binding energy on the following binding energy. These top three compounds show active reporting against PLA₂ protein.

SUMMARY AND CONCLUSION

The outcomes of our current docking simulations have unveiled encouraging prospects in the pursuit of potential inhibitors for phospholipase A2 (PLA₂). Particularly noteworthy are aristolochic acid and quercetin, which exhibited substantial binding energies of -105.37 (Kcal/mol) and -108.07 (Kcal/mol), respectively. These values signify a robust affinity for the target site, comparable to the co-crystallized ligand. Significantly, both compounds demonstrated





Lurdhu mary.Kunduri et al.,

interactions with critical amino acid residues HIS48 and ASP49, underscoring their potential as effective inhibitors of PLA2. Equally important is the observation that all the top compounds identified in our screening process displayed favorable properties of ADME (Absorption, Distribution, Metabolism, Excretion) and a promising pharmacokinetic profile. This implies that these compounds possess attributes conducive to good bioavailability and efficacy, rendering them promising candidates for further development. To conclude, compounds such as aristolochic acid and quercetin have not only demonstrated remarkable binding affinity but also exhibit favorable pharmacokinetic properties. Their interactions with key amino acid residues, coupled with advantageous ADME profiles, position these compounds as promising candidates for extended exploration in the realm of PLA2 inhibitor development. This study provides a robust foundation for future research and endeavors in the development of effective therapies targeting PLA2-associated conditions.

REFERENCES

1. Isabel Gómez-Betancur, Vedanjali Gogineni, Andrea Salazar-Ospina and Francisco León, Perspective on the Therapeutics of Anti-Snake Venom, *Molecules* 2019; 24:3276.
2. Ana L. Oliveira, Matilde F. Viegas, Saulo L. da Silva, Andreimar M. Soares Maria J. Ramos and Pedro A. Fernandes, The chemistry of snake venom and its medicinal potential, *Nature Reviews chemistry*, 2022; 6: 451 - 469.
3. Aisha Munawar, Syed Abid Ali, Ahmed Akrem and Christian Betzel, Snake Venom Peptides: Tools of Biodiscovery, *Toxins* 2018; 10: 474.
4. Saulo França Amui, Renato David Puga, Andreimar Martins Soares, Silvana Giuliani, Plant-antivenom: Database of anti-venom medicinal plants, *Electronic Journal of Biotechnology*, 2011; 14: 1-9.
5. Asenate A. X. Adrião, Aline O. dos Santos, Emilly J. S. P. de Lima, Jessica B. Maciel, Weider H. P. Paz, Felipe M. A. da Silva, Manuela B. Pucca, Ana M. Moura-da-Silva, Wuelton M. Monteiro, Marco A. Sartim and Hector H. F. Koolen, Plant-Derived Toxin Inhibitors as Potential Candidates to Complement Antivenom Treatment in Snakebite Envenomations, *Frontiers in Immunology*, 2022, 13: 842576
6. J.-M. Yang and C.-C. Chen, "GEMDOCK: A generic evolutionary method for molecular docking", *Proteins: Structure, Function and Bioinformatics*, vol. 55, pp. 288-304, 2004.
7. J.-M. Yang, "Development and evaluation of a generic evolutionary method for protein-ligand docking", *Journal of Computational Chemistry*, vol. 25, pp. 843-857, 2004.
8. Antoine Daina, Olivier Michielin, Vincent Zoete, Swiss ADME: a free web tool to evaluate pharmacokinetics, drug-likeness and medicinal chemistry friendliness of small molecules, *Scientific reports*, 2017, 7:42717.

Table 1: Reported Anti PLA2 compounds

S.No	Plant Species	Reported Anti PLA2 compounds
1.	H.indicus ^R	Anisic Acid
2.	Aristolochia Indica ^r , A.Sprucei ^s	Aristolochic Acid
3.	Pluchea Indica ^r	Beta Sitosterol
4.	Butea Monosperma	Butein
5.	-	Corticosterone
6.	Baccharis Uncinella ^a	Ferulic Acid
7.	Schizolobium Parahyba ^l	Gallocathechin





Lurdhu mary.Kunduri et al.,

8.	-	Gramine
9.	H.indicus ^R	Lupelol acetate
10.	Thea Sinensis Linn. ^{Bt}	Melanin
11.	B. Uncinella ^a	Oleanolic Acid
12.	-	Quercitin
13.	-	Resveratrol
14.	-	Umbelliferone
15.	B. Uncinella ^R	Ursolic acid
16.	Eclipta Prostrate ^{sy}	Wedelolactone

Table 2:

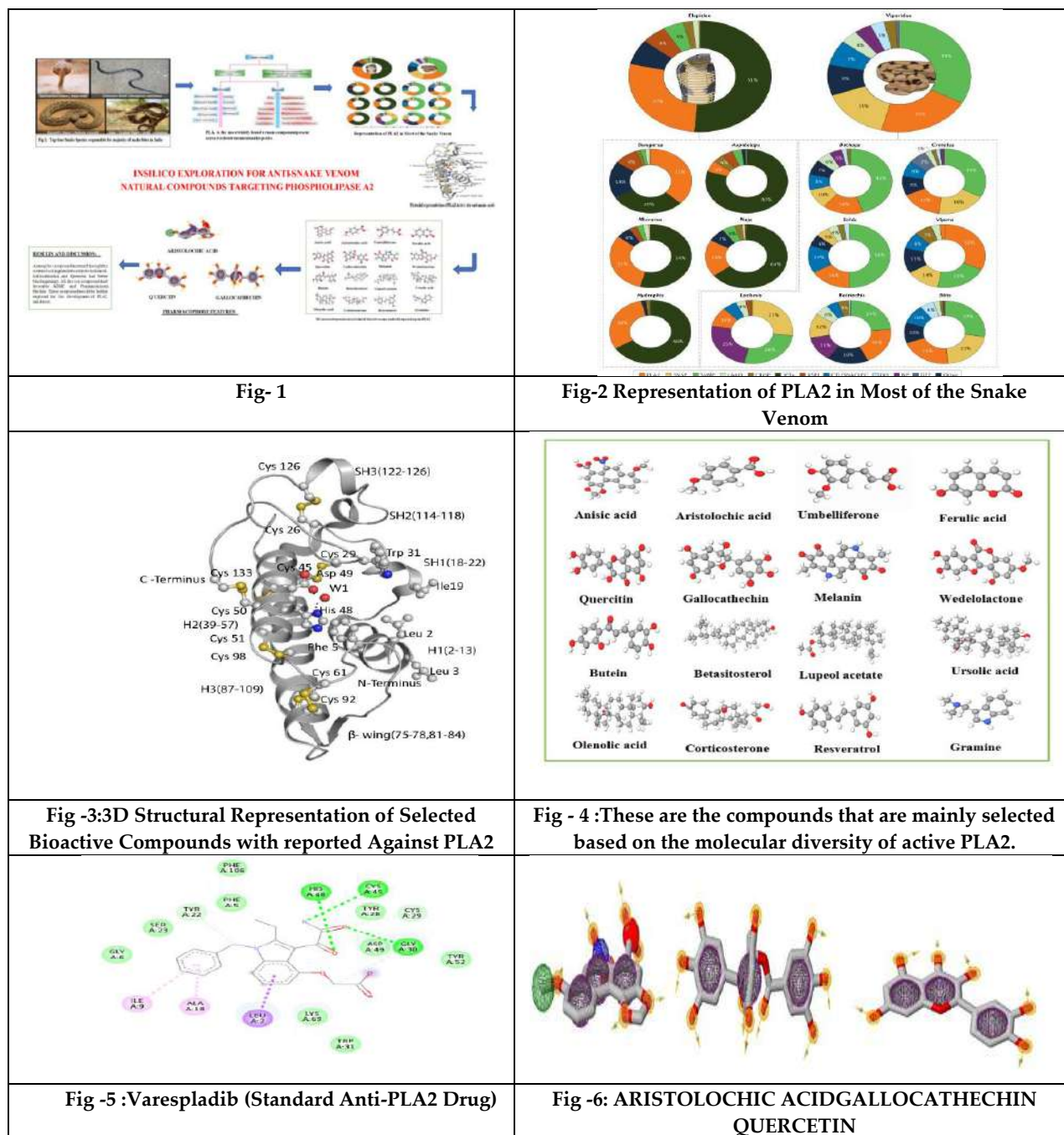
Compounds	Binding Energy (K.cal/mol)
Anisic acid	-90.32
Aristolochic acid	-105.37
Beta-Sitosterol	-82.54
Butein	-97.41
Corticosterone	-84.22
Ferulic acid	-83.67
Gallocatechin	-108.07
Gramine	-80.73
Lupeol acetate	-73.28
Melanin	-92.66
Oleanolic acid	-74.55
Quercitin	-103.58
Resveratrol	-95.28
Umbelliferone	-86.19
Ursolic acid	-77.4
Wedelolactone	-85.32



**Table 3: Reported plant species and compounds against PLA2 activity Molecular Interactions:**

<p>Fig 6 : Anisic Acid</p>	<p>Fig 7: Aristolochic acid</p>	<p>Fig 8 : B - Sitosterol</p>	<p>Fig 9: Butein</p>
<p>Binding Energy: -82.54 (K.cal/mol)</p>	<p>Binding Energy:-97.41(K.cal/mol)</p>	<p>Binding Energy: -90.32(K.cal/mol)</p>	<p>Binding Energy:- 105.37(K.cal/mol)</p>
<p>Fig 10: Corticosterone</p>	<p>Fig 11: Ferulic Acid</p>	<p>Fig 12: Gallochechin</p>	<p>Fig 13: Gramine</p>
<p>Binding Energy: -108.07 (K.cal/mol)</p>	<p>Binding Energy: -80.73(K.cal/mol)</p>	<p>Binding Energy: -84.22(K.cal/mol)</p>	<p>Binding Energy: -83.67(K.cal/mol)</p>
<p>Fig 14:Lupeol Acetate</p>	<p>Fig 15: Melanin</p>	<p>Fig 16 : Oleonic acid</p>	<p>Fig 17: Quercetin</p>
<p>Binding Energy: -74.55(K.cal/mol)</p>	<p>Binding Energy:-103.58(K.cal/mol)</p>	<p>Binding Energy: -73.28(K.cal/mol)</p>	<p>Binding Energy: -92.66(K.cal/mol)</p>
<p>Fig 18 : Resveratrol</p>	<p>Fig 19: Umbelliferone</p>	<p>Fig 20 Ursolic Acid</p>	<p>Fig 21 : Wedelolactone</p>
<p>Binding Energy: -95.28(K.cal/mol)</p>	<p>Binding Energy: -86.19(K.cal/mol)</p>	<p>Binding Energy: -77.4(K.cal/mol)</p>	<p>Binding Energy: -85.32(K.cal/mol)</p>







On b-gp (b-gsp)-Closed Sets in Binary Topological Spaces

P.Sathishmohan^{1*}, R.Nesarajithamani², K.Rajalakshmi³ and V.Rajendran⁴

^{1,2}Assistant Professor, Department of Mathematics, Kongunadu Arts and Science College (Autonomous), (Affiliated to Bharathiar University) Coimbatore, Tamil Nadu, India.

³Assistant Professor, Department of Mathematics, Sri Krishna College of Engineering and Technology, Kuniyamuthur, Coimbatore, India.

⁴Guest Lecturer, Department of Mathematics, PuratchiThalaivi Amma Government Arts and Science College, Palladam, (Affiliated to Bharathiar University) Coimbatore, Tamil Nadu, India.

Received: 20 Jan 2024

Revised: 09 Feb 2024

Accepted: 14 May 2024

*Address for Correspondence

P. Sathishmohan

Assistant Professor,

Department of Mathematics,

Kongunadu Arts and Science College (Autonomous),

(Affiliated to Bharathiar University)

Coimbatore, Tamil Nadu, India.

Email: nesarajimsc@gmail.com



This is an Open Access Journal / article distributed under the terms of the **Creative Commons Attribution License** (CC BY-NC-ND 3.0) which permits unrestricted use, distribution, and reproduction in any medium, provided the original work is properly cited. All rights reserved.

ABSTRACT

In this paper, we introduce the concept of binary generalized pre closed (binary generalized pre-open) sets and binary generalized semi pre closed (binary generalized semi pre-open) sets in binary topological spaces and investigates some of its basic characterizations.

Keywords: b-gp(b-gsp)-closed set, b-gp(b-gsp)-openset b-gp(b-gsp)-interior

INTRODUCTION

In 1970, Levine [2] introduced the concept of generalized closed sets as a generalization of closed sets in topological spaces. This concept was found to be the origin to develop many results in general topology. In [3] Noiri *et.al.*, introduced the concept of generalized pre closed sets in topological spaces. The initiation of binary topological spaces was done by Nithyanantha Jothi and Thangavelu [4] in the year 2011 and followed by the authors [5] introduced the concept of generalized binary closed sets in binary topological spaces and study some of its basic properties. In 2016, Nithyanantha Jothi [7] introduced binary semi open sets in binary topological spaces and obtained some basic results. Recently, Sathishmohan *et.al.*, [8,9] concentrated the notion of b-gs-closed sets and b-sg-closed sets in binary topological spaces and obtained many interesting results.





PRELIMINARIES

Definition 2.1.[4] Let X and Y be any two non empty sets. A binary topology from X to Y is a binary structure $\mathcal{M} \subseteq \mathcal{P}(X) \times \mathcal{P}(Y)$ that satisfies the axioms.

1. (ϕ, ϕ) and $(X, Y) \in \mathcal{M}$.
2. $(A_1 \cap A_2, B_1 \cap B_2) \in \mathcal{M}$ whenever $(A_1, B_1) \in \mathcal{M}$ and $(A_2, B_2) \in \mathcal{M}$.
3. If $\{(A_\alpha, B_\alpha) : \alpha \in \Delta\}$ is a family of members of \mathcal{M} then $(\bigcup_{\alpha \in \Delta} A_\alpha, \bigcup_{\alpha \in \Delta} B_\alpha) \in \mathcal{M}$.

Definition 2.2. [4] If \mathcal{M} is a binary topology from X to Y then the triplet (X, Y, \mathcal{M}) is called a binary topological space and the members of \mathcal{M} are called the binary open subsets of the binary topological space (X, Y, \mathcal{M}) . The elements of $X \times Y$ are called the binary points of the binary topological space (X, Y, \mathcal{M}) . If $Y = X$ then \mathcal{M} is called a binary topology on X in which case we write (X, \mathcal{M}) as a binary topological space.

Definition 2.3.[4] Let (X, Y, \mathcal{M}) be a binary topological space and $A \subseteq X, B \subseteq Y$. Then (A, B) is called binary closed in (X, Y, \mathcal{M}) if $(X/A, Y/B) \in \mathcal{M}$.

Proposition 2.4.[4] Let (X, Y, \mathcal{M}) be a binary topological space and $(A, B) \subseteq (X, Y)$. Let $(A, B) \subseteq (X, Y)$. Let $(A, B)^{1*} = \bigcap \{A_\alpha : (A_\alpha, B_\alpha) \text{ is binary closed and } (A, B) \subseteq (A_\alpha, B_\alpha)\}$ and $(A, B)^{2*} = \bigcap \{B_\alpha : (A_\alpha, B_\alpha) \text{ is binary closed and } (A, B) \subseteq (A_\alpha, B_\alpha)\}$. Then $((A, B)^{1*}, (A, B)^{2*})$ is binary closed and $(A, B) \subseteq ((A, B)^{1*}, (A, B)^{2*})$.

Definition 2.5.[4] The ordered pair $((A, B)^{1*}, (A, B)^{2*})$ is called the binary closure of (A, B) , denoted by $b\text{-cl}(A, B)$ in the binary space (X, Y, \mathcal{M}) where $(A, B) \subseteq (X, Y)$.

Definition 2.6.[4]

- (i) $(A, B)^{1^\circ} = \bigcup \{A_\alpha : (A_\alpha, B_\alpha) \text{ is binary open and } (A_\alpha, B_\alpha) \subseteq (A, B)\}$.
- (ii) $(A, B)^{2^\circ} = \bigcup \{B_\alpha : (A_\alpha, B_\alpha) \text{ is binary open and } (A_\alpha, B_\alpha) \subseteq (A, B)\}$.

Definition 2.7. [4] Let (X, Y, \mathcal{M}) be a binary topological space and $(A, B) \subseteq (X, Y)$. The ordered pair $((A, B)^{1^\circ}, (A, B)^{2^\circ})$ is called the binary interior of (A, B) , denoted by $b\text{-int}(A, B)$.

Definition 2.8. [4] Let (X, Y, \mathcal{M}) be a binary topological space. Let $(A, B) \subseteq (X, Y)$. Define $\mathcal{M}_{(A, B)} = \{A \cap U, B \cap V : (U, V) \in \mathcal{M}\}$. Then $\mathcal{M}_{(A, B)}$ is a binary topology from A to B . The binary topological space $(A, B, \mathcal{M}_{(A, B)})$ is called a binary subspace of (X, Y, \mathcal{M}) .

Definition 2.9. A subset (A, B) of a binary topological space (X, Y, \mathcal{M}) is called

1. binary semi-closed [7], if $b\text{-int}(b\text{-cl}(A, B)) \subseteq (A, B)$.
2. binary pre-closed [1], if $b\text{-cl}(b\text{-int}(A, B)) \subseteq (A, B)$.
3. binary α -closed [1], if $b\text{-int}(b\text{-cl}(b\text{-int}(A, B))) \subseteq (A, B)$.
4. binary semi pre-closed [1], if $b\text{-cl}(b\text{-int}(b\text{-cl}(A, B))) \subseteq (A, B)$.
5. binary regular closed [6], if $(A, B) = b\text{-cl}(b\text{-int}(A, B))$.
6. Generalized binary closed [5], if $b\text{-cl}(A, B) \subseteq (U, V)$ whenever $(A, B) \subseteq (U, V)$ and (U, V) is binary open.

Definition 2.10.[5] Let X and Y be any two non empty sets and let (A, B) and $(C, D) \in \mathcal{P}(X) \times \mathcal{P}(Y)$. We say that $(A, B) \subseteq (C, D)$ if $A \subseteq C$ and $B \subseteq D$.

Definition 2.11.[5] Let X and Y be any two nonempty sets and let (A, B) and $(C, D) \in \mathcal{P}(X) \times \mathcal{P}(Y)$. We say that $(A, B) \not\subseteq (C, D)$ if one of the following holds:

1. $A \subseteq C$ and $B \not\subseteq D$
2. $A \not\subseteq C$ and $B \subseteq D$





3. $A \not\subseteq C$ and $B \not\subseteq D$

Definition 2.12. [4] Let (X, Y, \mathcal{M}) be a binary topological space and let $(x, y) \in X \times Y$. The binary open set (A, B) is called a binary neighbourhood of (x, y) if $x \in A$ and $y \in B$.

Definition 2.13. [8] Let (X, Y, \mathcal{M}) be a binary topological space. Let $(A, B) \subseteq (X, Y)$. Then (A, B) is called binary generalized semi closed (briefly, b-gs-closed) if $b\text{-scl}(A, B) \subseteq (U, V)$ whenever $(A, B) \subseteq (U, V)$ and (U, V) is binary open.

Definition 2.14. [8] Let (X, Y, \mathcal{M}) be a binary topological space. Let $(A, B) \subseteq (X, Y)$. Then (A, B) is called binary semi generalized closed (briefly, b-sg-closed) if $b\text{-scl}(A, B) \subseteq (U, V)$ whenever $(A, B) \subseteq (U, V)$ and (U, V) is binary semi open.

Definition 2.15. [9] Let (X, Y, \mathcal{M}) be a binary topological space and let (x, y) be a point of (X, Y) . A subset (N_x, N_y) of (X, Y) is called binary g-neighbourhood of (x, y) iff there exists a binary g-open set (U, V) such that for $(x, y) \in (U, V) \subseteq (N_x, N_y)$.

Binary generalized pre-closed and Binary generalized semi pre-closed sets

This section is to introduce a new type of binary closed sets in binary topological spaces called binary generalized pre closed sets and binary generalized semi pre closed sets and to study some of its characterizations.

Definition 3.1. Let (X, Y, \mathcal{M}) be a binary topological space. Let $(A, B) \subseteq (X, Y)$. Then (A, B) is called binary generalized pre closed (briefly b-gp-closed) if $b\text{-pcl}(A, B) \subseteq (U, V)$ whenever $(A, B) \subseteq (U, V)$ and (U, V) is binary open.

Theorem 3.2. Every binary closed set is b-gp-closed.

Proof: Let (A, B) be a binary closed set and (U, V) be any binary open set such that $(A, B) \subseteq (U, V)$. We know that $b\text{-cl}(A, B) = (A, B)$. Since every binary closed set is binary pre closed, $b\text{-pcl}(A, B) \subseteq b\text{-cl}(A, B) = (A, B) \subseteq (U, V)$. That is $b\text{-pcl}(A, B) \subseteq (U, V)$. Hence (A, B) is b-gp-closed.

The converse of the above theorem need not be true as seen from the subsequent example.

Example 3.3. Let $X = \{a, b\}, Y = \{a, b, c\}$ clearly $\mathcal{M} = \{(\phi, \phi), (\{a\}, \{b\}), (\{a\}, \{a, c\}), (\{a\}, Y), (\{a, \phi\}, (X, Y))\}$ is a binary topology from X to Y . Also $(X, Y), (\{b\}, \{a, c\}), (\{b\}, \{b\}), (\{b\}, \phi), (\{b\}, Y)$ and (ϕ, ϕ) are the binary closed sets in (X, Y, \mathcal{M}) . Then the subsets $(X, \{b\})$ and $(\{b\}, \{a, b\})$ are b-gp - closed sets but not binary closed.

Theorem 3.4. Every binary semi closed set is b-gp-closed.

Proof: Let (A, B) be a binary semi closed set and (U, V) be any binary open set such that $(A, B) \subseteq (U, V)$. Since every binary open set is binary semi open, we have $b\text{-pcl}(A, B) = (A, B) \subseteq (U, V)$. Hence (A, B) is b-gp-closed.

The converse of the above theorem need not be true as seen from the subsequent example.

Example 3.5. Let $X = \{a, b\}, Y = \{a, b, c\}$ clearly $\mathcal{M} = \{(\phi, \phi), (\{b\}, \{a, c\}), (\{a\}, \{a, bc\}), (\phi, c), (X, Y)\}$ is a binary topology from X to Y . Also $(X, Y), (\{a\}, \{b\}), (\{b\}, \{a\}), (X, \{a, b\})$ and (ϕ, ϕ) are the binary closed sets in (X, Y, \mathcal{M}) . Then the subsets (X, ϕ) and $(X, \{a, c\})$ are b-gp-closed sets but not binary semi closed.

Theorem 3.6. Every binary α -closed set is b-gp-closed.

Proof: Let (A, B) be a binary α -closed set and (U, V) be any binary open set such that $(A, B) \subseteq (U, V)$. Since every binary open set is binary α -open, we have $b\text{-pcl}(A, B) \subseteq b\text{-}\alpha\text{-cl}(A, B) \subseteq (U, V)$. Hence (A, B) is b-gp-closed.

The converse of the above theorem need not be true as seen from the subsequent example.





Sathishmohan et al.,

Example 3.7. Let $X = \{a, b\}$, $Y = \{a, b, c\}$

clearly $\mathcal{M} = \{(\phi, \phi), (\{a\}, \{c\}), (\{a\}, \{a\}), (\{a\}, \{a, c\}), (\{a\}, \phi), (X, Y)\}$ is a binary topology from X to Y . Also $(X, Y), (\{b\}, \{a, b\}), (\{b\}, \{b, c\}), (\{b\}, \{b\}), (\{b\}, Y)$ and (ϕ, ϕ) are the binary closed sets in (X, Y, \mathcal{M}) . Then the subsets $(\{a\}, \{b, c\})$ and $(X, \{a, c\})$ are b-gp-closed sets but not binary α -closed.

Theorem 3.8. Every generalized binary closed set is b-gp-closed.

Proof: Let (A, B) be a generalized binary closed set and (U, V) be any binary open set such that $(A, B) \subseteq (U, V)$. Since (A, B) is generalized binary closed set, we have $b\text{-pcl}(A, B) \subseteq b\text{-cl}(A, B) \subseteq (U, V)$. Hence (A, B) is binary gp-closed.

The converse of the above theorem need not be true as seen from the subsequent example.

Example 3.9. Let $X = \{a, b\}$, $Y = \{a, b, c\}$ clearly $\mathcal{M} = \{(\phi, \phi), (\phi, \{c\}), (\{b\}, \{c\}), (X, Y)\}$ is a binary topology from X to Y . Also $(X, Y), (X, \{a, b\}), (\{a\}, \{a, b\})$ and (ϕ, ϕ) are the binary closed sets in (X, Y, \mathcal{M}) . Then the subsets $(\phi, Y), (\{a\}, \phi), (\{b\}, \phi)$ and (X, ϕ) are b-gp - closed sets but not generalized binary closed.

Theorem 3.10. Every binary r-closed set is b-gp-closed.

Proof: Let (A, B) be a binary r-closed set and (U, V) be any binary open set such that $(A, B) \subseteq (U, V)$. Since (U, V) is binary open set, we have $b\text{-pcl}(A, B) \subseteq b\text{-cl}(A, B) \subseteq$

$b\text{-rcl}(A, B) \subseteq (U, V)$. Therefore $b\text{-pcl}(A, B) \subseteq b\text{-rcl}(A, B) \subseteq (U, V)$. Hence (A, B) is binary gp-closed.

The converse of the above theorem need not be true as seen from the subsequent example.

Example 3.11. Let $X = \{a, b\}$, $Y = \{a, b, c\}$

clearly $\mathcal{M} = \{(\phi, \phi), (\{a\}, \{b\}), (\{a\}, \{a, c\}), (\{a\}, Y), (\{a\}, \phi), (X, Y)\}$ is a binary topology from X to Y . Also $(X, Y), (\{b\}, \{a, c\}), (\{b\}, \{b\}), (\{b\}, \phi), (\{b\}, Y)$ and (ϕ, ϕ) are the binary closed sets in (X, Y, \mathcal{M}) . Then the subsets $(\{b\}, \{a, b\})$ and (ϕ, Y) are b-gp closed sets but not binary r-closed.

Theorem 3.12. Union of any two b-gp-closed subsets is b-gp-closed.

Proof: Let (A, B) and (C, D) be any two b-gp-closed sets in (X, Y) , $(A, B) \subseteq (U, V)$ and $(C, D) \subseteq (U, V)$ where (U, V) is binary open in (X, Y) and so $(A, B) \cup (C, D) \subseteq (U, V)$. Since (A, B) and (C, D) are b-gp-closed. $(A, B) \subseteq b\text{-pcl}(A, B)$ and $(C, D) \subseteq b\text{-pcl}(C, D)$ and hence $(A, B) \cup (C, D) \subseteq b\text{-pcl}(A, B) \cup b\text{-pcl}(C, D) \subseteq b\text{-pcl}((A, B) \cup (C, D))$. Thus $(A, B) \cup (C, D)$ is b-gp-closed set in (X, Y, \mathcal{M}) .

Remark 3.13. Intersection of any two b-gp-closed subsets is b-gp-closed.

Example 3.14. Let $X = \{a, b\}$, $Y = \{a, b, c\}$ clearly $\mathcal{M} = \{(\phi, \phi), (\{a\}, \{c\}), (\{a\}, \{a\}), (\{a\}, \{a, c\}), (\{a\}, \phi), (X, Y)\}$ is a binary topology from X to Y . If $(A, B) = (\{a\}, \{c\})$ and $(C, D) = (\{a\}, \{a, c\})$. Then (A, B) and (C, D) are b-gp-closed sets in (X, Y) , $(A, B) \cap (C, D) = (\{a\}, \{c\})$ is also b-gp-closed sets in (X, Y) .

Theorem 3.15. Let (A, B) be a b-gp-closed subset of (X, Y) . If $(A, B) \subseteq (C, D) \subseteq b\text{-pcl}(A, B)$ then (C, D) is also b-gp-closed subset of (X, Y) .

Proof: Let (U, V) be a binary open sets of (X, Y) such that $(C, D) \subseteq (U, V)$. Then $(A, B) \subseteq (U, V)$. Since (A, B) is b-gp-closed sets $b\text{-pcl}(A, B) \subseteq (U, V)$. Also $(C, D) \subseteq b\text{-pcl}(A, B)$, $b\text{-pcl}(C, D) \subseteq b\text{-pcl}(A, B) \subseteq (U, V)$. Hence (C, D) is also b-gp-closed subset of (X, Y) .

Theorem 3.16. Let (X, Y, \mathcal{M}) be a binary topological space and $A \subseteq X$, $B \subseteq Y$. Then if (A, B) is b-gp-closed in (X, Y, \mathcal{M}) then A is b-gp-closed in (X, \mathcal{M}_X) and B is b-gp-closed in (Y, \mathcal{M}_Y)

Proof: Since (A, B) is b-gp-closed, we have $((X/A), (Y/B))$ is b-gp-open. Also, since (X, Y, \mathcal{M}) is a binary topological space, we have (X/A) is b-gp-open in X and (Y/B) is b-gp-open in Y . Therefore, A is b-gp-closed in X and B is b-gp-closed in Y .





Sathishmohan et al.,

Theorem 3.17. Let (X, Y, \mathcal{M}) be a binary topological spaces and $(A, B, \mathcal{M}_{(A,B)})$ is binary subspace of (X, Y, \mathcal{M}) . Let (C, D) be a b-gp-closed set in (X, Y, \mathcal{M}) and $(C, D) \subseteq (A, B)$. Then (C, D) is a b-gp-closed in $(A, B, \mathcal{M}_{(A,B)})$.

Proof: Since (C, D) is a b-gp-closed set in (X, Y, \mathcal{M}) , we have $\text{b-pcl}(C, D) \subseteq (U, V)$ where (U, V) is binary open in (X, Y, \mathcal{M}) and hence it should be in (\mathcal{M}) by definition of a binary subspace, $(U \cap A, V \cap B) \subseteq (\mathcal{M}_{(A,B)})$. Let (U, V) is a binary open sets in $(A, B, \mathcal{M}_{(A,B)})$, since $(C, D) \subseteq (A, B)$. $(C, D) \subseteq (U, V)$, so $\text{b-pcl}(C, D) = \text{b-pcl}(C \cap A, D \cap B) \subseteq \text{b-pcl}(U \cap C, V \cap D) \subseteq (U, V)$. Thus (C, D) is a b-gp-closed set in $(A, B, \mathcal{M}_{(A,B)})$.

Definition 3.18. A subset (A, B) of a binary topological space (X, Y, \mathcal{M}) is called binary generalized pre open set (briefly b-gp-open set) if its complement is b-gp-closed.

Theorem 3.19. Let be a (X, Y, \mathcal{M}) binary topological space, then the following statements hold.

1. Every binary open set is b-gp-open.
2. Every binary semi open set is b-gp-open.
3. Every binary α -open set is b-gp-open.
4. Every generalized binary open set is b-gp-open.
5. Every binary r-open set is b-gp-open.

Proof: It follows from the Theorems 3.2,3.4,3.6,3.8,3.10.

Definition 3.20. Let (X, Y, \mathcal{M}) be a binary topological space. Let $(A, B) \subseteq (X, Y)$. Then (A, B) is called binary generalized semi pre closed (briefly b-gsp-closed) if $\text{b-spcl}(A, B) \subseteq (U, V)$ whenever $(A, B) \subseteq (U, V)$ and (U, V) is binary open.

Theorem 3.21. Every binary closed set is b-gsp-closed.

Proof: Let (A, B) be a binary closed set and (U, V) be any binary open set such that $(A, B) \subseteq (U, V)$. We know that $\text{b-cl}(A, B) = (A, B)$. Since every binary closed set is binary semi pre closed, we have $\text{b-spcl}(A, B) \subseteq \text{b-cl}(A, B) = (A, B) \subseteq (U, V)$. Hence (A, B) is b-gsp-closed.

The converse of the above theorem need not be true as seen from the subsequent example.

Example 3.22. Let $X = \{a, b\}$, $Y = \{a, b, c\}$ clearly $\mathcal{M} = \{(\phi, \phi), (\{a\}, \{b\}), (\{a\}, \{a, c\}), (\{a\}, Y), (\{a\}, \phi), (X, Y)\}$ is a binary topology from X to Y . Also $(X, Y), (\{a\}, \{a, c\}), (\{b\}, \{b\}), (\{b\}, \phi), (\{b\}, Y)$ and (ϕ, ϕ) are the binary closed sets in (X, Y, \mathcal{M}) . Then the subsets $(X, \{b\})$ and $(\{b\}, \{a, b\})$ are b-gsp-closed sets but not binary closed.

Theorem 3.23. Every binary semi closed set is b-gsp-closed.

Proof:

Let (A, B) be a binary semi closed set and (U, V) be any binary open set such that $(A, B) \subseteq (U, V)$. Since every binary open set is binary semi open, we have $\text{b-spcl}(A, B) \subseteq \text{b-scl}(A, B) \subseteq (U, V)$. Hence (A, B) is b-gsp-closed.

The converse of the above theorem need not be true as seen from the subsequent example.

Example 3.24. Let $X = \{a, b\}$, $Y = \{a, b, c\}$. clearly $\mathcal{M} = \{(\phi, \phi), (\{b\}, \{a, c\}), (\{a\}, \{a, bc\}), (\phi, c), (X, Y)\}$ is a binary topology from X to Y . Also $(X, Y), (\{a\}, \{b\}), (\{b\}, \{a\}), (X, \{a, b\})$ and (ϕ, ϕ) are the binary closed sets in (X, Y, \mathcal{M}) . Then the subsets (X, ϕ) and $(X, \{a, c\})$ are b-gsp-closed sets but not binary semi closed.

Theorem 3.25. Every binary α -closed set is b-gsp-closed.

Proof: Let (A, B) be a binary α -closed set and (U, V) be any binary open set such that $(A, B) \subseteq (U, V)$. Since every binary open set is binary α -open, we have $\text{b-spcl}(A, B) \subseteq \text{b-scl}(A, B) \subseteq \text{b-}\alpha\text{cl}(A, B) \subseteq (U, V)$. Hence (A, B) is b-gsp-closed.

The converse of the above theorem need not be true as seen from the subsequent example.





Sathishmohan et al.,

Example 3.26. Let $X=\{a,b\}, Y=\{a,b,c\}$. Clearly $\mathcal{M}=\{(\phi, \phi), (\{a\}, \{c\}), (\{a\}, \{a\}), (\{a\}, \{a, c\}), (\{a\}, \phi), (X, Y)\}$ is a binary topology from X to Y . Also $(X, Y), (\{b\}, \{a, b\}), (\{b\}, \{b, c\}), (\{b\}, \{b\}), (\{b\}, Y)$ and (ϕ, ϕ) are the binary closed sets in (X, Y, \mathcal{M}) . Then the subsets $(\{a\}, \{b, c\})$ and $(X, \{a, c\})$ are b-gsp-closed sets but not binary α -closed.

Theorem 3.27. Every generalized binary closed set is b-gsp-closed.

Proof: Let (A, B) be a generalized binary closed set and (U, V) be any binary open set such that $(A, B) \subseteq (U, V)$. Since (A, B) is generalized binary closed set, we have $b-cl(A, B) \subseteq (U, V)$. Then $b-spcl(A, B) \subseteq b-cl(A, B) \subseteq (U, V)$. Hence (A, B) is b-gsp-closed.

The converse of the above theorem need not be true as seen from the subsequent example.

Example 3.28. Let $X = \{a, b\}, Y = \{a, b, c\}$ clearly $\mathcal{M} = \{(\phi, \phi), (\phi, \{c\}), (\{b\}, \{c\}), (X, Y)\}$ is a binary topology from X to Y . Also $(X, Y), (X, \{a, b\}), (\{a\}, \{a, b\})$ and (ϕ, ϕ) are the binary closed sets in (X, Y, \mathcal{M}) . Then the subsets $(\phi, Y), (\{a\}, \phi), (\{b\}, \phi)$ and (X, ϕ) are b-gsp closed sets but not generalized binary closed.

Theorem 3.29. Every binary r-closed set is b-gsp-closed.

Proof: Let (A, B) be a binary r-closed set and (U, V) be any binary open set such that $(A, B) \subseteq (U, V)$. Since every binary open set is binary r-open, we have $b-spcl(A, B) \subseteq b-scl(A, B) \subseteq b-rcl(A, B) \subseteq (U, V)$. Hence (A, B) is b-gsp-closed.

The converse of the above theorem need not be true as seen from the sub sequent example.

Example 3.30. Let $X=\{a,b\}, Y=\{a,b,c\}$. Clearly $\mathcal{M}=\{(\phi, \phi), (\{a\}, \{b\}), (\{a\}, \{a, c\}), (\{a\}, Y), (\{a\}, \phi), (X, Y)\}$ is a binary topology from X to Y . Also $(X, Y), (\{b\}, \{a, c\}), (\{b\}, \{b\}), (\{b\}, \phi), (\{b\}, Y)$ Then the subsets $(\{b\}, \{a, b\})$ and (ϕ, Y) are b-gsp-closed sets but not binary r-closed.

Theorem 3.31. Every binary sg-closed set is b-gsp-closed.

Proof: Let (A, B) be b-sg closed set. Let (U, V) be binary semi open set containing (A, B) . Since every binary open set is binary semi open set, we have $b-spcl(A, B) \subseteq b-scl(A, B) \subseteq (U, V)$. Hence (A, B) is b-gsp-closed.

The converse of the above theorem need not be true as seen from the sub sequent example.

Example 3.32. Let $X = \{a, b\}, Y = \{a, b, c\}$. Clearly $\mathcal{M} = \{(\phi, \phi), (X, \{a, c\}), (\{b\}, \{c\}), (X, Y)\}$ is a binary topology from X to Y . Also $(X, Y), (\phi, \{b\}), (\{a\}, \{a, ab\})$ and (ϕ, ϕ) are the binary closed sets in (X, Y, \mathcal{M}) . Then the subsets $(\{a\}, \{b, c\}), (\phi, \{b\}, \{b, c\})$ and (ϕ, Y) are b-gsp-closed sets but not b-sg-closed.

Theorem 3.33. Union of any two b-gsp-closed subset is b-gsp-closed.

Proof: Let (A, B) and (C, D) be any two b-gsp-closed sets in (X, Y) , $(A, B) \subseteq (U, V)$ and $(C, D) \subseteq (U, V)$ where (U, V) is binary open in (X, Y) and so $(A, B) \cup (C, D) \subseteq (U, V)$. Since (A, B) and (C, D) are b-gsp-closed. $(A, B) \subseteq b-spcl(A, B)$ and $(C, D) \subseteq b-spcl(C, D)$ and hence $(A, B) \cup (C, D) \subseteq b-spcl(A, B) \cup b-spcl(C, D) \subseteq b-spcl((A, B) \cup (C, D))$. Thus $(A, B) \cup (C, D)$ is b-gsp-closed set in (X, Y, \mathcal{M}) .

Remark 3.34. Intersection of any two b-gsp-closed subset is b-gsp-closed.

Example 3.35. Let $X = \{a, b\}, Y = \{a, b, c\}$ clearly $\mathcal{M} = \{(\phi, \phi), (\{a\}, \{c\}), (\{a\}, \{a\}), (\{a\}, \{a, c\}), (\{a\}, \phi), (X, Y)\}$ is a binary topology from X to Y . If $(A, B) = (\{a\}, \{c\})$ and $(C, D) = (\{a\}, \{a, c\})$. Then (A, B) and (C, D) are b-gsp-closed sets in (X, Y) , $(A, B) \cap (C, D) = (\{a\}, \{c\})$ is also b-gsp-closed sets in (X, Y) .

Theorem 3.36. Let (A, B) be a b-gsp-closed subset of (X, Y) . If $(A, B) \subseteq (C, D) \subseteq b-spcl(A, B)$ then (C, D) is also b-gsp-closed subset of (X, Y) .





Proof: Let (U,V) be a binary open sets of (X,Y) such that $(C,D) \subseteq (U,V)$. Then $(A,B) \subseteq (U,V)$. Since (A,B) is b-gsp-closed sets $b\text{-spcl}(A,B) \subseteq (U,V)$. Also $(C,D) \subseteq b\text{-spcl}(A,B)$, $b\text{-spcl}(C,D) \subseteq b\text{-spcl}(A,B) \subseteq (U,V)$. Hence (C,D) is also b-gsp-closed subset of (X,Y) .

Theorem 3.37. Let (X,Y,\mathcal{M}) be a binary topological space and $A \subseteq X$, $B \subseteq Y$. Then if (A,B) is b-gsp-closed in (X,Y,\mathcal{M}) then A is b-gsp-closed in (X,\mathcal{M}_X) and B is b-gsp-closed in (Y,\mathcal{M}_Y) .

Proof: Since (A,B) is b-gsp-closed, we have $((X/A),(Y/B))$ is b-gsp-open. Also, since (X,Y,\mathcal{M}) is a binary topological space, we have (X/A) is b-gsp-open in X and (Y/B) is b-gsp-open in Y . Therefore, A is b-gsp-closed in X and B is b-gsp-closed in Y .

Theorem 3.38. Let (X,Y,\mathcal{M}) be a binary topological spaces and $(A,B,\mathcal{M}_{(A,B)})$ is binary subspace of (X,Y,\mathcal{M}) . Let (C,D) be a b-gsp-closed set in (X,Y,\mathcal{M}) and $(C,D) \subseteq (A,B)$. Then (C,D) is a b-gsp-closed in $(A,B,\mathcal{M}_{(A,B)})$.

Proof: Since (C,D) is a b-gsp-closed set in (X,Y,\mathcal{M}) , we have $b\text{-spcl}(C,D) \subseteq (U,V)$ where (U,V) is binary open in (X,Y,\mathcal{M}) and hence it should be in (\mathcal{M}) by definition of a binary subspace, $(U \cap A, V \cap B) \subseteq (\mathcal{M}_{(A,B)})$. Let (U,V) is a binary open sets in $(A,B,\mathcal{M}_{(A,B)})$, since $(C,D) \subseteq (A,B)$, $(C,D) \subseteq (U,V)$, so $b\text{-spcl}(C,D) = b\text{-spcl}(C \cap A, D \cap B) \subseteq b\text{-spcl}(U \cap A, V \cap B) \subseteq (U,V)$. Thus (C,D) is a b-gsp-closed set in $(A,B,\mathcal{M}_{(A,B)})$.

Definition 3.39. A subset (A,B) of a binary topological space (X,Y,\mathcal{M}) is called binary generalized semi pre open set (briefly b-gsp-open set) if its complement is b-gsp-closed.

Theorem 3.40 Let be a (X,Y,\mathcal{M}) binary topological space, then the following statements hold.

1. Every binary open set is b-gsp-open.
2. Every binary semi open set is b-gsp-open.
3. Every binary α -open set is b-gsp-open.
4. Every generalized binary open set is b-gsp-open.
5. Every binary r -open set is b-gsp-open.
6. Every binary sg -open set is b-gsp-open.

Proof: Proof follows from the Theorems 3.21, 3.23, 3.25, 3.27, 3.29, 3.31.

b-gp(b-gsp)-neighbourhood, b-gp(b-gsp)-interior and b-gp(b-gsp)-closure

In this section, we initiate the concept of b-gp(b-gsp)-neighbourhood and we introduce the concept of b-gp(b-gsp)-interior and b-gp(b-gsp)-closure and study some of their characterizations.

Definition 4.1. Let (X,Y,\mathcal{M}) be a binary topological space and let (x,y) be a point of (X,Y) . A subset (N_x, N_y) of (X,Y) is called binary pre neighbourhood of (X,Y) iff there exists a binary pre open set (U,V) such that for $(x,y) \in (U,V) \subseteq (N_x, N_y)$.

Definition 4.2. Let (X,Y,\mathcal{M}) be a binary topological space and let (x,y) be a point of (X,Y) . A subset (N_x, N_y) of (X,Y) is called b-gp-neighbourhood of (X,Y) iff there exists a b-gp-open set (U,V) such that for $(x,y) \in (U,V) \subseteq (N_x, N_y)$.

Example 4.3. Let $X = \{a,b\}$, $Y = \{a,b,c\}$.

Clearly $\mathcal{M} = \{(\phi, \phi), (\{a\}, \{b,c\}), (\{b\}, \{a\}), (X,Y)\}$ is binary topology from X to Y .

b-gp open set = $\{(\phi, \phi), (X, \{b,c\}), (X, \{a,c\}), (X, \{a,b\}), (X, \{c\}), (X, \{b\}), (X, \{a\}), (X, \phi), (\{b\}, Y), (\{b\}, \{b,c\}), (\{b\}, \{a,c\}), (\{b\}, \{a,b\}), (\{b\}, \{c\}), (\{b\}, \{b\}), (\{b\}, \{a\}), (\{b\}, \phi), (\{a\}, Y), (\{a\}, \{b,c\}), (\{a\}, \{a,c\}), (\{a\}, \{a,b\}), (\{a\}, \{c\}), (\{a\}, \{b\}), (\{a\}, \{a\}), (\{a\}, \phi), (\phi, \{a,b\}), (\phi, \{c\}), (\phi, \{b\}), (\phi, \{a\}), (X,Y)\}$. Then

- b-gp-nbhds $(\{a\}, \{a\}) = \{(X, \{a,c\}), (X, \{a,b\}), (X, \{a\}), (\{a\}, Y), (\{a\}, \{a,c\}), (\{a\}, \{a,b\}), (\{a\}, \{a\}), (X,Y)\}$





- $b\text{-gp-nbhds}(\{a\},\{b\})=\{(X,\{b,c\}), (X,\{a,b\}), (X,\{b\}), (\{a\},Y), (\{a\},\{b,c\}), (\{a\},\{a,b\}), (\{a\},\{b\}), (X,Y)\}$
- $b\text{-gp-nbhds}(\{a\},\{c\})=\{(X,\{b,c\}), (X,\{a,c\}), (X,\{c\}), (\{a\},Y), (\{a\},\{b,c\}), (\{a\},\{a,c\}), (\{a\},\{c\}), (X,Y)\}$
- $b\text{-gp-nbhds}(\{b\},\{a\})=\{(X,\{a,c\}), (X,\{a,b\}), (X,\{a\}), (\{b\},Y), (\{b\},\{a,c\}), (\{b\},\{a,b\}), (\{b\},\{a\}), (X,Y)\}$
- $b\text{-gp-nbhds}(\{b\},\{b\})=\{(X,\{b,c\}), (X,\{a,b\}), (X,\{b\}), (\{b\},Y), (\{b\},\{b,c\}), (\{b\},\{a,b\}), (\{b\},\{b\}), (X,Y)\}$
- $b\text{-gp-nbhds}(\{b\},\{c\})=\{(X,\{b,c\}), (X,\{a,c\}), (X,\{c\}), (\{b\},Y), (\{b\},\{b,c\}), (\{b\},\{a,c\}), (\{b\},\{c\}), (X,Y)\}$

Theorem 4.4. Every binary neighbourhood (N_X, N_Y) of (x,y) in (X,Y) is a $b\text{-gp-neighbourhood}$ of (X,Y) .

Proof: Let (N_X, N_Y) be a neighbourhood of point $(x,y) \in (X,Y)$. To prove that (N_X, N_Y) is a $b\text{-gp-neighbourhood}$ of (x,y) by definition of binary neighbourhood, there exists a binary open set (U,V) , such that $(x,y) \in (U,V) \subseteq (N_X, N_Y)$. Hence (N_X, N_Y) is $b\text{-gp-neighbourhood}$ of (X,Y) .

Remark 4.5. For the most part $b\text{-gp-neighbourhood}$ (N_X, N_Y) of $(x,y) \in (X,Y)$ need not be a binary neighbourhood of (x,y) in (X,Y) , as seen from the following example.

Example 4.6. Let $X = \{a,b\}$, $Y = \{a,b,c\}$. Clearly $\mathcal{M} = \{(\phi,\phi), (\{a\},\{c\}), (\{a\},\{a\}), (\{a\},\{a,c\}), (\{a\},\phi), (X,Y)\}$ is a binary topology from X to Y . $b\text{-gp-open} = \{(\phi,\phi), (X,\{b,c\}), (X,\{a,c\}), (X,\{a,b\}), (X,\{c\}), (X,\{b\}), (X,\{a\}), (X,\phi), (\{b\},\{a,c\}), (\{b\},\{c\}), (\{b\},\{a\}), (\{b\},\phi), (\{a\},Y), (\{a\},\{b,c\}), (\{a\},\{a,c\}), (\{a\},\{a,b\}), (\{a\},\{c\}), (\{a\},\{b\}), (\{a\},\{a\}), (\{a\},\phi), (\phi,Y), (\phi,\{b,c\}), (\phi,\{a,c\}), (\phi,\{a,b\}), (\phi,\{c\}), (\phi,\{b\}), (\phi,\{a\}), (X,Y)\}$. Then set $(\{b\},Y)$ is $b\text{-gp-neighbourhood}$ of point $(\{b\},\{c\})$, since the $b\text{-gp open set}$ $(\{b\},\{c\})$ is such that $(\{b\},\{c\}) \in (\{b\},\{c\}) \subseteq (\{b\},Y)$. However the set $(\{b\},Y)$ is not a binary neighbourhood of the point $(\{b\},\{c\})$, since no binary open set (U,V) exists such that $(\{b\},\{c\}) \in (U,V) \subseteq (\{b\},Y)$.

Theorem 4.7. If a subset (N_X, N_Y) of a space (X,Y,\mathcal{M}) is $b\text{-gp open}$ then (N_X, N_Y) is $b\text{-gp neighbourhood}$ of each of its points.

Proof: Suppose (N_X, N_Y) is $b\text{-gp open}$. Let $(x,y) \in (N_X, N_Y)$ we claim that (N_X, N_Y) is $b\text{-gp-neighbourhood}$ of (x,y) for (N_X, N_Y) is a $b\text{-gp open set}$ such that $(x,y) \in (N_X, N_Y) \subseteq (N_X, N_Y)$. Since (x,y) is an arbitrary point of (N_X, N_Y) , it follows that (N_X, N_Y) is a $b\text{-gp-neighbourhood}$ of each of its points.

Theorem 4.8. Let (X,Y,\mathcal{M}) be a binary topological space. If (F,G) is a $b\text{-gp-closed}$ subset of (X,Y) and $(x,y) \in (F,G)^c$, then there exists a $b\text{-gp-neighbourhood}$ (N_X, N_Y) of (x,y) such that $(N_X, N_Y) \cap (F,G) = \phi$.

Proof: Let (F,G) be $b\text{-gp-closed}$ subset of (X,Y) and $(x,y) \in (F,G)^c$. Then $(F,G)^c$ is $b\text{-gp-open}$ subset of (X,Y) so by above theorem, $(F,G)^c$ contains a $b\text{-gp-neighbourhood}$ of each of its points. Hence there exists a $b\text{-gp-neighbourhood}$ (N_X, N_Y) of (x,y) such that $(N_X, N_Y) \subseteq (F,G)^c$. That is $(N_X, N_Y) \cap (F,G) = \phi$.

Definition 4.9. Let (A,B) be a subset of (X,Y) . A point $(x,y) \in (A,B)$ is said to be $b\text{-gp- interior point}$ of (A,B) is a $b\text{-gp-neighbourhood}$ of (x,y) . The set of all $b\text{-gp-interior point}$ (A,B) is called the $b\text{-gp-interior}$ of (A,B) and is denoted by $b\text{-gp-int}(A,B)$.

Theorem 4.10. If (A,B) be a subset of (X,Y) . Then $b\text{-gp-int}(A,B) = \cup\{(U,V) : (U,V) \text{ is } b\text{-gp-open}(U,V) \subseteq (A,B)\}$.

Proof: Let (A,B) be a subset of (X,Y) , $(x,y) \in b\text{-gp-int}(A,B) \Leftrightarrow (x,y)$ is a $b\text{-gp-interior point}$ of $(A,B) \Leftrightarrow (A,B)$ is a $b\text{-gp-neighbourhood point}$ of $(x,y) \Leftrightarrow$ there exists $b\text{-gp- open set}$ (U,V) such that $(x,y) \in (U,V) \subseteq (A,B) \Leftrightarrow (x,y) \in \cup\{(U,V) : (U,V) \text{ is } b\text{-gp- open}, (U,V) \subseteq (A,B)\}$. Hence $b\text{-gp-int}(A,B) = \cup\{(U,V) : (U,V) \text{ is } b\text{-gp-open}, (U,V) \subseteq (A,B)\}$.

Theorem 4.11. Let (A,B) and (C,D) be subset of (X,Y) . Then

1. $b\text{-gp-int}(X,Y) = (X,Y)$ and $b\text{-gp-int}(\phi,\phi) = (\phi,\phi)$.
2. $b\text{-gp-int}(A,B) \subseteq (A,B)$.
3. If (C,D) is any $b\text{-gp-open set}$ contained in (A,B) , then $(C,D) \subseteq b\text{-gp-int}(A,B)$.
4. If $(A,B) \subseteq (C,D)$, then $b\text{-gp-int}(A,B) \subseteq b\text{-gp-int}(C,D)$.





5. $b\text{-gp-int}(b\text{-gp-int}(A,B)) = b\text{-gp-int}(A,B)$.

Proof:

1. Since (X,Y) and (ϕ,ϕ) are $b\text{-gp-open}$ sets, by Theorem 4.10 $b\text{-gp-int}(X,Y) = \bigcup \{(U,V) : (U,V) \text{ is } b\text{-gp-open}, (U,V) \subseteq (X,Y)\} = (X,Y) \cup \{\text{all } b\text{-gp-open sets}\} = (X,Y)$. That is $b\text{-gp-int}(X,Y) = (X,Y)$. Since (ϕ,ϕ) is the only $b\text{-gp-open}$ set contained in (ϕ,ϕ) , $b\text{-gp-int}(\phi,\phi) = (\phi,\phi)$.
2. Let $(x,y) \in b\text{-gp-int}(A,B) \Rightarrow (x,y)$ is a $b\text{-gp-interior point}$ of $(A,B) \Rightarrow (A,B)$ is a $b\text{-gp-neighbourhood}$ of $(x,y) \Rightarrow (x,y) \in (A,B)$. Thus $(x,y) \in b\text{-gp-int}(A,B) \Rightarrow (x,y) \in (A,B)$. Hence $b\text{-gp-int}(A,B) \subseteq (A,B)$.
3. Let (C,D) be any $b\text{-gp-open}$ sets such that $(C,D) \subseteq (A,B)$. Let $(x,y) \in (C,D)$, then since (C,D) is a $b\text{-gp-open}$ set contained in (A,B) , (x,y) is a $b\text{-gp-interior point}$ of (A,B) . That is $(x,y) \in b\text{-gp-int}(A,B)$. Hence $(C,D) \subseteq b\text{-gp-int}(A,B)$.
4. Let (A,B) and (C,D) be subset of (X,Y) such that $(A,B) \subseteq (C,D)$. Let $(x,y) \in b\text{-gp-int}(A,B)$. Then (x,y) is a $b\text{-gp-interior point}$ of (A,B) and so (A,B) is $b\text{-gp-neighbourhood}$ of (x,y) . Since $(A,B) \subseteq (C,D)$, (C,D) is also a $b\text{-gp-neighbourhood}$ of (x,y) . This implies that $(x,y) \in b\text{-gp-int}(C,D)$. Thus we have shown that $(x,y) \in b\text{-gp-int}(A,B) \Rightarrow (x,y) \in b\text{-gp-int}(C,D)$. Hence $b\text{-gp-int}(A,B) \subseteq b\text{-gp-int}(C,D)$.
5. Let (A,B) be any subset of (X,Y) . By the definition of $b\text{-gp-interior}$, $b\text{-gp-int}(A,B)$ is $b\text{-gp-open}$ and hence $b\text{-gp-int}(b\text{-gp-int}(A,B)) = b\text{-gp-int}(A,B)$.

Theorem 4.12. If a subset (A,B) of space (X,Y) is $b\text{-gp-open}$, then $b\text{-gp-int}(A,B) = (A,B)$.

Proof: Let (A,B) be $b\text{-gp-open}$ subset of (X,Y) . We know that $b\text{-gp-int}(A,B) \subseteq (A,B)$. Also, (A,B) is $b\text{-gp-open}$ set contained in (A,B) . From Theorem 4.11.(3) $(A,B) \subseteq b\text{-gp-int}(A,B)$. Hence $b\text{-gp-int}(A,B) = (A,B)$.

Theorem 4.13. If (A,B) and (C,D) are subsets of (X,Y) , then $b\text{-gp-int}(A,B) \cup b\text{-gp-int}(C,D) \subseteq b\text{-gp-int}((A,B) \cup (C,D))$.

Proof: We know that $(A,B) \subseteq ((A,B) \cup (C,D))$ and $(C,D) \subseteq ((A,B) \cup (C,D))$. We have, by Theorem 4.11.(4), $b\text{-gp-int}(A,B) \subseteq b\text{-gp-int}((A,B) \cup (C,D))$ and $b\text{-gp-int}(C,D) \subseteq b\text{-gp-int}((A,B) \cup (C,D))$. This implies that $b\text{-gp-int}(A,B) \cup b\text{-gp-int}(C,D) \subseteq b\text{-gp-int}((A,B) \cup (C,D))$.

Theorem 4.14. If (A,B) and (C,D) are subsets of space (X,Y) then $b\text{-gp-int}((A,B) \cap (C,D)) = b\text{-gp-int}(A,B) \cap b\text{-gp-int}(C,D)$.

Proof: We know that $(A,B) \cap (C,D) \subseteq (A,B)$ and $(A,B) \cap (C,D) \subseteq (C,D)$. We have, by Theorem 4.11.(4), $b\text{-gp-int}((A,B) \cap (C,D)) \subseteq b\text{-gp-int}(A,B)$ and $b\text{-gp-int}((A,B) \cap (C,D)) \subseteq b\text{-gp-int}(C,D)$. This implies that $b\text{-gp-int}((A,B) \cap (C,D)) \subseteq b\text{-gp-int}(A,B) \cap b\text{-gp-int}(C,D) \rightarrow (1)$. Again, let $(x,y) \in b\text{-gp-int}(A,B) \cap b\text{-gp-int}(C,D)$. Then $(x,y) \in b\text{-gp-int}(A,B)$ and $(x,y) \in b\text{-gp-int}(C,D)$. Hence (x,y) is a $b\text{-gp-interior point}$ of each of sets (A,B) and (C,D) . It follows that (A,B) and (C,D) are $b\text{-gp-neighbourhoods}$ of (x,y) , so that their intersection $(A,B) \cap (C,D)$ is also a $b\text{-gp-neighbourhood}$ of (x,y) . Hence $(x,y) \in b\text{-gp-int}((A,B) \cap (C,D))$. Thus $(x,y) \in b\text{-gp-int}(A,B) \cap b\text{-gp-int}(C,D)$ implies that $(x,y) \in b\text{-gp-int}((A,B) \cap (C,D))$. Therefore $b\text{-gp-int}(A,B) \cap b\text{-gp-int}(C,D) \subseteq b\text{-gp-int}((A,B) \cap (C,D)) \rightarrow (2)$. From (1) and (2), we get $b\text{-gp-int}((A,B) \cap (C,D)) = b\text{-gp-int}(A,B) \cap b\text{-gp-int}(C,D)$.

Theorem 4.15. If (A,B) is a subset of (X,Y) , then $b\text{-int}(A,B) \subseteq b\text{-gp-int}(A,B)$.

Proof: Let (A,B) be a subset of a space (X,Y) . Let $(x,y) \in b\text{-int}(A,B)$

$\Rightarrow (x,y) \in \bigcup \{(U,V) : (U,V) \text{ is binary open}, (U,V) \subseteq (A,B)\}$.

\Rightarrow there exists a binary open set (U,V) such that $(x,y) \in (U,V) \subseteq (A,B)$.

\Rightarrow there exists a $b\text{-gp-open}$ set (U,V) such that $(x,y) \in (U,V) \subseteq (A,B)$, as every binary open set is a $b\text{-gp-open}$ set in (X,Y) .

$\Rightarrow (x,y) \in \bigcup \{(U,V) : (U,V) \text{ is } b\text{-gp-open}, (U,V) \subseteq (A,B)\}$.

$\Rightarrow (x,y) \in b\text{-gp-int}(A,B)$. Thus $(x,y) \in b\text{-int}(A,B) \Rightarrow (x,y) \in b\text{-gp-int}(A,B)$.

Hence $b\text{-int}(A,B) \subseteq b\text{-gp-int}(A,B)$.





Definition 4.16. Let (A,B) be a subset of a space (X,Y) . We define the b -gp-closure of (A,B) to be the intersection of all b -gp-closed sets containing (A,B) , is denoted by $b\text{-gp-cl}(A,B) = \cap\{(F,G) : (A,B) \subseteq (F,G) \in b\text{-gp-C}(X,Y)\}$.

Theorem 4.17. If (A,B) and (C,D) are subsets of a space (X,Y) . Then

1. $b\text{-gp-cl}(X,Y) = (X,Y)$ and $b\text{-gp-cl}(\phi, \phi) = (\phi, \phi)$.
2. $(A,B) \subseteq b\text{-gp-cl}(A,B)$.
3. If (C,D) is any b -gp-closed set containing (A,B) then $b\text{-gp-cl}(A,B) \subseteq (C,D)$.
4. If $(A,B) \subseteq (C,D)$ then $b\text{-gp-cl}(A,B) \subseteq b\text{-gp-cl}(C,D)$.
5. $b\text{-gp-cl}(A,B) = b\text{-gp-cl}(b\text{-gp-cl}(A,B))$.

Proof:

1. By the definition of b -gp closure, (X,Y) is the only b -gp closed set containing (X,Y) . Therefore $b\text{-gp-cl}(X,Y) = \text{Intersection of all the } b\text{-gp closed sets containing } (X,Y) = \cap\{X,Y\} = (X,Y)$. That is $b\text{-gp-cl}(X,Y) = (X,Y)$. By the definition of b -gp-closure, $b\text{-gp-cl}(\phi, \phi) = \text{Intersection of all the } b\text{-gp closed sets containing } (\phi, \phi) = (\phi, \phi)$. That is $b\text{-gp-cl}(\phi, \phi) = (\phi, \phi)$.
2. By the definition of b -gp-closure of (A,B) , it is obvious that $(A,B) \subseteq b\text{-gp-cl}(A,B)$.
3. Let (C,D) be any b -gp-closed set containing (A,B) . Since $b\text{-gp-cl}(A,B)$ is the intersection of all b -gp-closed sets containing (A,B) , $b\text{-gp-cl}(A,B)$ is contained in every b -gp-closed set containing (A,B) . Hence in particular $b\text{-gp-cl}(A,B) \subseteq (C,D)$.
4. Let (A,B) and (C,D) be subsets of (X,Y) such that $(A,B) \subseteq (C,D)$. By the definition of b -gp-closure, $b\text{-gp-cl}(C,D) = \cap\{(F,G) : (C,D) \subseteq (F,G) \in b\text{-gp-C}(X,Y)\}$. If $(C,D) \subseteq (F,G) \in b\text{-gp-C}(X,Y)$, then $b\text{-gp-cl}(C,D) \subseteq (F,G)$. Since $(A,B) \subseteq (C,D)$, $(A,B) \subseteq (C,D) \subseteq (F,G) \in b\text{-gp-C}(X,Y)$, we have $b\text{-gp-cl}(A,B) \subseteq (F,G)$. Therefore $b\text{-gp-cl}(A,B) \subseteq \cap\{(F,G) : (C,D) \subseteq (F,G) \in b\text{-gp-C}(X,Y)\} = b\text{-gp-cl}(C,D)$. That is $b\text{-gp-cl}(A,B) \subseteq b\text{-gp-cl}(C,D)$.
5. Let (A,B) be any subset of (X,Y) . By the definition of b -gp-closure, $b\text{-gp-cl}(A,B) = \cap\{(F,G) : (A,B) \subseteq (F,G) \in b\text{-gp-C}(X,Y)\}$. If $(A,B) \subseteq (F,G) \in b\text{-gp-C}(X,Y)$, then $b\text{-gp-cl}(A,B) \subseteq (F,G)$. Since (F,G) is b -gp-closed set containing $b\text{-gp-cl}(A,B)$, by (3) $b\text{-gp-cl}(b\text{-gp-cl}(A,B)) \subseteq (F,G)$. Hence $b\text{-gp-cl}(b\text{-gp-cl}(A,B)) \subseteq \cap\{(F,G) : (A,B) \subseteq (F,G) \in b\text{-gp-C}(X,Y)\} = b\text{-gp-cl}(A,B)$. That is $b\text{-gp-cl}(b\text{-gp-cl}(A,B)) = b\text{-gp-cl}(A,B)$.

Definition 4.18. Let (X,Y,\mathcal{M}) be a binary topological space and let (x,y) be a point of (X,Y) . A subset (N_x, N_y) of (X,Y) is called b -gsp-neighbourhood of (X,Y) iff there exists a b -gsp-openset (U,V) such that for $(x,y) \in (U,V) \subseteq (N_x, N_y)$.

Example 4.19. Let $tX = \{a,b\}$, $Y = \{a,b,c\}$. Clearly $\mathcal{M} = \{(\phi, \phi), (\{a\}, \{b,c\}), (\{b\}, \{a\}), (X,Y)\}$ is a binary topology from X to Y . b -gsp-openset $= \{(\phi, \phi), (X, \{b,c\}), (X, \{a,c\}), (X, \{a,b\}), (X, \{c\}), (X, \{b\}), (X, \{a\}), (X, \phi), (\{b\}, Y), (\{b\}, \{b,c\}), (\{b\}, \{a,c\}), (\{b\}, \{a,b\}), (\{b\}, \{c\}), (\{b\}, \{b\}), (\{b\}, \{a\}), (\{b\}, \phi), (\{a\}, Y), (\{a\}, \{b,c\}), (\{a\}, \{a,c\}), (\{a\}, \{a,b\}), (\{a\}, \{c\}), (\{a\}, \{b\}), (\{a\}, \{a\}), (\{a\}, \phi), (\phi, \{a,b\}), (\phi, \{c\}), (\phi, \{b\}), (\phi, \{a\}), (X,Y)\}$. Then

- $b\text{-gsp-nbhds}(\{a\}, \{a\}) = \{(X, \{a,c\}), (X, \{a,b\}), (X, \{a\}), (\{a\}, Y), (\{a\}, \{a,c\}), (\{a\}, \{a,b\}), (\{a\}, \{a\}), (X,Y)\}$
- $b\text{-gsp-nbhds}(\{a\}, \{b\}) = \{(X, \{b,c\}), (X, \{a,b\}), (X, \{b\}), (\{a\}, Y), (\{a\}, \{b,c\}), (\{a\}, \{a,b\}), (\{a\}, \{b\}), (X,Y)\}$
- $b\text{-gsp-nbhds}(\{a\}, \{c\}) = \{(X, \{b,c\}), (X, \{a,c\}), (X, \{c\}), (\{a\}, Y), (\{a\}, \{b,c\}), (\{a\}, \{a,c\}), (\{a\}, \{c\}), (X,Y)\}$
- $b\text{-gsp-nbhds}(\{b\}, \{a\}) = \{(X, \{a,c\}), (X, \{a,b\}), (X, \{a\}), (\{b\}, Y), (\{b\}, \{a,c\}), (\{b\}, \{a,b\}), (\{b\}, \{a\}), (X,Y)\}$
- $b\text{-gsp-nbhds}(\{b\}, \{b\}) = \{(X, \{b,c\}), (X, \{a,b\}), (X, \{b\}), (\{b\}, Y), (\{b\}, \{b,c\}), (\{b\}, \{a,b\}), (\{b\}, \{b\}), (X,Y)\}$
- $b\text{-gsp-nbhds}(\{b\}, \{c\}) = \{(X, \{b,c\}), (X, \{a,c\}), (X, \{c\}), (\{b\}, Y), (\{b\}, \{b,c\}), (\{b\}, \{a,c\}), (\{b\}, \{c\}), (X,Y)\}$

Theorem 4.20. Every binary neighbourhood (N_x, N_y) of (x,y) in (X,Y) is a b -gsp neighbourhood of (X,Y) .

Proof: Let (N_x, N_y) be a neighbourhood of point $(x,y) \in (X,Y)$. To prove that (N_x, N_y) is a b -gsp-neighbourhood of (x,y) by definition of binary neighbourhood, there exists a binary open set (U,V) , such that $(x,y) \in (U,V) \subseteq (N_x, N_y)$. Hence (N_x, N_y) is b -gsp- neighbourhood of (X,Y) .





Remark 4.21. For the most part $b\text{-gsp-neighbourhood } (N_x, N_y)$ of $(x, y) \in (X, Y)$ need not be a binary neighbourhood of (x, y) in (X, Y) as seen from the following example.

Example 4.22. Let $X = \{a, b\}$, $Y = \{a, b, c\}$. Clearly $\mathcal{M} = \{(\phi, \phi), (\{a\}, \{c\}), (\{a\}, \{a\}), (\{a\}, \{a, c\}), (\{a\}, \phi), (X, Y)\}$ is a binary topology from X to Y . $b\text{-gsp-open} = \{(\phi, \phi), (X, \{b, c\}), (X, \{a, c\}), (X, \{a, b\}), (X, \{c\}), (X, \{b\}), (X, \{a\}), (X, \phi), (\{b\}, \{a, c\}), (\{b\}, \{c\}), (\{b\}, \{a\}), (\{b\}, \phi), (\{a\}, Y), (\{a\}, \{b, c\}), (\{a\}, \{a, c\}), (\{a\}, \{a, b\}), (\{a\}, \{c\}), (\{a\}, \{b\}), (\{a\}, \{a\}), (\{a\}, \phi), (\phi, Y), (\phi, \{b, c\}), (\phi, \{a, c\}), (\phi, \{a, b\}), (\phi, \{c\}), (\phi, \{b\}), (\phi, \{a\}), (X, Y)\}$. Then set $(\{b\}, Y)$ is $b\text{-gsp-neighbourhood}$ of point $(\{b\}, \{c\})$, since the $b\text{-gsp-open}$ set $(\{b\}, \{c\})$ is such that $(\{b\}, \{c\}) \in (\{b\}, \{c\}) \subseteq (\{b\}, Y)$. However the set $(\{b\}, Y)$ is not a binary neighbourhood of the point $(\{b\}, \{c\})$, since no $b\text{-gsp-open}$ set (U, V) exists such that $(\{b\}, \{c\}) \in (U, V) \subseteq (\{b\}, Y)$.

Theorem 4.23. If a subset (N_x, N_y) of a space (X, Y, \mathcal{M}) is $b\text{-gsp-open}$ then (N_x, N_y) is $b\text{-gsp neighbourhood}$ of each of its points.

Proof: Suppose (N_x, N_y) is $b\text{-gsp-open}$. Let $(x, y) \in (N_x, N_y)$ we claim that (N_x, N_y) is $b\text{-gsp-neighbourhood}$ of (x, y) for (N_x, N_y) is a $b\text{-gsp-open}$ set such that $(x, y) \in (N_x, N_y) \subseteq (N_x, N_y)$. Since (x, y) is an arbitrary point of (N_x, N_y) , it follows that (N_x, N_y) is a $b\text{-gsp-neighbourhood}$ of each of its points.

Theorem 4.24. Let (X, Y, \mathcal{M}) be a binary topological space. If (F, G) is a $b\text{-gsp-closed}$ subset of (X, Y) and $(x, y) \in (F, G)^c$, then there exists a $b\text{-gsp-neighbourhood } (N_x, N_y)$ of (x, y) such that $(N_x, N_y) \cap (F, G) = \phi$.

Proof: Let (F, G) be $b\text{-gsp-closed}$ subset of (X, Y) and $(x, y) \in (F, G)^c$. Then $(F, G)^c$ is $b\text{-gsp-open}$ subset of (X, Y) so by above theorem, $(F, G)^c$ contains a $b\text{-gsp-neighbourhood}$ of each of its points. Hence there exists a $b\text{-gsp-neighbourhood } (N_x, N_y)$ of (x, y) such that $(N_x, N_y) \subseteq (F, G)^c$. That is $(N_x, N_y) \cap (F, G) = \phi$.

Definition 4.25. Let (A, B) be a subset of (X, Y) . A point $(x, y) \in (A, B)$ is said to be $b\text{-gsp- interior point}$ of (A, B) is a $b\text{-gsp-neighbourhood}$ of (x, y) . The set of all $b\text{-gsp- interior point}$ (A, B) is called the $b\text{-gsp-interior}$ of (A, B) and is denoted by $b\text{-gsp- int}(A, B)$.

Theorem 4.26. If (A, B) be a subset of (X, Y) . Then $b\text{-gsp-int}(A, B) = \bigcup \{(U, V) : (U, V) \text{ is } b\text{-gsp-open}, (U, V) \subseteq (A, B)\}$.

Proof: Let (A, B) be a subset of (X, Y) , $(x, y) \in b\text{-gsp-int}(A, B) \Leftrightarrow (x, y)$ is a $b\text{-gsp-interior point}$ of $(A, B) \Leftrightarrow (A, B)$ is a $b\text{-gsp-neighbourhood point}$ of $(x, y) \Leftrightarrow$ there exists $b\text{-gsp-open}$ set (U, V) such that $(x, y) \in (U, V) \subseteq (A, B) \Leftrightarrow (x, y) \in \bigcup \{(U, V) : (U, V) \text{ is } b\text{-gsp-open}, (U, V) \subseteq (A, B)\}$. Hence $b\text{-gsp-int}(A, B) = \bigcup \{(U, V) : (U, V) \text{ is } b\text{-gsp-open}, (U, V) \subseteq (A, B)\}$.

Theorem 4.26. Let (A, B) and (C, D) be subset of (X, Y) . Then

1. $b\text{-gsp-int}(X, Y) = (X, Y)$ and $b\text{-gsp-int}(\phi, \phi) = (\phi, \phi)$.
2. $b\text{-gsp-int}(A, B) \subseteq (A, B)$.
3. If (C, D) is any $b\text{-gsp-open}$ set contained in (A, B) , then $(C, D) \subseteq b\text{-gsp-int}(A, B)$.
4. If $(A, B) \subseteq (C, D)$, then $b\text{-gsp-int}(A, B) \subseteq b\text{-gsp-int}(C, D)$.
5. $b\text{-gsp-int}(b\text{-gsp-int}(A, B)) = b\text{-gsp-int}(A, B)$.

Proof:

1. Since (X, Y) and (ϕ, ϕ) are $b\text{-gsp-open}$ sets, by Theorem 4.10 $b\text{-gsp-int}(X, Y) = \bigcup \{(U, V) : (U, V) \text{ is } b\text{-gsp-open}, (U, V) \subseteq (X, Y)\} = (X, Y) \cup \{\text{all } b\text{-gsp-open sets}\} = (X, Y)$. That is $b\text{-gsp-int}(X, Y) = (X, Y)$. Since (ϕ, ϕ) is the only $b\text{-gsp-open}$ set contained in (ϕ, ϕ) , $b\text{-gsp-int}(\phi, \phi) = (\phi, \phi)$.
2. Let $(x, y) \in b\text{-gsp-int}(A, B) \Rightarrow (x, y)$ is a $b\text{-gsp-interior point}$ of $(A, B) \Rightarrow (A, B)$ is a $b\text{-gsp-neighbourhood}$ of $(x, y) \Rightarrow (x, y) \in (A, B)$. Thus $(x, y) \in b\text{-gsp-int}(A, B) \Rightarrow (x, y) \in (A, B)$. Hence $b\text{-gsp-int}(A, B) \subseteq (A, B)$.
3. Let (C, D) be any $b\text{-gsp-open}$ sets such that $(C, D) \subseteq (A, B)$. Let $(x, y) \in (C, D)$, then since (C, D) is a $b\text{-gsp-open}$ set contained in (A, B) , (x, y) is a $b\text{-gsp-interior point}$ of (A, B) . That is $(x, y) \in b\text{-gsp-int}(A, B)$. Hence $(C, D) \subseteq b\text{-gsp-int}(A, B)$.





4. Let (A,B) and (C,D) be subset of (X,Y) such that $(A,B) \subseteq (C,D)$. Let $(x,y) \in \text{b-gsp-int}(A,B)$. Then (x,y) is a b-gsp-interior point of (A,B) and so (A,B) is b-gsp-neighbourhood of (x,y) . Since $(A,B) \subseteq (C,D)$, (C,D) is also a b-gsp-neighbourhood of (x,y) . This implies that $(x,y) \in \text{b-gsp-int}(C,D)$. Thus we have shown that $(x,y) \in \text{b-gsp-int}(A,B) \Rightarrow (x,y) \in \text{b-gsp-int}(C,D)$. Hence $\text{b-gsp-int}(A,B) \subseteq \text{b-gsp-int}(C,D)$.
5. Let (A,B) be any subset of (X,Y) . By the definition of b-gsp-interior, $\text{b-gsp-int}(A,B)$ is b-gsp-open and hence $\text{b-gsp-int}(\text{b-gsp-int}(A,B)) = \text{b-gsp-int}(A,B)$.

Theorem 4.27. If a subset (A,B) of space (X,Y) is b-gsp-open, then $\text{b-gsp-int}(A,B) = (A,B)$.

Proof: Let (A,B) be b-gsp-open subset of (X,Y) . We know that $\text{b-gsp-int}(A,B) \subseteq (A,B)$. Also, (A,B) is b-gsp-open set contained in (A,B) . From Theorem 4.26.(3) $(A,B) \subseteq \text{b-gsp-int}(A,B)$. Hence $\text{b-gsp-int}(A,B) = (A,B)$.

Theorem 4.28. If (A,B) and (C,D) are subsets of (X,Y) , then $\text{b-gsp-int}(A,B) \cup \text{b-gsp-int}(C,D) \subseteq \text{b-gsp-int}((A,B) \cup (C,D))$.

Proof: We know that $(A,B) \subseteq ((A,B) \cup (C,D))$ and $(C,D) \subseteq ((A,B) \cup (C,D))$. We have, by Theorem 4.26.(4), $\text{b-gsp-int}(A,B) \subseteq \text{b-gsp-int}((A,B) \cup (C,D))$ and $\text{b-gsp-int}(C,D) \subseteq \text{b-gsp-int}((A,B) \cup (C,D))$. This implies that $\text{b-gsp-int}(A,B) \cup \text{b-gsp-int}(C,D) \subseteq \text{b-gsp-int}((A,B) \cup (C,D))$.

Theorem 4.29. If (A,B) and (C,D) are subsets of space (X,Y) then $\text{b-gsp-int}((A,B) \cap (C,D)) = \text{b-gsp-int}(A,B) \cap \text{b-gsp-int}(C,D)$.

Proof: We know that $(A,B) \cap (C,D) \subseteq (A,B)$ and $(A,B) \cap (C,D) \subseteq (C,D)$. We have, by Theorem 4.26.(4), $\text{b-gsp-int}((A,B) \cap (C,D)) \subseteq \text{b-gsp-int}(A,B)$ and $\text{b-gsp-int}((A,B) \cap (C,D)) \subseteq \text{b-gsp-int}(C,D)$. This implies that $\text{b-gsp-int}((A,B) \cap (C,D)) \subseteq \text{b-gsp-int}(A,B) \cap \text{b-gsp-int}(C,D) \rightarrow (1)$. Again, let $(x,y) \in \text{b-gsp-int}(A,B) \cap \text{b-gsp-int}(C,D)$. Then $(x,y) \in \text{b-gsp-int}(A,B)$ and $(x,y) \in \text{b-gsp-int}(C,D)$. Hence (x,y) is a b-gsp-interior point of each of sets (A,B) and (C,D) . It follows that (A,B) and (C,D) are b-gsp-neighbourhoods of (x,y) , so that their intersection $(A,B) \cap (C,D)$ is also a b-gsp-neighbourhood of (x,y) . Hence $(x,y) \in \text{b-gsp-int}((A,B) \cap (C,D))$. Thus $(x,y) \in \text{b-gsp-int}(A,B) \cap \text{b-gsp-int}(C,D)$ implies that $(x,y) \in \text{b-gsp-int}((A,B) \cap (C,D))$. Therefore $\text{b-gsp-int}(A,B) \cap \text{b-gsp-int}(C,D) \subseteq \text{b-gsp-int}((A,B) \cap (C,D)) \rightarrow (2)$. From (1) and (2), we get $\text{b-gsp-int}((A,B) \cap (C,D)) = \text{b-gsp-int}(A,B) \cap \text{b-gsp-int}(C,D)$.

Theorem 4.30. If (A,B) is a subset of (X,Y) , then $\text{b-int}(A,B) \subseteq \text{b-gsp-int}(A,B)$.

Proof: Let (A,B) be a subset of a space (X,Y) . Let $(x,y) \in \text{b-int}(A,B)$

$\Rightarrow (x,y) \in \bigcup \{(U,V) : (U,V) \text{ is binary open, } (U,V) \subseteq (A,B)\}$.

\Rightarrow there exists a binary open set (U,V) such that $(x,y) \in (U,V) \subseteq (A,B)$.

\Rightarrow there exists a b-gsp open set (U,V) such that $(x,y) \in (U,V) \subseteq (A,B)$, as every binary open set is a b-gsp open set in (X,Y) .

$\Rightarrow (x,y) \in \bigcup \{(U,V) : (U,V) \text{ is b-gsp open, } (U,V) \subseteq (A,B)\}$.

$\Rightarrow (x,y) \in \text{b-gsp-int}(A,B)$. Thus $(x,y) \in \text{b-int}(A,B) \Rightarrow (x,y) \in \text{b-gsp-int}(A,B)$.

Hence $\text{b-int}(A,B) \subseteq \text{b-gsp-int}(A,B)$.

Definition 4.31. Let (A,B) be a subset of a space (X,Y) . We define the b-gsp closure of (A,B) to be the intersection of all b-gsp closed sets containing (A,B) , is denoted by $\text{b-gsp cl}(A,B) = \bigcap \{(F,G) : (A,B) \subseteq (F,G) \in \text{b-gsp } C(X,Y)\}$.

Theorem 4.32. If (A,B) and (C,D) are subsets of a space (X,Y) . Then

1. $\text{b-gsp cl}(X,Y) = (X,Y)$ and $\text{b-gsp cl}(\phi, \phi) = (\phi, \phi)$.
2. $(A,B) \subseteq \text{b-gsp cl}(A,B)$.
3. If (C,D) is any b-gsp closed set containing (A,B) then $\text{b-gsp cl}(A,B) \subseteq (C,D)$.
4. If $(A,B) \subseteq (C,D)$ then $\text{b-gsp cl}(A,B) \subseteq \text{b-gsp cl}(C,D)$.
5. $\text{b-gsp cl}(A,B) = \text{b-gsp cl}(\text{b-gsp cl}(A,B))$.



**Proof:**

1. By the definition of b-gsp closure, (X, Y) is the only b-gsp closed set containing (X, Y) . Therefore $\text{b-gsp cl}(X, Y) = \text{Intersection of all the b-gsp closed sets containing } (X, Y) = \cap\{X, Y\} = (X, Y)$. That is $\text{b-gsp cl}(X, Y) = (X, Y)$. By the definition of b-gsp closure, $\text{b-gp cl}(\phi, \phi) = \text{Intersection of all the b-gsp closed sets containing } (\phi, \phi) = \cap(\phi, \phi) = (\phi, \phi)$. That is $\text{b-gp cl}(\phi, \phi) = (\phi, \phi)$.
2. By the definition of b-gsp closure of (A, B) , it is obvious that $(A, B) \subseteq \text{b-gsp cl}(A, B)$.
3. Let (C, D) be any b-gsp closed set containing (A, B) . Since $\text{b-gsp cl}(A, B)$ is the intersection of all b-gsp closed sets containing (A, B) , $\text{b-gsp cl}(A, B)$ is contained in every b-gsp closed set containing (A, B) . Hence in particular $\text{b-gsp cl}(A, B) \subseteq (C, D)$.
4. Let (A, B) and (C, D) be subsets of (X, Y) such that $(A, B) \subseteq (C, D)$. By the definition of b-gsp closure, $\text{b-gsp cl}(C, D) = \cap\{(F, G) : (C, D) \subseteq (F, G) \in \text{b-gsp } C(X, Y)\}$. If $(C, D) \subseteq (F, G) \subseteq \text{b-gsp } C(X, Y)$, then $\text{b-gsp cl}(C, D) \subseteq (F, G)$. Since $(A, B) \subseteq (C, D)$, $(A, B) \subseteq (C, D) \subseteq (F, G) \in \text{b-gsp } C(X, Y)$, we have $\text{b-gsp cl}(A, B) \subseteq (F, G)$. Therefore $\text{b-gsp cl}(A, B) \subseteq \cap\{(F, G) : (C, D) \subseteq (F, G) \in \text{b-gsp } C(X, Y)\} = \text{b-gsp cl}(C, D)$. That is $\text{b-gsp cl}(A, B) \subseteq \text{b-gsp cl}(C, D)$.
5. Let (A, B) be any subset of (X, Y) . By the definition of b-gsp closure, $\text{b-gsp cl}(A, B) = \cap\{(F, G) : (A, B) \subseteq (F, G) \in \text{b-gsp } C(X, Y)\}$. If $(A, B) \subseteq (F, G) \in \text{b-gsp } C(X, Y)$, then $\text{b-gsp cl}(A, B) \subseteq (F, G)$. Since (F, G) is b-gsp closed set containing $\text{b-gsp cl}(A, B)$, by (3) $\text{b-gsp cl}(\text{b-gsp cl}(A, B)) \subseteq (F, G)$. Hence $\text{b-gsp cl}(\text{b-gsp cl}(A, B)) \subseteq \cap\{(F, G) : (A, B) \subseteq (F, G) \in \text{b-gsp } C(X, Y)\} = \text{b-gsp cl}(A, B)$. That is $\text{b-gsp cl}(\text{b-gsp cl}(A, B)) = \text{b-gsp cl}(A, B)$.

CONCLUSION

In this paper, we had introduced and studied the concept of b-gp(b-gsp) closed sets, b-gp(b-gsp) open sets, b-gp(b-gsp) neighbourhoods, b-gp(b-gsp) interior and b-gp(b-gsp) closure of a set using the concept of b-gp(b-gsp) open sets in binary topological spaces and interrogate some of their characterizations. Further we obtained some important results, such as for every binary neighbourhood is b-gp(b-gsp) neighbourhood, binary gp(b-gsp) interior of space $(X, Y) = (X, Y)$ and binary gp(b-gsp) interior of empty set is empty set. Also we found the subset (C, D) is any b-gp(b-gsp) closed set containing (A, B) then $\text{b-gp(b-gsp) cl}(A, B) \subseteq (C, D)$.

ACKNOWLEDGEMENT

The authors would like to thank the referees for this beneficial approach which led to the enhancement of this paper.

REFERENCES

1. Jayalakshmi. S and Manonmani. A, Binary regular beta closed sets and Binary regular beta open sets in Binary topological spaces, The International Journal of Analytical and Experimental Modal Analysis, 12(4), 2020, 494-497.
2. Levine. N, Generalized closed sets in topology, Rendiconti del Circolo Matematico di Palermo, 19(2), 1970, 89-96.
3. Noiri. T, Maki. H and Umehara. J, Generalized pre closed functions, Memoirs of the faculty of science, Kochi University Series A Mathematics, 19, 1998, 13-20.
4. Nithyanantha Jothi. S and Thangavelu. P, Topology between two sets, Journal of Mathematical Sciences and Computer Applications, 1(3), 2011, 95-107.
5. Nithyanantha Jothi. S and Thangavelu. P, Generalized binary closed sets in binary topological spaces, Ultra Scientist of Physical Sciences, 26(1)A, 2014, 25-30.
6. Nithyanantha Jothi. S and Thangavelu. P, Generalized Binary Regular Closed Sets, IRA International Journal





Sathishmohan et al.,

- of Applied Sciences, 4(2), 2016, 259-263
7. Nithyanantha Jothi. S, Binary Semi Open Sets in Binary Topological Spaces, International Journal of Mathematical Archive, 7(9), 2016, 73-76.
 8. Sathishmohan. P, Lavanya. K and Mehar sudha. U, On b-gs-closed and b-sg-closed sets in Binary Topological spaces, Strad Research, 8(3), 2021, 20-24.
 9. Sathishmohan. P, Rajendran.V, Lavanya.K and Rajalakshmi.K ,On b-gs(b-sg) closure and b-gs(b-sg) interior of a sets in Binary Topological Spaces, Gedrag & Organisatie Review, 34(1), 2021, 359-366.





Between $N\theta$ -Closed Sets and N-Closed Sets

T. Chandralekha^{1*} and P. Periyasamy²

¹Research Scholar (Reg. No: 20212102092007), PG and Research Department of Mathematics, Kamaraj College, Thoothukudi, (Affiliated to Manonmaniam Sundaranar University, Abishekapatti, Tirunelveli) Tamil Nadu, India.

²Associate Professor, PG and Research Department of Mathematics, Kamaraj College, Thoothukudi, (Affiliated to Manonmaniam Sundaranar University, Abishekapatti, Tirunelveli) Tamil Nadu, India.

Received: 22 Jan 2024

Revised: 09 Feb 2024

Accepted: 04 May 2024

*Address for Correspondence

T. Chandralekha

Research Scholar (Reg. No: 20212102092007),

PG and Research Department of Mathematics,

Kamaraj College, Thoothukudi,

(Affiliated to Manonmaniam Sundaranar University, Abishekapatti, Tirunelveli)

Tamil Nadu, India.

Email: lekhanila@gmail.com.



This is an Open Access Journal / article distributed under the terms of the **Creative Commons Attribution License** (CC BY-NC-ND 3.0) which permits unrestricted use, distribution, and reproduction in any medium, provided the original work is properly cited. All rights reserved.

ABSTRACT

We investigate the notion of $N\theta$ -I closed sets in nano ideal topological space using the nano ideal closure operator $Ncl_{\theta}^*(F) = \{x \in U / Ncl^*(Z) \cap F \neq \emptyset, \text{ for every } Z \in N(x)\}$. Also, study some topological properties of $N\theta$ -I-interior, $N\theta$ -I-derived set, $N\theta$ -I-border, $N\theta$ -I-frontier and $N\theta$ -I-exterior in this space. The collection described here are properly lies in the middle of $N\theta$ -closed sets and N-closed sets.

Keywords: nano ideal topological space, N-closed set, $N\theta$ -closed set, $N\theta$ -I-closed sets, $N\theta$ -I-open sets.

1. INTRODUCTION

In a topological space, introduced ideals [10] were done by Kuratowski. A non-empty sub-collection I of $P(U)$ is defined as an ideal if it satisfies: 1. Heredity: $F \in I$ and $H \subseteq F$ implies $H \in I$, and 2. Finite additivity: $F \in I$, $H \in I$ implies $H \cup F \in I$. It was the work of Vaidhyanathaswamy [14], Joseph et al. [6], and Dontchev et al. [5] which was explored the characteristics of ideal topological spaces. The first step of nano topological space was initiated by Lellis Thivagar et al. [8] in the year of 2013. Let U be a universe and R be an equivalence relation on U . Take $X \subseteq U$ which is defined in terms of lower and upper approximations and boundary region on it. The pair (U, N) is called the nano topological space. The members of nano topological space are said to be nano open sets in U , and its complements are denoted by nano closed sets or simply write N-opn sets and N-cld sets, respectively. They also defined the nano interior and nano closure, namely $Nint$ and Ncl , respectively. The structure of nano ideal topological space was





found by Parimala et al. [11, 12, 13] and also discussed its basic characteristics in this space. A nano topological space (U, N) with ideal I on U is called a nano ideal topological space [13] or simply mentioned by (U, N, I) . In 1968, a subclass of closed set namely θ -closed set was defined by Velicko [15]. Dickman et al. [3, 4], Joseph [7], Long et al. [9], and M. Caldas et al. [2] continued the work of Velicko. Akdag [1] introduced and investigated the concept of θ -I-open sets. In a topological space (X, τ) , a subset F is defined as θ -I-closed if $\text{cl}_\theta^*(F) = F$ where $\text{cl}_\theta^*(F) = \{x \in X / \text{cl}^*(U) \cap F \neq \emptyset \text{ for every } U \in \tau(x)\}$. The motive of this article is to investigate the concept of $N\theta$ -I-open sets and the important properties of $N\theta$ -I-interior, $N\theta$ -I-derived set, $N\theta$ -I-border, $N\theta$ -I-frontier and $N\theta$ -I-exterior of nano ideal topological space or simply NITS.

2. $N\theta$ -I-OPEN SETS

Definition 2.1 In an NITS (U, N, I) , $F \subseteq U$. Then, the closure operator called nano ideal theta closure of $F \subseteq U$ is defined as: 1. $\text{Ncl}_\theta^*(F) = \{x \in U / \text{Ncl}^*(Z) \cap F \neq \emptyset \text{ for every } Z \in N(x)\}$. Where $N(x) = \{Z / Z \text{ is } N\text{-opn}, x \in Z\}$. If $\text{Ncl}_\theta^*(F) = F$, then F is known as $N\theta$ -I-closed set, or simply $N\theta$ -I-cld and its complement is $N\theta$ -I-open set or simply write $N\theta$ -I-opn. We denote $N_{\theta-I}(x) = \{Z / Z \text{ is } N\theta\text{-I-opn}, x \in Z\}$.

Example 2.2 Let $U = \{d_1, d_2, d_3, d_4\}$, $X = \{d_3, d_4\} \subseteq U$, $U/R = \{\{d_1, d_3\}, \{d_2\}, \{d_4\}\}$, $N = \{U, \emptyset, \{d_4\}, \{d_1, d_3\}, \{d_1, d_3, d_4\}\}$, and an ideal $I = \{\emptyset, \{d_4\}\}$. Let $F = \{d_1, d_2, d_3\}$, then $\text{Ncl}_\theta^*(F) = \{d_1, d_2, d_3\}$. Hence F is $N\theta$ -I-cld and $F^c = \{d_4\}$ is $N\theta$ -I-opn.

Theorem 2.3 $\text{Ncl}(F) \subseteq \text{Ncl}_\theta^*(F)$, for any $F \subseteq U$.

Proof If $x \in \text{Ncl}(F)$, then $Z \cap F \neq \emptyset$ for every $Z \in N(x)$. Since $Z \subseteq \text{Ncl}^*(Z)$, $Z \cap F \subseteq \text{Ncl}^*(Z) \cap F$ and hence $\text{Ncl}^*(Z) \cap F \neq \emptyset$. Therefore, $x \in \text{Ncl}_\theta^*(F)$. Thus, $\text{Ncl}(F) \subseteq \text{Ncl}_\theta^*(F)$.

Remark 2.4 $\text{Ncl}(F) \neq \text{Ncl}_\theta^*(F)$. For example, Let $U = \{q_1, q_2, q_3, q_4\}$, $X = \{q_3, q_4\} \subseteq U$, $U/R = \{\{q_2\}, \{q_4\}, \{q_1, q_3\}\}$, $N = \{U, \emptyset, \{q_4\}, \{q_1, q_3\}, \{q_1, q_3, q_4\}\}$, and an ideal $I = \{\emptyset, \{q_4\}\}$. Let $F = \{q_2, q_4\}$, $\text{Ncl}(F) = \{q_2, q_4\}$, and $\text{Ncl}_\theta^*(F) = U$ then $\text{Ncl}(F) \neq \text{Ncl}_\theta^*(F)$.

Theorem 2.5 $\text{Ncl}_\theta^*(F) = \text{Ncl}(F)$, if F is N -opn set.

Proof Let $F \subseteq U$, F be an N -opn set. We know that $\text{Ncl}(F) \subseteq \text{Ncl}_\theta^*(F)$. Let $x \in \text{Ncl}_\theta^*(F)$, then $F \cap \text{Ncl}^*(Z) \neq \emptyset$ for every $Z \in N(x)$. If $F \cap Z = \emptyset$, $Z \subseteq F^c$. Since F is N -opn set, F^c is N -cld set. That is, F^c is an N -cld set containing Z . But $\text{Ncl}(Z)$ is the smallest N -cld set containing Z . Hence $\text{Ncl}(Z) \subseteq F^c$. Thus, $\text{Ncl}(Z) \cap F = \emptyset$. There is a contradiction. Therefore, $F \cap Z \neq \emptyset$ for every $Z \in N(x)$. Therefore, $\text{Ncl}(F) \supseteq \text{Ncl}_\theta^*(F)$. Hence, $\text{Ncl}_\theta^*(F) = \text{Ncl}(F)$.

Theorem 2.6 $\text{Ncl}_\theta^*(F) \subseteq \text{Ncl}_\theta^*(\text{Ncl}_\theta^*(F))$, for any $F \subseteq U$.

Proof Let $x \in \text{Ncl}_\theta^*(F)$. For any $Z \in N(x)$, $x \in \text{Ncl}^*(Z)$. Thus, $x \in \text{Ncl}_\theta^*(F) \cap \text{Ncl}^*(Z)$ and therefore, $\text{Ncl}_\theta^*(F) \cap \text{Ncl}^*(Z) \neq \emptyset$ for every $Z \in N(x)$. Hence $x \in \text{Ncl}_\theta^*(\text{Ncl}_\theta^*(F))$. That is $\text{Ncl}_\theta^*(F) \subseteq \text{Ncl}_\theta^*(\text{Ncl}_\theta^*(F))$.

Remark 2.7 $\text{Ncl}_\theta^*(F) \neq \text{Ncl}_\theta^*(\text{Ncl}_\theta^*(F))$. That is, $\text{Ncl}_\theta^*(F)$ is not $N\theta$ -I-cld set. For example, If $U = \{q_1, q_2, q_3, q_4\}$, $X = \{q_3, q_4\} \subseteq U$, $U/R = \{\{q_2\}, \{q_4\}, \{q_1, q_3\}\}$, $N = \{U, \emptyset, \{q_4\}, \{q_1, q_3\}, \{q_1, q_3, q_4\}\}$, and an ideal $I = \{\emptyset, \{q_4\}\}$. Let $F = \{q_4\}$, $\text{Ncl}_\theta^*(F) = \{q_3, q_4\}$, and $\text{Ncl}_\theta^*(\text{Ncl}_\theta^*(F)) = U$ then $\text{Ncl}_\theta^*(F) \neq \text{Ncl}_\theta^*(\text{Ncl}_\theta^*(F))$.

Theorem 2.8 $\text{Ncl}_\theta^*(F)$ is N -cld, for any subset F of U .

Proof We know that $\text{Ncl}_\theta^*(F) \subseteq \text{Ncl}(\text{Ncl}_\theta^*(F))$ and it is enough to prove $\text{Ncl}(\text{Ncl}_\theta^*(F)) \subseteq \text{Ncl}_\theta^*(F)$. Let $x \in \text{Ncl}(\text{Ncl}_\theta^*(F))$. Then $\text{Ncl}_\theta^*(F) \cap Z \neq \emptyset$ for every $Z \in N(x)$. Let $t \in \text{Ncl}_\theta^*(F) \cap Z$, then $t \in Z$ and $t \in \text{Ncl}_\theta^*(F)$. Since $Z \in N(t)$ and $t \in \text{Ncl}_\theta^*(F)$, $F \cap \text{Ncl}^*(Z) \neq \emptyset$. Hence, $x \in \text{Ncl}_\theta^*(F)$ and so $\text{Ncl}_\theta^*(F)$ is N -cld.

Theorem 2.9 In an NITS (U, N, I) and $F, H \subseteq U$. For the nano ideal theta closure operator $\text{Ncl}_\theta^*(F)$, the following properties hold:





- (i) $Ncl_{\theta}^*(\emptyset) = \emptyset$ and $Ncl_{\theta}^*(U) = U$.
- (ii) $F \subseteq Ncl_{\theta}^*(F)$.
- (iii) If $F \subseteq H$, then $Ncl_{\theta}^*(F) \subseteq Ncl_{\theta}^*(H)$.
- (iv) $Ncl_{\theta}^*(F \cup H) = Ncl_{\theta}^*(F) \cup Ncl_{\theta}^*(H)$.
- (v) $Ncl_{\theta}^*(F \cap H) \subseteq Ncl_{\theta}^*(F) \cap Ncl_{\theta}^*(H)$.

Proof

- (i) Obvious.
- (ii) Let $x \in F$. Then $Z \cap F \neq \emptyset$ for any $Z \in N(x)$. Hence $Ncl^*(Z) \cap F \neq \emptyset$, since $F \cap Z \subseteq Ncl^*(F) \cap F$. Therefore, $x \in Ncl_{\theta}^*(F)$.
- (iii) Suppose $x \notin Ncl_{\theta}^*(H)$, then \exists a $Z \in N(x)$ such that $Ncl^*(Z) \cap H = \emptyset$ and so $Ncl^*(Z) \cap F = \emptyset$. There is a contradiction.
- (iv) Since $F \subseteq F \cup H$ and $H \subseteq F \cup H$, by (iii) $Ncl_{\theta}^*(F) \subseteq Ncl_{\theta}^*(F \cup H)$ and $Ncl_{\theta}^*(H) \subseteq Ncl_{\theta}^*(F \cup H)$. Therefore, $Ncl_{\theta}^*(F) \cup Ncl_{\theta}^*(H) \subseteq Ncl_{\theta}^*(F \cup H)$. For the reverse, let $x \in Ncl_{\theta}^*(F \cup H)$. Then for every $Z \in N(x)$, such that $Ncl^*(Z) \cap (F \cup H) \neq \emptyset$. Therefore, $Ncl^*(Z) \cap F \neq \emptyset$ or $Ncl^*(Z) \cap H \neq \emptyset$, and so $x \in Ncl_{\theta}^*(F)$ or $x \in Ncl_{\theta}^*(H)$. Hence, $x \in Ncl_{\theta}^*(F) \cup Ncl_{\theta}^*(H)$. Therefore, $Ncl_{\theta}^*(F \cup H) \subseteq Ncl_{\theta}^*(F) \cup Ncl_{\theta}^*(H)$.
- (v) Since $F \cap H \subseteq F$ and $F \cap H \subseteq H$, by (iii) $Ncl_{\theta}^*(F \cap H) \subseteq Ncl_{\theta}^*(F)$ and $Ncl_{\theta}^*(F \cap H) \subseteq Ncl_{\theta}^*(H)$. Therefore, $Ncl_{\theta}^*(F \cap H) \subseteq Ncl_{\theta}^*(F) \cap Ncl_{\theta}^*(H)$.

Corollary 2.10 If F and H are $N\theta$ -I-cld sets, then $F \cup H$ is an $N\theta$ -I-cld set.

Proof If F and H are $N\theta$ -I-cld sets. Then $Ncl_{\theta}^*(F) = F$ and $Ncl_{\theta}^*(H) = H$. Therefore, $Ncl_{\theta}^*(F \cup H) = Ncl_{\theta}^*(F) \cup Ncl_{\theta}^*(H) = F \cup H$ and hence, $F \cup H$ is $N\theta$ -I-cld set.

Corollary 2.11 If F and H are $N\theta$ -I-closed sets, then $F \cap H$ is a $N\theta$ -I-cld set.

Proof $Ncl_{\theta}^*(F) = F$ and $Ncl_{\theta}^*(H) = H$, since F and H are $N\theta$ -I-cld sets. Therefore, $Ncl_{\theta}^*(F \cap H) \subseteq Ncl_{\theta}^*(F) \cap Ncl_{\theta}^*(H) = F \cap H$. Hence $F \cap H$ is $N\theta$ -I-cld set.

Remark 2.12 $N\theta$ -I-closed sets forms topology from Corollary 2.10 and Corollary 2.11.

From the given example, it is clear that the reversal direction(v) of Theorem 2.9. is not always true. Let $U = \{m_1, m_2, m_3, m_4\}$, $X = \{m_3, m_4\} \subseteq U$, $U/R = \{\{m_2\}, \{m_4\}, \{m_1, m_3\}\}$, $N = \{U, \emptyset, \{m_4\}, \{m_1, m_3\}, \{m_1, m_3, m_4\}\}$ and an ideal $I = \{\emptyset, \{m_4\}\}$. Let $F = \{m_1\}$, $H = \{m_2\}$. Then $F \cap H = \emptyset$, $Ncl_{\theta}^*(F) = \{m_1, m_2, m_3\}$, $Ncl_{\theta}^*(H) = \{m_1, m_2, m_3\}$, $Ncl_{\theta}^*(F) \cap Ncl_{\theta}^*(H) = \{m_1, m_2, m_3\}$ and $Ncl_{\theta}^*(F \cap H) = \emptyset$. Therefore, $Ncl_{\theta}^*(F \cap H) \not\subseteq Ncl_{\theta}^*(F) \cap Ncl_{\theta}^*(H)$.

3. $N\theta$ -I-DERIVED SET, $N\theta$ -I-INTERIOR AND $N\theta$ -I-BORDER

Definition 3.1 In an NITS (U, N, I) , $F \subseteq U$. If $(F - \{x\}) \cap Z \neq \emptyset$ for each $Z \in N_{\theta-I}(x) = \{Z / Z \text{ is } N\theta\text{-I-open, } x \in Z\}$, then x is an $N\theta$ -I-limit point of F , and $NDr_{\theta}^*(F)$ mentions all its collection of F .

Theorem 3.2 For the subsets F and H of an NITS (U, N, I) , the given below are true:

- (i) If $F \subseteq H$, then $NDr_{\theta}^*(F) \subseteq NDr_{\theta}^*(H)$.
- (ii) $NDr_{\theta}^*(F) \cup NDr_{\theta}^*(H) \subseteq NDr_{\theta}^*(F \cup H)$.
- (iii) $NDr_{\theta}^*(F \cap H) \subseteq NDr_{\theta}^*(F) \cap NDr_{\theta}^*(H)$.
- (iv) $NDr_{\theta}^*(NDr_{\theta}^*(F)) - F \subseteq NDr_{\theta}^*(F)$.

Proof (i) If $x \notin NDr_{\theta}^*(H)$, then x is not an $N\theta$ -I-limit point of H . Therefore, \exists a $Z \in N_{\theta-I}(x)$, such that $(H - \{x\}) \cap Z = \emptyset$. But $Z \cap (F - \{x\}) \subseteq (H - \{x\}) \cap Z = \emptyset$. Hence, $x \notin NDr_{\theta}^*(F)$. Therefore, there is a contradiction.

(ii) Since $F \subseteq F \cup H$ and $H \subseteq F \cup H$, by (i) $NDr_{\theta}^*(F) \subseteq NDr_{\theta}^*(F \cup H)$ and $NDr_{\theta}^*(H) \subseteq NDr_{\theta}^*(F \cup H)$. Hence $NDr_{\theta}^*(F) \cup NDr_{\theta}^*(H) \subseteq NDr_{\theta}^*(F \cup H)$.

(iii) Since $H \cap F \subseteq F$ and $H \cap F \subseteq H$ again by (i), the proof is complete.





Chandralekha and Periyasamy

(iv) If $x \in \text{NDR}_0^*(\text{NDR}_0^*(F)) - F$, then $(\text{NDR}_0^*(F) - \{x\}) \cap Z \neq \emptyset$ for $Z \in \mathcal{N}_{\theta-1}(x)$. Let $y \in (\text{NDR}_0^*(F) - \{x\}) \cap Z$. Since $y \in \text{NDR}_0^*(F) - \{x\}$ and y belongs to Z , $Z \cap (F - \{y\}) \neq \emptyset$. Let $j \in Z \cap (F - \{y\})$. Then $x \neq j$ for $x \notin F$ and $j \in F$. Therefore, $x \in \text{NDR}_0^*(F)$.

The given below example illustrates the reversal part of Theorem 3.2 (iv), which may not be true in general. Let $U = \{q_1, q_2, q_3, q_4\}$, $X = \{q_3, q_4\} \subseteq U$, $U/R = \{\{q_2\}, \{q_4\}, \{q_1, q_3\}\}$, $N = \{U, \emptyset, \{q_4\}, \{q_1, q_3\}, \{q_1, q_3, q_4\}\}$, and an ideal $I = \{\emptyset, \{q_4\}\}$. Take $F = \{q_3\}$. Then $\text{NDR}_0^*(\text{NDR}_0^*(F)) - F \not\subseteq \text{NDR}_0^*(F)$.

Definition 3.3 Let a point $x \in U$ be $\mathcal{N}\theta$ -I-interior point or simply $\mathcal{N}\theta$ -I-IP of F if $\exists Z \in \mathcal{N}_{\theta-1}(x)$, such that $Z \subseteq F$. $\text{Nint}_0^*(F)$ is the collection of $\mathcal{N}\theta$ -I-IP's of F .

Theorem 3.4 For the subsets F and H of an NITS (U, N, I) , the given below holds:

- (i) $\text{Nint}_0^*(F)$ is the for most $\mathcal{N}\theta$ -I-opn set contained in F .
- (ii) F is $\mathcal{N}\theta$ -I-opn set iff $F = \text{Nint}_0^*(F)$.
- (iii) If $F \subseteq H$, then $\text{Nint}_0^*(F) \subseteq \text{Nint}_0^*(H)$.
- (iv) $\text{Nint}_0^*(F) = F - \text{NDR}_0^*(F^c)$.
- (v) $(\text{Nint}_0^*(F))^c = \text{Ncl}_0^*(F^c)$.
- (vi) $\text{Nint}_0^*(\text{Nint}_0^*(F)) \subseteq \text{Nint}_0^*(F)$.
- (vii) $\text{Nint}_0^*(F) \cup \text{Nint}_0^*(H) \subseteq \text{Nint}_0^*(F \cup H)$.
- (viii) $\text{Nint}_0^*(F) \cap \text{Nint}_0^*(H) = \text{Nint}_0^*(F \cap H)$.

Proof

- i) If $x \in Z$ and Z is an $\mathcal{N}\theta$ -I-opn subset of F , then $x \in Z \subseteq F$. Since Z is an $\mathcal{N}\theta$ -I-opn set, x is the $\mathcal{N}\theta$ -I-IP of F . Therefore, for $x \in Z$ implies that $x \in \text{Nint}_0^*(F)$. This implies that every $\mathcal{N}\theta$ -I-opn subset of F is contained in $\text{Nint}_0^*(F)$. Therefore, $\text{Nint}_0^*(F)$ is the for most $\mathcal{N}\theta$ -I-opn set contained in F .
- (ii) Let F be an $\mathcal{N}\theta$ -I-opn set. Since $\text{Nint}_0^*(F)$ is the for most $\mathcal{N}\theta$ -I-opn subset of F , $\text{Nint}_0^*(F) = F$. Converse is clear by (i).
- (iii) Let $F \subseteq H$, $x \in \text{Nint}_0^*(F)$. Then $\exists Z \in \mathcal{N}_{\theta-1}(x)$, such that $x \in Z \subseteq F$. Therefore, $x \in Z \subseteq F \subseteq H$ that is $x \in Z \subseteq H$ and hence $x \in \text{Nint}_0^*(H)$. Therefore, $\text{Nint}_0^*(F) \subseteq \text{Nint}_0^*(H)$.
- (iv) If $x \in F - \text{NDR}_0^*(F^c)$, then $x \notin \text{NDR}_0^*(F^c)$ and so $\exists Z \in \mathcal{N}_{\theta-1}(x)$, such that for $(F^c) \cap Z = \emptyset$ and $x \in Z \subseteq F$. Hence $x \in \text{Nint}_0^*(F)$. (i.e.) $F - \text{NDR}_0^*(F^c) \subseteq \text{Nint}_0^*(F)$. For the reverse, if $x \in \text{Nint}_0^*(F)$, then $x \notin \text{NDR}_0^*(F^c)$, since $\text{Nint}_0^*(F)$ is $\mathcal{N}\theta$ -I-opn set and $\text{Nint}_0^*(F) \cap (F^c) = \emptyset$. Hence, $\text{Nint}_0^*(F) \subseteq F - \text{NDR}_0^*(F^c)$. Therefore, $\text{Nint}_0^*(F) = F - \text{NDR}_0^*(F^c)$.
- (v) $U - \text{Nint}_0^*(F) = U - (F - \text{NDR}_0^*(F^c)) = (F^c) \cup \text{NDR}_0^*(F^c) = \text{Ncl}_0^*(F^c)$.
- (vi) Since $\text{Nint}_0^*(F) \subseteq F$, by (iii), $\text{Nint}_0^*(\text{Nint}_0^*(F)) \subseteq \text{Nint}_0^*(F)$.
- (vii) Since $F \subseteq (F \cup H)$ and $H \subseteq (F \cup H)$ by (iv), $\text{Nint}_0^*(F) \subseteq \text{Nint}_0^*(F \cup H)$ and $\text{Nint}_0^*(H) \subseteq \text{Nint}_0^*(F \cup H)$. Therefore, $\text{Nint}_0^*(F) \cup \text{Nint}_0^*(H) \subseteq \text{Nint}_0^*(F \cup H)$.
- (viii) Since $(\text{Nint}_0^*(F \cap H))^c = \text{Ncl}_0^*(F \cap H)^c = \text{Ncl}_0^*(F^c \cup H^c) = \text{Ncl}_0^*(F^c) \cup \text{Ncl}_0^*(H^c) = (\text{Nint}_0^*(F))^c \cup (\text{Nint}_0^*(H))^c$. Hence, $\text{Nint}_0^*(F) \cap \text{Nint}_0^*(H) = \text{Nint}_0^*(F \cap H)$.

Theorem 3.5 $\mathcal{N}_{\theta-1}(U) = \{Z \in U / Z \text{ is } \mathcal{N}\theta\text{-I-opn}\}$ is a topology.

Proof (i) Since \emptyset and U are $\mathcal{N}\theta$ -I-cld, they are $\mathcal{N}\theta$ -I-opn, and hence \emptyset and $U \in \mathcal{N}_{\theta-1}(U)$.

(ii) If $F_i \in \mathcal{N}_{\theta-1}(U)$, then each F_i is $\mathcal{N}\theta$ -I-opn in U , and hence $\text{Nint}_0^*(F_i) = F_i$ for each i . Let $F = \cup_i F_i$. Consider $\text{Nint}_0^*(F) = \text{Nint}_0^*(\cup_i F_i) \supseteq \cup_i \text{Nint}_0^*(F_i) = \cup_i F_i = F$. (i.e.) $F \subseteq \text{Nint}_0^*(F)$. But $\text{Nint}_0^*(F)$ is a subset of F . Therefore, $\text{Nint}_0^*(F) = F$. Thus, F is $\mathcal{N}\theta$ -I-opn. Hence, arbitrary union of members of $\mathcal{N}_{\theta-1}(U)$ belong to $\mathcal{N}_{\theta-1}(U)$.

(iii) Let F and $H \in \mathcal{N}_{\theta-1}(U)$. Then F, H are $\mathcal{N}\theta$ -I-opn and hence $\text{Nint}_0^*(F) = F$ and $\text{Nint}_0^*(H) = H$. Consider $\text{Nint}_0^*(F \cap H) \subseteq \text{Nint}_0^*(F) \cap \text{Nint}_0^*(H) = F \cap H$ and hence $F \cap H \in \mathcal{N}_{\theta-1}(U)$ whenever $F, H \in \mathcal{N}_{\theta-1}(U)$. Thus, $\mathcal{N}_{\theta-1}(U)$ is a topology.

Remark 3.6 $\mathcal{N}_{\theta-1}(U) \subseteq \mathcal{N}(U)$, since every $\mathcal{N}\theta$ -I-opn set is \mathcal{N} -opn.

Definition 3.7 The $\mathcal{N}\theta$ -I-border of F is defined by $\text{NBr}_0^*(F) = F - \text{Nint}_0^*(F)$.





Chandralekha and Periyasamy

Theorem 3.8 In an NITS (U, N, I) , for any subsets F and H of U , the given below holds:

- (i) $Nint_{\theta}^*(F) \cap NBr_{\theta}^*(F) = \emptyset$.
- (ii) F is $N\theta$ -I-opn set iff $NBr_{\theta}^*(F) = \emptyset$.
- (iii) $NBr_{\theta}^*(Nint_{\theta}^*(F)) = \emptyset$.
- (iv) $Nint_{\theta}^*(NBr_{\theta}^*(F)) = \emptyset$.
- (v) $NBr_{\theta}^*(NBr_{\theta}^*(F)) = NBr_{\theta}^*(F)$.
- (vi) $NBr_{\theta}^*(F) = Ncl_{\theta}^*(F^c) \cap F$.
- (vii) $NBr_{\theta}^*(F) = NDr_{\theta}^*(F^c)$

Proof (i) $Nint_{\theta}^*(F) \cap NBr_{\theta}^*(F) = Nint_{\theta}^*(F) \cap (F - Nint_{\theta}^*(F)) = Nint_{\theta}^*(F) \cap (F \cap (U - Nint_{\theta}^*(F))) = Nint_{\theta}^*(F) \cap \emptyset = \emptyset$.

(ii) The proof is obvious.

(iii) $NBr_{\theta}^*(Nint_{\theta}^*(F)) = Nint_{\theta}^*(F) - Nint_{\theta}^*(Nint_{\theta}^*(F)) = Nint_{\theta}^*(F) - Nint_{\theta}^*(F) = \emptyset$.

(iv) Let $x \in Nint_{\theta}^*(NBr_{\theta}^*(F))$, then $x \in NBr_{\theta}^*(F)$. Since $NBr_{\theta}^*(F) \subseteq F$, $x \in Nint_{\theta}^*(NBr_{\theta}^*(F)) \subseteq Nint_{\theta}^*(F)$. Hence, $x \in Nint_{\theta}^*(F) \cap NBr_{\theta}^*(F)$ which contradicts (i). Thus, $Nint_{\theta}^*(NBr_{\theta}^*(F)) = \emptyset$.

(v) $NBr_{\theta}^*(NBr_{\theta}^*(F)) = NBr_{\theta}^*(F) - Nint_{\theta}^*(NBr_{\theta}^*(F)) = NBr_{\theta}^*(F)$, by (iv).

(vi) $NBr_{\theta}^*(F) = F - Nint_{\theta}^*(F) = F - (U - Ncl_{\theta}^*(F^c)) = Ncl_{\theta}^*(F^c) \cap F$.

(vii) $NBr_{\theta}^*(F) = F - Nint_{\theta}^*(F) = F - (F - NDr_{\theta}^*(F^c)) = NDr_{\theta}^*(F^c)$.

4. $N\theta$ -I-FRONTIER AND $N\theta$ -I-EXTERIOR

Definition 4.1 $NFr_{\theta}^*(F) = Ncl_{\theta}^*(F) - Nint_{\theta}^*(F)$ is the $N\theta$ -I-frontier of F .

Theorem 4.2 In an NITS (U, N, I) , the given below are holds for $F \subseteq U$.

- (i) $Ncl_{\theta}^*(F) = Nint_{\theta}^*(F) \cup NFr_{\theta}^*(F)$.
- (ii) $Nint_{\theta}^*(F) \cap NFr_{\theta}^*(F) = \emptyset$.
- (iii) $NBr_{\theta}^*(F) \subseteq NFr_{\theta}^*(F)$.
- (iv) $NFr_{\theta}^*(F) = Ncl_{\theta}^*(F) \cap Ncl_{\theta}^*(F^c)$.
- (v) $NFr_{\theta}^*(Nint_{\theta}^*(F)) \subseteq NFr_{\theta}^*(F)$.
- (vi) $Nint_{\theta}^*(F) = F - NFr_{\theta}^*(F)$.

Proof

(i) $Nint_{\theta}^*(F) \cup NFr_{\theta}^*(F) = Nint_{\theta}^*(F) \cup (Ncl_{\theta}^*(F) - Nint_{\theta}^*(F)) = Ncl_{\theta}^*(F)$.

(ii) $Nint_{\theta}^*(F) \cap NFr_{\theta}^*(F) = Nint_{\theta}^*(F) \cap (Ncl_{\theta}^*(F) - Nint_{\theta}^*(F)) = \emptyset$.

(iii) $NBr_{\theta}^*(F) = F - Nint_{\theta}^*(F) \subseteq Ncl_{\theta}^*(F) - Nint_{\theta}^*(F) = NFr_{\theta}^*(F)$.

(iv) $NFr_{\theta}^*(F) = Ncl_{\theta}^*(F) - Nint_{\theta}^*(F) = Ncl_{\theta}^*(F) \cap Ncl_{\theta}^*(F^c)$.

(v) $NFr_{\theta}^*(Nint_{\theta}^*(F)) = Ncl_{\theta}^*(Nint_{\theta}^*(F)) - Nint_{\theta}^*(Nint_{\theta}^*(F)) \subseteq Ncl_{\theta}^*(F) - Nint_{\theta}^*(F) = NFr_{\theta}^*(F)$.

(vi) $F - NFr_{\theta}^*(F) = F \cap (NFr_{\theta}^*(F))^c = F \cap (Ncl_{\theta}^*(F) - Nint_{\theta}^*(F))^c = F \cap ((Ncl_{\theta}^*(F))^c \cap (Nint_{\theta}^*(F))^c) = F \cap ((Ncl_{\theta}^*(F))^c \cup (Nint_{\theta}^*(F))^c) = \emptyset \cup Nint_{\theta}^*(F) = Nint_{\theta}^*(F)$.

The reverse implication of Theorem 4.2 (iii) fails the given below example. Let $U = \{m_1, m_2, m_3, m_4\}$ be the universe, $X = \{m_1, m_3\} \subseteq U$, $U/R = \{\{m_1\}, \{m_2, m_3\}, \{m_4\}\}$, $N = \{U, \emptyset, \{m_1\}, \{m_2, m_3\}, \{m_1, m_3, m_3\}\}$, and an ideal $I = \{\emptyset\}$. Take $F = \{m_1\}$. Then $NFr_{\theta}^*(F) = \{m_1, m_4\}$ and $NBr_{\theta}^*(F) = \{m_1\}$. Therefore, $NBr_{\theta}^*(F) \not\subseteq NFr_{\theta}^*(F)$.

Definition 4.3 $N\theta$ -I-exterior of F is denoted by $NExt_{\theta}^*(F) = Nint_{\theta}^*(F^c)$.

Theorem 4.4 In an NITS, the given below holds for $F \subseteq U$.

- (i) $NExt_{\theta}^*(F) = (Ncl_{\theta}^*(F))^c$.
- (ii) $NExt_{\theta}^*(F)$ is $N\theta$ -I-opn set.
- (iii) $NExt_{\theta}^*(NExt_{\theta}^*(F)) = Nint_{\theta}^*(Ncl_{\theta}^*(F))$.
- (iv) If $F \subseteq H$, then $NExt_{\theta}^*(F) \supseteq NExt_{\theta}^*(H)$.
- (v) $NExt_{\theta}^*(F \cup H) = NExt_{\theta}^*(F) \cap NExt_{\theta}^*(H)$.
- (vi) $NExt_{\theta}^*(F \cap H) \supseteq NExt_{\theta}^*(F) \cup NExt_{\theta}^*(H)$.





(vii) $NExt_{\theta}^*(U) = \emptyset$ and $NExt_{\theta}^*(\emptyset) = U$.

(viii) $Nint_{\theta}^*(F) \subseteq NExt_{\theta}^*(NExt_{\theta}^*(F))$.

(ix) $NExt_{\theta}^*(F) = NExt_{\theta}^*(NExt_{\theta}^*(F))^c$.

Proof

(i) $NExt_{\theta}^*(F) = Nint_{\theta}^*(F^c) = (Ncl_{\theta}^*(F))^c$.

(ii) By Definition 4.3, the proof is clear.

(iii) $NExt_{\theta}^*(NExt_{\theta}^*(F)) = NExt_{\theta}^*(Nint_{\theta}^*(F^c)) = NExt_{\theta}^*(Ncl_{\theta}^*(F))^c = Nint_{\theta}^*((Ncl_{\theta}^*(F))^c) = Nint_{\theta}^*(Ncl_{\theta}^*(F))$.

(iv) Since $F \subseteq H$, $Nint_{\theta}^*(H^c) \subseteq Nint_{\theta}^*(F^c)$. Hence, clear by Definition 4.3.

(v) $NExt_{\theta}^*(F \cup H) = Nint_{\theta}^*(F \cap H)^c = Nint_{\theta}^*(F^c \cap H^c) = Nint_{\theta}^*(F^c) \cap Nint_{\theta}^*(H^c) = NExt_{\theta}^*(F) \cap NExt_{\theta}^*(H)$.

(vi) $NExt_{\theta}^*(F \cap H) = Nint_{\theta}^*(F \cup H)^c = Nint_{\theta}^*(F^c \cup H^c) \supseteq Nint_{\theta}^*(F^c) \cup Nint_{\theta}^*(H^c) = NExt_{\theta}^*(F) \cup NExt_{\theta}^*(H)$.

(vii) The proof is obvious.

(viii) $Nint_{\theta}^*(F) \subseteq Nint_{\theta}^*(Ncl_{\theta}^*(F)) = Nint_{\theta}^*(Nint_{\theta}^*(F^c))^c = Nint_{\theta}^*(NExt_{\theta}^*(F))^c = NExt_{\theta}^*(NExt_{\theta}^*(F))$.

(ix) $NExt_{\theta}^*(NExt_{\theta}^*(F))^c = NExt_{\theta}^*(Nint_{\theta}^*(F^c))^c = Nint_{\theta}^*((Nint_{\theta}^*(F^c))^c) = Nint_{\theta}^*(Nint_{\theta}^*(F^c)) = Nint_{\theta}^*(F^c) = NExt_{\theta}^*(F)$.

DISCUSSION AND CONCLUSION

The outcomes of this study have provided insights into the $N\theta$ -I-closed sets in nano ideal topological space. We investigated the closure operator $Ncl_{\theta}^*(F)$ for a subset F of the universe U . The collection of $N\theta$ -I-open sets created topology. The collection described here properly lies between $N\theta$ -closed sets and N -closed sets. The correlation of $Nint_{\theta}^*(F)$ with $Ncl_{\theta}^*(F)$ also deduced. $N\theta$ -derived set of F is defined as the set of $N\theta$ -I-limit point of F and studied its basic properties. Also studied the $N\theta$ -I-exterior, $N\theta$ -I-frontier and $N\theta$ -I-border of subset F and their important properties.

REFERENCES

1. M. Akdag, " θ -I-open sets", *Kochi Journal of Math*, pp. 217-229, (3), 2008.
2. M. Caldas, S. Jafari, and M. M. Kovar, "Some properties of θ -open sets", *Divulgaciones Math*, pp. 161-169, (12), 2004.
3. R. F. Dickman, Jr. and J. R. Porter, " θ -closed subsets of Hausdorff spaces", *Pacific Journal Math*, pp. 407-415, (59), 1975.
4. R. F. Dickman, Jr. and J. R. Porter, " θ -perfect and θ -absolutely closed functions", *Illinois Journal. Math*, pp. 42-60, (21), 1977.
5. J. Dontchev, M. Ganster, and D. Rose, "Ideal Resolvability", *Topology and its Application*, pp. 1-16, (93), 1999.
6. D. Jankovic and T. R. Hamlett, "New topologies from old via ideals", *Amer. Math. Monthly*, pp. 295-310, 97(1990).
7. J. E. Joseph, " θ -closure and θ -sub closed graphs", *Math. Chronicle*, pp. 99-117, (8), 1979.
8. M. Lellis Thivagar and Carmel Richard, "On nano forms of weakly open sets", *International Journal of Mathematics and Statistics Invention*, pp. 31-37, 1(1), 2013.
9. P. E. Long and L. L. Herrington, "The τ_{θ} -topology and faintly continuous functions", *Kyungpook Math. Journal*, pp. 7-14, 22, 1982.
10. K. Kuratowski, "Topology", *Academic Press. New York*, Vol. 1. 1966.
11. M. Parimala and R. Perumal, "Weaker form of open sets in nano ideal topological spaces", *Global Journal of Pure and Applied Mathematics*, pp. 302-305, 12(1), 2016.
12. M. Parimala and S. Jafari, "On some new notions in nano ideal topological spaces", *Eurasian Bulletin of Mathematics*, pp. 85-93, 1(3), 2018.
13. M. Parimala, Noiri and S. Jafari, "New types of nano topological spaces via ideals" (August 2016).
14. V. Vaidhyathanaswamy, "The localization theory in set topology", *Proc. Indian Acad. Sci.*, 20, 1945.
15. N. V. Velicko, "H-closed topological spaces", *Amer. Math. Soc. Transl.*, pp. 103-118, 78, 1968.





Stability Analysis of Different Chilli Hybrids (*Capsicum annuum* L.) for their Yield and Yield Components

Gokulakrishnan J^{1*}, K. Saranya², P. Abinash² and S. Ranjith Raja Ram³

¹Associate Professor, Department of Genetics and Plant Breeding, Faculty of Agriculture, Annamalai University, Cuddalore, Tamil Nadu, India.

²PG Scholar, Department of Genetics and Plant Breeding, Faculty of Agriculture, Annamalai University, Cuddalore, Tamil Nadu, India.

³Assistant Professor, Plant Breeding and Genetics, TNAU, TCRS-Yethapur, Salem, Tamil Nadu, India.

Received: 22 Jan 2024

Revised: 09 Feb 2024

Accepted: 29 Apr 2024

*Address for Correspondence

Gokulakrishnan J

Associate Professor,

Department of Genetics and Plant Breeding,

Faculty of Agriculture,

Annamalai University,

Cuddalore, Tamil Nadu, India.

Email: gokulayamuna@gmail.com



This is an Open Access Journal / article distributed under the terms of the **Creative Commons Attribution License** (CC BY-NC-ND 3.0) which permits unrestricted use, distribution, and reproduction in any medium, provided the original work is properly cited. All rights reserved.

ABSTRACT

Chilli (*Capsicum annuum* L.), an important vegetable crop in India. It is sensitive to climate changes and environmental conditions. The aim of this study was to assess the stability of 19 test hybrids for their yield and yield components along with two commercial check hybrids (Indam-5 and Tejaswini) at three different locations. Genotype × Environment interaction were estimated by three methods viz., Eberhart and Russell model. Variance due to Genotype × Environment Interactions (G×E) were significant for all the characters except days to fifty percent flowering and fruit width. Among the above studied hybrids, the hybrid AUCH-16 showed stable performance with high mean, non-significant deviation from regression (S^2_{di}) and regression around unity so they are advised for commercial cultivation. The hybrid AUCH-13 recorded as most stable hybrid in poor unfavourable environments and AUCH-3 as stable hybrid with a low mean value in favourable environments. Therefore, the stability models such as mean, regression coefficient, squared deviation, indicated that AUCH-16 could be recommended for commercial cultivation under varied environments.

Keywords: *Capsicum annuum*, Chilli, Genotype × Environments, Stability analysis.





INTRODUCTION

Chilli (*Capsicum annuum* L.) is one of the most important commercial crops of India. It is grown almost throughout the country. There are more than 400 different varieties of chillies found all over the world. It is also known as hot pepper, cayenne pepper, sweet pepper, bell pepper, *etc.*, chilli is one of the spices and vegetable crops of Solanaceae family. Capsicum species have been widely used in food as well as in pharmaceutical Industries. Its properties comprise high antioxidant capacity and content of several healthy related compounds including Vitamin C, Carotenoids and Capsaicinoids (Maria de Lourdes Reyes-Escogido *et al.*, 2011). Chilli is valued for its pungency and colour aspects in food industries. Most of the economic traits in chilli are vulnerable to environmental fluctuations (WANI *et al.*, 2013). Pungency is due to crystalline alkaloid called capsaicin, present in the placenta of fruits. The red colour of chilli pigment is due to capsanthin. Given the economic importance of Chilli, it is imperative that the released chilli hybrids exhibit consistent yield per unit area. However, due to environmental effects the genotypes tend to perform in a varied manner at each environment. Thereby, an assessment of the trait yield and its components are necessary in the wake of unprecedented climate change events. Stable chilli hybrids can be identified under different environment conditions by employing various stability models. The most widely used model was proposed by Eberhart and Russell (1966). Identification of the climatic variables that contribute most to genotype \times environment (G \times E) interactions could help breeders to understand the pattern of these interactions. The present study was undertaken to identify high yielding and stable chilli hybrids in different environmental conditions for its cultivation. The main objectives are to evaluate 19 chilli hybrids for yield and yield components under various growing environments to identify the best performing and stable hybrids for recommendations to farmers and to estimate (G \times E) interaction for grain yield and its components. Multi-environmental or multi-locational testing of genotypes provides an opportunity to plant breeders to identify the adaptability of a genotype to a particular environment and also stability of genotype over different environments.

MATERIALS AND METHODS

The present investigation “Studies on stability analysis for yield and yield components in chilli hybrids (*Capsicum annuum* L.) was undertaken during 2019-2021. Stability analysis was carried out at three locations namely, Chidambaram (E₁), Namakkal (E₂) and Attur (E₃). Seventeen hybrids with two checks were sown at the nursery area separately in rows and the 40 days young seedlings were transplanted to the main field. The chilli seedlings were planted in a single row of 5m length with the spacing of 45 \times 30 cm. The experiments were laid out in Randomized Block Design (RBD) with three replications. For each hybrid a total of fifteen plants per replication were maintained. Recommended package of practice and plant protection measures were followed to raise the crop to obtain good yield and yield attributing components. The observations were recorded after field evaluation studied from five randomly selected plants from each hybrid per replication for the following characters. Nine traits *viz.*, days to 50 percent flowering, plant height, plant width, fruit length, fruit width, average number of fruits per plant, average number of seeds per fruit, thousand seed weight, dry chilli fruit yield per plot genotypes were assessed for stability of performance over in environments in accordance with method described by Eberhart and Russel Model (1966).

RESULTS AND DISCUSSION

The mean data averaged over replications for the genotypes over three environments for each of the nine characters were subjected to pooled analysis and their results were subjected to pooled analysis and their result were presented in Table 2. The mean sum of squares due to genotypes, environments and G \times E were tested against mean squares due to pooled error and were highly significant for all the characters except days to 50% flowering and fruit width and satisfied the requirement of stability. Significant G \times E for maximum characters indicate select a stable genotypes from this



Gokulakrishnan *et al.*,

group of materials. The mean sum of squares due to treatments was highly significant for all the nine characters studied in this experiment. Analysis revealed that, the genotypes and environments were significant for all the characters studied and environments were significant for all the characters studied except days to fifty percent flowering and fruit width, indicating the diversity among the genotypes and environments studied. The G×E interactions were significant for the characters plant height, plant width, fruit length, average number of fruits per plant, average number of seeds per fruit, thousand seed weight and dry chilli fruit yield per plant implying different behaviour of genotypes under three locations for these characters. The G×E interactions for the remaining two characters were found non-significant. Therefore, further analysis of stability was not carried out for these characters. Partitioning of sum of squares into that of varieties, Environments + (Genotype × Environment) and pooled error revealed that mean squares due to Environments + (Genotypes × Environments) were significant for the characters *viz.*, plant height, plant width, fruit length, average number of fruits per plant, average number of seeds per fruit, thousand seed weight and dry chilli fruit yield per plot reemphasizing the existence of G×E interactions for these traits. These results are in agreement with the previous observations of Lohithaswa *et al.* (2001), Tembrune and Rao (2013) and Kranthi Rekha *et al.* (2016) in chilli.

Environmental index

Environmental indices of nine characters *viz.*, days to fifty percent flowering, plant height, plant width, fruit length, fruit width, average number of fruits per fruit, average number of seeds per fruit, thousand seed weight and dry chilli fruit yield per plot are presented in Table 17. The environmental indices for three environments revealed that among the nine characters, eight characters were negative and only thousand seed weight was positive in E₁. E₂ was best for plant height, fruit length, fruit width, average number of fruits per plant, average number of seeds per fruit, thousand seed weight and dry chilli fruit yield per fruit. E₃ was best for days to fifty percent flowering, plant weight, plant width and dry chilli fruit yield per fruit. Among the three environments E₂ found to be more favourable in comparison with E₁ and E₃. A perusal of the results on environmental index for various traits under different environments suggested variable response of the environments to the different traits studied. Lohithaswa *et al.* (2001) and Temabhrune and Rao (2013) in chilli who also reported variable response of the environments to different traits.

Eberhart and Russell Model

The genotypes were grouped into four categories namely, Group I - High mean and low variation Group II - High mean and high variation Group III - Low mean and low variation Group IV - Low mean and high variation. Group I includes several parameters they are, days to fifty percent flowering includes group I and II, plant height, dry chilli fruit yield per plot includes group I, II, III and IV, plant width includes group I and II, fruit length includes group I, II and III, fruit width includes group I and II, average number of fruits per plant, average number of seeds per fruit, Thousand seed weight includes group I and II. The hybrids falling in Group I will have average responsiveness and highly stable over environments. Hybrids in Group II will have above or below average responsiveness that is they will be suited for stress or favourable environments and will be stable in respective environments. Behaviour of hybrids falling in Groups III and IV cannot be predicted and are highly unstable. The hybrids are placed in their respective groups in Table 4. Considering the overall performance, G₁₃ (AUCH -13) was found promising with stable performance (Group II) and may be used for general cultivation in unfavourable environments. G₃ (AUCH-3) showed stable performance with a low mean value for yield in favourable environments. The hybrid G₁₆ (AUCH-16) showed stable performance with high mean value for yield therefore it is advised for commercial exploitation and these hybrids are better than the commercial check variety.

CONCLUSION

Considering the environmental indices, E₂ was deemed to be better one than the other two for all the traits studied. Eberhart and Russell model showed (AUCH-16) G₁₆ as stable genotype for yield with high mean value whereas the hybrid (AUCH-13) G₁₃ showed stable performance in unfavourable environments. They indicated five hybrids *viz.*, G₅



Gokulakrishnan *et al.*,

(AUCH-5), G₁₁ (AUCH-11), G₁₃ (AUCH-13), G₁₆ (AUCH-16) and G₁₇ (AUCH-17) as phenotypically stable hybrids across environments. Genotype grouping technique identified G₁₆ (AUCH-16), G₁₃ (AUCH-13) and G₁₇ (AUCH-17) as stable due to its less fluctuations across environments for yield and its contributing characters.

REFERENCES

1. Allard, R.W. and Bradshaw, A.D. 1964. Implications of genotype-environment interactions in applied plant breeding 1. *Crop Science*, 4(5): 503–508.
2. Comstock, R.E. and Moll, R.H. 1963. Genotype environment interactions. *Statistical Genetics and Plant Breeding*, pp. 164-197.
3. Datta, L.S. and Dey, A.N. 2009. Stability analysis in chilli (*Capsicum annuum* L.) under open and mahogany (*Swietenia mahagoni* L.) based agroforestry system. *Journal of Spices and Aromatic Crops*, 18(2): 84-87.
4. Eberhart, S.A. and Russell, W.A. 1966. Stability parameters for comparing varieties 1. *Crop Science*, 6(1): 36–40.
5. Finlay, K.W. and Wilkinson, G.N. 1963. The analysis of adaptation in a plant-breeding programme. *Australian Journal of Agricultural Research*, 14(6): 742–754.
6. Fisher, R.A. and Mackenzie, W.A. 1923. Studies in crop variation. II. The manurial response of different potato varieties. *The Journal of Agricultural Science*, 13(3): 311–320.
7. Kranthi Rekha, G., Naram Naidu, L., Venkata Ramana, C., Umajyothi, K., Paratap Rao, M. and Sasikala, K. 2016. Heterosis studies for yield and yield attributing characters in chilli (*Capsicum annuum* L.) over environments. *Plant Archives*, 16(1): 243-251.
8. Lohithaswa, H.C., Kulkarni, R.S. and Manjunath, A. 2000. Combining ability analysis for fruit yield, capsaicin and other quantitative traits in chillies (*Capsicum annuum* L.). *Botanical Review*, 32(1): 24-55.
9. Maria de Lourdes Reyes-Escogido, Edith G. Gonzalez-Mondragon and Erika Vazquez-Tzompantzi. 2011. Chemical and pharmacological aspects of capsaicin. *Molecules*, 16: 1253-1270.
10. Tembrune, B.V. and Rao, S.K. 2013. Stability analysis in chilli (*Capsicum annuum* L.). *Journal of Spices and Aromatic Crops*, 22(2): 154-164.
11. Wani, K.P., Ahmed, N., Wani, S.A., Abeen, N.J., Mushtaq, F., Afroza, B., Singh, P.K. and Hussain, K. 2013. Comparative performance of various chilli genotypes under temperate conditions of Kashmir. *SKUAST Journal of Research*, 15: 117-122.

Table 1. List of hybrids selected for stability analysis

S.No	Genotype	Name
1	G1	AUCH-1
2	G2	AUCH-2
3	G3	AUCH-3
4	G4	AUCH-4
5	G5	AUCH-5
6	G6	AUCH-6
7	G7	AUCH-7
8	G8	AUCH-8
9	G9	AUCH-9
10	G10	AUCH-10
11	G11	AUCH-11
12	G12	AUCH-12
13	G13	AUCH-13
14	G14	AUCH-14
15	G15	AUCH-15





Gokulakrishnan et al.,

16	G16	AUCH-16
17	G17	AUCH-17
18	C 1	Indam-5
19	C2	Tejaswini

Table 2. Analysis of variance for Eberhart and Russel model

Sources	Df	MSS								
		Days to 50 % Flowering	Plant Height	Plant Width	Fruit Length	MSS Fruit Width	Average Number of fruits per plant	Average Number of seeds per Fruit	Thousand Seed Weight	Dry chilli Yield per Plant
Genotypes	18	15.3711**	1531.0370**	152.9254**	12.2787**	0.0681**	2849.3149**	414.1632**	0.3618*	1189025.2500**
Environment	2	3.6120	80.7829*	6.2467*	1.1046**	0.0014	30550.2891**	72.2319**	0.0699*	1865674.1250**
G x E	36	0.8421	56.8495*	13.5110**	0.1498**	0.0009	1771.3196**	18.4854*	0.0205*	116325.9375*
E + (G x E)	38	0.9879	58.1091*	13.1287**	0.2001**	0.0009	3286.0020**	21.3141**	0.0231*	208396.8906**
Environment linear	1	7.2241	161.5658**	12.4934**	2.2092**	0.0027	61100.5781**	144.4638**	0.1397*	3731348.2500**
G X E (Linear)	18	0.9687	45.1757*	18.0627**	2.6995**	0.0007	1640.2622**	14.9685*	0.0313*	80022.2344*
Pooled Deviation	19	0.6773	64.9206*	8.4896**	2.6945**	0.0011	1802.2416**	20.8435**	0.0092	144604.3438*
Pooled Error	108	7.7394	39.9241	4.3604	6.3047	0.0021	264.9155	30.8809	0.0289	249978.9063

Table 3. Environmental Indices for Nine characters

S. No.	Characters	E1	E2	E3
1	Days to 50 % flowering	-0.3941	-0.0749	0.4690
2	Plant Height	-2.1747	0.2495	1.9252
3	Plant Width	-0.3988	-0.2577	0.6565
4	Fruit Length	-0.0133	0.2474	-0.2342
5	Fruit Width	-0.0074	0.0093	-0.0019
6	Average Number of fruits per plant	-32.5044	44.8092	-12.3048
7	Average Number of seeds per fruit	-1.8346	2.0468	-0.2122
8	Thousand seed weight	0.0352	0.0349	-0.0701
9	Dry chilli fruit yield per plot	-348.970	91.6782	257.2922



Gokulakrishnan *et al.*,

Table 4. Grouping of Hybrids based on Stability parameters

Characters	Group I	Group II	Group III	Group III	Group IV
		b <1	b >1		
Days to fifty					
percent flowering	Nil	Nil	G ₁₆ , G ₁₇	Nil	Nil
Plant height	Nil	G ₅ , G ₁₀ , G ₁₁ , G ₁₇	G ₁₆ , C ₂	G ₁	Nil
Plant width	Nil	G ₁₂ , G ₁₃ , G ₁₄ , G ₁₆	G ₃		G ₁₅
Fruit length	G ₄	G ₁₃	G ₇ , G ₁₀ , G ₁₂ , C ₁	G ₁ , G ₃ , G ₁₅ , G ₁₆	Nil
Fruit width	Nil	G ₁ , G ₃ , G ₆ , G ₉ , G ₁₀ , C ₁	G ₁₂ , G ₁₃ , G ₁₅	G ₁₂	Nil
Average					
number of fruits per plant	Nil	Nil	Nil	G ₁₃ , G ₁₆ , G ₁₇	Nil
Average number of					
seeds per fruit	Nil	G ₁ , G ₂ , G ₄	G ₁₅	Nil	Nil
Thousand seed weight	Nil	G ₁ , G ₉ , G ₁₀ , C ₁	G ₇ , G ₁₂ , G ₁₃	Nil	Nil
Dry chilli fruit yield					
per plot	G ₁₆	G ₁₃	Nil	Nil	Nil





The Perception and Acceptance Level of Wellness Products (Nutraceuticals) in Central Kerala

Antony George*

Assistant Professor, Department of Commerce, Naipunnaya Institute of Management and Information Technology, Thrissur, (Affiliated to University of Calicut), Kerala, India.

Received: 30 Jan 2024

Revised: 09 Feb 2024

Accepted: 26 Apr 2024

*Address for Correspondence

Antony George

Assistant Professor,

Department of Commerce,

Naipunnaya Institute of Management and Information Technology,

Thrissur, (Affiliated to University of Calicut), Kerala, India.

Email: antonygeorge@naipunnaya.ac.in



This is an Open Access Journal / article distributed under the terms of the **Creative Commons Attribution License** (CC BY-NC-ND 3.0) which permits unrestricted use, distribution, and reproduction in any medium, provided the original work is properly cited. All rights reserved.

ABSTRACT

This study was conducted to find out the consumers' perception and acceptance level of Health supplements / Wellness products / Nutraceuticals in the districts of Ernakulam and Thrissur in Central Kerala. In recent years, there has been a significant increase in the use of wellness products among people of all ages. Health supplements are commonly used to improve overall health and wellness, boost immunity, and prevent diseases. However, with the rise of the health supplement industry, there has also been an increase in concerns about the safety and effectiveness of these products. The study aims to determine the factors that influence people's decision to use or not use wellness products, as well as the attitudes and perceptions they have towards these products. The study will be based on the following six dimensions, which are internationally accepted concerning wellness products - Better health, Better fitness, Better nutrition, Better appearance, Better sleep, and Better mindfulness. By analyzing these factors, the project aims to provide insights into how to improve the acceptance and overall well-being of individuals who use wellness products.

Keywords: Better health, Better fitness, Better nutrition, Better appearance, Better sleep, and Better mindfulness, Nutraceuticals

INTRODUCTION

Wellness products and nutraceuticals are specially designed to promote an individual's overall well-being, including their physical, emotional, and internal health. These products cover a broad range of items, including supplements, herbal remedies, fitness gear, skincare products, and more. Their goal is to provide support for wellness and help



**Antony George**

lead a healthy life. Wellness products and nutraceuticals often claim to offer benefits similar to improved health conditions, better physical strength, stress reduction, and enhanced mental clarity. Many of these products are marketed as natural or holistic alternatives to traditional healthcare products, appealing to consumers who prefer a proactive approach to their health. The wellness industry has experienced significant growth in recent years due to increased consumer interest in health and well-being, as well as a growing awareness of the importance of self-care. However, consumers need to be cautious when selecting wellness products, as the market can be flooded with misleading claims and ineffective products. Consulting with healthcare professionals and researching product ingredients and claims can help consumers make informed decisions about which wellness products are right for them. These days, consumers view wellness from a much broader and more sophisticated perspective, encompassing not only fitness and nutrition but also overall well-being. Consumers also have more choices in the types of products and services they buy and the way they buy them.

REVIEW OF LITERATURE

Researchers have conducted several studies to identify consumer behavior patterns in relation to purchasing wellness products. Saini and C. Chaudhari (2021) have emphasized the importance of conducting a thorough analysis to provide practical and relevant information about consumer preferences among different wellness product categories such as personal care, nutritional care, dietary supplements, and weight loss products. The COVID-19 pandemic has led to an increase in the marketing of health products to raise public awareness of their health benefits. Hidayat et al. (2021) have found that attitude significantly influences purchasing intention. Therefore, businesses should focus on product quality and regularly evaluate it to meet consumer expectations and develop a positive marketing strategy. They should also emphasize group references. Kengpol et al. (2021) have discovered that, while the marketing mix has a direct impact on consumer behavior, factors such as reference group, motivation, and knowledge have an indirect impact. Additionally, the sensitivity analysis has revealed that consumer behavior variables can be influenced by increasing or decreasing place and lowering knowledge. The study has also shown that consumers in the new normal market are interested in quality, brands, and health, which poses a significant challenge for small and medium-sized enterprises (SMEs) in creating a strong brand and raising brand awareness.

Indriani et al. (2021) have studied the impact of the COVID-19 epidemic on human life and how it has influenced people's attitudes and intentions to buy healthcare brands during the epidemic. According to the analysis, the low-level and high-mortality-salience groups respond differently to luxury healthcare brands, with the low-level group demonstrating a growing mindset and a preference for budget-friendly items. Uttama (2021) has claimed that the future growth of the health and wellness food market in the Asian market depends heavily on health trends and digital technologies. The study has shown that while the concentration of distribution channels has a major negative impact on food intake for health and wellbeing, health trends and digital technologies have positive and significant impacts. The study has also suggested using a consumer-driven open innovation model to build the health and wellness food industry. Sai Manideep, et al. (2019) claimed that while customers' perceptions of wellness items are based on factors like health, safety, and environmental consciousness, their perceptions of product quality are independent of their level of education. To reach wellness in life, consumers' intentions to purchase organic products are influenced by their demographic characteristics and educational backgrounds; nevertheless, there is no dependent relationship between customer qualification and purchase intention. The research problem and research gap have been identified based on these reviews.

Statement of the Problem

The latest research (April 2021) shows that consumers care deeply about wellness and that their interest is growing rapidly. In a survey of roughly 7,500 consumers by McKinsey in six countries (India not included), 79 percent of the respondents said they believe that wellness is important, and 42 percent consider it a top priority. The estimated global wellness market will be more than \$1.5 trillion, with annual growth of 5 to 10 percent. In every market researched, consumers' prioritization of wellness has shown a substantial increase over the past two to three years.





Antony George

At the same time, the wellness sector is getting more competitive, wellness is here to stay as consumers across nations plan to increase their spending on personal health, appearance, fitness, and more. The pandemic has taught us that physical and mental health will remain a priority for millions of people across the globe for a long time to come. With this huge market potential in the place, it is high time to tap the Indian market. So, this study was carried out to analyse the perception and acceptance level of potential Indian consumers towards wellness products.

Objectives of the Study

- To conduct a research study to measure and analyse the perception and acceptance level of wellness products in central Kerala.
- To understand and analyse the dimensions on which people are spending for wellness products.
- To identify the target market and also to suggest strategies to penetrate the target market.

RESEARCH METHODOLOGY

Total number of respondents were 225, and these respondents were selected based on their lifestyle. Since the wellness products are highly-priced, people with a higher lifestyle are considered as respondents. The sampling group consists of individuals who have an age of 35 years and above. The data for the research were collected through the convenience sampling method. A detailed structured Schedule was developed and after the approval by the experts, the data were collected by personally meeting the respondents and recording their responses. Acceptable Statistical methods and percentage analysis were used to measure the perception and awareness level and the information was presented through graphs and tables for easy understanding.

Sample Distribution

Nature of Respondents		Number of Respondents	Percentage of Respondents	Total
District-wise	Ernakulam	120	53.3	225
	Thrissur	105	46.7	
Gender-wise	Female	56	24.9	225
	Male	169	75.1	
Age-wise	35 - 45	118	52.4	225
	46 - 55	47	20.9	
	55 - 65	23	10.2	
	66 & Above	37	16.4	
Marital Status	Married	170	75.6	225
	Unmarried	55	24.4	
Employment-wise	Business	90	40.0	225
	Retired	37	16.4	
	Salaried professional	56	24.9	





Antony George

	Self Employed Professional	33	14.7	
	Unemployed	9	4.0	

RESULTS AND DISCUSSION

22.2% is the market penetration of wellness products among the target group, and only 7 % of the respondents are using it on a regular basis. 34% of the respondents are not at all aware about the product. Source of information for 31% of the respondents is internet and for 27% is through word of mouth / relatives and for 19% it is TV advertisement. Prescription by a doctor to use wellness products will be more convincing to buy and use the products. Majority of the respondents prefer to buy wellness products from pharmacies. OTT platforms, TV channels, newspapers and magazines play a major role in creating awareness about the product. Social media advertisement is another major tool for creating awareness and expanding the market. Since more than 70% of the respondents consider wellness as very important in their life, 44% perceive wellness as 'better health', and the regular usage rate is only 7% among the respondents. Business has to develop strategies that convince people about the various benefits of taking wellness products needs to spend on advertising and promotion through various print as well as electronic media to create a better awareness level about wellness products and thus increase the market share. Companies have to develop strategies that convince people about the various benefits of taking wellness products. Since the awareness level about the wellness products is very low in the market, it is much needed to create awareness about the benefits of wellness products among the public.

Awareness can be created by advertisements through social media, particularly Facebook, OTT platforms like, YouTube, Amazon Prime and Netflix. Wellness awareness campaigns can also be setup with the help of local authorities (by sponsoring such campaigns). Print media advertisement is also necessary to create awareness about these products. India Today, The Week and Vanitha are the most appropriate among the weeklies / Magazines and The Hindu and Malayala Manorama are the most preferred among newspapers. Promoting these products through doctors will be much more beneficial since these products have impact on the health of people. Prescription by a doctor to use wellness products will create more trust and demand for the products. Wellness products have to be made available in pharmacies rather than in specialized stores. Awareness programmes to nurses who are working as freelancers / personal health consultants can also be considered. Now a days wellness has become top priority and lots of wellness clinics and centers are coming up. Proper strategies to promote the product through these centers will also be beneficial. Since online shoppers are on the rise, apart from just giving advertisement on the social media, management can think of starting virtual shops, like Facebook shop, Shoppify store, etc.

Limitations of the Study

The study only focuses on consumer perception and acceptance level, it may not explore other factors influencing consumer behavior like pricing, availability, and marketing strategies. The study relies on self-reported data from respondents, which may be subject to bias or inaccuracies. The study does not account for cultural and regional differences in consumer behavior and preferences, which may vary across different parts of Kerala.

CONCLUSION

With the aging Kerala population and rates of many diseases continuing to soar, consumers are in need of new products that promote health and wellness. Wellness products (nutraceuticals), with their emphasis on natural health benefits, are one popular option. Nutraceuticals, which have been positioned as a natural alternative to medical treatments of physiological problems, have seen substantially growing in recent years. When developing a nutraceutical marketing strategy, company should focus on health and wellness websites, patient support groups





Antony George

and any channel where large numbers of people with medical issues come together. Company should focus their marketing efforts on the segment of the nutraceutical audience that is motivated more by wellness, fitness and preventive medicine. Nutraceutical marketing should make an effort to target and activate consumers and patients who are being poorly served by traditional healthcare approaches. Some diseases simply do not have a long list of viable medical treatments. Patients who fall within these groups, naturally, are highly motivated to seek impactful supplements. The nutraceutical market is highly fragmented, with a few large multinationals at the top and many small players operating in the industry. In order to stand out in this landscape, companies need to differentiate. The problem is, most companies are selling variations on the same products. This means that branding is a critically important differentiator. The brand should be developed to perceive as a valuable brand and appropriate awareness building strategies should be adopted to be in the strongest competitive position.

REFERENCES

1. Bárbara Franco Lucas, Franziska Götze, Jorge Alberto Vieira Costa & Thomas A. Brunner (2022): Consumer Perception Toward "Superfoods": A Segmentation Study, *Journal of International Food & Agribusiness Marketing*, DOI: 10.1080/08974438.2022.2044955, <https://doi.org/10.1080/08974438.2022.2044955>
2. Chaturvedi, A., Chand, M. R., & Rahman, M. (2021). Impact of the COVID-19 on Consumer Behaviour towards Organic Food in India. In *Predictive and Preventive Measures for COVID-19 Pandemic* (pp. 127-148). Springer, Singapore. DOI : https://doi.org/10.1007/978-981-33-4236-1_8
3. Chauhan NS, Alam S, Mittal A, Sahoo J (2017) Survey on Awareness, Perception, and Extent of Usage of Nutraceuticals in Local Region of Uttar Pradesh, India. *J Pharma Sci* 02: 129. DOI: 10.29011/2574-7711.
4. Hidayat, S., Wibowo, W., Gunawan, Y. L., Dewi, G. C., & Wijayaningtyas, M. (2021). Factors Influencing Purchase Intention of Healthcare Products during the COVID-19 Pandemic: An Empirical Study in Indonesia. *Journal of Asian Finance, Economics and Business*, 8(6). <http://eprints.itn.ac.id/id/eprint/5480>
5. Indriani, F., & Sukresna, I. M. (2021). Does Health Anxiety Influences Brand Engagement? An Experimental Approach on Healthcare Brands During COVID-19 Pandemic in Indonesia. *Journal of Resilient Economies* (ISSN: 2653-1917), 1(1). DOI: <https://doi.org/10.25120/jre.1.1.2021.3816>
6. Kaveh MH, Ostovarfar J, Keshavarzi S, Ghahramani L. Validation of perceived wellness survey in a sample of Iranian population. *Malays J Med Sci*. 2016; 23(4):46–53. doi: 10.21315/mjms2016.23.4.6
7. Kengpol, A., Pichitkarnkar, T., & Elfvengren, K. (2021). A Decision Support System for Consumer Behaviour of Chinese In-bound Tourists on Functional Beverage: An Empirical Study during COVID-19 with Thailand Sandbox. *Applied Science and Engineering Progress*. DOI: 10.14416/j.asep.2021.09.001
8. Latip, M. S. A., Newaz, F. T., Latip, S. N. N. A., May, R. Y. Y., & Rahman, A. E. A. (2021). The Sustainable Purchase Intention in a New Normal of COVID-19: An Empirical Study in Malaysia. *The Journal of Asian Finance, Economics and Business*, 8(5), 951-959. <https://doi.org/10.13106/jafeb.2021.vol.8.no5.0951>
9. Limsuwan, P. (2021). The Importance of Packaging Communication Interfaces on Intention to Purchase Super foods Healthy. *Vidyabharati International Interdisciplinary Research Journal* 13(1) ISSN 2319-4979 Sept. 2021 781 www.viirj.org Products: Tapping to Rising Healthy Food Trends in Times of COVID-19 Epidemic. *Psychology and Education Journal*, 58(2), 3947- 3953. DOI: <https://doi.org/10.17762/pae.v58.i2.2661>
10. Palau-Saumell, R., Matute, J., Derqui, B., & Meyer, J. H. (2021). The impact of the perceived risk of COVID-19 on consumers' attitude and behaviour toward locally produced food. *British Food Journal*. Vol. 123 No. 13, pp. 281-301. <https://doi.org/10.1108/BFJ-04-2021-0380>
11. Rawel Kerketta, A. O. (2020). Market Survey and Research on Ozone Generators, Factors Influencing Consumer Behaviour and the Effect of COVID-19 on the same in India. *Psychology and Education Journal*, 57(9), 5847-5860. DOI: <https://doi.org/10.17762/pae.v57i9.25.29>
12. Shaun Callaghan, Martin Lösch, Anna Pione, and Warren Teichner April 8, 2021 : Feeling good: The future of the \$1.5 trillion wellness market, McKinsey an Company, [https://www.mckinsey.com/industries/consumer-](https://www.mckinsey.com/industries/consumer-76095)





Antony George

packaged-goods/our-insights/feeling-good-the-future-of-the-1-5-trillion-wellness-market#download/%2F~%2Fmedia%2Fmckinsey%2Findustries%2Fconsumer%20packaged%20goods%2Four%20insights%2Ffeeling%20good%20the%20future%20of%20the%201%205%20trillion%20wellness%20market%2Ffeelinggoodthefutureofthe15trilliondollarwellnessmarket.pdf%3FshouldIndex%3Dfalse

13. Tiwari, P., Raychaudhuri, P.S., & Rastogi, A. (2020). Understanding the Market Demand Pattern and Prescribing Behavior of Doctors for Vitamin Drugs in the Indian Pharmaceutical Market under the COVID19 Pandemic Situation: A Case Study of Vitamin D3 and its Promotional Strategy. Perspectives on Business Management & Economics. Vol. III, pp. 47-56. <http://www.pbme.in/papers/68.pdf>
14. Uttama, N. P. (2021). Open innovation and business model of health food industry in Asia. Journal of Open Innovation: Technology, Market, and Complexity, 7(3), 174. <https://doi.org/10.3390/joitmc7030174>
15. Yun YH, Sim JA, Kim Y, et al. Consumers' consciousness of health friendly products and services and its association with sociodemographic characteristics and health status: a cross-sectional survey of the South Korean population. BMJ Open 2020;10:e035591. doi:10.1136/bmjopen-2019-035591.

Table 1 - Importance of wellness for Uses and Non users

			Fairly Important	Important	Not at all important	Slightly important	Very important	Total
Used or not	No	Count	22	20	1	8	124	175
		% of Total	9.8%	8.9%	0.4%	3.6%	55.1%	77.8%
	Yes	Count	7	4	1	4	34	50
		% of Total	3.1%	1.8%	0.4%	1.8%	15.1%	22.2%
Total		Count	29	24	2	12	158	225
		% of Total	12.9%	10.7%	0.9%	5.3%	70.2%	100.0%

Table 2 - Perception about wellness among Users and Non users

			Better appearance	Better Fitness	Better Health	Better Mindfulness	Better Nutrition	Better Sleep	Total
Used or not	No	Count	6	28	75	10	29	27	175
		% of Total	2.7%	12.4%	33.3%	4.4%	12.9%	12.0%	77.8%
	Yes	Count	8	5	23	5	7	2	50
		% of Total	3.6%	2.2%	10.2%	2.2%	3.1%	0.9%	22.2%
Total		Count	14	33	98	15	36	29	225
		% of Total	6.2%	14.7%	43.6%	6.7%	16.0%	12.9%	100.0%

Table 3 - Familiarity of the wellness products among Users and Non users

			I am aware but have never used it	Not aware of it	Use it on a regular basis	Use it only sometimes	Total
Used or not	No	Count	99	76	0	0	175
		% of Total	44.0%	33.8%	0.0%	0.0%	77.8%
	Yes	Count	0	0	16	34	50
		% of Total	0.0%	0.0%	7.3%	14.3%	22.2%





Antony George

		% of Total	0.0%	0.0%	7.1%	15.1%	22.2%
Total		Count	99	76	16	34	225
		% of Total	44.0%	33.8%	7.1%	15.1%	100.0%

Table 4 - Source of awareness about wellness products among Users and Non users

			Friends/ Relatives	Internet	Magazine	News- paper	Not sure	Others	Radio	TV	Total
Used or not	No	Count	24	31	9	3	5	1	2	24	99
		% of Total	16.1%	20.8%	6.0%	2.0%	3.4%	0.7%	1.3%	16.1%	66.4%
	Yes	Count	16	15	3	5	6	0	1	4	50
		% of Total	10.7%	10.1%	2.0%	3.4%	4.0%	0.0%	0.7%	2.7%	33.6%
Total		Count	40	46	12	8	11	1	3	28	149
		% of Total	26.8%	30.9%	8.1%	5.4%	7.4%	0.7%	2.0%	18.8%	100.0%

Table 5 - Strategies that convince the Users and Non users to buy wellness products

			Advertisement	In store promotions	Prescription by a doctor	Total
Used or not	No	Count	23	9	143	175
		% of Total	10.2%	4.0%	63.6%	77.8%
	Yes	Count	13	3	34	50
		% of Total	5.8%	1.3%	15.1%	22.2%
Total		Count	36	12	177	225
		% of Total	16.0%	5.3%	78.7%	100.0%

Table 6 - Comfortable mode of buying wellness products for Users and Non users

			Online	Pharmacy	Supermarket	Total
Used or not	No	Count	51	115	9	175
		% of Total	22.7%	51.1%	4.0%	77.8%
	Yes	Count	13	33	4	50
		% of Total	5.8%	14.7%	1.8%	22.2%
Total		Count	64	148	13	225
		% of Total	28.4%	65.8%	5.8%	100.0%

Table 7 - Most preferred social media platform among Users and Non users

			Faceboo k	Instagra m	LinkedI n	Not using	Snapch at	Twitte r	WhatsAp p	Total
Use d or not	No	Coun t	105	10	10	40	5	1	4	175
		% of Total	46.7%	4.4%	4.4%	17.8 %	2.2%	0.4%	1.8%	77.8%



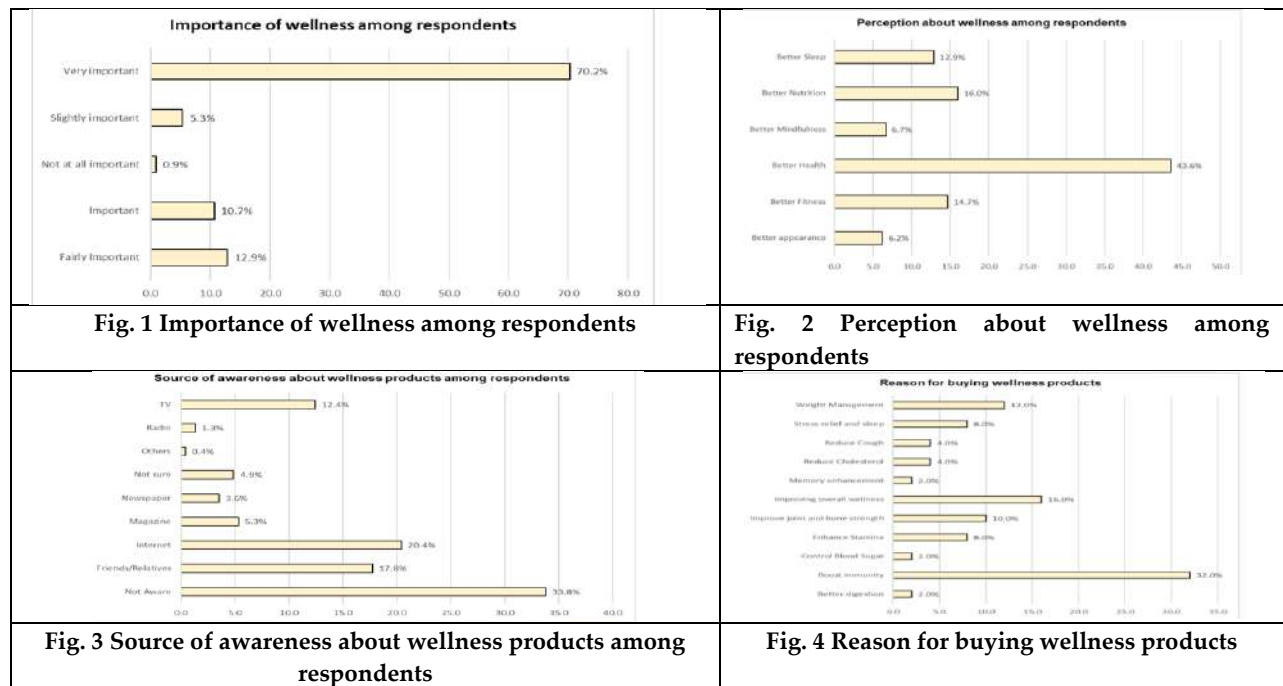


Antony George

	Yes	Count	37	5	5	2	0	0	1	50
		% of Total	16.4%	2.2%	2.2%	0.9%	0.0%	0.0%	0.4%	22.2%
Total		Count	142	15	15	42	5	1	5	225
		% of Total	63.1%	6.7%	6.7%	18.7%	2.2%	0.4%	2.2%	100.0%

Table 8 - Influence of social media advertisement on buying decisions

			No	Yes	Total
Used or not	No	Count	108	67	175
		% of Total	48.0%	29.8%	77.8%
	Yes	Count	23	27	50
		% of Total	10.2%	12.0%	22.2%
Total		Count	131	94	225
		% of Total	58.2%	41.8%	100.0%





Antony George

